ISOLATION AND CHARACTERIZATION OF BIOACTIVE COMPOUNDS FROM MARINE MACROALGAE *KAPPAPHYCUS ALVAREZII* AND *GRACILARIA OPUNTIA*

Thesis submitted in partial fulfilment of the requirement for the degree of

DOCTOR OF PHILOSOPHY

in

CHEMISTRY

BY

Mrs. FASINA MAKKAR
(Ref.No. MU/ACC/Ph.D./CR.40/2014-15/A3, dated 7.03.2015)

Guided By
Dr. KAJAL CHAKRABORTY
Senior Scientist (Organic Chemistry),
Central Marine Fisheries Research Institute (CMFRI)

Under the Faculty of Science and Technology

MANGALORE UNIVERSITY
MANGALAGANGOTHRI – 574 199
Dakshina Kannada Dist. Karnataka, India

भारतीय कृषि अनुसंधान परिषद
केन्द्रीय समुद्री मात्स्यिकी अनुसंधान संस्थान
[कृषि अनुसंधान एवं शिक्षा विभाग, कृषि मंत्रालय,भारत सरकार]
Indian Council of Agricultural Research
Central Marine Fisheries Research Institute
[Department of Agricultural Research and Education, Ministry of Agriculture, Govt. of India]
पोस्ट बॉक्स सं.1603, एरणाकुलम नोर्त पी.ओ.,कोच्ची–682018, केरल, भारत
Post Box No.1603, Ernakulam North P.O., Kochi - 682018, Kerala, India

December 2018

Declaration

*I do hereby declare that the thesis entitled "**Isolation and Characterization of Bioactive Compounds from Marine Macroalgae Kappaphycus alvarezii and Gracilaria opuntia**" is an authentic record of research work carried out by me under the guidance and supervision of Dr. Kajal Chakraborty, Senior Scientist, Central Marine Fisheries Research Institute, Cochin-682018 and the same has not previously formed the basis for the award of any degree or diploma.*

Whenever the work described is based on the findings of other researchers, due acknowledgement is made in keeping with the general practice of reporting scientific observations. However, errors and unintentional oversights, if any are regretted.

Fasina Makkar

Place: Cochin
Date:

भारतीय कृषि अनुसंधान परिषद
केन्द्रीय समुद्री मात्स्यिकी अनुसंधान संस्थान
[कृषि अनुसंधान एवं शिक्षा विभाग, कृषि मंत्रालय,भारत सरकार]
Indian Council of Agricultural Research
Central Marine Fisheries Research Institute
[Department of Agricultural Research and Education, Ministry of Agriculture, Govt. of India]
पोस्ट बोक्स सं.1603, एरणाकुलम नोर्त पी.ओ.,कोच्ची–682018, केरल, भारत
Post Box No.1603, Ernakulam North P.O., Kochi - 682018, Kerala, India
Phone: 91 484 2394867/2391407 Fax: 91 484 2394909/2396685 Email: director@cmfri.org.in Web: www.cmfri.org.in

Dr. Kajal Chakraborty
Senior Scientist (Organic Chemistry)

Certificate

This is to certify that this thesis entitled ***"Isolation and Characterization of Bioactive Compounds from Marine Macroalgae Kappaphycus alvarezii and Gracilaria opuntia"*** *submitted by* ***Mrs. FASINA MAKKAR,*** *Research Scholar of Marine Biotechnology Division of Central Marine Fisheries Research Institute, for the award of the degree of Doctor of Philosophy in Chemistry is the result of bonafide research work carried out by her in the Central Marine Fisheries Research Institute in* ***Chemistry****, Cochin-682018, under my guidance and direct supervision. I further certify that this thesis or part thereof has not previously formed the basis for the award of any degree, diploma, or associateship of any other University or Institution.*

Kajal Chakraborty

Place: Cochin
Date:

Acknowledgements

The successful completion of any task would be incomplete without mentioning the people who made it possible. I take this privilege to express a few words of gratitude and respect to all those who helped me in completion of this work.

Firstly I humbly bow before the almighty God for showering his blessings upon me and giving me the strength, wisdom, health and luck to accomplish this endeavor.

It is with profound joy that I express my heartfelt gratitude to my supervising guide and mentor Dr. Kajal Chakraborty, Senior Scientist, Central Marine Fisheries Research Institute for his inspiring and excellent guidance, valuable suggestions, ceaseless encouragement and intellectual support. He has been my constant inspiration throughout the investigation and I am deeply obliged to him for providing all the necessary facilities and above all the freedom provided in doing the experiment. I record my deep sense of gratitude to him for all the efforts he has put in and the moral support extended for the successful completion of this thesis.

I feel extremely privileged to thank Dr. A. Gopalakrishnan, Director, Central Marine Fisheries Research Institute for being kind enough to extend all the necessary facilities and support required to carry out my research work. I record my deep sense of respect and gratitude to Dr. A. Gopalakrishnan for providing me with the absolute freedom to successfully complete this thesis. I extend my deep sense of gratitude and respect to Dr. G. Syda Rao, former Director of Central Marine Fisheries Research Institute for being kind enough to permit me to register for the Ph.D. programme and providing me with all the necessary facilities required to carry out this doctoral programme. I feel extremely privileged to place on record my sincere respect and gratitude for Dr. P. Vijayagopal, Head, Marine Biotechnology Division, Central Marine Fisheries Research Institute for facilitating my research activities, and for his valuable suggestions and support rendered during the doctoral work.

I am thankful to Dr. Boby Ignatius, Principal Scientist and Scientist-in-Charge, HRD cell of CMFRI for their kind support and constant encouragement extended throughout the investigation. I feel privileged to place on record my sincere gratitude for Dr. P.C. Thomas, former Scientist-in-Charge, HRD cell of CMFRI for kindly facilitating my research activities during the doctoral work.

I feel privileged to place on record my sincere respect and gratitude to the scientists of Marine Biotechnology Division, Dr. P. Jayasankar, Dr. N. K. Sanil, Dr. Sandhya Sukumaran, and Dr. M. A. Pradeep. I wish to express my heartful thanks to Dr. M. P. Paulton (Senior Technical Officer), Shri K.M. David (Technical Assistant), SIC librarian, library support staff, staff members of the HRD Cell, the canteen, security personnel and employees of CMFRI, Cochin, for their sincere help and cooperation extended during the tenure.

I express my sincere thanks to all the staff members of the Indus Digital Press (Cochin) for the final professional setting and printing of the documents of the thesis in an impressive format.

I express my deep sense of gratitude for the support extended by my labmates and colleagues, Anusree Maneesh, Dexy Joseph, Vamshi Krishna Raola, Minju Joy, Soumya Salas, Soumya Krishnan, Tima Antony, and Vinaya K. K. during the study.

I acknowledge the staffs of SAIF, IIT Chennai, especially, Dr. C. Baby, Mr. Bhaskar, and staffs of STIC, Cochin University of Science and Technology (CUSAT), especially, Dr. Shibu Eapen, Mr. Saji T. K for their help and support extended towards the spectroscopic studies.

I take this opportunity to thank Indian Council of Agricultural Research, New Delhi for providing Research Fellowships under different schemes.

I remember my parents, C. S. Makkar & V. M. Nabeesa with profound sense of gratitude whose selfless sacrifice and their great efforts with pain, tears and unceasing prayers has enabled me to successfully complete the research work. I am forever indebted to their understanding, endless patience and encouragement when it was most required.

My express my gratitude to my brother Dilshad M and my sister Ashna Makkar, for their loving support. I extend my deep sense of gratitude to all the family members for their prayers and good wishes.

My special gratitude is due to my beloved husband Mr. Muhammed Sha C A for his love, sacrifice and constant support which made my task much easier. Words fail me to express the sort of heavenly benediction he has been to me. Thanks to my little naughty, Muhammed Mubariz, for always soothing me with a smiling and inspiring face.

Finally, I thank all those who have helped me directly or indirectly in the successful completion of my thesis.

Fasina Makkar

Place: Cochin
Date:

List of Contents

CHAPTER 3: BIOACTIVE POTENTIAL OF *KAPPAPHYCUS ALVAREZII* AND *GRACILARIA OPUNTIA*

CHAPTER 4: ISOLATION AND CHARACTERIZATION OF SECONDARY METABOLITES FROM *KAPPAPHYCUS ALVAREZII* AND *GRACILARIA OPUNTIA*

CHAPTER 5: ISOLATION AND CHARACTERIZATION OF SULFATED POLYSACCHARIDES FROM *KAPPAPHYCUS ALVAREZII* AND *GRACILARIA OPUNTIA* AND THEIR PHARMACOLOGICAL APPLICATIONS

List of Tables

List of Figures

Abstract

Marine macroalgae can be considered as a major resource of bioactive leads. Species of the red marine macroalgae (class Rhodophyceae) were proven to be rich sources of structurally unique and biologically active secondary metabolites endowed with antioxidant, anti-bacterial, anti-inflammatory and anti-carcinogenic activities for applications in functional food and pharmaceuticals. In recent days, macroalgae emerge as a subject area of interest in the biomedical applications owing to the presence of pharmacologically active substances with potential health benefits. Antioxidant compounds exhibit a predominant functional role in attenuating the overproduction of free radicals formed during the regular metabolic processes. Therefore, antioxidant compounds play a vital role in the pathogenesis of oxidative stress induced diseases, such as inflammation, hypertension and diabetics. The present study demonstrated the potential of red marine macroalgae as a source of bioactive leads. *Kappaphycus alvarezii* and *Gracilaria opuntia* registered significant antioxidant potential along with *in vitro* enzyme inhibitory potential with respect to anti-diabetics, anti-hypertension and anti-inflammation. The organic ethylacetate-methanol (EtOAc: MeOH) extracts of the studied marine macroalgae *K. alvarezii* and *G. opuntia* from the Gulf of Mannar region of Mandapam were screened for various pharmacological activities by using different *in vitro* model assays. The organic extracts obtained from *K. alvarezii* and *G. opuntia* was found to possess bioactivities against different disease targets, namely hypertension, type-2 diabetes and inflammation. The ethylacetate-methanol extract of the thalli of *K. alvarezii* and *G. opuntia* was fractionated by repeated column chromatography to afford a number of previously undescribed compounds. The structures of these compounds were established by exhaustive spectroscopic experiments, including mass and two-dimensional nuclear magnetic resonance. The antioxidative and anti-inflammatory activities of the newly reported compounds were evaluated by different *in vitro* assays. Structure-bioactivity correlation analyses of the studied compounds were carried out using different electronic and hydrophobic molecular descriptor variables.

Bioactivity-guided chromatographic fractionation of the ethyl acetate: methanol extract obtained from the thalli of *K. alvarezii* afforded two previously undescribed biogenic halogen analogues, 2-butyl-7-4-(chloromethyl) cyclooct-1-enyl) hept-5-en-1-ol (compound **K1**) and 4-(2-chloroethyl)-5-7-(methoxymethyl) undec-3-enyl) cyclooct-4-enone (compound **K2**) were extracted from the ethyl acetate-methanol extract of *K. alvarezii*, which demonstrated the rare skeletal framework featuring C_{20}-cyclooctene and C_{23}-cyclooctenyl ring system from marine environment. The characteristic isotopic molecular ion peaks with typical isotopic pattern of 3:1 at *m/z* 326 and *m/z* 328 appropriately attributed the existence of one chlorine atom in compound **K1**. The mass spectroscopic experiments of compound **K2** showed a molecular isotopic ion peak at *m/z* 382, having four degrees of unsaturation (molecular formula $C_{23}H_{39}ClO_2$) and were associated with two olefinic bonds, along with one each of carbonyl group and ring system. The studied halogen derivatives demonstrated potential anti-inflammatory and radical scavenging properties and therefore, could be the candidate pharmacophores for as selective inhibitor against pro-inflammatory COX-2 and 5-LOX enzymes. Three oxygenated meroterpenoids, characterized as 1-(3-methoxypropyl)-2-propylcyclohexane (compound **K3**), 3-(methoxymethyl) heptyl-3-(cyclohex-3-enyl) propanoate (compound **K4**) and 2-ethyl-6-(4-methoxy-2-((2-oxotetrahydro-*2H*-pyran-4-yl) methyl) butoxy)-6-oxohexyl-5-ethyloct-4-enoate (compound **K5**) were purified

from the ethyl acetate-methanol fraction of *K. alvarezii*. The highly oxygenated C_{29} meroterpenoid compound **K5** with potential radical quenching and anti-inflammatory potential might qualify this compound as candidate pharmacological lead against oxidative stress and inflammation. An unprecedented non-isoprenoid oxocine carboxylate cyclic ether characterized as (3, 4, 5, 6)-3-(hexan-2'-yl)-3, 4, 5, 8-tetrahydro-4-methyl-2*H*-oxocin-5-yl acetate (compound **K6**) with potential antioxidative and anti-inflammatory activities. The compound **K6** selectively inhibited COX-2 and therefore, has significantly greater selectivity than the NSAIDs. The target bioactivities of the compound **K6** were directed by the electronic and lipophilicity parameters.

Chromatographic purification of the MeOH-EtOAc extract of the thalli of the red marine macroalga *G. opuntia* yielded two unprecedented furanyl derivatives, named 5-(7-(5-ethyl-3, 4-dimethoxycyclooctyl) benzofuran-6-yl)-7-methyl-tetrahydro-2*H*-oxocin-2-one (compound **G1**) and 2-(3-ethyl-9-(2- methoxyethoxy)-1-oxo-tetrahydro-1*H*-xanthen-2-yl) ethyl-5-hydroxy-9-methoxy-7, 8-dimethyl-8-(5-methylfuran-2-yl) nona-3, 6-dienoate (compound **G2**) with significant pharmacological properties in the antioxidant, anti-inflammatory, anti-diabetic and anti-hypertensive model systems. Greater anti-inflammatory selectivity against proinflammatory COX-2 isoform along with significantly greater activity against pro-inflammatory 5-lipoxygenase demonstrated the potential of the newly reported furanyl derivatives as candidates for use against inflammatory disorders. Likewise, the potential antioxidative, anti-diabetic and angiotensin I-converting enzyme inhibitory activities of the isolated compounds showed their utilities in functional food and pharmaceutical preparations to attenuate type-2 diabetes and hypertension. The identified furanyl derivatives isolated from the organic extract of *G. opuntia* have potential pharmacological activities and could be used as future drug leads following toxicity and safety studies. A rare antioxidative azocinyl morpholinone alkaloid 3-(2-ethyl-6-((3, 7)-1, 2, 5, 6-tetrahydroazocin-5-yl) hexyl) morpholin-6-one (compound **G3**) was isolated from the organic extract of *G. opuntia* was found to possess significantly greater antioxidant and anti-inflammatory activities compared to the commercially available antioxidants and nonsteroidal anti-inflammatory drugs. A greater selectivity index of the studied azocinyl morpholinone isolated from *G. opuntia* signified the greater selectivity and significantly lesser side effect profiles than the present therapies by using nonsteroidal anti-inflammatory drugs used to combat inflammatory disorders. Chromatographic purification of the MeOH-EtOAc extract of the thalli of *G. opuntia* also yielded previously undescribed 2*H*-chromen derivative with highly oxygenated carbon skeleton, characterized as 2-acetoxy-2-(5-acetoxy-4-methyl-2-oxotetrahydro-2*H*-pyran-4-yl)ethyl-4-(3-methoxy-2-(methoxymethyl)-7-methyl-hexahydro-2*H*-chromen-4-yloxy)-5-methylheptanoate (compound **G4**), from *G. opuntia*. The target bioactivities of the compound **G4** were directed by the electronic and lipophilicity parameters. The highly oxygenated dimethoxy-2*H*-chromenyloxy methoxy framework bearing the 5-acetoxy-4-methyl-2-oxotetrahydro-2*H*-pyran-4-yl) ethyl acetate skeleton of the title compound isolated from *G. opuntia* might occupy a major space in the design and development of potentially selective new generation antioxidative and anti-inflammatory pharmacophore lead molecules.

The present study demonstrated that sulfated polygalactan characterized as →4)-4-*O*-sulfonato-(2-*O*-methyl)-β-D-galactopyranosyl-(1→4)-3, 6-anhydro-(2-*O*-methyl)-α-D-galactopyranan (**KA-1**) from *K. alvarezii* displayed significantly greater antioxidative and ACE inhibitory activities than →3)-4-*O*-sulfonato-(6-*O*-acetyl)-β-D-galactopyranosyl-(1→4)-3, 6-anhydro-(2-*O*-sulfonato)-α-D-galactopyranosyl-(1→3)-4-

O-sulfonato-(6-*O*-acetyl)-β-D-xylosyl-(1→3)-4-*O*-sulfonato-(6-*O*-acetyl)-β-D-galactopyranosyl-(1→4)-3, 6-anhydro-(2-*O*-sulfonato)-α-D-galactopyranan (**GO-1**), which was isolated from *G. opuntia*. The sulfated polygalactan from *K. alvarezii* (**KA-1**) was found to be a potential therapeutic candidate to prevent the pathologies of hypertensive disorders. The sulfated polygalactans isolated from *K. alvarezii* (**KA-2**) and *G. opuntia* (**GO-2**) possess a number of bioactivities against different disease targets, namely, inflammation and type-2 diabetes. The sulfated polygalactan obtained from *G. opuntia* (**GO-2**) showed greater anti-inflammatory activities than that from *K. alvarezii* as determined by *in vitro* cyclooxygenase/lipoxygenase inhibitory activities. The activities showed significant positive correlation with the anti-diabetic activities as determined by *in vitro* α-amylase, α-glucosidase and dipeptidyl peptidase-4 inhibitory properties.

Marine macroalgae-derived bioactive leads with potential therapeutic properties demonstrated to possess advantageous as functional food with added health benefits. Considering the promising perspective for the utilization of the marine macroalgae, their pharmaceutical potential began to receive considerable attention. The present study demonstrated the presence of library of small molecular weight bioactive compounds of two major species of red marine macroalgae *K. alvarezii* and *G. opuntia*, for use against various oxidative stress-induced diseases with a focus on hypertension, diabetes and inflammation. The lead molecules were isolated to homogeneity and characterized using combined chromatographic and spectroscopic experiments, whereas the novel leads were validated through bioassay and structure-activity relationship analyses to enrich the pool of bioactive leads. This research work also developed protocols to isolate and characterize polysaccharide compounds with bioactive properties against various drug targets for use against hypertension, diabetes, oxidants and inflammatory pathologies. The development of new bioactive compounds from marine metabolites would form the basis for new drug leads and would compose an abundant resource for future bioactivity research.

Abbreviations

^{13}C NMR	-	Carbon-13 Nuclear Magnetic Resonance
1D-NMR	-	One Dimensional-NMR
^{1}H-^{1}H COSY	-	Correlation spectroscopy
^{1}H NMR	-	Proton Nuclear Magnetic Resonance
$^{1}O_2$	-	Singlet Oxygen
2D-NMR	-	Two Dimensional- Nuclear Magnetic Resonance
ABTS	-	2, 2-Azino-Bis-3ethylbenzothiozoline-6-Sulfonic Acid
ACE	-	Angiotensin-Converting Enzyme
ANOVA	-	Analysis of Variance
BHA	-	Butylated Hydroxyanisole
BHT	-	Butylated Hydroxytoluene
CAT	-	Catalase
COSY	-	Correlation Spectroscopy
COX	-	Cyclooxygenase
DCF	-	Dichlorofluorescein
DCM	-	Dichloromethane
DEAE	-	Diethylaminoethyl
DEPT	-	Distortionless Enhancement by Polarization Transfer
DMSO	-	Dimethyl Sulfoxide
DNA	-	Deoxyribo Nucleic Acid
DPP-4	-	Dipeptidyl-Peptidase-4
DPPH	-	1, 1-Diphenyl-2-Picrylhydrazyl
EI	-	Electron Ionization
EI-MS	-	Electron Ionization Mass Spectrometry
EtOAc	-	Ethyl Acetate
FAPGG	-	Furanacryloyl-l-Phenylalanylglycylglycine
FT-IR	-	Fourier Transform Infra Red
GAE	-	Gallic Acid Equivalence
GC-MS	-	Gas Chromatography-Mass Spectrometry
GLP	-	Glucagon Like Peptide
GRx	-	Glutathione peroxidase
GSHPx	-	Glutathione peroxidase
H_2O_2	-	Hydrogen Peroxide
HMBC	-	Heteronuclear Multiple Bond Correlation
HPLC	-	High-Performance Liquid Chromatography
HREIMS	-	High Resolution Electron Ionisation Mass Spectrometry
HRESIMS	-	High Resolution Electrospray Ionisation Mass Spectrometry
HSQC	-	Heteronuclear Single Quantum Coherence
IC_{50}	-	Inhibition Concentration at 50 %
KBr	-	Potassium Bromide
LCMS	-	Liquid Chromatography Mass Spectroscopy
LOX	-	Lipoxygenase
m/z	-	Mass-to-Charge Ratio
MDAEQ	-	Malondialdehyde Equivalent Compounds
MeOH	-	Methanol
MS	-	Mass Spectroscopy
NADPH	-	Nicotinamide Adenine Dinucleotide Phosphate (reduced form)
NMR	-	Nuclear Magnetic Resonance
NOESY	-	Nuclear Overhauser Effect Spectroscopy
$NSAID_S$	-	Non-Steroidal Anti-Inflammatory Drugs
O^2	-	Superoxide Anion
OG	-	Octyl Gallate

$OH^{\cdot}$	-	Hydroxyl Radical
PC	-	Principle Components
PCA	-	Principal Component Analysis
PG	-	Propyl Gallate
ppm	-	Parts Per Million
P-TLC	-	Preparative Thin Layer Chromatography
QSAR	-	Quantitative Structure-Activity Relationship
R	-	Alkyl Radicals
Rf	-	Retardation Factor
ROS	-	Reactive Oxygen Species
RP-HPLC	-	Reverse Phase High-Performance Liquid Chromatography
Rt	-	Retention Time
SD	-	Standard Deviation
SOD	-	Superoxide Dismutase
SPSS	-	Statistical Program for Social Sciences
TBA	-	Thiobarbituric Acid
TBARS	-	Thiobarbituric Acid Reactive Species
tBHQ	-	Tertbutylhydroquinone
TLC	-	Thin Layer Chromatography
TMS	-	Tetramethylsilane
TNF-α	-	Tumor Necrosis Factor-α
TPC	-	Total Phenolic Content
tPSA	-	topological Polar Surface Area
UV-Vis	-	Ultra Violet-Visible
VCC	-	Vacuum Column Chromatography

Chapter 1

INTRODUCTION

Contents

1.1. Marine Macroalgae

Marine life is fascinating, and considered to have great potential for its intrinsic values, as well for the development of new pharmacophore leads. Marine macroalgae are photosynthetic organisms, and there were reports of occurrence of bioactive metabolites. The natural products of marine macroalgae and other marine organisms represent one of the new frontiers in the exploration for valuable bioactive compounds with interesting pharmacological characteristics. Notably, these marine flora have the unique ability to withstand salt-triggered oxidative stress conditions, which is governed by multiple biochemical mechanisms facilitating cell homeostasis and retention of water ability. It is apparent that higher salt concentrations induce disturbances in osmotic and oxidative state of these marine organisms (Zhu 2001). They survive the unfavorable stressed environment by synthesizing various compatible osmolyte derivatives and accumulation of antioxidant molecules. Absence of oxidative damage in the stress-induced biochemical parameters of marine macroalgae suggested that their cells are the store house of bioactive metabolites with potential radical scavenging properties, which provide competitive advantages against various oxidative stress factors leading to the development of harmful reactive oxygen species (Blunt et al.

2006). Antioxidant effects have been reported from various macroalgae due to phenolic compounds, terpenoids and sulfated polysaccharides (Chakraborty et al. 2010a). Novel secondary bioactive metabolites from red marine macroalgae are attracting attention because of the growing demand for new compounds of marine natural origin, having potential applications in pharmaceutical fields and concerns about the toxic effects by synthetic drugs (Kladi et al. 2005; Kladi et al. 2006; Konig and Wright 1997a). The biofunction of small molecular weight molecules including polysaccharides in these organisms as bioactive metabolites is yet poorly understood. Considering the importance of these groups and paucity of information, a systematic search of these candidates for the development of new sources of chemical compounds will be helpful for the design and development of novel bioactive molecules harbored in these species with respect to their antioxidant properties for use in human health and medication. The knowledge on the structural features responsible for bioactivities will guide us to synthesize the molecules in commercial scale for use as new generation bioactive leads as potential drug candidates.

1.2. Marine Macroalgae as Potential Sources of Bioactive Compounds

Bioactive compounds have been reported from marine macroalgae due to various lipid analogues, terpenoids and sulfated polysaccharides (Blunt et al. 2016; Leal et al. 2013; Chakraborty et al. 2015; Newman and Cragg 2012). It is important to note that small molecular weight bioactives and polysaccharides constitute a major share of bioactives in marine organisms including marine macroalgae (Blunt et al. 2016). The predominant classes of novel small molecular weight marine natural leads in these organisms were found to be lactones, phenolics, hydroxybenzene and quinones (Blunt et al. 2014; Liu et al. 2012). The polysaccharides found in the marine macroalgae are known to have many physiological and biological activities including anti-coagulant, anti-viral, anti-tumor and anti-inflammatory and antioxidant effects (De Sousa et al. 2013). In addition, oligosaccharides obtained by depolymerization of marine macroalgal polysaccharides also were found to induce protection against viral, fungal and bacterial infections in plants. The reactive oxygen species are formed during the regular metabolic activities and their overproduction plays vital role in the pathogenesis of oxidative stress-induced diseases, such as chronic inflammation, neurodegenerative disorders, and certain types of cancer

(Yangthong et al. 2009). Antioxidant compounds exhibited a major role to attenuate these diseases, which reveal their extensive commercial potential in pharmaceutical and food industry. Therefore, consumption and addition of antioxidant compounds in food materials prevent the oxidative degradation of biomolecules. It is also important to note that the antioxidants assumed greater importance in controlling the initiation and development of inflammatory diseases. However, oxidative stress-induced molecular damages were found to be due to the overproduction of uncontrolled level of free radicals in the living cells (Florence 1995).

The modern studies have showed that marine macroalgae produced promising bioactive molecules for a range of diseases, such as oxidative stress, hypertension, cancer and inflammatory processes (Minelli et al. 2009). Inflammation is a convoluted mechanism, which includes cellular events and tissue recovery (Aller and Arias 2006). However, distraction of the balance between the free radicals and antioxidant concentration cause cellular oxidative stress, and therefore, antioxidative compounds displayed a prominent role as health defensive factors. They could retard or inhibit lipid oxidation by preventing the initiation or propagation of oxidizing chain reactions, and also by the process of free radicals scavenging (Piccolella et al. 2008). Therefore, there has been increased attention to search for the naturally derived antioxidant compounds from the marine environment during the last few decades. Nevertheless, there were many natural products that showed anti-inflammatory potential, and have comparably lesser extent of side effects. The marine organisms were found to be rich sources of both biological and chemical diversity along with numerous compounds produced by them with useful pharmacological activities (Mayer and Lehmann 1998). A number of bioactive compounds produced by red marine macroalgae were found to prevent the gastric ulcers and cancers caused by the oxidative stress along with inflammatory activities by lowering the production of inflammatory modulators in stomach and colon (Gonzalez et al. 1999). The bioactive natural compounds extracted from edible marine macroalgae would be safer to be used as anti-inflammatory therapeutics in food and traditional medicines. Marine macroalgae have drawn relevant attention in recent years in the search for bioactive compounds, which showed great potential as anti-inflammatory, anti-microbial, anti-viral and anti-tumor drugs (Souza et al. 2012). These groups of marine flora were found to be a rich source of antioxidant compounds (Wang et al. 2009), which could act against lipid oxidation in foods and oxidative stress in target tissues. A polysaccharide fraction of marine macroalga *Padina* sp, was found to

contain anti-inflammatory activities, and was demonstrated to be active against inflammatory enzymes, such as cyclooxygenase-1, 2 (COX) and 5-lipoxygenase (5-LOX) (Praveen and Chakraborty 2013). An anti-inflammatory concentrate enriched with substituted oligofucans was purified from the brown marine macroalgae (Praveen and Chakraborty 2013). Rhodophytan marine macroalgae were acknowledged as bounteous source of various biologically active lead molecules (Blunt et al. 2005). Small molecular weight pharmacophores from the red marine macroalgae were classified as terpenoids (Amico et al. 1991; Rochfort and Capon 1996), halogenated cyclic ether (Wright and Konig 1997a, b), acetogenins (Wael et al. 2010), phlorotannins (Yan et al. 1996), bromophenols, bromoindoles, as well as fucoxanthin (Yan et al. 1999) and phenolics (Chakraborty et al. 2014).

Macroalgae-derived bioactive compounds were found to exhibit extensive pharmacological properties, including antioxidative (Chakraborty et al. 2016; Chakraborty et al. 2014; Chakraborty and Paulraj 2010), cytotoxicity (Yotsu-Yamashita et al. 2004), anti-helmintic (Daigo 1959), anti-malarial (Topcu et al. 2003), anti-microbial (Vairappan et al. 2004), quorum-sensing inhibition (Manefield et al. 1999), and have been considered as potential sources of new therapeutic agents. Small molecular weight molecules isolated from marine macroalge were found to possess various bioactive potentials, such as anti-inflammatory and anti-proliferative (Pereira 2011). The structures of these secondary metabolites were found to vary from acyclic moieties with a linear chain to complex molecules and constituted of biogenic alkaloids, polysaccharides, terpenes and fatty acids (Nunnery 2010). Marine macroalgae are rich source of secondary metabolites, such as polyphenols and soluble polysaccharides with strong anti-microbial and antioxidant activities (Ananthi et al. 2010). The natural antioxidants in macroalgae were reported to include phenolics, phlorotannins, carotenoid, fucoxanthin and isoprenoids (Swanson and Druehl 2002), which were reported to have potential pharmacological importance

Turbinaria conoides *Turbinaria ornata*

Figure 1.1. Examples of brown marine macroalgae

Laurencia papillosa *Jania rubens*

Figure 1.2. Examples of red marine macroalgae

The biologically active compounds in marine macroalgae were found to include polysaccharides comprising galactans, fucoidan, laminarin and alginates (Ferreira et al. 2012). The macroalgal polysaccharides, especially sulfated derivatives were reported to have strong antioxidative properties, and have greater potential to be applied in pharmaceutical and food industries (Pangestuti and Kim 2011). Potential antioxidative and free radical scavenging activities (Ganesan et al. 2008) along with *in vitro* anti-proliferative activity in cancer cell lines (Vallinayagam et al. 2009) were also reported in *K. alvarezii*.

1.3. Free Radicals and Oxidative Agents as Major Causal Agent of Life-Threatening Diseases

Radicals are atoms, molecules or ions with minimum one unpaired electron in the outermost orbit, and are able to exist independentently. Free radicals are highly reactive due to the existence of unpaired electron. Any free radical associated with oxygen can be assigned as reactive oxygen species (ROS). The numerous ROS constitute the radicals, such as hydroxyl ($OH^{\cdot}$), hydrogen peroxides (H_2O_2), singlet oxygen ($^1O_2$), hydroxyl radical and super oxide anion (O^2). Oxidative stress is described as the state in which the increased level of toxic reactive oxygen species defeats the endogenous antioxidant resistance of the host. This resulted in the excessive generation of free radicals, which could interact with the cellular lipids, proteins and nucleic acids, leading to injury and subsequent organ dysfunction. Therefore, the free radicals have been involved in the pathogenesis of life-threatening diseases, such as Alzheimer's, Parkinson's, cancer and cardiovascular disorders (Chew et al. 2008). Free radicals were found to be either endogenous or exogenous. Endogenous free radicals are formed in the body by abnormal metabolism of oxygen, destruction of blood cells by parasites, bacteria and viruses using oxidants, such as nitric oxide, super oxide and hydrogen peroxide. The degradation of fatty acids and other molecules often result in the formation of cellular component (peroxisomes) producing hydrogen peroxide (Slater 1979; Lobo et al. 2010). Exogenous sources of free radicals, which comprise air pollutants including trace metals (lead, mercury, iron and copper) were found to be responsible for free radical generation. The mechanisms of oxidative cellular damage are summarized in Figure 1.3.

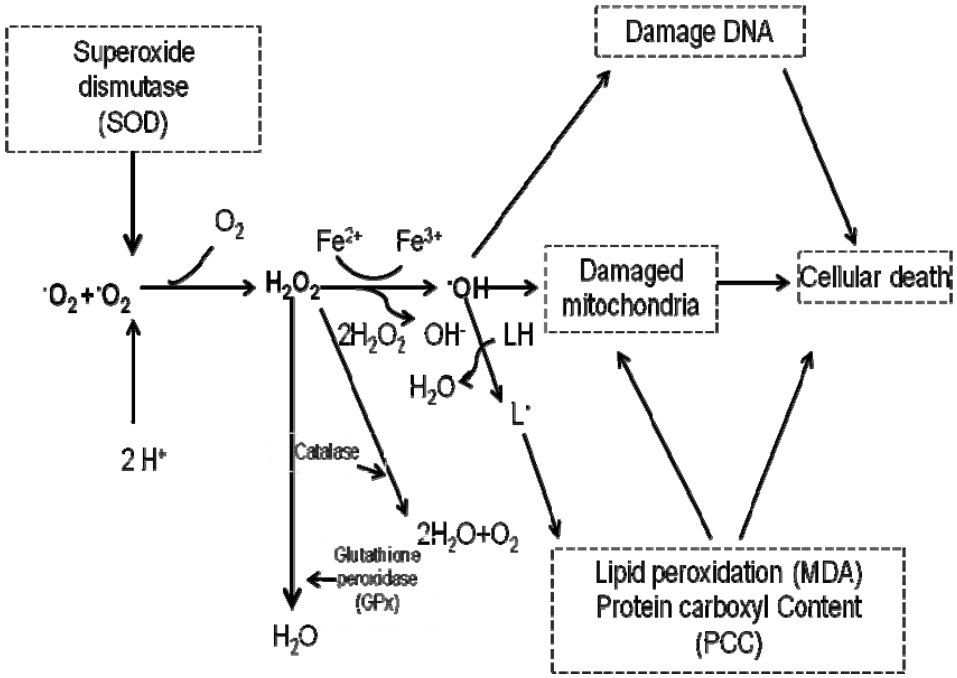

Figure 1.3. Mechanisms of oxidative cellular damage

Free radicals are reduced into water with the co-operation of the three main antioxidant enzymes, such as superoxide dismutase (SOD), catalase and glutathione peroxidases (GSHPx). The hydroxyl radicals generated from hydrogen peroxide induce the production of oxidative cell injury that include carboxylation of protein, DNA damage and lipid peroxidation. By these pathways, oxidative damage leads to cellular death. Excessive production of free radicals is often correlated with lipid and protein peroxidation leading to cell structural damage, tissue injury or gene mutation that finally led to the generation of different health disorders. ROS are the arbitrator of inflammation and other cells were found to be associated with the generation of eicosanoids along with the activation/release of different cytokines, and proliferate the inflammatory action from one organ (liver) to another (kidney, lungs, etc.). The Figure 1.4 illustrated the free radical induced diseases in human biological system leading to the oxidative stress in tissues and multiple-system organ failure (Parke and Parke 1995).

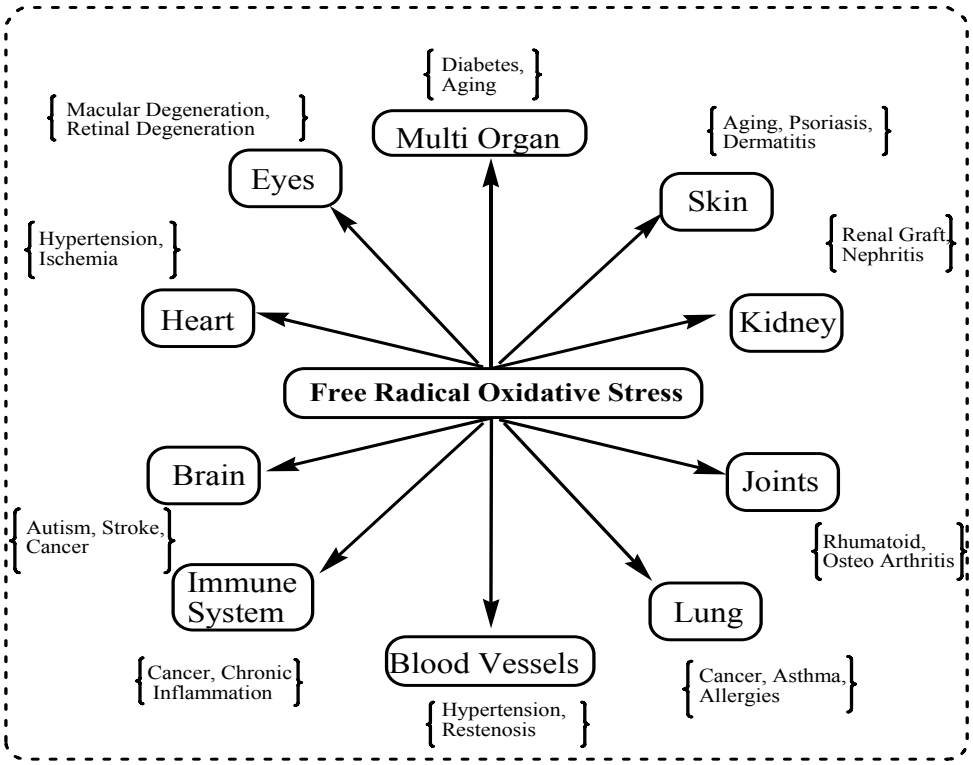

Figure 1.4. Free radical induced diseases in humans

The ROS interfering with the pathogenesis of inflammatory diseases is a concern in immune and autoimmune disorders, which include inflammatory bowel disease, cancer (Ames et al. 1993; Parke 1994), hepatitis (Elliot and Strunin 1993), AIDS (Baruchel and Wainberg 1992), Alzheimer's dementia, multiple-system organ failure (Fry 1992; Parke and Parke 1995) and respiratory distress syndrome (McLean and Byrick 1993).

1.4. Biological Protection Against ROS-Mediated Diseases

The human body has in-built biological processes in place to defend oxidative stress by generating antioxidants, either naturally originated *in situ* (endogenous antioxidants) or externally supplied through diet (exogenous antioxidants).

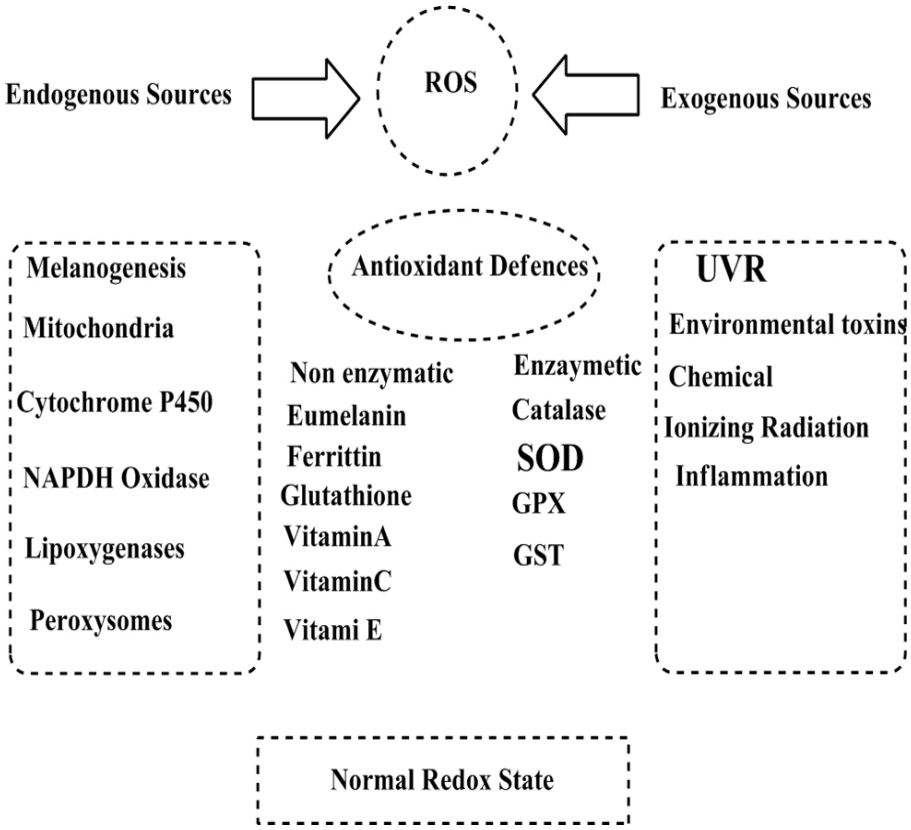

Figure 1.5. Reactive oxygen species (ROS) are derived from multiple sources (endogenous and exogenous) and are counter-balanced by enzymatic and non-enzymatic antioxidants. The antioxidant defenses overwhelmed ROS production resulting in prevention of diseases

The enzymatic and non-enzymatic antioxidant defenses minimize the generation of ROS leading to prevention of diseases. Substances that inhibit oxidation and are able to counteract the damaging effects of oxidation in body tissue are termed as antioxidants. There are biogenic antioxidative enzymes, such as superoxide dismutase (SOD), catalase (CAT), glutathione peroxidase and glutathione reductase (GRx) that are free radical scavengers (Fig. 1.5), and neutralize various types of reactive oxygen species.

1.5. Synthetic Alternatives and Their Adverse Effects

Butylated hydroxy anisole (BHA), butylated hydroxy toluene (BHT), propyl gallate (PG), teritiary butyl hydroquinone (TBHQ), octyl gallate (OG), 2, 4, 5-trihydroxy butapyranone, nordihydroguaiaretic acid and 4-hexyl resorcinol are the few common examples of synthetic antioxidants (Carocho 2013; Aguillar et al. 2012; Gharavi and El-Kadi 2005; Anton et al. 2004; Kubo et al. 2001; Astill et al. 1959; Evan and Gardner 1979; Chen et al. 2004). They are widely used in lipid-containing foods for reducing rancidity, arresting lipid oxidation or peroxidation, cosmetic, and pharma industries. During the last few years, researchers questioned the safety of these synthetic antioxidants in the food systems, and there have been continuous efforts to search for green antioxidant alternatives. Therefore, the pharmaceutical and functional food industries have been focused on developing and marketing natural antioxidants with greater safety thresholds. ROS-mediated inflammation is mainly treated by using non-steroidal anti-inflammatory drugs (NSAIDs) by inhibiting pro-inflammatory cyclooxygenase-1 (COX-1) (a constitutive isoform) along with cyclooxygenase-2 (COX-2). The major side-effects of these drugs are often destructive, which include gastrointestinal ulcers and cardiovascular diseases (Quan 2008). Hence, in recent years, efforts in searching naturally antioxidant and anti-inflammatory compounds in functional food or drugs to replace synthetic products are major thrust areas of research.

1.6. Marine Natural Leads from the Marine Macroalgae: Potential Pharmacophore Candidates Against Several Diseases

Marine flora was recognized as potential natural sources of bioactive compounds with antioxidant and anti-inflammatory properties (Kornprobst 2005). Marine macroalgae constitute a major share of marine flora, and they were reported to be valuable reservoirs of bioactive compound with antioxidant, anti-bacterial, anti-inflammatory and anti-carcinogenic activities (Kornprobst 2005).

Marine macroalgae are photosynthetic organisms, and are resolved to a conjunction of stressful factors, *viz*., light and oxygen at the origin of the evolution of free radicals and other oxidative reagents. The absence of oxidative destruction in their structural components evidently recommended that their cells generate bioactive metabolites with antioxidative resistance systems (Escrig et al. 2001). The reactive

oxygen species (ROS) *viz*., hydroxyl radical (HO), hydrogen peroxide (H_2O_2) etc, are metabolites generated during the aerobic life as an outcome of the metabolism of oxygen. DNA, cell membranes, proteins and other cellular fragments are target sites of the free radical stimulated oxidative degradation processes, resulting in serious human diseases, such as chronic inflammation, atherosclerosis, cancer, cardiovascular disorders and ageing. Clinical studies established that oxidative stress through free radical generation assumes a significant role in the inception of hypertension. Reactive oxygen species and inflammatory markers were found to be greater in the patients with hypertension (Savoia and Schiffrin 2007). It has been reported that extended generation of ROS substantially adds to the dysregulation of physiological processes, which evoke structural and functional variations in hypertension. Increased levels of ROS also potentiate the pathogenic factors leading to type-2 diabetes, and chronic subclinical inflammation was found to be associated with the insulin resistance syndrome (Festa et al. 2000). Diabetes is the most frequent endocrine disorder and, it has been predicted that greater than 200 million people in the world will have diabetes mellitus and 300 million will decisively have the disorder by the year of 2025 (King et al. 1998). The remedial measures to treat the pathogenesis of diabetes are to diminish the post-prandial hyperglycemia in order to prevent the actions of carbohydrate-hydrolyzing enzymes, such as α-amylase and α-glucosidase along with dipeptidyl peptidase 4 (DPP-4). Marine macroalgae were found to be rich sources of bioactive compounds, such as terpenoids, phloroglucinol, phenolics, fucoidans, sterols, glycolipids and halogenated compounds, whereas the extracts or isolated components derived from these marine species exhibited a wide range of pharmaceutical properties, such as anti-cancer, anti-bacterial, anti-viral, anti-fungal, anti-inflammatory, antioxidant, hypoglycaemic, hypolipidemic, hepatoprotective and neuroprotective activities (Liu et al. 2012; Chakraborty et al. 2015).

Antioxidant compounds play an immense role against these disorders, which described their significant economic potential in medicine (Blunt et al. 2016), food production (Blouin et al. 2011) and cosmetic industry (Wang et al. 2015). Chemical compounds with oxidation-inhibiting properties are present in the tropical sessile macroalgae as a protective mechanism against oxidative stress factors in the oceanic ecosystems (Chakraborty et al. 2010a). Investigation of curative metabolites, such as benzene acetamide, methyl-ethyl ketone derivatives and bromophenols extracted from marine macroalgae (red and brown) with significant inhibitory activity towards α-

glucosidase enzymes were described in the previous reports of literature (Seung et al. 2013). In the last few years, numerous investigations have shown that low-grade inflammation were identified with the possibility of developing type-2 diabetes (Crook 2004).

1.7. Antioxidant and Anti-inflammatory Potentials of Bioactives from Red Marine Macroalgae

Bioactive properties of the marine macroalgae were reported to be due to the presence of sulfated polysaccharides, phenolics and terpenoids (Chakraborty and Paulraj 2010; Chakraborty et al. 2015). Polyphenols and sulfated polysaccharides present in macroalgae showed potential anti-viral, anti-tumoral, anti-inflammatory and anti-coagulant activities (Cumashi et al. 2007). Different investigations prescribed that antioxidant and other bioactive properties fundamentally reliant on the level of sulfation, position of sulfate groups on the sugar backbone, sugar composition and glycosidic branching (Leonard et al. 2010). The reported bioactivities of polysaccharides from marine macroalgae incorporated antioxidant, immunomodulatory, anti-coagulant, anti-thrombotic, blood lipid reducing and anti-inflammatory activities (Li et al. 2008). Antioxidant capacities of polysaccharide or polysaccharide-complex were observed in the fucoidan and fucans isolated from *Fucus vesiculosus* and *Padina gymnospora* displaying inhibitory properties towards hydroxy radical and superoxide radical formation (De Souza et al. 2007). The red marine macroalga *Kappaphycus alvarezii* is an economically significant and extensively cultivated red macroalga under the class of Rhodophyceae. *K. alvarezii* has been reported for its antioxidant potential (Ganesan et al. 2008) and *in vitro* anti-proliferative activity in the cancer cell lines (Vallinayagam et al. 2009). The genus *Gracilaria* is the largest in the order Gracilariales, and was found to include more than 150 species, which were distributed in the tropical and temperate sea (Guiry and Guiry 2016). The most common bioactivities known in *Gracilaria* are anti-bacterial, anti-viral, and have been best described in *Gracilaria cornea* (Bansemir et al. 2006) and *Gracilaria changii* (Sasidharan et al. 1991).

Figure 1.6. Marine macroalgae and their collection site at the Gulf of Mannar of Southeast coast of India

Among different species of the genus *Gracilaria*, *Gracilaria opuntia* is one of the predominantly available red marine macroalga grown in the Gulf of Mannar region of the south-east coast of India. There were no reports of the occurrence of naturally occurring antioxidative and anti-inflammatory compounds from this marine macroalgal species.

1.8. Objectives

The red marine macroalgae comprise a large collection of species that are abundant in the coastal areas of Gulf of Mannar region in Mandapam. Among various red macroalgae, *Kappaphycus alvarezii* and *Gracilaria opuntia* (Phylum Rhodophyta) are abundantly available in this area throughout different seasons. Therefore, these species were shortlisted for the present study to evaluate their bioactive properties. Based on this background the objectives of the present study were as follows:

- To collect the red marine macroalgae, *Kappaphycus alvarezii* and *Gracilaria opuntia* (Rhodophyta) from the coastline of India and making extracts, fractions.
- To screen the extracts/fractions from the studied macroalgae for antioxidant and anti-inflammatory properties.
- To isolate the lead molecules belonging to small molecular bioactives and polysaccharides from the crude extracts/fractions of the studied macroalgae using various chromatographic techniques coupled with evaluation of target bioactivities.
- To characterize the bioactive leads using detailed spectroscopic techniques, such as infrared, extensive nuclear magnetic resonance, and mass spectroscopic experiments.
- To predict the biological properties of the studied compounds by structure-activity relationship analyses and generation of database of potential lead molecules as tool box to combat inflammation.

1.9. Thesis Outline

Based on the above objectives the present thesis is divided into a total of six chapters. The importance of the study on the bioactive properties of the red marine macroalgae with objectives are discussed and explained in the Introduction under Chapter 1. Chapter 2 deals with the detail review of the works with regard to the significance of macroalgae as potential sources of antioxidative and anti-inflammatory bioactivities. The pharmaceutical and medicinal values of these species are covered under this chapter. Subsequently, Chapter 3 describes the bioactive properties (with reference to antioxidant, anti-inflammatory, anti-diabetic and anti-hypertension) of the organic extracts derived from *K. alvarezii* and *G. opuntia*. Chapter 4 describes the isolation and characterization of secondary metabolites responsible for antioxidant and

anti-inflammatory activities, for the development of new sources of bioactive pharmacophores, from the studied marine macroalgae. The evaluation of the antioxidant, anti-inflammatory, anti-diabetic and anti-hypertension potentials of the polysaccharides derived from *K. alvarezii* and *G. opuntia* along with their structural characterization and applications are described in Chapter 5. The entire work in this Thesis, along with the discussion regarding the new research findings are summarized in Chapter 6.

Chapter 2

REVIEW OF LITERATURE

Contents

2.1. General Background and Importance

Oxidative stress-induced molecular damages of living cells are caused due to the uncontrolled production of free radicals. Traditionally, macroalgae are considered as valuable marine flora, which are preferred delicacies in the South-east Asian countries, particularly in Japan, China, Korea and Indonesia due to their potential antioxidant and therapeutic properties (Wang et al. 2009). Marine macroalgae developed self resistance mechanisms to inhibit oxidative stress dependent disorders in coastal environment by generating biogenic compounds with antioxidant properties. Therefore, researchers have developed interests in the isolation of bioactive compounds with potential pharmacological properties from marine macroalgae. These group of marine species are the abundant sources of natural bioactive metabolites, in which many of them constitute a novel chemical classification, which has been unexplored in the terrestrial ecosystem. This describes the use of marine macroalgae as potential resources of naturally available antioxidant compounds. Notably, the marine macroalgae do not require freshwater for their production, and these macroalgal species completely depend on saline water for their growth and reproduction.

In recent years, macroalgae have drawn considerable attention to the food technologists as renewable natural resources of novel bioactive compounds and functional food ingredients with potential antioxidative, anti-inflammatory, anti-microbial, anti-viral and anti-tumor activities (Blouin et al. 2011; Holdt and Kraan 2011; Souza et al. 2012; Blunt et al. 2016). This might describe the application potential of these marine species as sustainable sources to bestow valuable 'natural' antioxidant molecules for use as treatment against a host of oxidative stress-induced diseases, which include inflammation, arthritis, type-2 diabetes, obesity and cancer. Therefore, it is important to explore these underutilized and natural resources, based on their bioactive potential.

2.2. Marine Macroalgae as Natural Renewable Resources of Bioactive Compounds

During the last few decades, there is an increased interest in the search of natural antioxidants to replace the synthetic alternatives. There were reports of utilizing marine macroalgae as natural renewable resources to derive potent bioactive compounds and nutraceutical supplements. During the past few years, nutraceutical and agricultural food industries were more focused on the use of macroalgae to develop valuable bioactives and pharmaceutical natural leads. Macroalgae comprises a leading proportion in to the marine flora, and they were recorded to possess structurally distinct metabolites with diverse biogenic potential endowed with hypolipidemic, antioxidant, anti-viral, anti-cancer, anti-bacterial, anti-inflammatory, hypoglycaemic, anti-fungal, hepatoprotective and neuroprotective properties (Liu et al. 2012; Chakraborty et al. 2013). The applications of these marine resources as constituent in functional food are convincing due to presence of structurally diverse bioactive principles. In the ocean environment, light energy absorbs much faster than it can be scattered leading to the generation of free radicals and stimulates lipid oxidation. Marine macroalgae are photosynthetic plants, which are exposed to a fusion of increased oxygen concentration and sunlight. The reduced structural destructions in the cells of marine macroalgae even after the constant exposure to the sunlight, assigned to the significance of natural antioxidative metabolites in macroalgae to neutralize these hazardous free radicals (Swanson and Druehl 2002; Burritt et al. 2002). The antioxidative potential of marine macroalgae could be utilized to interrupt the radical aggregation and propagation.

Therefore, it is of interest to examine the bioactive leads from marine macroalgae for use as potential antioxidant and anti-inflammatory agents. The marine macroalgae were located in intertidal locale, which represents an abundant source of structurally distinct bioactive leads with potent biomedical and pharmaceutical applications (Marina Barbosa et al. 2014). However, there were limited reports in relation to the structural knowledge of bioactive leads in marine macroalgae from the Indian waters. The report on the structural characteristics would help us to develop the molecules in commercial scale, and facilitate explaining their mode of action. The isolation and characterization of newer leads from marine macroalgae will be guiding us to the development of antioxidant compounds to increase the prolonged storage of food ingredients.

2.3. Classifications of Marine Macroalgae

On the basis of pigmentation, marine macroalgae can be classified as green, brown and red belonging to the family of Chlorophyceae, Phaeophyceae and Rhodophyceae, respectively.

2.3.1. Green Marine Macroalgae

Green marine macroalgae are smaller in size, and they exhibited different shapes, such as hair-like filaments, flat sheets, cylinders, spheres and strings of beads. These species of macroalgae are widely present in the marine ecosystem, and green color of this particular macroalgae has been due to the presence of pigments, such as chlorophyll *a* and chlorophyll *b. Bryopsis* and *Caulerpa* are some common examples of green macroalgae (Fig. 2.1).

2.3.2. Brown Marine Macroalgae

Brown macroalgae of marine origin are usually larger in size when compared to other classes of macroalgae. The length of this group of macroalgae is about 20 m with thick leather-like appearance. Traditionally the classes of Phaeophyte are considered as photosynthetic marine algae. However, the class of phaeophytes is not closer to the terrestrial plants, due to the presence of cell wall pigments including fucoxanthin and

chlorophyll-*c*. The genus belonging to *Sargassum* and *Padina* are some of the common examples (Fig. 2.2).

2.3.3. Red Marine Macroalgae

Red marine macroalgae belonging to the class of Rhodophta are generally smaller in size, varying between few centimeters to one meter in length. They exhibited variety of shapes including filamentous, encrusting, tube-like string-like and flat sheets. The red marine macroalgae appear in different colors, such as red, purple, and brownish red due to the presence of pigment phycoerythrin and other characteristics. In addition to phycoerythrin they possess other photosynthetic pigments like R-phycocyanin and chlorophyll-*a.* Red macroalgae are generally comprise filamentous forms, however when compared to other algal species they do not have flagellated cells during the complex life cycles (McHugh 2003). In addition, these macroalgae are usually multicellular and mainly attached with the rocks. *Kappaphycus* and *Gracilaria* are the common examples of red marine macroalgae (Fig. 2.3).

2.4. Red Marine Macroalgae: Prospective Sources of Bioactive Compounds

Species of the red marine macroalgae (class Rhodophyceae) were proven to be rich sources of structurally unique and biologically active secondary metabolites for applications in functional food and pharmaceuticals (Kladi et al. 2004). Terpenoids (Chakraborty and Paulraj 2010), phylopheophylin (Cahyana et al. 1992), fucoxanthin (Yan et al. 1999) and phlorotannins (Yan et al. 1996) are some of the antioxidative compounds were isolated from these species. The bioactive compounds extracted from the macroalgae are used as safer anti-inflammatory therapeutics.

Caulerapa cetruloidis *Bryopsis plumosa*

Figure 2.1. Examples of green marine macroalgae

Padina gymnospora *Sargassum wightii*

Figure 2.2. Examples of brown marine macroalgae

Kappaphycus alvarezii *Gracilaria opuntia*

Figure 2.3. Examples of red marine macroalgae

The vast majority of the red macroalgae of marine origin were found to possess bioactive compounds belonging to diterpenes (Rochfort and Capon 1996), sesquiterpenes (Amico et al. 1991) and C_{15} non-terpenoids containing ether rings of different sizes including halogenated cyclic ether enynes and related allenes (Erickson 1983; Konig and Wright 1997a, b; Iliopoulou et al. 2002). These groups of marine macroalgae were reported for their potential antioxidant properties, and *in vitro* anti-proliferative activity in the cancer cell lines (Chakraborty et al. 2015). *Kappaphycus alvarezii* (Doty ex Silva et al. 1996) (class Rhodophyceae, family Solieriaceae, order Gigartinales) is economically significant and predominantly farmed red macroalga in the shallow tropical marine habitats around the South-east Asian countries, particularly Philippines, Taiwan, Malaysia, Indonesia and India (Ask and Azanza 2002; Chandrasekaran et al. 2008). Despite the fact that red macroalgae, particularly *Laurencia* sp., have been studied extensively with respect to secondary metabolite chemistry (Amico et al. 1991; Rochfort and Capon 1996; Manta 2001; Iliopoulou et al. 2002), studies on members of the genus *K. alvarezii* have been rare with regard to the isolation of novel intriguing structures. Rhodophytan macroalgae were acknowledged as bounteous source of various biologically active lead molecules (Blunt et al. 2005).

Small molecular weight pharmacophores from the macroalgae were classified as terpenoids (Amico et al. 1991; Rochfort and Capon 1996), halogenated cyclic ethers (Konig and Wright 1997a, b), C_{15}-acetogenins (Wael et al. 2010; Rochfort and Capon 1996; Erickson 1983; Konig and Wright 1997a, b), phlorotannins (Yan et al. 1996a), bromophenols, and bromoindoles as well as fucoxanthins (Yan et al. 1999a, b), and phenolics (Chakraborty et al. 2015). Rarely occurring halogenated furanone metabolites were isolated from the Australian red macroalgae, *Delisea fimbriata* and *Delisea pulchra* (Kazlauskas et al. 1977a; De-Nys et al. 1993). Bioactive compounds isolated from macroalgae were found to exhibit extensive pharmacological properties, including antioxidative (Chakraborty et al. 2015; Chakraborty et al. 2016; Chakraborty and Paulraj 2010), cytotoxicity (e.g., halomon) (Yotsu-Yamashita et al. 2004), anti-helmintic (Daigo 1959), anti-malarial (Topcu et al. 2003), anti-microbial (Vairappan et al. 2004), quorum-sensing inhibition (Manefield et al. 1999), and have been considered as potential sources of new therapeutic agents. The red macroalga, *Gracilaria opuntia* Durairatnam (family Gracilariaceae, phylum Rhodophyta) is abundantly available throughout the subtropical and tropical climatic zones (Guiry and Guiry 2016). No natural products were reported from this red macroalga, suggesting *G. opuntia* is an important source to characterize novel bioactive compounds of potential medicinal significance.

2.5. Cultural and Economic Importance of Macroalgae

Marine macroalgae, which were found to possess both industrial and ecological importance in various parts of the World, are one of the major marine resources among marine flora. Traditionally, they were harvested from the wild, but presently, the growing percentage of the production is performed from the cultivation of marine macroalgae. The cultivation of this group of marine flora is one of the means of livelihood among the coastal fishermen populace, and has been used to deliver integrated coastal management (Sievanen et al. 2005). During the year of 2000s, trial farming of marine macroalgae such as *Kappaphycus alvarezii* and *Eucheuma denticulatum* were started in the southern coast of Kenya (Wakibia et al. 2006).

With the increasing requirement of marine macroalgae resources, natural populations regularly become insufficient. Experiments are being invented to accelerate the reproduction of macroalgae by resource administration methods including artificial

farming, advanced collection techniques, expelling challenging species, including artificial habitation. The world's largest favorable macroalgae farming industries are located in Asia, where there is a great necessity for macroalgae-based products and intensify society to organize market growth. Immense ranges of systems are used to culture the macroalgae controlled by biogeographical features and life cycle of the cultivated species (Luning 1990; Kain 1991; Critchley and Ohno 1997).

In the year of 1960s, culturing of the species *Gracilaria* was established in China for the production of raw material for agar industry. At the beginning, cultivation of marine macroalgae was performed on ropes in channel involving fish pond sewage, but by on the year of 1967 this was passed towards the fish ponds themselves (Troell et al. 1999; Bushmann et al. 2001). The novel large scale cultivation of macroalgae such as *Hypnea, Gracilaria, Gelidiella, Enteromorpha* and *Kappaphycus* in Indian coastal water was developed by the Mandapam regional centres of ICAR-Central Marine Fisheries Research Institute and CSIR-Central Salt and Marine Chemical Research Institute. Previously, they were cultivated by vegetative fragment on stones or a floating system and deposit spores on to the nets. A tissue culture method was adapted to some of the algal species particularly for *Kappaphycus,* to enhance its biological productivity. In addition the industrial production techniques were implemented in the species *Gelidiella* and *Kappaphycus* for the extraction of phycocolloids, such as agar and carrageenan, and it was transferred to the industries (Ganesan et al. 2009).

Many species of macroalgae are edible and few of them are deliberated to be a great delicacy. The macroalgae-based industries contributed a wide variety of products with an approximated annual income of US $ 5.5-6.0 billion. Marine macroalgae played very prominent role in human diet in various countries, particularly in China, Japan and other Asian countries due to the valuable components, such as minerals and vitamins (Nisizawa et al. 1987; Fleurence 1999). Other than hydrocolloid-based products, fertilizers, miscellaneous uses and animal feed additives were also contributed significant economic value to the industries (McHugh 2003). Marine macroalgae possess distinct uses in various industries, such as food and feed, fertilizers and pharmaceutical industry (Chapman and Chapman 1980).

The green macroalga *Ulva* that is also known in the name of 'Sea lettuce' has found to be rich in protein content in comparison with *Enteromolpha* and *Monostroma* spp. (Ohno 1993). Due to the presence of rich protein content, *Ulva* is considered as a fresh ingredient in salads. Other than *Ulva*, macroalgae such as *Caulerpa lentillifera*

and *Caulerpa racemosa* are the other famous edible macroalgae that were used in fresh salads (McHugh 2003).

As compared to green macroalgae, brown macroalgae are mainly considered for the extraction of hydrocolloid named as alginate, which exist in the cell wall material. The species of brown macroalgae such as *Lessonia, Ecklonia, Lalllinaria* and *Macrocystis* are generally used in foreign countries for the extraction of alginate, although the species of *Turbinaria ornata* and *Turbinaria conoides* are considered for the industrial production of alginate in India. In addition to the production of phycocolloids, some species of brown macroalgae, such as *Hizikia, Laminaria* and *Undaria* were considered as the preferred food items (Cordero 2003; McHugh 2003). Red marine macroalgae have been considered as a food product, and was consumed by the coastal populace during the last 200 years. There are approximately 344 available species, which were found to possess economic value, but few of them includes *Eucheuma, Porphyra, Gleopeltis, Gracilaria* and *Gelidium* have been farmed to a significant extent. The red macroalgae were found to be prominent sources of agar and carrageenan.

2.6. Structural Diversity of Bioactive Compounds from Marine Macroalgae

Red marine macroalgae are known to be an unprecedented source of different terpenoid and non terpenoid secondary metabolites, including halogenated cyclic ethers and related allenes with prominent bioactivities (Blunt et al. 2006). Sulfated polysaccharides from macroalga *Fucus vesiculosus* were known to have antioxidant importance, and advocation of sulfated polysaccharides enhanced the antioxidant status, thereby preventing membrane injury and free radical formation (Veena et al. 2007). A previous report of literature described the antioxidant property in the sulfoglycolipid fraction of red marine macroalga *Porphyridum creuntum* (Berge et al. 2002). Fucoxanthin, which is a polysaccharide analogue, was reported to be the major antioxidant metabolite in the edible marine macroalga *Hijikia fusiformis* (Yan et al. 1999a). The sesquiterpenes (majapolene B) (Blunt et al. 2008); diterpenes (neorogioldiol B) (Blunt et al. 2005) and C_{15}-acetogenins (laurenyne) were isolated from the red marine macroalgae, and their structural description on the basis of halogen atoms (Konig and Wright 1997b) were detailed. These compounds were reported to possess antioxidative, anti-cancer and cytotoxic properties. Among the antioxidants from marine macroalgae,

phenolic acids, flavonoids, anthocyanins, hydroxycinnamic acid derivatives, alkaloids and terpenoids (Bandoniene and Murkovic 2002) were reported to have major share among others (Ragan and Glombitza 1986).

The marine macroalgae deliver a cocktail of halogenated secondary metabolites with significant industrial values and pharmaceutical importance (Holdt and Kraan 2011). The structures of these algal secondary metabolites were found to range from non cyclic linear chain moiety to complex cyclic entities. Halogenations generally bring these metabolites with intriguing characteristics, and macroalgae displayed distinct and individual anabolism pathways for the generation of halogen-substituted compounds with pharmacological potentials, such as anti-inflammation, anti-bacterial, ichthyotoxic, cytotoxic, anti-fungal, and insecticidal properties. Red macroalgae are the main source of halogenated metabolites, which include callicladol (Holdt and Kraan 2011), laurenterol (Castro and Huber 2013) and halomon (Lordan et al. 2011). Red marine macroalga of the genus *Laurencia* were found to be rich sources of broad-ranging halogenated compounds including C_{15}-acetogenins, terpenoids, sesquiterpene alcohol, and elatol with potential bioactivities (Laurienzo 2010). A series of C_{15} acetogenin enynes displaying anti-staphylococcal activity, were isolated from *Laurencia glandulifera* (Kladi et al. 2008). 5-Acetoxypalisadin B (Jiao et al. 2011), palisadin A (Pomin et al. 2008), and palisadin B (Ngo et al. 2013) were the anti-microbial compounds, which were isolated from *Laurencia saitoi* (Ji et al. 2009). Anti-bacterial potential of Malaysian macroalga *Laurencia pannosa* was tested against different marine bacterial species, such as *Chromobacterium violaceum*, *Proteus mirabilis* and *Vibrio cholerae*. The halogenated sesquiterpenes, pannosanol, pannosane and chlorofucin (Güven 2010; Takaichi 2011) were found to display potential anti-bacterial activity.

Chromenes are one of the distinctive classes of bioactive compounds and functional food component exhibiting various pharmacological properties, such as antioxidant (Milan et al. 2011), anti-viral (Mori et al. 2003), anti-inflammatory, anti-coagulant, and TNF-α inhibitor (Cheng et al. 2003) activities. This group of benzopyran derivatives represents the basic nucleus of various marine natural products, particularly belonging to polyphenols, alkaloids, small molecular weight compounds, and are ubiquitously distributed among marine organisms including coelenterates, macroalgae, sponges and tunicates (Blunt et al. 2005). There were reports of the presence of chromene metabolites with antioxidative and cytotoxic properties in macroalgae (Kato et al. 1975). Notably, the greater bioactivity of the chromene derivatives was attributed

to the lipophilic properties, which lead to the higher permeability across cell membranes (Nicolaou et al. 2000). Anti-inflammatory compounds and cyclooxygenase inhibitors, such as SC-75416, 6-chloro-8-methyl-2-(trifluoromethyl)-2*H*-chromene-3-carboxylic acid, 6-chloro-2-(trifluoromethyl)-4-phenyl-2*H*-chromene-3-carboxylic acid, 6-(4-hydroxybenzoyl)-2-(trifluoromethyl)-*2H*-chromene-3-carboxylic acid and 6-chloro-7-(4-nitrophenoxy)-2-(trifluoromethyl)-2*H*-chromene-3-carboxylic acid were reported to contain chromene pharmacophore (Kwangwoo et al. 2008). Plastoquinones, chromanols and chromenes reside in a common class of natural compounds containing polyprenyl chain bound to a hydroquinone framework, and were reported to occur in marine macroalgae (Pereira et al. 2011). Mojabanchromanol is an example of an antioxidative chromene derivative isolated from macroalga *Sargassum siliquastrum*, and was reported to display free radical scavenging activity (Toth and Pavia 2000). Chromene derivatives from marine macroalga *Sargassum micracanthum* with potential antioxidative and anti-ulcer properties were reported in a previous literature (Mori et al. 2003). Chromene derivatives was also found to be an interesting template for the discovery of potential anti-cancer agents (Vosooghi et al. 2010), such as acronycine (lung, colon and ovary cancer).

Terpenoids are structurally diverse secondary metabolites with more than 40,000 reported structural diversity possessing valuable bioactive properties (Gershenzon and Dudareva 2007). Terpenoids were recognized to possess potential pharmacological properties against deadly diseases, such as malaria (Parshikov et al. 2012), cardiovascular ailments (Liebgott et al. 2000) and cancer (Ebada et al. 2010). These marine organisms were found to be potential reservoir of bioactive secondary metabolites including terpenes, sterols, polyphenols, acetogenins, etc., and the most prominent among these are meroterpenoid group of compounds (Chakraborty et al. 2016). The meroditerpene, 11-hydroxy-11-*O*-methylamentadione, isolated from the macroalga *Cystoseira usneoides* showed anti-inflammatory effects in dextran sodium sulfate-persuade colitis in a murine model. The terpenoid compound was found to significantly inhibit the generation of the cytokine (a type of inflammatory signaling molecule) and tumor necrosis factor in lipopolysaccharide-induced human monocytic leukaemia cell line. Three antioxidative aryl meroterpenoids were previously isolated from the red macroalga *Hypnea musciformis* (Chakraborty et al. 2016).

The C_{15} acetogenins bearing cyclic ether skeletons have been isolated as the major secondary metabolites from red macroalga *Laurencia* sp (Erickson 1983), and were reported to be anti-microbial (Konig and Wright 1997a, b), anti-feedant (Kurata et al. 1998), anti-helmintic (Davyt et al. 2001) and cytotoxic properties (Juagdan et al. 1997). A range of chlorinated compounds, C_{15} acetogenin en-ynes, were isolated from *Laurencia glandulifera* and were reported to be moderately cytotoxic towards various human tumour cell lines (Kladi et al. 2009). However, there was no literature report for the antioxidant and anti-inflammatory activities of the laurefurenynes A–F and cyclic ether acetogenins isolated and characterized from red macroalgae. Anti-inflammatory potential of the chromene sargachromanol G from the Korean macroalga *Sargassum siliquastrum* (Fucales) (Yoon et al. 2012); halogenated compounds from the red macroalga *Laurencia snackeyi* (Vairappan et al. 2013) along with the porphyrin derivatives pheophorbide and pheophytin from the macroalga *Sargassum japonica* were reported in previous literature (Islam et al. 2013). Antioxidative compounds from macroalga *Eisenia bicyclis* were identified as phylopheophylin in (Cahyana et al. 1992), whereas phlorotannins in *Sargassum kjellamanianum* (Yan et al. 1996) and fucoxanthin in *Hijikia fusiformis* were characterized as predominant secondary metabolites (Yan et al. 1999a). Laureatin, isolaureatin and deoxyprepacifenol were other related compounds obtained from the red marine alga *Laurencia nipponica* (Masuda et al. 1997). They exhibited significant insecticidal activity against the mosquito larvae *Culex pipens pallens* (Watanabe 1989). Cytotoxic compounds belonging to (+)-α-isobromocuparene and (-)-α-bromocuparene along with cyclolaurane sesquiterpenes were extracted from marine macroalgae (Kladi et al. 2006). Flavonoid compounds, such as quercetin, catechin, tiliroside, acanthophorins and acid derivates were described as the principle bioactive components of the red marine macroalgae (Blunt et al. 2006). Antioxidant properties of phenolic and polysaccharide components from methanolic and aqueous extracts and their fractions were reported from marine macroalgae (Chakraborty et al. 2013; Ganesan et al. 2008). Phlorotannins (polyphenols) from marine macroalga *Ecklonia stolonifera* and *Ecklonia kurome* were reported to be potent antioxidants (Kang et al. 2003). Phlorotannins of *Ecklonia kurome* were reported to be composed of phloroglucinol, eckol, phlorofucofuroeckol, dieckol and 8,8''-bieckol with some other unknown phenolic compounds (Kang et al. 2004). Laurefurenynes A **(1)** described from the red marine macroalga *Laurencia* sp (Abdel-Mageed et al. 2010). The chamigrane sesquiterpenes Yicterpene A and B **(2)** isolated

from marine macroalga *Laurencia composita* (Pingtan Is., China) and the other seven compounds were described from *Laurencia similis* (Sepanggar Is., Kota Kinabalu, Sabah), whereas ent-1(10)-aristolen-9b-ol **(3)** claimed as an enantiomer of a known compound (Kamada et al. 2013). Two bromophenols **(4-7)** with radical scavenging activities were obtained from marine macroalga *Symphyocladia latiuscula* (Qingdao, Shandong Province, China) (Xu et al. 2013a). This same collection of *Symphyocladia latiuscula* also provided the weakly anti-fungal bromophenol sulfoxide (Xu et al. 2013b). The bromophenols isolated from *Vertebrata lanosa* (Oldervik, Ullsfjorden, Norway) and found to possess cellular antioxidant activities (Olsen et al. 2013). The unprecedented polybrominated spiro-trisindole similisine A **(8)** and its enantiomer similisine B obtained from *Laurencia similis* (S. China Sea) (Sun et al. 2013). Five known bromophenols from a variety of red macroalgae were reported to possess inhibitory activity against glucose 6-phosphate dehydrogenase (Mikami et al. 2013). Bioactive metabolites isolated from *Asparagopsis taxiformis* were found to have potential for therapy to fish infected with *Streptococcus iniae* (Mata et al. 2013). An anti-fungal aldehyde **(9)** isolated from *Laurencia papillosa* (Jeddah, Red Sea) (Alarif et al. 2011). Maneonenes were reported from red macroalga *Laurencia obtusa* (Jeddah, Red Sea) (Ayyad et al. 2011). It was found that the structure of *cis*-maneonene D had the similar structure with lembyne A (Vairappan et al. 2001) or the product obtained from treatment of *cis*-maneonene C with p-toluenesulfonic acid (Waraszkiewicz et al. 1978). Apoptotic activity was shown for compounds *cis*-maneonenes E **(10)** and maneonenes (3Z) and (3E) **(11)**.

The oxidized levuglandin D2 **(12)** obtained from marine macroalga *Gracilaria edulis* (La Union, Philippines) (Kanai et al. 2011). Eight halogenated nonterpenoid acetogenins **(13)**, 12-epoxyobtusallene IV **(14)**, obtusallene X **(15)**, marilzallene **(16)**, (-)-4-acetoxymarilzallene **(17)**, (Z)-adrienyne **(18)** and (E)-adrienyne **(19)** isolated from marine macroalga *Laurencia marilzae* (Paraiso Floral, Canary Is.) (Gutierrez-Cepeda et al. 2011a). This same collection of *Laurencia marilzae* also yielded marilzabicycloallenes A–D **(20-21)** which posesse an unprecedented bicyclotridecane ring skeleton, when present in *Laurencia* species (Gutierrez-Cepeda et al. 2011b). The halogenated monoterpenes A **(22)** and B **(23)** derived from *Plocamium suhrii* (Port Elizabeth, Africa). Along with other similar known compounds from this extract, they had significant cytotoxic effects on an esophageal cell line (Antunes et al. 2011).

Two chamigrenes, such as cycloelatanene A **(24)** and cycloelatanene B **(25)** isolated from marine macroalga *Laurencia elata* (St. Pauls Beach, Vic., Australia) using high performance liquid chromatography. Three cytotoxic oxasqualenoids, prethyrsenol A, 15 dehydroxythyrsenol A, 13-hydroxyprethyrsenol A, Iubol **(26)**, venustatriol **(27)** and thyrsiferol **(28-29)** derived from *Laurencia viridis* (Cen Pacheco et al. 2011). Bromophenols **(30-34)** isolated from *Rhodomela confervoides* (Dalian, China), and the same exhibited potent antioxidant activities (Li et al. 2011). Lithothamnin A **(35)** isolated from *Lithothamnion fragilissimum* (Lighthouse Reef, Palau Is.) as a modestly cytoxic compound. This metabolite is an unusual bastadin-like molecule with a unique meta–meta linkage between the aromatic rings (Van Wyk et al. 2011). An extract from *Callophycus oppositifolius* (Pugh Shoal, NT, Australia) yielded the cytotoxic tetrahydro-carboline callophycin A (ovenden et al. 2011). Marine macroalga-derived bioactive compound callophycin A **(36)** synthesized along with fifty other variously functionalized tetrahydro carboline derivatives for evaluation as chemopreventive and anti-cancer agents (Shen et al. 2011). Previously reported red algal metabolites continue to be the targets of synthesis. Polysiphenol was generated by intramolecular regioselective oxidative coupling reactions (Aknin et al. 1992; Clausen et al. 2011).

A pharmacologically active nucleoside, 5-iodo-5'-deoxytubercidin **(37)** isolated from marine macroalga *Hypnea valendie* (Kazlauskas et al. 1983). The monoterpene **(38)** obtained from species of the genus *Plocamium* and the structural determination was defined by X-ray analysis (Stierle et al. 1979). Three monoterpenes **(39-41)** described as the principle bioactive components of the species *Plocamium* (Crews 1977). Polyhalogenated anti-microbial bisnormonoterpenoid **(42)** and monoterpene **(43)** reported from marine macroalga *Plocamium cruciferum* (Faulkner 1984). Two linear monoterpenes **(44-45)** and preplocamenes, **(46-48)** isolated from marine macroalgae *Plocamium angustum* (Dunlop et al. 1979) and *Plocamium viofaceum* (Crews and Kho-Wiseman 1977) respectively. The species of the genus *Plocamium* contains monocyclic polyhalogenated monoterpenes **(49)** and **(50)** (Mynderse and Faulkner 1974). The secondary metabolites, plocamene E **(51)**, plocamene D **(52)**, plocamene D' **(53)** reported from red macroalga *Plocamium violaceurn* (Crews et al. 1978). Plocamene D' **(54)**, 4-bromo-analogue **(55)** of violacene along with **(56)** and its isomer **(57)** also extracted from an Antarctic specimen of *Plocamium cartilagineum* (Higgs et al. 1977).

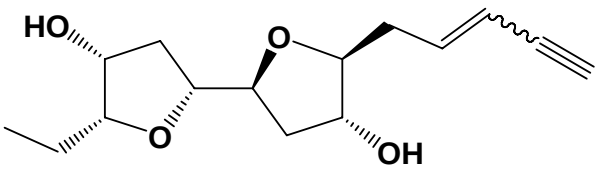
HO
O
O
OH

1

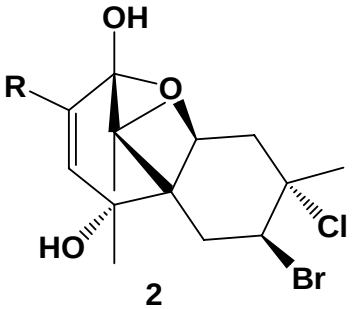
OH
R
O
HO
Cl
Br

2

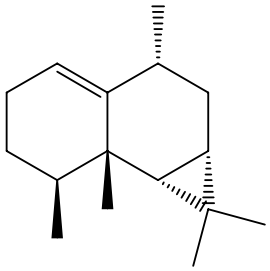

3

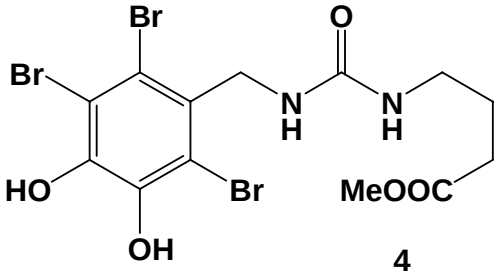
Br
O
Br
N
H
N
H
HO
Br
MeOOC
OH

4

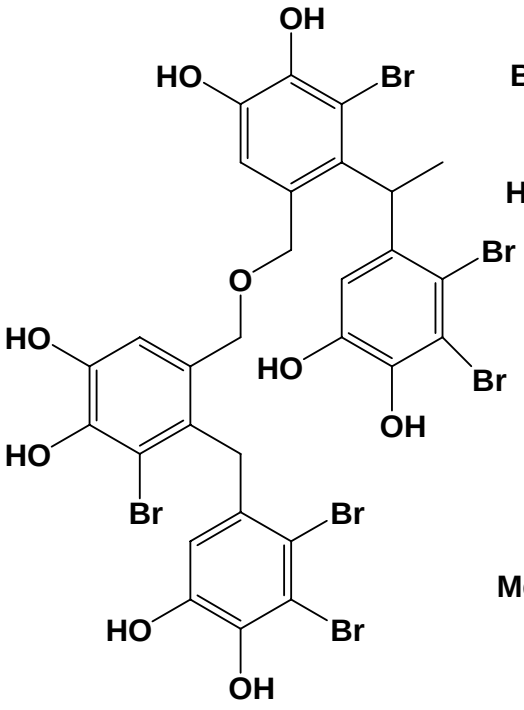
OH
HO
Br
Br
O
HO
Br
OH
HO
Br
Br
HO
Br
OH

5

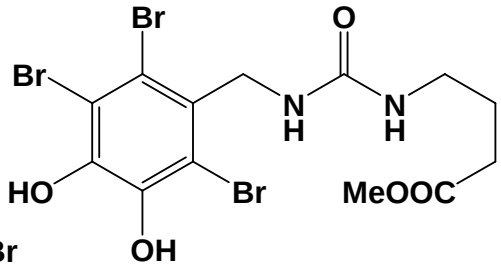
Br
O
Br
N
H
N
H
HO
Br
MeOOC
OH

6

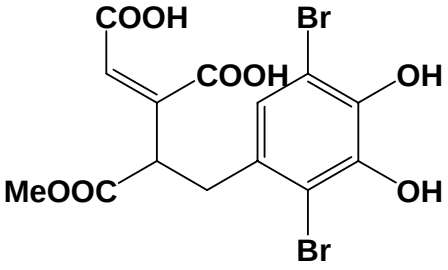
COOH
Br
COOH
OH
MeOOC
OH
Br

7

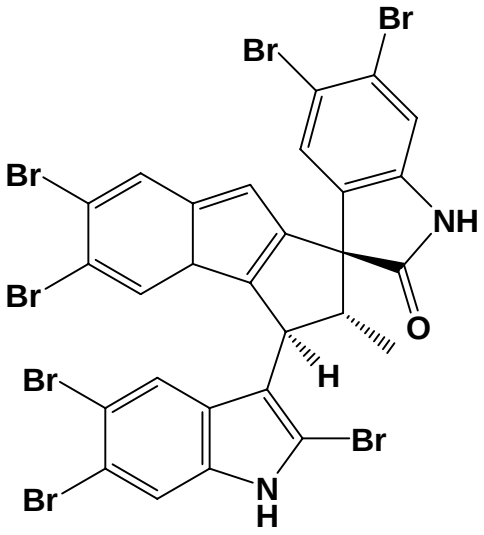

8

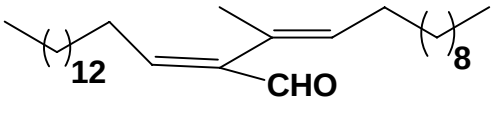

9

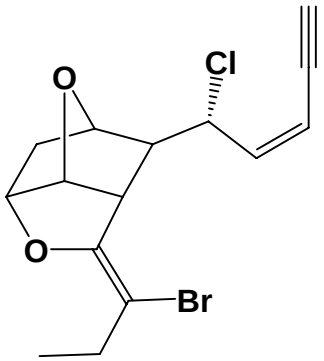

10

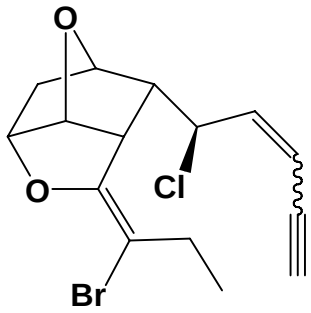

11

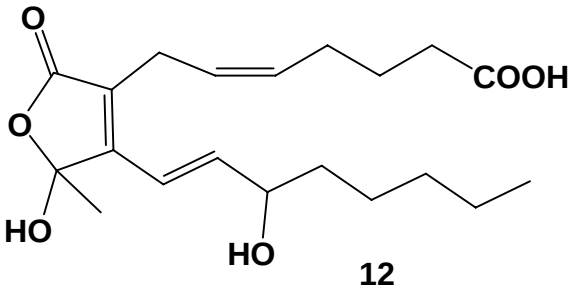

12

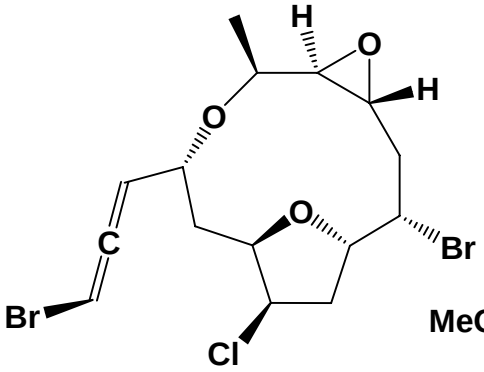

13

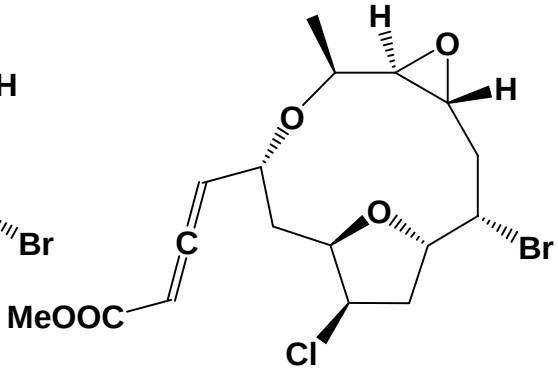

14

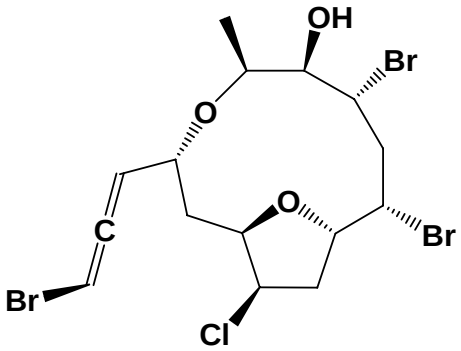

15

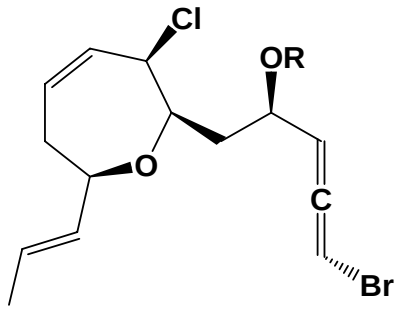

16

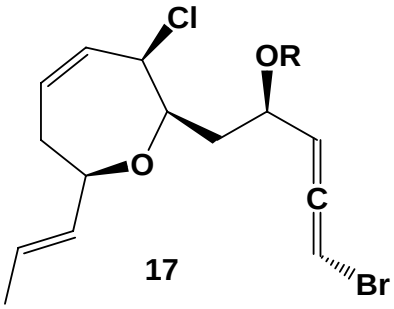

17

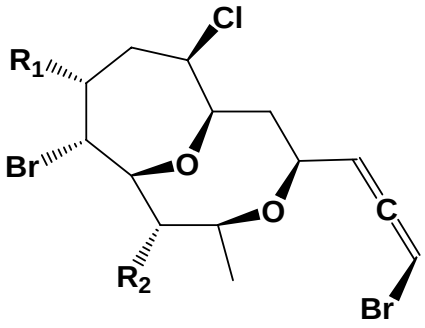

20

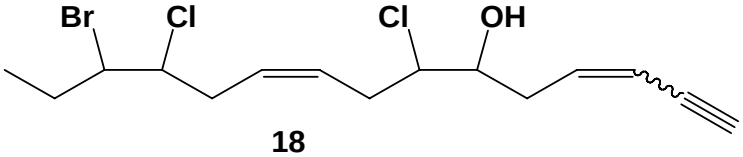

18

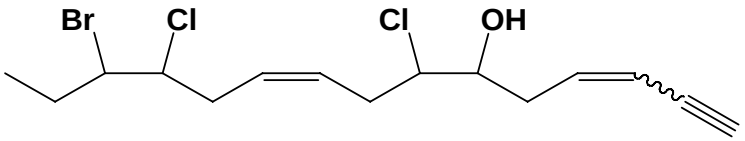

19

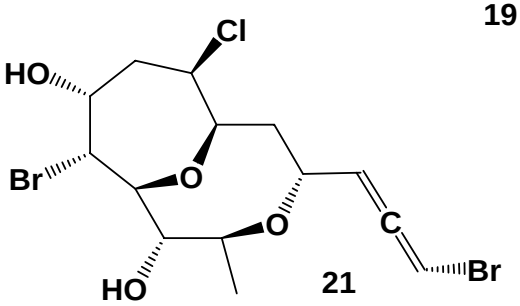

21

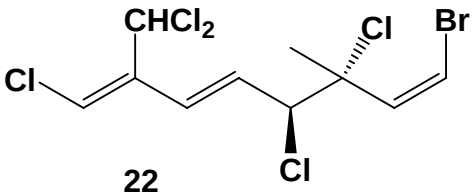

22

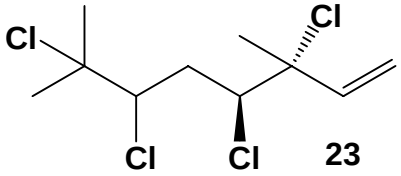

23

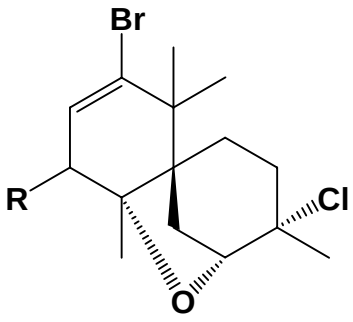

24

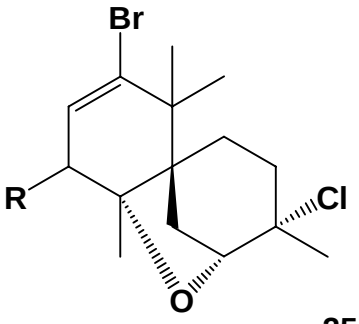

25

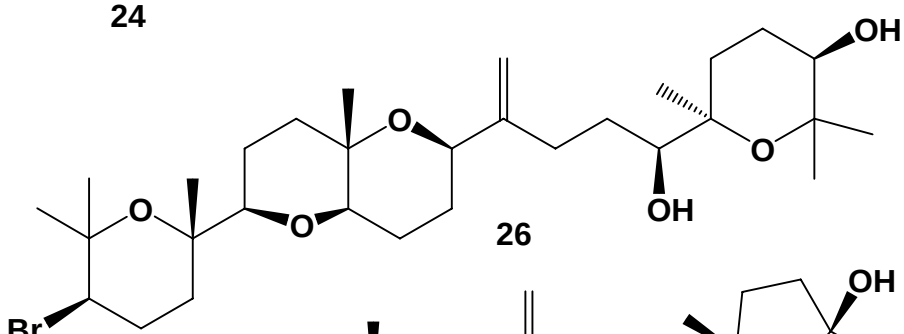

26

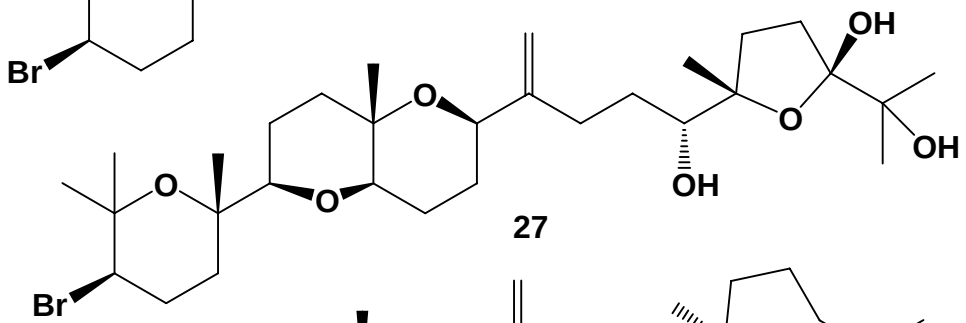

27

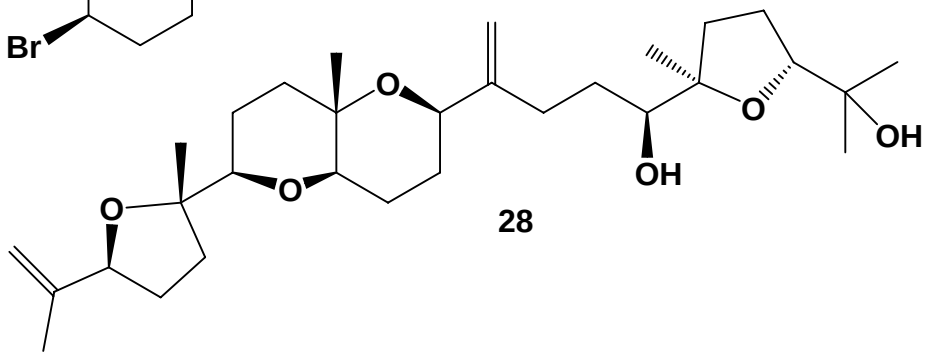

28

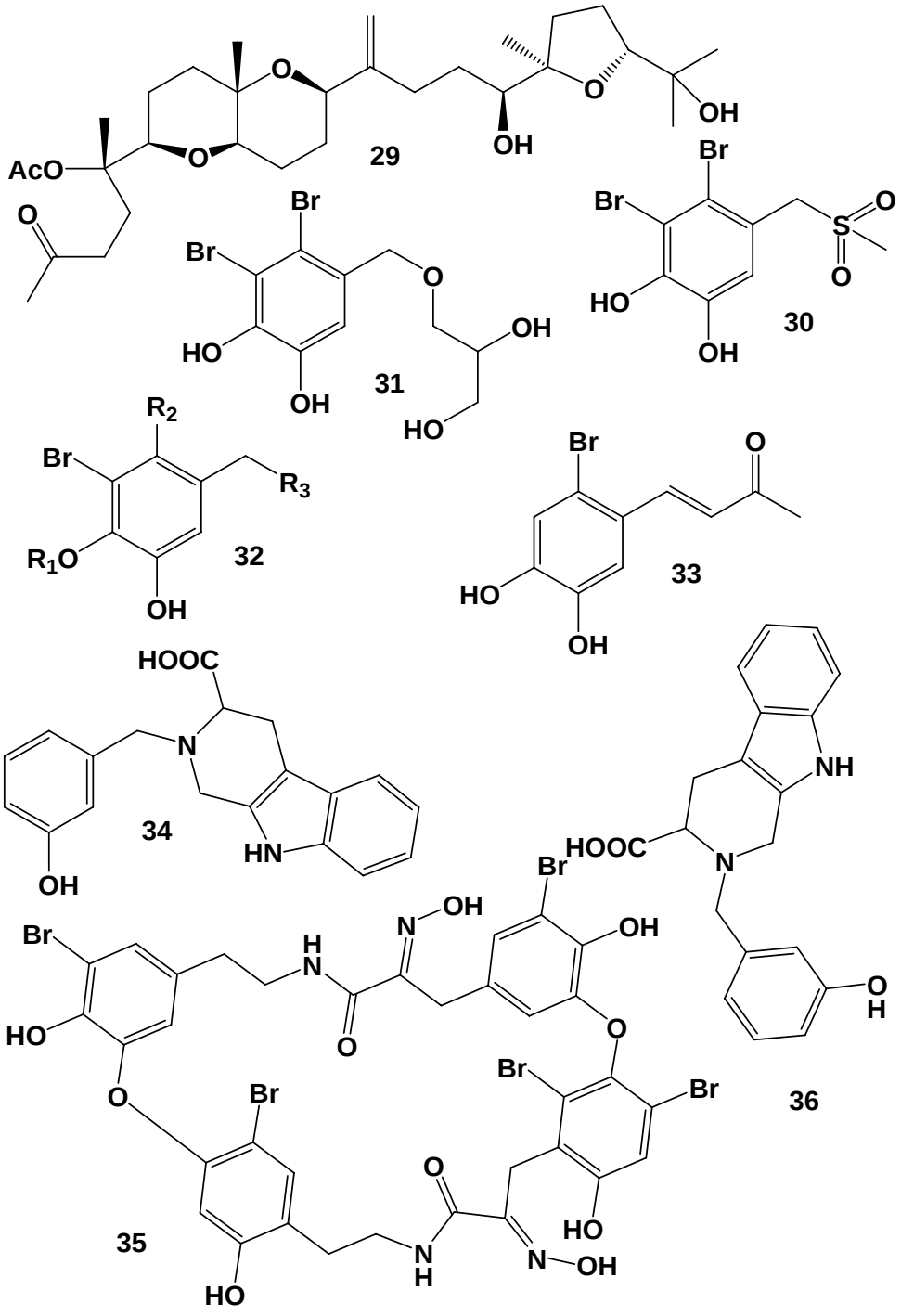
29
30
31
32
33
34
35
36

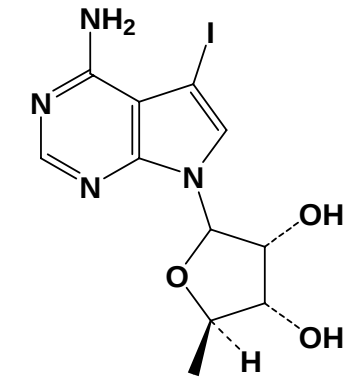

37

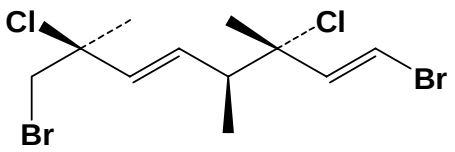

38

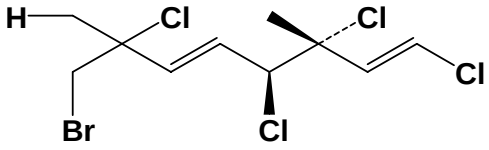

39

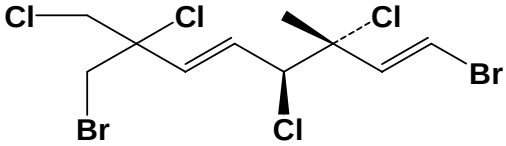

40

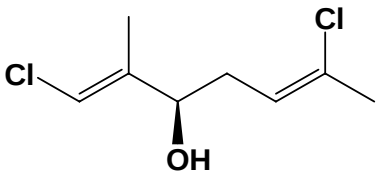

42

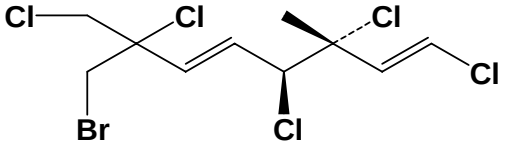

41

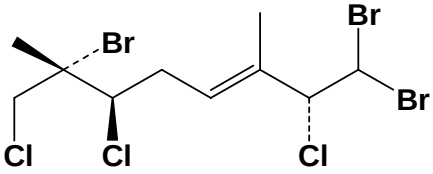

43

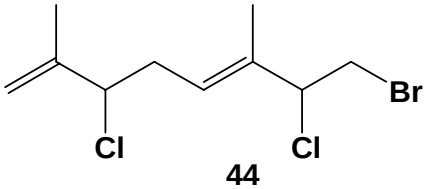

44

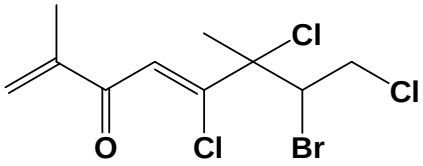

45

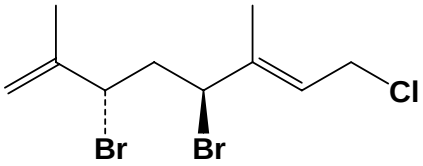

46

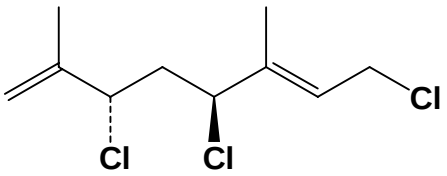

47

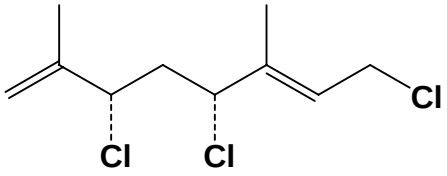

48

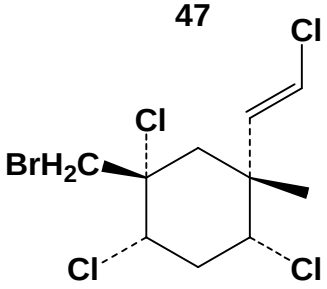

49

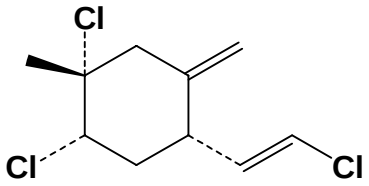

50

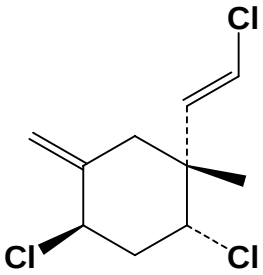

51

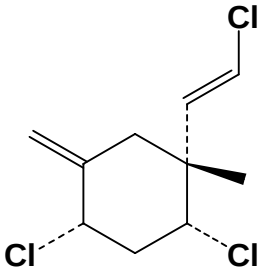

52

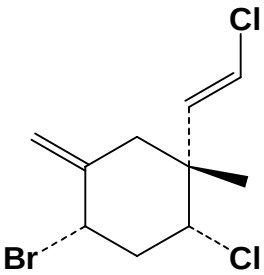

53

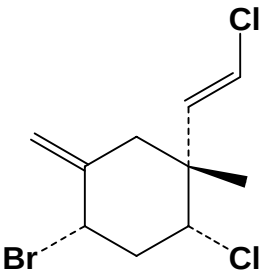

54

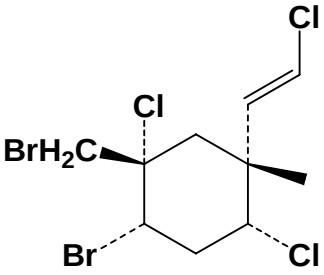

55

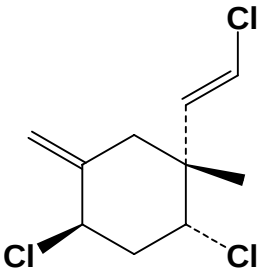

56

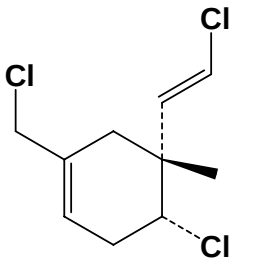

57

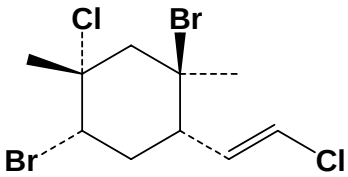

58

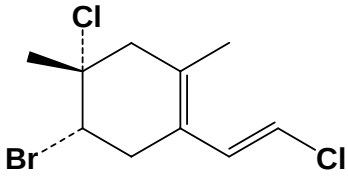

59

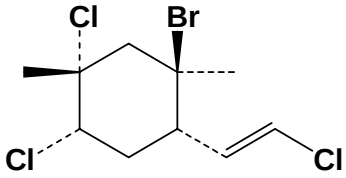

60

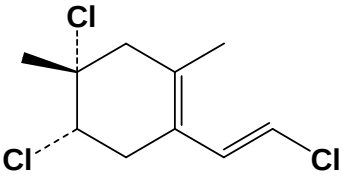

61

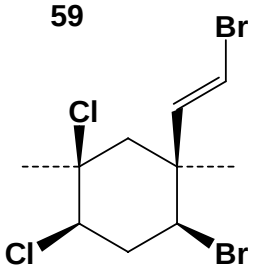

62

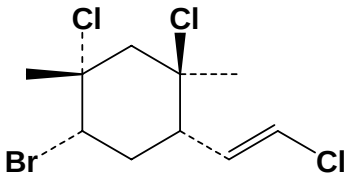

63

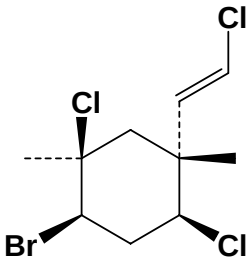

64

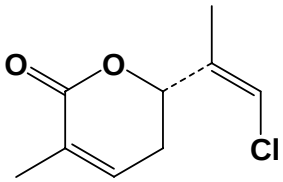

65

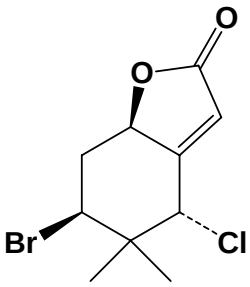

66

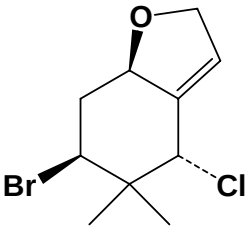

67

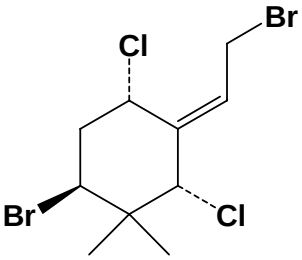

68

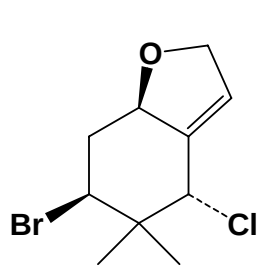

69

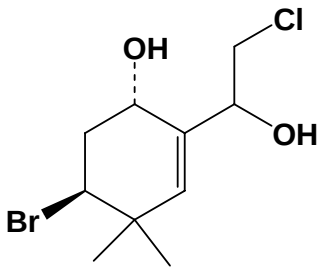

70

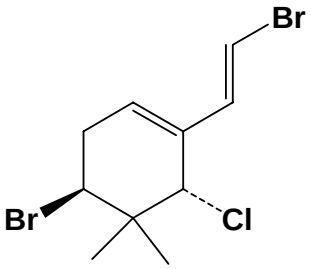

71

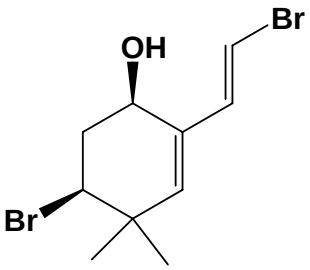

72

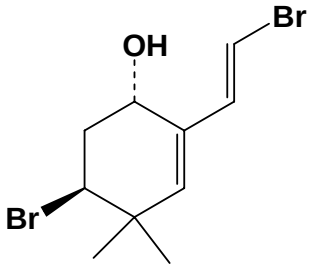

73

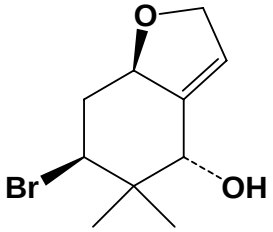

74

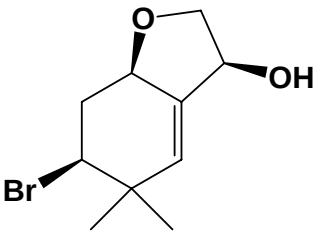

75

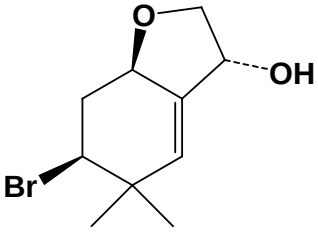

76

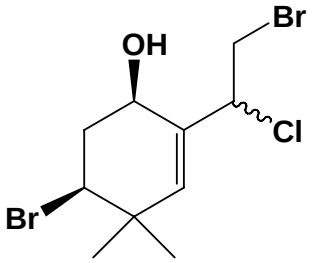

77

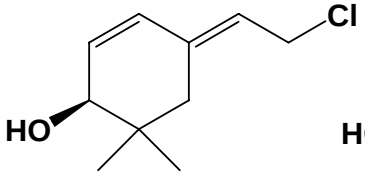

78

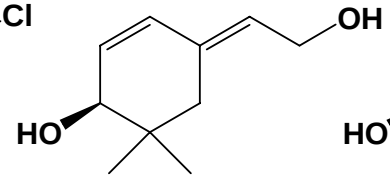

79

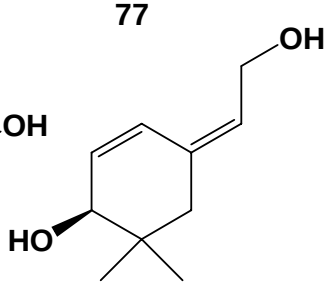

80

Two compounds **(58)** and **(59)** derived from *Plocamium cartilagineum,* were related to the metabolites of *Plocamium violaceim* **(60)** and **(61)** (Faulkner 1984). An unusual bromoviny monoterpene **(62)** and monoterpene **(63)** isolated from the Spanish and Australian sample respectively (Norton et al. 1977). The monoterpene **(64)** and polyhalogenated monoterpene, costatolide **(65)** yielded from red macroalga *Plocamium*

merrensii (Mynderse and Faulkner 1978) and *Plocamium costatum* (Williard et al. 1983) respectively. The new secondary metabolite isolated from *Chondrococcus horrxmanni* is chondrocolactone **(66)**, (Woolard et al. 1978) which is synthesized from chondrocole A **(67)** (Burreson et al. 1975). *Ochtodes secundirarnea* contains, ochtodene **(68)** along with chondrocole A **(69)** and the minor metabolite ochtodiol **(70)** (McConnell and Fenical 1978).

Thirteen novel monoterpenes **(71-83)** reported from marine macroalga *Ochtodes crockeri.* Brominated diterpenes (1S)-1, 2-dihydro-l-hydroxybromosphaerol **(84)** (Faulkner 1984), bromosphaerodiol **(85)** (Cafieri et al. 1977), (12S)-12-hydroxybromosphaerol **(86)** (Cafieri et al. 1982), bromosphaerene A **(87)** and bromosphaerene B **(88)** (Cafieri et al. 1983) related to bromosphaerol **(89)** derived from species *Sphaerococcus coronopifolius*. The anti-microbial metabolites such as (5Z*,* 8E, 10E)-11-fomylundeca-5, 8, 10-trienoic acid **(90)**, (2Z, 5Z, 7E, 11Z, 14Z)-9-hydroxyeicosa-2, 5, 7, 11, 14-pentaenoic acid **(91)** (Higgs and Mulheirn 1981) and cyclic lipid compound hybridalactone **(92)** isolated from macroalga *Burencia hybrid* (Higgs and Mulheirn 1981).

The red marine macroalga *Gracilaria lichenoides* contains prostaglandins PGE_2 **(93)** and $PGF_{2\alpha}$ **(94)** (Gregson et al. 1979). Four metabolites isolated from *Liagora farinosa* in which, three of these compounds, (7Z, 9Z, 12Z)-octadeca-7, 9, 12-trien-5-ynoic acid **(95)**, 4-hydroxynon-2-enal **(96)**, and (9Z, 12Z)-7-hydroxyoctadeca-9, 12-dien-5-ynoic acid **(97)**, exhibited potent ichthyotoxic activities, where as the glyceride **(98)** is not toxic (Paul and Fenical 1980b). Three macrocyclic lipids such as (14Z, 17Z)-3, 20-dibromo-21-ethyl-2, 6-epoxy-l-oxacycloheneicosa-2, 5, 14, 17-tetraen-11-yn-4one **(99)**, (14Z, 17Z)-21-ethyl-2, 6-epoxy-l-oxacycloheneicosa-2, 5, 14, 17, 20-pentaen-11-yn-4-one **(100)**, (12Z, 15Z)-19-ethy1-2, 6-epoxy-1-oxacyclononadeca-2, 5, 12, 15, 18-pentaen-9-yn-4-one **(101)** and acyclic lactone **(102)** isolated from *Phacelocarpus labillardieri* (Kazlauskas et al. 1982b). The metabolite delesserine **(103)** yielded from macroalga *Delesseria sanguine* (Yvin et al. 1982). *Rhabdonia verticillata* contains six halogenated derivatives of phloroglucinol **(104-109)** (Blackman and Matthews 1982). Halogenated diphenylmethanes **(110)** and **(111)** obtained from macroalga *Rhodomela larix* (Kurata and Amiya 1977) where as similar diphenylmethane **(112)** reported from *Rytiphlea tinctoria* (Chevolot-Magueur et al. 1976). *Symphocladia latiuscula* contains anti-fungal dibenzyl ether **(113)** (Kurata and Amiya 1980). A symmetrical trimer cyclotribromoveratrylene **(114)** with 3, 4-di

hydroxybenzyl unit and 2, 6-dibromo-3, 5-dihydroxy phenylacetic acid **(115)** isolated from macroalga *Hulopitys pinastroides* (Combaut et al. 1978). The anti-microbial brominated indoles **(116-119)** reported from *Burencia brongniartii* (Carter et al. 1978). Indole alkaloids such as mertensine A **(120)**, mertensine B **(121)** and fragilamide **(122)** yielded from *Martensia fragilis* (Kirkup and Moore 1983). *Palythoa tuberculosa* contains *Chndrus yendoi* consist of palythine **(123)** (Tsujino et al. 1978). The major metabolite, epoxide isolated from *Bonnemaisonia nootkana* **(124)**. Iodinated octen-3-ones **(125-127)** obtained from macroalga *Delisea Jimbriata*. 1, 1, 2, 6, 6-Pentabromo-octa-l, 4 dien-3-one and the pyrones **(128)** and **(129)** mainly present in the macroalga *Ptilonia australasica* (Kazlauskas et al. 1978). The compound, trans-3, 4-dibromo-5-methylenecyclopent-3-ene-l, 2 diol **(130)** derived from the species *Vidalia spiralis* (Kazlauskas et al. 1982a).

Secondary compounds were generated from (3Z) or (3E)-laurencenyne **(131)**, (3Z) and (3E) neolaurencenyne **(132)** isolated from macroalga *Laurencia okamurai* (Kigoshi et al. 1981). The isomers rhodophytin, (12Z) of (3Z) and (3E) venustin **(133)**, epoxyrhodophytin, (3Z) and (3E) epoxyvenustin **(134)** and (3Z) venustinene **(135)** 1, 3-diene derived from *Laurencia venusta* (Suzuki et al. 1983a; Suzuki and Kurosawa 1980). The *cis* and *trans*-pinnatifidenyne **(136)** derived from *Laurencia pinnatifida* (Gonzalez et al. 1982). Halogenated C_1 lipid laurencienyne **(137)** and laurenyne **(138)** isolated from macroalga *Laurencia obtusa* (Caccamese et al. 1980). The species *Laurencia pinnata* contains eight and seven membered ethers, such as laurepinnacin **(139)** and isolaurepinnacin **(140)** respectively (Fukuzawa and Masamune 1981).

The compound laurepinnacin **(141)** and laurencin **(142)** displayed close structural similarity were derived from *Laurencia glandulifera* (Murai et al. 1977). Eleven halogenated C_1 lipids, intricenyne **(143)** isolated from macroalga *Laurencia intricata* (White and Hager 1978). Similarly, bermudenynol **(144)** corresponding acetate **(145)** identified from same species (Cardellina et al. 1982). The *Laurencia thyrsiferra* contains (3E) and (3Z) chlorodiols **(146)** (Blunt et al. 1981). A nine-membered cyclic ether compound was named as obtusenyene **(147)** extracted from *Laurencia obtusa* (King et al. 1979; Howard et al. 1980). The metabolites such as chlorofucin **(148)** and poiteol **(149)** derived from macroalgae *Laurencia snyderae* and *Laurencia poitei* respectively (Howard et al. 1980). The compounds *cis* maneone-B **(150)** *cis* maneone-A **(151)** isolated from macroalga *Laurencia nidijica* (Waraszkiewicz et al. 1978). The compounds isolaurallene **(152)**, laureepoxide **(153)**, 4-epi-laurallene

(154) and laurallene **(155)** reported from *Burencia nipponica* (Kurata et al. 1982). The species *Laurencia nipponica* contains brominated allene, kumausallene **(156)**, deacetylkumausyne **(157)** and kumausyne **(158)** (Suzuki et al. 1983b). The metabolite obtusallene **(159)** exhibited an unusual bridged twelve-membered ring, obtained from macroalga *Laurencia obtuse* (Cox et al. 1982). Three 1-bromoallenes such as deoxyokamurallene **(160)**, okamurallene **(161**) and iso-okamurallene **(162)** derived from *Laurencia okamurai* (Suzuki and Kurosawa 1981). Tricyclic ketal, obtusin **(163)** extracted from macroalga *Laurencia obtuse* (Faulkner 1984). Twelve-membered cyclic ether compound poitediene **(164)** isolated from *Laurencia poitei* (Wright et al. 1983). The metabolite thyrsiferol **(165)** derived from the species *Laurencia thyrsifera* (Blunt et al. 1978). (10E*,* 11R) Squalene 10, 11-epoxide **(166**) isolated from *Laurencia okamurai* (Kigoshi et al. 1982). Two ecdysone derivatives acetylpinnasterol **(167)** and pinnasterol **(168)** reported from *Laurencia pinnata* (Fukuzawa et al. 1981). The metabolite chilenone **(169)** derived from the species *Laurencia chilensis* (San Martin et al. 1983). Several new aromatic sesquiterpenes such as caraibical **(170)**, 10-bromo-7-hydroxy-11-iodolaurene **(171)**, 10-bromo-7, 12-dihydroxy-laurene **(172)** and the iodo-ether **(173)** obtained from *Laurencia caraibica* (Izac and Sims 1979). Similarly new aromatic sesquiterpenes, isoaplysin **(174)** and neolaurinterol **(175)** isolated from macroalga *Laurencia okamurai. Laurencia okamurai* contains two aromatic sesquiterpenes, debromoaplysinol **(176)** and 8-bromolaurinterol **(177)** which are minor metabolites of the species. *Laurencia glandulifera* contains minor metabolites 10-bromolaurenisol **(178)**, ethers **(179)** and **(180)** (Suzuki and Kurosawa 1979). A species of *Laurencia nipponica* contains three laurene derivatives **(181-183)** and three dihydrolaurene derivatives **(184-186)** (Ohta and Takagi 1977). The compounds glanduliferol **(187)**, 10-bromo-α-chamigren-4-one **(188)**, 10-bromo-α-chamigrene **(189)**, 10-bromo-3, 4-epoxy-α-chamigrene **(190)** and 4, 10-dibromo-3-chloro-α-chamigrene **(191)** isolated from macroalga *Laurencia glanddifera* (Suzuki et al. 1979). 3-Chloro-4, l0-di bromo-7 and 8-epoxy-α-chamigrene **(192)** obtained from *Laurencia nipponica* (Faulkner 1984). The structures of iso-obtusol **(193)** and of the corresponding 10-debromo derivatives **(194)**, **(195)** and obtusol **(196)** elucidated by X-ray analysis (Gonzalez et al. 1979a). The compounds isofurocaespitane **(197)** and obtusane **(198)** isolated from macroalga *Laurencia caespitosa* (Gonzalez et al. 1979b). The compound bromohydrin **(199)** obtained from macroalga *Laurencia majuscula,* was converted into the acetate **(200)** for

X-ray analysis (Suzuki and Kurosawa 1978). The metabolite nidifocene **(201)** isolated from *Laurencia nidijica* (Waraszkiewicz et al. 1977).

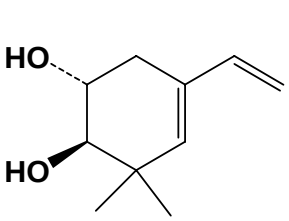

81

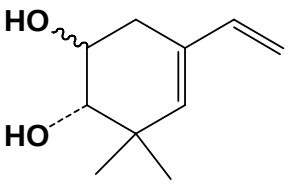

82

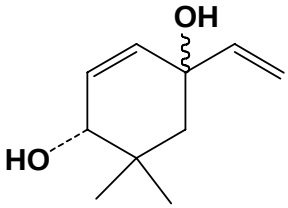

83

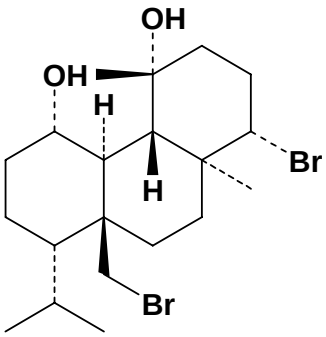

84

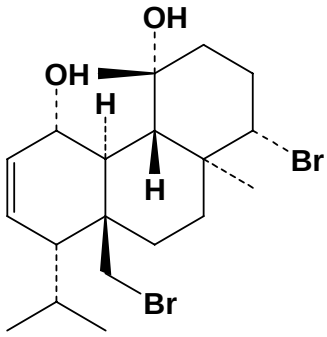

85

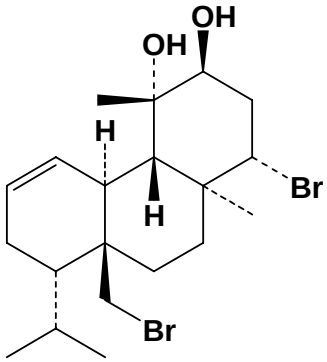

86

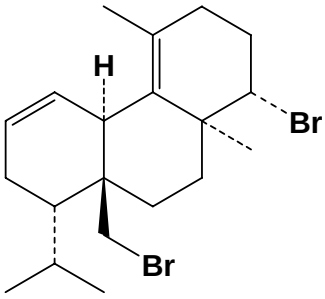

87

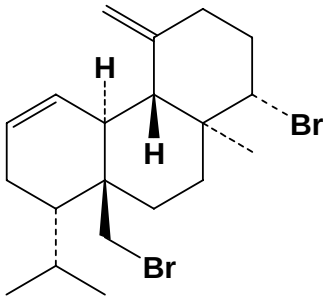

88

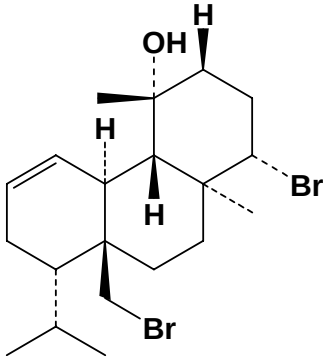

89

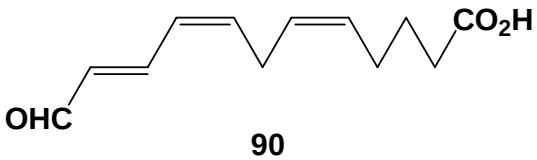

90

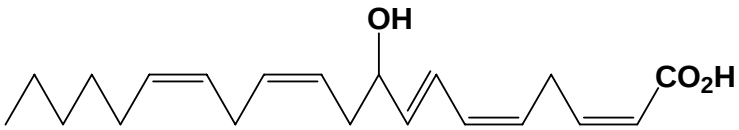

91

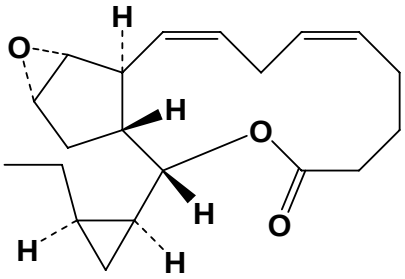

92

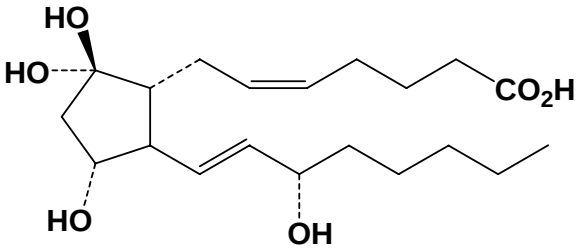

93

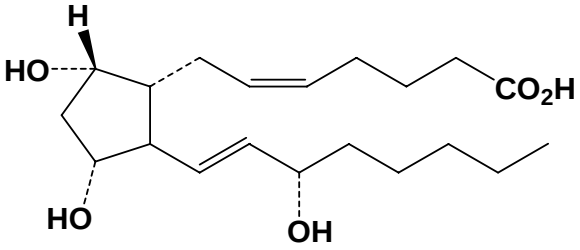

94

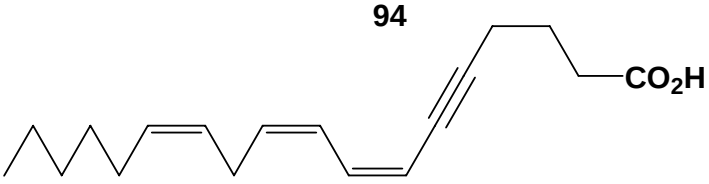

95

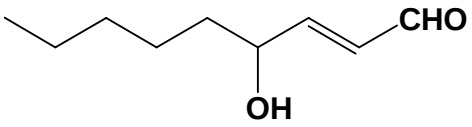

96

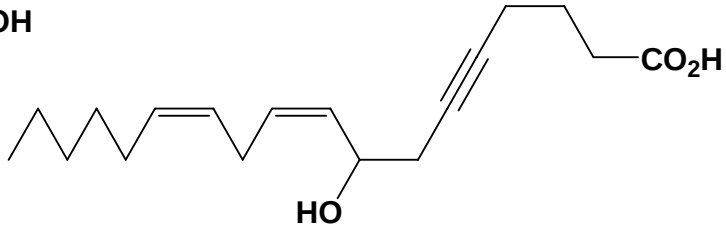

97

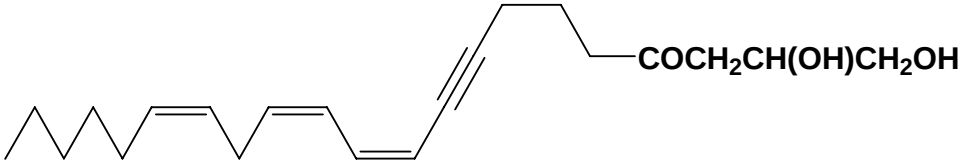

98

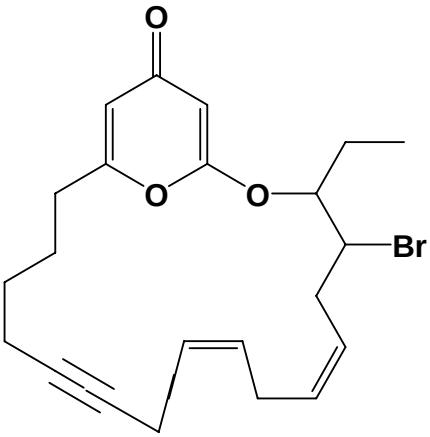

99

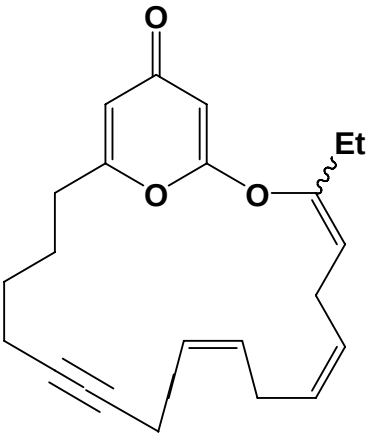

100

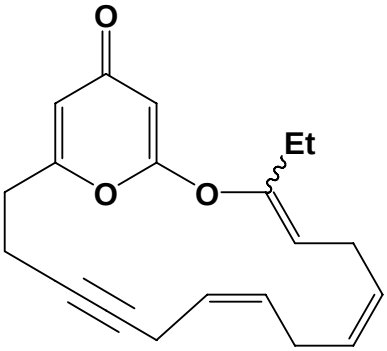

101

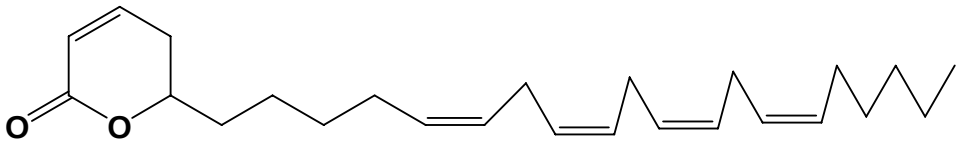

102

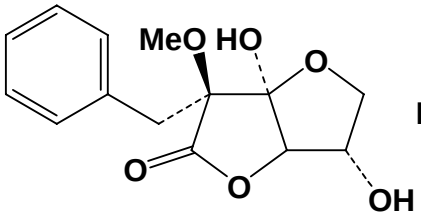

103

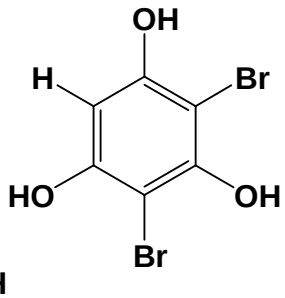

104

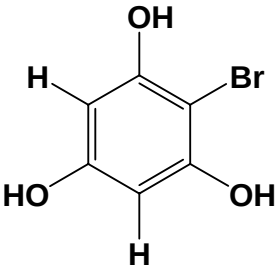

105

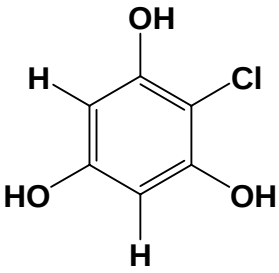

106

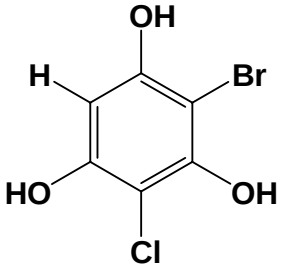

107

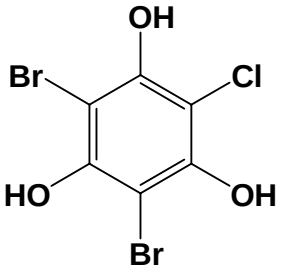

108

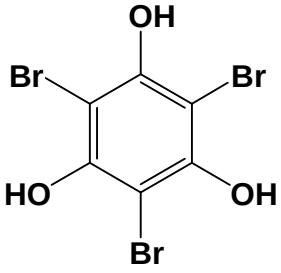

109

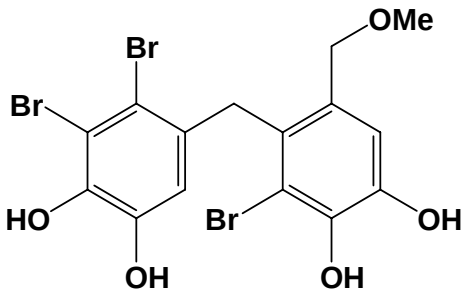

110

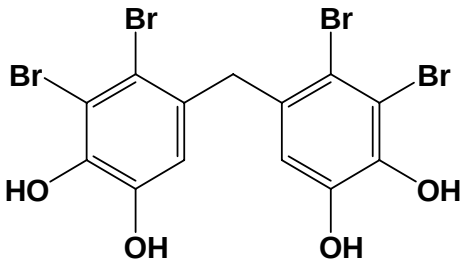

111

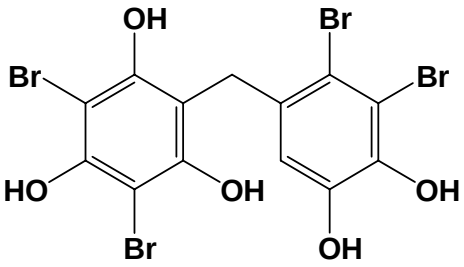

112

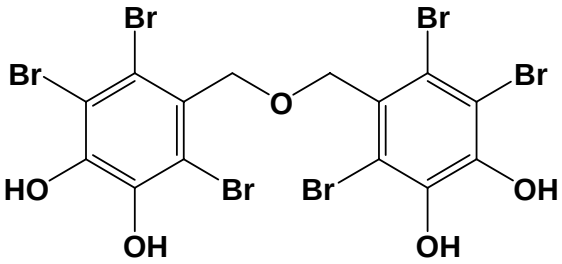

113

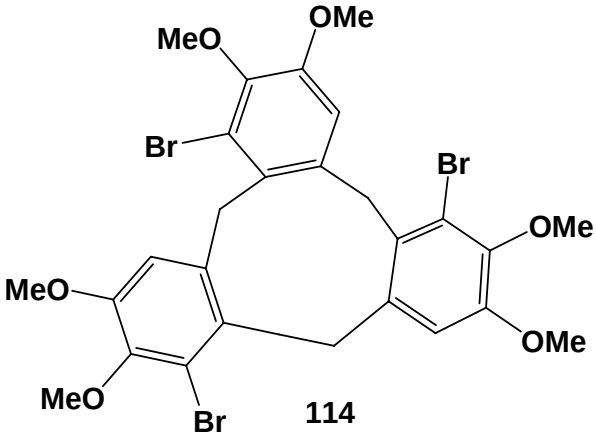

114

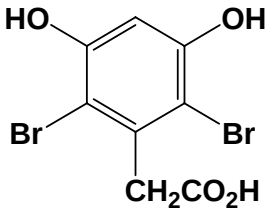

115

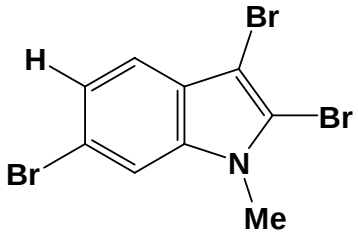

116

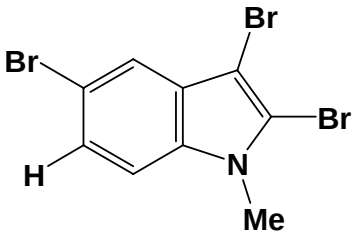

117

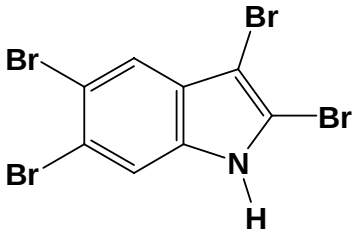

118

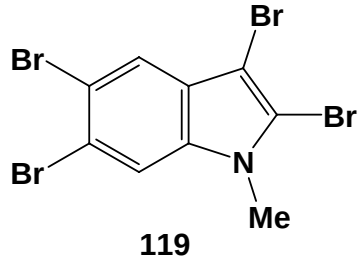

119

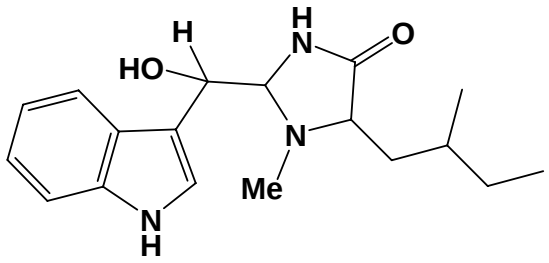

120

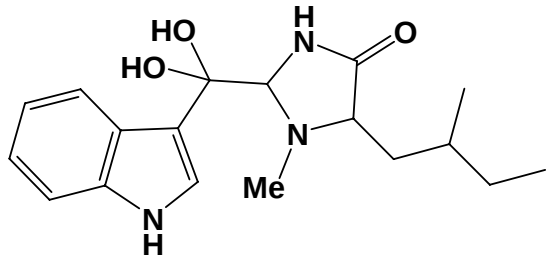

121

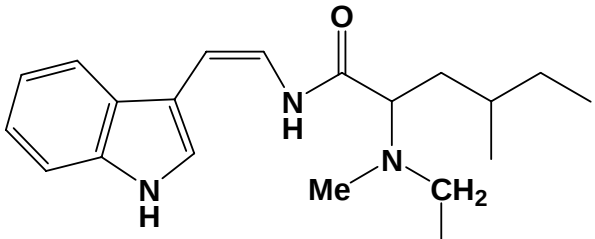

122

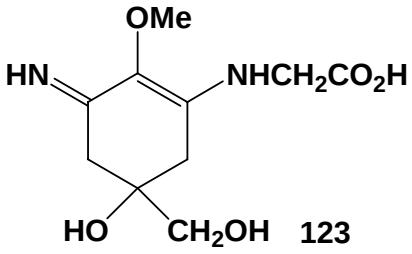

123

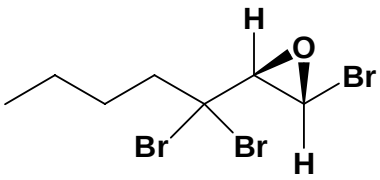

124

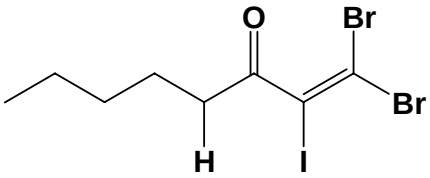

125

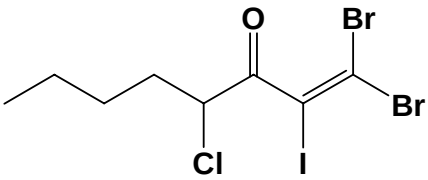

126

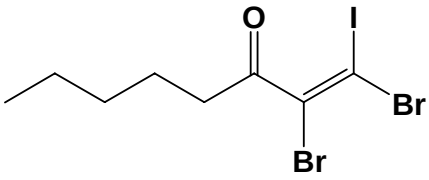

127

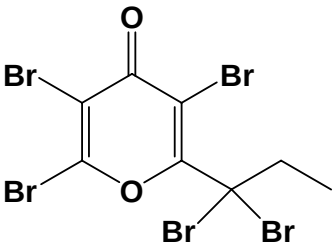

128

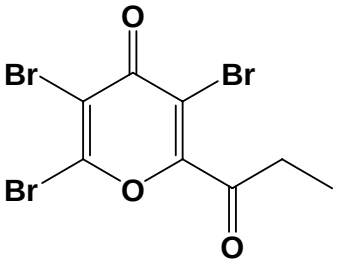

129

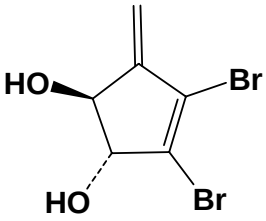

130

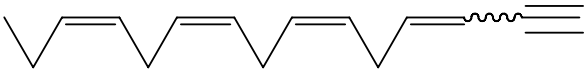

131

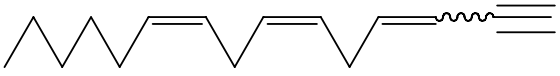

132

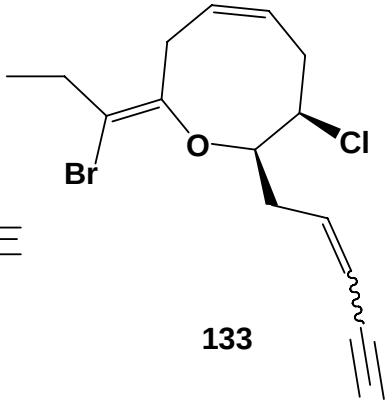

133

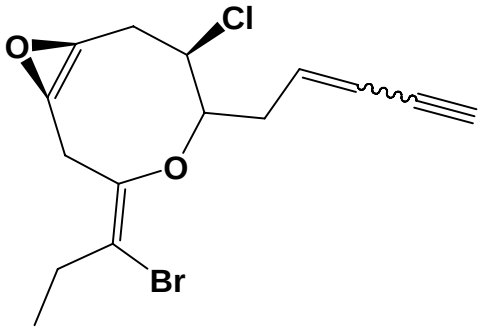

134

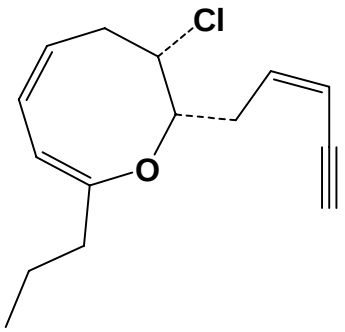

135

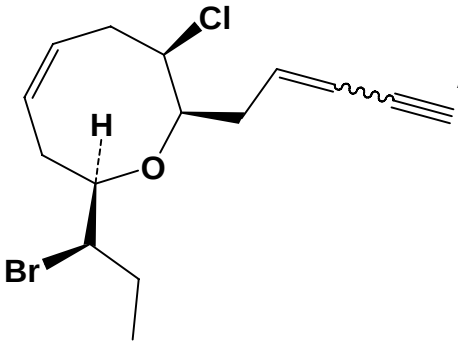

136

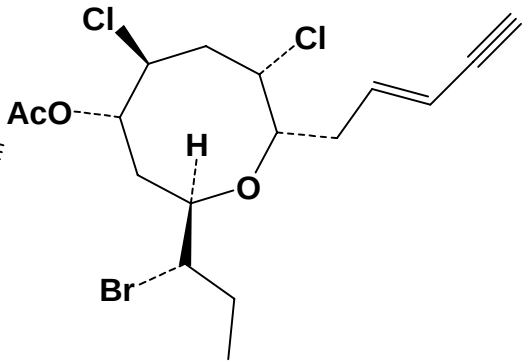

137

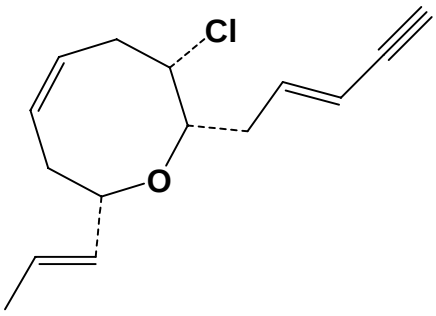

138

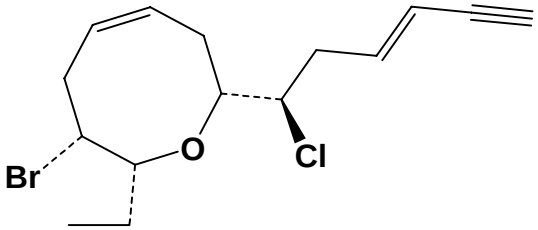

139

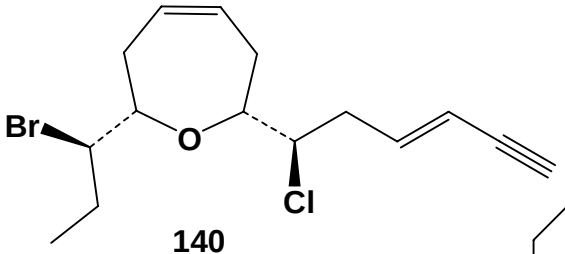

140

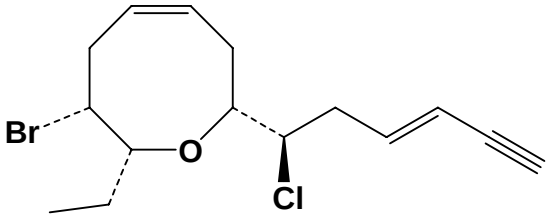

141

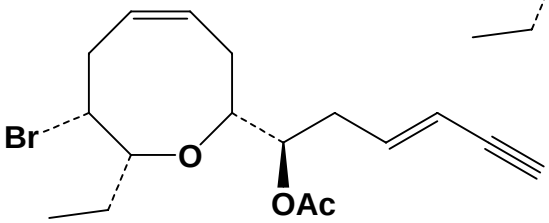

142

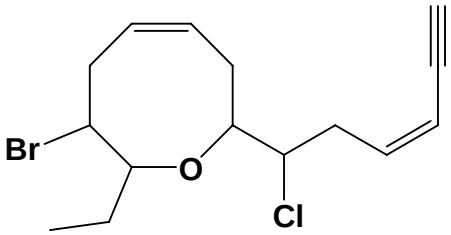

143

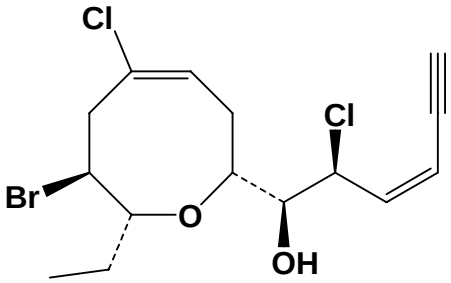

144

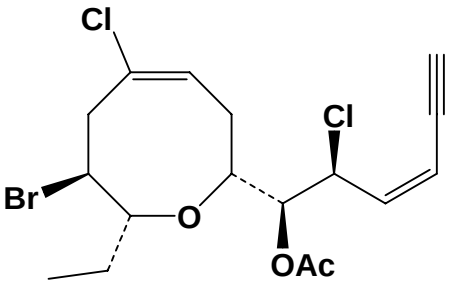

145

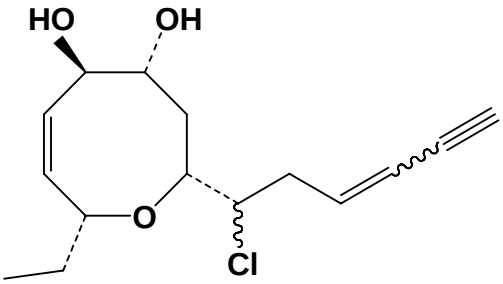

146

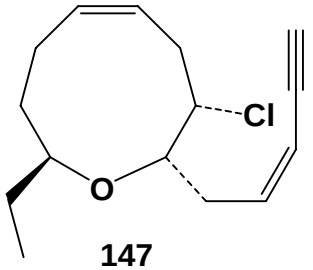

147

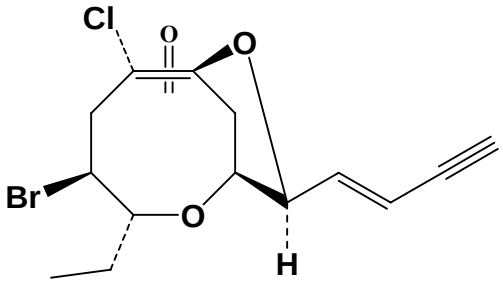

148

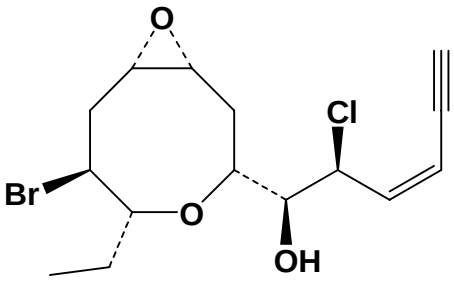

149

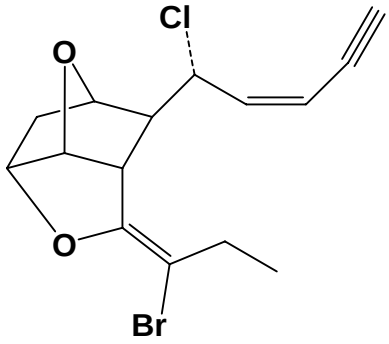

150

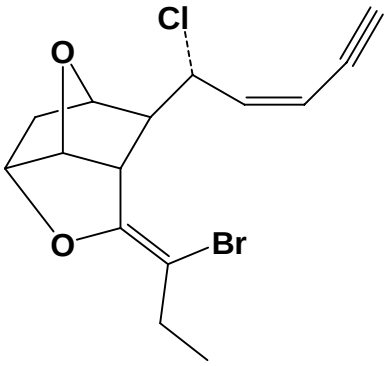

151

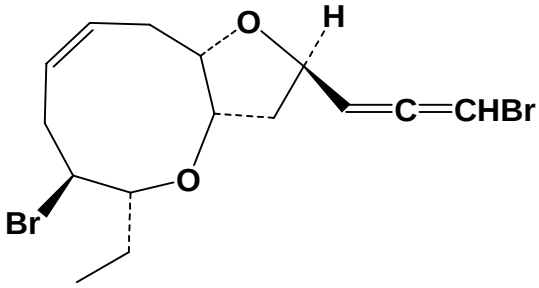

152

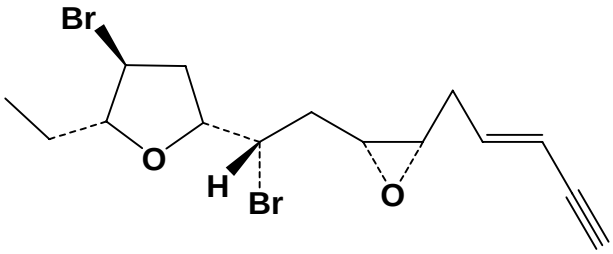

153

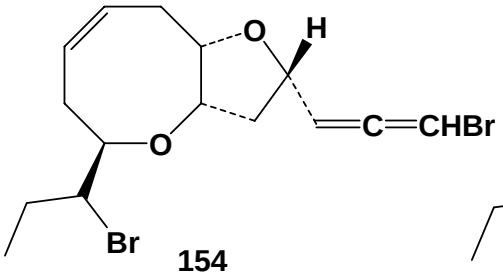

154

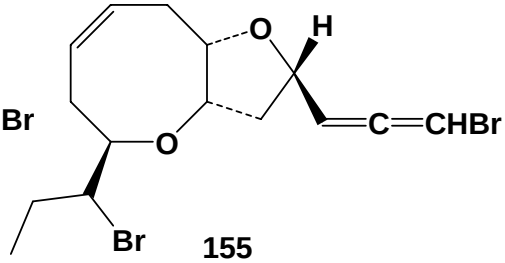

155

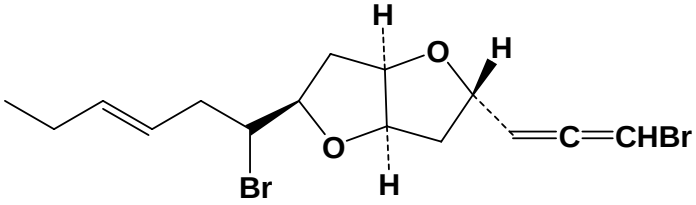

156

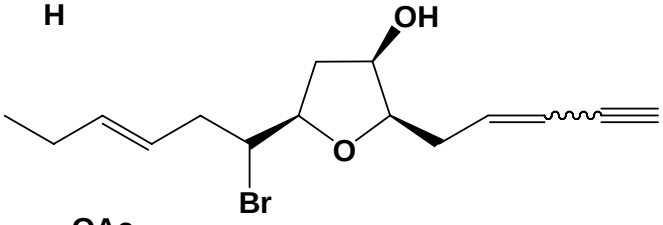

157

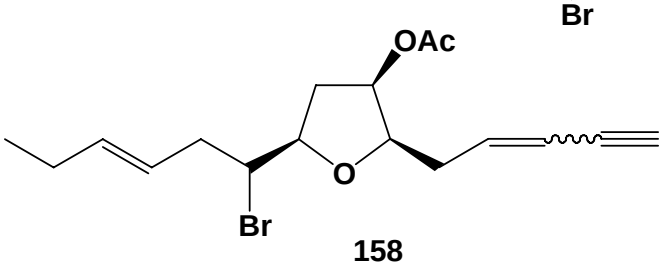

158

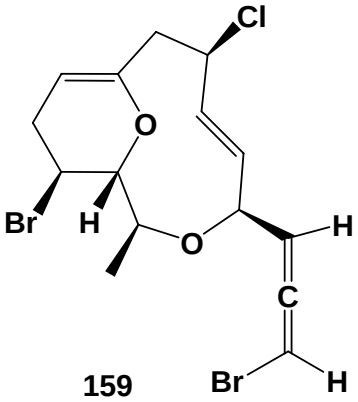

159

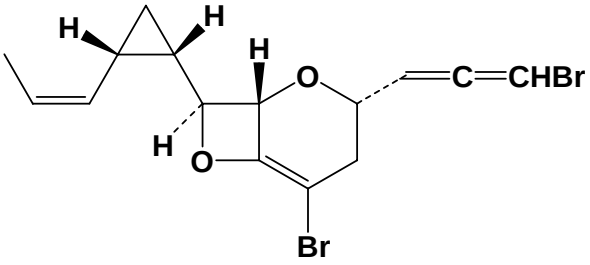

160

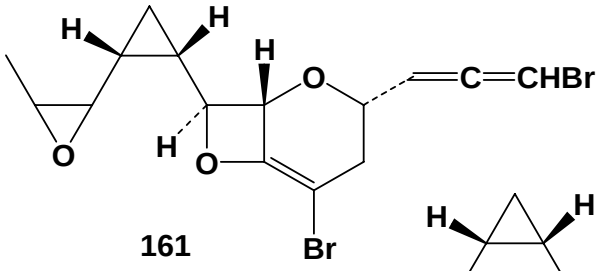

161

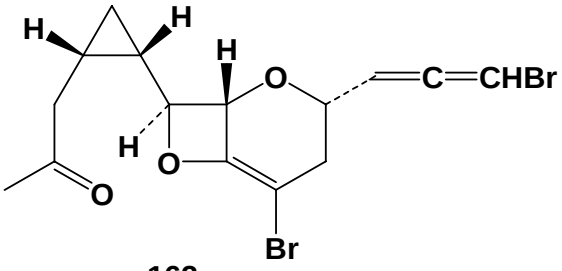

162

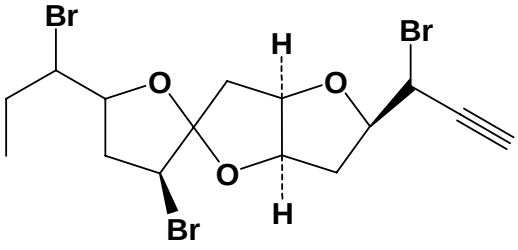

163

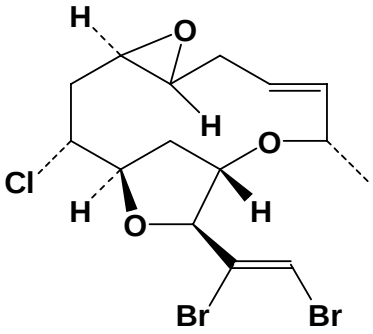

164

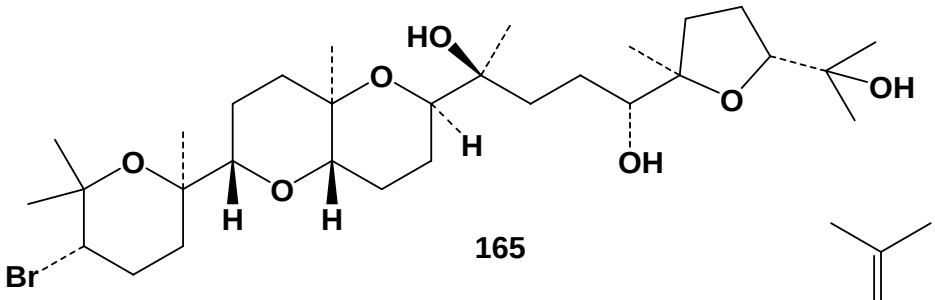

165

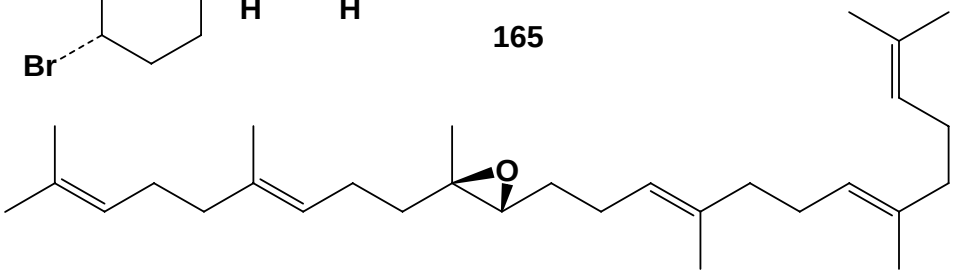

166

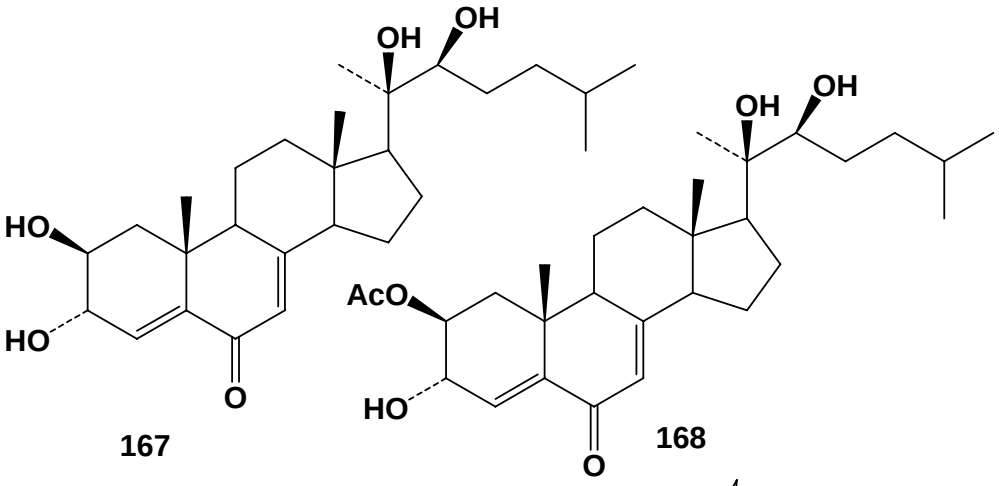

167 168

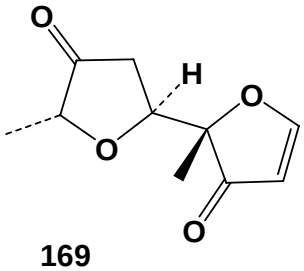

169

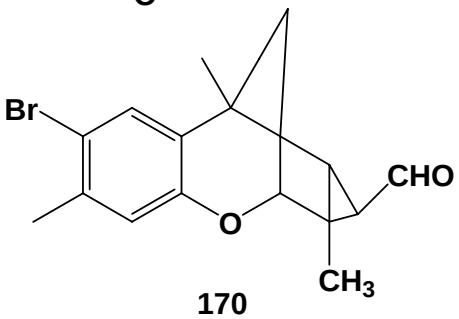

170

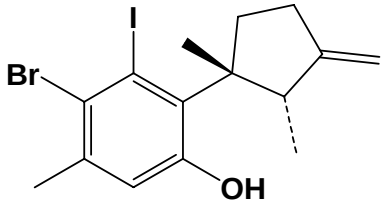

171

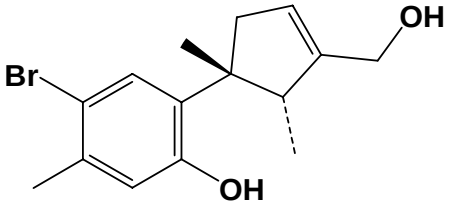

172

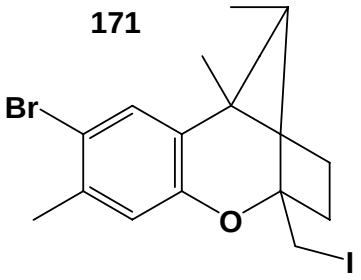

173

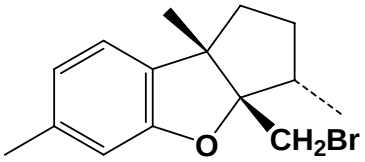

174

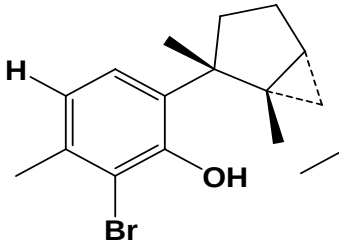

175

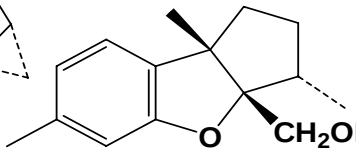

176

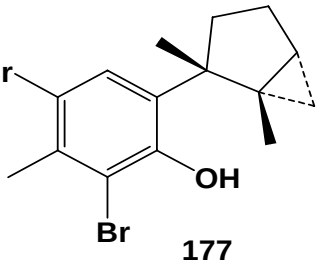

177

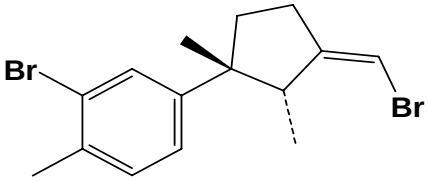

178

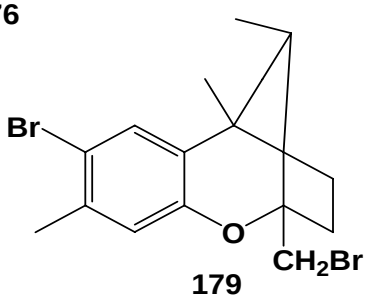

179

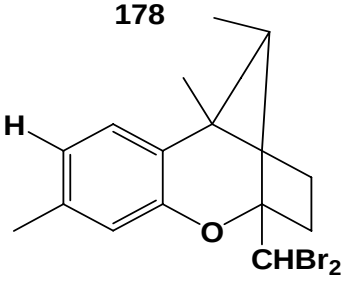

180

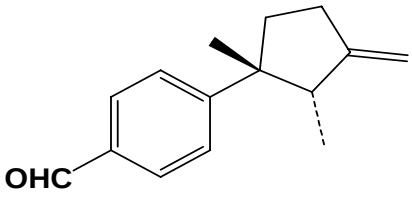

183

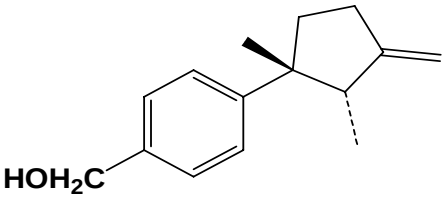

181

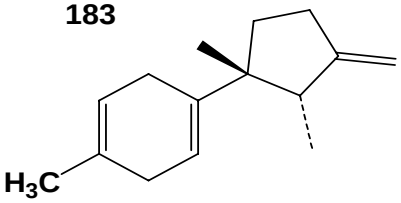

184

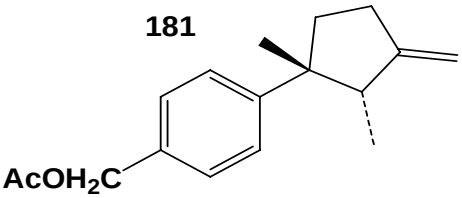

182

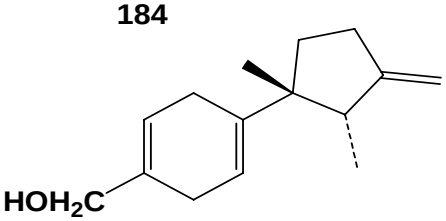

185

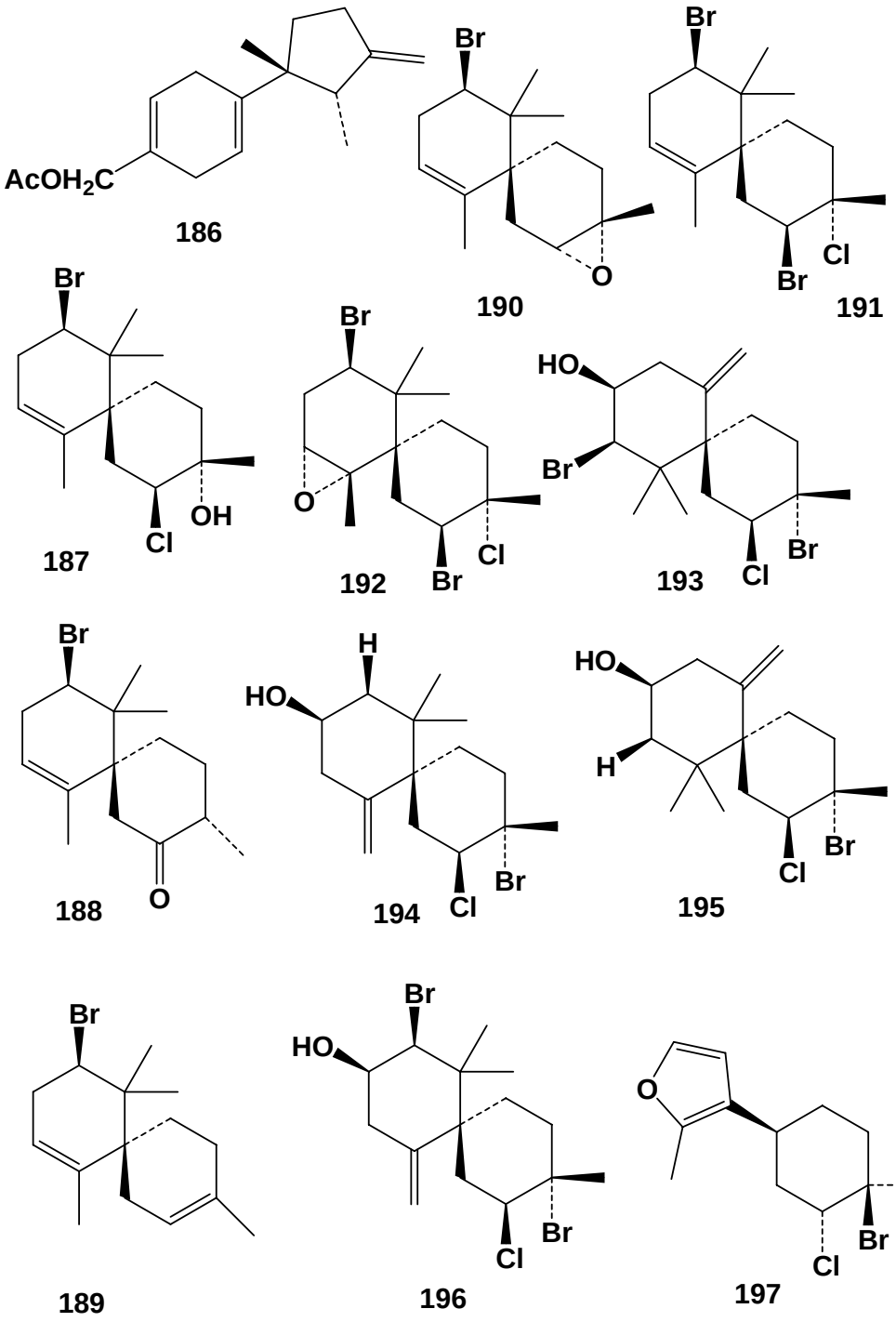

A thermolabile diol **(202)**, pacifenol **(203)**, a dibromodiol **(204)** and bromo-alcohol **(205)** yielded from macroalga *Laurencia nipponica* (Kurata et al. 1981). Laurencial **(206)** isolated from macroalga *Laurencia nipponica,* has chamigrene skeleton (Kurata et al. 1983). The metabolite, kylinone **(207)**, obtained from macroalga *Laurencia pacifica* (Selover and Crews 1980). Guadalupol **(208)** and epiguadalupol

(209) isolated from macroalga *Laurencia snyderae* (Howard and Fenical 1979). Several molecules such as rhodolaureol **(210)**, perforenol **(211)** and rhodolauradiol **(212)** found in *Laurencia perforate* (Gonzalez et al. 1978). A ring-contracted chamigrene derivative, spirolaurenone **(213)** isolated from macroalga *Laurencia glandulifera* (Suzuki et al. 1980a). (E)-Bisabolene 8, 9-epoxide **(214)** derived from macroalga *Laurencia nipponica* (Suzuki et al. 1980b). The bisabolene derivative, 8-desoxyisocaespitaol **(215)** isolated from macroalga *Laurencia caespitosa* (Gonzalez et al. 1980). The metabolite, dibromide **(216)** found in *Laurencia obtusa* (Faulkner 1984). Cyclic ether of nerolidol, obtusenol **(217)** isolated from macroalga *Laurencia obtuse* (Faulkner 1984). Metabolite conjugated diene **(218)**, the corresponding acetate **(219)** and palisol **(220)** isolated from *Laurencia palisade* (Paul and Fenical 1980a). The species *Laurencia palisada* also contains palisadin A **(221)**, aplysistatin **(222)** and palisadin B **(223)**. 12-hydroxypalisadin B **(224)** and 5-acetoxypalisadin B **(225)** isolated from *Laurencia palisade.* Aplysistatin **(226)** and 6P-hydroxyaplysistatin **(227)** derived from *Laurencia filiformis* (Capon et al. 1981). Metabolites such as α-snyderol **(228)** and bicyclolaurencenol **(229)** produced from macroalga *Laurencia intricate* (Horsley et al. 1981). Heterocladol **(230)** obtained from macroalga *Laurencia fliformis* (Kazlauskas et al. 1977b). (lS, 4R, 7R)-l-Bromo-4-hydroxy-7-chloroselinane **(231)** (Rose et al. 1978) and its dehydrochlorination product (1S, 4R)-1-bromo-4-hydroxyselin-7-ene **(232)** isolated from the species *Laurencia* (Rose and Sims 1977). Secondary metabolites such as austradiol diacetate **(233)**, austradiol acetate **(234)** (Brennan and Erickson 1982) and (+)-selina-4, 7(11)-diene **(235)** yielded from *Laurencia* species (Sun and Erickson 1978). The unusual sesquiterpene poitediol **(236)** isolated from a species of the genus *Laurencia* is *Laurencia poitei* (Fenica et al. 1978). Brominated diterpenes such as irieol D **(237)**, irieol **(238)**, irieol G **(239)**, irieol E **(240)**, irieol F **(241)** and neoireone **(242)** reported from macroalga *Laurencia irieii* (Howard and Fenical 1978b; Faulkner 1984).

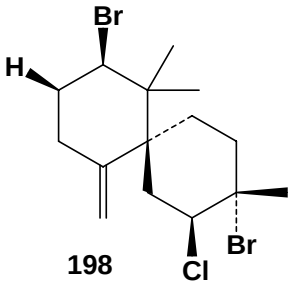

198

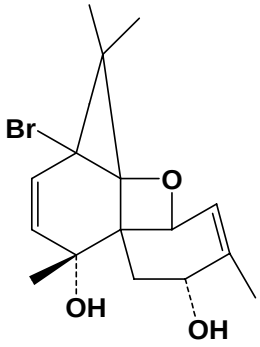

202

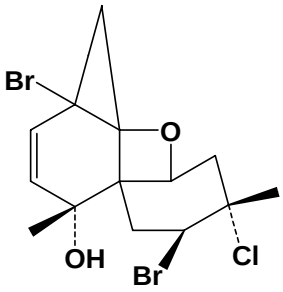

203

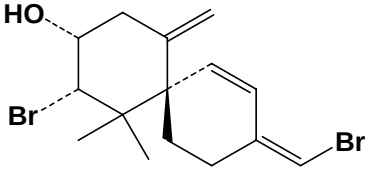

199

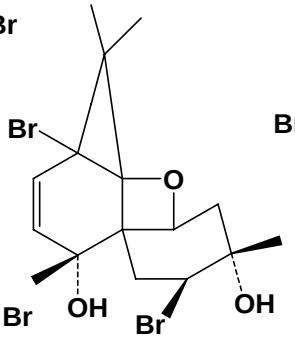

204

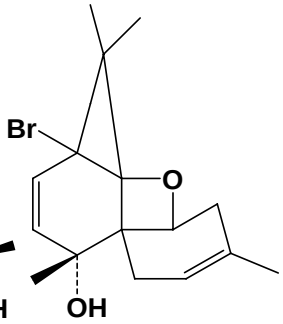

205

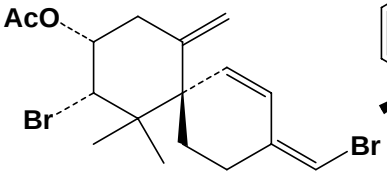

200

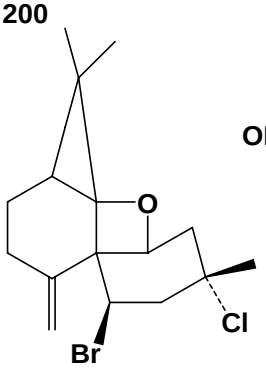

201

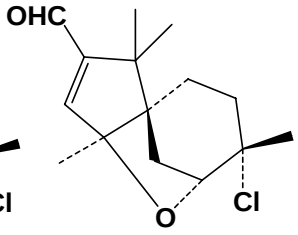

206

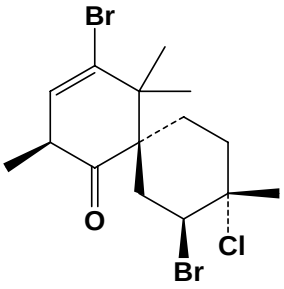

207

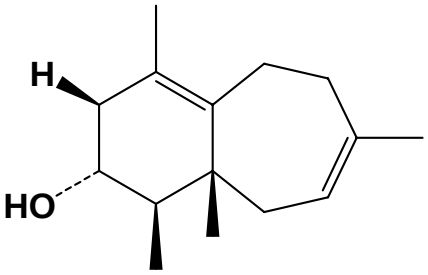

208

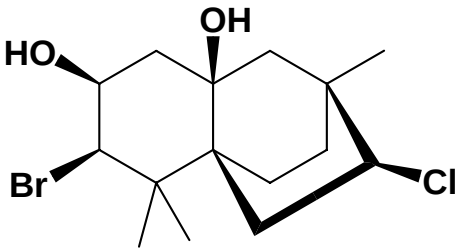

212

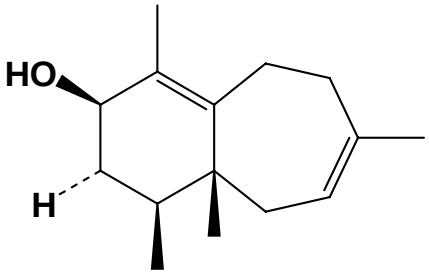

209

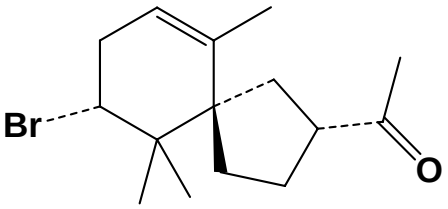

213

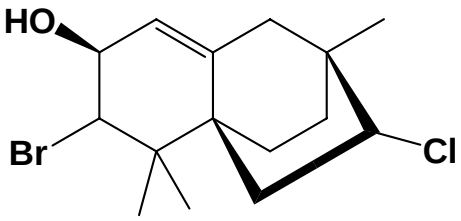

210

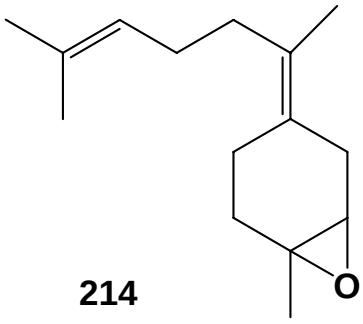

214

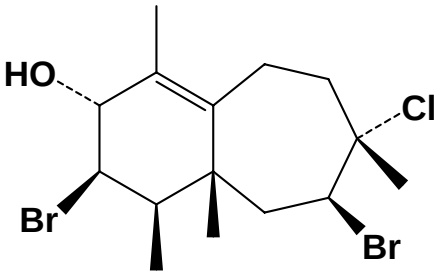

211

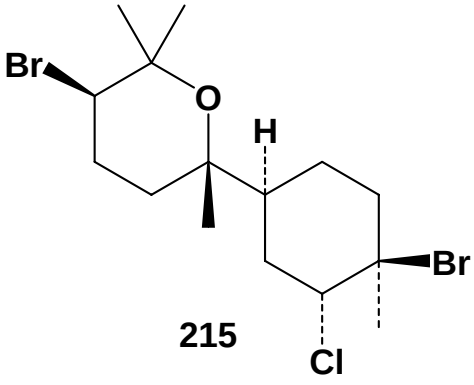

215

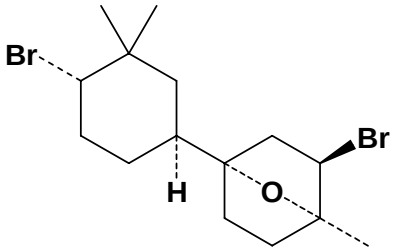

216

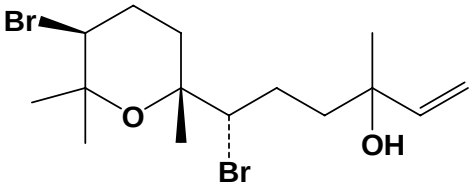

217

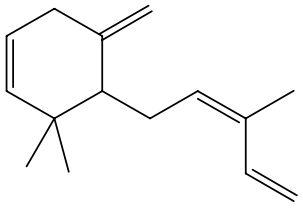

218

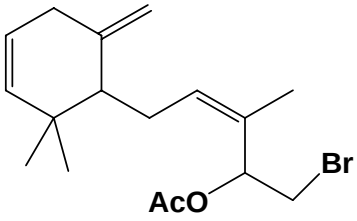

219

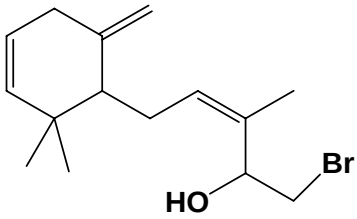

220

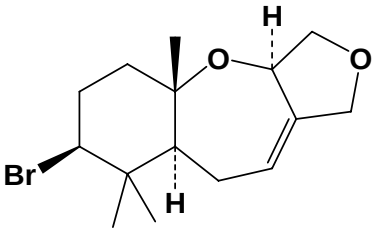

221

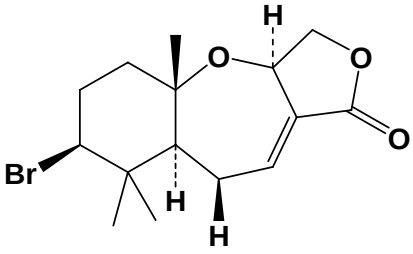

222

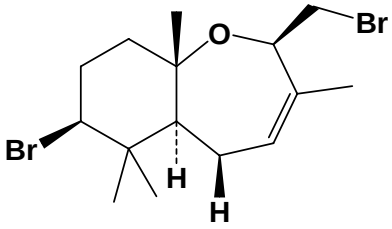

223

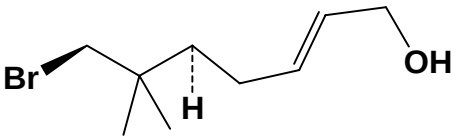

224

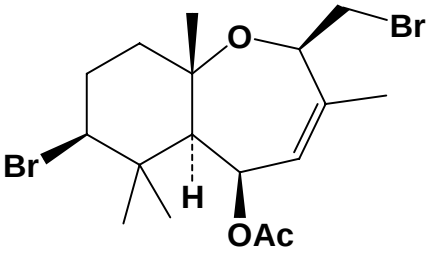

225

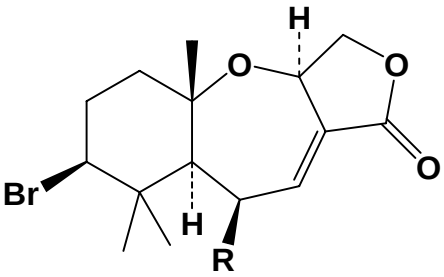

226

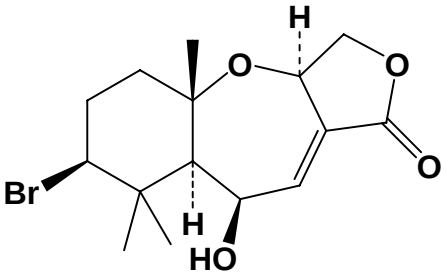

227

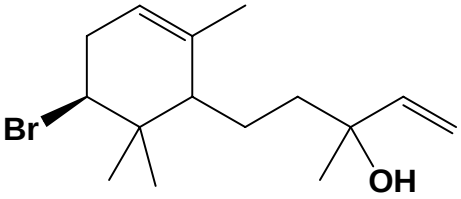

228

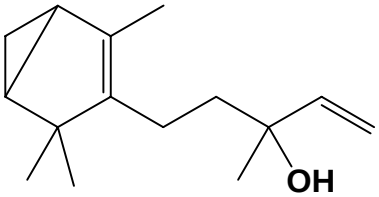

229

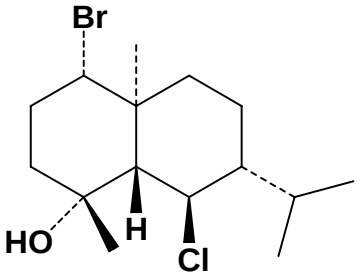

230

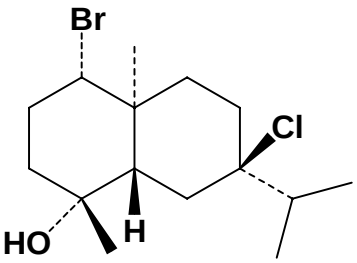

231

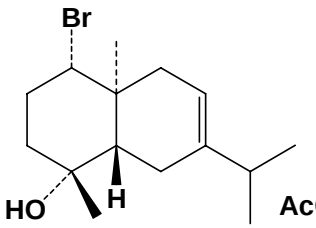

232

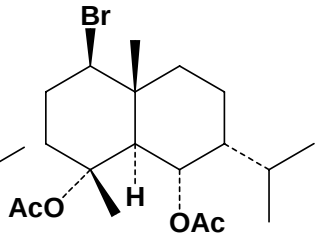

233

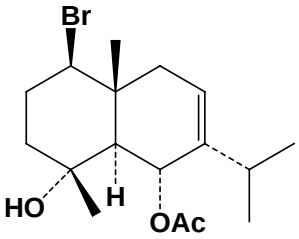

234

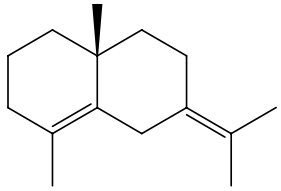

235

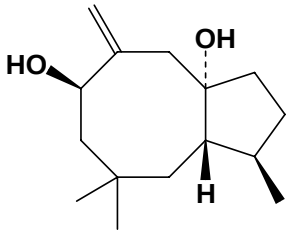

236

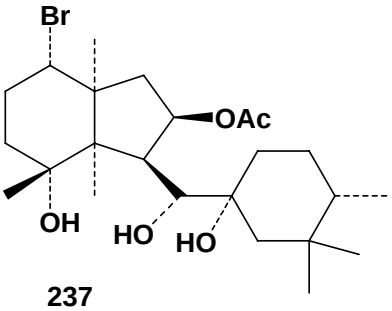

237

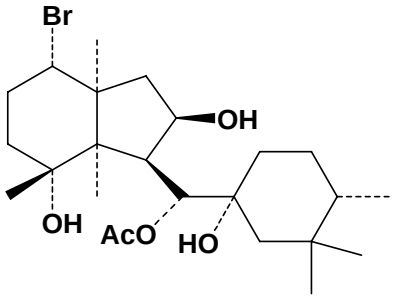

239

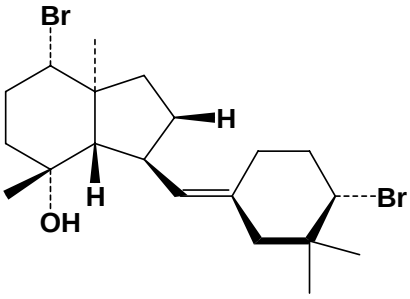

238

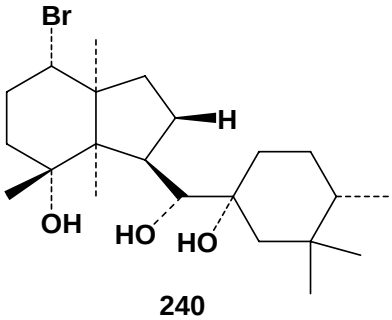

240

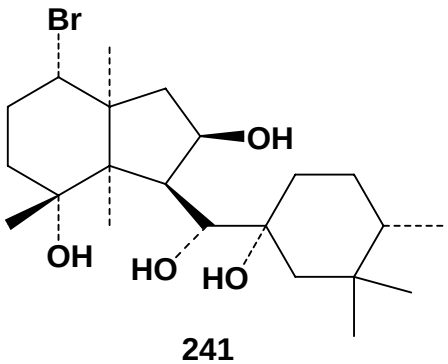

241

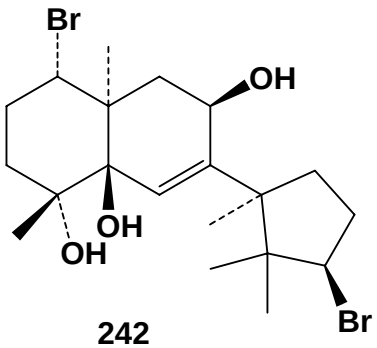

242

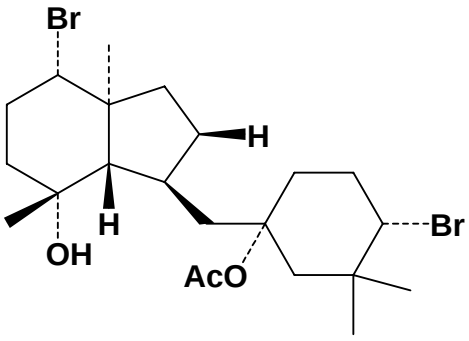

243

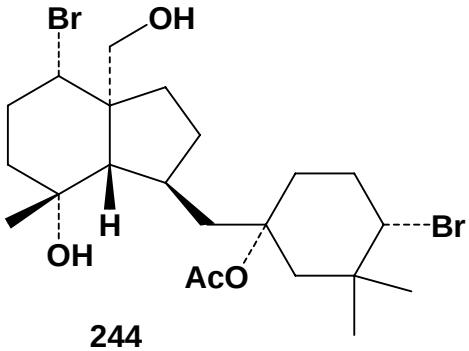

244

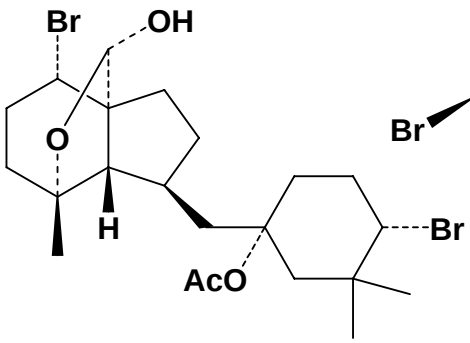

245

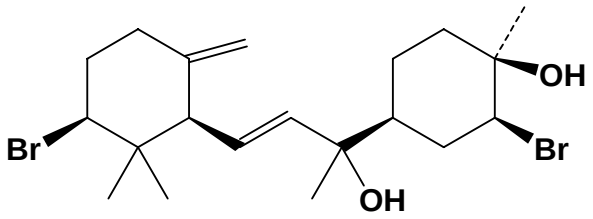

246

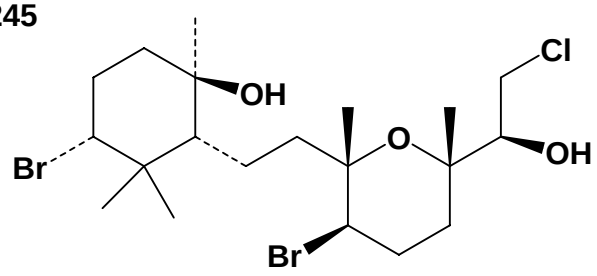

247

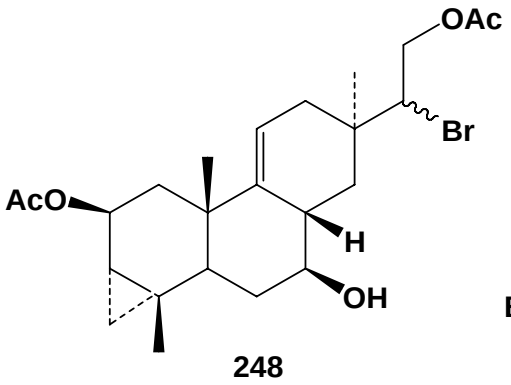

248

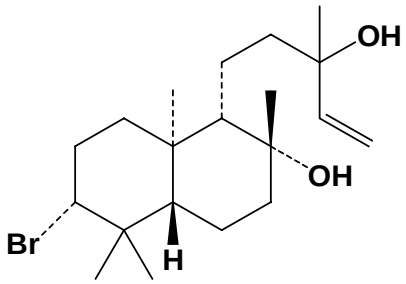

249

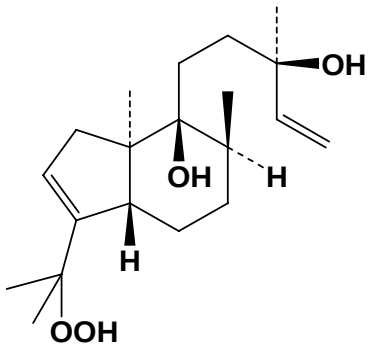

250

Three cyclic ether includes pinnaterpene A **(243)**, pinnaterpene B **(244)** and pinnaterpene C **(245)** obtained from *Laurencia pinnata* (Fukuzawa et al. 1982). Halogenated diterpenes such as obtusadiol **(246)**, laurencianol **(247)** and 15-bromo-2, 16-diacetoxy-7-hydroxy-9 (11)-paraguerene **(248)** derived from *Laurencia obtuse* (Howard and Fenical 1978a). Two diterpenes isoconcinndiol **(249)** and neoconcinndiol hydroperoxide **(250)** isolated from *Laurencia snyderae* (Howard and Fenical 1980).

2.7. Structural Diversity of Polysaccharides from Marine Macroalgae

Algal sulfated polysaccharides, until recently, were largely ignored as sources of antioxidant activities. For example, fucans from *F. vesiculosus* exhibited considerable ferric reducing/antioxidant power and superoxide radical scavenging abilities (De Souza et al. 2007). Fucan fractions from *Laurencia japonica* also showed significant antioxidant capabilities in superoxide radical and hydroxyl radical scavenging assays (Zhao et al. 2005). Positive correlation was observed between superoxide radical scavenging activity and the sulfate content of the polysaccharide fractions (De Souza et al. 2007).

Antioxidative potential of carrageenans (De Souza et al. 2007) and *ulvans* appeared to be associated with the sulfate content, and previous report of literature showed enhanced antioxidant potential of polysaccharide due to the presence of high sulfate content (Zhang et al. 2005). Sulfated polysaccharides derived from macroalgae showed immunomodulatory potential that might be useful in stimulating the immune response (Chen et al. 2008). Sulfated polysaccharide from marine macroalgae (Fig. 2.4) used as anti-inflammatory agents displayed their potential to impede with the relocation of leukocytes to the inflammatory sites. Polysaccharide fucans derived from the marine macroalgae, such as *Cladosiphon okamuranus*, *Fucus* spp, *Laminaria* spp and *Ascophyllum nodosum* were displayed to inhibit leukocyte recruitment to the abdominal cavity throughout acute peritonitis in rats (Cumashi et al. 2007). Moreover, sulfated polysaccharides inhibit heparanase and elastases, which are the tissue degradative enzymes that are intricate in the breakdown of basement membrane integrity during inflammation (Senni et al. 2006). The fucoidan fractions isolated from marine macroalga *Ascophyllum nodosum* eventualy constitutes the classical and alternative pathways in human serum (Blondin et al. 1994). The algal sulfated polysaccharides were found to effectively interact with the complement system proposing that they may have applicability in regulating indigenous immunity to lower the pro-inflammatory occurrence or other unfavorable conditions, such as allergic reflections originating during the inherent immune response.

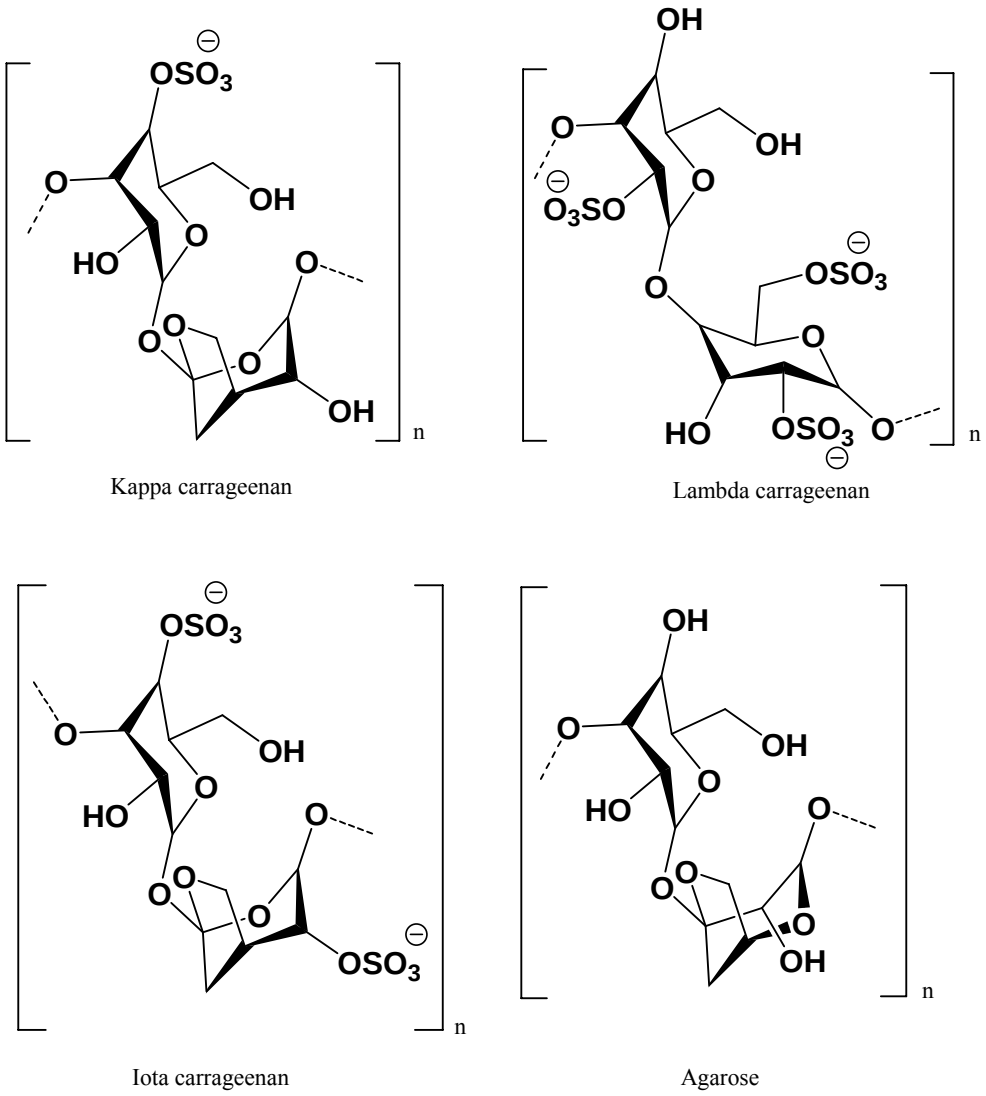

Figure 2.4. Structure of polysaccharides from red macroalgae

Algal polysaccharides were found to attenuate the generation of nitric oxide and pro-inflammatory cytokines during the initiation of inductive nitric oxide synthase (Leiro et al. 2007). According to previous reports, sulfated polysaccharides derived from the marine algal species could directly stimulate the immune system to result in reduced inflammation (Leiro et al. 2007). Algal derived sulfated polysaccharides like carrageenans and fucoidans were found to increase the cytotoxic ability of natural killer cells, such as macrophages and lymphocytes towords the carcinogenic tumors (Choi et al. 2005). Polysaccharides isolated from marine macroalga *Ulva rigida*

demonstrated reduced immune stimulatory potential after desulfation (Leiro et al. 2007). However, some of the marine algal species were reported to generate toxic compounds that stimulate neurodegenerative disorders (Turkez et al. 2012). Ethanol extracts extracted from the red marine macroalage *Callophyllis japonica* (Kang et al. 2005) and *Gracilaria tenuistipitata* (Yang et al. 2012) have significant antioxidant properties. Radical scavenging potential has been evaluated for enzymatic extracts of various marine macroalgae. Oxidative stress plays a prominent roles in various disorders includes, endothelial dysfunction (Schramm et al. 2012), lung disease (Rosanna and Salvatore 2012), gastrointestinal dysfunction (Kim et al. 2012) and atherosclerosis (Hulsmans et al. 2012), all of which involve inflammatory reactions. Marine natural products that possess antioxidant compounds were also known to have anti-inflammatory potential (Abad et al. 2008). However, anti-inflammatory properties have been reported for two species of red algae such as, *Gracilaria verrucosa* and *Gracilaria textorii.* An aqueous extract of *Gracilaria tenuistipitata* lower the virus-induced inflammation. Similarly, the polysaccharide obtained from *Porphyridium* sp. inhibited the replication of retro viruses, and an ethanol extract of *Polyopes affinis* suppressed asthmatic reactions in a disease (Lee et al. 2011). Neorogioltriol, a tricyclic brominated diterpenoid metabolite derived from the marine macroalga *Laurencia glandulifera* have showed significant anti-inflammatory potential (Chatter et al. 2011). (E)-10-Oxooctadec-8-enoic acid and (E)-9-Oxooctadec-10-enoic acid isolated from *Gracilaria verrucosa*, were the two enone fatty acids, which were reported to prevent the generation of inflammatory analogues (Lee et al. 2009). Significant antinociceptive and anti-inflammatory activities were demonstrated by the methanol extract of *Bryothamnion triquetrum* (Cavalcante et al. 2012) and sulfated polysaccharides from *Delesseria sanguinea* (Hudson) Lamouroux in *in vivo* experiments. Anti-inflammatory and antinociceptive properties were exhibited by the distinct secondary metabolites, such as a lectin from *Pterocladiella capillacea* (Silva et al. 2010), galactan from *Gelidium crinale* (De Sousa et al. 2013), sulfated polysaccharide from *Gracilaria caudate* (Chaves et al. 2013), and agglutinin isolated from marine macroalga *Hypnea cervicornis* (Bitencourt et al. 2008).

2.8. Health Benefits of Macroalgae: Prospective Candidate in Food and Pharmaceutical Industries

Marine macroalgae have drawn relevant attention in recent years in the search for bioactive compounds, which show great potential as anti-inflammatory, anti-microbial, anti-viral, and anti-tumor drugs (Souza et al. 2012). Marine macroalgae were found to be rich sources of antioxidant compounds (Wang et al. 2009), which could act against lipid oxidation in foods and oxidative stress in the target tissues. The macroalgal polysaccharides, especially those with sulfated residues were reported to have strong antioxidative properties, and have greater potential as pharmacophore candidates (Pangestuti and Kim 2011). The polysaccharide fraction of marine macroalga *Padina* sp, was found to contains anti-inflammatory activities, and was demonstrated to be active against inflammatory enzymes, such as cyclooxygenase-2 (COX-2) and 5-lipoxygenase (5-LOX) (Praveen and Chakraborty 2013). An anti-inflammatory concentrate enriched with substituted oligofucans was purified from the brown macroalgae (Praveen and Chakraborty 2013). The marine macroalga *Gracilaria* sp. is the largest in the order Gracilariales (class Florideophyceae), and were found to include more than 150 species in the tropical and temperate sea (Guiry and Guiry 2016). The most common bioactivities known in *Gracilaria* were anti-bacterial and anti-viral, and have been best described in *Gracilaria cornea* (Bansemir et al. 2006) and *Gracilaria changii* (Sasidharan et al. 2008). There were reports of biogenic alkaloids from marine invertebrates, and few of them were found to be active against various disease molecular targets. The nitrogen containing bioactive compounds were found to comprise a major share of about 40 % of the marine natural products, and are ubiquitous in various marine flora and fauna (Blunt et al. 2008). Some of the bioactive secondary metabolites purified from marine origin were often used as drugs or biological probes for different physiological studies (Bansemir et al. 2006). Indole alkaloids were characterized from marine macroalga *Enteromorpha intestinalis* (Numata et al. 1993) and leptosins from *Sargassum tortillae* (Takahashi et al. 1995). Hordenine was reported to be the first alkaloid isolated from marine algae in 1969 (Guven et al. 1969). These red and green macroalgae of marine origin were found to be potential inhibitors of the carbolytic enzyme α-glucosidase (Seung et al. 2013). Bromophenols, 2-piperidione, benzene acetamide, *n*-hexadecanoic acid and polysaccharide derivatives were found in red marine macroalgae, such as *Rhodomela*

confervoides, *Symphyocladia latiuscula*, *Polysiphonia urceolata*, and were found to exhibit pivotal hypoglycemic potentials by inhibiting α-glucosidase (Seung et al. 2013). Bioactive properties of the marine macroalgae were reported to be due to the presence of sulfated polysaccharides, phenolics, and terpenoids (Chakraborty and Paulraj 2010; Chakraborty et al. 2016). There were additional reports of marine macroalgae possessing α-amylase and α-glucosidase inhibitory activities (Apostolidis et al. 2011), which appropriately substantiated the results obtained in the present study that these macroalgal species are good source for anti-diabetic agents. The synthetic dipeptidyl peptidase-4 (DPP-4) inhibitors, such as vildagliptin, sitagliptin, saxagliptin, etc, were reported to have multiple adverse effects, such as headache, dizziness, hypoglycemic disorders, nausea, weight gain and swelling of the legs and ankles due to excess fluid retention (Idris and Donnelly 2007). Similarly, other synthetic hypoglycemic agents (acarbose and voglibose) that inhibit α-amylase and α-glucosidase were found to cause hepatic and gastrointestinal disorders (Murai et al. 2002). The bioactive compounds from macroalgae were reported to be effective for the treatment of major chronic diseases, such as diabetes through the inhibition of starch digesting enzymes and the regulation of glucose-induced oxidative stress (Lee et al. 2010). Different investigations prescribed that antioxidant and other bioactive properties fundamentally reliant on the level of sulfation, position of sulfate groups on the sugar backbone, sugar composition and glycosidic branching (Leonard et al. 2010). The reported bioactivities of polysaccharides from marine macroalgae incorporate antioxidant, immunomodulatory, anti-coagulant, anti-thrombotic, blood lipid reducing, and anti-inflammatory activities (Li et al. 2008). Antioxidant capacities of polysaccharide or polysaccharide-complex were observed in the fucoidan and fucans isolated from marine macroalgae *Fucus vesiculosus* and *Padina gymnospora* (De Souza et al. 2007). Sulfated polysaccharides extracted from marine macroalgae were found to exhibit promising antioxidant activities (Li et al. 2008). Oxidative stress is known to assume a significant role in causing chronic diseases, for example, hypertension (Savoia and Schiffrin 2007).

Figure 2.5. Photographs of macroalgae collection site in Southeast coast of India

Despite several side effects, such as hypotension, cough and reduced renal function connected with the utilization of synthetic ACE-I inhibitors, e.g., Captopril (Bristol-Myers Squibb Co., New York, NY, USA), Enalapril (Biovail Pharmaceuticals, Ontario, Canada) and Alacepril (LGM Pharma, Boca Raton, FL, USA), they are still broadly utilized for the treatment of hypertension (Lordan et al. 2011). Owing to these symptoms, there were continuous searches for alternative sources of ACE-I inhibitors from natural sources including macroalgae (Paiva et al. 2016). The marine macroalga ‘‘Wakame’’ (*Undaria pinnatifida*), which is consumed in Japan, has been accounted for *in vitro* ACE-I inhibitory and *in vivo* anti-

hypertensive effects (Suetsuna and Nakano 2000). Sato and colleagues identified seven types of ACE-I inhibitory peptides from the butanol portion of Wakame hydrolysate (Sato et al. 2002). The aqueous extracts of the red marine macroalgae, *Gracilaria verrucosa, Gracilaria textorii, Grateloupia filicina, Polysiphonia japonica, Euchema kappaphycus* and *Gracilaria edulis* displayed noteworthy DPPH radical scavenging properties (Heo et al. 2006). There was a previous report that accounted for the molecules with electronegative groups, such as hydroxyl, sulfate, and sulfated ester residues possessing potential Fe^{2+} chelating abilities (Lindsay 1996). Toth and Pavia (2000) reported that polysaccharides derived from marine macroalgae were more biologically active than phlorotannins (phenolics) for the detoxification and imperviousness to transition metal accumulation (Toth and Pavia 2000). The inhibition of lipid peroxidation might be due to the presence of multiple hydroxyl groups on the polysaccharide chain. The polygalactans separated from the red marine macroalgae were disclosed to disrupt free-radical chain reaction by giving a proton to unsaturated fat radicals to end the chain reactions, and therefore, might play prominent role to inhibit lipid peroxidation. As of late, much consideration has been paid by the consumers towards natural bioactive compounds as functional ingredients, and that the marine-inferred ACE inhibitors are alternative tools, which that can add to customer's well-being. The bioactive compounds derived from the food matrices were found to be more effective in promoting health leading to the reduction of disease risk. Particularly, the bioactive compounds derived from marine macroalgae have served as a rich source of health-promoting components. Among them, oligosaccharides and their derivatives are rich sources of natural health enhancers, and this suggests their potential as a functional ingredient in future nutraceutical and pharmaceutical products. However, substantial medical and pharmaceutical researches are required to expand therapeutic agents from these marine sources. All in all, it could be proposed that macroalgae-derived bioactives belonging to sulfated polygalactans are potential therapeutic candidates to prevent various human ailments.

2.9. Conclusions

During the last decades, efforts were undertaken to develop potent antioxidant compounds from the marine origin as food supplements in the food and pharmaceutical industries. These naturally occurring leads were considered as valuable alternatives to the commercially available synthetic compounds due to their effectiveness and safety. There were reports that described the utilization of the antioxidant compounds from marine resources (Li et al. 2008; Liu et al. 2012; Yoon et al. 2012). The regular intake of macroalgae based diet can lower the risk facts of cardiovascular diseases, cancer and diabetes (Yang et al. 2010; Lee et al. 2010). Keeping this fact as background information, the present study has undertaken to develop an optimized protocol for the isolation and purification of the bioactives belonging to small molecular bioactives and polysaccharides. These compounds were characterized using exhaustive spectroscopic techniques, and the novel leads were validated through selective bioassay, structure optimization and chemiinformatic experiments to enrich the pool of bioactive leads for use against oxidants and inflammatory mediators.

Chapter 3

BIOACTIVE POTENTIAL OF *KAPPAPHYCUS ALVAREZII AND GRACILARIA OPUNTIA*

Contents

3.1. Background

Macroalgae of marine origin are photosynthetic organisms, and are resolved to a conjunction of stressful factors, *viz*., light and oxygen at the origin of the evolution of free radicals and other oxidative reagents. Although the absence of oxidative damage in their structural components evidently suggested that their cells generate bioactive metabolites with antioxidative resistance systems (Escrig et al. 2001). The reactive oxygen species (ROS) *viz*., hydroxyl radical ($HO^{\cdot}$), hydrogen peroxide (H_2O_2) etc. are metabolites, which are generated during aerobic life as an outcome of the metabolism of oxygen. DNA, cell membranes, proteins and other cellular fragments are target sites of the free radical-stimulated oxidative degradation processes, resulting in serious human diseases, such as chronic inflammation, atherosclerosis, cancer, cardiovascular disorders and ageing. Clinical studies established that oxidative stress, through free radical generation, assumes a prominent role in the inception of hypertension (Savoia and Schiffrin 2007). It has been established that extended generation of ROS substantially adds to the dysregulation of physiological processes, which evoke structural and functional variations in hypertension. Increased levels of ROS and chronic subclinical inflammation could also potentiate the pathogenic factors leading to type-2 diabetes associated with the insulin resistance syndrome (Festa et al. 2000). Diabetes is the most frequent endocrine disorder, and by the year 2010, it is predicted that greater than 200 million people in the world will have diabetes mellitus and 300 million will decisively have the disorder by 2025 (King et al. 1998). The methods to treat diabetes is to diminish the post-prandial hyperglycemia in order to prevent the actions of carbohydrate hydrolyzing enzymes, such as α-amylase and α-glucosidase. Among various algae found in the Gulf of Mannar regions, *K. alvarezii* and *G. opuntia* are abundantly available throughout the different seasons. The present work anticipated the evaluation of antioxidant, anti-hypertension anti-diabetics and anti-inflammatory potential of the solvent extracts derived from *K. alvarezii* and *G. opuntia* from the Gulf of Mannar at South-Eastern Coast of the Indian Peninsula. The bioactivities of the solvent extracts were also correlated with the presence of various auxochromes, and their chemical properties responsible for the target bioactivities.

3.2. Materials and Methods

3.2.1. Chemicals and Reagents

All chemicals were of analytical, spectroscopic or chromatographic reagent grade, and were obtained from E-Merck (Darmstadt, Germany) and Sigma-Aldrich Chemical Co. Inc. (St. Louis, MO, USA). The reagents and chemical solvents were of analytical grade or higher.

3.2.2. Samples and Study Area

The two marine red marine macroalgae used in this study were *K. alvarezii* and *G. opuntia* {Fig. 3.1 (A-C)}. They were freshly collected from the Gulf of Mannar in Mandapam region located between 8º48′ N, 78º9′ E and 9º14′ N, 79º14′ E on the south east coast of India. The samples were washed in running water for 10 min, transported to the laboratory and shade-dried (35 ± 3 °C) for 36 h. The shade-dried macroalgae were powdered and used for further experiments. The powdered algal samples (100 g) were extracted three times with EtOAc-MeOH (50–60 °C, 3 h), filtered through Whatman No. 1 filter paper, and the pooled filtrate was concentrated (50 °C) in a rotary vacuum evaporator (Heidolf, Germany) to one-third of the original volume. All reagents and solvents were of analytical grade, and were acquired from E-Merck (Darmstadt, Germany) or Sigma-Aldrich Chemical Co. Inc. (St. Louis, MO).

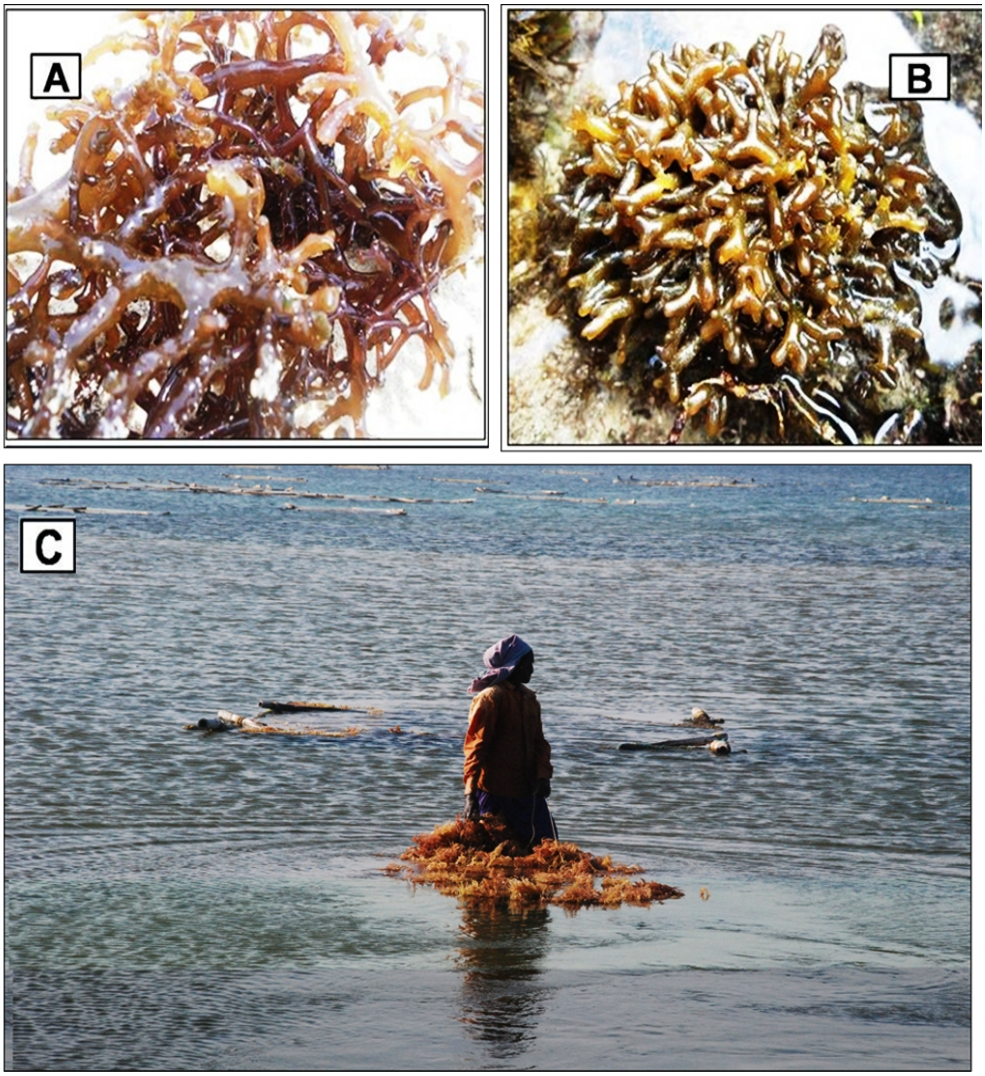

Figure 3.1. Photographs of marine red macroalgae (**A**) *Kappaphycus alvarezii* (**B**) *Gracilaria opuntia* (**C**) and their collection site at the Gulf of Mannar of Southeast coast of India

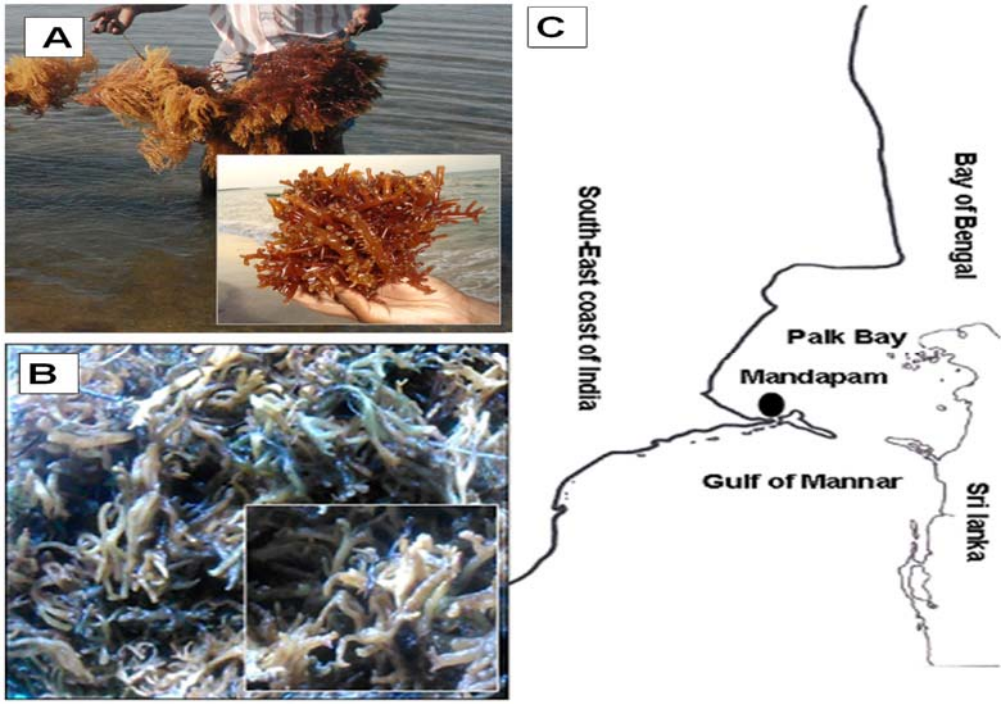

Figure 3.2. Red marine macroalgae collected from the intertidal zone of the Gulf of Mannar region (**A**) *Kappaphycus alvarezii* and (**B**) *Gracilaria opuntia.* The close-up views of the algae were shown as insets (**C**) The collection site of marine macroalgae at the Gulf of Mannar region in South-East coast of India (9° 17' 0" North, 79° 7' 0" East)

3.2.3. Antioxidant Activity Assays

3.2.3.1. Total Phenolic Contents (TPC)

Total phenolic content in the crude EtOAc-MeOH extracts of *K. alvarezii* and *G. opuntia* were determined by the Folin–Ciocalteu method (Wojdyło et al. 2007). Briefly, 0.5 mL of the EtOAc-MeOH extracts (5 mg/mL in MeOH) was added into a test tube containing 0.25 mL of Folin–Ciocalteu reagent. After the addition, the mixture was incubated for 8 min. About 1.0 mL of sodium carbonate (7.5 %, w/v) was added, and the contents were thereafter incubated at 25 ºC (for 120 min), and the absorbance was recorded at 756 nm. The results were depicted in milligram of gallic acid equivalents (mg GAE)/g of the solvent extracts.

3.2.3.2. 1, 1-Diphenyl-2-picryl-hydrazil Radical Scavenging Activity

DPPH (100 μM) was dissolved in methanol to prepare the stock solution. The EtOAc-MeOH extracts (1 mL in MeOH) of *K. alvarezii* and *G. opuntia* were mixed with DPPH solution (1 mL) and kept in the dark at room temperature for 10 min. The decrease in absorbance of the mixture was analyzed at 517 nm against a reagent blank by using a UV–VIS spectrophotometer. The percentage of DPPH radical scavenging potential was determined by scavenging activity (%) = $\{(A_0-A_s)/A_0\} \times 100$, where A_0 is the absorbance of control and A_s is the absorbance of the sample. The 50 % inhibitory concentration (IC_{50}) was calculated from the graph plotted with the concentrations of sample (x-axis) against the percentage inhibition (y-axis). The results were expressed as IC_{50}, the concentrations of samples at which they scavenge 50 % of radical activities, and were expressed in mg/mL.

3.2.3.3. 2, 2′-Azino-bis-3 ethylbenzothiozoline-6-sulfonic acid diammonium salt (ABTS) Radical Scavenging Activity

In brief, ABTS was dissolved in the deionized water to a concentration of 7 μM, and the content was mixed with potassium persulfate ($K_2S_2O_8$, 2.45 μM) before being kept in dark at room temperature for 12–16 h. The ABTS radical solution was diluted with MeOH to get an absorbance of 0.70 at 734 nm. The diluted $ABTS^{\cdot+}$ solution (3 mL) was mixed with the EtOAc-MeOH extracts of *K. alvarezii* and *G. opuntia* (30 μL), and the absorbance was recorded after 6 min at 734 nm. The percentage of ABTS radical scavenging potential was determined by scavenging activity (%) = $\{(A_0-A_s)/A_0\} \times 100$, where A_0 is the absorbance of control and A_s is the absorbance of the sample. The 50 % inhibitory concentration (IC_{50}) was calculated from the graph plotted with the concentrations of sample (x-axis) against the percentage inhibition (y-axis). The results were expressed as IC_{50}, the concentrations of samples at which they scavenge 50 % of radical activities, and were expressed in mg/mL.

3.2.3.4. Ferrous ion (Fe^{2+}) Chelating Activity

The ferrous ion chelating ability of the EtOAc-MeOH extracts of *K. alvarezii* and *G. opuntia* was determined as mentioned earlier (Lim et al. 2007) with suitable

modifications. $FeSO_4$ (1.0 mL, 0.125 mM) and ferrozine (1.0 mL, 0.3125 mM) were mixed with 1.0 mL of EtOAc-MeOH extracts of *K. alvarezii* and *G. opuntia*. The mixture was equilibrated for 10 min before measuring the absorbance at 562 nm. The ability of the EtOAc-MeOH extracts of *K. alvarezii* and *G. opuntia* to chelate Fe^{2+} was determined relative to the control (consisting of Fe and ferrozine only) by applying the equation: % chelating ability = $(A_0 - A_1) \times 100/A_0$, where A_0 is the absorbance of control, and A_1 is the absorbance of sample. The results were expressed as IC_{50}, the concentrations of samples at which 50 % of iron chelating activity, and were expressed in mg/mL.

3.2.3.5. Lipid Peroxidation Inhibition Activity

The activities of the EtOAc-MeOH extracts of *K. alvarezii* and *G. opuntia* to arrest lipid peroxidation were assessed by thiobarbituric acid-reactive species (TBARS) formation inhibitory assay (Kulisic et al. 2004). The model system used for this assay was lyophilized green mussel (*Perna viridis* L.) as a lipid source. The lyophilized powder of *P. viridis* meat (10 mg) was incubated with 1 mL of solvent extracts of *K. alvarezii* and *G. opuntia* (1 mL; 2 mg/mL). The incubation was terminated by cold acetic acid addition (pH 3.6, 2 mL, 20 % v/v), and the malondialdehyde production was followed by TBA addition (0.78 % w/v in acetic acid, 2 mL). The incubated (for 45 min at 95 ºC) mixture was cooled to room temperature, and centrifuged (10 min, 8000 rpm) before measuring the absorbance at 532 nm. The TBARS activity was expressed as mM of malondialdehyde equivalent compounds formed per kg sample (MDAEQ/kg sample), related to the control (lyophilized green mussel) with highest lipid peroxidation on the same assay conditions.

3.2.4. Anti-hypertensive Activities

The anti-hypertensive activities were determined by ACE-I inhibitory assay (Udenigwe et al. 2009). Briefly, the enzyme angiotensin converting enzyme-I (ACE-I, 20 µL, 1 U/mL) was mixed with the EtOAc-MeOH extracts of *K. alvarezii* and *G. opuntia* (0.2 mg), and the mixture was added with *N*-furanacryloyl-l-phenylalanylglycylglycine (FAPGG, 1 mL, 0.5 mM dissolved in 50 mM Tris-HCl buffer, pH 7.5) containing 300 µM of common salt (NaCl). The decreased absorbance

at 345 nm was recorded within a 1.5 min span at room temperature, whereas the anti-hypertensive activities were expressed as IC_{50}, the concentration at which it inhibit 50 % of ACE-I activity.

3.2.5. Anti-diabetic Activities

In vitro anti-diabetic studies by inhibition of dipeptidyl peptidase-4 (DPP-4) and carbolytic enzyme α-amylase were determined by following previous reports of literature (Kojima et al. 1980; Hamdan and Afifi 2004), whereas α-glucosidase inhibition assay was performed according to the previous literature (Dong et al. 2012) with suitable modifications.

3.2.5.1. Inhibition of α-Amylase Activity

To carry out α-amylase inhibitory activity, the EtOAc-MeOH extracts of *K. alvarezii* and *G. opuntia* were added to the phosphate buffer (500 µL, 0.20 mM, pH 6.9) containing α-amylase (0.5 mg/mL) solution before being incubated at 25 °C for 10 min. Thereafter, starch solution (500 µL, 1 % w/v in 0.02 M sodium phosphate buffer of pH 6.9) was added to the content, and the reaction mixture was incubated at 25 °C for 10 min. The reaction was quenched by addition of 3, 5 dinitrosalicylic acid reagent (1.0 mL) under heating condition for 5 min before being cooled at room temperature. The reaction mixture was diluted with distilled water (10 mL), and the absorbance was recorded at 540 nm.

3.2.5.2. Inhibition of α-Glucosidase Activity

To determine the α-glucosidase inhibitory activities of the EtOAc-MeOH extracts of *K. alvarezii* and *G. opuntia*, Tris-HCl buffer (500 µL, 0.2 M, pH 8) was prepared in different concentrations, and was added to the enzyme solution (1 U/mL prepared in 0.2 M Tris-HCl, pH 8.0). The reaction mixture was pre-incubated for 5 min at 37 °C before being added with the starch solution (500 µL, 2 % w/v) and incubated for 10 min at 37 °C. The reaction was stopped with 3, 5 dinitrosalicylic acid reagent (1 mL) under heating for 2 min in a boiling water bath before being cooled at room

temperature. The reaction mixture was then diluted with distilled water (9 mL), and the absorbance was measured at 540 nm.

3.2.5.3. Inhibition of DPP-4 Activity

The EtOAc-MeOH extracts of *K. alvarezii* and *G. opuntia* were prepared in Tris-HCl buffer (50 mM, pH 7.5) at different concentrations. The EtOAc-MeOH extract of *K. alvarezii* and *G. opuntia* (0.35 mL) were mixed with DPP-4 (15 µL, 0.05 U/mL), which was previously prepared in Tris-HCl buffer (100 mM, pH 8). The reaction mixture was pre-incubated for 10 min at 37 °C before being added with the substrate (gly-pro-p-nitroanilide, 50 µL, 0.2M in Tris-HCl buffer). The contents were incubated for 30 min at 37 °C, and the reaction was terminated by the addition of glacial acetic acid (25 µL). The absorbance of the reaction mixture was measured at 405 nm. The results were expressed as IC_{50}, the concentration at which it inhibits 50 % of the enzyme (α-amylase, α-glucosidase and DPP-4) activities.

3.2.6. Anti-inflammatory Activities

The anti-inflammatory properties were evaluated by COX-1 and COX-2 inhibition assays using 2, 7-dichlorofluorescein method (Larsen et al. 1996), and 5-LOX inhibition assay using the principle of 1, 4-diene and 1, 3-diene conversion of the polyunsaturated fatty acid (Baylac and Racine 2003).

3.2.6.1. Cyclooxygenase (COX-1 and COX-2) Inhibition Assay

In brief, leuco-2, 7-dichlorofluorescein diacetate (5 mg) was hydrolyzed at room temperature in NaOH (1 M, 50 µL, 10 min) and the excess of NaOH was neutralized by adding HCl (1 M, 30 µL) before the resulting 1-dichlorofluorescein (1-DCF) was diluted in Tris-HCl buffer (0.1 M, pH 8). The COX isoforms (COX-1 and COX-2) were diluted in 0.1 M Tris-buffer (pH 8), and the EtOAc-MeOH extracts of *K. alvarezii* and *G. opuntia* (the equivalent volume of MeOH, 20 µL) were pre-incubated with the enzymes at room temperature for 5 min in the presence of hematin. Premixed phenol, 1-DCF, and arachidonic acid (fatty acid) were added to the enzyme mixture to initiate the reaction, and to give a final reaction mixture (1 mL) of arachidonic acid (50

μM), phenol (500 μM), 1-DCF (20 μM), and hematin (1 μM) in the final volume of 0.1 M Tris-buffer (pH 8). The reaction was recorded spectrophotometrically over 1 min at 502 nm. The blank was analyzed against each test reaction to ascertain non-enzymatic activity due to the experimental samples.

3.2.6.2. Lipoxygenase (5-LOX) Inhibition Assay

The 5-LOX inhibitory assay was carried out by a previously described method (Baylac and Racine 2003). In brief, an aliquot of the stock solution (50 μL) prepared in solvent DMSO and a surfactant (tween 20) at a particular ratio (29:1, w/w) of each sample were added with potassium phosphate buffer (0.1 M, 2.95 mL, pH 6.3) and linoleic acid solution (48 μL) before being placed in a cuvette (3 mL). An ice-cold solution of potassium phosphate buffer (12 μL) was thereafter mixed with 5-LOX (100 U) in the cuvette. The absorbance of the content was recorded at 234 nm by using a spectrophotometer.

The inhibitory activities of the EtOAc-MeOH extracts of *K. alvarezii* and *G. opuntia* towards COX-1, 2 and 5-LOX were calculated as follows: $\{(Ab_C - Ab_S)/Ab_C\} \times 100$, where Ab_S and Ab_C depicted the absorbance of sample and control, respectively. The results were demonstrated as IC_{50}, the concentration at which it inhibits 50 % of COX and LOX activities.

3.2.7. Spectroscopic Methods

Fourier-transform infrared (FTIR) spectra of the KBr pellets were recorded by utilizing a Perkin–Elmer FTIR spectrophotometer scanning between 4000 and 400 cm^{-1} (Perkin–Elmer 2000, USA). Ultraviolet–visible (UV–VIS) data were acquired by Varian Cary 50 Conc UV–VIS spectrometer (Varian, Waltham, USA). The solvents were evaporated in a rotary vacuum evaporator (Heidolf, Germany). A table-top high speed refrigerated centrifuge (Sorvall, Biofuge Stratos, Thermo Scientific, Germany) was used for centrifugation. The crude EtOAc-MeOH extracts of *K. alvarezii* and *G. opuntia* (10 mg) were mixed with KBr (100 mg) and compressed to prepare as a salt disc. The frequencies of different components present in each sample were analyzed. Proton nuclear magnetic resonance (^{1}H-NMR) spectra were recorded on a Bruker

AVANCE DRX 600 MHz (AV 600) spectrometer (Bruker, Karlsruhe, Germany) in $CDCl_3$ as aprotic solvent at ambient temperature (27 ^oC) with tetramethylsilane (TMS) as the internal standard (δ 0 ppm) equipped with 5 mm probes.

3.2.8. Statistical Analysis

Data were expressed as mean of triplicate ± standard deviation. Statistical evaluation was carried out by SPSS software (SPSS Inc, Chicago, USA, ver. 13.0). Descriptive statistics were calculated for all the studied traits. The Pearson correlation coefficient (*r*) was calculated ($P < 0.05$) to assess the strength of the linear relationship between two variables. The selected variables for principal component analysis (PCA) were the different bioactivities, as exhibited by crude extracts prepared from the studied red marine macroalgae.

3.3. Results and Discussion

3.3.1. Yield

The yields of EtOAc-MeOH extracts of *K. alvarezii* and *G. opuntia* were found to be 60 g (6 %) and 40 g (4 %) of 1 kg of dry algae, respectively.

Table 3.1 *In vitro* bioactivity of EtOAc-MeOH (1:1 v/v) solvent extracts from the red marine macroalgae

Activities	***K. alvarezii***	***G. opuntia***
Total phenolic content	295.68 ± 0.01^a	380.33 ± 0.02^a
Antioxidant activities		
$DPPH^·$ radical scavenging	1.24 ± 0.06^b	1.28 ± 0.03^c
ABTS radical scavenging	1.26 ± 0.03^b	1.31 ± 0.05^c
Fe^{2+} ion chelating	1.30 ± 0.09^b	1.33 ± 0.01^c
Lipid peroxidation inhibitory	47.08 ± 0.05^a	53.81 ± 0.04^b
Anti-hypertensive activities (ACE)	2.10 ± 0.02^b	2.13 ± 0.09^c
Anti-diabetic activities		
α-amylase inhibitory	2.18 ± 0.04^b	2.20 ± 0.08^c

α-glucosidase inhibitory	2.20 ± 0.01^{b}	2.22 ± 0.03^{c}
DPP-4 inhibitory	2.18 ± 0.03^{b}	2.21 ± 0.02^{c}
Anti-inflammatory activities		
COX-1 inhibitory	1.38 ± 0.09^{b}	1.42 ± 0.02^{c}
COX-2 inhibitory	1.35 ± 0.05^{b}	1.39 ± 0.04^{b}
5-LOX inhibitory	1.49 ± 0.02^{b}	1.52 ± 0.03^{b}

Results were expressed in IC_{50} values (50 % inhibitory concentration as mg/mL; calculated from the graph plotted with concentrations of samples against percentage.

[a-c] Column wise values with different superscripts of this type indicate significant difference ($P < 0.05$).

Results were expressed as mean ± SD (n =3).

Lipid peroxidation inhibitory activity (TBARS assay) was expressed as m MDAEQ/kg.

3.3.2. Antioxidant Activities and Phenolic Contents of Organic Extracts of Macroalgae

The EtOAc-MeOH extracts from *G. opuntia* (380.33 mg of GAE/g) was found to possess greater content of total phenolics than that of *K. alvarezii* (295.68 mg of GAE/g). The DPPH radical scavenging activity of EtOAc-MeOH extracts derived from *K. alvarezii* was found to be greater (IC_{50} 1.24 mg/mL) than that displayed by *G. opuntia* (IC_{50} 1.28 mg/mL). $ABTS^{\cdot+}$ scavenging activity of EtOAc-MeOH extracts from *K. alvarezii* was greater (IC_{50} 1.26 mg/mL) than that from *G. opuntia* (IC_{50} 1.31 mg/mL). The EtOAc-MeOH extracts from *K. alvarezii* displayed significantly greater Fe^{2+} chelating abilities (IC_{50} 1.30 mg/mL) than that acquired from *G. opuntia* (IC_{50} 1.33 mg/mL). On account of lipid peroxidation inhibition assay, the EtOAc-MeOH extracts from *K. alvarezii* displayed greater lipid peroxidation inhibition activity (47.08 mM MDAEQ/kg) than that obtained from *G. opuntia* (53.81 mM MDAEQ/kg). TBARS activity was denoted as mM of malondialdehyde equivalent compounds formed per kg sample (MDAEQ/kg sample) related to the control (lyophilized green mussel) leading to maximum lipid peroxidation in the same assay conditions. The capability of the EtOAc-MeOH extracts derived from *K. alvarezii* and *G. opuntia* to induce lipid peroxidation was estimated by thiobarbituric acid reactive species (TBARS) assay.

3.3.3. ACE Inhibitory Activity

The ACE inhibitory activities of the EtOAc-MeOH extracts from *G. opuntia* was lesser (IC_{50} 2.13 mg/mL) than those from *K. alvarezii* (IC_{50} 2.10 mg/mL).

3.3.4. *In-vitro* Anti-diabetic Activities of EtOAc-MeOH Extracts from *K. alvarezii* and *G. opuntia*

3.3.4.1. Inhibition of α-Amylase and α-Glucosidase Activities

The results from the present study demonstrated that there were no significant difference in α-amylase and α-glucosidase inhibitory activity of the EtOAc-MeOH extracts from *K. alvarezii* and *G. opuntia* considered in the present study (Table 3.1). However, the EtOAc-MeOH extracts of *K. alvarezii* exhibited greater α-amylase inhibitory activity (IC_{50} 2.18 mg/mL) than that of *G. opuntia* (IC_{50} 2.20 mg/mL). Likewise, there was no significant difference in the α-glucosidase inhibitory activity of the EtOAc-MeOH extracts derived from these two red macroalgal species (*K. alvarezii* IC_{50} 2.20 mg/mL; *G. opuntia* IC_{50} 2.22 mg/mL). The macroalgae were reported to possess α-amylase and α-glucosidase inhibitory activities (Apostolidis et al. 2011), which substantiated the results obtained in the present study that these macroalgal species were good source for anti-diabetic agents.

3.3.4.2. Inhibition of Dipeptidyl-Peptidase-4 Enzyme Activity

Dipeptidyl peptidase-4 (DPP-4) is involved in the inactivation of glucagon like peptide-1 (GLP-1), a potent insulinotropic peptide. Thus, DPP-4 inhibition can be an efficient approach to treat type-2 diabetes mellitus by potentiating insulin secretion (Mentlein 1999). The present study described the biological effects of EtOAc-MeOH extracts from two different red macroalgae *K. alvarezii* and *G. opuntia*. DPP-4 inhibitory activity of the EtOAc-MeOH extracts of *K. alvarezii* was found to be significantly greater (IC_{50} 2.18 mg/mL) than that derived from *G. opuntia* (IC_{50} 2.21 mg/mL). The synthetic DPP-4 inhibitors such as vildagliptin, sitagliptin, saxagliptin, etc, were reported to have several side effects like headache, dizziness, hypoglycemic disorders, nausea, weight gain and swelling of the legs and ankles due to excess fluid

retention (Idris and Donnelly 2007). Similarly, other synthetic hypoglycemic agents (acarbose and voglibose) that inhibit α-amylase and α-glucosidase were found to cause hepatic and gastrointestinal disorders (Murai et al. 2002). The bioactive compounds from macroalgae were reported to be effective for the treatment of major chronic diseases like diabetes through the inhibition of starch digesting enzymes and the regulation of glucose-induced oxidative stress (Lee et al. 2010). The macroalgae considered in the present study can be used as potential alternative therapy for treatment of diabetes.

3.3.5. *In-vitro* Anti-inflammatory Activities of Organic Extracts from *K. alvarezii* and *G. opuntia*

The EtOAc-MeOH extracts from *K. alvarezii* exhibited significantly greater ($P < 0.05$) COX-1 and COX-2 inhibition activity (IC_{50} values of 1.38 mg/mL and 1.35 mg/mL, respectively) than that displayed by *G. opuntia* (IC_{50} values of 1.42 mg/mL and 1.39 mg/mL, respectively). EtOAc-MeOH extracts from *K. alvarezii* also exhibited greater 5-LOX inhibitory activity (1.49 mg/mL) than that of *G. opuntia* (IC_{50} 1.52 mg/mL) (Table 3.1).

3.3.6. Spectroscopic Fingerprinting of EtOAc-MeOH Extracts of *K. alvarezii* and *G. opuntia*

Spectrometric fingerprinting were used to de-replicate the pattern recognition of the resonances along with types and number of protons associated with structural classes involved in extracts

3.3.6.1. Fourier Transform Infrared Spectral (FT-IR) Analysis

FT-IR is a valuable tool for qualitative determination of the probable occurrences of various functional groups in the crude organic extracts (Ashokkumar and Ramaswamy 2014). In the present study, the FT-IR experiments were carried out to fingerprint the functional groups present in the EtOAc-MeOH extracts from *K. alvarezii* and *G. opuntia*. The intense band at 3429.39 cm^{-1} in the organic crude extract from *K. alvarezii* was attributed due to the N-H stretching or O-H stretching vibration

of phenols or alcohols. The absorption peaks were present in the EtOAc-MeOH crude extract from *G. opuntia* at 1715 cm^{-1} might be due to the C=O stretching vibration of saturated aliphatic groups and carbonyls. Absorption band in the FTIR spectrum of EtOAc-MeOH crude extracts of *K. alvarezii* (1363 cm^{-1}) and *G. opuntia* (1371.54 cm^{-1}, 1458.63 cm^{-1}) were attributed, which represented the C-C stretching vibrations of the aryl ring framework. The strong absorption bands in the 2920-2923 cm^{-1} region of the FT-IR spectra of the EtOAc-MeOH extracts of *K. alvarezii* and *G. opuntia* attributed the C-H stretching vibrations. In comparison with the FT-IR spectra of EtOAc-MeOH extracts of *K. alvarezii* and *G. opuntia*, both the extracts displayed prominent functional groups.

3.3.6.2. Nuclear Magnetic Resonance (NMR) Fingerprinting

The protons and carbons associated with different magnetic environments of the functional groups in the organic extracts of the studied marine macroalgal species were labeled and analyzed by ^{1}H and ^{13}C-NMR spectroscopy. The ^{1}H-NMR spectral data of EtOAc-MeOH extract obtained from *K. alvarezii* displayed greater proton integrals (>1000) at δ_H 0-2, which implied the existence of methine (-C<u>H</u>-), methylene (RC<u>H_2</u>-) and methyl (C<u>H_3</u>-C) protons correlated with saturated hydrocarbons, whereas the organic extract from *G. opuntia* was found to illustrate lesser number of proton integral (~579).

The signals at δ_H 1.08–1.38 in the organic extract of *G. opuntia* could be explained by the presence of methylene group {–(C<u>H_2</u>)$_n$} in the long alkyl chain. The ^{1}H-NMR spectra of *K. alvarezii* acquired well resolved, deshielded signals at about δ_H 4.5-5, than those displayed by *G. opuntia,* which appropriately signified the vicinity of the olefinic attachments in the former. The protons appeared at δ_H 2-2.5, apparently indicated acetyl or allylic substitution, which were found to be significantly higher in the EtOAc-MeOH extract of *K. alvarezii*, whilst EtOAc-MeOH extract of *G. opuntia* possessed lesser number of proton integral at this region. The presence of methoxy proton (R-OC<u>H_3</u>) was confirmed by the protons at δ_H 3.08, 3.66 and 3.18 in the NMR spectrum of the organic extracts of *K. alvarezii* and a peak at δ_H 3.54 with regard to the same of *G. opuntia*. The integral value of protons in the olefinic range (δ_H 4.5-6) of EtOAc-MeOH extract of *K. alvarezii* was greater (~341) when compared with the same obtained from *G. opuntia* (δ_H 4.8-4.9) (~76). The protons present in the region of δ_H

7.2-7.4 were typical of the aryl (aromatic) ring system. Proton integral at this aromatic region was found to be greater in EtOAc-MeOH extract of *K. alvarezii* (proton integral of ~330). There were no aldehydic protons at the characteristic region of δ_H 8.5-10 in the NMR spectra of EtOAc-MeOH extracts of *K. alvarezii* and *G. opuntia*. The pattern recognition and proton integration ^{1}H-NMR approach to de-replication could thus lead to a conclusion of the types and number of protons that might be associated with the compound(s) in the extracts. The number of carbon atoms associated to the saturated hydrocarbons (δ_C 10-40) was higher in the EtOAc-MeOH extracts of *K. alvarezii* than that of *G. opuntia.* The olefinic carbons at δ_C 114-136 were greater in the extract of *K. alvarezii.* Prominent ^{13}C-NMR signals were recorded in the carbonyl carbon region (δ_C 171-173) of the organic extract derived from *K. alvarezii*. Preliminary, the spectroscopic fingerprinting experiments, such as FT-IR and NMR of the organic extracts of *K. alvarezii* and *G. opuntia* provided with the preliminary information with regard to the different types of protons and carbons associated with different magnetic environments of the functional groups.

3.3.7. Correlation Analysis

The relationships between antioxidant, anti-inflammatory, anti-hypertension and anti-diabetic activities of the EtOAc-MeOH extracts of *K. alvarezii* and *G. opuntia* were statistically analyzed using PCA (Fig. 3.3). The loading of first and second principle components (PC1 and PC2) were accounted for 65.30 % and 30.10 % of the variance, respectively.

The component, PC1 was mainly influenced by inhibitory activities of EtOAc-MeOH derived from *G. opuntia* and *K. alvarezii* (GO, KA) towards the pro-inflammatory enzymes, COX-1 (denoted as C1; GO and C2; KA) and COX-2 (denoted as CO1; GO and CO2; KA), along with DPPH (DPP2; KA) and ACE (AC2; KA). On the other hand, 5-LOX (denoted as L1; GO and L2; KA), DPP-4 (DP1; GO and DP2; KA), DPPH (DPP1; GO), and ACE (AC1; GO) inhibiotory properties of the EtOAc-MeOH extracts of the marine macroalgae were mainly contributed to PC2 (Fig. 3.3).

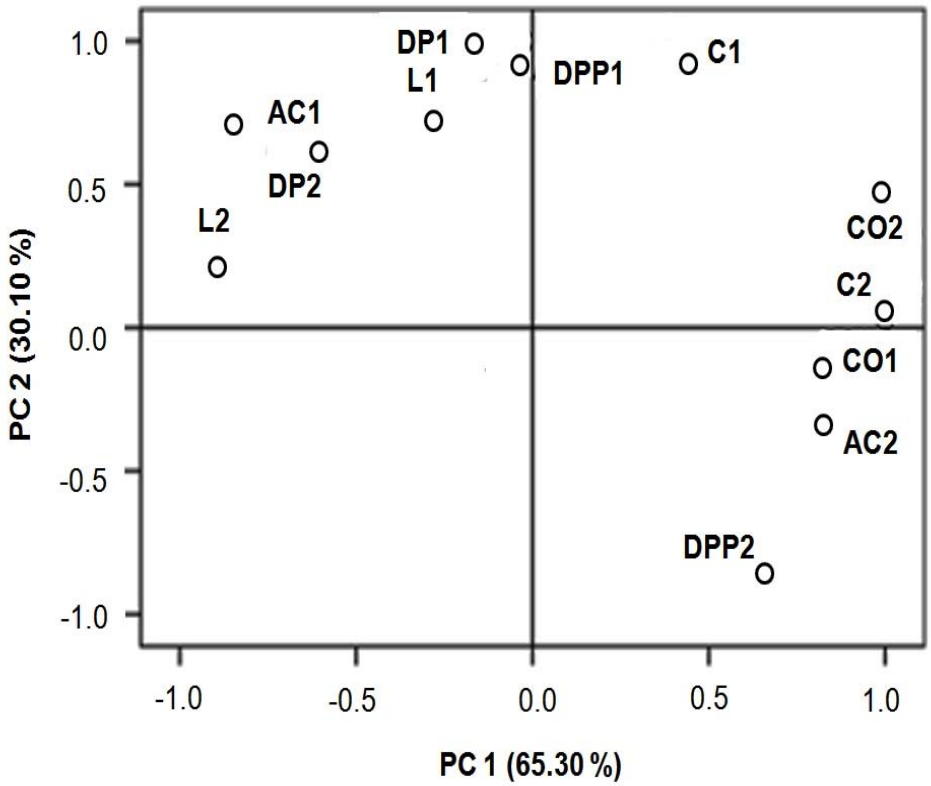

Figure 3.3. Loading plot diagram of various bioactivities

The similarity in the greater loading of DPPH, ACE, DPP-4, COX-2, 5-LOX inhibitory activities of the EtOAc-MeOH extracts derived from *G. opuntia* and *K. alvarezii* apparently demonstrated that these bioactivities were in close relation. The significant correlation of antioxidant activities with anti-diabetic, anti-inflammatory and anti-hypertensive properties of the EtOAc-MeOH extracts derived from the marine macroalgae *G. opuntia* and *K. alvarezii* also indicated that the bioactive compounds present in the extract were responsible for bioactivities.

3.4. Conclusions

The organic extracts obtained from the red macroalgae *K. alvarezii* and *G. opuntia* were found to possess a number of bioactivities against different disease targets, namely hypertension, type-2 diabetes, and inflammation. The current study revealed that the EtOAc-MeOH extract of *K. alvarezii* possessed greater anti-

oxidative activities, and exhibited significant positive correlation with the anti-inflammatory, anti-hypertensive and anti-diabetic activities. The organic extract of *K. alvarezii* possessed significantly greater antioxidative properties than those obtained from *G. opuntia*. The organic extract from *K. alvarezii* also showed greater angiotensin-I converting enzyme (ACE) inhibitory activity along with pro-inflammatory cyclooxygenase/lipoxygenase inhibitory activities than that exhibited by that acquired from *G. opuntia.* Likewise, EtOAc-MeOH crude extract obtained from *K. alvarezii* showed significant anti-diabetic activities as determined by *in vitro* α-amylase, α-glucosidase and dipeptidyl peptidase-4 inhibitory properties. The spectroscopic characterization of the solvent extracts provided the evidence regarding the occurrences of signature peaks and the prominent functional groups that were responsible for the target bioactivities. This study demonstrated the candidacy of red macroalga particularly, *K. alvarezii* as potential source of bioactive compounds for use as functional food supplements and pharmaceutical applications.

Chapter 4

ISOLATION AND CHARACTERIZATION OF SECONDARY METABOLITES FROM *KAPPAPHYCUS ALVAREZII AND GRACILARIA OPUNTIA*

Contents

4.1. Background

Traditionally, marine macroalgae have been considered as valuable marine flora, which are preferred delicacies in the South-east Asian countries, particularly Japan, China, Korea and Indonesia due to their potential antioxidant and therapeutic properties (Wang et al. 2009). Species of the red marine macroalgae were proven to be rich sources of structurally unique and biologically active secondary metabolites for applications in functional food and pharmaceuticals (Kladi et al. 2004). Antioxidative compounds obtained from these species were identified as phylopheophylin (Cahyana et al. 1992), phlorotannins (Yan et al. 1996), terpenoids (Chakraborty and Paulraj 2010) and fucoxanthin (Yan et al. 1999). The bioactive compounds extracted from marine macroalgae were used as safer anti-inflammatory therapeutics as well. The vast majority of the red marine macroalgae derived bioactive compounds were diterpenes (Rochfort and Capon 1996), sesquiterpenes (Amico et al. 1991) and C_{15} non-terpenoids containing ether rings of different sizes including halogenated cyclic ether enynes and related allenes (Erickson 1983; Iliopoulou et al. 2002). The red marine macroalgae were reported for their antioxidant potential and *in vitro* anti-proliferative activities in cancer cell lines (Chakraborty et al. 2015). *Kappaphycus alvarezii* (Silva et al. 1996) is economically significant and predominantly farmed red marine macroalga in the shallow tropical marine habitats around the South-east Asian countries, particularly Philippines, Taiwan, Malaysia, Indonesia and India (Ask and Azanza 2002; Chandrasekaran et al. 2008). Despite the fact that red marine macroalgae, particularly *Laurencia* species, have been studied extensively with respect to secondary metabolite chemistry (Amico et al. 1991; Rochfort and Capon 1996; Manta 2001; Iliopoulou et al. 2002), studies on members of the genus *K. alvarezii* and *G. opuntia* have been rare for the isolation of novel intriguing structures.

The marine macroalgae *K. alvarezii* and *G. opuntia* are abundantly available throughout the subtropical and tropical climatic zones from the south-east coast of Gulf of Mannar of India (Guiry and Guiry 2016). Despite the fact that red marine macroalgae have been extensively studied to isolate various classes of bioactive compounds (Iliopoulou et al. 2002), no natural products have been reported from the aforesaid red marine macroalgae, suggesting *K. alvarezii* and *G. opuntia* would be an attractive source for chemical investigation. The methanol-ethyl acetate extract

(MeOH: EtOAc 1:1 v/v) fraction of the thalli of *K. alvarezii* and *G. opuntia* was fractionated by repeated column chromatography to afford a number of previously undescribed compounds. The structures of these compounds were established by exhaustive spectroscopic experiments, including mass and two-dimensional nuclear magnetic resonance. The antioxidative and anti-inflammatory activities of the newly reported compounds were evaluated by different *in vitro* assays. Structure-bioactivity correlation analysis of the studied compounds was carried out using different electronic and hydrophobic molecular descriptor variables.

4.2. Materials and Methods

4.2.1. Chemicals and Reagents

All chemicals were of analytical, spectroscopic or chromatographic reagent grade, and were obtained from E-Merck (Darmstadt, Germany) and Sigma-Aldrich (St. Luois, MO, USA). All reagents and chemical solvents were of analytical grade or higher.

4.2.2. Isolation and Purification of Secondary Metabolites

4.2.2.1. Sample Preparation

This section described the preparation of crude extract of *K. alvarezii* and *G. opuntia* for the chromatographic purification and the isolation of bioactive compounds. Briefly, the marine macroalgae *K. alvarezii* and *G. opuntia* were freshly collected from Gulf of Mannar located between 8º48′ N, 78º9′ E and 9º14′ N, 79º14′ E on the south east coast of India. The samples were washed in running water for 10 min, transported to the laboratory before being shade dried (35±3 °C) for 24 h and powdered. The shade-dried material (1 kg dry wt) was ground and extracted with ethyl acetate: methanol (EtOAc: MeOH 1:1, v/v, 60–70 °C, 3 h) before being dried over sodium sulfate and concentrated by vacuum evaporation at 50 °C (Heidolph Instruments GmbH and Co., Schwabach, Germany) to yield a dark green extract (55 g and 40 g respectively). This crude extract was subjected to various chromatographic purification techniques.

4.2.2.2. Chromatographic Purification and Spectral Analysis of Purified Compounds from *K. alvarezii*

The EtOAc: MeOH fraction (55 g) of *K. alvarezii* was fractionated by vacuum liquid chromatography (VCC) (60-120 mesh) using 100 % *n*-hexane, with increasing polarity using EtOAc and MeOH to obtain a total of three column fractions, such as KA_1 through KA_3. The bioactivities of the fractions were checked, and based on the results; these three fractions were further purified.

The fraction KA_2 was obtained by eluting with 15 % EtOAc/MeOH. The column eluent concentration was gradually raised (EtOAc: *n*-hexane 1:99 to 70:30 v/v) to obtain 30 fractions (with each 35 mL), which were combined to 13 fractions ($KA_{2\text{-}1}$-$KA_{2\text{-}13}$) after TLC analysis (EtOAc: *n*-hexane 1:9 v/v). The first fraction ($KA_{2\text{-}1}$, 600 mg) was flash chromatographed (Biotage AB SP1-B1A; Biotage, Sweden) employing a step-gradient (0-5 % EtOAc) to acquire 170 fractions (each 12 mL) that were reduced to seven groups on the basis of analytical TLC (*n*-hexane/EtOAc 3:2 v/v) ($KA_{2\text{-}1\text{-}1}$-$KA_{2\text{-}1\text{-}7}$). The fraction $KA_{2\text{-}1\text{-}1}$, on subsequent purification using preparative HPLC (60:40 MeOH/ H_2O; flow rate: 10 mL/min), yielded 2-butyl-7-4-(chloromethyl) cyclooct-1-enyl) hept-5-en-1-ol (compound **K1**) and 4-(2-chloroethyl)-5-7-(methoxymethyl) undec-3-enyl) cyclooct-4-enone (compound **K2**) as homogenous compounds.

The fraction KA_3 was column fractionated with *n*-hexane and the solvent polarity was gradually increased with the gradual addition of solvent EtOAc (3:7 v/v *n*-hexane: EtOAc) to obtain a total of thirty fractions (20 mL) that were minimized to five homogeneous groups ($KA_{3\text{-}1}$- $KA_{3\text{-}5}$), whereas $KA_{3\text{-}2}$ (320.3 mg) was fractionated with *n*-hexane: EtOAc (4:1, v/v) to yield 1-(3-methoxypropyl)-2-propylcyclohexane (compound **K3**). The fraction $KA_{3\text{-}3}$ was flash chromatographed (Biotage SP1-B1A, Sweden) on a silica gel column (loaded with 230–400 mesh) by employing a step gradient of EtOAc/*n*-hexane (0–10 % EtOAc) to yield a total of ninety fractions (10 mL). Following thin layer chromatography (TLC) analyses, the identical fractions were pooled to obtain five fractions (50 mL, $KA_{3\text{-}3\text{-}1}$- $KA_{3\text{-}3\text{-}5}$). The fraction $KA_{3\text{-}3\text{-}2}$ was flash chromatographed on a column (230–400 meshed silica gel) with EtOAc/*n*-hexane (1:9 to 3:7, v/v) to yield 3-(methoxymethyl) heptyl-3-(cyclohex-3-enyl) propanoate (compound **K4**). The fraction $KA_{3\text{-}3\text{-}4}$ was fractionated with silica gel flash chromatography with EtOAc/*n*-hexane (1:1, v/v), and thereafter with MeOH/ DCM

(1:9, v/v) to yield fifty fractions (10 mL). Following TLC analyses, the identical fractions were pooled to yield $KA_{3\text{-}3\text{-}4\text{-}1}$ through $KA_{3\text{-}3\text{-}4\text{-}11}$. The fraction $KA_{3\text{-}3\text{-}4\text{-}1}$ was further purified by preparatory silica gel TLC, whereas the plate was eluted with DCM/MeOH (9:1, v/v) to afford 2-ethyl-6-(4-methoxy-2-((2-oxotetrahydro-2*H*-pyran-4-yl) methyl) butoxy)-6-oxohexyl-5-ethyloct-4-enoate (compound **K5)**.

The fraction KA_1 was slurried in silica gel (60–120 mesh) and loaded into a glass column (90 cm × 4 cm) before being subjected to VCC on silica gel (60–120 mesh, 50 g), using *n*-hexane with increasing amounts (*n*-hexane: EtOAc 99:1 to 3:7, v/v) of EtOAc as mobile phase, and finally with MeOH to furnish 30 fractions of 35 mL each, which were reduced to 12 groups ($KA_{1\text{-}1}$-$KA_{1\text{-}12}$) after TLC analysis (*n*-hexane: EtOAc, 9:1 v/v). The fraction $KA_{1\text{-}1}$ (600 mg) obtained by eluting with *n*-hexane: EtOAc (4:1 v/v) was found to be a mixture, which was flash chromatographed (Biotage AB SP1-B1A, 230–400 mesh, 12 g; Biotage AB, Uppsala, Sweden) on a silica gel column (Biotage, 230–400 mesh, 12 g; Sweden, Biotage No. 25 + M 0489-1) at a collection UV wavelength at 236 nm using a step gradient of EtOAc/*n*-hexane (0–5 % EtOAc) to afford 170 fractions (12 mL each). Based on analytical TLC, the fractions with similar patterns were pooled together to afford nine pooled fractions (80 mL, $KA_{1\text{-}1\text{-}1}$– $KA_{1\text{-}1\text{-}9}$). The fraction $KA_{1\text{-}1\text{-}2}$ (5 % EtOAc in *n*-hexane), which was found to be a mixture, was subjected to normal-phase flash chromatography using as mobile phase EtOAc/*n*-hexane (0–70 % EtOAc) followed by MeOH/CH_2Cl_2 (10 % MeOH) to afford 70 fractions (15 mL each). Based on analytical TLC, the fractions with similar patterns were pooled together to afford 10 pooled fractions ($KA_{1\text{-}1\text{-}2\text{-}1}$ – $KA_{1\text{-}1\text{-}2\text{-}10}$). The fraction, $KA_{1\text{-}1\text{-}2\text{-}3}$ was subjected to preparatory TLC on silica gel GF_{254}, using as mobile phase $CHCl_3$/MeOH (9:1, v/v) to yield pure compound as (3, 4, 5, 6)-3-(hexan-2'-yl)-3, 4, 5, 8-tetrahydro-4-methyl-2*H*-oxocin-5-yl acetate (compound **K6**) as the major component (Fig. 4.1).

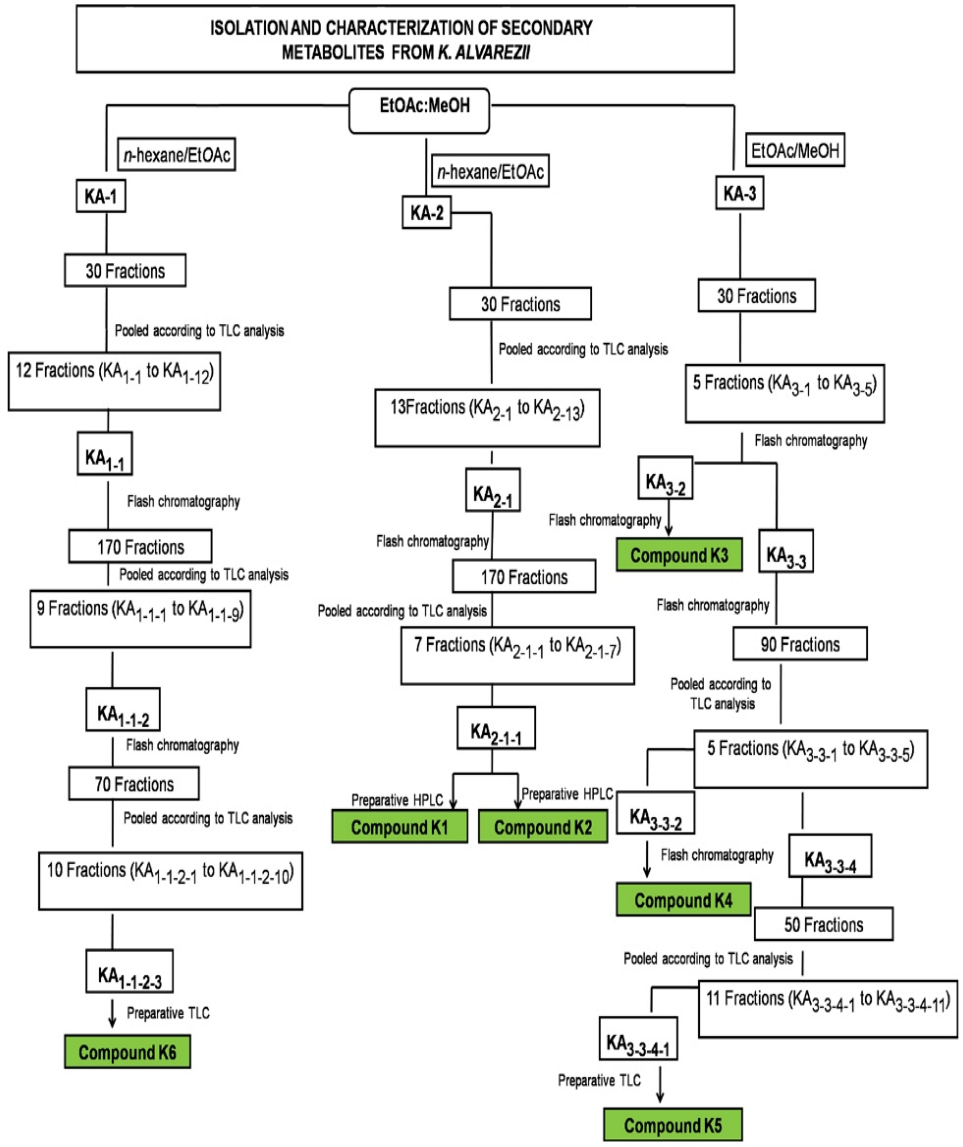

Figure 4.1. Schematic diagram representing the chromatographic purification of the EtOAc: MeOH (1:1) fraction of *K. alvarezii* (green highlights implied pure compounds with higher activity)

4.2.2.3. Chromatographic Purification and Spectral Analysis of Purified Compounds from *G. opuntia*

The EtOAc: MeOH (1:1) fraction (40 g) of *G. opuntia* was fractionated by vacuum liquid chromatography (60-120 mesh) and eluted using 100 % *n*-hexane with increasing polarity using EtOAc and MeOH to obtain a total of three column fractions, such as GO_1 through GO_3. The bioactivities of the column fractions were checked before being purified.

The fraction GO_1 was fractionated through vacuum liquid chromatography using silica gel as an adsorbent (8 g, 60–120 mesh size) on a column (90 × 4 cm), using *n*-hexane to ethyl acetate gradient solvent system (EtOAc: *n*-hexane, 1:99 to 7:3, v/v), and finally with MeOH to yield $GO_{1\text{-}1}$-$GO_{1\text{-}12}$ as twelve pooled fractions on the basis of TLC analysis (EtOAc: *n*-hexane 1:4, v/v). The fraction $GO_{1\text{-}2}$ (500 mg) was recovered by eluting with EtOAc: *n*-hexane (1:2, v/v), and was further fractionated by flash chromatography (Biotage SP1, 230–400 mesh, 12 g) on a Biotage No. 25+M 0489-1 column (silica gel 230–400 mesh, Biotage, Sweden) with a collection wavelength (UV) at 236 nm, and with the solvent gradient of CH_2Cl_2-MeOH (0–100 % MeOH) to furnish 145 fractions (15 mL). Similar fractions were mixed together to afford nine pooled fractions ($GO_{1\text{-}2\text{-}1}$-$GO_{1\text{-}2\text{-}9}$) after TLC analysis (10 % EtOAc in *n*-hexane). The fraction $GO_{1\text{-}2\text{-}4}$ was found to be a mixture, and was further purified with normal phase flash chromatography by using EtOAc/*n*-hexane (0–70 % EtOAc) as mobile phase, followed by MeOH/ EtOAc (15 % MeOH) to yield $GO_{1\text{-}2\text{-}4\text{-}1}$-$GO_{1\text{-}2\text{-}4\text{-}10}$ as ten pooled fractions based on TLC analysis (EtOAc: *n*-hexane 1:9, v/v). The sub-fraction $GO_{1\text{-}2\text{-}4\text{-}2}$ (145 mg), was a mixture of compounds, and therefore, was fractionated with preparatory thin layer chromatography (silica gel GF_{254}) using a step-wise gradient system of EtOAc/MeOH (9:1, v/v) to afford 5-(7-(5-ethyl-3, 4-dimethoxycyclooctyl) benzofuran-6-yl)-7-methyl-3, 4, 7, 8-tetrahydro-2*H*-oxocin-2-one as a homogenous compound (compound **G1**). The fraction, $GO_{1\text{-}2\text{-}4\text{-}8}$ was further purified by preparatory TLC on silica gel GF_{254} by using MeOH/EtOAc (3:7, v/v) as mobile phase to yield 2-(3-ethyl-9-(2-methoxyethoxy)-1-oxo-2, 3, 4, 9-tetrahydro-1*H*-xanthen-2-yl) ethyl-5-hydroxy-9-methoxy-7, 8-dimethyl-8-(5-methylfuran-2-yl) nona-3, 6-dienoate (compound **G2**) as the major component.

The fraction 2 (GO_2, 200 mg) was acquired by eluting with EtOAc: *n*-hexane (1:4, v/v) was found to be a mixture that was subjected to further purification with flash

chromatography (Biotage AB, Biotage AB SP1-B1A Uppsala, Sweden) on a silica gel column (Biotage, 230–400 mesh, 12 g; Sweden, 25 + M0489–1) at a collection UV wavelength at 236 nm using a step gradient of EtOAc/*n*-hexane (0–50 % EtOAc) to afford 160 fractions (9 mL each). On the basis of analytical TLC, the fractions with identical patterns were pooled together to yield five pooled fractions (GO_{2-1} through GO_{2-5}). The fraction GO_{2-3} was fractionated using preparatory TLC on silica gel GF_{254} using methanol: ethyl acetate (1:4, v/v) to afford 3-(2-ethyl-6-((3, 7)-1, 2, 5, 6-tetrahydroazocin-5-yl) hexyl) morpholin-6-one (compound **G3**) as the major component.

The fraction 3 (GO_3) acquired by eluting with EtOAc: *n*-hexane (1:4, v/v) was found to be a mixture. The latter was subjected to column chromatography on silica gel (6 g, 60–120 mesh) with a solvent gradient from *n*-hexane to EtOAc followed by EtOAc to MeOH. A total of 20 fractions (25 mL each) were further fractionated with 50 % EtOAc in *n*-hexane on a silica gel flash chromatograph (Biotage AB SP1-B1A, 230–400 mesh, 12 g; Biotage AB, Uppsala, Sweden) at a collection UV wavelength of 236 nm using a step gradient of MeOH/ EtOAc (0–5 % EtOAc) to afford 150 fractions (10 mL each). Based on analytical TLC, the fractions with similar patterns were pooled together to afford five pooled fractions (GO_{3-1}- GO_{3-5}, 60 mL each). The fraction GO_{3-5} eluted with 5 % EtOAc in *n*-hexane, was found to be a mixture, and therefore, was further subjected to normal-phase silica gel flash chromatography using 0–30 % EtOAc followed by 10 % MeOH in EtOAc to yield 40 fractions (15 mL each). Based on analytical TLC, the fractions with similar patterns were pooled together to afford five pooled fractions (GO_{3-5-1} through GO_{3-5-5}). The fraction GO_{3-5-3}, was subjected to preparatory TLC on silica gel GF_{254}, using as mobile phase MeOH/ EtOAc (1:1, v/v) to yield 2-acetoxy-2-(5-acetoxy-4-methyl-2-oxotetrahydro-2*H*-pyran-4-yl) ethyl-4-(3-methoxy-2-(methoxymethyl)-7-methyl-3, 4, 4a, 7, 8, 8a-hexahydro-2*H*-chromen-4-yloxy)-5-methylheptanoate (compound **G4**) as the major component (Fig. 4.2).

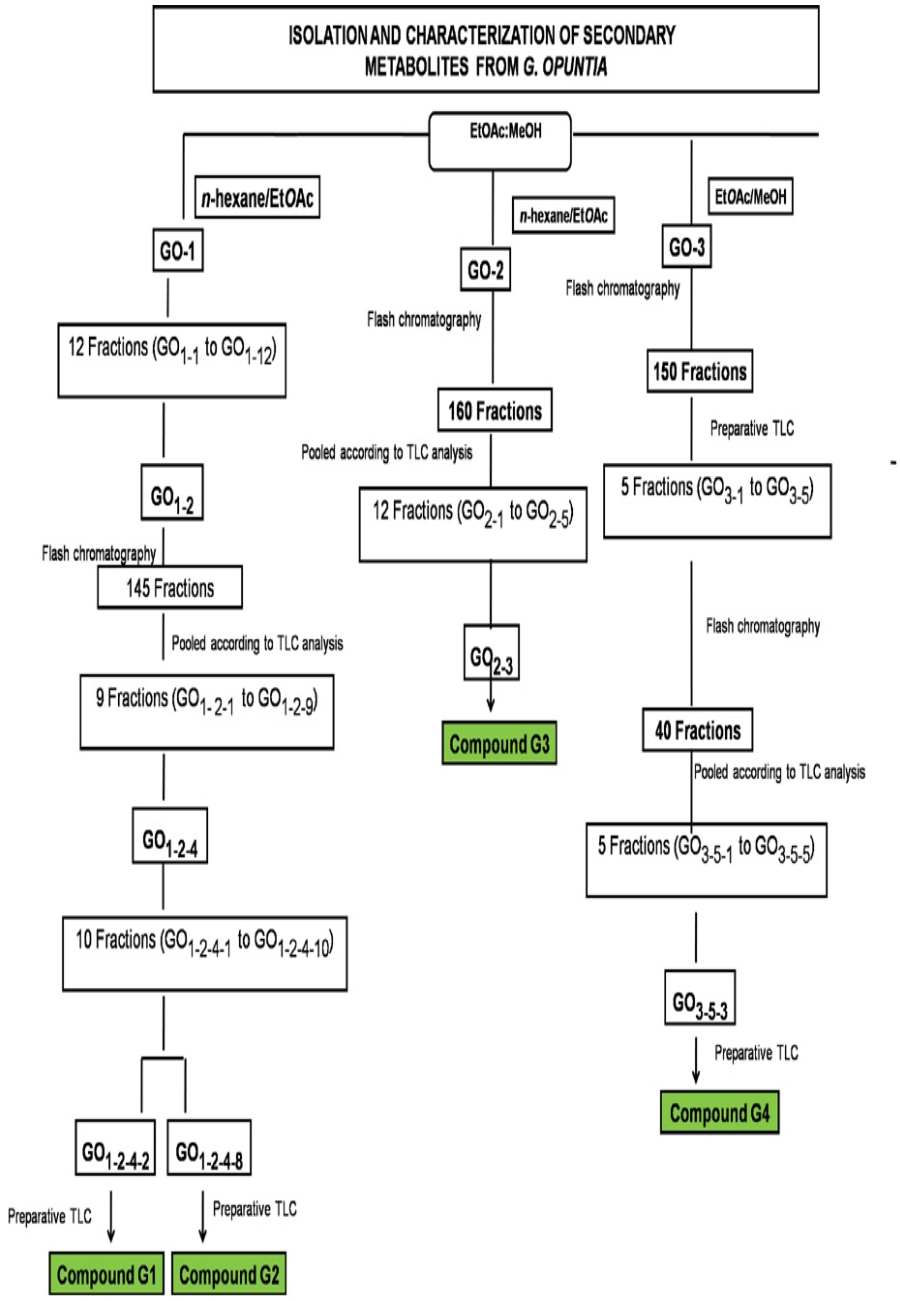

Figure 4.2. Schematic diagram representing the chromatographic purification of the EtOAc: MeOH (1:1) fraction of *G. opuntia* (green highlights implied the pure compounds with higher activity)

4.2.3. Instrumentation

FTIR spectra of the compounds under KBr pellets were recorded in a Thermo Nicolet Avatar 370 in the IR range between 4000 and 400 cm^{-1}. UV spectra were obtained on a Varian Cary 50 ultraviolet visible (UV–VIS) spectrometer (Varian Cary, USA). The gas chromatography–mass spectrometry (GC-MS) analyses were performed in electronic impact (EI) ionization mode in a PerkinElmer Clarus 680. GC-MS fitted with an Elite 5 MS non-polar, bonded phase capillary column (50 m × 0.22 mm i.d. × 0.25 μm film thicknesses). Helium (He) was used as the carrier gas, and the flow rate used was 1 mL min^{-1}. The temperature was programmed initially at 50 ° C for 2 min, then increased at a rate of 10 ° C min^{-1} to 180 °C and kept for 2 min and raised at 4° C min^{-1} to 280 °C and held for 15 min. Thin layer chromatographic analysis was carried out using silica gel GF_{254} plates and visualized with a documentation system operating at 254 and 366 nm wavelength regions. ESI-MS spectra were acquired on a liquid chromatography–mass spectrometry system (Applied Biosystems QTrap 2000, Applied Biosystems, Darmstadt, Germany). A table-top high speed refrigerated centrifuge (Sorvall, Biofuge Stratos, Thermo Scientific, Germany) was used for centrifugation. Flash chromatography was carried out with a Biotage instrument (AB SP1-B1A, Biotage AB, Uppsala, Sweden). High pressure liquid chromatographic analysis was carried out using high performance liquid chromatograph (Shimadzu SCL-10A vp, Shimadzu Co., Kyoto, Japan) equipped with a vacuum degasser, a binary pump (LC–20AD), a thermostated column compartment (CTO–20A) and a diode array detector (SPD–M20A), connected to an LC solution software. Chromatographic separation was carried out at 30 °C on a reverse phase Luna C_{18} (250 mm x 4.6 mm, 5 μm) phenomenex column. The ultra sonicator (Labline) was used for sonicating and a laboratory shaker (Shaker, Labline) was used for shaking. A rotary vacuum evaporator (Heidolf, Germany) was used for evaporation of solvents. ^{1}H and ^{13}C NMR spectra were recorded on a Bruker AVANCE III 500 MHz (AV 500) spectrometer (Bruker, Germany) in $CDCl_3$ as aprotic solvent at ambient temperature with TMS as the internal standard (δ 0 ppm). Two-dimensional ^{1}H-^{1}H COSY, DEPT, HSQC, HMBC and NOESY experiments were carried out using standard pulse sequences. The NMR data were acquired by using the BrukerTopSpin™ 2 software, and processed by MestReNova-7.1.1-9649 (Mestrelab Research S.L.). All the reagents and solvents used in this study were of analytical grade and purchased from E-Merck.

4.2.4. Pharmacological Activities of Secondary Metabolites Isolated from *K. alvarezii* and *G. opuntia*

The pharmacological activities of the compounds were determined based on the *in vitro* assays performed as explained in the previous chapter (Chapter 3). The *in vitro* antioxidant activities were determined by ABTS, DPPH radical scavenging assays along with ferrous ion chelating assay (Sivasothy et al. 2012; Chakraborty et al. 2014). The anti-inflammatory properties were evaluated by COX-1 and COX-2 inhibition assays (Larsen et al. 1996) and 5-LOX inhibition assay (Baylac and Racine 2003). *In vitro* anti-diabetic studies were carried out by inhibition of dipeptidyl peptidase-4, α-amylase (Kojima et al. 1980; Hamdan and Afifi 2004) and α-glucosidase (Dong et al. 2012) inhibition assays. The anti-hypertensive activities were determined by ACE-I inhibitory assay (Udenigwe et al. 2009).

Structure-biactivity relationship analyses have been conducted by different structural descriptors, such as electronic (polarizability α/topological polar surface area tPSA), hydrophobic–hydrophilic balance {logarithm (octanol/water partition coefficient) or log Pow), steric {parachor (Pr)/molar volume (Vm)/molar refractivity (MR)} (Chakraborty et al. 2016a, b; Joy and Chakraborty 2017a, b; Lipinski and Hopkins 2004) using ACD ChemSketch (Advanced Chemistry Development, Inc., Canada; ver. 12.0) and ChemDraw® Ultra (Cambridge Soft Corporation, Cambridge, MA, USA; ver. 8.0) softwares.

4.2.5. Statistical Analysis

One-way analysis of variance was carried out with the Statistical Program for Social Sciences 13.0 (SPSS, Inc., Chicago, USA, ver. 13.0) to assess for any significant differences between the means. The analyses were performed in triplicates, and the means of all variables were analyzed for significance by using analysis of variance. Differences between means at the 5 % ($P < 0.05$) level were considered significant.

4.3. Results and Discussion

4.3.1. Secondary Metabolites from *K. alvarezii*

4.3.1.1. Structural Characterization of Compound K1

2-Butyl-7-4-(chloromethyl) cyclooct-1-enyl) hept-5-en-1-ol (**K1**)

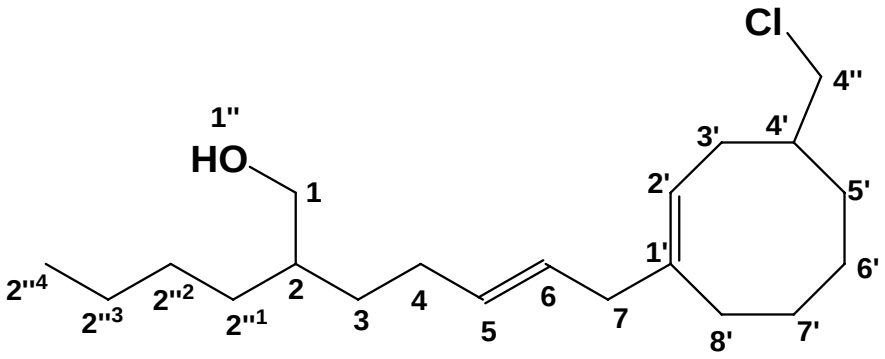

Sample yield	92 mg (0.92 %)
Physical description	White powder
Molecular formula	$C_{20}H_{35}ClO$
Molecular weight	326.2380

2-Butyl-7-4-(chloromethyl) cyclooct-1-enyl) hept-5-en-1-ol: White powder; UV (MeOH: EtOAc) λ_{max} (log ε): 285 nm (3.23); R_f: 0.62 (*n*-hexane: EtOAc 7:3, v/v); R_t (HPLC, ACN: MeOH, 2:3 v/v): 12.62 min; IR (KBr, cm^{-1}) ν_{max} (ν = stretching, δ= bending, ρ= rocking vibrations); 724.78 (CH_2 ρ), 979.37 (=C-H δ), 1252.02 (C-O ν), 1457.39 (C-H δ), 2857.37 (C-H ν), 2925.80 (C-H ν), 3430.23 (broad OH ν); ^{1}H NMR (500 MHz, $CDCl_3$) δ_H 5.39 (m, 2H), δ_H 5.37 (m, 1H), δ_H 3.74 (d, *J*=6.55 Hz, 2H), δ_H 3.67 (s, 1H), δ_H 3.61 (d, *J*=7.60 Hz, 2H), δ_H 3.27 (d, *J*=7.2 Hz, 2H), δ_H 2.81 (m, 2H), δ_H 2.35 (t, *J*=6.1 Hz, 2H), δ_H 2.13 (t, *J*=6.0 Hz, 2H), δ_H 2.05 (m, 1H), δ_H 1.72 (m, 1H), δ_H 1.63 (m, 2H), δ_H 1.30 (m, 6H), δ_H 1.25 (m, 6H), δ_H 0.88 (t, *J*=6.75 Hz, 3H); ^{13}C NMR (125 MHz, $CDCl_3$): δ_C 146.84 (C-1'), δ_C 130.51 (C-5), δ_C 128.77 (C-6), δ_C 128.58 (C-2'), δ_C 70.59 (C-1), δ_C 51.76 (C-4''), δ_C 44.88 (C-7), δ_C 38.19 (C-4'), δ_C 38.16 (C-2), δ_C

34.3 (C-3'), δ_C 34.06 (C-3), δ_C 33.63 (C-8'), δ_C 31.93 (C-5'), δ_C 31.52 (C-2"^{1}), δ_C 30.2 (C-4), δ_C 29.5 (C-2"^{2}), δ_C 29.33 (C-7'), δ_C 27.23 (C-6'), δ_C 22.58 (C-2"^{3}), δ_C 14.07 (C 2"^{4}).^{1}H-^{1}H-COSY and HMBC data (Fig. 4.3 to Fig. 4.11, Table 4.1); High-resolution electron ionization mass spectroscopy HR (EI) MS calcd for $C_{20}H_{35}ClO$ at *m/z* 326.2376, found 326.2380 $[M]^+$.

Table 4.1 NMR spectroscopic data of compound **K1** in $CDCl_3$[a]

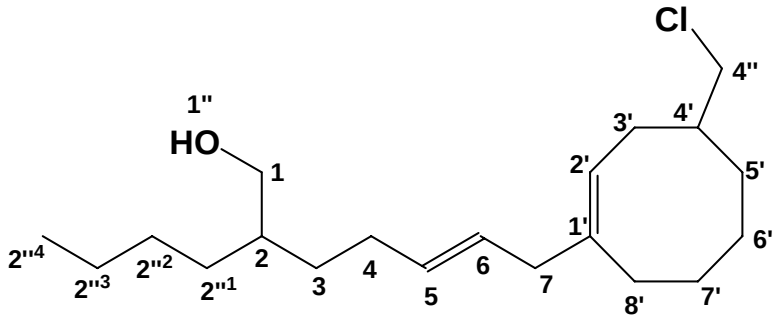

C. No	^{13}C (δ)	^{1}H-NMR[b] (int., mult., *J* in Hz)	^{1}H-^{1}H COSY	HMBC (^{1}H-^{13}C)
1	70.59	3.61 (2H, d, *J*=7.60 Hz)	-	–
1"		3.67 (1H, s)		
2	38.16	1.72 (1H, m)	-	C-2"^{1}
2"^{1}	31.52	1.25 (2H, m)		C-2"^{2}, C-2"^{3}
2"^{2}	29.5	1.25 (2H, m)		-
2"^{3}	22.58	1.30 (2H, m)		-
2"^{4}	14.07	0.88 (3H, t, *J*=6.75 Hz)		C-2"^{2}, C-2"^{3}
3	34.06	1.30 (2H, m)	-	-
4	30.2	2.81 (2H, m)	5-H	C-6
5	130.51	5.37 (1H, m)	4-H	-
6	128.77	5.39 (1H, m)	-	-
7	44.88	3.27 (2H, d, *J*=7.2 Hz)	-	C-1', C-5
1'	146.84	-	-	-
2'	128.58	5.39 (1H, m)	3'-H	-
3'	34.3	2.13 (2H, t, *J*=6.0 Hz)	2'-H	-
4'	38.19	2.05 (1H, m)	-	C-3'
4"	51.76	3.74 (2H, d, *J*=6.55 Hz)		
5'	31.93	1.30 (2H, m)	-	C-7'
6'	27.23	1.25 (2H, m)	-	-
7'	29.33	1.63 (2H, m)	8'-H	-
8'	33.63	2.35 (2H, t, *J*=6.1 Hz)	7'-H	C-7', C-6'

[a] NMR spectra recorded using Bruker AVANCE III 500 MHz (AV 500) spectrometer in $CDCl_3$ as aprotic solvent at ambient temperature with TMS as the internal standard (δ 0 ppm).

[b] Values in ppm, multiplicity and coupling constants (*J*=Hz) are indicated in parentheses. The assignments were made with the aid of the ^1H-^1H COSY, HSQC, HMBC and NOESY experiment

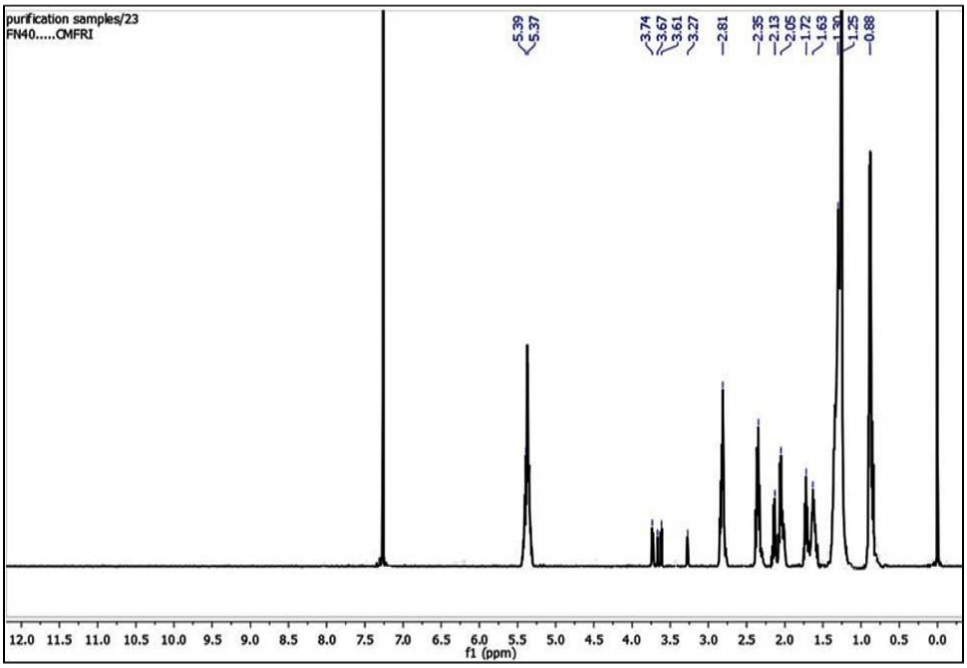

Figure 4.3. Figure showing the ^1H NMR spectrum of compound **K1**

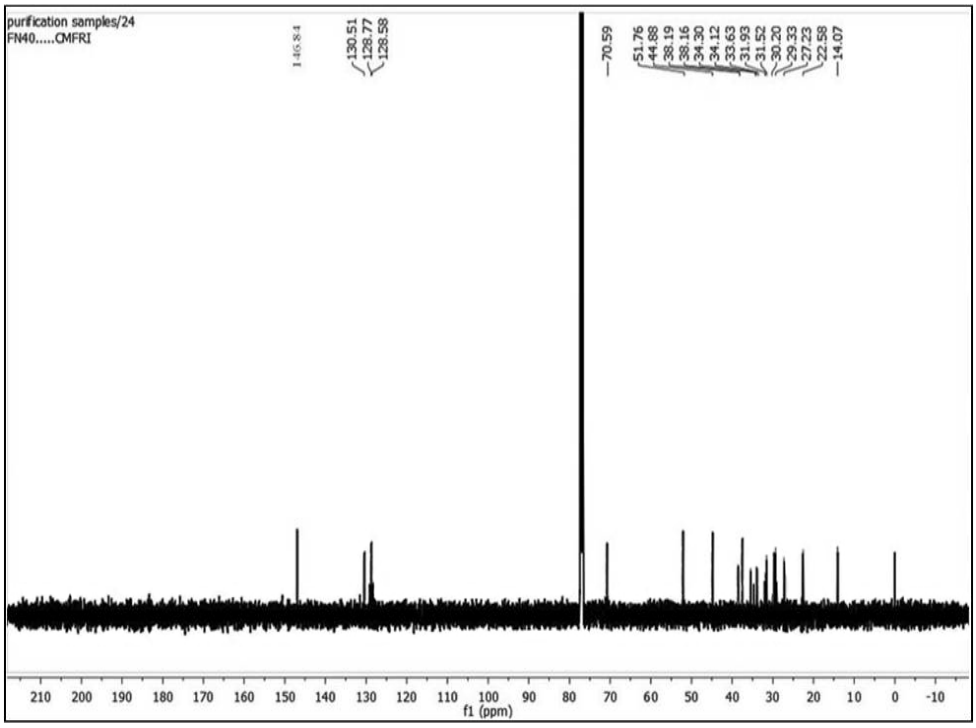

Figure 4.4. Figure showing the ^{13}C NMR spectrum of compound **K1**

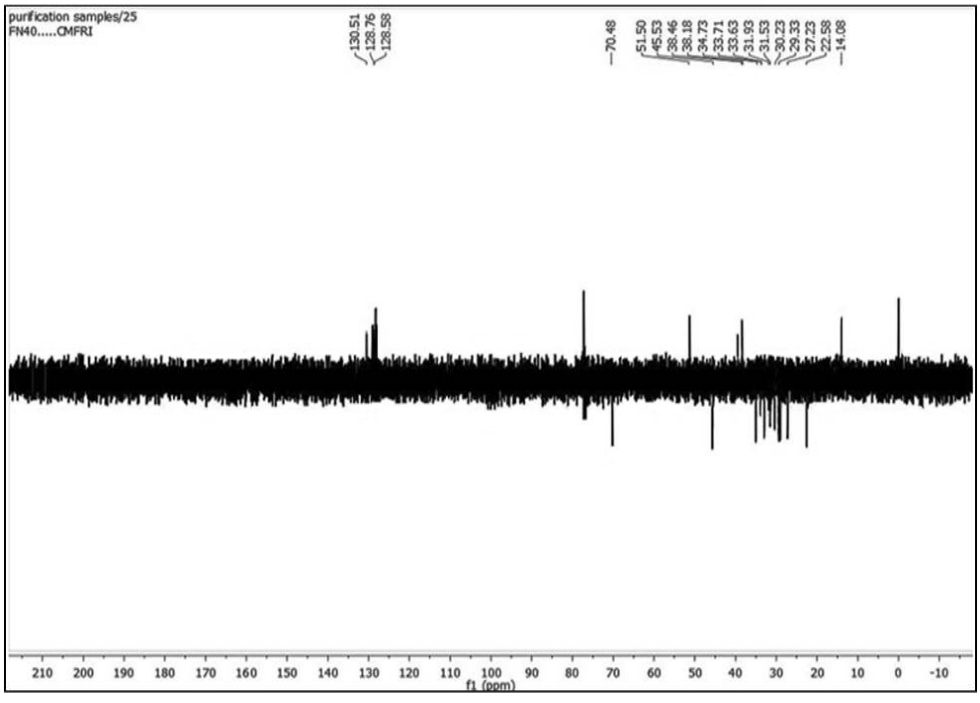

Figure 4.5. Figure showing the DEPT spectrum of compound **K1**

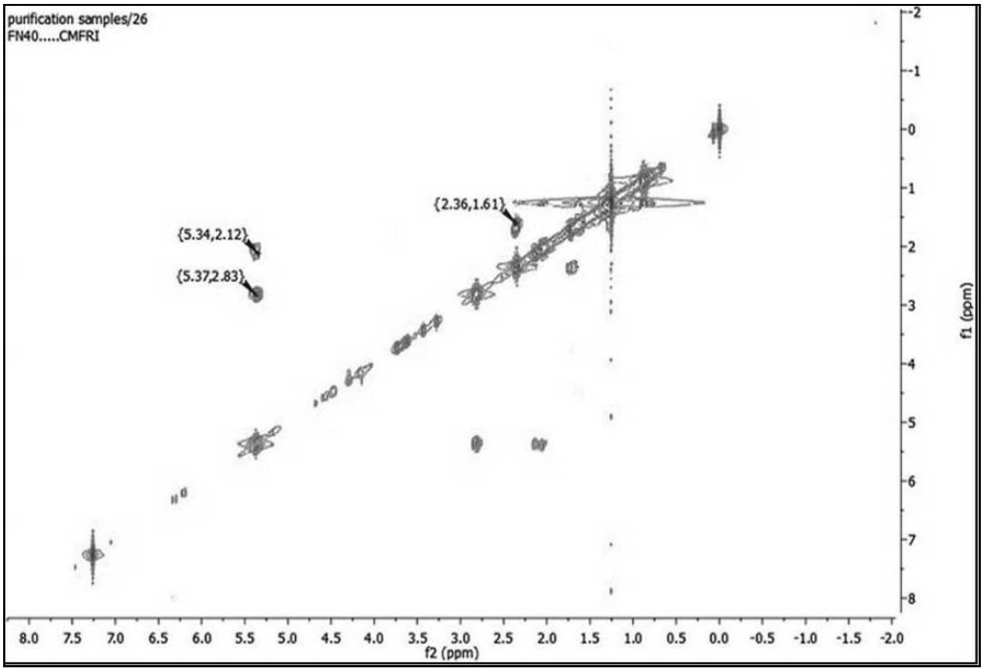

Figure 4.6. Figure showing the ^{1}H-^{1}H COSY spectrum of compound **K1**

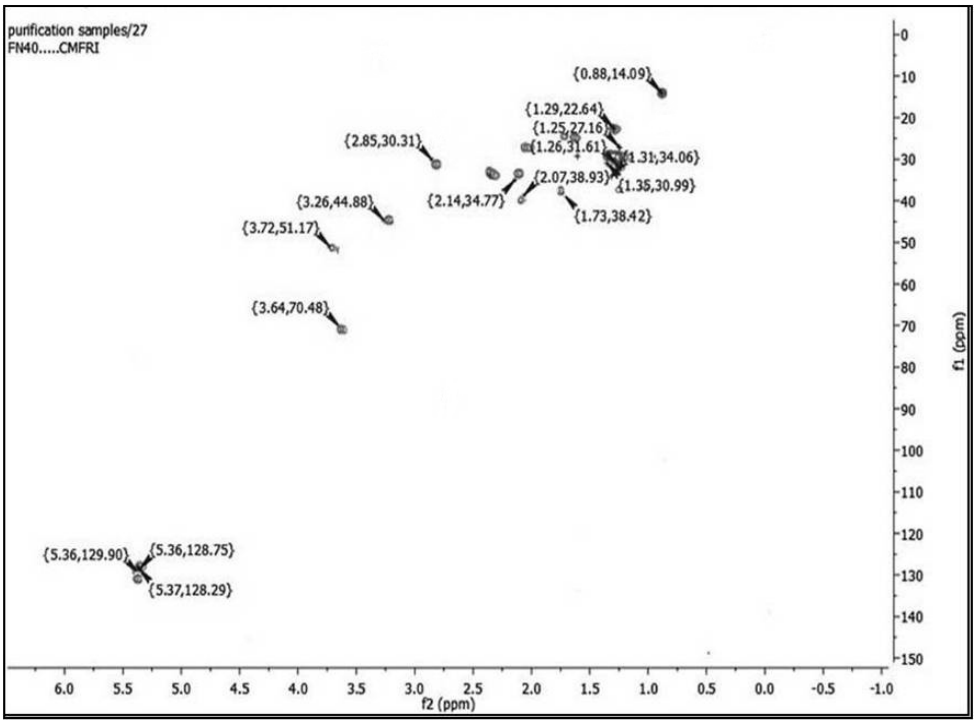

Figure 4.7. Figure showing the HSQC spectrum of compound **K1**

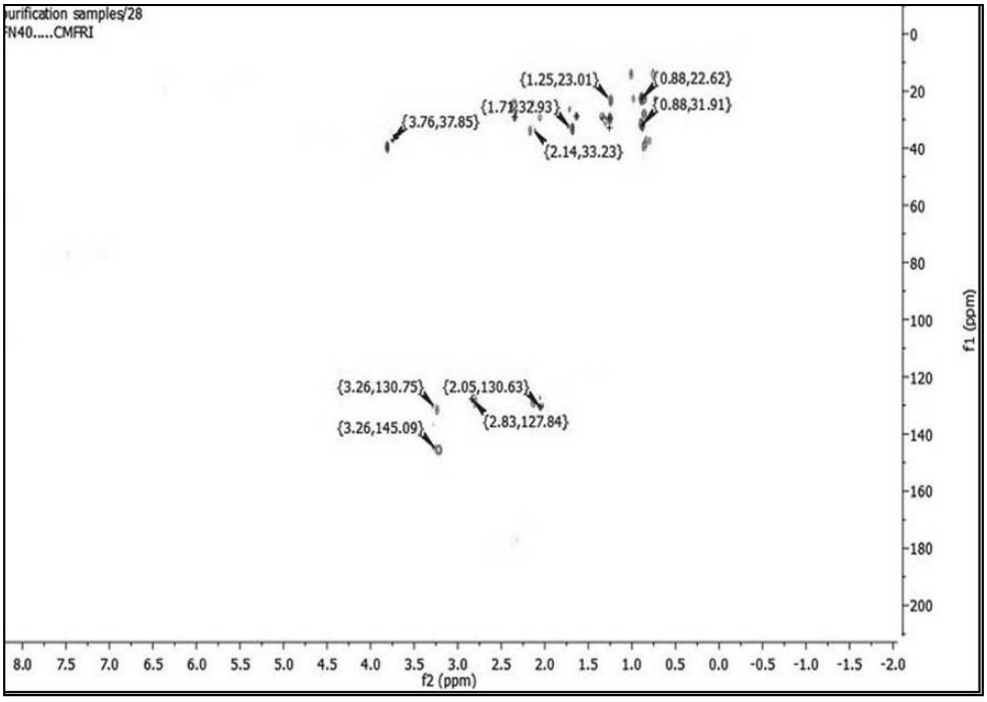

Figure 4.8. Figure showing the HMBC spectrum of compound **K1**

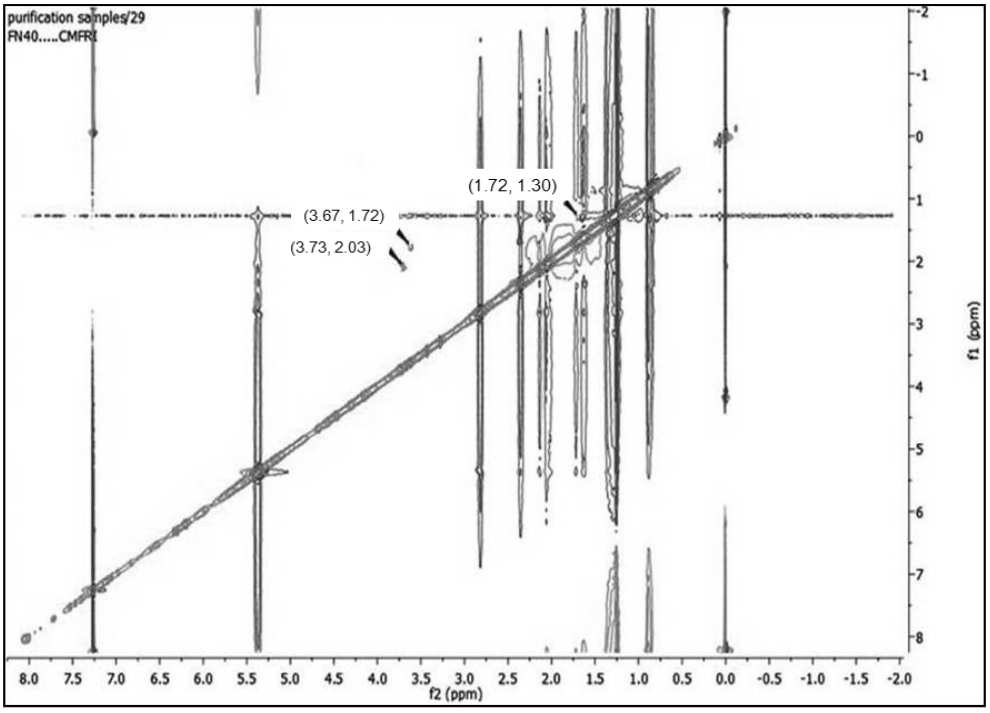

Figure 4.9. Figure showing the NOESY spectrum of compound **K1**

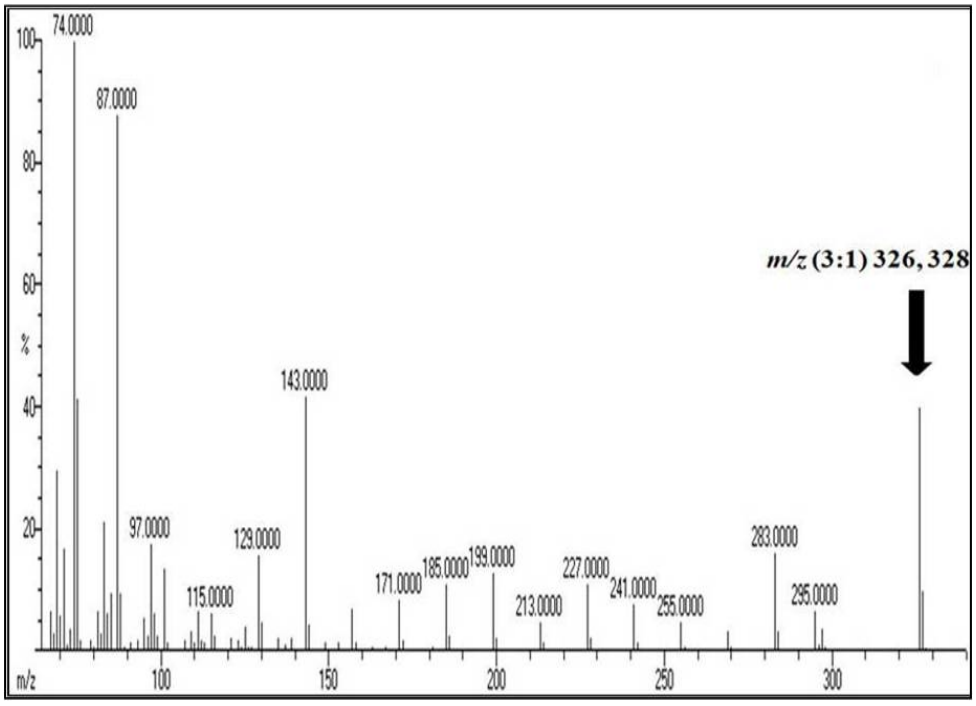

Figure 4.10. Mass spectrum of compound **K1**

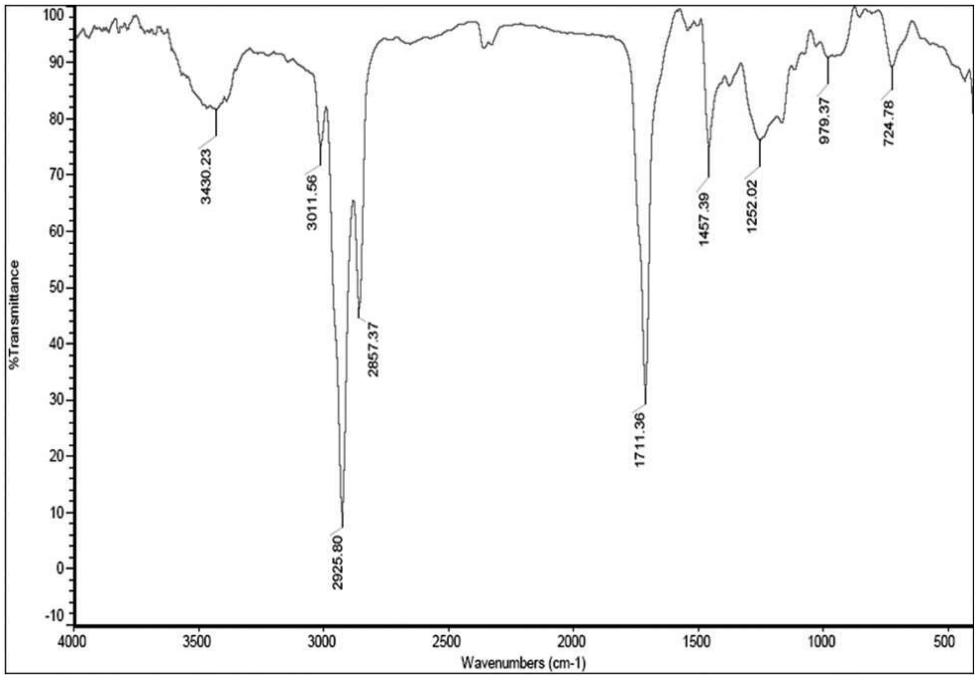

Figure 4.11. Figure showing the FTIR spectrum of compound **K1**

4.3.1.2. Structural Characterization of Compound K2

4-(2-Chloroethyl)-5-7-(methoxymethyl) undec-3-enyl) cyclooct-4-enone (**K2**)

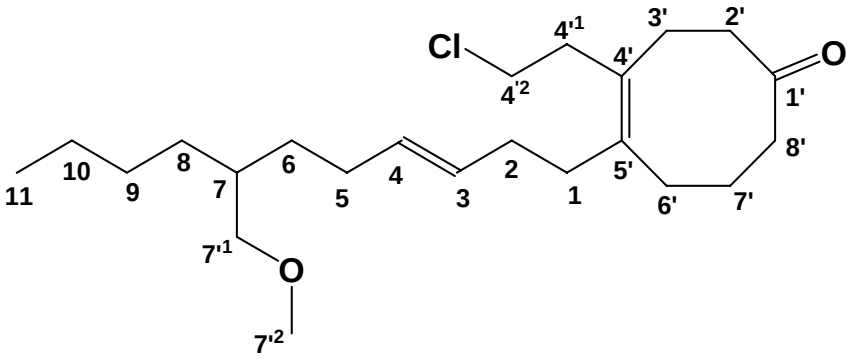

Sample yield	69 mg (0.69 %)
Physical description	Yellow oil
Molecular formula	$C_{23}H_{39}ClO_2$
Molecular weight	382.2641

4-(2-Chloroethyl)-5-7-(methoxymethyl) undec-3-enyl) cyclooct-4-enone: Yellow oil; UV (MeOH: EtOAc) λ_{max} (log ε): 290 nm (2.44); R_f: 0.57 (*n*-hexane: EtOAc 7:3, v/v); R_t (HPLC, ACN: MeOH, 2:3 v/v): 14.42 min; IR (KBr, cm^{-1}) ν_{max} (ν = stretching, δ= bending, ρ= rocking vibrations): 744.08 (C-Cl ν), 950.25 (=C-H δ), 1127.77 (CH_2 wag), 1284.33 (CH_2 ν), 1380.79 (CH_3 ν), 1457.32 (C-H δ), 1727.88 (C-CO-C ν), 2870.08 (C-H ν), 2961.87 (C-H ν), 3434.44 (broad OH ν); ^{1}H NMR (500 MHz, $CDCl_3$) δ_H 5.35 (m, 1H), δ_H 5.34 (m, 1H), δ_H 4.29 (d, *J*=7.46 Hz, 2H), δ_H 4.15 (t, *J*=7.50 Hz, 2H), δ_H 3.67 (s, 3H), δ_H 2.77 (t, *J*=6.65 Hz, 2H), δ_H 2.30 (t, *J*=6.1 Hz, 6H), δ_H 2.06 (t, *J*=6.0 Hz, 4H), δ_H 2.00 (m, 4H), δ_H 1.62 (m, 2H), δ_H 1.73 (m, 1H), δ_H 1.58 (m, 2H), δ_H 1.33 (m, 2H), δ_H 1.30 (m, 2H), δ_H 1.25 (m, 2H), δ_H 0.87 (t, *J*=6.70 Hz, 3H); ^{13}C NMR (125 MHz, $CDCl_3$): δ_C 209 (C-1'), δ_C 147.07 (C-4'), δ_C 139.28 (C-5'), δ_C 130 (C-4), δ_C 129.68 (C-3), δ_C 80.95 (C-7'^{1}), δ_C 62.11 (C-4'^{2}), δ_C 51.44 (C-7'^{2}), δ_C 41.5 (C-2'), δ_C 40.19 (C-8'), δ_C 38.86 (C-7), δ_C 34.13 (C-6), δ_C 33.83 (C-4'^{1}), δ_C 32.74 (C-2), δ_C 31.93 (C-1), δ_C 31.44 (C-5), δ_C 30.2 (C-8), δ_C 29.7 (C-6'), δ_C 29.6 (C-9), δ_C 29.37 (C-3'), δ_C 27.19 (C-7'), δ_C 22.7 (C-10), δ_C 14.11 (C-11). ^{1}H-^{1}H-COSY and HMBC data

(Fig. 4.12 to Fig. 4.20, Table 4.2); HR (EI) MS calcd for $C_{23}H_{39}ClO_2$ at *m/z* 382.2639, found 382.2641 $[M]^+$.

Table 4.2 NMR spectroscopic data of compound **K2** in $CDCl_3$[a]

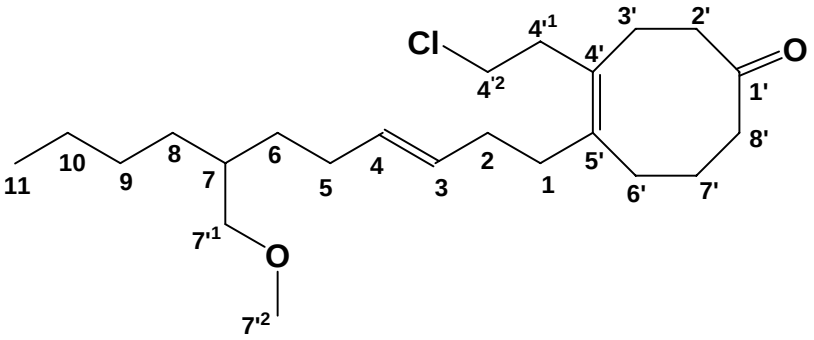

C. No	^{13}C (δ)	^1H-NMR[b] (int., mult., *J* in Hz)	^1H-^1H COSY	HMBC (^1H-^{13}C)
1	31.93	2.06 (2H, t, *J*=6.0 Hz)	-	C-2, C-5', C-6', C-4'
2	32.74	2.00 (2H, m)	-	-
3	129.68	5.34 (1H, m)	-	C-4, C-2'
4	130	5.35 (1H, m)	5-H	-
5	31.44	2.00 (2H, m)	4-H	C-4
6	34.13	1.58 (2H, m)	-	-
7	38.86	1.73 (1H, m)	-	C-6, C-5
7'[1]	80.95	4.29 (2H, d, *J*=7.46 Hz)	-	-
7'[2]	51.44	3.67 (3H, s)	-	C-7'[1]
8	30.2	1.30 (2H, m)	-	C-10, C-7
9	29.6	1.25 (2H, m)	-	C-10, C-7
10	22.7	1.33 (2H, m)	-	C-11, C-9, C-8
11	14.12	0.87 (3H, t, *J*=6.70 Hz)	-	C-10
1'	209	-	-	-
2'	41.5	2.77 (2H, t, *J*=6.65 Hz)	-	C-4'
3'	29.37	2.30 (2H, t, *J*=6.1 Hz)	-	C-2', C-4'[1]
4'	147.07	-	-	-
4'[1]	33.83	2.30 (2H, t, *J*=6.1 Hz)	-	-
4'[2]	62.11	4.15 (2H, t, *J*=7.50 Hz)		C-4'
5'	139.28	-	-	-
6'	29.7	2.06 (2H, t, *J*=6.0 Hz)	-	-
7'	27.19	1.62 (2H, m)	8'-H	C-1', C-6'
8'	40.19	2.30 (2H, t, *J*=6.1 Hz)	7'-H	C-1'

[a] NMR spectra recorded using Bruker AVANCE III 500 MHz (AV 500) spectrometer in $CDCl_3$ as aprotic solvent at ambient temperature with TMS as the internal standard (δ 0 ppm).

[b] Values in ppm, multiplicity and coupling constants (*J*=Hz) are indicated in parentheses. The assignments were made with the aid of the ^1H-^1H COSY, HSQC, HMBC and NOESY experiment

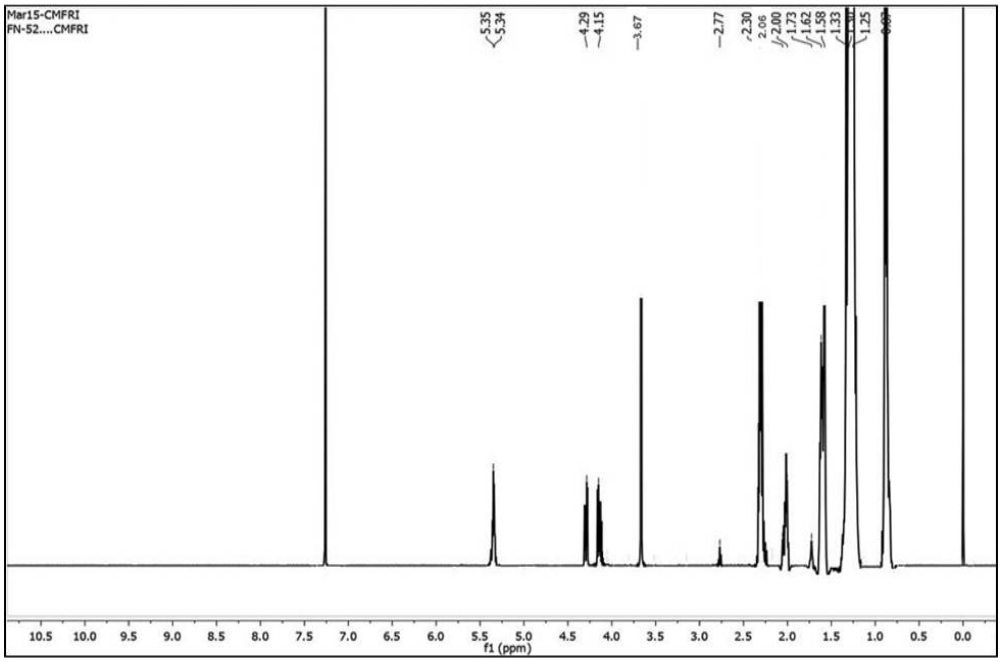

Figure 4.12. Figure showing the ^1H NMR spectrum of compound **K2**

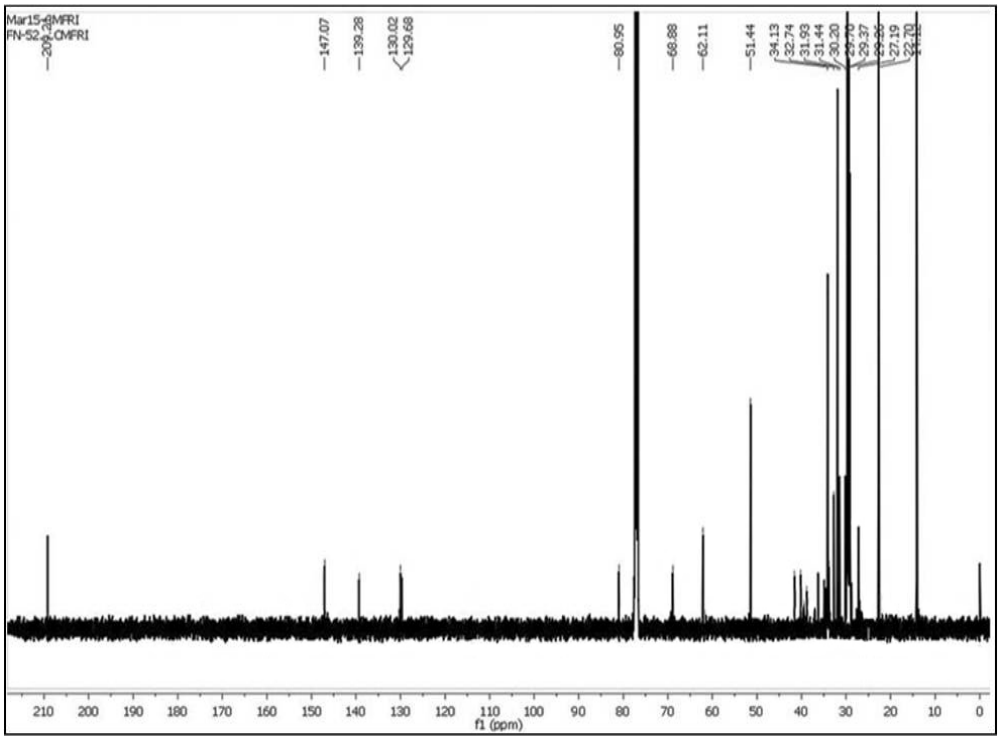

Figure 4.13. Figure showing the ^{13}C NMR spectrum of compound **K2**

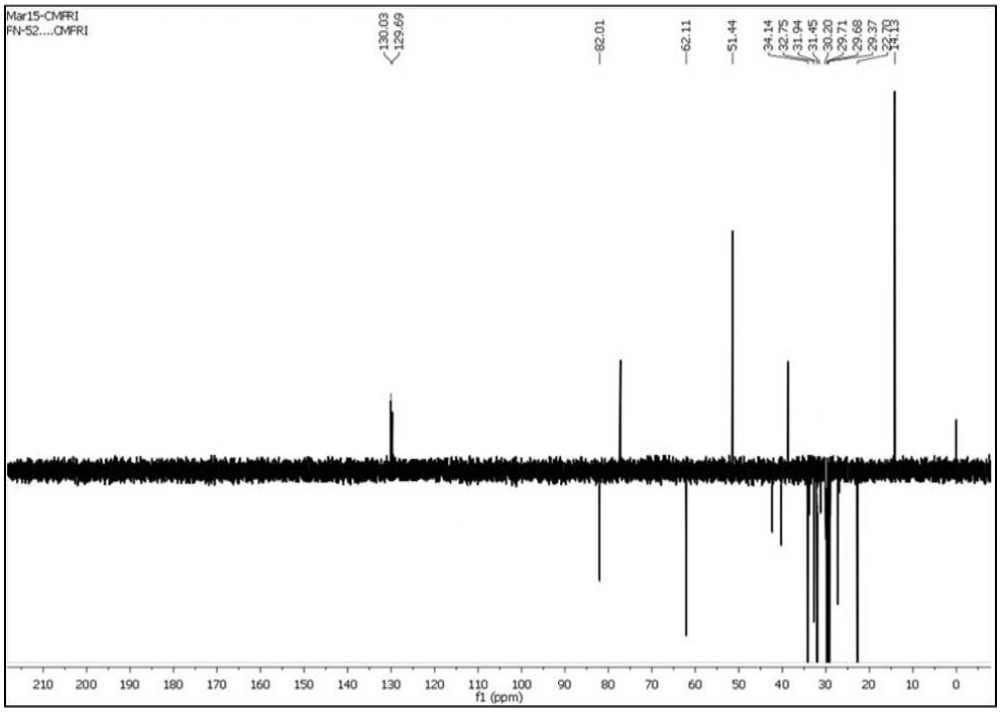

Figure 4.14. Figure showing the DEPT spectrum of compound **K2**

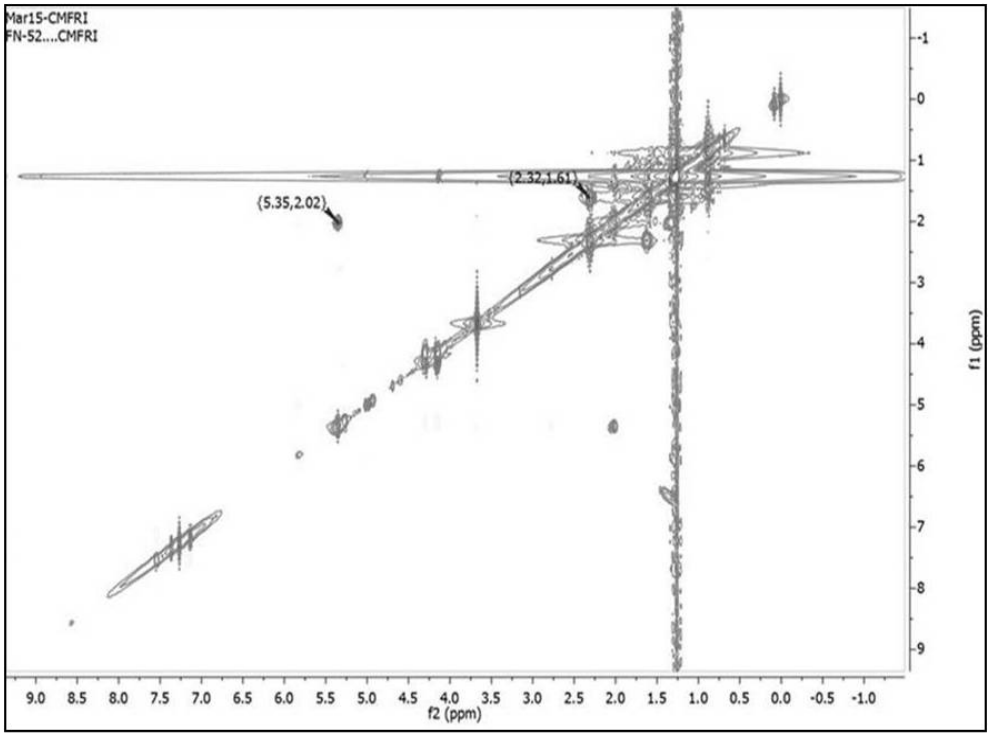

Figure 4.15. Figure showing the ^{1}H-^{1}H COSY spectrum of compound **K2**

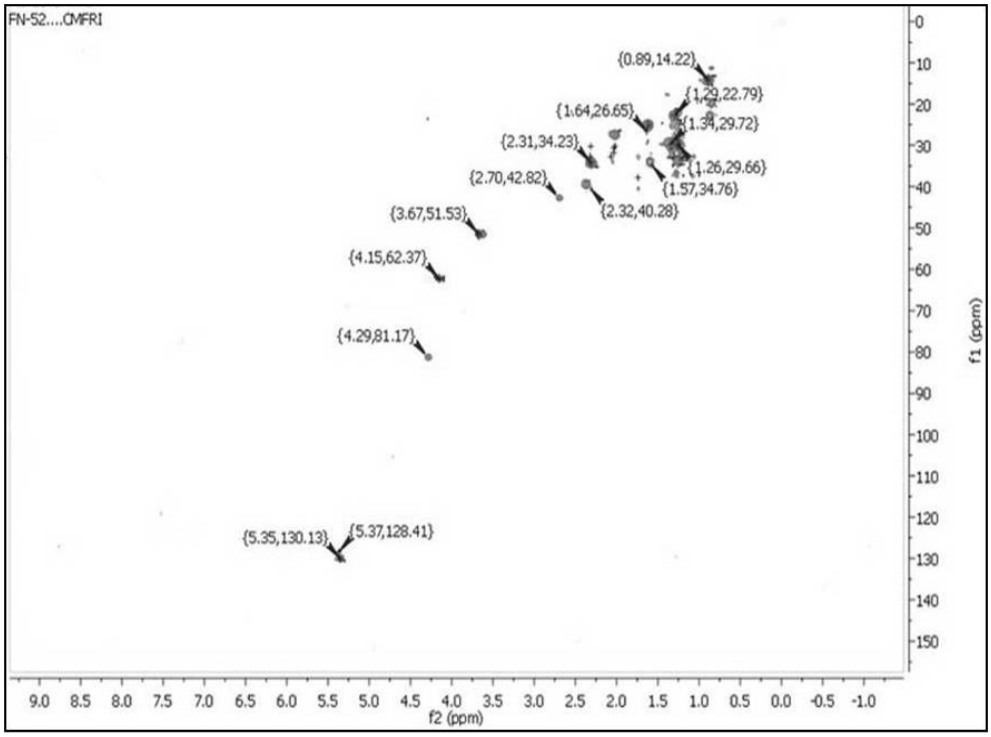

Figure 4.16. Figure showing the HSQC spectrum of compound **K2**

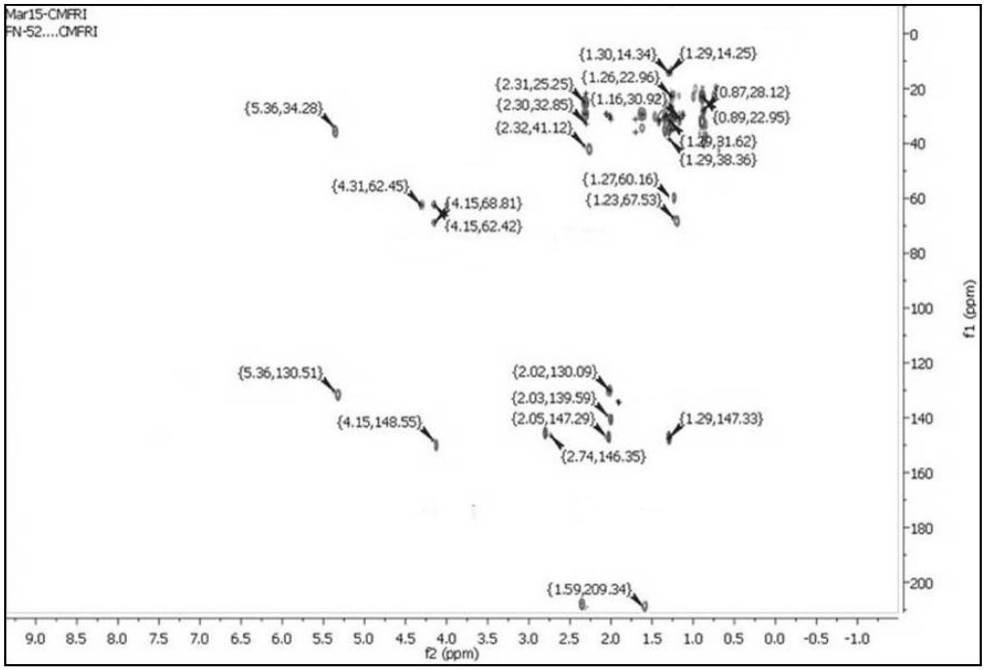

Figure 4.17. Figure showing the HMBC spectrum of compound **K2**

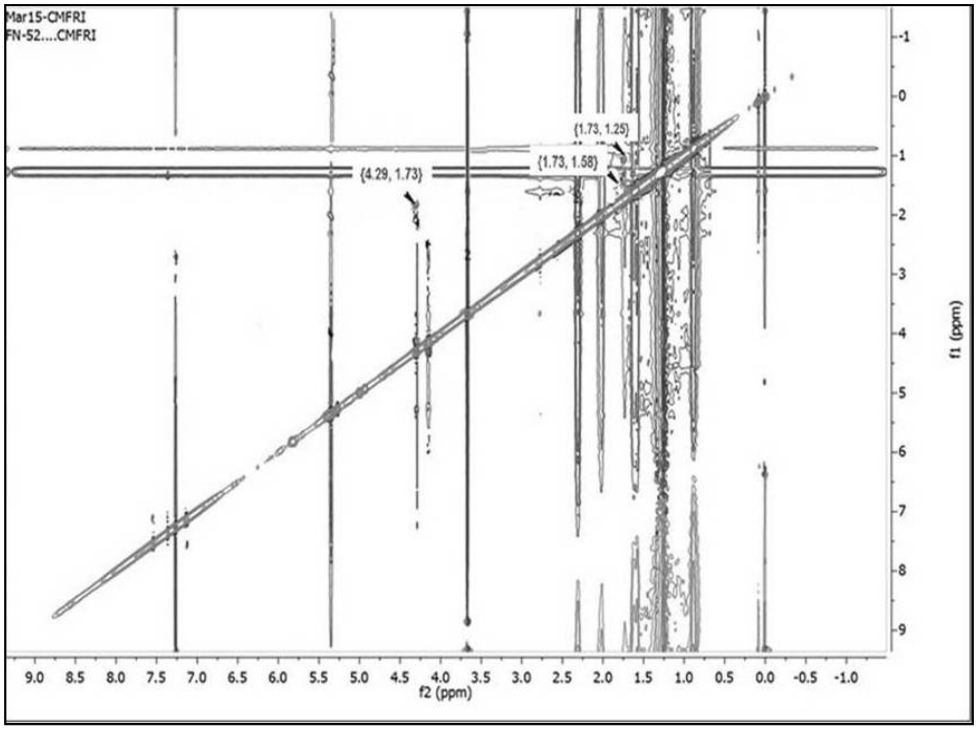

Figure 4.18. Figure showing the NOESY spectrum of compound **K2**

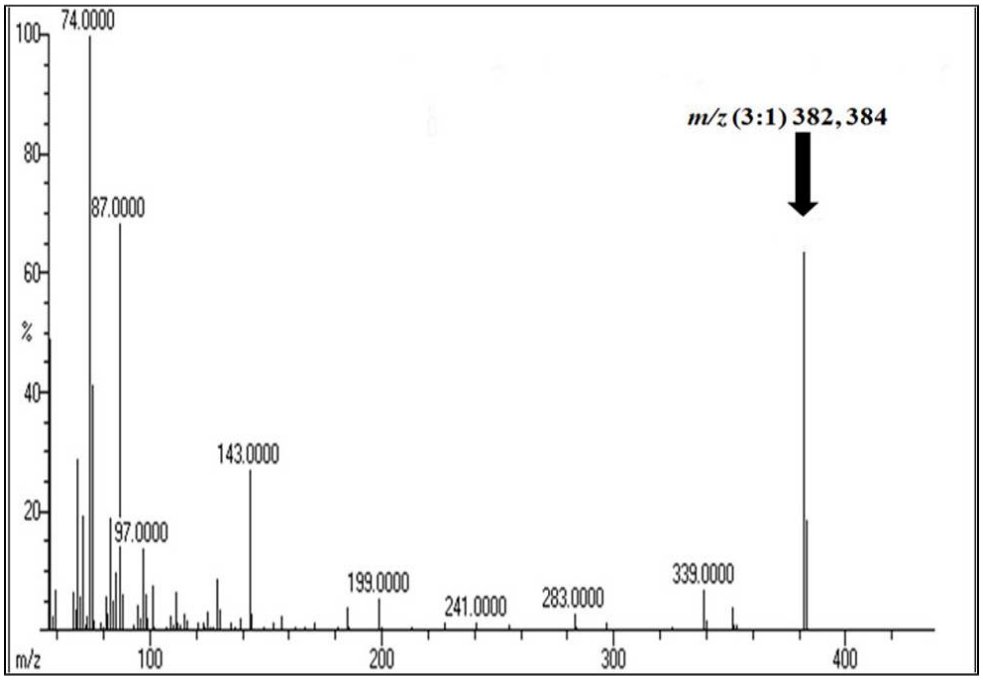

Figure 4.19. Mass spectrum of compound **K2**

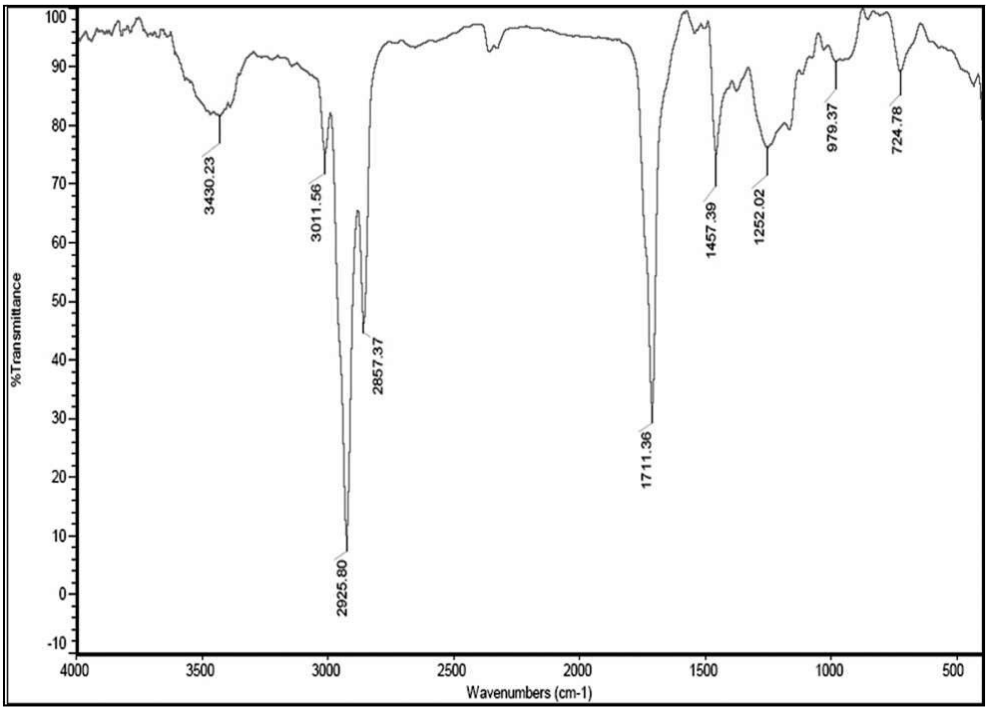

Figure 4.20. Figure showing the FTIR spectrum of compound **K2**

The preliminary studies with various solvents and mixture of solvents were carried out to identify the best solvent/solvent combination to extract the most active fraction in the studied marine macroalga *K. alvarezii*. In this process, the solvents EtOAc, MeOH, DCM and $CHCl_3$, along with various solvent combinations were used as extractants to distribute the extraction process throughout the entire scale of eleutropic solvent series. Among various solvents, EtOAc: MeOH at equal proportion (1:1, v/v) was appropriate to extract the crude with potentially higher bioactivities than other solvents (Table 4.4). Notably, the EtOAc: MeOH (1:1 v/v) fractions of *K. alvarezii* registered significantly higher antioxidant activities in terms of scavenging DPPH and ABTS radicals along with greater pro-inflammatory enzyme (5-LOX, COX-2) inhibitory properties than other extracts (Table 4.4).

Initial bioactivity-assisted fractionation of EtOAc: MeOH (1:1, v/v) extract of *K. alvarezii* over silica gel column resulted in various fractions, as detailed in the materials section. It was noted that the fraction $KA_{2\text{-}1}$ obtained at the solvent eluent gradient of EtOAc: *n*-hexane of 1:99 to 1:19 (v/v) displayed greater antioxidative and 5-lipoxygenase inhibition activities (IC_{50} DPPH scavenging 0.54 mg/mL; IC_{50} 5-LOX inhibition 0.98 mg/mL) than those recorded with other fractions (IC_{50} > 1 mg/mL) (Table 4.5). Therefore, the fraction $KA_{2\text{-}1}$ was selected for further chromatographic fractionation. Furthermore, the sub-fraction $KA_{2\text{-}1\text{-}1}$, which was obtained by step-gradient flash chromatography showed greater bioactivity (IC_{50} DPPH scavenging 0.45 mg/mL; IC_{50} 5-LOX inhibition 0.96 mg/mL) than other sub-fractions (IC_{50} > 1 mg/mL) (Table 4.5), and was therefore, used for downstream preparative HPLC (60:40 MeOH/H_2O) fractionation to yield the studied compounds.

Bioactivity-assisted fractionation of EtOAc: MeOH (1:1, v/v) extract of *K. alvarezii* yielded two previously unreported halogenated compounds, characterized as 2-butyl-7-4-(chloromethyl) cyclooct-1-enyl) hept-5-en-1-ol (compound **K1**) and 4-(2-chloroethyl)-5-7-(methoxymethyl) undec-3-enyl) cyclooct-4-enone (compound **K2**), which were found to constitute C_{20}-cyclooctene and C_{23}-cyclooctenyl frameworks, respectively.

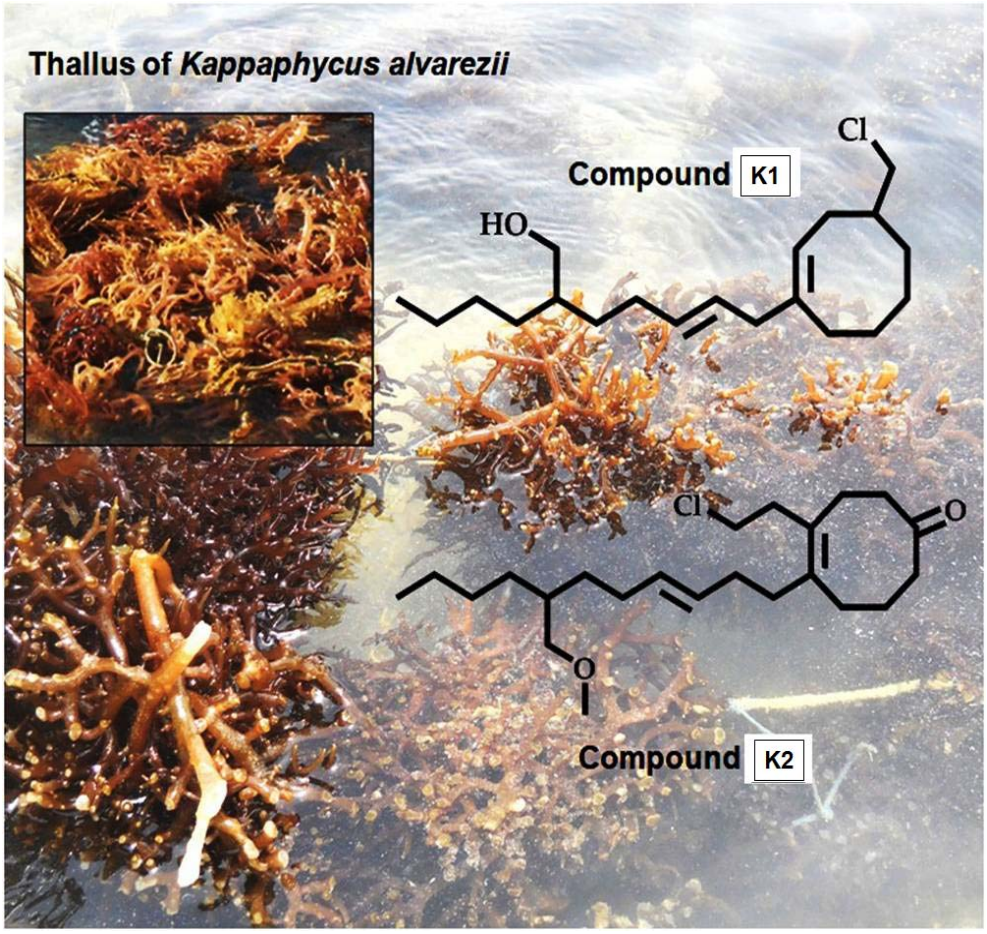

Figure 4.21. Figure showing the structures of compound **K1** and **K2**, isolated from the intertidal marine macroalga *K. alvarezii*. The thalli of the studied marine macroalga were displayed as inset

2-Butyl-7-4-(chloromethyl) cyclooct-1-enyl) hept-5-en-1-ol (compound **K1**) was purified from the EtOAc: MeOH (1:1, v/v) extract of red marine macroalga *K. alvarezii* by silica gel-based column chromatographic fractionation, and its structure was resolved by extensive 1D-2D NMR and mass spectral analyses. The mass spectroscopic data demonstrated a molecular ion peak at *m/z* 326, while the molecular formula $C_{20}H_{35}ClO$, implying three unsaturation degrees, and were associated with two olefinic bonds and one ring system. The infrared (IR) spectrum exhibited distinctive stretching vibration band for hydroxyl (3430 cm^{-1}) and olefinic group (3011 cm^{-1}). The existence of the hydroxyl proton at δ_H 3.67 was validated by ^1H NMR spectra and D_2O exchange reaction. The ^{13}C NMR spectroscopic data along with DEPT experiment of

compound **K1** demonstrated the presence of twenty ^{13}C signals including one terminal methyl group at δ_H 0.88 (H-2"^{4}, *J*=6.75 Hz), an oxygenated sp^2 methylene carbon (δ_H 3.61; *J*=7.60 Hz; attributed to H-1, δ_C 70.59), twelve methylene carbons δ_H 1.30 (H-2"^{3}, δ_C 22.58); δ_H 1.25 (H-2"^{2}, δ_C 29.50); δ_H 1.25 (H-2"^{1}, δ_C 31.52); δ_H 1.30 (H-3, δ_C 34.06); δ_H 2.81 (H-4, δ_C 30.20); δ_H 3.27 (H-7, d, *J*=7.2 Hz, δ_C 44.88); δ_H 2.35 (H-8', t, *J*=6.1 Hz, δ_C 33.63); δ_H 1.25 (H-6', δ_C 27.23); δ_H 1.30 (H-5', δ_C 31.93); δ_H 2.13 (H-3', t, *J*=6.0 Hz, δ_C 34.30)), olefinic carbons (δ_H 5.37 (H-5, δ_C 130.51); δ_H 5.39 (H-6, δ_C 128.77; H-2', 128.58), two methine carbons δ_H 1.72 (H-2, δ_C 38.16); δ_H 2.05 (H-4', δ_C 38.19)), one deshielded methylene carbon due to halogen at δ_H 3.74 (H-4", d, *J* = 6.55 Hz, δ_C 51.76), and one quaternary carbon at δ_C 146.84 (H-1'). The positions of hydroxyl and side chain substituent to the cyclooctene were established from the major HMBC and ^1H-^1H COSY correlations. The intense HMBC correlations between δ_H 1.25 (H-2"^{1}) to δ_C 22.58 (C-2"^{3})/δ_C 29.50 (C-2"^{2}); δ_H 0.88 (t, *J*=6.75 Hz; H-2"^{4}) to δ_C 22.58 (C-2"^{3})/δ_C 29.50 (C-2"^{2}); δ_H 1.72 (H-2) to δ_C 31.52 (C-2"^{1}); δ_H 2.81 (H-4) to δ_C 128.77 (C-6); δ_H 3.27 (d, *J*=7.2 Hz; H-7) to δ_C 146.84 (C-1')/δ_C 130.51 (C-5) and ^1H–^1H COSY correlations with δ_H 2.81 (H-4)/δ_H 5.37 (H-5) supported the presence of cycloctene framework. The existence of cyclooctene ring system was supported by additional HMBCs {δ_H 1.30 (H-5') to δ_C 29.33 (C-7'); δ_H 2.05 (H-4') to δ_C 34.30 (C-3'); δ_H 2.35 (t, *J*=6.1 Hz; H-8') to δ_C 29.33 (C-7')/δ_C 27.23 (C-6')} and ^1H–^1H COSY δ_H 2.13 {H-3')/δ_H 5.39 (H-2')}; δ_H 2.35 {H-8')/δ_H 1.63 (H-7')} correlations (Table 4.1).

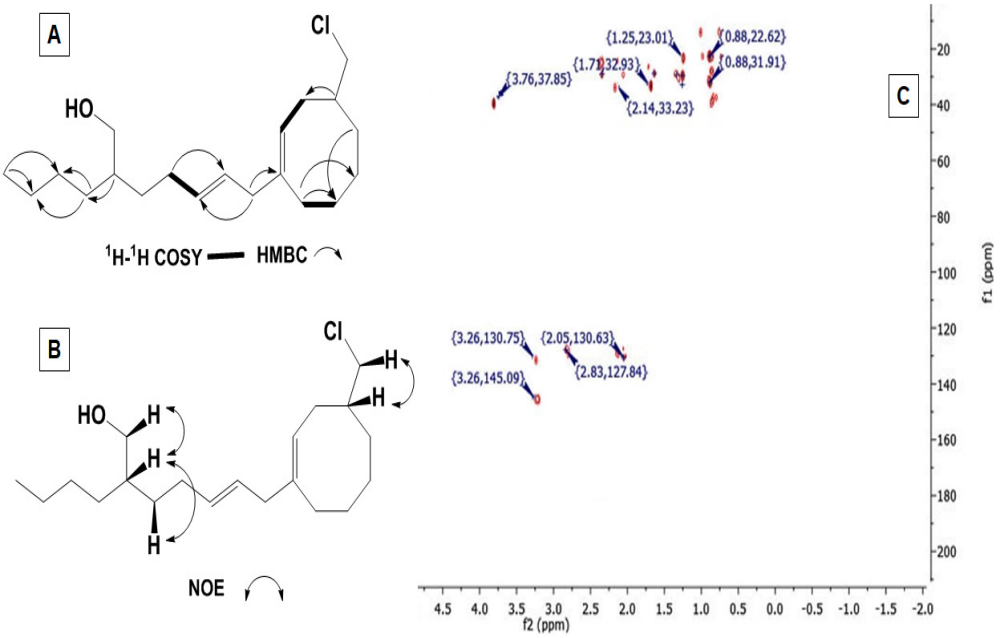

Figure 4.22. Figure showing the key (**A**) ^{1}H-^{1}H COSY, HMBC and (**B**) NOESY correlations of compound **K1**. (**C**) The spectral representation of long-range C-H correlations (showing prominent cross-peaks). The ^{1}H-^{1}H COSY cross peaks were displayed by bold face bonds, whereas the selected HMBC correlations were shown as double-barbed arrows. The β-orientation in the NOESY relations was presented as double-sided arrows

The NOE experiment of compound **K1** showed correlation peaks between the equatorial methine proton at δ_H 1.72, (H-2) and methylene proton at δ_H 3.61, t, *J*=7.60 Hz; (H-1), which proposed that these protons were arranged on the same side of the reference plane (cyclooctene) with β-faced interaction. In addition, NOESY correlations were observed between the equatorial methine proton at δ_H 1.72, (H-2) and methylene proton at δ_H 1.30, (H-3), which proposed that these protons were disposed on opposite to the plane of reference (cyclooctene). The proton at δ_H 3.74 (H-4") showed sharp NOE cross-peaks with the axial proton at δ_H 2.05 (H-4'), which displayed β-faced interaction with each other. The characteristic isotopic molecular ion peaks with typical isotopic pattern of 3:1 at *m/z* 326 and *m/z* 328 appropriately attributed the existence of one chlorine atom in compound **K1**.

4-(2-Chloroethyl)-5-7-(methoxymethyl) undec-3-enyl) cyclooct-4-enone (compound **K2**) was purified from the EtOAc-MeOH (1:1, v/v) extract of *K. alvarezii* by silica gel-based chromatographic techniques, and its structure was resolved by extensive 1D-2D NMR and mass spectral analyses. The mass spectroscopic experiments showed a molecular isotopic ion peak at *m/z* 382, having four degrees of unsaturation (molecular formula $C_{23}H_{39}ClO_2$), and were associated with two olefinic bonds, along with one each of carbonyl group and ring system. The infrared (IR) spectrum exhibited distinctive stretching vibration band for carbonyl stretching (1727.88 cm^{-1} (C–CO–C ν)) and olefinic group (3072.42 cm^{-1} (C–H)). The ^{13}C NMR spectroscopic data of compound **K2** along with DEPT experiment demonstrated the presence of twenty-three ^{13}C signals including fifteen methylene carbon {δ_H 1.33 (H-10, δ_C 22.70); δ_H 1.30 (H-8, δ_C 30.20); δ_H 1.58 (H-6, δ_C 34.13); δ_H 2.00 (H-5, δ_C 31.44); δ_H 2.00 (H-2, δ_C 32.74); δ_H 2.06 (H-1, δ_C 31.93); δ_H 1.62 (H-7', δ_C 27.19); δ_H 2.30 (H-8', t, *J*=6.1 Hz, δ_C 40.19); δ_H 2.77 (H-2', δ_C 41.50); δ_H 2.30 (t, *J*=6.1 Hz, H-3', δ_C 29.37); δ_H 2.30 (H-4'^{1}, δ_C 33.83); δ_H 1.25 (H-9, δ_C 29.6); δ_H 2.06 (H-6', δ_C 29.70)}, one terminal methyl group {δ_H 0.87, t, *J*=6.70 Hz; H-11; δ_C 14.12}, an oxygenated methylene carbon {δ_H 4.29; *J*=7.46 Hz; H-7'^{1} δ_C 80.95}, olefinic carbons {δ_H 5.35 (H-4, δ_C 130.0); δ_H 5.34 (H-3, δ_C 129.68)}, one methine carbon {δ_H 1.73 (H-7, δ_C 38.86)}, one deshielded methylene carbon due to halogen {δ_H 4.15 (H-4'^{2}, t, *J*=7.50 Hz, δ_C 62.11)}, one methoxy carbon {δ_H 3.67 (H-7'^{1}, δ_C 51.44)}, two quaternary carbons {δ_C 139.28 (H-5'); δ_C 147.07 (H-4')}, and one carbonyl carbon {δ_C 209 (H-1')}. The positions of methoxy group and side chain substituent to the cyclooctenone were established from the key ^1H–^1H COSY and HMBC correlations. The ^1H–^1H correlations spectroscopy observed between δ_H 5.35 (H-4)/δ_H 2.00 (H-5) and $J^{1\text{-}3}$ C–H correlations between δ_H 1.33 (H-10) to δ_C 30.20 (C-8)/δ_C 29.6 (C-9)/δ_C 14.12 (C-11); δ_H 1.30 (H-8) to δ_C 38.86 (C-7)/δ_C 22.70 (C-10); δ_H 3.67 (H-7'^{2}) to δ_C 80.95 (C-7'^{1}); δ_H 2.06 (H-1) to δ_C 32.74 (C-2); δ_H 1.25 (H-9) to δ_C 22.70 (C-10)/δ_C 38.86 (C-7); δ_H 0.87 (t, *J*=6.70 Hz; H-11) to δ_C 22.70 (C-10); δ_H 1.73 (H-7) to δ_C 34.13 (C-6)/δ_C 31.44 (C-5); δ_H 2.00 (H-5) to δ_C 130.0 (C-4); δ_H 5.34 (H-3) to δ_C 130.0 (C-4)/δ_C 32.74 (C-2) supported the presence of cyclooctenyl framework. The existence of cyclooctenyl ring system was corroborated by additional HMBCs {δ_H 2.30 (H-8') to δ_C 209 (C-1'); δ_H 1.62 (H-7') to δ_C 209 (C-1)/δ_C 29.70 (C-6'); δ_H 2.77 (H-2') to δ_C 147.07 (C-4'); δ_H 2.06 (t, *J*=6.10 Hz; H-1) to δ_C 29.70 (C-6')/δ_C 147.07 (C-4')/δ_C 139.28 (C-5'); δ_H 2.30 (H-3') to δ_C 33.83 (C-4'^{1})/δ_C 41.50 (C-

2'); δ_H 4.15 (H-4'^{2}) to δ_C 147.07 (C-4')} and ^{1}H–^{1}H COSY {(δ_H 2.30 (H-8')/δ_H 1.62 (H-7')} correlations. The NOE experiment showed correlation peaks between the oxygenated methine proton at δ_H 1.73 (H-7) and axial proton at δ_H 1.58 (H-6), which proposed that these protons were on the opposite to the reference plane (cyclooctenyl) with β-faced interaction. Intense NOE correlation were also observed between the equatorial proton at δ_H 4.29 (d, *J*=7.46 Hz; H-7'^{1}) with δ_H 1.73 (H-7), which suggested that these protons were di-equatorially oriented with β-faced interaction. Moreover intense NOE correlation were observed between the axially oriented proton δ_H 1.25 (H-9) with δ_H 1.73 (H-7), suggesting that these protons were disposed in the identical plane of reference. The characteristic isotopic molecular ion peaks with typical isotopic pattern of 3:1 at *m/z* 382 and *m/z* 384 appropriately attributed the existence of one chlorine atom in compound **K2**. It is of note that the halogen derivatives isolated in the present study from *K. alvarezii* represented the first examples of naturally occurring halogen derivative from the marine macroalga (Table 4.2). There were reports of halogenated compounds isolated from other species of red marine macroalgae. Therefore, we will confine our discussion with the closely related structures, such as laurefurenynes A-F and cyclic ether acetogenins isolated and characterized from the red marine macroalga *Laurentia* sp. The FT-IR spectral data of laurefurenynes A-F, which belonged to the class of C_{15} cyclic ether acetogenins, were purified from *Laurentia* sp, displayed strong absorption bands attributed to a terminal acetylene (2107 and 3315 cm^{-1}) functional groups, which were absent in the halogen derivatives isolated from *K. alvarezii*. The C_{15} acetogenin en-ynes, a group of chlorinated compounds with potential pharmacological properties, were isolated from *Laurencia glandulifera*, and were structurally similar to the studied compounds (Kladi et al. 2009). However, there was no previous report with regard to the antioxidant and anti-inflammatory activities of the laurefurenynes A-F and cyclic ether acetogenins from red marine macroalgae. The present study is the first of its kind to describe the halogen derivatives with anti-inflammatory and radical scavenging leads for use in the medicinal and functional food applications.

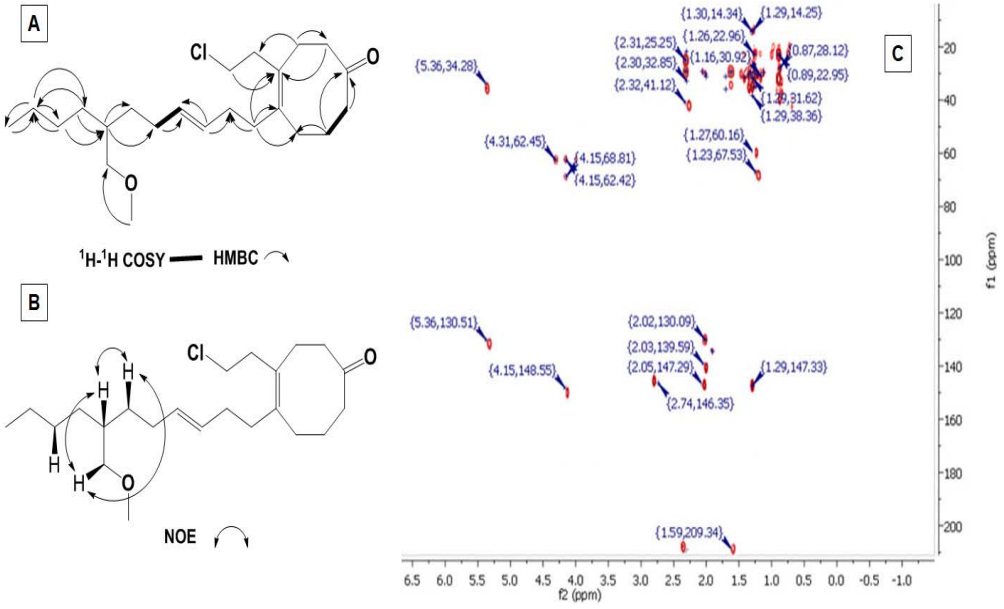

Figure 4.23. Figure showing the Key (**A**) ^{1}H-^{1}H COSY, HMBC and (**B**) NOESY correlations of compound **K2** (**C**) The spectral representation of long-range C-H correlations (showing prominent cross-peaks). The ^{1}H-^{1}H COSY cross peaks were displayed by bold face bonds, whereas the selected HMBC correlations were shown as double-barbed arrows. The β-orientation in the NOESY relations was presented as double-sided arrows

The signals obtained at δ_H 4.93 and δ_H 4.43 indicated the two hydroxyl groups, which were present at OH-7 and OH-12 (Wael et al. 2010). The studied halogenated compounds derived from the ethyl acetate-methanol extract of the red marine macroalga *K. alvarezii* displayed the presence of OH-1". The previously reported C_{15}-acetogenin from red marine macroalgae was found to differ with the isolated halogen compounds in the pattern of oxygenation and halogenations. The characteristic isotopic molecular ion peaks appropriately attributed the existence of one chlorine atom in the halogen derivatives isolated from *K. alvarezii*. Similarly, the C_{15}-acetogenin isolated from red marine macroalga *Laurencia* sp displayed brominated halogenations.

4.3.1.3. Bioactivities and Structure-Activity Relationship Analysis

The radical scavenging potentials of the isolated compounds were resolved by *in vitro* radical scavenging assays, such as 1, 1-diphenyl-2-picrylhydrazyl (DPPH) and 2, 2′-azino-bis(3-ethylbenzothiazoline-6-sulphonic acid (ABTS), whereas their activities were compared with the synthetic antioxidants (BHT, BHA) and α-tocopherol. Among the halogen derivatives, compound **K2** showed significant radical scavenging activity ($IC_{50\ DPPH}$ 0.23±0.06, $IC_{50\ ABTS}$ 0.25±0.18 mg/mL) when compared to compound **K1** ($IC_{50\ DPPH}$ 0.27±0.04, $IC_{50\ ABTS}$ 0.31±0.18 mg/mL), and than that of the commercial antioxidants. The anti-inflammatory activities of studied halogen derivatives were analyzed by pro-inflammatory 5-lipoxygenase, cyclooxygense-2 *in vitro* assays. Among the studied compounds, compound **K2** displayed higher 5-LOX inhibitory activities (IC_{50} 0.90±0.04 mg/mL) than synthetic ibuprofen (IC_{50} 0.93±0.11 mg/mL) (Fig. 4.24, Table 4.3). Notably, the studied halogen analogues presented significantly greater inhibitory activities against COX-2 than its COX-1 isoform. Similarly, their selectivity indices ($IC_{50\ anti\text{-}COX\text{-}1}/IC_{50\ anti\text{-}COX\text{-}2}$ ~ 1.06–1.07) were greater in comparison with synthetic NSAIDs (aspirin 0.02; ibuprofen 0.44). It is intriguing to note that the synthetically available anti-inflammatory drugs demonstrated comparable inhibitory activities against constitutive COX-1 and inducible COX-2, which might reveal their adverse effects (Fosslien 2005).

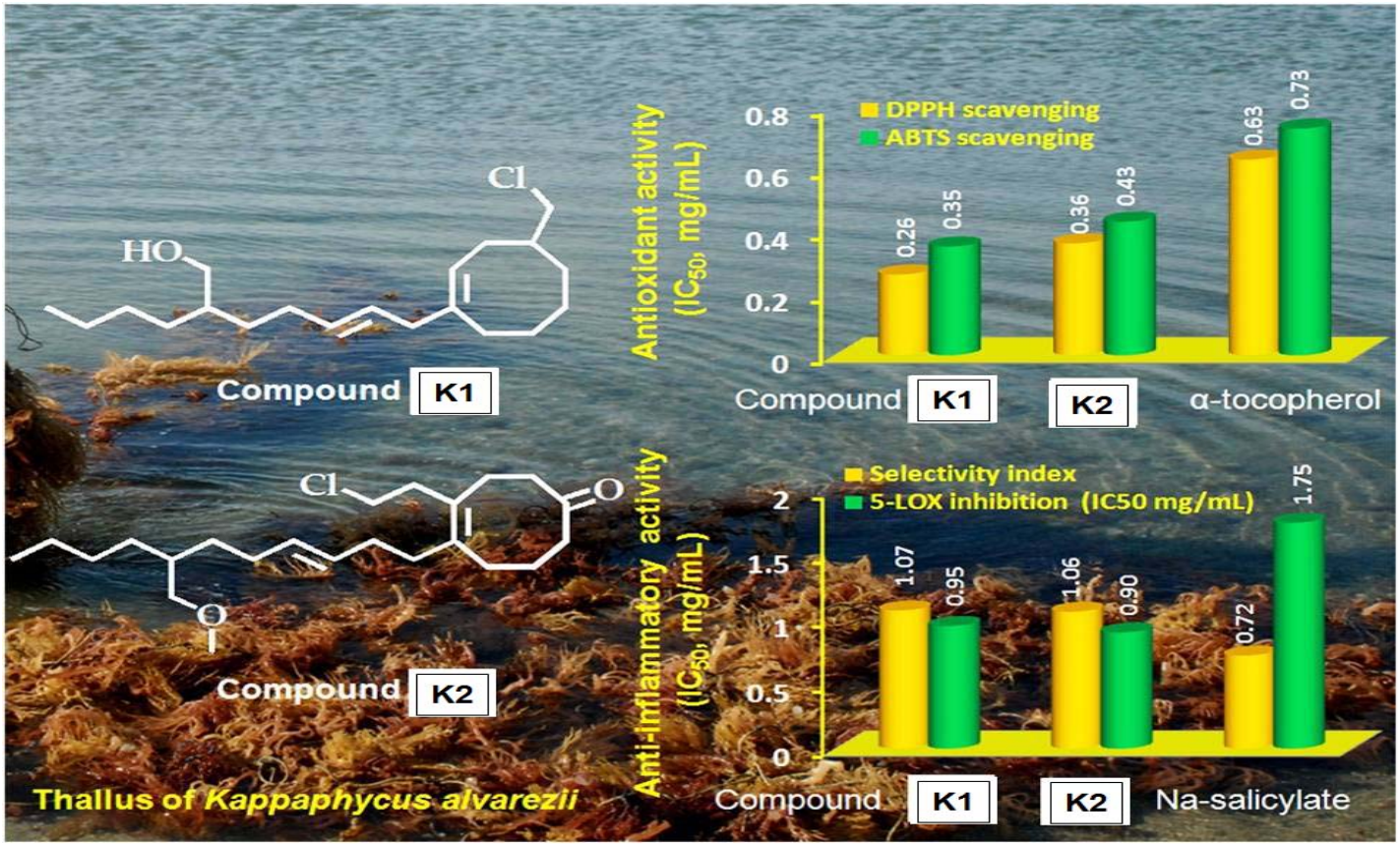

Figure 4.24. Graphical representation of bioactivities of compound **K1** and **K2**. The thalli of the studied marine macroalga were displayed as inset

Table 4.3 Antioxidative and inflammatory activities of the halogen derivatives (compounds **K1**-**K2**) isolated from *K. alvarezii vis-à-vis* the commercially available antioxidants and anti-inflammatory agents

Antioxidative activities[†] {IC_{50} (mg/mL)}

	Compound K1	**Compound K2**	**BHA**	**BHT**	**α-tocopherol**
$DPPH^{\cdot}$ scavenging	$0.27^{a} \pm 0.04$	$0.23^{a} \pm 0.06$	$0.26^{b} \pm 0.01$	$0.25^{b} \pm 0.02$	$0.63^{c} \pm 0.04$
$ABTS^{+\cdot}$ scavenging	$0.31^{a} \pm 0.18$	$0.25^{a} \pm 0.18$	$0.34^{b} \pm 0.02$	$0.26^{b} \pm 0.02$	$0.73^{c} \pm 0.05$

Anti-inflammatory activities[†] {IC_{50} (mg/mL)}

	Compound K1	**Compound K2**	**Aspirin**	**Na-salicylate**	**Ibuprofen**
COX-1 inhibition	$1.01^{a} \pm 0.04$	$0.94^{a} \pm 0.04$	$0.005^{a} \pm 0.00$	$1.93^{c} \pm 0.05$	$0.04^{a} \pm 0.00$
COX-2 inhibition	$0.94^{a} \pm 0.03$	$0.88^{a} \pm 0.09$	$0.21^{b} \pm 0.02$	$2.65^{c} \pm 0.05$	$0.09^{a} \pm 0.02$
Selectivity index[‡]	$1.07^{b} \pm 0.06$	$1.06^{b} \pm 0.03$	$0.02^{b} \pm 0.02$	$0.72^{b} \pm 0.01$	$0.44^{b} \pm 0.02$
5-LOX inhibition	$0.95^{a} \pm 0.11$	$0.90^{a} \pm 0.04$	$0.39^{a} \pm 0.02$	$1.75^{c} \pm 0.12$	$0.93^{b} \pm 0.11$

[†] The bioactivities were expressed as IC_{50} values (mg/mL). The samples were analyzed in triplicate (n=3) and expressed as mean ± standard deviation.

Means followed by the different superscripts (a–c) within the same row indicate significant differences ($P < 0.05$).

[‡] Selectivity index has been calculated as the ratio of anti-COX-1 (IC_{50}) to that of anti-COX-2 (IC_{50}).

Table 4.4 Yield, antioxidant and anti-inflammatory activities (IC_{50}, mg/mL)[†] of different solvent fractions extracted from the red marine macroalga *K. alvarezii*

	Solvent fractions					
Activities	**$CHCl_3$**	**DCM**	**EtOAc**	**MeOH**	**$CHCl_3$: MeOH**	**EtOAc: MeOH (1:1 v/v)**
Yield[‡]	1.1	1.0	3.8	4.32	2.5	6.0
DPPH radical scavenging	2.08 ± 0.12	1.97 ± 0.08	1.36 ± 0.06	1.38 ± 0.09	1.74 ± 0.06	1.24 ± 0.11
ABTS radical scavenging	2.05 ± 0.07	1.93 ± 0.05	1.32 ± 0.08	1.35 ± 0.12	1.72 ± 0.15	1.26 ± 0.06
5-LOX inhibitory	2.13 ± 0.11	2.01 ± 0.16	1.58 ± 0.14	1.52 ± 0.18	1.97 ± 0.20	1.49 ± 0.12
COX-2 inhibitory	2.08 ± 0.17	2.03 ± 0.08	1.52 ± 0.12	1.50 ± 0.13	1.92 ± 0.14	1.35 ± 0.15

[†] The samples were analyzed in triplicate (n = 3) and expressed as mean ± standard deviation. The IC_{50} values were expressed as mg/mL. $CHCl_3$-chloroform, DCM-dichloromethane, EtOAc-ethyl acetate, MeOH-methanol.

[‡] Yields of the extracts were represented as % w/w of marine macroalga on dry weight basis.

Table 4.5 Antioxidant and anti-inflammatory activities (IC_{50}, mg/mL)[†] of the column fraction and purified compounds from EtOAc-MeOH (1:1 v/v) extracts of the red marine macroalga *K. alvarezii*

	Activities			
Fractions	**DPPH scavenging**	**ABTS scavenging**	**5-LOX inhibitory**	**COX-2 inhibitory**
KA_{2-1}	**0.54±0.01**	**0.53±0.04**	**0.98±0.02**	**0.97±0.04**
KA_{2-2}	1.39±0.06	1.40±0.06	1.50±0.03	1.52±0.02
KA_{2-3}	1.36±0.03	1.35±0.02	1.48±0.02	1.46±0.05
KA_{2-4}	1.38±0.05	1.38±0.01	1.45±0.05	1.42±0.06
KA_{2-5}	1.41±0.01	1.42±0.01	1.52±0.02	1.54±0.03
KA_{2-6}	1.45±0.03	1.48±0.01	1.54±0.01	1.56±0.01
KA_{2-7}	1.48±0.02	1.50±0.08	1.60±0.09	1.59±0.04
KA_{2-8}	1.42±0.02	1.40±0.01	1.53±0.03	1.54±0.06
KA_{2-9}	1.45±0.02	1.42±0.01	1.56±0.02	1.54±0.02
KA_{2-10}	1.46±0.04	1.43±0.02	1.53±0.04	1.52±0.09
KA_{2-11}	1.43±0.04	1.40±0.02	1.50±0.01	1.52±0.05
KA_{2-12}	1.38±0.01	1.39±0.08	1.43±0.06	1.45±0.02
KA_{2-13}	1.49±0.01	1.47±0.03	1.52±0.04	1.52±0.02
KA_{2-1} Sub Fractions				
KA_{2-1-1}	**0.45±0.02**	**0.43±0.01**	**0.96±0.03**	**0.92±0.01**
KA_{2-1-2}	1.13±0.01	1.15±0.03	1.20±0.01	1.19±0.06
KA_{2-1-3}	1.15±0.02	1.18±0.01	1.22±0.03	1.20±0.04
KA_{2-1-4}	1.10±0.01	1.08±0.08	1.16±0.04	1.15±0.09
KA_{2-1-5}	1.11±0.02	1.10±0.03	1.18±0.01	1.17±0.04
KA_{2-1-6}	1.13±0.04	1.13±0.06	1.14±0.01	1.16±0.02
KA_{2-1-7}	1.18±0.02	1.16±0.06	1.20±0.06	1.21±0.03
KA_{2-1-1} Sub Fractions				
Compound K1	0.27±0.04	0.31±0.18	0.94±0.03	0.88±0.09
Compound K2	0.23±0.06	0.25±0.18	0.95±0.11	0.90±0.04

† The samples were analyzed in triplicate (n=3) and expressed as mean ± standard deviation.

The IC_{50} values were expressed as mg/mL.

Table 4.6. Antioxidative, anti-inflammatory, anti-diabetic and anti-hypertensive activities of the crude EtOAc: MeOH (1:1 v/v) extract and purified compounds isolated from the red marine macroalga *K. alvarezii*

Activities† IC_{50} values (mg/mL)	**EtOAc: MeOH (1:1 v/v)**	**Compound K1**	**Compound K2**
Antioxidant activities			
DPPH radical scavenging	1.24±0.06	0.27±0.04	0.23±0.06
ABTS radical scavenging	1.26±0.03	0.31±0.18	0.25±0.18
Anti-hypertensive activities			
ACE inhibitory	2.10±0.02	2.01±0.04	2.03±0.04
Anti-diabetic activities			
α-amylase inhibitory	2.18±0.04	2.01±0.02	2.08±0.01
α-glucosidase inhibitory	2.20±0.01	2.03±0.04	2.10±0.06
DPP-4 inhibitory	2.18±0.03	2.02±0.05	2.11±0.02
Anti-inflammatory activities			
COX-2 inhibitory	1.35±0.05	0.88±0.09	0.90±0.04
5-LOX inhibitory	1.49±0.02	0.94±0.03	0.95±0.11

†The bioactivities were expressed as IC_{50} values (mg/mL).

The samples were analyzed in triplicate (n=3) and expressed as mean ± standard deviation.

4.3.1.4. Structural Characterization of Compound K3

1-(3-Methoxypropyl)-2-propylcyclohexane (**K3**)

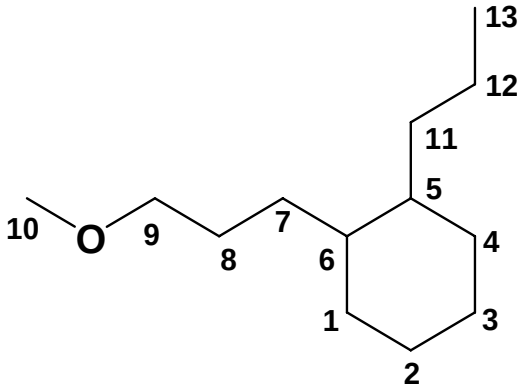

Sample yield	120 mg (1.2 %)
Physical description	Yellow oil
Molecular formula	$C_{13}H_{26}O$
Molecular weight	198.1984

1-(3-Methoxypropyl)-2-propylcyclohexane: Yellow oil; UV MeOH λmax (log ε): 245 nm (3.26), TLC (Si gel GF_{254} 15 mm; EtOAc/MeOH 19:1, v/v) Rf: 0.96; Rt (HPLC, ACN: MeOH, 2:4 v/v): 12.401 min; IR (vibrational spectra were measured between 4000 to 450 cm^{-1} for (KBr, cm^{-1}) νmax (ν = stretching, δ = bending, ρ = rocking vibrations)): 728.70 (C-H ρ), 1014.67 (C–O ν), 1256.18 (CH_2 ν), 1376.13 (C-H ρ), 1458.14 (C-H δ), 1644.58 (C=C ν), 2857.12, 2923.46 (C–H ν); ^{1}H NMR (500 MHz $CDCl_3$): δ_H 1.26 (2H, m, H-1), δ_H 1.26 (2H, m, H-2), δ_H 1.26 (2H, m, H-3), δ_H 1.62 (2H, m, H-4), δ_H 2.32 (1H, m, H-5), δ_H 2.04 (1H, m, H-6), δ_H 1.42 (2H, m, H-7), δ_H 1.72 (2H, m, H-8), δ_H 4.29 (2H, t, *J*=6.95 Hz, H-9), δ_H 3.67 (3H, s, H-10), δ_H 1.25 (2H, m, H-11), δ_H 1.31 (2H, m, H-12), δ_H 0.88 (3H, t, *J*=7.53 Hz, H-13); ^{13}C NMR (125 MHz, $CDCl_3$): δ_C 29.65 (C-1), δ_C 27.23 (C-2), δ_C 29.65 (C-3), δ_C 37.10 (C-4), δ_C 33.86 (C-5), δ_C 32.38 (C-6), δ_C 29.88 (C-7), δ_C 29.66 (C-8), δ_C 50.87 (C-9), δ_C 51.45 (C-10), δ_C 31.97 (C-11), δ_C 22.7 (C-12), δ_C 14.12 (C-13); HMBC and ^{1}H-^{1}H-COSY data (Fig. 4.26 to Fig. 4.34, Table 4.7); HR (EI) MS *m/z* measured value 198.1988 $[M]^+$, calcd for $C_{13}H_{26}O$ 198.1984.

1-(3-Methoxypropyl)-2-propylcyclohexane (compound **K3**), a methoxy-substituted C_{13} meroterpenoid, was purified as yellow oil by extensive column chromatography on adsorbent silica gel. The mass spectrum displayed the molecular ion peak at *m/z* 198 enclosing mono unsaturation (because of the ring system), and the molecular formula as $C_{13}H_{26}O$ based upon combined ^{1}H and ^{13}C NMR spectral data. The existence of 13 carbon signals constituting of nine methylenes, two methines and one each of methoxy and methyl carbons was supported by the ^{13}C NMR experiment. The deshielded resonance of H-9 (δ_H 4.29, *J*=6.95 Hz) of compound **K3** suggested the C-9 methylene groups remained attached to an electronegative group, possibly of oxygenated origin.

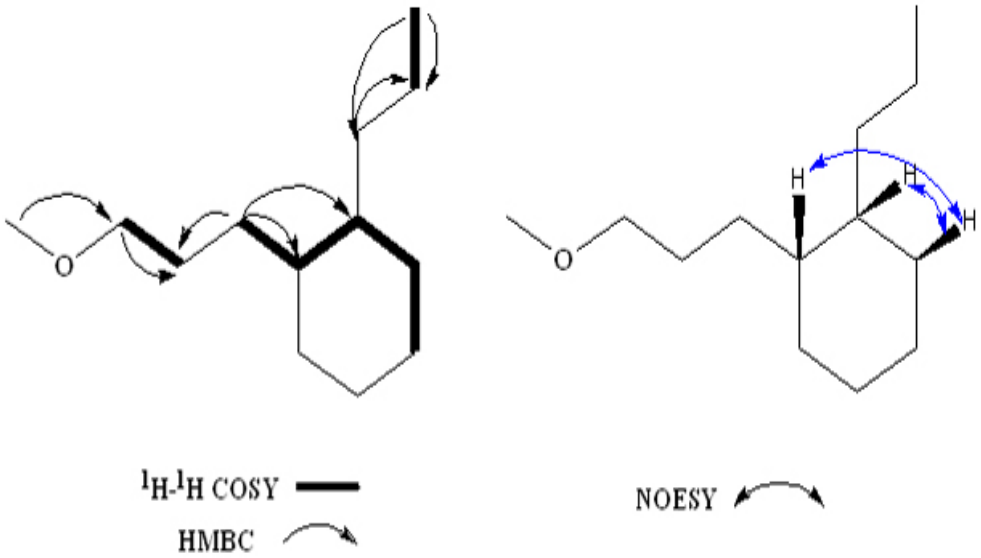

Figure 4.25. Figure showing Key ^{1}H-^{1}H COSY, HMBC and NOESY correlations of compound **K3.** The ^{1}H-^{1}H COSY cross peaks were displayed by bold face bonds, whereas the selected HMBC correlations were shown as double barbed arrows. The β orientation in the NOESY relations was presented as blue colored arrows

The ^{1}H-^{1}H COSY correlations were observed between δ_H 2.32 (H-5)/δ_H 2.04 (H-6); δ_H 1.62 (H-4)/δ_H 2.32 (H-5) were apparent, and were ascribed to the cyclohexane ring framework (Fig. 4.25). The methine (–CH) carbon signals were apparent at δ_C 33.86 (C-5) and C-6 (δ_C 32.38) that appropriately recognized the

junction point of cyclohexane ring system substituted with propane and the methoxypropane moieties, respectively. HMBC correlations from δ_H 1.25 (assigned as H-11) to δ_C 22.7 (C-12); δ_H 1.42 (H-7) to δ_C 33.86 (C-5)/δ_C 31.97 (C-6)/δ_C 29.66 (C-8); δ_H 0.88 (H-13) to δ_C 31.97 (C-11)/δ_C 22.7 (C-12); δ_H 4.29 (H-9) to δ_C 29.66 (C-8); δ_H 3.67 (H-10) to δ_C 50.87 (C-9) displayed the side chain substitutions of the cyclohexane ring system.

In addition, ^{1}H-^{1}H COSY correlations appeared at δ_H 4.29 (H-9)/δ_H 1.72 (H-8), δ_H 2.04 (H-6)/δ_H 1.42 (H-7), which were due to the 1-methoxypropane framework attached to the cyclohexane ring system, and was in accordance with the J^{1-3} HMBC attributions. Similarly, ^{1}H-^{1}H COSY correlation appeared at δ_H 1.31 (H-12)/δ_H 0.88 (H-13), which was due to the framework attached to the cyclohexane ring system. The combined ^{1}H/^{13}C NMR demonstrated highly deshielded oxymethylene protons at δ_H 4.29 (attributed to H-9) corresponding to the carbon resonance at δ_C 50.87 (C-9) to assign the propylcyclohexane ring system and side chain substitution in C_{13} meroterpenoid. The relative stereochemistries of compound **K3** were attributed by NOESY experiments. The reference plane of the compound **K3** was arbitrarily chosen as the cyclohexane ring system. NOESY cross peaks between δ_H 2.32 (H-5)/δ_H 1.62 (H-4) suggested their close proximity, and therefore, assigned to align on an identical plane of the cyclohexane ring system with di-equatorial β-faced interaction. Intense NOESY cross peaks between δ_H 1.62 (H-4)/δ_H 2.04 (H-6) appropriately indicated their equiplaner disposition (β-orientation).

Table 4.7 NMR spectroscopic data of compound **K3** in $CDCl_3$[a]

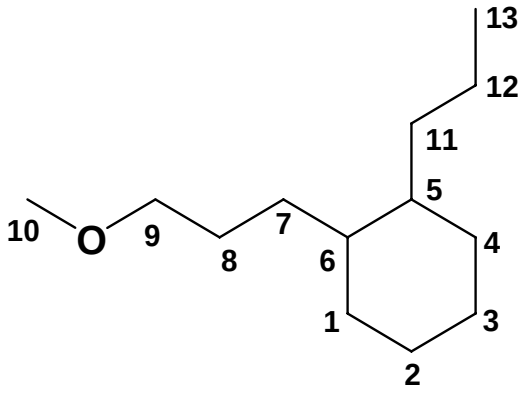

C. No	^{13}C (δ)	^{1}H-NMR[b] (int., mult., *J* in Hz)	^{1}H-^{1}H COSY	HMBC (^{1}H-^{13}C)
1	29.65	1.26 (2H, m)	-	-
2	27.23	1.26 (2H, m)	-	-
3	29.65	1.26 (2H, m)	4-H	-
4	37.10	1.62 (2H, m)	3-H, 5-H	-
5	33.86	2.32 (1H, m)	4-H, 6-H	-
6	32.38	2.04 (1H, m)	7-H	-
7	29.88	1.42 (2H, m)	6-H	C-5, C-6, C-8
8	29.66	1.72 (2H, m)	9-H	-
9	50.87	4.29 (2H, *J*=6.95 Hz, t)	8-H	C-8
10	51.45	3.67 (3H, s)	-	C-9
11	31.97	1.25 (2H, m)	-	C-12
12	22.7	1.31 (2H, m)	-	-
13	14.12	0.88 (3H, *J*=7.53 Hz, t)	12-H	C-11, C-12

[a] NMR spectra recorded using Bruker AVANCE III 500 MHz (AV 500) spectrometer in $CDCl_3$ as aprotic solvent at ambient temperature with TMS as the internal standard (δ 0 ppm).

[b] Values in ppm, multiplicity and coupling constants (*J*=Hz) are indicated in parentheses. The assignments were made with the aid of the ^{1}H-^{1}H COSY, HSQC, HMBC and NOESY experiment

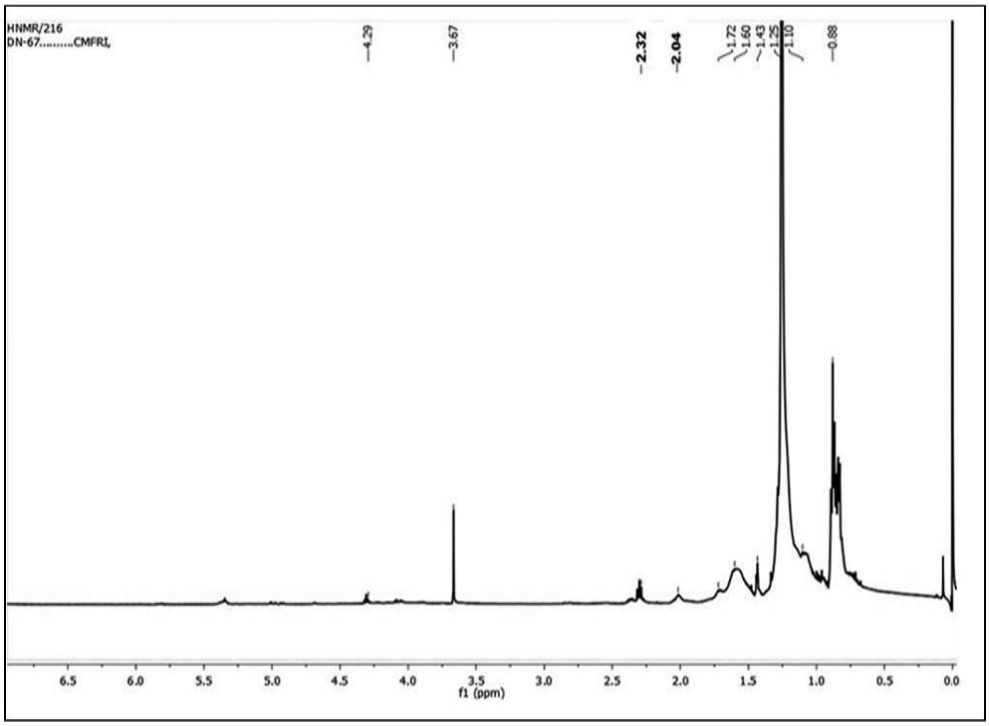

Figure 4.26. Figure showing the ^{1}H NMR spectrum of compound **K3**

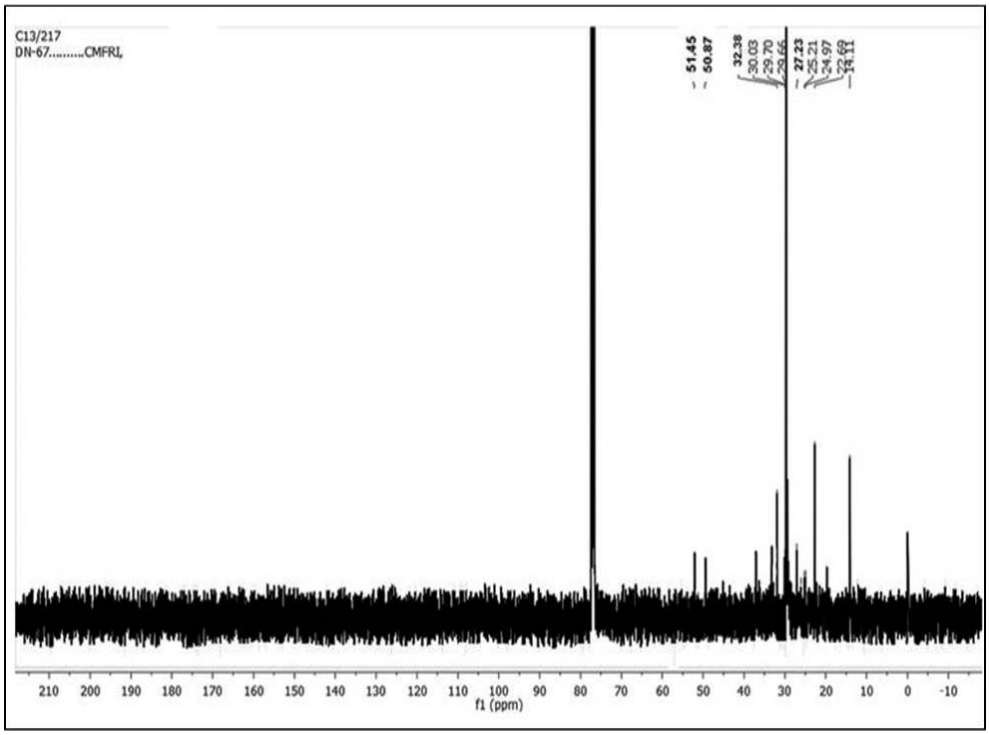

Figure 4.27. Figure showing the ^{13}C NMR spectrum of compound **K3**

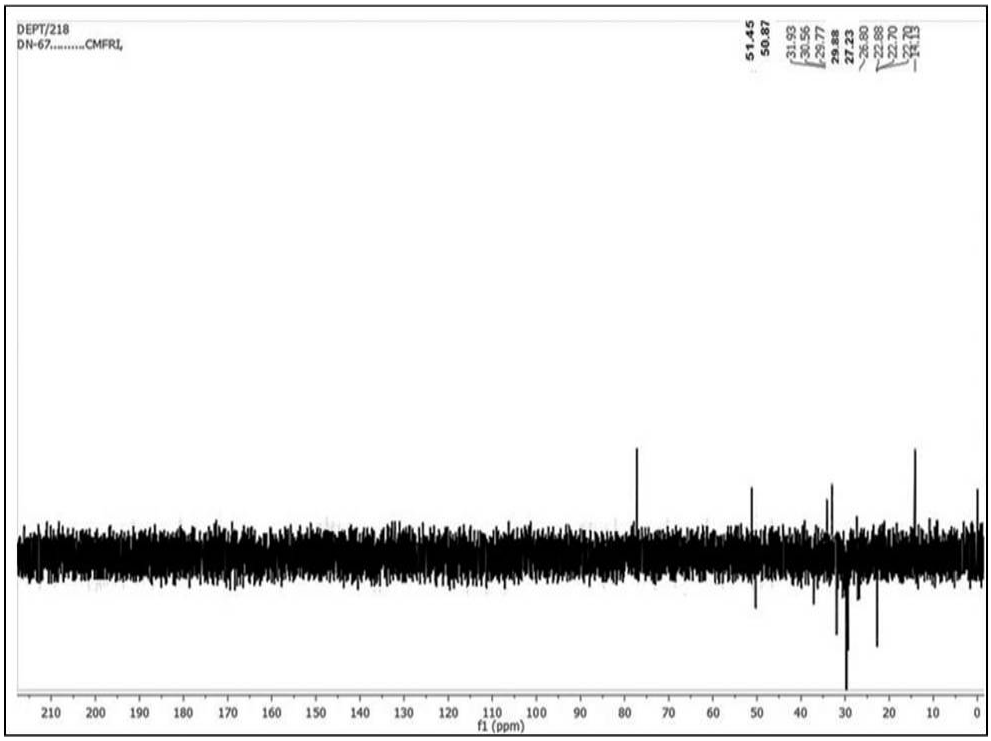

Figure 4.28. Figure showing the DEPT spectrum of compound **K3**

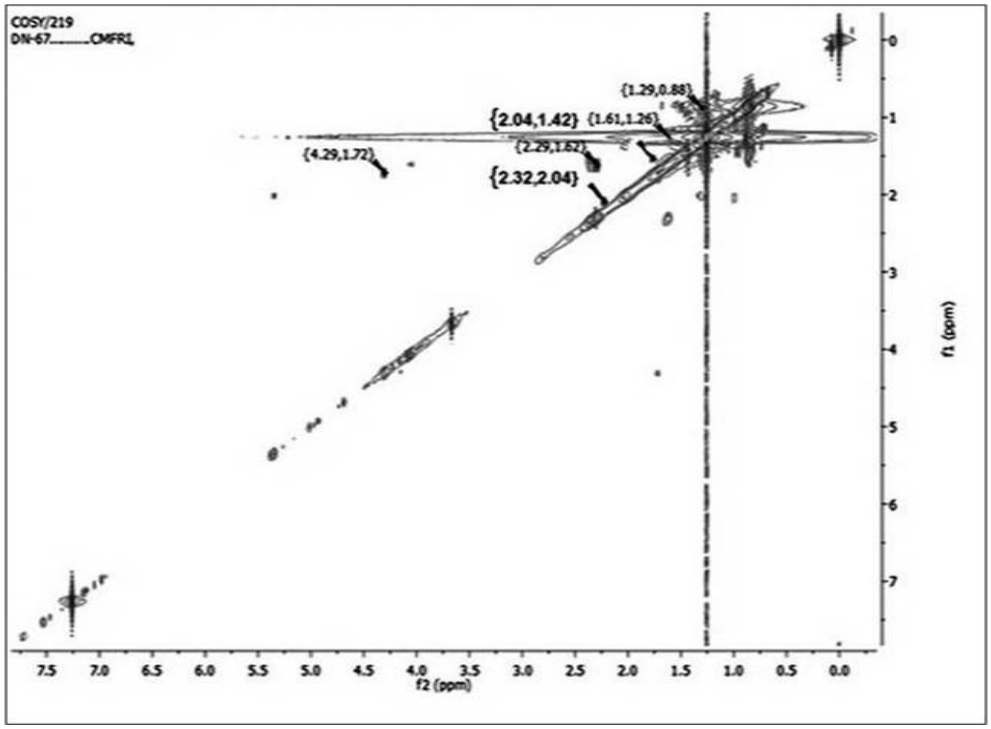

Figure 4.29. Figure showing the ^{1}H-^{1}H COSY spectrum of compound **K3**

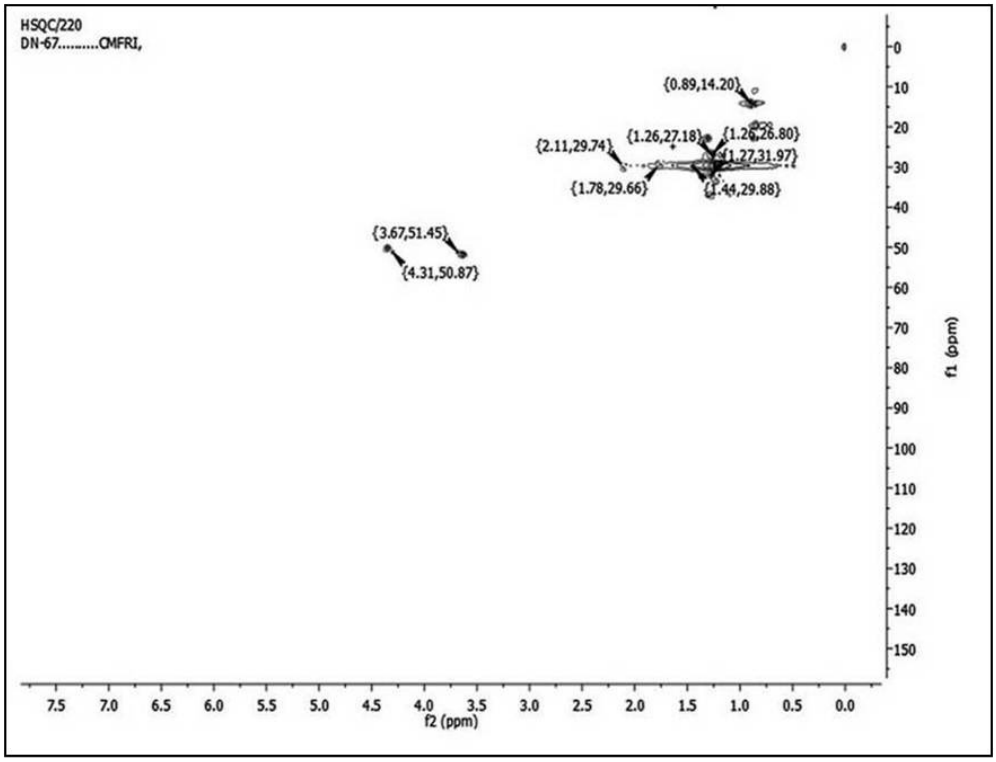

Figure 4.30. Figure showing the HSQC spectrum of compound **K3**

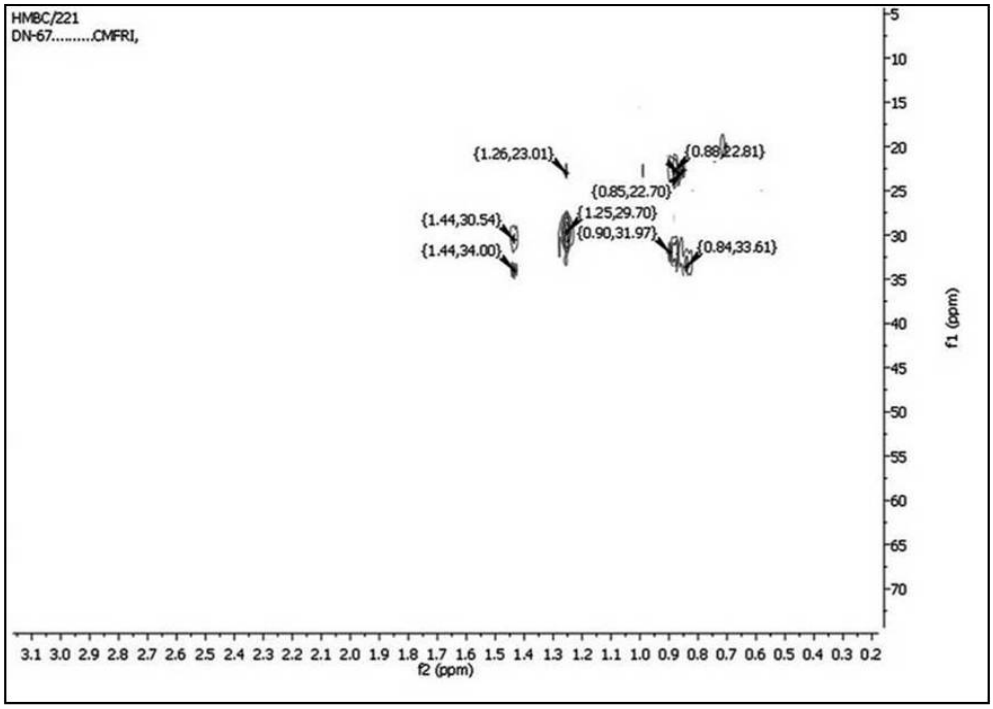

Figure 4.31. Figure showing the HMBC spectrum of compound **K3**

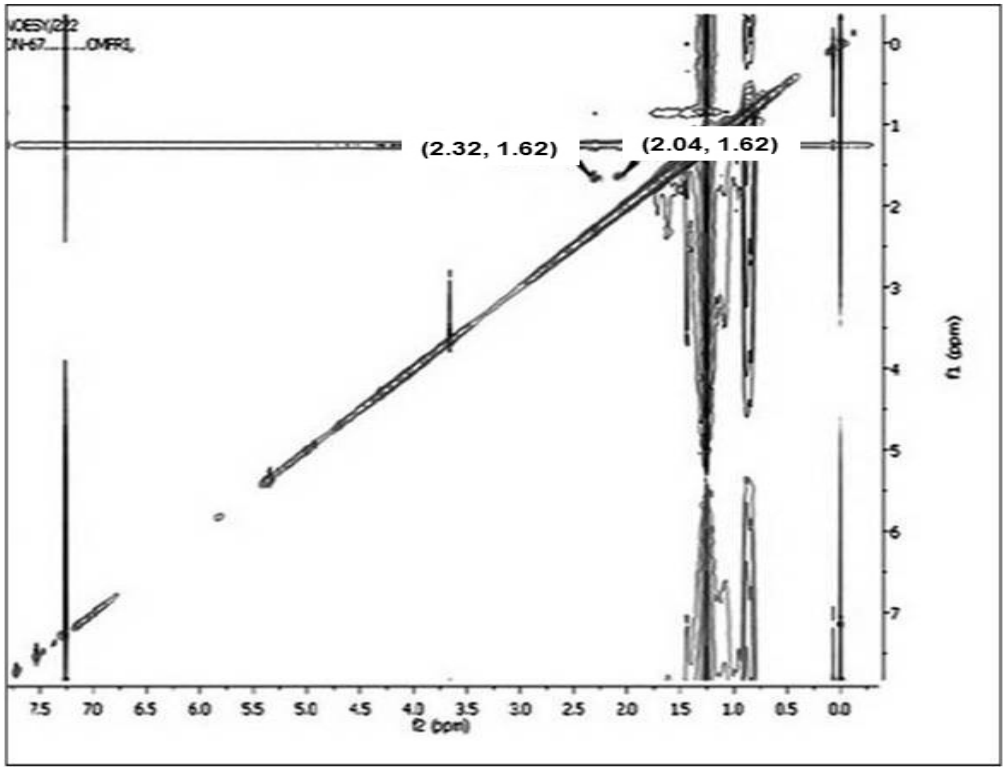

Figure 4.32. Figure showing the NOESY spectrum of compound **K3**

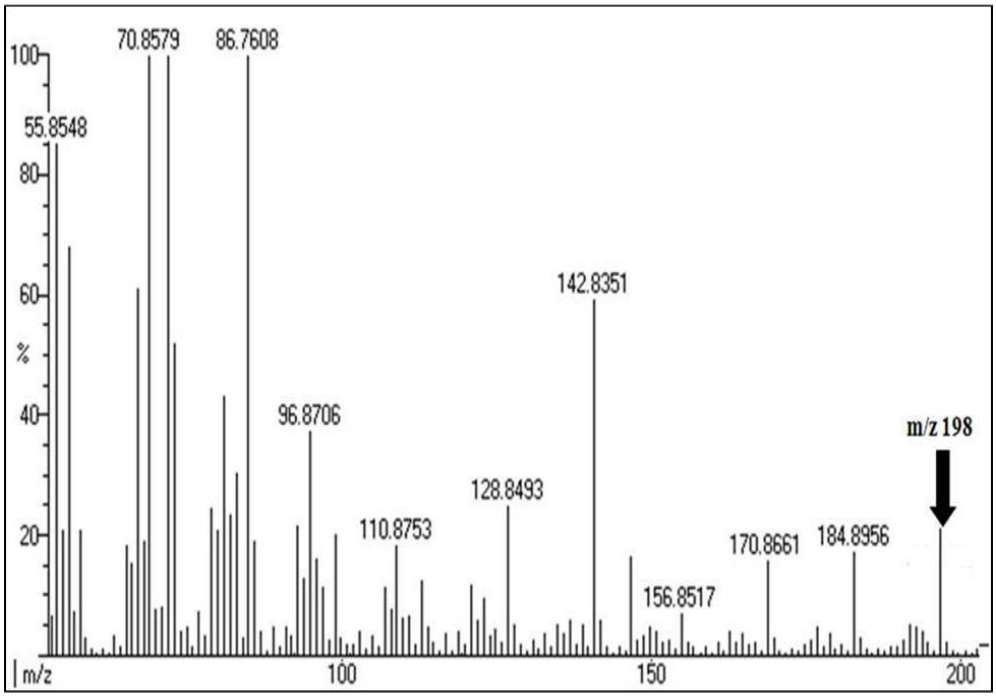

Figure 4.33. Mass spectrum of compound **K3**

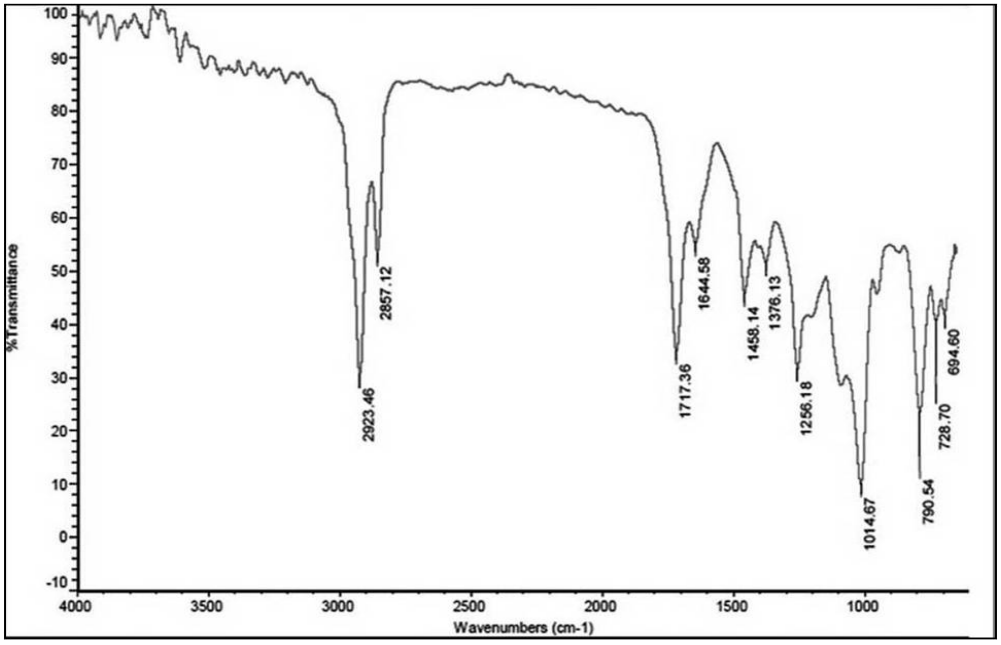

Figure 4.34. Figure showing the FTIR spectrum of compound **K3**

4.3.1.5. Structural Characterization of Compound K4

3-(Methoxymethyl) heptyl-3-(cyclohex-3-enyl) propanoate (**K4**)

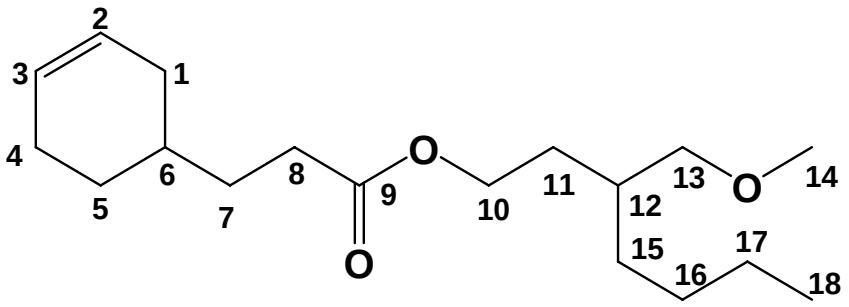

Sample yield	162 mg (1.35 %)
Physical description	Yellow oil
Molecular formula	$C_{18}H_{32}O_3$
Molecular weight	296.2354

3-(Methoxymethyl) heptyl-3-(cyclohex-3-enyl) propanoate: Yellow oil; UV $_{MeOH/DCM}$ λ_{max} (log ε): 238 nm (2.82), 262 nm (2.40); TLC (Si gel GF_{254} 15 mm; MeOH/DCM 1:99, v/v) R_f: 0.80.; R_t (HPLC, ACN: MeOH, 2:4 v/v): 14.2681 min; IR (KBr, cm^{-1}) νmax (ν = stretching, δ = bending, ρ = rocking vibrations): 724.66 (C-H ρ), 878.09 (C-H δ), 1018.99 (C-H ρ), 1114.25 (C-H δ), 1169.65 (C=C ν) 1249.94 (C-CO-C ν), 1366.49 (C=O ν), 1458.06 (C-H ν), 1743.11 (C=O ν), 2856.12 (C-H ν), 2925.01 (C-H ν); ^{1}H NMR (500 MHz $CDCl_3$): δ_H 1.94 (2H, t, *J*=6.13 Hz), δ_H 5.27 (1H, m), δ_H 5.28 (1H, m), δ_H 2.71 (2H, t, *J*=6.69 Hz), δ_H 1.65 (2H, m), δ_H 1.65 (1H, m), δ_H 1.54 (2H, m), δ_H 2.24 (2H, t, *J*=7.34 Hz), δ_H 4.05 (2H, t, *J*=6.85 Hz), δ_H 1.51 (2H, m), δ_H 2.02 (1H, m), δ_H 4.21 (2H, d, *J*=6.78 Hz), δ_H 3.59 (3H, s), δ_H 1.19 (2H, m), δ_H 1.26 (2H, m), δ_H 1.18 (2H, m), δ_H 0.80 (3H, t, *J*=6.77 Hz); ^{13}C NMR (125 MHz, $CDCl_3$): δ_C 27.15 (C-1), δ_C 129.93 (C-2), δ_C 129.92 (C-3), δ_C 25.5 (C-4), δ_C 32.73 (C-5), δ_C 40.19 (C-6), δ_C 24.97 (C-7), δ_C 34.13 (C-8), δ_C 174.37 (C-9), δ_C 62.04 (C-10), δ_C 37.61 (C-11), δ_C 31.50 (C-12), δ_C 62.20 (C-13), δ_C 51.43 (C-14), δ_C 29.56 (C-15), δ_C 28.82 (C-16), δ_C 26.34 (C-17), δ_C 14.11 (C-18); HMBC and ^{1}H-^{1}H-COSY data (Fig. 4.36 to Fig. 4.44, Table 4.8); HR (EI) MS *m/z* measured value 296.2354 $[M]^+$, calcd for $C_{18}H_{32}O_3$ 296.2351.

3-(Methoxymethyl) heptyl-3-(cyclohex-3-enyl) propanoate (compound **K4**), an oxygenated C_{18} meroterpenoid displayed the molecular ion peak at *m/z* 296 enclosing three degrees of unsaturation {due to the ester carbonyl group (δ_C 174.37), olefinic carbon at δ_C 129.92 (C-3), δ_C 129.93 (C-2) and a ring system}, and the molecular formula as $C_{18}H_{32}O_3$ based upon combined ^{1}H and ^{13}C NMR spectral data (Table 4.8). The IR-spectrum of compound **K4** displayed the presence of carbonyl group along with olefinic groups due to the bands recorded at 1458 and 2856 cm^{-1}. The ^{13}C NMR spectrum established the existence of 18 carbon signals constituting eleven methylene, two methine, along with one each of carbonyl, olefinic, methyl and methoxy carbons.

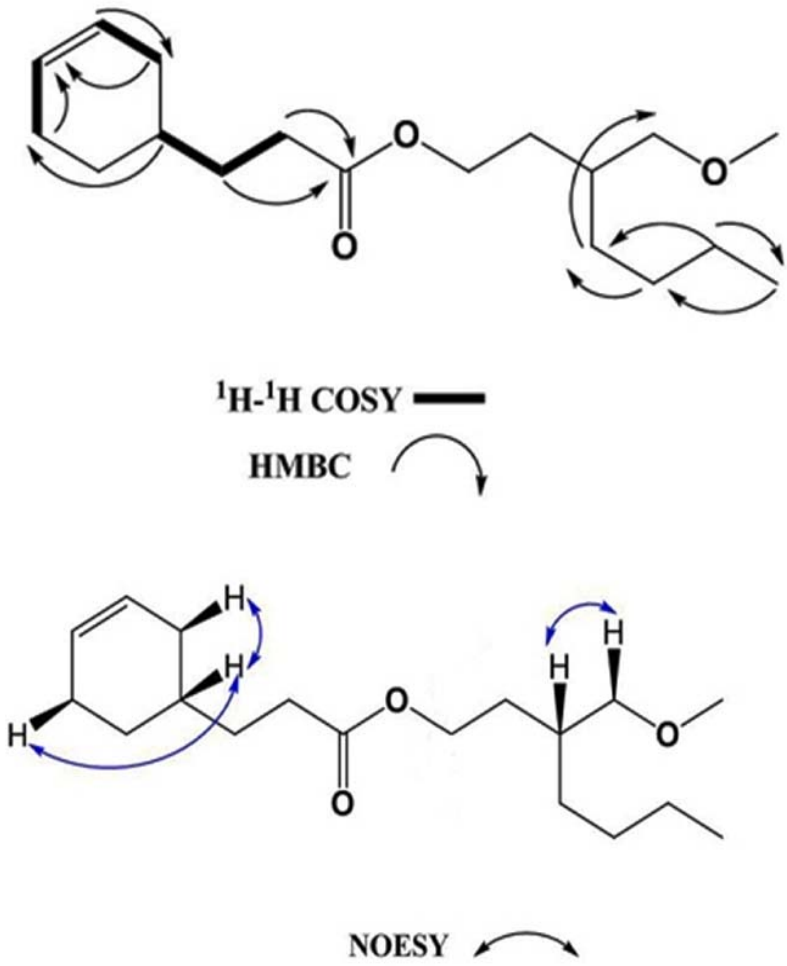

Figure 4.35. Figure showing key ^{1}H-^{1}H COSY, HMBC and NOESY correlations of compound **K4**. The ^{1}H-^{1}H COSY cross peaks were displayed by bold face bonds, whereas the selected HMBC correlations were shown as double barbed arrows. The β orientation in the NOESY relations was presented as blue colored arrows

The ^{1}H NMR in combination with ^{13}C NMR experiments demonstrated highly deshielded oxymethylene protons at H-10 (δ_H 4.05, *J*=6.85 Hz) and H-13 (δ_H 4.21, *J*=6.78 Hz) that were deduced to be correlated with the corresponding carbon signals at C-10 and C-13 methylene groups, and that was further corroborated based on the existence of an ester carbonyl {δ_C 174.37 (C-9)} and sharp singlet (integral of three) of O-CH_3 group in the NMR spectrum. The ^{1}H-^{1}H COSY correlations between δ_H 1.94 (denoted as H-1)/δ_H 5.27 (H-2) and δ_H 5.28 (assigned to H-3)/δ_H 2.71 (H-4) were

ascribed to the cyclohexane ring framework. The $J^{1\text{-}3}$ HMBC correlation between δ_H 1.94 (denoted as H-1) to δ_C 129.92 (C-3), δ_H 5.27 (H-2) to δ_C 27.15 (C-1) and δ_H 2.71 (H-4) to δ_C 129.92 (C-3) attributed the presence of cyclohexene ring system (Fig. 4.46).

The methine (-CH) carbon at C-6 (δ_C 40.19) recognized the junction of cyclohexene ring moiety and was substituted with 3-(methoxymethyl) heptyl butyrate skeleton. This was corroborated by the $^1H–^1H$ COSY and $J^{1\text{-}3}$ HMBC correlations. HMBC cross peaks between δ_H 1.54 (assigned as H-7) to δ_C 174.37 (C-9), δ_H 2.24 (H-8) to δ_C 174.37 (C-9) appropriately supported the presence of ester carbonyl carbon attached to the cyclohexene ring system. Additional $J^{1\text{-}3}$ HMBC correlations were displayed between δ_H 1.19 (assigned to H-15) to δ_C 62.20 (C-13), δ_H 1.26 (H-16) to δ_C 29.56 (C-15), δ_H 1.18 (H-17) to δ_C 29.56 (C-15)/δ_C 14.11 (C-18), δ_H 0.80 (H-18) to δ_C 28.82 (C-16), which apparently indicated the substitution of 3-(methoxymethyl) heptyl butyrate to the cyclohexene ring system. The methoxy group was found to appear as a singlet at δ_H 3.59 (attributed to H-14; HSQC δ_C 51.43 at C-14) to support the presence of 3-(methoxymethyl) heptyl butyrate framework. In addition, the olefinic group was found to appear as the multiplet at δ_H 5.27-5.28 (H2-H3) {HSQC, δ_C 129.93 (C-2), δ_C 129.92 (C-3)}, which attributed to the cyclohexene ring framework. The chemistries of the stereogenic centres bearing protons were derived using coupling constant values and NOESY experiments. An intense NOE correlation was displayed between the protons at δ_H 1.65 (H-6) and δ_H 1.94 (H-1; J=6.13 Hz)/δ_H 2.71 (H-4; J=6.69 Hz), which suggested their equi-planer disposition, and was arbitrarily attributed as β-oriented. Strong NOE correlation between δ_H 2.02 (H-12; J=6.69 Hz) and δ_H 4.21 (H-13; J=6.78 Hz) attributed the protons to dispose at the β-side of the reference plane, which suggested their diaxial orientation with reference to the plane of the symmetry.

Table 4.8 NMR spectroscopic data of compound **K4** in $CDCl_3$[a]

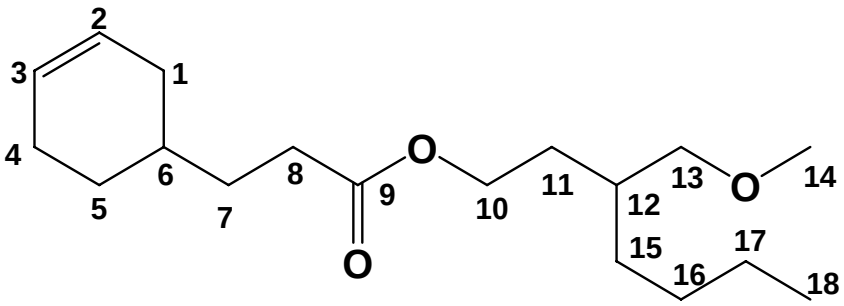

C. No	^{13}C (δ)	^{1}H-NMR[b] (int., mult., *J* in Hz)	^{1}H-^{1}H COSY	HMBC (^{1}H-^{13}C)
1	27.15	1.94 (t, *J*=6.13 Hz, 2H)	2-H	C-3
2	129.93	5.27 (m,1H)	1-H	C-1
3	129.92	5.28 (m,1H)	4-H	-
4	25.5	2.71 (t, *J*=6.69 Hz, 2H)	3-H	C-3
5	32.73	1.65 (m, 2H)	-	-
6	40.19	1.65 (m, 1H)	-	C-4
7	24.97	1.54 (m, 2H)	8-H	C-9
8	34.13	2.24 (t, *J*=7.34 Hz, 2H)	7-H	C-9
9	174.37	-	-	-
10	62.04	4.05 (t, *J*=6.85 Hz, 2H)	-	-
11	37.61	1.51 (m, 2H)	-	-
12	31.50	2.02 (m, 1H)	-	-
13	62.20	4.21 (d, *J*=6.78 Hz, 2H)	-	-
14	51.43	3.59 (s, 3H)	-	-
15	29.56	1.19 (m,2H)	-	C-13
16	28.82	1.26 (m, 2H)	-	C-15
17	26.34	1.18 (m, 2H)	-	C-15, C-18
18	14.11	0.80 (t, *J*=6.77 Hz, 3H)	-	C-16

[a] NMR spectra recorded using Bruker AVANCE III 500 MHz (AV 500) spectrometer in $CDCl_3$ as aprotic solvent at ambient temperature with TMS as the internal standard (δ 0 ppm).

[b] Values in ppm, multiplicity and coupling constants (*J*=Hz) are indicated in parentheses. The assignments were made with the aid of the ^1H-^1H COSY, HSQC, HMBC and NOESY experiment

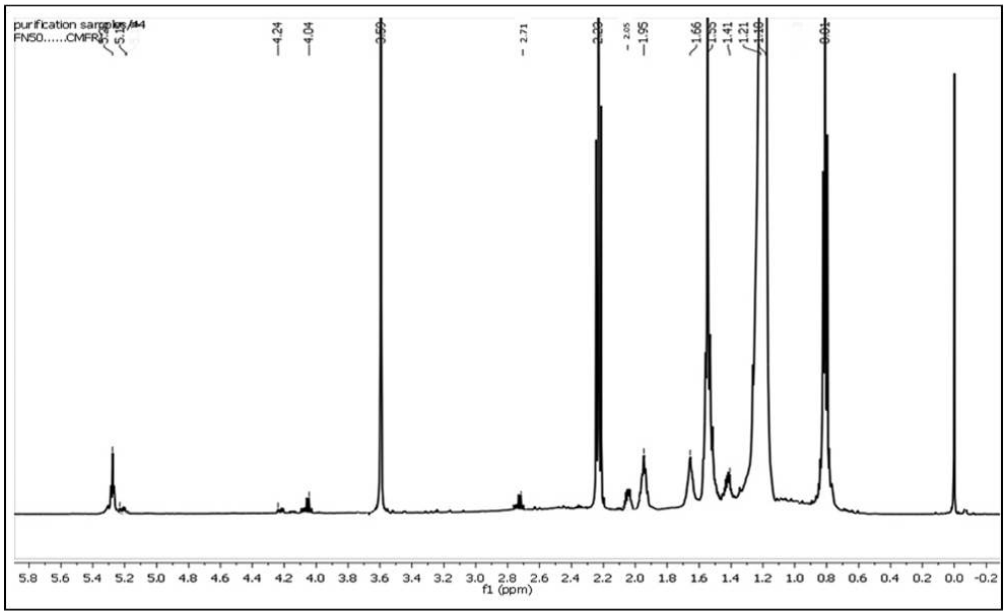

Figure 4.36. Figure showing the ^1H NMR spectrum of compound **K4**

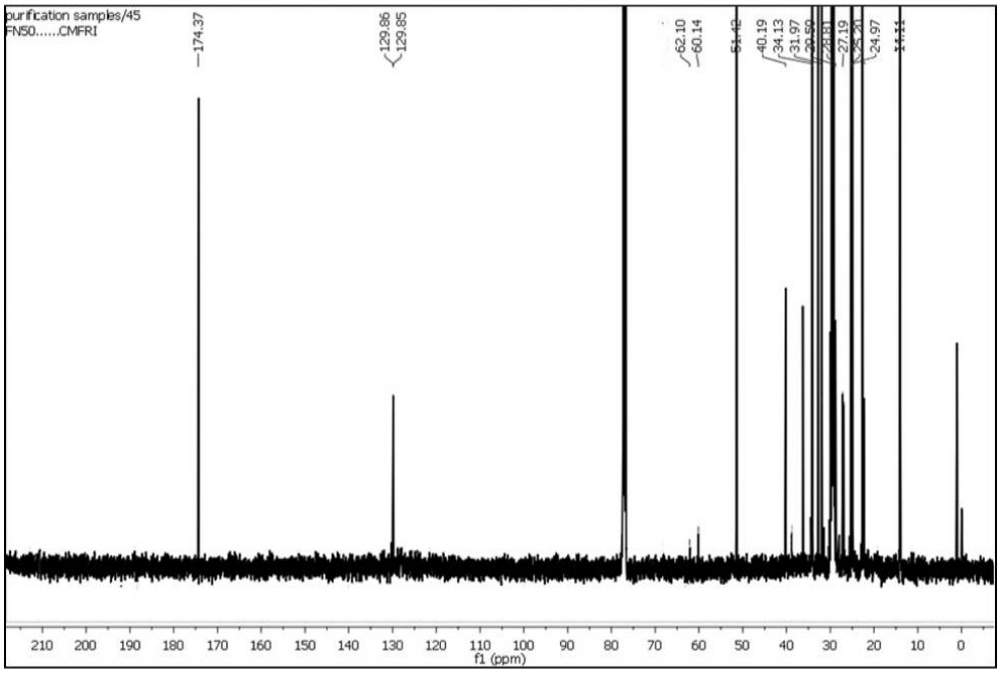

Figure 4.37. Figure showing the ^{13}C NMR spectrum of compound **K4**

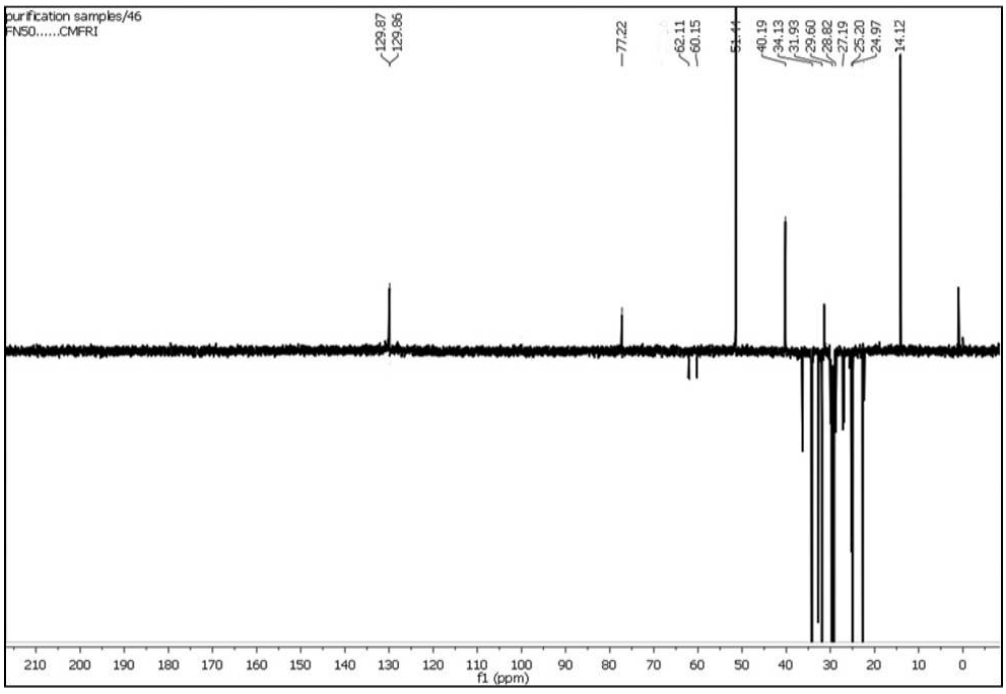

Figure 4.38. Figure showing the DEPT spectrum of compound **K4**

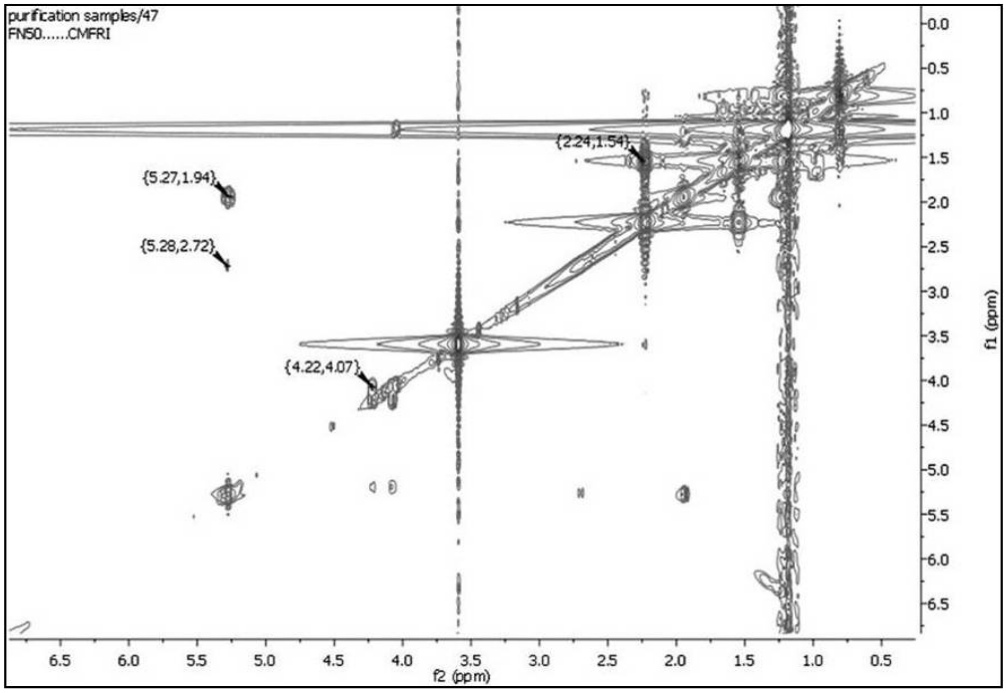

Figure 4.39. Figure showing the ^{1}H-^{1}H COSY spectrum of compound **K4**

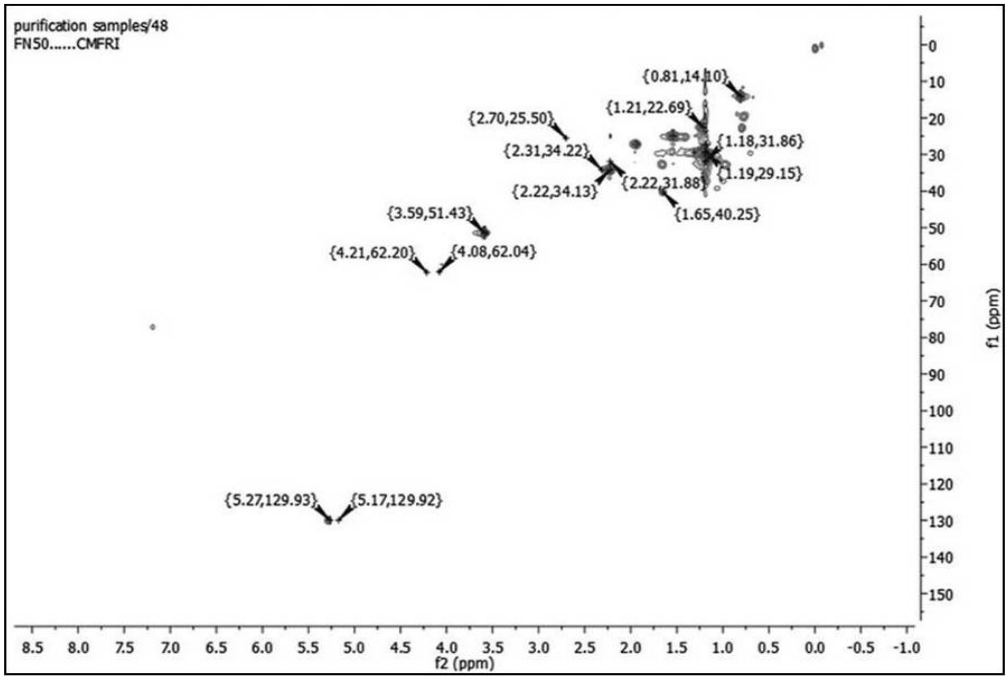

Figure 4.40. Figure showing the HSQC spectrum of compound **K4**

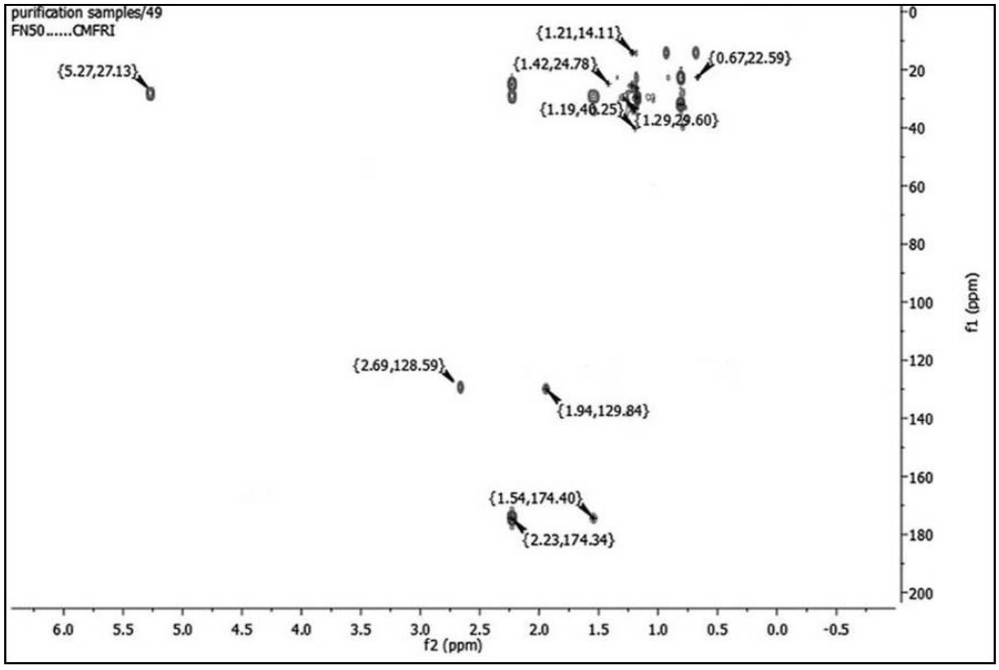

Figure 4.41. Figure showing the HMBC spectrum of compound **K4**

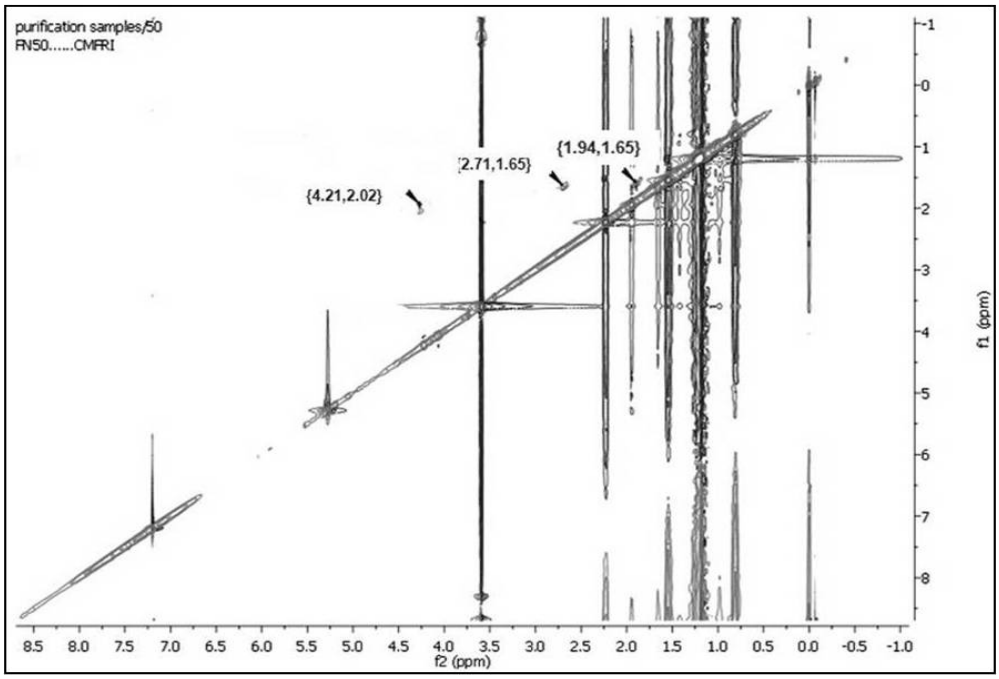

Figure 4.42. Figure showing the NOESY spectrum of compound **K4**

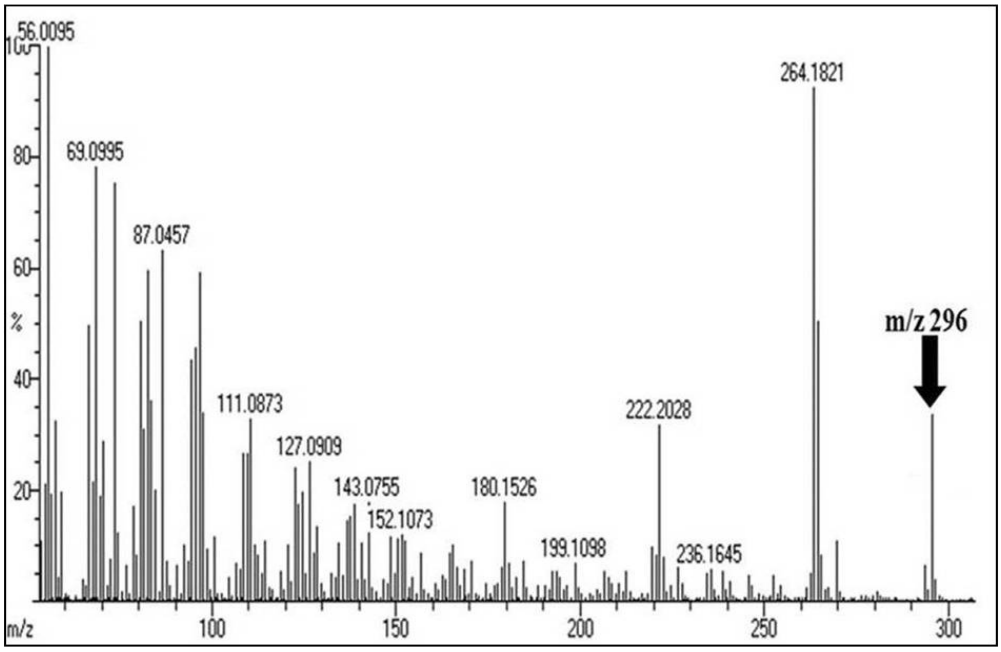

Figure 4.43. Mass spectrum of compound **K4**

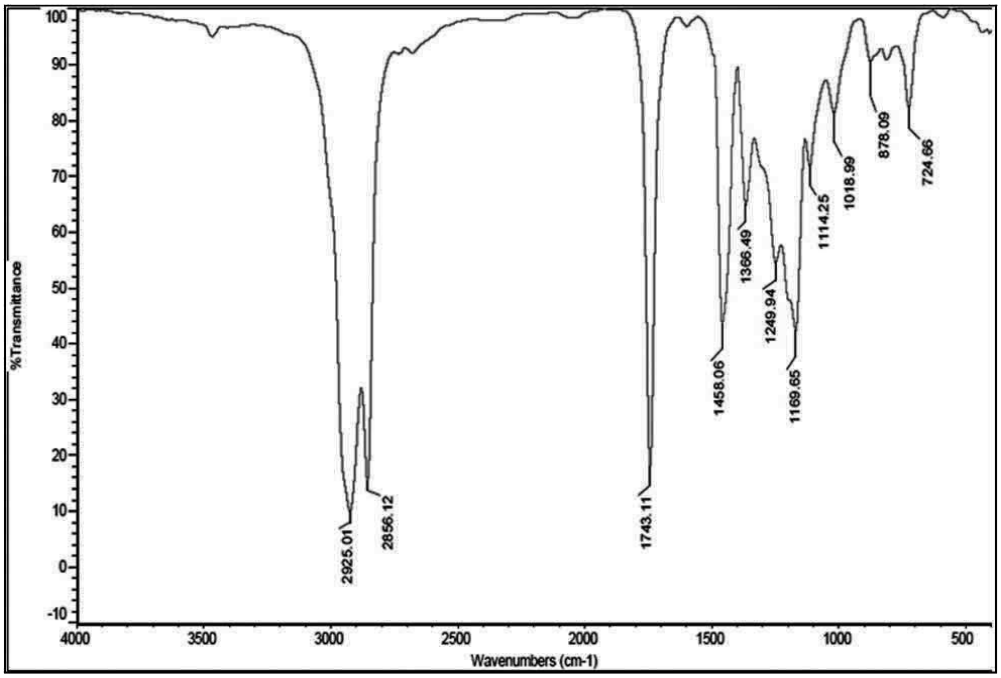

Figure 4.44. Figure showing the FTIR spectrum of compound **K4**

4.3.1.6. Structural Characterization of Compound K5

2-Ethyl-6-(4-methoxy-2-((2-oxotetrahydro-2*H*-pyran-4-yl) methyl) butoxy)-6-oxohexyl-5-ethyloct-4-enoate (**K5**)

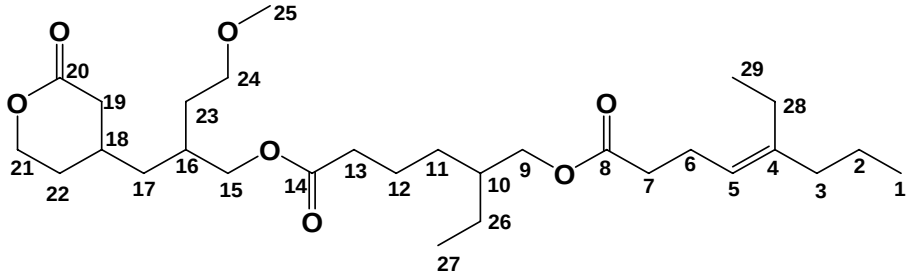

Sample yield	142 mg (1.18 %)
Physical description	Yellow oil
Molecular formula	$C_{29}H_{50}O_7$
Molecular weight	510.3557

2-Ethyl-6-(4-methoxy-2-((2-oxotetrahydro-2*H*-pyran-4-yl) methyl) butoxy)-6-oxohexyl-5-ethyloct-4-enoate : Yellow oil; UV $_{MeOH}$ λ_{max} (log ε): 245 nm (3.26); TLC (Si gel GF_{254} 15 mm; MeOH/$CHCl_3$ 1:19, v/v) R_f: 0.96; R_t (HPLC, MeOH: ACN, 2:1 v/v): 14.401 min; IR (KBr, cm^{-1}) νmax (ν = stretching, δ = bending, ρ = rocking vibrations): 738.89 (C-H ρ), 1073.42 (C-O ν), 1125.95 (CH_2 wag), 1170.14 (C-O ν), 1280.43 (CH_2 ν) 1369.88 (C-H ρ), 1455.83 (C-H δ), 1589.64 (C=C ν), 1736.56 (C=O ν), 2857.58, 2926.28 (C-H ν); ^{1}H NMR (500 MHz $CDCl_3$): δ_H 0.87 (3H, t, *J*=6.80 Hz), δ_H 1.30 (2H, m), δ_H 2.02 (2H, m), δ_H 5.35 (1H, t, *J*=5.68 Hz), δ_H 2.02 (2H, m), δ_H 2.32 (2H, t, *J*=7.80 Hz), δ_H 4.16 (2H, d, *J*=5.80 Hz), δ_H 1.73 (1H, m), δ_H 1.27 (2H, m), δ_H 1.62 (2H, m), δ_H 2.32 (2H, t, *J*=7.80 Hz), δ_H 4.26 (2H, d, *J*=9.08 Hz), δ_H 2.49 (1H, m), δ_H 1.50 (2H, m), δ_H 1.69 (1H, m), δ_H 2.32 (2H, t, *J*=7.80 Hz), δ_H 4.19 (2H, t, *J*=9.08 Hz), δ_H 1.69 (2H, m), δ_H 1.73 (2H, m), δ_H 4.30 (2H, t, *J*=7.44 Hz), δ_H 3.67 (3H, s), δ_H 1.42 (2H, m), δ_H 0.85 (3H, t, *J*=6.80 Hz), δ_H 2.13 (2H, m), δ_H 0.87 (3H, t, *J*=7.17 Hz); ^{13}C NMR (125 MHz, $CDCl_3$): δ_C 14.20 (C-1), δ_C 25.12 (C-2), δ_C 28.24 (C-3), δ_C 132.45 (C-4), δ_C 130.08 (C-5), δ_C 34.11 (C-6), δ_C 29.67 (C-7), δ_C 174.56 (C-8), δ_C 62.17 (C-9), δ_C 40.19 (C-10), δ_C 29.65 (C-11), δ_C 28.99 (C-12), δ_C 24.98 (C-13), δ_C 168.33 (C-14),

δ_C 68.24 (C-15), δ_C 34.39 (C-16), δ_C 29.26 (C-17), δ_C 38.88 (C-18), δ_C 32.14 (C-19), δ_C 173.48 (C-20), δ_C 60.14 (C-21), δ_C 30.78 (C-22), δ_C 32.73 (C-23), δ_C 65.68 (C-24), δ_C 51.42 (C-25), δ_C 29.85 (C-26), δ_C 19.70 (C-27), δ_C 30.07 (C-28), δ_C 22.80 (C-29) HMBC and ^{1}H-^{1}H-COSY data (Fig. 4.47 to Fig. 4.55, Table 4.9); HR (EI) MS *m/z* measured value 510.3557 $[M]^+$, calcd for $C_{29}H_{50}O_7$ 510.3552.

2-Ethyl-6-(4-methoxy-2-((2-oxotetrahydro-2*H*-pyran-4-yl) methyl) butoxy)-6-oxohexyl-5-ethyloct-4-enoate (compound **K5)**, a highly oxygenated C_{29} meroterpenoid, was purified as yellow oil with *m/z* 510 bearing five degrees of unsaturation, and its structure was characterized by combined ^{1}H and ^{13}C NMR spectral experiments. The IR bending vibration near 1736 cm^{-1} was associated with the carbonyl group, whereas the olefinic groups were assigned to the absorption bands at 1455 cm^{-1} and 2857 cm^{-1}. The ^{13}C NMR spectroscopic data deduced the existence of 29 carbon signals constituting three each of methyl, methylene and ester carbonyl groups along with seventeen methylene and one each of olefinic and methoxy carbons.

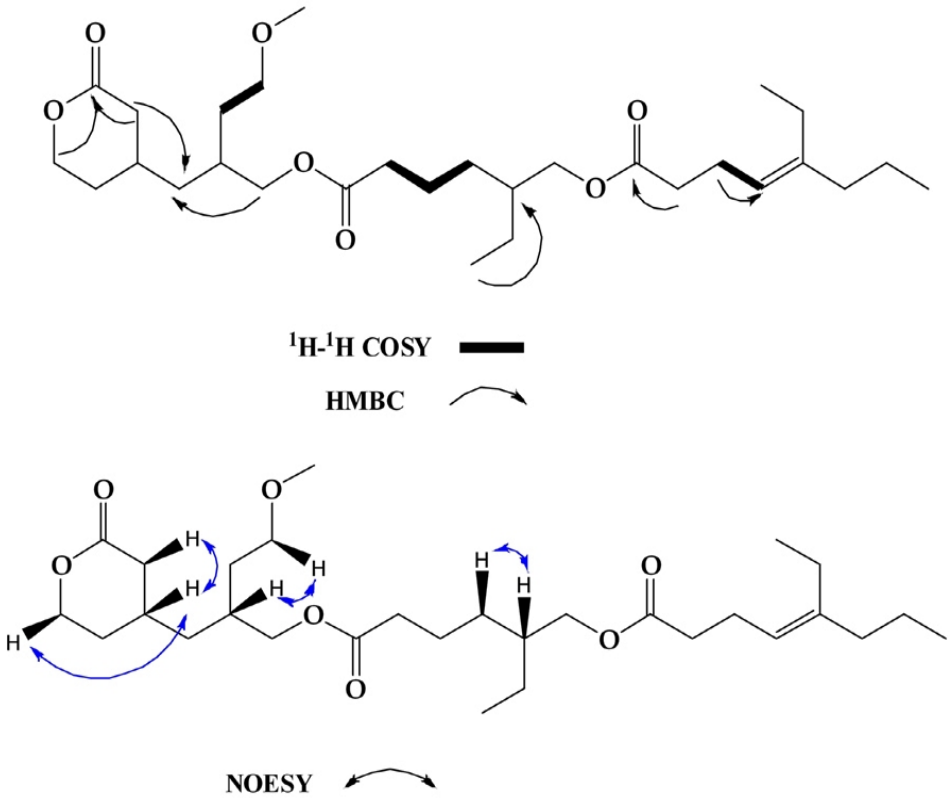

Figure 4.45. Key ^{1}H-^{1}H COSY, HMBC and NOESY correlations of compound **K5.** The ^{1}H-^{1}H COSY cross peaks were displayed by bold face bonds, whereas the selected

HMBC correlations were shown as double barbed arrows. The β orientation in the NOESY relations was presented as blue colored arrows. The ^{1}H NMR in combination with ^{13}C NMR demonstrated highly deshielded oxymethylene protons at δ_H 4.16 (attributed to H-9, *J*=5.80 Hz), δ_H 4.19 (H-21, *J*=9.08 Hz), δ_H 4.26 (H-15, *J*=9.08 Hz) and δ_H 4.30 (H-24, *J*=7.44 Hz) in the proton spectrum suggesting that the C-24, C-21, C-15 and C-9 methylene groups were attached to an electronegative group, possibly of oxygenated origin. This was further corroborated by the presence of ester carbonyl carbons {δ_C 174.56 (assigned to C-8), δ_C 168.33 (C-14), δ_C 173.48 (C-20)} and a singlet (integral of three) of O-CH_3 group {δ_C 51.42 (C-25)}, in the NMR spectrum. The proton-proton connections were apparent between δ_H 1.73 (ascribed to H-23)/δ_H 4.30 (H-24) that assigned the part of a tetrahydro-2*H*-pyran-2-one ring framework. The J^{1-3} HMBC correlations between δ_H 2.32 (ascribed to H-7) to δ_C 174.56 (C-8), δ_H 4.26 (H-15) to δ_C 29.26 (C-17), δ_H 4.19 (H-21) to δ_C 173.48 (C-20) and δ_H 2.32 (H-19) to δ_C 29.26 (C-17)/173.48 appropriately deduced the existence of highly deshielded oxymethylene protons and ester carbonyl carbon as part of the tetrahydro-2*H*-pyran-2-one ring framework. The ^{1}H–^{1}H COSY correlation between δ_H 1.27 (ascribed to H-11)/δ_H 1.62 (H-12)/δ_H 2.32 (H-13) were probably attributed to the part of substituted tetrahydro-2*H*-pyranone ring system (Fig. 4.56). In addition, an olefinic group was found to appear as the multiplet at δ_H 5.35 (H-4/H-5) {HSQC, δ_C 132.45 (C-4) and δ_C 130.08 (C-5)}, which was situated at the extended side chain of compound **K5**. The ^{1}H-^{1}H correlation between δ_H 5.35 (denoted as H-5)/δ_H 2.02 (H-6) and a HMBC correlation between δ_H 2.02 (assigned as H-6) to δ_C 130.08 (C-5) appropriately established the existence of the olefinic group (Fig. 4.56). The HMBC correlation from δ_H 1.42 (assigned as H-26) to δ_C 29.85 (C-10) deduced the substitution of 2-ethyl-6-(2-ethyl-4-methoxybutoxy)-6-oxohexyl-5-ethyloct-4-enoate to the pyran-2-one ring system in compound **K5**. The methoxy group was found to appear as singlet at δ_H 3.67 {attributed to H-25; HSQC δ_C 51.42 (C-25)}, which described the 2-ethyl-6-(2-ethyl-4-methoxybutoxy)-6-oxohexyl-5-ethyloct-4-enoate framework. The relative stereochemistries of the stereogenic centres in compound **K5** were deduced by NOESY experiments and coupling constant values (*J*). NOE cross peaks at δ_H 1.69 (H-18)/δ_H 4.19 (H-21; *J*=9.08 Hz)/δ_H 2.32 (H-19; *J*=7.80 Hz) appropriately suggested their close proximity and equi-planer orientation (arbitrarily assigned to β-faced). NOE correlation between the di-equatorial protons at δ_H 4.30 (H-24; *J*=7.44 Hz)/δ_H 2.49 (H-16) apparently attributed to their close spatial arrangements, and therefore, were assigned to

be at the β-face with reference to the molecular plane of symmetry. Likewise, an intense NOE correlation was observed between δ_H 1.73(H-10)/δ_H 1.27 (H-11) that implied their deposition on the same side of the plane with di-axial interaction.

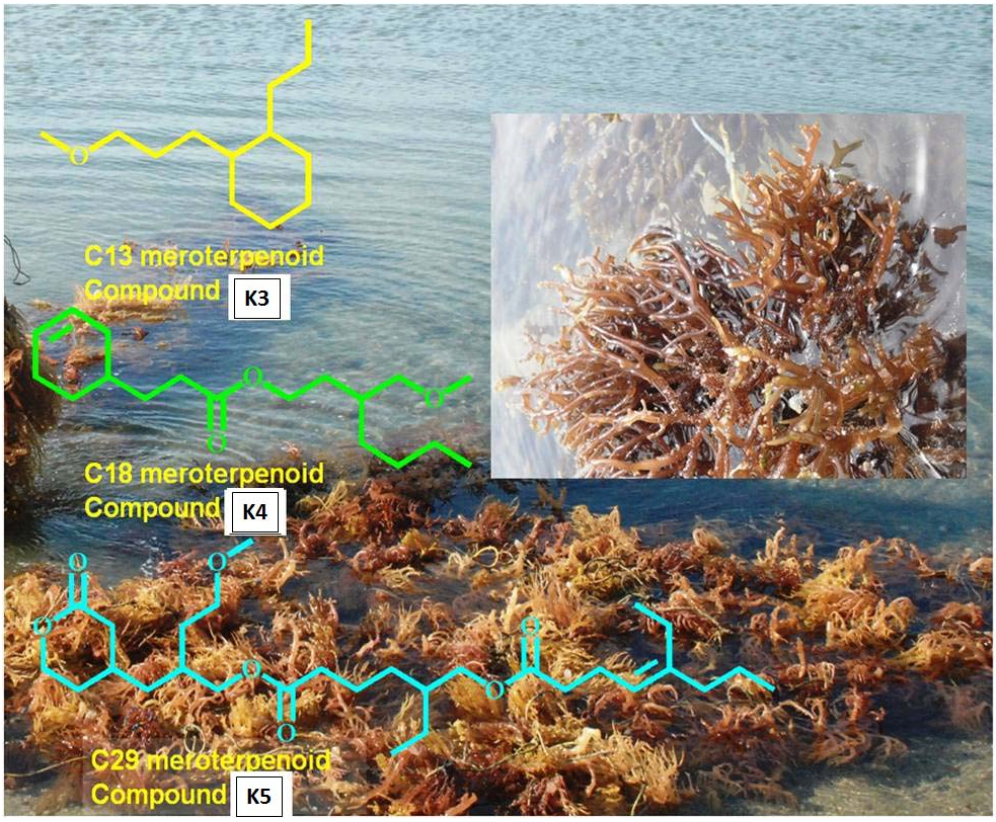

Figure 4.46. Oxygenated meroterpenoids, isolated from red marine macroalga *K. alvarezii.* The thalli of the studied macroalga were displayed as inset

Table 4.9 NMR spectroscopic data of compound **K5** in $CDCl_3$[a]

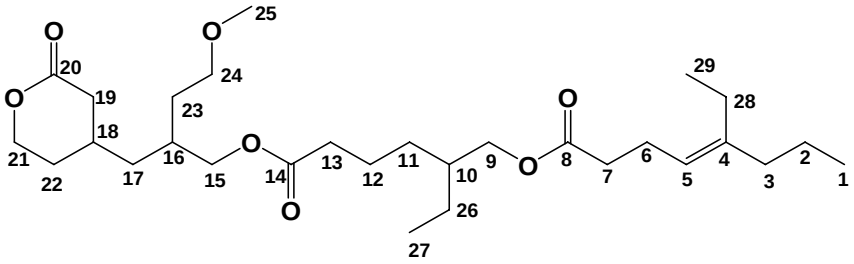

C. No	^{13}C (δ)	^{1}H-NMR[b] (int., mult., *J* in Hz)	^{1}H-^{1}H COSY	HMBC (^{1}H-^{13}C)
1	14.20	0.87(3H, *J*=6.80 Hz, t)		-
2	25.12	1.30 (2H, m)	-	-
3	28.24	2.02 (2H, m)	-	-
4	132.45	-	-	-
5	130.08	5.35 (1H, *J*=5.68 Hz, t)	6-H	-
6	34.11	2.02 (2H, m)	5-H	C-5
7	29.67	2.32 (2H, *J*=7.80 Hz, t)	-	C-8
8	174.56	-	-	-
9	62.17	4.16 (2H, *J*=5.80 Hz, d)	-	-
10	40.19	1.73 (1H, m)	-	-
11	29.65	1.27 (2H, m)	12-H	-
12	28.99	1.62 (2H, m)	11-H, 13-H	-
13	24.98	2.32 (2H, *J*=7.80 Hz, t)	12-H	-
14	168.33	-	-	-
15	68.24	4.26 (2H, *J*=9.08 Hz, d)	-	C-17
16	34.39	2.49 (1H, m)	-	-
17	29.26	1.50 (2H, m)	-	-
18	38.88	1.69 (1H, m)	-	-
19	32.14	2.32 (2H, *J*=7.80 Hz, t)	-	C-20, C-17
20	173.48	-	-	-
21	60.14	4.19 (2H, *J*=9.08 Hz, t)	-	C-20
22	30.78	1.69 (2H, m)	-	-
23	32.73	1.73 (2H, m)	24-H	-
24	65.68	4.30 (2H, *J*=7.44 Hz, t)	23-H	-
25	51.42	3.67 (3H, s)	-	-
26	29.85	1.42 (2H, m)	-	C-10
27	19.70	0.85 (3H, *J*=6.80 Hz, t)		
28	30.07	2.13 (2H, m)	-	–
29	22.80	0.87 (3H, *J*=7.17 Hz, t)	-	-

[a] NMR spectra recorded using Bruker AVANCE III 500 MHz (AV 500) spectrometer in $CDCl_3$ as aprotic solvent at ambient temperature with TMS as the internal standard (δ 0 ppm).

[b] Values in ppm, multiplicity and coupling constants (*J*=Hz) are indicated in parentheses. The assignments were made with the aid of the ^1H-^1H COSY, HSQC, HMBC and NOESY experiment

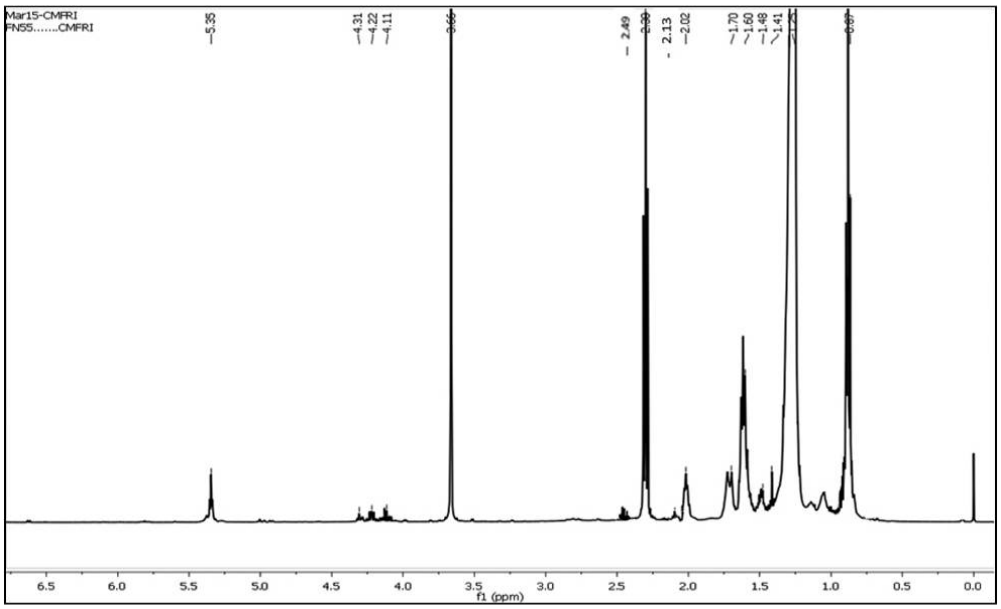

Figure 4.47. Figure showing the ^1H NMR spectrum of compound **K5**

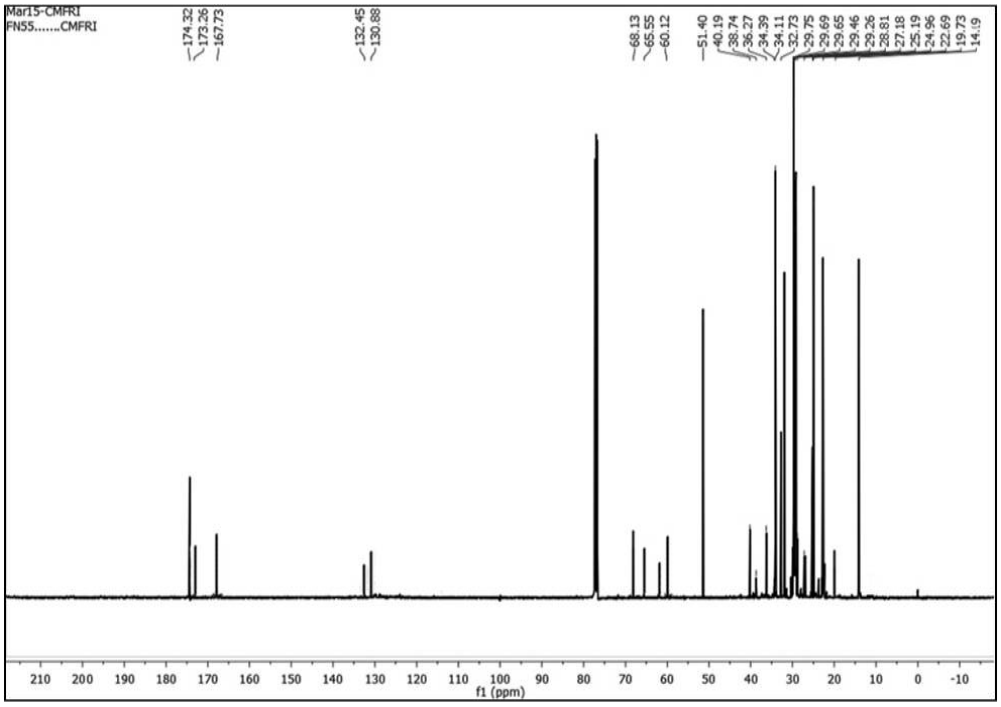

Figure 4.48. Figure showing the ^{13}C NMR spectrum of compound **K5**

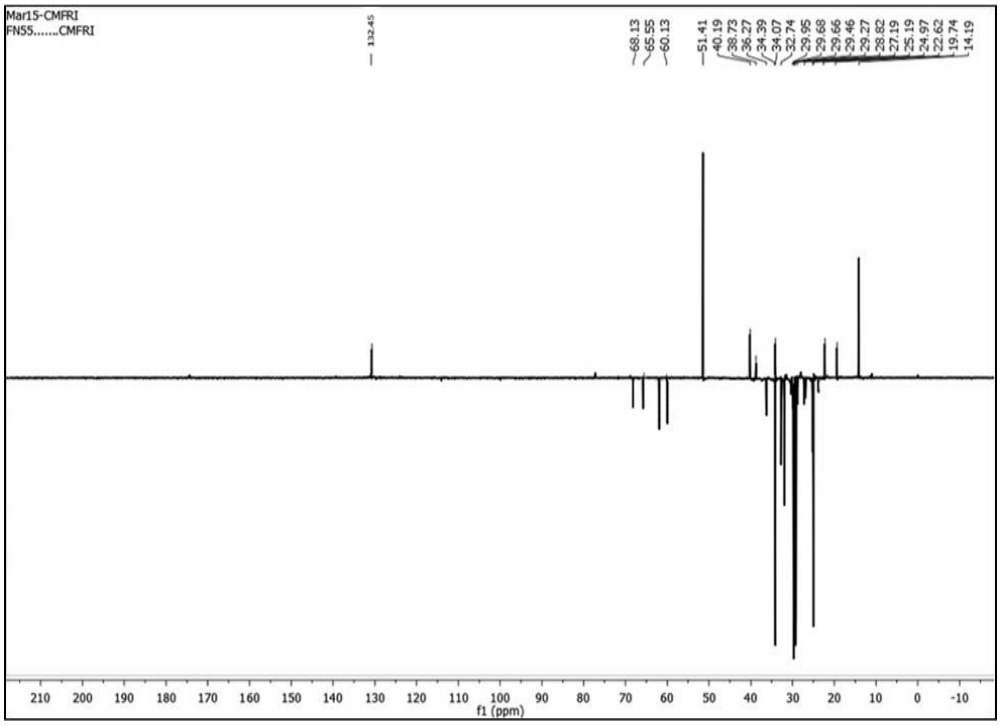

Figure 4.49. Figure showing the DEPT spectrum of compound **K5**

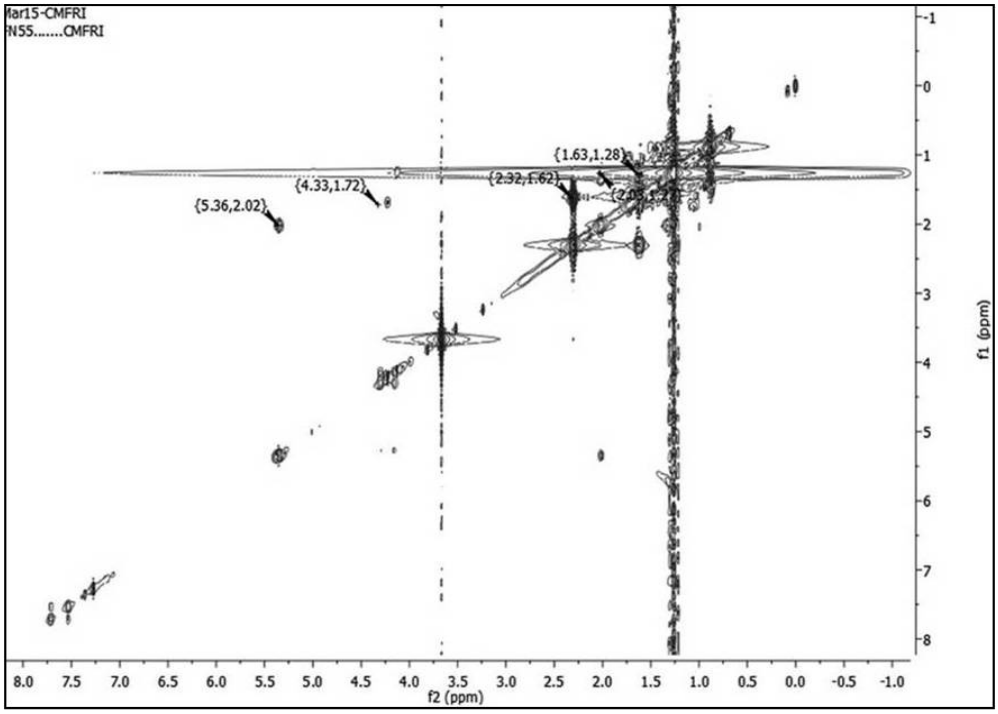

Figure 4.50. Figure showing the ^{1}H-^{1}H COSY spectrum of compound **K5**

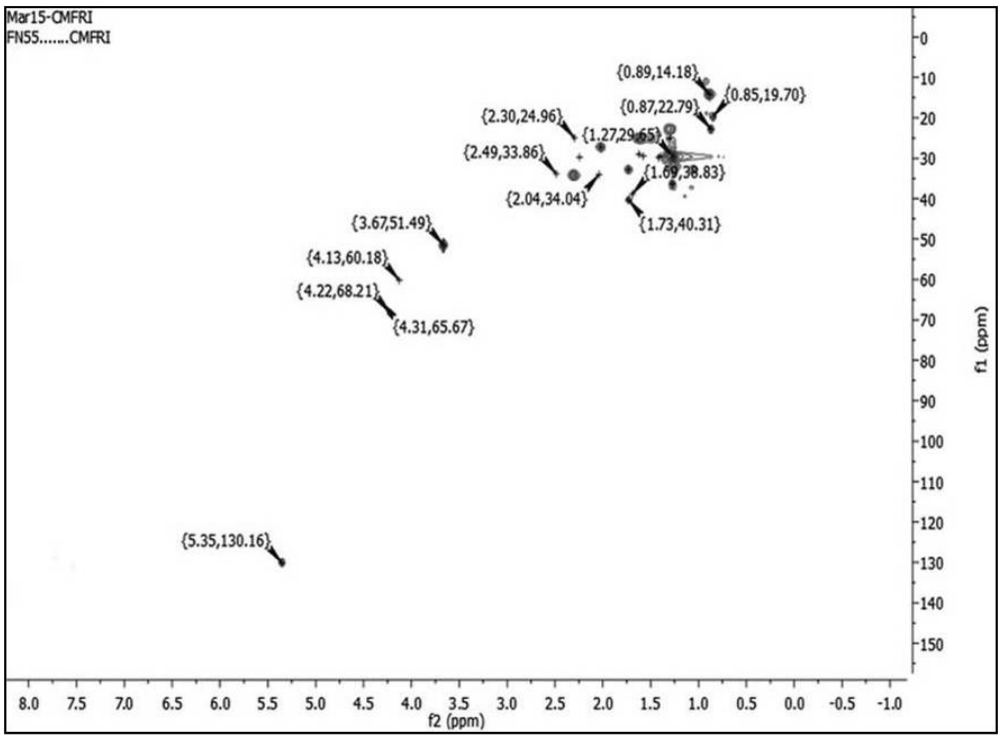

Figure 4.51. Figure showing the HSQC spectrum of compound **K5**

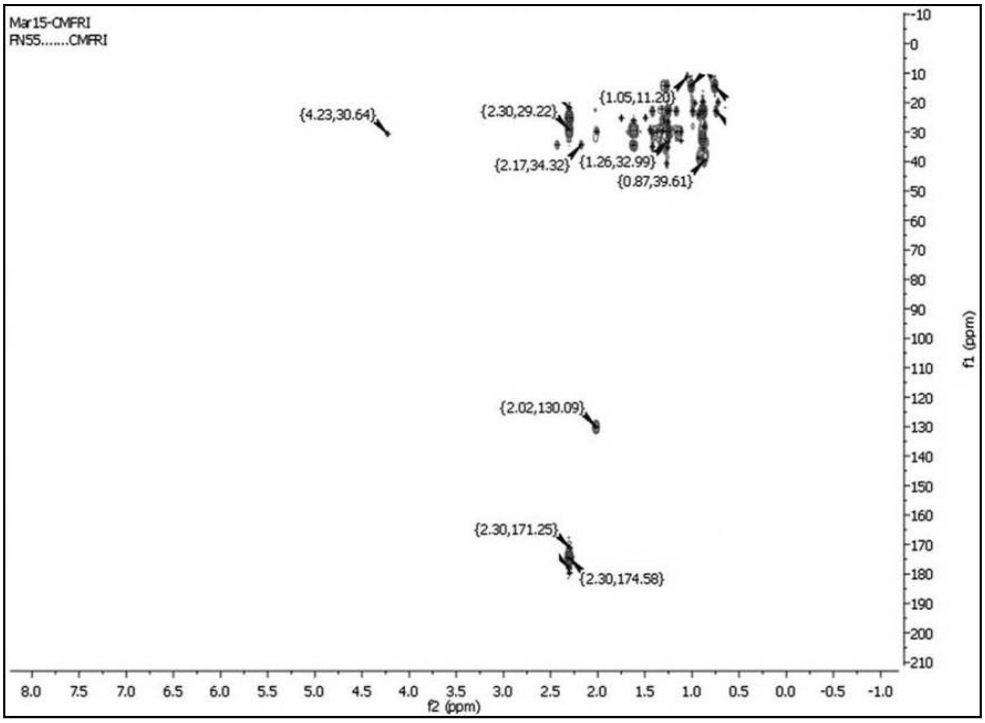

Figure 4.52. Figure showing the HMBC spectrum of compound **K5**

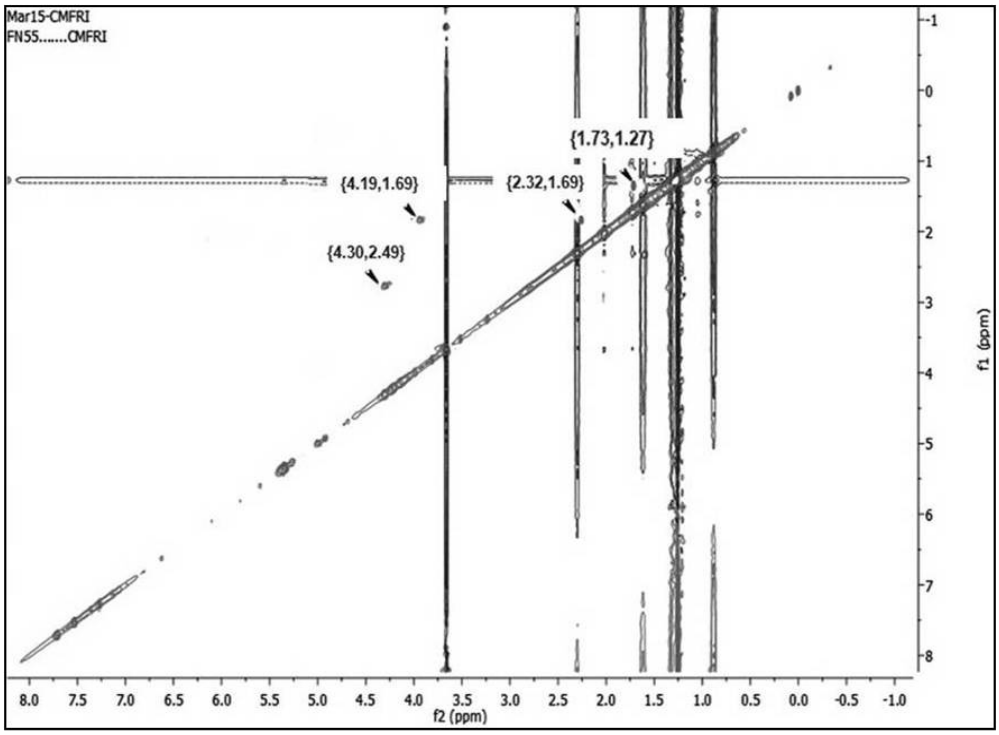

Figure 4.53. Figure showing the NOESY spectrum of compound **K5**

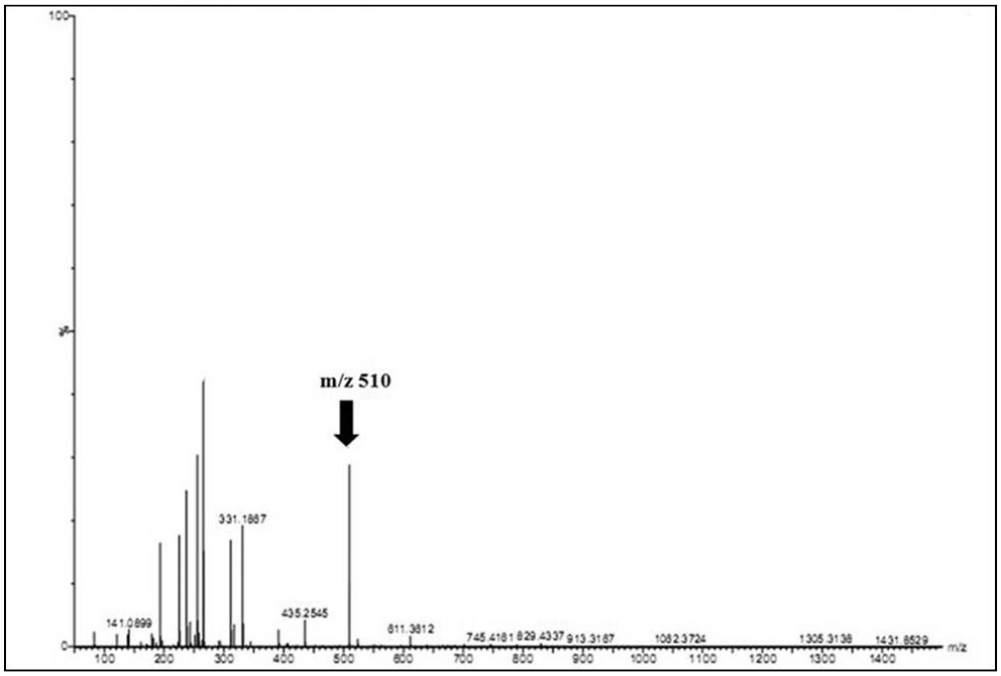

Figure 4.54. Mass spectrum of compound **K5**

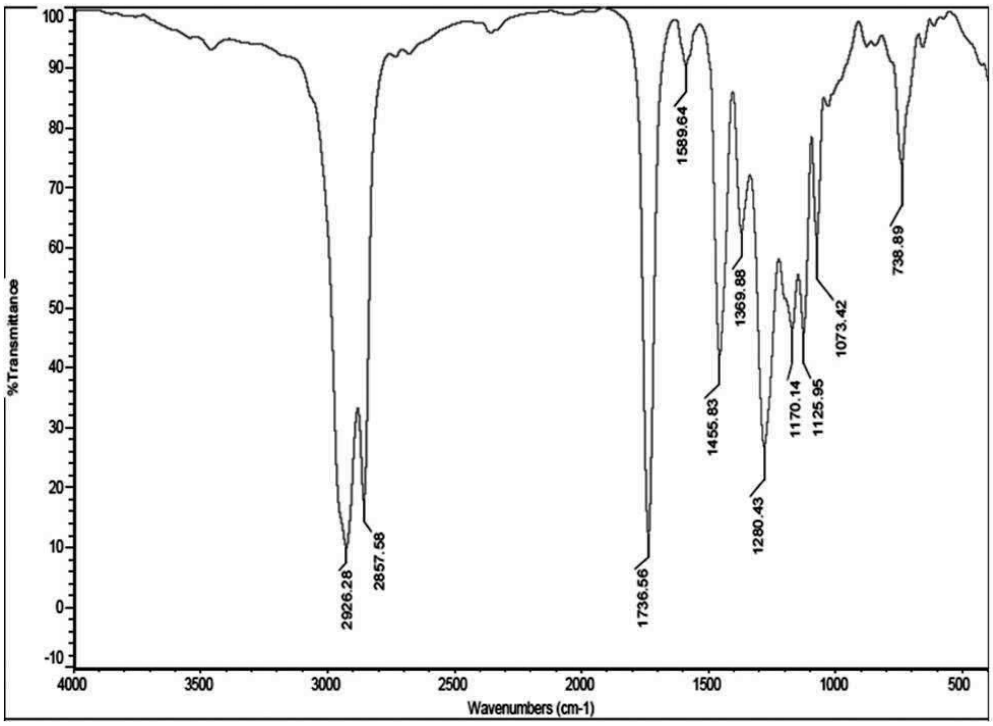

Figure 4.55. Figure showing the FTIR spectrum of compound **K5**

Table 4.10 Antioxidative and anti-inflammatory activities of the meroterpenoids isolated from *K. alvarezii vis-à-vis* the commercial agents

	Pharmacological activities {IC_{50} (mg/mL)}					
Antioxidative activities*	**Compound K3**	**K4**	**K5**	**BHA**	**BHT**	**α-tocopherol**
$DPPH^{\cdot}$ scavenging	$0.70^{a} \pm 0.01$	$0.52^{a} \pm 0.06$	$0.31^{a} \pm 0.03$	$0.26^{b} \pm 0.01$	$0.25^{b} \pm 0.02$	$0.63^{c} \pm 0.04$
$ABTS^{+\cdot}$ scavenging	$0.72^{a} \pm 0.11^{a}$	$0.58^{a} \pm 0.15^{a}$	$0.34^{a} \pm 0.13^{a}$	$0.34^{b} \pm 0.02$	$0.26^{b} \pm 0.02$	$0.73^{c} \pm 0.05$
Anti-inflammatory activities*	**Compound K3**	**K4**	**K5**	**Aspirin**	**Na-salicylate**	**Ibuprofen**
COX -1 inhibition	$1.20^{a} \pm 0.03$	$1.18^{a} \pm 0.04$	$1.12^{a} \pm 0.02$	$0.005^{a} \pm 0.00$	$1.93^{c} \pm 0.05$	$0.04^{a} \pm 0.00$
COX -2 inhibition	$1.09^{a} \pm 0.06$	$1.08^{a} \pm 0.09$	$1.05^{a} \pm 0.07$	$0.21^{b} \pm 0.02$	$2.65^{c} \pm 0.05$	$0.09^{a} \pm 0.02$
Selectivity Index**	$1.10^{a} \pm 0.06$	$1.09^{a} \pm 0.09$	$1.06^{a} \pm 0.07$	$0.02^{b} \pm 0.02$	$0.72^{c} \pm 0.05$	$0.44^{a} \pm 0.02$
5-LOX inhibition	$1.14^{a} \pm 0.05$	$1.10^{a} \pm 0.04$	$1.04^{a} \pm 0.02$	$0.39^{a} \pm 0.02$	$1.75^{c} \pm 0.12$	$0.93^{b} \pm 0.11$

* The bioactivities were expressed as IC_{50} values (mg/mL). The samples were analyzed in triplicate (n=3) and expressed as a mean ± standard deviation. Means followed by the different superscripts (a–c) within the same row indicate significant differences ($P < 0.05$).

**Selectivity index has been calculated as the ratio of anti-COX-1(IC_{50}) to that of anti-COX-2 (IC_{50}).

4.3.1.7. Bioactivities and Structure-Activity Relationship Analysis

The radical scavenging and anti-inflammatory properties of the oxygenated meroterpenoids isolated from *K. alvarezii* were compared with commercially available synthetic standards. The highly oxygenated C_{29} meroterpenoid (compound **K5**) displayed potential antioxidative activities as determined by ABTS and DPPH free radical scavenging potential (IC_{50} < 0.35 mg/mL), and was comparable with those exhibited by α-tocopherol (IC_{50} 0.6–0.7 mg/mL, $P < 0.05$). The electron delocalization between the carbonyl, methoxy, and olefinic bonds in the molecular structure of these compounds might probably contribute towards the potential free radical scavenging properties (Pietta 2000; Cai et al. 2006). These meroterpenoid derivatives showed significantly greater inhibition towards the inducible COX-2 than its constitutive cyclooxygenase isoform, and accordingly, their anti-inflammatory selectivity index (SI, anti-COX-1IC_{50}/anti- COX-2IC_{50}) were lower (1.06–1.10) than synthetic NSAIDs (ibuprofen and aspirin, SI: 0.44 and 0.02, respectively; $P < 0.05$). In particular, no significant variation in the *in vitro* inhibitory activities towards pro-inflammatory 5-lipoxygenase (IC_{50} 1.04–1.14 mg/mL) and cyclooxygenase-2 (IC_{50} 1.05–1.09 mg/mL) of compound **K5** indicated its potential anti-inflammatory properties against inducible inflammatory mediators causing an inflammatory response. Notably, sodium salicylate appeared to be a weaker inhibitor of the COX isoforms (anti-COX-2 IC_{50} 2.65 mg/mL, anti-COX-1 IC_{50} 1.93 mg/mL), and exhibited significantly lesser activity against 5-LOX (anti-LOX-5 IC_{50} 1.75 mg/mL) (Table 4.10).

The radical quenching along with cyclooxygenase and lipoxygenase inhibitory activities of the meroterpenoids were determined by lipophilic (log Pow, octanol-water partition coefficient), steric (molar refractivity, MR) and electronic (tPSA, topological polar surface area) parameters. The radical quenching and anti-inflammatory properties of the studied compounds were found to be directly related to their hydrophobic characters as determined by hydrophobicity-lipophilicity balance (log Pow). A greater value of log Pow indicated the higher molecular hydrophobicity. The compound **K3** showed lesser hydrophobicity (log Pow 4) than those displayed by compound **K4** (log Pow 4.26) and **K5** (log Pow 5.46). The hydrophobic property was deduced to ascribe the intermembrane permeability of compounds, the optimal range being 2–5 for appropriate lipophilic–hydrophobic characteristics (Lipinski and Hopkins 2004). The

decreased activity of compound **K3** might be corroborated with the lesser hydrophobicity and reduced membrane permeability. Resultantly, the lipophilic DPPH radical might easily be associated with meroterpenoids possessing greater hydrophobicity (greater log Pow value) and displaying higher radical scavenging property. On the basis of above attribution, it might be ascribed that the electronic and hydrophobic factors play significant roles to narrate the bioactive potential of the studied compounds. The electron-rich centers were found to constitute the methoxy-substituted side chain, hydroxyl and aryl substituents in the ring framework. These groups might possibly function as the centre of unsaturations, and were attributed to potential anti-inflammatory and radical quenching properties of the meroterpenoids. The aggregate number of electronegative centres and centre of unsaturation were lesser in compound **K3**, thereby resulting in lesser activity than those recorded in compounds **K4** and **K5**. The optimum log Pow of the highly oxygenated C_{29} meroterpenoid (compound **K5**) (~5.46) along with greater topological polar surface area (tPSA 88.13) might result in its potential anti-inflammatory activity in terms of inhibiting COX-2 (IC_{50} 1.05 mg/mL) and 5-LOX (IC_{50} 1.04 mg/mL).

4.3.1.8. Structural Characterization of Compound K6

(3, 4, 5, 6)-3-Hexan-2'-yl)-3, 4, 5, 8-tetrahydro-4-methyl-2*H*-oxocin-5-yl acetate (**K6**)

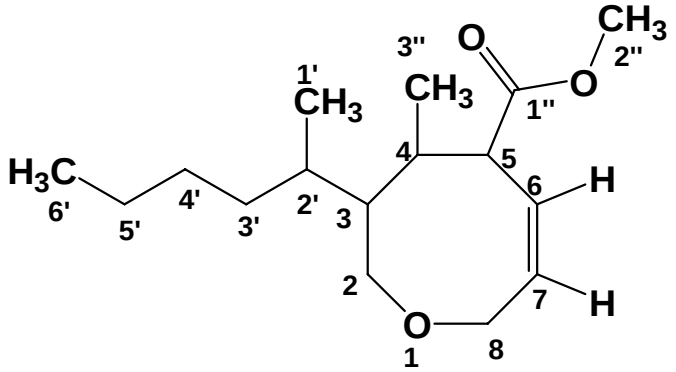

Sample yield	142 mg (1.775 %)
Physical description	Greenish oil
Molecular formula	$C_{16}H_{28}O_3$

Molecular weight	268.8363

(3, 4, 5, 6)-3-(Hexan-2'-yl)-3, 4, 5, 8-tetrahydro-4-methyl-2*H*-oxocin-5-yl acetate: Greenish oil; UV (EtOAc: MeOH) λmax (log ε): 268 nm (3.01); TLC (Si gel GF_{254} 15 mm; EtOAc: *n*-hexane 3:7, v/v) Rf: 0.52; Rt (HPLC, MeOH: ACN, 3:2 v/v): 14.16 min; IR (KBr, cm^{-1}) νmax (ν = stretching, δ = bending, ρ = rocking vibrations): 720.35 (C–Cl ν), 910.91 (alkene C–H δ), 1177.28 (C–O ν), 1297.86 (C–O ν), 1370.83 (CH_3 ν), 1458.44 (C–H δ), 1712.40 (C–CO–C ν), 2855.51 (C–H ν), 2922.32 (C–H ν). ^{1}H NMR (500 MHz, $CDCl_3$) δ_H 5.38 (m, 1H), δ_H 5.27 (m, 1H), δ_H 4.21 (m, 2H), δ_H 4.15 (m, 2H), δ_H 3.68 (s, 3H), δ_H 2.32 (m, 2H), δ_H 2.01 (m, 1H), δ_H 1.69 (m, 1H), δ_H 1.63 (m, 1H), δ_H 1.4 (m, 1H), δ_H 1.3 (m, 1H), δ_H 1.28 (m, 2H), δ_H 0.92 (m, 3H), δ_H 0.9 (m, 3H), δ_H 0.88 (m, 3H); ^{13}C NMR (125 MHz, $CDCl_3$): δ_C 162.79 (C-1"), δ_C 124.81 (C-6), δ_C 107.6 (C-7), δ_C 68.08 (C-2), δ_C 68.08 (C-8), δ_C 51.48 (C-2"), δ_C 38.78 (C-3), δ_C 34.08 (C-3'), δ_C 31.92 (C-5'), δ_C 29.18 (C-4'), δ_C 28.93 (C- 5), δ_C 23.48 (C-2'), δ_C 22.68 (C-4), δ_C 14.12 (C-1'), δ_C 13.88 (C-3"), δ_C 10.38 (C-6'); ^{1}H-^{1}H-COSY and HMBC data (Fig. 4.58 to Fig. 4.66, Table 4.11); High-resolution electrospray ionization mass spectrometry HR (ESI) MS *m/z* calcd for $C_{16}H_{28}O_3$ 268.8362, found 268.8363 $[M + H]^+$.

The ethyl acetate: methanol (EtOAc: MeOH 1:1, v/v) extract of the air-dried red marine macroalga *K. alvarezii* was subjected to a series of vacuum column chromatography (VCC) on silica gel, normal-phase flash chromatography and preparative thin layer chromatography (PTLC), using mixtures of *n*-hexane/EtOAc as mobile phase, to yield an unprecedented non-isoprenoid oxocine carboxylate cyclic ether (3, 4, 5, 6)-3-(hexan-2'-yl)-3, 4, 5, 8-tetrahydro-4-methyl-2*H*-oxocin-5-yl acetate in pure form. The structure of purified compound was proposed on the basis of comprehensive analysis of the ^{1}H NMR and ^{13}C NMR, including two-dimensional nuclear magnetic resonance spectroscopy experiments (^{1}H–^{1}H COSY; HSQC; HMBC; NOESY) and mass spectra. The ^{1}H-NMR in conjugation with ^{13}C NMR recorded the presence of methylene signals at δ_H 4.15, δ_H 4.21, δ_H 2.32, δ_H 1.63 and δ_H 1.28. ^{1}H–^{1}H COSY couplings were apparent between these protons attributed to H-3/H-4, H5/6, H2/3, H3'/4', H2'/1', H5'/6', which supported the presence of C-16 skeleton. The olefinic protons were assigned to be present at δ_H 5.27-5.38, and their proton integral revealed the presence of one olefinic bonds. The methylene group at δ_H 4.21 and δ_H 4.15 shifted downfield due to the electronegative group (oxygen) along with the presence of olefinic

group. The presence of the methoxy group has been confirmed by the singlet at δ_H 3.68. The ^1H–^1H COSY correlations indicated the presence of three spin systems in the molecule, including CH_2–CH= (from H-7 to H-8), –CH_2–CH–CH–CH–CH= (from H-2 to H-6) and CH–CH_2–CH_2–CH_2–CH_2 (from H-2' to H-5'). The above spectral evidences confirmed the planar structure for the compound. The ether bridge was placed on carbons C-2 and C-8 because of the long-range correlation between H-2 (δ_H 4.21) and C-2 (δ_C 68.08), and that between H-3 (δ_H 1.69) and C-2 (δ_C 68.08). The literature survey revealed that the chemical structure of the compound closely related to laureatin, a cyclic ether that was identified from *Laurencia nipponica* (Kurosawa et al. 1973). In the ^1H–^1H COSY spectrum, couplings were apparent between the protons at δ_H 2.01 (H5)/δ_H 1.3 (H4)/δ_H 1.69 (H3)/δ_H 4.21 (H2), δ_H 2.01 (H5)/δ_H 5.38 (H6) and δ_H 5.27 (H7)/δ_H 4.15 (H8), which supported the presence of 3, 4, 5, 8-tetrahydro-2*H*-oxocine moiety (Fig. 4.56). The methylene signal at δ_H 4.15 and δ_H 4.21 appeared downfield due to the presence of multiple electronegative systems at close proximity (Table 4.11). Two methylene groups have been assigned to occupy at the C-8, C-2 positions and were shifted at downfield position due to the presence of an extended conjugation. HMBC correlations were apparent between H-5 (δ_H 2.01) with that of a terminal methyl carbon at δ_C 174.34, which apparently indicated the presence of 3, 4, 5, 8-tetrahydro-2*H*-oxocine moiety. The carbonyl group at the C-1" position of the compound resulted in strong deshielding of the –CH– proton at δ_H 2.01, and therefore, has been assigned to be present at the C-5 position of the structure. The methane proton at δ_H 1.69 has been characteristic of the junction point of the 3, 4, 5, 8-tetrahydro-2*H*-oxocine moiety with that of the side chain 2-methyl hexane moiety. The low field methine signals (^{13}C NMR) was in agreement with that to a methine carbon signal carrying the methoxy groups at C-2" of the structure, and this was supported by the relatively downfield shift of the H-2" signal (δ_C 3.68), which referred to a possible oxygenation in its vicinity. In the HMBC spectrum, it was observed that H-5 (δ_H 2.01)/C-3" (δ_C 13.88); H-8 (δ_H 4.15)/C-1" (δ_C 174.34)/C-1' (δ_C 14.12); H-3 (δ_H 1.69)/C-3" (δ_C 13.88)/C-6' (δ_C 10.38); H-4 (δ_H 1.3)/C-1 (δ_C 14.12); H-3" (δ_H 0.9)/C-2' (δ_C 23.48); H-2' (δ_H 1.4)/C-6' (δ_C 10.38); H-6' (δ_H 0.88)/C-1' (δ_C 14.12) were correlated with each other. The detailed HMBC spectral analyses demonstrating the presence of (3, 4, 5, 6)-3-(hexan-2'-yl)-3, 4, 5, 8-tetrahydro-4-methyl-2*H*-oxocin-5-yl acetate has been represented under the Table 4.11. The relative stereochemistries of the chiral centres, particularly that of C-5, C-3, C-4 and C-2' were deduced from the ^1H-^1H COSY

and HMBC spectra of the compound. The mass spectrum supported the molecular formula $C_{16}H_{28}O_3$ (*m/z* calcd for $C_{16}H_{28}O_3$ 268.8362, found 268.8363 $[M+H]^+$) and the molecular ion peak at *m/z* 268 in the mass spectrum, which in combination with its ^1H and ^{13}C NMR data indicated the elemental composition of the compound as $C_{16}H_{28}O_3$ with three degrees of unsaturation. The molecular ion peak at *m/z* 268 ($[M+H]^+$) appeared to undergo elimination of three $–CH_2–$ groups to yield methyl-3-isopropy1-4-methyl-3, 4, 5, 8-tetrahydro-2*H*-oxocine-5-carboxylate (*m/z* 226). The elimination of two $–CH_2$ groups from the fragment ion at *m/z* 226 yielded the fragments with *m/z* 212 (attributed to (methyl 3-ethyl-4-methyl-3, 4, 5, 8-tetrahydro-2*H*-oxocine-5-carboxylate) and *m/z* 198 (methyl-3, 4-methyl-3, 4, 5, 8-tetrahydro-2*H*-oxocine-5-carboxylate). The elimination of one $–CH_2$ groups from the fragment ion at *m/z* 198 yielded the fragments with *m/z* 184 (attributed to methyl-3-methyl-3, 4, 5, 8-tetrahydro-2*H*-oxocine-5-carboxylate). The elimination of two $–CH_2$ groups from the fragment ion at *m/z* 170 yielded the fragments with *m/z* 156 attributed to (3, 4, 5, 8-tetrahydro-2*H*-oxocine-5-carboxylate) and *m/z* 142 (attributed to 3, 4, 5, 8-tetrahydro-2*H*-oxocine-5-carboxylate). The fragment peak at 142 (assigned to 3, 4, 5, 8-tetrahydro-2*H*-oxocine-5-carboxylate) was found to be the base peak. The olefinic (C=C) and alkyl (C–H) groups IR stretching vibrations were represented by the 1458 and 2855 cm^{-1} absorption bands, respectively. The strong bending vibration bands near 1712 cm^{-1} denoted the ester carbonyl absorption. The Fourier transform infrared (FTIR) spectral absorption bands at 1297 (C–C stretch), 910, 720 cm^{-1} (C–H bend alkene) substantiated the structure of the compound. The presence of a carbonyl group was indicated by the strong IR absorption at 1712.40 cm^{-1}. The relative stereochemical configuration of the asymmetric centres, such as C-3, C-2', C-4, and C-5 bearing the 3, 4, 5, 8-tetrahydro-2*H*-oxocine ring framework, was proposed on the basis of NOE enhancements along with the coupling constants (*J*-values) of the NMR spectrum. Both of the protons H-5 and H-3 exhibited NOESY correlations with the methyl protons H-3", which suggested the *cis* orientation for the methyl groups C-3", and methine group C-5/C-3. The H-6 should be trans-orientation with the methine protons at C-2' and C-3, since no cross-peak could be detected between the H-4 and H-3/H-2' in NOESY experiment. The double bond at C-6 apparently indicated the presence of *cis* configuration on the basis of small coupling constant observed for H-6 and H-7 (10.7 Hz). Additionally, the coupling constant of 10.5 Hz (each) between the pertinent olefinic protons H-6 and H-7 revealed the *cis* geometry (*Z* form) of the C6–C7 double bond.

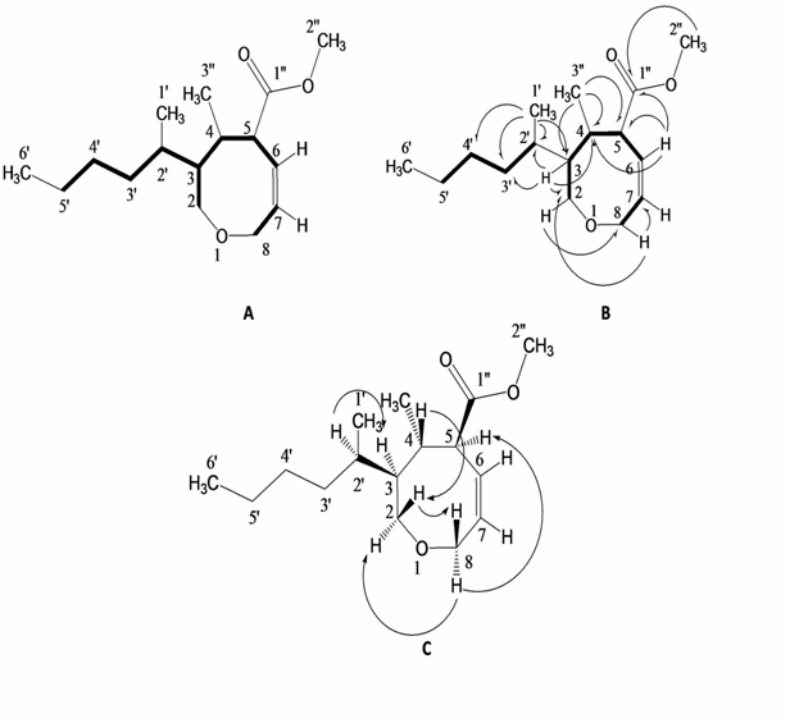

Figure 4.56. 2D NMR correlations of compound **K6** (**A**) Key $^{1}H–^{1}H$ COSY couplings (bold face bonds) (**B**) HMBC couplings (single-barbed arrow) (**C**) Key NOESY correlations (long range H–H couplings are indicated as double barbed arrow) of compound **K6**

The NOE correlation between H-2' and the proton of the H-4 supported the stereochemistry at C-2' and C-4. The axial proton Ha of C-2 resonates as a doublet with the equatorial proton He-3, having an axial–equatorial coupling (*J* a,b=2.64 Hz) subsequently the preference for the larger substituent 3, 4, 5, 8-tetrahydro-2*H*-oxocine group at C-3 to be equatorial. The strong NOE correlation between the methoxy proton at H-2" and at methylene proton at H-4' recommended that these protons are axial. Moreover, the coupling constants between H-2" and H-4' (10.5 Hz) indicated axial–axial orientations. It is of note that an NOE between the methine proton Ha-3, and the axial methylene proton Hd-2, implicated a boat chair conformation of substituted 3, 4, 5, 8-tetrahydro-2*H*-oxocine. In brief, the 3, 4, 5, 8-tetrahydro-2*H*-oxocine ring has been is represented as a boat–chair like conformation. The interpretation for the boat–chair conformation might be due to the bulky 3, 4, 5, 8-tetrahydro-2*H*-oxocine group as equatorially disposed.

Table 4.11 NMR spectroscopic data of compound K**6** in $CDCl_3$ [a]

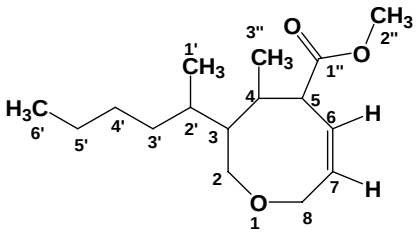

C. No.	^{13}C (δ)	^{1}H NMR (int.,mult.,*J* in Hz)[b]	^{1}H-^{1}H COSY	HMBC (^{1}H-^{13}C)
2	68.08	4.21 (2H, m)	3-H	-
3	38.78	1.69 (1H, m)	2-H, 4-H, 2'-H	C-3", C-6'
4	22.68	1.3 (1H, m)	5-H, 3-H, 3"-H	C-1'
5	28.93	2.01 (1H, m)	6-H, 4-H	C-3'
6	124.81	5.38 (1H, m)	5-H	-
7	107.6	5.27 (1H, m)	8-H	-
8	68.08	4.15 (2H, m)	7-H	C-1", C-1'
1'	14.12	0.92 (3H, t)	2'-H	-
2'	23.48	1.4 (1H, m)	3-H, 1'-H	C-6'
3'	34.08	2.32 (2H, m)	4'-H	-
4'	29.18	1.63 (1H, m)	3'-H, 5'-H	-
5'	31.92	1.28 (2H, m)	4'-H	C-1'
6'	10.38	0.88 (3H, m)	-	-
1"	174.34	-	-	-
2"	51.48	3.68 (3H, s)	-	-
3"	13.88	0.9 (3H, m)	4-H	C-2'

[a] NMR spectra recorded using Bruker AVANCE III 500 MHz (AV 500) spectrometer in $CDCl_3$ as aprotic solvent at ambient temperature with TMS as the internal standard (δ 0 ppm).

[b] Values in ppm, multiplicity and coupling constants (*J*=Hz) are indicated in parentheses. The assignments were made with the aid of the ^1H-^1H COSY, HSQC, HMBC and NOESY experiment

4.3.1.9. Bioactivities and Structure-Activity Relationship Analysis

The antioxidative activity of the compound was found to be significantly greater as determined by DPPH (1, 1-diphenyl-2-picryl-hydrazil) and ABTS (2, 2′-azino-bis-3 ethylbenzothiozoline-6-sulfonic acid) radical scavenging activities (IC_{50} ~ 0.3 mg/mL) compared to α-tocopherol (IC_{50} > 0.6 mg/mL) and was comparable to synthetic antioxidants BHT (Butylated hydroxytoluene) and BHA (Butylated hydroxyanisole) (IC_{50} ~ 0.35–0.34 mg/mL). Structure–activity relationship analysis of the newly isolated cyclic ether from the red alga *K. alvarezii* was performed by utilizing different structural descriptors (ACD Chemsketch, version 8.0 and ChemDraw Ultra version 8.0), such as molar volume (MV), parachor (Pr) and molar refractivity (MR) classified as bulk variables, octanol–water partition coefficient (log Pow) classified as hydrophobic and topological polar surface area (tPSA) and polarisability (Pl), which were classified as electronic descriptor variables. It is of note that whilst the log Pow of (3, 4, 5, 6)-3- (hexan-2'-yl)-3, 4, 5, 8-tetrahydro-4-methyl-2*H*-oxocin-5-yl acetate was recorded as 3.63, that of α-tocopherol (log Pow 9.98) was found to be considerably greater. This might significantly contribute to the greater antioxidant activity of the compound **K6** than α-tocopherol. The log Pow of the compound **K6** was comparable to those of BHA (log Pow 3.22), and BHT (log Pow 5.54), and therefore, their antioxidative properties were not different (IC_{50} 0.25–0.26 mg/mL).

The free radical scavenging activity of bioactive leads depends on the electron-transferring groups, such as –COOMe, –OH and –NH, which can easily abstract free radicals and can convert from highly reactive species to non-reactive compounds (Cai et al. 2006). The radical scavenging activities were also reported to increase with the presence of double bonds due to effective electron transfer through electron delocalisation (Pietta 2000), and these reasons might be attributed to the significant

antioxidative property of the compound. Cyclooxygenase (COX-1) has been known as a constitutive enzyme, which is essentially required for various metabolic functions. It is intriguing to note that aspirin, sodium salicylate and ibuprofen are commonly available non-steroidal anti-inflammatory drugs (NSAIDs), which recorded greater inhibitory properties towards COX-1 than COX-2 isoform. The compound exhibited greater activity against COX-2 than against COX-1 isoform, and therefore, the selectivity index remained significantly lesser (anti-COX-1 IC_{50}: anti-COX-2 IC_{50} 0.87) than the synthetic NSAIDs (0.02–0.44) (Fig. 4.57). No significant difference of *in vitro* 5-lipoxygenase (5-LOX) activity (IC_{50} 0.95 mg/mL) than ibuprofen (IC_{50} 0.93 mg/mL) indicated the potential anti-inflammatory properties of the compound **K6**. Sodium salicylate was found to be a weaker inhibitor of both COX isoforms (anti-COX-2 IC_{50} 2.65 mg/mL, anti-COX-1 IC_{50} 1.93 mg/mL) and demonstrated significantly lesser activity against 5-LOX (anti-COX-1 IC_{50} 1.75 mg/mL). Likewise, the log Pow and tPSA of (3, 4, 5, 6)-3-(hexan-2'-yl)-3, 4, 5, 8- tetrahydro-4-methyl-2*H*-oxocin-5-yl acetate were recorded as 3.63 and 35.53, respectively, whilst the values were found to be comparable with those noted for ibuprofen (3.75 and 37.30, respectively).

It is, therefore, the selectivity indices of the compound **K6**, and ibuprofen recorded greater values (0.87 and 0.44, respectively) than aspirin (0.02), and consequently, the compound **K6** appeared to be safer than that of the synthetic NSAIDs. The compound **K6** purified from the red marine macroalga might therefore be [†]used as a potential selective inhibitor of COX-2 with significantly lesser side effect profiles, such as renal and gastric damage than the present therapies by using NSAIDs used to combat inflammatory disorders (Table 4.12). There were reports of closely related structures, such as laurefurenynes A–F and cyclic ether acetogenins isolated and characterized from red marine macroalga *Laurencia* sp. The ^{1}H NMR of C_{15}-acetogenin derived from red marine macroalga *Laurencia* sp revealed the presence of a *cis*-ene-yne functionality (H-4 δ_H 6.05, H-3 δ_H 5.57, H-1 δ_H 3.10), which was proved by the respective ^{13}C NMR signals at C-4 (δ_C 139.9), C-3 (δ_C 111.3), C-2 (δ_C 80.0) and C-1 (δ_C 82.4) (Wael et al. 2010). The signals obtained at δ_H 4.93 and δ_H 4.43 indicated the two hydroxyl groups were at OH-7 and OH-12 (Wael et al. 2010), which are absent in the compound **K6** (non-isoprenoid oxocine carboxylate cyclic ether) isolated from the ethyl acetate–methanol extract of the red marine macroalga *K. alvarezii.*

The IR spectrum of laurefurenynes A–F broadly belongs to the group of C_{15} cyclic ether acetogenins that were isolated from *Laurencia* sp, showing an intense absorption bands attributed to a terminal acetylene functional group (3315 cm^{-1} and 2107 cm^{-1}), which is not present in the compound **K6** isolated from *K. alvarezii.* These groups of compounds exhibited non-selective cytotoxic activity, presumably due to the terminal acetylene. The C_{15} acetogenins bearing cyclic ether skeletons have been isolated as the main secondary metabolites from red marine macroalga *Laurencia* sp (Erickson 1983) and were reported to be anti-microbial (Konig and Wright 1997), anti-feedant (Kurata et al. 1998), anti-helmintic (Davyt et al. 2001) and cytotoxic (Juagdan et al. 1997). A range of chlorinated compounds, C_{15} acetogenin en-ynes, which are structurally similar to the compounds, were isolated from *Laurencia glandulifera* and were, reported to be moderately cytotoxic towards various human tumour cell lines (Kladi et al. 2009). However, there is no literature report for the antioxidant and anti-inflammatory activities of the laurefurenynes A–F and cyclic ether acetogenins isolated and characterized from red marine macroalgae. Anti-inflammatory potential of the chromene sargachromanol G from the Korean marine macroalga *Sargassum siliquastrum* (Fucales) (Yoon et al. 2012); halogenated compounds from the red marine macroalga *Laurencia snackeyi* (Vairappan et al. 2013) and the porphyrin derivatives; and pheophorbide and pheophytin from the marine macroalga *Sargassum japonica* were reported in previous literature (Islam et al. 2013). Antioxidative compounds from marine macroalgae were identified as phylopheophylin in *Eisenia bicyclis* (Cahyana et al. 1992), phlorotannins in *Sargassum kjellamanianum* (Yan et al. 1996) and fucoxanthin in *Hijikia fusiformis* (Yan et al. 1999). Laureatin, isolaureatin and deoxyprepacifenol are other related compounds obtained from the red alga *Laurencia nipponica* (Masuda et al. 1997). They exhibited significant insecticidal activity against the mosquito larvae *Culex pipens pallens* (Watanabe 1989). However, there is no literature report for the antioxidant and anti-inflammatory activities of the laurefurenynes A–F and cyclic ether acetogenins isolated and characterized from red marine macroalgae.

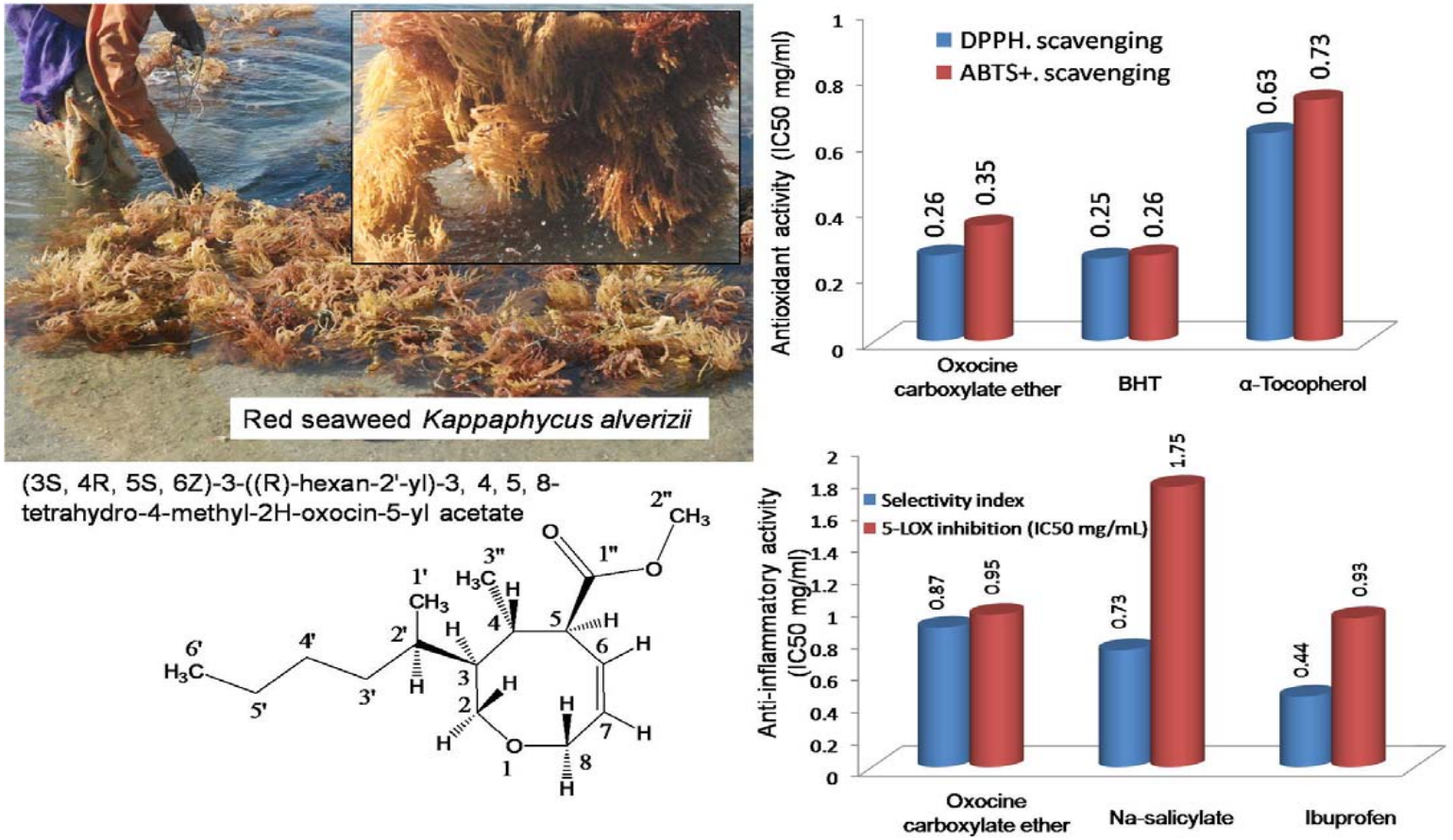

Figure 4.57. Graphical representation of bioactivities of compound **K6**. The thalli of the studied marine macroalga were displayed as inset

Table 4.12 Antioxidative and inflammatory activities of the compound from *K. alvarezii vis-à-vis* the commercially available natural and synthetic antioxidants and anti-inflammatory ingredients

	Bioactivity IC_{50} (mg/mL)			
Antioxidative activities*	**K6[x]**	**BHA**	**BHT**	**α-tocopherol**
$DPPH^{\cdot}$ scavenging	$0.26^{a} \pm 0.02$	$0.26^{b} \pm 0.01$	$0.25^{b} \pm 0.02$	$0.63^{c} \pm 0.04$
$ABTS^{+\cdot}$ scavenging	$0.35^{a} \pm 0.13$	$0.34^{b} \pm 0.02$	$0.26^{b} \pm 0.02$	$0.73^{c} \pm 0.05$
Anti-inflammatory activities*	**K6[x]**	**Aspirin**	**Na-salicylate**	**Ibuprofen**
COX -1 inhibition	$0.92^{a} \pm 0.02$	$0.01^{a} \pm 0.00$	$1.93^{c} \pm 0.05$	$0.04^{a} \pm 0.00$
COX -2 inhibition	$1.05^{a} \pm 0.07$	$0.21^{b} \pm 0.02$	$2.65^{c} \pm 0.05$	$0.09^{a} \pm 0.02$
Selectivity index**	$0.87^{b} \pm 0.08$	$0.02^{b} \pm 0.01$	$0.73^{b} \pm 0.02$	$0.44^{b} \pm 0.03$
5-LOX inhibition	$0.95^{a} \pm 0.14$	$0.39^{a} \pm 0.02$	$1.75^{c} \pm 0.12$	$0.93^{b} \pm 0.11$

* The bioactivities were expressed as IC_{50} values (mg/mL).

The samples were analyzed in triplicate (n=3) and expressed as mean ± standard deviation. Means followed by the different superscripts (a–c) within the same row indicate significant differences ($P < 0.05$).

**Selectivity index has been calculated as the ratio of anti-COX-1(IC_{50}) to that of anti-COX-2 (IC_{50}).

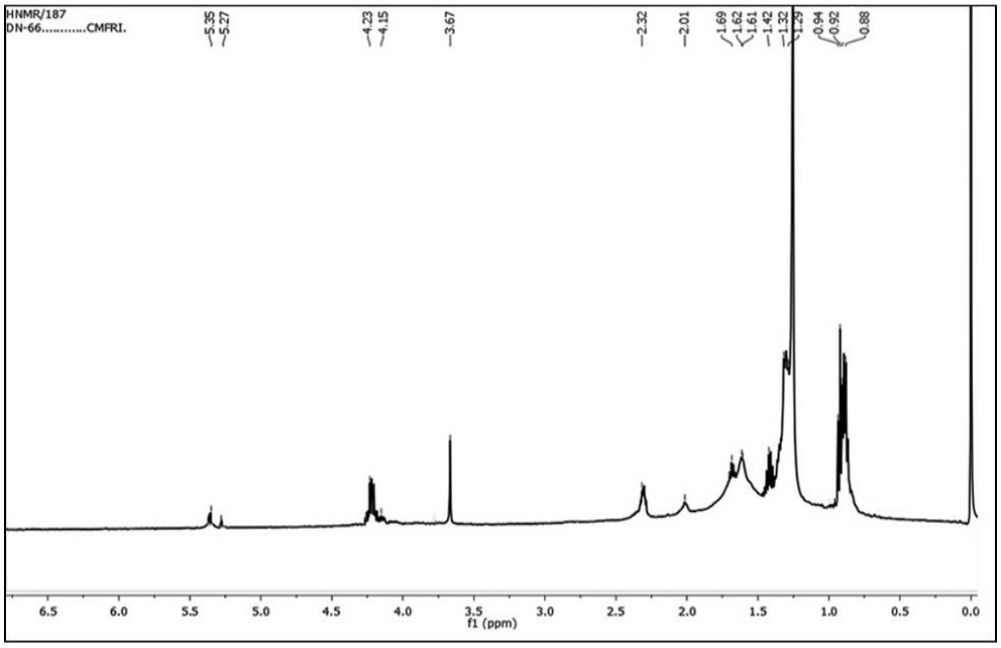

Figure 4.58. Figure showing the ^{1}H NMR spectrum of compound **K6**

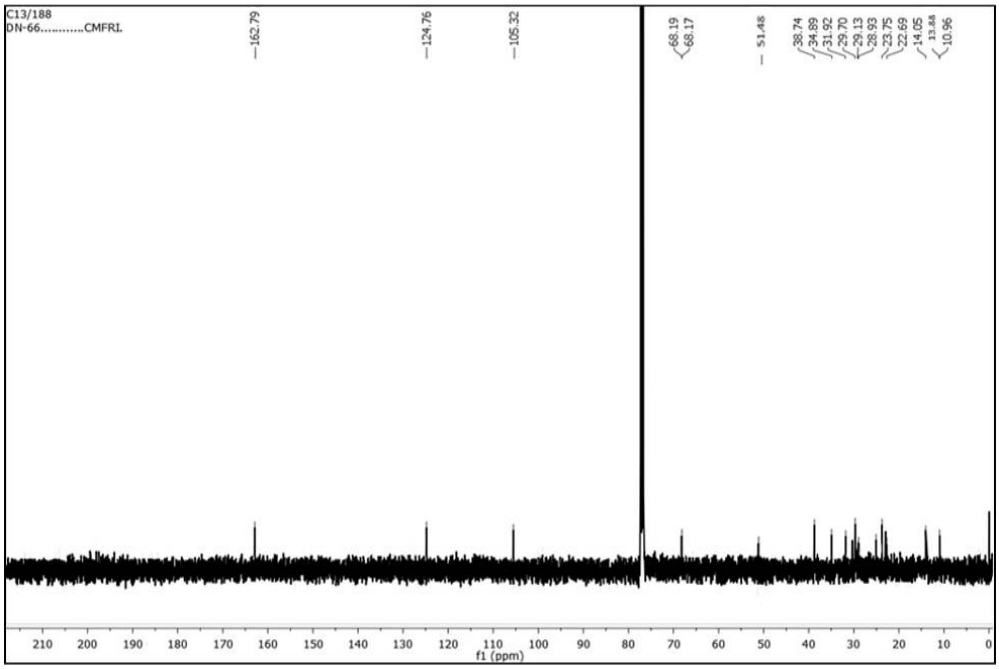

Figure 4.59. Figure showing the ^{13}C NMR spectrum of compound **K6**

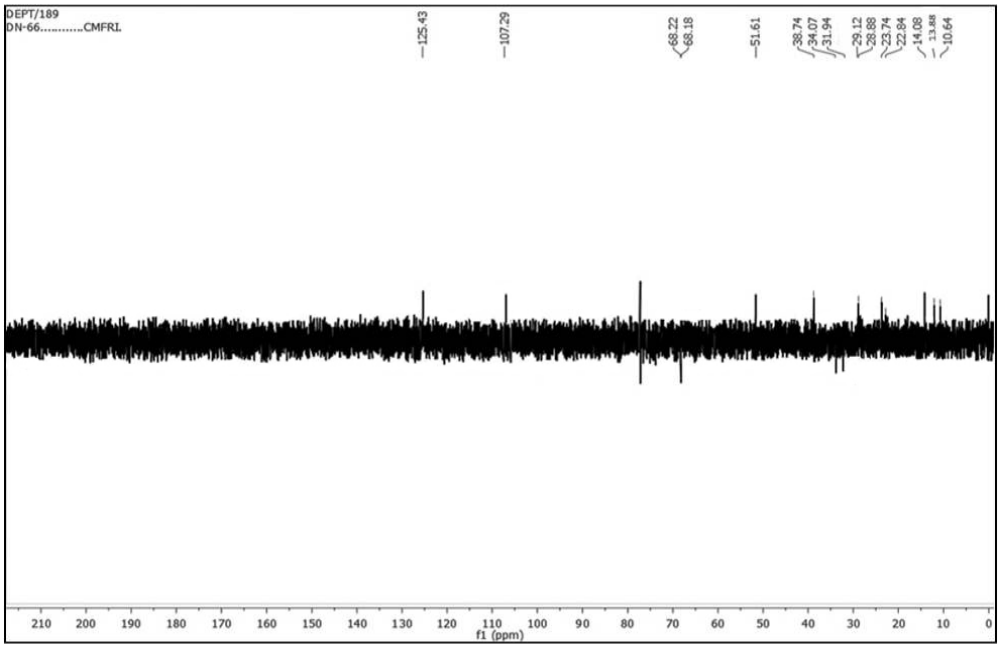

Figure 4.60. Figure showing the DEPT spectrum of compound **K6**

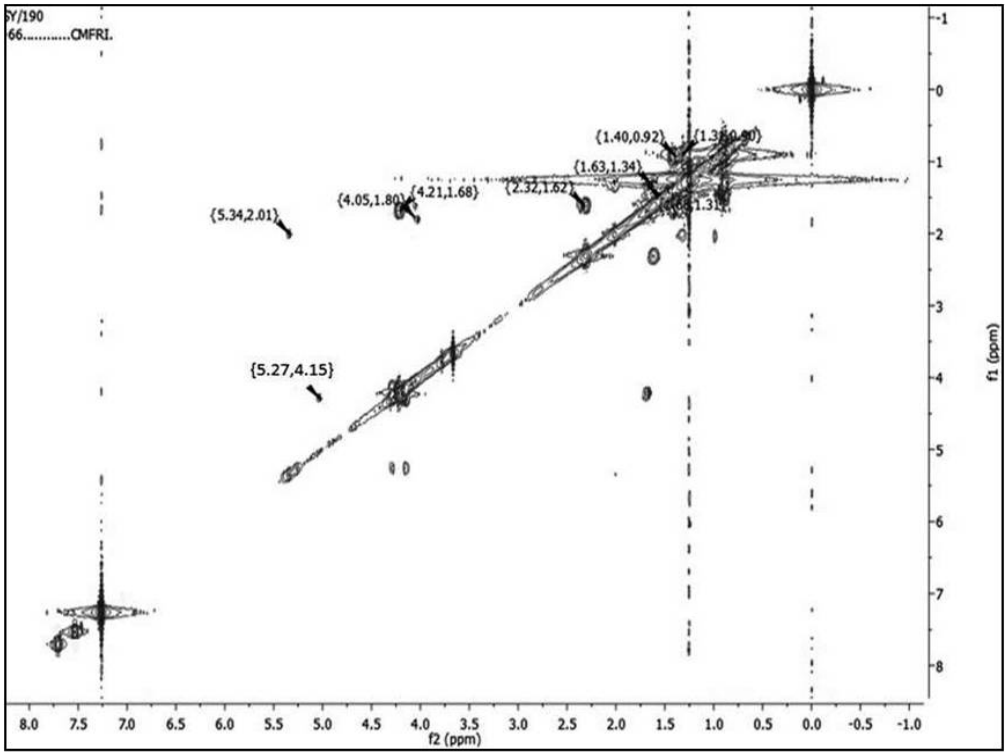

Figure 4.61. Figure showing the ^{1}H-^{1}H COSY spectrum of compound **K6**

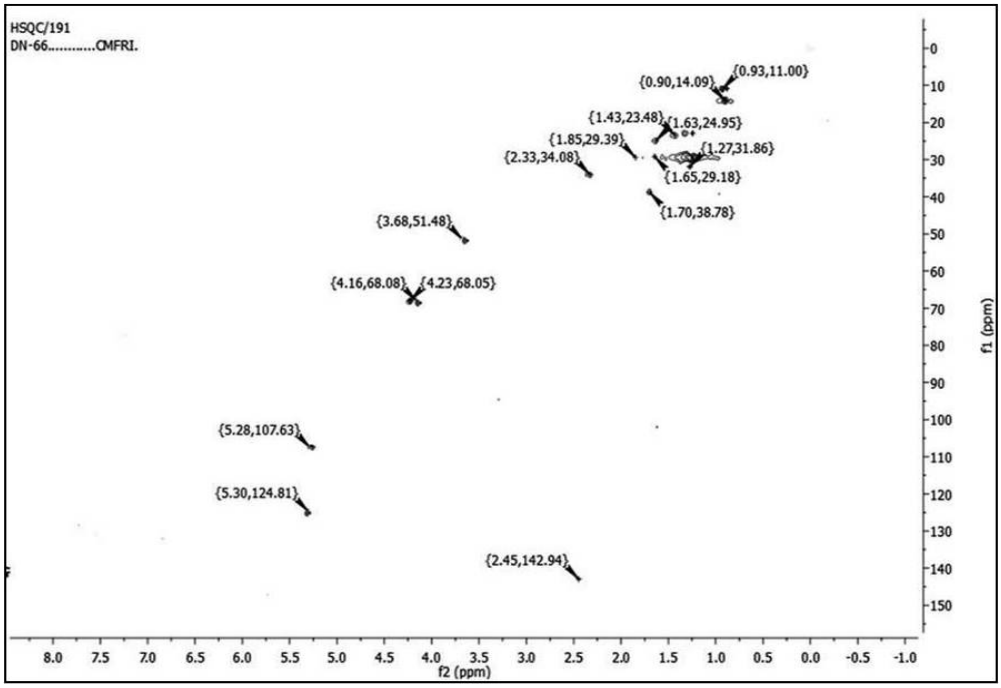

Figure 4.62. Figure showing the HSQC spectrum of compound **K6**

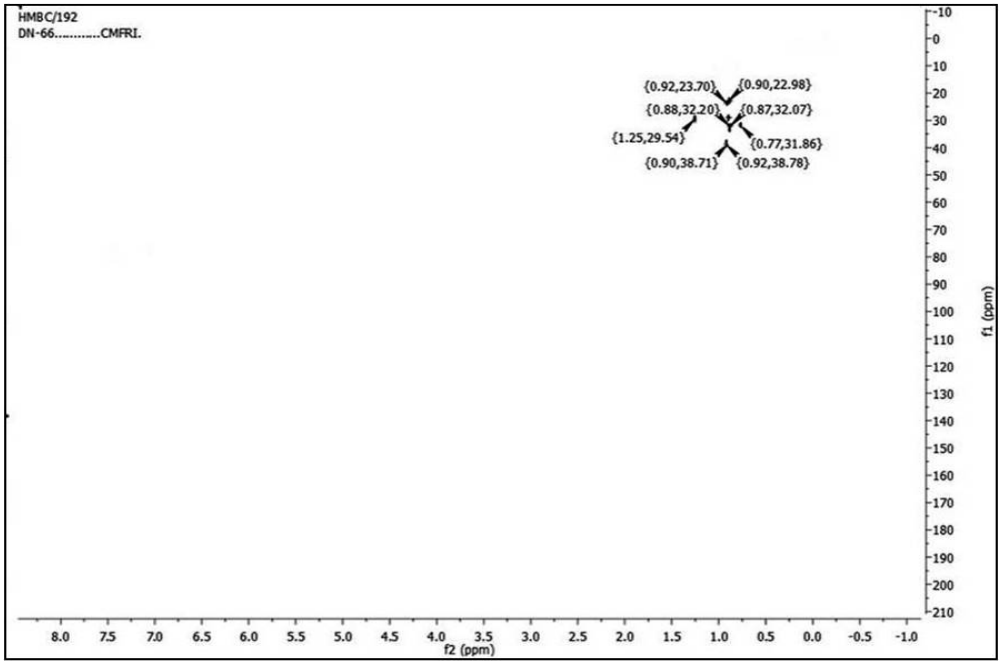

Figure 4.63. Figure showing the HMBC spectrum of compound **K6**

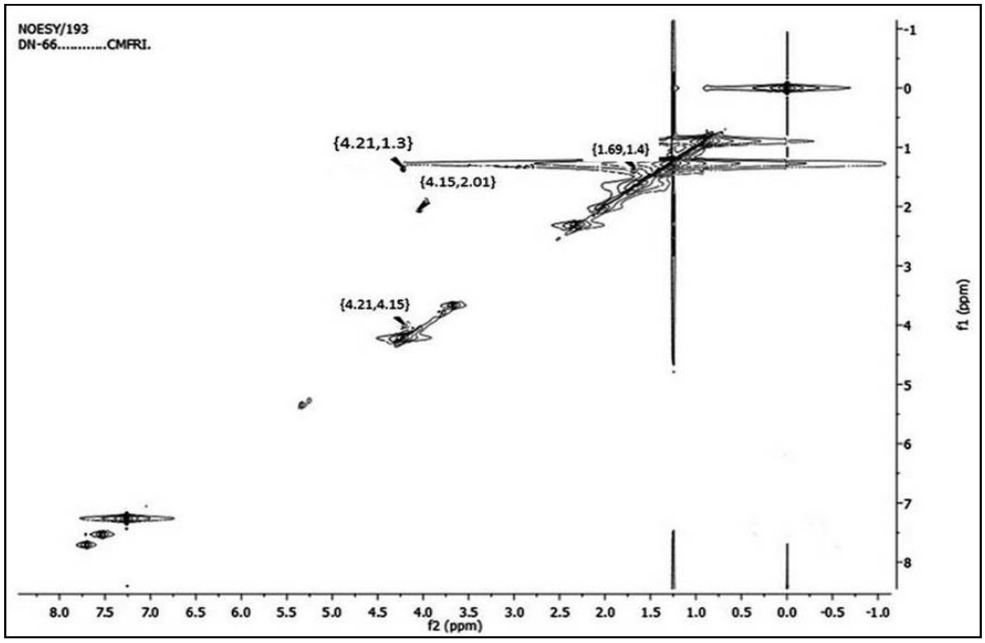

Figure 4.64. Figure showing the NOESY spectrum of compound **K6**

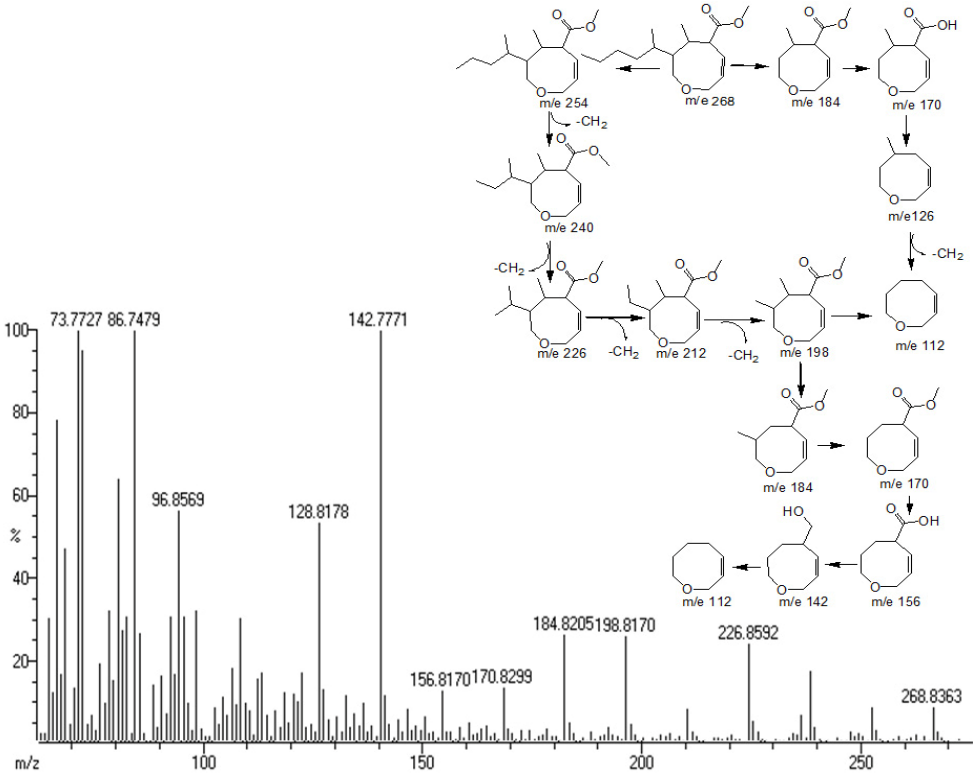

Figure 4.65. Mass spectrum of compound **K6**

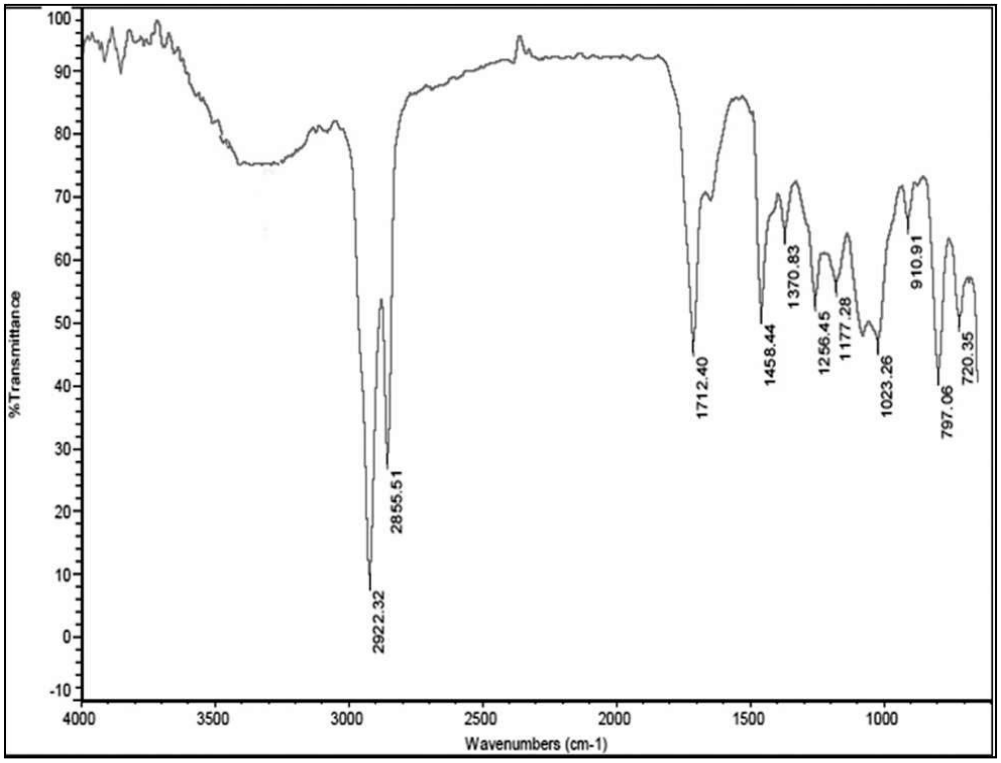

Figure 4.66. Figure showing the FTIR spectrum of compound **K6**

4.3.2. Secondary Metabolites from *G. opuntia*

4.3.2.1. Structural Characterization of Compound G1

5-(7-(5-Ethyl-3, 4-dimethoxycyclooctyl) benzofuran-6-yl)-7-methyl-3, 4, 7, 8-tetrahydro-2*H*-oxocin-2-one (**G1**)

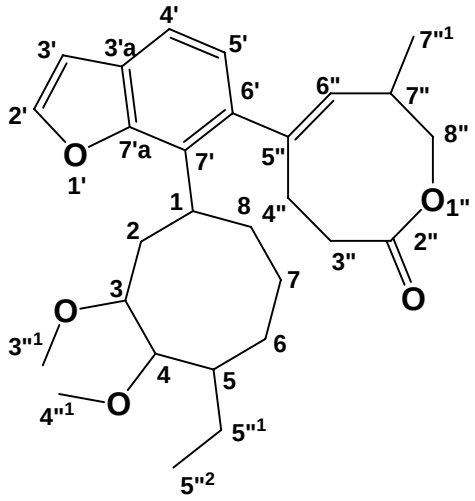

Sample yield	130 mg (1.625 %)
Physical description	Yellow oil
Molecular formula	$C_{28}H_{38}O_5$
Molecular weight	454.2728

5-(7-(5-Ethyl-3, 4-dimethoxycyclooctyl) benzofuran-6-yl)-7-methyl-3, 4, 7, 8-tetrahydro-2*H*-oxocin-2-one: Yellow oil; UV MeOH: EtOAc λmax (log ε): 237 nm (3.217), TLC (Si gel GF_{254} 15 mm; MeOH: EtOAc 7:3, v/v) Rf: 0.56.; Rt (HPLC, CH_3CN: MeOH, 2:3 v/v): 12.85 min; IR (KBr, expressed in cm^{-1}) νmax (ν = stretching, δ = bending, ρ = rocking vibrations): 2925.39, 2856.44 (C-H ν), 1741.18 (C=O ν), 1459.21 (C-H δ), 1370.58, 1257.96 (C-H ρ), 1170.92 (C-O ν), 1093.53 (CH δ), 968.11, 866.84, 806.67 (=C-H δ), 721.60 (C-H ρ); ^{1}H NMR (500 MHz $CDCl_3$): δ_H 1.72 (1H, m), δ_H 1.28 (2H, m), δ_H 0.88 (3H, t, *J*=7.04 Hz), δ_H 2.02 (2H, m), δ_H 1.72 (2H, m), δ_H 2.20 (2H, m), δ_H 1.61 (1H, t, *J*=7.98 Hz), δ_H 2.53 (2H, t, *J*=5.97 Hz), δ_H 4.19 (1H, m), δ_H 3.79 (3H, s), δ_H 4.32 (1H, t, *J*=6.93 Hz), δ_H 3.67 (3H, s), δ_H 6.82 (1H, d, *J*=2.31 Hz),

δ_H 6.09 (1H, d, *J*=2.17 Hz), δ_H 7.72 (1H, d, *J*=2.31 Hz), δ_H 7.54 (1H, d, *J*=3.38 Hz), δ_H 4.09 (2H, d, *J*=6.58 Hz), δ_H 2.02 (1H, m), δ_H 0.99 (3H, d, *J*=6.71 Hz), δ_H 5.35 (1H, d, *J*=5.15 Hz), δ_H 1.61 (2H, t, *J*=10 Hz), δ_H 2.32 (2H, t, *J*=7.60 Hz); ^{13}C NMR (125 MHz, $CDCl_3$): δ_C 32.85 (C-5), δ_C 29.70 (C-5"^{1}), δ_C 14.1 (C-5"^{2}), δ_C 32.39 (C-6), δ_C 34.55 (C-7), δ_C 34.58 (C-8), δ_C 27.73 (C-1), δ_C 40.06 (C-2), δ_C 70.46 (C-3), δ_C 52.47 (C-3"^{1}), δ_C 65.57 (C-4), δ_C 51.46 (C-4"^{1}), δ_C 147.23 (C-2'), δ_C 130.48 (C-3'), δ_C 147.04 (C-3a'), δ_C 128.78 (C- 4'), δ_C 130.91 (C-5'), δ_C 148.31 (C-6'), δ_C 149.4 (C-7'), δ_C 147.23 (C-7a'), δ_C 71.80 (C-8"), δ_C 27.93 (C-7"), δ_C 19.15 (C-7"^{1}), δ_C 130.32 (C-6"), δ_C 132.3 (C-5"), δ_C 34.45 (C-4"), δ_C 34.12 (C-3"); δ_C 174.35 (C-2"); ^{1}H-^{1}H COSY and HMBC (Fig. 4.67 to Fig. 4.77, Table 4.13); HR (EI) MS *m/z* found 454.2728 $[M]^+$, calcd for $C_{28}H_{38}O_5$ 454.2719.

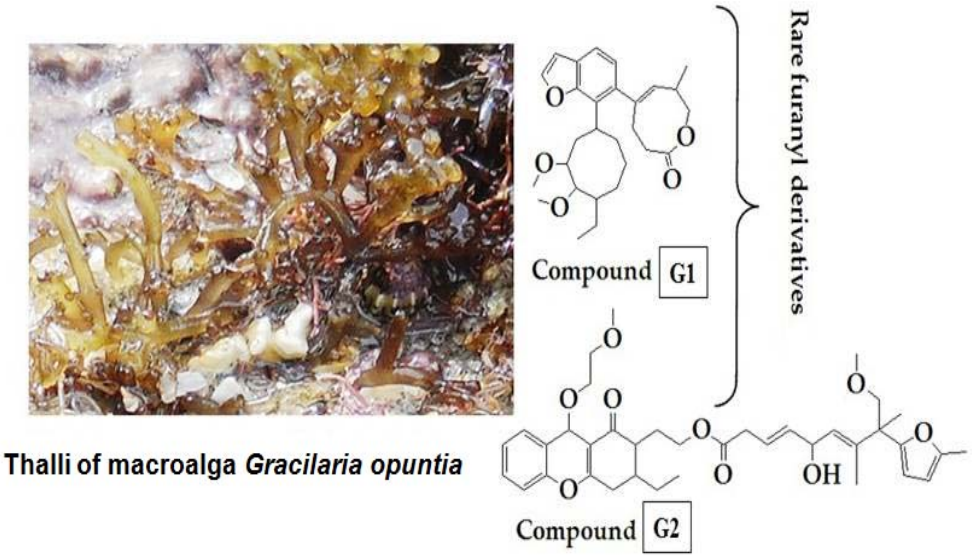

Figure 4.67. Figure showing red marine macroalga *G. opuntia* collected from the Palk Bay of south east coast of India, and two furanyl compounds isolated from the EtOAc: MeOH crude extract of marine macroalga

The compound 5-(7-(5-ethyl-3, 4-dimethoxycyclooctyl) benzofuran-6-yl)-7-methyl-3, 4, 7, 8-tetrahydro-2*H*-oxocin-2-one was obtained as yellow oil, and its molecular ion peak at *m/z* 454 was deduced from the mass spectrum (HR-EI-MS *m/z* 454.2728 $[M]^+$). The molecular formula of the isolated compounds was deduced as $C_{28}H_{38}O_5$ based on combined ^{1}H and ^{13}C NMR spectroscopic data.

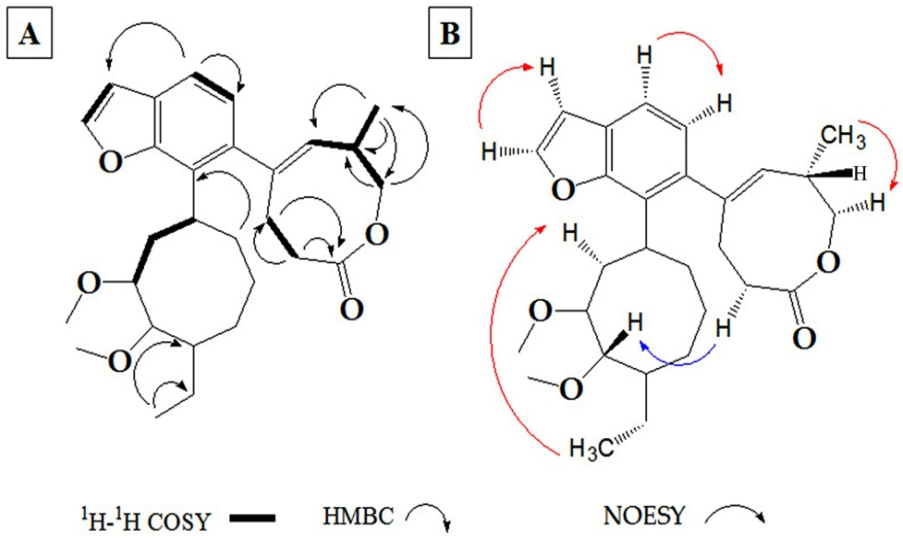

Figure 4.68. (**A**) Figure showing the ^{1}H-^{1}H COSY, HMBC, and (**B**) NOESY correlations of compound **G1**. The ^{1}H-^{1}H COSY cross peaks were displayed by bold face bonds, whereas the selected HMBC correlations were shown as double barbed arrows. The NOESY relations was presented as colored arrows

The IR spectrum displayed bending vibration appeared at 1741 cm^{-1}, which was attributed to the ester carbonyl group. The FTIR absorption bands at 1459 and 2856 cm^{-1} were attributed to the olefinic (>C=C<) as well as alkyl groups, respectively. The ^{13}C NMR spectral data showed 28 resolved signals that were classified into four aromatic methines, two methoxy group, one olefinic carbon, five methine, eight methylene, two methyl carbon, and six quaternary carbons, which were supported by the exhaustive 2D NMR experiments. Ultraviolet absorbance at λmax (log ε) 235 nm (3.24) was attributed to the furan chromophore that was further supported by the IR bending vibrations at about 1459 cm^{-1}. The isolated compounds displayed six quaternary carbons in which the carbon signals at δ_C 147.04 (ascribed to C-3a'), δ_C 147.23 (C- 7a'), δ_C 148.31 (C-6') and δ_C 149.40 (C-7') were associated with the benzyl furan moiety. The carbon at δ_C 174.35 (attributed to C-2') was due to the carbonyl group in the 7-methyl-3, 4, 7, 8-tetrahydro-2*H*-oxocin-2-one framework. The ^{1}H–^{1}H COSY spin system appeared between δ_H 1.72 (H-5)/δ_H 4.32 (H-4), δ_H 1.61 (H-1)/δ_H 2.53 (H-2), and δ_H 4.19 (H-3), which attributed to the methoxy substituted ethylcyclooctane ring skeleton (Fig. 4.68). Likewise, strong ^{1}H–^{1}H COSY cross peaks observed between δ_H 4.09 (H-8")/δ_H 2.02 (H-7")/δ_H 5.35 (H-6") and δ_H 2.02 (H-7")/δ_H

0.99 (H-7"[1]) supported the ring framework of 7-methyl-tetrahydro-2*H*-oxocin-2-one moiety. The ring framework was further supported by key HMBC correlation between oxymethine proton δ_H 4.09 (H-8") coupled with the methylene carbon δ_C 27.93 (C-7"), and methyl carbon at δ_C 19.15 (C-7"[1]). In addition, the HMBC cross peaks were observed between the methyl proton δ_H 0.99 (H-7"[1]) coupled to the methine carbon δ_C 27.93 (C-7") and oxymethine carbon at δ_C 71.80 (H-8") (Table 4.13). Key HMBC correlation between δ_H 0.88 (H-5"[2])/C-5(δ_C 32.85), δ_H 2.20 (H-8)/C-7' (δ_C 149.40), δ_H 7.72 (H-4')/C-5' (δ_C 130.91) supported the substituted 2*H*-oxocin-2-one ring framework. The terminal methyl group appeared as a triplet at H-5"[2]{δ_H 0.88 (*J*=7.04 Hz), δ_C 14.1 (C-5"[2])} associated with (1, 2, 3)-1-ethyl-2, 3-dimethoxycyclooctane and a carbonyl group at C-2" {δ_C 174.35 (C-2")} were deduced to be enclosed with the 7-methyl-tetrahydro-2*H*-oxocin-2-one ring framework. This was corroborated by intense HMBC couplings between H- 4" (δ_H 1.61)/C-2" (δ_C 174.35); H-3" (δ_H 2.32)/C-2" (δ_C 174.35) (Table 4.13). Two doublets at δ_H 6.82 (H-2', *J*=2.31 Hz) and δ_H 6.09 (H-3', *J*=2.17 Hz) due to the furanyl ring system were apparent in the ^{1}H NMR spectrum. In addition, aryl ring system appeared at δ_H 7.72 {H-4', *J*=2.31 Hz, δ_C 128.78} and δ_H 7.54 {H-5', *J*=3.38 Hz, δ_C 130.91}. The olefinic signals were detected at δ_H 5.35 {H-6", δ_C 130.32 (C-6")}. Methoxy groups were attributed to the proton signal at δ_H 3.79 (3H, H-3"[1]) and δ_H 3.67 (3H, H-4"[1]), which were assigned to form the part of ethylcyclooctane moiety. Additional oxymethylene signals H-8" {δ_H 4.09 (*J*=6.58 Hz), δ_C 71.80 (H-8")} were attributed to the 7-methyl-tetrahydro-2*H*-oxocin-2-one moieties. The ^{1}H NMR spectroscopic data displayed the occurrence of highly deshielded oxymethine protons at δ_H 4.19 (H-3) and δ_H 4.32 (H-4, *J*=6.93 Hz). Each of the two olefinic groups and carbonyl groups along with aromatic moieties (aryl and furyl) were accounted for ten degrees of unsaturation in compound **G1**. The relative stereochemical configuration of the asymmetric centers, C-5, C-4, C-3, C-1, and C-7" bearing the substituted furan ring framework were attributed by extensive NOESY experiments along with the coupling constants (*J*-values) in the ^{1}H NMR spectrum. The aromatic methine protons at H-5' (δ_H 7.54, *J*=3.38 Hz) displayed NOESY correlations with the neighboring aromatic methane protons at δ_H 7.74 (*J*=2.31 Hz) in the benzyl furan aromatic ring system. An additional NOE cross peak was recorded between δ_H 6.09 (H-3', *J*=2.17 Hz) and δ_H 6.82 (H-2', *J*=2.31 Hz), which apparently indicated that these protons were associated with the furanyl moiety. The oxymethine group at C-4 (δ_H 4.32, *J*=6.93 Hz) exhibited NOE cross peaks with δ_H 2.32 (H-3", *J*=7.60 Hz), which was situated at the junction

point with side chain methoxy substitution. The NOE relationships with δ_H 0.99 (assigned to H-7"[1], *J*=6.71 Hz) and δ_H 4.09 (assigned to H-8", *J*=6.58 Hz) were seen at the α-face of the molecule. In addition, the terminal methane protons at H-5"[2] (δ_H 0.88, *J*=7.04 Hz) displayed NOESY correlations with the methine protons at δ_H 2.53 (H-2, *J*=5.97 Hz) in the side chain substitution of 1-ethyl-2, 3-dimethoxycyclooctane ring system.

Table 4.13 NMR spectroscopic data of compound **G1** in $CDCl_3$[a]

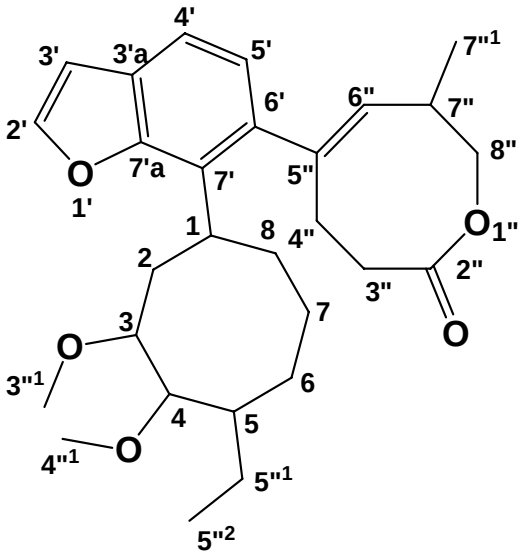

C. No	^{13}C (δ)	^{1}H NMR (mult., *J* in Hz, int.)[b]	^{1}H-^{1}H COSY	HMBC ($^{1}H^{13}C$)
1	27.73	1.61 (t, *J*=7.98 Hz, 1H)	2-H	-
2	40.06	2.53 (t, *J*=5.97Hz, 2H)	1-H, 3-H	
3	70.46	4.19 (m, 1H)	-	-
3"[1]	52.47	3.79 (s, 3H)	-	-
4	65.57	4.32 (t, *J*=6.93 Hz, 1H)	-	-
4"[1]	51.46	3.67 (s, 3H)	-	-
5	32.85	1.72 (m, 1H)	4-H	-
5"[1]	29.70	1.28 (m, 2H)	-	-
5"[2]	14.1	0.88 (t, *J*=7.04 Hz, 3H)	-	C-5"[1], C-5
6	32.39	2.02 (m, 2H)	-	-
7	34.55	1.72 (m, 2H)	-	-
8	34.58	2.20 (m, 2H)	-	C-7'
2'	147.23	6.82 (d, *J*=8.21 Hz, 1H)	3'-H	
3'	130.48	6.09 (d, *J*=2.17 Hz, 1H)	2'-H	-
3a'	147.04	-		-
4'	128.78	7.72 (d, *J*=2.31 Hz, 1H)	5'-H	C-3', C-5'
5'	130.91	7.54 (d, *J*=3.38 Hz, 1H)	4'-H	-
6'	148.31	-	-	-
7'	149.4	-	-	-
7a'	147.23	-		
2"	174.35	-	-	-

3"	34.12	2.32 (t, *J*=7.60 Hz, 2H)	-	C-2"
4"	34.45	1.61 (t, *J*=10 Hz, 2H)	-	C-3", C-2"
5"	132.3	-	-	-
6"	130.32	5.35 (d, *J*=5.15 Hz, 1H)	7"-H	-
7"	27.93	2.02 (m, 1H)	7"^{1}-H, 6'-H, 8"-H	C-6", C-7"^{1}
7"^{1}	19.15	0.99 (d, *J*=6.71 Hz, 3H)	-	C-7", C-8"
8"	71.80	4.09 (d, *J*=6.58 Hz, 2H)	7"-H	C-7"^{1}, C-7"

[a] NMR spectra recorded using Bruker AVANCE III 500 MHz (AV 500) spectrometer in $CDCl_3$ as aprotic solvent at ambient temperature with TMS as the internal standard (δ 0 ppm).

[b] Values in ppm, multiplicity and coupling constants (*J*=Hz) are indicated in parentheses. The assignments were made with the aid of the ^{1}H-^{1}H COSY, HSQC, HMBC and NOESY experiment

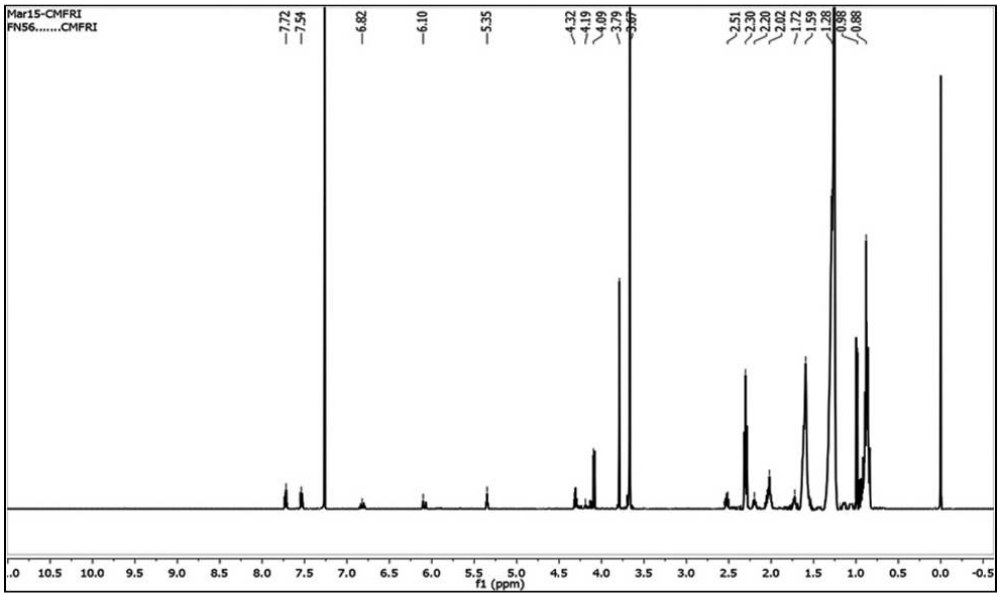

Figure 4.69. Figure showing the ^{1}H NMR spectrum of compound **G1**

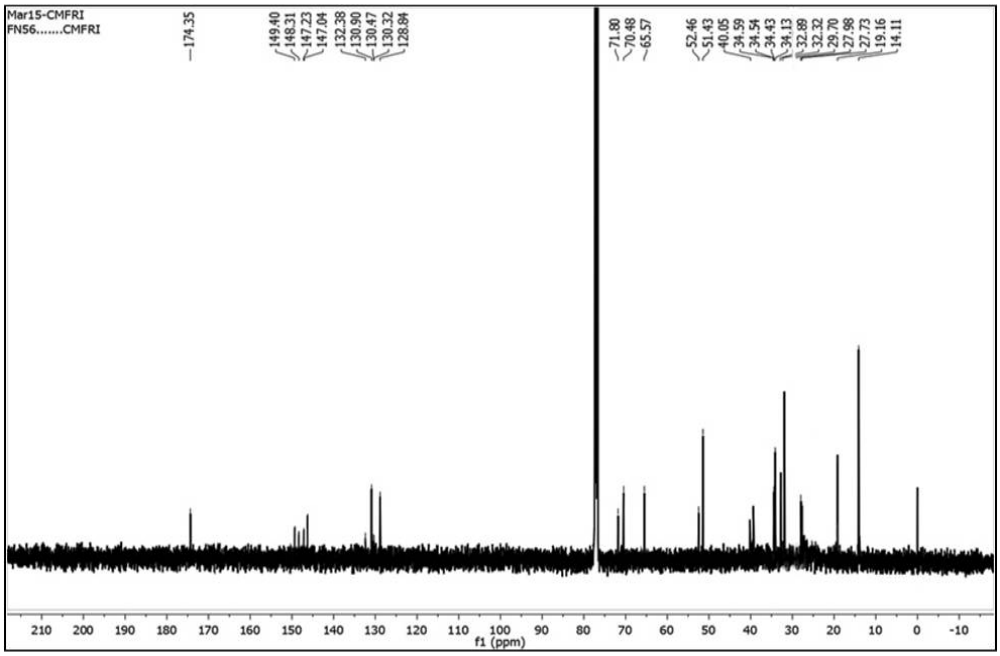

Figure 4.70. Figure showing the ^{13}C NMR spectrum of compound **G1**

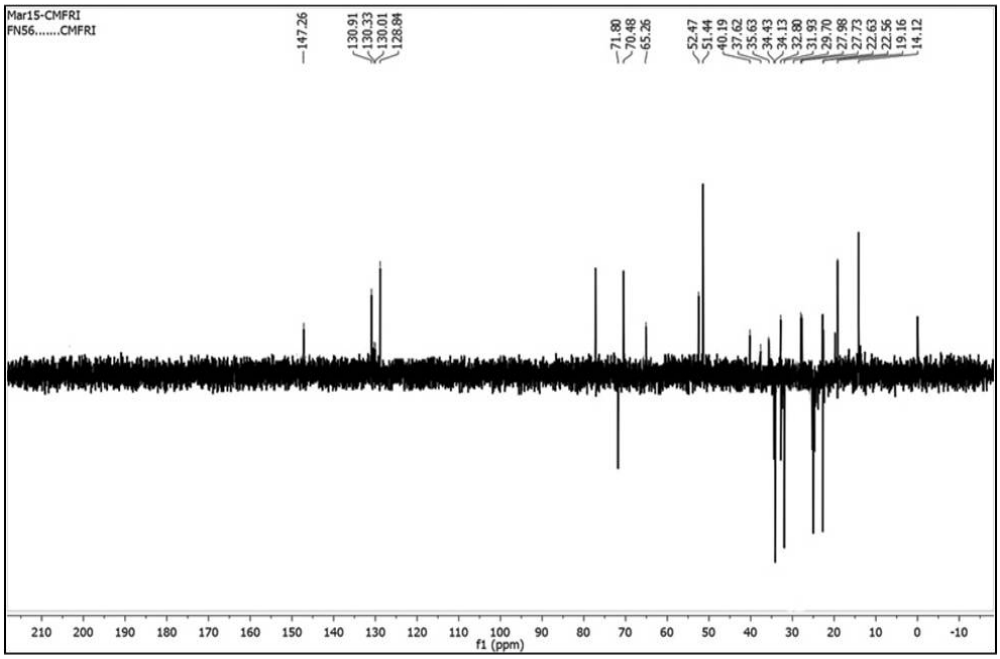

Figure 4.71. Figure showing the DEPT spectrum of compound **G1**

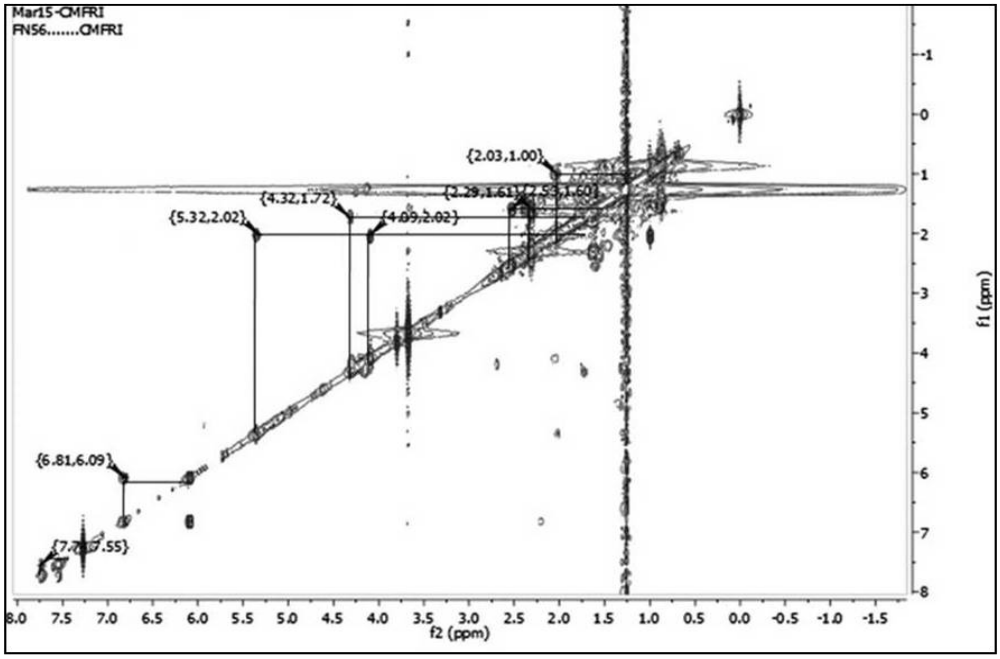

Figure 4.72. Figure showing the ^{1}H-^{1}H COSY spectrum of compound **G1**

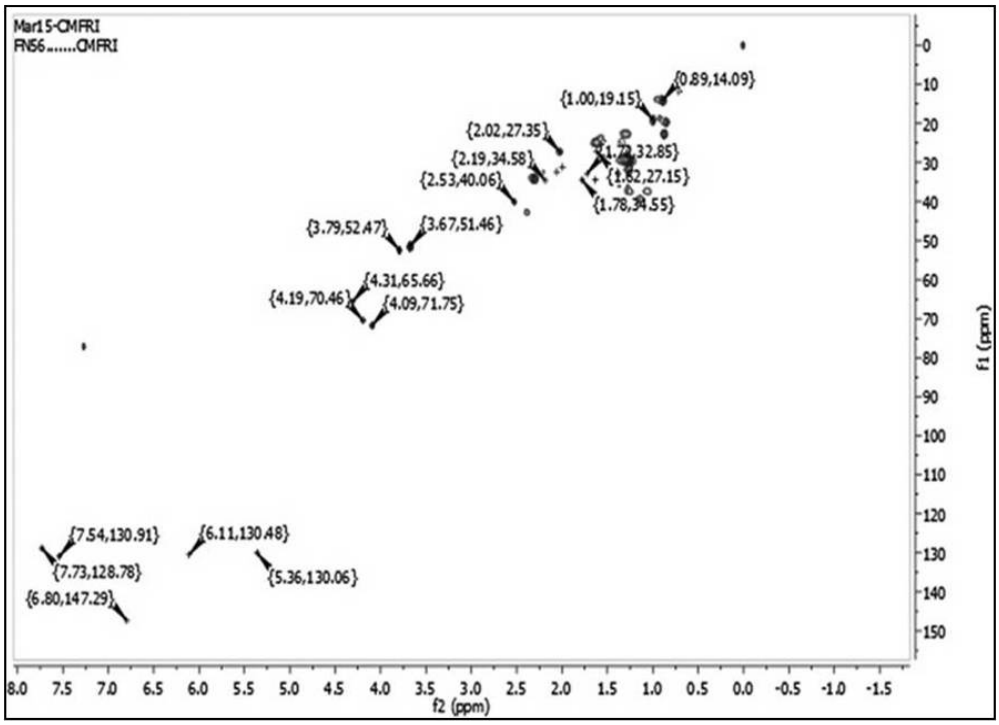

Figure 4.73. Figure showing the HSQC spectrum of compound **G1**

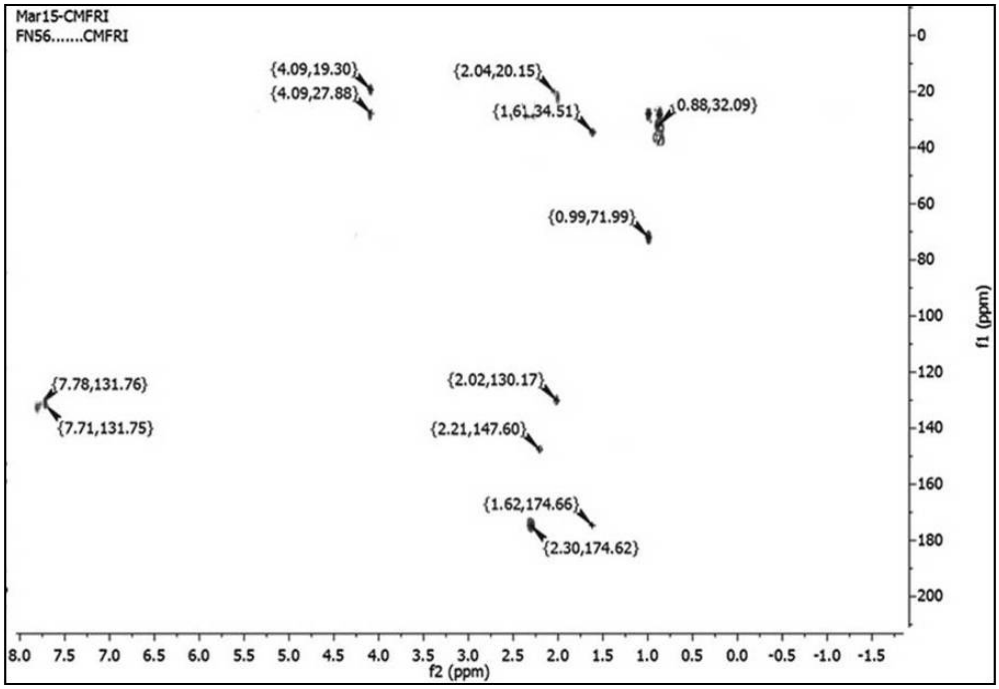

Figure 4.74. Figure showing the HMBC spectrum of compound **G1**

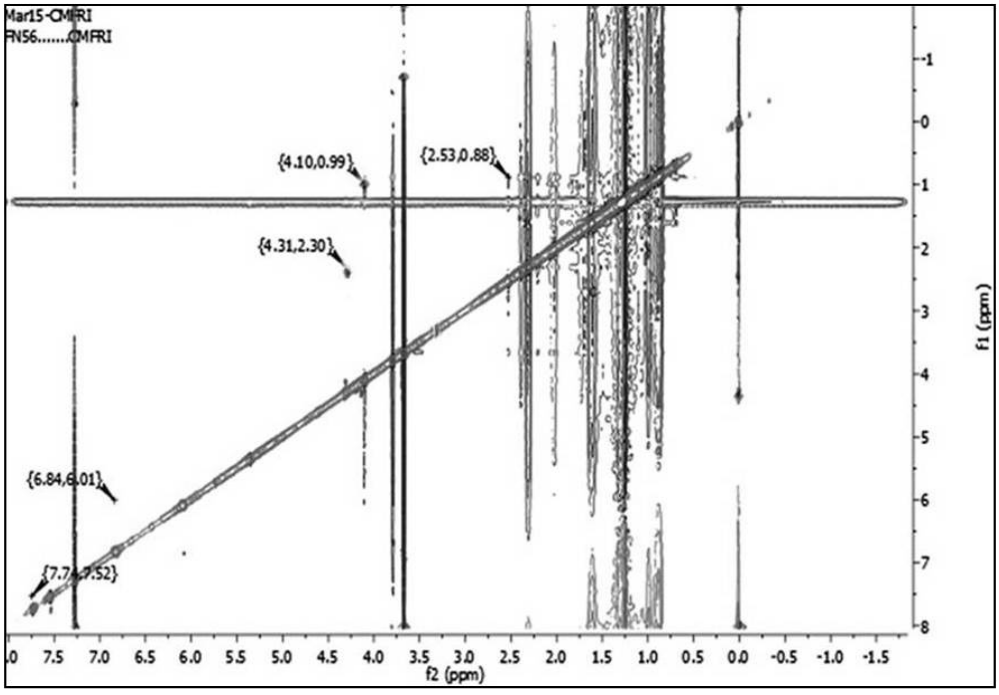

Figure 4.75. Figure showing the NOESY spectrum of compound **G1**

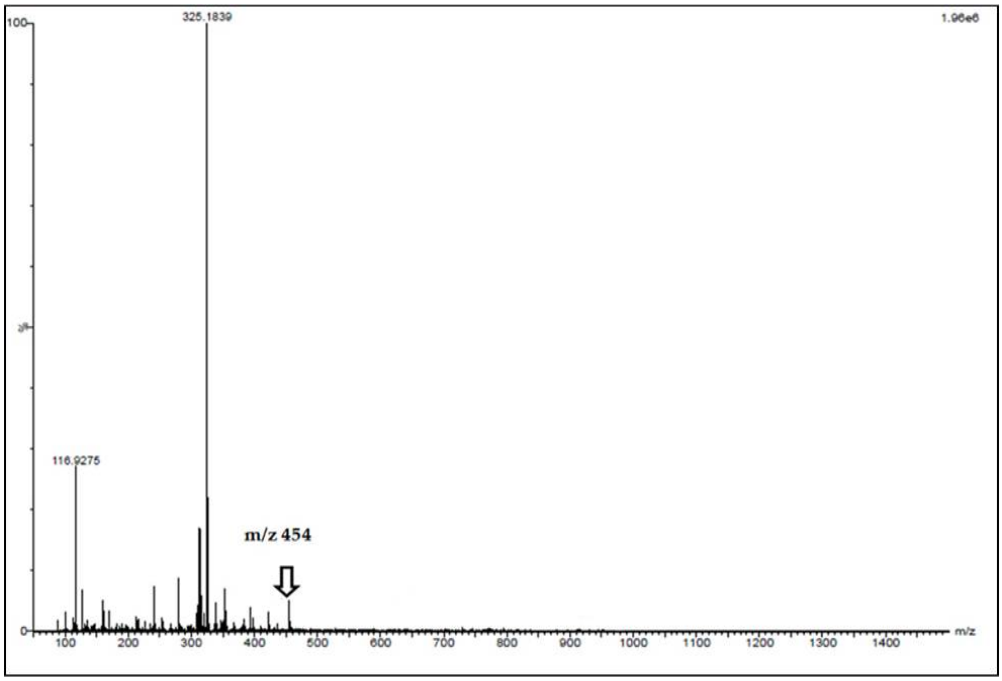

Figure 4.76. Mass spectrum of compound **G1**

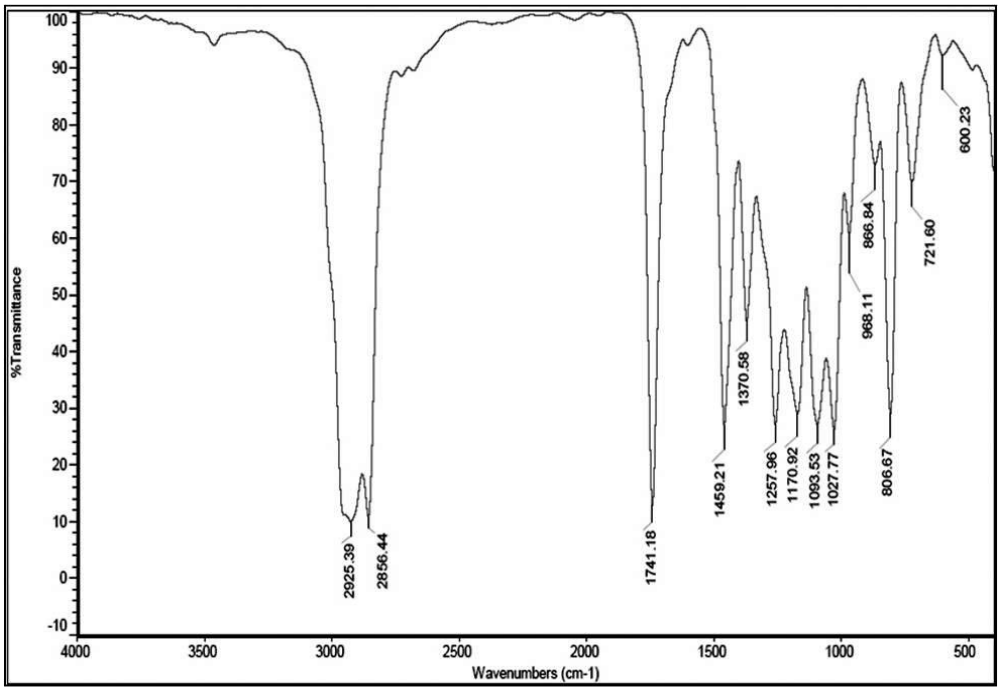

Figure 4.77. Figure showing the FTIR spectrum of compound **G1**

4.3.2.2. Structural Characterization of compound G2

2-(3-Ethyl-9-(2-methoxyethoxy)-1-oxo-2, 3, 4, 9-tetrahydro-1*H*-xanthen-2-yl) ethyl 5- hydroxy-9-methoxy-7, 8-dimethyl-8-(5-methylfuran- 2-yl) nona-3, 6-dienoate **(G2)**

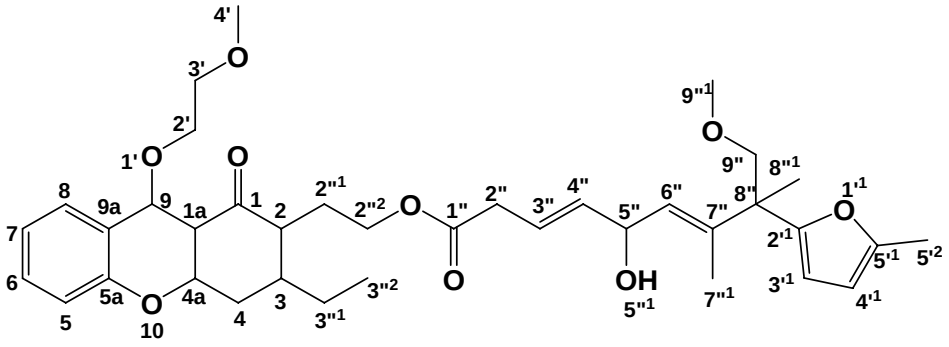

Sample yield	150 mg (0.625 %)
Physical description	Yellow oil
Molecular formula	$C_{37}H_{48}O_9$
Molecular weight	636.3308

2-**(3-Ethyl-9-(2-methoxyethoxy)-1-oxo-2, 3, 4, 9-tetrahydro-1*H*-xanthen-2-yl) ethyl 5-hydroxy-9-methoxy-7, 8-dimethyl-8-(5-methylfuran- 2-yl) nona-3, 6-dienoate :**Yellow oil; UV (MeOH: EtOAc) (log ε): 235 nm (3.237); TLC (Si gel GF_{254} 15 mm; MeOH: EtOAc 7:3, v/v) Rf: 0.76.; Rt (HPLC, CH_3CN: MeOH, 2:3 v/v): 14.147 min; IR (KBr, cm^{-1}) νmax (ν = stretching, δ = bending, ρ = rocking vibrations): 3425.10 (O-H ν), 2923.34, 2854.61 (C-H ν), 1708.08 (C=O ν), 1461.79 (C-H δ), 1297.86 (C-H ρ), 942.30 (=C-H δ), 724.28 (C-H ρ) ; ^{1}H NMR (500 MHz $CDCl_3$): δ_H 1.93 (2H, m), δ_H 1.93 (1H, m), δ_H 1.45 (2H, m), δ_H 0.80 (3H, t, *J*=6.88 Hz, H), δ_H 2.24 (1H, m), δ_H 1.54 (2H, m), δ_H 3.98 (2H, t, *J*=6.49 Hz), δ_H 2.75 (2H, d, *J*=4.62 Hz), δ_H 5.29 (1H, m), δ_H 5.26 (1H, t, *J*=8.19 Hz), δ_H 4.52 (1H, d, *J*=7.32 Hz), δ_H 3.24 (1H, s), δ_H 5.35 (1H, s), δ_H 1.62 (3H, s), δ_H 4.16 (1H, s), δ_H 4.06 (2H, t, *J*=7.18 Hz), δ_H 4.15 (2H, t, *J*=2.62 Hz), δ_H 3.59 (3H, s), δ_H 7.64 (1H, d, *J*=3.20 Hz), δ_H 7.29 (1H, t, *J*=2.05 Hz), δ_H 7.46 (1H, t,

J=3.07 Hz), δ_H 7.06 (1H, d, *J*=2.56 Hz), δ_H 2.06 (3H, s), δ_H 7.05 (1H, d, *J*=2.56 Hz), δ_H 7.06 (1H, d, *J*=2.56 Hz), δ_H 1.18 (3H, s), δ_H 3.92 (2H, s), δ_H 3.59 (3H, s); ^{13}C NMR (125 MHz, $CDCl_3$): δ_C 39.87 (C-4), δ_C 32.67 (C-3), δ_C 29.53 (C-3"^{1}), δ_C 14.1 (C-3"^{2}), δ_C 31.92 (C-2), δ_C 30.37 (C-2"^{1}), δ_C 64.39 (C-2"^{2}), δ_C 174.3 (C-1"), δ_C 25.63 (C-2"), δ_C 128.55 (C-3"), δ_C 128.99 (C-4"), δ_C 73.98 (C-5"), δ_C 128.18 (C-6"), δ_C 132.46 (C-7"), δ_C 38.76 (C-7"^{1}), δ_C 209.27 (C-1), δ_C 138.4 (C-1a), δ_C 74.75 (C-9), δ_C 60.8 (C-1'), δ_C 68.13 (C-2'), δ_C 51.39 (C-3'), δ_C 142.54 (C-9a), δ_C 128.85 (C-8), δ_C 124.44 (C-7), δ_C 130.83 (C-6), δ_C 125.09 (C-5), δ_C 147.67 (C-5a), δ_C 138.51 (C-4a), δ_C 147.07 (C-5'^{1}); δ_C 30.19 (C-5'^{2}), δ_C 123.42 (C-4'^{1}), δ_C 128.15 (C-3'^{1}), δ_C 142.6 (C-2'^{1}), δ_C 42.31 (C-8"), δ_C 31.79 (C-8"^{1}), δ_C 66.64 (C- 9"), δ_C 50.04 (C-9"^{1}); ^{1}H-^{1}H COSY and HMBC (Fig. 4.78 to Fig. 4.88, Table 4.14); HR (EI) MS *m/z* found 636.3308 $[M]^+$, calcd for $C_{37}H_{48}O_9$ 636.3305.

Compound **G2**, a previously undescribed furanyl derivative, was purified as yellow oil by extensive column chromatography on adsorbent silica gel. The mass spectral data of compound **G2** accounted for the molecular ion peak at *m/z* 636 (*m/z* 636.3308 $[M]^+$) enclosing fourteen degrees of unsaturation, and the molecular formula as $C_{37}H_{48}O_9$ was deduced from combined ^{1}H and ^{13}C NMR spectroscopic experiments. The IR spectrum showed bending vibration near 1708 cm^{-1}, which was attributed to the carbonyl group.

The absorption bands at 1461 and 2854 cm^{-1} in the FTIR spectrum showed the presence of olefinic (>C=C<) as well as alkyl groups, respectively. The characteristic hydroxyl stretching vibration appeared at 3425.10 cm^{-1}. The isolated compounds displayed ten quaternary carbons, in which, four carbons (δ_C 9a 142.54, δ_C 5a 147.67, δ_C 1a 138.4, δ_C 4a 138.51) were associated with substituted aromatic moiety, and two carbons {δ_C (C-1) 209.27, δ_C (C-1") 174.3} were attributed to the carbonyl groups in the side chain substitution of the aromatic framework, three carbons (δ_C 138.4, C-1a; δ_C 138.51, C-4a; and δ_C 132.46, C-7") were due to the olefinic groups, one quaternary carbon associated side chain substitution from furanyl moiety (δ_C 42.31, C-8") and remaining two carbons associated with furanyl skelton (δ_C 147.07, C-5'^{1} and δ_C 142.6, C-2'^{1}). These assignments supported the presence of 1*H*-xanthenyl methylfuranyl carbon skeleton. The ^{1}H-^{1}H COSY displayed the existence of three spin arrangements, H-6 to H-5{(δ_H 7.46 (H-6)/δ_H 7.06 (H-5)} which were due to the aromatic ring system, whereas the correlations between H-3"^{1} to H-3"^{2} {(δ_H 1.45 (H-3"^{1})/δ_H 0.80 (H-3"^{2})} designated ethyl substitution from xanthenyl moiety. ^{1}H-^{1}H COSY correlation between

H-2 to H-2"[1]/H-2"[2]{(δ_H 2.24 (H-2)/δ_H 1.54 (H-2"[1])/δ_H 3.98 (H-2"[2])}, H-2" to H-3" {(δ_H 2.75 (H-2")/δ_H 5.29 (H-3")} and H-4" to H-5" {(δ_H 5.26 (H-4")/δ_H 4.52 (H-5")} were assigned to the substitution from the furanyl framework, which were further confirmed from the detailed HMBC correlations.

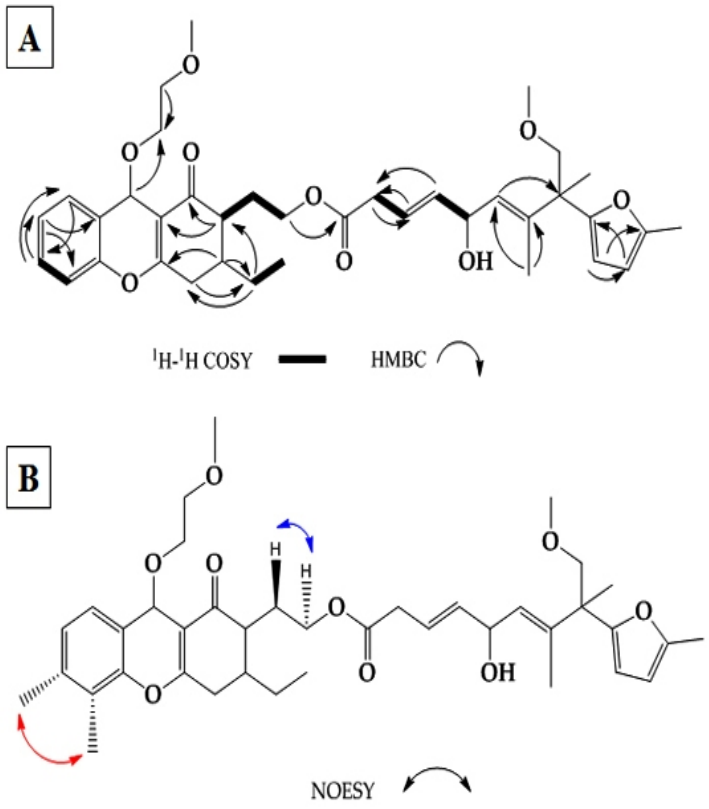

Figure 4.78. Figure showing key (**A**) ^{1}H-^{1}H COSY, HMBC, and (**B**) NOESY correlations of compound **G2**

Ultraviolet absorbance at λmax (log ε) 235 nm (3.237) was assigned to the xanthen chromophore, which was further supported by the IR bending vibrations at about 1461 cm^{-1} (Ochieng et al. 2012; Jiang et al. 2002). The ^{1}H NMR spectrum showed two doublets, and each integrated for one proton of furan with the same coupling constant (*J*=2.56 Hz) at δ_H 7.05 (H-4'[1]) and (*J*=2.56 Hz) at δ_H 7.06 (H-3'[1]) (Christoph et al. 2007). The ^{1}H NMR spectrum included eight methylene proton signals that appeared at H-1' {(δ_H 4.06 (H-1') corresponding to δ_C 60.18 (C-1') as deduced by HSQC experiments}, H-2' {(δ_H 4.15 (H-2'), δ_C 68.13 (C-2')}, H-4 {(δ_H 1.93 (H-4), δ_C

39.87 (C-4)}, H-3"^{1} {(δ_H 1.45 (H-3"^{1}), δ_C 29.53 (C-3"^{1})}, H-2"^{1} {(δ_H 1.54 (H-2"^{1}), δ_C 30.37 (C-2"^{1})}, H-2"^{2} {(δ_H 3.98 (H-2"^{2}), δ_C 64.39 (C-2"^{2})}, H-2" {(δ_H 2.75 (H-2"), δ_C 25.63 (C-2")} and H-9" {(δ_H 3.92 (H-9"), δ_C 66.64 (C-9")}, and terminal methyl group appeared as a triplet at H-3"^{2} {(δ_H 0.80 (H-3"^{2}, *J*=7 Hz), δ_C 14.1 (C-3"^{2})} attached to the xanthenyl ring framework (Table 4.14). The HMBC couplings between H-8 (δ_H 7.64)/C-6 (δ_C 130.83); H-7 (δ_H 7.29)/C-5 (δ_C 124.44); H-3 (δ_H 1.93)/C-3"^{1} (δ_C 29.53); H-3"^{1} (δ_H 1.45)/C-2 (δ_C 31.92), H-2" (δ_H 2.75)/C-3" (δ_C 128.55), H-3" (δ_H 5.29)/C-2" (δ_C 25.63), H- 4" (δ_H 5.26)/C-2" (δ_C 25.63) supported the above attributions. The ^{1}H NMR in combination with ^{13}C NMR exhibited highly deshielded oxymethylene protons at δ_H 4.06, H-1' (*J*=7.18 Hz) corresponding to C-1' (δ_C 60.18); δ_H 4.15, H-2' (*J*=2.62 Hz) C-2' (δ_C 68.13); δ_H 3.98, H-2"^{2} (*J*=6.49 Hz) C-2"^{2} (δ_C 64.39), and δ_H 3.92, H-9" (*J*=7.56 Hz) exhibiting HSQC correlation with C-9" (δ_C 66.64). Similarly highly deshielded oxymethine protons appeared at δ_H 4.16 H-9 (*J*=2.19 Hz) corresponding to C-9 (δ_C 74.75) due to the presence of electronegative oxygen and at δ_H 4.52 H-5" (*J*=7.32 Hz) C-5" (δ_C 73.83) due to the presence of neighboring –OH group, and therefore, were attributed to comprise the 1*H*-xanthenyl methylfuranyl ring system in compound **G2**. The additional olefinic signals were deduced at δ_H 5.29 (H-3", C-3"), δ_H 5.26 (H-4", *J*=8.19 Hz, C-4"), and δ_H 5.35 (H-6", *J*=5.35 Hz, C-6") whereas the methoxy group was found to appear as a singlet at δ_H 3.59 (H-3', 51.39 C-3'), δ_H 3.59 (H-9"^{1}, 50.04 C-9"^{1}), which were attributed to build the 2-(3-ethyl-9-(2-methoxyethoxy)-1-oxo-2, 3, 4, 9-tetrahydro-1*H*-xanthen-2-yl) ethyl-5-hydroxy-9-methoxy-7, 8-dimethyl-8-(5-methylfuran-2-yl) nona-3, 6-dienoate framework. The methyl protons at δ_H 7"^{1} (δ_H 1.62), 8"^{1} (δ_H 1.18) and 5'^{2} (δ_H 2.06) appeared as singlets. In addition hydroxyl group (-OH) appeared at H-5"^{1} (δ_H 3.24) as a singlet. The –CH proton at δ_H 2.24 {(H-2, C-2 (δ_C 31.92)}, δ_H 1.93 {(H-3, C- 3 (δ_C 32.67)}, and δ_H 4.16 {(H-9, C-9 (δ_C 74.75)} were distinct to the junction point of the substituted xanthenyl moiety with the side chain furanyl substitution. The intense HMBC interactions between H-3 (δ_H 1.93)/C-3"^{1} (δ_C 29.53)/C-4a (δ_C 138.51); H-3"^{1} (δ_H 1.45)/C-4 (δ_C 39.87); H-2 (δ_H 2.24)/C-1 (δ_C 209.27)/C-1a (δ_C 138.4); H-2"^{2} (δ_H 3.98)/C-1" (δ_C 174.3); H-7"^{1} (δ_H 1.62)/C-7" (δ_C 132.46)/C-6" (δc 128.18); H-6" (δ_H 5.35)/C-8" (δ_C 42.31); H-9 (δ_H 4.16)/C-1' (δ_C 60.18); H-2' (δ_H 4.15)/C-1' (δ_C 60.1); H-7 (δ_H 7.29)/C-9a (δ_C 142.54); H-6 (δ_H 7.46)/C-7 (δ_C 124.44)/C-8 (δc 128.85); H-4'^{1} (δ_H 7.05)/C-2'^{1} (δ_C 142.6); H-3'^{1} (δ_H 7.06)/C-4'^{1} (δ_C 123.42)/C-5'^{1} (δ_C 147.07) supported the above characteristics. The relative stereochemistries at C-3, C-2, C-9, and C-5" bearing the xanthenyl furanyl ring carbon

skeleton were attributed by detailed NOESY correlations and corresponding ^{1}H coupling constants (*J*-values). Notably, the aromatic protons at δ_H 7.46 {(H-6, C-6 (δ_C 130.83)} displayed NOESY correlations with the aromatic methine protons at δ_H 7.06 {(H-5, C-5 (δ_C 125.09)} in the xanthenyl furanyl ring skeleton. The proton at δ_H 1.54 {(H-2"^{1}, C-2"^{1} (δ_C 30.37)} resonated as a multiplet, which was at the α-face of the molecule having coupling at δ_H 3.98 {(H-2"^{2}, C-2"^{2} (δ_C 64.39)} (*J*=6.49 Hz), and subsequently the larger substituent 2, 3-diethyl-9-(2-methoxyethoxy)- tetrahydro-1*H*-xanthen-1-one at C-3 and C-2 was attributed to α-disposed.

Table 4.14 NMR spectroscopic data of compound **G2** in $CDCl_3$[a]

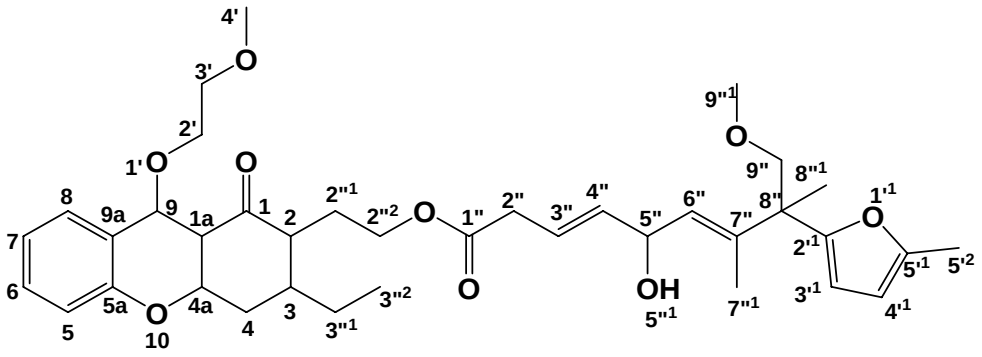

C. No	^{13}C (δ)	^{1}H NMR (mult., *J* in Hz, int.)[b]	^{1}H-^{1}H COSY	HMBC ($^{1}H^{13}C$)
1	209.27	-	-	-
1a	138.4	-	-	-
2	31.92	2.24 (m, 1H)	$2"^{1}$-H	C-1, C-1a
$2"^{1}$	30.37	1.54 (m, 2H)	2-H, $2"^{2}$-H	-
$2"^{2}$	64. 39	3.98 (t, *J*=6.49 Hz, 2H)	$2"^{1}$-H	C-1"
3	32.67	1.93 (m, 1H)	-	C-$3"^{1}$, C-4a
$3"^{1}$	29.53	1.45 (m, 2H)	$3"^{2}$-H	C-2, C-4
$3"^{2}$	14.1	0.80 (t, *J*=6.88 Hz, 3H)	$3"^{1}$-H	-
4	39.87	1.93 (m, 2H)	-	C-$3"^{1}$
4a	138.51	-	-	-
5	125.09	7.06 (d, *J*=2.56 Hz, 1H)	6-H	-
5a	147.67	-	-	-
6	130.83	7.46 (t, *J*=3.07 Hz, 1H)	5-H	C-7, C-8
7	124. 44	7.29 (t, *J*=2.05 Hz, 1H)	-	C-9a, C-5
8	128.85	7.64 (d, *J*=3.20 Hz, 1H)	-	C-6
9	74.75	4.16 (s, 1H)	-	C-1'
9a	142.54	-	-	-
1'	60.18	4.06 (t, *J*=7.18 Hz, 2H)		
2'	68.13	4.15 (t, *J*=2.62 Hz, 2H)		C-1'
3'	51.39	3.59 (s, 3H)		
1"	174.3	-		
2"	25.63	2.75 (d, *J*=4.62 Hz, 2H)	3"-H	C-3"
3"	128.55	5.29 (m, 1H)	2"-H	C-2"
4"	128.99	5.26 (t, *J*=8.19 Hz, 1H)	5"-H	C-2"
5"	73.98	4.52 (d, *J*=7.32 Hz, 1H)	4"-H	-
$5"^{1}$	-	3.24 (s, 1H)		
6"	128.18	5.35 (d, *J*=8.12 Hz,1H)		C-8"
7"	132.46	-		-
$7"^{1}$	38.76	1.62 (s, 3H)		C-6", C-7"
8"	42.31	-	-	
$8"^{1}$	31. 79	1.18 (s, 3H)	-	
9"	66.64	3.92 (s, 2H)	-	
$9"^{1}$	50.04	3.59 (s, 3H)	-	
$2'^{1}$	142.6	-	-	

$3'^{1}$	128.15	7.06 (d, *J*=2.56 Hz, 1H)	-	C-$4'^{1}$, C-$5'^{1}$
$4'^{1}$	123.42	7.05 (d, *J*=2.56 Hz, 1H)	-	C-$2'^{1}$
$5'^{1}$	147.07	-		
$5'^{2}$	30.19	2.06 (s, 3H)		

[a] NMR spectra recorded using Bruker AVANCE III 500 MHz (AV 500) spectrometer in $CDCl_3$ as aprotic solvent at ambient temperature with TMS as the internal standard (δ 0 ppm).

[b] Values in ppm, multiplicity and coupling constants (*J*=Hz) are indicated in parentheses. The assignments were made with the aid of the ^{1}H-^{1}H COSY, HSQC, HMBC and NOESY experiment

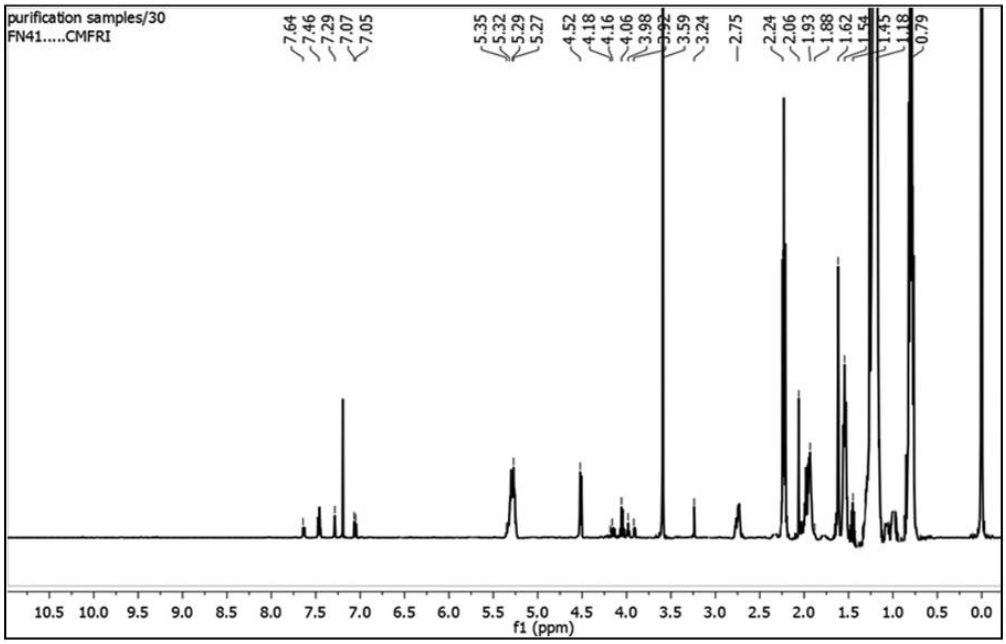

Figure 4.79. Figure showing the ^{1}H NMR spectrum of compound **G2**

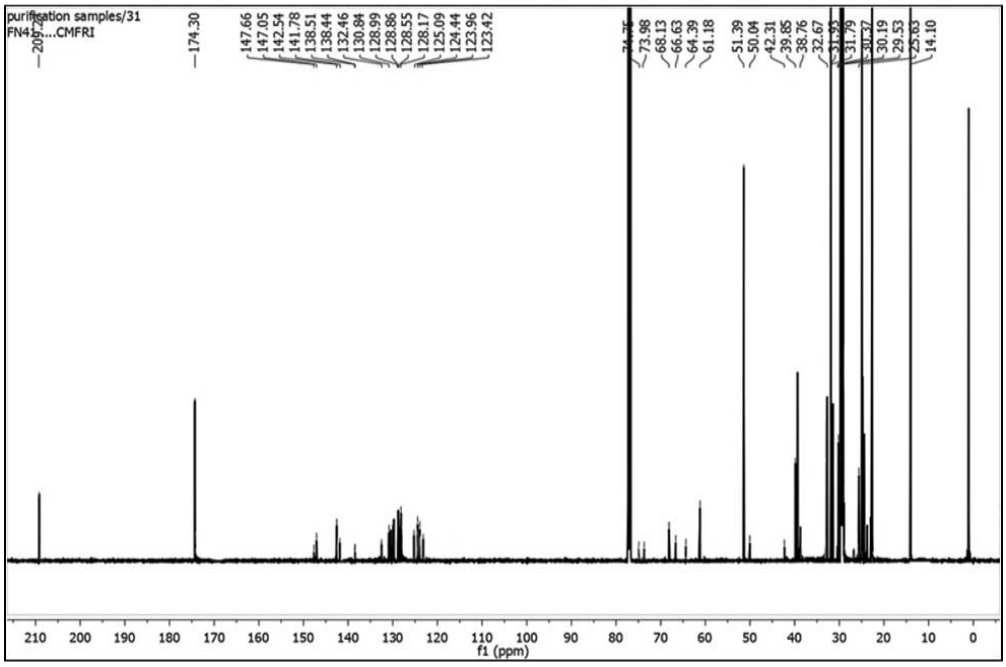

Figure 4.80. Figure showing the ^{13}C NMR spectrum of compound **G2**

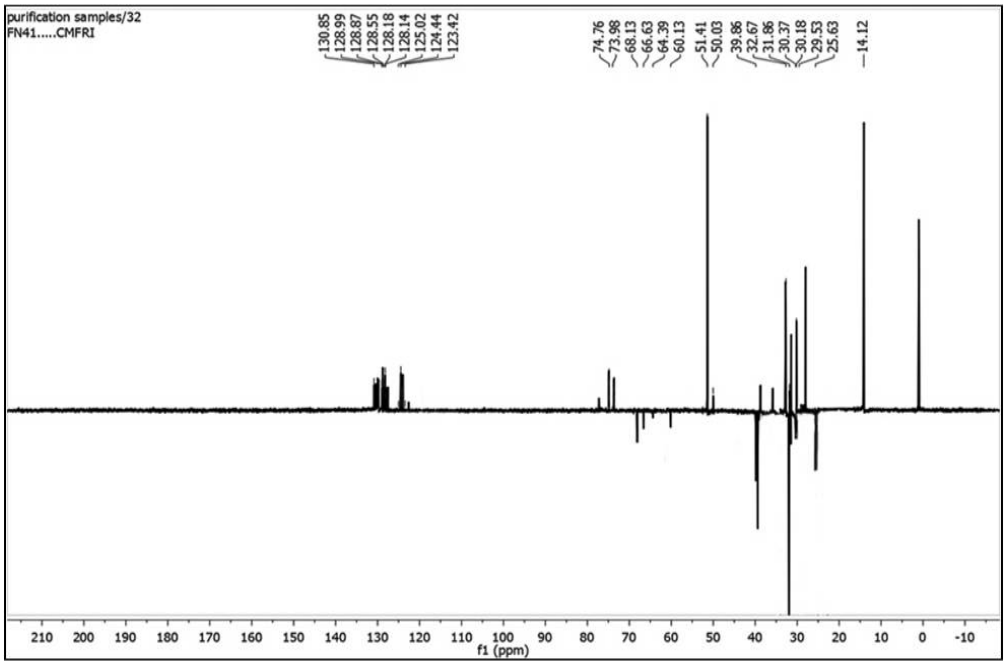

Figure 4.81. Figure showing the DEPT spectrum of compound **G2**

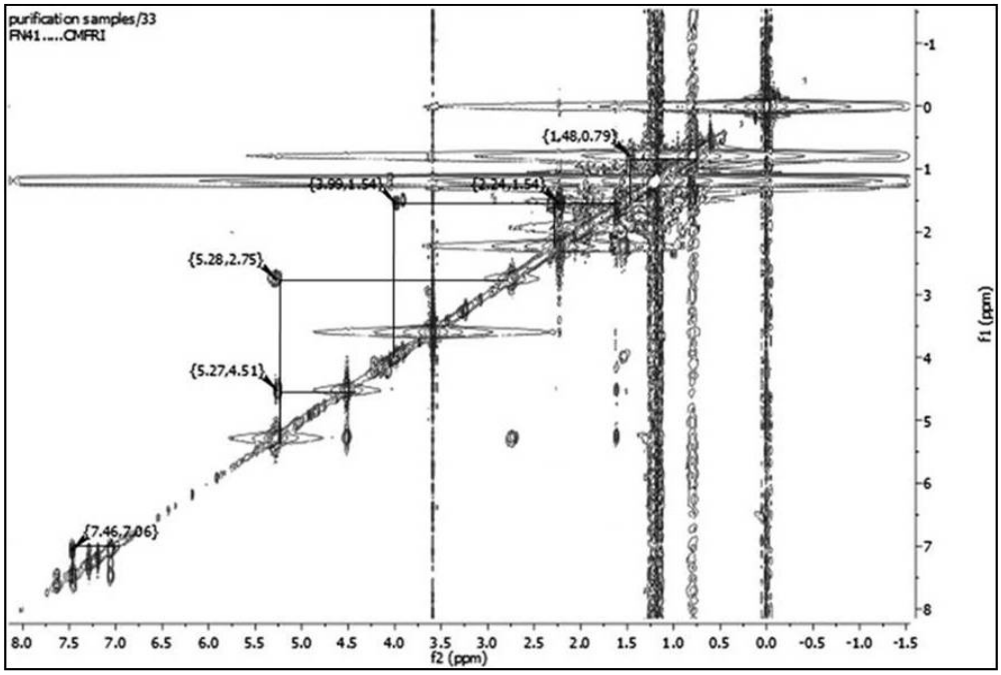

Figure 4.82. Figure showing the ^{1}H-^{1}H COSY spectrum of compound **G2**

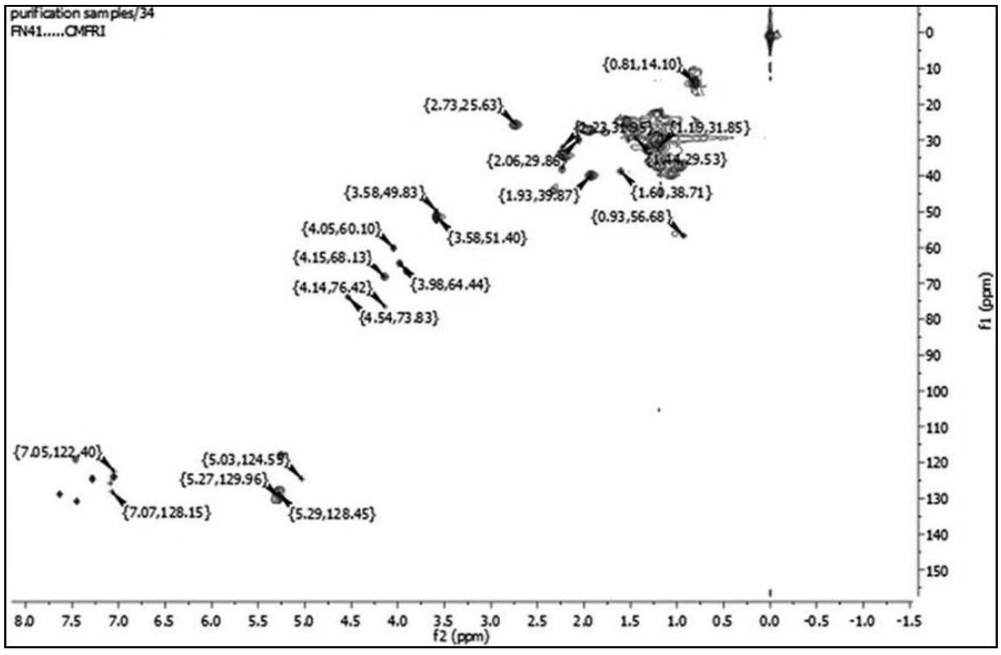

Figure 4.83. Figure showing the HSQC spectrum of compound **G2**

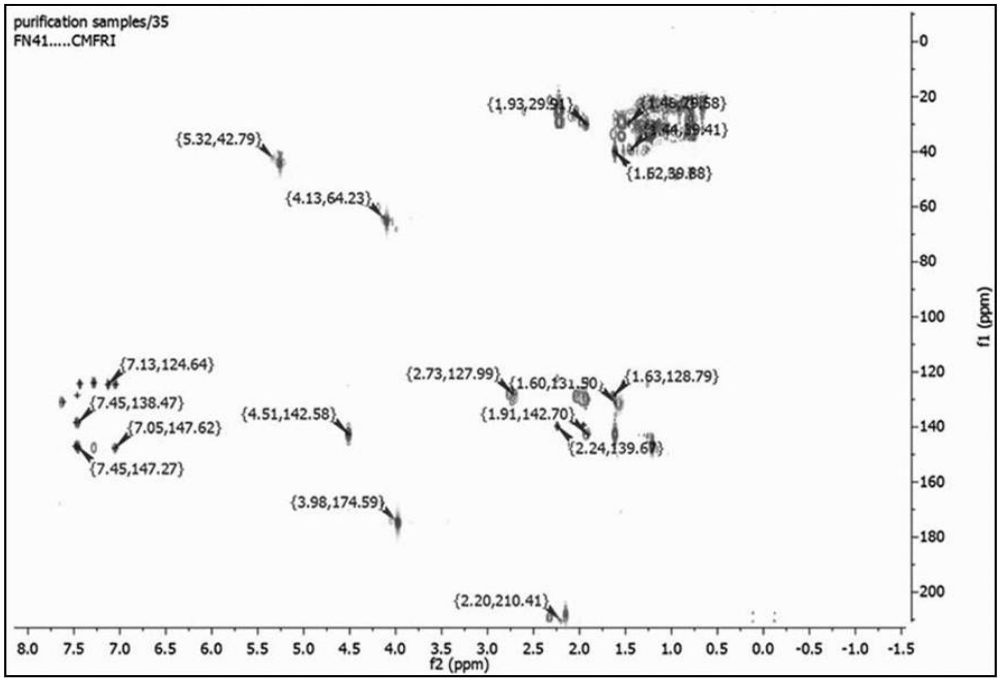

Figure 4.84. Figure showing the HMBC spectrum of compound **G2**

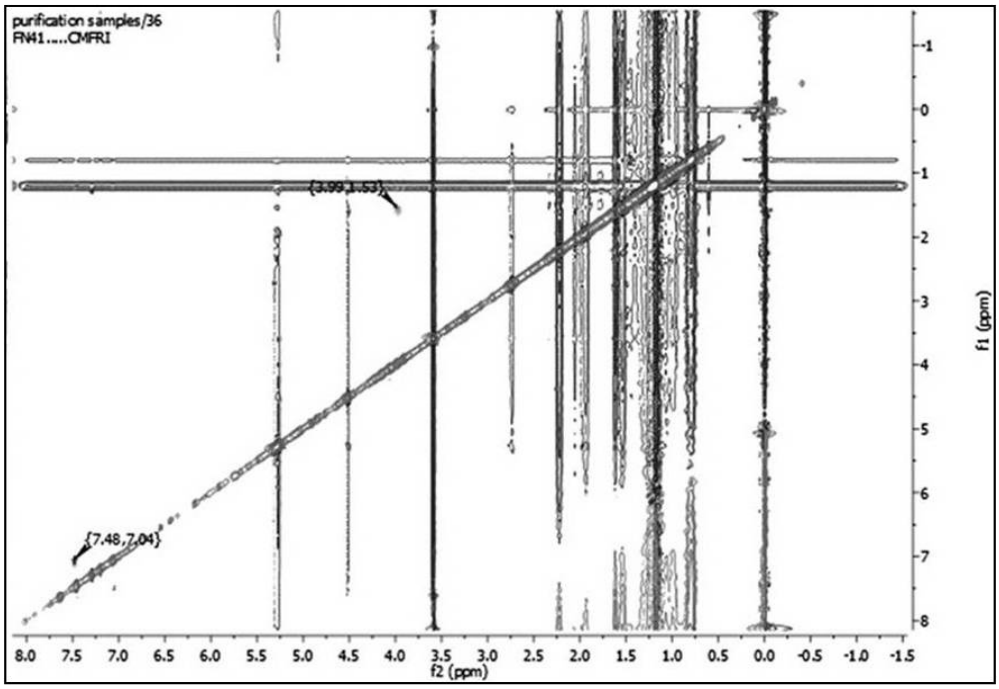

Figure 4.85. Figure showing the NOESY spectrum of compound **G2**

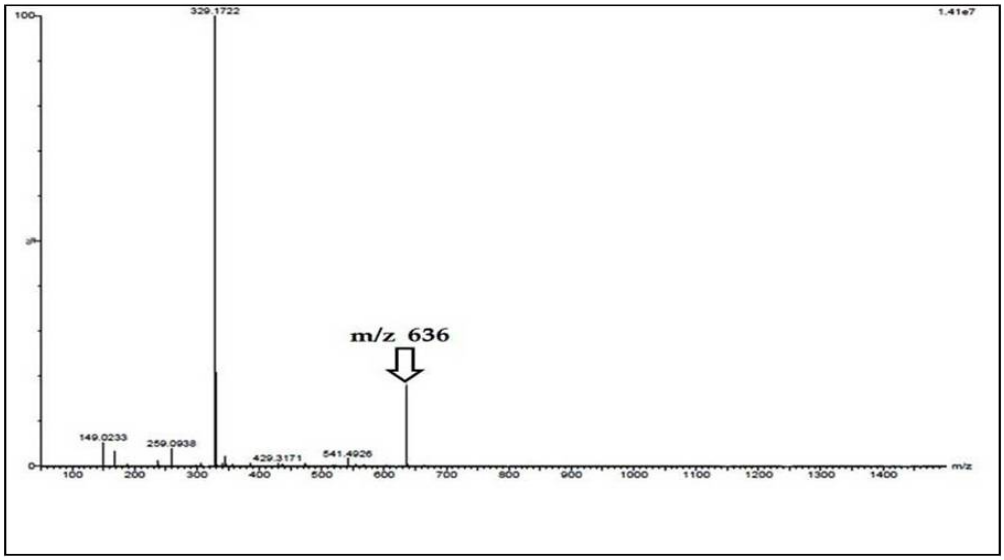

Figure 4.86. Mass spectrum of compound **G2**

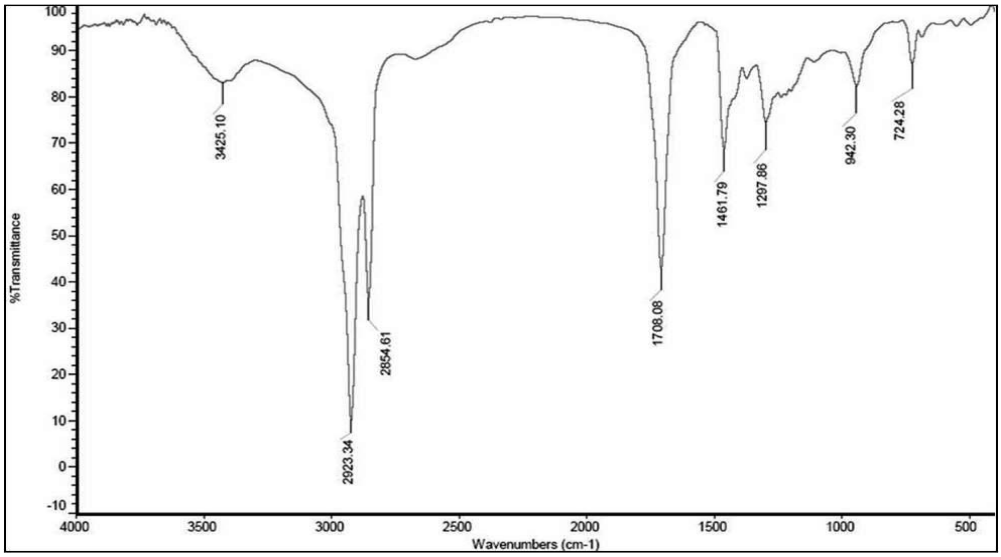

Figure 4.87. Figure showing the FTIR spectrum of compound **G2**

4.3.2.3. Bioactivities and Structure-Activity Relationship Analysis

The antioxidative properties of the furanyl derivatives as resolved by DPPH and ABTS free radical scavenging activities were found to be significantly greater (IC_{50}

~0.051–0.055 × 10^{-2} M) than those exhibited by α-tocopherol (IC_{50} > 0.146 × 10^{-2} M), and were similar to the synthetic antioxidants (BHT/BHA IC_{50} ~0.113–0.189 × 10^{-2} M, $P < 0.05$). It is of note that electron-delocalization through the electron-dense aromatic, carbonyl, methoxy, and olefinic bonds present in the molecular structure of the isolated compounds might apparently contribute towards their potential free radical scavenging properties (Pietta 2000; Cai et al. 2006).

The prostaglandins produced by proinflammatory constitutive enzyme COX-1 were reported to protect the stomach lining from gastric HCl secreted from the oxyntic and peptic glands, while blocking this enzyme isoform apparently increases the risk of stomach bleeding and ulcers. Notably, the commercially available NSAIDs, including salicylate analogs, aspirin and ibuprofen equally block two different cyclooxygenase isoforms, such as constitutive COX-1 and inducible COX-2. While this results in reduced pain and inflammation, it can potentially lead to serious gastrointestinal bleeding, heart attacks, and strokes. The furanyl derivatives isolated in this study displayed significantly greater inhibition towards COX-2 than its COX-1 isoform, and likewise, the selectivity indices (SI, anti-COX-1 IC_{50}/anti-COX-2 IC_{50}) of these compounds remained significantly lesser (1.08–1.09) than synthetic NSAIDs (aspirin and ibuprofen, SI: 0.02 and 0.44, respectively, $P < 0.05$), and consequently, appeared to be safer. The furanyl analogs exhibited no significant difference towards *in vitro* 5-LOX inhibitory activities (IC_{50} 0.209–0.173 × 10^{-2} M) with that displayed by ibuprofen (IC_{50} 0.451 × 10^{-2} M; $P < 0.05$). Sodium salicylate was found to be a weaker inhibitor of both COX isoforms (anti-COX-2 IC_{50} 1.655 × 10^{-2} M, anti-COX-1 IC_{50} 1.206 × 10^{-2} M), and demonstrated significantly lesser activity against 5-LOX (anti-LOX-5 IC_{50} 1.093 × 10^{-2} M) (Table 4.15-4.16). The hitherto undescribed furanyl derivatives from the red marine macroalga *G. opuntia*, might therefore, be used as potential anti-inflammatory and antioxidative pharmacophore leads in medicine and food. Structure–bioactivity correlation analyses of the furanyl derivatives isolated in this study were carried out by using different structural descriptor factors. The antioxidative properties of the isolated compounds were found to be directly proportional to their hydrophobic characters as resolved by octanol–water coefficient (log Pow). The larger the value of log Pow, the greater the molecular hydrophobicity of the compounds. Compound **G2** displayed lesser hydrophobic character (log Pow 3.37) than that recorded with **G1** (log Pow 4.59).

Table 4.15 Antioxidative and anti-inflammatory activities of the furanyl derivatives (**G1-G2**) from *G. opuntia vis-à-vis* the commercially available antioxidants and anti-inflammatory agents

Antioxidative activities†	**Bioactivities** {IC_{50} ($x10^{-2}$ M)}				
	Compound G1	**Compound G2**	**BHA**	**BHT**	**α-tocopherol**
$DPPH^{\cdot}$ scavenging	$0.051^{a} \pm 0.009$	$0.050^{a} \pm 0.009$	$0.144^{c} \pm 0.006$	$0.113^{b} \pm 0.009$	$0.146^{c} \pm 0.009$
$ABTS^{+\cdot}$ scavenging	$0.066^{a} \pm 0.004$	$0.055^{a} \pm 0.008$	$0.189^{c} \pm 0.011$	$0.118^{b} \pm 0.009$	$0.169^{c} \pm 0.116$
Anti-inflammatory activities†	**Compound G1**	**Compound G2**	**Aspirin**	**Na-salicylate**	**Ibuprofen**
COX -1 inhibition	$0.222^{b} \pm 0.009$	$0.185^{b} \pm 0.006$	$0.003^{a} \pm 0.00$	$1.206^{c} \pm 0.031$	$0.019^{a} \pm 0.00$
COX -2 inhibition	$0.202^{b} \pm 0.007$	$0.171^{b} \pm 0.014$	$0.117^{b} \pm 0.011$	$1.655^{c} \pm 0.031$	$0.044^{a} \pm 0.010$
Selectivity index††	$1.09^{c} \pm 0.06$	$1.08^{c} \pm 0.03$	$0.02^{a} \pm 0.02$	$0.72^{b} \pm 0.01$	$0.44^{b} \pm 0.02$
5-LOX inhibition	$0.209^{a} \pm 0.024$	$0.173^{a} \pm 0.006$	$0.216^{a} \pm 0.011$	$1.093^{c} \pm 0.075$	$0.451^{b} \pm 0.053$

† The samples were analyzed in triplicate (n=3) and expressed as mean ± standard deviation. Means followed by the different superscripts (a–c) within the same row indicate significant differences ($P < 0.05$).

†† Selectivity index has been calculated as the ratio of anti-COX-1(IC_{50}) to that of anti-COX-2 (IC_{50})

Table 4.16 Anti-diabetic and anti-hypertensive activities of the furanyl derivatives (**G1-G2**) from *G. opuntia vis-à-vis* the commercially available agents

	Bioactivities { $IC_{50}s\,(x10^{-2}\,M)$}		
Anti-diabetic activities[†]	**Compound G1**	**Compound G2**	**Standard**[††]
α-Amylase inhibitory	$0.062^{a} \pm 0.002$	$0.052^{a} \pm 0.002$	$0.062^{a} \pm 0.002$
α-Glucosidase inhibitory	$0.040^{a} \pm 0.007$	$0.031^{a} \pm 0.005$	$0.033^{a} \pm 0.002$
Inhibition of DPP-4	$0.002^{a} \pm 0.00$	$0.002^{a} \pm 0.009$	$0.003^{a} \pm 0.00$
Anti-hypertensive activities[†]	**Compound G1**	**Compound G2**	**Captopril**
ACE-1 inhibition	$0.024^{a} \pm 0.007$	$0.023^{a} \pm 0.005$	$0.037^{b} \pm 0.005$

[†] The samples were analyzed in triplicate (n=3) and expressed as mean ± standard deviation. Means followed by the different superscripts (a–b) within the same row indicate significant differences ($P < 0.05$).

[††] Acarbose was used as the standard for α-amylase and α-glucosidase inhibitory activities; whereas diprotin A was the reference towards inhibition of DPP-4.

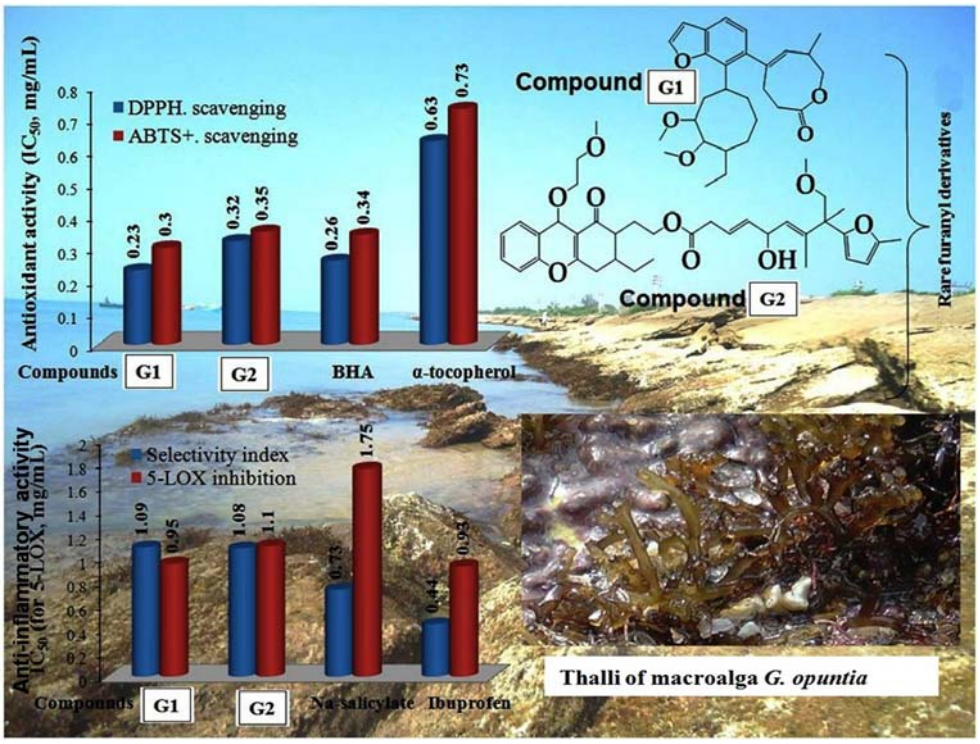

Figure 4.88. Graphical representation of bioactivities of compound **G1** and **G2**. The thalli of the studied marine macroalga were displayed as inset

The reduced activity of compound **G2** is justified based on the lesser hydrophobic properties and reduced membrane permeability and reactivity towards DPPH-free radical. It has been hypothesized that the free radical DPPH can easily interact with the compounds with greater hydrophobic coefficients (greater log Pow value), and therefore, exhibit higher radical scavenging ability towards lipophilic DPPH. Since antioxidants require diffusing into the liposomes to interact with the lipophilic free radicals in the biological systems, it is reasonable to expect that a greater hydrophobicity of antioxidants is related to their radical scavenging activity in liposomes and cells. On the basis of these results, it could be concluded that hydrophobicity has been the significant factor in determining the antioxidant and anti-inflammatory properties of the furanyl derivatives. Notably, acarbose and miglitol are competitive inhibitors of α-glucosidase, and were found to decrease the absorption of starch and disaccharides (Baylac and Racine 2003; Davis and Granner 2011). One of the remedial pathways for reducing the postprandial blood glucose levels in the patients with diabetes mellitus is to cut off carbohydrate consumption after food intake.

The α-amylase/α-glucosidase has been accepted as a family of endo-amylases catalyzing the initial hydrolysis of starch into smaller oligosaccharides by the cleavage of α-D-(1-4) glycosidic bonds. Inhibition of the enzymes, α-amylase and α-glucosidase appeared to minimize the increased postprandial blood glucose level in diabetes (Abu Soud et al. 2004; Conforty et al. 2005). The present study displayed that there were significant differences in α-glucosidase/α-amylase inhibitory activities of the purified compound **G1** than those recorded with compound **G2**. However, compound **G1** exhibited greater α-amylase inhibitory activity (IC_{50} 0.062 × 10^{-2} M) compared to compound **G2** (IC_{50} 0.052 × 10^{-2} M) and the activities were comparable with synthetic positive control (acarbose, IC_{50} 0.062 × 10^{-2} M) (Fig. 4.88, Table 4.15-4.16). Likewise, compound **G1** exhibited greater α-glucosidase inhibitory activity (IC_{50} 0.040 × 10^{-2} M) than that displayed by compound **G2** (IC_{50} 0.031 × 10^{-2} M) and the positive control (acarbose, IC_{50} 0.033 × 10^{-2} M). Marine macroalgae were reported to possess α-amylase and α-glucosidase inhibitory activities (Apostolidis et al. 2011), which appropriately substantiated the results obtained in the present study that the marine macroalgal species are potential source for anti-diabetic agents. DPP-4 inhibition was found to be a systematic approach to manage type 2 diabetes mellitus by potentiating insulin production (Mentlein 1999). The present study showed the biological effects of furanyl derivatives isolated from *G. opuntia*. The isolated compounds exhibited potential DPP-4 inhibitory activities (IC_{50} ~0.002 × 10^{-2} M) and were comparable with standard diprotin A (IC_{50} 0.003 × 10^{-2} M; $P < 0.05$). Vildagliptin, sitagliptin, saxagliptin, etc, are synthetic DPP-4 inhibitors available in market, and were reported to have several side effects, such as hypoglycemic disorders, headache, nausea, dizziness, weight gain, and swelling of the appendages due to excess fluid retention (Idris and Donnelly 2007). Likewise, other synthetic hypoglycemic agents, such as acarbose and voglibose that inhibit α-amylase and α-glycosidase were found to cause hepatic and gastrointestinal disorders (Murai et al. 2002). Bioactive potential of the isolated compounds was due to the interaction of functional groups in the furanyl derivative with DPP-4 by H-bonding and hydrophilic interactions. The isolated compounds showed significant number of electronegative functional groups, which could potentially form H-bond with DPP-4 resulting in greater anti-diabetic activity. The compounds in the present study can be effectively used for potential alternative therapy for treatment of diabetes. Notably, the isolated furanyl derivatives exhibited

potential ACE inhibitory activity (IC_{50} 0.023–0.024 × 10^{-2} M), and were comparable with the commercial ACE inhibitor, captopril (IC_{50} 0.037 × 10^{-2} M).

4.3.2.4. Structural Characterization of Compound G3

3-(2-Ethyl-6-((3, 7)-1, 2, 5, 6-tetrahydroazocin-5-yl) hexyl) morpholin-6-one (**G3**)

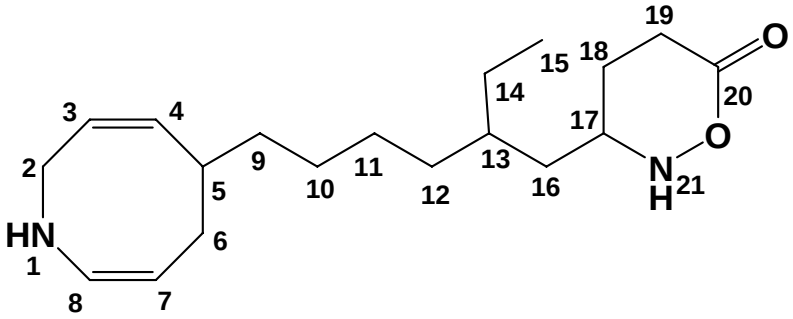

Sample yield	134 mg (1.34 %)
Physical description	Greenish oil
Molecular formula	$C_{19}H_{32}N_2O_2$
Molecular weight	320.2467

3-(2-Ethyl-6-((3, 7)-1, 2, 5, 6-tetrahydroazocin-5-yl) hexyl) morpholin-6-one: Greenish oil; UV (MeOH: EtOAc) λmax (log ε): 252 nm (3.76); TLC (Si gel GF_{254} 15 mm; EtOAc: *n*-hexane 3:7, v/v); Rf: 0.76.; Rt (HPLC, ACN: MeOH 2:3 v/v): 16.57 min; IR (KBr, cm^{-1}) ν_{max} (ν = stretching, δ = bending, ρ = rocking vibrations): 724.28 (C–H ρ), 942.30 (alkene C–H δ), 1297.86 (C–N ρ), 1461.79 (C–H δ), 1708.08 (C–CO–C ν), 2854.61 (C–H ν), 2923.34 (C–H ν), 3425.10 (N–H ν); ^{1}H-NMR ($CDCl_3$, 500 MHz), δ_H 2.64 (1H, s, NH), δ_H 4.16 (d, *J*=7.01 Hz, 2H), δ_H 5.4 (m, 1H), δ_H 5.43 (m, 1H), δ_H 2.81 (m, 1H), δ_H 2.01 (t, *J*=5.95 Hz, 2H), δ_H 5.34 (m, 1H), δ_H 5.36 (d, *J*=6.6 Hz, 1H), δ_H 1.5 (m, 2H), δ_H 1.11 (m, 2H), δ_H 1.26 (m, 2H), δ_H 1.26 (m, 2H), δ_H 1.32 (m, 1H), δ_H 1.28 (m, 2H), δ_H 0.88 (t, *J*=6.81 Hz, 3H), δ_H 1.25 (m, 2H), δ_H 4.16 (m, 1H), δ_H 1.62 (m, 2H), δ_H 2.36 (t, *J*=6.75 Hz, 2H), δ_H 3.79 (s, 1H); ^{13}C NMR (125 MHz, $CDCl_3$): δ_C 59.47 (C-2), δ_C 122.88 (C-3), δ_C 130.19 (C-4), δ_C 32.79 (C-5), δ_C 39.88 (C-6), δ_C 129.97 (C-7), δ_C 127.86 (C-8), δ_C 27.73 (C-9), δ_C 39.35 (C-10), δ_C 29.63 (C-11), δ_C 31.91 (C-12), δ_C 32.80 (C-13), δ_C 22.74 (C-14), δ_C 14.12 (C-15), δ_C 37.20 (C-16),

δ_C 61.62 (C-17), δ_C 24.72 (C-18), δ_C 33.83 (C-19), δ_C 178.6 (C-20); HMBC and ^1H-^1H-COSY data (Fig. 4.89 to Fig. 4.98, Table 4.17); HR (EI) MS *m/z* calcd for $C_{19}H_{32}N_2O_2$ 320.2464, found 320.2467 $[M]^+$.

In the present study, solvent methanol: ethyl acetate (1:1, v/v) soluble extract from the shade-dried thalli of red marine macroalga *G. opuntia* was submitted to repeated vacuum column chromatographic fractionation over silica gel, flash chromatography, and preparative thin layer chromatography (PTLC), using various combinations of mobile phase (*n*-hexane/EtOAc/MeOH) to afford hitherto unknown azocinyl morpholinone, named 3-(2-ethyl-6-((3, 7)-1, 2, 5, 6-tetrahydroazocin-5-yl) hexyl) morpholin-6-one. Furthermore, this novel bioactive lead from *G. opuntia* will be an abundant source for future research work. 3-(2-Ethyl-6-((3, 7)-1, 2, 5, 6-tetrahydroazocin-5-yl) hexyl) morpholin-6-one, a new derivative of the azocinyl morpholinone alkaloid, was purified as greenish oil by repeated chromatography (on adsorbent silica gel). The structure of the purified compound was attributed based on extensive 2D NMR experiments and mass spectra. The ^1H NMR along with ^{13}C NMR spectra recorded the presence of methylene protons at δ_H 1.62, δ_H 2.36, δ_H 1.25, δ_H 1.28, δ_H 1.26, δ_H 1.26, δ_H 1.11, δ_H 1.5, δ_H 2.01, δ_H 4.16 and the ^1H–^1H COSY cross peaks at H-18/H-19, H6/7, and H2/3 supported the occurrence of C-19 skeleton (Table 4.17). The downfield chemical shift of the $>CH_2$ signals at δ_H 2.36 and the C-19 carbon at δ_H 33.83 referred to a presence of ester carbonyl moiety. The olefinic protons were assigned at δ_H 5.32–5.45, and their proton integral values showed the existence of two olefinic bonds. The broad absorption band at 3425.10 cm^{-1} in the IR spectrum was attributed to the –NH groups, which has been supported by the ^1H NMR signal at δ_H 3.79 and δ_H 2.64. The presence of –NH protons was further validated by D_2O exchange. The occurrences of two nitrogen groups were also satisfied by nitrogen odd and even rule. The $>CH_2$ group of the protons at δ_H 4.16 and δ_H 2.36 were assigned to the C-2 and C-19 positions, respectively. Intense HMBC correlation was found between δ_H 2.01 (attributed to H-6) and δ_C 130.19 (assigned to C-4), which showed the existence of olefinic group near the $>CH_2$ group.

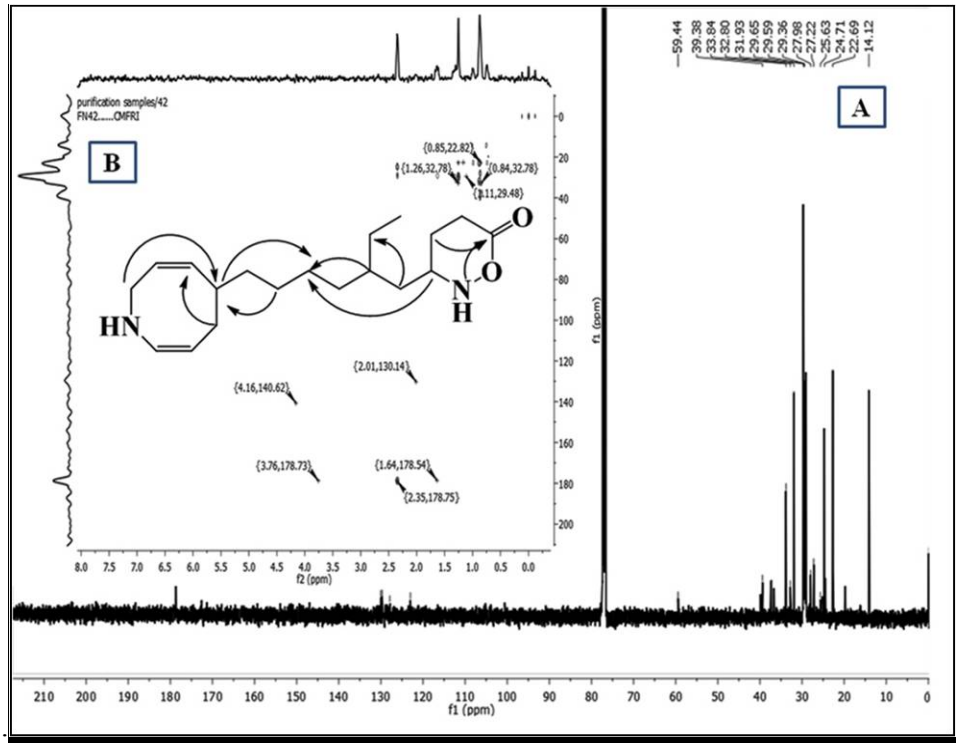

Figure 4.89. Figure showing the Key **(A)** ^{13}C-NMR, (**B**) HMBC spectra of compound **G3**

The proton due to methine group at δ_H 2.81 were deshielded due to the possible olefinic groups in their vicinity. Intense ^{1}H–^{1}H COSY cross peaks between H-6 (δ_H 2.01)/H-7 (δ_H 5.34), H-2 (δ_H 4.16)/H-3 (δ_H 5.4) along with the C/H connectivities (from the HMBC/HSQC experiments) attributed the tetrahydroazocine carbon skelton. The strong deshileding of the –NH protons at δ_H 3.79 was due to the presence of carboxyl ester group at C-20, and accordingly it was assigned to the junction point. The –CH– proton at δ_H 2.81 was attributed to the junction point of the tetrahydroazocinyl ring substituted with the side chain ethyl heptyl morpholine carbon skeleton. These assignments were further confirmed by ^{1}H–^{1}H COSY correlations and strong HMBC correlations. The location of the >NH proton at δ_H 3.79 was assisted by HMBC experiments. The cyclization point of the substituted morpholin ring was resolved by downfield shift of H-17 at δ_H 4.16, which was connected to the methylene protons at δ_H 1.62 (assigned to H-18) showing clear ^{1}H–^{1}H COSY correlation with H-19, thereby supporting the presence of the morpholin-6-one moiety. HSQC and HMBC experiments established the presence of tetrahydroazocinyl ring skelton connected to

the morpholin substitution at the C-9 carbon of the compound. Intense HMBC cross peaks were recorded between H-2 (δ_H 4.16)/C-5 (δ_C 32.79), H-5 (δ_H 2.81)/C-11 (δ_C 29.63), H-6 (δ_H 2.01)/C-4 (δ_C 130.19), H-10 (δ_H 1.11)/C-5 (δ_C 32.79), H-16 (δ_H 1.25)/C-14 (δ_C 22.74), H-13 (δ_H 1.32)/C-11 (δ_C 29.63), H-18 (δ_H 1.62)/C-20 (δ_C 178.6), H-21 (δ_H 3.79)/C-20 (δ_C 178.6), which supported the presence of 3-(2-ethyl-6-((3, 7)-1, 2, 5, 6-tetrahydro azocin-5-yl-hexyl) morpholin-6-one moiety. The –CH_2 signal at δ_H 1.62 (assigned to C-18) demonstrated HMBC connections with ester carbonyl carbon at δ_C 178.6 (attributed to C-20). The comparative stereochemical configuration of the chiral centers at C-5, C-13 belonging to 1, 2, 5, 6-tetrahydro azocin-5-yl-hexyl moiety, and C-17 of the morpholin- 6-one ring framework were summarized from the NOE spectral experiments and the coupling constant values. The equatorial proton Hb, of C-18b was found to resonate as a multiplet with the axial proton Ha-5, having an axial-axial coupling (*J*a,d=12 Hz) and axial equatorial coupling (*J*a,b=6 Hz) which attributed for the larger substituent 5-(5-methylheptyl)-1, 2, 5, 6-tetrahydroazocine group at C-16 as equatorially disposed. These assignments were established by a sequence of NOE cross peaks, which confirmed the C-17 proton as axial. Intense NOE correlation between the methine proton at Ha-5 and H-13, suggested that these protons were axial. The chair-like conformation might be due to intense 1,3-eclipsing interaction between the axial methylene proton at C-16 belonging to the bulky tetrahydro-5-(5-methylheptyl) azocine moiety and the He-19, which forced the latter into an equatorial disposition, and the morpholinone framework into a chair-like conformation. The existence of NOE between the axial –CH_2– proton Hd-19 and axial CH at Ha-5 indicated a chair-like configuration and these assignments were assisted by the absence of an NOE between the axial proton Hd-19, and the methylene proton Hc-18. The attributions for the chair-conformation might be explained by the lack of intense 1, 2-eclipsing interactions, since the equatorial position was occupied with bulky tetrahydro-5-(5-methylheptyl) azocine framework. The molecular ion peak at *m/z* 320 (HR-EI-MS *m/z* calcd. for $C_{19}H_{32}N_2O_2$ 320.2464, found 320.2467 $[M]^+$), which was combined with the detailed NMR experimental data to record the elemental composition of the compound **G3** with five degrees of unsaturation. Two degrees of unsaturation were due to the two olefinic double bonds (δ_H 5.32–5.42), whereas one degree of unsaturation was attributed to the carbonyl group (δ_C 178.6) and the remaining two were due to the two ring systems. The molecular ion peak at *m/z* 320 ($C_{19}H_{32}N_2O_2$, $[M]^+$) was found to undergo deamination yielding 6-ethyl-11-(prop-1-enyl) tetradec-13-enoic acid (*m/z*

294). Two $-CH_2$ groups eliminated from the fragment ion (*m/z* 294) to afford the fragments at *m/z* 280 (assigned to 6-ethyl-11-vinyltetradec-13-enoic acid) and *m/z* 266 (6-methyl-11-vinyltetradec-13-enoic acid). The fragment peak at *m/z* 148 (assigned to tetrahydro-6a*H*-cyclopenta azocine) was found to be the base peak. Intense IR stretching vibrations were apparent between 1461 and 2854 cm^{-1} that were attributed to the olefinic (C=C) and alkyl (C–H) groups. Intense ester carbonyl and N–H stretching vibrations were apparent near 1708 and 3425 cm^{-1}, respectively.

Table 4.17 NMR spectroscopic data of compound **G3** in $CDCl_3$[a]

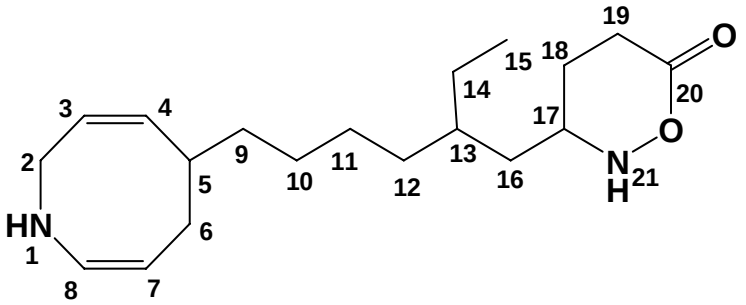

C. No	^{13}C (δ)	^{1}H-NMR[b] (int., mult., *J* in Hz)	^{1}H-^{1}H COSY	HMBC
1	-	2.64 (s, 1H)	-	-
2	59.47	4.16 (d, *J*=7.01 Hz, 2H)	3-H	C-5
3	122.88	5.4 (m, 1H)	2-H	-
4	130.19	5.43 (m, 1H)	-	-
5	32.79	2.81 (m, 1H)	-	C-11
6	39.88	2.01 (t, *J*=5.95 Hz, 2H)	7-H	C-4
7	129.97	5.34 (m, 1H)	6-H	-
8	127.86	5.36 (d, *J*=6.6 Hz, 1H)	-	-
9	27.73	1.5 (d, *J*=6.3 Hz, 2H)	-	-
10	39.35	1.11 (m, 2H)	-	C-5
11	29.63	1.26 (m, 2H)	-	-
12	31.91	1.26 (m, 2H)	-	-
13	32.80	1.32 (m, 1H)	-	C-11
14	22.74	1.28 (m, 2H)	-	-
15	14.12	0.88 (t, *J*=6.81 Hz, 3H)	-	-
16	37.20	1.25 (m, 2H)	-	C-14
17	61.62	4.16 (m, 1H)	-	-
18	24.72	1.62 (m, 2H)	19-H	C-20
19	33.83	2.36 (t, *J*=6.75 Hz, 2H)	18-H	-
20	178.6	-	-	-
21	-	3.79 (s, 1H)	-	C-20

[a] NMR spectra recorded using Bruker AVANCE III 500 MHz (AV 500) spectrometer in $CDCl_3$ as aprotic solvent at ambient temperature with TMS as the internal standard (δ 0 ppm).

[b] Values in ppm, multiplicity and coupling constants (*J*=Hz) are indicated in parentheses. The assignments were made with the aid of the ^1H-^1H COSY, HSQC, HMBC and NOESY experiment

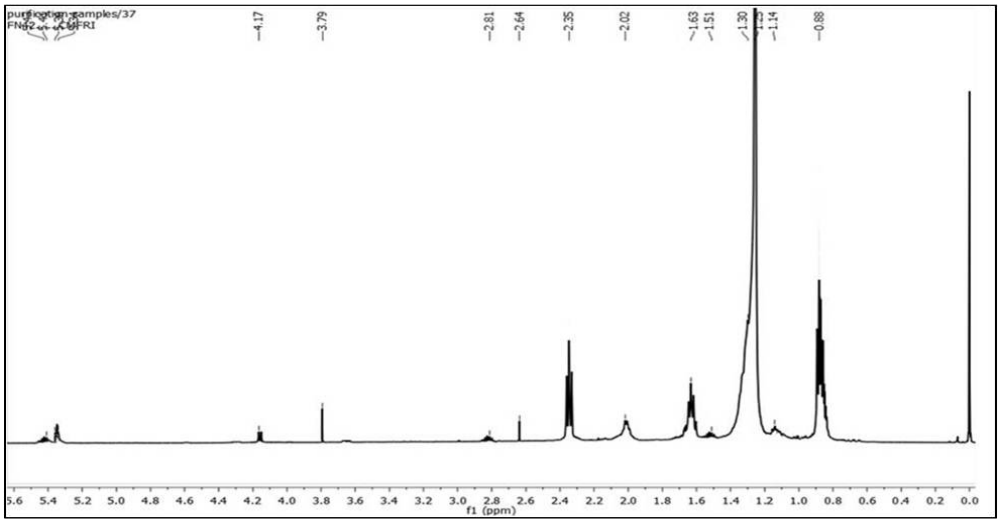

Figure 4.90. Figure showing the ^1H NMR spectrum of compound **G3**

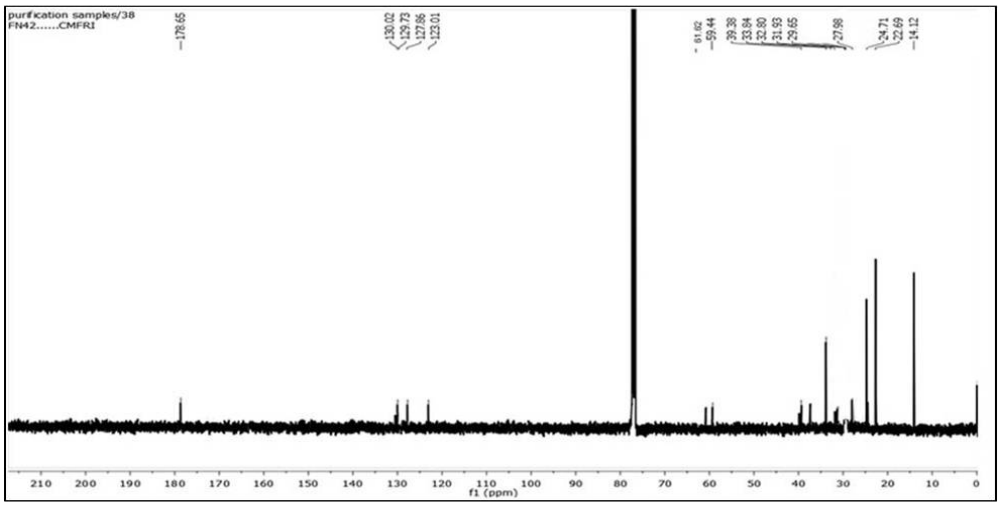

Figure 4.91. Figure showing the ^{13}C spectrum of compound **G3**

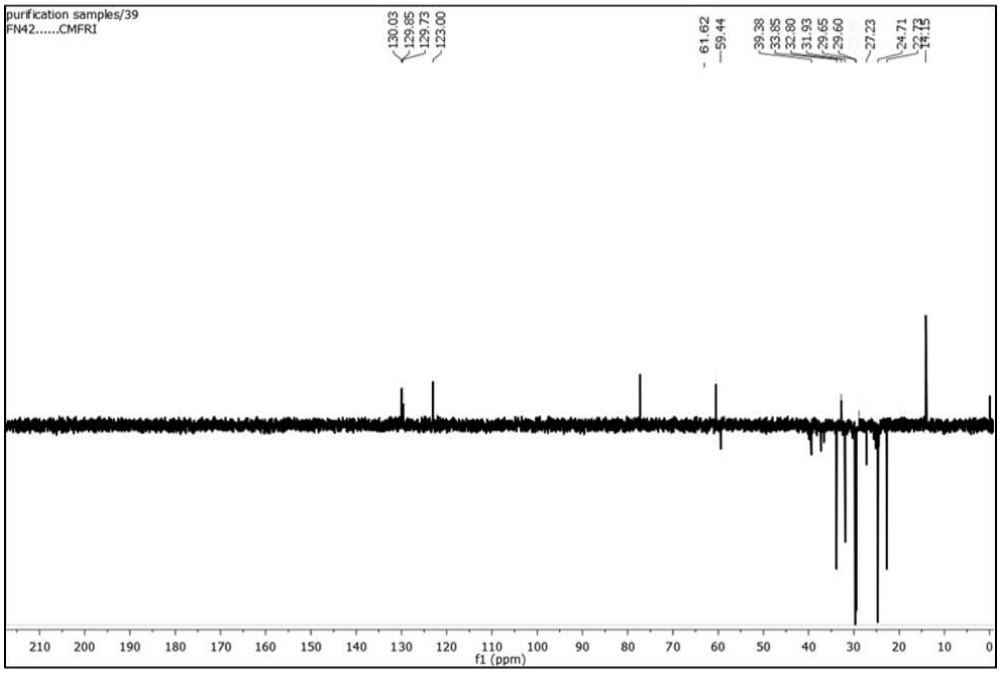

Figure 4.92. Figure showing the DEPT spectrum of compound **G3**

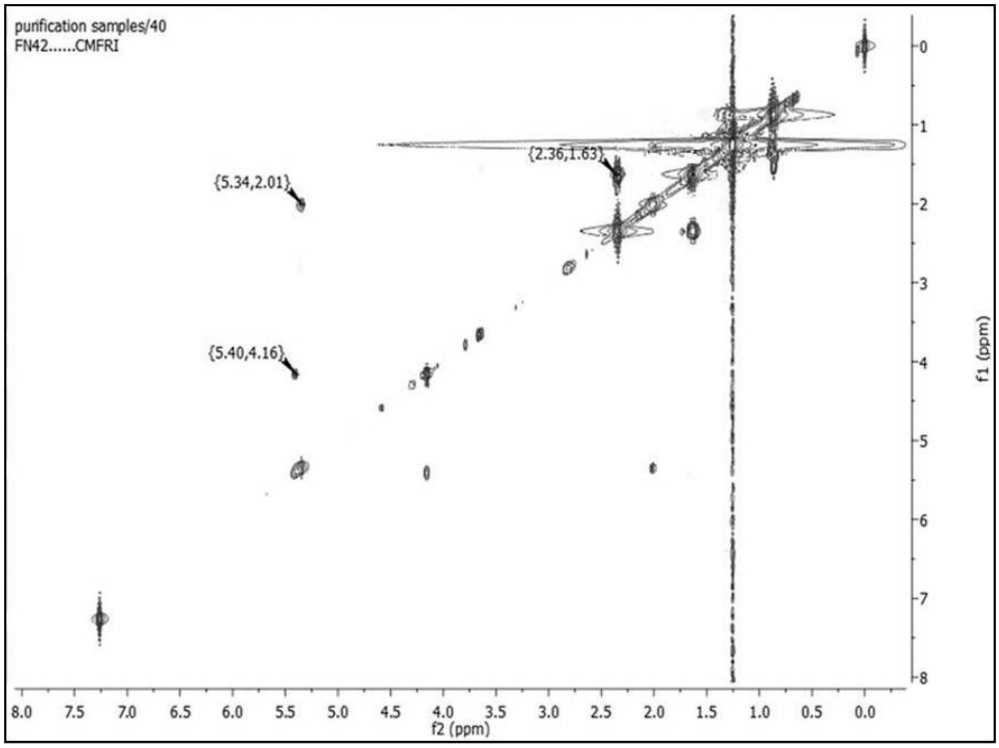

Figure 4.93. Figure showing the ^{1}H-^{1}H COSY spectrum of compound **G3**

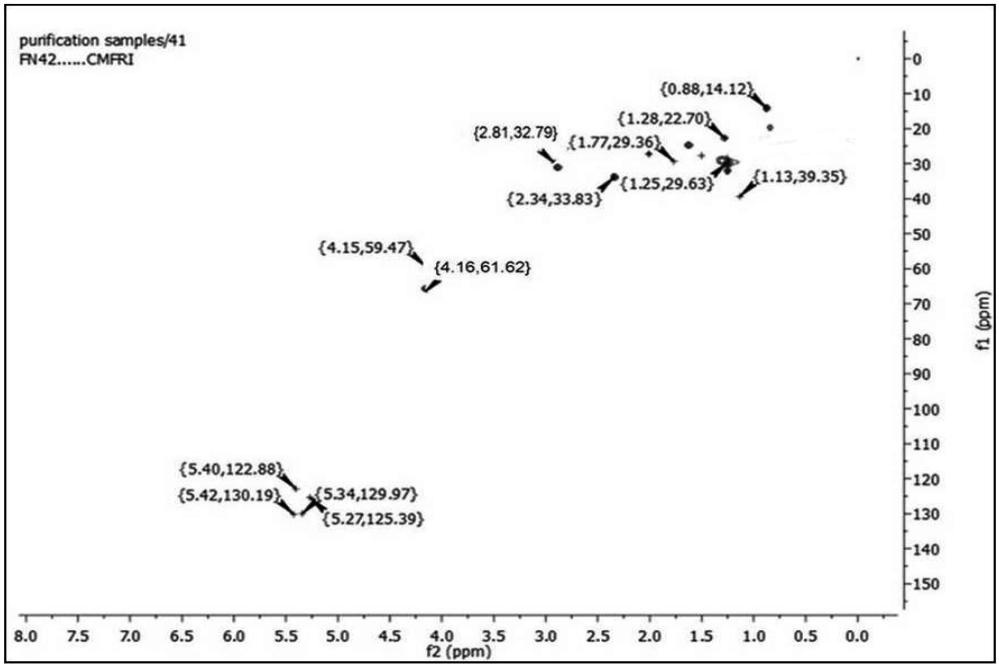

Figure 4.94. Figure showing the HSQC spectrum of compound **G3**

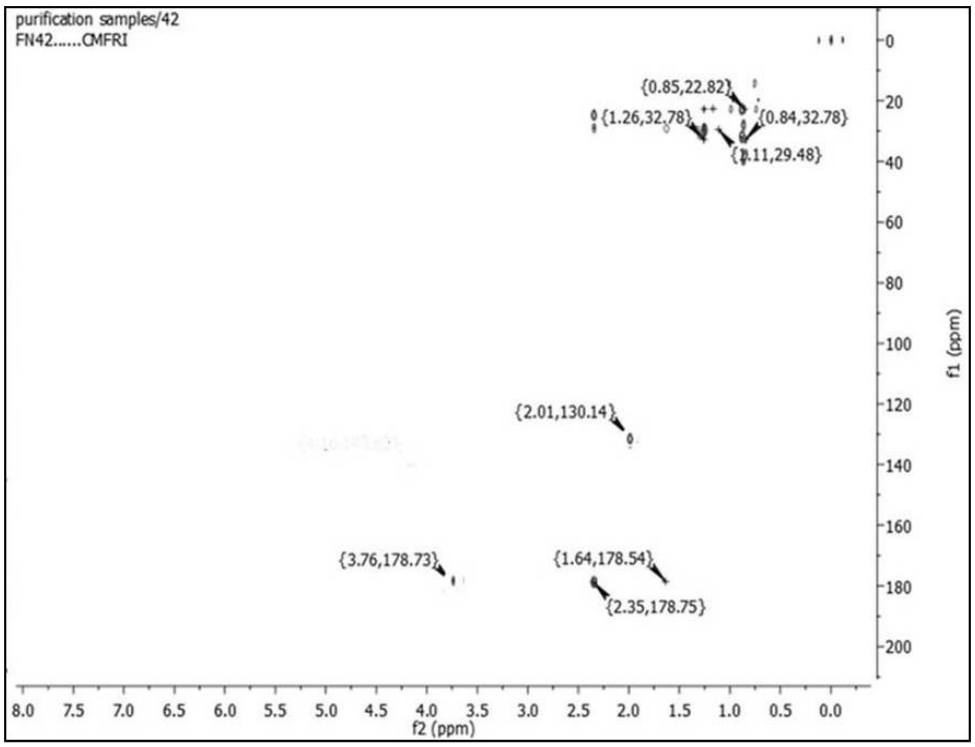

Figure 4.95. Figure showing the HMBC spectrum of compound **G3**

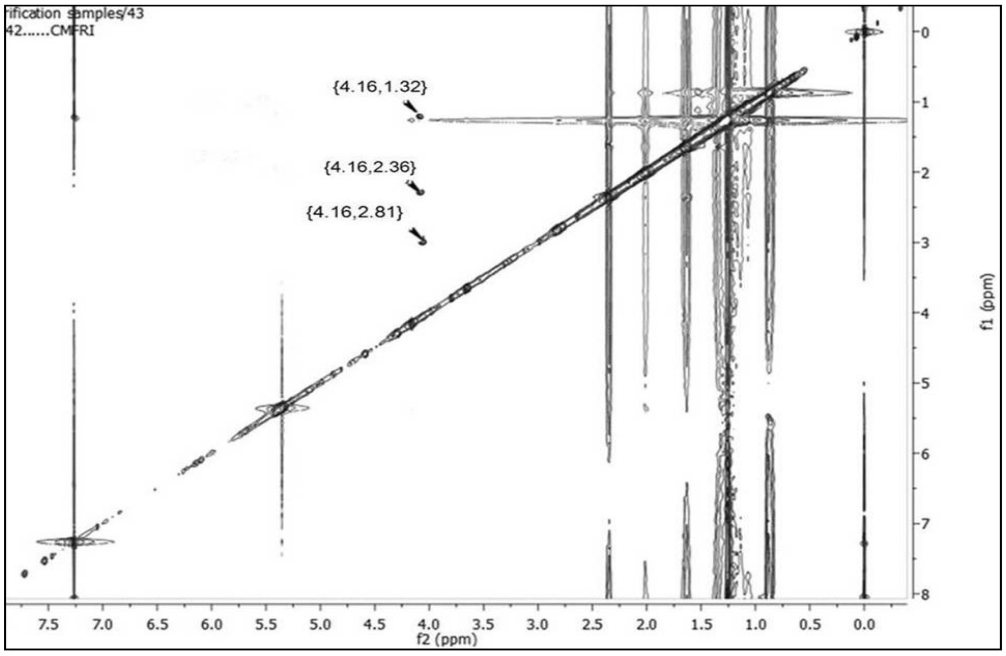

Figure 4.96. Figure showing the NOESY spectrum of compound **G3**

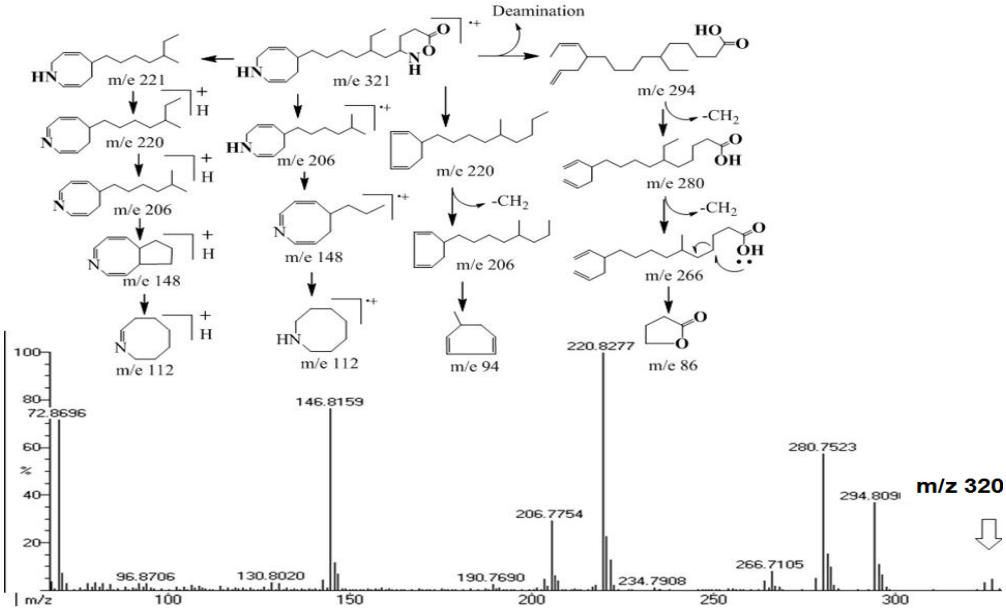

Figure 4.97. Mass spectrum of compound **G3**

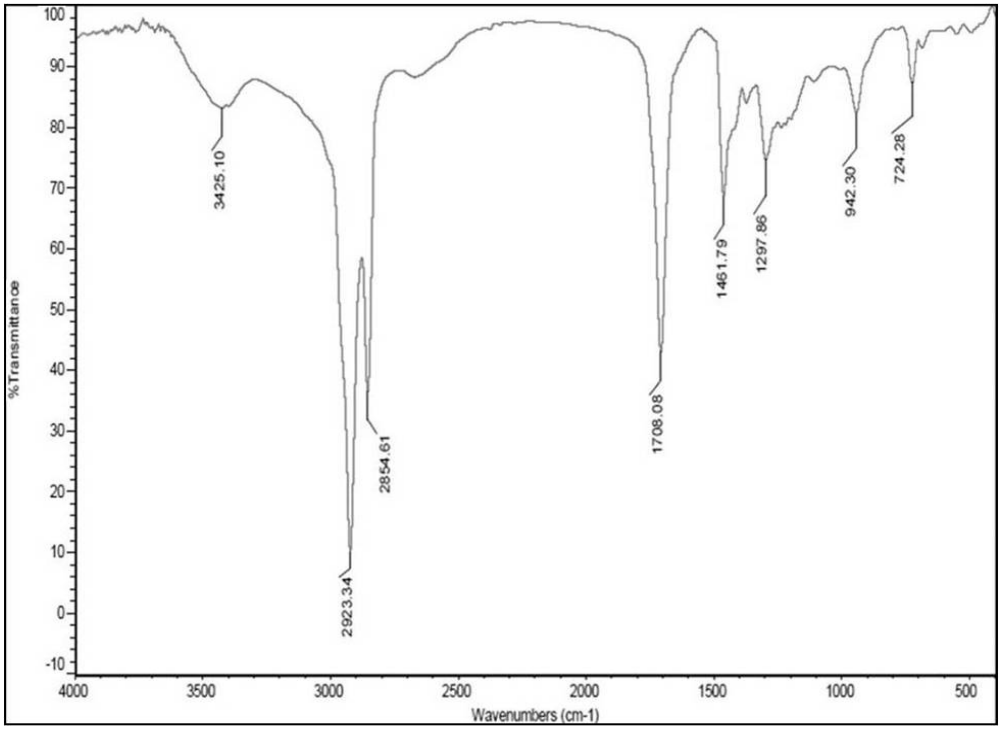

Figure 4.98. Figure showing the FTIR spectrum of compound **G3**

4.3.2.5. Bioactivities and Structure-Activity Relationship Analysis

The substituted azocinyl morpholinone recorded appreciably greater 1, 1-diphenyl-2-picryl-hydrazil (DPPH) free radical scavenging activities (IC_{50} ~ 0.086 mg/mL) compared to the commercially available synthetic antioxidants, butylated hydroxyanisole (BHA), butylated hydroxy toluene (BHT), and α-tocopherol (IC_{50} > 0.20 mg/mL). The lipophilic parameter Clog Pow (compound logarithmic scale of the octanol-water partition coefficient) was found to occupy a prominent part in determining the antioxidant property of the compounds. It is of note that while the Clog Pow of 3-(2-ethyl-6-((3, 7)-1, 2, 5, 6-tetrahydroazocin-5-yl) hexyl) morpholin-6-one was recorded as 0.55, the octanol-water partition coefficients of α-tocopherol (Clog Pow 120.4), BHA (Clog Pow 3.30), and BHT (Clog Pow 5.43) were found to be considerably greater, and this might considerably reflect towards the greater antioxidative potential of the compound **G3** than the commercially available synthetic and natural antioxidants. The antioxidant activity of α-tocopherol was found to be

considerably lesser apparently due to the greater steric bulk (Pr > 1000 cm^3) than the azocinyl morpholinone (Pr 783 cm^3) purified from *G. opuntia*. It is of note that the electronic parameter, topological polar surface area (tPSA) of the compound **G3** was significantly greater (tPSA 50.36) than the synthetic antioxidants, BHT (20.23), BHA (29.46) and α-tocopherol (29.46), and therefore, might contribute towards the higher DPPH radical scavenging activity (IC_{50} 0.086 mg/mL) than the synthetics (IC_{50} > 0.2 mg/mL). Likewise, no considerable variation in 2, 2′-azino-bis-3-ethylbenzothiozoline-6-sulfonic acid (ABTS) radical scavenging activity of the azocinyl morpholine (IC_{50} 0.42 mg/mL) was discernable with those of BHA and BHT (IC_{50} 0.34 and 0.26 mg/mL, respectively, $P > 0.05$), whilst, α-tocopherol recorded significantly lesser activity (IC_{50} 0.73 mg/mL) than the compound **G3** ($P > 0.05$). Apparently, the compound **G3** has two sp-hybridized –NH protons, which can be transferred to the free radicals (e.g. the hydrazinyl N – centered free radical of ABTS) by hydrogen atom transfer (HAT). It is evident that the HAT neutralize the free radicals (ABTS), as in phenolic antioxidants, is the mechanism of action of azocinyl morpholinone. In particular, the –NH proton that is a part of the morpholinone ring system, was deshielded, and appeared downfield at δ_H 3.79, which could be explained by the presence of the electronegative -O-C(=O) group at its vicinity. Earlier reports demonstrated that the radical scavenging activity of pharmacophore leads depends on electron donating groups, such as hydroxyl (-OH) and -NH group independent of their attachments, which can easily abstract free radicals and can potentially convert the highly reactive free radicals to their non-reactive forms (Cai et al. 2006). The radical scavenging activities of compounds were also reported to increase with the presence of double bonds due to effective electron-transfer through electron delocalization (Pietta 2000). It is interesting to note that the commercially available drugs, such as aspirin, sodium salicylate and ibuprofen along with COX-2 selective inhibitors {(Coxibs), celecoxib and rofecoxib} which were considered in the current study, displayed greater activities against cyclooxygenase-1 (COX-1) than cyclooxygenase-2 (COX-2), which might explain their undesirable side effects. Notably, greater inhibitory properties of the synthetic NSAIDs towards the constitutive enzyme COX-1 might lead to their shared therapeutic and side effects, which are undesirable, and lead to nephrotoxicity and gastrointestinal disorders (Rao and Knaus 2008). However, the compound **G3** exhibited greater activity against COX-2 (anti-COX-2 IC_{50} 0.84 mg/mL) than COX-1 isoform (COX-1 IC_{50} ~ 0.98 mg/mL). Sodium salicylate was found to be a weaker inhibitor of both COX isoforms (anti-COX-2 IC_{50}

2.65 mg/mL, anti- COX-1 IC_{50} 1.93 mg/mL) and demonstrated significantly lesser activity against 5-LOX (anti- LOX-5 IC_{50} 1.75 mg/mL). It was found that the synthetic NSAIDs, ibuprofen, sodium salicylate, and aspirin displayed significantly lesser activity against COX-2 than against COX-1 isoform, and the selectivity indices {ratio of anti-COX-1(IC_{50}) to that of anti-COX-2 (IC_{50})} remained considerably lesser (0.02–0.73 mg/mL) than the purified compounds (SI, 1.17). The azocinyl morpholinone exhibited potential COX-2 inhibitory activity/selectivity (IC_{50} 0.84 mg/mL) in conjunction with *in vitro* 5-LOX activity (IC_{50} 0.85 mg/mL) (Fig. 4.99, Table 4.18-4.19). The COX-2 selective inhibitors displayed potential selective COX-2 inhibitory activity (Celecoxib IC_{50} 29.60; Valdecoxib IC_{50} 61.50; Rofecoxib IC_{50} 272) (Tacconelli et al. 2002) than the purified compound. The selective COX-2 inhibitors were found to restrict the endothelial cell synthesis of prostacyclin (PGI2), an arachidonic acid product. PGI2 was reported to resist the effects of thromboxane leading to the disruption of physiological balance between thromboxane and prostacyclin resulting in the pathogenesis of atherosclerosis, thrombogenesis and other cardiovascular disorders (Fosslien 2005). These reports led to the restricted use of rofecoxib in 2004, followed by that of valdecoxib in 2005 (Fitz Gerald 2004). It was reported that rofecoxib induced nearly 28,000 heart attacks in the United States during the year 1999 and 2003 (Horton 2004). In addition COX-2 inhibitors, such as Celecoxib, with lesser selectivity, are also under restricted use (Fosslien 2005). The electronegative/hydrophilic groups in the compound **G3** appeared to inhibit the abstraction of hydrogen from arachidonic acid in the active site of cyclooxygenase (COX-1), thereby suppressing the synthesis of pro-inflammatory prostaglandins. Electronegative groups, such as NH in the compound **G3** can presumably be coordinated with the COX active site by ion pairing thereby preventing the prostaglandins synthesis. Notably, the animals challenged with the compound **G3** significantly mitigated the carrageenan-induced paw edema in a time-dependent manner till the end of the 6 h as compared to negative control animals. Structure-activity relationship analysis imparted that the bioactivities of azocinyl morpholinone were directed by the electronic and lipophilic parameters. Likewise, the greater anti-inflammatory potential of the compound **G3** was determined by the lesser Clog Pow value (0.55) as compared to the greater Clog Pow values of the synthetic NSAIDs, aspirin (1.02) and ibuprofen (3.68). The electronic parameter (polarizability, Pl and tPSA) also appeared to display significant role in determining the anti-inflammatory activity of the compound **G3**.

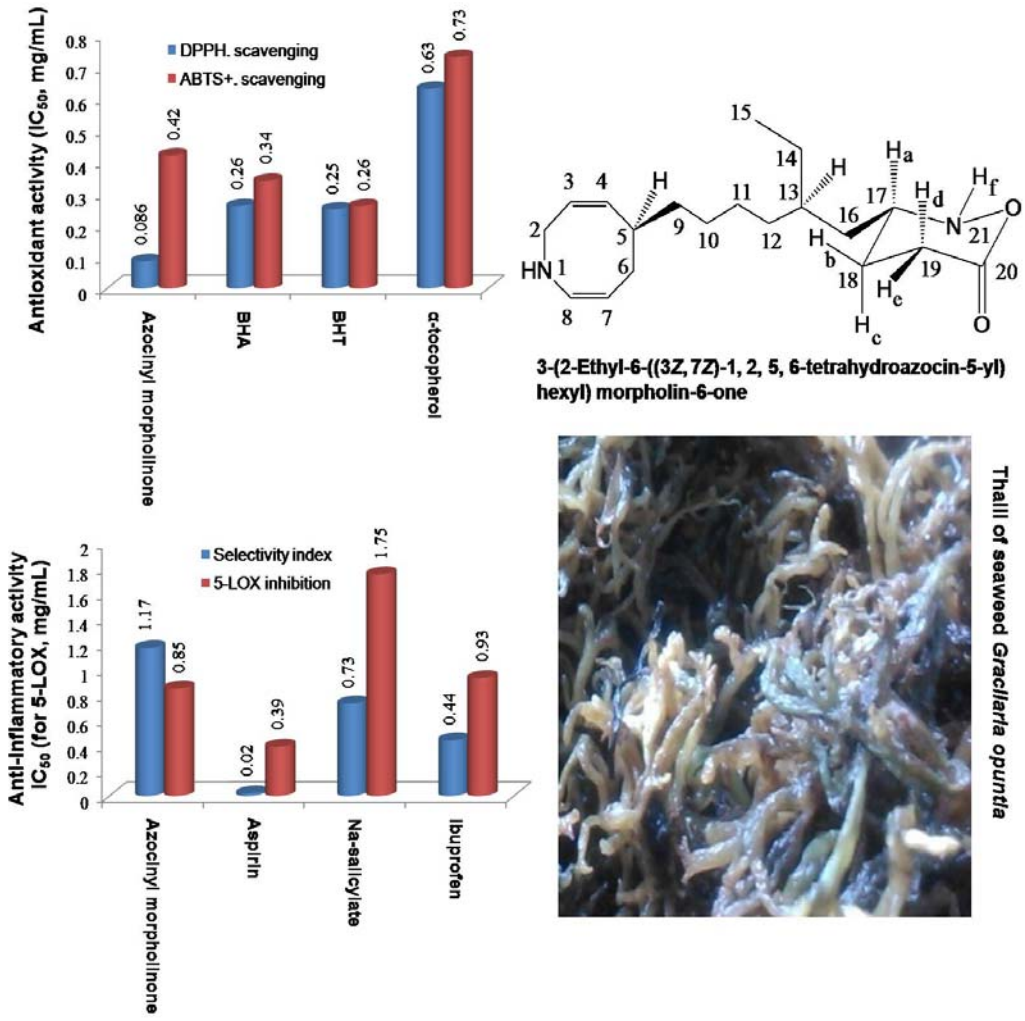

Figure 4.99. Graphical representation of bioactivities of compound **G3**. The thalli of the studied marine macroalga were displayed as inset

It is apparent that the electronic descriptor, Pl of the azocinyl morpholinone registered significantly greater value (~37 × 10^{-24} cm^3) than the NSAIDs (Pl aspirin 17.65 × 10^{-24} cm^3, Pl ibuprofen 24.09 × 10^{-24} cm^3), and therefore, the anti-inflammatory activity of the compound **G3** was found to be comparable to that of the synthetic NSAIDs. A greater selectivity index of the new azocinyl morpholinone isolated from *G. opuntia* signified the greater selectivity and significantly lesser side effect profiles than the current remedies by using nonsteroidal anti-inflammatory drugs used to combat the inflammatory diseases.

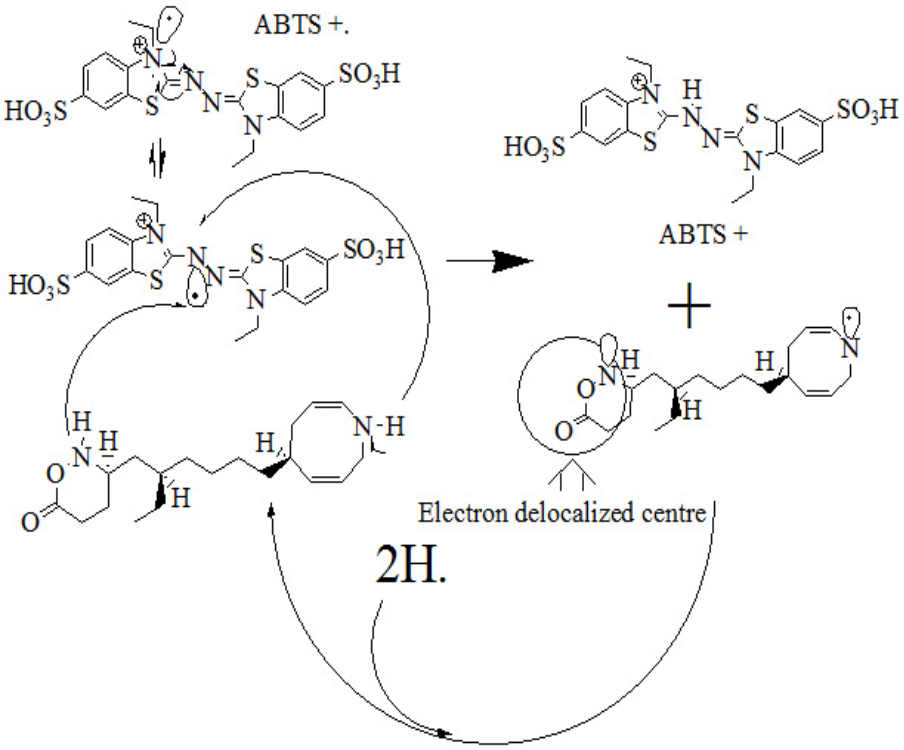

Figure 4.100. Antioxidative mechanism of the purified compound in the ABTS model system. The compound **G3** has two sp-hybridized –NH protons, which can be transferred to the free radicals (e.g., the hydrazinyl N –centered free radical of $ABTS^{+\cdot}$) by hydrogen atom transfer (HAT). HAT from the azocinyl morpholinone stabilized the free radicals ($ABTS^{+\cdot}$)

Table 4.18 Antioxidative and inflammatory activities of azocinyl morpholinone isolated from *G. opuntia vis-à-vis* the commercially available natural and synthetic antioxidants

Bioactivities*	**IC_{50} (mg/mL)**			
Antioxidative activities	**Azocinyl morpholinone**	**BHA**	**BHT**	**α-tocopherol**
DPPH scavenging	0.086^{a} ±0.07	0.26^{b} ± 0.01	0.25^{b} ± 0.02	0.63^{c} ± 0.04
ABTS scavenging	0.42^{b} ±0.23	0.34^{b} ± 0.02	0.26^{b} ± 0.02	0.73^{c} ± 0.05
Anti-inflammatory activities	**Azocinyl morpholinone**	**Aspirin**	**Na-salicylate**	**Ibuprofen**
COX -1 inhibition	0.98^{b} ±0.05	0.005^{a} ±0.00	1.93^{c} ±0.05	0.04^{a} ±0.00
COX -2 inhibition	0.84^{b} ±0.03	0.21^{b} ±0.02	2.65^{c} ±0.05	0.09^{a} ±0.02
Selectivity index**	1.17^{b} ±0.08	0.02^{b} ±0.01	0.73^{b} ±0.02	0.44^{b} ±0.03
5-LOX inhibition	0.85^{b} ±0.12	0.39^{a} ±0.02	1.75^{c} ±0.12	0.93^{b} ±0.11

* The bioactivities were expressed as IC_{50} values (mg/mL).

The samples were analyzed in triplicate (n=3) and expressed as mean ± standard deviation. Means followed by the different superscripts (a–c) within the same row indicate significant differences ($P < 0.05$).

**Selectivity index has been calculated as the ratio of anti-COX-1(IC_{50}) to that of anti-COX-2 (IC_{50}).

Table 4.19 Effect of the azocinyl morpholinone compared with the standard drug on carrageenan-induced hind paw edema in BALB/C mice at different time intervals.

	Paw edema (mm)*				
Samples					
Positive control (carrageenan induced)	**2h**	**3h**	**4h**	**5h**	**6h**
Normal saline	2.59^{bc} ±0.32	2.48^{b} ±0.27	2.53^{cd} ±0.24	2.62^{cd} ±0.26	2.65^{cd} ±0.21
Standard (ibuprofen)	1.98^{a} ±0.21	1.91^{a} ±0.16	1.84^{b} ±0.14	1.80^{a} ±0.13	1.79^{b} ±0.15
Azocinyl morpholinone	1.95^{a} ±0.18	1.87^{a} ±0.19	1.76^{a} ±0.20	1.72^{a} ±0.19	1.68^{a} ±0.11

*Initial paw diameter 1.38 mm (at 0^{th} h)

a-d: Column wise values with superscripts indicate significant differences ($P < 0.05$) within the samples.

4.3.2.6. Structural Characterization of Compound G4

2-Acetoxy-2-(5-acetoxy-4-methyl-2-oxotetrahydro-2*H*-pyran-4-yl) ethyl-4-(3-methoxy-2(methoxymethyl)-7-methyl-3, 4, 4a, 7, 8, 8a-hexahydro-2*H*-chromen-4-yloxy)-5 methylheptanoate (**G4**)

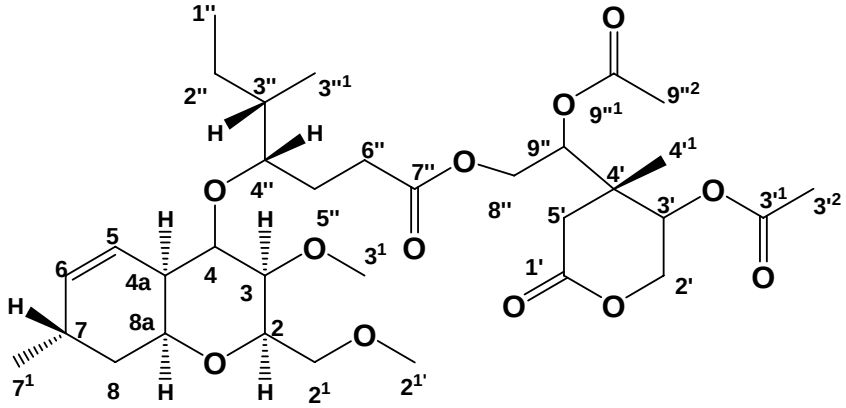

Sample yield	110 mg (1.0 %)
Physical description	Yellow oil
Molecular formula	$C_{33}H_{52}O_{12}$
Molecular weight	640.3182

2-Acetoxy-2-(5-acetoxy-4-methyl-2-oxotetrahydro-2*H*-pyran-4-yl) ethyl-4-(3-methoxy-2 (methoxymethyl)-7-methyl-3, 4, 4a, 7, 8, 8a-hexahydro-2*H*-chromen-4-yloxy)-5-methylheptanoate : Yellowish oil; UV (MeOH) λmax (log ε): 268 nm (3.01); TLC (Si gel GF_{254} 15 mm; EtOAc: *n*-hexane 3:7, v/v) Rf: 0.55; Rt (HPLC, MeOH: ACN, 3:2 *v/v*): 9.86 min; IR (KBr, cm^{-1}) *v*max (ν = stretching, δ = bending, ρ = rocking vibrations): 722.40 (C–H ρ), 794.82 (C–H ρ), 910.63 (alkene C–H δ), 1062.19 (C–O ν), 1252.45 (C–O ν), 1371.54 (CH_3 ν), 1458.63 (C–H δ), 1715.00 (C–CO–C ν), 2856.63 (C–H ν), 2923.39 (C–H ν); ^{1}H NMR (500 MHz, $CDCl_3$) δ_H 4.17 (m, 1H), δ_H 3.18 (*J*=4.40 Hz, d, 2H), δ_H 3.71 (s, 3H), δ_H 3.66 (*J*=3.10 Hz, t, 1H), δ_H 3.36 (s, 3H), δ_H 3.75 (*J*=5.55 Hz, t, 1H), δ_H 2.05 (m, 1H), δ_H 5.35 (*J*=7.36 Hz, t, 1H), δ_H 5.51 (*J*=7.87

Hz, t, 1H), δ_H 1.74 (m, 1H), δ_H 1.08 (*J*=4.16 Hz, d, 3H), δ_H 2.04 (*J*=3.13 Hz, t, 2H), δ_H 4.07 (m, 1H), δ_H 3.69 (*J*=3.10 Hz, d, 2H), δ_H 4.50 (*J*=8.11 Hz, t, 1H), δ_H 2.71 (s, 3H), δ_H 1.29 (s, 3H), δ_H 2.86 (s, 2H), δ_H 0.99 (*J*=6.07 Hz, t, 3H), δ_H 1.30 (m, 2H), δ_H 1.52 (m, 1H), δ_H 0.88 (*J*=6.64 Hz, d, 3H), δ_H 3.47 (m, 1H), δ_H 1.61 (m, 2H), δ_H 2.38 (*J*=7.87 Hz, t, 2H), δ_H 4.30 (*J*=8.97 Hz, d, 2H), δ_H 5.35 (*J*=7.36 Hz, t, 1H), δ_H 2.17 (s, 3H); ^{13}C NMR (125 MHz, methanol d4 δ in ppm): δ_C 75.21 (C-3), δ_C 73.45 (C-4), δ_C 73.32 (C-2^1), δ_C 65.13 (C-2), δ_C 53.96 (C-2$^{1'}$), δ_C 51.29 (C-3^1), δ_C 40.1 (C-4a), δ_C 129.55 (C-5), δ_C 132.53 (C-6), δ_C 40.07 (C-7), δ_C 26.56 (C-8), δ_C 71.62 (C-8a), δ_C 173.57 (C-1'), δ_C 70.31 (C-2'), δ_C 63.01 (C-3'), δ_C174.17 (C-3'^{1}), δ_C 39.07 (C-3'^{2}), δ_C 50.85 (C-4'), δ_C 14.03 (C-4'^{1}), δ_C 28.44 (C-5'), δ_C 21.63 (C-1"), δ_C 29.4 (C-2"), δ_C 27.77 (C-3"), δ_C 13.17 (C-3"^{1}), δ_C 72.01 (C-4"), δ_C 24.68 (C-5"), δ_C 33.62 (C-6"), δ_C 174.27 (C-7"), δ_C 65.77 (C-8"), δ_C 97.58 (C-9"), δ_C 184 (C-9"^{1}), δ_C 32.37 (C-9"^{2}), δ_C 18.16 (C-7^1). ^{1}H-^{1}H-COSY and HMBC data (Fig. 4.101 to Fig. 4.110, Table 4.20); HR (EI) MS *m/z* calcd for $C_{33}H_{52}O_{12}$ 640.3173, found 640.3182 $[M]^+$.

The EtOAc: MeOH extract of *G. opuntia* was subjected to repeated column chromatography over silica gel and preparative thin layer chromatography (PTLC) to yield the compound **G4** as yellowish oil. The compound showed absorption bands at 1715 cm^{-1} in the Fourier Transform Infrared (FTIR) spectrum due to the carbonyl functionalities. The olefinic (C=C) and alkyl (C–H) groups IR stretching vibrations were demonstrated by absorption bands at 1458 and 2856 cm^{-1}, respectively. The detailed ^{1}H, ^{13}C NMR and mass spectral analysis confirmed the structure. Its molecular formula, $C_{33}H_{52}O_{12}$, was deduced from the HR-EI-MS (*m/z* 640.3182) and ^{13}C NMR spectroscopic data, showing eight indices of hydrogen deficiency. The carbon signals at δ_C 174.27 (C-7"), δ_C 174.17 (C-3'^{1}), δ_C 173.57 (C-1') and δ_C 184 (C-9"^{1}) indicated the presence of four carbonyl carbons, and among them, one carbonyl groups formed the part of the 1-(5-acetoxy-4-methyl-2-oxotetrahydro-2*H*-pyran-4-yl) ethyl acetate moiety. The heteronuclear multiple- bond correlation spectroscopy (HMBC) relation between H-2^1 (δ_H 3.18; *J*=4.40 Hz)/C-2$^{1'}$ (δ_C 53.96)/C-2 (δ_C 65.13), H-3 (δ_H 3.66; *J*=3.10 Hz)/C-2^1 (δ_C 53.96), H-4a (δ_C 2.05)/C-5 (δ_C 129.55), H-6 (δ_H 5.51; *J*=7.87 Hz)/C-5 (δ_C 129.55), H-3"^{1} (δ_H 0.88; *J*=6.64 Hz)/C-2" (δ_C 29.4)/C-3" (δ_C 27.77), H-5" (δ_H 1.61)/C-7" (δ_C 174.27)/C-6" (δ_C 33.62), H-6" (δ_H 2.38; *J*=7.87 Hz)/C-7" (δ_C 129.55)/C-5" (δ_C 24.68), H-9" (δ_H 5.35; *J*=7.36 Hz)/C-8" (δ_C 65.77), H-9"^{2} (δ_H 2.17)/C-9"^{1} (δ_C 184)/C-9" (δ_C 97.58) established the side chain substitution of chromen (Table 4.20).

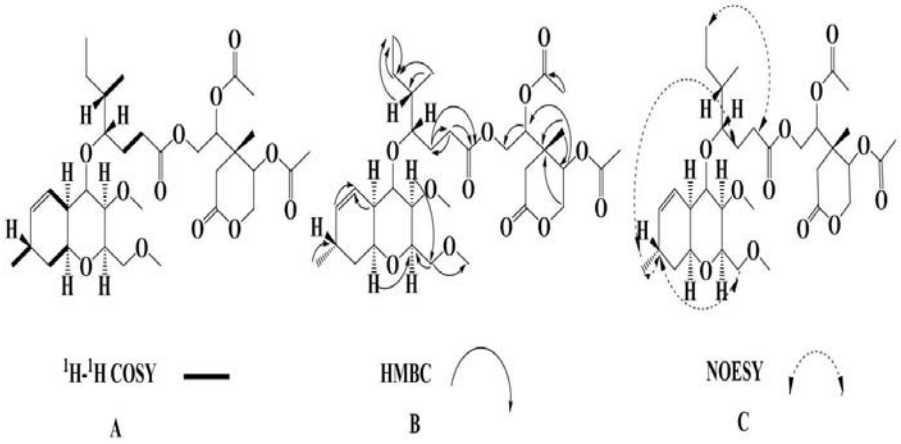

Figure 4.101. Figure showing the Key (**A**) ^{1}H-^{1}H COSY (**B**) HMBC and (**C**) NOESY correlations of compound **G4**

The ^{1}H NMR spectrum of the compound **G4** showed signals at δ_H 4.17 bearing carbon at δ_C 65.13 that unambiguously confirmed the presence of the characteristic signals of chromen carbons. The presence of the two acetyl groups has been confirmed by the singlet at δ_H 2.71 (H-3'^{2}) and δ_H 2.17 (H-9"^{2}). Intense HMBC correlation between H-9"^{2} (δ_H 2.17)/C-9"^{1} (δ_C 184)/C-9" (δ_C 97.58) established the side chain acetyl substitution of chromen. The ^{1}H-^{1}H COSY experiment displayed that the presence of three spin systems, H-4a to H-5 {(δ_H 2.05 (H-4a)/δ_C 5.35; *J*=7.36 Hz (H-5), H-7 to H-7^1 {δ_H 1.74(H-7)/δ_H 1.08; *J*=4.16 Hz (H-7^1)}, H-8 to H-8a {(δ_H 2.04; *J*=3.13 Hz (H-8)/δ_H 4.07(H-8a)} in the methylcyclohexene ring, H-3" to H-3"^{1} {(δ_H1.52 (H-3")/δ_H 0.88; *J*=6.64 Hz (H-3"^{1}), H-5" to H-6" (δ_H 1.61(H-5")/δ_H 2.38; *J*=7.87 Hz (H-6")} in the propyl 4-hydroxy-5-methylheptanoate framework, which indicated the presence of substitution in the chromen groups that were further confirmed by the detailed HMBC correlations. The HMBC correlations from H-3 (δ_H 3.66; *J*=3.10 Hz)/C-2$^{1'}$ (δ_C 53.96), H-2^1 (δ_H 3.18; *J*=4.40 Hz)/C-2$^{1'}$ (δ_C 53.96) suggested the position of a methoxy group substituted at C-2 position. The presence of methoxy groups were also supported by two singlets at δ_H 3.36 and 3.71 recorded in the ^{1}H NMR spectrum. Strong HMBC correlations were exhibited by H-2^1 (δ_H 3.18; *J*=4.40 Hz)/C-2$^{1'}$ (δ_C 53.96)/C-2 (δ_C 65.13), H-3 (δ_H 3.66; *J*=3.10 Hz)/C-2^1 (δ_C 53.96), H-4a (δ_H 2.05)/C-5 (δ_C 129.55), H-6" (δ_H 2.38; *J*=7.87 Hz)/C-7" (δ_C 129.55)/C-5" (δ_C 24.68), H-9" (δ_H 5.35; *J*=7.36 Hz)/C-8" (δ_C 65.77), H-9"^{2} (δ_H 2.17)/C-9"^{1} (δ_C 184)/C-9" (δ_C 97.58), which supported the

structural attributions. The ^{13}C NMR in combination with DEPT spectra revealed the occurrence of one quaternary carbon along with intense HMBC correlations of H-2' (δ_H 3.69; *J*=3.10 Hz)/C-4' (δ_C 50.85) and H-4'^{1} (δ_H 1.29) C-4' (δ_C 50.85), which substantiated the presence of quaternary carbon at C-4' position. The NMR spectra displayed the presence of highly deshielded seven oxymethine signals (δ_H 4.17, δ_H 4.07, δ_H 3.66, δ_H 3.75, δ_H 3.47, δ_H 4.50, δ_H 5.35 corresponding to δ_C 65.13, δ_C 71.62, δ_C 75.21, δ_C 73.45, δ_C 72.01, δ_C 63.01, δ_C 97.58), one oxymethylene signals at (δ_H 3.18/δ_C 73.32, δ_H 4.30; *J*=8.97 Hz/δ_C 65.77, δ_H 3.69; *J*=3.10 Hz/δ_C 70.31) with eight degrees of unsaturation associated with three each of ring systems and carbonyl groups, with the remaining one attributed to the presence of olefinic group. The olefinic protons were recorded at δ_H 5.35 (*J*=7.36 Hz) and at δ_H 5.51 (*J*=7.87 Hz) of the ^1H NMR spectrum. In the proton correlation spectroscopy (^1H-^1H COSY) spectrum of the compound **G4**, couplings were apparent between the protons at δ_H H-4a to H-5 {(δ_H 2.05 (H-4a)/δ_H 5.35*; J*=7.36 Hz (H-5), H-7 to H-7^1 {δ_H 1.74 (H-7)/δ_H 1.08; *J*=4.16 Hz (H-7^1)}, H-8 to H-8a {(δ_H 2.04; *J*=3.13 Hz (H-8)/δ_H 4.07 (H-8a)}, H-3" to H-3"^{1} {(δ_H 1.52 (H-3")/δ_H 0.88 (H-3"^{1}), H-5" to H-6" (δ_H 1.61 (H-5")/δ_H 2.38; *J*=7.87 Hz (H-6")}, which formed three spin systems. The chromen framework of the compound **G4** was further evident from the characteristic proton and carbon signals in the literature data (Rateb and Ebel 2011). A combined 2D NMR analysis, in particular, ^1H-^1H COSY, heteronuclear single-quantum correlation spectroscopy (HSQC) and HMBC experiment unambiguously attributed the rest of the structure. The relative stereochemistries of the chiral centres of the compound **G4**, particularly that of C-7 (δ_H 1.74), C-8a (δ_H 4.07), C-4a (δ_H 2.05), C-4 (δ_H 3.75; *J*=5.55 Hz), C-3" (δ_H 1.52), C-4" (δ_H 3.47) and C-9" (δ_H 5.35 *J*=7.36 Hz) carrying the methine protons, were deduced from the NOESY spectrum and their *J*-values. The NOESY correlations between H-7^1 (δ_H 1.08)/H-5" (δ_H 1.62)/H-7 (δ_H 1.78), H-7 (δ_H 1.76)/H-2^1 (δ_H 3.18; *J*=4.40 Hz), H-1" (δ_H 0.99; *J*=6.07 Hz)/H-6" (δ_H 2.38; *J*=7.87 Hz) assigned the chair-like conformation of the 2*H*-chromen derivative. In addition, the coupling constant between the olefinic protons (*J*=7.36 Hz) at H-5 and H-6 attributed their *cis* configuration. The ^{13}C NMR spectrum in combination with DEPT indicated the presence of a total of 33 carbons, which enclosed four carbonyl groups, four CH_3, eight CH_2, nine CH, one olefinic, two methoxy, two acetyl and one quaternary carbon. The molecular ion peak at *m/z* 640 {HR (EI) MS *m/z* calcd for $C_{33}H_{52}O_{12}$ 640.3173, found 640.3182 $[M]^+$}, which in combination with its ^1H and ^{13}C NMR data designated the elemental composition of the compound **G4** as

$C_{33}H_{52}O_{12}$. Plastoquinones, chromanols and chromenes reside in a common class of natural compounds containing polyprenyl chain bound to a hydroquinone framework, and were reported to occur in marine macroalgae (Pereira et al. 2011). Mojabanchromanol is an example of an antioxidative chromen derivative isolated from marine macroalga *Sargassum siliquastrum*, and was reported to display free radical scavenging activity (Toth and Pavia 2000). Chromen derivatives from marine macroalga *Sargassum micracanthum* with potential antioxidative and anti-ulcer properties were reported in previous literature (Mori et al. 2003). Although there have been scanty reports of the occurrence of substituted chromenes from marine realm, several bioactive leads found their place in the literature with regard to the terrestrial plants. For example, new classes of quinones, chromenes and isoprenoid acetogenins were isolated from certain members of the family *Cyperaceae* of Australian origin (Allan et al. 1969). Naturally occurring anti-fungal 5, 7-dimethoxy-2-methyl-2*H*-chromene and 5, 7-dimethoxy-2, 8-dimethyl-2*H*-chromene were isolated from the leaf essential oil of *Calyptranthes tricona*. 7-Hydroxy-6-methoxy-4*H*-chromene was an example for naturally occurring 4*H*-chromene, which was obtained from the flower of *Wisteria sinensis*, and was reported to possess organoleptic property (Willem et al. 2005). The 4*H* chromene uvafzlelin was isolated from the stems of *Uvaria ufielii*, and showed anti-microbial activity against gram-positive and acid-fast bacteria (Charles et al. 1980). Chromen derivatives was also found to be an interesting template for the discovery of potential anti-cancer agents (Vosooghi et al. 2010), such as acronycine (lung, colon and ovary cancer).

Table 4.20 NMR spectroscopic data of compound **G4** in methanol d_4[a]

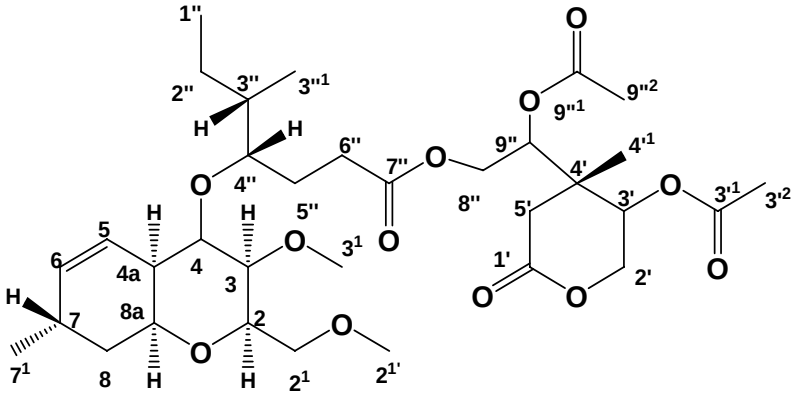

C. No	^{13}C (δ)	^{1}H-NMR[b] (int., mult., *J* in Hz)	^{1}H-^{1}H COSY	HMBC (^{1}H-^{13}C)
2	65.13	4.17 (1H, m)	-	–
2^{1}	73.32	3.18 (2H, *J*=4.40 Hz, d)	-	C-$2^{1'}$, C-2
$2^{1'}$	53.96	3.71 (3H, s)	-	-
3	75.21	3.66 (1H, *J*=3.10 Hz, t)	-	C-$2^{1'}$
3^{1}	51.29	3.36 (3H, s)	-	–
4	73.45	3.75 (1H, *J*=5.55 Hz, t)	-	-
4a	40.1	2.05 (1H, m)	5-H	C-5
5	129.55	5.35 (1H, *J*=7.36 Hz, t)	4a-H	–
6	132.53	5.51 (1H, *J*=7.87 Hz, t)	-	C-5
7	40.07	1.74 (1H, m)	7^{1}-H	-
7^{1}	18.16	1.08 (3H, *J*=4.16 Hz, d)	7-H	C-7
8	26.56	2.04 (2H, *J*=3.13 Hz, t)	8a-H	-
8a	71.62	4.07 (1H, m)	8-H	C-2
1'	173.57	-	-	-
2'	70.31	3.69 (2H, *J*=3.10 Hz, d)	-	C-4'
3'	63.01	4.50 (1H, *J*=8.11Hz, t)	-	C-9"
$3'^{1}$	174.17	-	-	-
$3'^{2}$	39.07	2.71 (3H, s)	-	-
4'	50.85	-	-	-
$4'^{1}$	14.03	1.29 (3H, s)	-	C-3', C-4'
5'	28.44	2.86 (2H, s)	-	-
1"	21.63	0.99 (3H, *J*=6.07 Hz, t)	-	C-2"
2"	29.4	1.30 (2H, m)	-	C-1"
3"	27.77	1.52 (1H, m)	$3"^{1}$-H	C-1"
$3"^{1}$	13.17	0.88 (3H, *J*=6.64 Hz, d)	3"-H	C-2", C-3"
4"	72.01	3.47 (1H, m)	-	-
5"	24.68	1.61 (2H, m)	6"-H	C-7", C-6"

6"	33.62	2.38 (2H, *J*=7.87 Hz, t)	5"-H	C-7", C-5"
7"	174.27	-	-	-
8"	65.77	4.30 (2H, *J*=8.97 Hz, d)	-	-
9"	97.58	5.35 (1H, *J*=7.36 Hz, t)	-	C-8"
9"[1]	184	-	-	-
9"[2]	32.37	2.17 (3H, s)		C-9"[1], C-9"

[a] NMR spectra recorded using Bruker AVANCE III 500 MHz (AV 500) spectrometer in methanol-d_4 as aprotic solvent at ambient temperature with TMS as the internal standard (δ 0 ppm).

[b]Values in ppm, multiplicity and coupling constants (*J*=Hz) are indicated in parentheses. The assignments were made with the aid of the ^{1}H-^{1}H COSY, HSQC, HMBC and NOESY experiments.

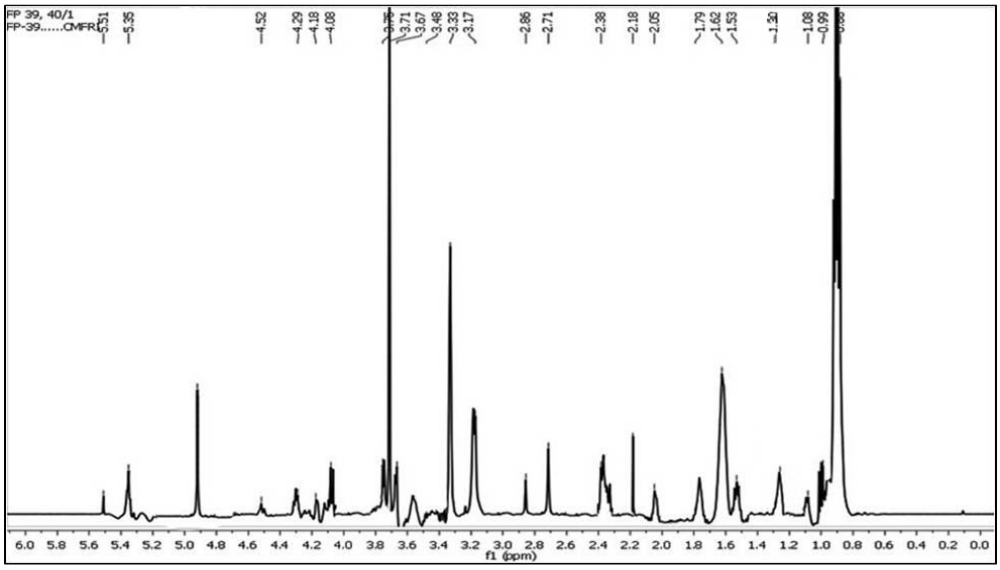

Figure 4.102. Figure showing the ^{1}H spectrum of compound **G4**

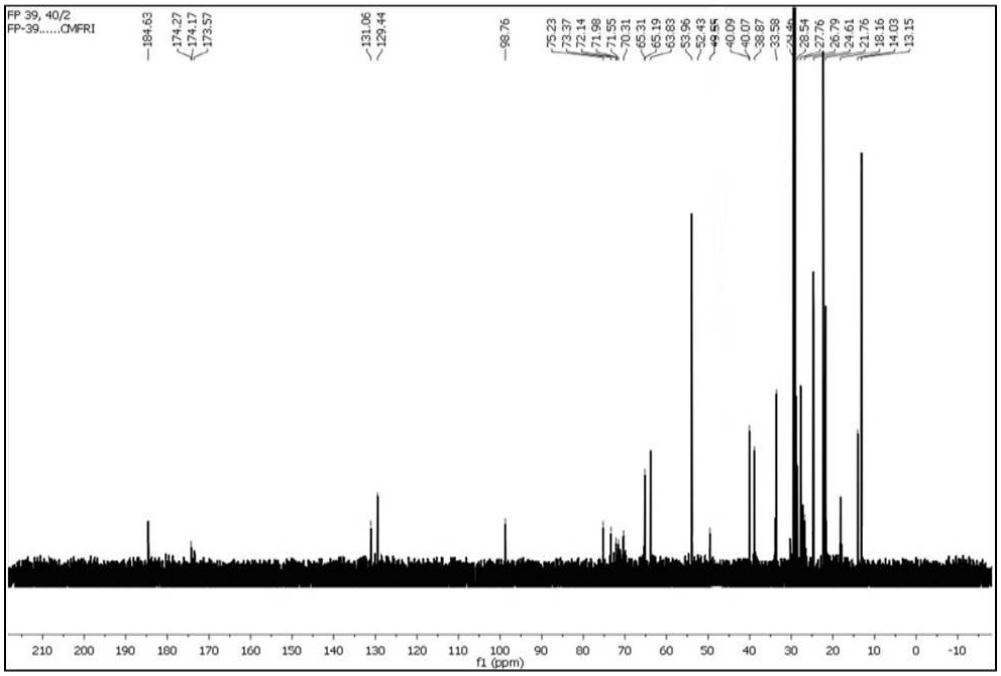

Figure 4.103. Figure showing the ^{13}C spectrum of compound **G4**

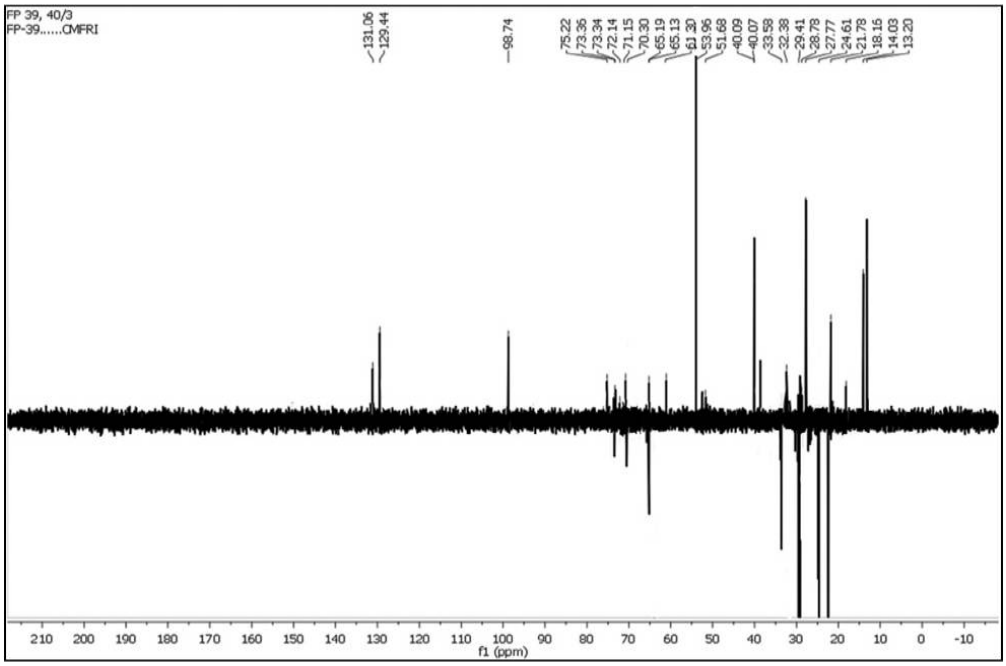

Figure 4.104. Figure showing the DEPT spectrum of compound **G4**

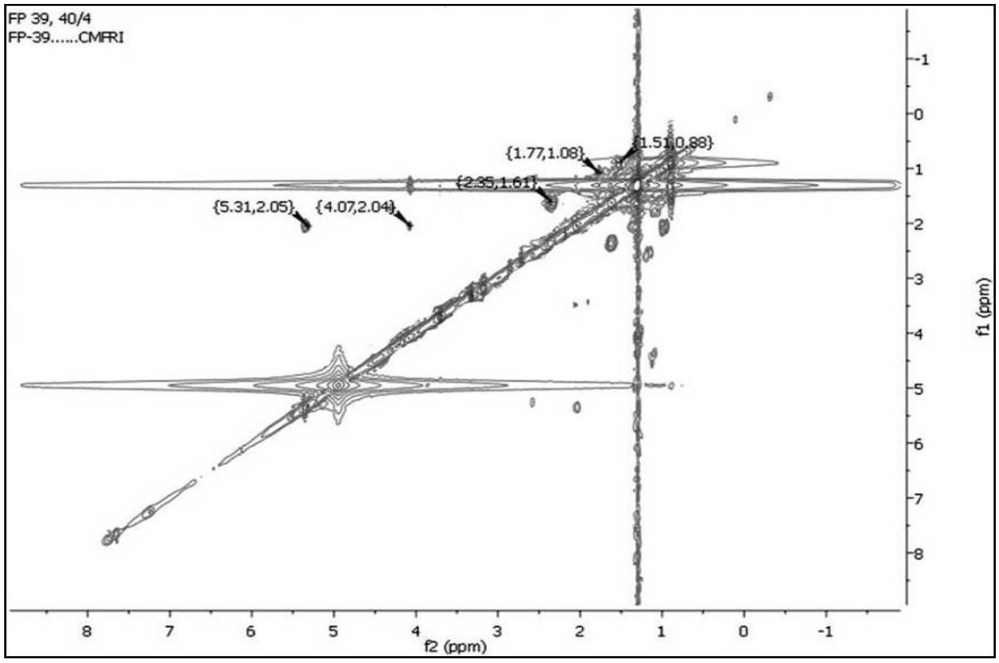

Figure 4.105. Figure showing the ^{1}H-^{1}H COSY spectrum of compound **G4**

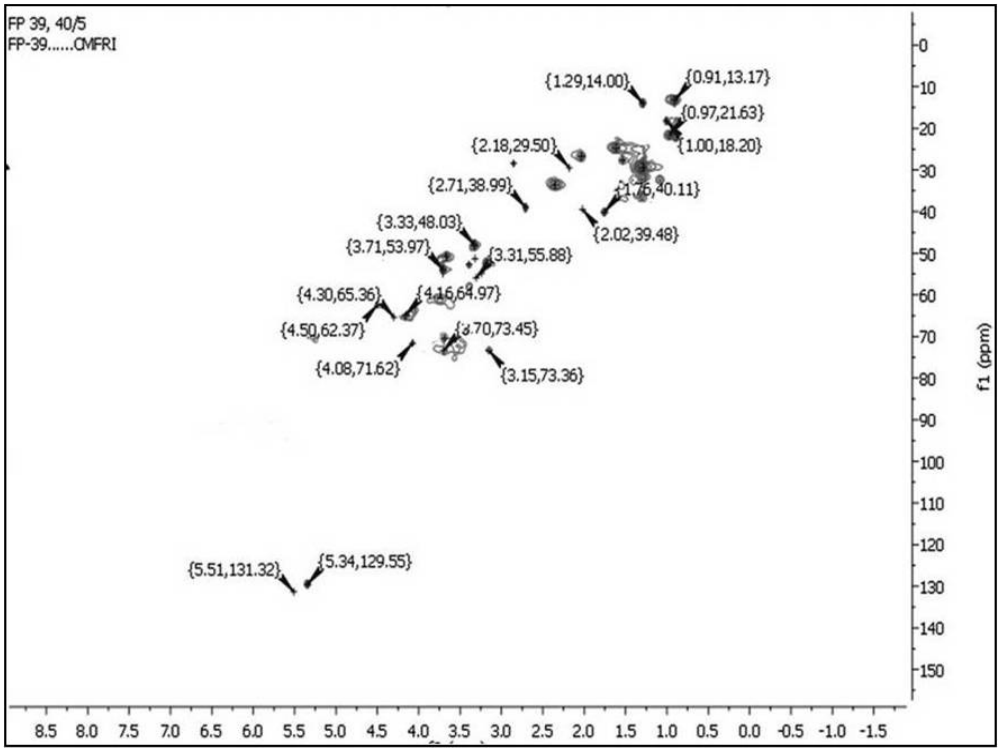

Figure 4.106. Figure showing the HSQC spectrum of compound **G4**

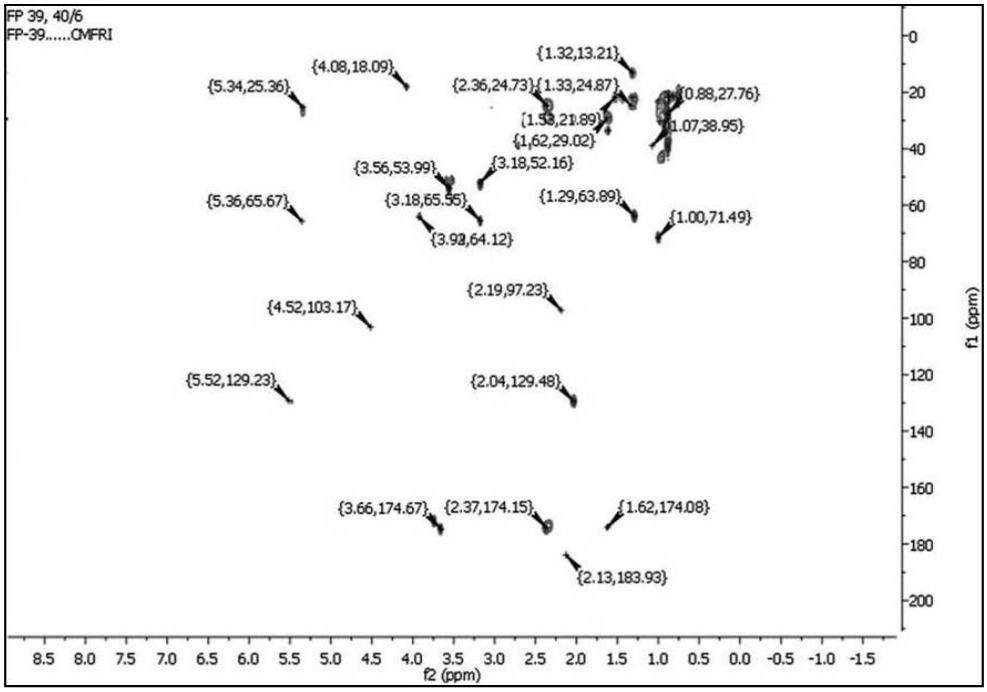

Figure 4.107. Figure showing the HMBC spectrum of compound **G4**

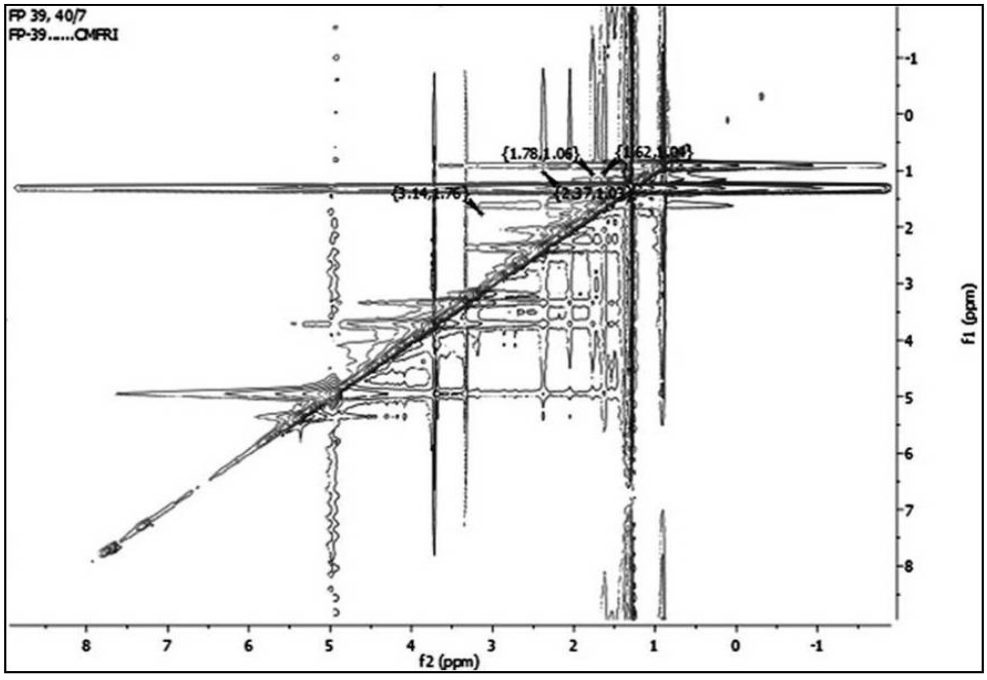

Figure 4.108. Figure showing the NOESY spectrum of compound **G4**

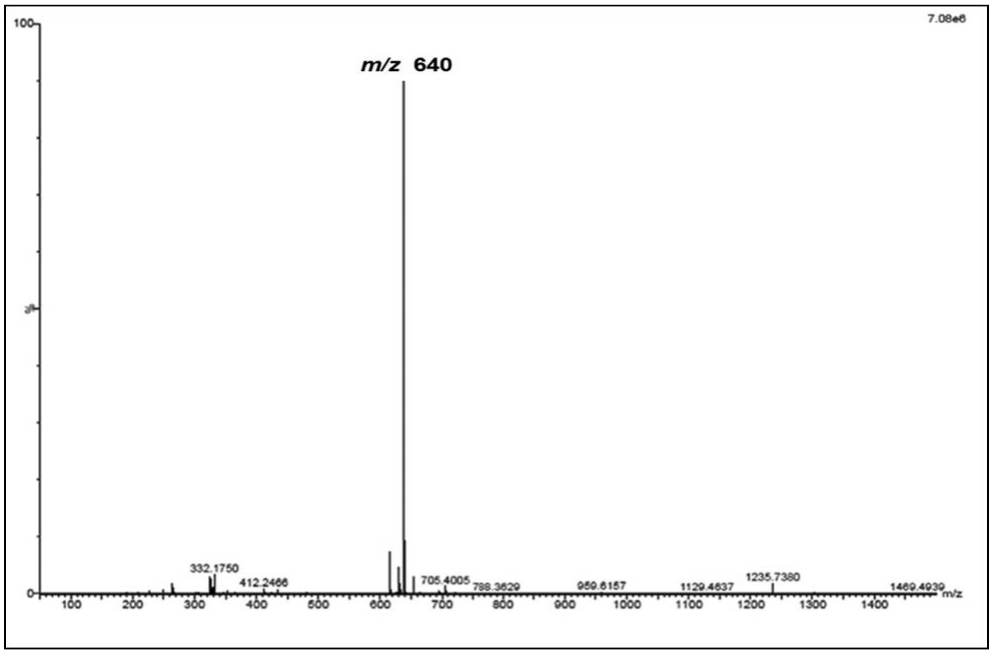

Figure 4.109. Mass spectrum of compound **G4**

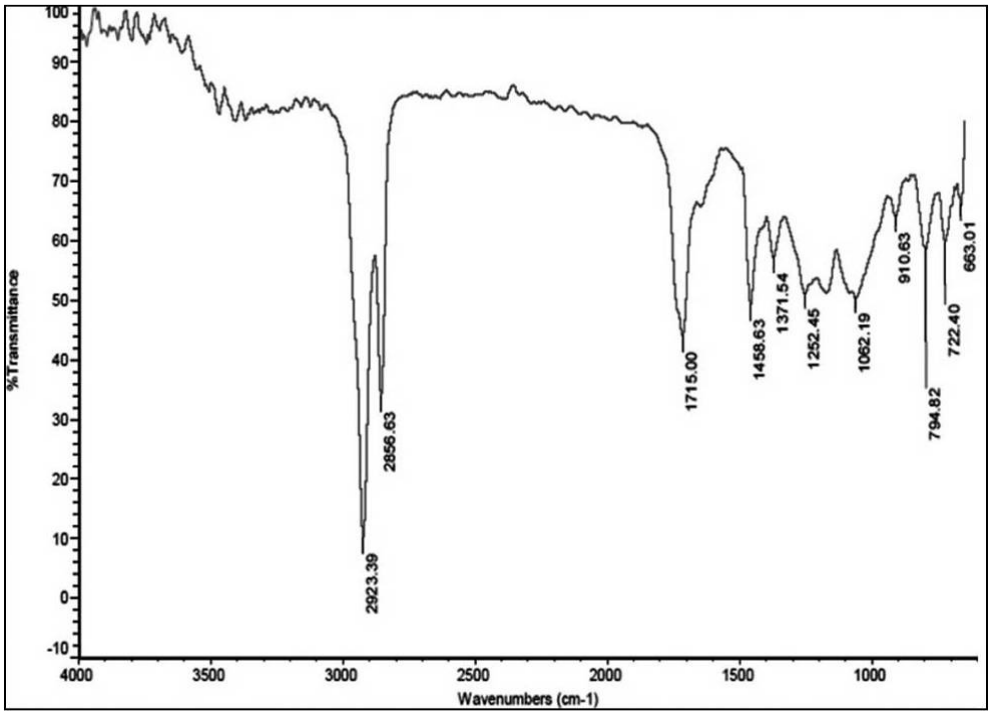

Figure 4.110. Figure showing the FTIR spectrum of compound **G4**

4.3.2.7. Bioactivities and Structure-Activity Relationship Analysis

Antioxidant activities have been displayed by various genera of marine macroalgae (Cornish and Garbary 2010; Kindleysides et al. 2012), although there were scanty reports of biogenic chromene derivatives with antioxidative and anti-inflammatory properties from this group of marine flora (Cornish and Garbary 2010). The antioxidative activity of the 2*H*-chromen derivative from the red marine macroalga *G. opuntia* was significantly greater as determined by DPPH and ABTS radical scavenging activities (IC_{50} 0.26–0.32 mg/mL) compared to α-tocopherol (IC_{50} > 0.6 mg/mL), and was comparable to the synthetic antioxidants BHT and BHA (IC_{50} ~ 0.25–0.34 mg/mL). The free radical scavenging property of the 2*H*-chromen derivative was found to be significantly influenced by the lipophilic descriptor (octanol-water coefficient, log Pow). It is of note that the octanol-water coefficient value of the compound **G4** was comparatively lesser (log Pow=2) as compared to those of the commercially available antioxidants (α-tocopherol log Pow 9.98, BHA log Pow 3.22, BHT log Pow 5.54), and this might be one of the factors leading to the significantly greater antioxidant activity of the 2*H*-chromen derivative. Although a greater lipophilic coefficient permits facile transportation of the molecule through the inter-membrane space, the lesser molecular hydrophobicity renders the molecule to harbor lesser radical scavenging properties. The log Pow of the chromene derivative is lesser apparently due to the presence of 1-(5-acetoxy-4-methyl-2-oxotetrahydro-2*H*-pyran-4-yl) ethyl acetate (log Pow 0.22) and dimethoxy-4-(methoxymethoxy)-2*H*-chromene (log Pow 1.23) frameworks. The majorities of the hydrophobicity and membrane permeability were imparted by the methylheptane moiety (log Pow 3.75) sandwiched between these two hydrophilic groups described earlier. It is of note that compounds with greater antioxidative properties in the *in vitro* systems might not prove themselves as potential radical scavengers in our metabolic systems, due to the fact that a balanced combination of hydrophilicity-lipophility is essential for antioxidative activities in the cellular framework. The 2*H*-chromen derivative isolated in the present study harbour 1-(5-acetoxy-4-methyl-2-oxotetrahydro-2*H*-pyran-4-yl) ethyl acetate and dimethoxy-4-(methoxymethoxy)-2*H*-chromene moieties, which might contribute towards the aggregate electronic property of the compound **G4** (aggregate topological surface area tPSA 142.12, polarisability Pl 53.26×10^{-24} cm^3).

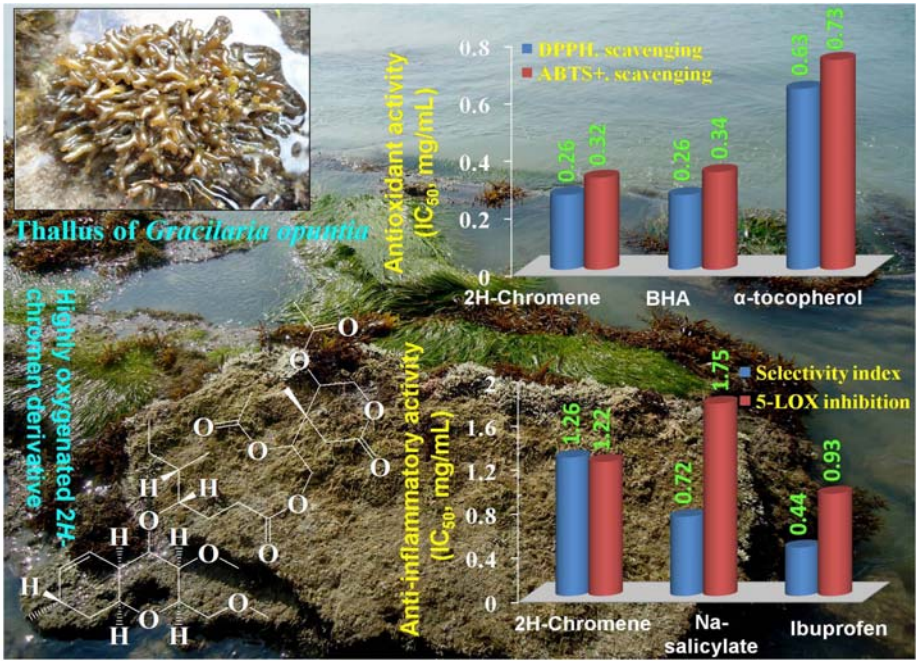

Figure 4.111. Graphical representation of bioactivities of compound **G4**. The thalli of the studied marine macroalga were displayed as inset

The antioxidative activity of the compound **G4** might be contributed by the presence of electron donating groups, such as $–CH_2O$, –OMe, >C=O, etc., which could abstract and convert the free radicals to their non-reactive forms (Pietta 2000; Cai et al. 2006). It is interesting to note that the chromen from marine macroalga recorded significantly greater electronic properties than α-tocopherol (tPSA 29.46), BHT (20.23) and BHA (29.46) along with acceptable hydrophobicity (log Pow 2.88), which is comparable to that of BHT and BHA (log Pow 3–5). Interestingly, the hydrophobicity of α-tocopherol is significantly greater (log Pow 9.98) than other synthetics and the 2*H*-chromen, which can be attributed to the significantly lesser antioxidative activities of the former (IC_{50} 0.6–0.7 mg/mL, $P < 0.05$). Notably, the inhibition of the COX-1 isoform is subjected to many side effects of the conventional NSAIDs, and therefore, there were efforts to search anti-inflammatory leads with selective anti-COX-2 activities and lesser side effects. The purified compound showed greater anti-inflammatory activity against COX-2 isoform (IC_{50} 0.96 mg/mL) than COX-1 (IC_{50} 1.21 mg/mL), and this phenomenon is inverse with regard to the traditional NSAIDs, such as aspirin (anti-COX-1 IC_{50} 0.005, anti-COX-2 IC_{50} 0.21 mg/mL) and ibuprofen (anti-COX-1 IC_{50} 0.04, anti-COX-2 IC_{50} 0.09 mg/mL) (Fig. 4.111, Table 4.21).

Therefore, the anti-inflammatory selectivity index of the substituted 2*H*-chromen was found to be greater (SI: anti-cyclooxygense-1 IC_{50}/anti-cyclooxygense-2 IC_{50} ~ 1.26) than synthetic NSAIDs (aspirin and ibuprofen, SI: 0.02 and 0.44, respectively), and consequently, appeared to be safer. The *in vitro* 5-lipoxygenase (5-LOX) activity of the 2*H*-chromen (IC_{50} 1.22 mg/mL) was comparable to that of synthetic ibuprofen (IC_{50} 0.93 mg/mL). Sodium salicylate was found to be a weaker inhibitor of both COX isoforms (anti-COX-2 IC_{50} 2.65 mg/mL, anti-COX-1 IC_{50} 1.93 mg/mL) and demonstrated significantly lesser activity against 5-LOX (anti-COX-1 IC_{50} 1.75 mg/mL) ($P < 0.05$). In this context, it is important to note that the polarity (or electronic attributes) of the oxygenated 2*H*-chromen recorded greater values (tPSA 88.13) than NSAIDs (tPSA aspirin 63.60, tPSA ibuprofen 37.30), along side comparable hydrophobic-lipophobic (HLB) balance {log Pow (aspirin) 1.21, log Pow (ibuprofen) 3.75, log Pow (oxygenated 2*H*-chromen) 2.3)}. While the acceptable HLB would be of help for the compound **G4** to cross inter-membrane barrier, the greater polarity might enable the compound to effectively interact with the cyclooxygenase/lipoxygenase active site residues, which in turn, would result in greater anti-inflammatory activity.

Table 4.21 Antioxidative and anti-inflammatory activities of the 2*H*-chromen from *G. opuntia vis-à-vis* the commercially available antioxidants and anti-inflammatory agents

Bioactivities*	**IC_{50} (mg/mL)**			
Antioxidative activities	**Substituted 2*H*-chromen**	**BHA**	**BHT**	**α-tocopherol**
DPPH· scavenging	0.26^{a} ±0.02	0.26^{b}± 0.01	0.25^{b}± 0.02	0.63^{c}±0.04
$ABTS^{+\cdot}$ scavenging	0.32^{b} ±0.11	0.34^{b}± 0.02	0.26^{b}± 0.02	0.73^{c}±0.05
Anti-inflammatory activities	**Substituted *2H*-chromen**	**Aspirin**	**Na-salicylate**	**Ibuprofen**
COX -1 inhibition	1.21^{a} ±0.03	0.005^{a} ±0.00	1.93^{c} ±0.05	0.04^{a} ±0.00
COX -2 inhibition	0.96^{a} ±0.04	0.21^{b} ±0.02	2.65^{c} ±0.05	0.09^{a} ±0.02
Selectivity index**	1.26^{b} ±0.04	0.02^{b} ±0.02	0.72^{b} ±0.01	0.44^{b} ±0.02
5-LOX inhibition	1.22^{a} ±0.07	0.39^{a} ±0.02	1.75^{c} ±0.12	0.93^{b} ±0.11

* The bioactivities were expressed as IC_{50} values (mg/mL).

The samples were analyzed in triplicate (n=3) and expressed as mean ± standard deviation. Means followed by the different superscripts (a–c) within the same row indicate significant differences ($P < 0.05$).

**Selectivity index has been calculated as the ratio of anti-COX-1(IC_{50}) to that of anti-COX-2 (IC_{50})

4.4. Conclusions

Bioactivity-guided chromatographic fractionation of the organic extract obtained from the thalli of the red marine macroalga *K. alvarezii* yielded two halogenated compounds named as 2-butyl-7-4-(chloromethyl) cyclooct-1-enyl) hept-5-en-1-ol and 4-(2-chloroethyl)-5-7-(methoxymethyl) undec-3-enyl) cyclooct-4-enone. Three oxygenated meroterpenoids, characterized as 1-(3-methoxypropyl)-2-propylcyclohexane, 3-(methoxymethyl) heptyl 3-(cyclohex-3-enyl) propanoate, and 2-ethyl-6-(4-methoxy-2-((2-oxotetrahydro-*2H*-pyran-4-yl) methyl) butoxy)-6-oxohexyl-5-ethyloct-4-enoate along with an unprecedented non-isoprenoid oxocine carboxylate cyclic ether characterized as (3, 4, 5, 6)-3-(hexan-2'-yl)-3, 4, 5, 8-tetrahydro-4-methyl-2*H*-oxocin-5-yl acetate were also purified to homogeneity from the organic extract of the marine macroalga. Likewise chromatographic purification of the organic solvent extract of the thalli of the red marine macroalga *G. opuntia* yielded two unprecedented furanyl derivatives, named as 5-(7-(5-ethyl-3, 4-dimethoxycyclooctyl) benzofuran-6-yl)-7-methyl-tetrahydro-2*H*-oxocin-2-one and 2-(3-ethyl-9-(2- methoxyethoxy)-1-oxo-tetrahydro-1*H*-xanthen-2-yl) ethyl-5-hydroxy-9-methoxy-7, 8-dimethyl-8-(5-methylfuran-2-yl) nona-3, 6-dienoate. A rare antioxidative azocinyl morpholinone alkaloid characterized as of 3-(2-ethyl-6-((3, 7)-1, 2, 5, 6-tetrahydroazocin-5-yl) hexyl) morpholin-6-one along with a chromen derivative with highly oxygenated carbon skeleton, characterized as 2-acetoxy-2-(5-acetoxy-4-methyl-2-oxotetrahydro-2*H*-pyran-4-yl) ethyl-4-(3-methoxy-2-(methoxymethyl)-7-methyl-hexahydro-2*H*-chromen-4-yloxy)-5-methylheptanoate. The compounds were found to selectively inhibit pro-inflammatory inducible enzymes cyclooxygenase-2 and 5-lipoxygenase, and possessed significantly greater selectivity than the non-steroidal anti-inflammatory drugs. The target bioactivities of the isolated secondary metabolites were predominantly directed by the electronic and lipophilicity parameters. The newly reported compounds from the two studied marine macroalgae were found to be endowed with valuable bioactive potential as natural antioxidant and anti-inflammatory leads for use in the pharmaceutical and food applications.

Chapter 5

ISOLATION AND CHARACTERIZATION OF SULFATED POLYSACCHARIDES FROM *KAPPAPHYCUS ALVAREZII* AND *GRACILARIA OPUNTIA* AND THEIR PHARMACOLOGICAL APPLICATIONS

Contents

5.1. Background

The marine macroalgal polysaccharides were reported to possess valuable pharmacological properties, and have been found to constitute a fascinating chemical diversity (Pangestuti and Kim 2011; Souza et al. 2012; Maneesh and Chakraborty 2018). Previous reports of literature found that the macroalgae-derived polysaccharides could stimulate the immune system resulting in the decreasing onset of various life-threatening diseases (Leiro et al. 2007; Choi et al. 2005). The chemical structures of macroalgal hydrocolloids bearing oligosaccharide framework are heterogeneous, whereas these large families of macroalgal hydrocolloids were made up of homogenous or heterogenous group of linear repeating chains of monomeric saccharide units, with repeated sequence of 1, 3 and 1, 4-connectivity. The monosaccharide units were found to possess various combinations of ester-sulfate groups in their repeating framework. These structural complexities of macroalgal polysaccharide were attributed to the occurrence of a mixture of monomeric units, and their repeating sequence along with uronic acid and sulfate content in the polysaccharide backbone (Vandevelde et al. 2002). The brown marine macroalga '*wakame*' (*Undaria pinnatifida*), which is customarily consumed in Japan, was accounted for to have *in vitro* Angiotensin-I-converting enzyme (ACE) inhibitory and *in vivo* anti-hypertensive effects (Suetsuna and Nakano 2000). ACE-I inhibitory peptides were reported from the butanol portion of marine macroalga *U. pinnatifida* hydrolysate (Sato et al. 2002). Bioactive properties of the macroalgae were reported to be due to the presence of sulfated polysaccharides, phenolics, and terpenoids (Chakraborty and Paulraj 2010; Chakraborty et al. 2015).

The marine macroalgae were found to be potential inhibitors of α-glucosidase (Seung-Hong and You-Jin 2013). Bromophenols, 2-piperidione, benzene acetamide, *n*-hexadecanoic acid, and polysaccharide derivatives were found in red marine macroalgae like *Rhodomela confervoides*, *Symphyocladia latiuscula*, *Polysiphonia urceolata* and were found to exhibit hypoglycemic potentials by inhibiting α-glucosidase (Seung-Hong and You-Jin 2013).

Red marine macroalgae (Rhodophyta) were found to constitute a predominant natural resource in the coastal areas of Indian penninsular. Among different red marine macroalgae found in the Gulf of Mannar of the Indian subcontinent, *Kappaphycus alvarezii* (Doty) Doty ex Silva (family Solieriaceae, phylum Rhodophyta; voucher

specimen number MA/RS/KA-005/2016–2017) and *Gracilaria opuntia* (family Gracilariaceae, phylum Rhodophyta; voucher specimen number MA/RS/GO-003/2016–2017) are available all through the distinctive seasons. These genera of macroalgae were widely used in traditional medicine, and have been considered to be economically important since they are used in the pharmaceutical, nutraceutical, cosmetic and food industries (Blouin et al. 2011; Gressler et al. 2010; Holdt and Kraan 2011). Numerous studies have been carried out to determine the antioxidant activities in the red marine macroalga *K. alvarezii* extract (Chew et al. 2008; Matanjun et al. 2008; Ganesan et al. 2008; Kumar et al. 2008). The acetone extract of *K. alvarezii* was found to possess significant antioxidative activity (Farah Diyana et al. 2015). The organic extracts of *K. alvarezii* displayed significant protection against DNA damage induced by H_2O_2, and enhanced antioxidant potential and protection against tissue lipid peroxidation and cell damage (Nagarani and Kumaraguru 2013). The methanol extract derived from *K. alvarezii* was screened for the anti-diabetic (α-amylase) anti-inflammatory activity (hyaluronidase inhibition) and cytotoxicity against the stannous chloride in *E. coli* AB 1157 (Nagarani and Kumaraguru 2013). The red marine macroalga belonging to *Gracilaria* sp were found to be rich in sulfated polysaccharides, and were generally related with anti-inflammatory property (Mendonca and Freitas 2000).

In this background, the objectives of the present study were to screen these marine macroalgae belonging to *K. alvarezii* (family Solieriaceae, phylum Rhodophyta) and *G. opuntia* (family Gracilariaceae, phylum Rhodophyta) for lead polysaccharide fractions containing different sulfated galactan motifs by chemical derivatization and spectroscopic analyses. The pharmacological properties with regard to antioxidant, anti-hypertensive, anti-inflammatory and anti-diabetic activities of the purified polygalactans were evaluated by various selective assays as described in the following sections.

5.2. Materials and Methods

5.2.1. Algal Material

The red marine macroalgae used in this study were *Kappaphycus alvarezii* (Doty) Doty ex Silva (family Solieriaceae, phylum Rhodophyta; voucher specimen number MA/RS/KA-005/2016-2017) and *Gracilaria opuntia* Durairatnam (1962) (family Gracilariaceae, phylum Rhodophyta; voucher specimen number MA/RS/GO-003/2016-2017), which were freshly collected from the Gulf of Mannar in Mandapam region situated between 8º48′ N, 78º9′ E and 9º14′ N, 79º14′ E in the south east coast of India. The samples were washed in running water for 10 min to remove epiphytes, dirt, and salt particles, before being transported to the laboratory and shade-dried (35 ± 3 °C) for 72 h and utilized for further experiments.

5.2.2. Instrumentation

FTIR spectra of the compounds under KBr pellets were recorded in a Thermo Nicolet Avatar 370 in the IR range between 4000 and 400 cm^{-1}. UV spectra were obtained on a Varian Cary 50 ultraviolet visible (UV–VIS) spectrometer (Varian Cary, USA). The Gas chromatography–Mass spectrometry (GC-MS) analyses were performed in electronic impact (EI) ionization mode in a Perkin Elmer Clarus 680. GC-MS fitted with an Elite 5 MS non-polar, bonded phase capillary column (50 m × 0.22 mm i.d. × 0.25 μm film thicknesses). Helium (He) was used as the carrier gas, and the flow rate used was 1 mL min^{-1}. The temperature was programmed initially at 50 °C for 2 min, then increased at a rate of 10 °C min^{-1} to 180° C and kept for 2 min and raised at 4° C min^{-1} to 280 °C and held for 15 min. Thin layer chromatographic analysis was carried out using silica gel GF_{254} plates and visualized with a documentation system operating at 254 and 366 nm wavelength regions. A table-top high speed refrigerated centrifuge (Sorvall, Biofuge Stratos, Thermo Scientific, Germany) was used for centrifugation. Flash Chromatography (Biotage AB SP1-B1A, Biotage AB, Uppsala, Sweden). Chromatographic analysis was carried out using High performance liquid chromatography (Shimadzu SCL-10A vp, Shimadzu Co., Kyoto, Japan) equipped with a vacuum degasser, a binary pump (LC–20AD), a thermostatic column compartment (CTO–20A) and a diode array detector (SPD–M20A), connected to an LC solution software. Chromatographic separation was carried out at 30 °C on a reverse phase Luna C_{18} (250 mm x 4.6 mm, 5μm) phenomenex column. The ultra sonicator (Labline) was used for sonicating and a laboratory shaker (Shaker, Labline) was used for shaking. A

rotary vacuum evaporator (Heidolf, Germany) was used for evaporation of solvents. ^{1}H and ^{13}C NMR spectra were recorded on a Bruker AVANCE III 500 MHz (AV 500) spectrometer (Bruker, Germany) in $CDCl_3$ as aprotic solvent at ambient temperature with TMS as the internal standard (δ 0 ppm). Two-dimensional ^{1}H-^{1}H COSY, DEPT, HSQC, HMBC and NOESY experiments were carried out using standard pulse sequences. The NMR data were acquired by using the BrukerTopSpin™ 2 software, and processed by MestReNova-7.1.1-9649 (Mestrelab Research S.L.). All the reagents and solvents used in this study were of analytical grade and purchased from E-Merck.

5.2.3. Isolation and Purification of the Various Polysaccharide Fractions from the Marine Macroalgae *K. alvarezii* and *G. opuntia*

The dried and powdered material (200 g) derived from the marine macroalgae was refluxed for 4 h in *n*-hexane (40-60 °C, 1000 mL). The residual material acquired after filtration (Whatman number 1) was air-dried for 24 h before being treated with an alkaline solution (6 % KOH w/w) at 80–90 °C for 3–4 h. The treated samples were repeatedly washed with deionized water (3 × 1000 mL) to remove the excess KOH before being dried. The dried macroalgal powder (200 g) was thereafter extracted with hot deionized water (1200 mL) at 80–90 °C for 3–4 h to yield an aqueous extract, which was cooled and centrifuged (8,500 rpm for 15 min, 4 °C, Sorvell Biofuge Stratos, Thermo Scientific, USA) to remove the solid residues. The clarified supernatant (1000 mL) obtained after centrifugation was concentrated to $1/4^{th}$ of the original volume (250 mL) by utilizing a rotational vacuum concentrator (Martin Christ RVC 2-33 IR, Martin Christ, Germany), cooled, and precipitated with three volumes of cold ethanol (750 mL, 3:1, v/v) overnight at 4 °C for the precipitation of mixture of sulfated polygalactan. Subsequently, ionic halide ($CaCl_2$ 1 % w/v, 15 g) was added to the supernatant, and the mixture was kept up overnight at 4 °C. The lyophilization of the precipitated material in a laboratory freeze-drier (Martin Christ alpha 1-4 LDplus, Germany) yielded sulfated polygalactan-enriched concentrate (**KA-1** from *K. alvarezii* and **GO-1** from *G. opuntia*) derived from the marine macroalgal species (yield based on powdered material, 72 %). The resultant polysaccharide concentrate was fractionated by anion-exchange chromatography (DEAE cellulose Cl^{-} previously equilibrated with 0.1 M NaCl, 3 × 10 cm, Bio-Rad, CA, USA), and the column was

continuously eluted with common salt (NaCl, 0-2 M). The polysaccharide fractions were vacuum-concentrated (Martin Christ RVC 2-33 IR, Germany) before being dialyzed for 48 h (against distilled water) and lyophilized (alpha 1-4 LD, Martin Christ, Germany). The purity of the fractionated polysaccharides were examined by reverse-phase high performance liquid chromatography (Shimadzu LC 20AD; Shimadzu Corp., Nakagyo-ku, Japan) accompanied by an reverse-phase amino column (SUPELCOSIL NH_2 column-5 µm, 25 cm × 4.6 mm; Supelco, Bellefonte, PA, USA) previously housed in an oven (maintained at 35 °C). Acetonitrile/water (3:1 v/v, flow rate of 0.5 mL/min) was used as the mobile phase to separate the polysaccharide fractions by using a refractive index detector. The purified polysaccharide fractions (**KA-1** from *K. alvarezii* and **GO-1** from *G. opuntia*) were further used for antioxidant and anti-hypertensive *in vitro* analysis.

In another process to fractionate the various polysaccharide fractions, the dried marine macroalgal powder (200 g) was extracted with hot water at 80–90 °C for 3–4 h to yield an aqueous extract (Praveen and Chakraborty 2013) which was cooled and centrifuged (8500 rpm for 15 min, 4 °C, Sorvell Biofuge Stratos, Thermo Scientific, USA) to remove the solid residues. The supernatant (1000 mL) obtained after centrifugation was concentrated to $1/10^{th}$ of the original volume (100 mL) by utilizing a rotational vacuum concentrator (Martin Christ RVC 2-33 IR, Germany), cooled, and precipitated with three volumes of ethanol (500 mL, 3:1, v/v) overnight at 4 °C for the precipitation of the sulfated polygalactans (**KA-2** from *K. alvarezii* and **GO-2** from *G. opuntia*). The lyophilization of the precipitated material in a laboratory freeze-drier (alpha 1-4 LD, Martin Christ, Germany) yielded sulfated polygalactan-enriched macroalgal concentrate (144 g; yield based on powdered macroalgae (72 %). The purified polysaccharide fractions (**KA-2** from *K. alvarezii* and **GO-2** from *G. opuntia*) were further used for anti-diabetic and anti-inflammatory *in vitro* analysis.

In a further different process to fractionate the various polysaccharides from the studied marine macroalga, the air-dried thalli of *K. alvarezii* (50 g) were extracted with alkali (1000 mL, 5 % KOH) at 80 °C (1 h), and were added with acid (1 M HCl) followed by extraction with mild alkaline solution of sodium bicarbonate ($NaHCO_3$, pH 8-9). The mild alkaline extract was treated with 1 % KCl solution to precipitate the polysaccharide fractions, which was freeze-dried (alpha 1-4 LD, Martin Christ, Germany) to yield a polysaccharide-concentrate (**KA-3** from *K. alvarezii*, 1000 g; 72 % yield on the basis of dry weight). Likewise, the air-dried thalli of *G. opuntia* (50 g)

were extracted with of mild alkaline solution of $NaHCO_3$ (1000 mL, pH 8-9). The extraction was carried out for 2 h, and the supernatant was collected. The clarified solution was evaporated to one-third of its original volume, and the polysaccharide fractions were precipitated by isopropyl alcohol. The centrifugation at 8000 rpm (4 °C for 20 min) was performed to recover precipitated polysaccharide fractions, which were freeze-dried to yield polysaccharide-enriched concentrate (**GO-3** from *G. opuntia*) (50 g; yield 75 %). The fractionation of polysaccharide concentrates using diethylaminoethyl cellulose (DEAE cellulose, Cl^-) anion-exchange chromatography (previously equilibrated with 0.1 M NaCl, 3 × 10 cm, Bio-Rad, CA, USA) with an increasing gradient of NaCl (0-2 M) was used to yield various fractions, which were vacuum-concentrated and dialyzed (against distilled water) before being freeze-dried. The reverse-phase high performance liquid chromatography (RP-HPLC; Shimadzu LC 20AD) with amino column (Supelcosil NH_2 column-5 μm) and mobile phase of acetonitrile/water (3:1 v/v) (flow rate of 0.6 mL/min) were used to analyze the homogeneity of the polysaccharides. The purified polysaccharide motifs were further used for anti-diabetic and anti-hypertensive *in vitro* analysis (**KA-3** from *K. alvarezii* and **GO-3** from *G. opuntia*). Monosaccharide composition was then measured by RP-HPLC with pulsed refractive index detector (RID detector), by external calibration with standard solutions of galactose (Sigma, St. Louis, MO, USA). In brief, trifluoro acetic acid (TFA, 1 M) was used to hydrolyze the sample (20 mg), and nitrogen gas was purged to remove the residues of TFA. The resulting hydrolysate was dissolved in 1 mL of HPLC-grade water, and was injected to the RP-HPLC mounted with an amino column and RI detector. Acetonitrile-water (80:20, v/v) mobile phase was used to separate the compounds, and methylation analyses of polysaccharides were performed by following previous reports of literature (Jun and Gray 1987; Kiwitt-Haschemie et al. 1993) with suitable modifications.

Methylated polysaccharide fractions (80 g) from *K. alvarezii* were recovered in EtOAc before being packed in glass column (90 cm X 4 cm) loaded with 60-120 meshed silica gel. Gradual increase of polarity of the mobile phase by addition of increasing gradient of EtOAc: *n*-hexane (1:99 to 7:3, v/v) yielded 10 fractions (8 mL each) that were combined to 4 fractions (FP_{10}- FP_{14}) on the basis of TLC experiments (EtOAc: *n*-hexane 1:4, v/v). The fraction FP_{11} (110 mg) recovered by using EtOAc: *n*-hexane (1:4, v/v) was a mixture that was flash chromatographed (Biotage AB SP1-B1A, Sweden) with a step-gradient of EtOAc/*n*-hexane (0-50 % EtOAc) to afford 160

sub-fractions (15 mL each). On the basis of analytical TLC experiments, the homogeneous fractions were combined to yield three fractions (FP_{15} – FP_{17}). The fraction $FP_{15\text{-}1}$ on further fractionation over preparatory RP-HPLC chromatography on a C_{18} RP column yielded 1, 3-*O*-diacetyl-2, 5, 6-tri hydroxyl-β-D-galactose-4-sulfate (**KA-3$_A$**; 85 mg, ~99 % purity).

The methylated polysaccharide fractions (80 g) from *G. opuntia* were recovered in EtOAc before being packed in glass column (90 cm X 4 cm) loaded with silica gel (60-120 mesh). Gradual increase of polarity of the mobile phase by addition of increasing gradient of EtOAc: *n*-hexane (1:99 to 7:3, v/v) yielded 15 fractions (15 mL each) that were combined to 5 fractions (FP_{30}- FP_{35}) on the basis of TLC experiments (EtOAc: *n*-hexane 1:4, v/v). The fraction FP_{33} (130 mg) recovered by using EtOAc: *n*-hexane (1:4, v/v) was a mixture that was flash chromatographed (Biotage AB SP1-B1A, Sweden) with a step-gradient of EtOAc/*n*-hexane (0-50 % EtOAc) to afford 150 sub-fractions (10 mL each). On the basis of analytical TLC experiments, the homogeneous fractions were combined to yield five fractions (FP_{36}–FP_{40}). The fraction $FP_{38\text{-}1}$ on further fractionation over preparatory RP-HPLC chromatography on a C_{18} RP column yielded 1, 3, 5-*O*-triacetyl-4-hydroxyl-6-*O*-methyl-D-galactose-2-sulfate (**GO-3$_A$**; 78 mg, ~ 99 % purity).

5.2.4. Analytical Methods

The polysaccharide fractions purified from the studied marine macroalgae were analyzed by the dinitrosalicyclic acid method, whereas uronic acid content was determined using the phenol-sulphuric acid reaction (Dubois et al. 1956). The sulfate content was evaluated by $BaCl_2$-gelatin method (Dodgson 1961). The yields were assessed from the dried weight of polysaccharide motifs. The pharmacological activities of the polysaccharide motifs were determined based on the *in vitro* assays performed as explained in the previous chapter (Chapter 3). The *in vitro* antioxidant activities were determined by ABTS, DPPH radical scavenging assays along with ferrous ion chelating assay (Sivasothy et al. 2012; Chakraborty et al. 2014). The anti-inflammatory properties were evaluated by COX-1 and COX-2 inhibition assays (Larsen et al. 1996) and 5-LOX inhibition assay (Baylac and Racine 2003). *In vitro* anti-diabetic studies were carried out by inhibition of dipeptidyl peptidase-4, α-amylase (Kojima et al. 1980; Hamdan and Afifi 2004) and α-glucosidase (Dong et al. 2012)

inhibition assays. The anti-hypertensive activities were determined by ACE-I inhibitory assay (Udenigwe et al. 2009). The IC_{50} value (mg/mL), named effective concentration, which is the concentration of the sulfated polygalactan enriched concentrate of *K. alvarezii* and *G. opuntia* inhibiting 50 % of the activity (COX-1 and COX-2), was calculated from the non linear regression curve. To calculate IC_{50}, a series of dose-response data have been used, whereas the simplest estimate of IC_{50} is to plot x-y and fit the data with a straight line. IC_{50} value was estimated using the fitted line, i.e., $y=mx+c$, and expressed as $IC_{50}= (0.5 - c)/m$.

5.2.5. Spectroscopic Methods

Fourier-transform infrared (FTIR) spectra of KBr pellets were recorded utilizing a Perkin–Elmer Series 400 FTIR spectrophotometer (Waltham, USA; scan range between 400-4000 cm^{-1}). The solid samples of dried sulfated polygalactan fraction (10 mg) were mixed with KBr (100 mg) and compressed to prepare as a salt disc. The frequencies of different components present in each sample were analyzed. Proton nuclear magnetic resonance (^{1}H-NMR) spectra were recorded on a Bruker AVANCE DRX 600 MHz (AV 600) spectrometer (Bruker, Karlsruhe, Germany) in deuterium oxide (D_2O) as aprotic solvent at ambient temperature (27 ^oC) with tetramethylsilane (TMS) as the internal standard (δ 0 ppm) equipped with 5 mm probes. The samples were deuterium exchanged by successive freeze-drying steps in D_2O (99.9 %) before being dissolved in D_2O (20-25 mg/mL).

5.2.6. Statistical Analysis

Data were expressed as mean values standard deviations. Statistical evaluation was carried out by Statistical Program for Social Sciences software (SPSS Inc, Chicago, USA, ver. 13.0). Analyses were carried out in triplicate and the means of all parameters were examined for significance ($P < 0.05$) by one-way analysis of variance (ANOVA). The Pearson correlation coefficient (r) was calculated ($P < 0.05$) to assess the strength of the linear relationship between two variables. The selected variables for principle component analysis (PCA) were the different bioactivities, as exhibited by different types of polysaccharides, which were extracted from the marine macroalgae.

5.3. Results and Discussion

5.3.1. Structural Characterization of Polysaccharide Fractions (KA-1 and GO-1) from Marine Macroalgae

The precipitation of polysaccharides from the crude extracts of *K. alvarezii* (**KA-1**) with ethanol brought about significantly greater yields (75 %) than that by utilizing $CaCl_2$ (56 %) ($P < 0.05$). Essentially, the aggregate recovery of polysaccharides from *G. opuntia* (**GO-1**) was recorded to be significantly lesser than those in *K. alvarezii* (**KA-1**) using ethanol (55 %) and $CaCl_2$ (50 %). The sulfated galactan was found to possess 34 % 3, 6-anhydro-D-galactose groups as a feature of its repeating structure and 25 % ester sulfate groups, which promptly diffused when warmed. Sulfated polygalactan was found to be the predominant polysaccharide acquired by $CaCl_2$ precipitation. It is evident that Ca^{2+} ions form bridges between the contiguous double helices through an electrostatic binding to two adjoining sulfate groups, consequently settling and reinforcing the polysaccharide system. The present examination demonstrated that a more significant yield of sulfated galactan could be obtained with alkaline (KOH) treatment.

The intense absorption bands in the 1210-1260 cm^{-1} region of the Fourier transform infrared (FT-IR) spectra showed the vicinity of S=O group of sulfate esters (ascribed to the glycosidic linkage) (Fig. 5.1). A particularly intense signal was recorded at 803-805 cm^{-1}, which was particular to 3, 6-anhydrogalactose-2-sulfate. The peaks were likewise identified at 925-935 cm^{-1} in the samples because of the vicinity of 3, 6-anhydro-D-galactose moieties (Villanueva et al. 2009). The S=O of the sulfate esters were obvious at 1258.92 and 1364.15 cm^{-1}, whilst the C-O-C of sugar and C-O-S sulfate ester were displayed at around 950-1100 cm^{-1}. The broad absorption band at 1240-1220 cm^{-1}, related to the ester sulfate group, is normal to every single sulfated polysaccharide. The ^{1}H-NMR spectra of polysaccharides derived from the marine macroalgae comprised of some well-resolved signals, tallying those of anomeric protons (δ_H 4.4-5.5), acetyl (δ_H 2) and methyl (δ_H 1.2) (Fig. 5.2 to Fig. 5.4). The ring protons connected to sulfate group showed up at δ_H 5.4-5.3, though the sulfated protons found at δ_H 6.1-6.8 was recorded in the ^{1}H-NMR spectra.

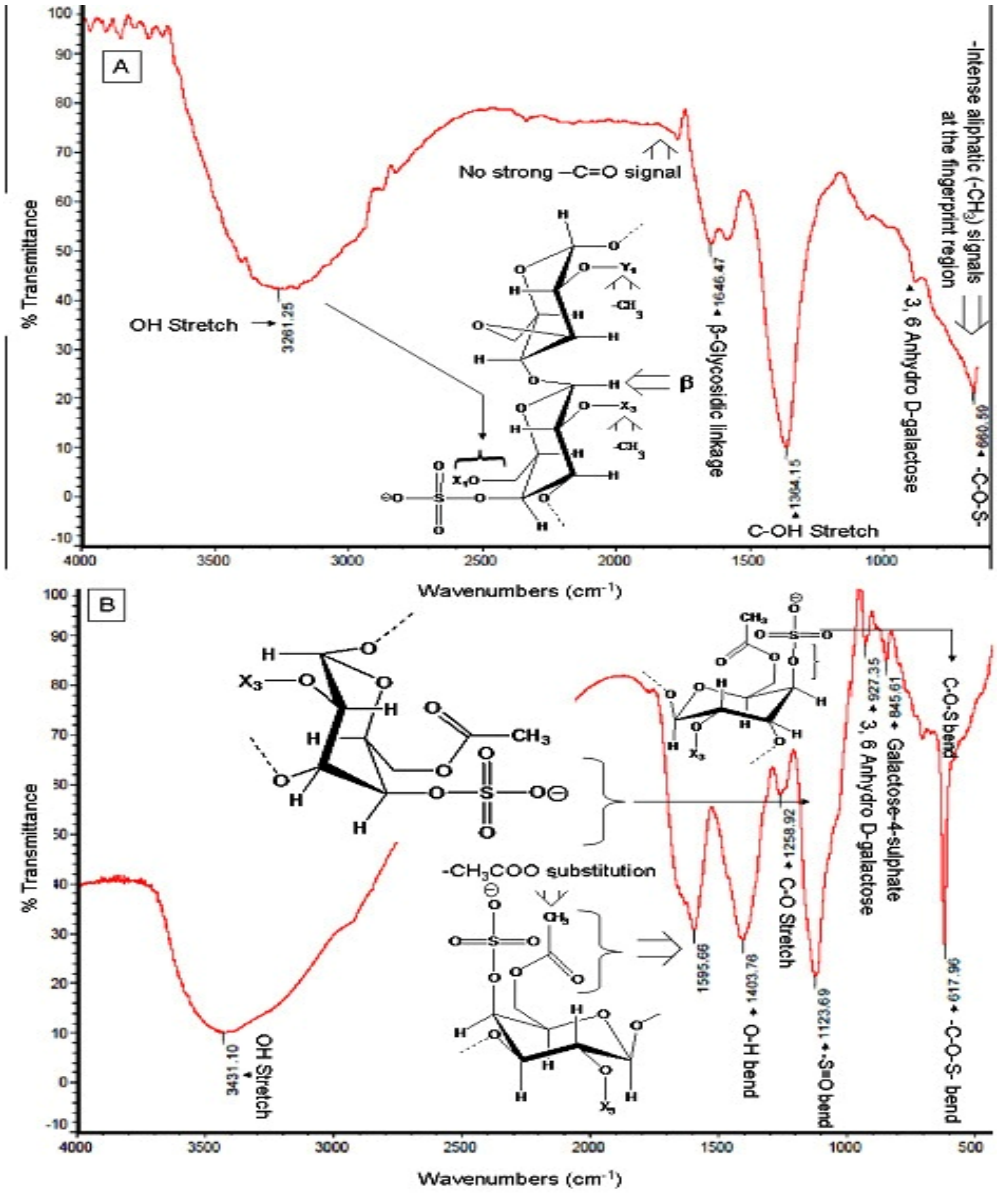

Figure 5.1. Infra red spectra of the sulfated polygalactans from (**A**) *K. alvarezii* (**KA-1**) and (**B**) *G. opuntia* (**GO-1**), the representative functional groups of the polysaccharides were indicated

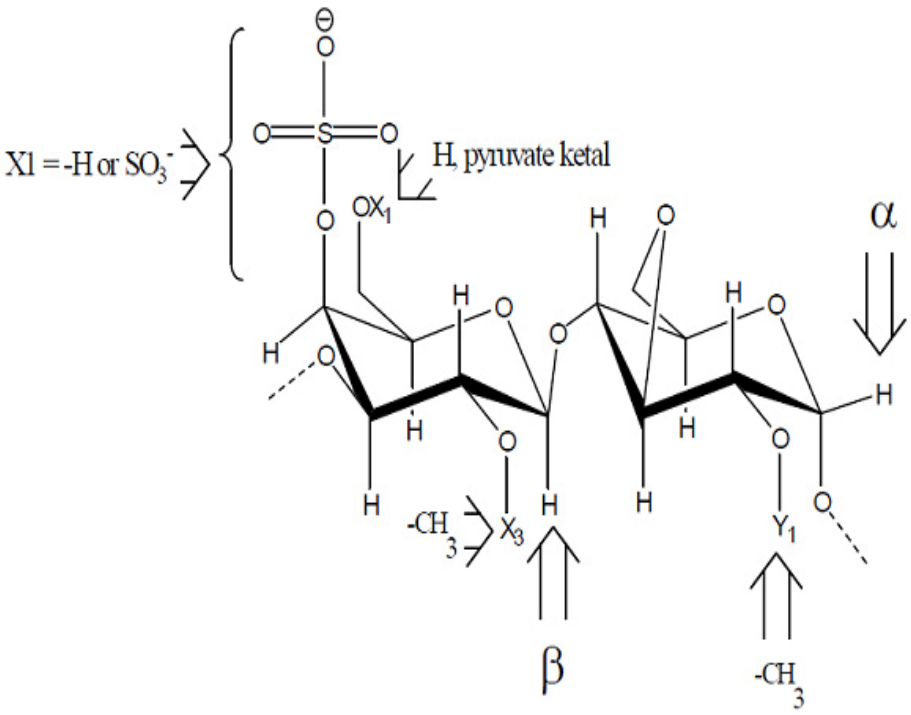

Figure 5.2. Schematic and global representation of sulfated polygalactans from *K. alvarezii* (**KA-1**)

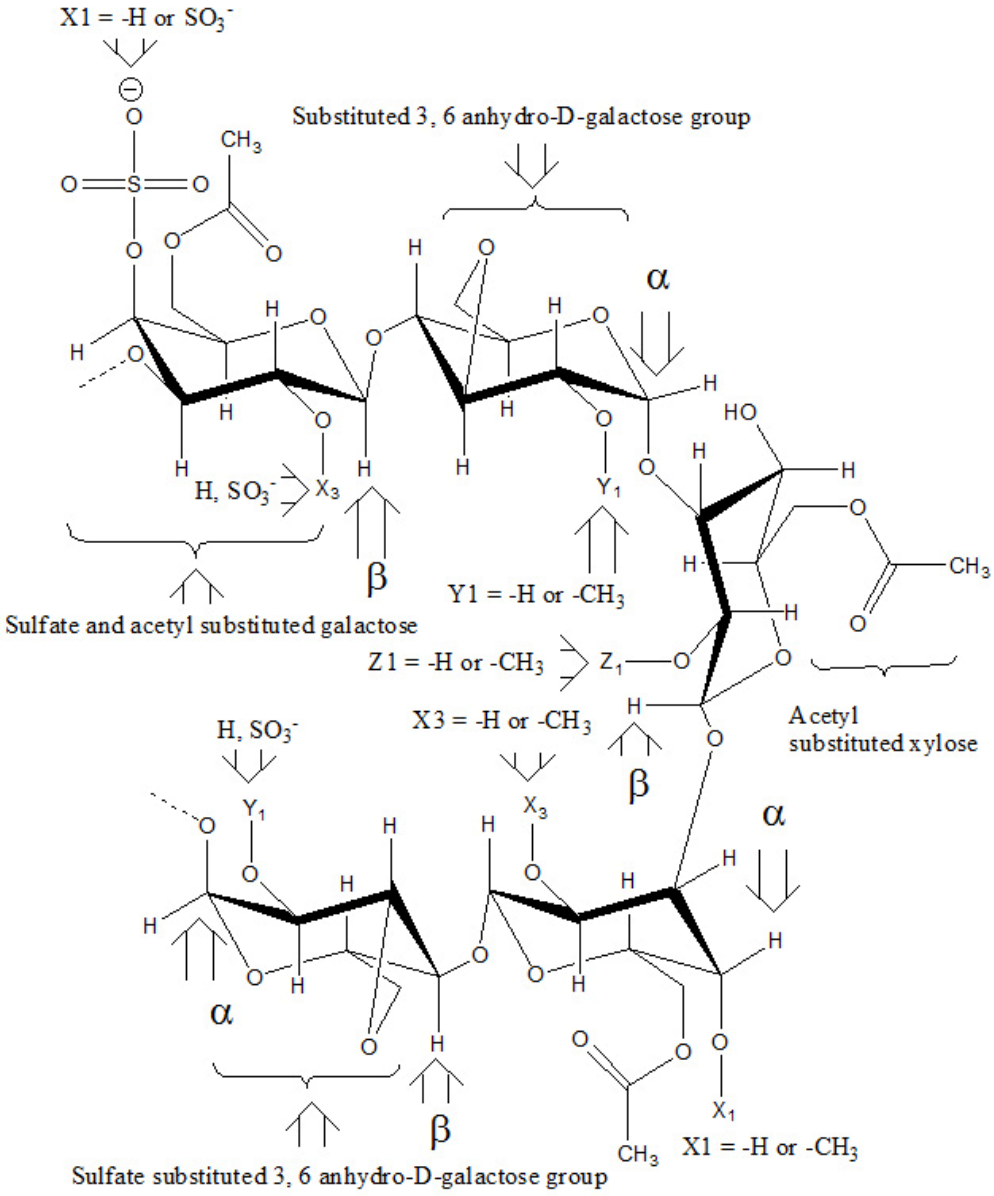

Figure 5.3. Schematic and global representation of sulfated polygalactans from *G. opuntia* (**GO-1**)

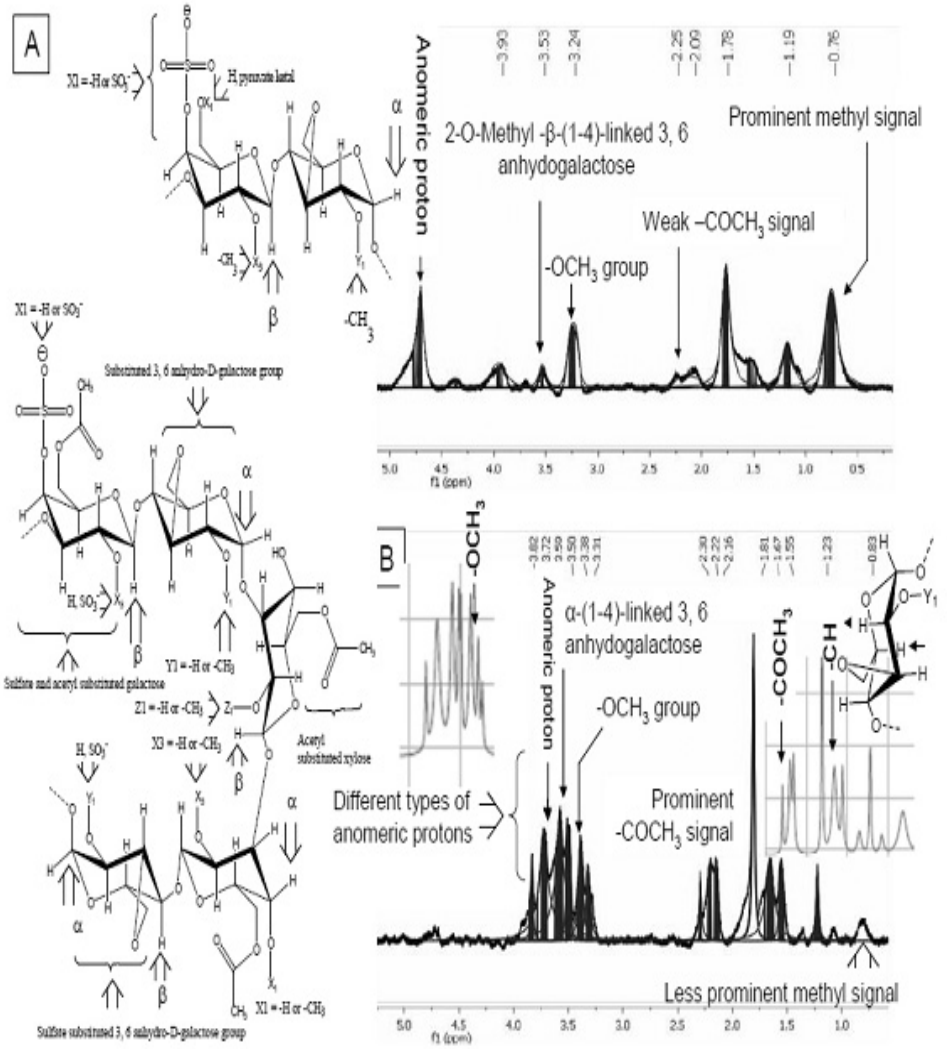

Figure 5.4. [1]H-NMR spectral representation of sulfated polygalactans motif from (**A**) *K. alvarezii* (**KA-1**) and (**B**) from *G. opuntia* (**GO-1**)

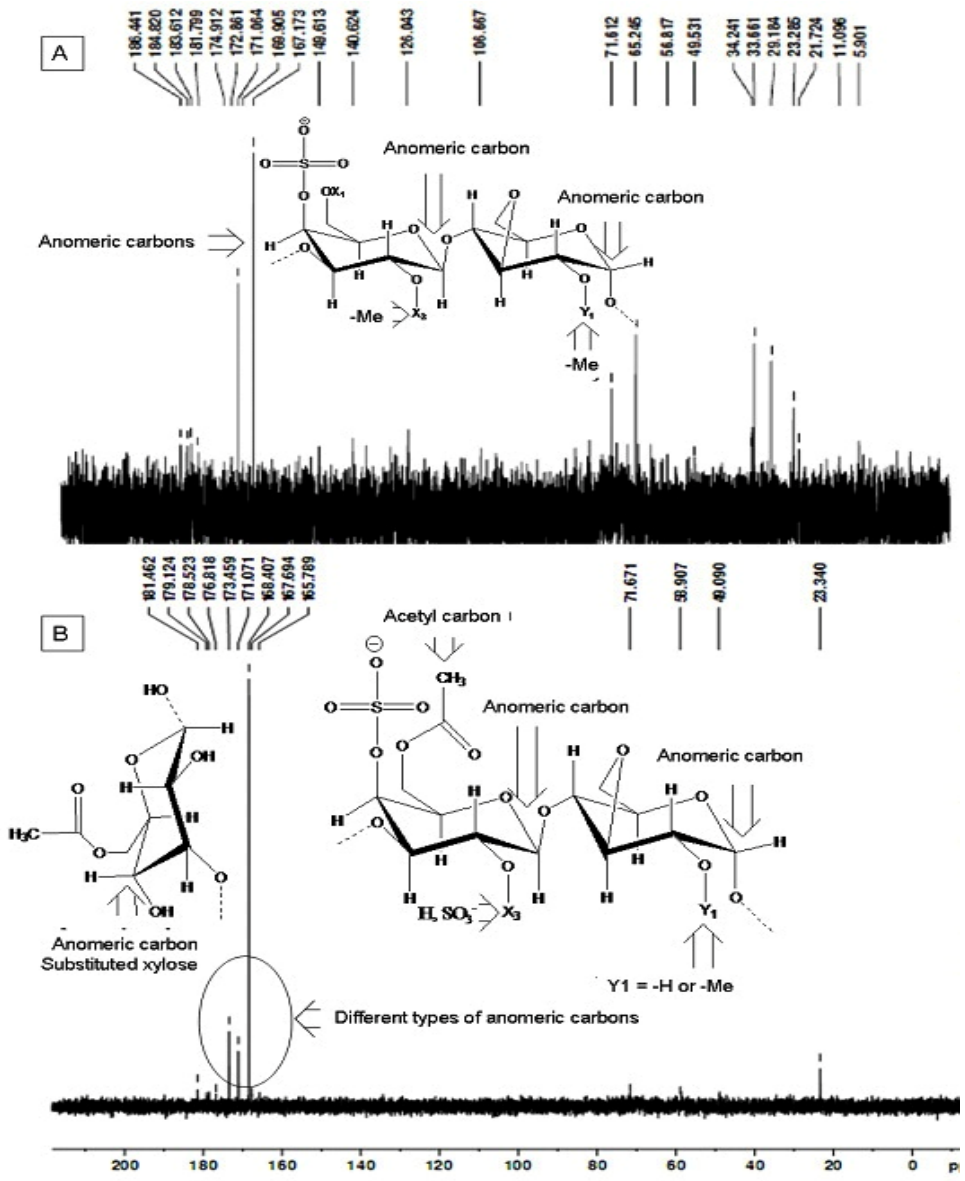

Figure 5.5. ^{13}C-NMR spectral representation of substituted galactan motifs from (**A**) *K. alvarezii* (**KA-1**) and (**B**) *G. opuntia* (**GO-1**)

The anomeric signals at δ_H 4.6 and δ_H 5.1 were characteristic of κ-sulfated polygalactan. The signal at δ_H 3.43 was assigned to the methyl proton of 6-*O*-methyl galactose. The sulfate group was situated at C-4 of (1→3)-linked galactopyranosyl residues of the native galactan, whereas the strong signals in the ^{1}H-NMR of *G. opuntia* (**GO-1**) at δ_H 2-2.5 attributed to the presence of strong -$COCH_3$ protons. Interestingly, very weak proton signals at δ_H 2-2.5 for *K. alvarezii* (**KA-1**) were assigned to be due to

the -$COCH_3$ protons. As diverged from *K. alvarezii* (**KA-1**), *G. opuntia* (**GO-1**) exhibited very sharp intense signals at δ_H 3.50 and δ_H 3.38, which ascribed to be due to the vicinity of 2-*O*-methyl α-(1-4)-linked 3, 6-anhydogalactose and 6-*O*-methyl-β-(1-3)-linked galactose residues, respectively. The anomeric carbon signals were found to be as C-1 of α-D-galactose-4-sulfate at δ_C 106.7, and this dyad was illustrative of a sulfated polygalactan. The ^{13}C-NMR chemical shifts of these characteristic signals were found at δ_C 27.6, δ_C 103.6 and δ_C 178, which showed the vicinity of methyl, acetyl and carboxyl carbon atoms, respectively (Fig. 5.5). The ^{13}C-NMR signals at δ_C 71.61, δ_C 71.67 and δ_C 65.25 were ascribed to the vicinity of C-5 and C-6 of 4-linked α-D-galactopyranoses (Fig. 5.5). The signals at δ_C 21.72 and δ_C 23.34 were because of the vicinity of methyl carbon atom of pyruvate moiety ($CH_3COCOOH$).

5.3.2. Structural Characterization of Polysaccharide Fractions (KA-2 and GO-2) from Marine Macroalgae

The precipitation of sulfated polygalactan from the crude extracts of *K. alvarezii* (**KA-2**) with ethanol brought about significantly greater recovery (75 %) than that in *G. opuntia* (55 %) (**GO-2**). The ethanol precipitated material was found to be rigid and crystalline. The elementary variables in extraction were the base used to generate the macroalgal material, and the temperature at which the reaction materialized, which affected the gelling properties and structure of sulfated galactan. The sulfated galactan was found to be a linear poly-galactose chain, where the galactose units integrate together and bear differing extent of sulfate entity (Fig. 5.6). A few of the D-galactoses involved a 6-sulfate ester group while some 3, 6-anhydro-D-galactoses consisting of a 2-sulfate ester group. In the presence of potassium ions, sulfated polygalactan gels dissolved by heating and subsequent cooling, resulting in the evolution of a three dimensional network by cationic interaction with sulfate group. The interesting aspects of mixture of sulfated polygalactan gel are its thermal reversibility, whereas it can gel and melt frequently, only defeating a little gel strength at each cycle. As potassium concentration increases, the gel stability was found to be increased until an optimum level is reached according to that potassium ions have a size and shape which comprise them fit into the mixture of sulfated polygalactan helix. This structure is sustained through the positively charged ions and the negatively charged sulfate groups in the sulfated galactan moiety.

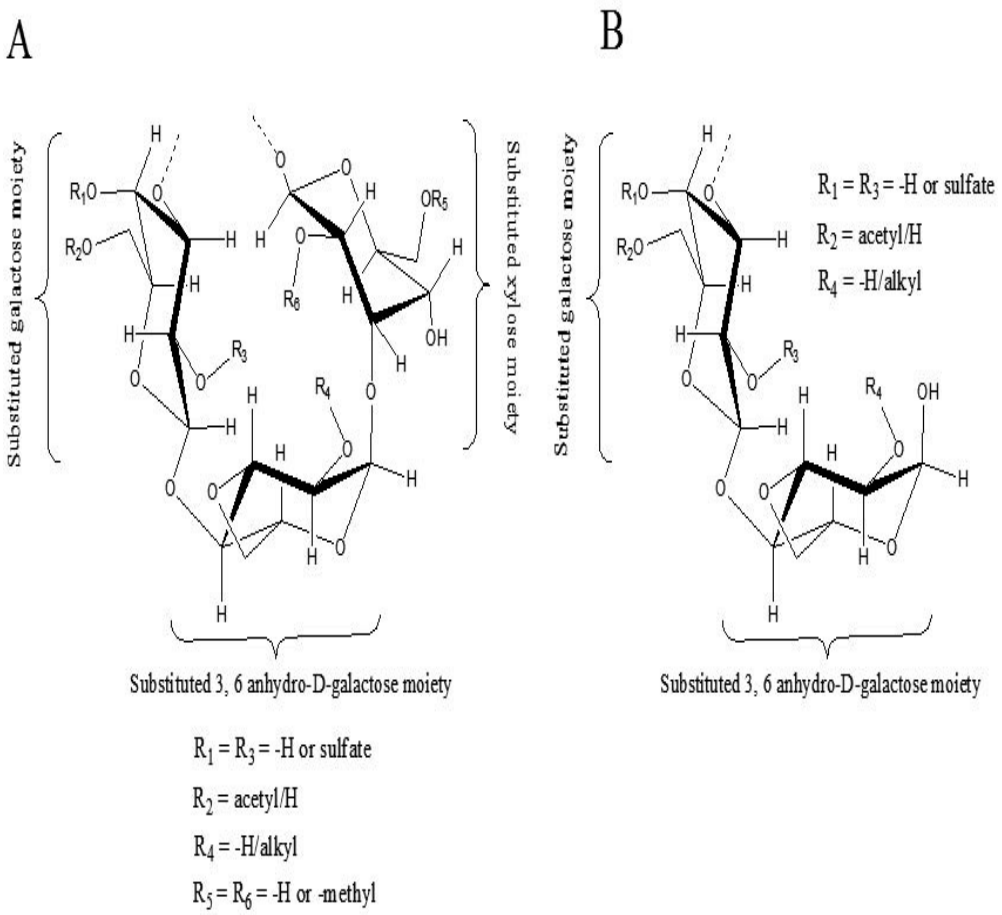

Figure 5.6. Structural representation of galactopyranan motifs of the sulfated polygalactans from (**A**) G. *opuntia* (**GO-2**) and (**B**) *K. alvarezii* (**KA-2**)

.

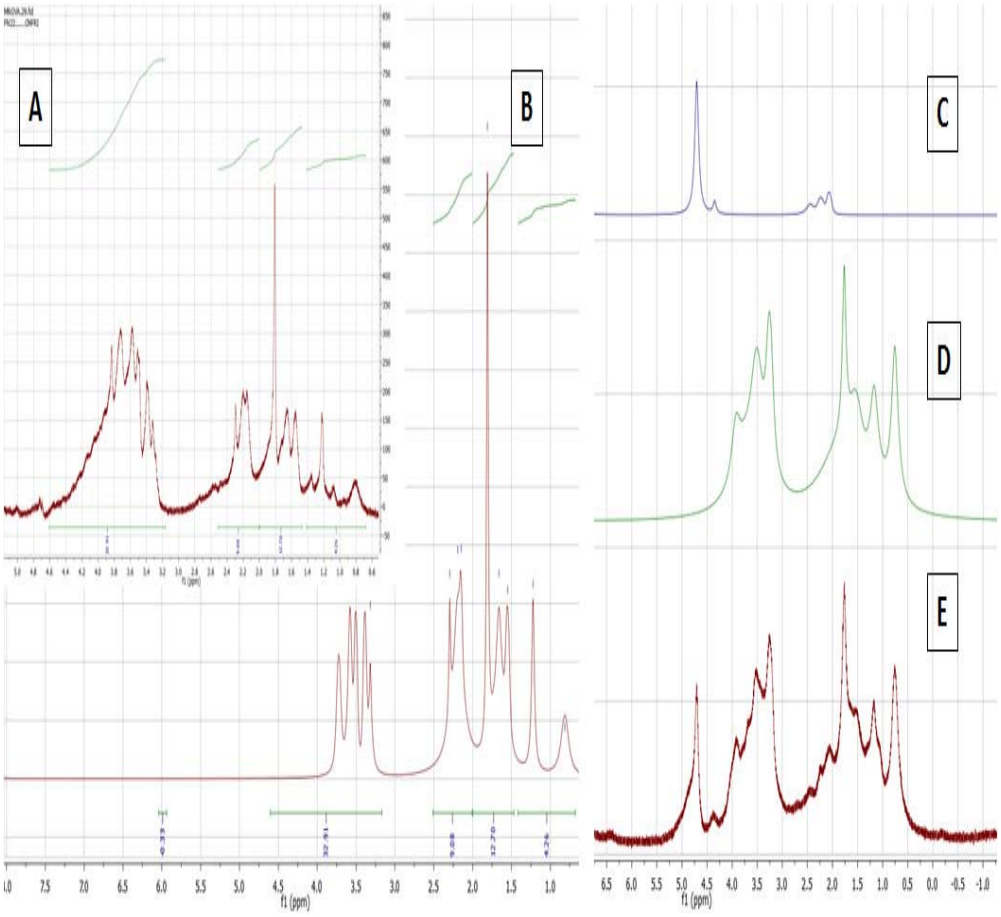

Figure 5.7. ^{1}H-NMR spectral representation of sulfated polygalactan from *G. opuntia* (**A-B**) (**GO-2**) and *K. alvarezii* (**C-E**) (**KA-2**)

The sulfated polygalactan has 34 % 3, 6 anhydro-D-galactose groups as segment of its repeating structure and 25 % ester sulfate groups, which promptly dispersed when heated. Thermo reversible gels engendered by polygalactan by the arrangement of the disjointed chains into double or triple helices. Hydrogen bonding, persuaded by aggregation of the ordered domains to form a firm, three dimensional stable gels. The gel strength of polysaccharides derived from the marine macroalgae *K. alvarezii* (**KA-2**) and *G. opuntia* (**GO-2**) was found to be greater, when heated in an alkaline solution of potassium hydroxide for about two hours. The hydroxide part of the reagent penetrates the macroalgae, diminished the amount of sulfate in the sulfated galactan and increasing the 3, 6-anhydro galactose unit, thereby developing the gel strength of the sulfated galactan. The contemporary inspection showed that greater yield of sulfated galactan could be achieved with KOH treatment. The conspicuous

attributes of the FT-IR spectra of sulfated polygalactan from the red marine macroalgae were because of the sulfate ester and carbohydrate groups in the infrared spectra. The strong absorption bands at 1210-1260 cm^{-1} of the FT-IR spectra demonstrated the region of S=O groups (attributed to the glycosidic linkage). The band at ~800 cm^{-1} was specific to 3, 6- anhydrogalactose-2-sulfate (Ganesan et al. 2008; Villanueva et al. 2009). The IR signals close to 3200-3400 cm^{-1} were credited to the region of -OH gatherings present in the sulfated polygalactans from the macroalgae. The S=O of the sulfate esters were showing up at 1250-1300 cm^{-1}, while the C-O-C of sugar and C-O-S sulfate ester were displayed at around 950-1100 cm^{-1}. The broad bands at 3200-3400 cm^{-1} were found to be a result of the sulfated polygalactan units. The C-H stretching vibrations were assigned to be present at around 2800-2900 cm^{-1}.

The absorbance peaks around 1050-1100 cm^{-1} displayed the pyranose ring structure. Intense absorbance at around 1700 cm^{-1} and bands of about 1420 cm^{-1} (C=O symmetric stretching vibrations), were due to carbonyl (acetyl) groups in the polysaccharide back bone chain. Three characteristic bands in the fingerprint anomeric region (950-700 cm^{-1}), connected to the ester sulfate bonds were attributed to a special feature of the sulfated polygalactan type of polysaccharides (Gomez-ordonez and Rupere 2011). The absorption bands at ~1400 cm^{-1} in FT-IR spectra deduced the normality of β-glycosidic linkages. Moreover, the IR absorption bands unique to the presence of anomeric locale (800-900 cm^{-1}), joined with the ester sulfate bonds are the special feature of the sulfated polygalactan type of polysaccharides (Kumar et al. 2008; Gomez-ordonez and Rupere 2011). NMR spectroscopy has been carried out for the structural prediction of any regular and complex polysaccharides. Intense signals acquired from the ^{1}H-NMR spectroscopy exhibited the region of hydrogen atoms at anomeric carbon (δ_H 5.4) (Fig. 5.7). The ^{1}H-NMR spectra of polysaccharides comprise of some well-resolved signals, counting those of anomeric protons (δ_H 4.4 - 5.5) (Fig. 5.7). By virtue of polysaccharides, the resonances due to the anomeric protons were grouped between δ_H 3-4. These results were in accordance to those reported in the literature (Cases et al. 1995). The Figure 5.7 exhibited the ^{1}H-NMR range of blend of sulfated polygalactans (κ-, ι-) separated from *K. alvarezii* (**KA-2**) and *G. opuntia* (**GO-2**). The peaks at δ_H 5 signified the vicinity of iota and κappa monomers of sulfated polygalactans (Nagarani and Kumaraguru 2013; Vandevelde et al. 2002). The ring protons associated with sulfate functionalities demonstrated ^{1}H-NMR signals at δ_H 5. The ^{1}H-NMR showed proton signal at δ_H 5.34, which was relegated to be a direct result

of the anomeric proton of the 3, 6- anhydrogalactose-2-sulfate (Cases et al. 1995). The anomeric proton signals at δ_H 4.5 and δ_H 5.0 were normal for κ-sulfated polygalactan. The ^{1}H-NMR signals in the scope of δ_H 3.6–4.9 were portrayed to whatever is left of the methylene and methine hydrogens of the sulfated polygalactan moiety. The ^{1}H-NMR spectrum of polysaccharides obtained from *K. alvarezii* (**KA-2**) got very much comprehended deshielded signals at δ_H 4.5-5, which demonstrated the region of κ and ι monomer of sulfated polygalactans. There absence of peaks at δ_H 5.26 indicated the absence of μ-monomers (precursor of κ-sulfated polygalactan) (Vandevelde et al. 2002). *Gracilaria opuntia* (**GO-2**) contains anomeric protons in the region between δ_H 3-4, which demonstrated that the sulfated polygalactan isolated from *G. opuntia* (**GO-2**) contains oligomeric building subunits, such as xylose and anhydro galactose besides κ and ι-type of monomeric units. Weak proton signals at δ_H 2-2.5 for *K. alvarezii* (**KA-2**) were relegated because of the acetyl protons. These outcomes have been supported by earlier studies (Chiovitti et al. 1998). Recognizable –*O*-alkyl signals (ideally -OCH_3) in the ^{1}H-NMR spectrum of galactan derivative from *G. opuntia* (**GO-2**) and *K. alvarezii* (**KA-2**) at δ_H 3.4 obviously revealed the region of more conspicuous number of alkoxy substitutions in the sulfated polygactans from the red macroalgae. The ^{13}C NMR spectrum of polygalactans sowed signals with specific multiplicities, which suggested the positional differences of 1→3 and 1→4 linked residues in the sulfation patterns. The anomeric region of ^{13}C-NMR exhibited the characteristic signals, and were relegated taking into account the data reported in the literature (Cases et al. 1995). Despite the normal sulfated polygalactan rehashing units, the samples were found to contain some minor constituents that were as often as possible experienced in carragenophytes. A small amount of 3-linked 6-*O*-methyl-D-galactose residues was found in the κ-sulfated polygalactan from *K. alvarezii* (**KA-2**) as additionally supported by past studies (Bellion et al. 1983). Pyruvic acid is a typical segment of numerous complex sulfated polygalactans. It outlines a cyclic acetal at positions C-4 and C-6 of the 3-linked galactose residues. The pyruvic acid ketals might likewise be experienced in the ^{1}H-NMR spectra of the polysaccharides in the present study as evident by the methyl proton resonances at δ_H 1.45. These outcomes have been supported by earlier studies (Chiovitti et al. 1998) .The anomeric region of ^{13}C-NMR exhibited the characteristic signals, and were assigned based on the literature data (Vandevelde et al. 2002). The ^{13}C-NMR signals at δ_C 58.91 and δ_C 65.25 were suggested as the –CH_2-groups on the C-6 of the 3-linked galactopyranosyl-4-sulfate moiety. In addition the

frail proton signals at δ_C 29.18 and δ_C 23.34 and carbon signals at δ_C 174-178 were related to the methyl and carboxyl carbons of the pyruvated galactopyranosyl residues. The ^{13}C-NMR chemical shift values in the present study were in accordance with the chemicals shifts reported for the basic sulfated polygalactan structure (Vandevelde et al. 2002). Based on the detailed NMR experiments the sulfated galactopyran motif of *G. opuntia* (**GO-2**) was designated as →3)-4-*O*-sulfonato-(6-*O*-acetyl)-β-D-galactopyranosyl-(1→4)-3, 6-anhydro-(2-*O*-sulfonato)-α-D-galactopyranosyl-(1→3)-4-*O*-sulfonato-(6-*O*-acetyl)-β-D-xylosyl-(1→3)-4-*O*-sulfonato-(6-*O*-acetyl)-β-D-galactopyranosyl-(1→4)-3, 6-anhydro-(2-*O*-sulfonato)-α-D- galactopyranan, whilst the one from *K. alvarezii* was demonstrated to be →4)-4-*O*-sulfonato-(2-*O*-methyl)-β-Dgalactopyranosyl-(1→4)-3, 6-anhydro-(2-*O*-methyl)-α-D-galactopyranan (Fig. 5.6).

5.3.3. Structural Characterization of Polysaccharide Fractions (KA-3$_A$ and GO-3$_A$) from Marine Macroalgae

NMR spectroscopy was used for the structural interpretation of polysaccharides (Bilan et al. 2004), whereas the pharmacological potential of this macropolymeric molecules were related with their structural parameters, such as series disposal of sugar units, branching arrangement, and orientation of functional groups (Rinaudo 2001). The HPLC profile of monosaccharide composition of polysaccharides revealed that they were mainly composed of galactose residues derived from the red marine macroalgae *K. alvarezii* (**KA-3**) and *G. opuntia* (**GO-3**) (Fig. 5.24).

5.3.3.1. Spectral Analysis of 1, 3-*O*-diacetyl-2, 5, 6-trihydroxyl-β-D-galactose-4-sulfate (KA-3$_A$)

White amorphous powder; HPLC R_t (H_2O: MeOH, 2:3 v/v): 7.21 min; TLC (15 mm Si gel GF_{254} *n*-hexane: EtOAc, 7:3 v/v); R_f: 0.82; UV (EtOAc) λ_{max} (log ε): 387 nm (1.722); IR (KBr, ν_{max} ν = stretching, δ= bending, ρ= rocking vibrations expressed in cm^{-1}): 720.35 (C-H ρ), 797.06 (C-H δ), 1023.26 (CH_3 ν), 1256.45 (C-CO-C ν, S=O ν), 1370.83 (CH_3 ν, S=O ν), 1458.44 (C-H δ), 1712.40 (-O-C=OCH_3 ν), 2855.51 (C-H ν), 2922.32 (C-H ν), 3339.03 (-OH ν); ^{1}H (500 MHz), ^{13}C-NMR (125 MHz) and 2D

NMR data (Table 5.1, Fig. 5.8 to 5.15); HR (EI) MS *m/z* calcd for $C_{10}H_{17}O_{11}S$ 345.0492; measured 345.0496 $[M]^+$ (Fig. 5.25).

1, 3-*O*-Diacetyl-2, 5, 6-trihydroxyl-β-D-galactose-4-sulfate was obtained as a white amorphous powder by methylation reaction of the polysaccharide fraction derived from *K. alvarezii* (**KA-3$_A$**). The spectrum displayed characteristic resonance of signals from ring protons between δ_H 4.01 {H-1/C-1 (δ_C 65.33)} and δ_H 5.08 {H-5/C-5 (δ_C 72.40)}. The ^1H–^1H COSY correlation between δ_H 4.24 (H-4)/δ_H 5.07 (H-3); δ_H 4.01 (H-6)/δ_H 5.08 (H-5) and strong HMBCs between δ_H 4.24 (H-4)/δ_C 59.90 (C-2)/δ_C 66.03 (H-3)/δ_C 72.40 (C-5) supported the backbone framework of the ring system. The proton NMR accompanied with carbon NMR documented the existence of anomeric carbon appeared at δ_C 65.33 (C-1). The very high intensity two sharp singlet protons in the NMR spectrum {δ_H 2.20 (H-1"^{1}) and δ_H 2.13 (H-3"^{1})} were attributed to the acetyl group substitution in the 1, 3-*O*-diacetyl-2, 5, 6-tri hydroxyl-β-D-galactose-4-sulfate (**KA-3$_A$**) residues. The strong HMBC correlations between δ_H 5.07 (H-1)/δ_C 167.7 (C-3"); δ_H 2.13 (H-3"^{1})/δ_C 167.7 (C-3"); δ_H 4.01 (H-1)/δ_C 167.02 (C-1"); δ_H 2.20 (H-1"^{1})/δ_C 167.02 (C-1") supported the above assignments.

It was inferred that the 3, 6-anhydro-galactose moiety were degraded during this particular reaction, and that supported the absence of IR signals at 845, 830 and 805 cm^{-1} (Mollet et al. 1998; Murano 1995; Murano et al. 1996). The characteristic absorption bands at 3339, 2922, 2855, 1712, 1458, 1370, 1256, 1177, 1023, 910, 797, 720 cm^{-1} in the FTIR spectrum of *K. alvarezii* (**KA-3$_A$**) recorded the existence of galactose residue. The absorption band of S=O vibration appeared at 1370 cm^{-1} in the FTIR spectrum indicated the presence of sulfate groups (Melo et al. 2002; Fournet et al. 1997). The presence of –OH group in the IR spectroscopy (3339 cm^{-1}) considered that all the OH groups did not undergo the methylation, reduction and acetylation reactions. The ^{13}C resonances at δ_C 167.02, 167.7, 38.05 and 45.15 appropriately indicated the presence of acetyl carbons associated with carboxyl group of the galactose unit. Strong bending vibrations of the carbonyl group associated with acetyl group were found near 1712 cm^{-1}, which was further corroborated by the presence of ^{13}C NMR peak at δ_C 167.02 (C-1") and 167.7 (C-3"). The primary -CH_2- protons were assigned at δ_H 4.01 (H-6, d, *J*=6.65 Hz, 2H) showing HSQC correlation with δ_C 71.8 (C-6). Characteristic OSO_3^- group in the moiety of 1, 3-*O*-diacetyl-2, 5, 6-trihydroxyl-β-D-galactose-4-sulfate (**KA-3$_A$**) were found to be situated at C-4 of the ring system, and these assignments was supported by the signals at δ_H 4.24 (H-4) showing HSQC cross-peak

with δ_C 65.56 (C-4). The 1, 3-*O*-diacetyl-2, 5, 6-trihydroxyl-β-D-galactose-4-sulfate were mainly unsubstituted with methoxy because the presence of -OH group were present in the primary alcoholic position (δ_H 3.70; H-6''). In addition, the unsubstituted -OH groups were recorded at δ_H 3.70 (H-6'') and δ_H 3.88 (H-2''). The mass spectrum showed the peak at *m/z* 345 (molecular ion peak) (HR EI MS *m/z* calcd. for $C_{10}H_{17}O_{11}S^-$ 345.0492, measured at 345.0496 $[M]^+$). The presence of the strong NOEs between δ_H 5.08 (H-5) with δ_H 4.01 (H-1 *J*=6.65 Hz; H-6 *J*=6.65 Hz)/δ_H 2.20 (H-1''^{1}) showed axial-equatorial orientation of these proton pairs in the chair conformation of 1, 3-*O*-diacetyl-2, 5, 6-trihydroxyl-β-D-galactose-4-sulfate residue. Similarly, strong NOEs were observed between δ_H 5.08 (H-5) with δ_H 4.24 (H-4, *J*=6.31 Hz) that indicated the axial-axial orientation of these protons in the same polymeric backbone. In addition, the axial proton at δ_H 4.01 (H-1, H-6) displayed NOE correlation with the equatorial proton at δ_H 2.13 (H-3''^{1}) having axial-equatorial interaction between these protons.

5.3.3.2. Spectral Analysis of 1, 3, 5-*O*-triacetyl-4-hydroxyl-6-*O*-methyl-D-galactose-2-sulfate (GO- 3_A)

White amorphous powder; HPLC R_t (H_2O: MeOH, 2:3 v/v): 6.76 min; TLC (15 mm Si gel GF_{254} *n*-hexane: EtOAc, 7:3 v/v); R_f: 0.76; UV (EtOAc) λ_{max} (log ε): 387 nm (1.608); IR (KBr, ν_{max} in cm^{-1}): 1045.98 (CH_3 ν), 1201.04 (C-CO-C ν), 1416.30 (C-H *δ*), 1689.30 (-O-C=OCH_3 ν), 34445.36 (-OH ν); ^{1}H (500 MHz), ^{13}C-NMR (125 MHz) and 2D NMR data (Table 5.2; Fig. 5.16 to 5.25); HR (EI) MS *m/z* calcd for $C_{13}H_{21}O_{12}S$ 401.0754; measured 401.0758 $[M]^+$ (Fig. 5.25).

1, 3, 5-*O*-Triacetyl-4-hydroxyl-6-*O*-methyl-D-galactose-2-sulfate **(GO-3_A)** was isolated as white powder by repeated chromatography over adsorbent silica gel. The spectrum displayed characteristic resonance of signals from ring protons between δ_H 3.65 {(H-5/C-5 (δ_C 69.89)} and δ_H 3.81{H-1/C-1 (δ_C 81.83)}. The ^{1}H–^{1}H COSY correlation between δ_H 3.81 (H-1)/δ_H 3.73 (H-4)/δ_H 3.38 (H-3)/δ_H 3.65 (H-2) and intense HMBCs between δ_H 3.38 (H-3)/δ_C 81.83 (C-1); δ_H 3.65 (H-5)/δ_C 83.51 (C-6); δ_H 3.81 (H-1)/δ_C 62.28 (C-3)/δ_C 69.88 (C-2); δ_H 3.73 (H-4)/δ_C 62.28 (C-3) were recorded. The high intensity sharp singlet protons in the NMR spectrum at δ_H 2.17 (H-1''^{1}), δ_H 2.62 (H-3''^{1}), and δ_H 2.02 (H-5''^{1}) attributed to the acetyl group substitution in

the 1, 3, 5-*O*-triacetyl-4-hydroxyl-6-*O*-methyl-D-galactose-2-sulfate (**GO-3$_A$**) residues. The strong HMBC correlation between δ_H 3.81 (H-1)/δ_C 179.66 (C-1"); δ_H 3.65 (H-5)/δ_C 172.51 (C-5"); δ_H 2.02 (H-5"^{1})/δ_C 172.51 (C-5") supported the above assignments. NMR analysis of methylated polysaccharide from *G. opuntia* attributed the presence of acetylated and 1, 3, 5-*O*-triacetyl-4-hydroxyl-3-*O*-methyl-D-galactose-2-sulfate (**GO-3$_A$**) units. The IR spectrum inferred the presence of residual -OH group (3445 cm^{-1}) that indicated that all the hydroxyl groups did not undergo methylation reactions. The strong bending vibrations of carbonyl group associated with acetyl group were found near 1689 cm^{-1}, which further corroborated by the peak at δ_C 172.51 (C-5"), δ_C 176.07 (C-3") and δ_C 179.66 (C-1"). The primary-CH_2- protons were assigned at δ_H 3.81 {H-6 displaying HSQC with C-6 (δ_C 83.51)}. Characteristic OSO_3^- group in the moiety were present at the 2nd position of the ring system, and these attributions were inferred by the presence of δ_H 3.65 (H-2; δ_C 69.88 (C-2)) in the HSQC spectrum. The mass spectrum showed the molecular ion peak peak at *m/z* 401 (HR EI MS *m/z* calcd. for $C_{13}H_{21}O_{12}S$ 401.0754, measured at 401.0758 $[M]^+$). The strong NOE correlations between δ_H 2.17 (H-1"^{1}) with δ_H 3.38 (H-3 *J*=6.50 Hz) and δ_H 3.65 (H-5, H-2) showed axial-axial and axial-equatorial orientation of these proton pairs, respectively in the chair structure of 1, 3, 5-*O*-triacetyl-4-hydroxyl-3-*O*-methyl-D-galactose-2-sulfate (**GO-3$_A$**) residue. Similarly, intense NOEs between δ_H 2.62 (H-3"^{1}) with δ_H 3.67 (H-5, H-2) and δ_H 3.49 (H-6") indicated the axial–axial orientation between the protons. In addition, the axial proton at δ_H 3.65 (H-2, H-5) displayed NOE correlation with the equatorial proton at δ_H 2.85 (H-4") having axial-equatorial interaction between the protons. The presence of the strong NOEs correlation between δ_H 3.65 (H-5, H-2), δ_H 3.73 (H-4, *J*=8.52 Hz), and δ_H 3.38 (H-3 *J*=6.50 Hz) inferred their axial-axial orientation. The present study characterized the major polysaccharide fractions obtained from the red marine macroalgae *K. alvarezii* and *G. opuntia* as 1, 3-*O*-diacetyl-2, 5, 6-trihydroxyl-β-D-galactose-4-sulfate (**KA-3$_A$**) and 1, 3, 5-*O*-triacetyl-4-hydroxyl-6-*O*-methyl-D-galactose-2-sulfate (**GO-3$_A$**), respectively.

Table 5.1. NMR spectroscopic data of **KA-3$_A$** in $CDCl_3$[a]

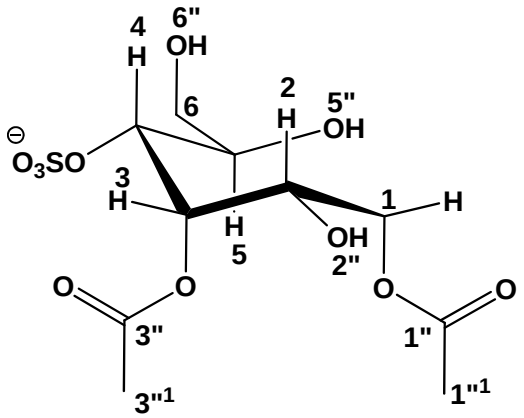

C. No	^{13}C (δ)	^{1}H-NMR[b] (int., mult., *J* in Hz)	^{1}H-^{1}H COSY	HMBC
1	65.33	4.01 (d, *J*=6.65 Hz, 2H)		C-1"
2	59.90	4.26 (m, 1H)		-
3	66.03	5.07 (t, *J*=6.89 Hz, 1H)	4-H	C-3"
4	65.56	4.24 (t, *J*=6.31 Hz, 1H)	3-H	C-5, C-3, C-2
5	72.40	5.08 (m, 1H)	6-H	-
6	71.8	4.01 (d, *J*=6.65 Hz, 2H)	5-H	-
1"	167.02	-	-	-
1"^{1}	38.05	2.20 (s, 3H)	-	C-1"
2"	-	3.88 (s, 1H)	-	
3"	167.7	-	-	-
3"^{1}	45.15	2.13 (s, 3H)	-	C-3"
5"	-	3.70 (s, 1H)		
6"	-	3.70 (s, 1H)	-	-

[a] NMR spectra recorded using Bruker AVANCE III 500 MHz (AV 500) spectrometers.

[b] Values in ppm, multiplicity and coupling constants (*J*=Hz) are indicated in parentheses. Assignments were made with the aid of the ^{1}H-^{1}H COSY, HSQC, HMBC and NOESY experiments.

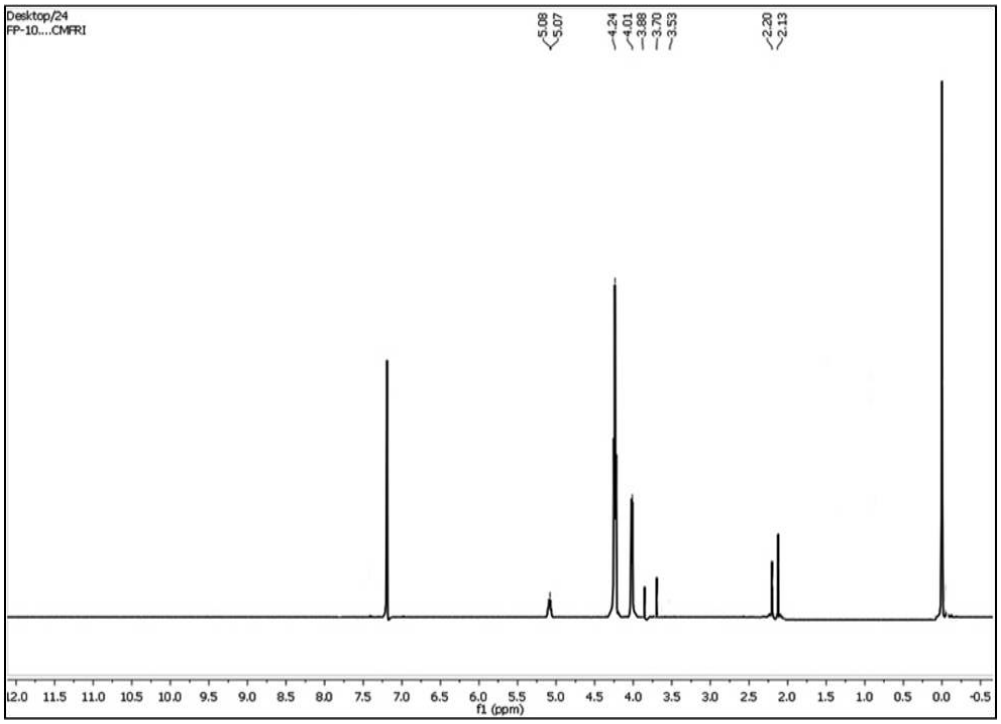

Figure 5.8. Figure showing the ^{1}H NMR spectrum of **KA-3$_A$**

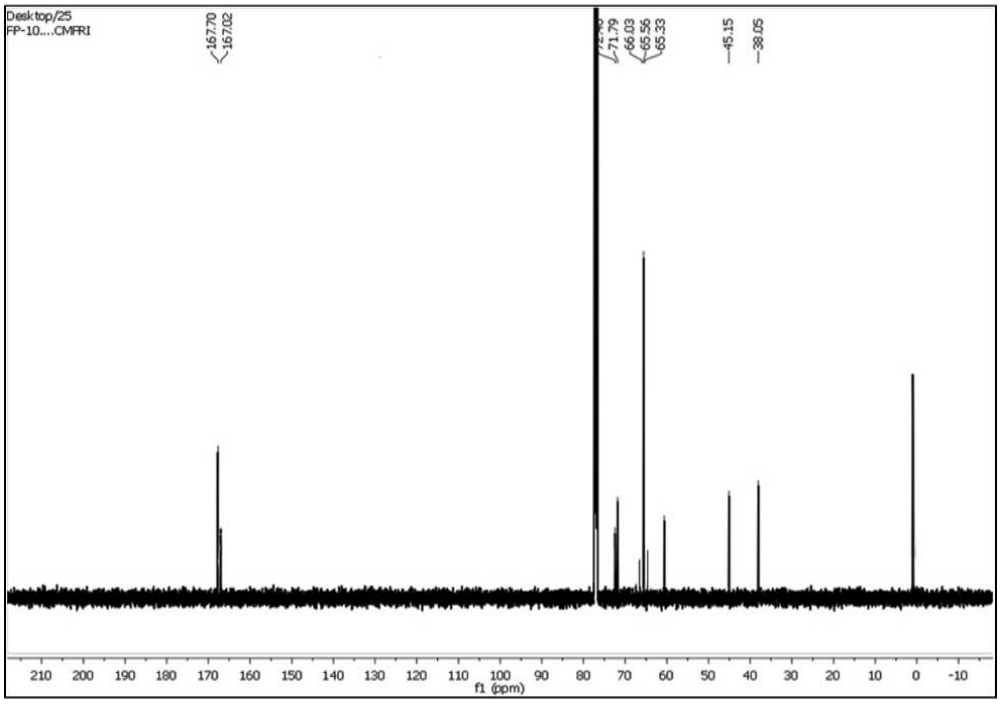

Figure 5.9. Figure showing the ^{13}C NMR spectrum of **KA-3$_A$**

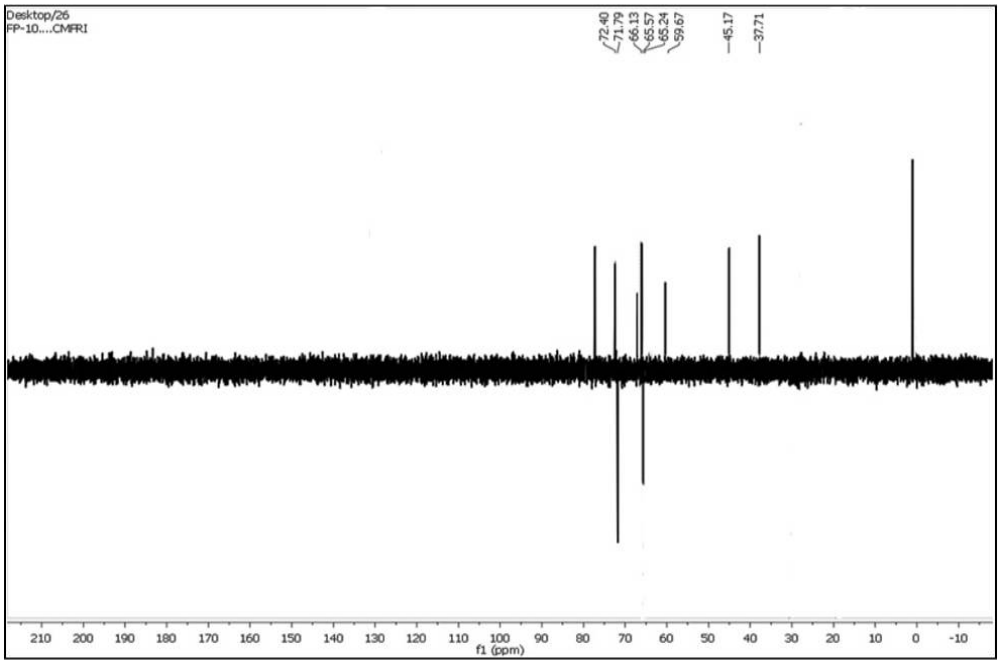

Figure 5.10. Figure showing the DEPT spectrum of **KA-3$_A$**

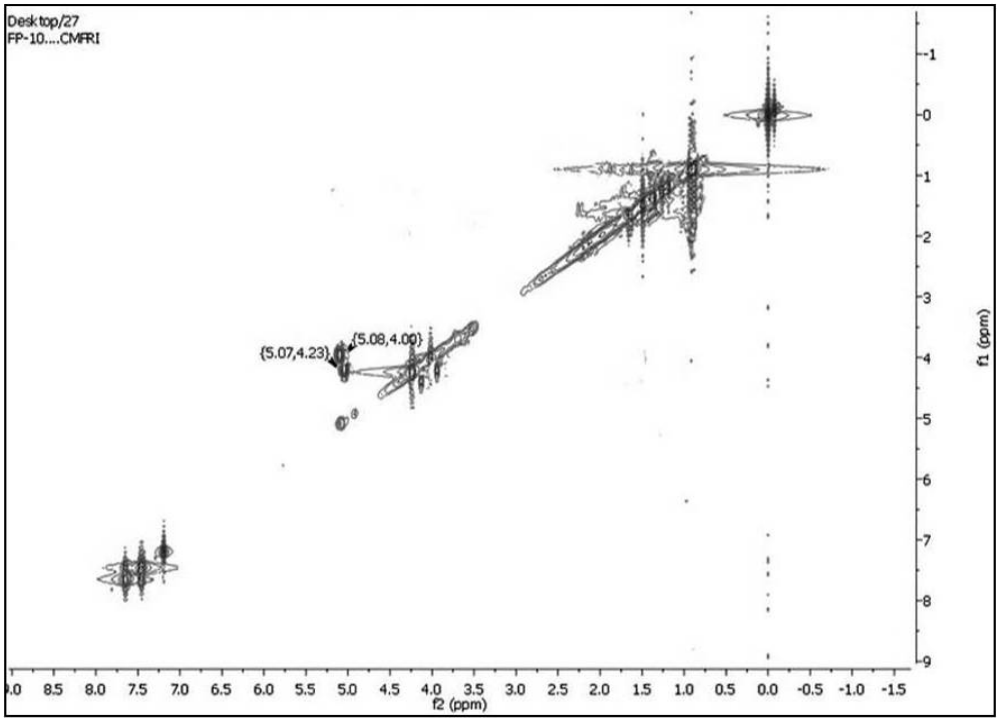

Figure 5.11. Figure showing the ^{1}H-^{1}H COSY spectrum of **KA-3$_A$**

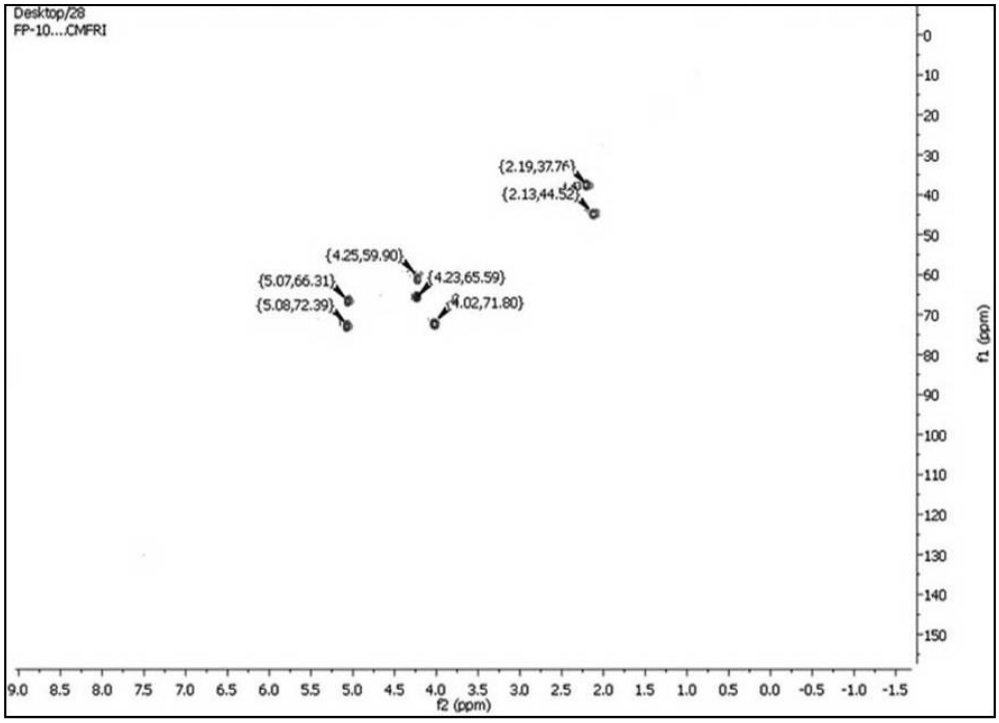

Figure 5.12. Figure showing the HSQC spectrum of **KA-3$_A$**

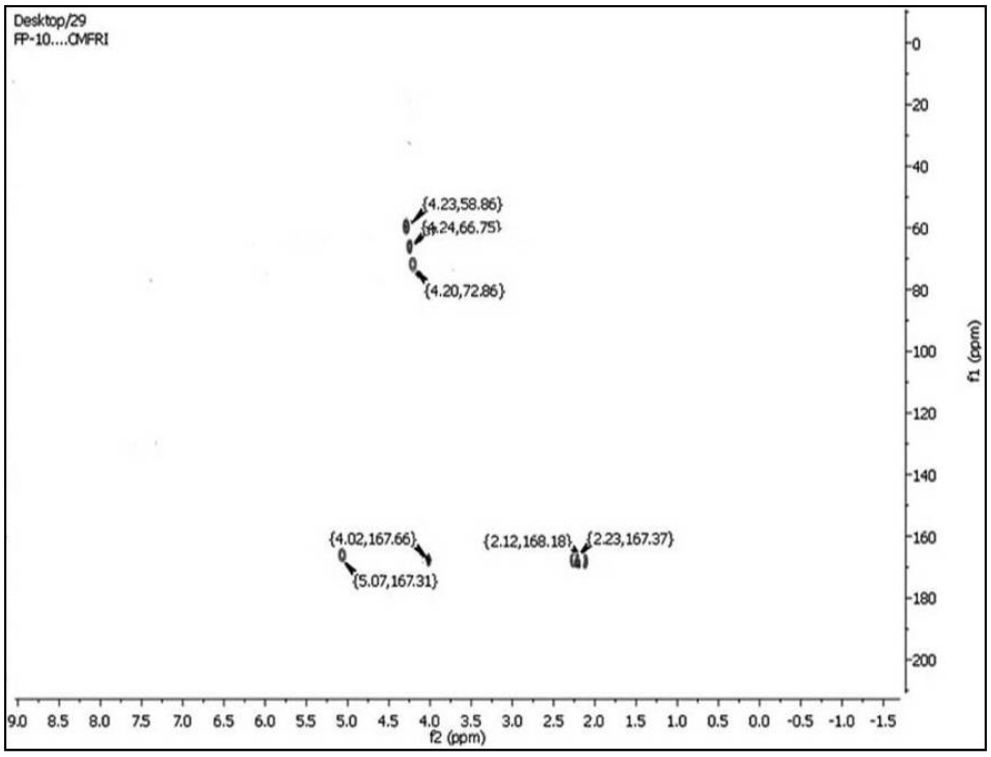

Figure 5.13. Figure showing the HMBC spectrum of **KA-3$_A$**

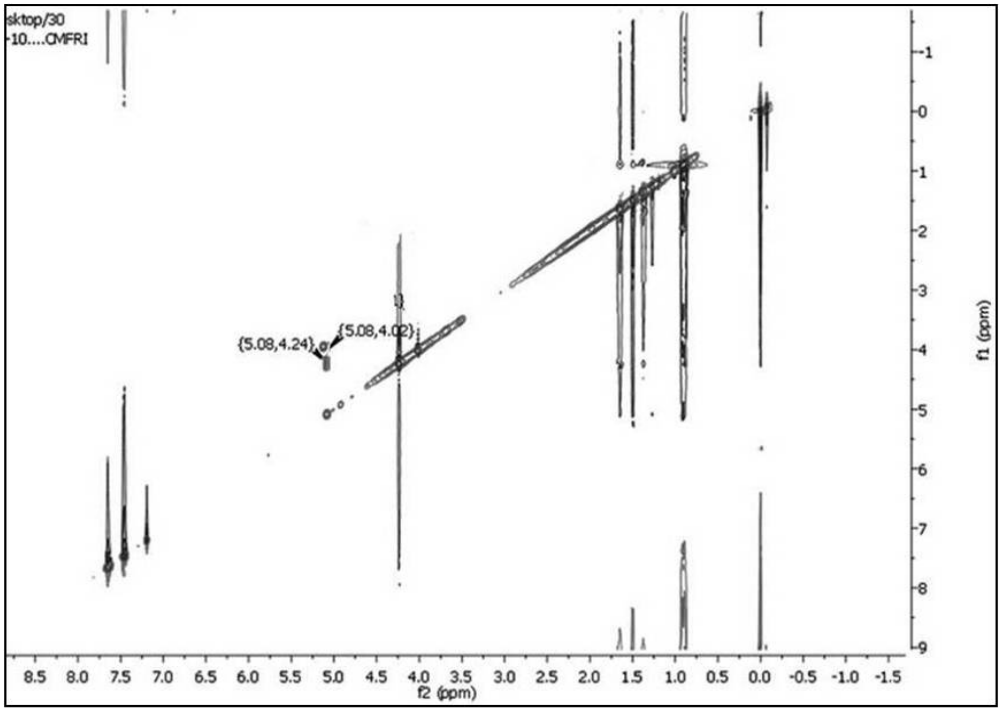

Figure 5.14. Figure showing the NOESY spectrum of **KA-3$_A$**

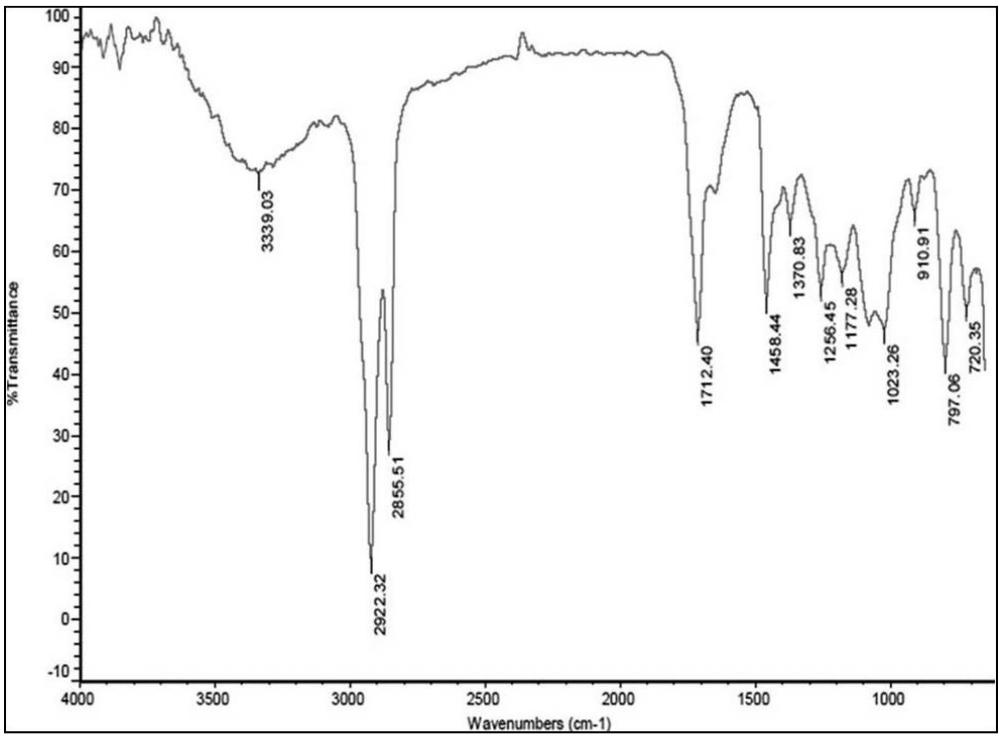

Figure 5.15. Figure showing the FTIR spectrum of **KA-3$_A$**

Table 5.2. NMR spectroscopic data of **GO-3$_A$** in $CDCl_3$[a]

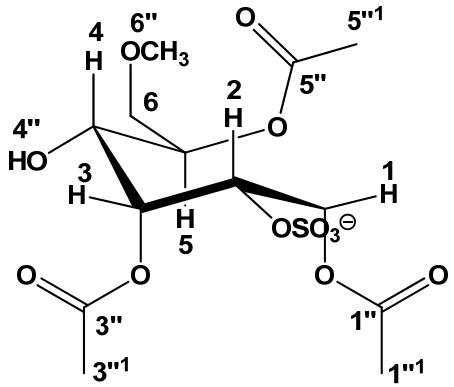

C. No	^{13}C (δ)	^{1}H-NMR[b] (int., mult., *J* in Hz)	^{1}H-^{1}H COSY	HMBC
1	81.83	3.81 (d, *J*=6.87 Hz, 2H)	2-H	C-3, C-2, C-1"
2	69.88	3.65 (m, 1H)	1-H, 3-H	
3	62.28	3.38 (t, *J*=6.50 Hz, 1H)	4-H, 2-H	C-1
4	74.7	3.73 (t, *J*=8.52 Hz, 1H)	3-H	C-3
5	69.89	3.65 (m, 1H)	-	C-6, C-5"
6	83.51	3.81 (d, *J*=6.87 Hz, 2H)	-	
1"	179.66	-	-	-
1"^{1}	30.93	2.17 (s, 3H)	-	-
3"	176.07	-	-	-
3"^{1}	40.98	2.62 (s, 3H)	-	-
4"	-	3.43 (s, 1H)	-	-
6"	59.84	3.49 (s, 3H)	-	-
5"	172.51			
5"^{1}	22.61	2.02 (s, 3H)		C-5"

[a]The NMR spectra were recorded using Bruker AVANCE III 500 MHz (AV 500) spectrometers.

[b] Values in ppm, multiplicity and coupling constants (*J*=Hz) are indicated in parentheses. Assignments were made with the aid of the ^{1}H-^{1}H COSY, HSQC, HMBC and NOESY experiments.

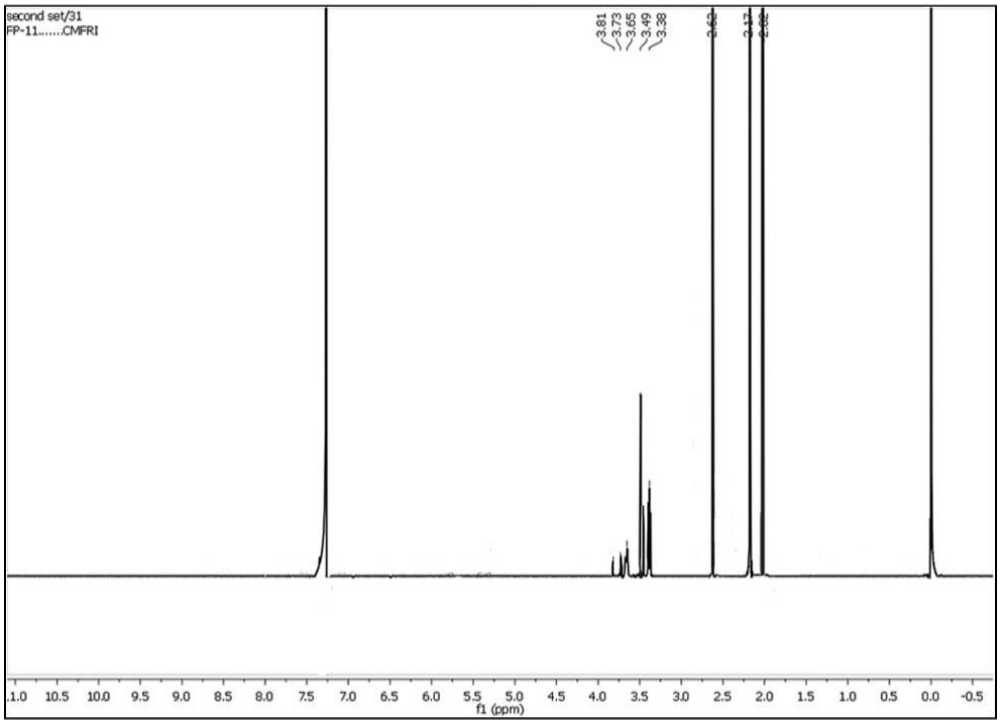

Figure 5.16. Figure showing the ^{1}H NMR spectrum of **GO-3$_A$**

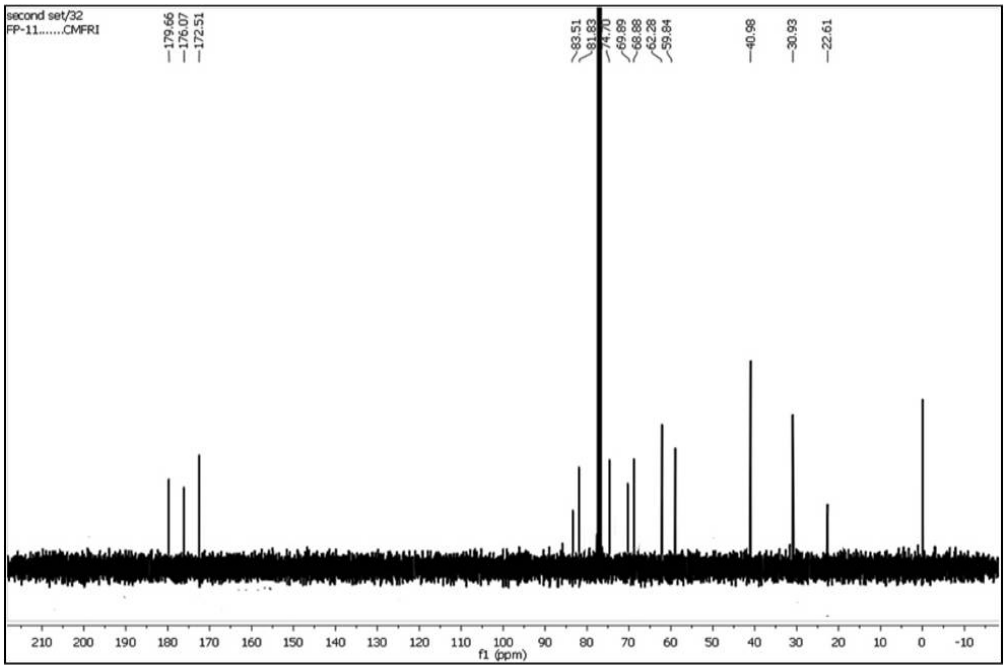

Figure 5.17. Figure showing the ^{13}C NMR spectrum of **GO-3$_A$**

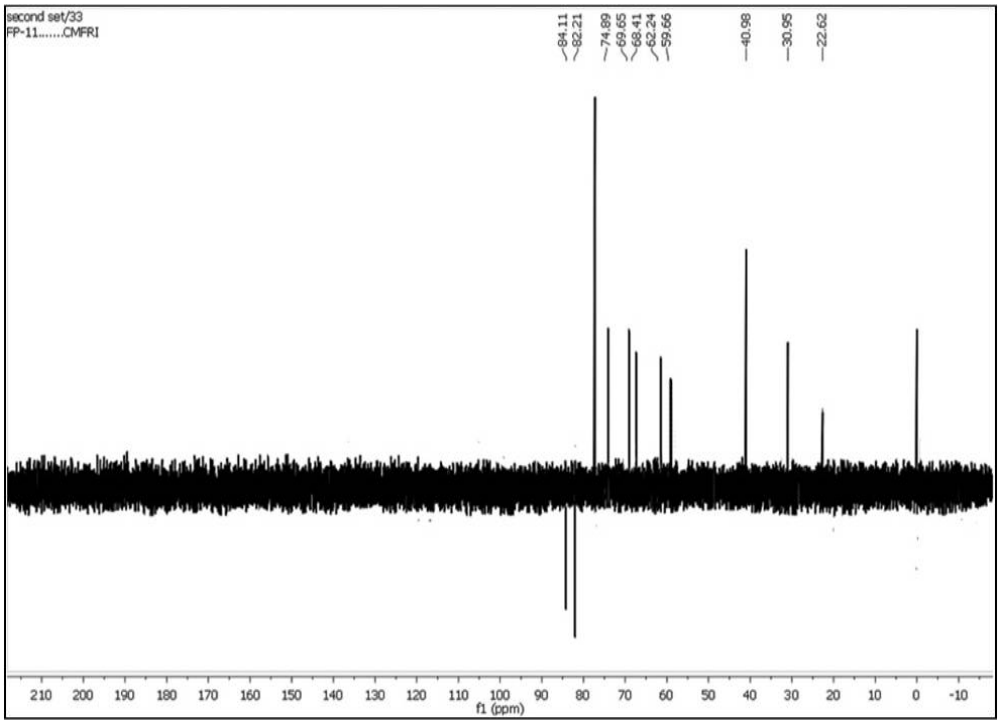

Figure 5.18. Figure showing the DEPT spectrum of **GO-3$_A$**

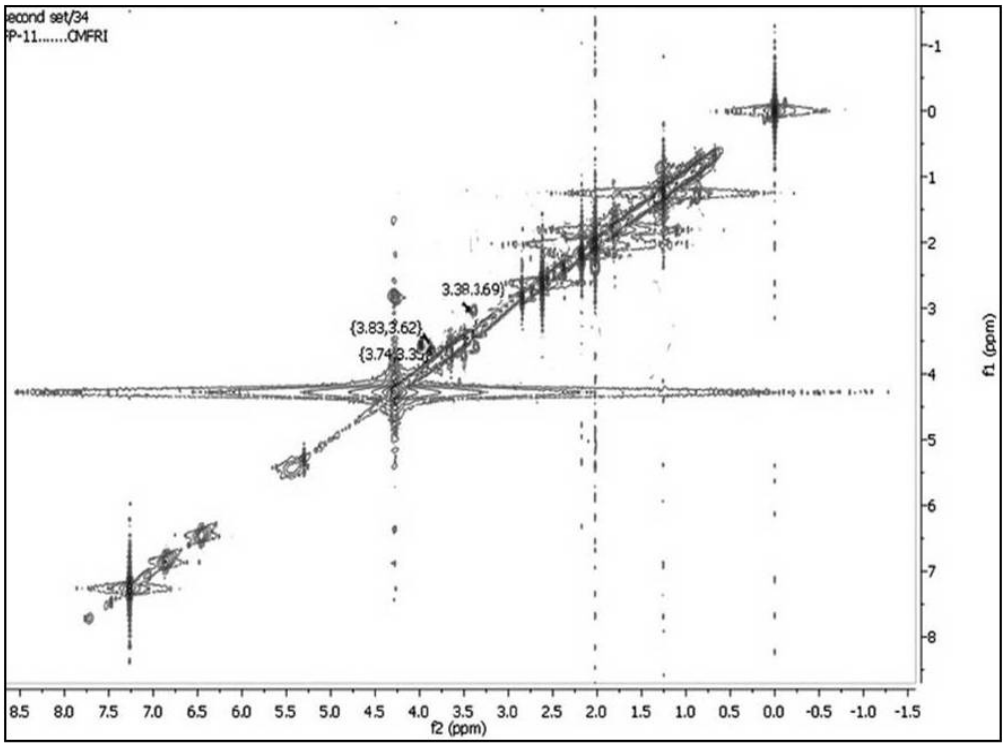

Figure 5.19. Figure showing the ^{1}H-^{1}H COSY spectrum of **GO-3$_A$**

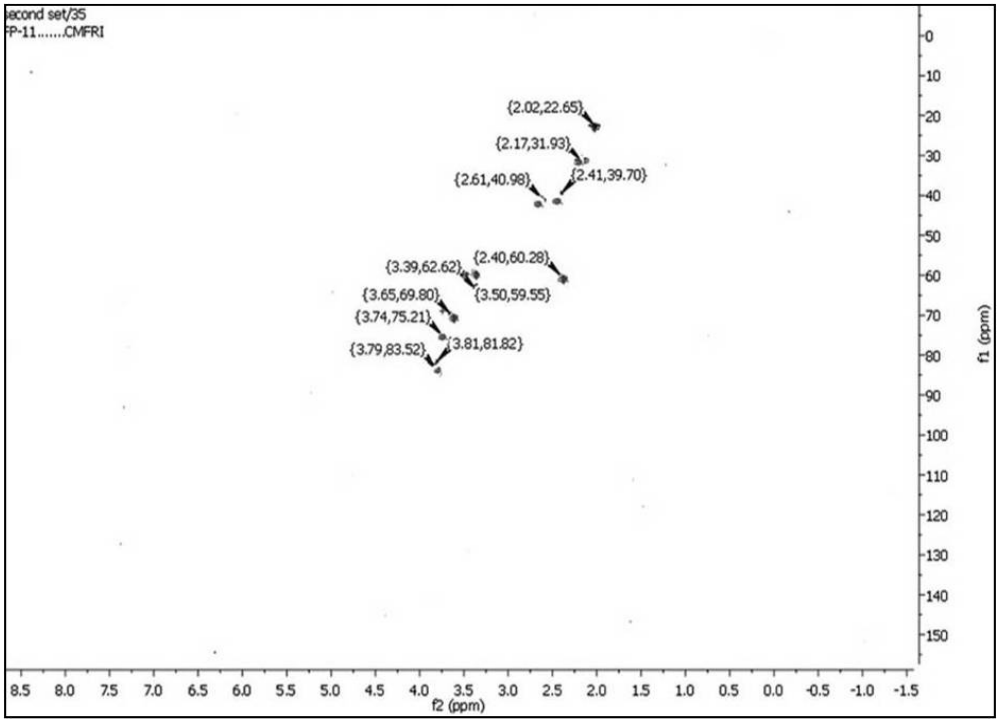

Figure 5.20. Figure showing the HSQC spectrum of **GO-3$_A$**

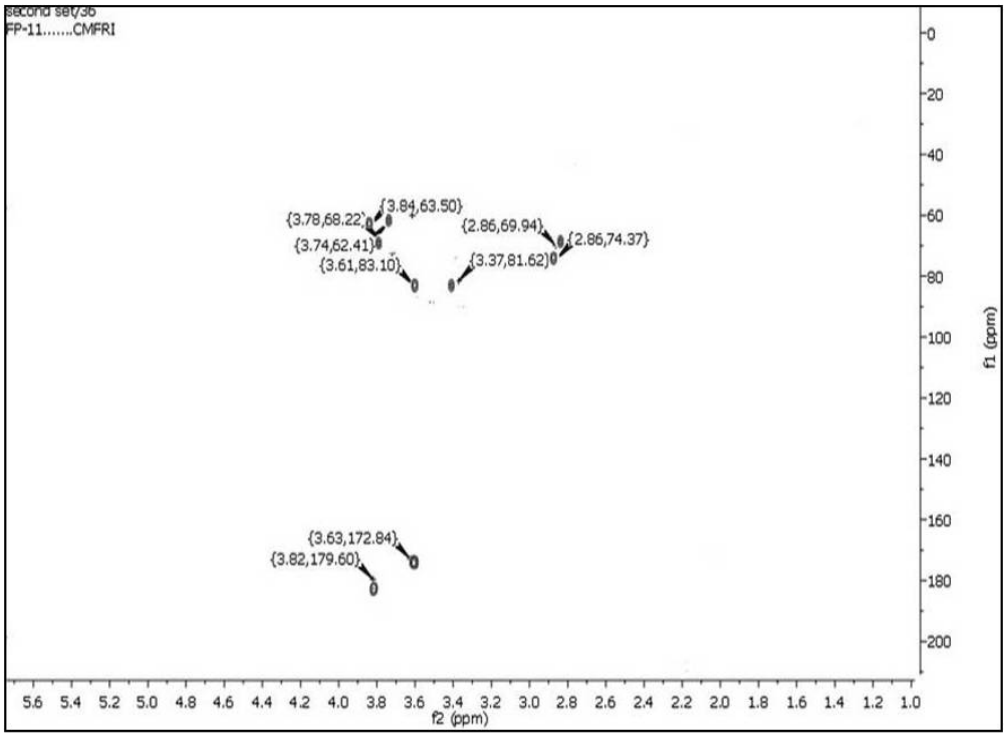

Figure 5.21. Figure showing the HMBC spectrum of **GO-3$_A$**

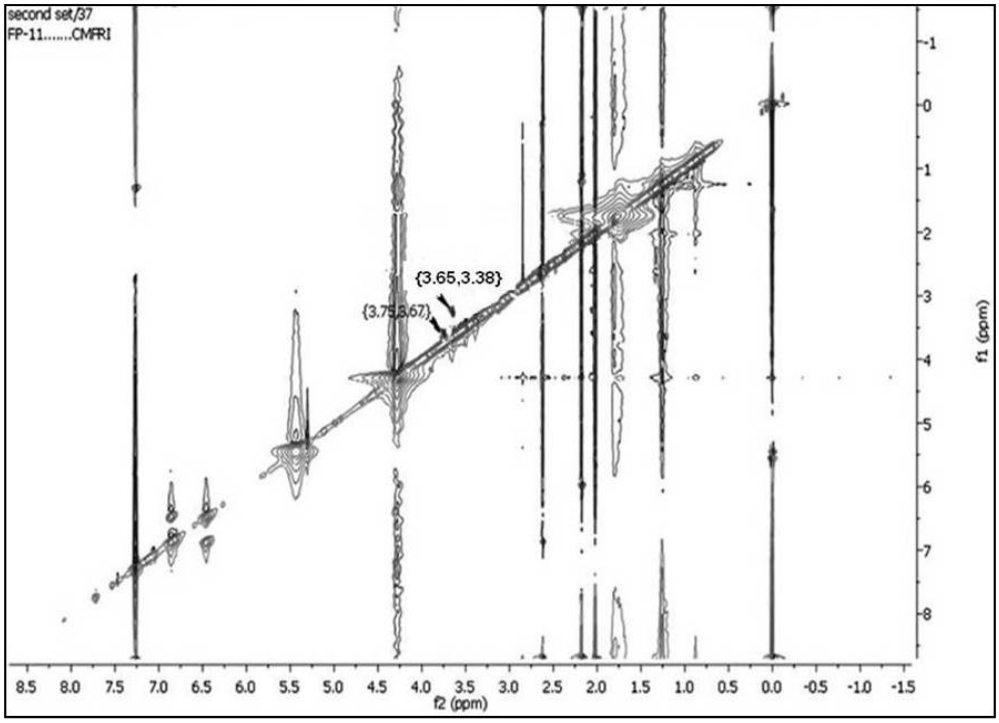

Figure 5.22. Figure showing the NOESY spectrum of **GO-3$_A$**

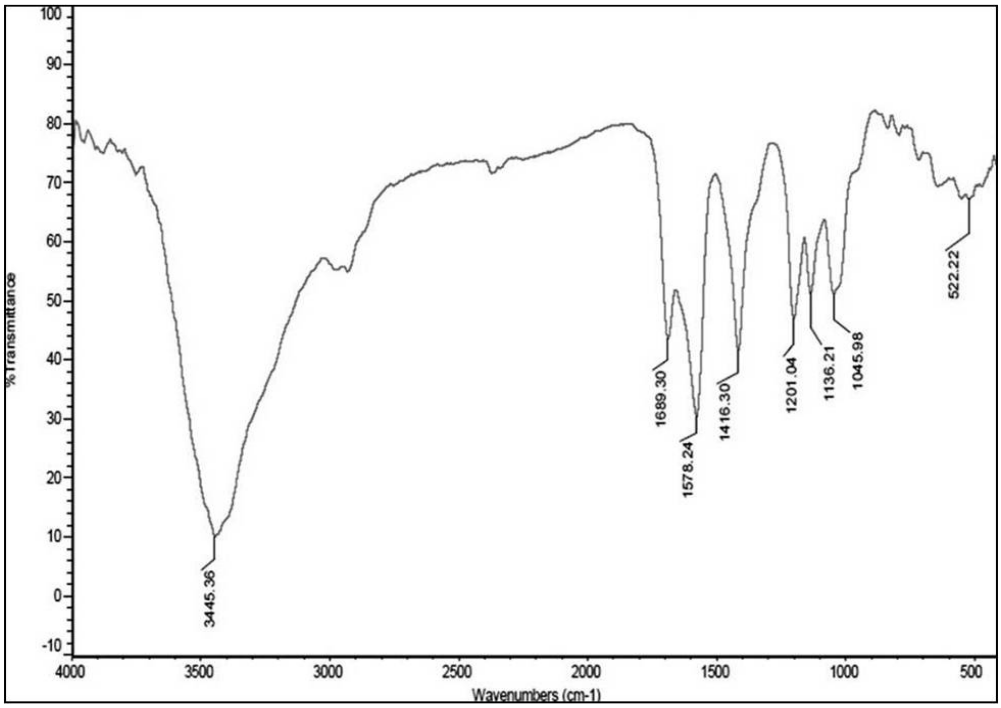

Figure 5.23. Figure showing the FTIR spectrum of **GO-3$_A$**

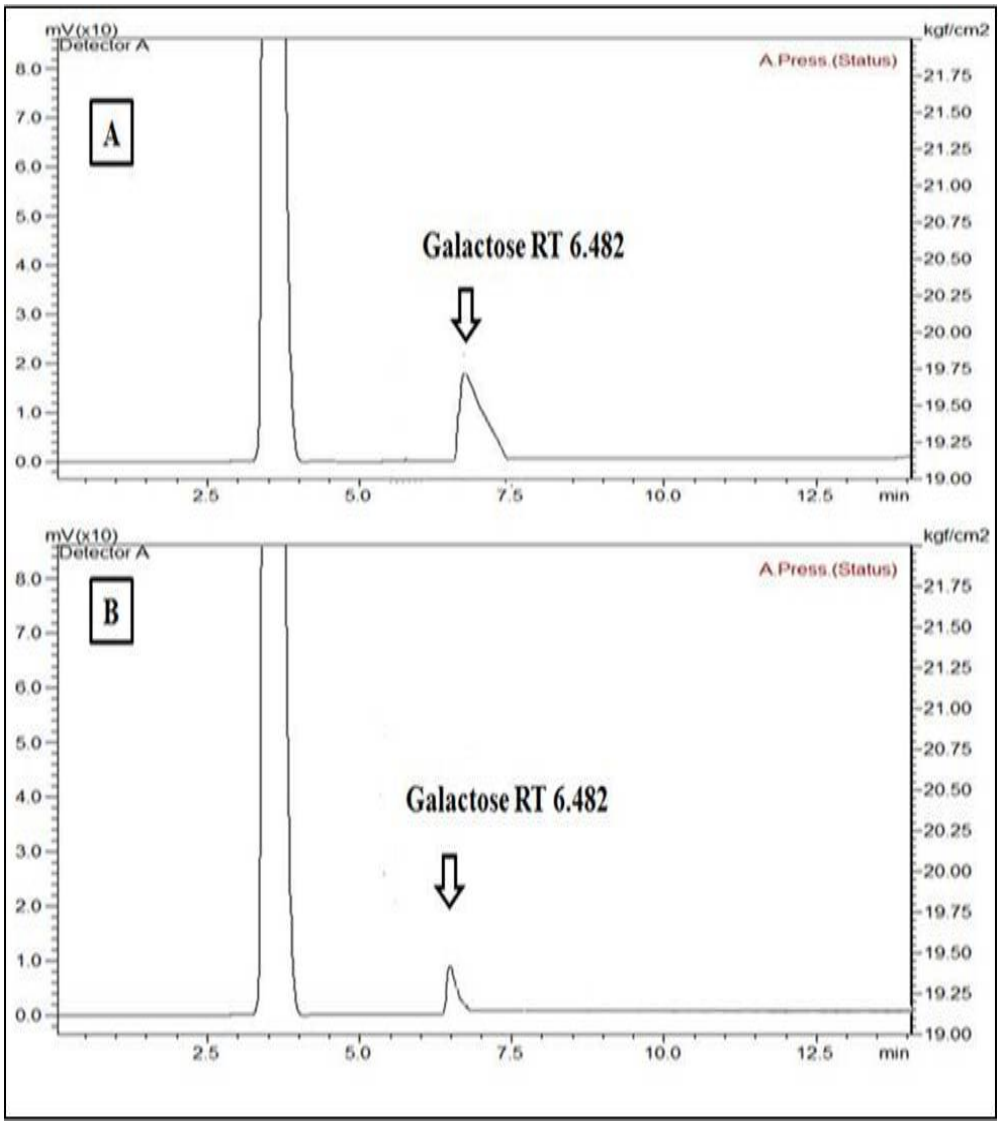

Figure 5.24. Figure showing Monosaccharide composition analysis of **KA-3$_A$** and **GO-3$_A$**

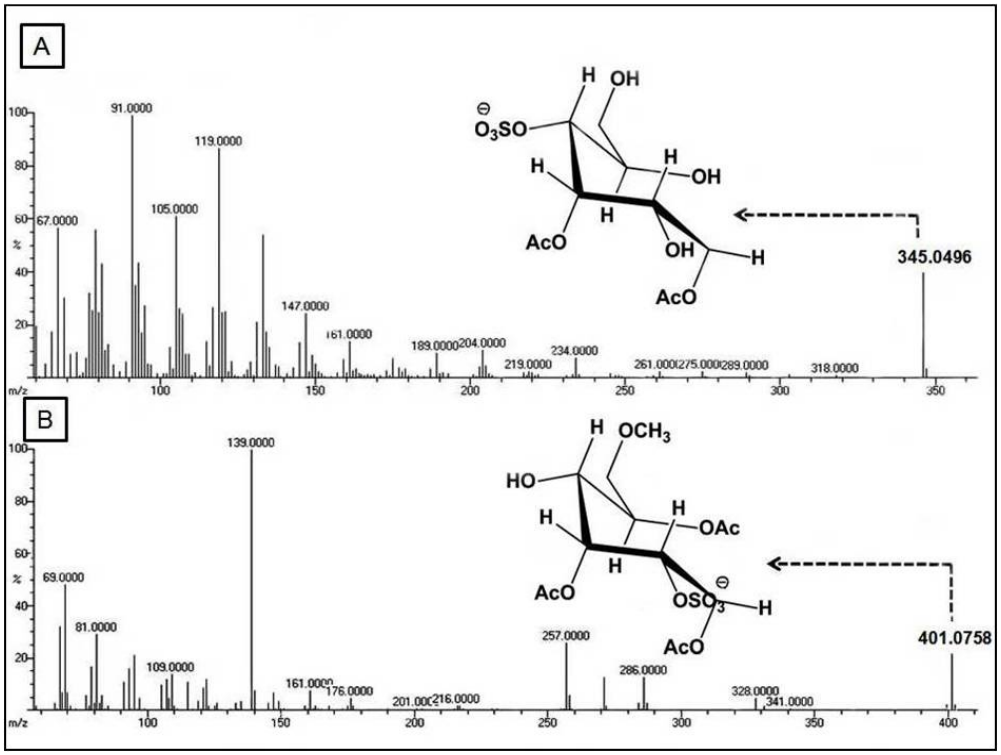

Figure 5.25. Mass spectrum of (**A**) from *K. alvarezii* (**KA-3$_A$**) (**B**) and *G. opuntia* (**GO-3$_A$**)

5.3.4. Pharmacological Potential of Various Polysaccharides from *K. alvarezii and G. opuntia*

The chemical analysis showed that the sulfated polygalactans derived from *K. alvarezii* (**KA-1**) was made essentially with carbohydrates (47 %) and showed higher sulfate content (> 70 %) than that recorded in *G. opuntia* (**GO-1**) (< 40 %). The aggregate content of carbohydrate in the latter was found to be 41.5 %, which was shown to be lesser than that in *K. alvarezii* (**KA-1**, Table 5.3). The uronic acid content in the sulfated polygalactan acquired from *K. alvarezii* (**KA-1**) by $CaCl_2$ precipitation was found to be significantly greater (7.2 %) than those in *G. opuntia* (**GO-1**) (6.6 %) ($P < 0.05$). There were other reports, which demonstrated that sulfated polysaccharides have been the major polysaccharides present in the marine algae (Ohno et al. 1994). The sulfated polygalactan from *G. opuntia* (**GO-1**) (> 400 mg of GAE/g) was found to possess greater content of total phenolics than that isolated from *K. alvarezii* (**KA-1**) (< 300 mg of GAE/g) (Table 5.3). ABTS scavenging activity of galactan separated from

K. alvarezii (**KA-1**) was greater (IC_{50} 0.72 mg/mL) than that from *G. opuntia* (**GO-1**) (IC_{50} 0.86 mg/mL) and commercially available antioxidant (gallic acid IC_{50} 0.92 mg/mL). The DPPH radical scavenging activity of sulfated polygalactan fraction derived from *K. alvarezii* (**KA-1**) was found to be greater (IC_{50} 0.97 mg/mL) than that in *G. opuntia* (**GO-1**, IC_{50} 1.20 mg/mL). The sulfated polygalactan from *K. alvarezii* displayed significantly greater Fe^{2+} chelating abilities (**KA-1**, IC_{50} 0.46 mg/mL) than that derived from *G. opuntia* (**GO-1**, IC_{50} 1.30 mg/mL). On account of lipid peroxidation inhibition assay, the sulfated polygalactan from the *G. opuntia* displayed greater lipid peroxidation inhibition activity (**GO-1**, 320.52 mM MDAEQ/kg) than that isolated from *K. alvarezii* (**KA-1**, 232.70 mM MDAEQ/kg). TBARS activity was denoted as mM of malondialdehyde equivalent compounds formed per kg sample (MDAEQ/kg sample) related to the control (lyophilised green mussel) leads to maximum lipid peroxidation on the same assay conditions. The capability of the polysaccharide fractions to capture lipid peroxidation was estimated by thiobarbituric acid reactive species (TBARS) assay. The guiding principles to determine the antioxidative activity of the sulfated polygalactans from the marine macroalgae could be attributed by utilizing different descriptor variables *viz.*, electronic, hydrophobic and steric parameters (Cinq-Mars et al. 2008). The electronic descriptors *viz.*, molecular polar surface area based on fragment contributions (aggregate topological polar surface area, tPSA), hydrophobic parameter Clog Pow to calculate *n*-octanol/water partition coefficient; steric (or bulk descriptor), molar refractivity (CMR) as computed by ChemDraw 12.0 were taken into consideration. We have considered 4-hydroxy-6-((3-hydroxy-4-methoxy-2, 6-dioxabicyclo [3.2.1] octan-8-yl) oxy)-2-(hydroxymethyl)-5-methoxytetrahydro-2*H*-pyran-3-yl sulfate moiety (designated as **KA-1**) of the galactan motif ((→4)-4-*O*-sulfonato-(2-*O*-methyl)-β-D-galactopyranosyl-(1→4)-3, 6-anhydro-(2-*O*-methyl)-α-D-galactopyranan) isolated from *K. alvarezii* for the accommodation to comprehend the atomic descriptors to adequately describe their anti-hypertensive properties. It is of note that, 2-(acetoxymethyl)-4, 5-dihydroxy-6-((3-hydroxy-4-methoxy-2, 6-dioxabicyclo [3.2.1] octan-8-yl) oxy) tetrahydro-2*H*-pyran-3-yl sulfate (designated as **GO-1**) was considered as a part of →3)-4-*O*-sulfonato-(6-*O*-acetyl)-β-D-galactopyranosyl-(1→4)-3, 6-anhydro-(2-*O*-sulfonato)-α-D-galactopyranosyl-(1→motif isolated from *G. opuntia*. The lipophilic (Clog Pow) and steric descriptors (CMR) were found to play a significant part to portray the greater antioxidative activities of sulfated galactan isolated from *K. alvarezii* **(KA-1)**. Although there were

no significant difference between the electronic descriptor (tPSA) variables (~188) in the macroalgal galactopyranan, the activity of the galactan extracted from *K. alvarezii (***KA-1)** displayed greater antioxidant activity than that obtained from *G. opuntia* **(GO-1)**, apparently due to greater steric bulk (estimated molar refractivity value, CMR = 9.10 cm^3) of **GO-1** than that exhibited by **KA-1** (CMR = 8.61 cm^3). Since MR is fundamentally a measure of the bulk of the substituent, the positive coefficient for this term indicates that molecules are contacting polar space in the enzyme (Hansch and Caldwell 1991) not the hydrophobic surface. A significant co-linearity was found to exist between CMR and Clog Pow. A positive correlation might propose an association with the polarisability of the substituents, albeit there is a little confirmation for the significance of such an effect. It is of note that unlike compound **KA-1** with 4, 6-dihydroxy-2-(hydroxymethyl)-5-methoxytetrahydro-2*H*-pyran-3-yl sulfate group, the compound **GO-1** with 2-(acetoxymethyl)-4, 5, 6-trihydroxytetrahydro-2*H*-pyran-3-yl sulfate moiety indicated more prominent lipophilic nature (Clog Pow -3.0628). The parameter Clog Pow of the compounds explained the hypothetically general computed lipophilicity of the molecule and governs the variations in activity. An increase in the lipophilicity apparently diminishes the antioxidative action of the galactans. The lipophilicity of the acetoxymethyl group was found to contribute towards reduced antioxidative property of the galactan isolated from *G. opuntia*. It was anticipated that the greater the acetyl substitution at the hydroxymethyl group of the galactan motif, lesser is the antioxidant activity. It can hence be induced that the stetric and lipophilic descriptors might essentially assume significant roles in determining the antioxidant activity. The electronic factor, such as tPSA was also found to significantly contribute towards the greater antioxidant activity of the macroalgal polygalactans.

The ACE inhibitory activities of the polygalactans from *G. opuntia* was lesser (**GO-1**, IC_{50} 0.70 µg/mL) than those separated from *K. alvarezii* (**KA-1**, IC_{50} 0.02 µg/mL) and the commercial ACE inhibitor, captopril (IC_{50} 0.05 µg/mL). The guiding principles to determine the anti-hypertensive activity of the sulfated polygalactans from the marine macroalgae was outlined by utilizing different descriptor variables *viz.*, electronic, hydrophobic and steric parameters. Despite the fact that the tPSA depicting the electronic descriptor were indistinguishable in the sulfated galactans isolated from *K. alvarezii* (**KA-1**) and *G. opuntia* (**GO-1**) the activity of the latter was lesser (IC_{50} 0.02 µg/mL) than of the previous (IC_{50} 0.70 µg/mL), evidently because of the greater steric values (CMR > 9 cm^3) of **GO-1** than that recorded in **KA-1** (CMR~ 8.6 cm^3). It

is intriguing to note that the lipophilicity of the 2-(acetoxymethyl)-4, 5, 6-trihydroxytetrahydro-2*H*-pyran-3-yl sulfate group has been double (Clog Pow 9.1058) than that of the corresponding 4, 6-dihydroxy-2-(hydroxymethyl)-5-methoxytetrahydro-*2H*-pyran-3-yl sulfate group of **KA-1** (Clog Pow 5.1021). Specifically, the tPSA of the polygalactans were recorded to be significantly greater (> 180) than the commercially available anti-hypertensive drug captopril with mercaptomethylpropanoyl pyrrolidine carboxylate moiety, which recorded a lesser tPSA value (tPSA 57.61). This might be due to the absence of the multiple electronegative sites (-OH, O-alkyl, $-SO_3^-$, etc.) in captopril.

The $–COCH_3$ group of the sulfated galactan might form a hydrogen bond with the imidazolyl proton of 2-amino-3-(1*H*-imidazol-4-yl) propanoic acid (His). The methoxy group on the anhydrogalactose ring fills the S3 pocket, and may conceivably shape a hydrogen bond with an auxiliary amine group of aromatic amino acid (such as Tyr). The terminal sulfate in position C-4 of the galactose ring grapples the tail in the dynamic site by framing a hydrogen bond with the aromatic amino acid (Tyr) and the enzyme metal cofactor Zn^{2+} in the S2' pocket of ACE (Fig. 5.26). The hydroxyl groups of the pyranose ring structure of sulfated polygalactan, at distinctive positions are different chemical attractions and hydroxyl group in the C-4 position was effectively supplanted by the sulfonato group, and a stronger interaction of $–SO_3^-$ with the Zn^{2+} (and tyrosyl –OH group) appeared to be responsible for anti-hypertensive activity. According to Ngo et al. (2008), the ACE inhibitory activity of aminoethyl-chitooligosaccharides (AE-COS) were greater than that of original chitooligosaccharides (COS). Essentially, Huang et al. (2005) have modified the structure of COS by carboxylation with $–COCH_2CH_2COO-$ groups to acquire particular structural features similar to captopril. Further, the greater ACE inhibitory activity of the 4-*O*-sulfonato-(2-*O*-methyl)-β-D-galactopyranosyl derivative (IC_{50} 0.02 μg/mL) than that of captopril (IC_{50} 0.51 μg/mL) might be due to the stronger electrostatic interactions between positively charged sites of enzymatic and negatively charged $–SO_3^-$ group of the latter. The sulfated polygalactan from *G. opuntia* (**GO-1**) was found to have additional $–COCH_3$ groups in the substituted galactose and anhydrogalactose units. It was, therefore, evident that the –OAc groups might have a negative effect on the target bioactivity.

Table 5.3. Yield, chemical compositions, antioxidative and ACE inhibitory activities of the sulfated polygalactans derived from *K. alvarezii* (**KA-1**) and *G. opuntia* (**GO-1**)

Activities	(**KA-1**)	(**GO-1**)
[†]**Yield (%)**	56.0	50.0
Biochemical contents		
[†]Uronic acid content	$7.20^{a} \pm 0.02$	$6.57^{b} \pm 0.12$
[†]Total sugar content	$46.99^{a} \pm 0.17$	$41.54^{a} \pm 0.10$
[†]Sulfate content	$75.0^{a} \pm 2.95$	$35.0^{b} \pm 1.37$
Total phenolic content (mg GAE/g)	$299.66^{b} \pm 0.04$	$480.45^{a} \pm 0.12$
Antioxidative activities		
[x‡]ABTS radical scavenging activity	$97.85^{a} \pm 0.68$ (0.72)	$90.67^{b} \pm 0.60$ (0.86)
[x‡]DPPH radical scavenging activity	$88.15^{a} \pm 0.63$ (0.97)	$83.04^{a} \pm 0.39$ (1.12)
[x‡]Fe^{2+} ion chelating ability	$73.15^{a} \pm 0.92$ (0.46)	$42.13^{b} \pm 0.56$ (1.30)
[y]Lipid peroxidation inhibitory	$232.70^{b} \pm 0.36$	$320.52^{a} \pm 0.36$
Anti-hypertensive activities		
[z]ACE inhibition	$82.69^{a} \pm 0.24$ (0.02)	$70.52^{b} \pm 1.11$ (0.70)

[†] The samples were analyzed in triplicate (n=3) and expressed as mean ± standard deviation. Means followed by the different superscripts within the same row indicate significant difference ($P < 0.05$).

[†]Percent mentioned in w/w

[‡] Percentage inhibition of radicals/peroxides/metal ion (%) was calculated by, scavenging activity (%) = (Bc-Bs)/Bc X 100, where, Bc is the absorbance of the control and Bs is the absorbance of the sample.

[x] The IC_{50} values (the concentration at which it inhibits 50 % of its activity) were presented within the parentheses, and expressed as mg/mL. The IC_{50} was calculated from the graph plotted with concentrations of sample against percentage inhibition.

[y] Lipid peroxidation inhibitory (TBARS assay) was expressed as mM MDAEQ /kg.

[z] The ACE inhibition (%) was calculated as follows: $[1 - (\Delta A_{sample}/min \div \Delta A_{blank}/min)] \times 100$ % as detailed in the Materials section. The IC_{50} values were presented within the parentheses, and expressed as µg/mL.

Competitive inhibitor of α-glucosidase is acarbose and miglitol, which reduces consumption of starch and disaccharides (Baylac and Racine 2003; Davis and Granner 2011). Hence one of the therapeutic pathways for contracting postprandial blood glucose levels in patient with diabetes mellitus is to impede carbohydrate absorption after food intake. The α-amylase established a family of endo-amylases catalyzing the initial hydrolysis of starch into shorter oligosaccharides through the cleavage of α-D-(1-4) glycosidic bonds. Inhibition of these enzymes (α-amylase and α-glucosidase) reduced the high postprandial blood glucose peaks in diabetes (Hamdan and Afifi 2004; Conforty et al. 2005). Acarbose and miglitol are competitive inhibitor of α-glucosidase resulting in lower absorption of starch and disaccharides. Vicinity of ^{13}C-NMR signals at δ_H 170 of the extracts derived from the macroalgae are a decent sign about the acyl carbonyl carbon that were accounted for to repress α-glucosidase protein (Dong et al. 2012; Matsui et al. 2001). The results from the present study demonstrated that there were no difference in α-glucosidase inhibitory activity (IC_{50} 0.09 mg/mL) of the sulfated polygalactans purified from two marine macroalgae species considered in the present study (Table 5.4). However, the sulfated galactans of *G. opuntia* (**GO-2**) exhibited greater α-amylase inhibitory activity (IC_{50} 0.04 mg/mL) than that of *K. alvarezii* (**KA-2**, IC_{50} 0.15 mg/mL) and the positive control (acarbose, IC_{50} 0.2 mg/mL). The anti-diabetic effect of the sulfated polysaccharides from macroalgae might attribute to their inhibitory effects against α-amylase that retard the digestion of carbohydrate to delay the postprandial rise in blood glucose. Likewise, there was no significant difference in the α-glucosidase inhibitory activity of the sulfated galactans (**KA-2** and **GO-2**) derived from these two red macroalgal species (IC_{50} ~0.09 mg/mL). Marine macroalgae were reported to possess α-amylase and α-glucosidase inhibitory activities, (Villanueva et al. 2009; Apostolidis et al. 2011) which substantiate the results obtained in the present study that these macroalgal species are good source for anti-diabetic agents.

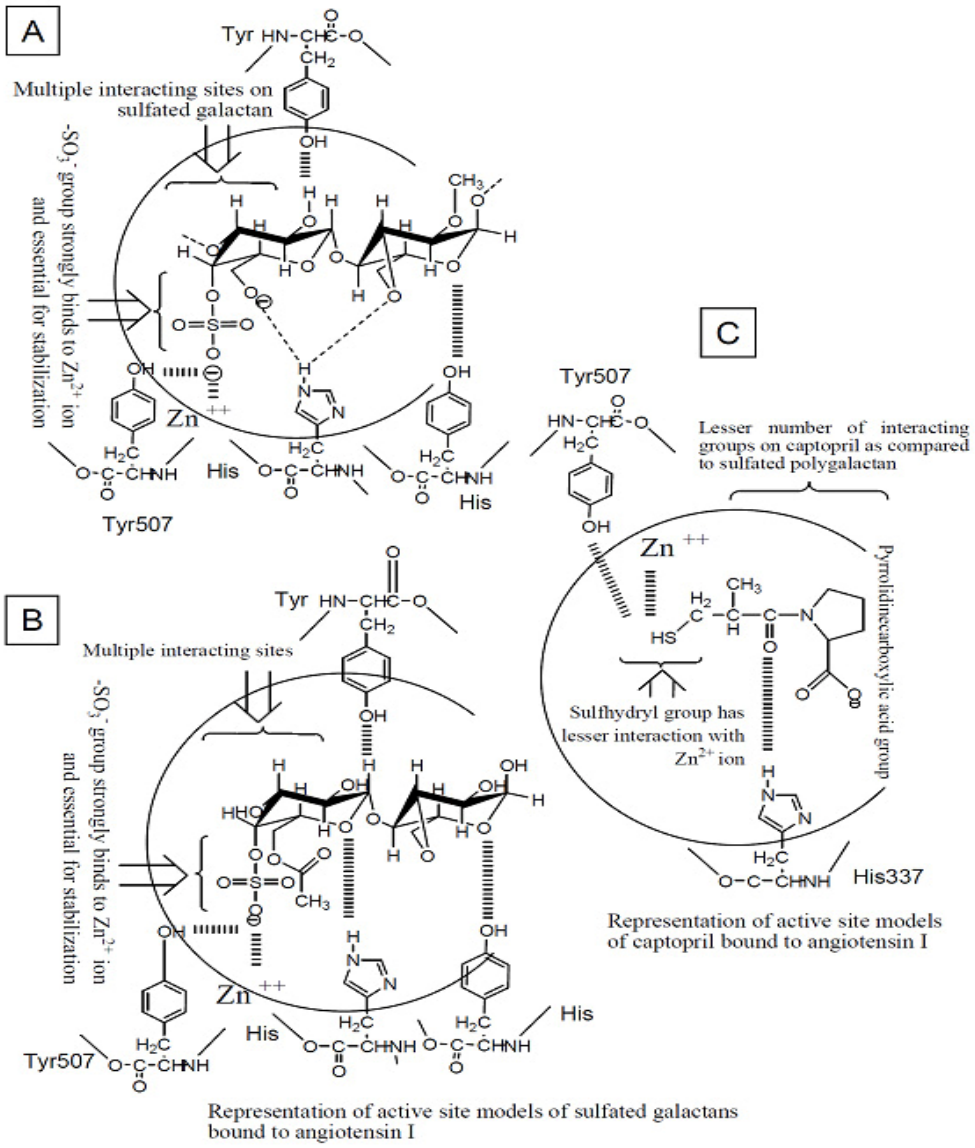

Figure 5.26. Representative active site models of substituted galactan motifs from (**A**) *K. alvarezii* (**KA-1**) (**B**) *G. opuntia* (**GO-1**) bound to the active centre of ACE (**C**) The ACE-ligand interaction of anti-hypertensive drug captopril has been shown

Dipeptidyl peptidase-4 (DPP-4) is involved in the inactivation of glucagon like peptide-1 (GLP-1), a potent insulinotropic peptide. Thus, DPP-4 inhibition can be an efficient approach to treat type-2 diabetes mellitus by potentiating insulin secretion (Mentlein 1999). The present study described the biological effects of sulfated polygalactan isolated from two different red marine macroalgae (**KA-2** and **GO-2**).

Significant differences were observed in the polysaccharide fractions, when compared with control.

Table 5.4. Anti-diabetic and anti-inflammatory inhibitory activities (IC_{50}) of the sulfated polygalactans derived from *K. alvarezii* (**KA-2)** and *G. opuntia* (**GO-2)**

Bioactivities	(**KA-2**)	(**GO-2**)
[x]**Anti-diabetic activities**		
α-Amylase	$0.15^{b} \pm 0.03$	$0.04^{a} \pm 0.02$
α-Glucosidase	$0.09^{a} \pm 0.02$	$0.09^{a} \pm 0.03$
DPP-4	$0.12^{b} \pm 0.01$	$0.09^{a} \pm 0.03$
[x]**Anti-inflammatory activities**		
COX-1	$0.01^{a} \pm 0.00$	$0.01^{a} \pm 0.00$
COX-2	$0.06^{b} \pm 0.01$	$0.03^{a} \pm 0.00$
5-LOX	$0.34^{b} \pm 0.02$	$0.24^{a} \pm 0.01$

The samples were analyzed in triplicate (n = 3) and expressed as mean ± standard deviation.

Means followed by the different superscripts within the same row indicate significant difference ($P < 0.05$).

[x] The IC_{50} values were expressed as mg/mL.

DPP-4 inhibitory activity of the sulfated galactans of *G. opuntia* (**GO-2)** was found to be significantly greater (IC_{50} 0.09 mg/mL) than that derived from *K. alvarezii* (**KA-2,** IC_{50} 0.12 mg/mL) and the standard diprotin A (IC_{50} 1.54 mg/mL) ($P < 0.05$). The synthetic DPP-4 inhibitors, such as, vildagliptin, sitagliptin, saxagliptin, etc, were reported to have several side effects like headache, dizziness, hypoglycemic disorders, nausea, weight gain and swelling of the legs and ankles due to excess fluid retention (Gomez-ordonez and Rupere 2011). Similarly, other synthetic hypoglycemic agents (acarbose and voglibose) that inhibit α-amylase and α-glucosidase were found to cause hepatic and gastrointestinal disorders (Cases et al. 1995; Murai et al. 2002). Polyphenols and sulfated polysaccharides present in macroalgae have been proven for anti-viral, anti-tumoral, anti-inflammatory and anti-coagulant activity (Vandevelde et

al. 2002; Cumashi et al. 2007). The bioactive compounds from macroalgae were reported to be effective for the treatment of major chronic diseases like diabetes through the inhibition of starch digesting enzymes and the regulation of glucose induced oxidative stress (Chiovitti et al. 1998; Lee et al. 2010). The bioactivity of the macroalgae extracts are due to the interaction of functional groups in the sulfated polygalactan with DPP-4 by H-bonding and hydrophilic interactions. The solvent fractions of *G. opuntia* were found to possess greater number of electronegative functional groups, which can form H-bond with DPP-4 resulting in greater anti-diabetic activity. The macroalgae considered in the present study can be used as potential alternative therapy for treatment of diabetes.

The sulfated polygalactan from *G. opuntia* **(GO-2)** exhibited significantly greater ($P < 0.05$) COX-1 and COX-2 inhibition activity (IC_{50} values of 0.01 and 0.03 mg/mL, respectively). *G. opuntia* **(GO-2),** polygalactan also exhibited greater 5-LOX inhibitory activity (**GO-2,** 0.24 mg/mL) than that of *K. alvarezii* (**KA-2,** IC_{50} 0.34 mg/mL) (Table 5.4). It is to be noted that sulfated polygalactan isolated in the present study showed greater anti-inflammatory activity in comparison with the positive control aspirin. Polysaccharides were reported to be one of the major bioactive components with selective activity against inflammation in the aqueous extract of macroalga *D. obtusata* (Frias et al. 2010; Silva et al. 1980). Red marine macroalgae were found to be the most important source of many biologically active metabolites in contrast to other algal classes (Frias et al. 2010). The sulfated galactans got from *G. opuntia* **(GO-2)** were found to have more prominent number of electronegative functional groups, which are characteristic of sulfated polygalactans, in the downfield space of the NMR spectra. These electronegative functional groups in the substituted polysaccharides derived from the macroalgae prevent abstraction of hydrogen from arachidonic acid in cyclooxygenases by ion pairing, and in this manner prevent synthesis of the pro-inflammatory prostaglandins.

The anti-diabetic potential of **KA-3** isolated from *K. alvarezii* measured in terms of the inhibitory activities against DPP-4 were deduced to be higher (IC_{50} 0.17 mg/mL) in comparison with that obtained from *G. opuntia* (**GO-3**, IC_{50} 0.21 mg/mL) and gold standard diprotein-A (IC_{50} 0.24 mg/mL). Similarly, the sulfated polygalactan derivatives showed significant increase in ($P > 0.05$) α-amylase inhibitory activities (**KA-3** and **GO-3**, $IC_{50} < 1$ mg/mL) when compared with the standard acarbose (IC_{50}

1.39 mg/mL). Notably, there has been a positive correlation between the sulfate content and anti-diabetic properties as reported previously (Cho et al. 2011).

Table 5.5. Pharmacological potential of sulfated polygalactan isolated from *K. alvarezii* (**KA-3**) and *G. opuntia* (**GO-3**)

Bioactivities	**Standard**	(**KA-3**)	(**GO-3**)
Anti-diabetic activity			
α-Amylase inhibitory activity	1.39 ± 0.06^{aC}	0.91 ± 0.04^{a}	0.93 ± 0.02^{b}
α-Glucosidase inhibitory activity	1.52 ± 0.03^{aC}	1.41 ± 0.02^{b}	1.43 ± 0.04^{b}
DPP-4 inhibitory activity	0.24 ± 0.01^{aD}	0.17 ± 0.02^{a}	0.21 ± 0.01^{b}
Anti-hypertensive activity			
ACE-I inhibitory activity	0.01 ± 0.01^{aE}	0.04 ± 0.01^{b}	0.07 ± 0.01^{b}

The samples were analyzed in triplicate (n=3) and expressed as mean ± standard deviation.

Means followed by the different superscripts (a-b) within the same row indicate significant difference ($P < 0.05$).

The IC_{50} values of anti-diabetic and anti-hypertensive activities were expressed as mg/mL.

Different superscripts (C-E) indicated the standards used for different activities; C-acarbose; D-diprotein-A; E-captopril

It was found that the α-amylase enzyme inhibitory activity of sulfated polysaccharide derived from *Ascophyllum nodosum* and *Saccharina longicruris* were lesser following complete removal of sulfate groups (Kim et al. 2014). Similarly, the polygalactan **KA-3** from *K. alvarezii* showed greater inhibitory properties against angiotensin-I (IC_{50} 0.04 mg/mL) when compared with **GO-3** (IC_{50} 0.07 mg/mL) (Table 5.5).

5.3.5. Correlation Analysis

A negative correlation was demonstrated between the total phenolic content (TPC) and different antioxidative activities of the sulfated polygalactans **(KA-1** and **GO-1)** isolated from the marine macroalgae, which apparently outlined that anti-hypertensive properties did not depend on aggregate phenol content, but rather additionally on other compounds, for instance, polysaccharides (Muzzarelli 1997).

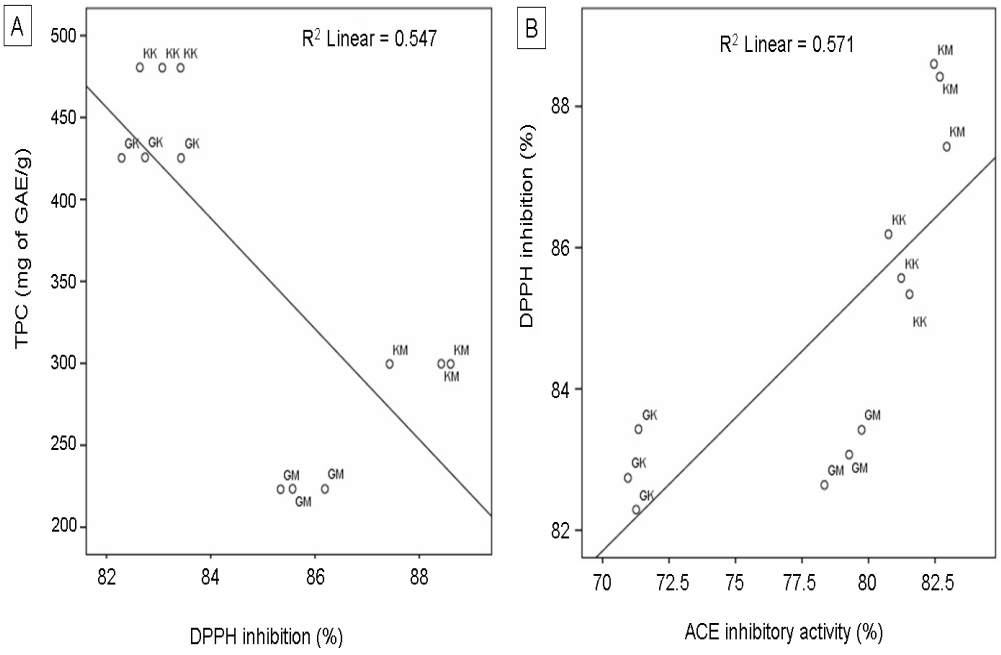

Figure 5.27. Correlation plot between (**A**) total phenolic contents (TPC) and antioxidative properties (DPPH inhibition) (**B**) antioxidative (DPPH inhibition) and anti-hypertensive properties (ACE inhibition)

The antioxidant activities as dictated by DPPH and ABTS activities were found to be significantly related to the anti-hypertension activity as displayed by ACE-I inhibitory properties (Fig. 5.27), which apparently demonstrated that the ACE-I inhibitory activities of the sulfated galactans **(KA-1** and **GO-1)** were due to their free radical scavenging properties. It is apparent that the multiple –OH and other electronegative groups bearing the hydrogen atoms contributed towards the hydrogen atom transfer (HAT), which resulted in the stabilization of the free radicals.

The relationships between anti-inflammatory and anti-diabetic activities of the sulfated polygalactan enriched concentrate of *K. alvarezii* **(KA-2)** and *G. opuntia* **(GO-2)** were statistically analyzed using PCA (Fig. 5.28). The loading of first and second principle components (PC1 and PC2) were accounted for 68.17 % and 31.8 % of the variance, respectively.

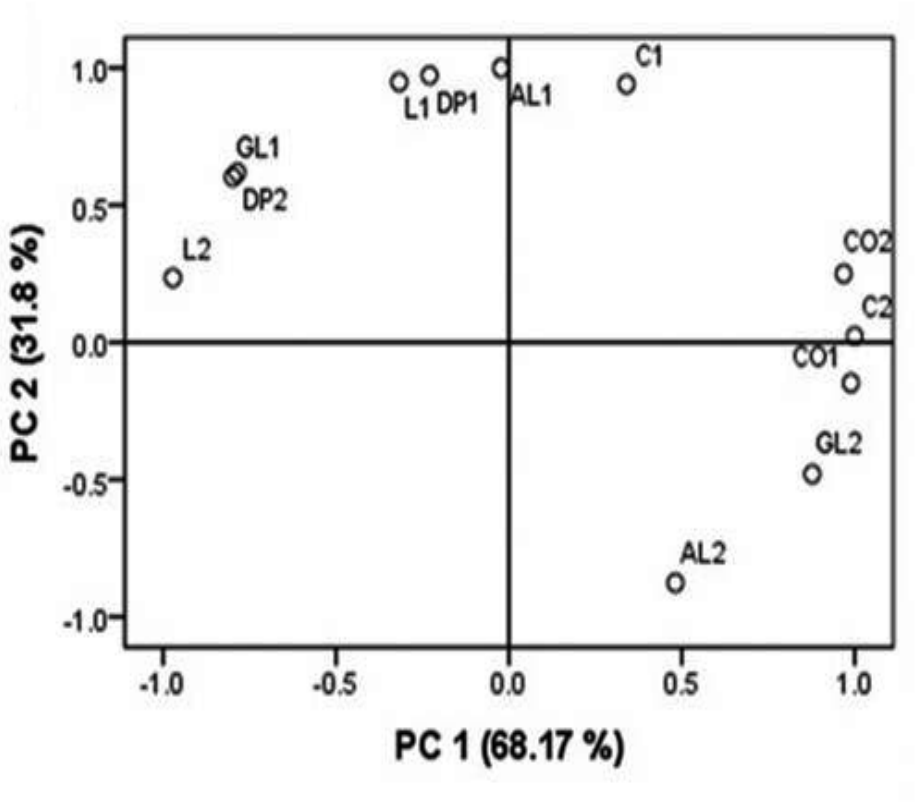

Figure 5.28. PCA loading plot diagrams showing the correlation between anti-diabetic and anti-inflammatory activities of the sulfated polygalactan fractions from *G. opuntia* **(GO-2)** and *K. alvarezii* **(KA-2)**.

The component, PC1 was mainly influenced by inhibitory activities of sulfated polygalactan derived from *G. opuntia* (**GO-2** and *K. alvarezii* (**KA-2**) towards the pro-inflammatory enzymes, COX-1 (denoted as C1; **GO-2** and C2; **KA-2**) and COX-2 (denoted as CO1; **GO-2** and CO2; **KA-2**), along with α-amylase (AL2; **KA-2**) and α-glucosidase (GL2; **KA-2**). On the other hand, 5-LOX (denoted as L1; **GO-2** and L2; **KA-2**), DPP-4 (DP1; **GO-2** and DP2; **KA-2**), α- amylase (AL1; **GO-2**), and α-

glucosidase (GL1; **GO-2**) inhibiotory properties of the sulfated polygalactans of the marine macroalgae were mainly contributed to PC2 (Fig. 5.28). The similarity in the greater loading of DPP-4, COX-2, 5-LOX·inhibitory activities, and a significant positive correlation between DPP-4 inhibition activity (DP1-DP2) with anti-COX and LOX properties of macroalgae derived sulfated polygalactans (**KA-2** and **GO-2)** apparently demonstrated that these bioactivities were in close relation. The significant correlation of anti-diabetic activities with anti-inflammatory properties of the sulfated polygalactans isolated from the macroalgae *G. opuntia* **(GO-2)** and *K. alvarezii* (**KA-2)** also indicated that these polysaccharides derived from macroalgae were responsible for potential anti-inflammatory and anti-diabetic properties.

5.4. Conclusions

The present study demonstrated that sulfated polygalactan characterized as→4)-4-*O*-sulfonato-(2-*O*-methyl)-β-D-galactopyranosyl-(1→4)-3, 6-anhydro-(2-*O*-methyl)-α-D-galactopyranan from *K. alvarezii* **(KA-1)** displayed significantly greater antioxidative and ACE inhibitory activities than →3)-4-*O*-sulfonato-(6-*O*-acetyl)-β-D-galactopyranosyl-(1→4)-3, 6-anhydro-(2-*O*-sulfonato)-α-D-galactopyranosyl-(1→3)-4-*O*-sulfonato-(6-*O*-acetyl)-β-D-xylosyl-(1→3)-4-*O*-sulfonato-(6-*O*-acetyl)-β-D-galactopyranosyl-(1→4)-3, 6-anhydro-(2-*O*-sulfonato)-α-D-galactopyranan from *G. opuntia* **(GO-1)**. The multiple hydroxyl groups of the pyranose ring structure of sulfated polygalactan from *K. alvarezii* **(KA-1)** and sulfonato group ($-SO_3^-$) at distinctive positions have stronger interactions with the Zn^{2+} (and tyrosyl –OH group), which were responsible for their anti-hypertensive activities. The sulfated polygalactan from *K. alvarezii* **(KA-1)** was found to be a potential therapeutic candidate to prevent the pathologies of hypertensive disorders.

The sulfated polygalactans isolated from the red marine macroalgae *K. alvarezii* **(KA-2)** and *G. opuntia* **(GO-2)** were found to possess a number of bioactivities against different disease targets, namely, inflammation and type-2 diabetes. The sulfated polygalactan enriched concentrate obtained from *G. opuntia* **(GO-2)** showed greater anti-inflammatory activities than that from *K. alvarezii* **(KA-2)** as determined by *in vitro* cyclooxygenase/lipoxygenase inhibitory activities. The activities showed significant positive correlation with the anti-diabetic activities as determined by *in vitro* α-amylase, α-glucosidase and dipeptidyl peptidase-4 inhibitory

properties. This study demonstrated the candidacy of red marine macroalgae particularly, *G. opuntia* **(GO-2)** as potential source of bioactive sulfated polygalactans for use as functional food supplements to deter inflammation and type-2 diabetes.

Further other polysaccharide fractions obtained from the red marine macroalgae *K. alvarezii* and *G. opuntia* were characterized as 1, 3-*O*-diacetyl-2, 5, 6-trihydroxyl-β-D-galactose-4-sulfate **(KA-3$_A$)** and 1, 3, 5-*O*-triacetyl-4-hydroxyl-6-*O*-methyl-D-galactose-2-sulfate **(GO-3$_A$)**, respectively, which were characterized by using extensive spectroscopic experiments. In particular, the polysaccharide fraction isolated from *K. alvarezii* **(KA-3)** exhibited potential DPP-4 and ACE-I enzyme inhibitory properties, and therefore, could function as candidate template for use in medicinal and food applications.

Chapter 6

SUMMARY

Marine macroalgae (otherwise named as seaweeds) were found to be the potential reservoir of bioactive secondary metabolites. Traditionally, marine macroalgae are considered as valuable marine flora, which are preferred delicacies in the South-east Asian countries due to their potential antioxidant and therapeutic properties. Species of the red marine macroalgae (class Rhodophyceae) were proven to be rich sources of structurally unique and biologically active secondary metabolites endowed with antioxidant, anti-bacterial, anti-inflammatory and anti-carcinogenic activities for applications in functional food and pharmaceuticals. The bioactive compounds extracted from the marine macroalgae are used as safer anti-inflammatory therapeutics. Marine macroalgae were found to be rich sources of bioactive compounds, such as terpenoids, phloroglucinol, phenolics, fucoidans, sterols, glycolipids and halogenated compounds, whereas the extracts or isolated components derived from these marine species exhibited a wide range of pharmaceutical properties. The potential applications offered by these valuable resources as ingredients in functional foods are significant because of their richness in bioactive principles, particularly antioxidants. Antioxidant effects have been reported from various macroalgae due to phenolic compounds, terpenoids and sulfated polysaccharides. Novel secondary bioactive metabolites from red marine macroalgae are attracting attention because of the growing demand for new compounds of marine natural origin, having potential applications in pharmaceutical fields and concerns about the toxic effects by synthetic drugs.

Among different red marine macroalgae, *Kappaphycus alvarezii* (Doty) (family Solieriaceae) and *Gracilaria opuntia* (Durairatnam) (family Gracilariaceae) are commercially important and cultivable species that are predominantly abundant in tropical coastal and marine habitats in the Southeast Asian countries. *K. alvarezii* is economically significant and predominantly farmed red marine macroalga in shallow tropical marine habitats. The genus *Gracilaria* is the largest in the order Gracilariales,

and was found to include more than 150 species, which were distributed in the tropical and temperate sea. Among different species of the genus *Gracilaria*, *G. opuntia* is one of the predominantly available red marine macroalga grown in the Gulf of Mannar region of the south-east coast of India. Despite the fact that red marine macroalgae, particularly *Laurencia* spp, have been studied extensively with respect to secondary metabolite chemistry, studies on members of the genus *K. alvarezii* and *G. opuntia* have been rare for the isolation of novel intriguing structures.

The organic ethyl acetate-methanol (EtOAc: MeOH) extracts of the studied marine macroalgae *K. alvarezii* and *G. opuntia* from the Gulf of Mannar region of Mandapam were screened for various pharmacological activities by different *in vitro* assays. The organic extracts obtained from the red macroalgae *K. alvarezii* and *G. opuntia* were found to possess a number of bioactivities against different disease targets, namely, hypertension, type-2 diabetes and inflammation. The organic extract of *K. alvarezii* possessed significantly greater antioxidative properties than those obtained from *G. opuntia*. The EtOAc: MeOH fraction of *K. alvarezii* registered greater Fe^{2+} ion chelating ability (IC_{50} 1.30 mg/mL), and were effective in stabilizing the ABTS (IC_{50} 1.26 mg/mL), and DPPH radicals (IC_{50} 1.24 mg/mL). The organic extract from *K. alvarezii* also showed greater angiotensin-I converting enzyme (ACE) inhibitory activity along with pro-inflammatory cyclooxygenase/lipoxygenase inhibitory activities than that exhibited by that acquired from *G. opuntia.* Likewise, EtOAc-MeOH crude extract obtained from *K. alvarezii* showed significant anti-diabetic activities as determined by *in vitro* α-amylase, α-glucosidase and dipeptidyl peptidase-4 inhibitory properties. The spectroscopic characterization of the solvent extracts provided the evidence regarding the occurrences of signature peaks and the prominent functional groups that were responsible for the target bioactivities.

The ethyl acetate-methanol extract of the thalli of *K. alvarezii* and *G. opuntia* was fractionated by repeated column chromatography to afford a number of previously undescribed compounds. The structures of these compounds were established by exhaustive spectroscopic experiments, including mass and two-dimensional nuclear magnetic resonance. The antioxidative and anti-inflammatory activities of the newly reported compounds were evaluated by different *in vitro* assays. Structure-bioactivity correlation analyses of the studied compounds were carried out using different electronic and hydrophobic molecular descriptor variables. Chromatographic fractionation of the organic extract obtained from the thalli of *K. alvarezii* yielded two

previously undescribed biogenic halogenated compounds named as 2-butyl-7-4-(chloromethyl) cyclooct-1-enyl) hept-5-en-1-ol (compound **K1**) and 4-(2-chloroethyl)-5-7-(methoxymethyl) undec-3-enyl) cyclooct-4-enone (compound **K2**), which demonstrated the rare skeletal framework featuring C_{20}-cyclooctene and C_{23}-cyclooctenyl ring system and three oxygenated meroterpenoids, characterized as 1-(3-methoxypropyl)-2-propylcyclohexane (C_{13}) (compound **K3**), 3-(methoxymethyl) heptyl 3-(cyclohex-3-enyl) propanoate (C_{18}) (compound **K4**) and 2-ethyl-6-(4-methoxy-2-((2-oxotetrahydro-*2H*-pyran-4-yl) methyl) butoxy)-6-oxohexyl-5-ethyloct-4-enoate (C_{29}) (compound **K5**) along with an unprecedented non-isoprenoid oxocine carboxylate cyclic ether characterized as (3, 4, 5, 6)-3-(hexan-2′-yl)-3, 4, 5, 8-tetrahydro-4-methyl-2*H*-oxocin-5-yl acetate (compound **K6**)

The mass spectroscopic data of compound **K1** demonstrated a molecular ion peak at *m/z* 326, while the molecular formula $C_{20}H_{35}ClO$, implying three unsaturation degrees, and were associated with two olefinic bonds and one ring system. The infrared (IR) spectrum exhibited distinctive stretching vibration band for hydroxyl (3430 cm^{-1}) and olefinic group (3011 cm^{-1}). The existence of the hydroxyl proton at δ_H 3.67 was validated by ^1H NMR spectra and D_2O exchange reaction. The characteristic isotopic molecular ion peaks with typical isotopic pattern of 3:1 at *m/z* 326 and *m/z* 328 appropriately attributed the presence of one chlorine atom in compound **K1**. The NOE experiment of compound **K1** showed correlation peaks between the equatorial methine proton and methylene proton, which proposed that these protons were arranged on the same side of the reference plane (cyclooctene) with β-faced interaction. The mass spectroscopic experiments of compound **K2** showed a molecular isotopic ion peak at *m/z* 382, having four degrees of unsaturation (molecular formula $C_{23}H_{39}ClO_2$), and were associated with two olefinic bonds, along with one each of carbonyl group and ring system. The infrared (IR) spectrum exhibited distinctive stretching vibration band for carbonyl stretching (1727.88 cm^{-1} for C-CO-C ν) and olefinic group {3072.42 cm^{-1} (C-H)}. The NOE experiment showed correlation peaks between the oxygenated methine proton and axial proton, which proposed that these protons were on the opposite of the reference plane (cyclooctenyl) with β-faced interaction. The characteristic isotopic molecular ion peaks with typical isotopic pattern of 3:1 at *m/z* 382 and *m/z* 384 appropriately attributed the existence of one chlorine atom in compound **K2**. It is of note that the halogen derivatives isolated in the present study from *K. alvarezii* represented the first examples of naturally occurring halogen

derivative from the marine macroalga. The halogenated cyclooctenone (compound **K2**) displayed greater 5-LOX (IC_{50} 0.90 mg/mL) inhibitory activity when compared to the non steroidal anti-inflammatory drug ibuprofen (IC_{50} 0.93 mg/mL). Similarly, selectivity indices of the studied halogenated compounds (compounds **K1** and **K2**) were higher (anti-cyclooxygense-1 IC_{50}/anti-cyclooxygense-2 IC_{50} ~ 1.06-1.07) when compared to those exhibited by ibuprofen (0.44) and aspirin (0.02). The antioxidative activities of the halogen derivatives (compounds **K1** and **K2**) were found to be greater (IC_{50} < 0.30 mg/mL) in comparison with that displayed by α-tocopherol (IC_{50} > 0.50 mg/mL). This is the first report on structural characterization of unusual halogen analogues from *K. alvarezii* with duel cyclooxygenase-2 and 5-lipoxygenase inhibitory activities.

Compound **K3**, a methoxy-substituted C_{13} meroterpenoid, was purified as yellow oil by extensive column chromatography on adsorbent silica gel. The mass spectrum displayed the molecular ion peak at *m/z* 198 enclosing mono unsaturation, and the molecular formula as $C_{13}H_{26}O$ based upon combined ^{1}H and ^{13}C NMR spectral data. NOESY cross-peaks suggested their close proximity, and therefore, assigned to align on an identical plane of the cyclohexane ring system with di-equatorial β-faced interaction. Compound **K4**, an oxygenated C_{18} meroterpenoid displayed the molecular ion peak at *m/z* 296 enclosing three degrees of unsaturation the molecular formula as $C_{18}H_{32}O_3$ based upon combined ^{1}H and ^{13}C NMR spectral data. The IR-spectrum of compound **K4** displayed the presence of carbonyl group along with olefinic groups due to the bands recorded at 1458 and 2856 cm^{-1}. The chemistries of the stereogenic centres bearing protons were derived using coupling constant values and NOESY experiments. An intense NOE correlation was displayed between the protons suggested their equi-planer disposition, and was arbitrarily attributed as β-oriented. Compound **K5**, a highly oxygenated C_{29} meroterpenoid, was purified as yellow oil with *m/z* 510 bearing five degrees of unsaturation, and its structure was characterized by combined ^{1}H and ^{13}C NMR spectral experiments. The IR bending vibration near 1736 cm^{-1} was associated with the carbonyl group, whereas the olefinic groups were assigned to the absorption bands at 1455 cm^{-1} and 2857 cm^{-1}. NOE correlations between the di-equatorial protons apparently attributed to their close spatial arrangements, and therefore, were assigned to be at the β-face with reference to the molecular plane of symmetry. The highly oxygenated C_{29} meroterpenoid (compound **K5**) displayed potential antioxidative activities (IC_{50} < 0.35 mg/mL) as evaluated by 2, 2'-azino-bis (3-ethylbenzothiazoline)-6-

sulfonic acid and 1, 1-diphenyl-2-picryl-hydrazil free radical scavenging assays. The compound **K5** also displayed potential *in vitro* inhibitory activities towards pro-inflammatory 5-lipoxygenase (IC_{50} 1.04 mg/mL), which indicated its potential anti-inflammatory properties against inducible inflammatory mediators causing an inflammatory response. Structure-activity relationship analyses displayed the functional roles of lipophilic-hydrophobic characteristics and electronic parameter to determine its potential anti-inflammatory activity in terms of inhibiting inducible inflammatory cyclooxygenase and lipoxygenase. The mass spectrum supported the molecular formula of $C_{16}H_{28}O_3$ and the molecular ion peak at *m/z* 268 in the mass spectrum, which in combination with its ^{1}H and ^{13}C NMR data indicated the elemental composition of the compound **K6** as $C_{16}H_{28}O_3$ with three degrees of unsaturation. The olefinic (C=C) and alkyl (C–H) groups IR stretching vibrations were represented by the 1458 and 2855 cm^{-1} absorption bands, respectively. The strong bending vibration bands near 1712 cm^{-1} denoted the ester carbonyl absorption. The relative stereochemical configuration of the asymmetric centers bearing the 3, 4, 5, 8-tetrahydro-2*H*-oxocine ring framework, was proposed on the basis of NOE enhancements along with the coupling constants (*J*-values) of the NMR spectrum. The interpretation for the boat–chair conformation might be due to the bulky 3, 4, 5 ,8-tetrahydro-2*H*-oxocine group as equatorially disposed. The antioxidative activity of the non-isoprenoid oxocine carboxylate cyclic ether was found to be significantly greater as determined by DPPH and ABTS radical scavenging activities (IC_{50} ~ 0.3 mg/mL) compared to that displayed by α-tocopherol (IC_{50} > 0.6 mg/mL). The compound exhibited greater anti-inflammatory activity against COX-2 than COX-1 isoform, and therefore, the selectivity index remained significantly lesser (anti-COX-1 IC_{50}: anti-COX-2 IC_{50} 0.87) than synthetic anti-inflammatory drugs (0.02–0.44). No significant difference of *in vivo* 5-lipoxygenase activity (IC_{50} 0.95 mg/mL) than ibuprofen (IC_{50} 0.93 mg/mL) indicated the potential anti-inflammatory properties of the compound **K6**.

Chromatographic fractionation of the organic extract obtained from the thalli of *G. opuntia* yielded two furanyl derivatives, characterized as 5-(7-(5-ethyl-3, 4-dimethoxycyclooctyl) benzofuran-6-yl)-7-methyl-3, 4, 7, 8-tetrahydro-2*H*-oxocin-2-one (compound **G1)** and 2-(3-ethyl-9-(2-methoxyethoxy)-1-oxo-2, 3, 4, 9-tetrahydro-1*H*-xanthen-2-yl) ethyl-5-hydroxy-9-methoxy-7, 8-dimethyl-8-(5-methylfuran-2-yl) nona-3, 6-dienoate (compound **G2**) along with 3-(2-ethyl-6-((3, 7)-1, 2, 5, 6-tetrahydroazocin-5-yl) hexyl) morpholin-6-one (compound **G3**) and 2-acetoxy-2-(5-

acetoxy-4-methyl-2-oxotetrahydro-2*H*-pyran-4-yl) ethyl-4-(3-methoxy-2-(methoxymethyl)-7-methyl-3, 4, 4a, 7, 8, 8a-hexahydro-*2H*-chromen-4-yloxy)-5-methylheptanoate (compound **G4**). The isolated compounds were found to be the first furanyl natural products featuring methoxycyclooctyl benzofuran with tetrahydro-2*H*-oxocin framework and tetrahydro-1*H*-xanthenyl methoxy methylfuran skeletons. The compound **G1** was obtained as yellow oil, and its molecular ion peak at *m/z* 454 was deduced from the mass spectrum. The molecular formula of the isolated compounds was deduced as $C_{28}H_{38}O_5$ based on combined ^1H and ^{13}C NMR spectroscopic data. The IR spectrum displayed bending vibration appeared at 1741 cm^{-1}, which was attributed to the ester carbonyl group. The FTIR absorption bands at 1459 and 2856 cm^{-1} were attributed to the olefinic (>C=C<) as well as alkyl groups, respectively. The relative stereochemical configuration of the asymmetric centers, bearing the substituted furan ring framework was attributed by extensive NOESY experiments along with the coupling constants (*J*-values) in the ^1H NMR spectrum. The aromatic methine protons displayed NOESY correlations with the neighboring aromatic methane protons in the benzyl furan aromatic ring system. Compound **G2**, a previously undescribed furanyl derivative, was purified as yellow oil by extensive column chromatography on adsorbent silica gel. The mass spectral data of compound **G2** accounted for the molecular ion peak at *m/z* 636 enclosing fourteen degrees of unsaturation, and the molecular formula as $C_{37}H_{48}O_9$ was deduced from combined ^1H and ^{13}C NMR spectroscopic experiments. The IR spectrum showed bending vibration near 1708 cm^{-1}, which was attributed to the carbonyl group. The characteristic hydroxyl stretching vibration was recorded at 3425.10 cm^{-1}. The relative stereochemistries at chiral centers bearing the xanthenyl furanyl ring carbon skeleton were attributed by detailed NOESY correlations.

These studied compounds were assessed for anti-inflammatory activities against pro-inflammatory cyclooxygenase-2/5-lipoxygenase (COX-1, 2, and 5-LOX) and antioxidative effects in various *in vitro* models. The antioxidative properties of the furanyl derivatives as resolved by DPPH and ABTS free radical scavenging activities were found to be significantly greater (IC_{50} ~ 0.051–0.055 × 10^{-2} M) than those exhibited by α-tocopherol (IC_{50} > 0.146 × 10^{-2} M), and were similar to those displayed by the synthetic antioxidants BHT/ BHA (IC_{50} ~ 0.144–0.189 × 10^{-2} M, $P < 0.05$). The anti-inflammatory selectivity indices of the isolated compounds recorded significantly greater values (SI: anti-COX-1 IC_{50}/anti-COX-2 IC_{50} ~1.08–1.09) than NSAIDs

(aspirin, and ibuprofen, SI: 0.02 and 0.44, respectively, $P < 0.05$), and consequently, appeared to be safer. The isolated compounds showed significant anti-diabetic properties as determined by α-amylase/α-glucosidase ($IC_{50} < 0.052 \times 10^{-2}$ M) and dipeptidyl peptidase-4 (DPP-4, $IC_{50} < 0.002 \times 10^{-2}$ M) inhibitory activities. The angiotensin converting enzyme-I (ACE-I) inhibitory activity of the compounds (IC_{50} 0.023–0.024 $\times 10^{-2}$ M) was found to be comparable with that recorded by commercial ACE inhibitor, captopril (IC_{50} 0.037 $\times 10^{-2}$ M).

The molecular ion peak at *m/z* 320, which was combined with the detailed NMR experimental data to record the elemental composition of the compound **G3** with five degrees of unsaturation. The broad absorption band at 3425 cm^{-1} in the IR spectrum was attributed to the –NH groups, which has been supported by the ^{1}H NMR signal. The presence of –NH protons was further validated by D_2O exchange. The occurrences of two nitrogen groups were also satisfied by nitrogen odd and even rule. The comparative stereochemical configuration of the chiral centers belonging to 1, 2, 5, 6-tetrahydro azocin-5-yl-hexyl moiety, and morpholin-6-one ring framework were summarized from the NOE spectral experiments and the coupling constant values. The substituted azocinyl morpholinone recorded significant DPPH free radical scavenging activities (IC_{50} ~ 0.086 mg/mL) compared to the commercially available antioxidants, butylated hydroxyanisole, butylated hydroxytoluene, and α-tocopherol ($IC_{50} > 0.20$ mg/mL). The compound **G3** showed greater COX-2 inhibitory activity (IC_{50} 0.84 mg/mL) in conjunction with *in vitro* 5-lipoxygenase inhibitory activity (IC_{50} 0.85 mg/mL) than non-steroidal anti-inflammatory drugs (NSAIDs). The test compound had better selectivity index (COX-1/COX-2 ratio) (1.17 mg/mL) compared to those displayed by aspirin (0.02 mg/mL), sodium salicylate (0.73 mg/mL) and ibuprofen (0.44 mg/mL). The animals challenged with the substituted azocinyl morpholinone significantly mitigated the carrageenan-induced paw edema in time-dependent manner till the end of 6 h.

The compound **G4** showed absorption bands at 1715 cm^{-1} in the Fourier Transform Infrared (FTIR) spectrum due to the carbonyl functionalities. The IR stretching vibrations due to olefinic (C=C) and alkyl (C–H) groups were demonstrated by the absorption bands at 1458 and 2856 cm^{-1}, respectively. The molecular ion peak at *m/z* 640 in combination with its ^{1}H and ^{13}C NMR data designated the elemental composition of the compound **G4** as $C_{33}H_{52}O_{12}$. The detailed ^{1}H, ^{13}C NMR and mass spectral analysis confirmed the structure. The relative stereochemistries of the chiral

centres of the compound **G4**, assigned the chair-like conformation of the 2*H*-chromen derivative. The anti-inflammatory selectivity index of the compound **G4** was greater (SI: anti-cyclooxygense-1 IC_{50}/anti-cyclooxygense-2 IC_{50} ~ 1.26) than those exhibited by synthetic NSAIDs (aspirin and ibuprofen, SI: 0.02 and 0.44, respectively). The antioxidative activity of the compound **G4** was significantly greater as determined by DPPH and ABTS radical scavenging activities (IC_{50} 0.26–0.32 mg/mL) compared to α-tocopherol (IC_{50} > 0.6 mg/mL), and was comparable to the synthetic antioxidants BHT and BHA (IC_{50} ~ 0.25–0.34 mg/mL).

Antioxidant and anti-hypertensive potential of the sulfated polygalactans (**KA-1** and **GO-1**) isolated from the marine macroalgae *K. alvarezii* (**KA-1**) and *G. opuntia* (**GO-1**) was assessed by utilizing different *in vitro* systems. The intense absorption bands in the 1210-1260 cm^{-1} region of the fourier transform infrared spectra showed the vicinity of S=O group of sulfate esters. The sulfate group was situated at C-4 of (1→3)-linked galactopyranosyl residues of the native galactan, whereas the strong signals in the ^{1}H-NMR spectrum of *G. opuntia* (**GO-1**) attributed to the presence of strong -$COCH_3$ protons. Interestingly, very weak proton signals for *K. alvarezii* (**KA-1**) were assigned to be due to the -$COCH_3$ protons. As compared to the sulfated polygalactan isolated from *K. alvarezii* (**KA-1**), the one isolated from *G. opuntia* (**GO-1**) exhibited very sharp intense signals, which ascribed to be due to the vicinity of 2-*O*-methyl-α-(1-4)-linked 3, 6-anhydogalactose and 6-*O*-methyl-β-(1-3)-linked galactose residues. The anomeric carbon signals were found to be C-1 of α-D-galactose-4-sulfate, and this dyad was illustrative of a sulfated polygalactan. The galactans isolated from *K. alvarezii* (**KA-1**) possessed significantly greater antioxidative properties as determined by DPPH (**KA-1:** IC_{50} 0.97 mg/mL) and ABTS (**KA-1:** IC_{50} 0.72 mg/mL) scavenging activities than those isolated from *G. opuntia* (**GO-1**: DPPH IC_{50} 1.2 mg/mL and ABTS 0.86 mg/mL). The sulfated polygalactan →4)-4-*O*-sulfonato-(2-*O*-methyl)-β-D-galactopyranosyl-(1→4)-3, 6-anhydro-(2-*O*-methyl)-α-D-galactopyranan from *K. alvarezii* (**KA-1**) showed greater angiotensin-I-converting enzyme (ACE) inhibitory activity (**KA-1:** IC_{50} 0.02 µg/mL) than that displayed by →3)-4-*O*-sulfonato-(6-*O*-acetyl)- β-D-galactopyranosyl-(1→4)-3, 6-anhydro-(2-*O*-sulfonato)-α-D-galactopyranosyl-(1→3)-4-*O*-sulfonato-(6-*O*-acetyl)-β-D-xylosyl-(1→3)-4-*O*-sulfonato-(6-*O*-acetyl)-β-D-galactopyranosyl (1→4)-3, 6-anhydro-(2-*O*-sulfonato)-α-D-galactopyranan motif extracted from *G. opuntia* (**GO-1**: IC_{50} 0.70 µg/mL). Structure-activity correlation studies displayed that the ACE inhibitory properties of isolated

polygalactans were directly proportional to their electronic properties and inversely with the steric and hydrophobic characteristics. Putative ACE inhibitory mechanism of action of sulfated galactans from marine macroalgae corroborated the structure bioactivity correlation analysis.

Anti-diabetic and anti-inflammatory potential of sulfated polygalactans isolated from the red marine macroalgae *K. alvarezii* (**KA-2**) and *G. opuntia* (**GO-2**) were acquired by employing different *in vitro* systems. The strong absorption bands at 1210-1260 cm^{-1} of the FT-IR spectra demonstrated the region of S=O groups (attributed to the glycosidic linkage). The IR signals close to 3200-3400 cm^{-1} were credited to the region of -OH groups present in the sulfated polygalactans from the macroalgae. The broad bands at 3200-3400 cm^{-1} were found to be a result of the sulfated polygalactan units. The ^{1}H-NMR spectra of polysaccharides comprise of some well-resolved signals, counting those of anomeric protons. The ^{1}H-NMR spectrum of polysaccharides obtained from *K. alvarezii* (**KA-2**) got deshielded signals demonstrating the region of κ and ι monomer of sulfated polygalactans. Recognizable -*O*-alkyl signals (ideally –OCH_3) in the ^{1}H-NMR spectrum of galactan derivative from *G. opuntia* (**GO-2**) and *K. alvarezii* (**KA-2**) appropriately recognized the region of more conspicuous number of alkoxy substitutions in the sulfated polygactans from the red macroalgae. The ^{13}C NMR spectrum of polygalactans showed signals with specific multiplicities, which suggested the positional differences of 1→3 and 1→4 linked residues in the sulfation patterns. Based on the detailed NMR experiments the sulfated galactopyran motif of *G. opuntia* (**GO-2**) was designated as →3)-4-*O*-sulfonato-(6-*O*-acetyl)-β-D-galactopyranosyl-(1→4)-3, 6-anhydro-(2-*O*-sulfonato)-α-D-galactopyranosyl-(1→3)-4-*O*-sulfonato-(6-*O*-acetyl)-β-D-xylosyl-(1→3)-4-*O*-sulfonato-(6-*O*-acetyl)-β-D-galactopyranosyl-(1→4)-3, 6-anhydro-(2-*O*-sulfonato)-α-D- galactopyranan, whilst the one from *K. alvarezii* was demonstrated to be →4)-4-*O*-sulfonato-(2-*O*-methyl)-β-Dgalactopyranosyl-(1→4)-3, 6-anhydro-(2-*O*-methyl)-α-D-galactopyranan.

The sulfated galactopyran motif derived from *G. opuntia* possessed significant anti-diabetic properties as identified by α-amylase (**GO-2:** IC_{50} 0.04 mg/mL), α-glucosidase (**GO-2:** IC_{50} 0.09 mg/mL) and dipeptidyl peptidase-4 (**GO-2:** IC_{50} 0.09 mg/mL) inhibitory activities. The sulfated galactans from *G. opuntia* showed greater anti-inflammatory inhibitory activities as determined by cyclooxygenase-1 (**GO-2:** COX-1, IC_{50} 0.01 mg/mL), cyclooxygenase-2 (**GO-2:** COX-2, IC_{50} 0.03 mg/mL) and 5-lipoxygenase inhibitory activities (**GO-2:** IC_{50} 0.24 mg/mL). This study revealed that

the sulfated polygalactan enriched concentrate from *G. opuntia* could be used as potential therapeutic candidate to suppress the hyperglycemic response in diabetic conditions and inflammatory activity.

Two sulfated polygalactan derivatives characterized as 1, 3-*O*-diacetyl-2, 5, 6-tri hydroxyl-β-D-galactose-4-sulfate (**KA-3$_A$**) and 1, 3, 5-*O*-triacetyl-4-hydroxyl-6-*O*-methyl-D-galactose-2-sulfate (**GO-3$_A$**), were furthermore purified from *K. alvarezii* and *G. opuntia*, respectively, and were spectroscopically characterized. The compound **KA-3$_A$** showed absorption bands at 1712 cm^{-1} in the Fourier Transform Infrared (FTIR) spectrum due to the carbonyl functionalities. The molecular ion peak at *m/z* 345 in combination with its ^{1}H and ^{13}C NMR data designated the elemental composition of the compound **KA-3$_A$** as $C_{10}H_{17}O_{11}S$. The compound **GO-3$_A$** showed molecular ion peak at *m/z* 401, which in combination with its ^{1}H and ^{13}C NMR data designated the elemental composition of the compound **GO-3$_A$** as $C_{13}H_{21}O_{12}S$. The polygalactan from *K. alvarezii* (**KA-3**) showed greater inhibitory properties against angiotensin-I (IC_{50} 0.04 mg/mL) in comparison with polygalactan from *G. opuntia* (**GO-3**: IC_{50} 0.07 mg/mL). The anti-diabetic potential of polygalactan (**KA-3**), measured in terms of the inhibitory activities against dipeptidyl peptidase-4 was found to be greater (**KA-3:** IC_{50} 0.17 mg/mL) when compared with standard diprotein-A (IC_{50} 0.24 mg/mL). Likewise, the polygalactan derivatives showed higher α-amylase inhibitory activities (**KA-3:** $IC_{50} < 1$ mg/mL) when compared with the standard acarbose (IC_{50} 1.39 mg/mL).

Marine macroalgae-derived bioactive leads with potential therapeutic properties demonstrated to possess advantageous as functional food with added health benefits. Novel secondary bioactive metabolites from the marine macroalgae are attracting attention because of the growing demand for new compounds of 'marine natural' origin, having potential applications in pharmaceutical fields, and concerns about the toxic effects by synthetic drugs and their derivatives. Considering the promising perspective for the utilization of these groups of organisms, and limited research reports on their utilization as potential health food, their pharmaceutical potential began to receive considerable attention. The present study envisaged a systematic approach involving chemical profiling of two major species of red marine macroalgae *K. alvarezii* and *G. opuntia*, for bioactive pharmacophore leads for activity against various oxidative stress-induced diseases with a focus on hypertension, diabetes, inflammation, and a library of small molecular weight compounds with bioactive potential. The lead molecules were isolated to homogeneity and characterized using combined

chromatographic and spectroscopic experiments, whereas the novel leads were validated through bioassay and structure-activity relationship analyses to enrich the pool of bioactive leads. This research work also developed protocols to isolate and characterize polysaccharide compounds with bioactive properties against various drug targets for use against hypertension, diabetes, antioxidants and inflammatory pathologies. Furthermore, the discovery of new bioactive compounds from marine metabolites will form the basis for new drug leads. Thus, the new compounds will absolutely compose an abundant resource for future bioactivity research and drug development.

REFERENCES

Abad MJ, Bedoya LM, Bermejo P (2008). Natural marine anti-inflammatory products. Mini Review in Medicinal Chemistry, 8:740-754.

Abdel-Mageed WM, Ebel R, Valeriote FA, Jaspars M (2010). Laurefurenynes A-F, new cyclic ether acetogenins from a marine red alga, *Laurencia* sp. Tetrahedron, 66:2855-2862.

Abu Soud RS, Hamdan II, Afifi FU (2004). Alpha amylase inhibitory activity of some plant extracts with hypoglycemic activity. Scientia Pharmaceutica, 72:25-53.

Aguillar F, Crebelli R, Dusemund B, Galtier P, Gilbert J, Gott DM, Gundert-Remi U, Koenig J, Lambre C, Leblanc JC, Mortensen A, Mossesso P, Parent-Massin D, Rietjens IMCM, Stankovic I, Tobbcak P, Waalkens-Berendsen I, Woutersen RA, Wright M (2012). Scientific opinion on the re-evaluation of butylated hydroxytoluene BHT (E321) as a food additive. European Food Safety Authority Journal, 10:2392-2588.

Aknin M, Samb A, Mirailles J, Costantino V, Fattorusso E, Mangoni A (1992). Polysiphenol, a new brominated 9, 10-dihydrophenanthrene from the Senegalese red alga *Polysyphonia ferulacea*. Tetrahedron Letters, 33:555-558.

Alarif WM, Al-Lihaibi SS, Abdel-Lateff A, Ayyad SE (2011). New antifungal cholestane and aldehyde derivatives from the red alga *Laurencia papillosa*. Natural Product Communication, 6:1821-1824.

Allan RD, Correl RL, Wells RJ (1969). A new class of quinones from certain members of the family *Cyperaceae*. Tetrahedron Letters, 53:4669-4672.

Aller MA, Arias JL (2006). The inflammatory response: An efficient way of life. Medical Science Monitor, 12:225-234.

Ames BN, Shinenaga MK, Hagen TM (1993). Oxidants antioxidants and the degenerative diseases of aging. Proceeding of the National Academy of Sciences, USA, 90:7915-7922.

Amico V, Caccamese S, Neri P, Russo G, Foti M (1991). Brasilane type sesquiterpenoids from the Mediterranean red alga *Laurencia obtusa*. Phytochemistry, 30:1921-1927.

Ananthi S, Rao H, Raghavendran B, Sunil AG, Gayathri V, Ramakrishnan G (2010). *In vitro* antioxidant and *in vivo* anti-inflammatory potential of crude

polysaccharide from *Turbinaria ornata* (Marine Brown Alga). Food and Chemical Toxicology, 48:187-192.

Anton R, Barlow S, Boskou D, Castle L, Crebelli R, Dekant W, Engel KH, Forsythe S, Grunow W, Larsen JC, Leclercq C, Mennes W, Milana MR, Rietjens I, Svensson K, Tobback P, Toldra F (2004). Opinion of the scientific palen on food additives, flavourings, processing aids and materials in contact with food on a request from the commission related to tertiary-butylhidroquinone (TBHQ). European Food Safety Authority Journal, 84:1-50.

Antunes AM, Afolayan AF, Chiwakata MT, Fakee J, Knott MG, Whibley CE, Hendricks DT, Bolton JJ, Beukes DR (2011). Identification and *in vitro* anti-esophageal cancer activity of a series of halogenated monoterpenes isolated from the South African seaweeds *Plocamium suhrii* and *Plocamium cornutum*. Phytochemistry, 72:769-772.

Apostolidis E, Karayannakidis PD, Kwon YI, Lee CM, Seeram NP (2011). Seasonal variation of phenolic antioxidant-mediated α-glucosidase inhibition of *Ascophyllum nodosum*. Plant Foods for Human Nutrition, 66:313-319.

Ashokkumar R, Ramaswamy M (2014). Phytochemical screening by FTIR spectroscopic analysis of leaf extracts of selected Indian medicinal plants. International Journal of Current Microbiology and Applied Sciences, 3:395-406.

Ask EI, Azanza RV (2002). Advances in cultivation technology of commercial eucheumatoid species: A review with suggestions for future research. Aquaculture, 206:257-277.

Astill BD, Fassett DW, Roudabush RL (1959). The metabolism of 2:4:5 trihydroxybutyrophenone in the rat and dog. Biochemical Journal, 72:451-459.

Ayyad SE, Al-Footy KO, Alarif WM, Sobahi TR, Bassaif SA, Makki MS, Asiri AM, Al Halwani AY, Badria AF, Badria FA (2011). Bioactive C_{15} acetogenins from the red alga *Laurencia obtusa*. Chemical and Pharmaceutical Bulletin, 59:1294-1298.

Bandoniene D, Murkovic M (2002). On-line HPLC-DPPH screening method for evaluation of radical scavenging phenols extracted from apples (*Malus domestica L*). Journal of Agricultural Food Chemistry, 50:2482-2487.

Bansemir A, Blume M, Schroder S, Lindequist U (2006). Screening of cultivated seaweeds for antibacterial activity against fish pathogenic bacteria. Aquaculture, 252:79-84.

Baruchel S, Wainberg MA (1992). The role of oxidative stress in disease. American Journal of Gastroenterology, 81:907-919.

Baylac S, Racine P (2003). Inhibition of 5-lipoxygenase by essential oils and other natural fragment extracts. International Journal of Aromatherapy, 13:138-142.

Bellion C, Brigand G, Prome JC, Welti D, Bociek S (1983). Identification characterization des precurseurs biologiques des carraghenanes par spectroscopie. Carbohydrate Research, 119:31-48.

Berge JP, Debiton E, Dumay J, Durand P, Barthomeuf C (2002). *In vitro* anti-inflammatory and anti-proliferative activity of sulfolipids from the red alga *Porphyridium cruentum*. Journal of Agricultural and Food Chemistry, 50:6227-6232.

Bilan MI, Grachev AA, Ustuzhanina NE, Shashkov AS, Nifantiev NE, Usov AI (2004). A highly regular fraction of a fucoidan from the brown seaweed *Fucus distichus L*. Carbohydrate Research, 339:511-517.

Bitencourt Fda S, Figueiredo JG, Mota MR, Bezerra CC, Silvestre PP, Vale MR, Nascimento KS, Sampaio AH, Nagano CS, Saker-Sampaio S (2008). Antinociceptive and anti-inflammatory effects of a mucin-binding agglutinin isolated from the red marine alga *Hypnea cervicornis*. Naunyn Schmiedebergs Archives of Pharmacology, 377:139-148.

Blackman J, Matthews DJ (1982). Halogenated phloroglucinols from *Rhabdonia verticillata*. Phytochemistry, 21:2141-2142.

Blondin C, Fischer E, Boisson-Vidal C, Kazatchkine MD, Jozefonvicz J (1994). Inhibition of complement activation by natural sulfated polysaccharides (fucans) from brown seaweed. Molecular Immunology, 31:247-253.

Blouin NA, Brodie JA, Grossman AC, Xu P, Brawley SH (2011). Porphyra: A marine crop shaped by stress. Trends in Plant Science, 16:29-37.

Blunt JW, Copp BR, Hu W, Munro MHG, Northcote PT, Prinsep M (2008). Marine natural products. Natural Product Report, 25:35-94.

Blunt JW, Copp BR, Keyzers RA, Munro MHG, Prinsep MR (2014). Marine natural products. Natural Product Report, 31:160-258.

Blunt JW, Copp BR, Munro MHG, Northcote PT, Prinsep M (2005). Marine natural products. Natural Product Report, 22:15-61.

Blunt JW, Copp BR, Munro MHG, Northcote PT, Prinsep MR (2006). Marine natural products. Natural Product Report, 23:26-78.

Blunt JW, Hartshorn MP, McLennan TJ, Munro MHG, Robinson WT, Yorke SC (1978). Thyrsiferol: A squalene-derived metabolite of *Laurencia thyrsifera*. Tetrahedron Letters, 1:69-72.

Blunt JW, Lake RJ, Munroe MHG, Yorke SC (1981). A new vinyl acetylene from the red alga *Laurencia thyrsifera.* Australian Journal of Chemistry, 34:2393-2400.

Blunt JW, Copp BR, Keyzers RA, Munro MH, Prinsep MR (2016). Marine natural products. Natural Product Report, 33:382-431.

Brennan MR, Erickson KL (1982). Austradiol acetate and austradiol diacetate, 4,6-dihydroxy-(+)-selinane derivatives from an Australian *Laurencia* sp. Journal of Organic Chemistry, 47:3917-3921.

Burreson BJ, Woolard FX, Moore RE (1975). Chondrocole A and B, two halogenated dimethylhexahydrobenzofurans from the red alga *Chondrococcus hornemanni* (mertens) Schmitz. Tetrahedron Letters, 26:2155-2158.

Burritt RL, Hahn T, Schaltegger St (2002). Towards a comprehensive framework for environmental management accounting-links between business actors and environmental management accounting tools. Australian Accounting Review, 12:39-50.

Buschmann AH, Correa JA, Westermeier R, Hernandez-Gonzalez MC, Norambuena R (2001). Red algal farming in chile: A review. Aquaculture, 194:203-220.

Caccamese S, Azzolina R, Duesler EN, Paul IC, Rinehart KL (1980). Laurencienyne, a new acetylenic cyclic ether from the marine red alga *Laurencia obtuse*. Tetrahedron Letters, 21:2299-2302.

Cafieri F, Ciminiello P, Santacroce C, Fattorusso E (1982). (1S)-1, 2-Dihydro-1-hydroxybromosphaerol, a minor bromoditerpene from the red alga *Sphaerococcus coronopifolius.* Phytochemistry, 21:2412-2413.

Cafieri F, Ciminiello P, Santacroce C, Fattorusso E (1983). Three diterpenes from the red alga *Sphaerococcus coronopifolius*. Phytochemistry, 22:1824-1825.

Cafieri F, De Napoli L, Fattorusso E, Impellizzeri G, Piattelli M, Sciuto S (1977). Bromosphaerodiol, a minor bromo compound from the red alga *Sphaerococcus coronopifolius.* Experientia, 33:1549-1550.

Cahyana AH, Shuto Y, Kinoshita Y (1992). Pyropheophytin as an antioxidative substance from the marine algae, *Arame* (*Eisenia bicyclis*). Bioscience Biotechnology and Biochemistry, 56:1533-1535.

Cai YZ, Mei S, Jie X, Luo Q, Corke H (2006). Structure-radical scavenging activity relationships of phenolic compounds from traditional Chinese medicinal plants. Life Sciences, 78:2872-2888.

Capon R, Ghisalberti EL, Jefferies PR, Skelton BW, White AH (1981). Sesquiterpene metabolites from *Laurencia filiformis*. Tetrahedron, 37:1613-1621.

Cardellina JH, Horsley SB, Clardy J, Leftow SR, Meinwald J (1982). Secondary metabolites from the red alga *Laurencia intricata*: Halogenated enynes. Canadian Journal of Chemistry, 60:2675-2677.

Carocho M, Ferreira ICFR (2013). A review on antioxidants, prooxidants and related controversy: Natural and synthetic compounds, screening and analysis methodologies and future perspectives. Food and Chemical Toxicology, 51:15-25.

Carter GT, Rinehart KL, Jr, Li LH, Kuentzel SL (1978). Brominated indoles from *Laurencia brongniartii*. Tetrahedron Letters, 46:4479-4482.

Cases MR, Cerezo AS, Stortz CA (1995). Separation and quantitation of enantiomeric galactoses and their mono-*O*-methylethers as their diastereomeric acetylated 1-deoxy-1-(2- hydroxypropylamino) alditols. Carbohydrate Research, 269:333-341.

Castro P, Huber ME (2013). Marine biology. McGraw-Hill, New York, pp 102-113.

Cavalcante-Silva LH, da Matta CB, de Araujo MV, Barbosa-Filho JM, de Lira DP, de Oliveira Santos BV, de Miranda GE, Alexandre-Moreira MS (2012). Ceptive and anti-inflammatory activities of crude methanolic extract of red alga *Bryothamnion triquetrum*. Marine Drugs, 10:1977-1992.

Cen Pacheco F, Villa–Pulgarin JA, Mollinedo F, Norte Martın M, Fernandez JJ, Daranas AH (2011). New polyether triterpenoids from *Laurencia viridis* and their biological evaluation. Marine Drugs, 9:2220-2235.

Chakraborty K, Joseph D (2013). Antioxidant activities and phenolic contents of three red seaweeds (Division: Rhodophyta) harvested from the Gulf of Mannar of Peninsular India. Journal of Food Science and Technology, 52:1924-1935.

Chakraborty K, Joseph D, Chakkalakal SJ (2014). Toxicity profile of a nutraceutical formulation derived from green mussel *Perna viridis*. BioMed Research International, 2016:1-14.

Chakraborty K, Joseph D, Joy M, Raola VK (2016). Characterization of substituted aryl meroterpenoids from red seaweed *Hypnea musciformis* as potential antioxidants. Food Chemistry, 212:778-788.

Chakraborty K, Joseph D, Praveen NK (2015). Antioxidant activities and phenolic contents of three red seaweeds (Division: Rhodophyta) harvested from the Gulf of Mannar of Peninsular India. Journal of Food Science and Technology, 52:1924-1935.

Chakraborty K, Lipton AP, Paulraj R, Chakraborty RD (2010). Guaiane sesquiterpenes from seaweed *Ulva fasciata Delile* and their antibacterial properties. European Journal of Medicinal Chemistry, 45:2237-2244.

Chakraborty K, Paulraj R (2010). Sesquiterpenoids with free-radical scavenging properties from marine macroalga *Ulva fasciata Delile*. Food Chemistry, 122:31-41.

Chandrasekaran S, Nagendran AN, Pandiaraja D, Krishnankutty N, Kamalakannan B (2008). Bioinvasion of *Kappaphycus alvarezii* on corals in the Gulf of Mannar, India. Current Science, 94:1167-1172.

Chapman V, Chapman DJ (1980). Sea vegetables (algae as food for man). In Seaweeds and their Uses, pp 62-97.

Charles DH, Babajide OO, Donna VE, David M, Jon C (1980). Vafzelin, uvafzelin novel constituents of *Uvaria afzelii*. Journal of the American Chemical Society, 102:7365-7367.

Chatter R, Ben Othman R, Rabhi S, Kladi M, Tarhouni S, Vagias C, Roussis V, Guizani-Tabbane L, Kharrat R (2011). *In vivo* and *in vitro* anti-inflammatory activity of neorogioltriol, a new diterpene extracted from the red algae *Laurencia glandulifera*. Marine Drugs, 9:1293-1306.

Chaves Lde S, Nicolau LA, Silva RO, Barros FC, Freitas AL, Aragao KS, Ribeiro Rde A, Souza MH, Barbosa AL, Medeiros JV (2013). Antiinflammatory and antinociceptive effects in mice of a sulfated polysaccharide fraction extracted from the marine red algae *Gracilaria caudata*. Immunopharmacology Immunotoxicology, 35:93-100.

Chen D, Wu XZ, Wen ZY (2008). Sulfated polysaccharides and immune response: Promoter or inhibitor. Panminerva Medica, 50:177-183.

Chen Q, Ke L, Song K, Huang H, Liu X (2004). Inhibitory effects of hexylresorcinol and dodecylresorcinol on mushroom (*Agaricus bisporus*) tyrosinase. The Protein Journal, 23:135-141.

Cheng JF, Ishikawa A, Ono Y, Thomas A, Alex N (2003). Novel chromen derivatives as TNF-α inhibitors. Bioorganic and Medicinal Chemistry Letters, 13:3647-3650.

Chevolot-Magueur M, Cave A, Potier P, Teste J, Chiaroni A, Riche C (1976). Composes bromes de *Rytiphlea tinctoria* (Rhodophyceae). Phytochemistry, 15:767-771.

Chew YL, Lim YY, Omar M, Khoo KS (2008). Antioxidant activity of three edible seaweeds from two areas in South East Asia. LWT Food Sciences and Technology, 41:1067-1072.

Chiovitti A, Bacic A, Craik DJ, Kraft GT, Liao ML, Falshaw R (1998). A pyruvated carrageenann from Australian specimens of the red alga *Sarconema filiforme*. Carbohydrate Research, 310:77-83.

Cho M, Han JH, You S (2011). Inhibitory effects of fucan sulfates on enzymatic hydrolysis of starch. Food Science and Technology, 44:1164-1171.

Choi EM, Kim AJ, Kim YO, Hwang JK (2005). Immunomodulating activity of arabinogalactan and focoidan *in vitro*. Journal of Medicinal Food, 8:446-453.

Christoph QS, Messmer Ruth, Bracher Franz, Krauss Jurgen (2007). A new approach to furan-containing macrolactones. Turkish Journal of Chemistry, 31:251-256.

Cinq-Mars CD, Hu C, Kitts DD, Li-Chan EC (2008). Investigations into inhibitor type and mode, simulated gastrointestinal digestion, and cell transport of angiotensin-I converting enzyme-inhibitory peptides in pacific hake (*Meriuccius productus*) fillet hydrolysate. Journal of Agricultural Food Chemistry, 56:410-419.

Clausen DJ, Wan S, Floreancig PE (2011). Total synthesis of the protein phosphatase 2A inhibitor lactodehydrothyrsiferol. Angewandte Chemie International Edition, 50:5178-5181.

Combaut G, Chantraine JM, Teste J, Soulier J, Glombitza KW (1978). Structure et conformation du dihydro-10, 15 tribromo-1, 6, 11 hexamethoxy-2, 3, 7, 8, 12, 13-5h-tribenzo [a,d,g] cyclononene. Tetrahedron Letters, 19:1699-1701.

Conforty F, Loizzo MR, Statty GA, Menichini F (2005). Comparative radical scavenging and antidiabetic activities of methanolic extract and fractions from *Achillea ligustica*. Biological and Pharmaceutical Bulletin, 28:1791-1794.

Cordero PA (2003). Encyclopedia of Food Sciences and Nutrition (Second Edition) 2003, pp 3726-3728.

Cornish ML, Garbary DJ (2010). Antioxidants from macroalgae: Potential applications in human health and nutrition. Algae, 25:155-171.

Cox PJ, Imre S, Islimyeli S, Thomson RH (1982). Obtusallene I, a new halogenated allene from *Laurencia Obtusa*. Tetrahedron Letters, 23:579-580.

Crews P (1977). Monoterpene halogenation by the red alga *Plocamium oregonum*. Journal of Organic Chemistry, 42:2634-2639.

Crews P, Kho-Wiseman E (1977). Acyclic polyhalogenated monoterpenes from the red algae *Plocamium violaceum*. Journal of Organic Chemistry, 42:2812-2815.

Crews P, Kho-Wiseman E, Montana P (1978). Halogenated alicyclic monoterpenes from the red algae (*Plocamium cartilagineum, Plocamium violaceum*). Journal of Organic Chemistry, 43:116-120.

Critchley AT, Ohno M (1998). Seaweed resources of the world. Yokosuka, Japan, Japan International Cooperation Agency, pp 429.

Crook M (2004). Type 2 diabetes mellitus: A disease of the innate immune system an update. Diabetic Medicine, 21:203-207.

Cumashi A, Ushakova NA, Preobrazhenskaya MEA (2007). Comparative study of the anti-inflammatory, anticoagulant, antiangiogenic, and antiadhesive activities of nine different fucoidans from brown seaweeds. Glycobiology, 17:541-552.

Daigo K (1959). Constituents of *Chondria arnata I*. Detection of anthelmintic constituents. Yakuga Zasshi, 79:350-353.

Davis SN, Granner DK (2001). Insulin, oral agents and the pharmacology of the endocrine pancreas. In: Hardman JG, Limbird LE, Gilman AG, editors. Goodman and Gilman's the pharmacological basis of therapeutics. 10th ed. New York: McGraw-Hill Co. Incorp, pp 1679-1714.

Davyt D, Fernandez R, Suescun L, Mombru AW, Saldana J, Dominguez L, Coll J, Fujii MT, Do Manta E (2001). New sesquiterpene derivatives from the red alga *Laurencia scoparia*. Isolation, structure determination and anthelmintic activity. Journal of Natural Product, 64:1552-1555.

De Sousa AA, Benevides NM, de Freitas Pires A, Fiuza FP, Queiroz MG, Morais TM, Pereira MG, Assreuy AM (2013). Galactan from marine alga *Gelidium crinale* with *in vivo* anti-inflammatory and antinociceptive effects. Fundamental and Clinical Pharmacology, 27:173-180.

De Souza MCR, Marques CT, Dore CMG, Da Silva FRF, Rocha HAO, Leite E (2007). Antioxidant activities of sulphated polysaccharides from brown and red seaweeds. Journal of Applied Phycology, 19:153-160.

De-Nys R, Wright AD, Konig GM, Sticher (1993). New halogenated furanones from the marine alga *Delisea pulchra* (cf. fmbriata). Tetrahedron, 49:11213-11220.

Dodgson KS (1961). Determination of inorganic sulphate in studies on the enzymic and non-enzymic hydrolysis of carbohydrate and other sulphate esters. Biochemical Journal, 78:312-319.

Dong HQ, Li M, Zhu F, Liu FL, Huang JB (2012). Inhibitory potential of trilobatin from *Lithocarpus polystachyus* Rehd against α-glucosidase and α-amylase linked to type 2 diabetes. Food Chemistry, 130:261-266.

Dubois M, Gilles KA, Hamilton JK, Rebers PA, Smith F (1956). Colorimetric method for determination of sugar and related substances. Analytical Chemistry, 28:350-356.

Dunlop RW, Murphy PT, Wells RJ (1979). A new polyhalogenated monoterpene from the red alga *Plocamium angustum*. Australian Journal of Chemistry, 32:2735-2739.

Ebada SS, Lin WH, Proksch P (2010). Bioactive sesterterpenes and triterpenes from marine sponges: Occurrence and pharmacological significance. Marine Drugs, 8:313-346.

Elliot RH, Strunin L (1993). Hepatotoxicity of volatile anaesthetics. British Journal of Anaesthaesia, 70:339-349.

Erickson KL (1983). Constituents of *Laurencia*. In: Scheuer PJ (ed) Marine Natural Products: Chemical and Biological Perspectives. Academic Press, New York, NY, pp 131-257.

Escrig AJ, Jimenez IJ, Pulido R, Calixto FS (2001). Antioxidant activity of fresh and processed edible seaweeds. Journal of the Science of Food and Agriculture, 81:530-534.

Evan AP, Gardner KD (1979). Nephron obstruction in nordihydroguaiaretic acid induced renalcystic disease. Kidney International, 15:7-19.

Farah Diyana A, Abdullah A, Shahrul Hisham ZA, Chan KM (2015). Antioxidant activity of red algae *Kappaphycus alvarezii* and *Kappaphycus striatum*. International Food Research Journal, 22:1977-1984.

Faulkner DJ (1984). Marine natural products: Metabolites of marine algae and herbivorous marine mollusks. Natural Product Reports, 1:251-280.

Fenical W, Schulte GR, Finer J, Clardy J (1978). Poitediol, a new nonisoprenoid sesquiterpene diol from the marine alga *Laurencia poitei*. Journal of Organic Chemistry, 43:3628-3630.

Ferreira ALG, Loureiro S, Soares AMVM (2012). Toxicity prediction of binary combinations of cadmium, carbendazim and low dissolved oxygen on *Daphniamagna.* Aquatic Toxicology*,* 89:28-39.

Festa AD, Agostino R, Howard G, Mykkanen L, Tracy, RP, Haffner SM (2000). Chronic subclinical inflammation as part of the insulin resistance syndrome: The Insulin Resistance Atherosclerosis Study (IRAS). Circulation, 102:42-47.

Fitz Gerald GA (2004). Coxibs and cardiovascular disease. The New England Journal of Medicine, 351:1709-1711.

Fleurence J (1999). Seaweed proteins: Biochemical, nutritional aspects and potential uses. Trends in Food science and Technology, 102:5-28.

Florence TM (1995). The role of free radicals in disease. Australian and New Zealand Journal of Ophthalmology, 23:3-7.

Fosslien E (2005). Cardiovascular complications of non-steroidal anti-inflammatory drugs. Annals of Clinical and Laboratory from red seaweed *Hypnea musciformis* as potential antioxidants. Food Chemistry, 212:778-788.

Fournet I, Gall EA, Deslandes E, Huvenne JP, Sombret B, Floch JY (1997). *In situ* measurements of cell wall components in the red alga *Solieria chordalis* (Solieriaceae, Rhodophyta) by FTIR micro spectrometry. Botanica Marina, 40:45-48.

Frias JP, Sobral P, Ferreira AM (2010). Organic pollutants in microplastics from two beaches of the Portuguese coast. Marine Pollution Bulletin, 60:1988-1992.

Fry DE (1992). Multiple system organ failure. In: Fry DE (ed). Mosby year book, St Louis, Missouri, pp 3-14.

Fukuzawa A, Kumagai Y, Masamune T, Furusaki A, Katayama C, Matsumoto T (1981). Acetylpinnasterol and pinnasterol, ecdysone-like metabolites, from the

marine red alga *Laurencia pinnata* Yamada. Tetrahedron Letters, 22:4085-4086.

Fukuzawa A, Kumagai Y, Masamune T, Furusaki A, Matsumoto T, Katayama C (1982). Pinnaterpenes A, B and C: New dibromoditerpenes from the red algal *Laurencia pinnata* Yamada. Chemistry Letters, 11:1389-1392.

Fukuzawa, Masamune T (1981). Laurepinnacin and isolaurepinnacin, new acetylenic cyclic ethers from the marine red alga *Laurencia pinnata* Yamada. Tetrahedron Letters, 22:4081-4084.

Ganesan P, Chandini SK, Bhaskar N (2008). Antioxidant properties of methanol extract and its solvent fractions obtained from selected Indian red seaweeds. Bioresource Technology, 99:2717-2723.

Ganesan S, Thiruppathi K, Eswaran CRK, Reddy B, Jha (2009). Cultivation of *Gelidiella acerosa* in the open sea on the southeastern coast of India. Marine Ecology Progress Series, 382:49-57.

Gershenzon J, Dudareva N (2007). The function of terpene natural products in the natural world. Nature Chemical Biology, 3:408-414.

Gharavi N, El-Kadi AOS (2005). Tert-Butylhydroquinone is a novel aryl hydrocarbon receptor ligand. Drug Metabolism and Disposition, 33:365-372.

Gomez-ordonez E, Rupere P (2011). FT-IR-ATR spectroscopy as a tool for polysaccharide identification in edible brown and red seaweeds. Food Hydrocolloids, 25:1514-1520.

Gonzalez AG, Aguiar JM, Darias J, Gonzalez E, Martin JD, Martin VS, Perez C, Fayos J, Martinez-Ripoll M (1978). Perforenol, a new polyhalogenated sesquiterpene from *Laurencia perforate*. Tetrahedron Letters, 19:3931-3934.

Gonzalez AG, Martin JD, Martin VS, Martinez-Ripoll M, Fayos J (1979a). X ray study of sesquiterpene constituents of the alga *Laurencia obtusa* leads to structure revision. Tetrahedron Letters, 20:2717-2718.

Gonzalez AG, Martin JD, Martin VS, Norte M (1979b). Carbon-13 NMR application to *Laurencia* polyhalogenated sesquiterpenes. Tetrahedron Letters, 20:2719-2722.

Gonzalez AG, Martin JD, Ptrez C, Ramirez MA, Ravelo P (1980). Total synthesis of 8-desoxy-isocaespitol, a new polyhalogenated sesquiterpene from *Laurencia caespitosa.* Tetrahedron Letters, 21:187-188.

Gonzalez G, Martin JD, Martin VS, Norte M, Perez R, Ruano JZ, Drexler SA, Clardy J (1982). Non-terpenoid C-15 metabolites from the red seaweed *Laurencia pinnatifida*. Tetrahedron, 38:1009-1014.

Gonzalez R, Rodriguez S, Romay C, Ancheta O, Gonzalez A, Armesta J, Remirez D, Merino N (1999). Anti-inflammatory activity of phycocyanin extract in acetic acid-induced colitis in rats. Pharmacological Research, 39:55-59.

Gregson RP, Marwood JF, Quinn RJ (1979). The occurrence of prostaglandins PGE_2 and $PGF_{2\alpha}$ in a plant-the red alga *Gracilaria lichenoides*. Tetrahedron Letters, 20:4505-4506.

Gressler V, Yokoya NS, Fujii MT, Colepicolo P, Mancini J, Torres RP, Pinto E (2010). Lipid, fatty acid, protein, amino acid and ash contents in four Brazilian red algae species. Food Chemistry, 120:585-590.

Guiry MD, Guiry GM (2016). Algae Base World-wide electronic publication. Galway: National University of Ireland.

Gutierrez-Cepeda A, Fernandez JJ, Gil LV, Opez- Rodrıguez ML, Norte M, Souto LM (2011a). Nonterpenoid C_{15} acetogenins from *Laurencia marilzae*. Journal of Natural Product, 74:441-448.

Gutierrez-Cepeda A, Fernandez JJ, Norte M, Souto ML (2011b). New Bicyclotridecane C_{15} Nonterpenoid Bromoallenes from *Laurencia marilzae*. Organic Letters, 13:2690-2693.

Guven KC, Bora A, Sunam G (1969). Alkaloid content of Marine algae. I. Hordenine from *Phyllophera nervosa*. Eczacihk Bulletin, 11:177-184.

Guven KC, Percot A, Sezik E (2010). Alkaloids in marine algae. Marine Drugs, 8:269-284.

Hamdan II, Afifi FU (2004). Studies on the *in vitro* and *in vivo* hypoglycemic activities of some medicinal plants used in treatment of diabetes in Jordanian traditional medicine. Journal of Ethnopharmacology, 93:117-121.

Hansch C, Caldwell J (1991). The structure-activity relationship of inhibitors of serotonin uptake and receptor binding. Journal of Computer Aided Molecular Design, 5:441-453.

Heo SJ, Cha SH, Lee KW, Jeon YJ (2006). Antioxidant activities of red algae from Jeju Island. Korean Society of Phycology, 21:149-156.

Higgs MD, Mulheirn LJ (1981). Hybridalactone, An unusual fatty acid metabolite from the red alga *Laurencia hybrida* (Rhodophyta, Rhodomelaceae). Tetrahedron, 37:4259-4262.

Higgs MD, Vanderah DJ, Faulkner DJ (1977). Polyhalogenated monoterpenes from *Plocamium cartilagineum* from the British coast. Tetrahedron, 33:2775-2780.

Holdt SL, Kraan S (2011). Bioactive compounds in seaweed: Functional food applications and legislation. Journal of Applied Phycology, 23:543-597.

Horsley SB, Cardellina JH, Meinwald J (1981). Secondary metabolites from a red alga (*Laurencia intricate*): Sesquiterpene alcohols. Journal of Organic Chemistry, 46:5033-5035.

Horton R (2004). Vioxx, the implosion of Merck, and aftershocks at the FDA. The Lancet, 364:1995-1996.

Howard BM, Fenical W (1978a). Obtusadiol, a unique bromoditerpenoid from the marine red alga *Laurencia obtusa*. Tetrahedron Letters, 19:2453-2456.

Howard BM, Fenical W (1978b). Structures of the irieols, new dibromoditerpenoids of a unique skeletal class from the marine red alga *Laurencia irieii*. Journal of Organic Chemistry, 43:4401-4408.

Howard BM, Fenical W (1979). Guadalupol and epiguadalupol, rearranged sesquiterpene alcohols from *Laurencia snyderiae var. guadalupensis.* Phytochemistry, 18:1224-1225.

Howard BM, Fenical W (1980). Isoconcinndiol, a brominated diterpenoid from *Laurencia snyderae var. guadalupensis*. Phytochemistry, 19:2774-2776.

Howard M, Schulte GR, Fenical W, Solheim B, Clardy J (1980). Three new vinyl acetylenes from the marine red alga *Laurencia*. Terrahedron, 36:1747-1751.

Huang R, Mendis E, Kim SK (2005). Improvement of ACE inhibitory activity of chitooligosaccharides (COS) by carboxyl modifications. Bioorganic Medicinal Chemistry, 13:3649-3655.

Hulsmans M, Van Dooren E, Holvoet P (2012). Mitochondrial reactive oxygen species and risk of atherosclerosis. Current Atherosclerosis Reports, 14:264-276.

Idris I, Donnelly R (2007). Dipeptidyl peptidase-4 inhibitors: A major new class of oral antidiabetic drug. Diabetes, Obesity and Metabolism, 9:153-165.

Iliopoulou D, Vagias C, Harvala C, Roussis V (2002). C_{15} acetogenins from the red alga *Laurencia obtusa*. Phytochemistry, 59:111-116.

Islam MN, Ishita IJ, Jin SE, Choi RJ, Lee CM, Kim YS, Jung HA, Choi JS (2013). Anti-inflammatory activity of edible brown alga *Saccharina japonica* and its constituents pheophorbide A and pheophytin A in LPS-stimulated RAW 264.7 macrophage cells. Food Chemical Toxicology, 55:541-548.

Izac RR, Sims JJ (1979). Marine natural products. 18. Iodinated sesquiterpenes from the red algal genus *Laurencia*. Journal of American Chemical Society, 101:6136-6137.

Ji NY, Wen W, Li XM, Xue QZ, Xiao HL, Wang BG (2009). Brominated selinane sesquiterpenes from the marine brown alga *Dictyopteris divaricata*. Marine Drugs, 7:355-360.

Jiang RW, Ma SC, He ZD, Huang XS, But PPH, Wang H, Chan SP, Ooi VEC, Xu HX, Mak TCW (2002). Molecular structures and antiviral activities of naturally occurring and modified cassane furanoditerpenoids and friedelane triterpenoids from *Caesalpinia minax*. Bioorganic and Medicinal Chemistry, 10:2161-2170.

Jiao N, Herndl GJ, Hansell DA, Benner R, Kattner G, Wilhelm SW, Kirchman DL, Weinbauer MG, Luo T, Chen F, Azam F (2011). The microbial carbon pump and the oceanic recalcitrant dissolved organic matter pool. Nature Reviews Microbiology, 9:555.

Joy M, Chakraborty K (2017a). Biogenic antioxidative and anti-inflammatory aryl polyketides from the venerid bivalve clam *Paphia malabarica*. Food Chemistry, 237:169-180.

Joy M, Chakraborty K (2017b). Previously undescribed antioxidative and anti-inflammatory chromenyls bearing 3*H*-isochromenone and furanyl-2*H*-chromenyl skeletons from the venerid clam, *Paphia malabarica*. Medicinal Chemistry Research, 26:1708-1722.

Juagdan EG, Kalidindi R, Scheuer P (1997). Two new chamigranes from Hawaiian red alga, *Laurencia cartilaginea*. Tetrahedron, 53:521-528.

Jun JG, Gray GR (1987). A new catalyst for reductive cleavage of methylated glycans. Carbohydrate Research, 163:247-261.

Kain JM (1991). Cultivation of attached seaweeds, In: Guiry, M.D. et al. (Ed.) Seaweed resources in Europe: Uses and potential, pp 309-377.

Kamada T, Vairappan CS (2013). New bioactive secondary metabolites from Bornean red alga, *Laurencia similis* (Ceramiales). Natural Product Communication, 8:287-288.

Kanai Y, Hiroki S, Koshino H, Konoki K, Cho Y, Cayme M, Fukuyo Y, Yotsu-Yamashita M (2011). Identification of novel oxidized levuglandin D_2 in marine red alga and mouse tissue. Journal of Lipid Research, 52:2245-2254.

Kang HS, Chung HY, Jung HA, Son BW, Choi JS (2003). A new phlorotannins from the brown alga *Ecklonia stolonifera*. Chemical and Pharmaceutical Bulletin, 51:1012-1014.

Kang HS, Chung HY, Kim JY, Son BW, Jung HA, Choi JS (2004). Inhibitory phlorotannins from the edible brown alga *Ecklonia stolonifera* on total reactive oxygen species (ROS) generation. Archives of Pharmacal Research, 27:194-198.

Kang KA, Bu HD, Park DS, Go GM, Jee Y, Shin T, Hyun JW (2005). Antioxidant activity of ethanol extract of *Callophyllis japonica*. Phytotherapy Research, 19:506-510.

Kato T, Kumanireng AS, Ichinose I, Kitahara Y, Kakinuma Y, Kato Y (1975). Structure and synthesis of active component from a marine alga, *Sargassum*. Chemistry Letters, 4:335-338.

Kazlauskas R, Lidgard RO, Wells RJ (1978). New polybrominated metabolites from the red alga *Ptilonia australasica*. Tetrahedron Letters, 34:3165-3168.

Kazlauskas R, Murphy PT, Qulnn RJ, U1ells RJ (1977a). A new class of halogenated lactones from the red alga *Delisea fimhriata* (Bonnemaisoneaceae). Tetrahedron Letters, 1:37-40.

Kazlauskas R, Murphy PT, Wells RJ (1982a). A brominated metabolite from the red alga *Vidalia spiralis*. Australian Journal of Chemistry, 35:219-220.

Kazlauskas R, Murphy PT, Wells RJ, Baird-Lambert JA, Jamieson DD (1983). Halogenated pyrrolo [2,3-d] pyrimidine nucleosides from marine organisms. Australian Journal of Chemistry, 36:165-170.

Kazlauskas R, Murphy PT, Wells RJ, Blackman A (1982b). Macrocyclic enol-ethers containing an acetylenic group from the red alga *Phacelocarpus labillardieri*. Australian Journal of Chemistry, 35:113-120.

Kazlauskas R, Murphy PT, Wells RJ, Daly JJ, Oberhansli WE (1977b). Heterocladol, a halogenated selinane sesquiterpene of biosynthetic significance from the red alga *Laurencia filiformis*: Its isolation, crystal structure andabsolute configuration. Australian Journal of Chemistry, 30:2679-2687.

Kigoshi H, Ojika M, Shizuri Y, Niwa H, Yamada K (1982).(10R, 11R)-(+)-squalene-10, 11-epoxide: Isolation from *Laurencia okamurai* and the asymmetric synthesis. Tetrahedron Letters, 23:5413-5414.

Kigoshi H, Shizuri Y, Niwa H, Yamada K (1981). Laurencenyne, a plausible precursor of various nonterpenoid C_{15}-compounds, and neolaurencenyne from the red alga *Laurencia okamurai*. Tetrahedron Letters, 22:4729-4732.

Kim KT, Rioux LE, Turgeon SL (2014). Alpha-amylase and alpha-glucosidase inhibition is differentially modulated by fucoidan obtained from *Fucus vesiculosus* and *Ascophyllum nodosum*. Phytochemistry, 98:27-33.

Kim SK, Pangestuti R (2011). Biological activities and potential health benefits of fucoxanthin derived from marine brown algae. Advances in Food and Nutrition Research, 64:111-128.

Kim YJ, Kim EH, Hahm KB (2012). Oxidative stress in inflammation-based gastrointestinal tract diseases: Challenges and opportunities. Journal of Gastroenterolgy Hepatology, 27:1004-1010.

Kindleysides S, Quek SY, Miller MR (2012). Inhibition of fish oil oxidation and the radical scavenging activity of New Zealand seaweed extracts. Food Chemistry, 133:1624-1631.

King H, Aubert RE, Herman WH (1998). Global burden of diabetes, 1995-2025: Prevalence, numerical estimates and projections. Diabetes Care, 2:1414-1431.

King TJ, Imre S, Oztuns A, Thomson RH (1979). Obtusenyne, a new acetylenic nine-membrered cyclic ether from *Laurenica obtuse*. Tetrahedron Letters, 20:1453-1454.

Kirkup MP, Moore RE (1983). Indole alkaloids from the marine red alga *Martensia fragilis*. Tetrahedron Letters, 24:2087-2090.

Kiwitt-Haschemie K, Heims H, Steinhart H, Mischnick P (1993). The analysis of agarose by the reductive cleavage method. Carbohydrate Research, 248:267-275.

Kladi M, Vagias C, Furnari G, Moreau D, Roussakis C, Roussis V (2005). Cytotoxic cuparene sesquiterpenes from *Laurencia microcladia*. Tetrahedron Letters, 46:5723-5726.

Kladi M, Vagias C, Papazafiri P, Brogi S, Tafi A, Roussis V (2009). Tetrahydrofuran acetogenins from *Laurencia glandulifera*. Journal of Natural Product, 72:190-193.

Kladi M, Vagias C, Roussis V (2004). Volatile halogenated metabolites from marine red algae. Phytochemistry Review, 3:337-366.

Kladi M, Vagias C, Stavri M, Rahman MM, Gibbons S, Roussis V (2008). C_{15} acetogenins with antistaphylococcal activity from the red alga *Laurencia glandulifera*. Phytochemistry Letters, 1:31-36.

Kladi M, Xenaki H, Vagias C, Papazafiri P, Roussis V (2006). New cytotoxic sesquiterpenes from the red algae *Laurencia obtusa* and *Laurencia microcladia*. Tetrahedron, 62:182-189.

Kojima K, Ham T, Kato T (1980). Rapid chromatographic purification of dipeptidyl peptidase-IV in human submaxiallry gland. Journal of Chromatography, 189:233-240.

Konig GM, Wright AD (1997a). *Laurencia rigida*: Chemical investigations of its antifouling dichloromethane extract. Journal of Natural Product, 60:967-970.

Konig GM, Wright AD (1997b). Sesquiterpene content of the antibacterial dichloromethane extract of the marine red alga *Laurencia obtusa*. Planta Medica, 63:186-187.

Kornprobst JM (2005). Substances naturelles d origine marine. Chimiodiversite-Pharmacodiversite-Biotechnologie. 1. Generalites-Micro-organismes-Algues. Lavoisier, Paris.

Kubo I, Xiao P, Fujita K (2001). Antifungal activity of octyl gallate: Structural criteria and mode of action. Bioorganic and Medicinal Chemistry Letters, 11:347-350.

Kulisic T, Radonic A, Katalinic V, Milos M (2004). Use of different methods for testing antioxidative activity of oregano essential oil. Food Chemistry, 85:633-640.

Kumar KS, Ganesan K, Subba Rao PV (2008). Antioxidant potential of solvent extracts of *Kappaphycus alvarezii* (Doty) Doty edible seaweed. Food Chemistry, 107:289-295.

Kurata K, Amiya T (1977). Two new bromophenols from the red alga, *Rhodomela larix*. Chemistry Letters, 6:1435-1438.

Kurata K, Amiya T (1980). Bis (2, 3, 6-tribromo-4, 5-dihydroxybenzyl) ether from the red alga, *Symphyocladia latiuscula.* Phytochemistry, 19:141-142.

Kurata K, Furusaki A, Katayama C, Kikuchi H, Suzuki T (1981). A new labile sesqiterpene diol having bromine from the marine red alga *Laurencia nipponica* Yamada. Chemistry Letters, 10:773-776.

Kurata K, Furusaki A, Suehiro K, Katayama C, Suzuki T (1982). Isolaurallene, a new nonterpenoid C_{15}-bromoallene, from the red alga *Laurencia nipponica* Yamada. Chemistry Letters, 11:1031-1034.

Kurata K, Suzuki T, Suzuki M, Kurosawa E, Furusaki A, Matsumoto T (1983). Constituents of marine plants. Laurenical, a novel sesquiterpene α, β-unsaturated aldehyde from the red alga *Laurencia Nipponica* Yamada. Chemistry Letters, 3:299-300.

Kurata K, Taniguchi K, Agatsuma Y, Suzuki M (1998). Diterpenoid feeding-deterrents from *Laurencia saitoi*. Phytochemistry, 47:363-369.

Kurosawa E, Fukuzawa A, Irie T (1973). Isoprelaurefucin, new bromo compound from *Laurencia nipponica Yamada*. Tetrahedron Letters, 14:4135-4138.

Kwangwoo C, Song-Kyu P, Hwan Mook K, Yongseok C, Myung-Hwa K, Chun-Ho P, Bo-Young J, Tae Gyu C, Hyun-Moo C, Hee-Yoon L (2008). Chromen-based TNF-α converting enzyme (TACE) inhibitors: Design, synthesis, and biological evaluation. Bioorganic and Medicinal Chemistry, 16:530-535.

Larsen LN, Dahl E, Bremer J (1996a). Peroxidative oxidation of leucodichloroluorescein by prostaglandin H synthase in prostaglandin biosynthesis from polyunsaturated fatty acids. Biochimica et Biophysica Acta, 1299:47-53.

Laurienzo (2010). Marine polysaccharides in pharmaceutical applications: An overview. Marine Drugs, 8:2435-2465.

Leal MC, Munro MHG, Blunt JW, Puga J, Jesus B, Calado R (2013). Biogeography and biodiscovery hotspots of macroalgal marine natural products. Natural Product Report, 30:1380-1390.

Lee DS, Park WS, Heo SJ, Cha SH, Kim D, Jeon YJ, Park SG, Seo SK, Choi JS, Park SJ (2011). Polyopes affinis alleviates airway inflammation in a murine model of allergic asthma. Journal of Bioscience, 36:869-877.

Lee HJ, Dang HT, Kang GJ, Yang EJ, Park SS, Yoon WJ, Jung JH, Kang HK, Yoo ES (2009). Two enone fatty acids isolated from *Gracilaria verrucosa* suppress the production of inflammatory mediators by down-regulating NF kappa B and STAT1 activity in lipopolysaccharide-stimulated RAW 264.7 cells. Archives of Pharmacal Research, 32:453-462.

Lee SH, Han JS, Heo SJ, Hwang JY, Jeon YJ (2010). Protective effects of dieckol isolated from *Ecklonia cava* against high glucose-induced oxidative stress in human umbilical vein endothelial cells. Toxicology in Vitro, 24:375-381.

Leiro JM, Castro R, Arranz JA, Lamas J (2007). Immunomodulating activities of acidic sulphated polysaccharides obtained from the seaweed *Ulva rigid*a C. Agardh. International Journal of Immunopharmacology, 7:879-888.

Leonard F, Collnot EM, Lehr CM (2010). A three-dimensional coculture of enterocytes, monocytes and dendritic cells to model inflamed intestinal mucosa *in vitro*. Molecular Pharmaceutics, 7:2103-2119.

Li K, Li XM, Gloer JB, Wang BG (2011). Isolation, characterization and antioxidant activity of bromophenols of the marine red alga *Rhodomela confervoides*. Journal of Agricultural Food Chemistry, 59:9916-9921.

Li F, Harmer P, Glasgow R, Mack KA, Sleet D, Fisher KJ (2008). Translation of an effective Tai Chi intervention into a community-based falls prevention program. American Journal of Public Health, 98:1195-1198.

Liebgott T, Miollan M, Berchadsky Y, Drieu K, Culcasi M, Pietri S (2000). Complementary cardioprotective effects of flavonoid metabolites and terpenoid constituents of Ginkgo biloba extract (EGb 761) during ischemia and reperfusion. Basic Research in Cardiology, 95:368-377.

Lindsay RC (1996). Food additives. In: Fennema OR, editor. Food chemistry. New York: Marcel Dekker, pp 778-780.

Lipinski C, Hopkins A (2004). Navigating chemical space for biology and medicine. Nature, 432:855-861.

Liu L, Heinrich M, Myers S, Dworjanyn SA (2012). Towards a better understanding of medicinal uses of the brown seaweed *Sargassum* in traditional Chinese medicine: A phytochemical and pharmacological review. Journal of Ethnopharmacology, 142:591-619.

Lobo V, Phatak A, Chandra N (2010). Free radicals and functional foods: Impact on human health. Pharmacognosy Reviews, 4:118-126.

Lordan S, Ross RP, Stanton C (2011). Marine bioactives as functional food ingredients: Potential to reduce the incidence of chronic diseases**.** Marine Drugs, 9:1056-1100.

Luning K (1990). Seaweeds: Their Environment, biogeography and ecophysiology. New York, John Wiely and sons.

Maneesh A, Chakraborty K (2018). Pharmacological potential of sulfated polygalactopyranosyl-fucopyranan from the brown seaweed *Sargassum wightii*. Journal of Applied Phycology, 30:1971-1988.

Manefield M, de Nys R, Kumar N, Read R, Givskov M, Steinberg P, Kjelleberg S (1999). Evidence that halogenated furanones from *Delisea pulchra* inhibit acylated homoserine lactone (AHL) - mediated gene expression by displacing the AHL signal from its receptor protein. Microbiology, 145:283-291.

Manta E (2001). New sesquiterpene derivatives from the red alga *Laurencia scoparia*. Isolation, structure determination and anthelmintic activity. Journal Natural Product, 64:1552-1555.

Mariana Barbosa, Patricia Valentao, Paula B, Andrade (2014). Bioactive Compounds from Macroalgae in the New Millennium: Implications for Neurodegenerative Diseases. Marine Drugs, 12:4934-4972.

Masuda M, Abe T, Sato S, Suzuki T, Suzuki M (1997). Diversity of halogenated secondary metabolites in the red alga *Laurencia nipponica* (Rhodomelaceae, Ceramiales). Journal of Phycology, 33:196-208.

Mata L, Wright E, Owens L, Paul N de Nys R (2013). Water soluble natural products from seaweed have limited potential in controlling bacterial pathogens in fish aquaculture. Journal of Applied Phycology, 25:1963-1973.

Matanjun P, Suhaila M, Noordin MM, Kharidah M, Ming CH (2008). Antioxidant activities and phenolic content of eight species of seaweeds from North Borneo. Journal of Applied Phycology, 20:367-373.

Matsui T, Ueda T, Sugita K, Terahara N, Matsumoto K (2001). α-Glucosidase inhibitory action of natural acylated anthocyanins. Journal of Agricultural Food Chemistry, 49:1952-1956.

Mayer AMS, Lehmann VKB (1998). Marine pharmacology in 1998: Marine compounds with antibacterial, anticoagulant, anti-inflammatory, anthelmintic, antiplatelet, antiprotozoal, and antiviral activities; with actions on the cardiovascular, endocrine, immune, and nervous systems; and other miscellaneous mechanisms of action. The Pharmacologist, 42:62-69.

McConnell OJ, Fenical W (1978). Ochtodene ochtodiol: Novel polyhalogenated cyclic monoterpenes from the red seaweed *Ochtodes secundiramea*. Journal of Organic Chemistry, 43:4238-4241.

McHugh DJ (2003). A guide to seaweed industry, FAO Fisheries Technical paper, No. 441. Rome, FAO, pp 105.

McLean JS, Byrick RJ (1993). ARDS and sepsis-definitions and new therapy. Canadian Journal of Anaesthaesia, 40:585-590.

Melo MRS, Feitosa JPA, Freitas ALP, de Paula RCM (2002). Isolation and characterization of soluble sulfated polysaccharide from the red seaweed *Gracilaria cornea*. Carbohydrate Polymers, 49:491-498.

Mendonca P, Freitas JC (2000). Topical antiedematous activity of the organic extract of *Liagora farinosa* algae (Rhodophyta, Nemaliales). Ciencia e Cultura, 52:175-178.

Mentlein R (1999). Dipeptidyl-peptidase IV (CD26): Role in the inactivation of regulatory peptides. Regulatory Peptides, 24:85-89.

Mikami D, Kurihara H, Kim SM, Takahashi K (2013). Red algal bromophenols as glucose 6-phosphate dehydrogenase inhibitors. Marine Drugs, 11:4050-4057.

Milan M, Mirjana M, Desanka B, Sanja M, Neda N, Vladimir M (2011). *In vitro* antioxidant of selected 4-hydroxy-chromen-2-one derivatives-SAR, QSAR and DFT studies. International Journal of Molecular Sciences, 12:2822-2841.

Minelli A, Chagas-junior A, Edgecombe GD (2009). Saltational evolution of trunk segment number in centipedes. Evolution and Development, 11:318-322.

Mollet JC, Rahaoui A, Lemoine Y (1998). Yield, chemical composition and gel strength of agarocolloids of *Gracilaria gracilis*, *Gracilariopsis longissima* and the newly reported *Gracilaria cf. vermiculophylla* from Roscoff (Brittany, France). Journal of Applied Phycology, 10:59-66.

Mori J, Hayashi T, Iwashima M, Matsunaga T, Saito H (2003). Effects of plastoquinones from the brown alga *Sargassum micracanthum* and a new chromen derivative converted from the plastoquinones on acute gastric lesions in rats. Biological and Pharmaceutical Bulletin, 29:1197-1201.

Murai A, Iwamura K, Takada M, Ogawa K, Usui T, Okumura JI (2002). Control of postprandial hyperglycaemia by galactosyl maltobionolactone and its novel anti-amylase effect in mice. Life Science, 71:1405-1415.

Murai, Murase H, Matsue H, Masamune T (1977). The synthesis of (±)-Laurencin. Tetrahedron Letters, 18:2507-2510.

Murano E (1995). Chemical structure and quality of agars from *Gracilaria*. Journal of Applied Phycology, 7:245-254.

Murano E, Toffanin R, Pedersini C, Carabot Cuervo A, Blunden G, Rizzo R (1996). Structure and properties of agar from two unexploited agarophytes from Venezuela. Hydrobiologia, 327:497-500.

Muzzarelli RAA (1997). Human enzymatic activities related to the therapeutical administration of chitin derivatives. Cellular and Molecular Life Science, 53:131-140.

Mynderse JS, Faulkner DJ (1974). Polyhalogenated acyclic and monocyclic monoterpenes have been found previously in red algae belonging to the genus *Plocamium*. Journal of American Chemical Society, 96:6771-6772.

Mynderse JS, Faulkner DJ (1978). Variations in the halogenated monoterpene metabolites of *Plocamium cartilagineum* and *Plocamium violaceum*. Phytochemistry, 17:237-240.

Nagarani N, Kumaraguru AK (2013). Evaluation of anti-inflammatory, antidiabetic, cytotoxic activity of *K. alvarezii*. International Journal of Pharma and Biosciences, 4:921-929.

Newman DJ, Cragg GM (2012). Natural products as sources of new drugs over the 30 years from 1981 to 2010. Journal of Natural Product, 75:311-335.

Ngo DH, Kim SK (2013). Sulfated polysaccharides as bioactive agents from marine algae. International Journal of Biological Macromolecules, 62:70-75.

Nicolaou KC, Pfefferkorn JA, Roecker AJ, Cao GQ, Barluenga S, Mitchell HJ (2000). Natural product-like combinatorial libraries based on privileged structures. 1. General principles and solid-phase synthesis of benzopyrans. Journal of American Chemical Society, 122:9939-9953.

Nisizawa K, Noda H, Kikuchi R, Watamaba T (1987). The main seaweeds food in Japan. Hydrobiologia, 151/152:5-29.

Numata A, Takahashi C, Ito Y, Takeda T, Kawai K, Osami Y, Matsumura E, Imachi M, Ito T, Hasegawa T (1993). Communesins, cytotoxic metabolites of a fungus isolated from a marine alga. Tetrahedron Letter, 34:2355-2358.

Nunnery JK, Mevers E, Gerwick WH (2010). Biologically active secondary metabolites from marine cyanobacteria. Current Opinion Biotechnology, 21:787-793.

Ochieng CO, Owuor PO, Manguro LAO, Akala H, Ishola IO (2012). Antinociceptive and antiplasmodial activities of cassane furanoditerpenes from *Caesalpinia volkensii H*. root bark. Fitoterapia, 83:74-80.

Ohno M (1993). Cultivation of the green alga, *Monostroma* and *Enteromorpha* "aonori", pp 51-56.

Ohno M, Largo DB, Ikumoto T (1994). Growth rate, sulphated galactan yield and gel properties of cultured kappa-carrageenan producing red alga *Kappaphycus alvarezii* (Doty) Doty in the subtropical waters of Shikoku, Japan. Journal of Applied Phycology, 6:1-5.

Olsen EK, Hansen E, Isaksson J, Andersen JH (2013). Cellular antioxidant effect of four bromophenols from the red algae, *Vertebrata lanosa*. Marine Drugs, 11:2769-2784.

Ovenden SPB , Nielson JL, Liptrot CH, Willis RH, Tapiolas DM, Wright AD, Motti CA, (2011). Callophycin A, a cytotoxic tetrahydro-beta-carboline from the red alga *Callophycus oppositifolius*. Phytochemistry Letters, 4:69-71.

Paiva L, Lima E, Neto AI, Baptista J (2016). Angiotensin I-converting enzyme (ACE) inhibitory activity of Fucus spiralis macroalgae and influence of the extracts storage temperature—A short report. Journal of Pharmaceutical and Biomedical Analysis, 131:503-507.

Pangestuti R, Kim SK (2011). Neuroprotective effects of marine algae. Marine Drugs, 9:803-818.

Parke A, Parke DV (1995). The pathogenisis of inflammatory disease: Surgical shock and multiple system organ failure. Inflammopharmacology, 3:149-168.

Parke DV (1994). The cyctochromes P450 and mechanisms of chemical carcinogenesis. Environmental Health Perspectives, 102:852-853.

Parshikov IA, Netrusov AI, Sutherland JB (2012). Microbial transformation of antimalarial terpenoids. Biotechnology Advances, 30:1516-1523.

Paul VJ, Fenical W (1980a). Palisadins A, B and related monocyclofarnesol-derived sesquiterpenoids from the red marine alga *Laurencia cf. palisade*. Tetrahedron Letters, 21:2787-2790.

Paul VJ, Fenical W (1980b). Toxic acetylene-containing lipids from the red marine alga *Liagorafarinosa lamouroux*. Tetrahedron Letters, 21:3327-3330.

Pereira DM, Cheel J, Areche C, San-Martin A, Rovirosa J, Silva LR, Valentao P, Andrade PB (2011). Antiproliferative activity of meroditerpenoids isolated from the brown alga *Stypopodium flabelliforme* against several cancer cell lines. Marine Drugs, 9:852-862.

Piccolella S, Fiorentino A, Pacifico S, D'Abrosca B, Uzzo P, Monaco P (2008). Antioxidant properties of sour cherries (Prunus cerasus L.): Role of colorless phytochemicals from the methanolic extract of ripe fruits. Journal of Agricultural Food Chemistry, 56:1928-1935.

Pietta PG (2000). Flavonoids as antioxidants. Journal of Natural Product, 63:1035-1042.

Pomin VH, Maurao PA (2008). Structure, biology, evolution, and medical importance of sulfated fucans and galactans. Glycobiology, 18:1016-1027.

Praveen NK, Chakraborty K (2013). Antioxidant and anti-inflammatory potential of the aqueous extract and polysaccharide fraction from brown marine macroalgae *Padina* sp from Gulf of Mannar of Peninsular India. Journal of Coastal Life Medicine, 1:38-48.

Quan (2008). Evolutionary and transcriptional analysis of karyopherin beta superfamily proteins. Molecular Cell Proteomics, 7:1254-69.

Ragan MA, Glombitza KW (1986). Phlorotannins, brown algal polyphenols. In: Round FE, Chapman DJ (eds) Progress in phycological research. Biopress, Bristol, pp 129-241.

Rao PNP, Knaus EE (2008). Evolution of nonsteroidal antiinflammatory drugs (NSAIDs): Cyclooxygenase (COX) inhibition and beyond. Journal of Pharmacy and Pharmaceutical Sciences, 11:81-110.

Rateb ME, Ebel R (2011). Secondary metabolites of fungi from marine habitats. Natural Product Report, 28:290-344.

Rinaudo M (2001). Relation between the molecular structure of some polysaccharides and original properties in sol and gel states. Food Hydrocolloids, 15:433-440.

Rochfort SJ, Capon RJ (1996). Parguerenes revisited: New brominated diterpenes from the southern Australian marine red alga *Laurencia filiformis*. Australian Journal of Chemistry, 49:19-26.

Rosanna DP, Salvatore C (2012). Reactive oxygen species, inflammation, and lung diseases. Current Pharmaceutical Design, 18:3889-3900.

Rose AF, Sims JJ (1977). Marine natural products XIV. 1-S-bromo-4-R-hydroxyselin-7-ene, a metabolite of the marine alga *Laurencia* sp. Tetrahedron Letters, 18:2935-2938.

Rose AF, Sims JJ, Wing RM, Wiger GM (1978). Marine natural products XVII. The structure of (1S, 4R, 7R)-1-bromo-4-hydroxy-7-chloroselinane, a metabolite of the marine alga *Laurencia* Sp. Tetrahedron Letters, 19:2533-2536.

San Martin A, Rovirosa J, Munoz O, Chen MHM, Guneratne RD, Clardy J (1983). The isolation and structure determination of chilenone A, a putative dimer of 2-methyl-3(2H)-furanone from the marine alga *Laurencia chilensis.* Tetrahedron Letters, 24:4063-4066.

Sasidharan S, Darah I, Jainc Witz K (1991). Antimicrobial activity and wound healing potential on infected rat of *Gracilaria Changii* methanolic extract. Pharmacologyonline, 2:661-670.

Sasidharan S, Darah I, Noordin MK (2008). Preliminary isolation and *in vitro* antiyeast activity of active fraction from crude extract of *Gracilaria changii*. Indian Journal of Pharmacology, 40:227-229.

Sato M, Hosokawa T, Yamaguchi T, Nakano K, Muramoto T, Kahara K, Funayama A, Kobayashi A (2002). Antihypertensive effects of hydrolysates of *wakame* (*Undaria pinnatifida*) and their angiotensin-I converting enzyme inhibitory activity. Annals of Nutrition and Metabolism, 46:259-267.

Savoia C, Schiffrin EL (2007). Vascular inflammation in hypertension and diabetes: Molecular mechanisms and therapeutic interventions. Clinical Sciences, 112:375-384.

Schramm A, Matusik P, Osmenda G, Guzik TJ (2012). Targeting NADPH oxidases in vascular pharmacology. Vascular Pharmacology, 56:216-231.

Selover SJ, Crews P (1980). Kylinone, a new sesqiterpene skeleton from the marine alga *Laurencia pacifica*. Journal of Organic Chemistry, 45:69-72.

Senni K, Gueniche F, Foucault-Bertaud A, Igondjo-Tchen S, Fioretti F, Colliec-Jouault S, Durand P, Guezennec J, Godeau G, Letourneur D (2006). Fucoidan a sulfated polysaccharide from brown algae is a potent modulator of connective tissue proteolysis. Archives of Biochemistry and Biophysics, 445:56-64.

Seung-Hong L, You-Jin J (2013). Anti-diabetic effects of brown algae derived phlorotannins, marine polyphenols through diverse mechanisms. Fitoterapia, 86:129-136.

Shen L, Park EJ, Kondratyuk TP, Guendisch D, Marler L, Pezzuto JM, Wright AD, Sun D (2011). Design, synthesis, and biological evaluation of callophycin A and

analogues as potential chemopreventive and anticancer agents. Bioorganic and Medicinal Chemistry, 19:6182-6195.

Sievanen L, Crawford B, Pollnac R, Lowe C (2005). Weeding through assumptions of livelihood approaches in ICM: Seaweed farming in the Philippines and Indonesia. Ocean and Coastal Management, 48:297-313.

Silva ED, Scheuer PJ (1980). Manoalide, an antibiotic sesterterpenoid from the marine sponge *Luffariella variabilis*. Tetrahedron Letters, 21:1611-1614.

Silva LM, Lima V, Holanda ML, Pinheiro PG, Rodrigues JA, Lima ME, Benevides NM (2010). Antinociceptive and anti-inflammatory activities of lectin from marine red alga *Pterocladiella* capillacea. Biological and Pharmaceutical Bulletin, 33:830-835.

Silva PC, Basson PW, Moe RL (1996). Catalogue of the benthic marine algae of the Indian Ocean. University of California Publications in Botany, 79:1-1259.

Sivasothy Y, Hadi AHA, Mohamad K, Leong KH, Ibrahim H, Sulaiman SF (2012). Spectaflavoside A, new potent iron chelating dimeric flavonol glycoside from the rhizomes of *Zingiber spectabile* Griff. Bioorganic and Medicinal Chemistry Letters, 22:3831-3836.

Slater TF (1979). Mechanisms of protection against the damage produced in biological systems by oxygen-derived radicals. Ciba Foundation Symposium, 65:143-162.

Souza BWS, Cerqueira MA, Bourbon AI, Pinheiro AC, Martins JT, Teixeira JA (2012). Chemical characterization and antioxidant activity of sulfated polysaccharide from the red seaweed *Gracilaria birdiae*. Food Hydrocolloid, 27:287-292.

Stierle DB, Wing RM, Sims JJ (1979). Marine natural products XV: Polyhalogenated cyclic monoterpenes from the red alga *Plocamium cartilegineum* of Antartica. Tetrahedron, 35:2855-2859.

Suetsuna K, Nakano T (2000). Identification of an antihypertensive peptide from peptic digest of *wakame* (*Undaria pinnatifida*). Journal of Nutritional Biochemistry, 11:450-454.

Sun HH, Erickson KL (1978). Sesquiterpenoids from the Hawaiian marine alga *Laurencia nidifica*. 7. (+)-selin-4, 7(11)-diene. Journal of Organic Chemistry, 43:1613-1614.

Sun WS, Su S, Zhu RX, Tu GZ, Cheng W, Liang H, Guo XY, Zhao YY, Zhang QY (2013). A pair of unprecedented spiro-trisindole enantiomers fused through a five-member ring from *Laurencia similis*. Tetrahedron Letters, 54:3617-3620.

Suzuki M, Furusaki A, Kurosawa E (1979). The absolute configurations of halogenated chamigrene derivatives from the marine alga, *Laurencia glandulifera*. Tetrahedron, 35:823-831.

Suzuki M, Kowata N, Kurosawa E (1980a). The structure of spirolaurenone, a halogenated sesquiterpenoid from the red alga *Laurencia glandulifera kutzing*. Tetrahedron, 36:1551-1556.

Suzuki M, Kurosawa E (1978). Two new halogenated sesquiterpenes from the red alga *Laurencia majuscule*. Tetrahedron Letters, 19:4805-4808.

Suzuki M, Kurosawa E (1979). Halogenated sesquiterpene phenols and ethers from the red alga *Laurencia glandulifera* Kutzing. Bulletin of the Chemical Society Japan, 52:3349-3351.

Suzuki M, Kurosawa E (1980). Venustin A and B, new halogenated C_{15} metabolites from the red alga *Laurencia venusta* Yamada. Chemistry Letters, 9:1177-1180.

Suzuki M, Kurosawa E (1981). Okamurallene, a novel halogenated C_{15} metabolite from the red alga *Laurencia okamuhai* Yamada. Tetrahedron Letters, 22:3853-3856.

Suzuki M, Kurosawa E, Furusaki A, Matsumoto T (1983a). The structures of (3Z)-epoxyvenustin, (3Z)-venustin and (3Z)-venustinene, new halogenated C_{15}-nonterpenoids from the red alga *Laurencia venusta* Yamada. Chemistry Letters, 12:779-782.

Suzuki T, Kikuchi H, Kurosawa E (1980b). (E)-γ-bisabolen-8, 9-epoxide and isocycloeudesmol, two new sesquiterpenoids from the marine red alga *Laurencia nipponica* Yamada. Chemistry Letters, 9:1267-1270.

Suzuki T, Koizumi K, Suzuki M, Kurosawa E (1983b). Kumausynes and deacetylkumausynes, four new halogenated C-15 acetylenes from the red alga *Laurencia nipponica* Yamada. Chemistry Letters, 12:1643-1644.

Swanson AK, Druehl LD (2002). Induction, exudation and the UV protective role of kelp phlorotannins. Aquatic Botany, 73:241-253.

Tacconelli S, Capone ML, Sciulli MG, Ricciotti E, Patrignani P (2002). The biochemical selectivity of novel COX-2 inhibitors in whole blood assays of COX-isozyme activity. Current Medicinal Research and Opinion, 18:503-511.

Takahashi C, Takai Y, Kimura Y, Numata A, Shigematsu N, Tanaka H (1995). Cytotoxic metabolites from a fungi adherent of a marine alga. Phytochemistry, 38:155-158.

Takaichi S (2011). Carotenoids in algae: Distributions, biosyntheses and functions. Marine Drugs, 9:1101-1118.

Topcu G, Aydogmus Z, Imre S, Goren AC, Pezzuto JM, Clement JA, Kingston DG (2003). Brominated sesquiterpenes from the red alga *Laurencia obtuse*. Journal of Natural Product, 66:1505-1508.

Toth G, Pavia H (2000). Lack of phlorotannin induction in the brown seaweed *Ascophyllum nodosum* in response to increased copper concentrations. Marine Ecology Progress Series, 192:119-126.

Troell M, Ronnback P, Halling C, Katusky, N, Buschmann A (1999). Ecological engineering in aquaculture: Use of seaweeds for removing nutrients from intensive mariculture. Journal of Applied Phycology, 11:89-97.

Tsujino I, Yabe K, Sekikawa I, Hamanaka N (1978). Isolation and structure of a mycosporine from the red alga *Chondrusyendoi*. Tetrahedron Letters, 16:1401-1402.

Turkez H, Gurbuz H, Aydin E, Aslan A, Dirican E (2012). The evaluation of the genotoxic and oxidative damage potentials of *Ulothrix tenuissima in vitro*. Toxicology and Industrial Health, 28:147-151.

Udenigwe CC, Lin Y, Hou W, Aluko RE (2009). Kinetic of the inhibition of renin angiotensin I-converting enzyme by flaxseed protein hydrolysate functions. Journal of Functional Food, 1:199-207.

Vairappan CS, Kamada T, Lee WW, Jeon YJ (2013). Anti-inflammatory activity of halogenated secondary metabolites of *Laurencia snackeyi* (Weber-van Bosse Masuda in LPS-stimulated RAW 264.7 macrophages). Journal of Applied Phycology, 25:1805-1813.

Vairappan CS, Kawamoto T, Miwa H, Suzuki M (2004). Potent antibacterial activity of halogenated compounds against antibiotic resistant bacteria. Planta Medica, 70:1087-1090.

Vairappan CS, Suzuki M, Abe T, Masuda M (2001). Halogenated metabolites with antibacterial activity from the *Okinawan Laurencia* species. Phytochemistry, 58:517-523.

Vallinayagam K, Arumugam R, Ragupathy raja kannan G (2009). Antibacterial activity of some selected seaweeds from Pudumadam coastal regions. Global Journal of Pharmacology, 3:50-52.

Van Wyk AWW, Zuck KM, McKee TC (2011). Lithothamnin A, the first bastadin-like metabolite from the red alga *Lithothamnion fragilissimum*. Journal of Natural Product, 74:1275-1280.

Vandevelde F, Knutsen SH, Usov AI, Rollema HS, Cerezo AS (2002). ^{1}H and ^{13}C high resolution NMR spectroscopy of carrageenans: Application in research and industry. Trends in Food Science and Technology International, 13:73-92.

Veena CK, Josephine A, Preetha SP, Varalakshmi P (2007). Beneficial role of sulfated polysaccharides from edible seaweed *Fucus vesiculosus* in experimental hyperoxaluria. Food Chemistry, 100:1552-1559.

Villanueva RD, Montano MNE, Romero JB (2009). Iota-carrageenan from a newly formed, rare variety of eucheumoid seaweed. Journal of Applied Phycology, 21:27-30.

Vosooghi M, Rajabalian S, Sorkhi M, Badinloo M, Nakhjiri M, Negahbani AS (2010). Synthesis and cytotoxic activity of some 2-amino-4-aryl-3-cyano-7-(dimethylamino)-4*H*-chromenes. Research in Pharmaceutical Sciences, 5:9-14.

Wael M, Abdel-Mageed AB, Rainer Ebel B, Fred A, Valeriote C, Jaspars M (2010). Laurefurenynes A-F, new cyclic ether acetogenins from a marine red alga, *Laurencia* sp. Tetrahedron, 66:2855-2862.

Wakibia JG, Bolton JJ, Keats DM, Rait LM (2006). Factors influencing the growth rate of three commercial eucheumoids grown in southern Kenya. Journal of Applied Phycology, 18:565-573.

Wang BG, Zhang WW, Duan XJ, Li XM (2009). *In vitro* antioxidative activities of extract and semi-purified fractions of the marine red alga, *Rhodomela confervoides* (Rhodomelaceae). Food Chemistry, 113:1101-1105.

Wang HMD, Chen, CC, Huynh, P, Chang JS (2015). Exploring the potential of using algae in cosmetics. Bioresource Technology, 184:355-362.

Waraszkiewicz SM, Erickson KL, Finer J, Clardy J (1977). Nidifocene: A reassignment of structure. Tetrahedron Letters, 18:2311-2314.

Waraszkiewicz SM, Sun HH, Erickson KL, Finer J, Clardy J (1978). C_{15}-Halogenated compounds from the Hawaiian marine alga *Laurencia nidifica*. Maneonenes and isomaneonenes. Journal of Organic Chemistry, 43:3194-3204.

Watanabe K, Umeda K, Miyakado M (1989). Isolation and identification of three insecticidal principles from the red algae *Laurencia nipponica* Yamada. Agricultural and Biological Chemistry, 53:2513-2515.

White RH, Hager LP (1978). Intricenyne and related halogenated compounds from *Laurencia intricate*. Phytochemistry, 17:939-941.

Willem AL, Lindani NE, Samuel K, Garreth LM, Simon SM, Charles BK (2005). Ring-closing metathesis for the synthesis of 2*H* and 4*H* chromenes. Tetrahedron, 61:9996-10006.

Williard PG, Grab LA, De Laszlo SE (1983). Synthesis of costatolide, a halogenated monoterpenoid from the red alga *Plocamium costatum*. Journal of Organic Chemistry, 48:1123-1125.

Wojdyło A, Oszmianski J, Czemerys R (2007). Antioxidant activity and phenolic compounds in 32 selected herbs. Food Chemistry, 105:940-949.

Woolard FX, Moore RE, Van Engen D, Clardy J (1978). The structure and absolute configuration of chondrocolactone, A halogenated monoterpene from the red alga *Chondrococcus hornemanni*, and a revised structure for chondrocole A. Tetrahedron Letters, 19:2367-2370.

Wright AE, Wing RM, Sims JJ (1983). Poitediene a new metabolite from the marine red alga *Laurencia Poitei*. Tetrahedron Letters, 24:4649-4652.

Xu X, Yin L, Gao L, Gao J, Chen J, Li J, Song F (2013a). Two new bromophenols with radical scavenging activity from marine red alga *Symphyocladia latiuscula*. Marine Drugs, 11:842-847.

Xu X, Yin L, Wang Y, Wang S, Song F (2013b). A new bromobenzyl methyl sulphoxide from marine red alga *Symphyocladia latiuscula*. Natural Product Research, 27:723-726.

Yan X, Chuda Y, Suzuki M, Nagata T (1999a). Fucoxanthin as the major antoxidant in *Hijikia fusiformis*, common edible seaweed. Bioscience, Biotechnology and Biochemistry, 63:605-607.

Yan XJ, Fang GM, Lou QX (1999b). Studies on free radical scavenging activity in Chinese seaweeds part I. screening results. Chinese Journal of Oceanology and Limnology, 17:240-246.

Yan XJ, Li XC, Zhou CX, Fan X (1996). Prevention of fish oil rancidity by phlorotannins from *Sargassum kjellmanianum*. Journal of Applied Phycology, 8:201-203.

Yang JI, Yeh CC, Lee JC, Yi SC, Huang HW, Tseng CN, Chang HW (2012). Aqueous extracts of the edible *Gracilaria tenuistipitata* are protective against H_2O_2-

induced DNA damage, growth inhibition, and cell cycle arrest. Molecules, 17:7241-7254.

Yangthong M, Nongporn HT, Phromkunthong W (2009). Antioxidant activities of four edible seaweeds from the southern coast of Thailand. Plant Foods Human Nutrition, 64:218-223.

Yoon WJ, Heo SJ, Han SC, Lee HJ, Kang GJ, Kang HK, Hyun JW, Koh YS, Yoo ES (2012). Anti-inflammatory effect of sargachromanol G isolated from *Sargassum siliquastrum* in RAW 264.7 cells. Archives of Pharmacal Research, 35:1421-1430.

Yotsu-Yamashita M, Yasumoto T, Yamada S, Bajarias FFA, Formeloza MA, Romero ML, Fukuyo Y (2004). Identification of polycavernoside A as the causative agent of the fatal food poisoning resulting from the ingestion of the red alga *Gracilaria edulis* in the Philippines. Chemical Research in Toxicology, 17:1265-1271.

Yvin JC, Chevolot-Magueur AM, Chevolot L, Lallemand JY, Potier P, Guilhem J (1982). Delesserine, a new metabolite of mixed biogenesis from the red marine Alga *Delesseria sanguinea* (Lamouroux). Journal of American Chemical Society, 104:4497-4498.

Zhang GN, Zhong LY, Bligh SWA, Guo YL, Zhang CF, Zhang M, Wang ZT, Xu LS (2005). Bi-bicyclic and bi-tricyclic compounds from *Dendrobium thyrsiûorum*. Phytochemistry, 66:1113-1120.

Zhao X, Xue C, Cai Y, Wang D, Fang Y (2005). Study of antioxidant activities of fucoidan from *Laminaria japonica*. High Technology Letters, 11:91-94.

Zhu JK (2001). Plant salt tolerance. Trends in Plant Science, 6:66-71.

LIST OF PUBLICATIONS

The list of published and accepted publications from the thesis work is detailed in this section.

1) Fasina Makkar, Kajal Chakraborty (2017). Antidiabetic and anti-inflammatory potential of sulphated polygalactans from red seaweeds *Kappaphycus alvarezii* and *Gracilaria opuntia*. International Journal of Food Properties, 20(6):1326-1337.
2) Fasina Makkar, Kajal Chakraborty (2017). Unprecedented antioxidative cyclic ether from the red seaweed *Kappaphycus alvarezii* with anti-cyclooxygenase and lipoxidase activities. Natural Product Research, 31:1131-1141.
3) Fasina Makkar, Kajal Chakraborty (2017). Antioxidative sulfated polygalactans from marine macroalgae as angiotensin-I converting enzyme inhibitors. Natural Product Research, 32(17): 2100-2106.
4) Fasina Makkar, Kajal Chakraborty (2017). Previously undescribed antioxidative azonicyl morpholinone alkaloid from red seaweed *Gracilaria opuntia* with anti-cyclooxygenase and lipoxidase properties. Natural Product Research, 32(10):1150-1160.
5) Fasina Makkar, Kajal Chakraborty (2018). Highly oxygenated antioxidative 2*H*-chromen derivative from the red seaweed *Gracilaria opuntia* with pro-inflammatory cyclooxygenase and lipoxygenase inhibitory properties. Natural Product Research, 32(23): 2756-2765.
6) Fasina Makkar, Kajal Chakraborty (2018). Novel furanyl derivatives from the red seaweed *Gracilaria opuntia* with pharmacological activities using different *in vitro* models. Medicinal Chemistry Research, 31:1131-1141.
7) Fasina Makkar, Kajal Chakraborty (2018). Antioxidant and anti-inflammatory oxygenated meroterpenoids from the thalli of red seaweed *Kappaphycus alvarezii*. Medicinal Chemistry Research, 27(8):2016-2026.
8) Fasina Makkar, Kajal Chakraborty (2018). First report of duel cyclooxygenase-2 and 5-lipoxygenase inhibitory halogen derivatives from the thallus of intertidal seaweed *Kappaphycus alvarezii*. Medicinal Chemistry Research, 27: 2331-2340.

PRESENTATION IN SEMINAR/SYMPOSIA

1) Fasina Makkar, Kajal Chakraborty (2017). Seminar presentation entitled "Previously undescribed and anti-inflammatory pharmacophores from red marine macroalga *Kappaphycus alvarezii*" in the National Seminar on Current Trends in Chemistry CTriC 2017 held at Cochin University of Science and Technology on 03rd and 4 th February 2017.
2) Fasina Makkar, Kajal Chakraborty (2017). Seminar presentation entitled "Antioxidative, anti-diabetic, anti-inflammatory and anti-hypertensive potential of sulfated polygalactans isolated from red macro algae *Kappaphycus alvarezii* and *Gracilaria opuntia*" in the National Seminar on Green Chemistry for Environmental Sustainability on 7 and 8 February 2017 held at Bharata Mata College, Thrikkakara , Kochi, Kerala.

ISOLATION AND CHARACTERIZATION OF BIOACTIVE COMPOUNDS FROM MARINE MACROALGAE *KAPPAPHYCUS ALVAREZII* AND *GRACILARIA OPUNTIA*

Thesis submitted in partial fulfilment of the requirement for the degree of

DOCTOR OF PHILOSOPHY

in

CHEMISTRY

BY

Mrs. FASINA MAKKAR
(Ref.No. MU/ACC/Ph.D./CR.40/2014-15/A3, dated 7.03.2015)

Guided By
Dr. KAJAL CHAKRABORTY
Senior Scientist (Organic Chemistry),
Central Marine Fisheries Research Institute (CMFRI)

Under the Faculty of Science and Technology

MANGALORE UNIVERSITY
MANGALAGANGOTHRI – 574 199
Dakshina Kannada Dist. Karnataka, India

भारतीय कृषि अनुसंधान परिषद
केन्द्रीय समुद्री मात्स्यिकी अनुसंधान संस्थान
[कृषि अनुसंधान एवं शिक्षा विभाग, कृषि मंत्रालय,भारत सरकार]
Indian Council of Agricultural Research
Central Marine Fisheries Research Institute
[Department of Agricultural Research and Education, Ministry of Agriculture, Govt. of India]
पोस्ट बॉक्स सं.1603, एरणाकुलम नॉर्त पी.ओ.,कोच्ची–682018, केरल, भारत
Post Box No.1603, Ernakulam North P.O., Kochi - 682018, Kerala, India

December 2018

Declaration

*I do hereby declare that the thesis entitled "**Isolation and Characterization of Bioactive Compounds from Marine Macroalgae Kappaphycus alvarezii and Gracilaria opuntia**" is an authentic record of research work carried out by me under the guidance and supervision of Dr. Kajal Chakraborty, Senior Scientist, Central Marine Fisheries Research Institute, Cochin-682018 and the same has not previously formed the basis for the award of any degree or diploma.*

Whenever the work described is based on the findings of other researchers, due acknowledgement is made in keeping with the general practice of reporting scientific observations. However, errors and unintentional oversights, if any are regretted.

Fasina Makkar

Place: Cochin
Date:

□□□□□□ □□□□ □□□□□□□□ □□□□□
□□□□□□□□□□ □□□□□□□□ □□□□□□□□□□ □□□□□□□□ □□□□□□□□
[□□□□ □□□□□□□□ □□□ □□□□□□ □□□□□, □□□□ □□□□□□□□,□□□□ □□□□□]
Indian Council of Agricultural Research
Central Marine Fisheries Research Institute
[Department of Agricultural Research and Education, Ministry of Agriculture, Govt. of India]
□□□□□ □□□□□ □□.1603, □□□□□□□□ □□□□□ □□.□.,□□□□□□□–682018, □□□□, □□□□
Post Box No.1603, Ernakulam North P.O., Kochi - 682018, Kerala, India
Phone: 91 484 2394867/2391407 Fax: 91 484 2394909/2396685 Email: director@cmfri.org.in Web: www.cmfri.org.in

Dr. Kajal Chakraborty
Senior Scientist (Organic Chemistry)

Certificate

This is to certify that this thesis entitled ***"Isolation and Characterization of Bioactive Compounds from Marine Macroalgae Kappaphycus alvarezii and Gracilaria opuntia"*** *submitted by* ***Mrs. FASINA MAKKAR****, Research Scholar of Marine Biotechnology Division of Central Marine Fisheries Research Institute, for the award of the degree of Doctor of Philosophy in Chemistry is the result of bonafide research work carried out by her in the Central Marine Fisheries Research Institute in* ***Chemistry****, Cochin-682018, under my guidance and direct supervision. I further certify that this thesis or part thereof has not previously formed the basis for the award of any degree, diploma, or associateship of any other University or Institution.*

Kajal Chakraborty

Place: Cochin
Date:

Acknowledgements

The successful completion of any task would be incomplete without mentioning the people who made it possible. I take this privilege to express a few words of gratitude and respect to all those who helped me in completion of this work.

Firstly I humbly bow before the almighty God for showering his blessings upon me and giving me the strength, wisdom, health and luck to accomplish this endeavor.

It is with profound joy that I express my heartfelt gratitude to my supervising guide and mentor Dr. Kajal Chakraborty, Senior Scientist, Central Marine Fisheries Research Institute for his inspiring and excellent guidance, valuable suggestions, ceaseless encouragement and intellectual support. He has been my constant inspiration throughout the investigation and I am deeply obliged to him for providing all the necessary facilities and above all the freedom provided in doing the experiment. I record my deep sense of gratitude to him for all the efforts he has put in and the moral support extended for the successful completion of this thesis.

I feel extremely privileged to thank Dr. A. Gopalakrishnan, Director, Central Marine Fisheries Research Institute for being kind enough to extend all the necessary facilities and support required to carry out my research work. I record my deep sense of respect and gratitude to Dr. A. Gopalakrishnan for providing me with the absolute freedom to successfully complete this thesis. I extend my deep sense of gratitude and respect to Dr. G. Syda Rao, former Director of Central Marine Fisheries Research Institute for being kind enough to permit me to register for the Ph.D. programme and providing me with all the necessary facilities required to carry out this doctoral programme. I feel extremely privileged to place on record my sincere respect and gratitude for Dr. P. Vijayagopal, Head, Marine Biotechnology Division, Central Marine Fisheries Research Institute for facilitating my research activities, and for his valuable suggestions and support rendered during the doctoral work.

I am thankful to Dr. Boby Ignatius, Principal Scientist and Scientist-in-Charge, HRD cell of CMFRI for their kind support and constant encouragement extended throughout the investigation. I feel privileged to place on record my sincere gratitude for Dr. P.C. Thomas, former Scientist-in-Charge, HRD cell of CMFRI for kindly facilitating my research activities during the doctoral work.

I feel privileged to place on record my sincere respect and gratitude to the scientists of Marine Biotechnology Division, Dr. P. Jayasankar, Dr. N. K. Sanil, Dr. Sandhya Sukumaran, and Dr. M. A. Pradeep. I wish to express my heartful thanks to Dr. M. P. Paulton (Senior Technical Officer), Shri K.M. David (Technical Assistant), SIC librarian, library support staff, staff members of the HRD Cell, the canteen, security personnel and employees of CMFRI, Cochin, for their sincere help and cooperation extended during the tenure.

I express my sincere thanks to all the staff members of the Indus Digital Press (Cochin) for the final professional setting and printing of the documents of the thesis in an impressive format.

I express my deep sense of gratitude for the support extended by my labmates and colleagues, Anusree Maneesh, Dexy Joseph, Vamshi Krishna Raola, Minju Joy, Soumya Salas, Soumya Krishnan, Tima Antony, and Vinaya K. K. during the study.

I acknowledge the staffs of SAIF, IIT Chennai, especially, Dr. C. Baby, Mr. Bhaskar, and staffs of STIC, Cochin University of Science and Technology (CUSAT),

especially, Dr. Shibu Eapen, Mr. Saji T. K for their help and support extended towards the spectroscopic studies.

I take this opportunity to thank Indian Council of Agricultural Research, New Delhi for providing Research Fellowships under different schemes.

I remember my parents, C. S. Makkar & V. M. Nabeesa with profound sense of gratitude whose selfless sacrifice and their great efforts with pain, tears and unceasing prayers has enabled me to successfully complete the research work. I am forever indebted to their understanding, endless patience and encouragement when it was most required.

My express my gratitude to my brother Dilshad M and my sister Ashna Makkar, for their loving support. I extend my deep sense of gratitude to all the family members for their prayers and good wishes.

My special gratitude is due to my beloved husband Mr. Muhammed Sha C A for his love, sacrifice and constant support which made my task much easier. Words fail me to express the sort of heavenly benediction he has been to me. Thanks to my little naughty, Muhammed Mubariz, for always soothing me with a smiling and inspiring face.

Finally, I thank all those who have helped me directly or indirectly in the successful completion of my thesis.

Fasina Makkar

Place: Cochin
Date:

Dedicated to my beloved husband……

Sha

Abstract

Marine macroalgae can be considered as a major resource of bioactive leads. Species of the red marine macroalgae (class Rhodophyceae) were proven to be rich sources of structurally unique and biologically active secondary metabolites endowed with antioxidant, anti-bacterial, anti-inflammatory and anti-carcinogenic activities for applications in functional food and pharmaceuticals. In recent days, macroalgae emerge as a subject area of interest in the biomedical applications owing to the presence of pharmacologically active substances with potential health benefits. Antioxidant compounds exhibit a predominant functional role in attenuating the overproduction of free radicals formed during the regular metabolic processes. Therefore, antioxidant compounds play a vital role in the pathogenesis of oxidative stress induced diseases, such as inflammation, hypertension and diabetics. The present study demonstrated the potential of red marine macroalgae as a source of bioactive leads. *Kappaphycus alvarezii* and *Gracilaria opuntia* registered significant antioxidant potential along with *in vitro* enzyme inhibitory potential with respect to anti-diabetics, anti-hypertension and anti-inflammation. The organic ethylacetate-methanol (EtOAc: MeOH) extracts of the studied marine macroalgae *K. alvarezii* and *G. opuntia* from the Gulf of Mannar region of Mandapam were screened for various pharmacological activities by using different *in vitro* model assays. The organic extracts obtained from *K. alvarezii* and *G. opuntia* was found to possess bioactivities against different disease targets, namely hypertension, type-2 diabetes and inflammation. The ethylacetate-methanol extract of the thalli of *K. alvarezii* and *G. opuntia* was fractionated by repeated column chromatography to afford a number of previously undescribed compounds. The structures of these compounds were established by exhaustive spectroscopic experiments, including mass and two-dimensional nuclear magnetic resonance. The antioxidative and anti-inflammatory activities of the newly reported compounds were evaluated by different *in vitro* assays. Structure-bioactivity correlation analyses of the studied compounds were carried out using different electronic and hydrophobic molecular descriptor variables.

Bioactivity-guided chromatographic fractionation of the ethyl acetate: methanol extract obtained from the thalli of *K. alvarezii* afforded two previously undescribed biogenic halogen analogues, 2-butyl-7-4-(chloromethyl) cyclooct-1-enyl) hept-5-en-1-ol (compound **K1**) and 4-(2-chloroethyl)-5-7-(methoxymethyl) undec-3-enyl) cyclooct-4-enone (compound **K2**) were extracted from the ethyl acetate-methanol extract of *K. alvarezii*, which demonstrated the rare skeletal framework featuring C_{20}-cyclooctene and C_{23}-cyclooctenyl ring system from marine environment. The characteristic isotopic molecular ion peaks with typical isotopic pattern of 3:1 at *m/z* 326 and *m/z* 328 appropriately attributed the existence of one chlorine atom in compound **K1**. The mass spectroscopic experiments of compound **K2** showed a molecular isotopic ion peak at *m/z* 382, having four degrees of unsaturation (molecular formula $C_{23}H_{39}ClO_2$) and were associated with two olefinic bonds, along with one each of carbonyl group and ring system. The studied halogen derivatives demonstrated potential anti-inflammatory and radical scavenging properties and therefore, could be the candidate pharmacophores for as selective inhibitor against pro-inflammatory COX-2 and 5-LOX enzymes. Three oxygenated meroterpenoids, characterized as 1-(3-methoxypropyl)-2-propylcyclohexane (compound **K3**), 3-(methoxymethyl) heptyl-3-(cyclohex-3-enyl) propanoate (compound **K4**) and 2-ethyl-6-(4-methoxy-2-((2-oxotetrahydro-*2H*-pyran-4-yl) methyl) butoxy)-6-oxohexyl-5-ethyloct-4-enoate (compound **K5**) were purified from the ethyl acetate-methanol fraction of *K. alvarezii*. The highly oxygenated C_{29} meroterpenoid compound **K5** with potential radical quenching and anti-inflammatory potential might qualify this compound as candidate pharmacological lead against oxidative stress and inflammation. An unprecedented non-isoprenoid oxocine carboxylate cyclic ether characterized as (3, 4, 5, 6)-3-(hexan-2'-yl)-3, 4, 5, 8-tetrahydro-4-methyl-2*H*-oxocin-5-yl acetate (compound **K6**) with potential antioxidative and anti-inflammatory activities. The compound **K6** selectively inhibited COX-2 and therefore, has significantly greater selectivity than the NSAIDs. The target bioactivities of the compound **K6** were directed by the electronic and lipophilicity parameters.

Chromatographic purification of the MeOH-EtOAc extract of the thalli of the red marine macroalga *G. opuntia* yielded two unprecedented furanyl derivatives, named 5-(7-(5-ethyl-3, 4-dimethoxycyclooctyl) benzofuran-6-yl)-7-methyl-tetrahydro-2*H*-oxocin-2-one (compound **G1**) and 2-(3-ethyl-9-(2- methoxyethoxy)-1-oxo-tetrahydro-1*H*-xanthen-2-yl) ethyl-5-hydroxy-9-methoxy-7, 8-dimethyl-8-(5-methylfuran-2-yl) nona-3, 6-dienoate (compound **G2**) with significant pharmacological properties in the antioxidant, anti-inflammatory, anti-diabetic and anti-hypertensive model systems. Greater anti-inflammatory selectivity against proinflammatory COX-2 isoform along with significantly greater activity against pro-inflammatory 5-lipoxygenase demonstrated the potential of the newly reported furanyl derivatives as candidates for use against inflammatory disorders. Likewise, the potential antioxidative, anti-diabetic and angiotensin I-converting enzyme inhibitory activities of the isolated compounds showed their utilities in functional food and pharmaceutical preparations to attenuate type-2 diabetes and hypertension. The identified furanyl derivatives isolated from the organic extract of *G. opuntia* have potential pharmacological activities and could be used as future drug leads following toxicity and safety studies. A rare antioxidative azocinyl morpholinone alkaloid 3-(2-ethyl-6-((3, 7)-1, 2, 5, 6-tetrahydroazocin-5-yl) hexyl) morpholin-6-one (compound **G3**) was isolated from the organic extract of *G. opuntia* was found to possess significantly greater antioxidant and anti-inflammatory activities compared to the commercially available antioxidants and nonsteroidal anti-inflammatory drugs. A greater selectivity index of the studied azocinyl morpholinone

isolated from *G. opuntia* signified the greater selectivity and significantly lesser side effect profiles than the present therapies by using nonsteroidal anti-inflammatory drugs used to combat inflammatory disorders. Chromatographic purification of the MeOH-EtOAc extract of the thalli of *G. opuntia* also yielded previously undescribed 2*H*-chromen derivative with highly oxygenated carbon skeleton, characterized as 2-acetoxy-2-(5-acetoxy-4-methyl-2-oxotetrahydro-2*H*-pyran-4-yl)ethyl-4-(3-methoxy-2-(methoxymethyl)-7-methyl-hexahydro-2*H*-chromen-4-yloxy)-5-methylheptanoate (compound **G4**), from *G. opuntia*. The target bioactivities of the compound **G4** were directed by the electronic and lipophilicity parameters. The highly oxygenated dimethoxy-2*H*-chromenyloxy methoxy framework bearing the 5-acetoxy-4-methyl-2-oxotetrahydro-2*H*-pyran-4-yl) ethyl acetate skeleton of the title compound isolated from *G. opuntia* might occupy a major space in the design and development of potentially selective new generation antioxidative and anti-inflammatory pharmacophore lead molecules.

The present study demonstrated that sulfated polygalactan characterized as →4)-4-*O*-sulfonato-(2-*O*-methyl)-β-D-galactopyranosyl-(1→4)-3, 6-anhydro-(2-*O*-methyl)-α-D-galactopyranan (**KA-1**) from *K. alvarezii* displayed significantly greater antioxidative and ACE inhibitory activities than →3)-4-*O*-sulfonato-(6-*O*-acetyl)-β-D-galactopyranosyl-(1→4)-3, 6-anhydro-(2-*O*-sulfonato)-α-D-galactopyranosyl-(1→3)-4-*O*-sulfonato-(6-*O*-acetyl)-β-D-xylosyl-(1→3)-4-*O*-sulfonato-(6-*O*-acetyl)-β-D-galactopyranosyl-(1→4)-3, 6-anhydro-(2-*O*-sulfonato)-α-D-galactopyranan (**GO-1**), which was isolated from *G. opuntia*. The sulfated polygalactan from *K. alvarezii* (**KA-1**) was found to be a potential therapeutic candidate to prevent the pathologies of hypertensive disorders. The sulfated polygalactans isolated from *K. alvarezii* (**KA-2**) and *G. opuntia* (**GO-2**) possess a number of bioactivities against different disease targets, namely, inflammation and type-2 diabetes. The sulfated polygalactan obtained from *G. opuntia* (**GO-2**) showed greater anti-inflammatory activities than that from *K. alvarezii* as determined by *in vitro* cyclooxygenase/lipoxygenase inhibitory activities. The activities showed significant positive correlation with the anti-diabetic activities as determined by *in vitro* α-amylase, α-glucosidase and dipeptidyl peptidase-4 inhibitory properties.

Marine macroalgae-derived bioactive leads with potential therapeutic properties demonstrated to possess advantageous as functional food with added health benefits. Considering the promising perspective for the utilization of the marine macroalgae, their pharmaceutical potential began to receive considerable attention. The present study demonstrated the presence of library of small molecular weight bioactive compounds of two major species of red marine macroalgae *K. alvarezii* and *G. opuntia*, for use against various oxidative stress-induced diseases with a focus on hypertension, diabetes and inflammation. The lead molecules were isolated to homogeneity and characterized using combined chromatographic and spectroscopic experiments, whereas the novel leads were validated through bioassay and structure-activity relationship analyses to enrich the pool of bioactive leads. This research work also developed protocols to isolate and characterize polysaccharide compounds with bioactive properties against various drug targets for use against hypertension, diabetes, oxidants and inflammatory pathologies. The development of new bioactive compounds from marine metabolites would form the basis for new drug leads and would compose an abundant resource for future bioactivity research.

Abbreviations

^{13}C NMR	-	Carbon-13 Nuclear Magnetic Resonance
1D-NMR	-	One Dimensional-NMR
^{1}H-^{1}H COSY	-	Correlation spectroscopy
^{1}H NMR	-	Proton Nuclear Magnetic Resonance
$^{1}O_2$	-	Singlet Oxygen
2D-NMR	-	Two Dimensional- Nuclear Magnetic Resonance
ABTS	-	2, 2-Azino-Bis-3ethylbenzothiozoline-6-Sulfonic Acid
ACE	-	Angiotensin-Converting Enzyme
ANOVA	-	Analysis of Variance
BHA	-	Butylated Hydroxyanisole
BHT	-	Butylated Hydroxytoluene
CAT	-	Catalase
COSY	-	Correlation Spectroscopy
COX	-	Cyclooxygenase
DCF	-	Dichlorofluorescein
DCM	-	Dichloromethane
DEAE	-	Diethylaminoethyl
DEPT	-	Distortionless Enhancement by Polarization Transfer
DMSO	-	Dimethyl Sulfoxide
DNA	-	Deoxyribo Nucleic Acid
DPP-4	-	Dipeptidyl-Peptidase-4
DPPH	-	1, 1-Diphenyl-2-Picrylhydrazyl
EI	-	Electron Ionization
EI-MS	-	Electron Ionization Mass Spectrometry
EtOAc	-	Ethyl Acetate
FAPGG	-	Furanacryloyl-l-Phenylalanylglycylglycine
FT-IR	-	Fourier Transform Infra Red
GAE	-	Gallic Acid Equivalence
GC-MS	-	Gas Chromatography-Mass Spectrometry
GLP	-	Glucagon Like Peptide
GRx	-	Glutathione peroxidase
GSHPx	-	Glutathione peroxidase
H_2O_2	-	Hydrogen Peroxide
HMBC	-	Heteronuclear Multiple Bond Correlation
HPLC	-	High-Performance Liquid Chromatography
HREIMS	-	High Resolution Electron Ionisation Mass Spectrometry
HRESIMS	-	High Resolution Electrospray Ionisation Mass Spectrometry
HSQC	-	Heteronuclear Single Quantum Coherence
IC_{50}	-	Inhibition Concentration at 50 %
KBr	-	Potassium Bromide
LCMS	-	Liquid Chromatography Mass Spectroscopy
LOX	-	Lipoxygenase
m/z	-	Mass-to-Charge Ratio
MDAEQ	-	Malondialdehyde Equivalent Compounds
MeOH	-	Methanol
MS	-	Mass Spectroscopy
NADPH	-	Nicotinamide Adenine Dinucleotide Phosphate (reduced form)
NMR	-	Nuclear Magnetic Resonance
NOESY	-	Nuclear Overhauser Effect Spectroscopy
$NSAID_S$	-	Non-Steroidal Anti-Inflammatory Drugs
O^2	-	Superoxide Anion
OG	-	Octyl Gallate

$OH^{\cdot}$	-	Hydroxyl Radical
PC	-	Principle Components
PCA	-	Principal Component Analysis
PG	-	Propyl Gallate
ppm	-	Parts Per Million
P-TLC	-	Preparative Thin Layer Chromatography
QSAR	-	Quantitative Structure-Activity Relationship
R	-	Alkyl Radicals
Rf	-	Retardation Factor
ROS	-	Reactive Oxygen Species
RP-HPLC	-	Reverse Phase High-Performance Liquid Chromatography
Rt	-	Retention Time
SD	-	Standard Deviation
SOD	-	Superoxide Dismutase
SPSS	-	Statistical Program for Social Sciences
TBA	-	Thiobarbituric Acid
TBARS	-	Thiobarbituric Acid Reactive Species
tBHQ	-	Tertbutylhydroquinone
TLC	-	Thin Layer Chromatography
TMS	-	Tetramethylsilane
TNF-α	-	Tumor Necrosis Factor-α
TPC	-	Total Phenolic Content
tPSA	-	topological Polar Surface Area
UV-Vis	-	Ultra Violet-Visible
VCC	-	Vacuum Column Chromatography

List of Contents

CHAPTER 3: BIOACTIVE POTENTIAL OF *KAPPAPHYCUS ALVAREZII* AND *GRACILARIA OPUNTIA*

CHAPTER 4: ISOLATION AND CHARACTERIZATION OF SECONDARY METABOLITES FROM *KAPPAPHYCUS ALVAREZII* AND *GRACILARIA OPUNTIA*

CHAPTER 5: ISOLATION AND CHARACTERIZATION OF SULFATED POLYSACCHARIDES FROM *KAPPAPHYCUS ALVAREZII* AND *GRACILARIA OPUNTIA* AND THEIR PHARMACOLOGICAL APPLICATIONS

List of Tables

List of Figures

Chapter 1

INTRODUCTION

Contents

1.1. Marine Macroalgae

Marine life is fascinating, and considered to have great potential for its intrinsic values, as well for the development of new pharmacophore leads. Marine macroalgae are photosynthetic organisms, and there were reports of occurrence of bioactive metabolites. The natural products of marine macroalgae and other marine organisms represent one of the new frontiers in the exploration for valuable bioactive compounds with interesting pharmacological characteristics. Notably, these marine flora have the unique ability to withstand salt-triggered oxidative stress conditions, which is governed by multiple biochemical mechanisms facilitating cell homeostasis and retention of water ability. It is apparent that higher salt concentrations induce disturbances in osmotic and oxidative state of these marine organisms (Zhu 2001). They survive the unfavorable stressed environment by synthesizing various compatible osmolyte derivatives and accumulation of antioxidant molecules. Absence of oxidative damage in the stress-induced biochemical parameters of marine macroalgae suggested that their cells are the store house of bioactive metabolites with potential radical scavenging properties, which provide competitive advantages against various oxidative stress factors leading to the development of harmful reactive oxygen species (Blunt et al.

2006). Antioxidant effects have been reported from various macroalgae due to phenolic compounds, terpenoids and sulfated polysaccharides (Chakraborty et al. 2010a). Novel secondary bioactive metabolites from red marine macroalgae are attracting attention because of the growing demand for new compounds of marine natural origin, having potential applications in pharmaceutical fields and concerns about the toxic effects by synthetic drugs (Kladi et al. 2005; Kladi et al. 2006; Konig and Wright 1997a). The biofunction of small molecular weight molecules including polysaccharides in these organisms as bioactive metabolites is yet poorly understood. Considering the importance of these groups and paucity of information, a systematic search of these candidates for the development of new sources of chemical compounds will be helpful for the design and development of novel bioactive molecules harbored in these species with respect to their antioxidant properties for use in human health and medication. The knowledge on the structural features responsible for bioactivities will guide us to synthesize the molecules in commercial scale for use as new generation bioactive leads as potential drug candidates.

1.2. Marine Macroalgae as Potential Sources of Bioactive Compounds

Bioactive compounds have been reported from marine macroalgae due to various lipid analogues, terpenoids and sulfated polysaccharides (Blunt et al. 2016; Leal et al. 2013; Chakraborty et al. 2015; Newman and Cragg 2012). It is important to note that small molecular weight bioactives and polysaccharides constitute a major share of bioactives in marine organisms including marine macroalgae (Blunt et al. 2016). The predominant classes of novel small molecular weight marine natural leads in these organisms were found to be lactones, phenolics, hydroxybenzene and quinones (Blunt et al. 2014; Liu et al. 2012). The polysaccharides found in the marine macroalgae are known to have many physiological and biological activities including anti-coagulant, anti-viral, anti-tumor and anti-inflammatory and antioxidant effects (De Sousa et al. 2013). In addition, oligosaccharides obtained by depolymerization of marine macroalgal polysaccharides also were found to induce protection against viral, fungal and bacterial infections in plants. The reactive oxygen species are formed during the regular metabolic activities and their overproduction plays vital role in the pathogenesis of oxidative stress-induced diseases, such as chronic inflammation, neurodegenerative disorders, and certain types of cancer

(Yangthong et al. 2009). Antioxidant compounds exhibited a major role to attenuate these diseases, which reveal their extensive commercial potential in pharmaceutical and food industry. Therefore, consumption and addition of antioxidant compounds in food materials prevent the oxidative degradation of biomolecules. It is also important to note that the antioxidants assumed greater importance in controlling the initiation and development of inflammatory diseases. However, oxidative stress-induced molecular damages were found to be due to the overproduction of uncontrolled level of free radicals in the living cells (Florence 1995).

The modern studies have showed that marine macroalgae produced promising bioactive molecules for a range of diseases, such as oxidative stress, hypertension, cancer and inflammatory processes (Minelli et al. 2009). Inflammation is a convoluted mechanism, which includes cellular events and tissue recovery (Aller and Arias 2006). However, distraction of the balance between the free radicals and antioxidant concentration cause cellular oxidative stress, and therefore, antioxidative compounds displayed a prominent role as health defensive factors. They could retard or inhibit lipid oxidation by preventing the initiation or propagation of oxidizing chain reactions, and also by the process of free radicals scavenging (Piccolella et al. 2008). Therefore, there has been increased attention to search for the naturally derived antioxidant compounds from the marine environment during the last few decades. Nevertheless, there were many natural products that showed anti-inflammatory potential, and have comparably lesser extent of side effects. The marine organisms were found to be rich sources of both biological and chemical diversity along with numerous compounds produced by them with useful pharmacological activities (Mayer and Lehmann 1998). A number of bioactive compounds produced by red marine macroalgae were found to prevent the gastric ulcers and cancers caused by the oxidative stress along with inflammatory activities by lowering the production of inflammatory modulators in stomach and colon (Gonzalez et al. 1999). The bioactive natural compounds extracted from edible marine macroalgae would be safer to be used as anti-inflammatory therapeutics in food and traditional medicines. Marine macroalgae have drawn relevant attention in recent years in the search for bioactive compounds, which showed great potential as anti-inflammatory, anti-microbial, anti-viral and anti-tumor drugs (Souza et al. 2012). These groups of marine flora were found to be a rich source of antioxidant compounds (Wang et al. 2009), which could act against lipid oxidation in foods and oxidative stress in target tissues. A polysaccharide fraction of marine macroalga *Padina* sp, was found to

contain anti-inflammatory activities, and was demonstrated to be active against inflammatory enzymes, such as cyclooxygenase-1, 2 (COX) and 5-lipoxygenase (5-LOX) (Praveen and Chakraborty 2013). An anti-inflammatory concentrate enriched with substituted oligofucans was purified from the brown marine macroalgae (Praveen and Chakraborty 2013). Rhodophytan marine macroalgae were acknowledged as bounteous source of various biologically active lead molecules (Blunt et al. 2005). Small molecular weight pharmacophores from the red marine macroalgae were classified as terpenoids (Amico et al. 1991; Rochfort and Capon 1996), halogenated cyclic ether (Wright and Konig 1997a, b), acetogenins (Wael et al. 2010), phlorotannins (Yan et al. 1996), bromophenols, bromoindoles, as well as fucoxanthin (Yan et al. 1999) and phenolics (Chakraborty et al. 2014).

Macroalgae-derived bioactive compounds were found to exhibit extensive pharmacological properties, including antioxidative (Chakraborty et al. 2016; Chakraborty et al. 2014; Chakraborty and Paulraj 2010), cytotoxicity (Yotsu-Yamashita et al. 2004), anti-helmintic (Daigo 1959), anti-malarial (Topcu et al. 2003), anti-microbial (Vairappan et al. 2004), quorum-sensing inhibition (Manefield et al. 1999), and have been considered as potential sources of new therapeutic agents. Small molecular weight molecules isolated from marine macroalge were found to possess various bioactive potentials, such as anti-inflammatory and anti-proliferative (Pereira 2011). The structures of these secondary metabolites were found to vary from acyclic moieties with a linear chain to complex molecules and constituted of biogenic alkaloids, polysaccharides, terpenes and fatty acids (Nunnery 2010). Marine macroalgae are rich source of secondary metabolites, such as polyphenols and soluble polysaccharides with strong anti-microbial and antioxidant activities (Ananthi et al. 2010). The natural antioxidants in macroalgae were reported to include phenolics, phlorotannins, carotenoid, fucoxanthin and isoprenoids (Swanson and Druehl 2002), which were reported to have potential pharmacological importance

Figure 1.1. Examples of brown marine macroalgae

Figure 1.2. Examples of red marine macroalgae

The biologically active compounds in marine macroalgae were found to include polysaccharides comprising galactans, fucoidan, laminarin and alginates (Ferreira et al. 2012). The macroalgal polysaccharides, especially sulfated derivatives were reported to have strong antioxidative properties, and have greater potential to be applied in pharmaceutical and food industries (Pangestuti and Kim 2011). Potential antioxidative and free radical scavenging activities (Ganesan et al. 2008) along with *in vitro* anti-proliferative activity in cancer cell lines (Vallinayagam et al. 2009) were also reported in *K. alvarezii*.

1.3. Free Radicals and Oxidative Agents as Major Causal Agent of Life-Threatening Diseases

Radicals are atoms, molecules or ions with minimum one unpaired electron in the outermost orbit, and are able to exist independentently. Free radicals are highly reactive due to the existence of unpaired electron. Any free radical associated with oxygen can be assigned as reactive oxygen species (ROS). The numerous ROS constitute the radicals, such as hydroxyl ($OH^{\cdot}$), hydrogen peroxides (H_2O_2), singlet oxygen ($^1O_2$), hydroxyl radical and super oxide anion (O^2). Oxidative stress is described as the state in which the increased level of toxic reactive oxygen species defeats the endogenous antioxidant resistance of the host. This resulted in the excessive generation of free radicals, which could interact with the cellular lipids, proteins and nucleic acids, leading to injury and subsequent organ dysfunction. Therefore, the free radicals have been involved in the pathogenesis of life-threatening diseases, such as Alzheimer's, Parkinson's, cancer and cardiovascular disorders (Chew et al. 2008). Free radicals were found to be either endogenous or exogenous. Endogenous free radicals are formed in the body by abnormal metabolism of oxygen, destruction of blood cells by parasites, bacteria and viruses using oxidants, such as nitric oxide, super oxide and hydrogen peroxide. The degradation of fatty acids and other molecules often result in the formation of cellular component (peroxisomes) producing hydrogen peroxide (Slater 1979; Lobo et al. 2010). Exogenous sources of free radicals, which comprise air pollutants including trace metals (lead, mercury, iron and copper) were found to be responsible for free radical generation. The mechanisms of oxidative cellular damage are summarized in Figure 1.3.

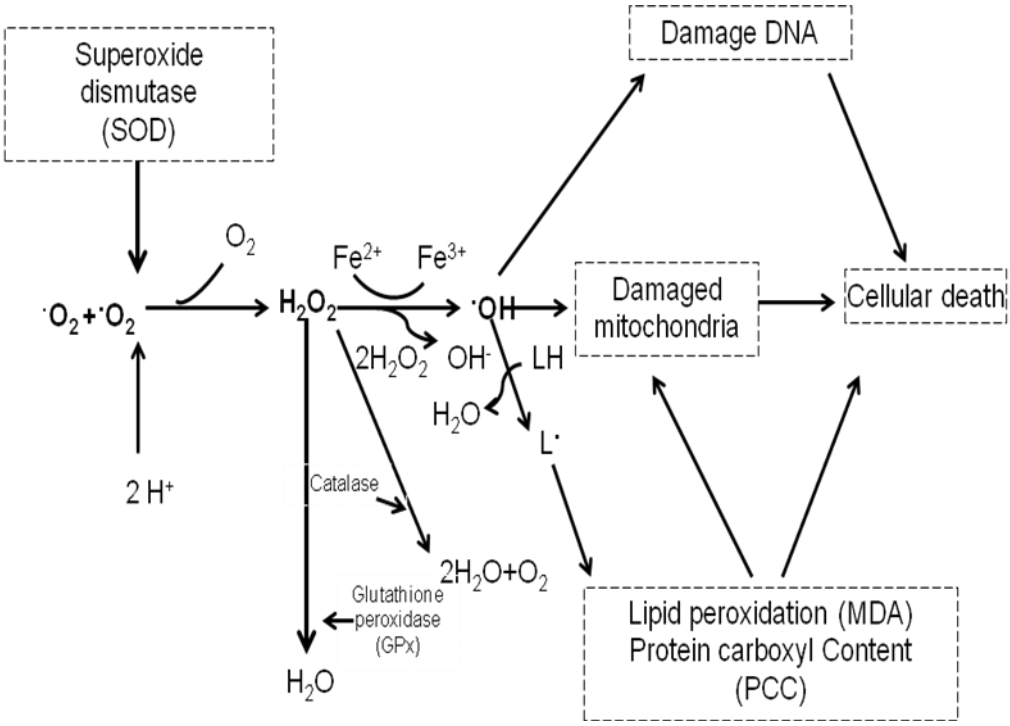

Figure 1.3. Mechanisms of oxidative cellular damage

Free radicals are reduced into water with the co-operation of the three main antioxidant enzymes, such as superoxide dismutase (SOD), catalase and glutathione peroxidases (GSHPx). The hydroxyl radicals generated from hydrogen peroxide induce the production of oxidative cell injury that include carboxylation of protein, DNA damage and lipid peroxidation. By these pathways, oxidative damage leads to cellular death. Excessive production of free radicals is often correlated with lipid and protein peroxidation leading to cell structural damage, tissue injury or gene mutation that finally led to the generation of different health disorders. ROS are the arbitrator of inflammation and other cells were found to be associated with the generation of eicosanoids along with the activation/release of different cytokines, and proliferate the inflammatory action from one organ (liver) to another (kidney, lungs, etc.). The Figure 1.4 illustrated the free radical induced diseases in human biological system leading to the oxidative stress in tissues and multiple-system organ failure (Parke and Parke 1995).

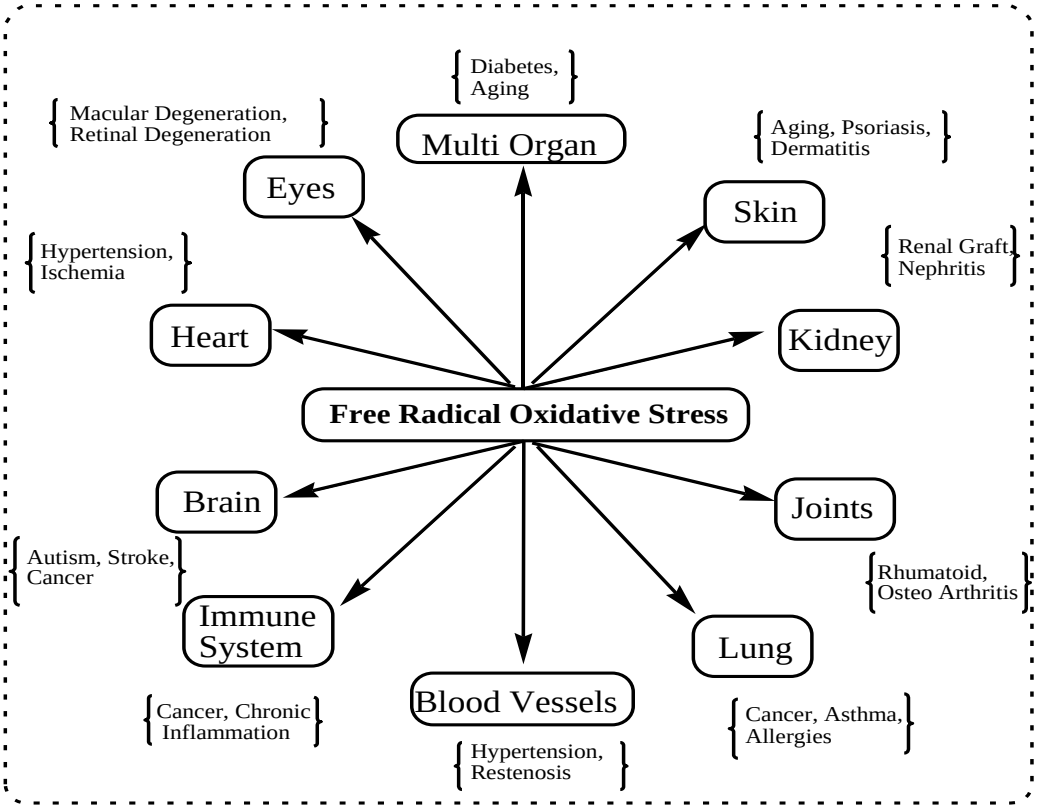

Figure 1.4. Free radical induced diseases in humans

The ROS interfering with the pathogenesis of inflammatory diseases is a concern in immune and autoimmune disorders, which include inflammatory bowel disease, cancer (Ames et al. 1993; Parke 1994), hepatitis (Elliot and Strunin 1993), AIDS (Baruchel and Wainberg 1992), Alzheimer's dementia, multiple-system organ failure (Fry 1992; Parke and Parke 1995) and respiratory distress syndrome (McLean and Byrick 1993).

1.4. Biological Protection Against ROS-Mediated Diseases

The human body has in-built biological processes in place to defend oxidative stress by generating antioxidants, either naturally originated *in situ* (endogenous antioxidants) or externally supplied through diet (exogenous antioxidants).

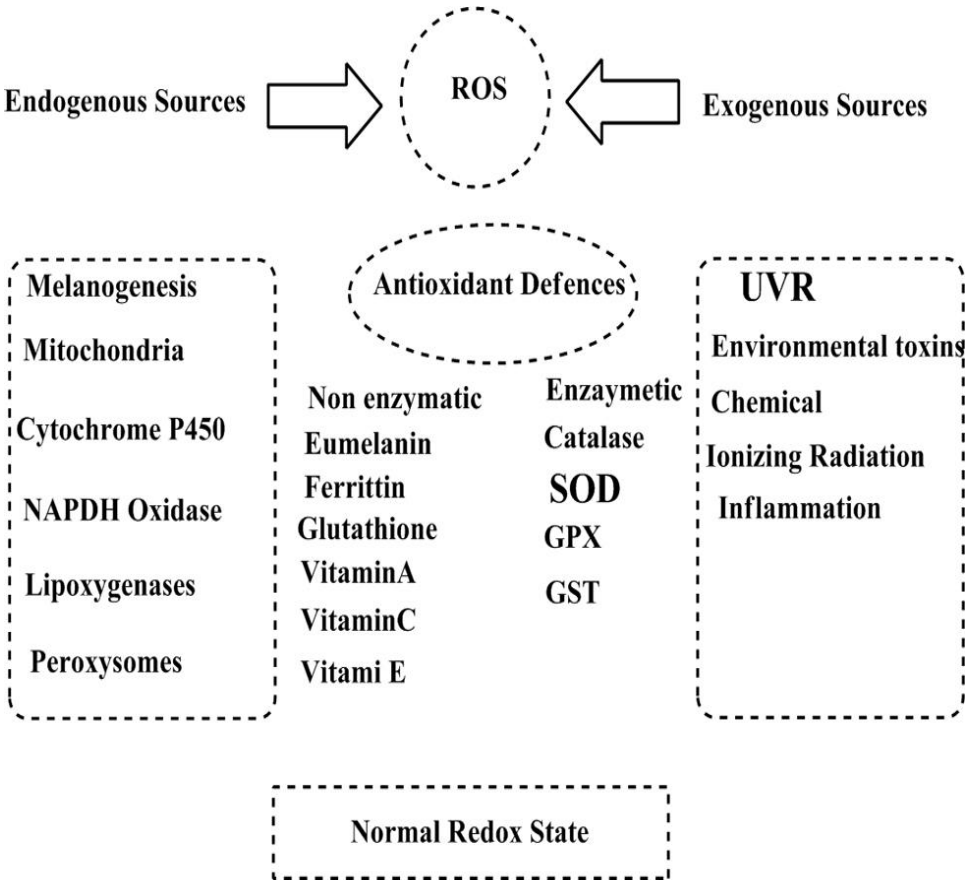

Figure 1.5. Reactive oxygen species (ROS) are derived from multiple sources (endogenous and exogenous) and are counter-balanced by enzymatic and non-enzymatic antioxidants. The antioxidant defenses overwhelmed ROS production resulting in prevention of diseases

The enzymatic and non-enzymatic antioxidant defenses minimize the generation of ROS leading to prevention of diseases. Substances that inhibit oxidation and are able to counteract the damaging effects of oxidation in body tissue are termed as antioxidants. There are biogenic antioxidative enzymes, such as superoxide dismutase (SOD), catalase (CAT), glutathione peroxidase and glutathione reductase (GRx) that are free radical scavengers (Fig. 1.5), and neutralize various types of reactive oxygen species.

1.5. Synthetic Alternatives and Their Adverse Effects

Butylated hydroxy anisole (BHA), butylated hydroxy toluene (BHT), propyl gallate (PG), teritiary butyl hydroquinone (TBHQ), octyl gallate (OG), 2, 4, 5-trihydroxy butapyranone, nordihydroguaiaretic acid and 4-hexyl resorcinol are the few common examples of synthetic antioxidants (Carocho 2013; Aguillar et al. 2012; Gharavi and El-Kadi 2005; Anton et al. 2004; Kubo et al. 2001; Astill et al. 1959; Evan and Gardner 1979; Chen et al. 2004). They are widely used in lipid-containing foods for reducing rancidity, arresting lipid oxidation or peroxidation, cosmetic, and pharma industries. During the last few years, researchers questioned the safety of these synthetic antioxidants in the food systems, and there have been continuous efforts to search for green antioxidant alternatives. Therefore, the pharmaceutical and functional food industries have been focused on developing and marketing natural antioxidants with greater safety thresholds. ROS-mediated inflammation is mainly treated by using non-steroidal anti-inflammatory drugs (NSAIDs) by inhibiting pro-inflammatory cyclooxygenase-1 (COX-1) (a constitutive isoform) along with cyclooxygenase-2 (COX-2). The major side-effects of these drugs are often destructive, which include gastrointestinal ulcers and cardiovascular diseases (Quan 2008). Hence, in recent years, efforts in searching naturally antioxidant and anti-inflammatory compounds in functional food or drugs to replace synthetic products are major thrust areas of research.

1.6. Marine Natural Leads from the Marine Macroalgae: Potential Pharmacophore Candidates Against Several Diseases

Marine flora was recognized as potential natural sources of bioactive compounds with antioxidant and anti-inflammatory properties (Kornprobst 2005). Marine macroalgae constitute a major share of marine flora, and they were reported to be valuable reservoirs of bioactive compound with antioxidant, anti-bacterial, anti-inflammatory and anti-carcinogenic activities (Kornprobst 2005).

Marine macroalgae are photosynthetic organisms, and are resolved to a conjunction of stressful factors, *viz*., light and oxygen at the origin of the evolution of free radicals and other oxidative reagents. The absence of oxidative destruction in their structural components evidently recommended that their cells generate bioactive metabolites with antioxidative resistance systems (Escrig et al. 2001). The reactive

oxygen species (ROS) *viz*., hydroxyl radical (HO), hydrogen peroxide (H_2O_2) etc, are metabolites generated during the aerobic life as an outcome of the metabolism of oxygen. DNA, cell membranes, proteins and other cellular fragments are target sites of the free radical stimulated oxidative degradation processes, resulting in serious human diseases, such as chronic inflammation, atherosclerosis, cancer, cardiovascular disorders and ageing. Clinical studies established that oxidative stress through free radical generation assumes a significant role in the inception of hypertension. Reactive oxygen species and inflammatory markers were found to be greater in the patients with hypertension (Savoia and Schiffrin 2007). It has been reported that extended generation of ROS substantially adds to the dysregulation of physiological processes, which evoke structural and functional variations in hypertension. Increased levels of ROS also potentiate the pathogenic factors leading to type-2 diabetes, and chronic subclinical inflammation was found to be associated with the insulin resistance syndrome (Festa et al. 2000). Diabetes is the most frequent endocrine disorder and, it has been predicted that greater than 200 million people in the world will have diabetes mellitus and 300 million will decisively have the disorder by the year of 2025 (King et al. 1998). The remedial measures to treat the pathogenesis of diabetes are to diminish the post-prandial hyperglycemia in order to prevent the actions of carbohydrate-hydrolyzing enzymes, such as α-amylase and α-glucosidase along with dipeptidyl peptidase 4 (DPP-4). Marine macroalgae were found to be rich sources of bioactive compounds, such as terpenoids, phloroglucinol, phenolics, fucoidans, sterols, glycolipids and halogenated compounds, whereas the extracts or isolated components derived from these marine species exhibited a wide range of pharmaceutical properties, such as anti-cancer, anti-bacterial, anti-viral, anti-fungal, anti-inflammatory, antioxidant, hypoglycaemic, hypolipidemic, hepatoprotective and neuroprotective activities (Liu et al. 2012; Chakraborty et al. 2015).

Antioxidant compounds play an immense role against these disorders, which described their significant economic potential in medicine (Blunt et al. 2016), food production (Blouin et al. 2011) and cosmetic industry (Wang et al. 2015). Chemical compounds with oxidation-inhibiting properties are present in the tropical sessile macroalgae as a protective mechanism against oxidative stress factors in the oceanic ecosystems (Chakraborty et al. 2010a). Investigation of curative metabolites, such as benzene acetamide, methyl-ethyl ketone derivatives and bromophenols extracted from marine macroalgae (red and brown) with significant inhibitory activity towards α-

glucosidase enzymes were described in the previous reports of literature (Seung et al. 2013). In the last few years, numerous investigations have shown that low-grade inflammation were identified with the possibility of developing type-2 diabetes (Crook 2004).

1.7. Antioxidant and Anti-inflammatory Potentials of Bioactives from Red Marine Macroalgae

Bioactive properties of the marine macroalgae were reported to be due to the presence of sulfated polysaccharides, phenolics and terpenoids (Chakraborty and Paulraj 2010; Chakraborty et al. 2015). Polyphenols and sulfated polysaccharides present in macroalgae showed potential anti-viral, anti-tumoral, anti-inflammatory and anti-coagulant activities (Cumashi et al. 2007). Different investigations prescribed that antioxidant and other bioactive properties fundamentally reliant on the level of sulfation, position of sulfate groups on the sugar backbone, sugar composition and glycosidic branching (Leonard et al. 2010). The reported bioactivities of polysaccharides from marine macroalgae incorporated antioxidant, immunomodulatory, anti-coagulant, anti-thrombotic, blood lipid reducing and anti-inflammatory activities (Li et al. 2008). Antioxidant capacities of polysaccharide or polysaccharide-complex were observed in the fucoidan and fucans isolated from *Fucus vesiculosus* and *Padina gymnospora* displaying inhibitory properties towards hydroxy radical and superoxide radical formation (De Souza et al. 2007). The red marine macroalga *Kappaphycus alvarezii* is an economically significant and extensively cultivated red macroalga under the class of Rhodophyceae. *K. alvarezii* has been reported for its antioxidant potential (Ganesan et al. 2008) and *in vitro* anti-proliferative activity in the cancer cell lines (Vallinayagam et al. 2009). The genus *Gracilaria* is the largest in the order Gracilariales, and was found to include more than 150 species, which were distributed in the tropical and temperate sea (Guiry and Guiry 2016). The most common bioactivities known in *Gracilaria* are anti-bacterial, anti-viral, and have been best described in *Gracilaria cornea* (Bansemir et al. 2006) and *Gracilaria changii* (Sasidharan et al. 1991).

Figure 1.6. Marine macroalgae and their collection site at the Gulf of Mannar of Southeast coast of India

Among different species of the genus *Gracilaria*, *Gracilaria opuntia* is one of the predominantly available red marine macroalga grown in the Gulf of Mannar region of the south-east coast of India. There were no reports of the occurrence of naturally occurring antioxidative and anti-inflammatory compounds from this marine macroalgal species.

1.8. Objectives

The red marine macroalgae comprise a large collection of species that are abundant in the coastal areas of Gulf of Mannar region in Mandapam. Among various red macroalgae, *Kappaphycus alvarezii* and *Gracilaria opuntia* (Phylum Rhodophyta) are abundantly available in this area throughout different seasons. Therefore, these species were shortlisted for the present study to evaluate their bioactive properties. Based on this background the objectives of the present study were as follows:

- To collect the red marine macroalgae, *Kappaphycus alvarezii* and *Gracilaria opuntia* (Rhodophyta) from the coastline of India and making extracts, fractions.
- To screen the extracts/fractions from the studied macroalgae for antioxidant and anti-inflammatory properties.
- To isolate the lead molecules belonging to small molecular bioactives and polysaccharides from the crude extracts/fractions of the studied macroalgae using various chromatographic techniques coupled with evaluation of target bioactivities.
- To characterize the bioactive leads using detailed spectroscopic techniques, such as infrared, extensive nuclear magnetic resonance, and mass spectroscopic experiments.
- To predict the biological properties of the studied compounds by structure-activity relationship analyses and generation of database of potential lead molecules as tool box to combat inflammation.

1.9. Thesis Outline

Based on the above objectives the present thesis is divided into a total of six chapters. The importance of the study on the bioactive properties of the red marine macroalgae with objectives are discussed and explained in the Introduction under Chapter 1. Chapter 2 deals with the detail review of the works with regard to the significance of macroalgae as potential sources of antioxidative and anti-inflammatory bioactivities. The pharmaceutical and medicinal values of these species are covered under this chapter. Subsequently, Chapter 3 describes the bioactive properties (with reference to antioxidant, anti-inflammatory, anti-diabetic and anti-hypertension) of the organic extracts derived from *K. alvarezii* and *G. opuntia*. Chapter 4 describes the isolation and characterization of secondary metabolites responsible for antioxidant and anti-inflammatory activities, for the development of new sources of bioactive pharmacophores, from the studied marine macroalgae. The evaluation of the antioxidant, anti-inflammatory, anti-diabetic and anti-hypertension potentials of the polysaccharides derived from *K. alvarezii* and *G. opuntia* along with their structural characterization and applications are described in Chapter 5. The entire work in this Thesis, along with the discussion regarding the new research findings are summarized in Chapter 6.

Chapter 2

REVIEW OF LITERATURE

Contents

2.1. General Background and Importance

Oxidative stress-induced molecular damages of living cells are caused due to the uncontrolled production of free radicals. Traditionally, macroalgae are considered as valuable marine flora, which are preferred delicacies in the South-east Asian countries, particularly in Japan, China, Korea and Indonesia due to their potential antioxidant and therapeutic properties (Wang et al. 2009). Marine macroalgae developed self resistance mechanisms to inhibit oxidative stress dependent disorders in

coastal environment by generating biogenic compounds with antioxidant properties. Therefore, researchers have developed interests in the isolation of bioactive compounds with potential pharmacological properties from marine macroalgae. These group of marine species are the abundant sources of natural bioactive metabolites, in which many of them constitute a novel chemical classification, which has been unexplored in the terrestrial ecosystem. This describes the use of marine macroalgae as potential resources of naturally available antioxidant compounds. Notably, the marine macroalgae do not require freshwater for their production, and these macroalgal species completely depend on saline water for their growth and reproduction.

In recent years, macroalgae have drawn considerable attention to the food technologists as renewable natural resources of novel bioactive compounds and functional food ingredients with potential antioxidative, anti-inflammatory, anti-microbial, anti-viral and anti-tumor activities (Blouin et al. 2011; Holdt and Kraan 2011; Souza et al. 2012; Blunt et al. 2016). This might describe the application potential of these marine species as sustainable sources to bestow valuable 'natural' antioxidant molecules for use as treatment against a host of oxidative stress-induced diseases, which include inflammation, arthritis, type-2 diabetes, obesity and cancer. Therefore, it is important to explore these underutilized and natural resources, based on their bioactive potential.

2.2. Marine Macroalgae as Natural Renewable Resources of Bioactive Compounds

During the last few decades, there is an increased interest in the search of natural antioxidants to replace the synthetic alternatives. There were reports of utilizing marine macroalgae as natural renewable resources to derive potent bioactive compounds and nutraceutical supplements. During the past few years, nutraceutical and agricultural food industries were more focused on the use of macroalgae to develop valuable bioactives and pharmaceutical natural leads. Macroalgae comprises a leading proportion in to the marine flora, and they were recorded to possess structurally distinct metabolites with diverse biogenic potential endowed with hypolipidemic, antioxidant, anti-viral, anti-cancer, anti-bacterial, anti-inflammatory, hypoglycaemic, anti-fungal, hepatoprotective and neuroprotective properties (Liu et al. 2012; Chakraborty et al. 2013). The applications of these marine resources as constituent in functional food are

convincing due to presence of structurally diverse bioactive principles. In the ocean environment, light energy absorbs much faster than it can be scattered leading to the generation of free radicals and stimulates lipid oxidation. Marine macroalgae are photosynthetic plants, which are exposed to a fusion of increased oxygen concentration and sunlight. The reduced structural destructions in the cells of marine macroalgae even after the constant exposure to the sunlight, assigned to the significance of natural antioxidative metabolites in macroalgae to neutralize these hazardous free radicals (Swanson and Druehl 2002; Burritt et al. 2002). The antioxidative potential of marine macroalgae could be utilized to interrupt the radical aggregation and propagation. Therefore, it is of interest to examine the bioactive leads from marine macroalgae for use as potential antioxidant and anti-inflammatory agents. The marine macroalgae were located in intertidal locale, which represents an abundant source of structurally distinct bioactive leads with potent biomedical and pharmaceutical applications (Marina Barbosa et al. 2014). However, there were limited reports in relation to the structural knowledge of bioactive leads in marine macroalgae from the Indian waters. The report on the structural characteristics would help us to develop the molecules in commercial scale, and facilitate explaining their mode of action. The isolation and characterization of newer leads from marine macroalgae will be guiding us to the development of antioxidant compounds to increase the prolonged storage of food ingredients.

2.3. Classifications of Marine Macroalgae

On the basis of pigmentation, marine macroalgae can be classified as green, brown and red belonging to the family of Chlorophyceae, Phaeophyceae and Rhodophyceae, respectively.

2.3.1. Green Marine Macroalgae

Green marine macroalgae are smaller in size, and they exhibited different shapes, such as hair-like filaments, flat sheets, cylinders, spheres and strings of beads. These species of macroalgae are widely present in the marine ecosystem, and green color of this particular macroalgae has been due to the presence of pigments, such as chlorophyll *a* and chlorophyll *b*. *Bryopsis* and *Caulerpa* are some common examples of green macroalgae (Fig. 2.1).

2.3.2. Brown Marine Macroalgae

Brown macroalgae of marine origin are usually larger in size when compared to other classes of macroalgae. The length of this group of macroalgae is about 20 m with thick leather-like appearance. Traditionally the classes of Phaeophyte are considered as photosynthetic marine algae. However, the class of phaeophytes is not closer to the terrestrial plants, due to the presence of cell wall pigments including fucoxanthin and chlorophyll-*c*. The genus belonging to *Sargassum* and *Padina* are some of the common examples (Fig. 2.2).

2.3.3. Red Marine Macroalgae

Red marine macroalgae belonging to the class of Rhodophta are generally smaller in size, varying between few centimeters to one meter in length. They exhibited variety of shapes including filamentous, encrusting, tube-like string-like and flat sheets. The red marine macroalgae appear in different colors, such as red, purple, and brownish red due to the presence of pigment phycoerythrin and other characteristics. In addition to phycoerythrin they possess other photosynthetic pigments like R-phycocyanin and chlorophyll-*a*. Red macroalgae are generally comprise filamentous forms, however when compared to other algal species they do not have flagellated cells during the complex life cycles (McHugh 2003). In addition, these macroalgae are usually multicellular and mainly attached with the rocks. *Kappaphycus* and *Gracilaria* are the common examples of red marine macroalgae (Fig. 2.3).

2.4. Red Marine Macroalgae: Prospective Sources of Bioactive Compounds

Species of the red marine macroalgae (class Rhodophyceae) were proven to be rich sources of structurally unique and biologically active secondary metabolites for applications in functional food and pharmaceuticals (Kladi et al. 2004). Terpenoids (Chakraborty and Paulraj 2010), phylopheophylin (Cahyana et al. 1992), fucoxanthin (Yan et al. 1999) and phlorotannins (Yan et al. 1996) are some of the antioxidative compounds were isolated from these species. The bioactive compounds extracted from the macroalgae are used as safer anti-inflammatory therapeutics.

Figure 2.1. Examples of green marine macroalgae

Figure 2.2. Examples of brown marine macroalgae

Figure 2.3. Examples of red marine macroalgae

The vast majority of the red macroalgae of marine origin were found to possess bioactive compounds belonging to diterpenes (Rochfort and Capon 1996), sesquiterpenes (Amico et al. 1991) and C_{15} non-terpenoids containing ether rings of different sizes including halogenated cyclic ether enynes and related allenes (Erickson 1983; Konig and Wright 1997a, b; Iliopoulou et al. 2002). These groups of marine macroalgae were reported for their potential antioxidant properties, and *in vitro* anti-proliferative activity in the cancer cell lines (Chakraborty et al. 2015). *Kappaphycus alvarezii* (Doty ex Silva et al. 1996) (class Rhodophyceae, family Solieriaceae, order Gigartinales) is economically significant and predominantly farmed red macroalga in the shallow tropical marine habitats around the South-east Asian countries, particularly Philippines, Taiwan, Malaysia, Indonesia and India (Ask and Azanza 2002; Chandrasekaran et al. 2008). Despite the fact that red macroalgae, particularly *Laurencia* sp., have been studied extensively with respect to secondary metabolite chemistry (Amico et al. 1991; Rochfort and Capon 1996; Manta 2001; Iliopoulou et al. 2002), studies on members of the genus *K. alvarezii* have been rare with regard to the isolation of novel intriguing structures. Rhodophytan macroalgae were acknowledged as bounteous source of various biologically active lead molecules (Blunt et al. 2005).

Small molecular weight pharmacophores from the macroalgae were classified as terpenoids (Amico et al. 1991; Rochfort and Capon 1996), halogenated cyclic ethers (Konig and Wright 1997a, b), C_{15}-acetogenins (Wael et al. 2010; Rochfort and Capon 1996; Erickson 1983; Konig and Wright 1997a, b), phlorotannins (Yan et al. 1996a), bromophenols, and bromoindoles as well as fucoxanthins (Yan et al. 1999a, b), and phenolics (Chakraborty et al. 2015). Rarely occurring halogenated furanone metabolites were isolated from the Australian red macroalgae, *Delisea fimbriata* and *Delisea pulchra* (Kazlauskas et al. 1977a; De-Nys et al. 1993). Bioactive compounds isolated from macroalgae were found to exhibit extensive pharmacological properties, including antioxidative (Chakraborty et al. 2015; Chakraborty et al. 2016; Chakraborty and Paulraj 2010), cytotoxicity (e.g., halomon) (Yotsu-Yamashita et al. 2004), anti-helmintic (Daigo 1959), anti-malarial (Topcu et al. 2003), anti-microbial (Vairappan et al. 2004), quorum-sensing inhibition (Manefield et al. 1999), and have been considered as potential sources of new therapeutic agents. The red macroalga, *Gracilaria opuntia* Durairatnam (family Gracilariaceae, phylum Rhodophyta) is abundantly available throughout the subtropical and tropical climatic zones (Guiry and Guiry 2016). No natural products were reported from this red macroalga, suggesting *G. opuntia* is an important source to characterize novel bioactive compounds of potential medicinal significance.

2.5. Cultural and Economic Importance of Macroalgae

Marine macroalgae, which were found to possess both industrial and ecological importance in various parts of the World, are one of the major marine resources among marine flora. Traditionally, they were harvested from the wild, but presently, the growing percentage of the production is performed from the cultivation of marine macroalgae. The cultivation of this group of marine flora is one of the means of livelihood among the coastal fishermen populace, and has been used to deliver integrated coastal management (Sievanen et al. 2005). During the year of 2000s, trial farming of marine macroalgae such as *Kappaphycus alvarezii* and *Eucheuma denticulatum* were started in the southern coast of Kenya (Wakibia et al. 2006).

With the increasing requirement of marine macroalgae resources, natural populations regularly become insufficient. Experiments are being invented to accelerate the reproduction of macroalgae by resource administration methods including artificial

farming, advanced collection techniques, expelling challenging species, including artificial habitation. The world's largest favorable macroalgae farming industries are located in Asia, where there is a great necessity for macroalgae-based products and intensify society to organize market growth. Immense ranges of systems are used to culture the macroalgae controlled by biogeographical features and life cycle of the cultivated species (Luning 1990; Kain 1991; Critchley and Ohno 1997).

In the year of 1960s, culturing of the species *Gracilaria* was established in China for the production of raw material for agar industry. At the beginning, cultivation of marine macroalgae was performed on ropes in channel involving fish pond sewage, but by on the year of 1967 this was passed towards the fish ponds themselves (Troell et al. 1999; Bushmann et al. 2001). The novel large scale cultivation of macroalgae such as *Hypnea, Gracilaria, Gelidiella, Enteromorpha* and *Kappaphycus* in Indian coastal water was developed by the Mandapam regional centres of ICAR-Central Marine Fisheries Research Institute and CSIR-Central Salt and Marine Chemical Research Institute. Previously, they were cultivated by vegetative fragment on stones or a floating system and deposit spores on to the nets. A tissue culture method was adapted to some of the algal species particularly for *Kappaphycus,* to enhance its biological productivity. In addition the industrial production techniques were implemented in the species *Gelidiella* and *Kappaphycus* for the extraction of phycocolloids, such as agar and carrageenan, and it was transferred to the industries (Ganesan et al. 2009).

Many species of macroalgae are edible and few of them are deliberated to be a great delicacy. The macroalgae-based industries contributed a wide variety of products with an approximated annual income of US $ 5.5-6.0 billion. Marine macroalgae played very prominent role in human diet in various countries, particularly in China, Japan and other Asian countries due to the valuable components, such as minerals and vitamins (Nisizawa et al. 1987; Fleurence 1999). Other than hydrocolloid-based products, fertilizers, miscellaneous uses and animal feed additives were also contributed significant economic value to the industries (McHugh 2003). Marine macroalgae possess distinct uses in various industries, such as food and feed, fertilizers and pharmaceutical industry (Chapman and Chapman 1980).

The green macroalga *Ulva* that is also known in the name of 'Sea lettuce' has found to be rich in protein content in comparison with *Enteromolpha* and *Monostroma* spp. (Ohno 1993). Due to the presence of rich protein content, *Ulva* is considered as a fresh ingredient in salads. Other than *Ulva,* macroalgae such as *Caulerpa lentillifera*

and *Caulerpa racemosa* are the other famous edible macroalgae that were used in fresh salads (McHugh 2003).

As compared to green macroalgae, brown macroalgae are mainly considered for the extraction of hydrocolloid named as alginate, which exist in the cell wall material. The species of brown macroalgae such as *Lessonia, Ecklonia, Lalllinaria* and *Macrocystis* are generally used in foreign countries for the extraction of alginate, although the species of *Turbinaria ornata* and *Turbinaria conoides* are considered for the industrial production of alginate in India. In addition to the production of phycocolloids, some species of brown macroalgae, such as *Hizikia, Laminaria* and *Undaria* were considered as the preferred food items (Cordero 2003; McHugh 2003). Red marine macroalgae have been considered as a food product, and was consumed by the coastal populace during the last 200 years. There are approximately 344 available species, which were found to possess economic value, but few of them includes *Eucheuma, Porphyra, Gleopeltis, Gracilaria* and *Gelidium* have been farmed to a significant extent. The red macroalgae were found to be prominent sources of agar and carrageenan.

2.6. Structural Diversity of Bioactive Compounds from Marine Macroalgae

Red marine macroalgae are known to be an unprecedented source of different terpenoid and non terpenoid secondary metabolites, including halogenated cyclic ethers and related allenes with prominent bioactivities (Blunt et al. 2006). Sulfated polysaccharides from macroalga *Fucus vesiculosus* were known to have antioxidant importance, and advocation of sulfated polysaccharides enhanced the antioxidant status, thereby preventing membrane injury and free radical formation (Veena et al. 2007). A previous report of literature described the antioxidant property in the sulfoglycolipid fraction of red marine macroalga *Porphyridum creuntum* (Berge et al. 2002). Fucoxanthin, which is a polysaccharide analogue, was reported to be the major antioxidant metabolite in the edible marine macroalga *Hijikia fusiformis* (Yan et al. 1999a). The sesquiterpenes (majapolene B) (Blunt et al. 2008); diterpenes (neorogioldiol B) (Blunt et al. 2005) and C_{15}-acetogenins (laurenyne) were isolated from the red marine macroalgae, and their structural description on the basis of halogen atoms (Konig and Wright 1997b) were detailed. These compounds were reported to possess antioxidative, anti-cancer and cytotoxic properties. Among the antioxidants from marine macroalgae,

phenolic acids, flavonoids, anthocyanins, hydroxycinnamic acid derivatives, alkaloids and terpenoids (Bandoniene and Murkovic 2002) were reported to have major share among others (Ragan and Glombitza 1986).

The marine macroalgae deliver a cocktail of halogenated secondary metabolites with significant industrial values and pharmaceutical importance (Holdt and Kraan 2011). The structures of these algal secondary metabolites were found to range from non cyclic linear chain moiety to complex cyclic entities. Halogenations generally bring these metabolites with intriguing characteristics, and macroalgae displayed distinct and individual anabolism pathways for the generation of halogen-substituted compounds with pharmacological potentials, such as anti-inflammation, anti-bacterial, ichthyotoxic, cytotoxic, anti-fungal, and insecticidal properties. Red macroalgae are the main source of halogenated metabolites, which include callicladol (Holdt and Kraan 2011), laurenterol (Castro and Huber 2013) and halomon (Lordan et al. 2011). Red marine macroalga of the genus *Laurencia* were found to be rich sources of broad-ranging halogenated compounds including C_{15}-acetogenins, terpenoids, sesquiterpene alcohol, and elatol with potential bioactivities (Laurienzo 2010). A series of C_{15} acetogenin enynes displaying anti-staphylococcal activity, were isolated from *Laurencia glandulifera* (Kladi et al. 2008). 5-Acetoxypalisadin B (Jiao et al. 2011), palisadin A (Pomin et al. 2008), and palisadin B (Ngo et al. 2013) were the anti-microbial compounds, which were isolated from *Laurencia saitoi* (Ji et al. 2009). Anti-bacterial potential of Malaysian macroalga *Laurencia pannosa* was tested against different marine bacterial species, such as *Chromobacterium violaceum*, *Proteus mirabilis* and *Vibrio cholerae*. The halogenated sesquiterpenes, pannosanol, pannosane and chlorofucin (Güven 2010; Takaichi 2011) were found to display potential anti-bacterial activity.

Chromenes are one of the distinctive classes of bioactive compounds and functional food component exhibiting various pharmacological properties, such as antioxidant (Milan et al. 2011), anti-viral (Mori et al. 2003), anti-inflammatory, anti-coagulant, and TNF-α inhibitor (Cheng et al. 2003) activities. This group of benzopyran derivatives represents the basic nucleus of various marine natural products, particularly belonging to polyphenols, alkaloids, small molecular weight compounds, and are ubiquitously distributed among marine organisms including coelenterates, macroalgae, sponges and tunicates (Blunt et al. 2005). There were reports of the presence of chromene metabolites with antioxidative and cytotoxic properties in macroalgae (Kato et al. 1975). Notably, the greater bioactivity of the chromene derivatives was attributed

to the lipophilic properties, which lead to the higher permeability across cell membranes (Nicolaou et al. 2000). Anti-inflammatory compounds and cyclooxygenase inhibitors, such as SC-75416, 6-chloro-8-methyl-2-(trifluoromethyl)-2*H*-chromene-3-carboxylic acid, 6-chloro-2-(trifluoromethyl)-4-phenyl-2*H*-chromene-3-carboxylic acid, 6-(4-hydroxybenzoyl)-2-(trifluoromethyl)-*2H*-chromene-3-carboxylic acid and 6-chloro-7-(4-nitrophenoxy)-2-(trifluoromethyl)-2*H*-chromene-3-carboxylic acid were reported to contain chromene pharmacophore (Kwangwoo et al. 2008). Plastoquinones, chromanols and chromenes reside in a common class of natural compounds containing polyprenyl chain bound to a hydroquinone framework, and were reported to occur in marine macroalgae (Pereira et al. 2011). Mojabanchromanol is an example of an antioxidative chromene derivative isolated from macroalga *Sargassum siliquastrum*, and was reported to display free radical scavenging activity (Toth and Pavia 2000). Chromene derivatives from marine macroalga *Sargassum micracanthum* with potential antioxidative and anti-ulcer properties were reported in a previous literature (Mori et al. 2003). Chromene derivatives was also found to be an interesting template for the discovery of potential anti-cancer agents (Vosooghi et al. 2010), such as acronycine (lung, colon and ovary cancer).

Terpenoids are structurally diverse secondary metabolites with more than 40,000 reported structural diversity possessing valuable bioactive properties (Gershenzon and Dudareva 2007). Terpenoids were recognized to possess potential pharmacological properties against deadly diseases, such as malaria (Parshikov et al. 2012), cardiovascular ailments (Liebgott et al. 2000) and cancer (Ebada et al. 2010). These marine organisms were found to be potential reservoir of bioactive secondary metabolites including terpenes, sterols, polyphenols, acetogenins, etc., and the most prominent among these are meroterpenoid group of compounds (Chakraborty et al. 2016). The meroditerpene, 11-hydroxy-11-*O*-methylamentadione, isolated from the macroalga *Cystoseira usneoides* showed anti-inflammatory effects in dextran sodium sulfate-persuade colitis in a murine model. The terpenoid compound was found to significantly inhibit the generation of the cytokine (a type of inflammatory signaling molecule) and tumor necrosis factor in lipopolysaccharide-induced human monocytic leukaemia cell line. Three antioxidative aryl meroterpenoids were previously isolated from the red macroalga *Hypnea musciformis* (Chakraborty et al. 2016).

The C_{15} acetogenins bearing cyclic ether skeletons have been isolated as the major secondary metabolites from red macroalga *Laurencia* sp (Erickson 1983), and were reported to be anti-microbial (Konig and Wright 1997a, b), anti-feedant (Kurata et al. 1998), anti-helmintic (Davyt et al. 2001) and cytotoxic properties (Juagdan et al. 1997). A range of chlorinated compounds, C_{15} acetogenin en-ynes, were isolated from *Laurencia glandulifera* and were reported to be moderately cytotoxic towards various human tumour cell lines (Kladi et al. 2009). However, there was no literature report for the antioxidant and anti-inflammatory activities of the laurefurenynes A–F and cyclic ether acetogenins isolated and characterized from red macroalgae. Anti-inflammatory potential of the chromene sargachromanol G from the Korean macroalga *Sargassum siliquastrum* (Fucales) (Yoon et al. 2012); halogenated compounds from the red macroalga *Laurencia snackeyi* (Vairappan et al. 2013) along with the porphyrin derivatives pheophorbide and pheophytin from the macroalga *Sargassum japonica* were reported in previous literature (Islam et al. 2013). Antioxidative compounds from macroalga *Eisenia bicyclis* were identified as phylopheophylin in (Cahyana et al. 1992), whereas phlorotannins in *Sargassum kjellamanianum* (Yan et al. 1996) and fucoxanthin in *Hijikia fusiformis* were characterized as predominant secondary metabolites (Yan et al. 1999a). Laureatin, isolaureatin and deoxyprepacifenol were other related compounds obtained from the red marine alga *Laurencia nipponica* (Masuda et al. 1997). They exhibited significant insecticidal activity against the mosquito larvae *Culex pipens pallens* (Watanabe 1989). Cytotoxic compounds belonging to (+)-α-isobromocuparene and (-)-α-bromocuparene along with cyclolaurane sesquiterpenes were extracted from marine macroalgae (Kladi et al. 2006). Flavonoid compounds, such as quercetin, catechin, tiliroside, acanthophorins and acid derivates were described as the principle bioactive components of the red marine macroalgae (Blunt et al. 2006). Antioxidant properties of phenolic and polysaccharide components from methanolic and aqueous extracts and their fractions were reported from marine macroalgae (Chakraborty et al. 2013; Ganesan et al. 2008). Phlorotannins (polyphenols) from marine macroalga *Ecklonia stolonifera* and *Ecklonia kurome* were reported to be potent antioxidants (Kang et al. 2003). Phlorotannins of *Ecklonia kurome* were reported to be composed of phloroglucinol, eckol, phlorofucofuroeckol, dieckol and 8,8"-bieckol with some other unknown phenolic compounds (Kang et al. 2004). Laurefurenynes A **(1)** described from the red marine macroalga *Laurencia* sp (Abdel-Mageed et al. 2010). The chamigrane sesquiterpenes Yicterpene A and B **(2)** isolated

from marine macroalga *Laurencia composita* (Pingtan Is., China) and the other seven compounds were described from *Laurencia similis* (Sepanggar Is., Kota Kinabalu, Sabah), whereas ent-1(10)-aristolen-9b-ol **(3)** claimed as an enantiomer of a known compound (Kamada et al. 2013). Two bromophenols **(4-7)** with radical scavenging activities were obtained from marine macroalga *Symphyocladia latiuscula* (Qingdao, Shandong Province, China) (Xu et al. 2013a). This same collection of *Symphyocladia latiuscula* also provided the weakly anti-fungal bromophenol sulfoxide (Xu et al. 2013b). The bromophenols isolated from *Vertebrata lanosa* (Oldervik, Ullsfjorden, Norway) and found to possess cellular antioxidant activities (Olsen et al. 2013). The unprecedented polybrominated spiro-trisindole similisine A **(8)** and its enantiomer similisine B obtained from *Laurencia similis* (S. China Sea) (Sun et al. 2013). Five known bromophenols from a variety of red macroalgae were reported to possess inhibitory activity against glucose 6-phosphate dehydrogenase (Mikami et al. 2013). Bioactive metabolites isolated from *Asparagopsis taxiformis* were found to have potential for therapy to fish infected with *Streptococcus iniae* (Mata et al. 2013). An anti-fungal aldehyde **(9)** isolated from *Laurencia papillosa* (Jeddah, Red Sea) (Alarif et al. 2011). Maneonenes were reported from red macroalga *Laurencia obtusa* (Jeddah, Red Sea) (Ayyad et al. 2011). It was found that the structure of *cis*-maneonene D had the similar structure with lembyne A (Vairappan et al. 2001) or the product obtained from treatment of *cis*-maneonene C with p-toluenesulfonic acid· (Waraszkiewicz et al. 1978). Apoptotic activity was shown for compounds *cis*-maneonenes E **(10)** and maneonenes (3Z) and (3E) **(11)**.

The oxidized levuglandin D2 **(12)** obtained from marine macroalga *Gracilaria edulis* (La Union, Philippines) (Kanai et al. 2011). Eight halogenated nonterpenoid acetogenins **(13)**, 12-epoxyobtusallene IV **(14)**, obtusallene X **(15)**, marilzallene **(16)**, (-)-4-acetoxymarilzallene **(17)**, (Z)-adrienyne **(18)** and (E)-adrienyne **(19)** isolated from marine macroalga *Laurencia marilzae* (Paraiso Floral, Canary Is.) (Gutierrez-Cepeda et al. 2011a). This same collection of *Laurencia marilzae* also yielded marilzabicycloallenes A–D **(20-21)** which posesse an unprecedented bicyclotridecane ring skeleton, when present in *Laurencia* species (Gutierrez-Cepeda et al. 2011b). The halogenated monoterpenes A **(22)** and B **(23)** derived from *Plocamium suhrii* (Port Elizabeth, Africa). Along with other similar known compounds from this extract, they had significant cytotoxic effects on an esophageal cell line (Antunes et al. 2011).

Two chamigrenes, such as cycloelatanene A **(24)** and cycloelatanene B **(25)** isolated from marine macroalga *Laurencia elata* (St. Pauls Beach, Vic., Australia) using high performance liquid chromatography. Three cytotoxic oxasqualenoids, prethyrsenol A, 15 dehydroxythyrsenol A, 13-hydroxyprethyrsenol A, Iubol **(26)**, venustatriol **(27)** and thyrsiferol **(28-29)** derived from *Laurencia viridis* (Cen Pacheco et al. 2011). Bromophenols **(30-34)** isolated from *Rhodomela confervoides* (Dalian, China), and the same exhibited potent antioxidant activities (Li et al. 2011). Lithothamnin A **(35)** isolated from *Lithothamnion fragilissimum* (Lighthouse Reef, Palau Is.) as a modestly cytoxic compound. This metabolite is an unusual bastadin-like molecule with a unique meta–meta linkage between the aromatic rings (Van Wyk et al. 2011). An extract from *Callophycus oppositifolius* (Pugh Shoal, NT, Australia) yielded the cytotoxic tetrahydro-carboline callophycin A (ovenden et al. 2011). Marine macroalga-derived bioactive compound callophycin A **(36)** synthesized along with fifty other variously functionalized tetrahydro carboline derivatives for evaluation as chemopreventive and anti-cancer agents (Shen et al. 2011). Previously reported red algal metabolites continue to be the targets of synthesis. Polysiphenol was generated by intramolecular regioselective oxidative coupling reactions (Aknin et al. 1992; Clausen et al. 2011).

A pharmacologically active nucleoside, 5-iodo-5'-deoxytubercidin **(37)** isolated from marine macroalga *Hypnea valendie* (Kazlauskas et al. 1983). The monoterpene **(38)** obtained from species of the genus *Plocamium* and the structural determination was defined by X-ray analysis (Stierle et al. 1979). Three monoterpenes **(39-41)** described as the principle bioactive components of the species *Plocamium* (Crews 1977). Polyhalogenated anti-microbial bisnormonoterpenoid **(42)** and monoterpene **(43)** reported from marine macroalga *Plocamium cruciferum* (Faulkner 1984). Two linear monoterpenes **(44-45)** and preplocamenes, **(46-48)** isolated from marine macroalgae *Plocamium angustum* (Dunlop et al. 1979) and *Plocamium viofaceum* (Crews and Kho-Wiseman 1977) respectively. The species of the genus *Plocamium* contains monocyclic polyhalogenated monoterpenes **(49)** and **(50)** (Mynderse and Faulkner 1974). The secondary metabolites, plocamene E **(51)**, plocamene D **(52)**, plocamene D' **(53)** reported from red macroalga *Plocamium violaceurn* (Crews et al. 1978). Plocamene D' **(54)**, 4-bromo-analogue **(55)** of violacene along with **(56)** and its isomer **(57)** also extracted from an Antarctic specimen of *Plocamium cartilagineum* (Higgs et al. 1977).

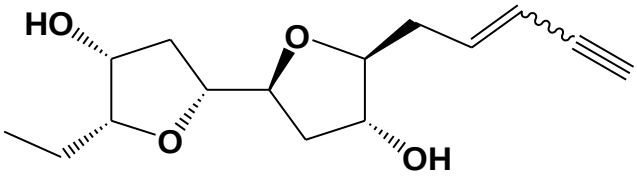
HO
O
O
OH

1

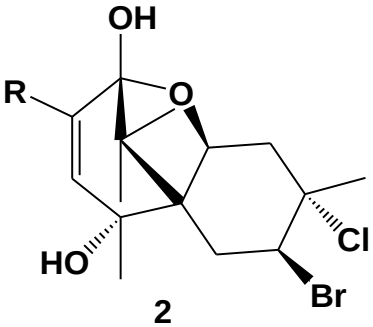
OH
R
O
HO
Cl
Br

2

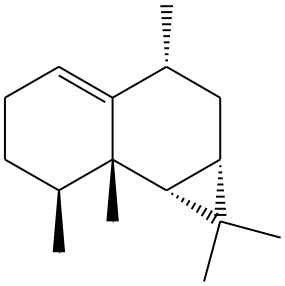

3

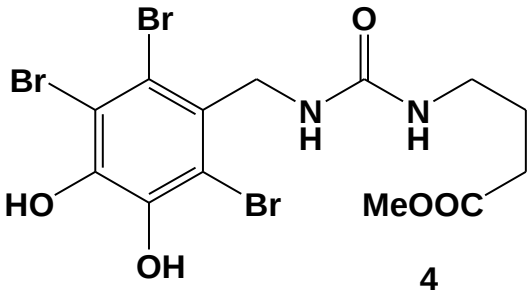
Br
O
Br
N
H
N
H
HO
Br
MeOOC
OH

4

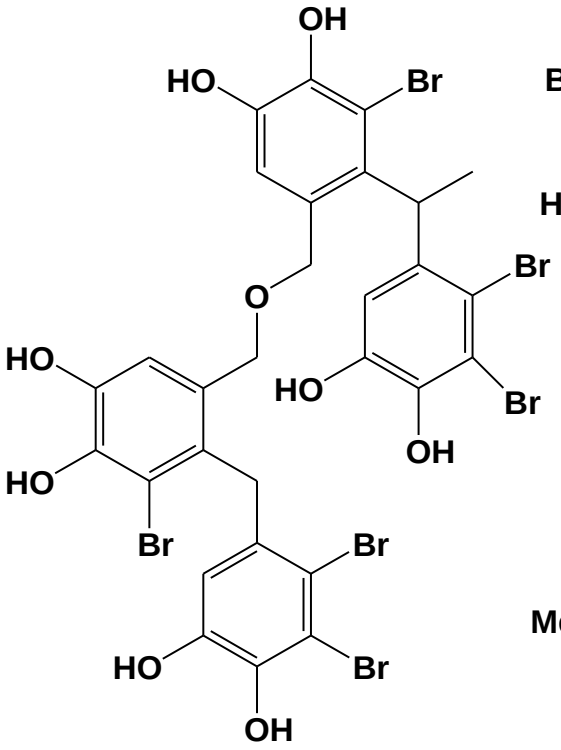
OH
HO
Br
Br
O
HO
Br
HO
OH
HO
Br
Br
HO
Br
OH

5

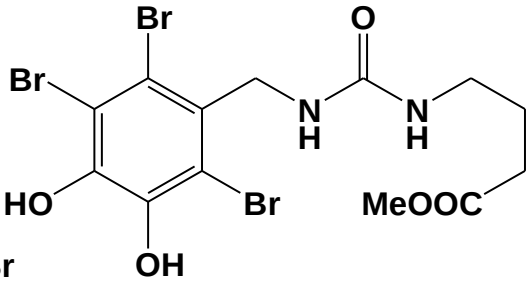
Br
O
Br
N
H
N
H
HO
Br
MeOOC
OH

6

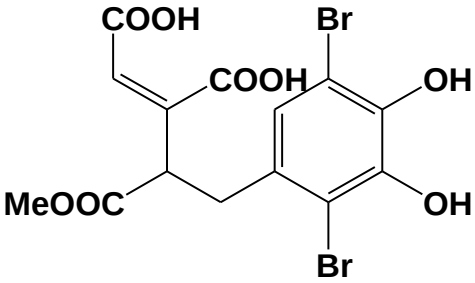
COOH
Br
COOH
OH
MeOOC
OH
Br

7

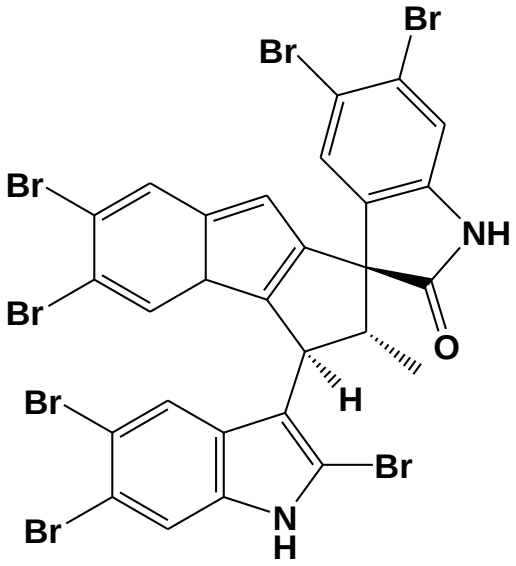

8

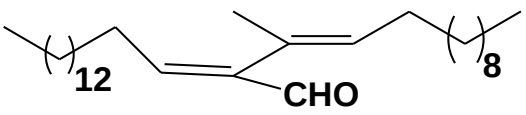

9

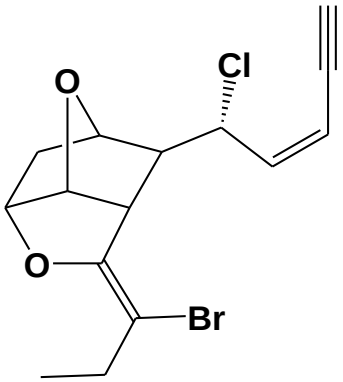

10

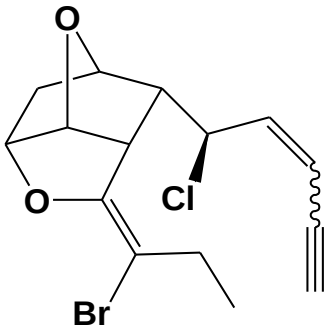

11

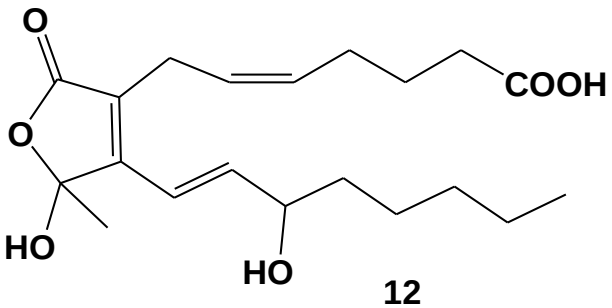

12

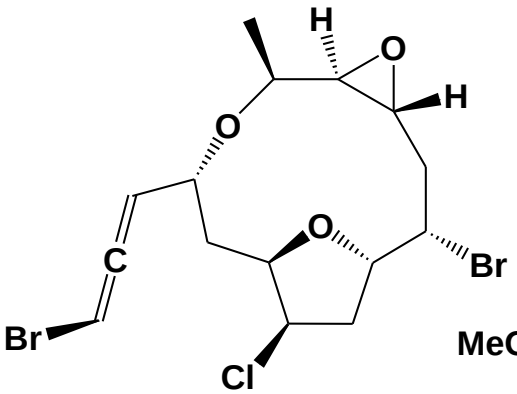

13

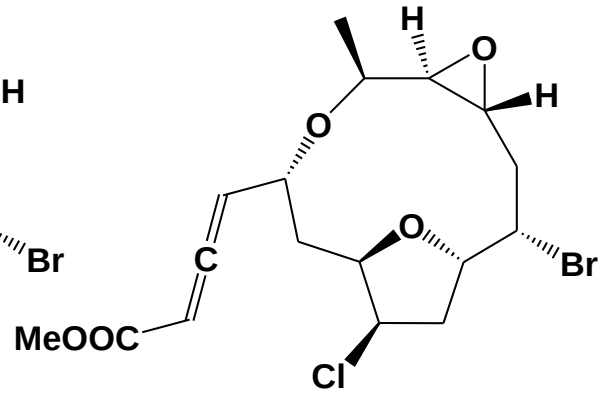

14

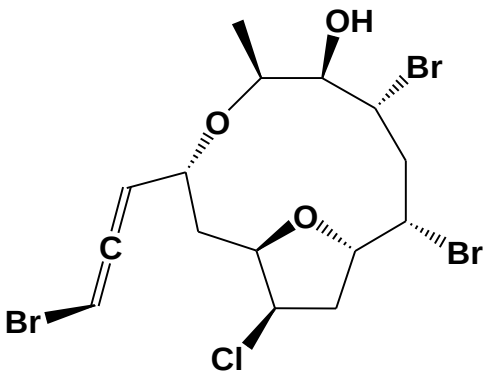

15

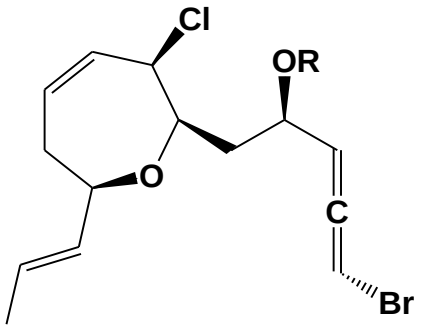

16

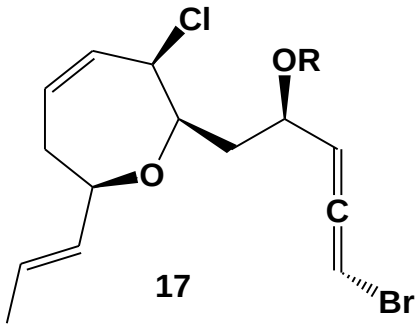

17

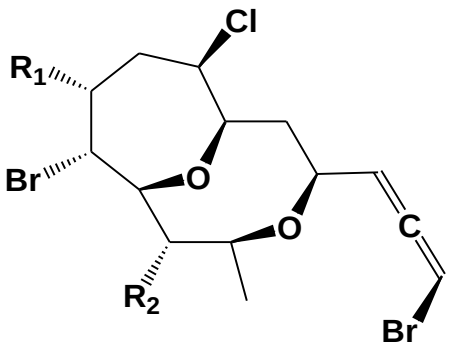

20

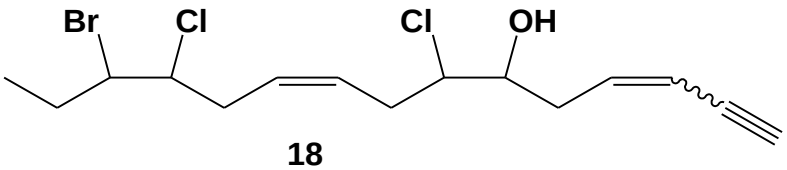

18

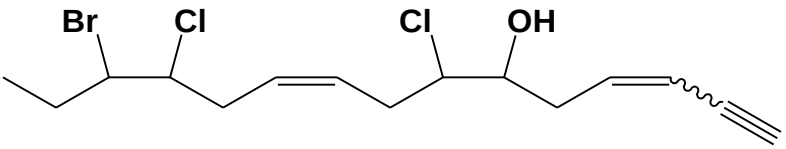

19

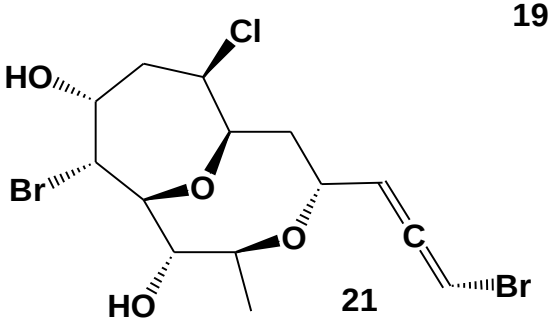

21

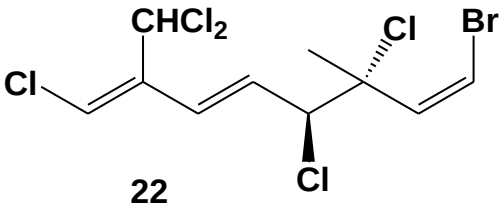

22

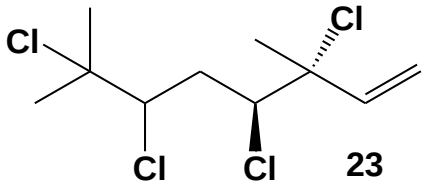

23

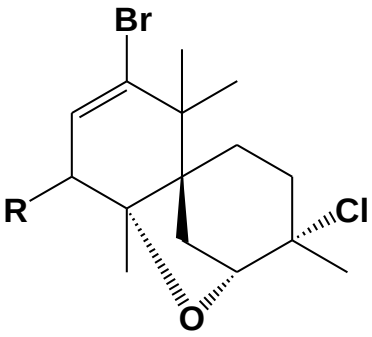

24

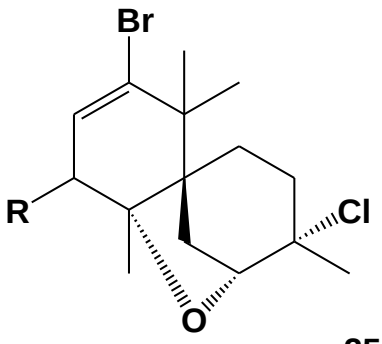

25

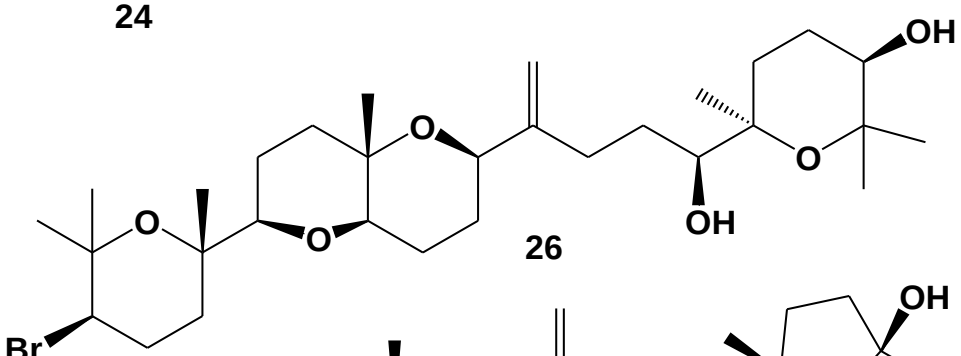

26

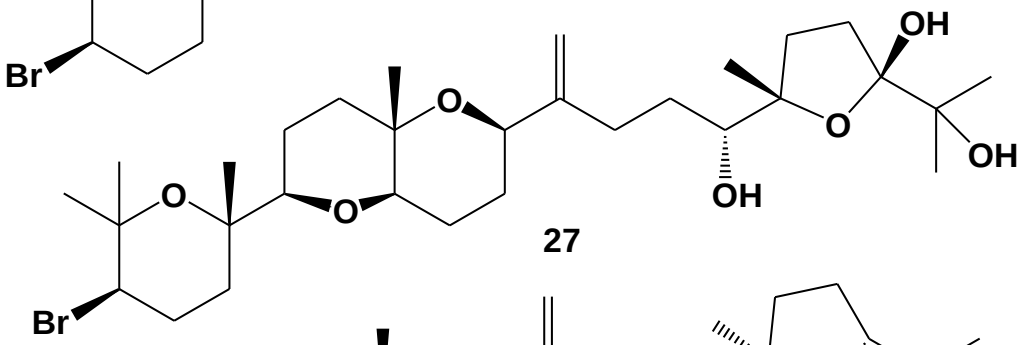

27

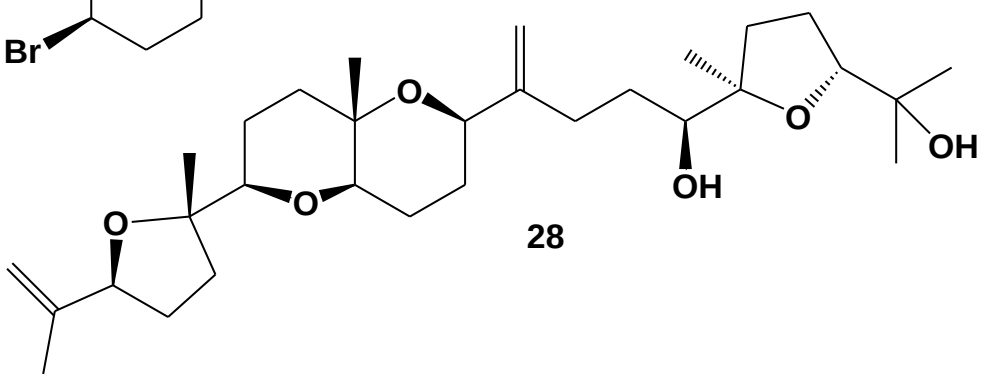

28

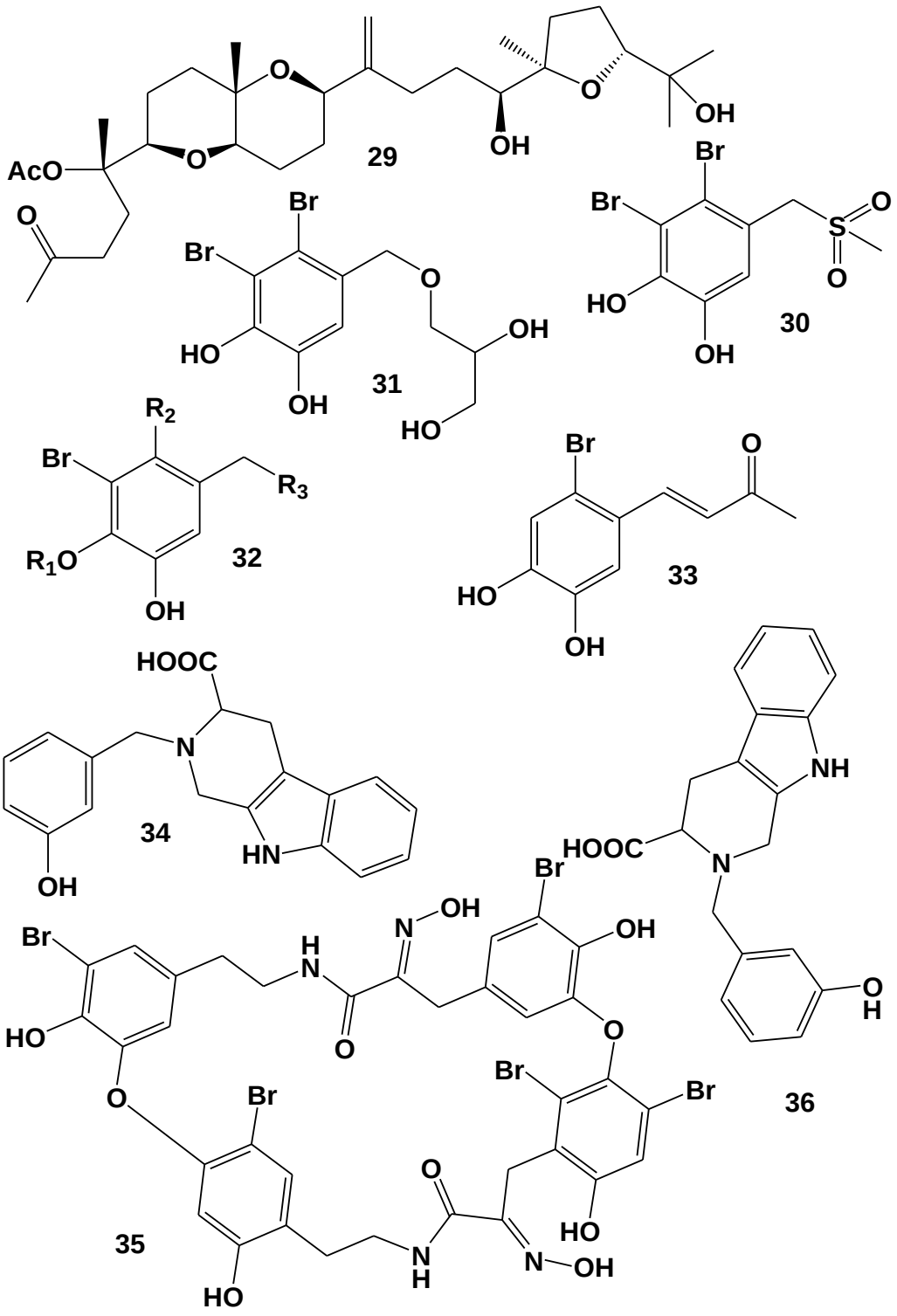
29
30
31
32
33
34
35
36

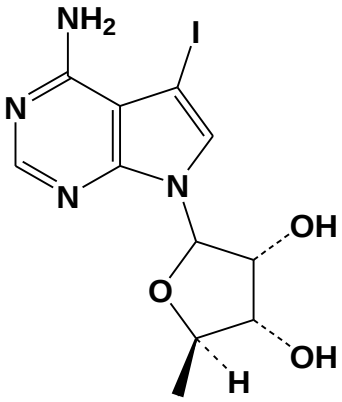

37

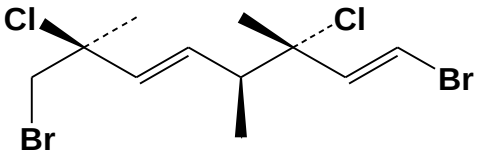

38

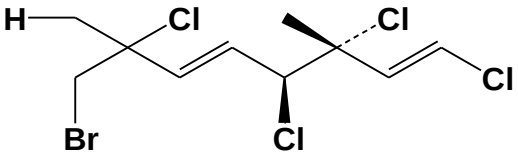

39

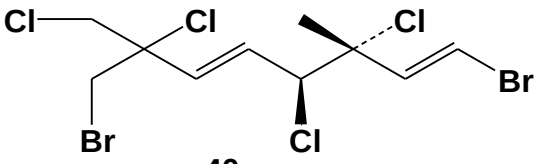

40

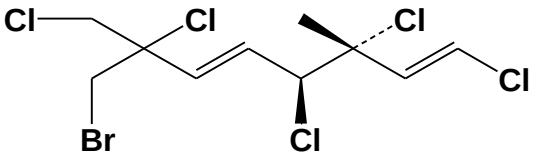

41

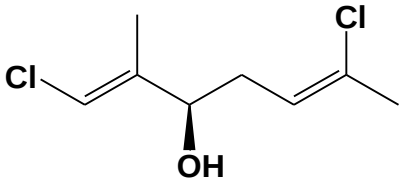

42

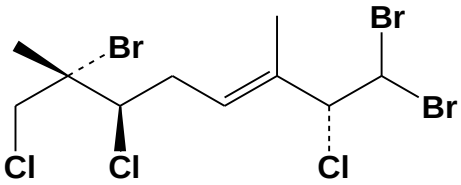

43

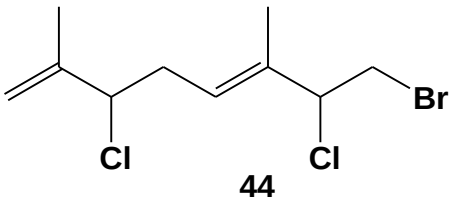

44

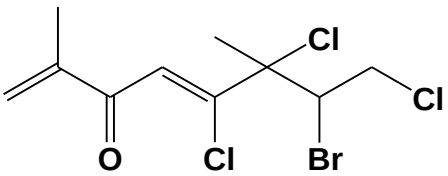

45

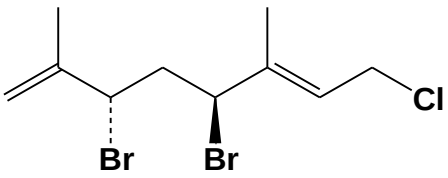

46

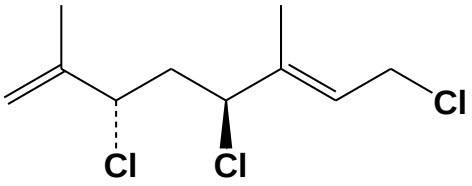

47

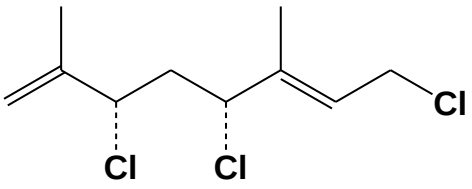

48

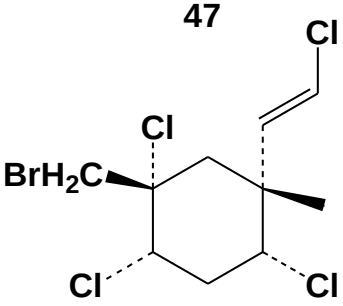

49

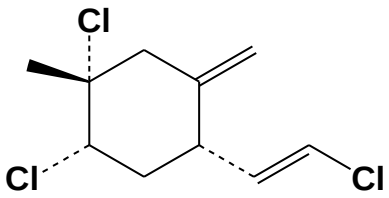

50

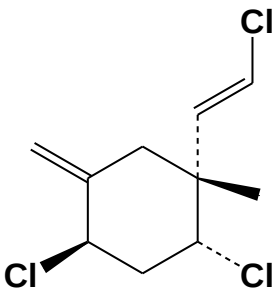

51

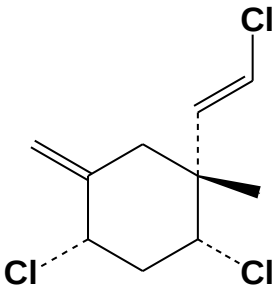

52

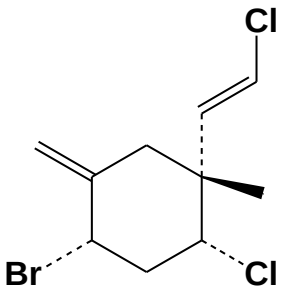

53

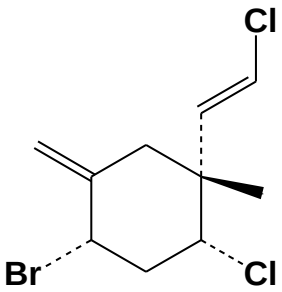

54

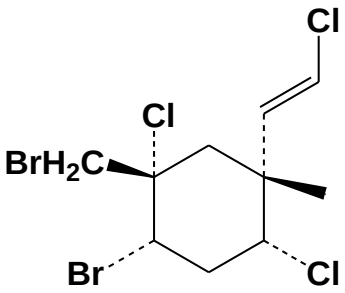

55

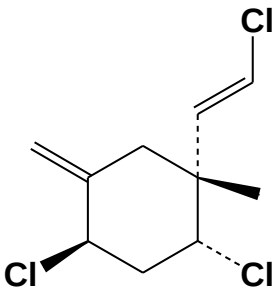

56

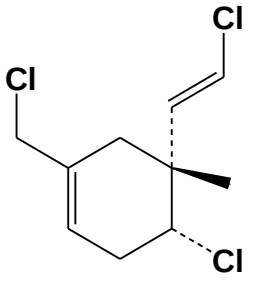

57

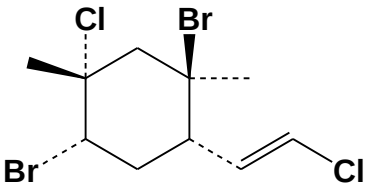

58

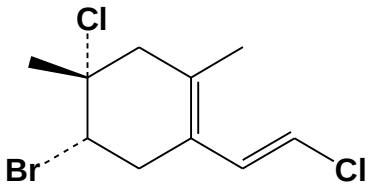

59

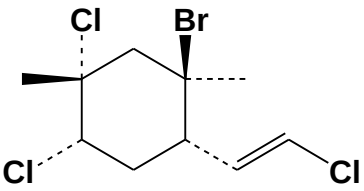

60

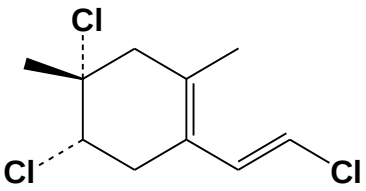

61

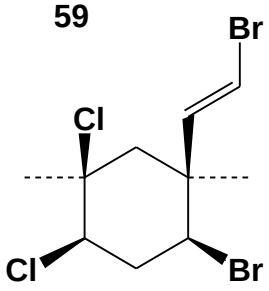

62

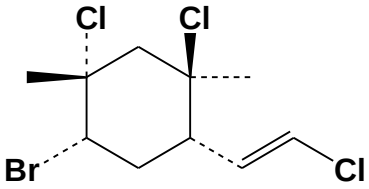

63

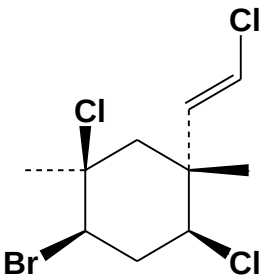

64

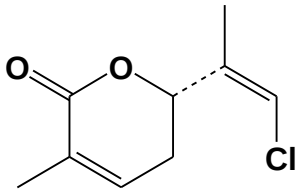

65

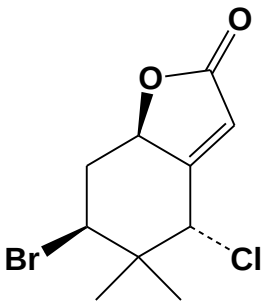

66

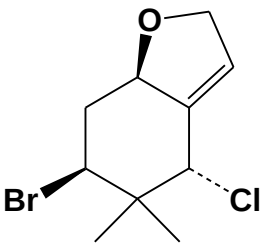

67

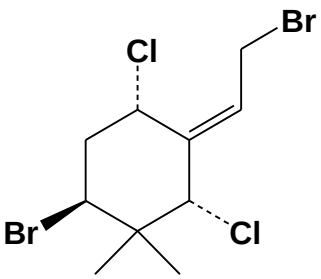

68

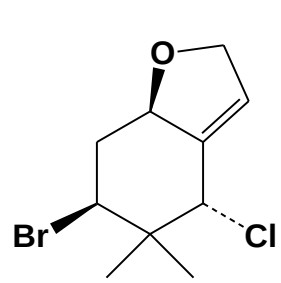

69

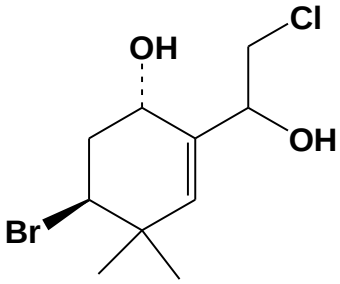

70

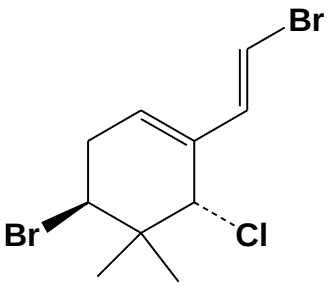

71

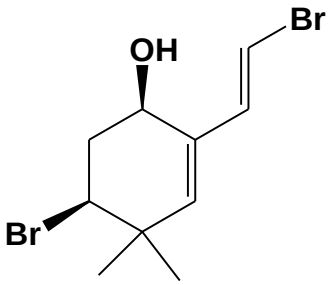

72

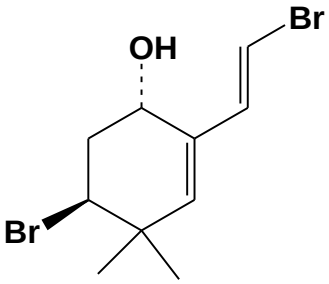

73

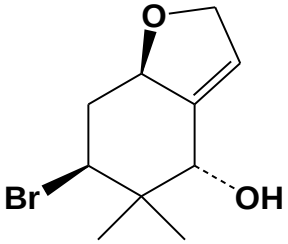

74

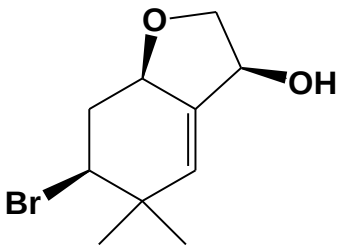

75

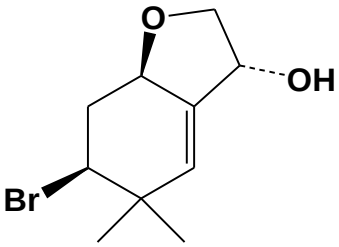

76

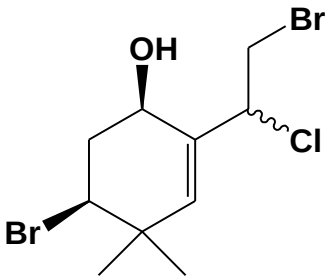

77

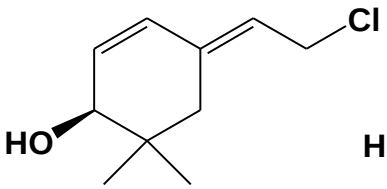

78

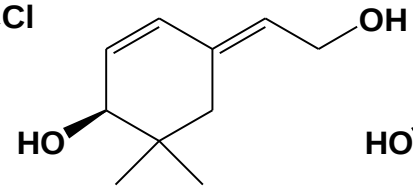

79

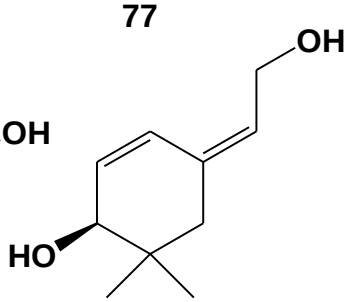

80

Two compounds **(58)** and **(59)** derived from *Plocamium cartilagineum*, were related to the metabolites of *Plocamium violaceim* **(60)** and **(61)** (Faulkner 1984). An unusual bromoviny monoterpene **(62)** and monoterpene **(63)** isolated from the Spanish and Australian sample respectively (Norton et al. 1977). The monoterpene **(64)** and polyhalogenated monoterpene, costatolide **(65)** yielded from red macroalga *Plocamium*

merrensii (Mynderse and Faulkner 1978) and *Plocamium costatum* (Williard et al. 1983) respectively. The new secondary metabolite isolated from *Chondrococcus horrxmanni* is chondrocolactone **(66)**, (Woolard et al. 1978) which is synthesized from chondrocole A **(67)** (Burreson et al. 1975). *Ochtodes secundirarnea* contains, ochtodene **(68)** along with chondrocole A **(69)** and the minor metabolite ochtodiol **(70)** (McConnell and Fenical 1978).

Thirteen novel monoterpenes **(71-83)** reported from marine macroalga *Ochtodes crockeri.* Brominated diterpenes (1S)-1, 2-dihydro-l-hydroxybromosphaerol **(84)** (Faulkner 1984), bromosphaerodiol **(85)** (Cafieri et al. 1977), (12S)-12-hydroxybromosphaerol **(86)** (Cafieri et al. 1982), bromosphaerene A **(87)** and bromosphaerene B **(88)** (Cafieri et al. 1983) related to bromosphaerol **(89)** derived from species *Sphaerococcus coronopifolius*. The anti-microbial metabolites such as (5Z, 8E, 10E)-11-fomylundeca-5, 8, 10-trienoic acid **(90)**, (2Z, 5Z, 7E, 11Z, 14Z)-9-hydroxyeicosa-2, 5, 7, 11, 14-pentaenoic acid **(91)** (Higgs and Mulheirn 1981) and cyclic lipid compound hybridalactone **(92)** isolated from macroalga *Burencia hybrid* (Higgs and Mulheirn 1981).

The red marine macroalga *Gracilaria lichenoides* contains prostaglandins PGE_2 **(93)** and $PGF_{2\alpha}$ **(94)** (Gregson et al. 1979). Four metabolites isolated from *Liagora farinosa* in which, three of these compounds, (7Z, 9Z, 12Z)-octadeca-7, 9, 12-trien-5-ynoic acid **(95)**, 4-hydroxynon-2-enal **(96)**, and (9Z, 12Z)-7-hydroxyoctadeca-9, 12-dien-5-ynoic acid **(97)**, exhibited potent ichthyotoxic activities, where as the glyceride **(98)** is not toxic (Paul and Fenical 1980b). Three macrocyclic lipids such as (14Z, 17Z)-3, 20-dibromo-21-ethyl-2, 6-epoxy-l-oxacycloheneicosa-2, 5, 14, 17-tetraen-11-yn-4one **(99)**, (14Z, 17Z)-21-ethyl-2, 6-epoxy-l-oxacycloheneicosa-2, 5, 14, 17, 20-pentaen-11-yn-4-one **(100)**, (12Z, 15Z)-19-ethy1-2, 6-epoxy-1-oxacyclononadeca-2, 5, 12, 15, 18-pentaen-9-yn-4-one **(101)** and acyclic lactone **(102)** isolated from *Phacelocarpus labillardieri* (Kazlauskas et al. 1982b). The metabolite delesserine **(103)** yielded from macroalga *Delesseria sanguine* (Yvin et al. 1982). *Rhabdonia verticillata* contains six halogenated derivatives of phloroglucinol **(104-109)** (Blackman and Matthews 1982). Halogenated diphenylmethanes **(110)** and **(111)** obtained from macroalga *Rhodomela larix* (Kurata and Amiya 1977) where as similar diphenylmethane **(112)** reported from *Rytiphlea tinctoria* (Chevolot-Magueur et al. 1976). *Symphocladia latiuscula* contains anti-fungal dibenzyl ether **(113)** (Kurata and Amiya 1980). A symmetrical trimer cyclotribromoveratrylene **(114)** with 3, 4-di

hydroxybenzyl unit and 2, 6-dibromo-3, 5-dihydroxy phenylacetic acid **(115)** isolated from macroalga *Hulopitys pinastroides* (Combaut et al. 1978). The anti-microbial brominated indoles **(116-119)** reported from *Burencia brongniartii* (Carter et al. 1978). Indole alkaloids such as mertensine A **(120)**, mertensine B **(121)** and fragilamide **(122)** yielded from *Martensia fragilis* (Kirkup and Moore 1983). *Palythoa tuberculosa* contains *Chndrus yendoi* consist of palythine **(123)** (Tsujino et al. 1978). The major metabolite, epoxide isolated from *Bonnemaisonia nootkana* **(124)**. Iodinated octen-3-ones **(125-127)** obtained from macroalga *Delisea Jimbriata*. 1, 1, 2, 6, 6-Pentabromo-octa-l, 4 dien-3-one and the pyrones **(128)** and **(129)** mainly present in the macroalga *Ptilonia australasica* (Kazlauskas et al. 1978). The compound, trans-3, 4-dibromo-5-methylenecyclopent-3-ene-l, 2 diol **(130)** derived from the species *Vidalia spiralis* (Kazlauskas et al. 1982a).

Secondary compounds were generated from (3Z) or (3E)-laurencenyne **(131)**, (3Z) and (3E) neolaurencenyne **(132)** isolated from macroalga *Laurencia okamurai* (Kigoshi et al. 1981). The isomers rhodophytin, (12Z) of (3Z) and (3E) venustin **(133)**, epoxyrhodophytin, (3Z) and (3E) epoxyvenustin **(134)** and (3Z) venustinene **(135)** 1, 3-diene derived from *Laurencia venusta* (Suzuki et al. 1983a; Suzuki and Kurosawa 1980). The *cis* and *trans*-pinnatifidenyne **(136)** derived from *Laurencia pinnatifida* (Gonzalez et al. 1982). Halogenated C_1 lipid laurencienyne **(137)** and laurenyne **(138)** isolated from macroalga *Laurencia obtusa* (Caccamese et al. 1980). The species *Laurencia pinnata* contains eight and seven membered ethers, such as laurepinnacin **(139)** and isolaurepinnacin **(140)** respectively (Fukuzawa and Masamune 1981).

The compound laurepinnacin **(141)** and laurencin **(142)** displayed close structural similarity were derived from *Laurencia glandulifera* (Murai et al. 1977). Eleven halogenated C_1 lipids, intricenyne **(143)** isolated from macroalga *Laurencia intricata* (White and Hager 1978). Similarly, bermudenynol **(144)** corresponding acetate **(145)** identified from same species (Cardellina et al. 1982). The *Laurencia thyrsiferra* contains (3E) and (3Z) chlorodiols **(146)** (Blunt et al. 1981). A nine-membered cyclic ether compound was named as obtusenyene **(147)** extracted from *Laurencia obtusa* (King et al. 1979; Howard et al. 1980). The metabolites such as chlorofucin **(148)** and poiteol **(149)** derived from macroalgae *Laurencia snyderae* and *Laurencia poitei* respectively (Howard et al. 1980). The compounds *cis* maneone-B **(150)** *cis* maneone-A **(151)** isolated from macroalga *Laurencia nidijica* (Waraszkiewicz et al. 1978). The compounds isolaurallene **(152)**, laureepoxide **(153)**, 4-epi-laurallene

(154) and laurallene **(155)** reported from *Burencia nipponica* (Kurata et al. 1982). The species *Laurencia nipponica* contains brominated allene, kumausallene **(156)**, deacetylkumausyne **(157)** and kumausyne **(158)** (Suzuki et al. 1983b). The metabolite obtusallene **(159)** exhibited an unusual bridged twelve-membered ring, obtained from macroalga *Laurencia obtuse* (Cox et al. 1982). Three 1-bromoallenes such as deoxyokamurallene **(160)**, okamurallene **(161**) and iso-okamurallene **(162)** derived from *Laurencia okamurai* (Suzuki and Kurosawa 1981). Tricyclic ketal, obtusin **(163)** extracted from macroalga *Laurencia obtuse* (Faulkner 1984). Twelve-membered cyclic ether compound poitediene **(164)** isolated from *Laurencia poitei* (Wright et al. 1983). The metabolite thyrsiferol **(165)** derived from the species *Laurencia thyrsifera* (Blunt et al. 1978). (10E, 11R) Squalene 10, 11-epoxide **(166**) isolated from *Laurencia okamurai* (Kigoshi et al. 1982). Two ecdysone derivatives acetylpinnasterol **(167)** and pinnasterol **(168)** reported from *Laurencia pinnata* (Fukuzawa et al. 1981). The metabolite chilenone **(169)** derived from the species *Laurencia chilensis* (San Martin et al. 1983). Several new aromatic sesquiterpenes such as caraibical **(170)**, 10-bromo-7-hydroxy-11-iodolaurene **(171)**, 10-bromo-7, 12-dihydroxy-laurene **(172)** and the iodo-ether **(173)** obtained from *Laurencia caraibica* (Izac and Sims 1979). Similarly new aromatic sesquiterpenes, isoaplysin **(174)** and neolaurinterol **(175)** isolated from macroalga *Laurencia okamurai. Laurencia okamurai* contains two aromatic sesquiterpenes, debromoaplysinol **(176)** and 8-bromolaurinterol **(177)** which are minor metabolites of the species. *Laurencia glandulifera* contains minor metabolites 10-bromolaurenisol **(178)**, ethers **(179)** and **(180)** (Suzuki and Kurosawa 1979). A species of *Laurencia nipponica* contains three laurene derivatives **(181-183)** and three dihydrolaurene derivatives **(184-186)** (Ohta and Takagi 1977). The compounds glanduliferol **(187)**, 10-bromo-α-chamigren-4-one **(188)**, 10-bromo-α-chamigrene **(189)**, 10-bromo-3, 4-epoxy-α-chamigrene **(190)** and 4, 10-dibromo-3-chloro-α-chamigrene **(191)** isolated from macroalga *Laurencia glanddifera* (Suzuki et al. 1979). 3-Chloro-4, l0-di bromo-7 and 8-epoxy-α-chamigrene **(192)** obtained from *Laurencia nipponica* (Faulkner 1984). The structures of iso-obtusol **(193)** and of the corresponding 10-debromo derivatives **(194)**, **(195)** and obtusol **(196)** elucidated by X-ray analysis (Gonzalez et al. 1979a). The compounds isofurocaespitane **(197)** and obtusane **(198)** isolated from macroalga *Laurencia caespitosa* (Gonzalez et al. 1979b). The compound bromohydrin **(199)** obtained from macroalga *Laurencia majuscula,* was converted into the acetate **(200)** for

X-ray analysis (Suzuki and Kurosawa 1978). The metabolite nidifocene **(201)** isolated from *Laurencia nidijica* (Waraszkiewicz et al. 1977).

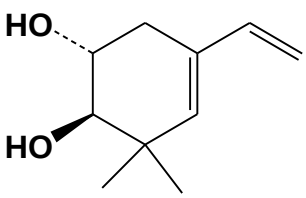

81

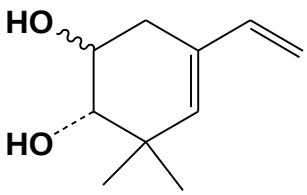

82

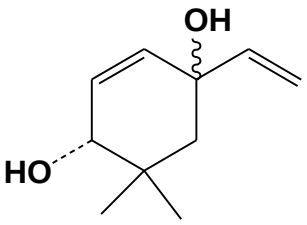

83

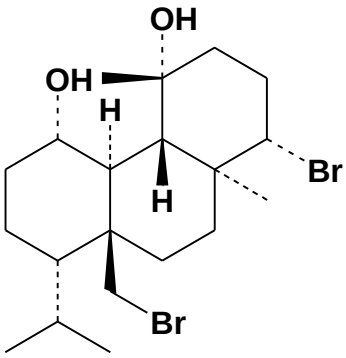

84

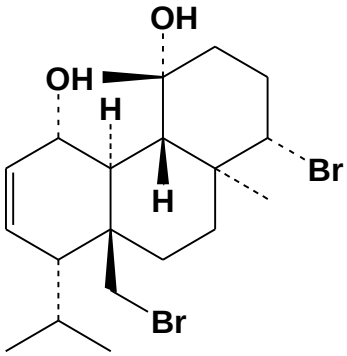

85

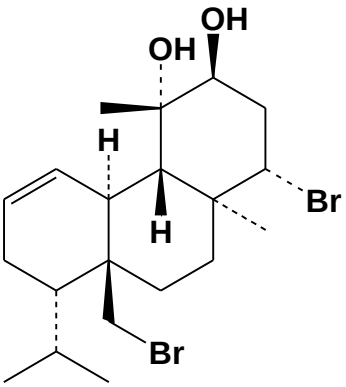

86

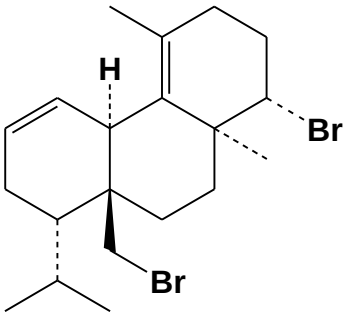

87

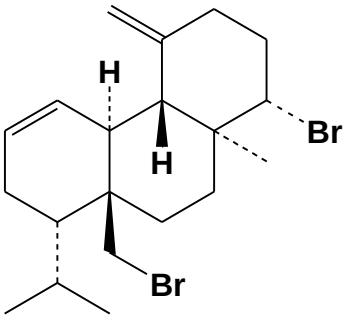

88

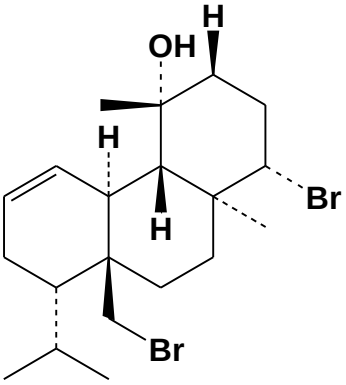

89

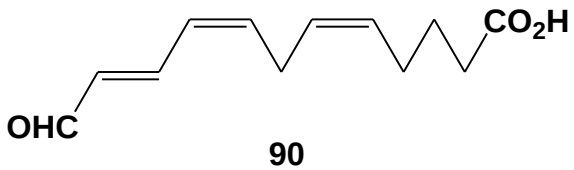

90

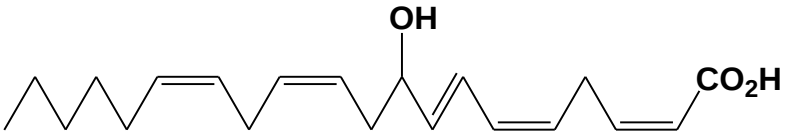

91

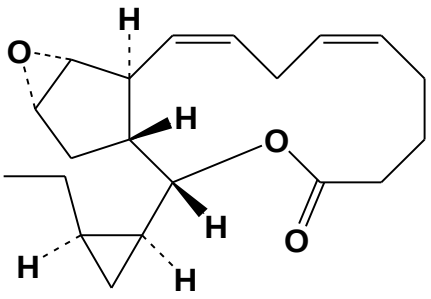

92

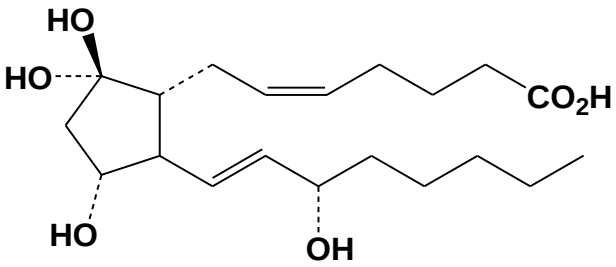

93

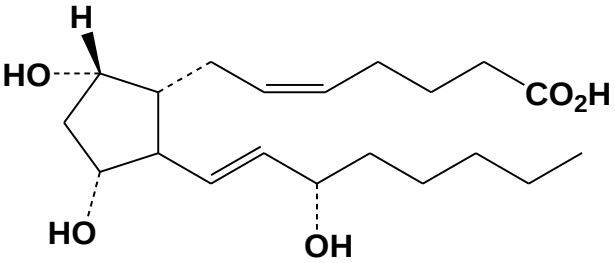

94

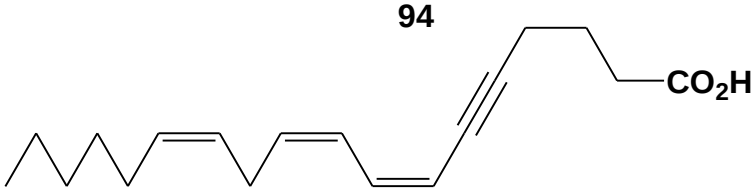

95

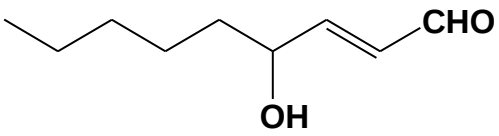

96

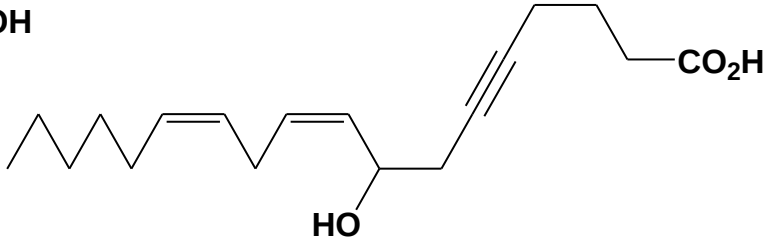

97

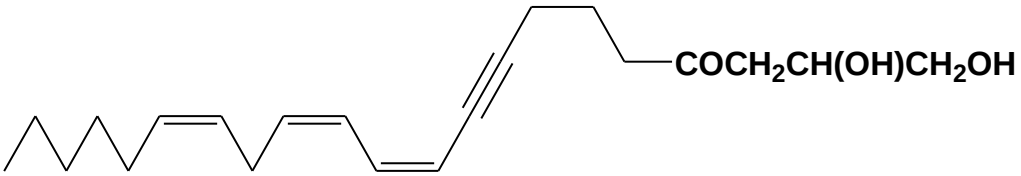

98

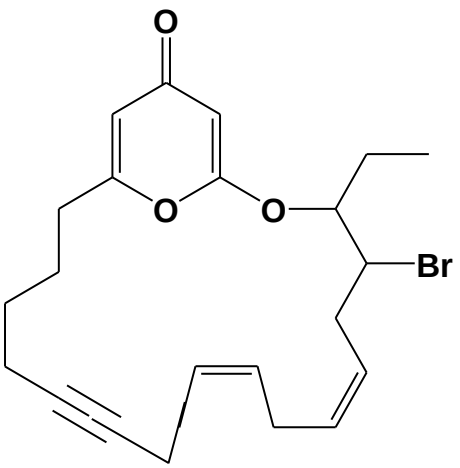

99

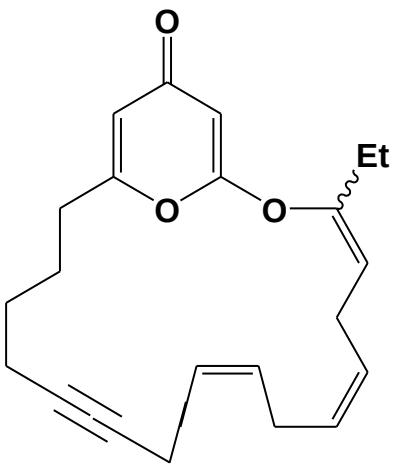

100

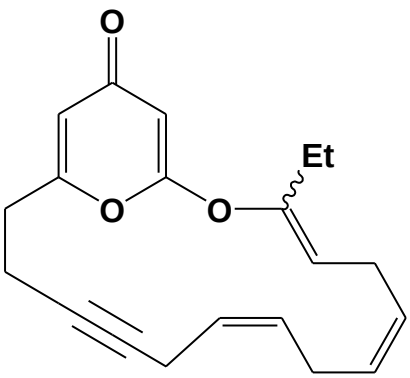

101

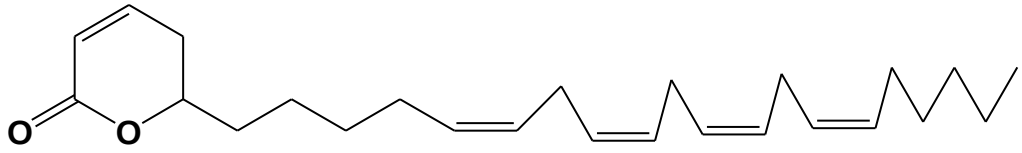

102

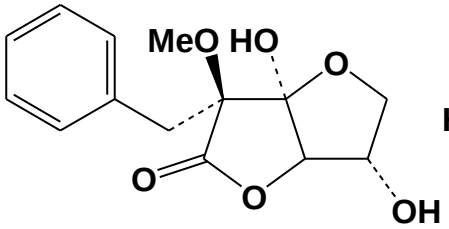

103

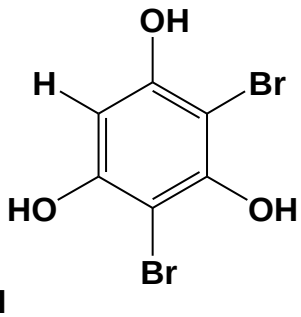

104

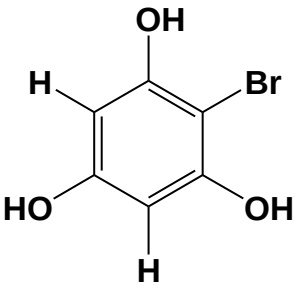

105

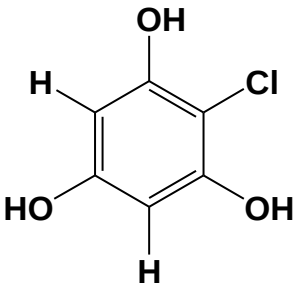

106

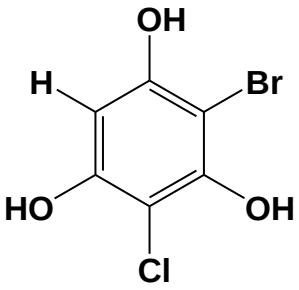

107

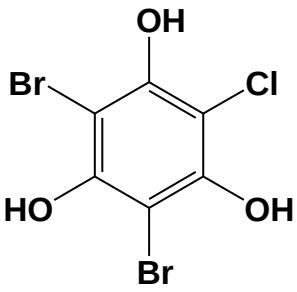

108

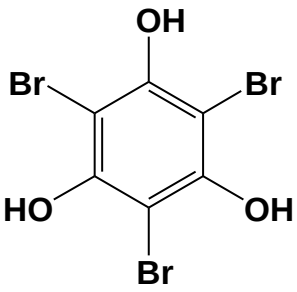

109

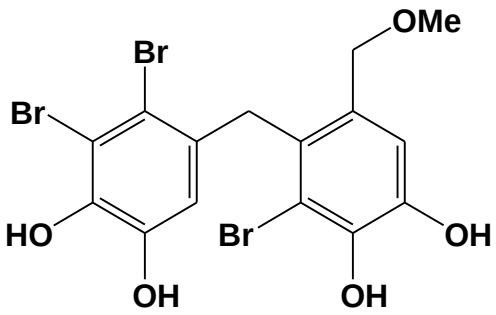

110

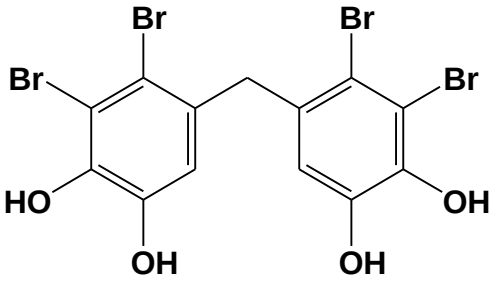

111

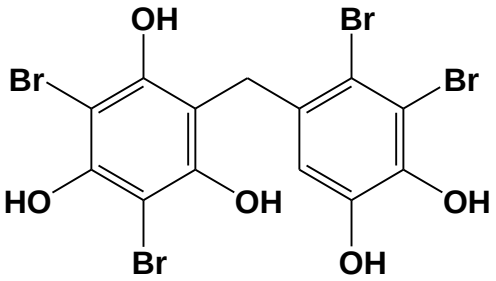

112

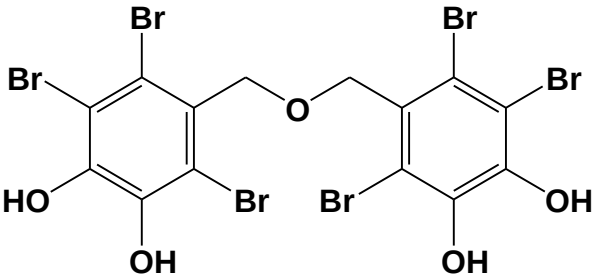

113

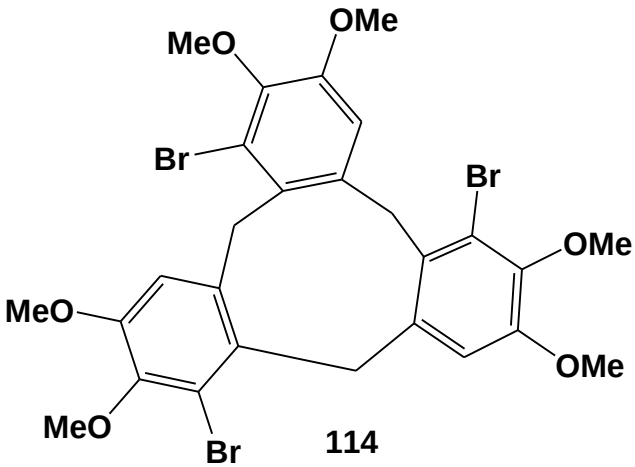

114

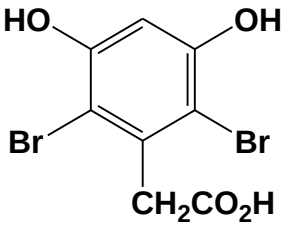

115

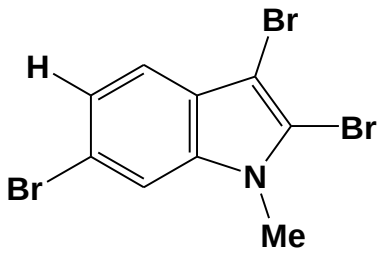

116

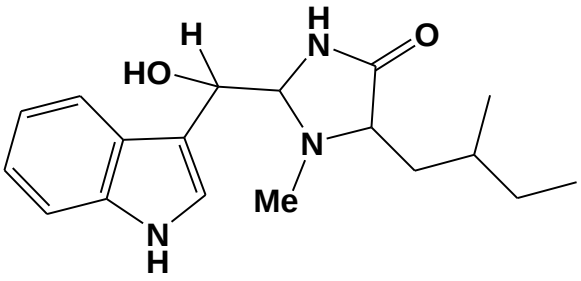

120

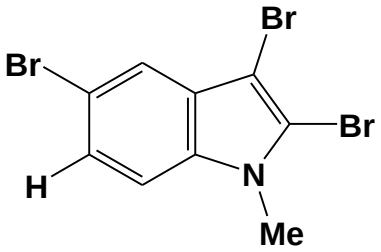

117

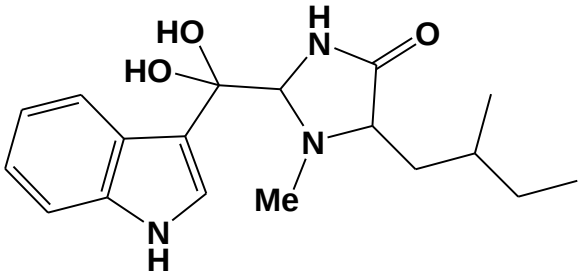

121

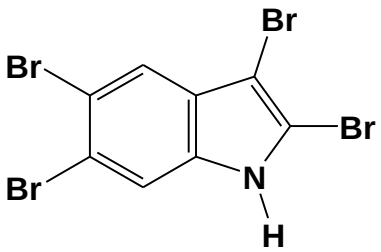

118

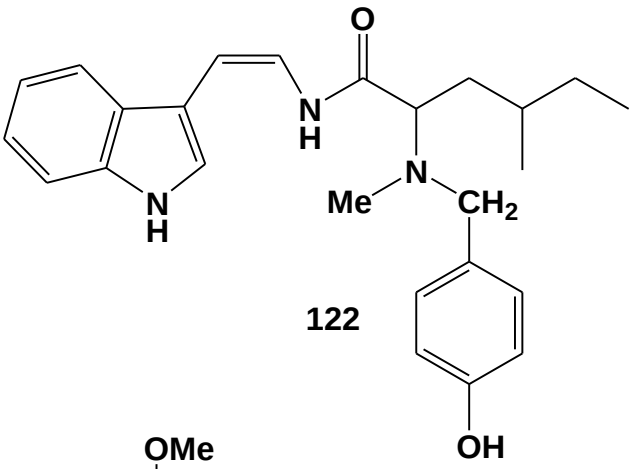

122

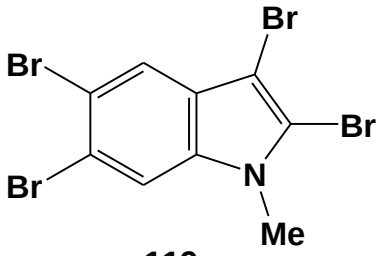

119

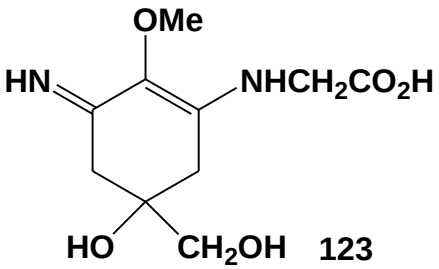

123

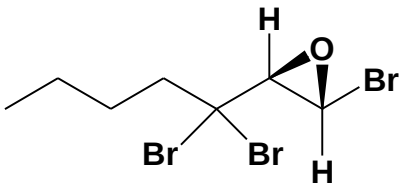

124

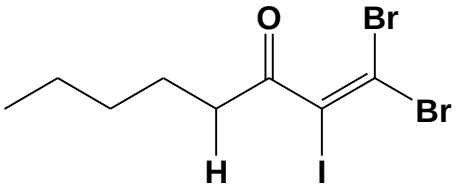

125

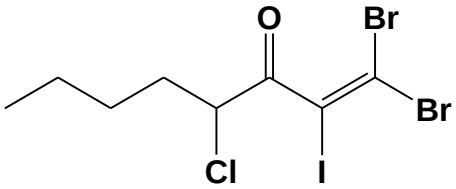

126

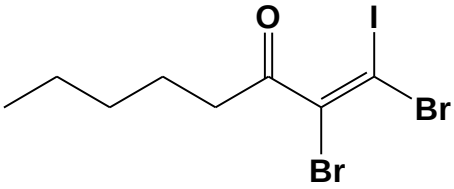

127

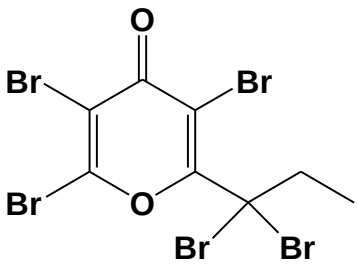

128

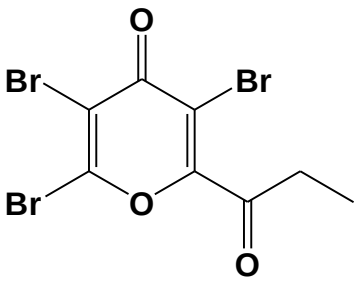

129

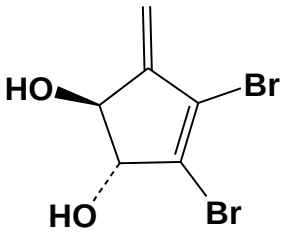

130

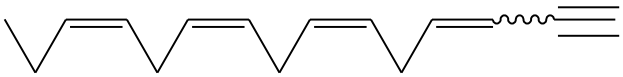

131

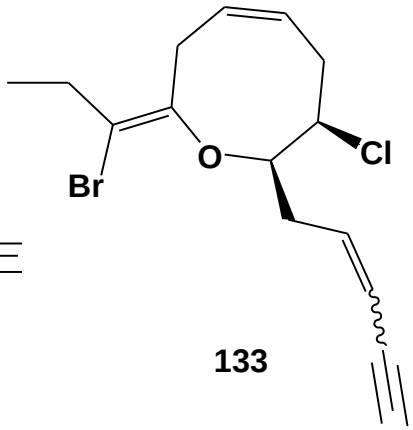

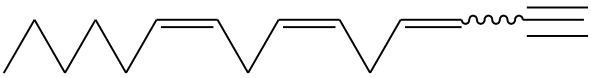

132

133

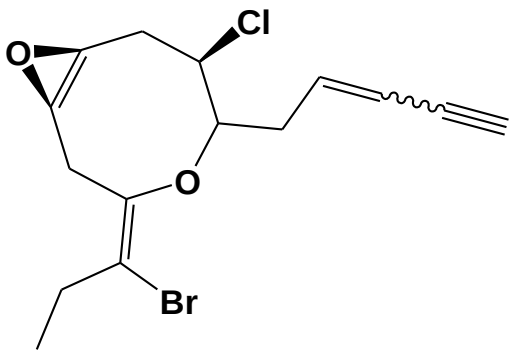

134

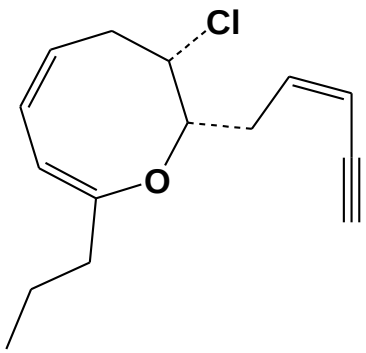

135

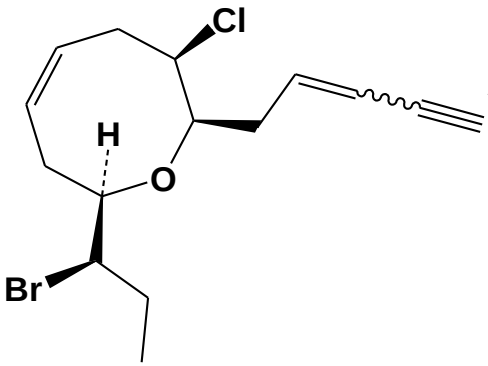

136

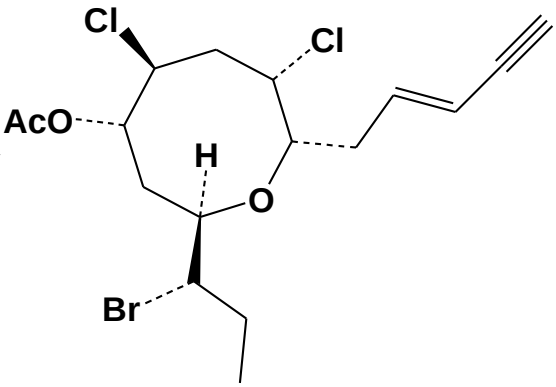

137

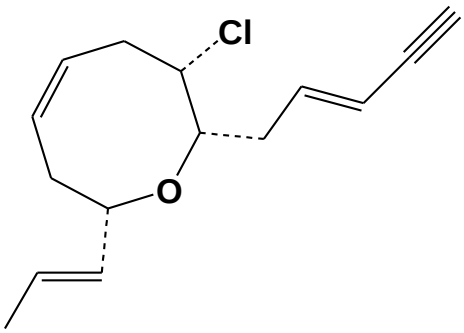

138

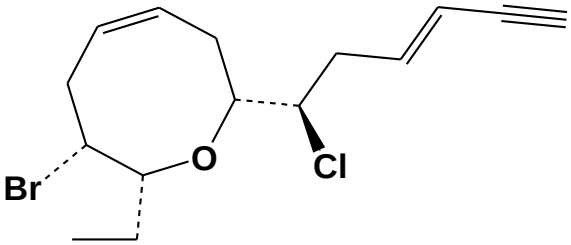

139

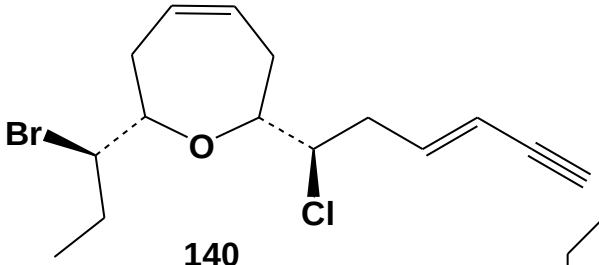

140

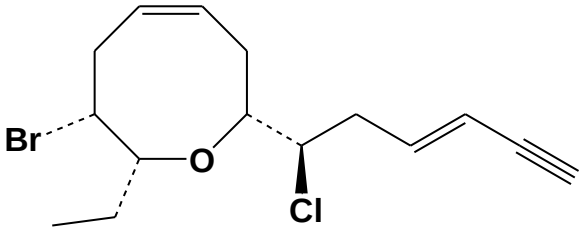

141

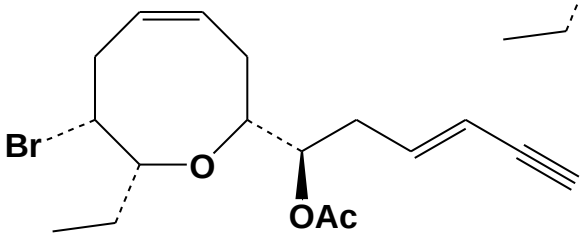

142

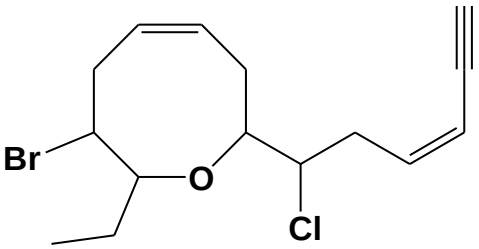

143

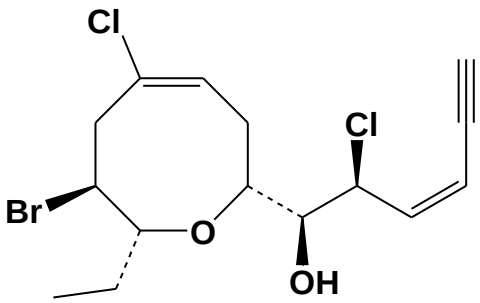

144

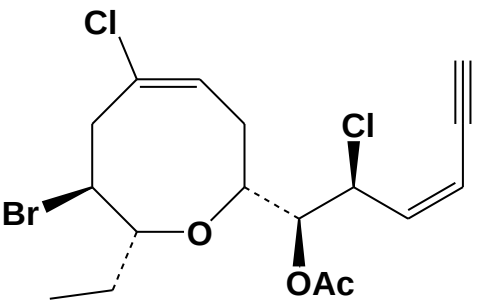

145

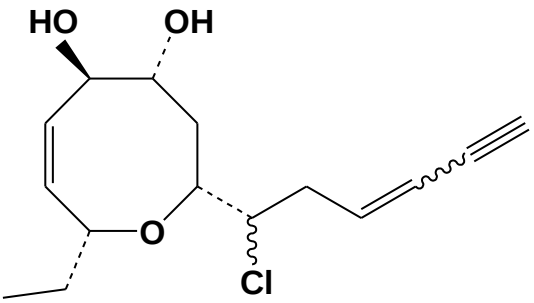

146

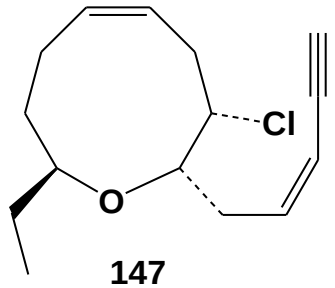

147

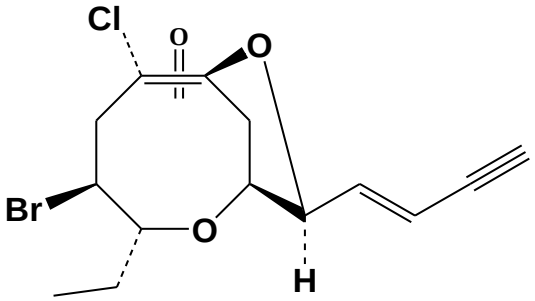

148

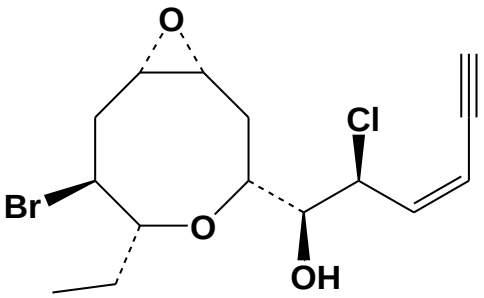

149

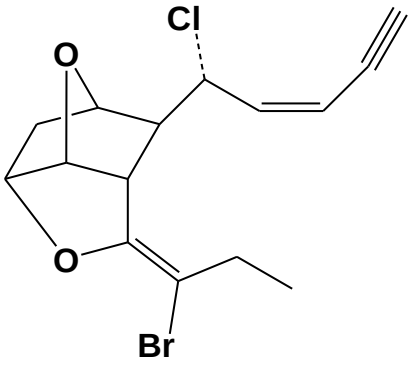

150

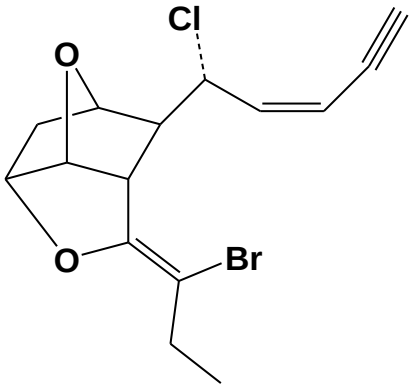

151

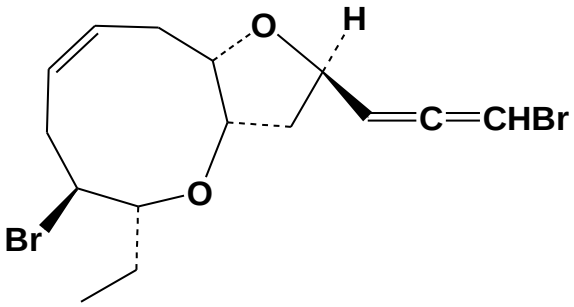

152

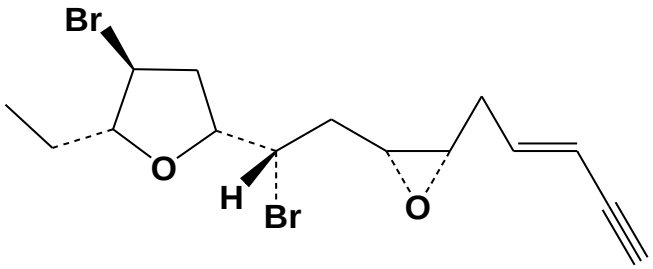

153

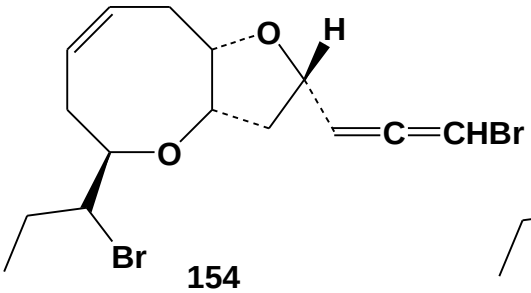

154

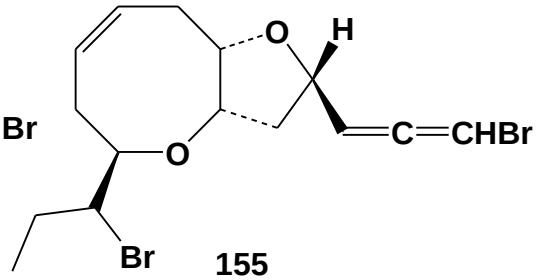

155

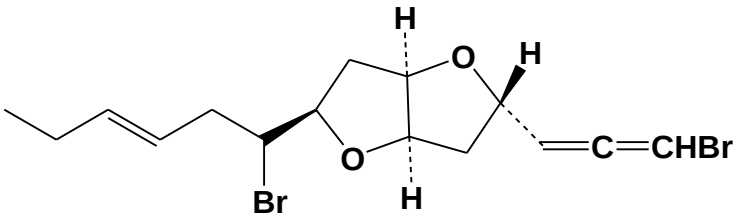

156

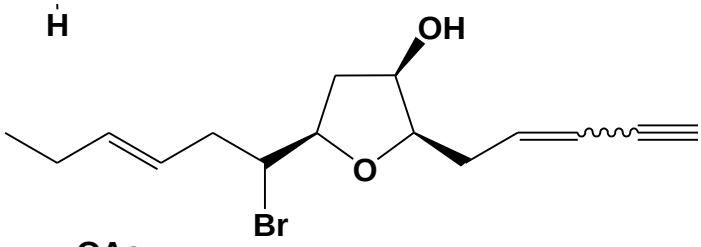

157

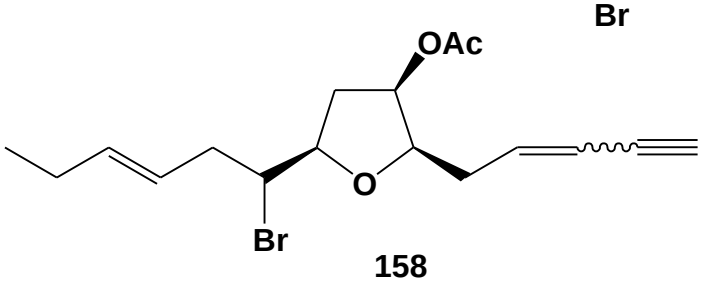

158

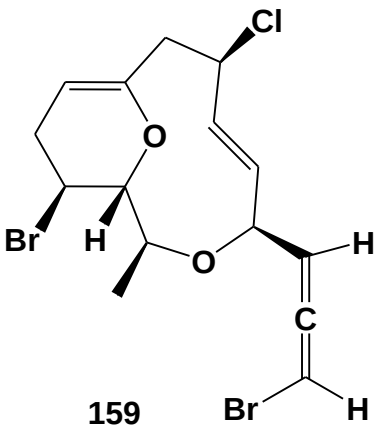

159

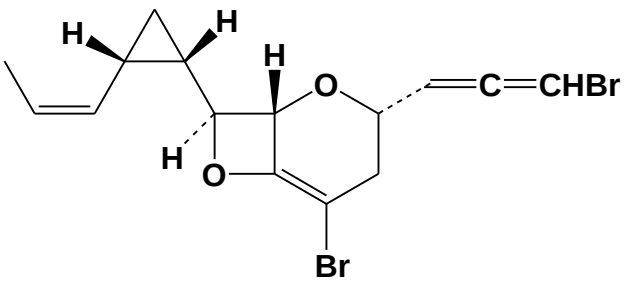

160

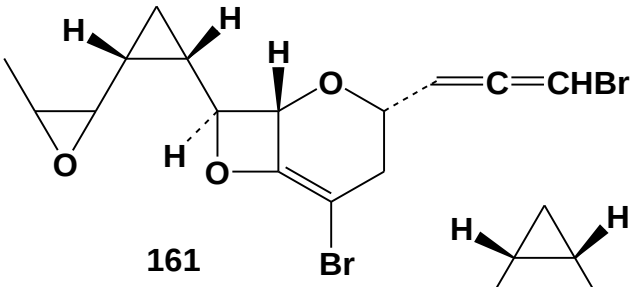

161

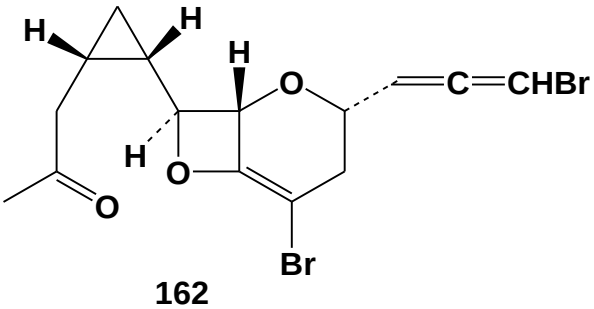

162

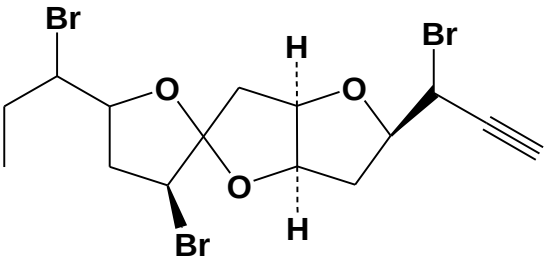

163

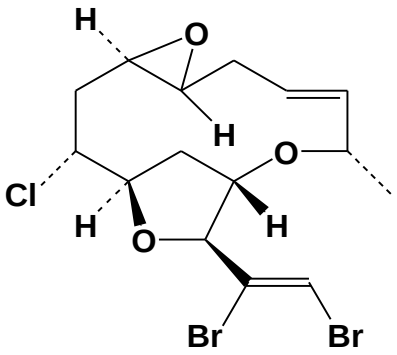

164

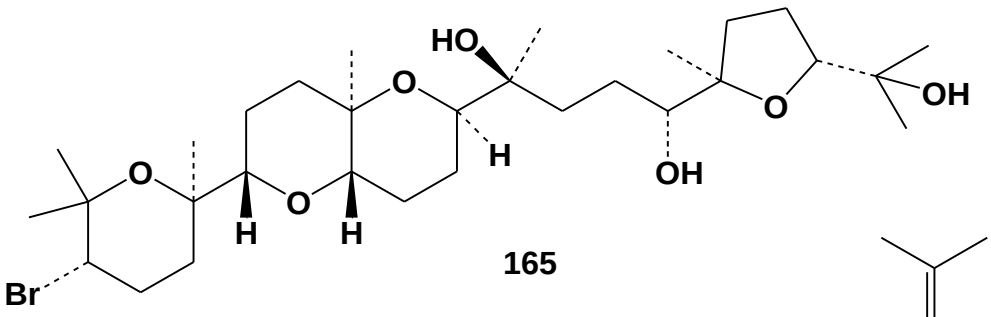

165

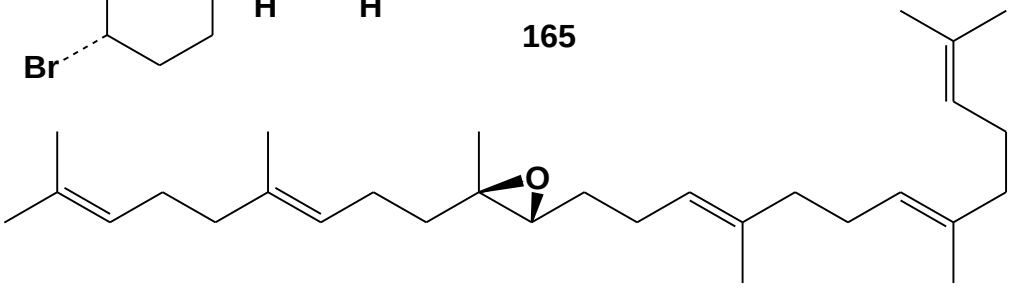

166

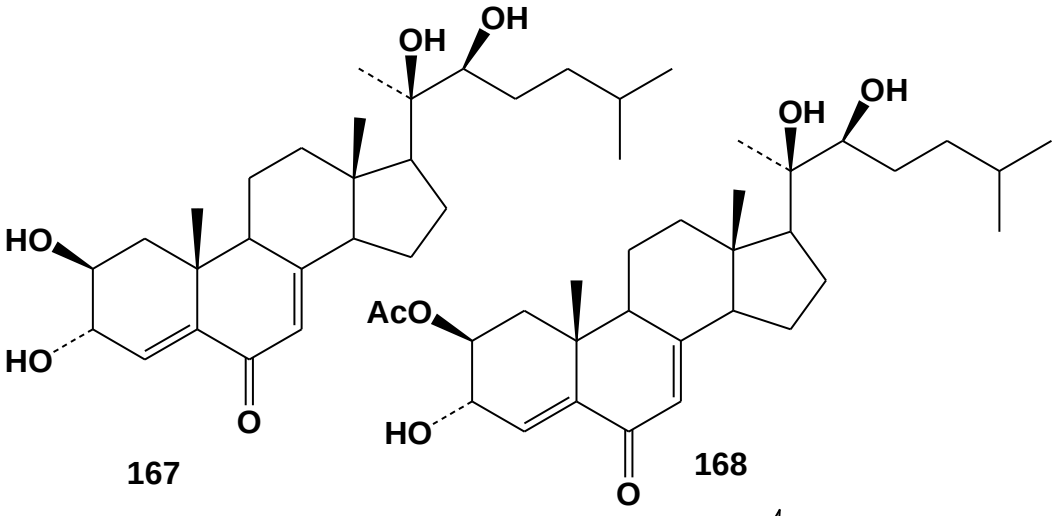

167 168

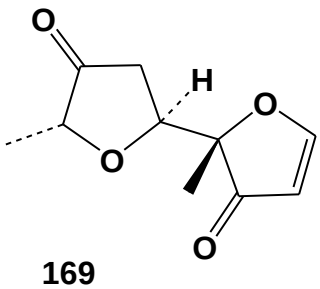

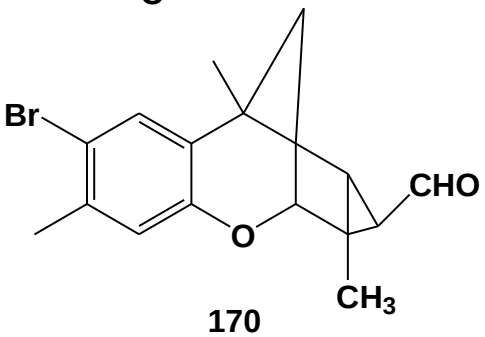

169 170

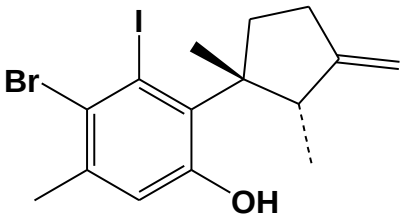

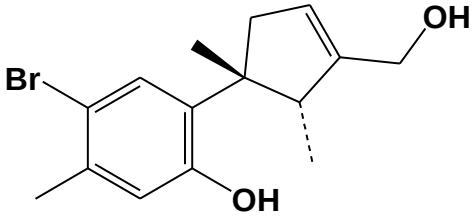

171 172

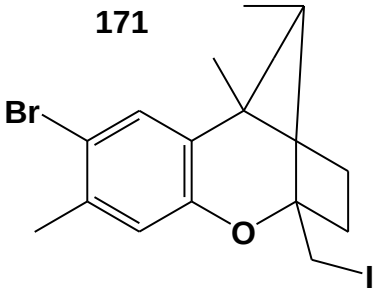

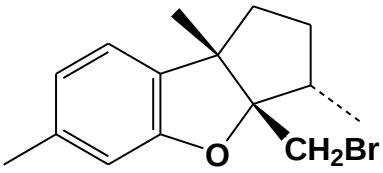

173 174

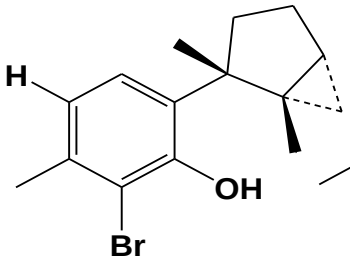

175

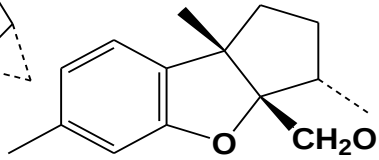

176

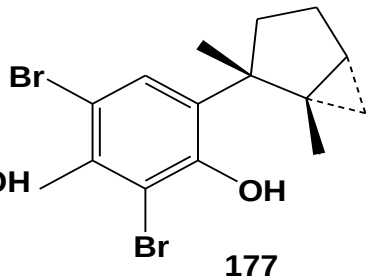

177

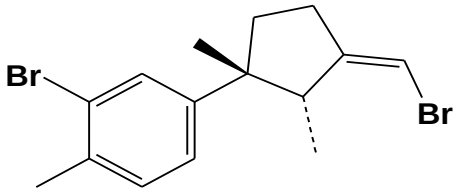

178

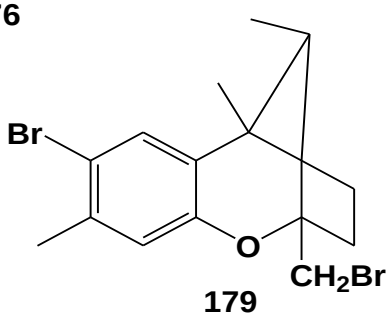

179

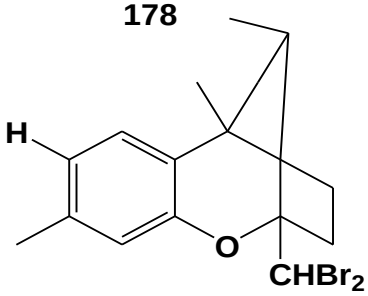

180

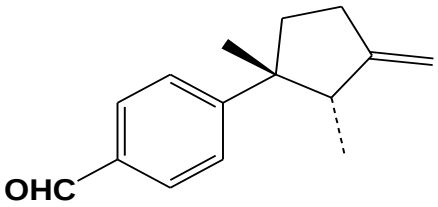

183

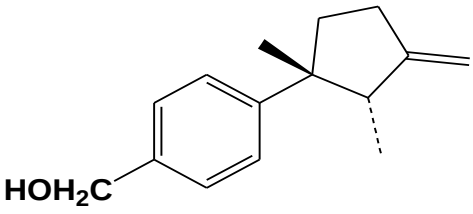

181

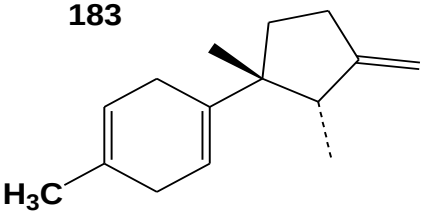

184

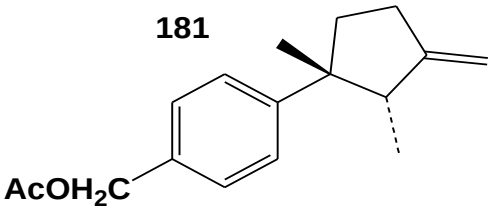

182

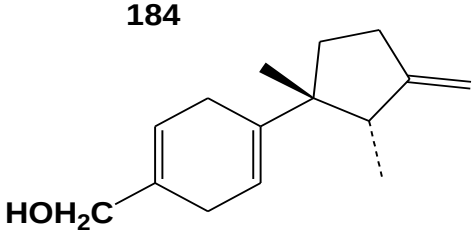

185

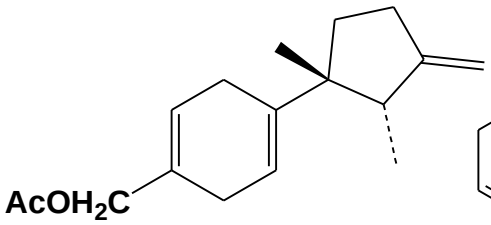

186

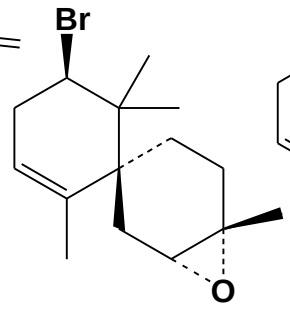

190

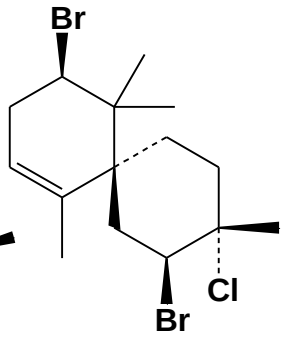

191

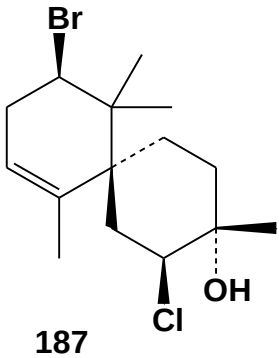

187

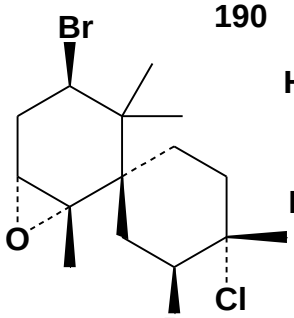

192

Br

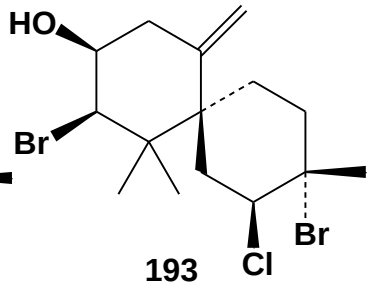

193

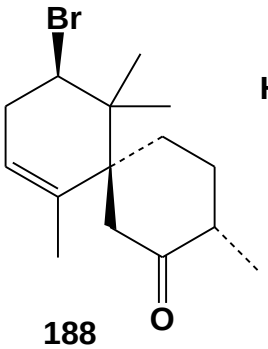

188

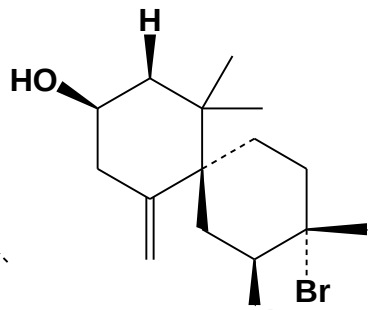

194

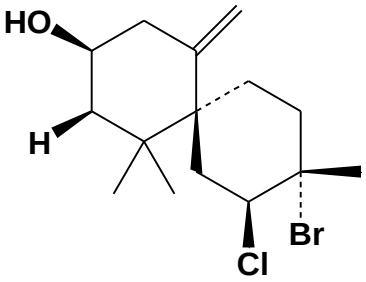

195

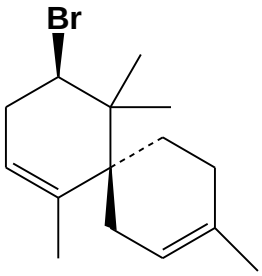

189

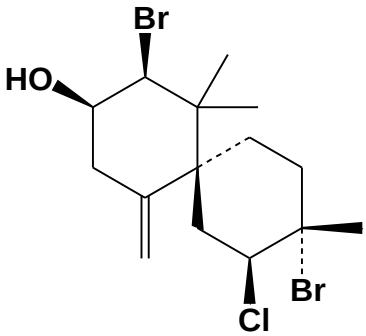

196

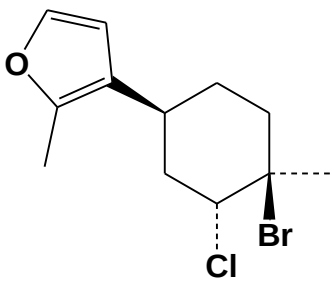

197

A thermolabile diol **(202)**, pacifenol **(203)**, a dibromodiol **(204)** and bromo-alcohol **(205)** yielded from macroalga *Laurencia nipponica* (Kurata et al. 1981). Laurencial **(206)** isolated from macroalga *Laurencia nipponica*, has chamigrene skeleton (Kurata et al. 1983). The metabolite, kylinone **(207)**, obtained from macroalga *Laurencia pacifica* (Selover and Crews 1980). Guadalupol **(208)** and epiguadalupol

(209) isolated from macroalga *Laurencia snyderae* (Howard and Fenical 1979). Several molecules such as rhodolaureol **(210)**, perforenol **(211)** and rhodolauradiol **(212)** found in *Laurencia perforate* (Gonzalez et al. 1978). A ring-contracted chamigrene derivative, spirolaurenone **(213)** isolated from macroalga *Laurencia glandulifera* (Suzuki et al. 1980a). (E)-Bisabolene 8, 9-epoxide **(214)** derived from macroalga *Laurencia nipponica* (Suzuki et al. 1980b). The bisabolene derivative, 8-desoxyisocaespitaol **(215)** isolated from macroalga *Laurencia caespitosa* (Gonzalez et al. 1980). The metabolite, dibromide **(216)** found in *Laurencia obtusa* (Faulkner 1984). Cyclic ether of nerolidol, obtusenol **(217)** isolated from macroalga *Laurencia obtuse* (Faulkner 1984). Metabolite conjugated diene **(218)**, the corresponding acetate **(219)** and palisol **(220)** isolated from *Laurencia palisade* (Paul and Fenical 1980a). The species *Laurencia palisada* also contains palisadin A **(221)**, aplysistatin **(222)** and palisadin B **(223)**. 12-hydroxypalisadin B **(224)** and 5-acetoxypalisadin B **(225)** isolated from *Laurencia palisade.* Aplysistatin **(226)** and 6P-hydroxyaplysistatin **(227)** derived from *Laurencia filiformis* (Capon et al. 1981). Metabolites such as α-snyderol **(228)** and bicyclolaurencenol **(229)** produced from macroalga *Laurencia intricate* (Horsley et al. 1981). Heterocladol **(230)** obtained from macroalga *Laurencia fliformis* (Kazlauskas et al. 1977b). (lS, 4R, 7R)-l-Bromo-4-hydroxy-7-chloroselinane **(231)** (Rose et al. 1978) and its dehydrochlorination product (1S, 4R)-1-bromo-4-hydroxyselin-7-ene **(232)** isolated from the species *Laurencia* (Rose and Sims 1977). Secondary metabolites such as austradiol diacetate **(233)**, austradiol acetate **(234)** (Brennan and Erickson 1982) and (+)-selina-4, 7(11)-diene **(235)** yielded from *Laurencia* species (Sun and Erickson 1978). The unusual sesquiterpene poitediol **(236)** isolated from a species of the genus *Laurencia* is *Laurencia poitei* (Fenica et al. 1978). Brominated diterpenes such as irieol D **(237)**, irieol **(238)**, irieol G **(239)**, irieol E **(240)**, irieol F **(241)** and neoireone **(242)** reported from macroalga *Laurencia irieii* (Howard and Fenical 1978b; Faulkner 1984).

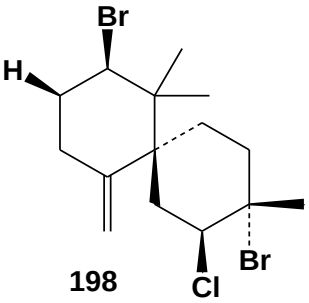

198

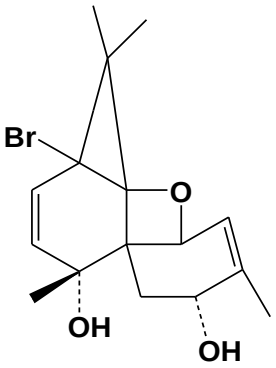

202

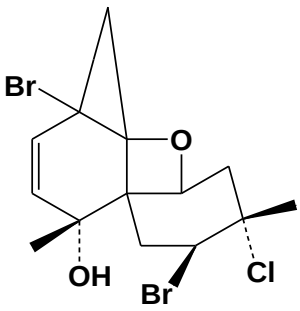

203

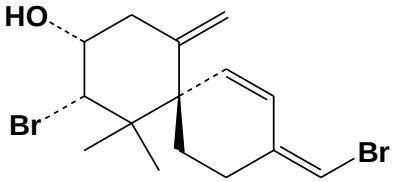

199

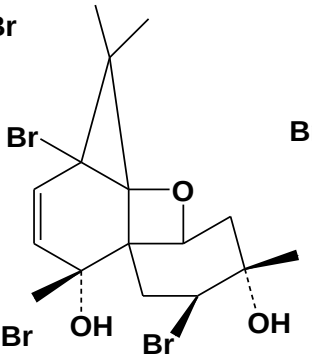

204

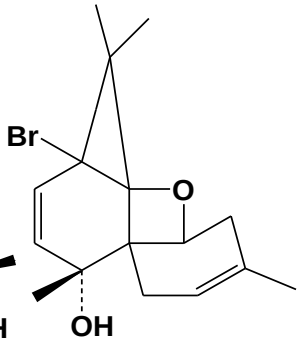

205

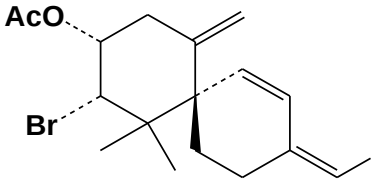

200

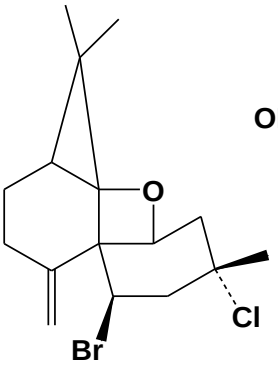

201

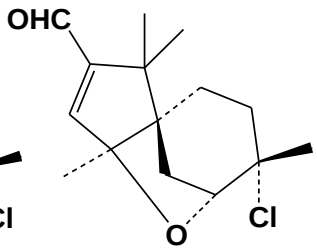

206

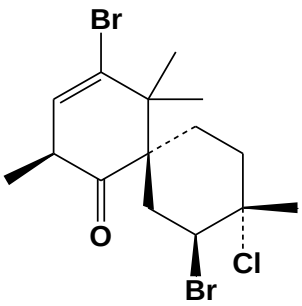

207

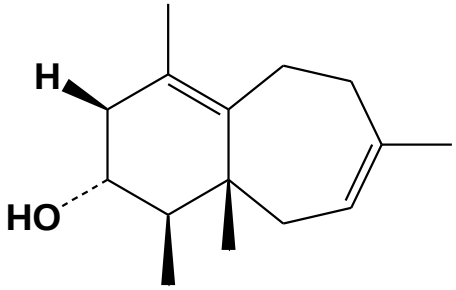

208

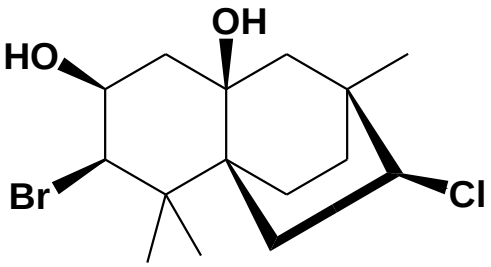

212

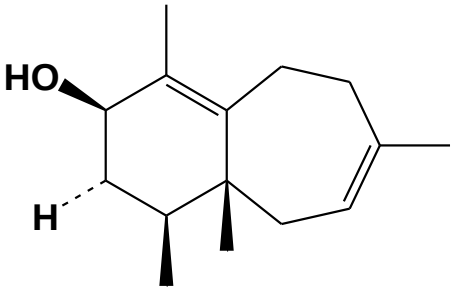

209

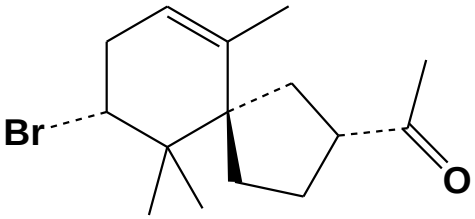

213

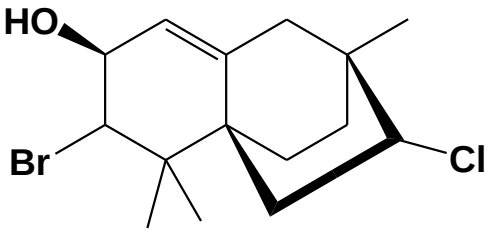

210

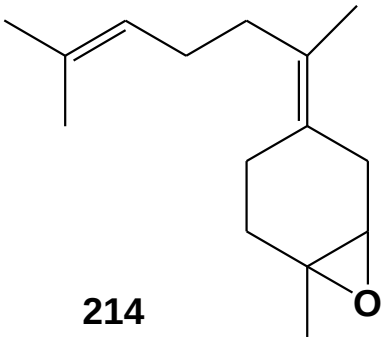

214

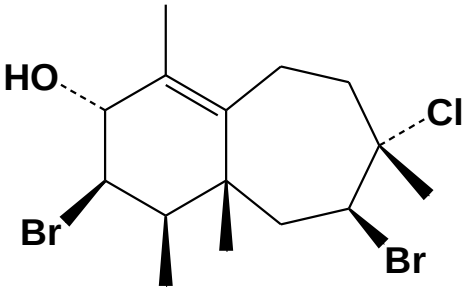

211

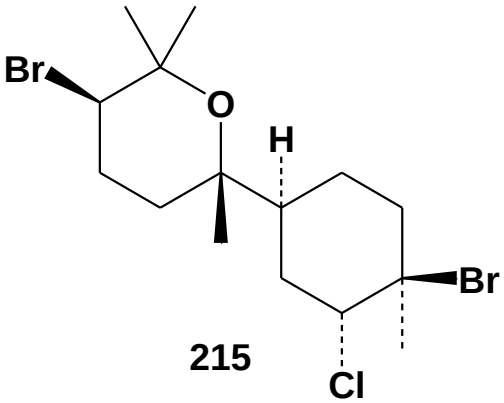

215

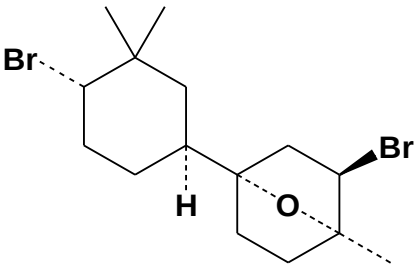

216

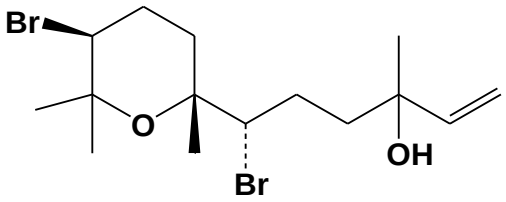

217

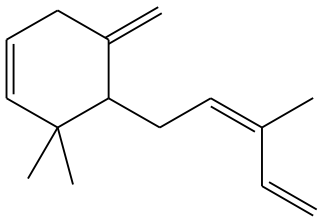

218

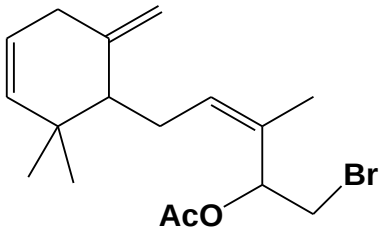

219

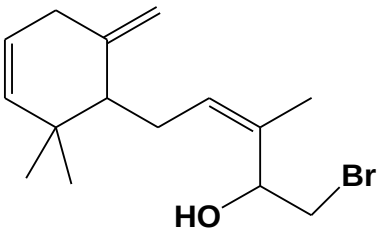

220

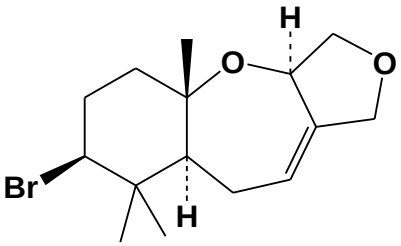

221

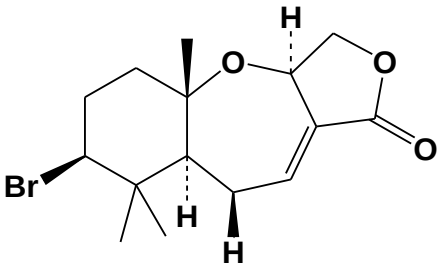

222

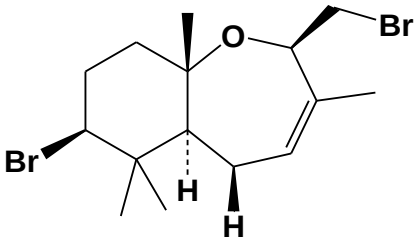

223

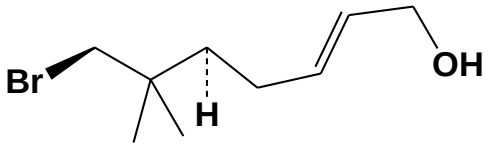

224

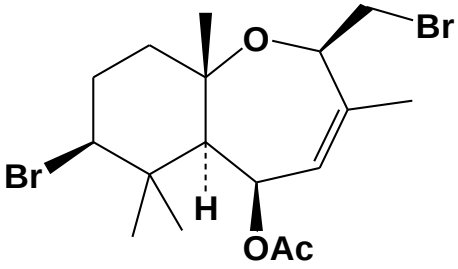

225

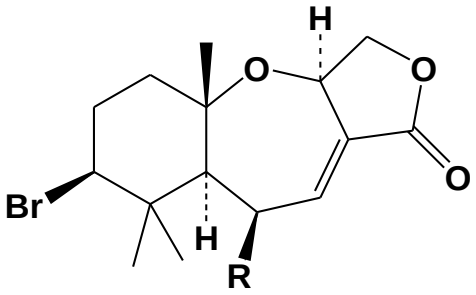

226

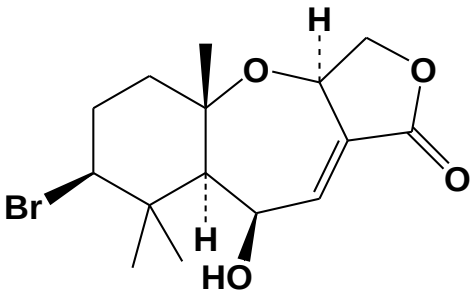

227

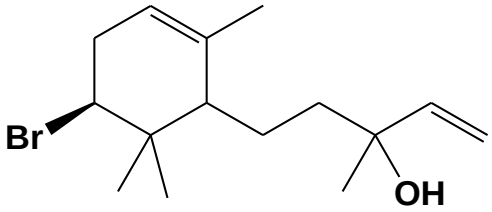

228

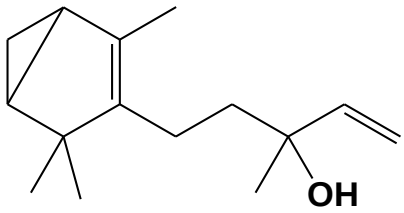

229

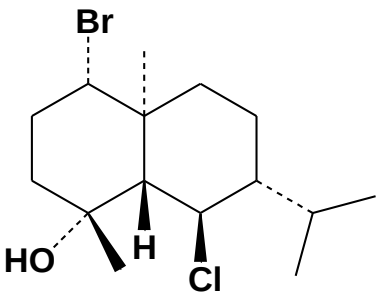

230

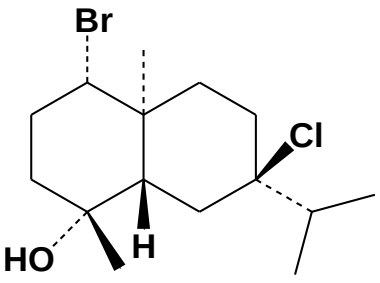

231

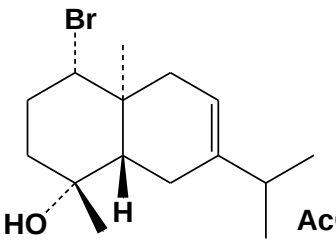

232

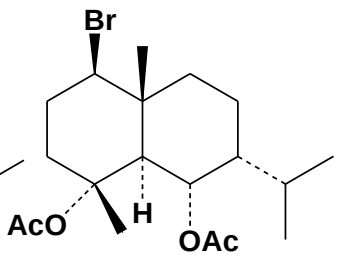

233

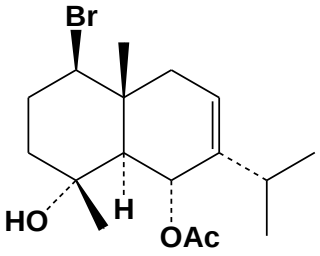

234

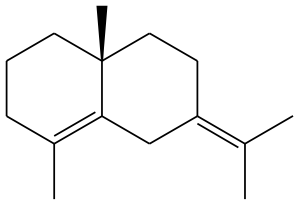

235

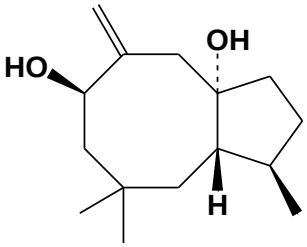

236

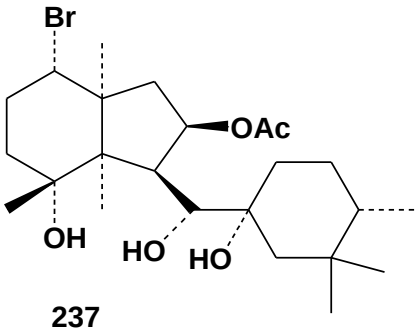

237

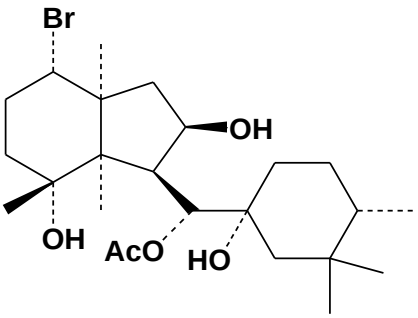

239

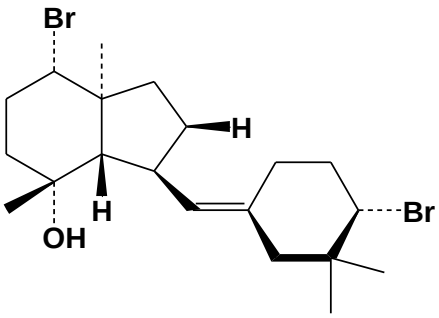

238

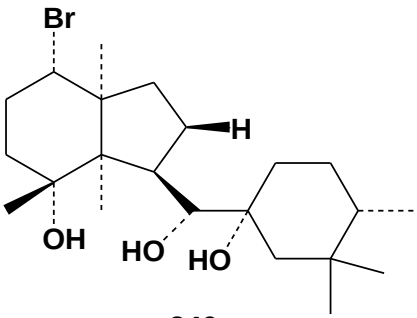

240

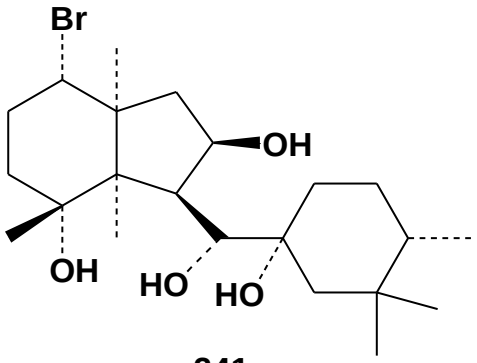

241

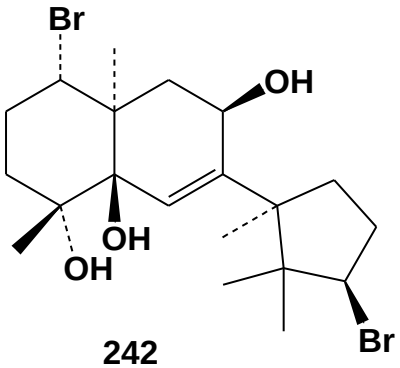

242

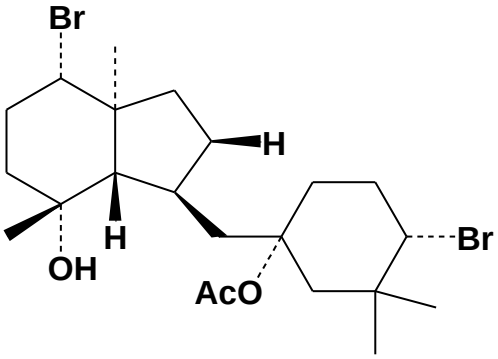

243

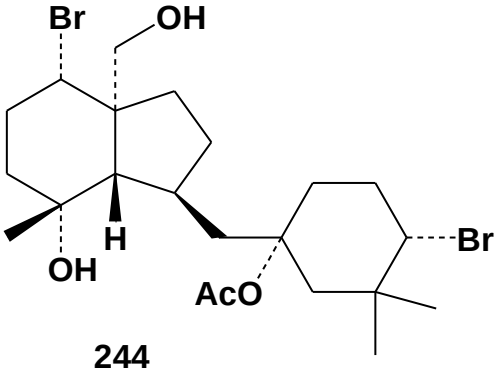

244

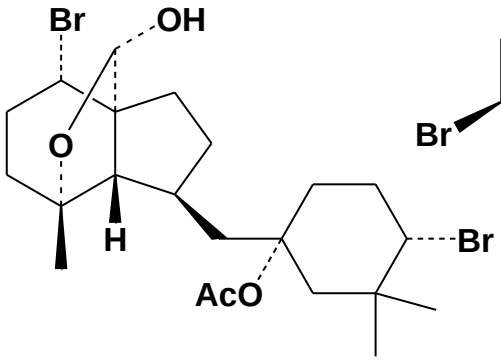

245

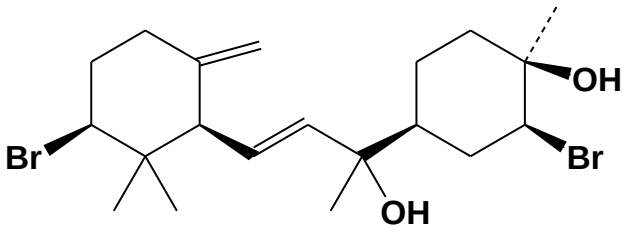

246

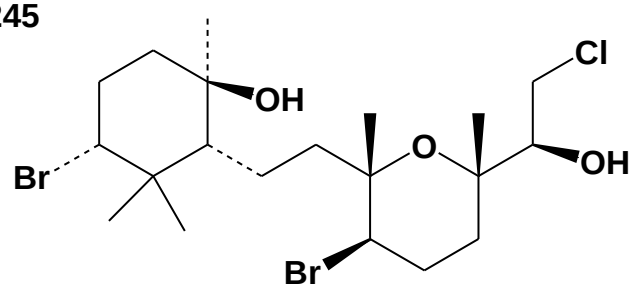

247

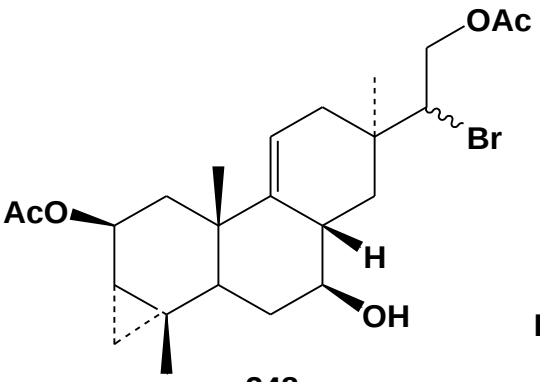

248

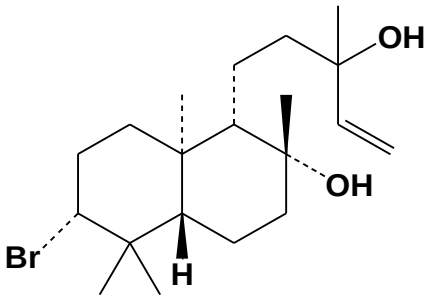

249

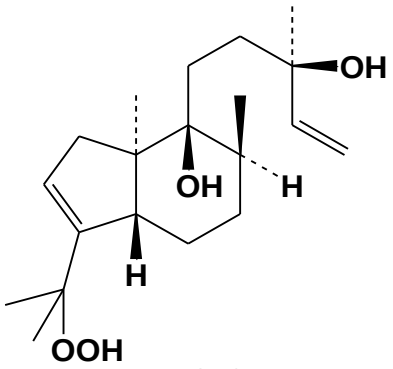

250

Three cyclic ether includes pinnaterpene A **(243)**, pinnaterpene B **(244)** and pinnaterpene C **(245)** obtained from *Laurencia pinnata* (Fukuzawa et al. 1982). Halogenated diterpenes such as obtusadiol **(246)**, laurencianol **(247)** and 15-bromo-2, 16-diacetoxy-7-hydroxy-9 (11)-paraguerene **(248)** derived from *Laurencia obtuse* (Howard and Fenical 1978a). Two diterpenes isoconcinndiol **(249)** and neoconcinndiol hydroperoxide **(250)** isolated from *Laurencia snyderae* (Howard and Fenical 1980).

2.7. Structural Diversity of Polysaccharides from Marine Macroalgae

Algal sulfated polysaccharides, until recently, were largely ignored as sources of antioxidant activities. For example, fucans from *F. vesiculosus* exhibited considerable ferric reducing/antioxidant power and superoxide radical scavenging abilities (De Souza et al. 2007). Fucan fractions from *Laurencia japonica* also showed significant antioxidant capabilities in superoxide radical and hydroxyl radical scavenging assays (Zhao et al. 2005). Positive correlation was observed between superoxide radical scavenging activity and the sulfate content of the polysaccharide fractions (De Souza et al. 2007).

Antioxidative potential of carrageenans (De Souza et al. 2007) and *ulvans* appeared to be associated with the sulfate content, and previous report of literature showed enhanced antioxidant potential of polysaccharide due to the presence of high sulfate content (Zhang et al. 2005). Sulfated polysaccharides derived from macroalgae showed immunomodulatory potential that might be useful in stimulating the immune response (Chen et al. 2008). Sulfated polysaccharide from marine macroalgae (Fig. 2.4) used as anti-inflammatory agents displayed their potential to impede with the relocation of leukocytes to the inflammatory sites. Polysaccharide fucans derived from the marine macroalgae, such as *Cladosiphon okamuranus*, *Fucus* spp, *Laminaria* spp and *Ascophyllum nodosum* were displayed to inhibit leukocyte recruitment to the abdominal cavity throughout acute peritonitis in rats (Cumashi et al. 2007). Moreover, sulfated polysaccharides inhibit heparanase and elastases, which are the tissue degradative enzymes that are intricate in the breakdown of basement membrane integrity during inflammation (Senni et al. 2006). The fucoidan fractions isolated from marine macroalga *Ascophyllum nodosum* eventualy constitutes the classical and alternative pathways in human serum (Blondin et al. 1994). The algal sulfated polysaccharides were found to effectively interact with the complement system proposing that they may have applicability in regulating indigenous immunity to lower the pro-inflammatory occurrence or other unfavorable conditions, such as allergic reflections originating during the inherent immune response.

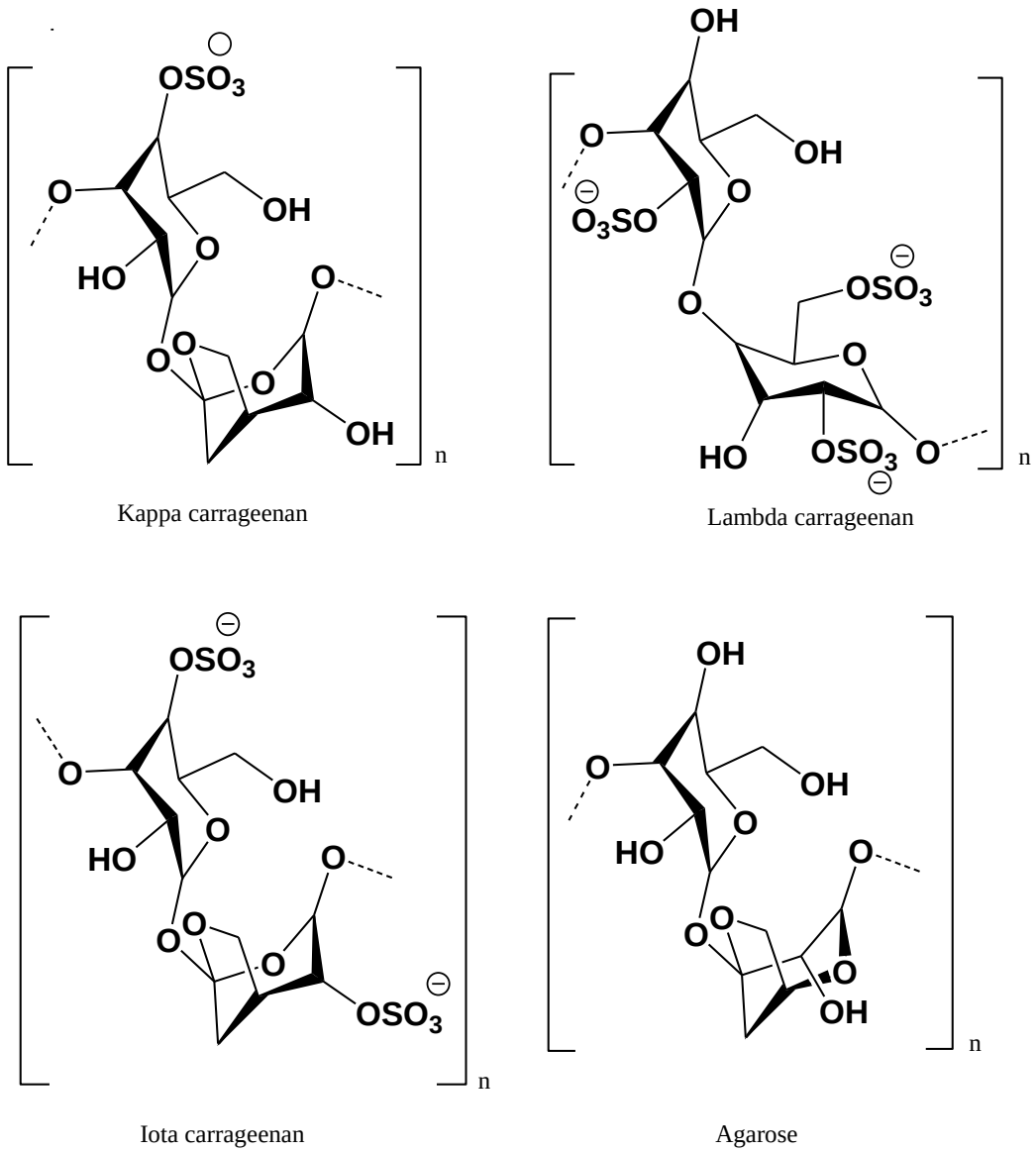

Figure 2.4. Structure of polysaccharides from red macroalgae

Algal polysaccharides were found to attenuate the generation of nitric oxide and pro-inflammatory cytokines during the initiation of inductive nitric oxide synthase (Leiro et al. 2007). According to previous reports, sulfated polysaccharides derived from the marine algal species could directly stimulate the immune system to result in reduced inflammation (Leiro et al. 2007). Algal derived sulfated polysaccharides like carrageenans and fucoidans were found to increase the cytotoxic ability of natural killer cells, such as macrophages and lymphocytes towords the carcinogenic tumors (Choi et al. 2005). Polysaccharides isolated from marine macroalga *Ulva rigida*

demonstrated reduced immune stimulatory potential after desulfation (Leiro et al. 2007). However, some of the marine algal species were reported to generate toxic compounds that stimulate neurodegenerative disorders (Turkez et al. 2012). Ethanol extracts extracted from the red marine macroalage *Callophyllis japonica* (Kang et al. 2005) and *Gracilaria tenuistipitata* (Yang et al. 2012) have significant antioxidant properties. Radical scavenging potential has been evaluated for enzymatic extracts of various marine macroalgae. Oxidative stress plays a prominent roles in various disorders includes, endothelial dysfunction (Schramm et al. 2012), lung disease (Rosanna and Salvatore 2012), gastrointestinal dysfunction (Kim et al. 2012) and atherosclerosis (Hulsmans et al. 2012), all of which involve inflammatory reactions. Marine natural products that possess antioxidant compounds were also known to have anti-inflammatory potential (Abad et al. 2008). However, anti-inflammatory properties have been reported for two species of red algae such as, *Gracilaria verrucosa* and *Gracilaria textorii*. An aqueous extract of *Gracilaria tenuistipitata* lower the virus-induced inflammation. Similarly, the polysaccharide obtained from *Porphyridium* sp. inhibited the replication of retro viruses, and an ethanol extract of *Polyopes affinis* suppressed asthmatic reactions in a disease (Lee et al. 2011). Neorogioltriol, a tricyclic brominated diterpenoid metabolite derived from the marine macroalga *Laurencia glandulifera* have showed significant anti-inflammatory potential (Chatter et al. 2011). (E)-10-Oxooctadec-8-enoic acid and (E)-9-Oxooctadec-10-enoic acid isolated from *Gracilaria verrucosa*, were the two enone fatty acids, which were reported to prevent the generation of inflammatory analogues (Lee et al. 2009). Significant antinociceptive and anti-inflammatory activities were demonstrated by the methanol extract of *Bryothamnion triquetrum* (Cavalcante et al. 2012) and sulfated polysaccharides from *Delesseria sanguinea* (Hudson) Lamouroux in *in vivo* experiments. Anti-inflammatory and antinociceptive properties were exhibited by the distinct secondary metabolites, such as a lectin from *Pterocladiella capillacea* (Silva et al. 2010), galactan from *Gelidium crinale* (De Sousa et al. 2013), sulfated polysaccharide from *Gracilaria caudate* (Chaves et al. 2013), and agglutinin isolated from marine macroalga *Hypnea cervicornis* (Bitencourt et al. 2008).

2.8. Health Benefits of Macroalgae: Prospective Candidate in Food and Pharmaceutical Industries

Marine macroalgae have drawn relevant attention in recent years in the search for bioactive compounds, which show great potential as anti-inflammatory, anti-microbial, anti-viral, and anti-tumor drugs (Souza et al. 2012). Marine macroalgae were found to be rich sources of antioxidant compounds (Wang et al. 2009), which could act against lipid oxidation in foods and oxidative stress in the target tissues. The macroalgal polysaccharides, especially those with sulfated residues were reported to have strong antioxidative properties, and have greater potential as pharmacophore candidates (Pangestuti and Kim 2011). The polysaccharide fraction of marine macroalga *Padina* sp, was found to contains anti-inflammatory activities, and was demonstrated to be active against inflammatory enzymes, such as cyclooxygenase-2 (COX-2) and 5-lipoxygenase (5-LOX) (Praveen and Chakraborty 2013). An anti-inflammatory concentrate enriched with substituted oligofucans was purified from the brown macroalgae (Praveen and Chakraborty 2013). The marine macroalga *Gracilaria* sp. is the largest in the order Gracilariales (class Florideophyceae), and were found to include more than 150 species in the tropical and temperate sea (Guiry and Guiry 2016). The most common bioactivities known in *Gracilaria* were anti-bacterial and anti-viral, and have been best described in *Gracilaria cornea* (Bansemir et al. 2006) and *Gracilaria changii* (Sasidharan et al. 2008). There were reports of biogenic alkaloids from marine invertebrates, and few of them were found to be active against various disease molecular targets. The nitrogen containing bioactive compounds were found to comprise a major share of about 40 % of the marine natural products, and are ubiquitous in various marine flora and fauna (Blunt et al. 2008). Some of the bioactive secondary metabolites purified from marine origin were often used as drugs or biological probes for different physiological studies (Bansemir et al. 2006). Indole alkaloids were characterized from marine macroalga *Enteromorpha intestinalis* (Numata et al. 1993) and leptosins from *Sargassum tortillae* (Takahashi et al. 1995). Hordenine was reported to be the first alkaloid isolated from marine algae in 1969 (Guven et al. 1969). These red and green macroalgae of marine origin were found to be potential inhibitors of the carbolytic enzyme α-glucosidase (Seung et al. 2013). Bromophenols, 2-piperidione, benzene acetamide, *n*-hexadecanoic acid and polysaccharide derivatives were found in red marine macroalgae, such as *Rhodomela confervoides*, *Symphyocladia latiuscula*, *Polysiphonia urceolata*, and were found to exhibit pivotal hypoglycemic potentials by inhibiting α-glucosidase (Seung et

al. 2013). Bioactive properties of the marine macroalgae were reported to be due to the presence of sulfated polysaccharides, phenolics, and terpenoids (Chakraborty and Paulraj 2010; Chakraborty et al. 2016). There were additional reports of marine macroalgae possessing α-amylase and α-glucosidase inhibitory activities (Apostolidis et al. 2011), which appropriately substantiated the results obtained in the present study that these macroalgal species are good source for anti-diabetic agents. The synthetic dipeptidyl peptidase-4 (DPP-4) inhibitors, such as vildagliptin, sitagliptin, saxagliptin, etc, were reported to have multiple adverse effects, such as headache, dizziness, hypoglycemic disorders, nausea, weight gain and swelling of the legs and ankles due to excess fluid retention (Idris and Donnelly 2007). Similarly, other synthetic hypoglycemic agents (acarbose and voglibose) that inhibit α-amylase and α-glucosidase were found to cause hepatic and gastrointestinal disorders (Murai et al. 2002). The bioactive compounds from macroalgae were reported to be effective for the treatment of major chronic diseases, such as diabetes through the inhibition of starch digesting enzymes and the regulation of glucose-induced oxidative stress (Lee et al. 2010). Different investigations prescribed that antioxidant and other bioactive properties fundamentally reliant on the level of sulfation, position of sulfate groups on the sugar backbone, sugar composition and glycosidic branching (Leonard et al. 2010). The reported bioactivities of polysaccharides from marine macroalgae incorporate antioxidant, immunomodulatory, anti-coagulant, anti-thrombotic, blood lipid reducing, and anti-inflammatory activities (Li et al. 2008). Antioxidant capacities of polysaccharide or polysaccharide-complex were observed in the fucoidan and fucans isolated from marine macroalgae *Fucus vesiculosus* and *Padina gymnospora* (De Souza et al. 2007). Sulfated polysaccharides extracted from marine macroalgae were found to exhibit promising antioxidant activities (Li et al. 2008). Oxidative stress is known to assume a significant role in causing chronic diseases, for example, hypertension (Savoia and Schiffrin 2007).

Figure 2.5. Photographs of macroalgae collection site in Southeast coast of India

Despite several side effects, such as hypotension, cough and reduced renal function connected with the utilization of synthetic ACE-I inhibitors, e.g., Captopril (Bristol-Myers Squibb Co., New York, NY, USA), Enalapril (Biovail Pharmaceuticals, Ontario, Canada) and Alacepril (LGM Pharma, Boca Raton, FL, USA), they are still broadly utilized for the

treatment of hypertension (Lordan et al. 2011). Owing to these symptoms, there were continuous searches for alternative sources of ACE-I inhibitors from natural sources including macroalgae (Paiva et al. 2016). The marine macroalga ‘‘Wakame’’ (*Undaria pinnatifida*), which is consumed in Japan, has been accounted for *in vitro* ACE-I inhibitory and *in vivo* anti-hypertensive effects (Suetsuna and Nakano 2000). Sato and colleagues identified seven types of ACE-I inhibitory peptides from the butanol portion of Wakame hydrolysate (Sato et al. 2002). The aqueous extracts of the red marine macroalgae, *Gracilaria verrucosa, Gracilaria textorii, Grateloupia filicina, Polysiphonia japonica, Euchema kappaphycus* and *Gracilaria edulis* displayed noteworthy DPPH radical scavenging properties (Heo et al. 2006). There was a previous report that accounted for the molecules with electronegative groups, such as hydroxyl, sulfate, and sulfated ester residues possessing potential Fe^{2+} chelating abilities (Lindsay 1996). Toth and Pavia (2000) reported that polysaccharides derived from marine macroalgae were more biologically active than phlorotannins (phenolics) for the detoxification and imperviousness to transition metal accumulation (Toth and Pavia 2000). The inhibition of lipid peroxidation might be due to the presence of multiple hydroxyl groups on the polysaccharide chain. The polygalactans separated from the red marine macroalgae were disclosed to disrupt free-radical chain reaction by giving a proton to unsaturated fat radicals to end the chain reactions, and therefore, might play prominent role to inhibit lipid peroxidation. As of late, much consideration has been paid by the consumers towards natural bioactive compounds as functional ingredients, and that the marine-inferred ACE inhibitors are alternative tools, which that can add to customer's well-being. The bioactive compounds derived from the food matrices were found to be more effective in promoting health leading to the reduction of disease risk. Particularly, the bioactive compounds derived from marine macroalgae have served as a rich source of health-promoting components. Among them, oligosaccharides and their derivatives are rich sources of natural health enhancers, and this suggests their potential as a functional ingredient in future nutraceutical and pharmaceutical products. However, substantial medical and pharmaceutical researches are required to expand therapeutic agents from these marine sources. All in all, it could be proposed that macroalgae-derived bioactives belonging to sulfated polygalactans are potential therapeutic candidates to prevent various human ailments.

2.9. Conclusions

During the last decades, efforts were undertaken to develop potent antioxidant compounds from the marine origin as food supplements in the food and pharmaceutical industries. These naturally occurring leads were considered as valuable alternatives to the commercially available synthetic compounds due to their effectiveness and safety. There were reports that described the utilization of the antioxidant compounds from marine resources (Li et al. 2008; Liu et al. 2012; Yoon et al. 2012). The regular intake of macroalgae based diet can lower the risk facts of cardiovascular diseases, cancer and diabetes (Yang et al. 2010; Lee et al. 2010). Keeping this fact as background information, the present study has undertaken to develop an optimized protocol for the isolation and purification of the bioactives belonging to small molecular bioactives and polysaccharides. These compounds were characterized using exhaustive spectroscopic techniques, and the novel leads were validated through selective bioassay, structure optimization and chemiinformatic experiments to enrich the pool of bioactive leads for use against oxidants and inflammatory mediators.

Chapter 3

BIOACTIVE POTENTIAL OF *KAPPAPHYCUS ALVAREZII AND GRACILARIA OPUNTIA*

Contents

3.1. Background

Macroalgae of marine origin are photosynthetic organisms, and are resolved to a conjunction of stressful factors, *viz*., light and oxygen at the origin of the evolution of free radicals and other oxidative reagents. Although the absence of oxidative damage in their structural components evidently suggested that their cells generate bioactive metabolites with antioxidative resistance systems (Escrig et al. 2001). The reactive oxygen species (ROS) *viz*., hydroxyl radical ($HO^{\cdot}$), hydrogen peroxide (H_2O_2) etc. are metabolites, which are generated during aerobic life as an outcome of the metabolism of oxygen. DNA, cell membranes, proteins and other cellular fragments are target sites of the free radical-stimulated oxidative degradation processes, resulting in serious human diseases, such as chronic inflammation, atherosclerosis, cancer, cardiovascular disorders and ageing. Clinical studies established that oxidative stress, through free radical generation, assumes a prominent role in the inception of hypertension (Savoia and Schiffrin 2007). It has been established that extended generation of ROS substantially adds to the dysregulation of physiological processes, which evoke structural and functional variations in hypertension. Increased levels of ROS and chronic subclinical inflammation could also potentiate the pathogenic factors leading to type-2 diabetes associated with the insulin resistance syndrome (Festa et al. 2000). Diabetes is the most frequent endocrine disorder, and by the year 2010, it is predicted that greater than 200 million people in the world will have diabetes mellitus and 300 million will decisively have the disorder by 2025 (King et al. 1998). The methods to treat diabetes is to diminish the post-prandial hyperglycemia in order to prevent

the actions of carbohydrate hydrolyzing enzymes, such as α-amylase and α-glucosidase. Among various algae found in the Gulf of Mannar regions, *K. alvarezii* and *G. opuntia* are abundantly available throughout the different seasons. The present work anticipated the evaluation of antioxidant, anti-hypertension anti-diabetics and anti-inflammatory potential of the solvent extracts derived from *K. alvarezii* and *G. opuntia* from the Gulf of Mannar at South-Eastern Coast of the Indian Peninsula. The bioactivities of the solvent extracts were also correlated with the presence of various auxochromes, and their chemical properties responsible for the target bioactivities.

3.2. Materials and Methods

3.2.1. Chemicals and Reagents

All chemicals were of analytical, spectroscopic or chromatographic reagent grade, and were obtained from E-Merck (Darmstadt, Germany) and Sigma-Aldrich Chemical Co. Inc. (St. Louis, MO, USA). The reagents and chemical solvents were of analytical grade or higher.

3.2.2. Samples and Study Area

The two marine red marine macroalgae used in this study were *K. alvarezii* and *G. opuntia* {Fig. 3.1 (A-C)}. They were freshly collected from the Gulf of Mannar in Mandapam region located between 8º48′ N, 78º9′ E and 9º14′ N, 79º14′ E on the south east coast of India. The samples were washed in running water for 10 min, transported to the laboratory and shade-dried (35 ± 3 °C) for 36 h. The shade-dried macroalgae were powdered and used for further experiments. The powdered algal samples (100 g) were extracted three times with EtOAc-MeOH (50–60 °C, 3 h), filtered through Whatman No. 1 filter paper, and the pooled filtrate was concentrated (50 °C) in a rotary vacuum evaporator (Heidolf, Germany) to one-third of the original volume. All reagents and solvents were of analytical grade, and were acquired from E-Merck (Darmstadt, Germany) or Sigma-Aldrich Chemical Co. Inc. (St. Louis, MO).

Figure 3.1. Photographs of marine red macroalgae (**A**) *Kappaphycus alvarezii* (**B**) *Gracilaria opuntia* (**C**) and their collection site at the Gulf of Mannar of Southeast coast of India

Figure 3.2. Red marine macroalgae collected from the intertidal zone of the Gulf of Mannar region (**A**) *Kappaphycus alvarezii* and (**B**) *Gracilaria opuntia.* The close-up views of the algae were shown as insets (**C**) The collection site of marine macroalgae at the Gulf of Mannar region in South-East coast of India (9° 17' 0" North, 79° 7' 0" East)

3.2.3. Antioxidant Activity Assays

3.2.3.1. Total Phenolic Contents (TPC)

Total phenolic content in the crude EtOAc-MeOH extracts of *K. alvarezii* and *G. opuntia* were determined by the Folin–Ciocalteu method (Wojdyło et al. 2007). Briefly, 0.5 mL of the EtOAc-MeOH extracts (5 mg/mL in MeOH) was added into a test tube containing 0.25 mL of Folin–Ciocalteu reagent. After the addition, the mixture was incubated for 8 min. About 1.0 mL of sodium carbonate (7.5 %, w/v) was added, and the contents were thereafter incubated at 25 ºC (for 120 min), and the absorbance was recorded at 756 nm. The results were depicted in milligram of gallic acid equivalents (mg GAE)/g of the solvent extracts.

3.2.3.2. 1, 1-Diphenyl-2-picryl-hydrazil Radical Scavenging Activity

DPPH (100 μM) was dissolved in methanol to prepare the stock solution. The EtOAc-MeOH extracts (1 mL in MeOH) of *K. alvarezii* and *G. opuntia* were mixed with DPPH solution (1 mL) and kept in the dark at room temperature for 10 min. The decrease in absorbance of the mixture was analyzed at 517 nm against a reagent blank by using a UV–VIS spectrophotometer. The percentage of DPPH radical scavenging potential was determined by scavenging activity (%) = $\{(A_0-A_s)/A_0\} \times 100$, where A_0 is the absorbance of control and A_s is the absorbance of the sample. The 50 % inhibitory concentration (IC_{50}) was calculated from the graph plotted with the concentrations of sample (x-axis) against the percentage inhibition (y-axis). The results were expressed as IC_{50}, the concentrations of samples at which they scavenge 50 % of radical activities, and were expressed in mg/mL.

3.2.3.3. 2, 2′-Azino-bis-3 ethylbenzothiozoline-6-sulfonic acid diammonium salt (ABTS) Radical Scavenging Activity

In brief, ABTS was dissolved in the deionized water to a concentration of 7 μM, and the content was mixed with potassium persulfate ($K_2S_2O_8$, 2.45 μM) before being kept in dark at room temperature for 12–16 h. The ABTS radical solution was diluted with MeOH to get an absorbance of 0.70 at 734 nm. The diluted $ABTS^{\cdot+}$ solution (3 mL) was mixed with the EtOAc-MeOH extracts of *K. alvarezii* and *G. opuntia* (30 μL), and the absorbance was recorded after 6 min at 734 nm. The percentage of ABTS radical scavenging potential was determined by scavenging activity (%) = $\{(A_0-A_s)/A_0\} \times 100$, where A_0 is the absorbance of control and A_s is the absorbance of the sample. The 50 % inhibitory concentration (IC_{50}) was calculated from the graph plotted with the concentrations of sample (x-axis) against the percentage inhibition (y-axis). The results were expressed as IC_{50}, the concentrations of samples at which they scavenge 50 % of radical activities, and were expressed in mg/mL.

3.2.3.4. Ferrous ion (Fe^{2+}) Chelating Activity

The ferrous ion chelating ability of the EtOAc-MeOH extracts of *K. alvarezii* and *G. opuntia* was determined as mentioned earlier (Lim et al. 2007) with suitable

modifications. $FeSO_4$ (1.0 mL, 0.125 mM) and ferrozine (1.0 mL, 0.3125 mM) were mixed with 1.0 mL of EtOAc-MeOH extracts of *K. alvarezii* and *G. opuntia*. The mixture was equilibrated for 10 min before measuring the absorbance at 562 nm. The ability of the EtOAc-MeOH extracts of *K. alvarezii* and *G. opuntia* to chelate Fe^{2+} was determined relative to the control (consisting of Fe and ferrozine only) by applying the equation: % chelating ability = $(A_0 - A_1) \times 100/A_0$, where A_0 is the absorbance of control, and A_1 is the absorbance of sample. The results were expressed as IC_{50}, the concentrations of samples at which 50 % of iron chelating activity, and were expressed in mg/mL.

3.2.3.5. Lipid Peroxidation Inhibition Activity

The activities of the EtOAc-MeOH extracts of *K. alvarezii* and *G. opuntia* to arrest lipid peroxidation were assessed by thiobarbituric acid-reactive species (TBARS) formation inhibitory assay (Kulisic et al. 2004). The model system used for this assay was lyophilized green mussel (*Perna viridis* L.) as a lipid source. The lyophilized powder of *P. viridis* meat (10 mg) was incubated with 1 mL of solvent extracts of *K. alvarezii* and *G. opuntia* (1 mL; 2 mg/mL). The incubation was terminated by cold acetic acid addition (pH 3.6, 2 mL, 20 % v/v), and the malondialdehyde production was followed by TBA addition (0.78 % w/v in acetic acid, 2 mL). The incubated (for 45 min at 95 ^oC) mixture was cooled to room temperature, and centrifuged (10 min, 8000 rpm) before measuring the absorbance at 532 nm. The TBARS activity was expressed as mM of malondialdehyde equivalent compounds formed per kg sample (MDAEQ/kg sample), related to the control (lyophilized green mussel) with highest lipid peroxidation on the same assay conditions.

3.2.4. Anti-hypertensive Activities

The anti-hypertensive activities were determined by ACE-I inhibitory assay (Udenigwe et al. 2009). Briefly, the enzyme angiotensin converting enzyme-I (ACE-I, 20 µL, 1 U/mL) was mixed with the EtOAc-MeOH extracts of *K. alvarezii* and *G. opuntia* (0.2 mg), and the mixture was added with *N*-furanacryloyl-l-phenylalanylglycylglycine (FAPGG, 1 mL, 0.5 mM dissolved in 50 mM Tris-HCl buffer, pH 7.5) containing 300 µM of common salt (NaCl). The decreased absorbance

at 345 nm was recorded within a 1.5 min span at room temperature, whereas the anti-hypertensive activities were expressed as IC_{50}, the concentration at which it inhibit 50 % of ACE-I activity.

3.2.5. Anti-diabetic Activities

In vitro anti-diabetic studies by inhibition of dipeptidyl peptidase-4 (DPP-4) and carbolytic enzyme α-amylase were determined by following previous reports of literature (Kojima et al. 1980; Hamdan and Afifi 2004), whereas α-glucosidase inhibition assay was performed according to the previous literature (Dong et al. 2012) with suitable modifications.

3.2.5.1. Inhibition of α-Amylase Activity

To carry out α-amylase inhibitory activity, the EtOAc-MeOH extracts of *K. alvarezii* and *G. opuntia* were added to the phosphate buffer (500 µL, 0.20 mM, pH 6.9) containing α-amylase (0.5 mg/mL) solution before being incubated at 25 °C for 10 min. Thereafter, starch solution (500 µL, 1 % w/v in 0.02 M sodium phosphate buffer of pH 6.9) was added to the content, and the reaction mixture was incubated at 25 °C for 10 min. The reaction was quenched by addition of 3, 5 dinitrosalicylic acid reagent (1.0 mL) under heating condition for 5 min before being cooled at room temperature. The reaction mixture was diluted with distilled water (10 mL), and the absorbance was recorded at 540 nm.

3.2.5.2. Inhibition of α-Glucosidase Activity

To determine the α-glucosidase inhibitory activities of the EtOAc-MeOH extracts of *K. alvarezii* and *G. opuntia*, Tris-HCl buffer (500 µL, 0.2 M, pH 8) was prepared in different concentrations, and was added to the enzyme solution (1 U/mL prepared in 0.2 M Tris-HCl, pH 8.0). The reaction mixture was pre-incubated for 5 min at 37 °C before being added with the starch solution (500 µL, 2 % w/v) and incubated for 10 min at 37 °C. The reaction was stopped with 3, 5 dinitrosalicylic acid reagent (1 mL) under heating for 2 min in a boiling water bath before being cooled at room

temperature. The reaction mixture was then diluted with distilled water (9 mL), and the absorbance was measured at 540 nm.

3.2.5.3. Inhibition of DPP-4 Activity

The EtOAc-MeOH extracts of *K. alvarezii* and *G. opuntia* were prepared in Tris-HCl buffer (50 mM, pH 7.5) at different concentrations. The EtOAc-MeOH extract of *K. alvarezii* and *G. opuntia* (0.35 mL) were mixed with DPP-4 (15 μL, 0.05 U/mL), which was previously prepared in Tris-HCl buffer (100 mM, pH 8). The reaction mixture was pre-incubated for 10 min at 37 °C before being added with the substrate (gly-pro-p-nitroanilide, 50 μL, 0.2M in Tris-HCl buffer). The contents were incubated for 30 min at 37 °C, and the reaction was terminated by the addition of glacial acetic acid (25 μL). The absorbance of the reaction mixture was measured at 405 nm. The results were expressed as IC_{50}, the concentration at which it inhibits 50 % of the enzyme (α-amylase, α-glucosidase and DPP-4) activities.

3.2.6. Anti-inflammatory Activities

The anti-inflammatory properties were evaluated by COX-1 and COX-2 inhibition assays using 2, 7-dichlorofluorescein method (Larsen et al. 1996), and 5-LOX inhibition assay using the principle of 1, 4-diene and 1, 3-diene conversion of the polyunsaturated fatty acid (Baylac and Racine 2003).

3.2.6.1. Cyclooxygenase (COX-1 and COX-2) Inhibition Assay

In brief, leuco-2, 7-dichlorofluorescein diacetate (5 mg) was hydrolyzed at room temperature in NaOH (1 M, 50 μL, 10 min) and the excess of NaOH was neutralized by adding HCl (1 M, 30 μL) before the resulting 1-dichlorofluorescein (1-DCF) was diluted in Tris-HCl buffer (0.1 M, pH 8). The COX isoforms (COX-1 and COX-2) were diluted in 0.1 M Tris-buffer (pH 8), and the EtOAc-MeOH extracts of *K. alvarezii* and *G. opuntia* (the equivalent volume of MeOH, 20 μL) were pre-incubated with the enzymes at room temperature for 5 min in the presence of hematin. Premixed phenol, 1-DCF, and arachidonic acid (fatty acid) were added to the enzyme mixture to initiate the reaction, and to give a final reaction mixture (1 mL) of arachidonic acid (50

μM), phenol (500 μM), 1-DCF (20 μM), and hematin (1 μM) in the final volume of 0.1 M Tris-buffer (pH 8). The reaction was recorded spectrophotometrically over 1 min at 502 nm. The blank was analyzed against each test reaction to ascertain non-enzymatic activity due to the experimental samples.

3.2.6.2. Lipoxygenase (5-LOX) Inhibition Assay

The 5-LOX inhibitory assay was carried out by a previously described method (Baylac and Racine 2003). In brief, an aliquot of the stock solution (50 μL) prepared in solvent DMSO and a surfactant (tween 20) at a particular ratio (29:1, w/w) of each sample were added with potassium phosphate buffer (0.1 M, 2.95 mL, pH 6.3) and linoleic acid solution (48 μL) before being placed in a cuvette (3 mL). An ice-cold solution of potassium phosphate buffer (12 μL) was thereafter mixed with 5-LOX (100 U) in the cuvette. The absorbance of the content was recorded at 234 nm by using a spectrophotometer.

The inhibitory activities of the EtOAc-MeOH extracts of *K. alvarezii* and *G. opuntia* towards COX-1, 2 and 5-LOX were calculated as follows: $\{(Ab_C - Ab_S)/Ab_C\} \times 100$, where Ab_S and Ab_C depicted the absorbance of sample and control, respectively. The results were demonstrated as IC_{50}, the concentration at which it inhibits 50 % of COX and LOX activities.

3.2.7. Spectroscopic Methods

Fourier-transform infrared (FTIR) spectra of the KBr pellets were recorded by utilizing a Perkin–Elmer FTIR spectrophotometer scanning between 4000 and 400 cm^{-1} (Perkin–Elmer 2000, USA). Ultraviolet–visible (UV–VIS) data were acquired by Varian Cary 50 Conc UV–VIS spectrometer (Varian, Waltham, USA). The solvents were evaporated in a rotary vacuum evaporator (Heidolf, Germany). A table-top high speed refrigerated centrifuge (Sorvall, Biofuge Stratos, Thermo Scientific, Germany) was used for centrifugation. The crude EtOAc-MeOH extracts of *K. alvarezii* and *G. opuntia* (10 mg) were mixed with KBr (100 mg) and compressed to prepare as a salt disc. The frequencies of different components present in each sample were analyzed. Proton nuclear magnetic resonance (^{1}H-NMR) spectra were recorded on a Bruker

AVANCE DRX 600 MHz (AV 600) spectrometer (Bruker, Karlsruhe, Germany) in $CDCl_3$ as aprotic solvent at ambient temperature (27 ^oC) with tetramethylsilane (TMS) as the internal standard (δ 0 ppm) equipped with 5 mm probes.

3.2.8. Statistical Analysis

Data were expressed as mean of triplicate ± standard deviation. Statistical evaluation was carried out by SPSS software (SPSS Inc, Chicago, USA, ver. 13.0). Descriptive statistics were calculated for all the studied traits. The Pearson correlation coefficient (*r*) was calculated ($P < 0.05$) to assess the strength of the linear relationship between two variables. The selected variables for principal component analysis (PCA) were the different bioactivities, as exhibited by crude extracts prepared from the studied red marine macroalgae.

3.3. Results and Discussion

3.3.1. Yield

The yields of EtOAc-MeOH extracts of *K. alvarezii* and *G. opuntia* were found to be 60 g (6 %) and 40 g (4 %) of 1 kg of dry algae, respectively.

Table 3.1 *In vitro* bioactivity of EtOAc-MeOH (1:1 v/v) solvent extracts from the red marine macroalgae

Activities	***K. alvarezii***	***G. opuntia***
Total phenolic content	295.68 ± 0.01^a	380.33 ± 0.02^a
Antioxidant activities		
$DPPH^{\cdot}$ radical scavenging	1.24 ± 0.06^b	1.28 ± 0.03^c
ABTS radical scavenging	1.26 ± 0.03^b	1.31 ± 0.05^c
Fe^{2+} ion chelating	1.30 ± 0.09^b	1.33 ± 0.01^c
Lipid peroxidation inhibitory	47.08 ± 0.05^a	53.81 ± 0.04^b
Anti-hypertensive activities (ACE)	2.10 ± 0.02^b	2.13 ± 0.09^c
Anti-diabetic activities		
α-amylase inhibitory	2.18 ± 0.04^b	2.20 ± 0.08^c

α-glucosidase inhibitory	2.20 ± 0.01[b]	2.22 ± 0.03[c]
DPP-4 inhibitory	2.18 ± 0.03[b]	2.21 ± 0.02[c]
Anti-inflammatory activities		
COX-1 inhibitory	1.38 ± 0.09[b]	1.42±0.02[c]
COX-2 inhibitory	1.35 ± 0.05[b]	1.39 ± 0.04[b]
5-LOX inhibitory	1.49 ± 0.02[b]	1.52 ± 0.03[b]

Results were expressed in IC_{50} values (50 % inhibitory concentration as mg/mL; calculated from the graph plotted with concentrations of samples against percentage.

[a-c] Column wise values with different superscripts of this type indicate significant difference ($P < 0.05$).

Results were expressed as mean ± SD (n =3).

Lipid peroxidation inhibitory activity (TBARS assay) was expressed as m MDAEQ/kg.

3.3.2. Antioxidant Activities and Phenolic Contents of Organic Extracts of Macroalgae

The EtOAc-MeOH extracts from *G. opuntia* (380.33 mg of GAE/g) was found to possess greater content of total phenolics than that of *K. alvarezii* (295.68 mg of GAE/g). The DPPH radical scavenging activity of EtOAc-MeOH extracts derived from *K. alvarezii* was found to be greater (IC_{50} 1.24 mg/mL) than that displayed by *G. opuntia* (IC_{50} 1.28 mg/mL). $ABTS^{\cdot+}$ scavenging activity of EtOAc-MeOH extracts from *K. alvarezii* was greater (IC_{50} 1.26 mg/mL) than that from *G. opuntia* (IC_{50} 1.31 mg/mL). The EtOAc-MeOH extracts from *K. alvarezii* displayed significantly greater Fe^{2+} chelating abilities (IC_{50} 1.30 mg/mL) than that acquired from *G. opuntia* (IC_{50} 1.33 mg/mL). On account of lipid peroxidation inhibition assay, the EtOAc-MeOH extracts from *K. alvarezii* displayed greater lipid peroxidation inhibition activity (47.08 mM MDAEQ/kg) than that obtained from *G. opuntia* (53.81 mM MDAEQ/kg). TBARS activity was denoted as mM of malondialdehyde equivalent compounds formed per kg sample (MDAEQ/kg sample) related to the control (lyophilized green mussel) leading to maximum lipid peroxidation in the same assay conditions. The capability of the EtOAc-MeOH extracts derived from *K. alvarezii* and *G. opuntia* to induce lipid peroxidation was estimated by thiobarbituric acid reactive species (TBARS) assay.

3.3.3. ACE Inhibitory Activity

The ACE inhibitory activities of the EtOAc-MeOH extracts from *G. opuntia* was lesser (IC_{50} 2.13 mg/mL) than those from *K. alvarezii* (IC_{50} 2.10 mg/mL).

3.3.4. *In-vitro* Anti-diabetic Activities of EtOAc-MeOH Extracts from *K. alvarezii* and *G. opuntia*

3.3.4.1. Inhibition of α-Amylase and α-Glucosidase Activities

The results from the present study demonstrated that there were no significant difference in α-amylase and α-glucosidase inhibitory activity of the EtOAc-MeOH extracts from *K. alvarezii* and *G. opuntia* considered in the present study (Table 3.1). However, the EtOAc-MeOH extracts of *K. alvarezii* exhibited greater α-amylase inhibitory activity (IC_{50} 2.18 mg/mL) than that of *G. opuntia* (IC_{50} 2.20 mg/mL). Likewise, there was no significant difference in the α-glucosidase inhibitory activity of the EtOAc-MeOH extracts derived from these two red macroalgal species (*K. alvarezii* IC_{50} 2.20 mg/mL; *G. opuntia* IC_{50} 2.22 mg/mL). The macroalgae were reported to possess α-amylase and α-glucosidase inhibitory activities (Apostolidis et al. 2011), which substantiated the results obtained in the present study that these macroalgal species were good source for anti-diabetic agents.

3.3.4.2. Inhibition of Dipeptidyl-Peptidase-4 Enzyme Activity

Dipeptidyl peptidase-4 (DPP-4) is involved in the inactivation of glucagon like peptide-1 (GLP-1), a potent insulinotropic peptide. Thus, DPP-4 inhibition can be an efficient approach to treat type-2 diabetes mellitus by potentiating insulin secretion (Mentlein 1999). The present study described the biological effects of EtOAc-MeOH extracts from two different red macroalgae *K. alvarezii* and *G. opuntia*. DPP-4 inhibitory activity of the EtOAc-MeOH extracts of *K. alvarezii* was found to be significantly greater (IC_{50} 2.18 mg/mL) than that derived from *G. opuntia* (IC_{50} 2.21 mg/mL). The synthetic DPP-4 inhibitors such as vildagliptin, sitagliptin, saxagliptin, etc, were reported to have several side effects like headache, dizziness, hypoglycemic disorders, nausea, weight gain and swelling of the legs and ankles due to excess fluid

retention (Idris and Donnelly 2007). Similarly, other synthetic hypoglycemic agents (acarbose and voglibose) that inhibit α-amylase and α-glucosidase were found to cause hepatic and gastrointestinal disorders (Murai et al. 2002). The bioactive compounds from macroalgae were reported to be effective for the treatment of major chronic diseases like diabetes through the inhibition of starch digesting enzymes and the regulation of glucose-induced oxidative stress (Lee et al. 2010). The macroalgae considered in the present study can be used as potential alternative therapy for treatment of diabetes.

3.3.5. *In-vitro* Anti-inflammatory Activities of Organic Extracts from *K. alvarezii* and *G. opuntia*

The EtOAc-MeOH extracts from *K. alvarezii* exhibited significantly greater ($P < 0.05$) COX-1 and COX-2 inhibition activity (IC_{50} values of 1.38 mg/mL and 1.35 mg/mL, respectively) than that displayed by *G. opuntia* (IC_{50} values of 1.42 mg/mL and 1.39 mg/mL, respectively). EtOAc-MeOH extracts from *K. alvarezii* also exhibited greater 5-LOX inhibitory activity (1.49 mg/mL) than that of *G. opuntia* (IC_{50} 1.52 mg/mL) (Table 3.1).

3.3.6. Spectroscopic Fingerprinting of EtOAc-MeOH Extracts of *K. alvarezii* and *G. opuntia*

Spectrometric fingerprinting were used to de-replicate the pattern recognition of the resonances along with types and number of protons associated with structural classes involved in extracts

3.3.6.1. Fourier Transform Infrared Spectral (FT-IR) Analysis

FT-IR is a valuable tool for qualitative determination of the probable occurrences of various functional groups in the crude organic extracts (Ashokkumar and Ramaswamy 2014). In the present study, the FT-IR experiments were carried out to fingerprint the functional groups present in the EtOAc-MeOH extracts from *K. alvarezii* and *G. opuntia*. The intense band at 3429.39 cm^{-1} in the organic crude extract from *K. alvarezii* was attributed due to the N-H stretching or O-H stretching vibration

of phenols or alcohols. The absorption peaks were present in the EtOAc-MeOH crude extract from *G. opuntia* at 1715 cm^{-1} might be due to the C=O stretching vibration of saturated aliphatic groups and carbonyls. Absorption band in the FTIR spectrum of EtOAc-MeOH crude extracts of *K. alvarezii* (1363 cm^{-1}) and *G. opuntia* (1371.54 cm^{-1}, 1458.63 cm^{-1}) were attributed, which represented the C-C stretching vibrations of the aryl ring framework. The strong absorption bands in the 2920-2923 cm^{-1} region of the FT-IR spectra of the EtOAc-MeOH extracts of *K. alvarezii* and *G. opuntia* attributed the C-H stretching vibrations. In comparison with the FT-IR spectra of EtOAc-MeOH extracts of *K. alvarezii* and *G. opuntia*, both the extracts displayed prominent functional groups.

3.3.6.2. Nuclear Magnetic Resonance (NMR) Fingerprinting

The protons and carbons associated with different magnetic environments of the functional groups in the organic extracts of the studied marine macroalgal species were labeled and analyzed by ^{1}H and ^{13}C-NMR spectroscopy. The ^{1}H-NMR spectral data of EtOAc-MeOH extract obtained from *K. alvarezii* displayed greater proton integrals (>1000) at δ_H 0-2, which implied the existence of methine (-C<u>H</u>-), methylene (RC<u>H_2</u>-) and methyl (C<u>H_3</u>-C) protons correlated with saturated hydrocarbons, whereas the organic extract from *G. opuntia* was found to illustrate lesser number of proton integral (~579).

The signals at δ_H 1.08–1.38 in the organic extract of *G. opuntia* could be explained by the presence of methylene group {–(C<u>H_2</u>)$_n$} in the long alkyl chain. The ^{1}H-NMR spectra of *K. alvarezii* acquired well resolved, deshielded signals at about δ_H 4.5-5, than those displayed by *G. opuntia*, which appropriately signified the vicinity of the olefinic attachments in the former. The protons appeared at δ_H 2-2.5, apparently indicated acetyl or allylic substitution, which were found to be significantly higher in the EtOAc-MeOH extract of *K. alvarezii*, whilst EtOAc-MeOH extract of *G. opuntia* possessed lesser number of proton integral at this region. The presence of methoxy proton (R-OC<u>H_3</u>) was confirmed by the protons at δ_H 3.08, 3.66 and 3.18 in the NMR spectrum of the organic extracts of *K. alvarezii* and a peak at δ_H 3.54 with regard to the same of *G. opuntia*. The integral value of protons in the olefinic range (δ_H 4.5-6) of EtOAc-MeOH extract of *K. alvarezii* was greater (~341) when compared with the same obtained from *G. opuntia* (δ_H 4.8-4.9) (~76). The protons present in the region of δ_H

7.2-7.4 were typical of the aryl (aromatic) ring system. Proton integral at this aromatic region was found to be greater in EtOAc-MeOH extract of *K. alvarezii* (proton integral of ~330). There were no aldehydic protons at the characteristic region of δ_H 8.5-10 in the NMR spectra of EtOAc-MeOH extracts of *K. alvarezii* and *G. opuntia*. The pattern recognition and proton integration ^{1}H-NMR approach to de-replication could thus lead to a conclusion of the types and number of protons that might be associated with the compound(s) in the extracts. The number of carbon atoms associated to the saturated hydrocarbons (δ_C 10-40) was higher in the EtOAc-MeOH extracts of *K. alvarezii* than that of *G. opuntia.* The olefinic carbons at δ_C 114-136 were greater in the extract of *K. alvarezii.* Prominent ^{13}C-NMR signals were recorded in the carbonyl carbon region (δ_C 171-173) of the organic extract derived from *K. alvarezii*. Preliminary, the spectroscopic fingerprinting experiments, such as FT-IR and NMR of the organic extracts of *K. alvarezii* and *G. opuntia* provided with the preliminary information with regard to the different types of protons and carbons associated with different magnetic environments of the functional groups.

3.3.7. Correlation Analysis

The relationships between antioxidant, anti-inflammatory, anti-hypertension and anti-diabetic activities of the EtOAc-MeOH extracts of *K. alvarezii* and *G. opuntia* were statistically analyzed using PCA (Fig. 3.3). The loading of first and second principle components (PC1 and PC2) were accounted for 65.30 % and 30.10 % of the variance, respectively.

The component, PC1 was mainly influenced by inhibitory activities of EtOAc-MeOH derived from *G. opuntia* and *K. alvarezii* (GO, KA) towards the pro-inflammatory enzymes, COX-1 (denoted as C1; GO and C2; KA) and COX-2 (denoted as CO1; GO and CO2; KA), along with DPPH (DPP2; KA) and ACE (AC2; KA). On the other hand, 5-LOX (denoted as L1; GO and L2; KA), DPP-4 (DP1; GO and DP2; KA), DPPH (DPP1; GO), and ACE (AC1; GO) inhibiotory properties of the EtOAc-MeOH extracts of the marine macroalgae were mainly contributed to PC2 (Fig. 3.3).

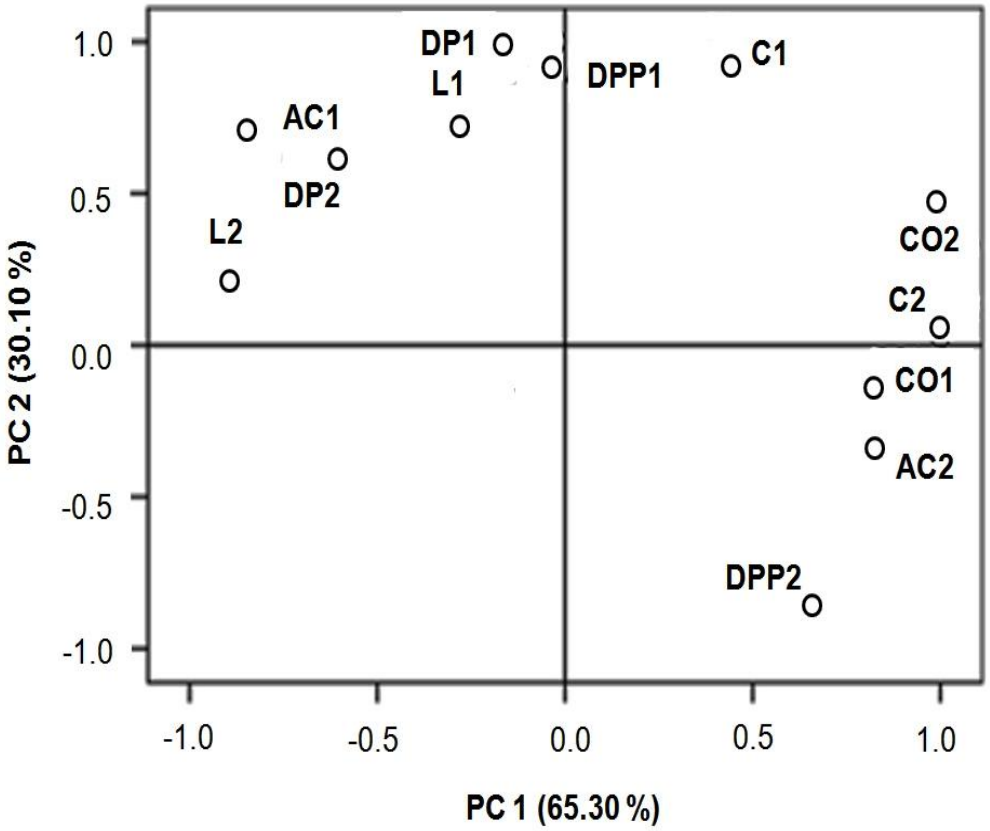

Figure 3.3. Loading plot diagram of various bioactivities

The similarity in the greater loading of DPPH, ACE, DPP-4, COX-2, 5-LOX inhibitory activities of the EtOAc-MeOH extracts derived from *G. opuntia* and *K. alvarezii* apparently demonstrated that these bioactivities were in close relation. The significant correlation of antioxidant activities with anti-diabetic, anti-inflammatory and anti-hypertensive properties of the EtOAc-MeOH extracts derived from the marine macroalgae *G. opuntia* and *K. alvarezii* also indicated that the bioactive compounds present in the extract were responsible for bioactivities.

3.4. Conclusions

The organic extracts obtained from the red macroalgae *K. alvarezii* and *G. opuntia* were found to possess a number of bioactivities against different disease targets, namely hypertension, type-2 diabetes, and inflammation. The current study revealed that the EtOAc-MeOH extract of *K. alvarezii* possessed greater anti-

oxidative activities, and exhibited significant positive correlation with the anti-inflammatory, anti-hypertensive and anti-diabetic activities. The organic extract of *K. alvarezii* possessed significantly greater antioxidative properties than those obtained from *G. opuntia*. The organic extract from *K. alvarezii* also showed greater angiotensin-I converting enzyme (ACE) inhibitory activity along with pro-inflammatory cyclooxygenase/lipoxygenase inhibitory activities than that exhibited by that acquired from *G. opuntia.* Likewise, EtOAc-MeOH crude extract obtained from *K. alvarezii* showed significant anti-diabetic activities as determined by *in vitro* α-amylase, α-glucosidase and dipeptidyl peptidase-4 inhibitory properties. The spectroscopic characterization of the solvent extracts provided the evidence regarding the occurrences of signature peaks and the prominent functional groups that were responsible for the target bioactivities. This study demonstrated the candidacy of red macroalga particularly, *K. alvarezii* as potential source of bioactive compounds for use as functional food supplements and pharmaceutical applications.

Chapter 4

ISOLATION AND CHARACTERIZATION OF SECONDARY METABOLITES FROM *KAPPAPHYCUS ALVAREZII AND GRACILARIA OPUNTIA*

Contents

4.1. Background

Traditionally, marine macroalgae have been considered as valuable marine flora, which are preferred delicacies in the South-east Asian countries, particularly Japan, China, Korea and Indonesia due to their potential antioxidant and therapeutic properties (Wang et al. 2009). Species of the red marine macroalgae were proven to be rich sources of structurally unique and biologically active secondary metabolites for applications in functional food and pharmaceuticals (Kladi et al. 2004). Antioxidative compounds obtained from these species were identified as phylopheophylin (Cahyana et al. 1992), phlorotannins (Yan et al. 1996), terpenoids (Chakraborty and Paulraj 2010) and fucoxanthin (Yan et al. 1999). The bioactive compounds extracted from marine macroalgae were used as safer anti-inflammatory therapeutics as well. The vast majority of the red marine macroalgae derived bioactive compounds were diterpenes (Rochfort and Capon 1996), sesquiterpenes (Amico et al. 1991) and C_{15} non-terpenoids containing ether rings of different sizes including halogenated cyclic ether enynes and related allenes (Erickson 1983; Iliopoulou et al. 2002). The red marine macroalgae were reported for their antioxidant potential and *in vitro* anti-proliferative activities in cancer cell lines (Chakraborty et al. 2015). *Kappaphycus alvarezii* (Silva et al. 1996) is economically significant and predominantly farmed red marine macroalga in the shallow tropical marine habitats around the South-east Asian countries, particularly Philippines, Taiwan, Malaysia, Indonesia and India (Ask and Azanza 2002; Chandrasekaran et al. 2008). Despite the fact that red marine macroalgae, particularly *Laurencia* species, have been studied extensively with respect to secondary metabolite chemistry (Amico et al. 1991; Rochfort and Capon 1996; Manta 2001; Iliopoulou et al. 2002), studies on members of the genus *K. alvarezii* and *G. opuntia* have been rare for the isolation of novel intriguing structures.

The marine macroalgae *K. alvarezii* and *G. opuntia* are abundantly available throughout the subtropical and tropical climatic zones from the south-east coast of Gulf of Mannar of India (Guiry and Guiry 2016). Despite the fact that red marine macroalgae have been extensively studied to isolate various classes of bioactive compounds (Iliopoulou et al. 2002), no natural products have been reported from the aforesaid red marine macroalgae, suggesting *K. alvarezii* and *G. opuntia* would be an attractive source for chemical investigation. The methanol-ethyl acetate extract

(MeOH: EtOAc 1:1 v/v) fraction of the thalli of *K. alvarezii* and *G. opuntia* was fractionated by repeated column chromatography to afford a number of previously undescribed compounds. The structures of these compounds were established by exhaustive spectroscopic experiments, including mass and two-dimensional nuclear magnetic resonance. The antioxidative and anti-inflammatory activities of the newly reported compounds were evaluated by different *in vitro* assays. Structure-bioactivity correlation analysis of the studied compounds was carried out using different electronic and hydrophobic molecular descriptor variables.

4.2. Materials and Methods

4.2.1. Chemicals and Reagents

All chemicals were of analytical, spectroscopic or chromatographic reagent grade, and were obtained from E-Merck (Darmstadt, Germany) and Sigma-Aldrich (St. Luois, MO, USA). All reagents and chemical solvents were of analytical grade or higher.

4.2.2. Isolation and Purification of Secondary Metabolites

4.2.2.1. Sample Preparation

This section described the preparation of crude extract of *K. alvarezii* and *G. opuntia* for the chromatographic purification and the isolation of bioactive compounds. Briefly, the marine macroalgae *K. alvarezii* and *G. opuntia* were freshly collected from Gulf of Mannar located between 8º48′ N, 78º9′ E and 9º14′ N, 79º14′ E on the south east coast of India. The samples were washed in running water for 10 min, transported to the laboratory before being shade dried (35±3 °C) for 24 h and powdered. The shade-dried material (1 kg dry wt) was ground and extracted with ethyl acetate: methanol (EtOAc: MeOH 1:1, v/v, 60–70 °C, 3 h) before being dried over sodium sulfate and concentrated by vacuum evaporation at 50 °C (Heidolph Instruments GmbH and Co., Schwabach, Germany) to yield a dark green extract (55 g and 40 g respectively). This crude extract was subjected to various chromatographic purification techniques.

4.2.2.2. Chromatographic Purification and Spectral Analysis of Purified Compounds from *K. alvarezii*

The EtOAc: MeOH fraction (55 g) of *K. alvarezii* was fractionated by vacuum liquid chromatography (VCC) (60-120 mesh) using 100 % *n*-hexane, with increasing polarity using EtOAc and MeOH to obtain a total of three column fractions, such as KA_1 through KA_3. The bioactivities of the fractions were checked, and based on the results; these three fractions were further purified.

The fraction KA_2 was obtained by eluting with 15 % EtOAc/MeOH. The column eluent concentration was gradually raised (EtOAc: *n*-hexane 1:99 to 70:30 v/v) to obtain 30 fractions (with each 35 mL), which were combined to 13 fractions ($KA_{2\text{-}1}$-$KA_{2\text{-}13}$) after TLC analysis (EtOAc: *n*-hexane 1:9 v/v). The first fraction ($KA_{2\text{-}1}$, 600 mg) was flash chromatographed (Biotage AB SP1-B1A; Biotage, Sweden) employing a step-gradient (0-5 % EtOAc) to acquire 170 fractions (each 12 mL) that were reduced to seven groups on the basis of analytical TLC (*n*-hexane/EtOAc 3:2 v/v) ($KA_{2\text{-}1\text{-}1}$-$KA_{2\text{-}1\text{-}7}$). The fraction $KA_{2\text{-}1\text{-}1}$, on subsequent purification using preparative HPLC (60:40 MeOH/ H_2O; flow rate: 10 mL/min), yielded 2-butyl-7-4-(chloromethyl) cyclooct-1-enyl) hept-5-en-1-ol (compound **K1**) and 4-(2-chloroethyl)-5-7-(methoxymethyl) undec-3-enyl) cyclooct-4-enone (compound **K2**) as homogenous compounds.

The fraction KA_3 was column fractionated with *n*-hexane and the solvent polarity was gradually increased with the gradual addition of solvent EtOAc (3:7 v/v *n*-hexane: EtOAc) to obtain a total of thirty fractions (20 mL) that were minimized to five homogeneous groups ($KA_{3\text{-}1}$- $KA_{3\text{-}5}$), whereas $KA_{3\text{-}2}$ (320.3 mg) was fractionated with *n*-hexane: EtOAc (4:1, v/v) to yield 1-(3-methoxypropyl)-2-propylcyclohexane (compound **K3**). The fraction $KA_{3\text{-}3}$ was flash chromatographed (Biotage SP1-B1A, Sweden) on a silica gel column (loaded with 230–400 mesh) by employing a step gradient of EtOAc/*n*-hexane (0–10 % EtOAc) to yield a total of ninety fractions (10 mL). Following thin layer chromatography (TLC) analyses, the identical fractions were pooled to obtain five fractions (50 mL, $KA_{3\text{-}3\text{-}1}$- $KA_{3\text{-}3\text{-}5}$). The fraction $KA_{3\text{-}3\text{-}2}$ was flash chromatographed on a column (230–400 meshed silica gel) with EtOAc/*n*-hexane (1:9 to 3:7, v/v) to yield 3-(methoxymethyl) heptyl-3-(cyclohex-3-enyl) propanoate (compound **K4**). The fraction $KA_{3\text{-}3\text{-}4}$ was fractionated with silica gel flash chromatography with EtOAc/*n*-hexane (1:1, v/v), and thereafter with MeOH/ DCM

(1:9, v/v) to yield fifty fractions (10 mL). Following TLC analyses, the identical fractions were pooled to yield $KA_{3\text{-}3\text{-}4\text{-}1}$ through $KA_{3\text{-}3\text{-}4\text{-}11}$. The fraction $KA_{3\text{-}3\text{-}4\text{-}1}$ was further purified by preparatory silica gel TLC, whereas the plate was eluted with DCM/MeOH (9:1, v/v) to afford 2-ethyl-6-(4-methoxy-2-((2-oxotetrahydro-2*H*-pyran-4-yl) methyl) butoxy)-6-oxohexyl-5-ethyloct-4-enoate (compound **K5)**.

The fraction KA_1 was slurried in silica gel (60–120 mesh) and loaded into a glass column (90 cm × 4 cm) before being subjected to VCC on silica gel (60–120 mesh, 50 g), using *n*-hexane with increasing amounts (*n*-hexane: EtOAc 99:1 to 3:7, v/v) of EtOAc as mobile phase, and finally with MeOH to furnish 30 fractions of 35 mL each, which were reduced to 12 groups ($KA_{1\text{-}1}$-$KA_{1\text{-}12}$) after TLC analysis (*n*-hexane: EtOAc, 9:1 v/v). The fraction $KA_{1\text{-}1}$ (600 mg) obtained by eluting with *n*-hexane: EtOAc (4:1 v/v) was found to be a mixture, which was flash chromatographed (Biotage AB SP1-B1A, 230–400 mesh, 12 g; Biotage AB, Uppsala, Sweden) on a silica gel column (Biotage, 230–400 mesh, 12 g; Sweden, Biotage No. 25 + M 0489-1) at a collection UV wavelength at 236 nm using a step gradient of EtOAc/*n*-hexane (0–5 % EtOAc) to afford 170 fractions (12 mL each). Based on analytical TLC, the fractions with similar patterns were pooled together to afford nine pooled fractions (80 mL, $KA_{1\text{-}1\text{-}1}$– $KA_{1\text{-}1\text{-}9}$). The fraction $KA_{1\text{-}1\text{-}2}$ (5 % EtOAc in *n*-hexane), which was found to be a mixture, was subjected to normal-phase flash chromatography using as mobile phase EtOAc/*n*-hexane (0–70 % EtOAc) followed by MeOH/CH_2Cl_2 (10 % MeOH) to afford 70 fractions (15 mL each). Based on analytical TLC, the fractions with similar patterns were pooled together to afford 10 pooled fractions ($KA_{1\text{-}1\text{-}2\text{-}1}$ – $KA_{1\text{-}1\text{-}2\text{-}10}$). The fraction, $KA_{1\text{-}1\text{-}2\text{-}3}$ was subjected to preparatory TLC on silica gel GF_{254}, using as mobile phase $CHCl_3$/MeOH (9:1, v/v) to yield pure compound as (3, 4, 5, 6)-3-(hexan-2'-yl)-3, 4, 5, 8-tetrahydro-4-methyl-2*H*-oxocin-5-yl acetate (compound **K6**) as the major component (Fig. 4.1).

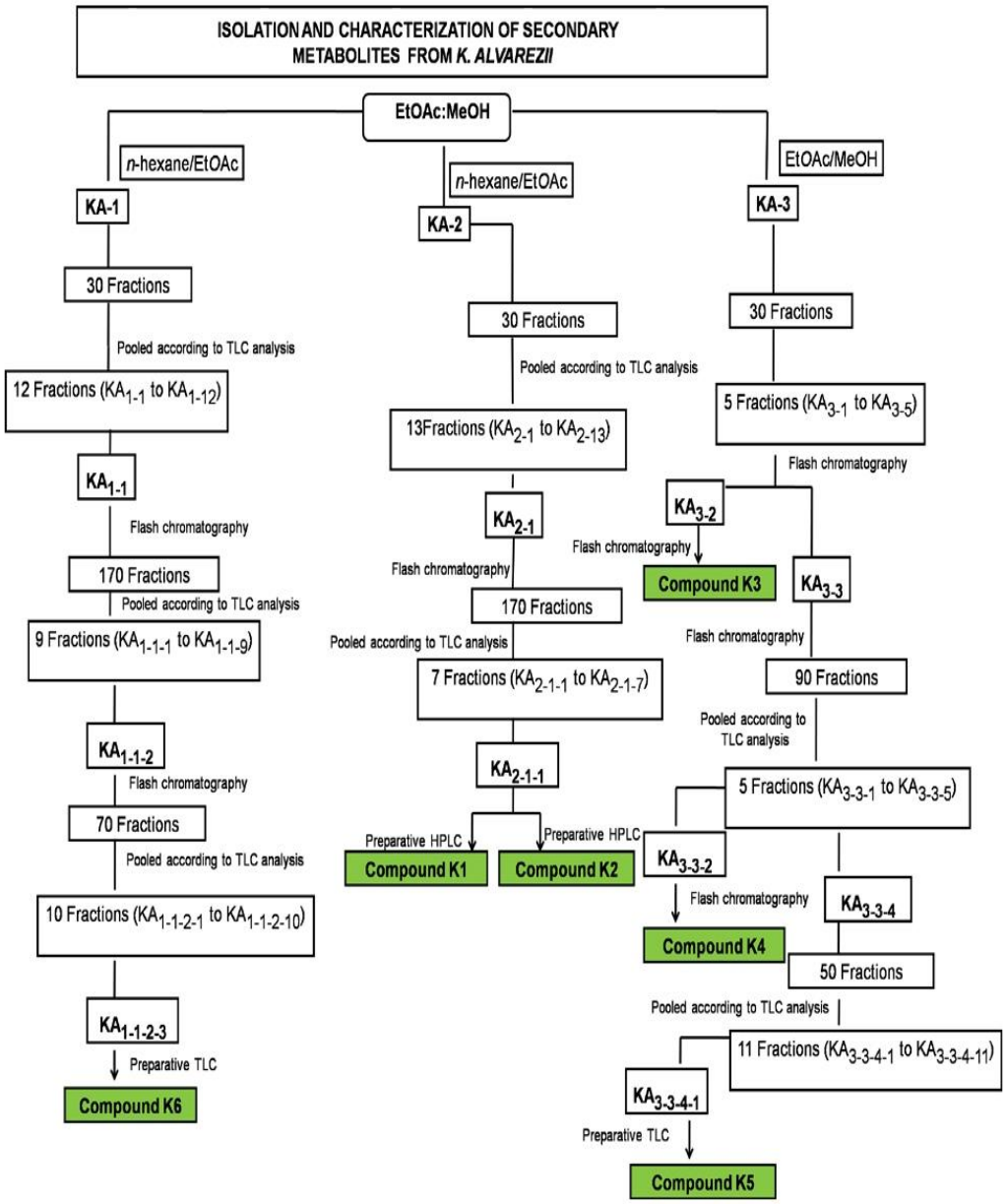

Figure 4.1. Schematic diagram representing the chromatographic purification of the EtOAc: MeOH (1:1) fraction of *K. alvarezii* (green highlights implied pure compounds with higher activity)

4.2.2.3. Chromatographic Purification and Spectral Analysis of Purified Compounds from *G. opuntia*

The EtOAc: MeOH (1:1) fraction (40 g) of *G. opuntia* was fractionated by vacuum liquid chromatography (60-120 mesh) and eluted using 100 % *n*-hexane with increasing polarity using EtOAc and MeOH to obtain a total of three column fractions, such as GO_1 through GO_3. The bioactivities of the column fractions were checked before being purified.

The fraction GO_1 was fractionated through vacuum liquid chromatography using silica gel as an adsorbent (8 g, 60–120 mesh size) on a column (90 × 4 cm), using *n*-hexane to ethyl acetate gradient solvent system (EtOAc: *n*-hexane, 1:99 to 7:3, v/v), and finally with MeOH to yield $GO_{1\text{-}1}$-$GO_{1\text{-}12}$ as twelve pooled fractions on the basis of TLC analysis (EtOAc: *n*-hexane 1:4, v/v). The fraction $GO_{1\text{-}2}$ (500 mg) was recovered by eluting with EtOAc: *n*-hexane (1:2, v/v), and was further fractionated by flash chromatography (Biotage SP1, 230–400 mesh, 12 g) on a Biotage No. 25+M 0489-1 column (silica gel 230–400 mesh, Biotage, Sweden) with a collection wavelength (UV) at 236 nm, and with the solvent gradient of CH_2Cl_2-MeOH (0–100 % MeOH) to furnish 145 fractions (15 mL). Similar fractions were mixed together to afford nine pooled fractions ($GO_{1\text{-}2\text{-}1}$-$GO_{1\text{-}2\text{-}9}$) after TLC analysis (10 % EtOAc in *n*-hexane). The fraction $GO_{1\text{-}2\text{-}4}$ was found to be a mixture, and was further purified with normal phase flash chromatography by using EtOAc/*n*-hexane (0–70 % EtOAc) as mobile phase, followed by MeOH/ EtOAc (15 % MeOH) to yield $GO_{1\text{-}2\text{-}4\text{-}1}$-$GO_{1\text{-}2\text{-}4\text{-}10}$ as ten pooled fractions based on TLC analysis (EtOAc: *n*-hexane 1:9, v/v). The sub-fraction $GO_{1\text{-}2\text{-}4\text{-}2}$ (145 mg), was a mixture of compounds, and therefore, was fractionated with preparatory thin layer chromatography (silica gel GF_{254}) using a step-wise gradient system of EtOAc/MeOH (9:1, v/v) to afford 5-(7-(5-ethyl-3, 4-dimethoxycyclooctyl) benzofuran-6-yl)-7-methyl-3, 4, 7, 8-tetrahydro-2*H*-oxocin-2-one as a homogenous compound (compound **G1**). The fraction, $GO_{1\text{-}2\text{-}4\text{-}8}$ was further purified by preparatory TLC on silica gel GF_{254} by using MeOH/EtOAc (3:7, v/v) as mobile phase to yield 2-(3-ethyl-9-(2-methoxyethoxy)-1-oxo-2, 3, 4, 9-tetrahydro-1*H*-xanthen-2-yl) ethyl-5-hydroxy-9-methoxy-7, 8-dimethyl-8-(5-methylfuran-2-yl) nona-3, 6-dienoate (compound **G2**) as the major component.

The fraction 2 (GO_2, 200 mg) was acquired by eluting with EtOAc: *n*-hexane (1:4, v/v) was found to be a mixture that was subjected to further purification with flash

chromatography (Biotage AB, Biotage AB SP1-B1A Uppsala, Sweden) on a silica gel column (Biotage, 230–400 mesh, 12 g; Sweden, 25 + M0489–1) at a collection UV wavelength at 236 nm using a step gradient of EtOAc/*n*-hexane (0–50 % EtOAc) to afford 160 fractions (9 mL each). On the basis of analytical TLC, the fractions with identical patterns were pooled together to yield five pooled fractions ($GO_{2\text{-}1}$ through $GO_{2\text{-}5}$). The fraction $GO_{2\text{-}3}$ was fractionated using preparatory TLC on silica gel GF_{254} using methanol: ethyl acetate (1:4, v/v) to afford 3-(2-ethyl-6-((3, 7)-1, 2, 5, 6-tetrahydroazocin-5-yl) hexyl) morpholin-6-one (compound **G3**) as the major component.

The fraction 3 (GO_3) acquired by eluting with EtOAc: *n*-hexane (1:4, v/v) was found to be a mixture. The latter was subjected to column chromatography on silica gel (6 g, 60–120 mesh) with a solvent gradient from *n*-hexane to EtOAc followed by EtOAc to MeOH. A total of 20 fractions (25 mL each) were further fractionated with 50 % EtOAc in *n*-hexane on a silica gel flash chromatograph (Biotage AB SP1-B1A, 230–400 mesh, 12 g; Biotage AB, Uppsala, Sweden) at a collection UV wavelength of 236 nm using a step gradient of MeOH/ EtOAc (0–5 % EtOAc) to afford 150 fractions (10 mL each). Based on analytical TLC, the fractions with similar patterns were pooled together to afford five pooled fractions ($GO_{3\text{-}1}$- $GO_{3\text{-}5}$, 60 mL each). The fraction $GO_{3\text{-}5}$ eluted with 5 % EtOAc in *n*-hexane, was found to be a mixture, and therefore, was further subjected to normal-phase silica gel flash chromatography using 0–30 % EtOAc followed by 10 % MeOH in EtOAc to yield 40 fractions (15 mL each). Based on analytical TLC, the fractions with similar patterns were pooled together to afford five pooled fractions ($GO_{3\text{-}5\text{-}1}$ through $GO_{3\text{-}5\text{-}5}$). The fraction $GO_{3\text{-}5\text{-}3}$, was subjected to preparatory TLC on silica gel GF_{254}, using as mobile phase MeOH/ EtOAc (1:1, v/v) to yield 2-acetoxy-2-(5-acetoxy-4-methyl-2-oxotetrahydro-2*H*-pyran-4-yl) ethyl-4-(3-methoxy-2-(methoxymethyl)-7-methyl-3, 4, 4a, 7, 8, 8a-hexahydro-2*H*-chromen-4-yloxy)-5-methylheptanoate (compound **G4**) as the major component (Fig. 4.2).

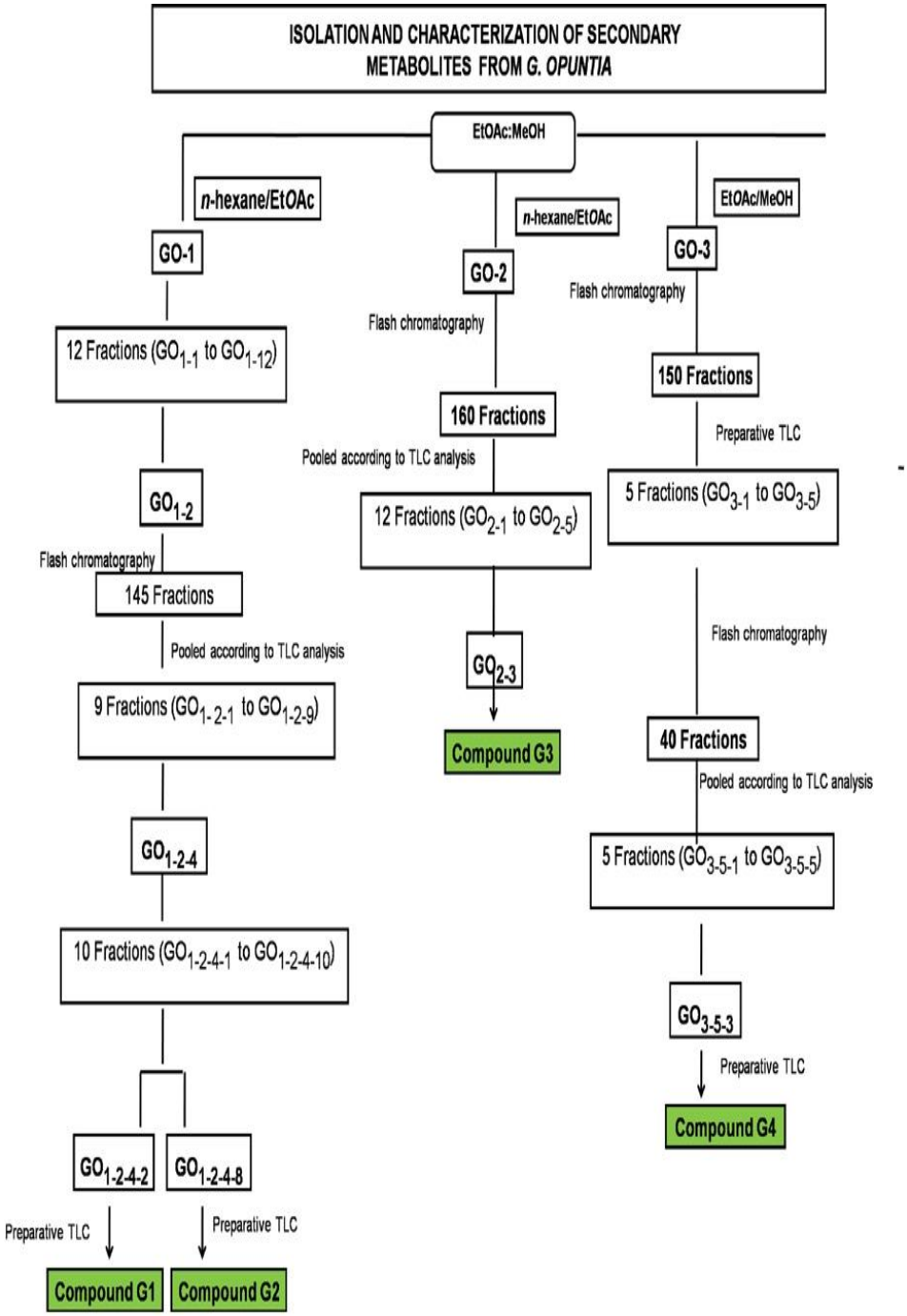

Figure 4.2. Schematic diagram representing the chromatographic purification of the EtOAc: MeOH (1:1) fraction of *G. opuntia* (green highlights implied the pure compounds with higher activity)

4.2.3. Instrumentation

FTIR spectra of the compounds under KBr pellets were recorded in a Thermo Nicolet Avatar 370 in the IR range between 4000 and 400 cm^{-1}. UV spectra were obtained on a Varian Cary 50 ultraviolet visible (UV–VIS) spectrometer (Varian Cary, USA). The gas chromatography–mass spectrometry (GC-MS) analyses were performed in electronic impact (EI) ionization mode in a PerkinElmer Clarus 680. GC-MS fitted with an Elite 5 MS non-polar, bonded phase capillary column (50 m × 0.22 mm i.d. × 0.25 μm film thicknesses). Helium (He) was used as the carrier gas, and the flow rate used was 1 mL min^{-1}. The temperature was programmed initially at 50 ° C for 2 min, then increased at a rate of 10 ° C min^{-1} to 180 °C and kept for 2 min and raised at 4° C min^{-1} to 280 °C and held for 15 min. Thin layer chromatographic analysis was carried out using silica gel GF_{254} plates and visualized with a documentation system operating at 254 and 366 nm wavelength regions. ESI-MS spectra were acquired on a liquid chromatography–mass spectrometry system (Applied Biosystems QTrap 2000, Applied Biosystems, Darmstadt, Germany). A table-top high speed refrigerated centrifuge (Sorvall, Biofuge Stratos, Thermo Scientific, Germany) was used for centrifugation. Flash chromatography was carried out with a Biotage instrument (AB SP1-B1A, Biotage AB, Uppsala, Sweden). High pressure liquid chromatographic analysis was carried out using high performance liquid chromatograph (Shimadzu SCL-10A vp, Shimadzu Co., Kyoto, Japan) equipped with a vacuum degasser, a binary pump (LC–20AD), a thermostated column compartment (CTO–20A) and a diode array detector (SPD–M20A), connected to an LC solution software. Chromatographic separation was carried out at 30 °C on a reverse phase Luna C_{18} (250 mm x 4.6 mm, 5 μm) phenomenex column. The ultra sonicator (Labline) was used for sonicating and a laboratory shaker (Shaker, Labline) was used for shaking. A rotary vacuum evaporator (Heidolf, Germany) was used for evaporation of solvents. ^{1}H and ^{13}C NMR spectra were recorded on a Bruker AVANCE III 500 MHz (AV 500) spectrometer (Bruker, Germany) in $CDCl_3$ as aprotic solvent at ambient temperature with TMS as the internal standard (δ 0 ppm). Two-dimensional ^{1}H-^{1}H COSY, DEPT, HSQC, HMBC and NOESY experiments were carried out using standard pulse sequences. The NMR data were acquired by using the BrukerTopSpin™ 2 software, and processed by MestReNova-7.1.1-9649 (Mestrelab Research S.L.). All the reagents and solvents used in this study were of analytical grade and purchased from E-Merck.

4.2.4. Pharmacological Activities of Secondary Metabolites Isolated from *K. alvarezii* and *G. opuntia*

The pharmacological activities of the compounds were determined based on the *in vitro* assays performed as explained in the previous chapter (Chapter 3). The *in vitro* antioxidant activities were determined by ABTS, DPPH radical scavenging assays along with ferrous ion chelating assay (Sivasothy et al. 2012; Chakraborty et al. 2014). The anti-inflammatory properties were evaluated by COX-1 and COX-2 inhibition assays (Larsen et al. 1996) and 5-LOX inhibition assay (Baylac and Racine 2003). *In vitro* anti-diabetic studies were carried out by inhibition of dipeptidyl peptidase-4, α-amylase (Kojima et al. 1980; Hamdan and Afifi 2004) and α-glucosidase (Dong et al. 2012) inhibition assays. The anti-hypertensive activities were determined by ACE-I inhibitory assay (Udenigwe et al. 2009).

Structure-biactivity relationship analyses have been conducted by different structural descriptors, such as electronic (polarizability α/topological polar surface area tPSA), hydrophobic–hydrophilic balance {logarithm (octanol/water partition coefficient) or log Pow), steric {parachor (Pr)/molar volume (Vm)/molar refractivity (MR)} (Chakraborty et al. 2016a, b; Joy and Chakraborty 2017a, b; Lipinski and Hopkins 2004) using ACD ChemSketch (Advanced Chemistry Development, Inc., Canada; ver. 12.0) and ChemDraw® Ultra (Cambridge Soft Corporation, Cambridge, MA, USA; ver. 8.0) softwares.

4.2.5. Statistical Analysis

One-way analysis of variance was carried out with the Statistical Program for Social Sciences 13.0 (SPSS, Inc., Chicago, USA, ver. 13.0) to assess for any significant differences between the means. The analyses were performed in triplicates, and the means of all variables were analyzed for significance by using analysis of variance. Differences between means at the 5 % ($P < 0.05$) level were considered significant.

4.3. Results and Discussion

4.3.1. Secondary Metabolites from *K. alvarezii*

4.3.1.1. Structural Characterization of Compound K1

2-Butyl-7-4-(chloromethyl) cyclooct-1-enyl) hept-5-en-1-ol (**K1**)

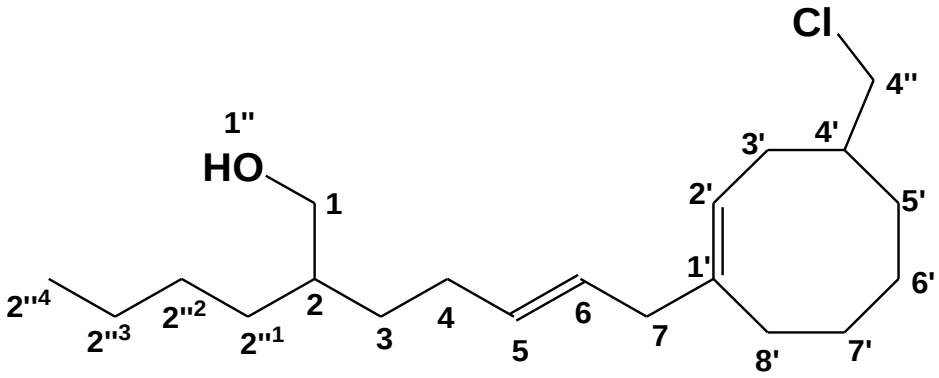

Sample yield	92 mg (0.92 %)
Physical description	White powder
Molecular formula	$C_{20}H_{35}ClO$
Molecular weight	326.2380

2-Butyl-7-4-(chloromethyl) cyclooct-1-enyl) hept-5-en-1-ol: White powder; UV (MeOH: EtOAc) λ_{max} (log ε): 285 nm (3.23); R_f: 0.62 (*n*-hexane: EtOAc 7:3, v/v); R_t (HPLC, ACN: MeOH, 2:3 v/v): 12.62 min; IR (KBr, cm^{-1}) ν_{max} (ν = stretching, δ= bending, ρ= rocking vibrations); 724.78 (CH_2 ρ), 979.37 (=C-H δ), 1252.02 (C-O ν), 1457.39 (C-H δ), 2857.37 (C-H ν), 2925.80 (C-H ν), 3430.23 (broad OH ν); ^{1}H NMR (500 MHz, $CDCl_3$) δ_H 5.39 (m, 2H), δ_H 5.37 (m, 1H), δ_H 3.74 (d, *J*=6.55 Hz, 2H), δ_H 3.67 (s, 1H), δ_H 3.61 (d, *J*=7.60 Hz, 2H), δ_H 3.27 (d, *J*=7.2 Hz, 2H), δ_H 2.81 (m, 2H), δ_H 2.35 (t, *J*=6.1 Hz, 2H), δ_H 2.13 (t, *J*=6.0 Hz, 2H), δ_H 2.05 (m, 1H), δ_H 1.72 (m, 1H), δ_H 1.63 (m, 2H), δ_H 1.30 (m, 6H), δ_H 1.25 (m, 6H), δ_H 0.88 (t, *J*=6.75 Hz, 3H); ^{13}C NMR (125 MHz, $CDCl_3$): δ_C 146.84 (C-1'), δ_C 130.51 (C-5), δ_C 128.77 (C-6), δ_C 128.58 (C-2'), δ_C 70.59 (C-1), δ_C 51.76 (C-4''), δ_C 44.88 (C-7), δ_C 38.19 (C-4'), δ_C 38.16 (C-2), δ_C

34.3 (C-3'), δ_C 34.06 (C-3), δ_C 33.63 (C-8'), δ_C 31.93 (C-5'), δ_C 31.52 (C-2''^{1}), δ_C 30.2 (C-4), δ_C 29.5 (C-2''^{2}), δ_C 29.33 (C-7'), δ_C 27.23 (C-6'), δ_C 22.58 (C-2''^{3}), δ_C 14.07 (C 2''^{4}).^{1}H-^{1}H-COSY and HMBC data (Fig. 4.3 to Fig. 4.11, Table 4.1); High-resolution electron ionization mass spectroscopy HR (EI) MS calcd for $C_{20}H_{35}ClO$ at *m/z* 326.2376, found 326.2380 $[M]^+$.

Table 4.1 NMR spectroscopic data of compound **K1** in $CDCl_3$[a]

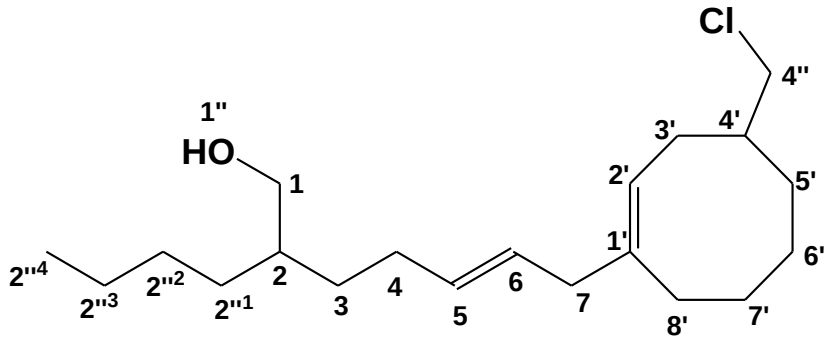

C. No	^{13}C (δ)	^{1}H-NMR[b] (int., mult., *J* in Hz)	^{1}H-^{1}H COSY	HMBC (^{1}H-^{13}C)
1	70.59	3.61 (2H, d, *J*=7.60 Hz)	-	-
1"		3.67 (1H, s)		
2	38.16	1.72 (1H, m)	-	C-2''^{1}
2''^{1}	31.52	1.25 (2H, m)		C-2''^{2}, C-2''^{3}
2''^{2}	29.5	1.25 (2H, m)		-
2''^{3}	22.58	1.30 (2H, m)		-
2''^{4}	14.07	0.88 (3H, t, *J*=6.75 Hz)		C-2''^{2}, C-2''^{3}
3	34.06	1.30 (2H, m)	-	-
4	30.2	2.81 (2H, m)	5-H	C-6
5	130.51	5.37 (1H, m)	4-H	-
6	128.77	5.39 (1H, m)	-	-
7	44.88	3.27 (2H, d, *J*=7.2 Hz)	-	C-1', C-5
1'	146.84	-	-	-
2'	128.58	5.39 (1H, m)	3'-H	-
3'	34.3	2.13 (2H, t, *J*=6.0 Hz)	2'-H	-
4'	38.19	2.05 (1H, m)	-	C-3'
4"	51.76	3.74 (2H, d, *J*=6.55 Hz)		
5'	31.93	1.30 (2H, m)	-	C-7'
6'	27.23	1.25 (2H, m)	-	-
7'	29.33	1.63 (2H, m)	8'-H	-
8'	33.63	2.35 (2H, t, *J*=6.1 Hz)	7'-H	C-7', C-6'

[a] NMR spectra recorded using Bruker AVANCE III 500 MHz (AV 500) spectrometer in $CDCl_3$ as aprotic solvent at ambient temperature with TMS as the internal standard (δ 0 ppm).

[b] Values in ppm, multiplicity and coupling constants (*J*=Hz) are indicated in parentheses. The assignments were made with the aid of the ^1H-^1H COSY, HSQC, HMBC and NOESY experiment

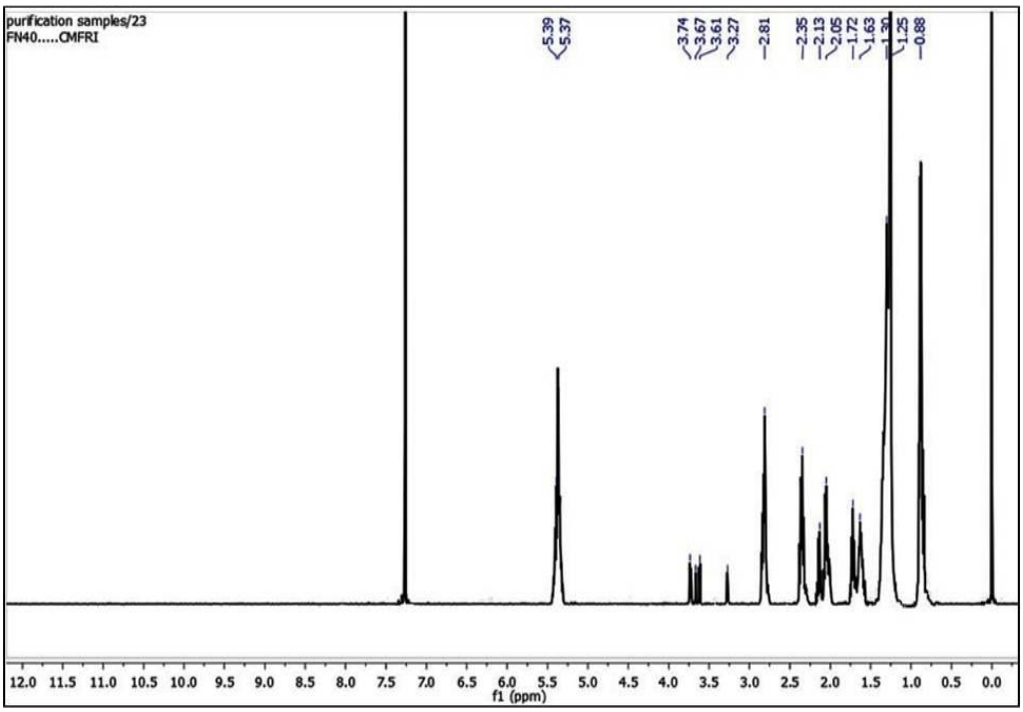

Figure 4.3. Figure showing the ^1H NMR spectrum of compound **K1**

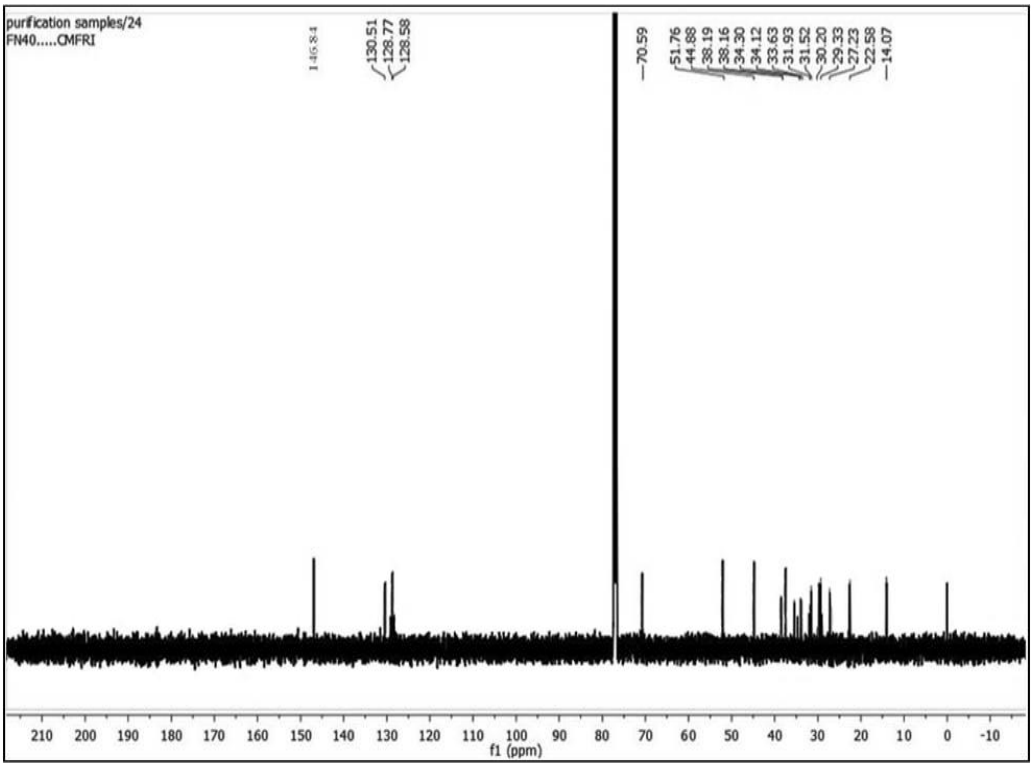

Figure 4.4. Figure showing the ^{13}C NMR spectrum of compound **K1**

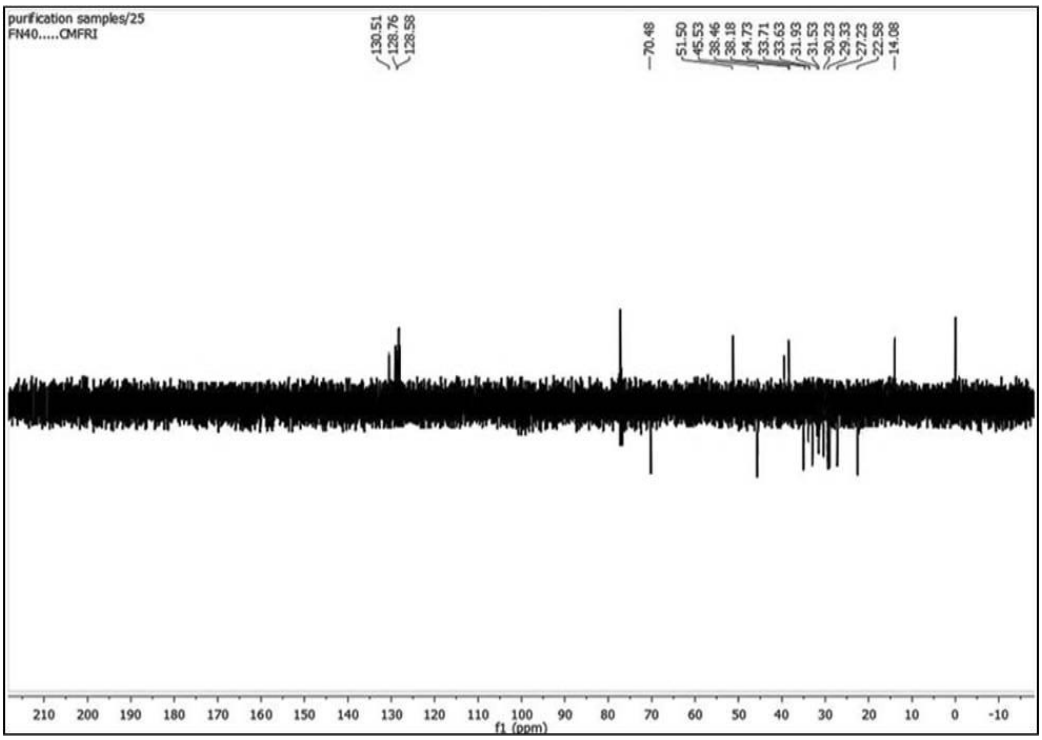

Figure 4.5. Figure showing the DEPT spectrum of compound **K1**

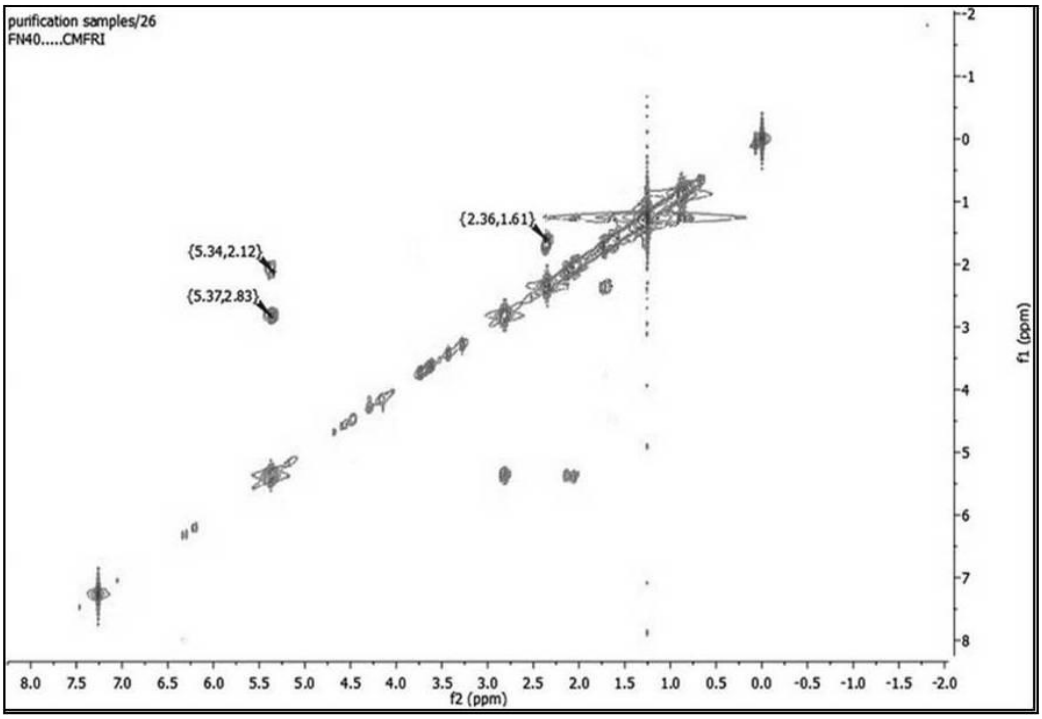

Figure 4.6. Figure showing the ^{1}H-^{1}H COSY spectrum of compound **K1**

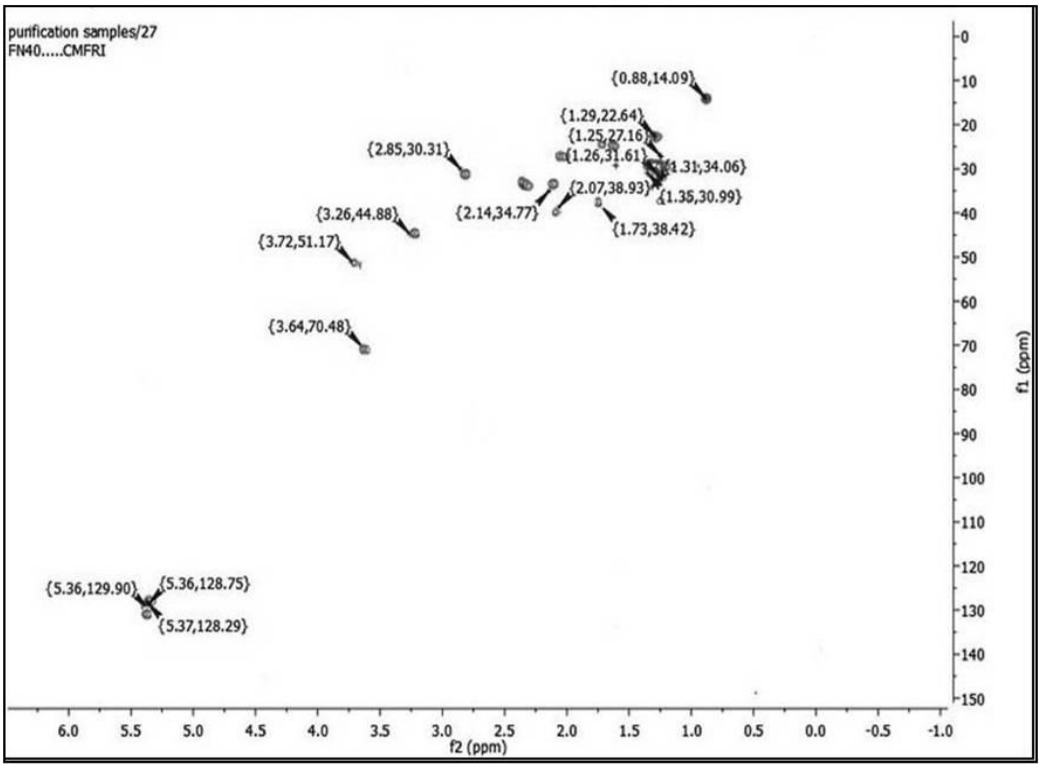

Figure 4.7. Figure showing the HSQC spectrum of compound **K1**

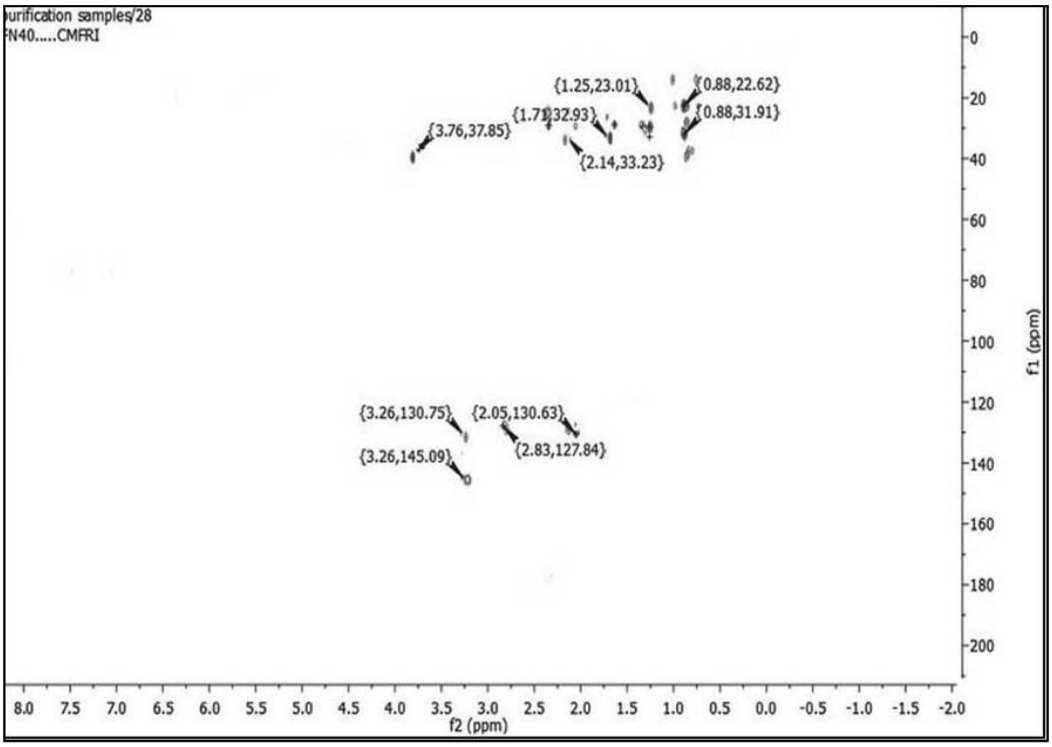

Figure 4.8. Figure showing the HMBC spectrum of compound **K1**

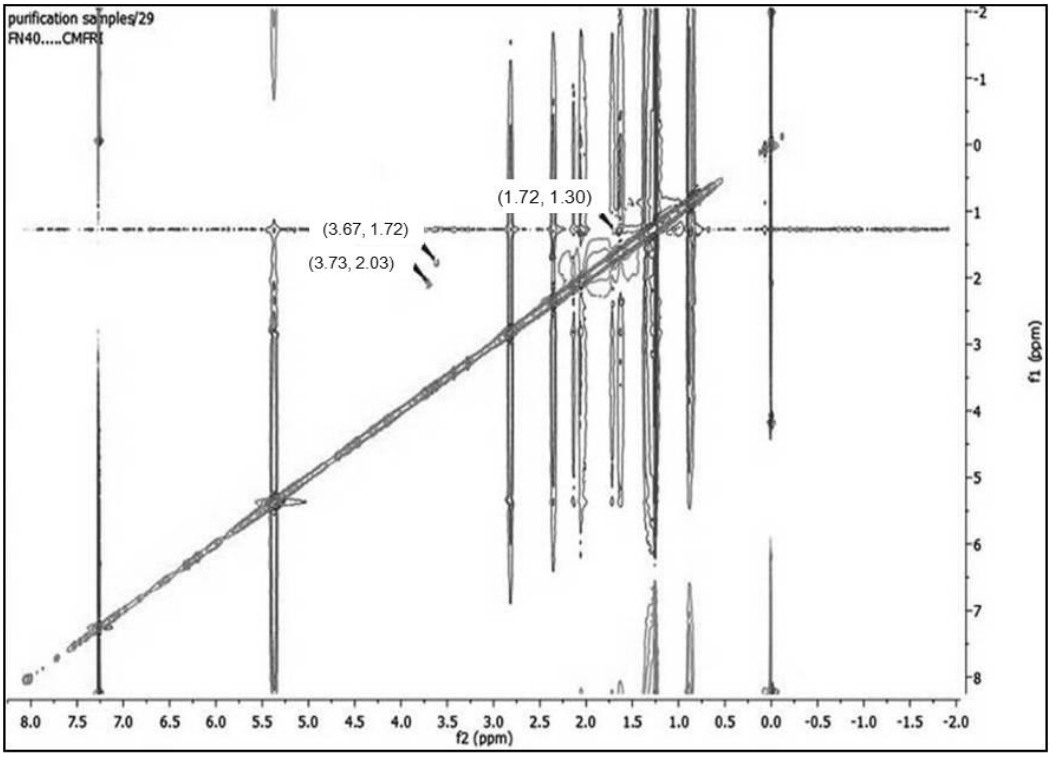

Figure 4.9. Figure showing the NOESY spectrum of compound **K1**

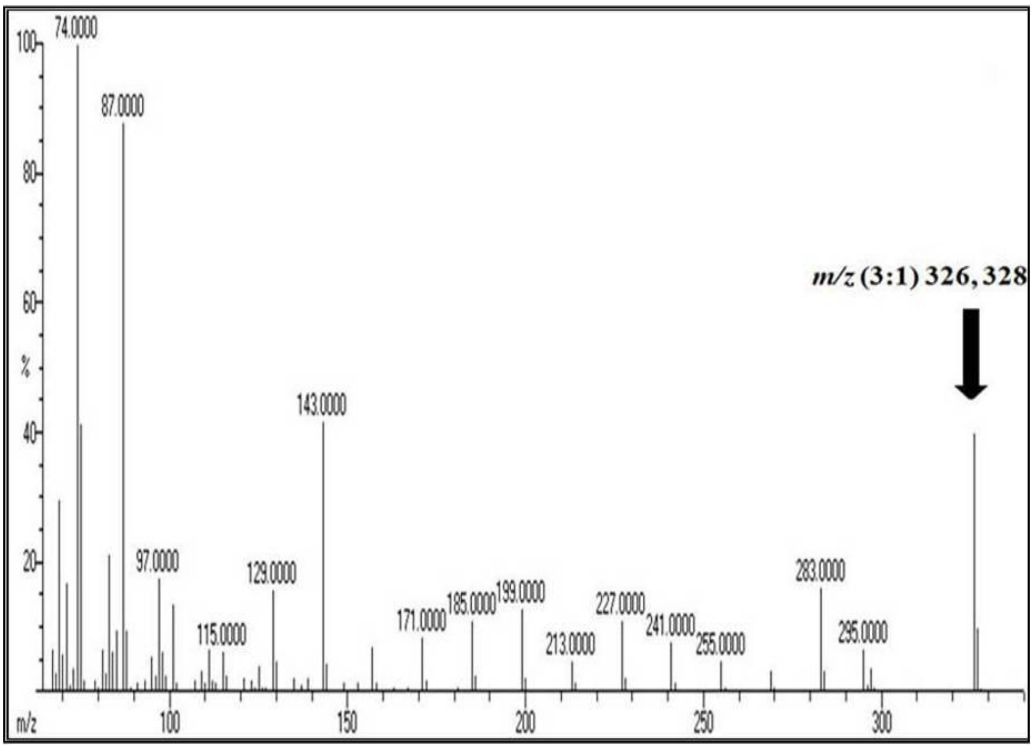

Figure 4.10. Mass spectrum of compound **K1**

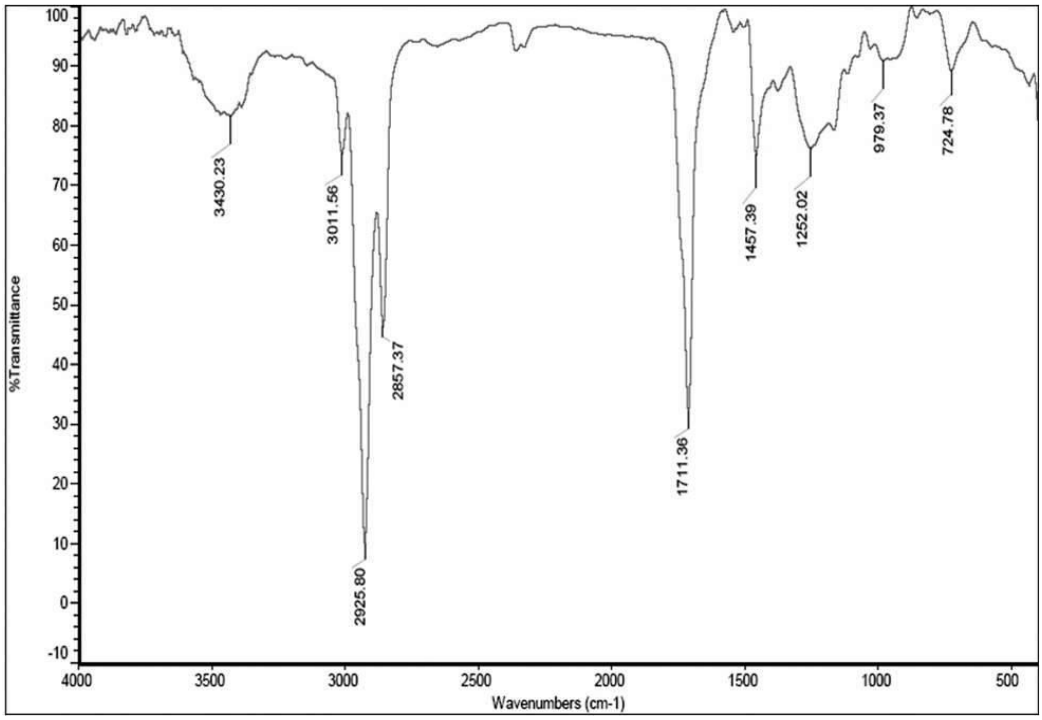

Figure 4.11. Figure showing the FTIR spectrum of compound **K1**

4.3.1.2. Structural Characterization of Compound K2

4-(2-Chloroethyl)-5-7-(methoxymethyl) undec-3-enyl) cyclooct-4-enone (**K2**)

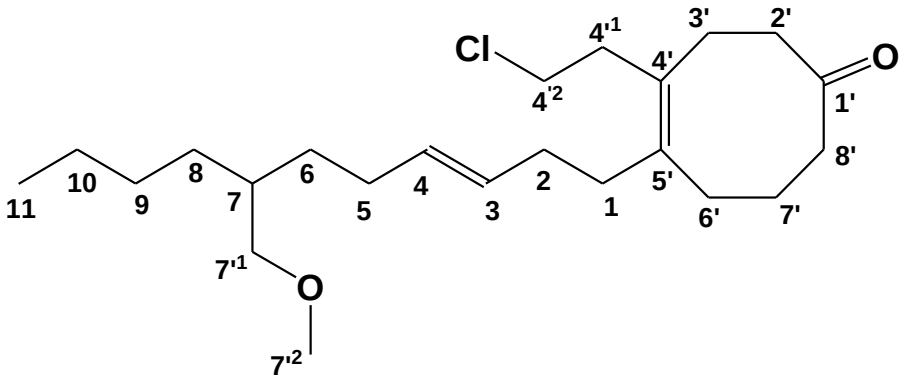

Sample yield	69 mg (0.69 %)
Physical description	Yellow oil
Molecular formula	$C_{23}H_{39}ClO_2$
Molecular weight	382.2641

4-(2-Chloroethyl)-5-7-(methoxymethyl) undec-3-enyl) cyclooct-4-enone: Yellow oil; UV (MeOH: EtOAc) λ_{max} (log ε): 290 nm (2.44); R_f: 0.57 (*n*-hexane: EtOAc 7:3, v/v); R_t (HPLC, ACN: MeOH, 2:3 v/v): 14.42 min; IR (KBr, cm^{-1}) ν_{max} (ν = stretching, δ= bending, ρ= rocking vibrations): 744.08 (C-Cl ν), 950.25 (=C-H δ), 1127.77 (CH_2 wag), 1284.33 (CH_2 ν), 1380.79 (CH_3 ν), 1457.32 (C-H δ), 1727.88 (C-CO-C ν), 2870.08 (C-H ν), 2961.87 (C-H ν), 3434.44 (broad OH ν); ^{1}H NMR (500 MHz, $CDCl_3$) δ_H 5.35 (m, 1H), δ_H 5.34 (m, 1H), δ_H 4.29 (d, *J*=7.46 Hz, 2H), δ_H 4.15 (t, *J*=7.50 Hz, 2H), δ_H 3.67 (s, 3H), δ_H 2.77 (t, *J*=6.65 Hz, 2H), δ_H 2.30 (t, *J*=6.1 Hz, 6H), δ_H 2.06 (t, *J*=6.0 Hz, 4H), δ_H 2.00 (m, 4H), δ_H 1.62 (m, 2H), δ_H 1.73 (m, 1H), δ_H 1.58 (m, 2H), δ_H 1.33 (m, 2H), δ_H 1.30 (m, 2H), δ_H 1.25 (m, 2H), δ_H 0.87 (t, *J*=6.70 Hz, 3H); ^{13}C NMR (125 MHz, $CDCl_3$): δ_C 209 (C-1'), δ_C 147.07 (C-4'), δ_C 139.28 (C-5'), δ_C 130 (C-4), δ_C 129.68 (C-3), δ_C 80.95 (C-7'^{1}), δ_C 62.11 (C-4'^{2}), δ_C 51.44 (C-7'^{2}), δ_C 41.5 (C-2'), δ_C 40.19 (C-8'), δ_C 38.86 (C-7), δ_C 34.13 (C-6), δ_C 33.83 (C-4'^{1}), δ_C 32.74 (C-2), δ_C 31.93 (C-1), δ_C 31.44 (C-5), δ_C 30.2 (C-8), δ_C 29.7 (C-6'), δ_C 29.6 (C-9), δ_C 29.37 (C-3'), δ_C 27.19 (C-7'), δ_C 22.7 (C-10), δ_C 14.11 (C-11). ^{1}H-^{1}H-COSY and HMBC data

(Fig. 4.12 to Fig. 4.20, Table 4.2); HR (EI) MS calcd for $C_{23}H_{39}ClO_2$ at *m/z* 382.2639, found 382.2641 $[M]^+$.

Table 4.2 NMR spectroscopic data of compound **K2** in $CDCl_3$[a]

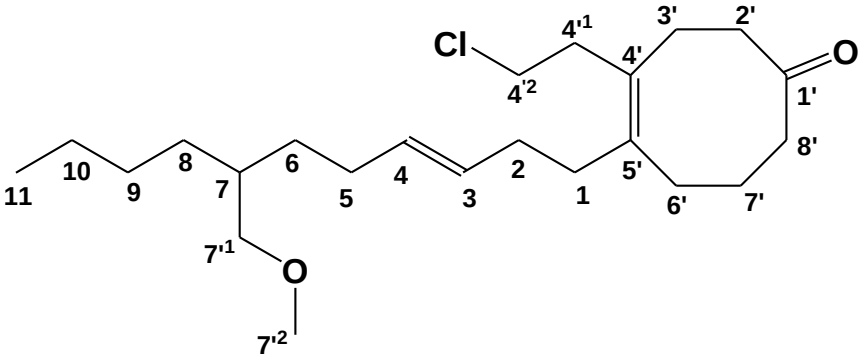

C. No	^{13}C (δ)	^{1}H-NMR[b] (int., mult., *J* in Hz)	^{1}H-^{1}H COSY	HMBC (^{1}H-^{13}C)
1	31.93	2.06 (2H, t, *J*=6.0 Hz)	-	C-2, C-5', C-6', C-4'
2	32.74	2.00 (2H, m)	-	-
3	129.68	5.34 (1H, m)	-	C-4, C-2'
4	130	5.35 (1H, m)	5-H	-
5	31.44	2.00 (2H, m)	4-H	C-4
6	34.13	1.58 (2H, m)	-	-
7	38.86	1.73 (1H, m)	-	C-6, C-5
7'[1]	80.95	4.29 (2H, d, *J*=7.46 Hz)	-	-
7'[2]	51.44	3.67 (3H, s)	-	C-7'[1]
8	30.2	1.30 (2H, m)	-	C-10, C-7
9	29.6	1.25 (2H, m)	-	C-10, C-7
10	22.7	1.33 (2H, m)	-	C-11, C-9, C-8
11	14.12	0.87 (3H, t, *J*=6.70 Hz)	-	C-10
1'	209	-	-	-
2'	41.5	2.77 (2H, t, *J*=6.65 Hz)	-	C-4'
3'	29.37	2.30 (2H, t, *J*=6.1 Hz)	-	C-2', C-4'[1]
4'	147.07	-	-	-
4'[1]	33.83	2.30 (2H, t, *J*=6.1 Hz)	-	-
4'[2]	62.11	4.15 (2H, t, *J*=7.50 Hz)		C-4'
5'	139.28	-	-	-
6'	29.7	2.06 (2H, t, *J*=6.0 Hz)	-	-
7'	27.19	1.62 (2H, m)	8'-H	C-1', C-6'
8'	40.19	2.30 (2H, t, *J*=6.1 Hz)	7'-H	C-1'

[a] NMR spectra recorded using Bruker AVANCE III 500 MHz (AV 500) spectrometer in $CDCl_3$ as aprotic solvent at ambient temperature with TMS as the internal standard (δ 0 ppm).

[b] Values in ppm, multiplicity and coupling constants (*J*=Hz) are indicated in parentheses. The assignments were made with the aid of the ^1H-^1H COSY, HSQC, HMBC and NOESY experiment

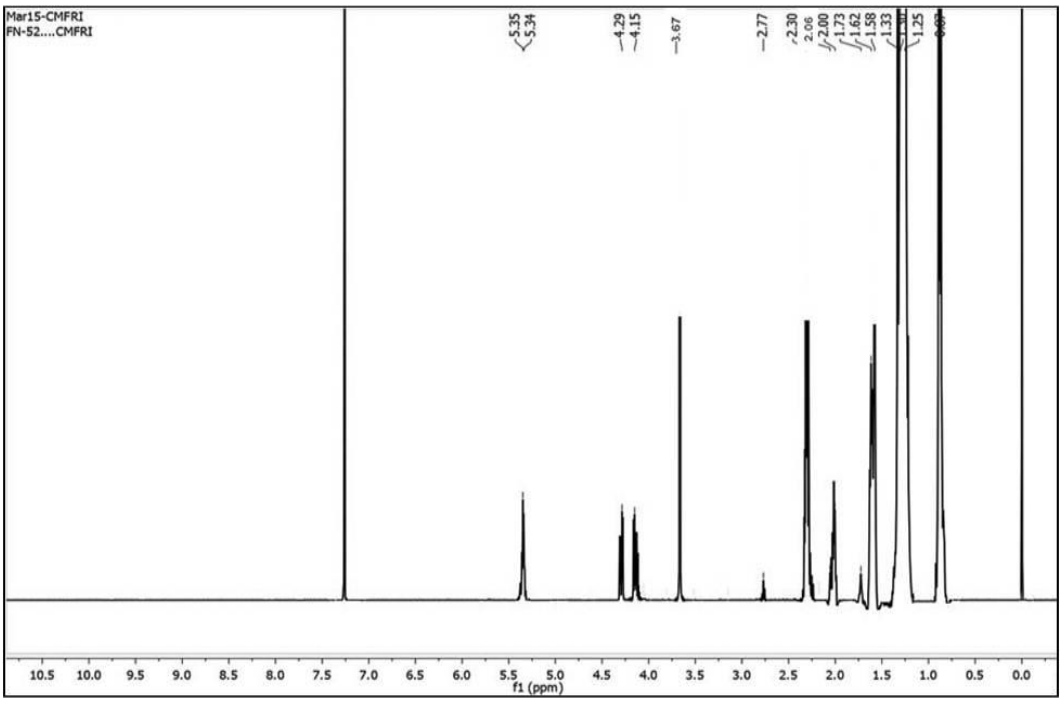

Figure 4.12. Figure showing the ^1H NMR spectrum of compound **K2**

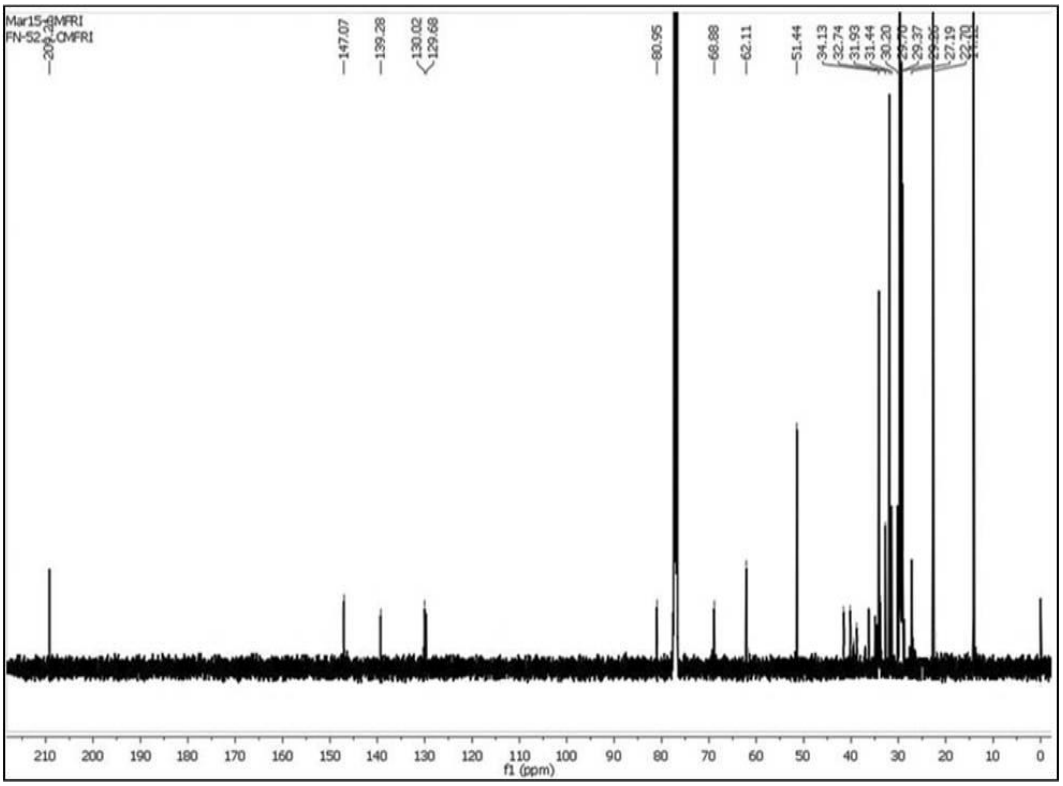

Figure 4.13. Figure showing the ^{13}C NMR spectrum of compound **K2**

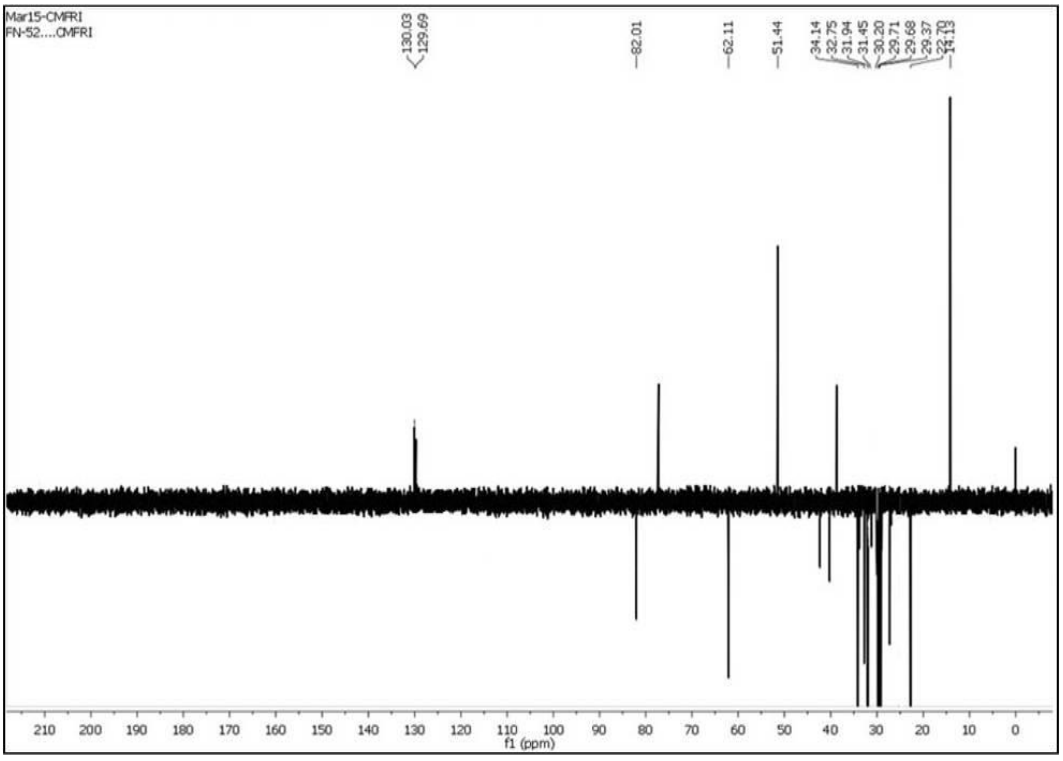

Figure 4.14. Figure showing the DEPT spectrum of compound **K2**

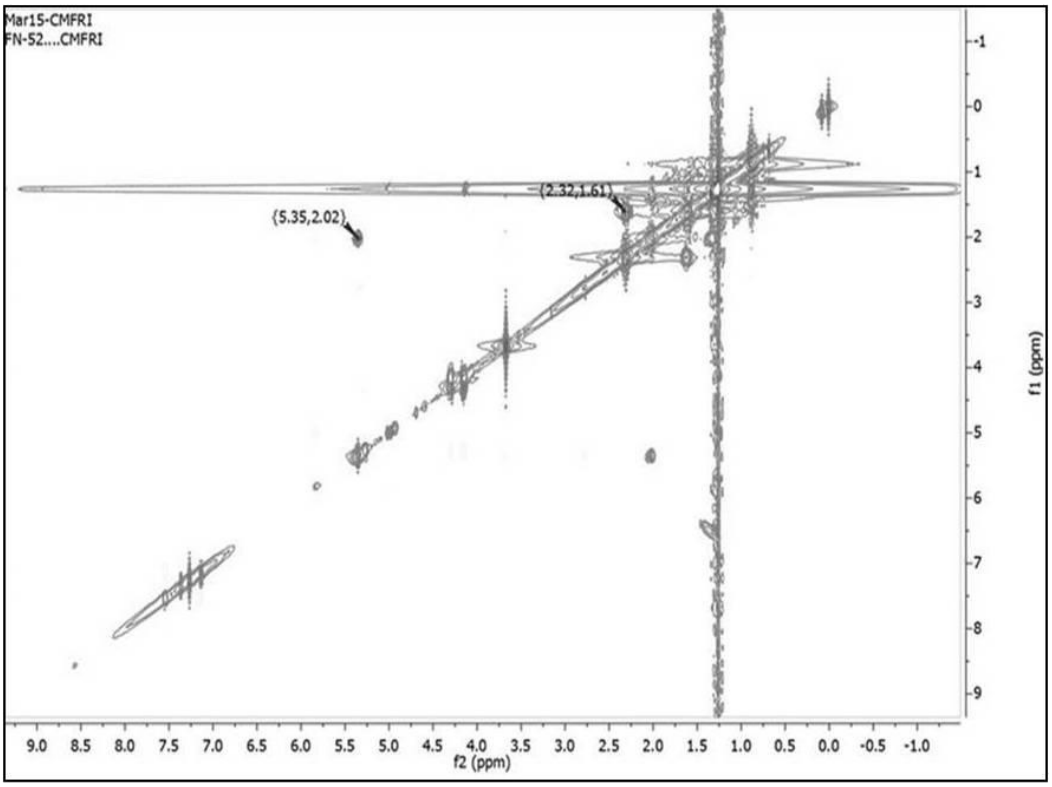

Figure 4.15. Figure showing the ^{1}H-^{1}H COSY spectrum of compound **K2**

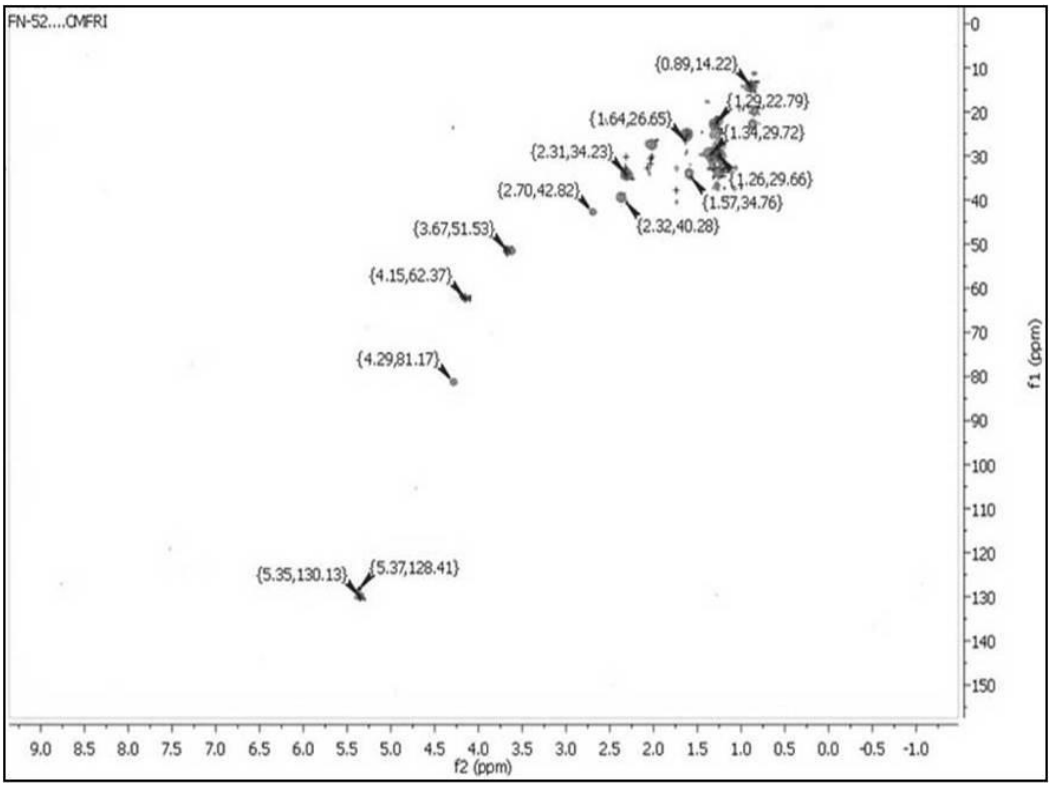

Figure 4.16. Figure showing the HSQC spectrum of compound **K2**

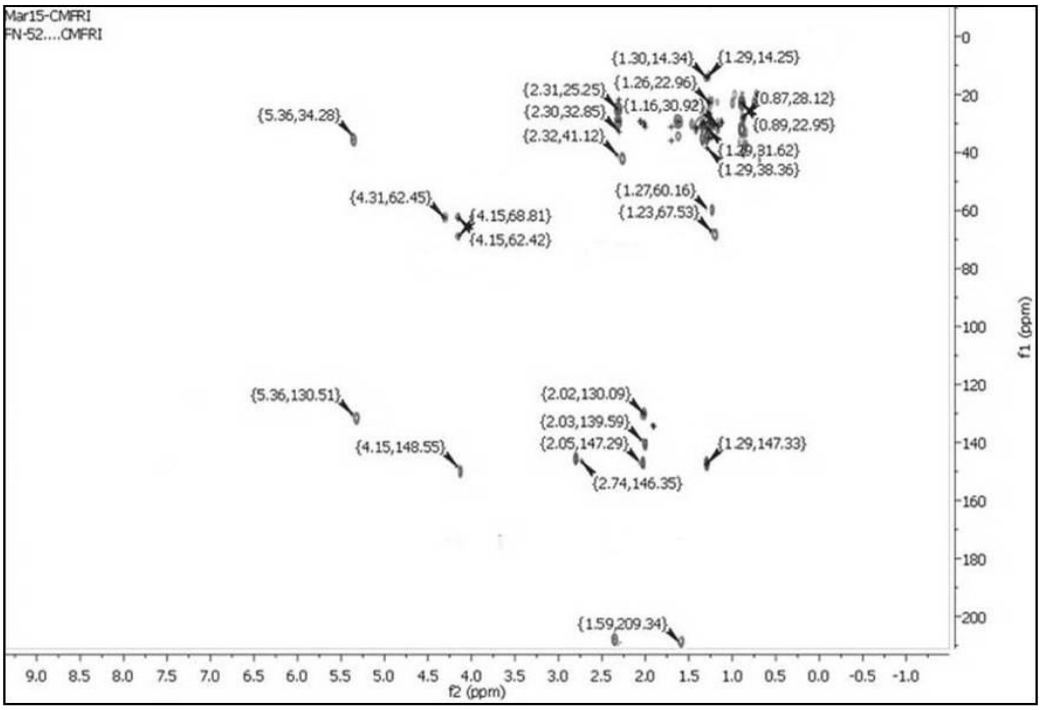

Figure 4.17. Figure showing the HMBC spectrum of compound **K2**

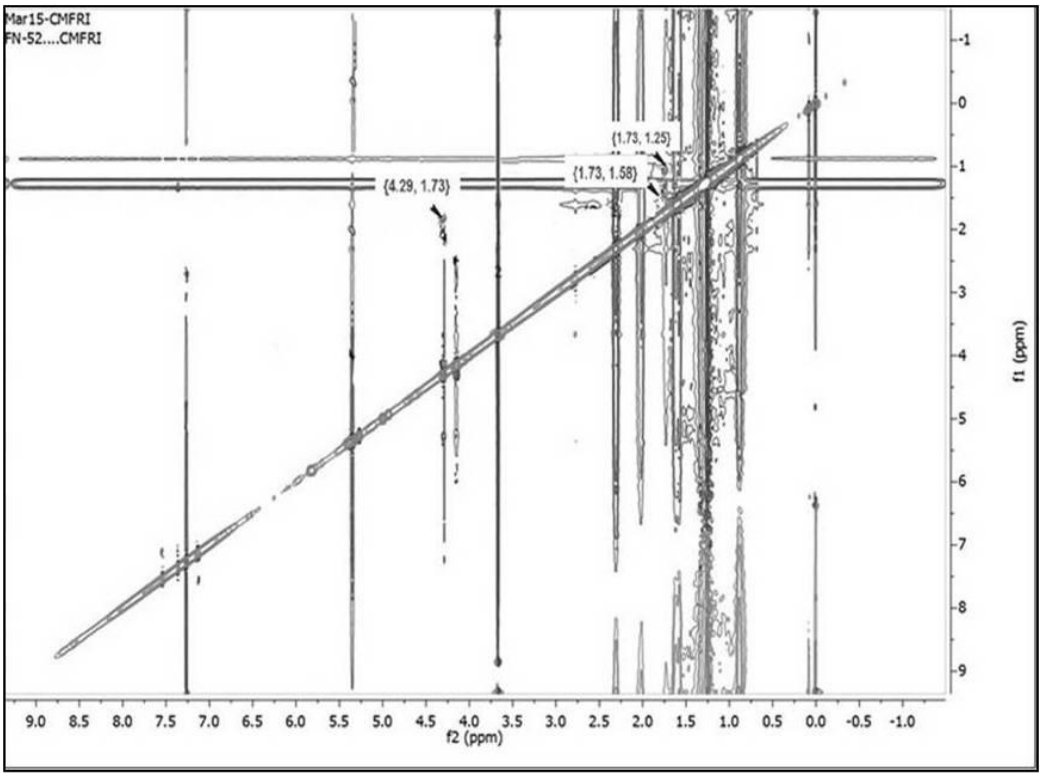

Figure 4.18. Figure showing the NOESY spectrum of compound **K2**

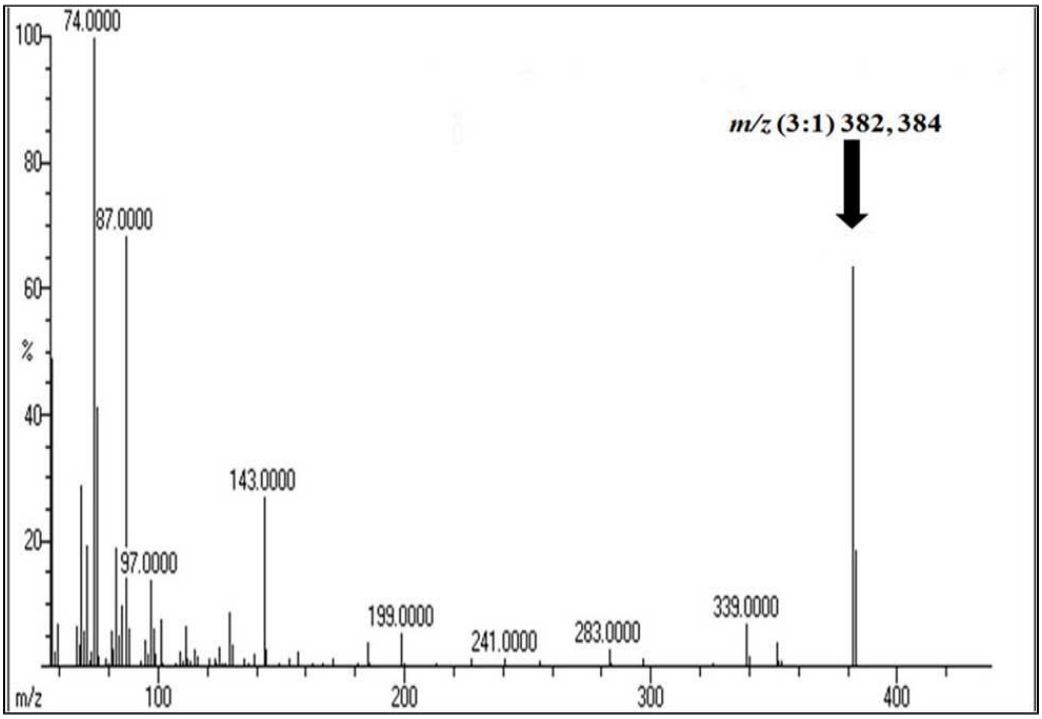

Figure 4.19. Mass spectrum of compound **K2**

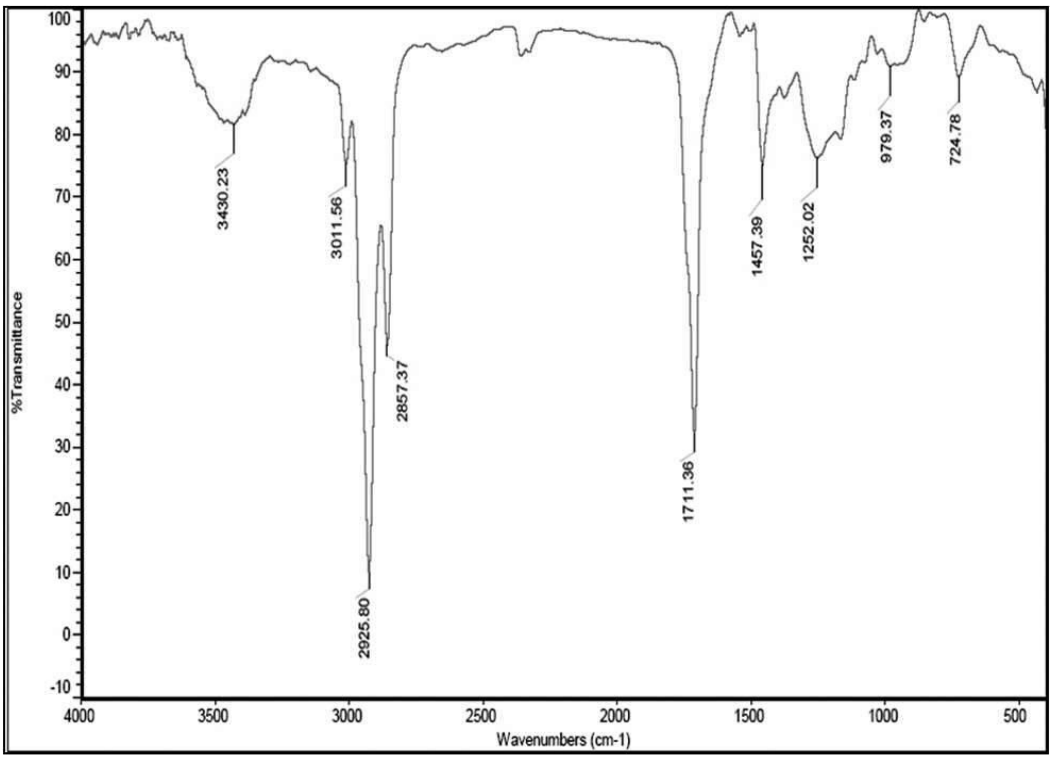

Figure 4.20. Figure showing the FTIR spectrum of compound **K2**

The preliminary studies with various solvents and mixture of solvents were carried out to identify the best solvent/solvent combination to extract the most active fraction in the studied marine macroalga *K. alvarezii*. In this process, the solvents EtOAc, MeOH, DCM and $CHCl_3$, along with various solvent combinations were used as extractants to distribute the extraction process throughout the entire scale of eleutropic solvent series. Among various solvents, EtOAc: MeOH at equal proportion (1:1, v/v) was appropriate to extract the crude with potentially higher bioactivities than other solvents (Table 4.4). Notably, the EtOAc: MeOH (1:1 v/v) fractions of *K. alvarezii* registered significantly higher antioxidant activities in terms of scavenging DPPH and ABTS radicals along with greater pro-inflammatory enzyme (5-LOX, COX-2) inhibitory properties than other extracts (Table 4.4).

Initial bioactivity-assisted fractionation of EtOAc: MeOH (1:1, v/v) extract of *K. alvarezii* over silica gel column resulted in various fractions, as detailed in the materials section. It was noted that the fraction $KA_{2\text{-}1}$ obtained at the solvent eluent gradient of EtOAc: *n*-hexane of 1:99 to 1:19 (v/v) displayed greater antioxidative and 5-lipoxygenase inhibition activities (IC_{50} DPPH scavenging 0.54 mg/mL; IC_{50} 5-LOX inhibition 0.98 mg/mL) than those recorded with other fractions (IC_{50} > 1 mg/mL) (Table 4.5). Therefore, the fraction $KA_{2\text{-}1}$ was selected for further chromatographic fractionation. Furthermore, the sub-fraction $KA_{2\text{-}1\text{-}1}$, which was obtained by step-gradient flash chromatography showed greater bioactivity (IC_{50} DPPH scavenging 0.45 mg/mL; IC_{50} 5-LOX inhibition 0.96 mg/mL) than other sub-fractions (IC_{50} > 1 mg/mL) (Table 4.5), and was therefore, used for downstream preparative HPLC (60:40 MeOH/H_2O) fractionation to yield the studied compounds.

Bioactivity-assisted fractionation of EtOAc: MeOH (1:1, v/v) extract of *K. alvarezii* yielded two previously unreported halogenated compounds, characterized as 2-butyl-7-4-(chloromethyl) cyclooct-1-enyl) hept-5-en-1-ol (compound **K1**) and 4-(2-chloroethyl)-5-7-(methoxymethyl) undec-3-enyl) cyclooct-4-enone (compound **K2**), which were found to constitute C_{20}-cyclooctene and C_{23}-cyclooctenyl frameworks, respectively.

Figure 4.21. Figure showing the structures of compound **K1** and **K2**, isolated from the intertidal marine macroalga *K. alvarezii*. The thalli of the studied marine macroalga were displayed as inset

2-Butyl-7-4-(chloromethyl) cyclooct-1-enyl) hept-5-en-1-ol (compound **K1**) was purified from the EtOAc: MeOH (1:1, v/v) extract of red marine macroalga *K. alvarezii* by silica gel-based column chromatographic fractionation, and its structure was resolved by extensive 1D-2D NMR and mass spectral analyses. The mass spectroscopic data demonstrated a molecular ion peak at *m/z* 326, while the molecular formula $C_{20}H_{35}ClO$, implying three unsaturation degrees, and were associated with two olefinic bonds and one ring system. The infrared (IR) spectrum exhibited distinctive stretching vibration band for hydroxyl (3430 cm^{-1}) and olefinic group (3011 cm^{-1}). The existence of the hydroxyl proton at δ_H 3.67 was validated by ^1H NMR spectra and D_2O exchange reaction. The ^{13}C NMR spectroscopic data along with DEPT experiment of compound **K1** demonstrated the presence of twenty ^{13}C signals including one terminal methyl group at δ_H 0.88 (H-2"^{4}, *J*=6.75 Hz), an oxygenated sp^2 methylene carbon (δ_H 3.61; *J*=7.60 Hz; attributed to H-1, δ_C 70.59), twelve methylene carbons δ_H 1.30 (H-2"^{3}, δ_C 22.58); δ_H 1.25 (H-2"^{2}, δ_C 29.50); δ_H 1.25 (H-2"^{1}, δ_C 31.52); δ_H 1.30 (H-3, δ_C 34.06); δ_H 2.81 (H-4, δ_C 30.20); δ_H 3.27 (H-7, d, *J*=7.2 Hz, δ_C 44.88); δ_H 2.35 (H-8', t, *J*=6.1 Hz, δ_C 33.63); δ_H 1.25 (H-6', δ_C 27.23); δ_H 1.30 (H-5', δ_C 31.93); δ_H 2.13 (H-3', t, *J*=6.0 Hz, δ_C 34.30)), olefinic carbons (δ_H 5.37 (H-5, δ_C 130.51); δ_H 5.39 (H-6, δ_C 128.77; H-2', 128.58), two methine carbons δ_H 1.72 (H-2, δ_C 38.16); δ_H 2.05 (H-4', δ_C 38.19)), one deshielded methylene carbon due to halogen at δ_H 3.74 (H-4", d, *J* = 6.55 Hz, δ_C 51.76), and one quaternary carbon at δ_C 146.84 (H-1'). The positions of hydroxyl and side chain substituent to the cyclooctene were established from the major HMBC and ^1H-^1H COSY correlations. The intense HMBC correlations between δ_H 1.25 (H-2"^{1}) to δ_C 22.58 (C-2"^{3})/δ_C 29.50 (C-2"^{2}); δ_H 0.88 (t, *J*=6.75 Hz; H-2"^{4}) to δ_C 22.58 (C-2"^{3})/δ_C 29.50 (C-2"^{2}); δ_H 1.72 (H-2) to δ_C 31.52 (C-2"^{1}); δ_H 2.81 (H-4) to δ_C 128.77 (C-6); δ_H 3.27 (d, *J*=7.2 Hz; H-7) to δ_C 146.84 (C-1')/δ_C 130.51 (C-5) and ^1H–^1H COSY correlations with δ_H 2.81 (H-4)/δ_H 5.37 (H-5) supported the presence of cycloctene framework. The existence of cyclooctene ring system was supported by additional HMBCs {δ_H 1.30 (H-5') to δ_C 29.33 (C-7'); δ_H 2.05 (H-4') to δ_C 34.30 (C-3'); δ_H 2.35 (t, *J*=6.1 Hz; H-8') to δ_C 29.33 (C-7')/δ_C 27.23 (C-6')} and ^1H–^1H COSY δ_H 2.13 {H-3')/δ_H 5.39 (H-2')}; δ_H 2.35 {H-8')/δ_H 1.63 (H-7')} correlations (Table 4.1).

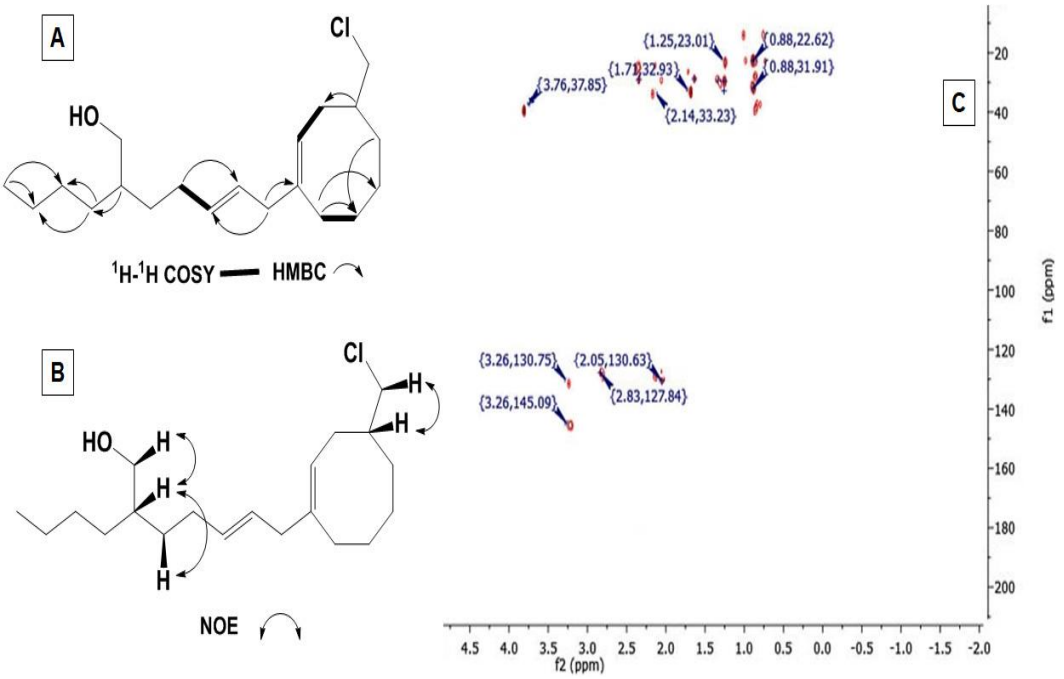

Figure 4.22. Figure showing the key (**A**) ^{1}H-^{1}H COSY, HMBC and (**B**) NOESY correlations of compound **K1**. (**C**) The spectral representation of long-range C-H correlations (showing prominent cross-peaks). The ^{1}H-^{1}H COSY cross peaks were displayed by bold face bonds, whereas the selected HMBC correlations were shown as double-barbed arrows. The β-orientation in the NOESY relations was presented as double-sided arrows

The NOE experiment of compound **K1** showed correlation peaks between the equatorial methine proton at δ_H 1.72, (H-2) and methylene proton at δ_H 3.61, t, *J*=7.60 Hz; (H-1), which proposed that these protons were arranged on the same side of the reference plane (cyclooctene) with β-faced interaction. In addition, NOESY correlations were observed between the equatorial methine proton at δ_H 1.72, (H-2) and methylene proton at δ_H 1.30, (H-3), which proposed that these protons were disposed on opposite to the plane of reference (cyclooctene). The proton at δ_H 3.74 (H-4") showed sharp NOE cross-peaks with the axial proton at δ_H 2.05 (H-4'), which displayed β-faced interaction with each other. The characteristic isotopic molecular ion peaks with typical isotopic pattern of 3:1 at *m/z* 326 and *m/z* 328 appropriately attributed the existence of one chlorine atom in compound **K1**.

4-(2-Chloroethyl)-5-7-(methoxymethyl) undec-3-enyl) cyclooct-4-enone (compound **K2**) was purified from the EtOAc-MeOH (1:1, v/v) extract of *K. alvarezii* by silica gel-based chromatographic techniques, and its structure was resolved by extensive 1D-2D NMR and mass spectral analyses. The mass spectroscopic experiments showed a molecular isotopic ion peak at *m/z* 382, having four degrees of unsaturation (molecular formula $C_{23}H_{39}ClO_2$), and were associated with two olefinic bonds, along with one each of carbonyl group and ring system. The infrared (IR) spectrum exhibited distinctive stretching vibration band for carbonyl stretching (1727.88 cm^{-1} (C–CO–C ν)) and olefinic group (3072.42 cm^{-1} (C–H)). The ^{13}C NMR spectroscopic data of compound **K2** along with DEPT experiment demonstrated the presence of twenty-three ^{13}C signals including fifteen methylene carbon {δ_H 1.33 (H-10, δ_C 22.70); δ_H 1.30 (H-8, δ_C 30.20); δ_H 1.58 (H-6, δ_C 34.13); δ_H 2.00 (H-5, δ_C 31.44); δ_H 2.00 (H-2, δ_C 32.74); δ_H 2.06 (H-1, δ_C 31.93); δ_H 1.62 (H-7', δ_C 27.19); δ_H 2.30 (H-8', t, *J*=6.1 Hz, δ_C 40.19); δ_H 2.77 (H-2', δ_C 41.50); δ_H 2.30 (t, *J*=6.1 Hz, H-3', δ_C 29.37); δ_H 2.30 (H-4'^{1}, δ_C 33.83); δ_H 1.25 (H-9, δ_C 29.6); δ_H 2.06 (H-6', δ_C 29.70)}, one terminal methyl group {δ_H 0.87, t, *J*=6.70 Hz; H-11; δ_C 14.12}, an oxygenated methylene carbon {δ_H 4.29; *J*=7.46 Hz; H-7'^{1} δ_C 80.95}, olefinic carbons {δ_H 5.35 (H-4, δ_C 130.0); δ_H 5.34 (H-3, δ_C 129.68)}, one methine carbon {δ_H 1.73 (H-7, δ_C 38.86)}, one deshielded methylene carbon due to halogen {δ_H 4.15 (H-4'^{2}, t, *J*=7.50 Hz, δ_C 62.11)}, one methoxy carbon {δ_H 3.67 (H-7'^{1}, δ_C 51.44)}, two quaternary carbons {δ_C 139.28 (H-5'); δ_C 147.07 (H-4')}, and one carbonyl carbon {δ_C 209 (H-1')}. The positions of methoxy group and side chain substituent to the cyclooctenone were established from the key ^1H–^1H COSY and HMBC correlations. The ^1H–^1H correlations spectroscopy observed between δ_H 5.35 (H-4)/δ_H 2.00 (H-5) and $J^{1\text{-}3}$ C–H correlations between δ_H 1.33 (H-10) to δ_C 30.20 (C-8)/δ_C 29.6 (C-9)/δ_C 14.12 (C-11); δ_H 1.30 (H-8) to δ_C 38.86 (C-7)/δ_C 22.70 (C-10); δ_H 3.67 (H-7'^{2}) to δ_C 80.95 (C-7'^{1}); δ_H 2.06 (H-1) to δ_C 32.74 (C-2); δ_H 1.25 (H-9) to δ_C 22.70 (C-10)/δ_C 38.86 (C-7); δ_H 0.87 (t, *J*=6.70 Hz; H-11) to δ_C 22.70 (C-10); δ_H 1.73 (H-7) to δ_C 34.13 (C-6)/δ_C 31.44 (C-5); δ_H 2.00 (H-5) to δ_C 130.0 (C-4); δ_H 5.34 (H-3) to δ_C 130.0 (C-4)/δ_C 32.74 (C-2) supported the presence of cyclooctenyl framework. The existence of cyclooctenyl ring system was corroborated by additional HMBCs {δ_H 2.30 (H-8') to δ_C 209 (C-1'); δ_H 1.62 (H-7') to δ_C 209 (C-1)/δ_C 29.70 (C-6'); δ_H 2.77 (H-2') to δ_C 147.07 (C-4'); δ_H 2.06 (t, *J*=6.10 Hz; H-1) to δ_C 29.70 (C-6')/δ_C 147.07 (C-4')/δ_C 139.28 (C-5'); δ_H 2.30 (H-3') to δ_C 33.83 (C-4'^{1})/δ_C 41.50 (C-

2'); δ_H 4.15 (H-4'^{2}) to δ_C 147.07 (C-4')} and ^{1}H–^{1}H COSY {(δ_H 2.30 (H-8')/δ_H 1.62 (H-7')} correlations. The NOE experiment showed correlation peaks between the oxygenated methine proton at δ_H 1.73 (H-7) and axial proton at δ_H 1.58 (H-6), which proposed that these protons were on the opposite to the reference plane (cyclooctenyl) with β-faced interaction. Intense NOE correlation were also observed between the equatorial proton at δ_H 4.29 (d, *J*=7.46 Hz; H-7'^{1}) with δ_H 1.73 (H-7), which suggested that these protons were di-equatorially oriented with β-faced interaction. Moreover intense NOE correlation were observed between the axially oriented proton δ_H 1.25 (H-9) with δ_H 1.73 (H-7), suggesting that these protons were disposed in the identical plane of reference. The characteristic isotopic molecular ion peaks with typical isotopic pattern of 3:1 at *m/z* 382 and *m/z* 384 appropriately attributed the existence of one chlorine atom in compound **K2**. It is of note that the halogen derivatives isolated in the present study from *K. alvarezii* represented the first examples of naturally occurring halogen derivative from the marine macroalga (Table 4.2). There were reports of halogenated compounds isolated from other species of red marine macroalgae. Therefore, we will confine our discussion with the closely related structures, such as laurefurenynes A-F and cyclic ether acetogenins isolated and characterized from the red marine macroalga *Laurentia* sp. The FT-IR spectral data of laurefurenynes A-F, which belonged to the class of C_{15} cyclic ether acetogenins, were purified from *Laurentia* sp, displayed strong absorption bands attributed to a terminal acetylene (2107 and 3315 cm^{-1}) functional groups, which were absent in the halogen derivatives isolated from *K. alvarezii*. The C_{15} acetogenin en-ynes, a group of chlorinated compounds with potential pharmacological properties, were isolated from *Laurencia glandulifera*, and were structurally similar to the studied compounds (Kladi et al. 2009). However, there was no previous report with regard to the antioxidant and anti-inflammatory activities of the laurefurenynes A-F and cyclic ether acetogenins from red marine macroalgae. The present study is the first of its kind to describe the halogen derivatives with anti-inflammatory and radical scavenging leads for use in the medicinal and functional food applications.

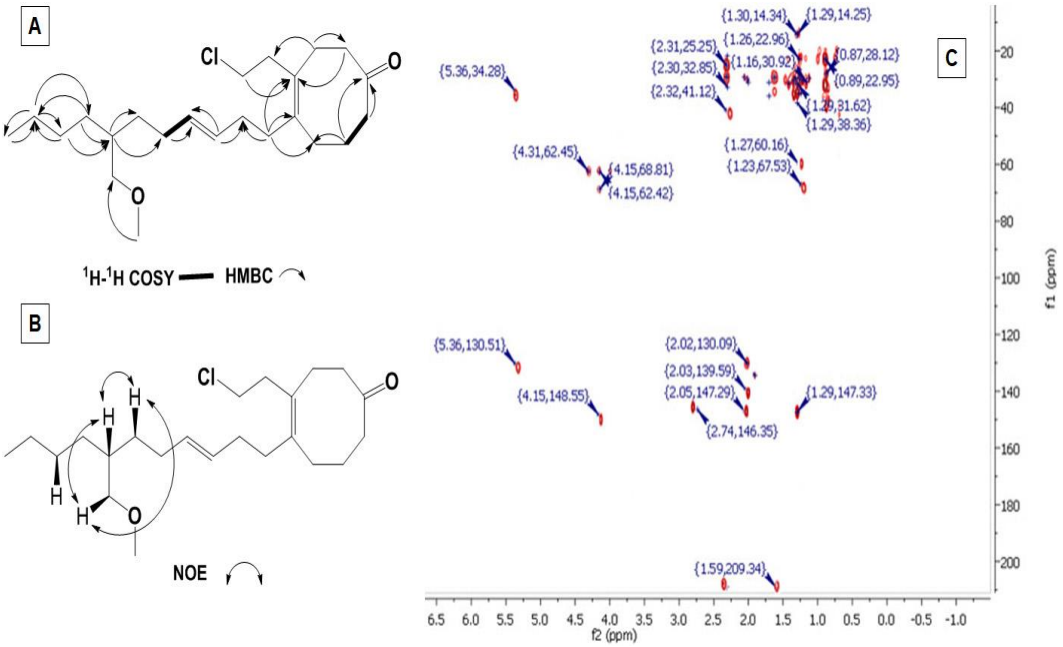

Figure 4.23. Figure showing the Key (**A**) ^{1}H-^{1}H COSY, HMBC and (**B**) NOESY correlations of compound **K2** (**C**) The spectral representation of long-range C-H correlations (showing prominent cross-peaks). The ^{1}H-^{1}H COSY cross peaks were displayed by bold face bonds, whereas the selected HMBC correlations were shown as double-barbed arrows. The β-orientation in the NOESY relations was presented as double-sided arrows

The signals obtained at δ_H 4.93 and δ_H 4.43 indicated the two hydroxyl groups, which were present at OH-7 and OH-12 (Wael et al. 2010). The studied halogenated compounds derived from the ethyl acetate-methanol extract of the red marine macroalga *K. alvarezii* displayed the presence of OH-1". The previously reported C_{15}-acetogenin from red marine macroalgae was found to differ with the isolated halogen compounds in the pattern of oxygenation and halogenations. The characteristic isotopic molecular ion peaks appropriately attributed the existence of one chlorine atom in the halogen derivatives isolated from *K. alvarezii*. Similarly, the C_{15}-acetogenin isolated from red marine macroalga *Laurencia* sp displayed brominated halogenations.

4.3.1.3. Bioactivities and Structure-Activity Relationship Analysis

The radical scavenging potentials of the isolated compounds were resolved by *in vitro* radical scavenging assays, such as 1, 1-diphenyl-2-picrylhydrazyl (DPPH) and 2, 2′-azino-bis(3-ethylbenzothiazoline-6-sulphonic acid (ABTS), whereas their activities were compared with the synthetic antioxidants (BHT, BHA) and α-tocopherol. Among the halogen derivatives, compound **K2** showed significant radical scavenging activity ($IC_{50\ DPPH}$ 0.23±0.06, $IC_{50\ ABTS}$ 0.25±0.18 mg/mL) when compared to compound **K1** ($IC_{50\ DPPH}$ 0.27±0.04, $IC_{50\ ABTS}$ 0.31±0.18 mg/mL), and than that of the commercial antioxidants. The anti-inflammatory activities of studied halogen derivatives were analyzed by pro-inflammatory 5-lipoxygenase, cyclooxygense-2 *in vitro* assays. Among the studied compounds, compound **K2** displayed higher 5-LOX inhibitory activities (IC_{50} 0.90±0.04 mg/mL) than synthetic ibuprofen (IC_{50} 0.93±0.11 mg/mL) (Fig. 4.24, Table 4.3). Notably, the studied halogen analogues presented significantly greater inhibitory activities against COX-2 than its COX-1 isoform. Similarly, their selectivity indices ($IC_{50\ anti\text{-}COX-1}/IC_{50\ anti\text{-}COX-2}$ ~ 1.06–1.07) were greater in comparison with synthetic NSAIDs (aspirin 0.02; ibuprofen 0.44). It is intriguing to note that the synthetically available anti-inflammatory drugs demonstrated comparable inhibitory activities against constitutive COX-1 and inducible COX-2, which might reveal their adverse effects (Fosslien 2005).

Figure 4.24. Graphical representation of bioactivities of compound **K1** and **K2**. The thalli of the studied marine macroalga were displayed as inset

Table 4.3 Antioxidative and inflammatory activities of the halogen derivatives (compounds **K1-K2**) isolated from *K. alvarezii vis-à-vis* the commercially available antioxidants and anti-inflammatory agents

Antioxidative activities† {IC_{50} (mg/mL)}					
	Compound K1	**Compound K2**	**BHA**	**BHT**	**α-tocopherol**
$DPPH^{\cdot}$ scavenging	$0.27^{a} \pm 0.04$	$0.23^{a} \pm 0.06$	$0.26^{b} \pm 0.01$	$0.25^{b} \pm 0.02$	$0.63^{c} \pm 0.04$
$ABTS^{+\cdot}$ scavenging	$0.31^{a} \pm 0.18$	$0.25^{a} \pm 0.18$	$0.34^{b} \pm 0.02$	$0.26^{b} \pm 0.02$	$0.73^{c} \pm 0.05$
Anti-inflammatory activities† {IC_{50} (mg/mL)}					
	Compound K1	**Compound K2**	**Aspirin**	**Na-salicylate**	**Ibuprofen**
COX-1 inhibition	$1.01^{a} \pm 0.04$	$0.94^{a} \pm 0.04$	$0.005^{a} \pm 0.00$	$1.93^{c} \pm 0.05$	$0.04^{a} \pm 0.00$
COX-2 inhibition	$0.94^{a} \pm 0.03$	$0.88^{a} \pm 0.09$	$0.21^{b} \pm 0.02$	$2.65^{c} \pm 0.05$	$0.09^{a} \pm 0.02$
Selectivity index‡	$1.07^{b} \pm 0.06$	$1.06^{b} \pm 0.03$	$0.02^{b} \pm 0.02$	$0.72^{b} \pm 0.01$	$0.44^{b} \pm 0.02$
5-LOX inhibition	$0.95^{a} \pm 0.11$	$0.90^{a} \pm 0.04$	$0.39^{a} \pm 0.02$	$1.75^{c} \pm 0.12$	$0.93^{b} \pm 0.11$

† The bioactivities were expressed as IC_{50} values (mg/mL). The samples were analyzed in triplicate (n=3) and expressed as mean ± standard deviation.

Means followed by the different superscripts (a–c) within the same row indicate significant differences ($P < 0.05$).

‡ Selectivity index has been calculated as the ratio of anti-COX-1 (IC_{50}) to that of anti-COX-2 (IC_{50}).

Table 4.4 Yield, antioxidant and anti-inflammatory activities (IC_{50}, mg/mL)[†] of different solvent fractions extracted from the red marine macroalga *K. alvarezii*

	Solvent fractions					
Activities	**$CHCl_3$**	**DCM**	**EtOAc**	**MeOH**	**$CHCl_3$: MeOH**	**EtOAc: MeOH (1:1 v/v)**
Yield[‡]	1.1	1.0	3.8	4.32	2.5	6.0
DPPH radical scavenging	2.08 ± 0.12	1.97 ± 0.08	1.36 ± 0.06	1.38 ± 0.09	1.74 ± 0.06	1.24 ± 0.11
ABTS radical scavenging	2.05 ± 0.07	1.93 ± 0.05	1.32 ± 0.08	1.35 ± 0.12	1.72 ± 0.15	1.26 ± 0.06
5-LOX inhibitory	2.13 ± 0.11	2.01 ± 0.16	1.58 ± 0.14	1.52 ± 0.18	1.97 ± 0.20	1.49 ± 0.12
COX-2 inhibitory	2.08 ± 0.17	2.03 ± 0.08	1.52 ± 0.12	1.50 ± 0.13	1.92 ± 0.14	1.35 ± 0.15

[†] The samples were analyzed in triplicate (n = 3) and expressed as mean ± standard deviation. The IC_{50} values were expressed as mg/mL. $CHCl_3$-chloroform, DCM-dichloromethane, EtOAc-ethyl acetate, MeOH-methanol.

[‡] Yields of the extracts were represented as % w/w of marine macroalga on dry weight basis.

Table 4.5 Antioxidant and anti-inflammatory activities (IC_{50}, mg/mL)[†] of the column fraction and purified compounds from EtOAc-MeOH (1:1 v/v) extracts of the red marine macroalga *K. alvarezii*

	Activities			
Fractions	**DPPH scavenging**	**ABTS scavenging**	**5-LOX inhibitory**	**COX-2 inhibitory**
KA_{2-1}	**0.54±0.01**	**0.53±0.04**	**0.98±0.02**	**0.97±0.04**
KA_{2-2}	1.39±0.06	1.40±0.06	1.50±0.03	1.52±0.02
KA_{2-3}	1.36±0.03	1.35±0.02	1.48±0.02	1.46±0.05
KA_{2-4}	1.38±0.05	1.38±0.01	1.45±0.05	1.42±0.06
KA_{2-5}	1.41±0.01	1.42±0.01	1.52±0.02	1.54±0.03
KA_{2-6}	1.45±0.03	1.48±0.01	1.54±0.01	1.56±0.01
KA_{2-7}	1.48±0.02	1.50±0.08	1.60±0.09	1.59±0.04
KA_{2-8}	1.42±0.02	1.40±0.01	1.53±0.03	1.54±0.06
KA_{2-9}	1.45±0.02	1.42±0.01	1.56±0.02	1.54±0.02
KA_{2-10}	1.46±0.04	1.43±0.02	1.53±0.04	1.52±0.09
KA_{2-11}	1.43±0.04	1.40±0.02	1.50±0.01	1.52±0.05
KA_{2-12}	1.38±0.01	1.39±0.08	1.43±0.06	1.45±0.02
KA_{2-13}	1.49±0.01	1.47±0.03	1.52±0.04	1.52±0.02
KA_{2-1} Sub Fractions				
KA_{2-1-1}	**0.45±0.02**	**0.43±0.01**	**0.96±0.03**	**0.92±0.01**
KA_{2-1-2}	1.13±0.01	1.15±0.03	1.20±0.01	1.19±0.06
KA_{2-1-3}	1.15±0.02	1.18±0.01	1.22±0.03	1.20±0.04
KA_{2-1-4}	1.10±0.01	1.08±0.08	1.16±0.04	1.15±0.09
KA_{2-1-5}	1.11±0.02	1.10±0.03	1.18±0.01	1.17±0.04
KA_{2-1-6}	1.13±0.04	1.13±0.06	1.14±0.01	1.16±0.02
KA_{2-1-7}	1.18±0.02	1.16±0.06	1.20±0.06	1.21±0.03
KA_{2-1-1} Sub Fractions				
Compound K1	0.27±0.04	0.31±0.18	0.94±0.03	0.88±0.09
Compound K2	0.23±0.06	0.25±0.18	0.95±0.11	0.90±0.04

† The samples were analyzed in triplicate (n=3) and expressed as mean ± standard deviation.

The IC_{50} values were expressed as mg/mL.

Table 4.6. Antioxidative, anti-inflammatory, anti-diabetic and anti-hypertensive activities of the crude EtOAc: MeOH (1:1 v/v) extract and purified compounds isolated from the red marine macroalga *K. alvarezii*

Activities† IC_{50} values (mg/mL)	**EtOAc: MeOH (1:1 v/v)**	**Compound K1**	**Compound K2**
Antioxidant activities			
DPPH radical scavenging	1.24±0.06	0.27±0.04	0.23±0.06
ABTS radical scavenging	1.26±0.03	0.31±0.18	0.25±0.18
Anti-hypertensive activities			
ACE inhibitory	2.10±0.02	2.01±0.04	2.03±0.04
Anti-diabetic activities			
α-amylase inhibitory	2.18±0.04	2.01±0.02	2.08±0.01
α-glucosidase inhibitory	2.20±0.01	2.03±0.04	2.10±0.06
DPP-4 inhibitory	2.18±0.03	2.02±0.05	2.11±0.02
Anti-inflammatory activities			
COX-2 inhibitory	1.35±0.05	0.88±0.09	0.90±0.04
5-LOX inhibitory	1.49±0.02	0.94±0.03	0.95±0.11

†The bioactivities were expressed as IC_{50} values (mg/mL).

The samples were analyzed in triplicate (n=3) and expressed as mean ± standard deviation.

4.3.1.4. Structural Characterization of Compound K3

1-(3-Methoxypropyl)-2-propylcyclohexane (**K3**)

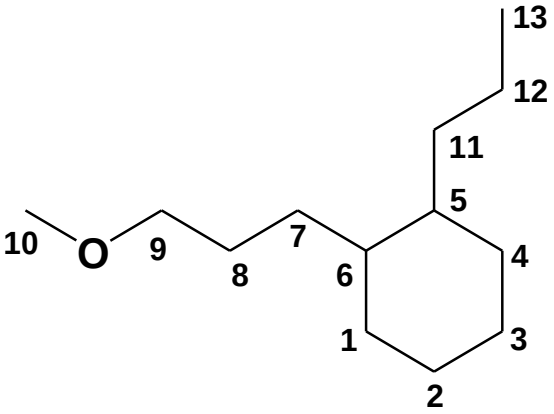

Sample yield	120 mg (1.2 %)
Physical description	Yellow oil
Molecular formula	$C_{13}H_{26}O$
Molecular weight	198.1984

1-(3-Methoxypropyl)-2-propylcyclohexane: Yellow oil; UV MeOH λmax (log ε): 245 nm (3.26), TLC (Si gel GF_{254} 15 mm; EtOAc/MeOH 19:1, v/v) Rf: 0.96; Rt (HPLC, ACN: MeOH, 2:4 v/v): 12.401 min; IR (vibrational spectra were measured between 4000 to 450 cm^{-1} for (KBr, cm^{-1}) νmax (ν = stretching, δ = bending, ρ = rocking vibrations)): 728.70 (C-H ρ), 1014.67 (C–O ν), 1256.18 (CH_2 ν), 1376.13 (C-H ρ), 1458.14 (C-H δ), 1644.58 (C=C ν), 2857.12, 2923.46 (C–H ν); ^{1}H NMR (500 MHz $CDCl_3$): δ_H 1.26 (2H, m, H-1), δ_H 1.26 (2H, m, H-2), δ_H 1.26 (2H, m, H-3), δ_H 1.62 (2H, m, H-4), δ_H 2.32 (1H, m, H-5), δ_H 2.04 (1H, m, H-6), δ_H 1.42 (2H, m, H-7), δ_H 1.72 (2H, m, H-8), δ_H 4.29 (2H, t, *J*=6.95 Hz, H-9), δ_H 3.67 (3H, s, H-10), δ_H 1.25 (2H, m, H-11), δ_H 1.31 (2H, m, H-12), δ_H 0.88 (3H, t, *J*=7.53 Hz, H-13); ^{13}C NMR (125 MHz, $CDCl_3$): δ_C 29.65 (C-1), δ_C 27.23 (C-2), δ_C 29.65 (C-3), δ_C 37.10 (C-4), δ_C 33.86 (C-5), δ_C 32.38 (C-6), δ_C 29.88 (C-7), δ_C 29.66 (C-8), δ_C 50.87 (C-9), δ_C 51.45 (C-10), δ_C 31.97 (C-11), δ_C 22.7 (C-12), δ_C 14.12 (C-13); HMBC and ^{1}H-^{1}H-COSY data (Fig. 4.26 to Fig. 4.34, Table 4.7); HR (EI) MS *m/z* measured value 198.1988 $[M]^+$, calcd for $C_{13}H_{26}O$ 198.1984.

1-(3-Methoxypropyl)-2-propylcyclohexane (compound **K3**), a methoxy-substituted C_{13} meroterpenoid, was purified as yellow oil by extensive column chromatography on adsorbent silica gel. The mass spectrum displayed the molecular ion peak at *m/z* 198 enclosing mono unsaturation (because of the ring system), and the molecular formula as $C_{13}H_{26}O$ based upon combined ^{1}H and ^{13}C NMR spectral data. The existence of 13 carbon signals constituting of nine methylenes, two methines and one each of methoxy and methyl carbons was supported by the ^{13}C NMR experiment. The deshielded resonance of H-9 (δ_H 4.29, *J*=6.95 Hz) of compound **K3** suggested the C-9 methylene groups remained attached to an electronegative group, possibly of oxygenated origin.

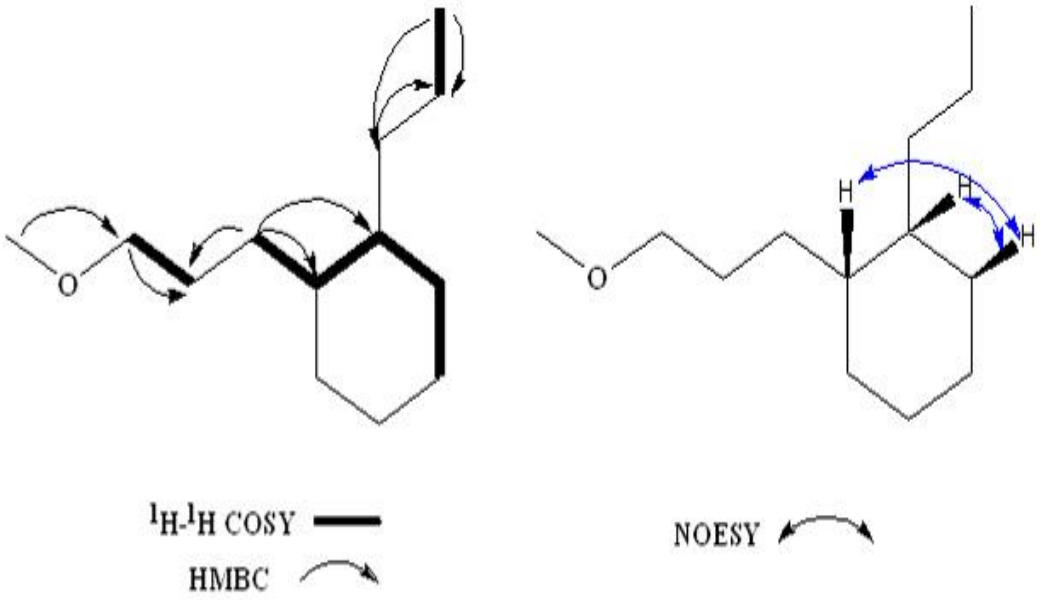

Figure 4.25. Figure showing Key ^{1}H-^{1}H COSY, HMBC and NOESY correlations of compound **K3.** The ^{1}H-^{1}H COSY cross peaks were displayed by bold face bonds, whereas the selected HMBC correlations were shown as double barbed arrows. The β orientation in the NOESY relations was presented as blue colored arrows

The ^{1}H-^{1}H COSY correlations were observed between δ_H 2.32 (H-5)/δ_H 2.04 (H-6); δ_H 1.62 (H-4)/δ_H 2.32 (H-5) were apparent, and were ascribed to the cyclohexane ring framework (Fig. 4.25). The methine (–CH) carbon signals were apparent at δ_C 33.86 (C-5) and C-6 (δ_C 32.38) that appropriately recognized the

junction point of cyclohexane ring system substituted with propane and the methoxypropane moieties, respectively. HMBC correlations from δ_H 1.25 (assigned as H-11) to δ_C 22.7 (C-12); δ_H 1.42 (H-7) to δ_C 33.86 (C-5)/δ_C 31.97 (C-6)/δ_C 29.66 (C-8); δ_H 0.88 (H-13) to δ_C 31.97 (C-11)/δ_C 22.7 (C-12); δ_H 4.29 (H-9) to δ_C 29.66 (C-8); δ_H 3.67 (H-10) to δ_C 50.87 (C-9) displayed the side chain substitutions of the cyclohexane ring system.

In addition, ^{1}H-^{1}H COSY correlations appeared at δ_H 4.29 (H-9)/δ_H 1.72 (H-8), δ_H 2.04 (H-6)/δ_H 1.42 (H-7), which were due to the 1-methoxypropane framework attached to the cyclohexane ring system, and was in accordance with the $J^{1\text{-}3}$ HMBC attributions. Similarly, ^{1}H-^{1}H COSY correlation appeared at δ_H 1.31 (H-12)/δ_H 0.88 (H-13), which was due to the framework attached to the cyclohexane ring system. The combined ^{1}H/^{13}C NMR demonstrated highly deshielded oxymethylene protons at δ_H 4.29 (attributed to H-9) corresponding to the carbon resonance at δ_C 50.87 (C-9) to assign the propylcyclohexane ring system and side chain substitution in C_{13} meroterpenoid. The relative stereochemistries of compound **K3** were attributed by NOESY experiments. The reference plane of the compound **K3** was arbitrarily chosen as the cyclohexane ring system. NOESY cross peaks between δ_H 2.32 (H-5)/δ_H 1.62 (H-4) suggested their close proximity, and therefore, assigned to align on an identical plane of the cyclohexane ring system with di-equatorial β-faced interaction. Intense NOESY cross peaks between δ_H 1.62 (H-4)/δ_H 2.04 (H-6) appropriately indicated their equiplaner disposition (β-orientation).

Table 4.7 NMR spectroscopic data of compound **K3** in $CDCl_3$[a]

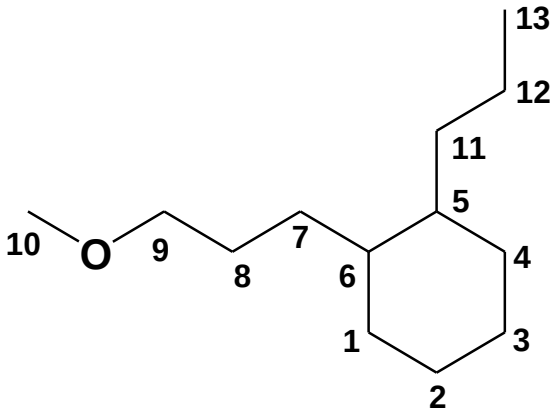

C. No	^{13}C (δ)	^{1}H-NMR[b] (int., mult., *J* in Hz)	^{1}H-^{1}H COSY	HMBC (^{1}H-^{13}C)
1	29.65	1.26 (2H, m)	-	-
2	27.23	1.26 (2H, m)	-	-
3	29.65	1.26 (2H, m)	4-H	-
4	37.10	1.62 (2H, m)	3-H, 5-H	-
5	33.86	2.32 (1H, m)	4-H, 6-H	-
6	32.38	2.04 (1H, m)	7-H	-
7	29.88	1.42 (2H, m)	6-H	C-5, C-6, C-8
8	29.66	1.72 (2H, m)	9-H	-
9	50.87	4.29 (2H, *J*=6.95 Hz, t)	8-H	C-8
10	51.45	3.67 (3H, s)	-	C-9
11	31.97	1.25 (2H, m)	-	C-12
12	22.7	1.31 (2H, m)	-	-
13	14.12	0.88 (3H, *J*=7.53 Hz, t)	12-H	C-11, C-12

[a] NMR spectra recorded using Bruker AVANCE III 500 MHz (AV 500) spectrometer in $CDCl_3$ as aprotic solvent at ambient temperature with TMS as the internal standard (δ 0 ppm).

[b] Values in ppm, multiplicity and coupling constants (*J*=Hz) are indicated in parentheses. The assignments were made with the aid of the ^{1}H-^{1}H COSY, HSQC, HMBC and NOESY experiment

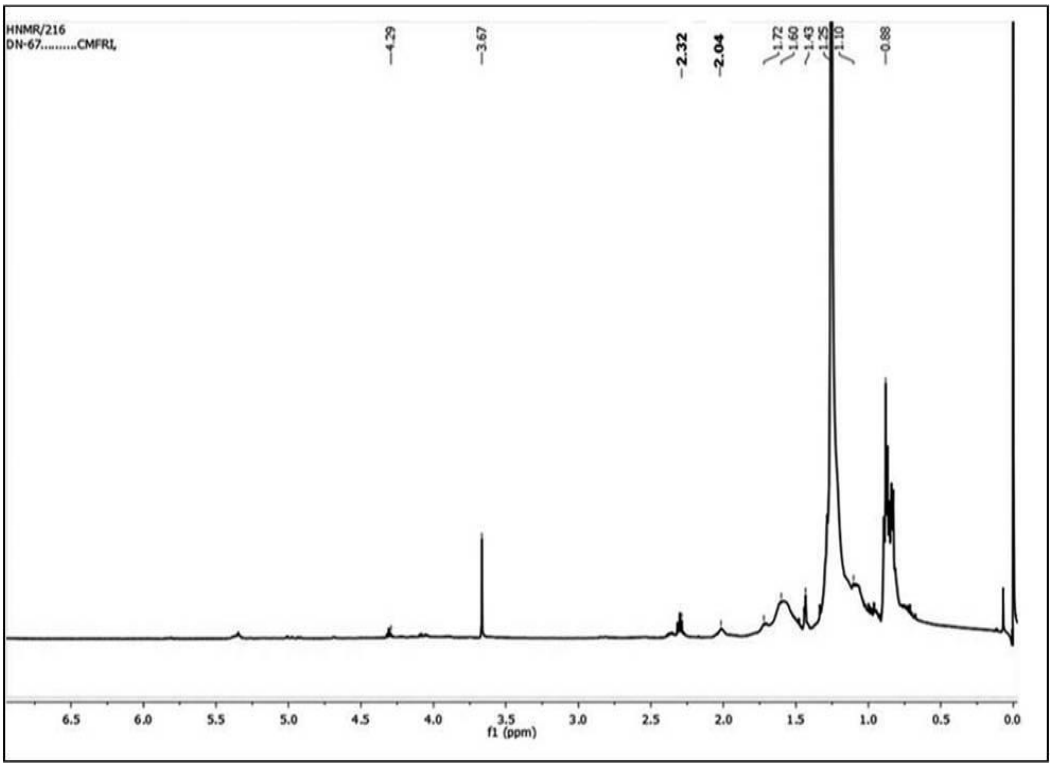

Figure 4.26. Figure showing the ^{1}H NMR spectrum of compound **K3**

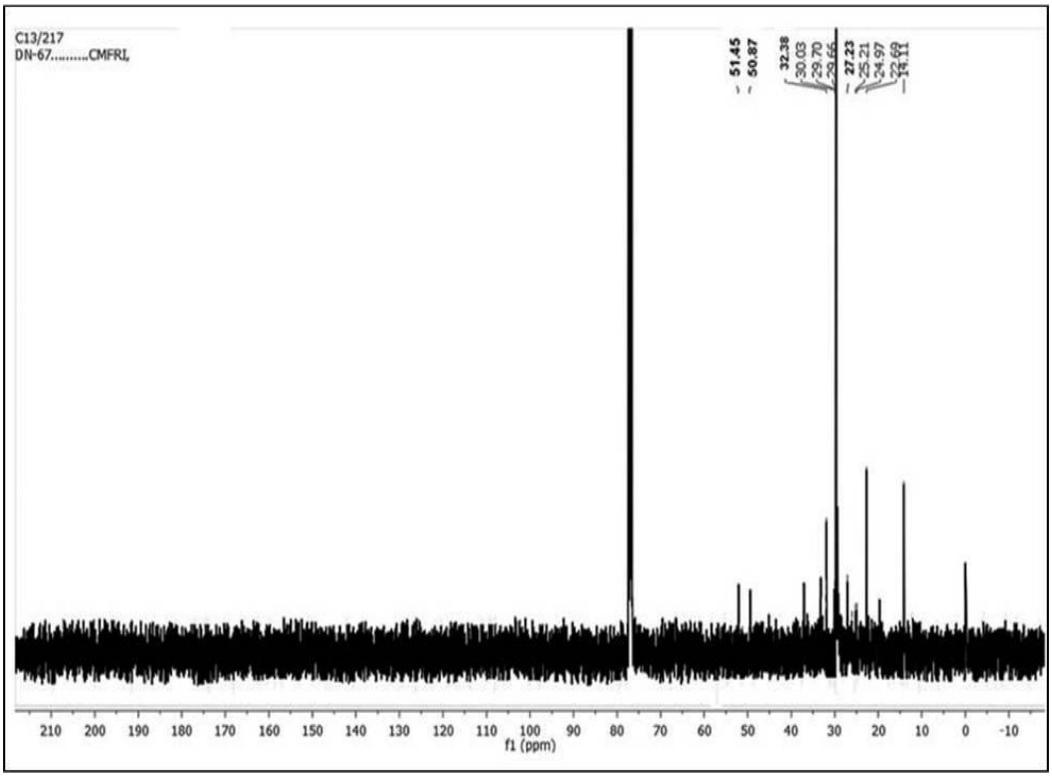

Figure 4.27. Figure showing the ^{13}C NMR spectrum of compound **K3**

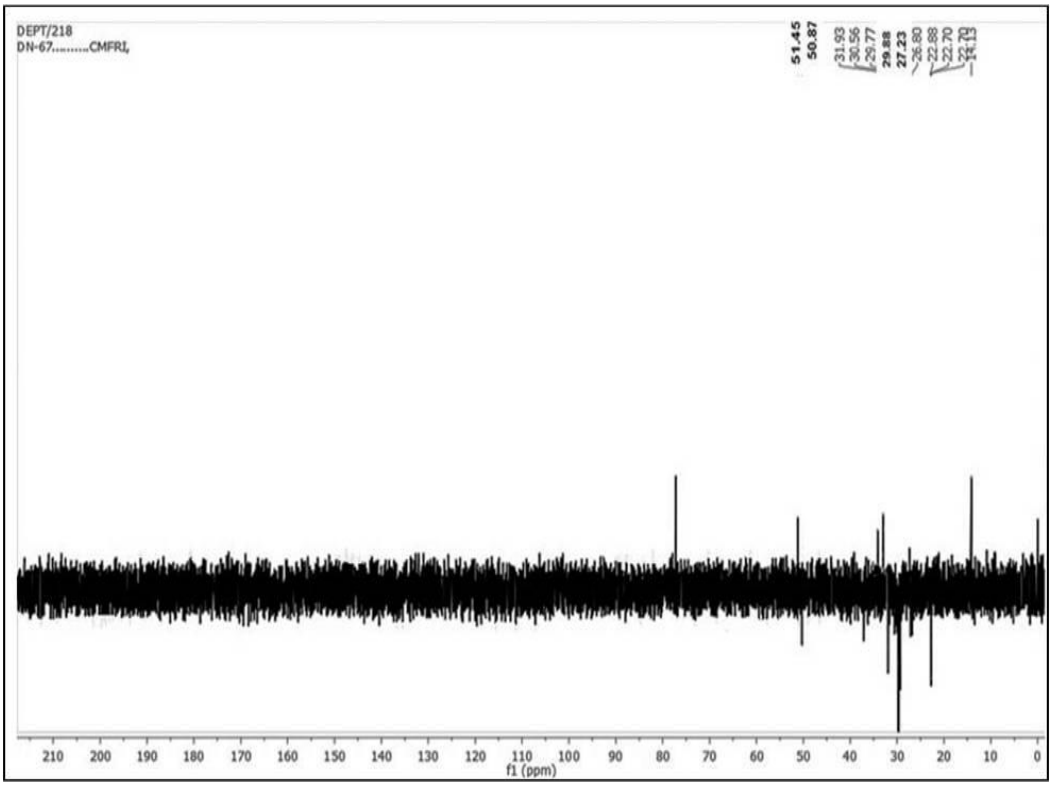

Figure 4.28. Figure showing the DEPT spectrum of compound **K3**

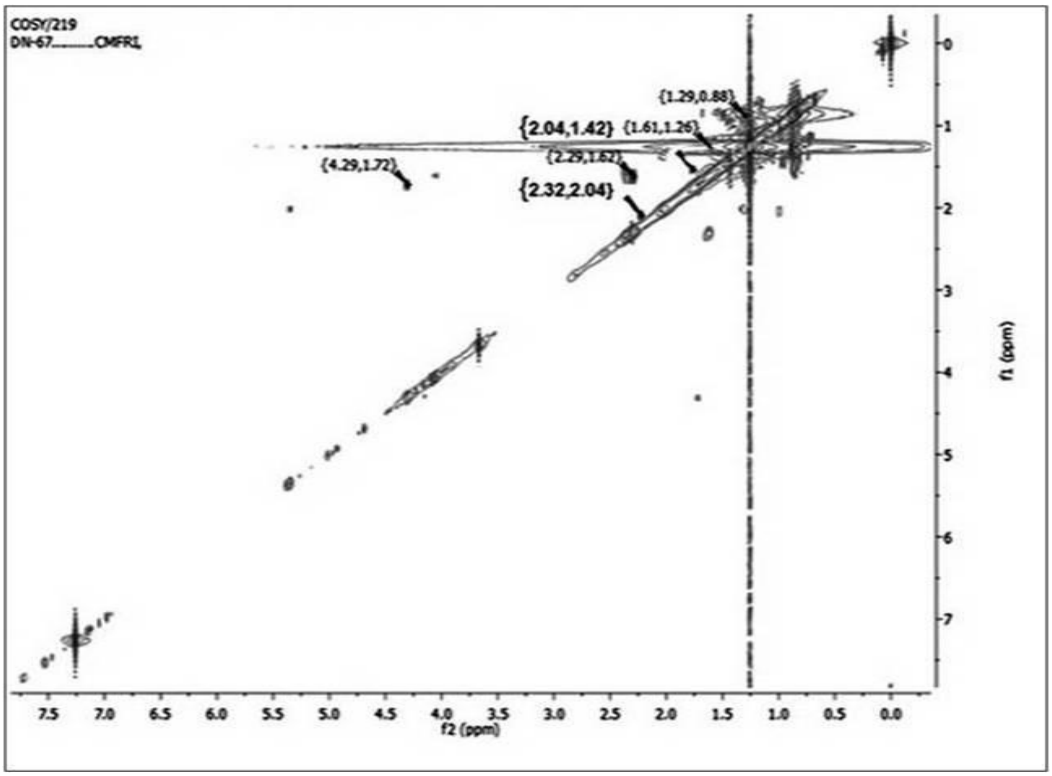

Figure 4.29. Figure showing the ^{1}H-^{1}H COSY spectrum of compound **K3**

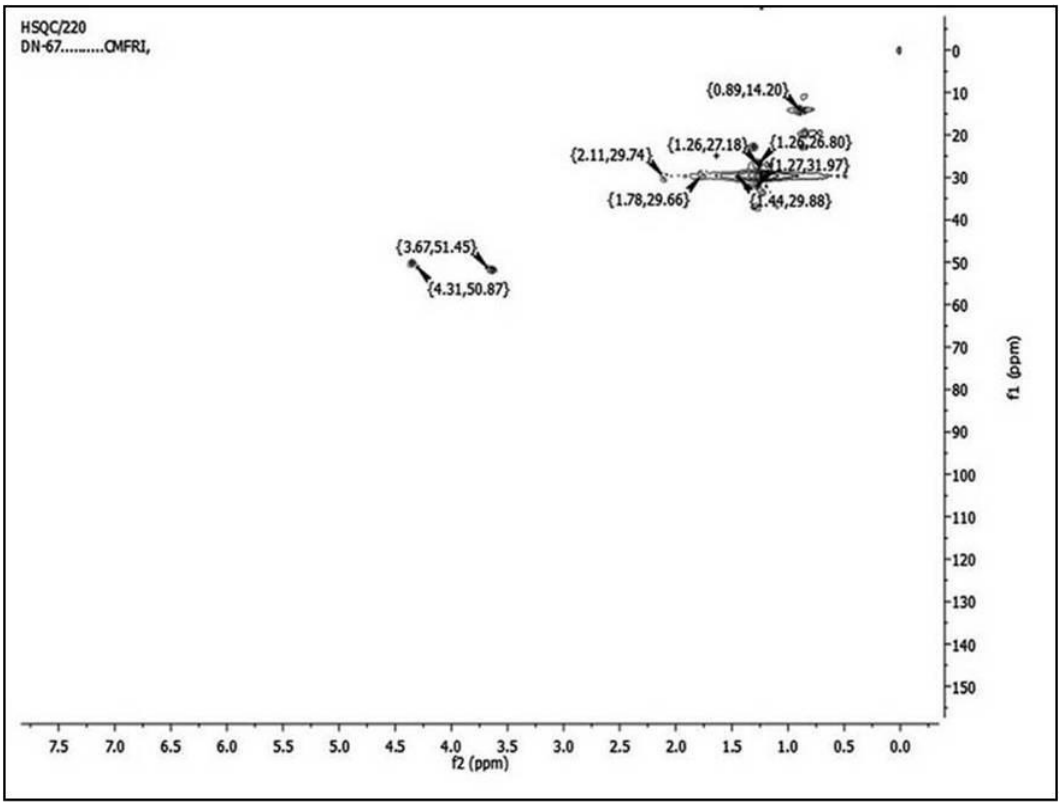

Figure 4.30. Figure showing the HSQC spectrum of compound **K3**

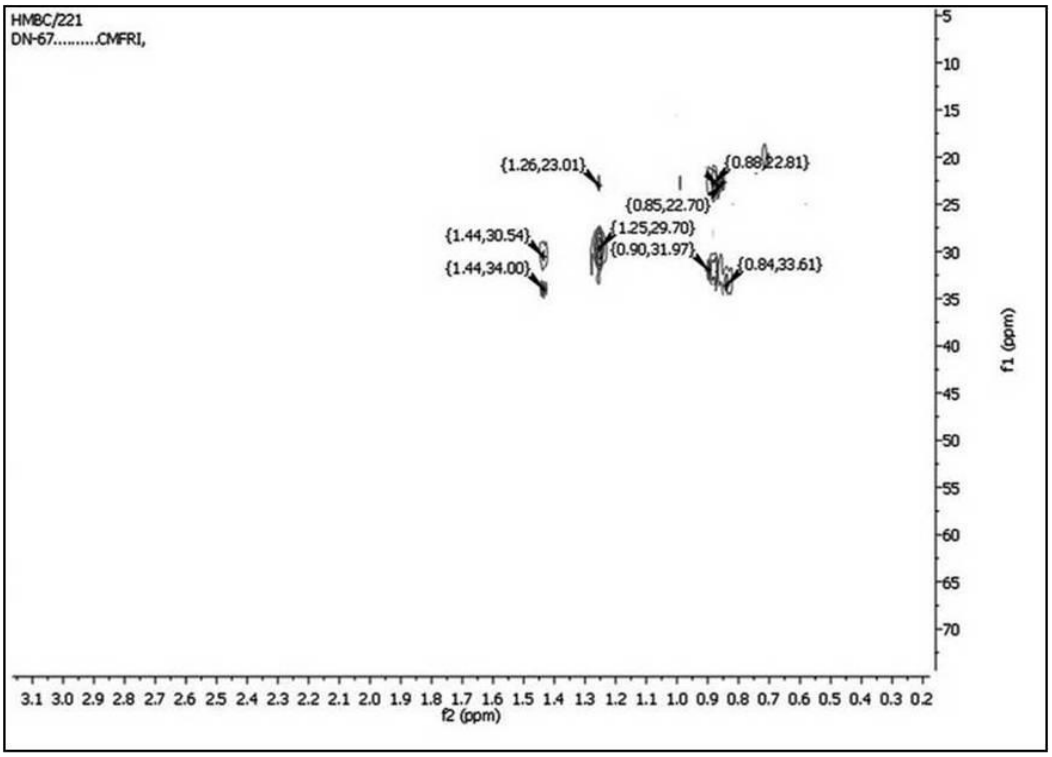

Figure 4.31. Figure showing the HMBC spectrum of compound **K3**

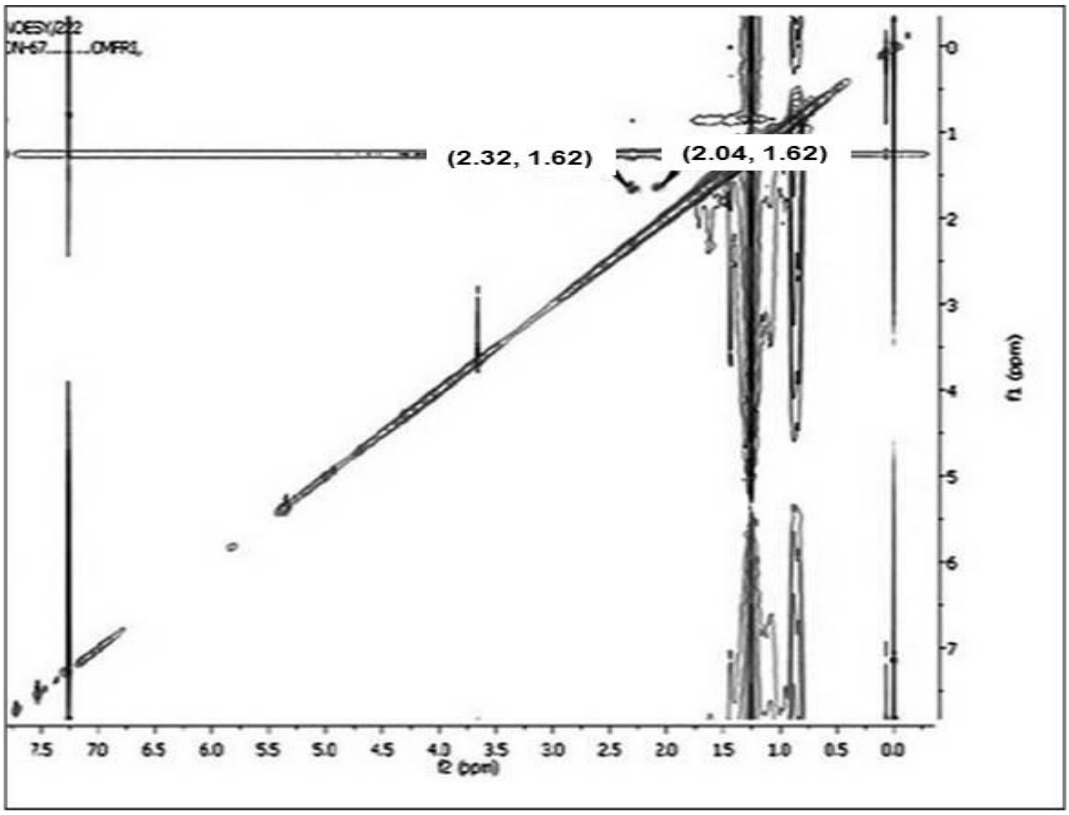

Figure 4.32. Figure showing the NOESY spectrum of compound **K3**

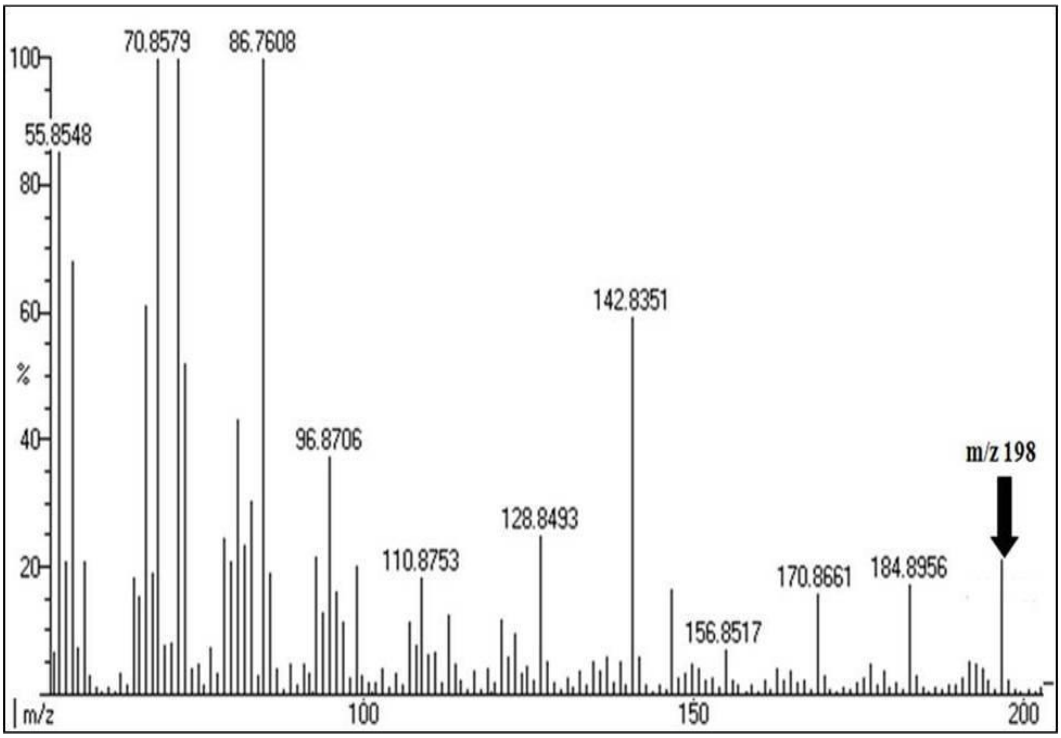

Figure 4.33. Mass spectrum of compound **K3**

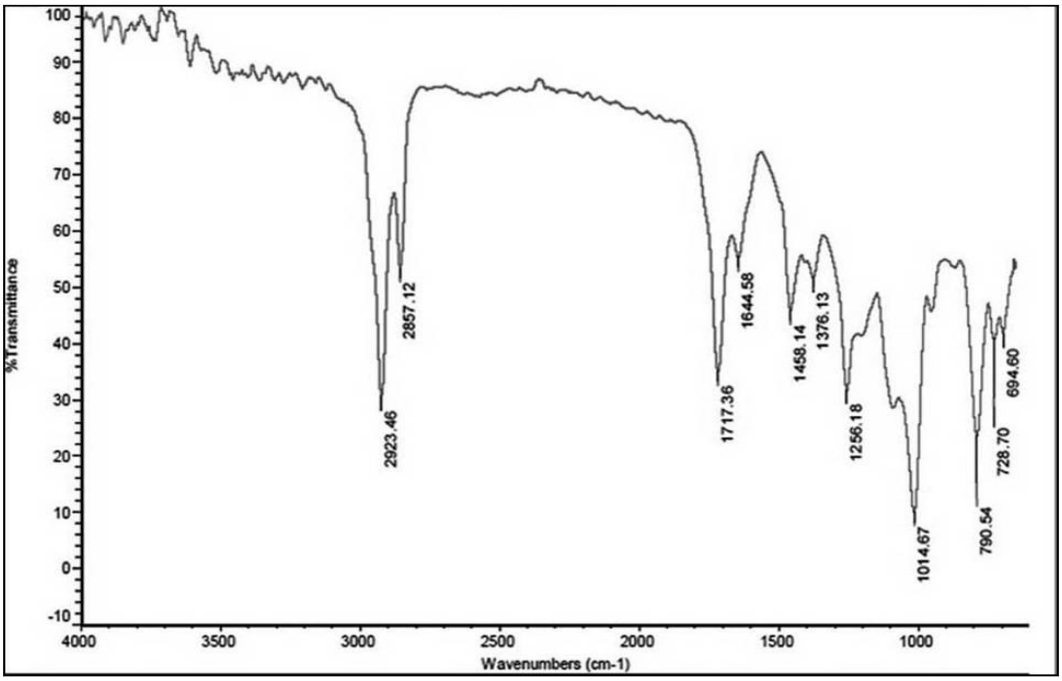

Figure 4.34. Figure showing the FTIR spectrum of compound **K3**

4.3.1.5. Structural Characterization of Compound K4

3-(Methoxymethyl) heptyl-3-(cyclohex-3-enyl) propanoate (**K4**)

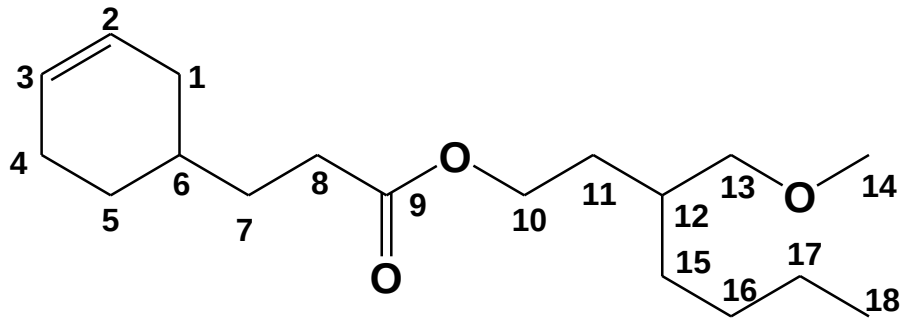

Sample yield	162 mg (1.35 %)
Physical description	Yellow oil
Molecular formula	$C_{18}H_{32}O_3$
Molecular weight	296.2354

3-(Methoxymethyl) heptyl-3-(cyclohex-3-enyl) propanoate: Yellow oil; UV $_{MeOH/DCM}$ λ_{max} (log ε): 238 nm (2.82), 262 nm (2.40); TLC (Si gel GF_{254} 15 mm; MeOH/DCM 1:99, v/v) R_f: 0.80.; R_t (HPLC, ACN: MeOH, 2:4 v/v): 14.2681 min; IR (KBr, cm^{-1}) νmax (ν = stretching, δ = bending, ρ = rocking vibrations): 724.66 (C-H ρ), 878.09 (C-H δ), 1018.99 (C-H ρ), 1114.25 (C-H δ), 1169.65 (C=C ν) 1249.94 (C-CO-C ν), 1366.49 (C=O ν), 1458.06 (C-H ν), 1743.11 (C=O ν), 2856.12 (C-H ν), 2925.01 (C-H ν); ^{1}H NMR (500 MHz $CDCl_3$): δ_H 1.94 (2H, t, *J*=6.13 Hz), δ_H 5.27 (1H, m), δ_H 5.28 (1H, m), δ_H 2.71 (2H, t, *J*=6.69 Hz), δ_H 1.65 (2H, m), δ_H 1.65 (1H, m), δ_H 1.54 (2H, m), δ_H 2.24 (2H, t, *J*=7.34 Hz), δ_H 4.05 (2H, t, *J*=6.85 Hz), δ_H 1.51 (2H, m), δ_H 2.02 (1H, m), δ_H 4.21 (2H, d, *J*=6.78 Hz), δ_H 3.59 (3H, s), δ_H 1.19 (2H, m), δ_H 1.26 (2H, m), δ_H 1.18 (2H, m), δ_H 0.80 (3H, t, *J*=6.77 Hz); ^{13}C NMR (125 MHz, $CDCl_3$): δ_C 27.15 (C-1), δ_C 129.93 (C-2), δ_C 129.92 (C-3), δ_C 25.5 (C-4), δ_C 32.73 (C-5), δ_C 40.19 (C-6), δ_C 24.97 (C-7), δ_C 34.13 (C-8), δ_C 174.37 (C-9), δ_C 62.04 (C-10), δ_C 37.61 (C-11), δ_C 31.50 (C-12), δ_C 62.20 (C-13), δ_C 51.43 (C-14), δ_C 29.56 (C-15), δ_C 28.82 (C-16), δ_C 26.34 (C-17), δ_C 14.11 (C-18); HMBC and ^{1}H-^{1}H-COSY data (Fig. 4.36 to Fig. 4.44, Table 4.8); HR (EI) MS *m/z* measured value 296.2354 $[M]^+$, calcd for $C_{18}H_{32}O_3$ 296.2351.

3-(Methoxymethyl) heptyl-3-(cyclohex-3-enyl) propanoate (compound **K4**), an oxygenated C_{18} meroterpenoid displayed the molecular ion peak at *m/z* 296 enclosing three degrees of unsaturation {due to the ester carbonyl group (δ_C 174.37), olefinic carbon at δ_C 129.92 (C-3), δ_C 129.93 (C-2) and a ring system}, and the molecular formula as $C_{18}H_{32}O_3$ based upon combined ^{1}H and ^{13}C NMR spectral data (Table 4.8). The IR-spectrum of compound **K4** displayed the presence of carbonyl group along with olefinic groups due to the bands recorded at 1458 and 2856 cm^{-1}. The ^{13}C NMR spectrum established the existence of 18 carbon signals constituting eleven methylene, two methine, along with one each of carbonyl, olefinic, methyl and methoxy carbons.

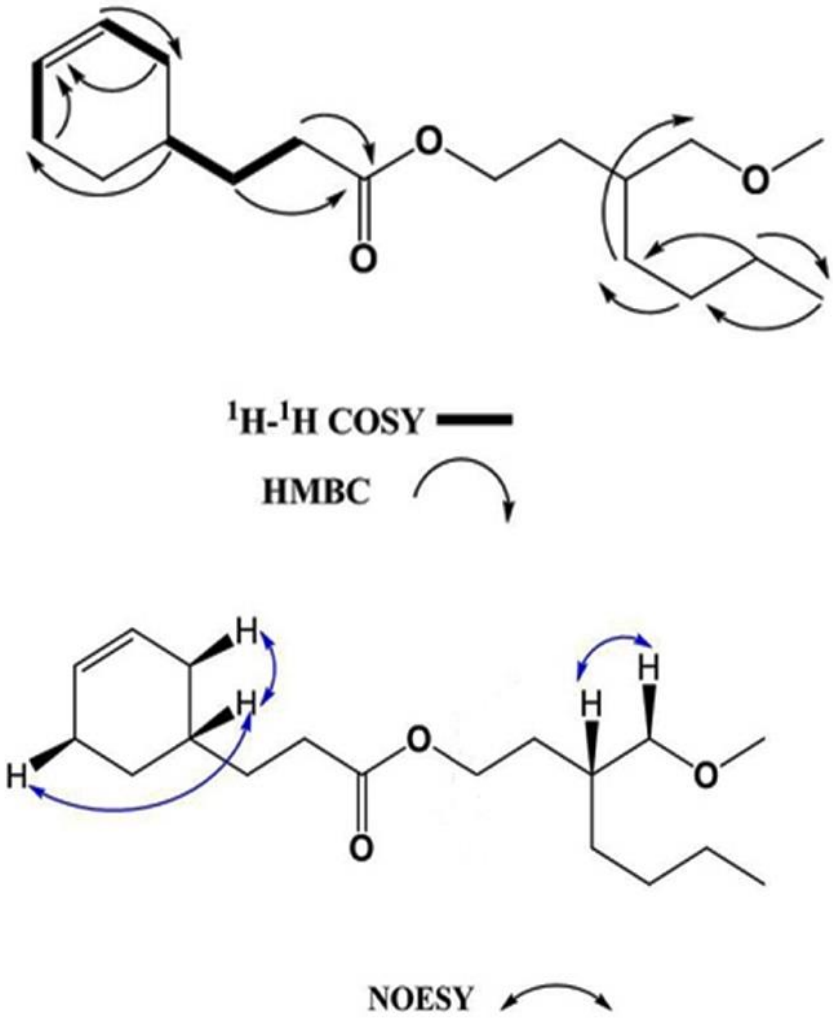

Figure 4.35. Figure showing key ^{1}H-^{1}H COSY, HMBC and NOESY correlations of compound **K4**. The ^{1}H-^{1}H COSY cross peaks were displayed by bold face bonds, whereas the selected HMBC correlations were shown as double barbed arrows. The β orientation in the NOESY relations was presented as blue colored arrows

The ^{1}H NMR in combination with ^{13}C NMR experiments demonstrated highly deshielded oxymethylene protons at H-10 (δ_H 4.05, *J*=6.85 Hz) and H-13 (δ_H 4.21, *J*=6.78 Hz) that were deduced to be correlated with the corresponding carbon signals at C-10 and C-13 methylene groups, and that was further corroborated based on the existence of an ester carbonyl {δ_C 174.37 (C-9)} and sharp singlet (integral of three) of O-CH_3 group in the NMR spectrum. The ^{1}H-^{1}H COSY correlations between δ_H 1.94 (denoted as H-1)/δ_H 5.27 (H-2) and δ_H 5.28 (assigned to H-3)/δ_H 2.71 (H-4) were

ascribed to the cyclohexane ring framework. The J^{1-3} HMBC correlation between δ_H 1.94 (denoted as H-1) to δ_C 129.92 (C-3), δ_H 5.27 (H-2) to δ_C 27.15 (C-1) and δ_H 2.71 (H-4) to δ_C 129.92 (C-3) attributed the presence of cyclohexene ring system (Fig. 4.46).

The methine (-CH) carbon at C-6 (δ_C 40.19) recognized the junction of cyclohexene ring moiety and was substituted with 3-(methoxymethyl) heptyl butyrate skeleton. This was corroborated by the $^1H–^1H$ COSY and J^{1-3} HMBC correlations. HMBC cross peaks between δ_H 1.54 (assigned as H-7) to δ_C 174.37 (C-9), δ_H 2.24 (H-8) to δ_C 174.37 (C-9) appropriately supported the presence of ester carbonyl carbon attached to the cyclohexene ring system. Additional J^{1-3} HMBC correlations were displayed between δ_H 1.19 (assigned to H-15) to δ_C 62.20 (C-13), δ_H 1.26 (H-16) to δ_C 29.56 (C-15), δ_H 1.18 (H-17) to δ_C 29.56 (C-15)/δ_C 14.11 (C-18), δ_H 0.80 (H-18) to δ_C 28.82 (C-16), which apparently indicated the substitution of 3-(methoxymethyl) heptyl butyrate to the cyclohexene ring system. The methoxy group was found to appear as a singlet at δ_H 3.59 (attributed to H-14; HSQC δ_C 51.43 at C-14) to support the presence of 3-(methoxymethyl) heptyl butyrate framework. In addition, the olefinic group was found to appear as the multiplet at δ_H 5.27-5.28 (H2-H3) {HSQC, δ_C 129.93 (C-2), δ_C 129.92 (C-3)}, which attributed to the cyclohexene ring framework. The chemistries of the stereogenic centres bearing protons were derived using coupling constant values and NOESY experiments. An intense NOE correlation was displayed between the protons at δ_H 1.65 (H-6) and δ_H 1.94 (H-1; J=6.13 Hz)/δ_H 2.71 (H-4; J=6.69 Hz), which suggested their equi-planer disposition, and was arbitrarily attributed as β-oriented. Strong NOE correlation between δ_H 2.02 (H-12; J=6.69 Hz) and δ_H 4.21 (H-13; J=6.78 Hz) attributed the protons to dispose at the β-side of the reference plane, which suggested their diaxial orientation with reference to the plane of the symmetry.

Table 4.8 NMR spectroscopic data of compound **K4** in $CDCl_3$[a]

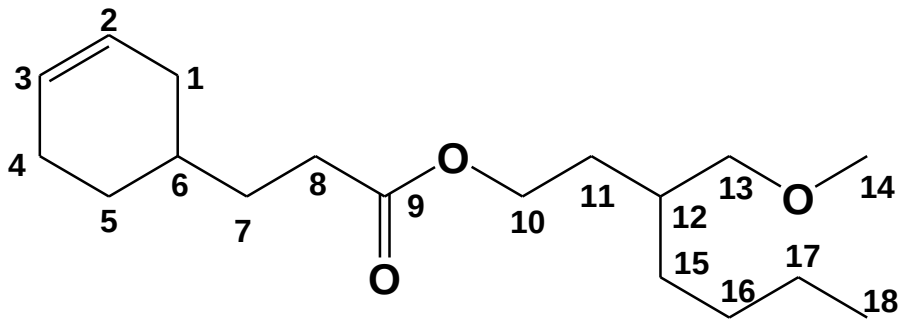

C. No	^{13}C (δ)	^{1}H-NMR[b] (int., mult., *J* in Hz)	^{1}H-^{1}H COSY	HMBC (^{1}H-^{13}C)
1	27.15	1.94 (t, *J*=6.13 Hz, 2H)	2-H	C-3
2	129.93	5.27 (m,1H)	1-H	C-1
3	129.92	5.28 (m,1H)	4-H	-
4	25.5	2.71 (t, *J*=6.69 Hz, 2H)	3-H	C-3
5	32.73	1.65 (m, 2H)	-	-
6	40.19	1.65 (m, 1H)	-	C-4
7	24.97	1.54 (m, 2H)	8-H	C-9
8	34.13	2.24 (t, *J*=7.34 Hz, 2H)	7-H	C-9
9	174.37	-	-	-
10	62.04	4.05 (t, *J*=6.85 Hz, 2H)	-	-
11	37.61	1.51 (m, 2H)	-	-
12	31.50	2.02 (m, 1H)	-	-
13	62.20	4.21 (d, *J*=6.78 Hz, 2H)	-	-
14	51.43	3.59 (s, 3H)	-	-
15	29.56	1.19 (m,2H)	-	C-13
16	28.82	1.26 (m, 2H)	-	C-15
17	26.34	1.18 (m, 2H)	-	C-15, C-18
18	14.11	0.80 (t, *J*=6.77 Hz, 3H)	-	C-16

[a] NMR spectra recorded using Bruker AVANCE III 500 MHz (AV 500) spectrometer in $CDCl_3$ as aprotic solvent at ambient temperature with TMS as the internal standard (δ 0 ppm).

[b] Values in ppm, multiplicity and coupling constants (*J*=Hz) are indicated in parentheses. The assignments were made with the aid of the ^1H-^1H COSY, HSQC, HMBC and NOESY experiment

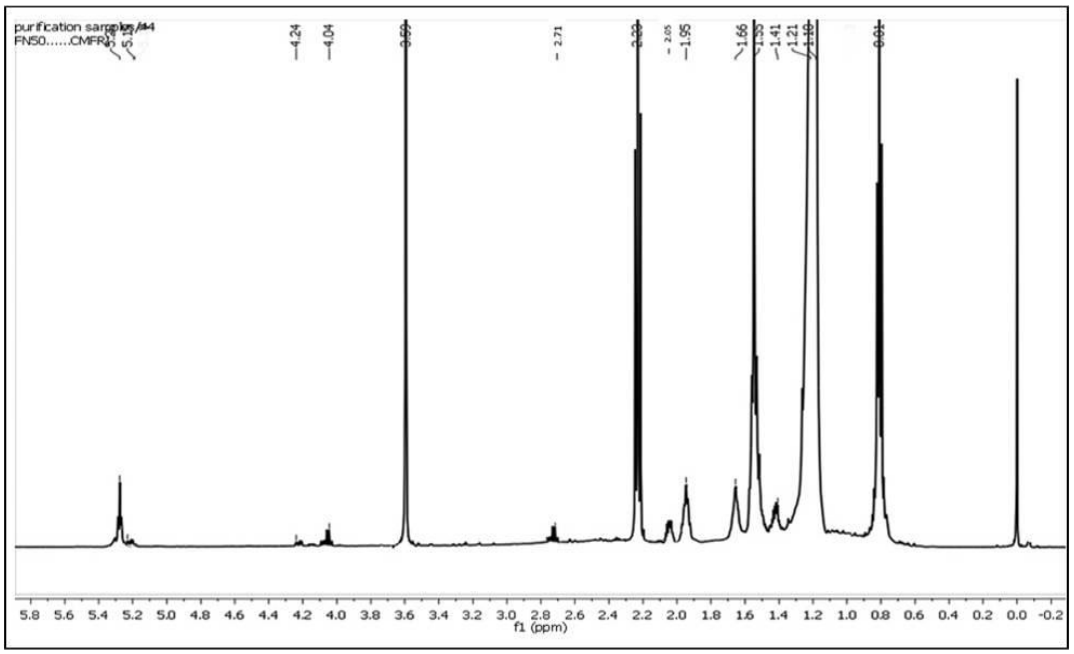

Figure 4.36. Figure showing the ^1H NMR spectrum of compound **K4**

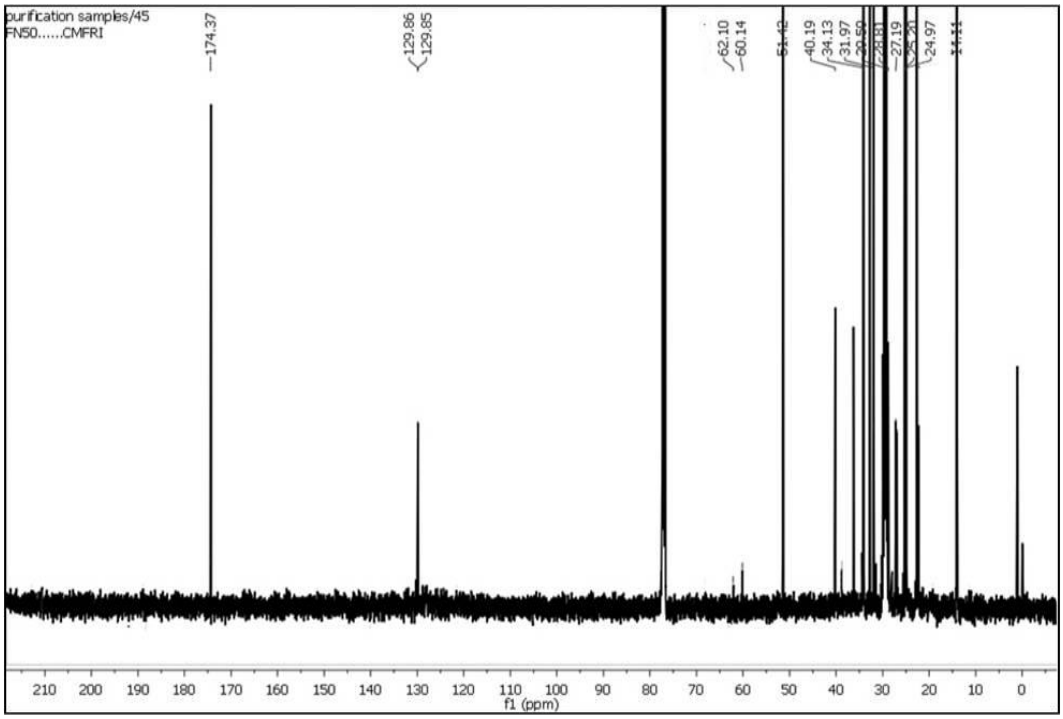

Figure 4.37. Figure showing the ^{13}C NMR spectrum of compound **K4**

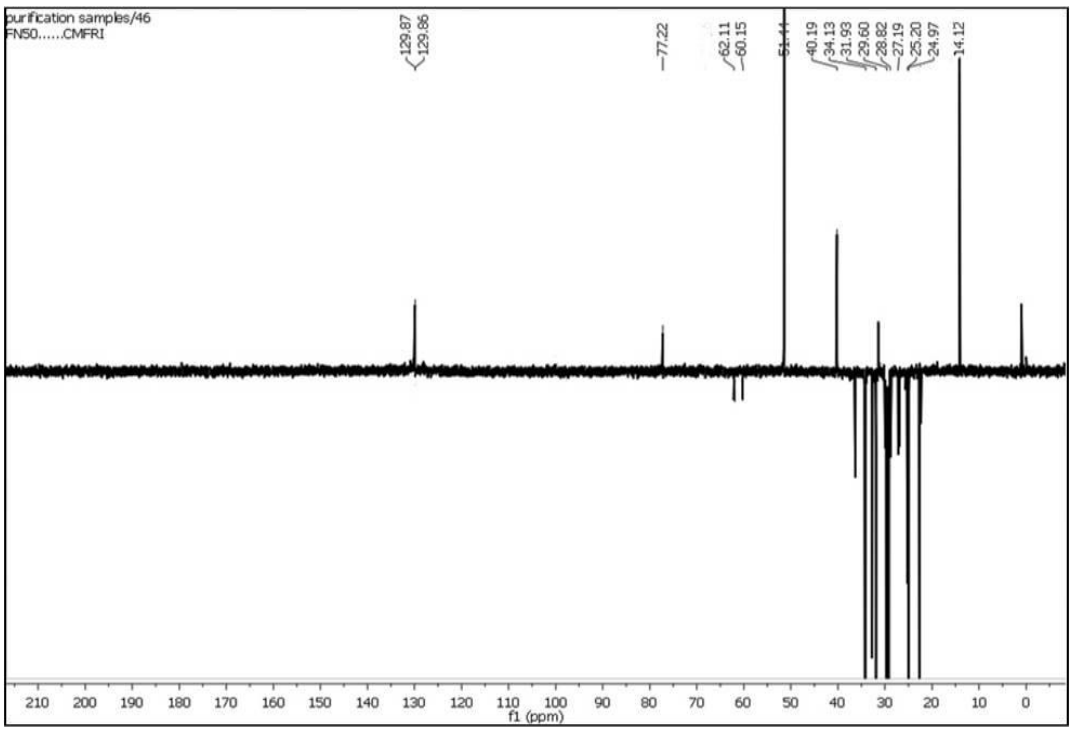

Figure 4.38. Figure showing the DEPT spectrum of compound **K4**

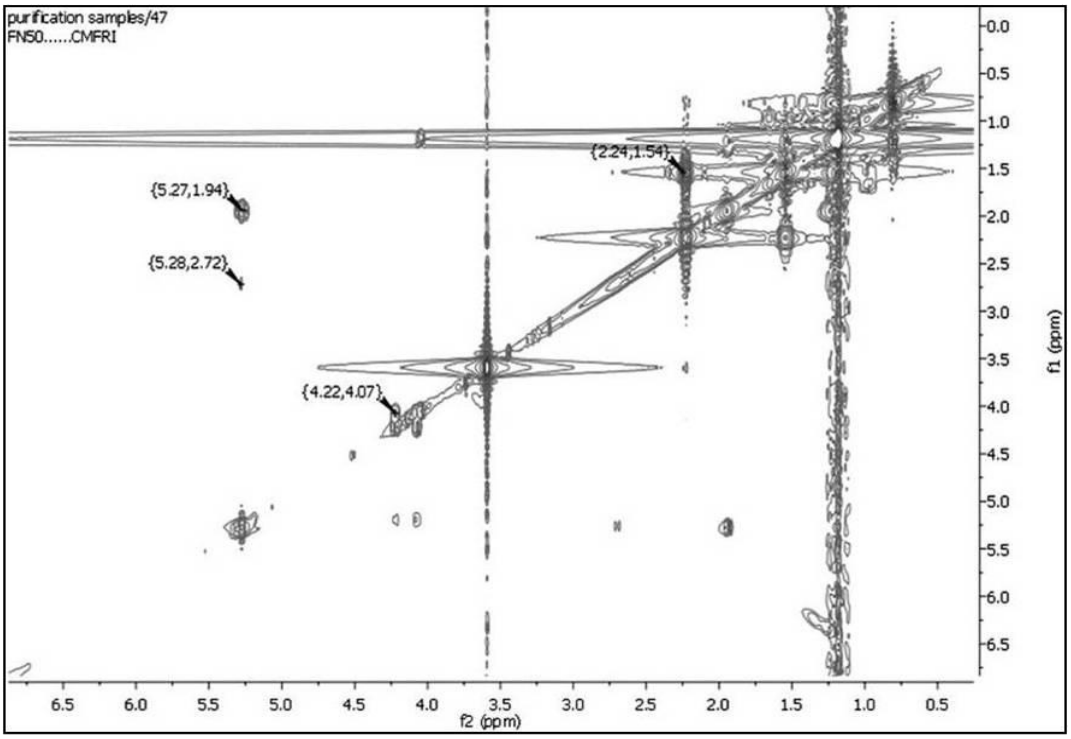

Figure 4.39. Figure showing the ^{1}H-^{1}H COSY spectrum of compound **K4**

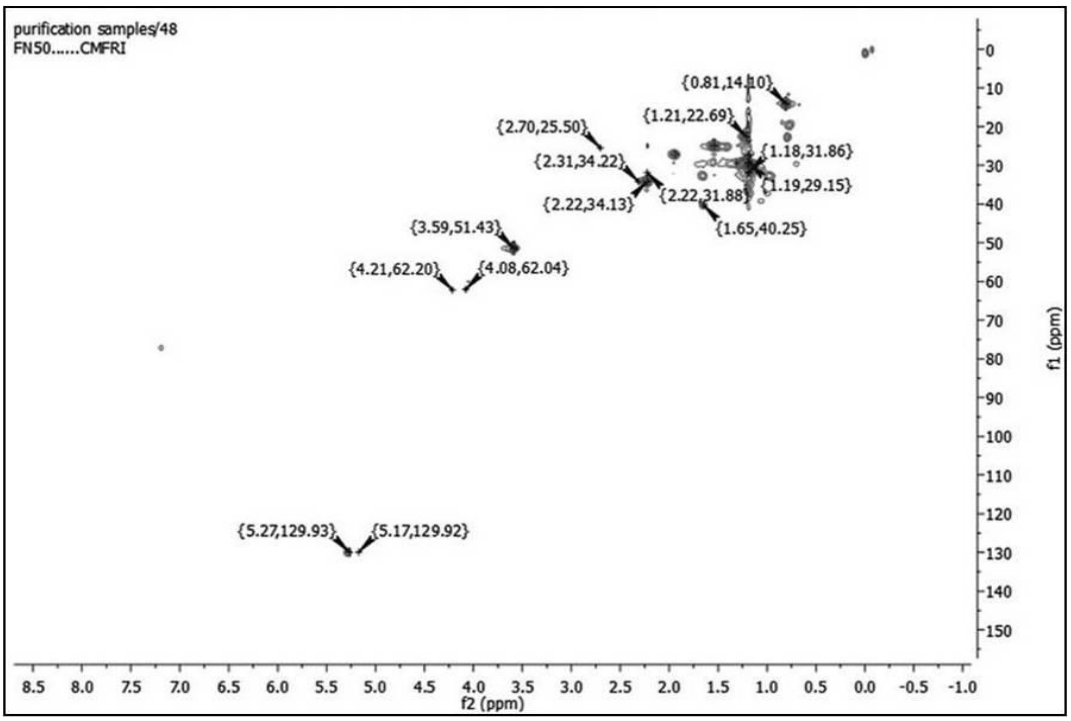

Figure 4.40. Figure showing the HSQC spectrum of compound **K4**

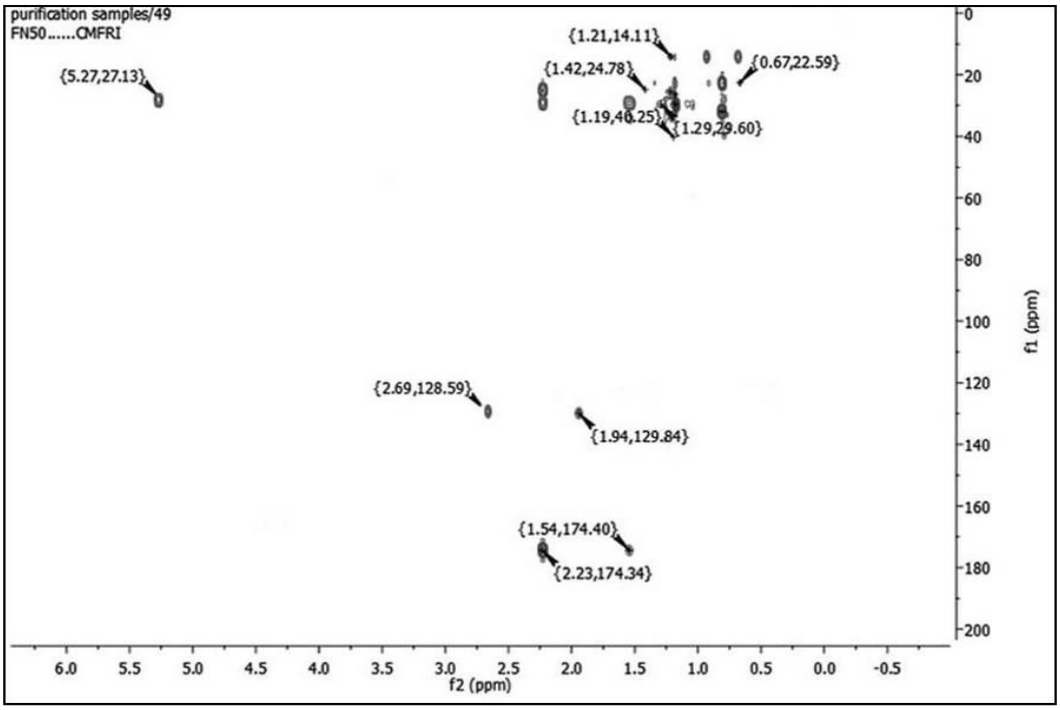

Figure 4.41. Figure showing the HMBC spectrum of compound **K4**

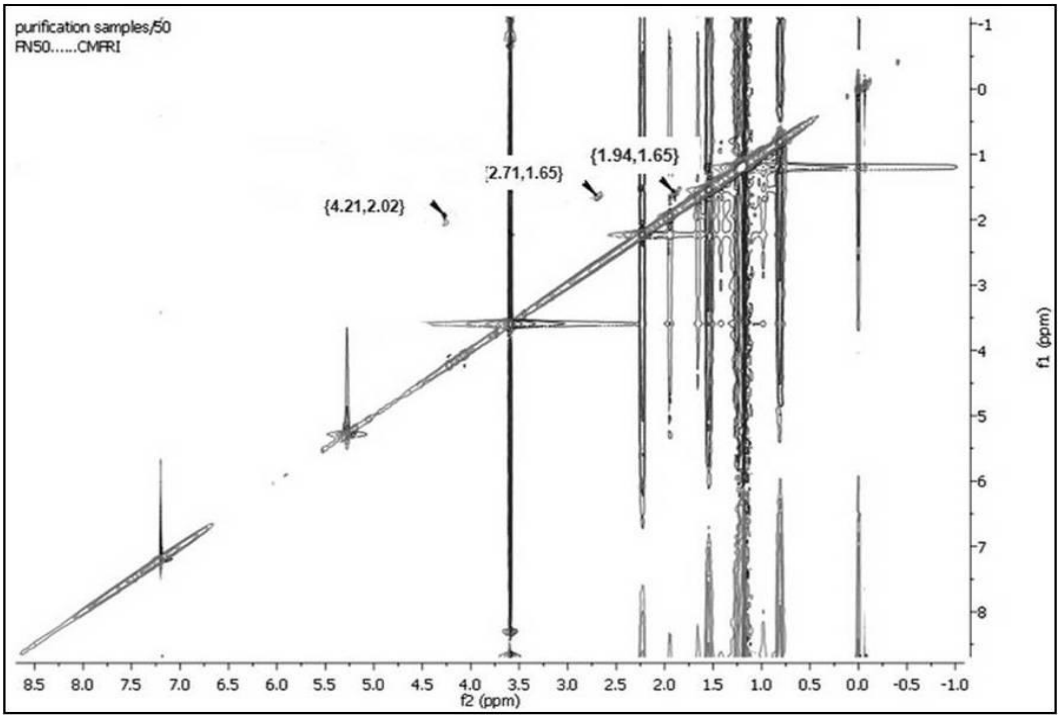

Figure 4.42. Figure showing the NOESY spectrum of compound **K4**

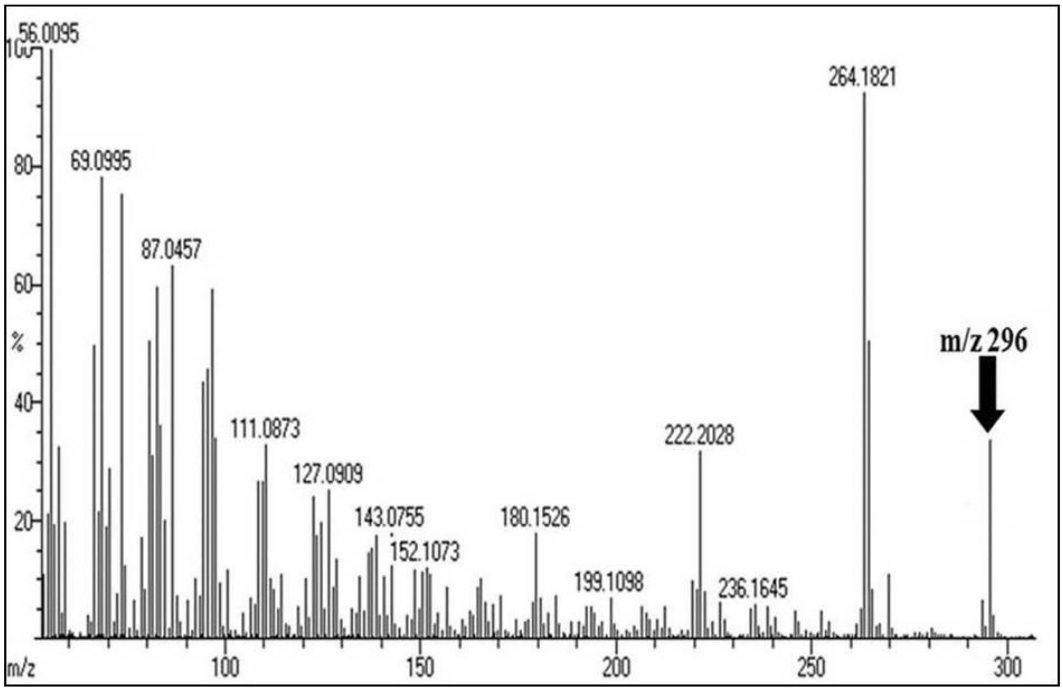

Figure 4.43. Mass spectrum of compound **K4**

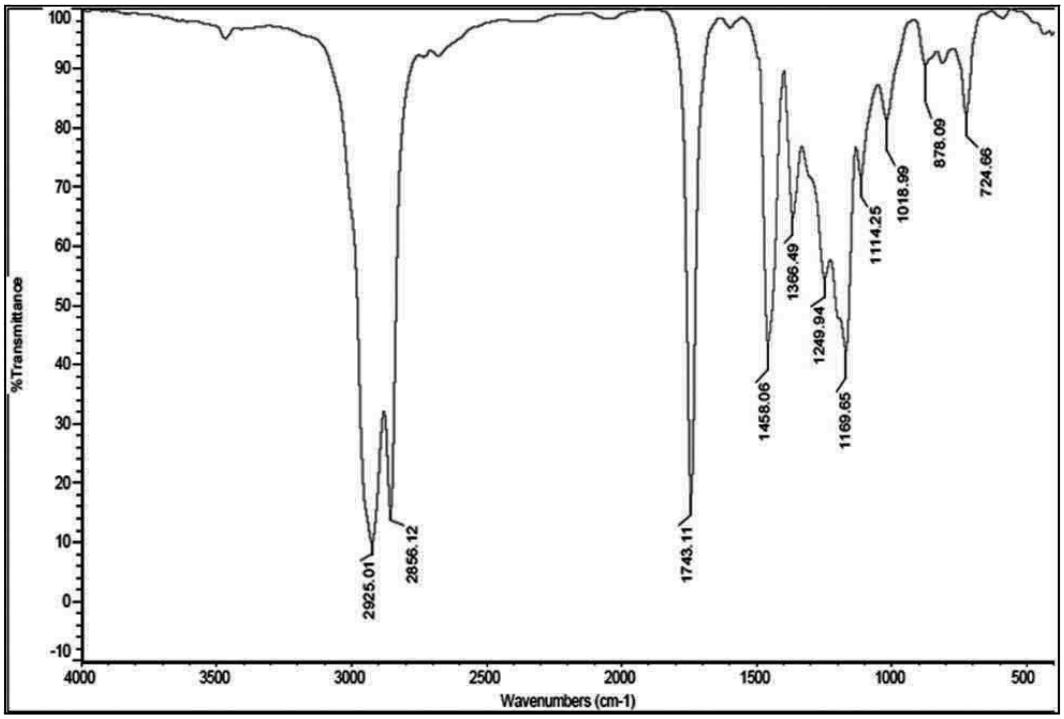

Figure 4.44. Figure showing the FTIR spectrum of compound **K4**

4.3.1.6. Structural Characterization of Compound K5

2-Ethyl-6-(4-methoxy-2-((2-oxotetrahydro-2*H*-pyran-4-yl) methyl) butoxy)-6-oxohexyl-5-ethyloct-4-enoate (**K5**)

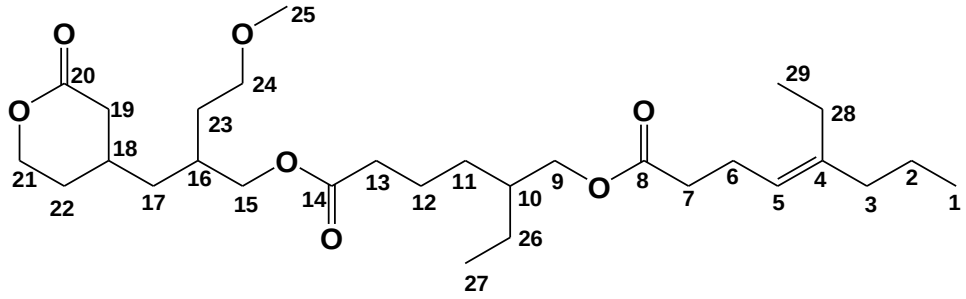

Sample yield	142 mg (1.18 %)
Physical description	Yellow oil
Molecular formula	$C_{29}H_{50}O_7$
Molecular weight	510.3557

2-Ethyl-6-(4-methoxy-2-((2-oxotetrahydro-2*H*-pyran-4-yl) methyl) butoxy)-6-oxohexyl-5-ethyloct-4-enoate : Yellow oil; UV $_{MeOH}\lambda_{max}$ (log ε): 245 nm (3.26); TLC (Si gel GF_{254} 15 mm; MeOH/$CHCl_3$ 1:19, v/v) R_f: 0.96; R_t (HPLC, MeOH: ACN, 2:1 v/v): 14.401 min; IR (KBr, cm^{-1}) νmax (ν = stretching, δ = bending, ρ = rocking vibrations): 738.89 (C-H ρ), 1073.42 (C-O ν), 1125.95 (CH_2 wag), 1170.14 (C-O ν), 1280.43 (CH_2 ν) 1369.88 (C-H ρ), 1455.83 (C-H δ), 1589.64 (C=C ν), 1736.56 (C=O ν), 2857.58, 2926.28 (C-H ν); ^{1}H NMR (500 MHz $CDCl_3$): δ_H 0.87 (3H, t, *J*=6.80 Hz), δ_H 1.30 (2H, m), δ_H 2.02 (2H, m), δ_H 5.35 (1H, t, *J*=5.68 Hz), δ_H 2.02 (2H, m), δ_H 2.32 (2H, t, *J*=7.80 Hz), δ_H 4.16 (2H, d, *J*=5.80 Hz), δ_H 1.73 (1H, m), δ_H 1.27 (2H, m), δ_H 1.62 (2H, m), δ_H 2.32 (2H, t, *J*=7.80 Hz), δ_H 4.26 (2H, d, *J*=9.08 Hz), δ_H 2.49 (1H, m), δ_H 1.50 (2H, m), δ_H 1.69 (1H, m), δ_H 2.32 (2H, t, *J*=7.80 Hz), δ_H 4.19 (2H, t, *J*=9.08 Hz), δ_H 1.69 (2H, m), δ_H 1.73 (2H, m), δ_H 4.30 (2H, t, *J*=7.44 Hz), δ_H 3.67 (3H, s), δ_H 1.42 (2H, m), δ_H 0.85 (3H, t, *J*=6.80 Hz), δ_H 2.13 (2H, m), δ_H 0.87 (3H, t, *J*=7.17 Hz); ^{13}C NMR (125 MHz, $CDCl_3$): δ_C 14.20 (C-1), δ_C 25.12 (C-2), δ_C 28.24 (C-3), δ_C 132.45 (C-4), δ_C 130.08 (C-5), δ_C 34.11 (C-6), δ_C 29.67 (C-7), δ_C 174.56 (C-8), δ_C 62.17 (C-9), δ_C 40.19 (C-10), δ_C 29.65 (C-11), δ_C 28.99 (C-12), δ_C 24.98 (C-13), δ_C 168.33 (C-14),

δ_C 68.24 (C-15), δ_C 34.39 (C-16), δ_C 29.26 (C-17), δ_C 38.88 (C-18), δ_C 32.14 (C-19), δ_C 173.48 (C-20), δ_C 60.14 (C-21), δ_C 30.78 (C-22), δ_C 32.73 (C-23), δ_C 65.68 (C-24), δ_C 51.42 (C-25), δ_C 29.85 (C-26), δ_C 19.70 (C-27), δ_C 30.07 (C-28), δ_C 22.80 (C-29) HMBC and ^{1}H-^{1}H-COSY data (Fig. 4.47 to Fig. 4.55, Table 4.9); HR (EI) MS *m/z* measured value 510.3557 $[M]^+$, calcd for $C_{29}H_{50}O_7$ 510.3552.

2-Ethyl-6-(4-methoxy-2-((2-oxotetrahydro-2*H*-pyran-4-yl) methyl) butoxy)-6-oxohexyl-5-ethyloct-4-enoate (compound **K5)**, a highly oxygenated C_{29} meroterpenoid, was purified as yellow oil with *m/z* 510 bearing five degrees of unsaturation, and its structure was characterized by combined ^{1}H and ^{13}C NMR spectral experiments. The IR bending vibration near 1736 cm^{-1} was associated with the carbonyl group, whereas the olefinic groups were assigned to the absorption bands at 1455 cm^{-1} and 2857 cm^{-1}. The ^{13}C NMR spectroscopic data deduced the existence of 29 carbon signals constituting three each of methyl, methylene and ester carbonyl groups along with seventeen methylene and one each of olefinic and methoxy carbons.

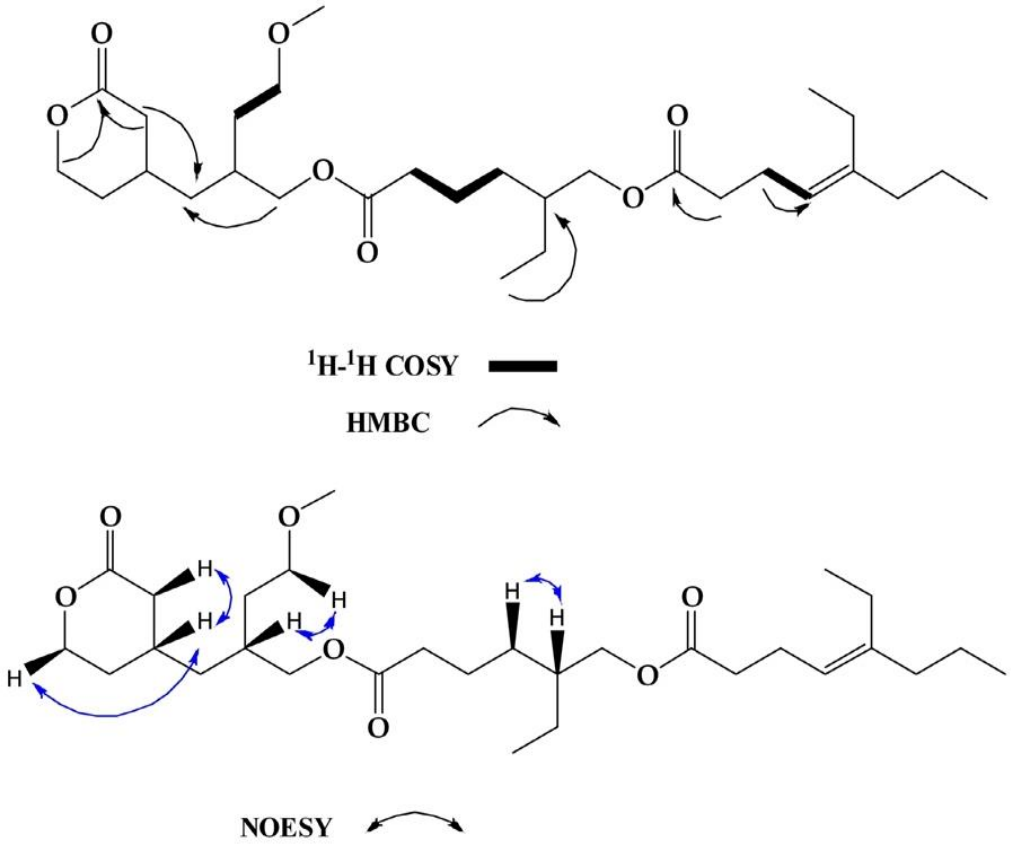

Figure 4.45. Key ^{1}H-^{1}H COSY, HMBC and NOESY correlations of compound **K5.** The ^{1}H-^{1}H COSY cross peaks were displayed by bold face bonds, whereas the selected

HMBC correlations were shown as double barbed arrows. The β orientation in the NOESY relations was presented as blue colored arrows. The ^{1}H NMR in combination with ^{13}C NMR demonstrated highly deshielded oxymethylene protons at δ_H 4.16 (attributed to H-9, *J*=5.80 Hz), δ_H 4.19 (H-21, *J*=9.08 Hz), δ_H 4.26 (H-15, *J*=9.08 Hz) and δ_H 4.30 (H-24, *J*=7.44 Hz) in the proton spectrum suggesting that the C-24, C-21, C-15 and C-9 methylene groups were attached to an electronegative group, possibly of oxygenated origin. This was further corroborated by the presence of ester carbonyl carbons {δ_C 174.56 (assigned to C-8), δ_C 168.33 (C-14), δ_C 173.48 (C-20)} and a singlet (integral of three) of O-CH_3 group {δ_C 51.42 (C-25)}, in the NMR spectrum. The proton-proton connections were apparent between δ_H 1.73 (ascribed to H-23)/δ_H 4.30 (H-24) that assigned the part of a tetrahydro-2*H*-pyran-2-one ring framework. The $J^{1\text{-}3}$ HMBC correlations between δ_H 2.32 (ascribed to H-7) to δ_C 174.56 (C-8), δ_H 4.26 (H-15) to δ_C 29.26 (C-17), δ_H 4.19 (H-21) to δ_C 173.48 (C-20) and δ_H 2.32 (H-19) to δ_C 29.26 (C-17)/173.48 appropriately deduced the existence of highly deshielded oxymethylene protons and ester carbonyl carbon as part of the tetrahydro-2*H*-pyran-2-one ring framework. The ^{1}H–^{1}H COSY correlation between δ_H 1.27 (ascribed to H-11)/δ_H 1.62 (H-12)/δ_H 2.32 (H-13) were probably attributed to the part of substituted tetrahydro-2*H*-pyranone ring system (Fig. 4.56). In addition, an olefinic group was found to appear as the multiplet at δ_H 5.35 (H-4/H-5) {HSQC, δ_C 132.45 (C-4) and δ_C 130.08 (C-5)}, which was situated at the extended side chain of compound **K5**. The ^{1}H-^{1}H correlation between δ_H 5.35 (denoted as H-5)/δ_H 2.02 (H-6) and a HMBC correlation between δ_H 2.02 (assigned as H-6) to δ_C 130.08 (C-5) appropriately established the existence of the olefinic group (Fig. 4.56). The HMBC correlation from δ_H 1.42 (assigned as H-26) to δ_C 29.85 (C-10) deduced the substitution of 2-ethyl-6-(2-ethyl-4-methoxybutoxy)-6-oxohexyl-5-ethyloct-4-enoate to the pyran-2-one ring system in compound **K5**. The methoxy group was found to appear as singlet at δ_H 3.67 {attributed to H-25; HSQC δ_C 51.42 (C-25)}, which described the 2-ethyl-6-(2-ethyl-4-methoxybutoxy)-6-oxohexyl-5-ethyloct-4-enoate framework. The relative stereochemistries of the stereogenic centres in compound **K5** were deduced by NOESY experiments and coupling constant values (*J*). NOE cross peaks at δ_H 1.69 (H-18)/δ_H 4.19 (H-21; *J*=9.08 Hz)/δ_H 2.32 (H-19; *J*=7.80 Hz) appropriately suggested their close proximity and equi-planer orientation (arbitrarily assigned to β-faced). NOE correlation between the di-equatorial protons at δ_H 4.30 (H-24; *J*=7.44 Hz)/δ_H 2.49 (H-16) apparently attributed to their close spatial arrangements, and therefore, were assigned to

be at the β-face with reference to the molecular plane of symmetry. Likewise, an intense NOE correlation was observed between δ_H 1.73(H-10)/δ_H 1.27 (H-11) that implied their deposition on the same side of the plane with di-axial interaction.

Figure 4.46. Oxygenated meroterpenoids, isolated from red marine macroalga *K. alvarezii*. The thalli of the studied macroalga were displayed as inset

Table 4.9 NMR spectroscopic data of compound **K5** in $CDCl_3$[a]

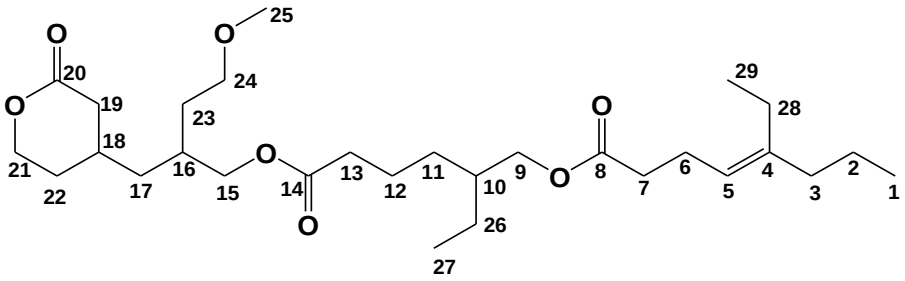

C. No	^{13}C (δ)	^{1}H-NMR[b] (int., mult., *J* in Hz)	^{1}H-^{1}H COSY	HMBC (^{1}H-^{13}C)
1	14.20	0.87(3H, *J*=6.80 Hz, t)		-
2	25.12	1.30 (2H, m)	-	-
3	28.24	2.02 (2H, m)	-	-
4	132.45	-	-	-
5	130.08	5.35 (1H, *J*=5.68 Hz, t)	6-H	-
6	34.11	2.02 (2H, m)	5-H	C-5
7	29.67	2.32 (2H, *J*=7.80 Hz, t)	-	C-8
8	174.56	-	-	-
9	62.17	4.16 (2H, *J*=5.80 Hz, d)	-	-
10	40.19	1.73 (1H, m)	-	-
11	29.65	1.27 (2H, m)	12-H	-
12	28.99	1.62 (2H, m)	11-H, 13-H	-
13	24.98	2.32 (2H, *J*=7.80 Hz, t)	12-H	-
14	168.33	-	-	-
15	68.24	4.26 (2H, *J*=9.08 Hz, d)	-	C-17
16	34.39	2.49 (1H, m)	-	-
17	29.26	1.50 (2H, m)	-	-
18	38.88	1.69 (1H, m)	-	-
19	32.14	2.32 (2H, *J*=7.80 Hz, t)	-	C-20, C-17
20	173.48	-	-	-
21	60.14	4.19 (2H, *J*=9.08 Hz, t)	-	C-20
22	30.78	1.69 (2H, m)	-	-
23	32.73	1.73 (2H, m)	24-H	-
24	65.68	4.30 (2H, *J*=7.44 Hz, t)	23-H	-
25	51.42	3.67 (3H, s)	-	-
26	29.85	1.42 (2H, m)	-	C-10
27	19.70	0.85 (3H, *J*=6.80 Hz, t)		
28	30.07	2.13 (2H, m)	-	-
29	22.80	0.87 (3H, *J*=7.17 Hz, t)	-	-

[a] NMR spectra recorded using Bruker AVANCE III 500 MHz (AV 500) spectrometer in $CDCl_3$ as aprotic solvent at ambient temperature with TMS as the internal standard (δ 0 ppm).

[b] Values in ppm, multiplicity and coupling constants (*J*=Hz) are indicated in parentheses. The assignments were made with the aid of the ^1H-^1H COSY, HSQC, HMBC and NOESY experiment

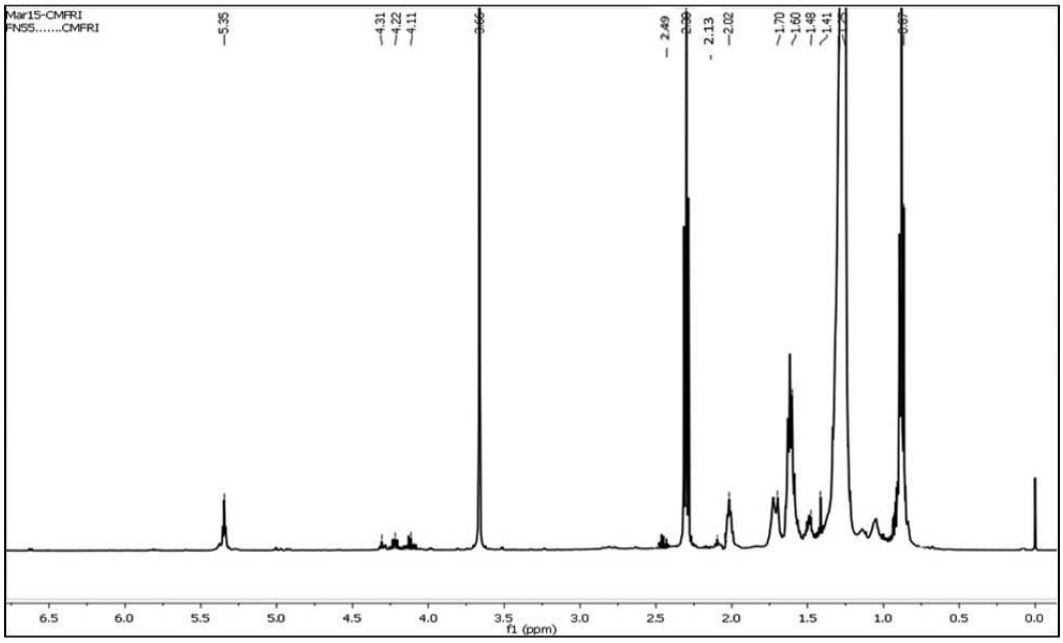

Figure 4.47. Figure showing the ^1H NMR spectrum of compound **K5**

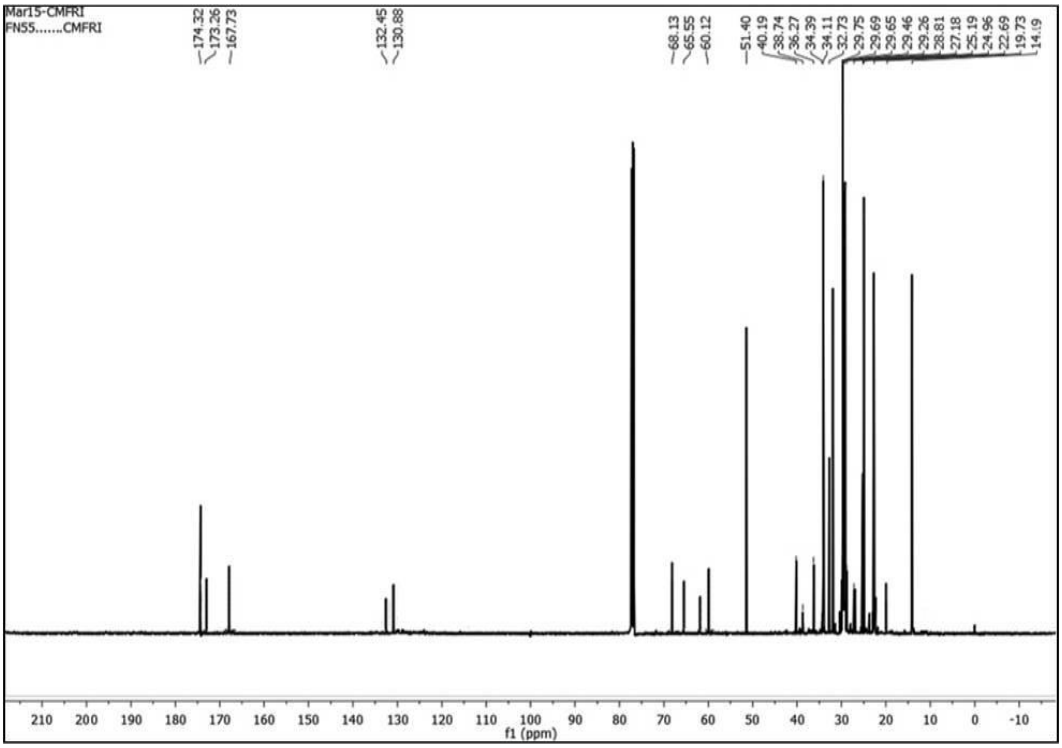

Figure 4.48. Figure showing the ^{13}C NMR spectrum of compound **K5**

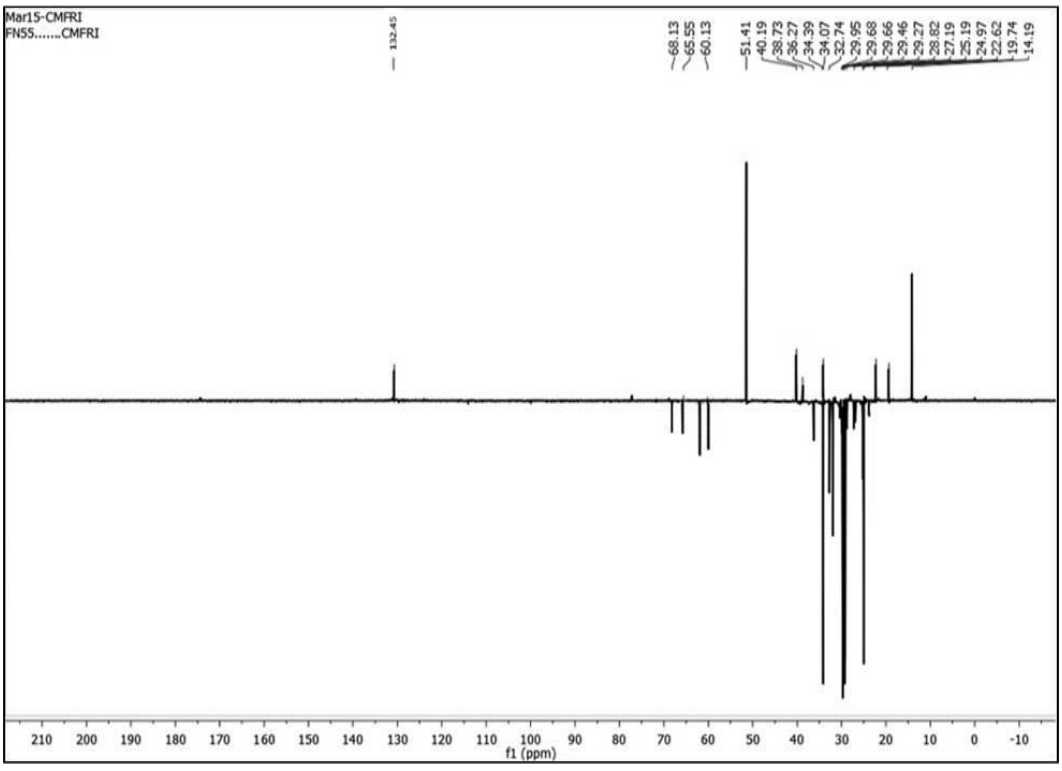

Figure 4.49. Figure showing the DEPT spectrum of compound **K5**

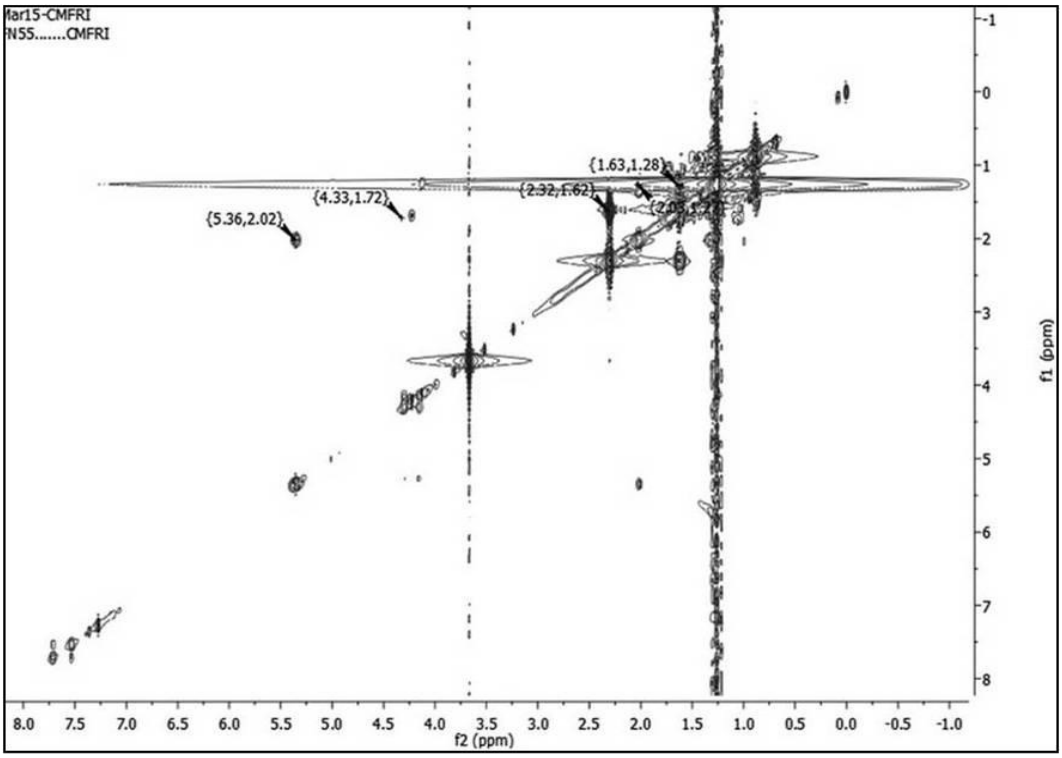

Figure 4.50. Figure showing the ^{1}H-^{1}H COSY spectrum of compound **K5**

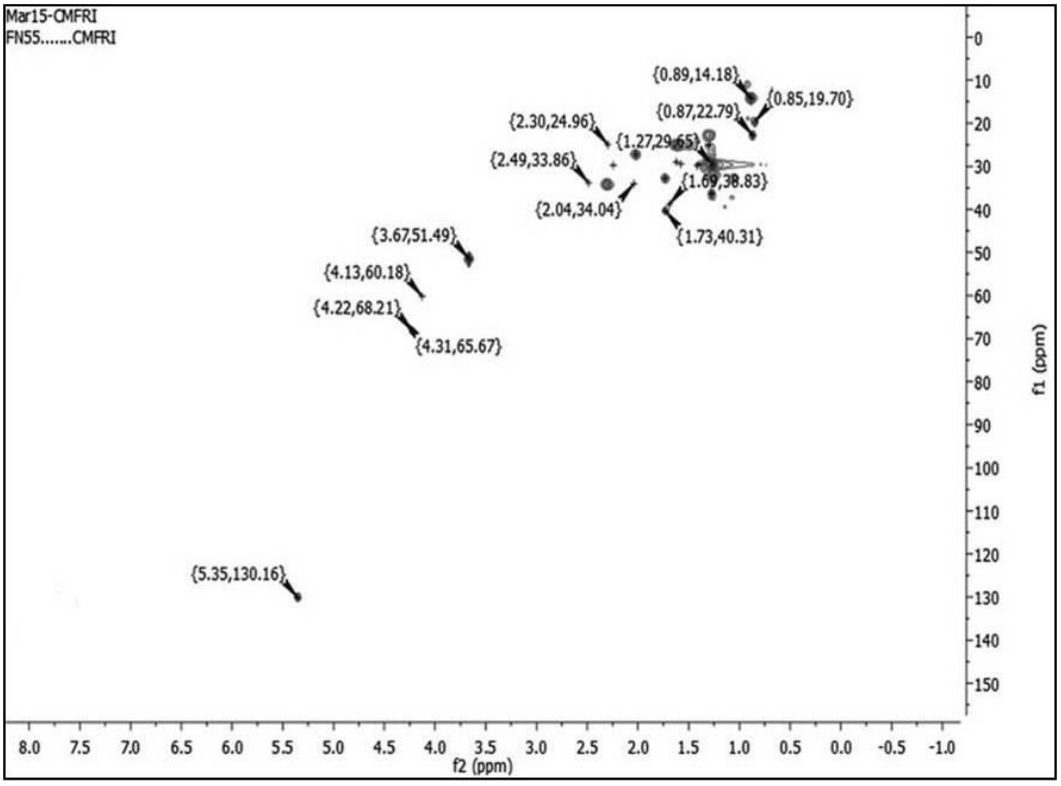

Figure 4.51. Figure showing the HSQC spectrum of compound **K5**

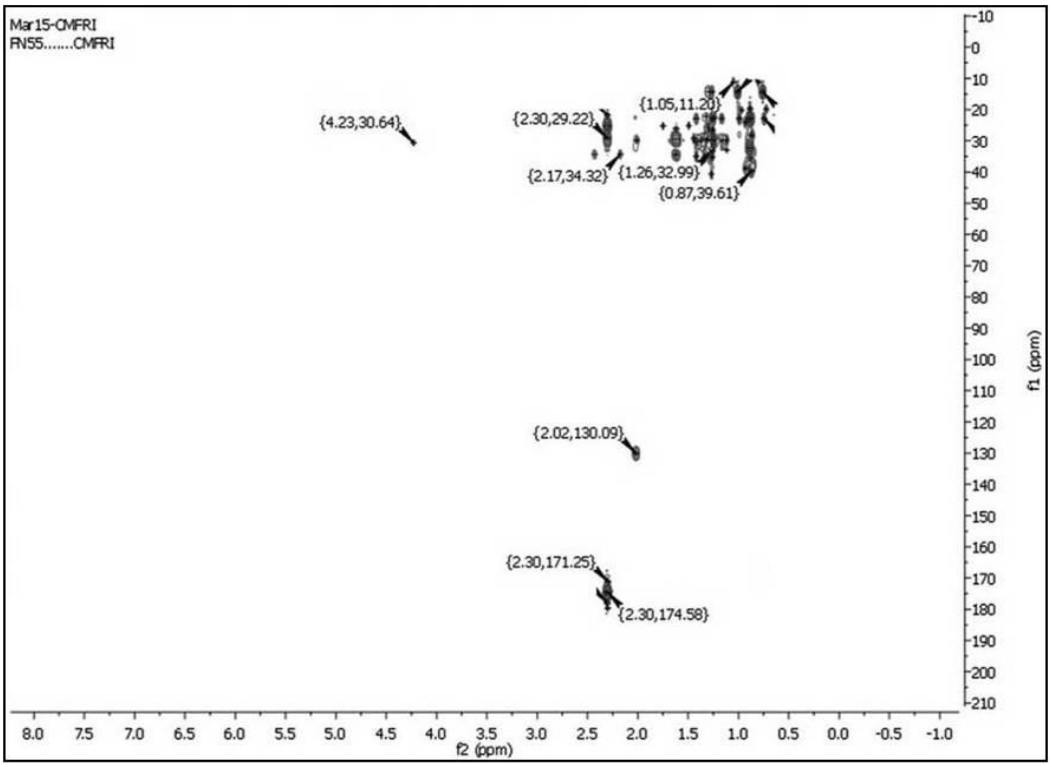

Figure 4.52. Figure showing the HMBC spectrum of compound **K5**

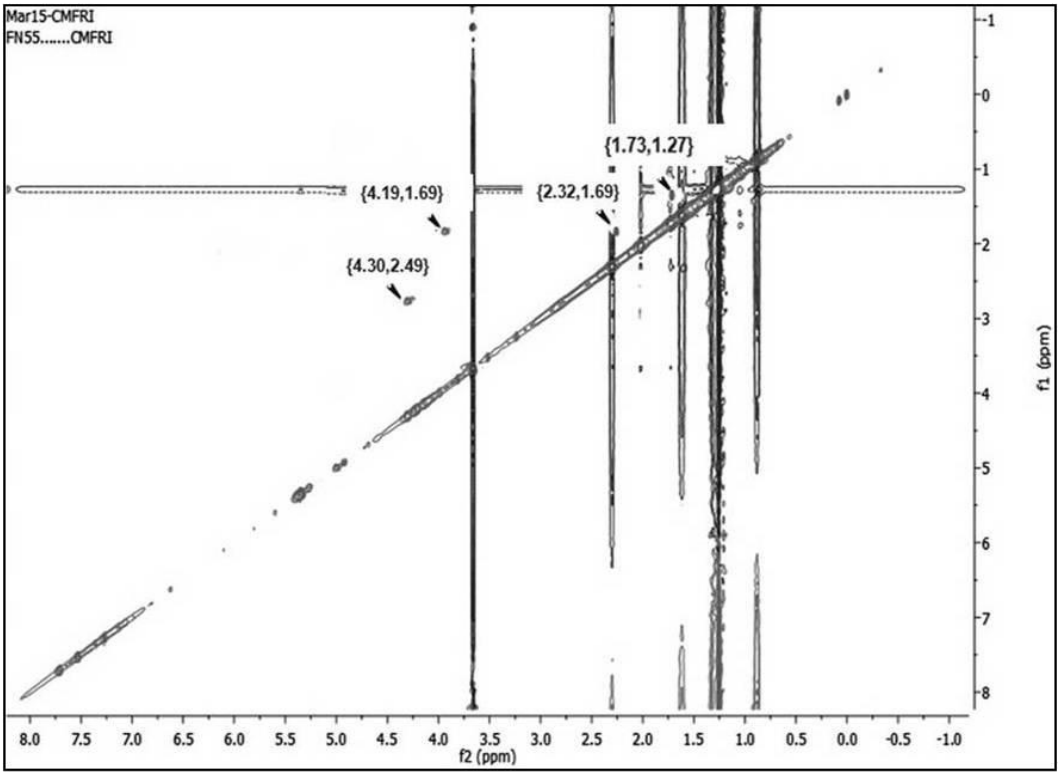

Figure 4.53. Figure showing the NOESY spectrum of compound **K5**

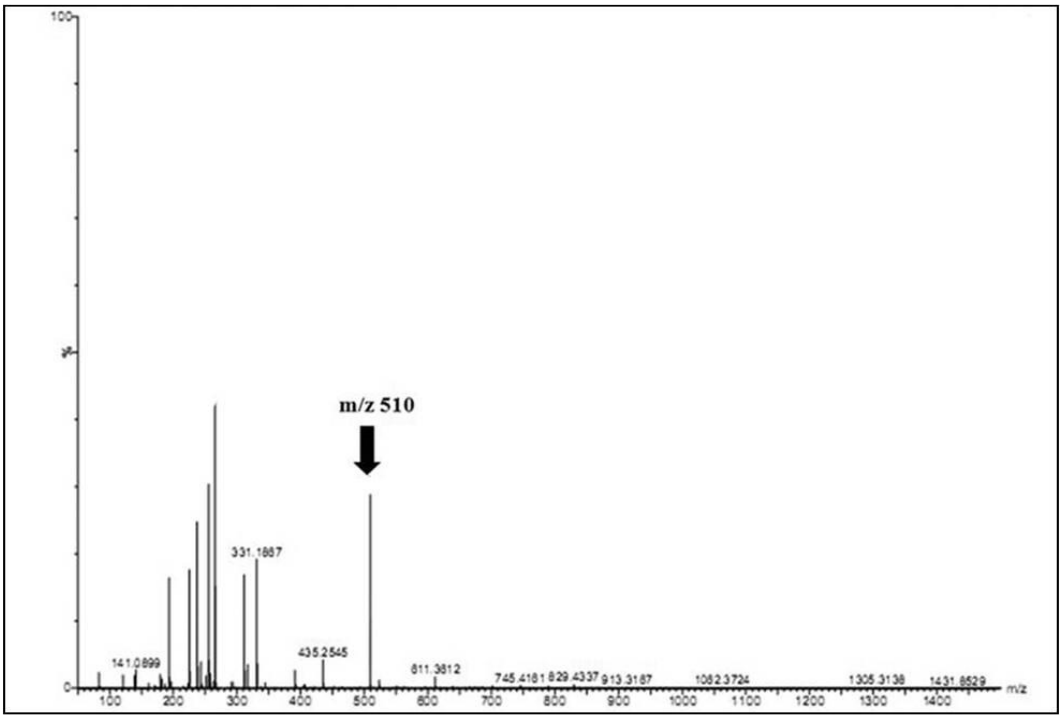

Figure 4.54. Mass spectrum of compound **K5**

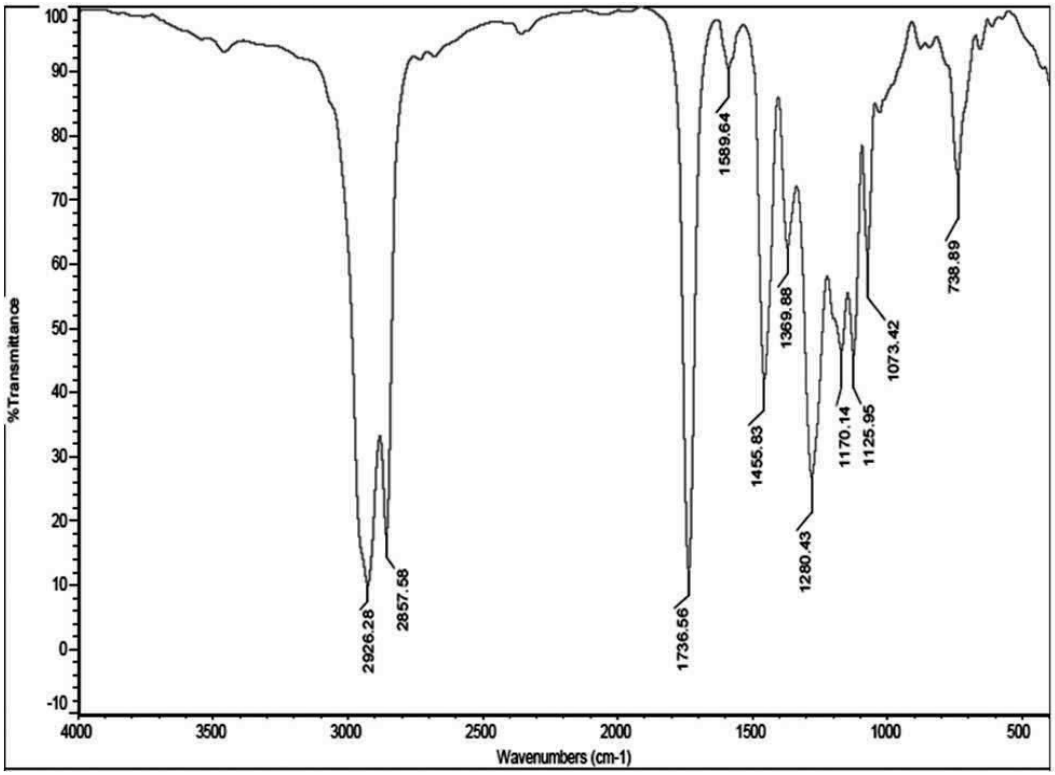

Figure 4.55. Figure showing the FTIR spectrum of compound **K5**

Table 4.10 Antioxidative and anti-inflammatory activities of the meroterpenoids isolated from *K. alvarezii vis-à-vis* the commercial agents

	Pharmacological activities {IC_{50} (mg/mL)}					
Antioxidative activities*	**Compound K3**	**K4**	**K5**	**BHA**	**BHT**	**α-tocopherol**
DPPH· scavenging	$0.70^{a} \pm 0.01$	$0.52^{a} \pm 0.06$	$0.31^{a} \pm 0.03$	$0.26^{b} \pm 0.01$	$0.25^{b} \pm 0.02$	$0.63^{c} \pm 0.04$
$ABTS^{+\cdot}$ scavenging	$0.72^{a} \pm 0.11^{a}$	$0.58^{a} \pm 0.15^{a}$	$0.34^{a} \pm 0.13^{a}$	$0.34^{b} \pm 0.02$	$0.26^{b} \pm 0.02$	$0.73^{c} \pm 0.05$
Anti-inflammatory activities*	**Compound K3**	**K4**	**K5**	**Aspirin**	**Na-salicylate**	**Ibuprofen**
COX -1 inhibition	$1.20^{a} \pm 0.03$	$1.18^{a} \pm 0.04$	$1.12^{a} \pm 0.02$	$0.005^{a} \pm 0.00$	$1.93^{c} \pm 0.05$	$0.04^{a} \pm 0.00$
COX -2 inhibition	$1.09^{a} \pm 0.06$	$1.08^{a} \pm 0.09$	$1.05^{a} \pm 0.07$	$0.21^{b} \pm 0.02$	$2.65^{c} \pm 0.05$	$0.09^{a} \pm 0.02$
Selectivity Index**	$1.10^{a} \pm 0.06$	$1.09^{a} \pm 0.09$	$1.06^{a} \pm 0.07$	$0.02^{b} \pm 0.02$	$0.72^{c} \pm 0.05$	$0.44^{a} \pm 0.02$
5-LOX inhibition	$1.14^{a} \pm 0.05$	$1.10^{a} \pm 0.04$	$1.04^{a} \pm 0.02$	$0.39^{a} \pm 0.02$	$1.75^{c} \pm 0.12$	$0.93^{b} \pm 0.11$

* The bioactivities were expressed as IC_{50} values (mg/mL). The samples were analyzed in triplicate (n=3) and expressed as a mean ± standard deviation. Means followed by the different superscripts (a–c) within the same row indicate significant differences ($P < 0.05$).

**Selectivity index has been calculated as the ratio of anti-COX-1(IC_{50}) to that of anti-COX-2 (IC_{50}).

4.3.1.7. Bioactivities and Structure-Activity Relationship Analysis

The radical scavenging and anti-inflammatory properties of the oxygenated meroterpenoids isolated from *K. alvarezii* were compared with commercially available synthetic standards. The highly oxygenated C_{29} meroterpenoid (compound **K5**) displayed potential antioxidative activities as determined by ABTS and DPPH free radical scavenging potential (IC_{50} < 0.35 mg/mL), and was comparable with those exhibited by α-tocopherol (IC_{50} 0.6–0.7 mg/mL, $P < 0.05$). The electron delocalization between the carbonyl, methoxy, and olefinic bonds in the molecular structure of these compounds might probably contribute towards the potential free radical scavenging properties (Pietta 2000; Cai et al. 2006). These meroterpenoid derivatives showed significantly greater inhibition towards the inducible COX-2 than its constitutive cyclooxygenase isoform, and accordingly, their anti-inflammatory selectivity index (SI, anti-COX-1IC_{50}/anti- COX-2IC_{50}) were lower (1.06–1.10) than synthetic NSAIDs (ibuprofen and aspirin, SI: 0.44 and 0.02, respectively; $P < 0.05$). In particular, no significant variation in the *in vitro* inhibitory activities towards pro-inflammatory 5-lipoxygenase (IC_{50} 1.04–1.14 mg/mL) and cyclooxygenase-2 (IC_{50} 1.05–1.09 mg/mL) of compound **K5** indicated its potential anti-inflammatory properties against inducible inflammatory mediators causing an inflammatory response. Notably, sodium salicylate appeared to be a weaker inhibitor of the COX isoforms (anti-COX-2 IC_{50} 2.65 mg/mL, anti-COX-1 IC_{50} 1.93 mg/mL), and exhibited significantly lesser activity against 5-LOX (anti-LOX-5 IC_{50} 1.75 mg/mL) (Table 4.10).

The radical quenching along with cyclooxygenase and lipoxygenase inhibitory activities of the meroterpenoids were determined by lipophilic (log Pow, octanol-water partition coefficient), steric (molar refractivity, MR) and electronic (tPSA, topological polar surface area) parameters. The radical quenching and anti-inflammatory properties of the studied compounds were found to be directly related to their hydrophobic characters as determined by hydrophobicity-lipophilicity balance (log Pow). A greater value of log Pow indicated the higher molecular hydrophobicity. The compound **K3** showed lesser hydrophobicity (log Pow 4) than those displayed by compound **K4** (log Pow 4.26) and **K5** (log Pow 5.46). The hydrophobic property was deduced to ascribe the intermembrane permeability of compounds, the optimal range being 2–5 for appropriate lipophilic–hydrophobic characteristics (Lipinski and Hopkins 2004). The

decreased activity of compound **K3** might be corroborated with the lesser hydrophobicity and reduced membrane permeability. Resultantly, the lipophilic DPPH radical might easily be associated with meroterpenoids possessing greater hydrophobicity (greater log Pow value) and displaying higher radical scavenging property. On the basis of above attribution, it might be ascribed that the electronic and hydrophobic factors play significant roles to narrate the bioactive potential of the studied compounds. The electron-rich centers were found to constitute the methoxy-substituted side chain, hydroxyl and aryl substituents in the ring framework. These groups might possibly function as the centre of unsaturations, and were attributed to potential anti-inflammatory and radical quenching properties of the meroterpenoids. The aggregate number of electronegative centres and centre of unsaturation were lesser in compound **K3**, thereby resulting in lesser activity than those recorded in compounds **K4** and **K5**. The optimum log Pow of the highly oxygenated C_{29} meroterpenoid (compound **K5**) (~5.46) along with greater topological polar surface area (tPSA 88.13) might result in its potential anti-inflammatory activity in terms of inhibiting COX-2 (IC_{50} 1.05 mg/mL) and 5-LOX (IC_{50} 1.04 mg/mL).

4.3.1.8. Structural Characterization of Compound K6

(3, 4, 5, 6)-3-Hexan-2'-yl)-3, 4, 5, 8-tetrahydro-4-methyl-2*H*-oxocin-5-yl acetate (**K6**)

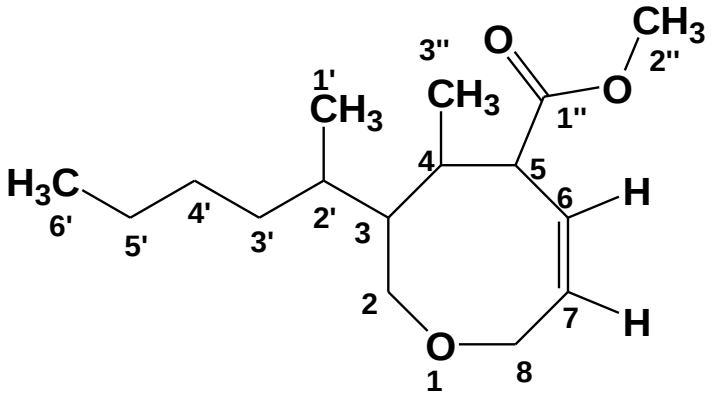

Sample yield	142 mg (1.775 %)
Physical description	Greenish oil
Molecular formula	$C_{16}H_{28}O_3$

Molecular weight	268.8363

(3, 4, 5, 6)-3-(Hexan-2'-yl)-3, 4, 5, 8-tetrahydro-4-methyl-2*H*-oxocin-5-yl acetate: Greenish oil; UV (EtOAc: MeOH) λmax (log ε): 268 nm (3.01); TLC (Si gel GF_{254} 15 mm; EtOAc: *n*-hexane 3:7, v/v) Rf: 0.52; Rt (HPLC, MeOH: ACN, 3:2 v/v): 14.16 min; IR (KBr, cm^{-1}) νmax (ν = stretching, δ = bending, ρ = rocking vibrations): 720.35 (C–Cl ν), 910.91 (alkene C–H δ), 1177.28 (C–O ν), 1297.86 (C–O ν), 1370.83 (CH_3 ν), 1458.44 (C–H δ), 1712.40 (C–CO–C ν), 2855.51 (C–H ν), 2922.32 (C–H ν). ^{1}H NMR (500 MHz, $CDCl_3$) δ_H 5.38 (m, 1H), δ_H 5.27 (m, 1H), δ_H 4.21 (m, 2H), δ_H 4.15 (m, 2H), δ_H 3.68 (s, 3H), δ_H 2.32 (m, 2H), δ_H 2.01 (m, 1H), δ_H 1.69 (m, 1H), δ_H 1.63 (m, 1H), δ_H 1.4 (m, 1H), δ_H 1.3 (m, 1H), δ_H 1.28 (m, 2H), δ_H 0.92 (m, 3H), δ_H 0.9 (m, 3H), δ_H 0.88 (m, 3H); ^{13}C NMR (125 MHz, $CDCl_3$): δ_C 162.79 (C-1''), δ_C 124.81 (C-6), δ_C 107.6 (C-7), δ_C 68.08 (C-2), δ_C 68.08 (C-8), δ_C 51.48 (C-2''), δ_C 38.78 (C-3), δ_C 34.08 (C-3'), δ_C 31.92 (C-5'), δ_C 29.18 (C-4'), δ_C 28.93 (C- 5), δ_C 23.48 (C-2'), δ_C 22.68 (C-4), δ_C 14.12 (C-1'), δ_C 13.88 (C-3''), δ_C 10.38 (C-6'); ^{1}H-^{1}H-COSY and HMBC data (Fig. 4.58 to Fig. 4.66, Table 4.11); High-resolution electrospray ionization mass spectrometry HR (ESI) MS *m/z* calcd for $C_{16}H_{28}O_3$ 268.8362, found 268.8363 $[M + H]^+$.

The ethyl acetate: methanol (EtOAc: MeOH 1:1, v/v) extract of the air-dried red marine macroalga *K. alvarezii* was subjected to a series of vacuum column chromatography (VCC) on silica gel, normal-phase flash chromatography and preparative thin layer chromatography (PTLC), using mixtures of *n*-hexane/EtOAc as mobile phase, to yield an unprecedented non-isoprenoid oxocine carboxylate cyclic ether (3, 4, 5, 6)-3-(hexan-2'-yl)-3, 4, 5, 8-tetrahydro-4-methyl-2*H*-oxocin-5-yl acetate in pure form. The structure of purified compound was proposed on the basis of comprehensive analysis of the ^{1}H NMR and ^{13}C NMR, including two-dimensional nuclear magnetic resonance spectroscopy experiments (^{1}H–^{1}H COSY; HSQC; HMBC; NOESY) and mass spectra. The ^{1}H-NMR in conjugation with ^{13}C NMR recorded the presence of methylene signals at δ_H 4.15, δ_H 4.21, δ_H 2.32, δ_H 1.63 and δ_H 1.28. ^{1}H–^{1}H COSY couplings were apparent between these protons attributed to H-3/H-4, H5/6, H2/3, H3'/4', H2'/1', H5'/6', which supported the presence of C-16 skeleton. The olefinic protons were assigned to be present at δ_H 5.27-5.38, and their proton integral revealed the presence of one olefinic bonds. The methylene group at δ_H 4.21 and δ_H 4.15 shifted downfield due to the electronegative group (oxygen) along with the presence of olefinic

group. The presence of the methoxy group has been confirmed by the singlet at δ_H 3.68. The ^1H–^1H COSY correlations indicated the presence of three spin systems in the molecule, including CH_2–CH= (from H-7 to H-8), –CH_2–CH–CH–CH–CH= (from H-2 to H-6) and CH–CH_2–CH_2–CH_2–CH_2 (from H-2' to H-5'). The above spectral evidences confirmed the planar structure for the compound. The ether bridge was placed on carbons C-2 and C-8 because of the long-range correlation between H-2 (δ_H 4.21) and C-2 (δ_C 68.08), and that between H-3 (δ_H 1.69) and C-2 (δ_C 68.08). The literature survey revealed that the chemical structure of the compound closely related to laureatin, a cyclic ether that was identified from *Laurencia nipponica* (Kurosawa et al. 1973). In the ^1H–^1H COSY spectrum, couplings were apparent between the protons at δ_H 2.01 (H5)/δ_H 1.3 (H4)/δ_H 1.69 (H3)/δ_H 4.21 (H2), δ_H 2.01 (H5)/δ_H 5.38 (H6) and δ_H 5.27 (H7)/δ_H 4.15 (H8), which supported the presence of 3, 4, 5, 8-tetrahydro-2*H*-oxocine moiety (Fig. 4.56). The methylene signal at δ_H 4.15 and δ_H 4.21 appeared downfield due to the presence of multiple electronegative systems at close proximity (Table 4.11). Two methylene groups have been assigned to occupy at the C-8, C-2 positions and were shifted at downfield position due to the presence of an extended conjugation. HMBC correlations were apparent between H-5 (δ_H 2.01) with that of a terminal methyl carbon at δ_C 174.34, which apparently indicated the presence of 3, 4, 5, 8-tetrahydro-2*H*-oxocine moiety. The carbonyl group at the C-1" position of the compound resulted in strong deshielding of the –CH– proton at δ_H 2.01, and therefore, has been assigned to be present at the C-5 position of the structure. The methane proton at δ_H 1.69 has been characteristic of the junction point of the 3, 4, 5, 8-tetrahydro-2*H*-oxocine moiety with that of the side chain 2-methyl hexane moiety. The low field methine signals (^{13}C NMR) was in agreement with that to a methine carbon signal carrying the methoxy groups at C-2" of the structure, and this was supported by the relatively downfield shift of the H-2" signal (δ_C 3.68), which referred to a possible oxygenation in its vicinity. In the HMBC spectrum, it was observed that H-5 (δ_H 2.01)/C-3" (δ_C 13.88); H-8 (δ_H 4.15)/C-1" (δ_C 174.34)/C-1' (δ_C 14.12); H-3 (δ_H 1.69)/C-3" (δ_C 13.88)/C-6' (δ_C 10.38); H-4 (δ_H 1.3)/C-1 (δ_C 14.12); H-3" (δ_H 0.9)/C-2' (δ_C 23.48); H-2' (δ_H 1.4)/C-6' (δ_C 10.38); H-6' (δ_H 0.88)/C-1' (δ_C 14.12) were correlated with each other. The detailed HMBC spectral analyses demonstrating the presence of (3, 4, 5, 6)-3-(hexan-2'-yl)-3, 4, 5, 8-tetrahydro-4-methyl-2*H*-oxocin-5-yl acetate has been represented under the Table 4.11. The relative stereochemistries of the chiral centres, particularly that of C-5, C-3, C-4 and C-2' were deduced from the ^1H-^1H COSY

and HMBC spectra of the compound. The mass spectrum supported the molecular formula $C_{16}H_{28}O_3$ (*m/z* calcd for $C_{16}H_{28}O_3$ 268.8362, found 268.8363 $[M+H]^+$) and the molecular ion peak at *m/z* 268 in the mass spectrum, which in combination with its ^1H and ^{13}C NMR data indicated the elemental composition of the compound as $C_{16}H_{28}O_3$ with three degrees of unsaturation. The molecular ion peak at *m/z* 268 ($[M+H]^+$) appeared to undergo elimination of three $–CH_2–$ groups to yield methyl-3-isopropy1-4-methyl-3, 4, 5, 8-tetrahydro-2*H*-oxocine-5-carboxylate (*m/z* 226). The elimination of two $–CH_2$ groups from the fragment ion at *m/z* 226 yielded the fragments with *m/z* 212 (attributed to (methyl 3-ethyl-4-methyl-3, 4, 5, 8-tetrahydro-2*H*-oxocine-5-carboxylate) and *m/z* 198 (methyl-3, 4-methyl-3, 4, 5, 8-tetrahydro-2*H*-oxocine-5-carboxylate). The elimination of one $–CH_2$ groups from the fragment ion at *m/z* 198 yielded the fragments with *m/z* 184 (attributed to methyl-3-methyl-3, 4, 5, 8-tetrahydro-2*H*-oxocine-5-carboxylate). The elimination of two $–CH_2$ groups from the fragment ion at *m/z* 170 yielded the fragments with *m/z* 156 attributed to (3, 4, 5, 8-tetrahydro-2*H*-oxocine-5-carboxylate) and *m/z* 142 (attributed to 3, 4, 5, 8-tetrahydro-2*H*-oxocine-5-carboxylate). The fragment peak at 142 (assigned to 3, 4, 5, 8-tetrahydro-2*H*-oxocine-5-carboxylate) was found to be the base peak. The olefinic (C=C) and alkyl (C–H) groups IR stretching vibrations were represented by the 1458 and 2855 cm^{-1} absorption bands, respectively. The strong bending vibration bands near 1712 cm^{-1} denoted the ester carbonyl absorption. The Fourier transform infrared (FTIR) spectral absorption bands at 1297 (C–C stretch), 910, 720 cm^{-1} (C–H bend alkene) substantiated the structure of the compound. The presence of a carbonyl group was indicated by the strong IR absorption at 1712.40 cm^{-1}. The relative stereochemical configuration of the asymmetric centres, such as C-3, C-2', C-4, and C-5 bearing the 3, 4, 5, 8-tetrahydro-2*H*-oxocine ring framework, was proposed on the basis of NOE enhancements along with the coupling constants (*J*-values) of the NMR spectrum. Both of the protons H-5 and H-3 exhibited NOESY correlations with the methyl protons H-3", which suggested the *cis* orientation for the methyl groups C-3", and methine group C-5/C-3. The H-6 should be trans-orientation with the methine protons at C-2' and C-3, since no cross-peak could be detected between the H-4 and H-3/H-2' in NOESY experiment. The double bond at C-6 apparently indicated the presence of *cis* configuration on the basis of small coupling constant observed for H-6 and H-7 (10.7 Hz). Additionally, the coupling constant of 10.5 Hz (each) between the pertinent olefinic protons H-6 and H-7 revealed the *cis* geometry (*Z* form) of the C6–C7 double bond.

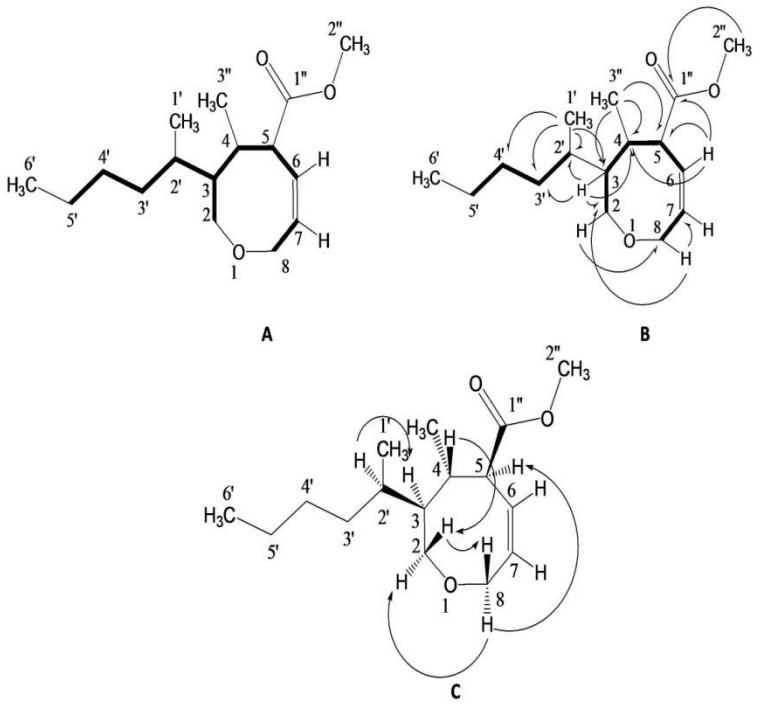

Figure 4.56. 2D NMR correlations of compound **K6** (**A**) Key $^{1}H-^{1}H$ COSY couplings (bold face bonds) (**B**) HMBC couplings (single-barbed arrow) (**C**) Key NOESY correlations (long range H–H couplings are indicated as double barbed arrow) of compound **K6**

The NOE correlation between H-2' and the proton of the H-4 supported the stereochemistry at C-2' and C-4. The axial proton Ha of C-2 resonates as a doublet with the equatorial proton He-3, having an axial–equatorial coupling (*J* a,b=2.64 Hz) subsequently the preference for the larger substituent 3, 4, 5, 8-tetrahydro-2*H*-oxocine group at C-3 to be equatorial. The strong NOE correlation between the methoxy proton at H-2'' and at methylene proton at H-4' recommended that these protons are axial. Moreover, the coupling constants between H-2'' and H-4' (10.5 Hz) indicated axial–axial orientations. It is of note that an NOE between the methine proton Ha-3, and the axial methylene proton Hd-2, implicated a boat chair conformation of substituted 3, 4, 5, 8-tetrahydro-2*H*-oxocine. In brief, the 3, 4, 5, 8-tetrahydro-2*H*-oxocine ring has been is represented as a boat–chair like conformation. The interpretation for the boat–chair conformation might be due to the bulky 3, 4, 5, 8-tetrahydro-2*H*-oxocine group as equatorially disposed.

Table 4.11 NMR spectroscopic data of compound K**6** in $CDCl_3$ [a]

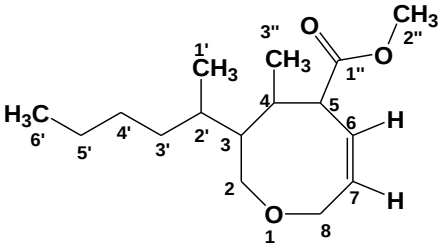

C. No.	^{13}C (δ)	^{1}H NMR (int.,mult.,*J* in Hz)[b]	^{1}H-^{1}H COSY	HMBC (^{1}H-^{13}C)
2	68.08	4.21 (2H, m)	3-H	-
3	38.78	1.69 (1H, m)	2-H, 4-H, 2'-H	C-3", C-6'
4	22.68	1.3 (1H, m)	5-H, 3-H, 3"-H	C-1'
5	28.93	2.01 (1H, m)	6-H, 4-H	C-3'
6	124.81	5.38 (1H, m)	5-H	-
7	107.6	5.27 (1H, m)	8-H	-
8	68.08	4.15 (2H, m)	7-H	C-1", C-1'
1'	14.12	0.92 (3H, t)	2'-H	-
2'	23.48	1.4 (1H, m)	3-H, 1'-H	C-6'
3'	34.08	2.32 (2H, m)	4'-H	-
4'	29.18	1.63 (1H, m)	3'-H, 5'-H	-
5'	31.92	1.28 (2H, m)	4'-H	C-1'
6'	10.38	0.88 (3H, m)	-	-
1"	174.34	-	-	-
2"	51.48	3.68 (3H, s)	-	-
3"	13.88	0.9 (3H, m)	4-H	C-2'

[a] NMR spectra recorded using Bruker AVANCE III 500 MHz (AV 500) spectrometer in $CDCl_3$ as aprotic solvent at ambient temperature with TMS as the internal standard (δ 0 ppm).

[b] Values in ppm, multiplicity and coupling constants (*J*=Hz) are indicated in parentheses. The assignments were made with the aid of the ^1H-^1H COSY, HSQC, HMBC and NOESY experiment

4.3.1.9. Bioactivities and Structure-Activity Relationship Analysis

The antioxidative activity of the compound was found to be significantly greater as determined by DPPH (1, 1-diphenyl-2-picryl-hydrazil) and ABTS (2, 2′-azino-bis-3 ethylbenzothiozoline-6-sulfonic acid) radical scavenging activities (IC_{50} ~ 0.3 mg/mL) compared to α-tocopherol (IC_{50} > 0.6 mg/mL) and was comparable to synthetic antioxidants BHT (Butylated hydroxytoluene) and BHA (Butylated hydroxyanisole) (IC_{50} ~ 0.35–0.34 mg/mL). Structure–activity relationship analysis of the newly isolated cyclic ether from the red alga *K. alvarezii* was performed by utilizing different structural descriptors (ACD Chemsketch, version 8.0 and ChemDraw Ultra version 8.0), such as molar volume (MV), parachor (Pr) and molar refractivity (MR) classified as bulk variables, octanol–water partition coefficient (log Pow) classified as hydrophobic and topological polar surface area (tPSA) and polarisability (Pl), which were classified as electronic descriptor variables. It is of note that whilst the log Pow of (3, 4, 5, 6)-3- (hexan-2'-yl)-3, 4, 5, 8-tetrahydro-4-methyl-2*H*-oxocin-5-yl acetate was recorded as 3.63, that of α-tocopherol (log Pow 9.98) was found to be considerably greater. This might significantly contribute to the greater antioxidant activity of the compound **K6** than α-tocopherol. The log Pow of the compound **K6** was comparable to those of BHA (log Pow 3.22), and BHT (log Pow 5.54), and therefore, their antioxidative properties were not different (IC_{50} 0.25–0.26 mg/mL).

The free radical scavenging activity of bioactive leads depends on the electron-transferring groups, such as –COOMe, –OH and –NH, which can easily abstract free radicals and can convert from highly reactive species to non-reactive compounds (Cai et al. 2006). The radical scavenging activities were also reported to increase with the presence of double bonds due to effective electron transfer through electron delocalisation (Pietta 2000), and these reasons might be attributed to the significant

antioxidative property of the compound. Cyclooxygenase (COX-1) has been known as a constitutive enzyme, which is essentially required for various metabolic functions. It is intriguing to note that aspirin, sodium salicylate and ibuprofen are commonly available non-steroidal anti-inflammatory drugs (NSAIDs), which recorded greater inhibitory properties towards COX-1 than COX-2 isoform. The compound exhibited greater activity against COX-2 than against COX-1 isoform, and therefore, the selectivity index remained significantly lesser (anti-COX-1 IC_{50}: anti-COX-2 IC_{50} 0.87) than the synthetic NSAIDs (0.02–0.44) (Fig. 4.57). No significant difference of *in vitro* 5-lipoxygenase (5-LOX) activity (IC_{50} 0.95 mg/mL) than ibuprofen (IC_{50} 0.93 mg/mL) indicated the potential anti-inflammatory properties of the compound **K6**. Sodium salicylate was found to be a weaker inhibitor of both COX isoforms (anti-COX-2 IC_{50} 2.65 mg/mL, anti-COX-1 IC_{50} 1.93 mg/mL) and demonstrated significantly lesser activity against 5-LOX (anti-COX-1 IC_{50} 1.75 mg/mL). Likewise, the log Pow and tPSA of (3, 4, 5, 6)-3-(hexan-2'-yl)-3, 4, 5, 8- tetrahydro-4-methyl-2*H*-oxocin-5-yl acetate were recorded as 3.63 and 35.53, respectively, whilst the values were found to be comparable with those noted for ibuprofen (3.75 and 37.30, respectively).

It is, therefore, the selectivity indices of the compound **K6**, and ibuprofen recorded greater values (0.87 and 0.44, respectively) than aspirin (0.02), and consequently, the compound **K6** appeared to be safer than that of the synthetic NSAIDs. The compound **K6** purified from the red marine macroalga might therefore be [†]used as a potential selective inhibitor of COX-2 with significantly lesser side effect profiles, such as renal and gastric damage than the present therapies by using NSAIDs used to combat inflammatory disorders (Table 4.12). There were reports of closely related structures, such as laurefurenynes A–F and cyclic ether acetogenins isolated and characterized from red marine macroalga *Laurencia* sp. The ^{1}H NMR of C_{15}-acetogenin derived from red marine macroalga *Laurencia* sp revealed the presence of a *cis*-ene-yne functionality (H-4 δ_H 6.05, H-3 δ_H 5.57, H-1 δ_H 3.10), which was proved by the respective ^{13}C NMR signals at C-4 (δ_C 139.9), C-3 (δ_C 111.3), C-2 (δ_C 80.0) and C-1 (δ_C 82.4) (Wael et al. 2010). The signals obtained at δ_H 4.93 and δ_H 4.43 indicated the two hydroxyl groups were at OH-7 and OH-12 (Wael et al. 2010), which are absent in the compound **K6** (non-isoprenoid oxocine carboxylate cyclic ether) isolated from the ethyl acetate–methanol extract of the red marine macroalga *K. alvarezii*.

The IR spectrum of laurefurenynes A–F broadly belongs to the group of C_{15} cyclic ether acetogenins that were isolated from *Laurencia* sp, showing an intense absorption bands attributed to a terminal acetylene functional group (3315 cm^{-1} and 2107 cm^{-1}), which is not present in the compound **K6** isolated from *K. alvarezii*. These groups of compounds exhibited non-selective cytotoxic activity, presumably due to the terminal acetylene. The C_{15} acetogenins bearing cyclic ether skeletons have been isolated as the main secondary metabolites from red marine macroalga *Laurencia* sp (Erickson 1983) and were reported to be anti-microbial (Konig and Wright 1997), anti-feedant (Kurata et al. 1998), anti-helmintic (Davyt et al. 2001) and cytotoxic (Juagdan et al. 1997). A range of chlorinated compounds, C_{15} acetogenin en-ynes, which are structurally similar to the compounds, were isolated from *Laurencia glandulifera* and were, reported to be moderately cytotoxic towards various human tumour cell lines (Kladi et al. 2009). However, there is no literature report for the antioxidant and anti-inflammatory activities of the laurefurenynes A–F and cyclic ether acetogenins isolated and characterized from red marine macroalgae. Anti-inflammatory potential of the chromene sargachromanol G from the Korean marine macroalga *Sargassum siliquastrum* (Fucales) (Yoon et al. 2012); halogenated compounds from the red marine macroalga *Laurencia snackeyi* (Vairappan et al. 2013) and the porphyrin derivatives; and pheophorbide and pheophytin from the marine macroalga *Sargassum japonica* were reported in previous literature (Islam et al. 2013). Antioxidative compounds from marine macroalgae were identified as phylopheophylin in *Eisenia bicyclis* (Cahyana et al. 1992), phlorotannins in *Sargassum kjellamanianum* (Yan et al. 1996) and fucoxanthin in *Hijikia fusiformis* (Yan et al. 1999). Laureatin, isolaureatin and deoxyprepacifenol are other related compounds obtained from the red alga *Laurencia nipponica* (Masuda et al. 1997). They exhibited significant insecticidal activity against the mosquito larvae *Culex pipens pallens* (Watanabe 1989). However, there is no literature report for the antioxidant and anti-inflammatory activities of the laurefurenynes A–F and cyclic ether acetogenins isolated and characterized from red marine macroalgae.

Figure 4.57. Graphical representation of bioactivities of compound **K6**. The thalli of the studied marine macroalga were displayed as inset

Table 4.12 Antioxidative and inflammatory activities of the compound from *K. alvarezii vis-à-vis* the commercially available natural and synthetic antioxidants and anti-inflammatory ingredients

	Bioactivity IC_{50} (mg/mL)			
Antioxidative activities*	**K6[x]**	**BHA**	**BHT**	**α-tocopherol**
$DPPH^{\cdot}$ scavenging	$0.26^{a} \pm 0.02$	$0.26^{b} \pm 0.01$	$0.25^{b} \pm 0.02$	$0.63^{c} \pm 0.04$
$ABTS^{+\cdot}$ scavenging	$0.35^{a} \pm 0.13$	$0.34^{b} \pm 0.02$	$0.26^{b} \pm 0.02$	$0.73^{c} \pm 0.05$
Anti-inflammatory activities*	**K6[x]**	**Aspirin**	**Na-salicylate**	**Ibuprofen**
COX -1 inhibition	$0.92^{a} \pm 0.02$	$0.01^{a} \pm 0.00$	$1.93^{c} \pm 0.05$	$0.04^{a} \pm 0.00$
COX -2 inhibition	$1.05^{a} \pm 0.07$	$0.21^{b} \pm 0.02$	$2.65^{c} \pm 0.05$	$0.09^{a} \pm 0.02$
Selectivity index**	$0.87^{b} \pm 0.08$	$0.02^{b} \pm 0.01$	$0.73^{b} \pm 0.02$	$0.44^{b} \pm 0.03$
5-LOX inhibition	$0.95^{a} \pm 0.14$	$0.39^{a} \pm 0.02$	$1.75^{c} \pm 0.12$	$0.93^{b} \pm 0.11$

* The bioactivities were expressed as IC_{50} values (mg/mL).

The samples were analyzed in triplicate (n=3) and expressed as mean ± standard deviation. Means followed by the different superscripts (a–c) within the same row indicate significant differences ($P < 0.05$).

**Selectivity index has been calculated as the ratio of anti-COX-1(IC_{50}) to that of anti-COX-2 (IC_{50}).

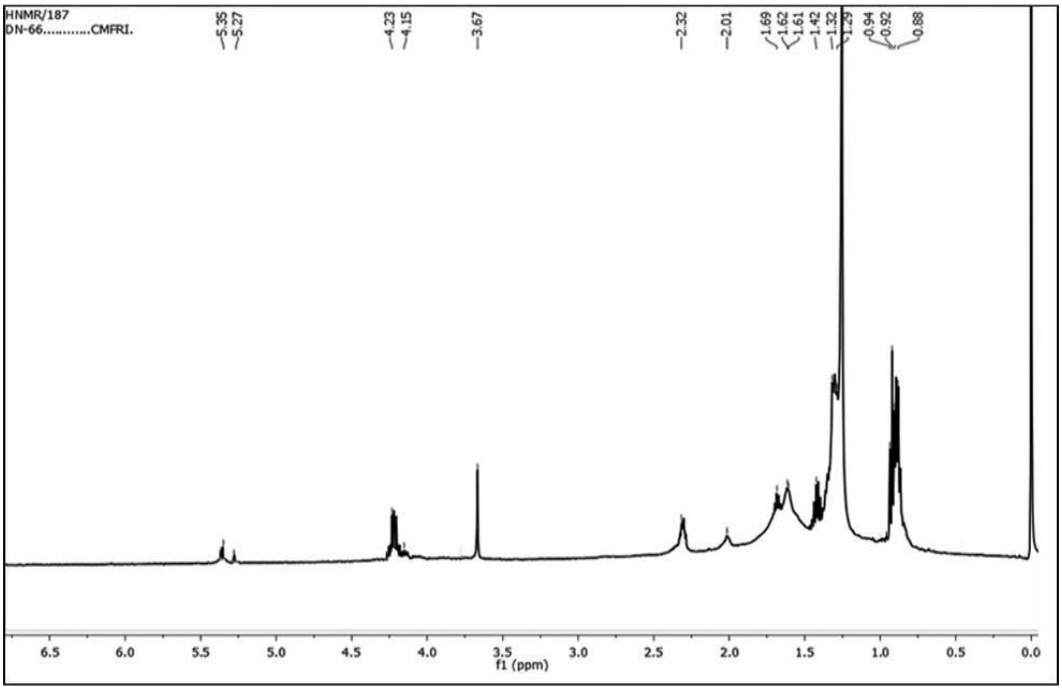

Figure 4.58. Figure showing the ^{1}H NMR spectrum of compound **K6**

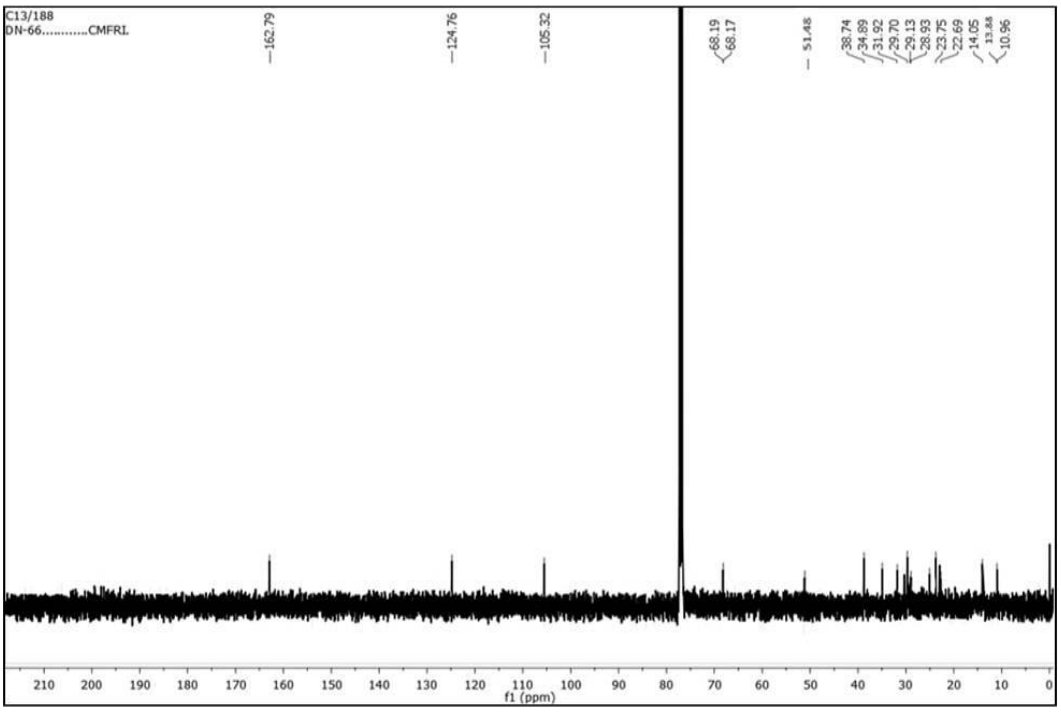

Figure 4.59. Figure showing the ^{13}C NMR spectrum of compound **K6**

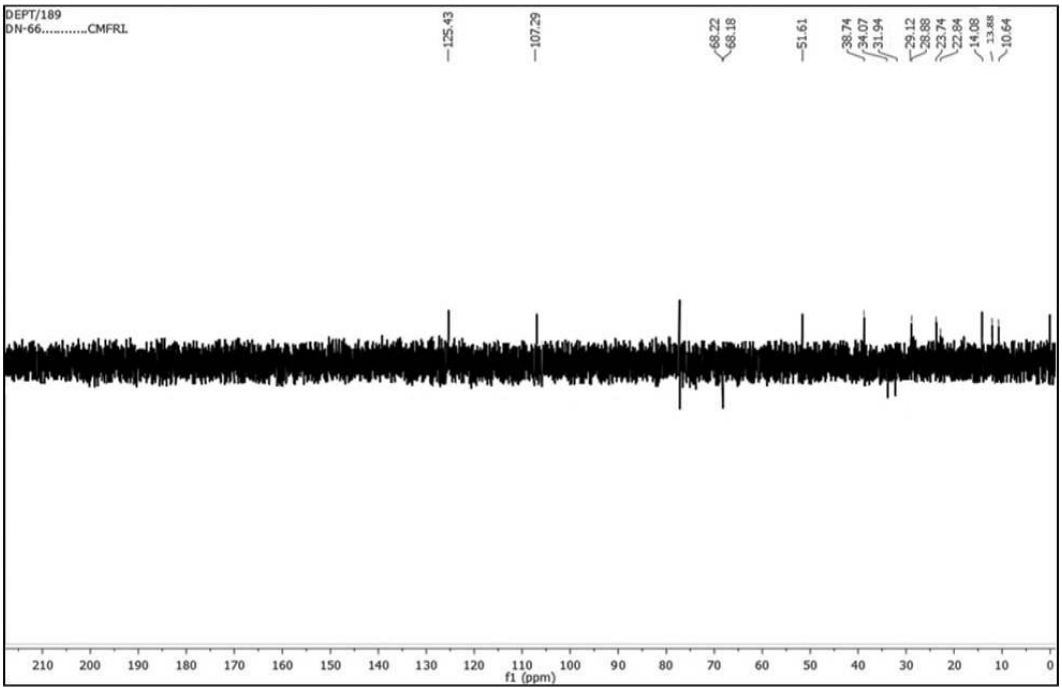

Figure 4.60. Figure showing the DEPT spectrum of compound **K6**

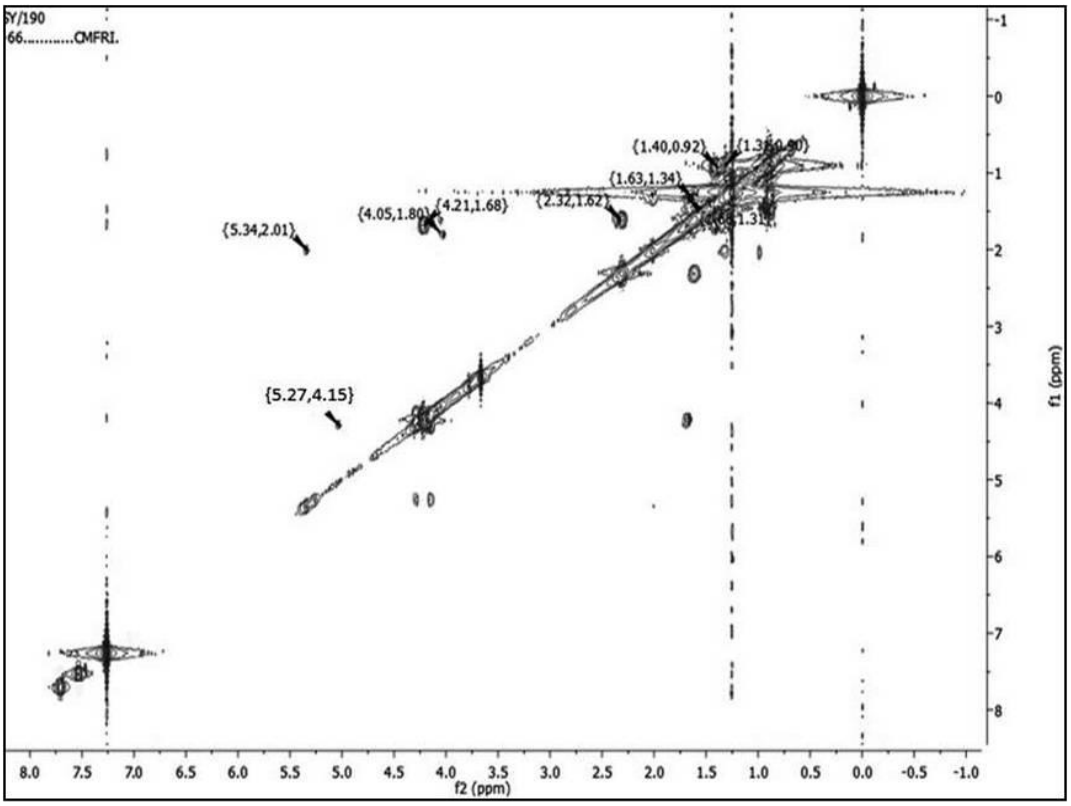

Figure 4.61. Figure showing the ^{1}H-^{1}H COSY spectrum of compound **K6**

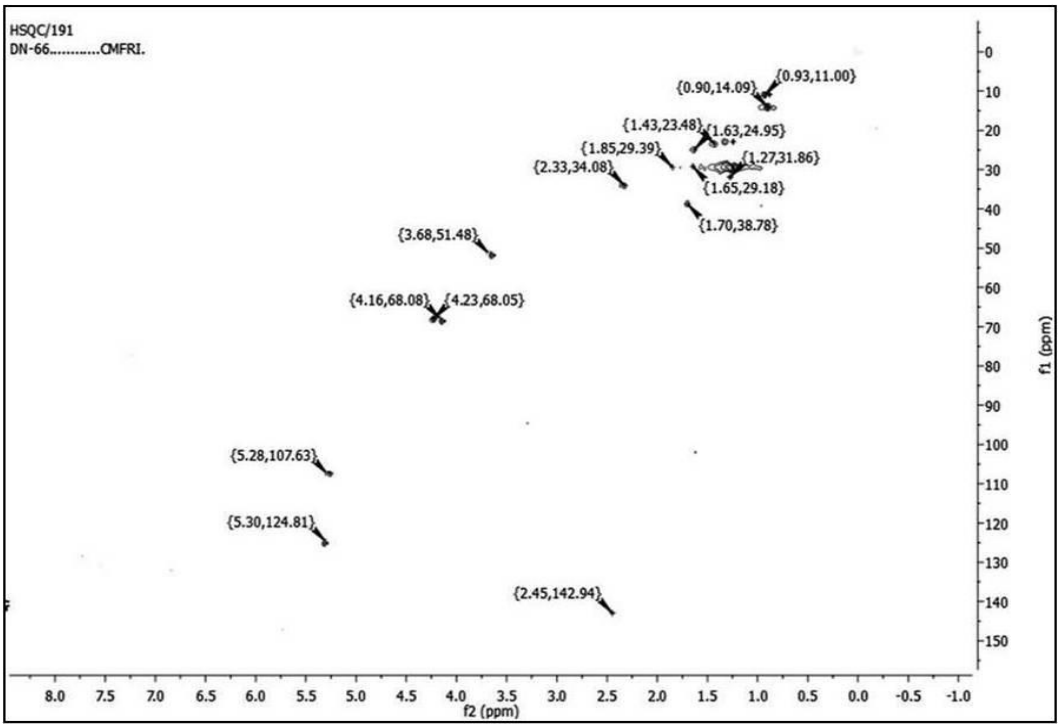

Figure 4.62. Figure showing the HSQC spectrum of compound **K6**

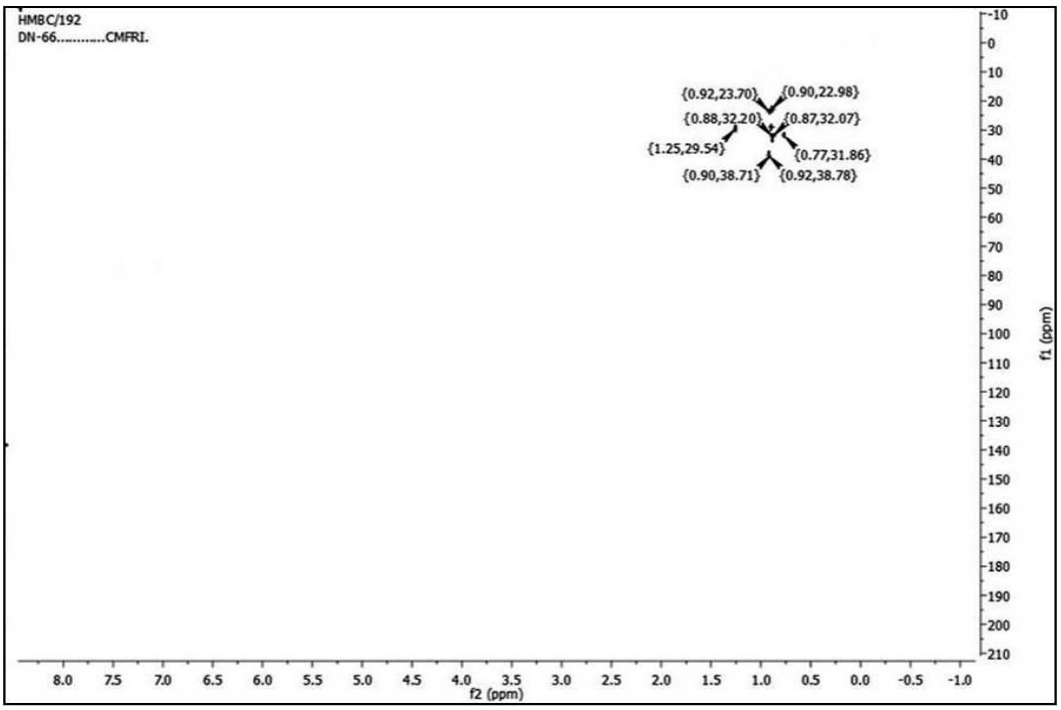

Figure 4.63. Figure showing the HMBC spectrum of compound **K6**

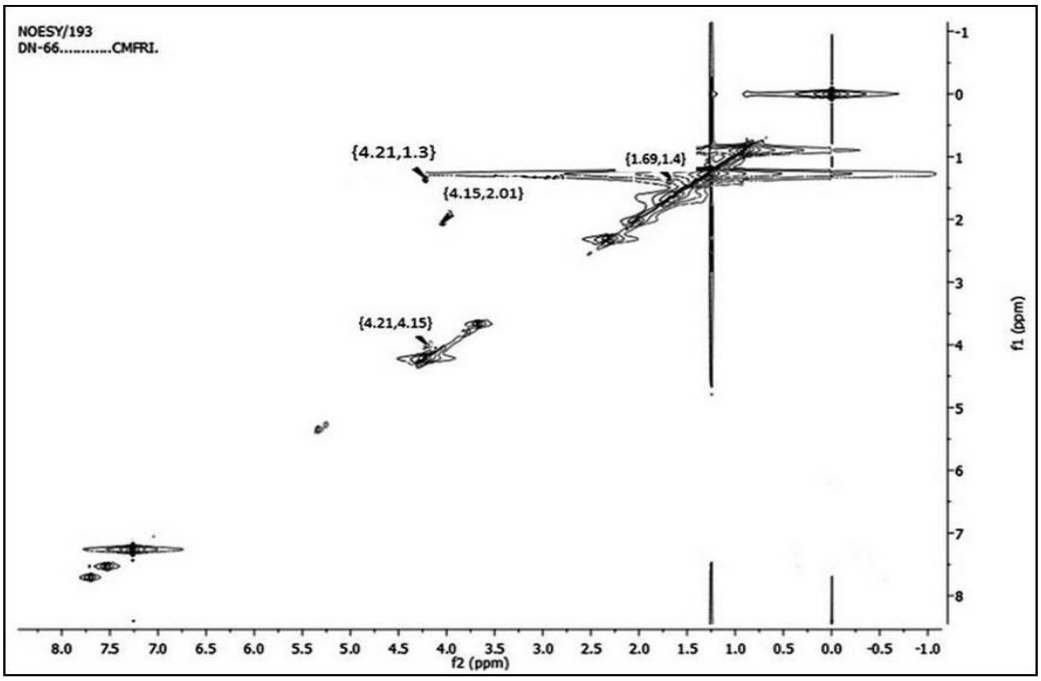

Figure 4.64. Figure showing the NOESY spectrum of compound **K6**

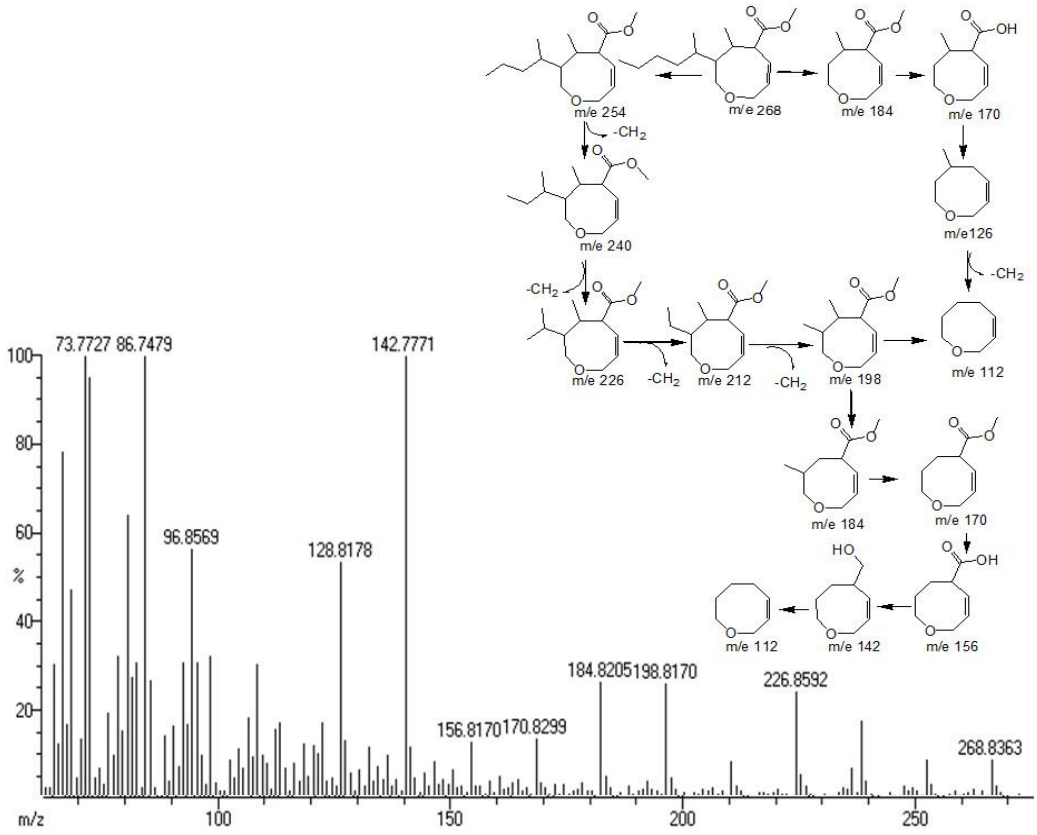

Figure 4.65. Mass spectrum of compound **K6**

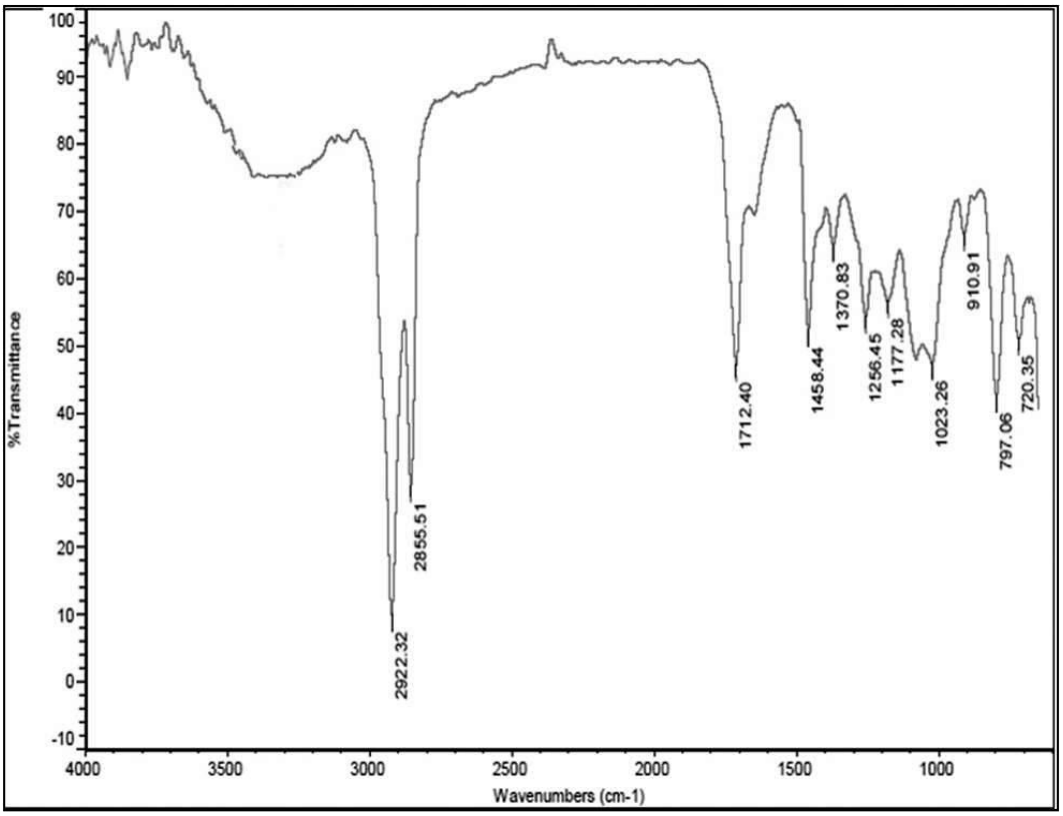

Figure 4.66. Figure showing the FTIR spectrum of compound **K6**

4.3.2. Secondary Metabolites from *G. opuntia*

4.3.2.1. Structural Characterization of Compound G1

5-(7-(5-Ethyl-3, 4-dimethoxycyclooctyl) benzofuran-6-yl)-7-methyl-3, 4, 7, 8-tetrahydro-2*H*-oxocin-2-one (**G1**)

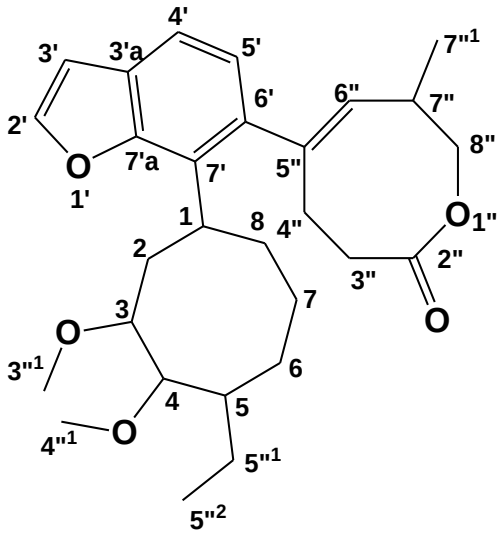

Sample yield	130 mg (1.625 %)
Physical description	Yellow oil
Molecular formula	$C_{28}H_{38}O_5$
Molecular weight	454.2728

5-(7-(5-Ethyl-3, 4-dimethoxycyclooctyl) benzofuran-6-yl)-7-methyl-3, 4, 7, 8-tetrahydro-2*H*-oxocin-2-one: Yellow oil; UV MeOH: EtOAc λmax (log ε): 237 nm (3.217), TLC (Si gel GF_{254} 15 mm; MeOH: EtOAc 7:3, v/v) Rf: 0.56.; Rt (HPLC, CH_3CN: MeOH, 2:3 v/v): 12.85 min; IR (KBr, expressed in cm^{-1}) νmax (ν = stretching, δ = bending, ρ = rocking vibrations): 2925.39, 2856.44 (C-H ν), 1741.18 (C=O ν), 1459.21 (C-H δ), 1370.58, 1257.96 (C-H ρ), 1170.92 (C-O ν), 1093.53 (CH δ), 968.11, 866.84, 806.67 (=C-H δ), 721.60 (C-H ρ); ^{1}H NMR (500 MHz $CDCl_3$): δ_H 1.72 (1H, m), δ_H 1.28 (2H, m), δ_H 0.88 (3H, t, *J*=7.04 Hz), δ_H 2.02 (2H, m), δ_H 1.72 (2H, m), δ_H 2.20 (2H, m), δ_H 1.61 (1H, t, *J*=7.98 Hz), δ_H 2.53 (2H, t, *J*=5.97 Hz), δ_H 4.19 (1H, m), δ_H 3.79 (3H, s), δ_H 4.32 (1H, t, *J*=6.93 Hz), δ_H 3.67 (3H, s), δ_H 6.82 (1H, d, *J*=2.31 Hz),

δ_H 6.09 (1H, d, *J*=2.17 Hz), δ_H 7.72 (1H, d, *J*=2.31 Hz), δ_H 7.54 (1H, d, *J*=3.38 Hz), δ_H 4.09 (2H, d, *J*=6.58 Hz), δ_H 2.02 (1H, m), δ_H 0.99 (3H, d, *J*=6.71 Hz), δ_H 5.35 (1H, d, *J*=5.15 Hz), δ_H 1.61 (2H, t, *J*=10 Hz), δ_H 2.32 (2H, t, *J*=7.60 Hz); ^{13}C NMR (125 MHz, $CDCl_3$): δ_C 32.85 (C-5), δ_C 29.70 (C-5"^{1}), δ_C 14.1 (C-5"^{2}), δ_C 32.39 (C-6), δ_C 34.55 (C-7), δ_C 34.58 (C-8), δ_C 27.73 (C-1), δ_C 40.06 (C-2), δ_C 70.46 (C-3), δ_C 52.47 (C-3"^{1}), δ_C 65.57 (C-4), δ_C 51.46 (C-4"^{1}), δ_C 147.23 (C-2'), δ_C 130.48 (C-3'), δ_C 147.04 (C-3a'), δ_C 128.78 (C- 4'), δ_C 130.91 (C-5'), δ_C 148.31 (C-6'), δ_C 149.4 (C-7'), δ_C 147.23 (C-7a'), δ_C 71.80 (C-8"), δ_C 27.93 (C-7"), δ_C 19.15 (C-7"^{1}), δ_C 130.32 (C-6"), δ_C 132.3 (C-5"), δ_C 34.45 (C-4"), δ_C 34.12 (C-3"); δ_C 174.35 (C-2"); ^{1}H-^{1}H COSY and HMBC (Fig. 4.67 to Fig. 4.77, Table 4.13); HR (EI) MS *m/z* found 454.2728 $[M]^+$, calcd for $C_{28}H_{38}O_5$ 454.2719.

Figure 4.67. Figure showing red marine macroalga *G. opuntia* collected from the Palk Bay of south east coast of India, and two furanyl compounds isolated from the EtOAc: MeOH crude extract of marine macroalga

The compound 5-(7-(5-ethyl-3, 4-dimethoxycyclooctyl) benzofuran-6-yl)-7-methyl-3, 4, 7, 8-tetrahydro-2*H*-oxocin-2-one was obtained as yellow oil, and its molecular ion peak at *m/z* 454 was deduced from the mass spectrum (HR-EI-MS *m/z* 454.2728 $[M]^+$). The molecular formula of the isolated compounds was deduced as $C_{28}H_{38}O_5$ based on combined ^{1}H and ^{13}C NMR spectroscopic data.

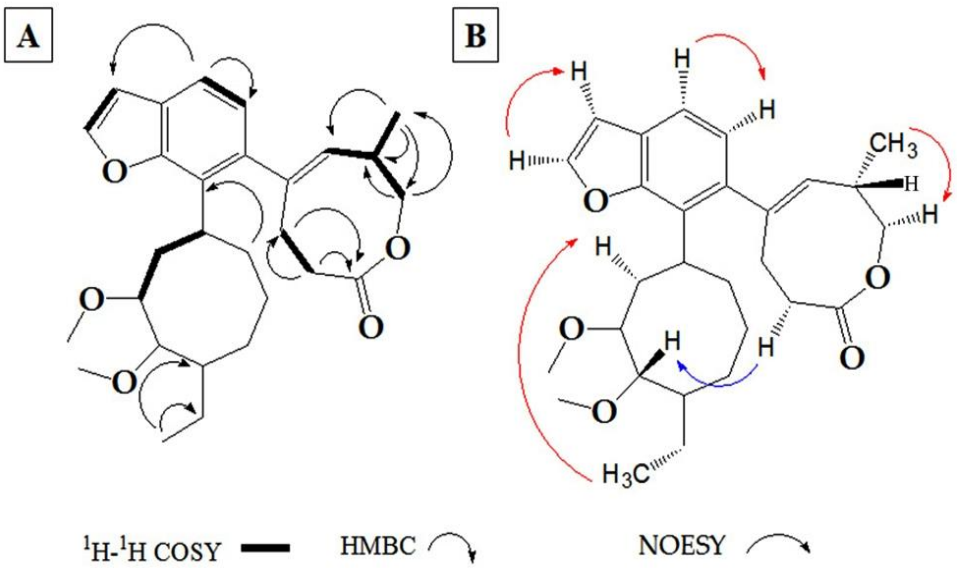

Figure 4.68. (**A**) Figure showing the ^{1}H-^{1}H COSY, HMBC, and (**B**) NOESY correlations of compound **G1**. The ^{1}H-^{1}H COSY cross peaks were displayed by bold face bonds, whereas the selected HMBC correlations were shown as double barbed arrows. The NOESY relations was presented as colored arrows

The IR spectrum displayed bending vibration appeared at 1741 cm^{-1}, which was attributed to the ester carbonyl group. The FTIR absorption bands at 1459 and 2856 cm^{-1} were attributed to the olefinic (>C=C<) as well as alkyl groups, respectively. The ^{13}C NMR spectral data showed 28 resolved signals that were classified into four aromatic methines, two methoxy group, one olefinic carbon, five methine, eight methylene, two methyl carbon, and six quaternary carbons, which were supported by the exhaustive 2D NMR experiments. Ultraviolet absorbance at λmax (log ε) 235 nm (3.24) was attributed to the furan chromophore that was further supported by the IR bending vibrations at about 1459 cm^{-1}. The isolated compounds displayed six quaternary carbons in which the carbon signals at δ_C 147.04 (ascribed to C-3a'), δ_C 147.23 (C- 7a'), δ_C 148.31 (C-6') and δ_C 149.40 (C-7') were associated with the benzyl furan moiety. The carbon at δ_C 174.35 (attributed to C-2') was due to the carbonyl group in the 7-methyl-3, 4, 7, 8-tetrahydro-2*H*-oxocin-2-one framework. The ^{1}H–^{1}H COSY spin system appeared between δ_H 1.72 (H-5)/δ_H 4.32 (H-4), δ_H 1.61 (H-1)/δ_H 2.53 (H-2), and δ_H 4.19 (H-3), which attributed to the methoxy substituted ethylcyclooctane ring skeleton (Fig. 4.68). Likewise, strong ^{1}H–^{1}H COSY cross peaks observed between δ_H 4.09 (H-8")/δ_H 2.02 (H-7")/δ_H 5.35 (H-6") and δ_H 2.02 (H-7")/δ_H 0.99 (H-7"^{1}) supported the ring framework of 7-methyl-tetrahydro-2*H*-oxocin-2-one moiety. The ring framework was further supported by key HMBC correlation between oxymethine proton δ_H 4.09 (H-8") coupled with the methylene carbon δ_C 27.93 (C-7"), and methyl carbon at δ_C 19.15 (C-7"^{1}). In addition, the HMBC cross peaks were observed between the methyl proton δ_H 0.99 (H-7"^{1}) coupled to the methine carbon δ_C 27.93 (C-7") and oxymethine carbon at δ_C 71.80 (H-8") (Table 4.13). Key HMBC correlation between δ_H 0.88 (H-5"^{2})/C-5(δ_C 32.85), δ_H 2.20 (H-8)/C-7' (δ_C 149.40), δ_H 7.72 (H-4')/C-5' (δ_C 130.91) supported the substituted 2*H*-oxocin-2-one ring framework. The terminal methyl group appeared as a triplet at H-5"^{2}{δ_H 0.88 (*J*=7.04 Hz), δ_C 14.1 (C-5"^{2})} associated with (1, 2, 3)-1-ethyl-2, 3-dimethoxycyclooctane and a carbonyl group at C-2" {δ_C 174.35 (C-2")} were deduced to be enclosed with the 7-

methyl-tetrahydro-2*H*-oxocin-2-one ring framework. This was corroborated by intense HMBC couplings between H- 4" (δ_H 1.61)/C-2" (δ_C 174.35); H-3" (δ_H 2.32)/C-2" (δ_C 174.35) (Table 4.13). Two doublets at δ_H 6.82 (H-2', *J*=2.31 Hz) and δ_H 6.09 (H-3', *J*=2.17 Hz) due to the furanyl ring system were apparent in the ^{1}H NMR spectrum. In addition, aryl ring system appeared at δ_H 7.72 {H-4', *J*=2.31 Hz, δ_C 128.78} and δ_H 7.54 {H-5', *J*=3.38 Hz, δ_C 130.91}. The olefinic signals were detected at δ_H 5.35 {H-6", δ_C 130.32 (C-6")}. Methoxy groups were attributed to the proton signal at δ_H 3.79 (3H, H-3"^{1}) and δ_H 3.67 (3H, H-4"^{1}), which were assigned to form the part of ethylcyclooctane moiety. Additional oxymethylene signals H-8" {δ_H 4.09 (*J*=6.58 Hz), δ_C 71.80 (H-8")} were attributed to the 7-methyl-tetrahydro-2*H*-oxocin-2-one moieties. The ^{1}H NMR spectroscopic data displayed the occurrence of highly deshielded oxymethine protons at δ_H 4.19 (H-3) and δ_H 4.32 (H-4, *J*=6.93 Hz). Each of the two olefinic groups and carbonyl groups along with aromatic moieties (aryl and furyl) were accounted for ten degrees of unsaturation in compound **G1**. The relative stereochemical configuration of the asymmetric centers, C-5, C-4, C-3, C-1, and C-7" bearing the substituted furan ring framework were attributed by extensive NOESY experiments along with the coupling constants (*J*-values) in the ^{1}H NMR spectrum. The aromatic methine protons at H-5' (δ_H 7.54, *J*=3.38 Hz) displayed NOESY correlations with the neighboring aromatic methane protons at δ_H 7.74 (*J*=2.31 Hz) in the benzyl furan aromatic ring system. An additional NOE cross peak was recorded between δ_H 6.09 (H-3', *J*=2.17 Hz) and δ_H 6.82 (H-2', *J*=2.31 Hz), which apparently indicated that these protons were associated with the furanyl moiety. The oxymethine group at C-4 (δ_H 4.32, *J*=6.93 Hz) exhibited NOE cross peaks with δ_H 2.32 (H-3", *J*=7.60 Hz), which was situated at the junction point with side chain methoxy substitution. The NOE relationships with δ_H 0.99 (assigned to H-7"^{1}, *J*=6.71 Hz) and δ_H 4.09 (assigned to H-8", *J*=6.58 Hz) were seen at the α-face of the molecule. In addition, the terminal methane protons at H-5"^{2} (δ_H 0.88, *J*=7.04 Hz) displayed NOESY correlations with the methine protons at δ_H 2.53 (H-2, *J*=5.97 Hz) in the side chain substitution of 1-ethyl-2, 3-dimethoxycyclooctane ring system.

Table 4.13 NMR spectroscopic data of compound **G1** in $CDCl_3$[a]

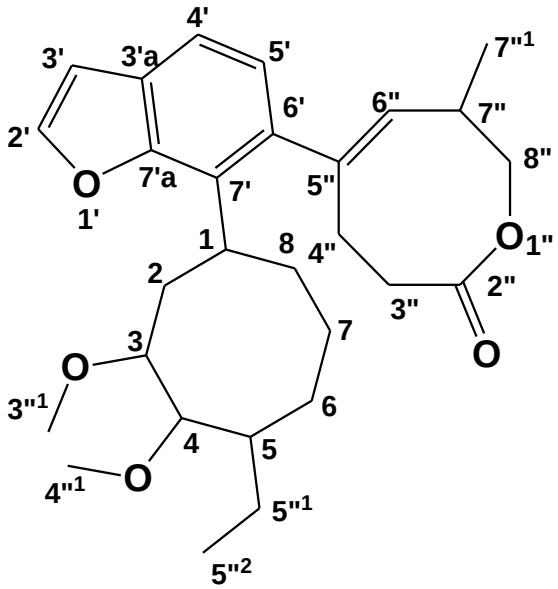

C. No	^{13}C (δ)	^{1}H NMR (mult., *J* in Hz, int.)[b]	^{1}H-^{1}H COSY	HMBC (^{1}H^{13}C)
1	27.73	1.61 (t, *J*=7.98 Hz, 1H)	2-H	-
2	40.06	2.53 (t, *J*=5.97Hz, 2H)	1-H, 3-H	
3	70.46	4.19 (m, 1H)	-	-
3"^{1}	52.47	3.79 (s, 3H)	-	-
4	65.57	4.32 (t, *J*=6.93 Hz, 1H)	-	-
4"^{1}	51.46	3.67 (s, 3H)	-	-
5	32.85	1.72 (m, 1H)	4-H	-
5"^{1}	29.70	1.28 (m, 2H)	-	-
5"^{2}	14.1	0.88 (t, *J*=7.04 Hz, 3H)	-	C-5"^{1}, C-5
6	32.39	2.02 (m, 2H)	-	-
7	34.55	1.72 (m, 2H)	-	-
8	34.58	2.20 (m, 2H)	-	C-7'
2'	147.23	6.82 (d, *J*=8.21 Hz, 1H)	3'-H	
3'	130.48	6.09 (d, *J*=2.17 Hz, 1H)	2'-H	-
3a'	147.04	-		-
4'	128.78	7.72 (d, *J*=2.31 Hz, 1H)	5'-H	C-3', C-5'
5'	130.91	7.54 (d, *J*=3.38 Hz, 1H)	4'-H	-
6'	148.31	-	-	-
7'	149.4	-	-	-
7a'	147.23	-		
2"	174.35	-	-	-
3"	34.12	2.32 (t, *J*=7.60 Hz, 2H)	-	C-2"
4"	34.45	1.61 (t, *J*=10 Hz, 2H)	-	C-3", C-2"
5"	132.3	-	-	-
6"	130.32	5.35 (d, *J*=5.15 Hz, 1H)	7"-H	-
7"	27.93	2.02 (m, 1H)	7"^{1}-H, 6'-H, 8"-H	C-6", C-7"^{1}
7"^{1}	19.15	0.99 (d, *J*=6.71 Hz, 3H)	-	C-7", C-8"
8"	71.80	4.09 (d, *J*=6.58 Hz, 2H)	7"-H	C-7"^{1}, C-7"

[a] NMR spectra recorded using Bruker AVANCE III 500 MHz (AV 500) spectrometer in $CDCl_3$ as aprotic solvent at ambient temperature with TMS as the internal standard (δ 0 ppm).

[b] Values in ppm, multiplicity and coupling constants (*J*=Hz) are indicated in parentheses. The assignments were made with the aid of the ^1H-^1H COSY, HSQC, HMBC and NOESY experiment

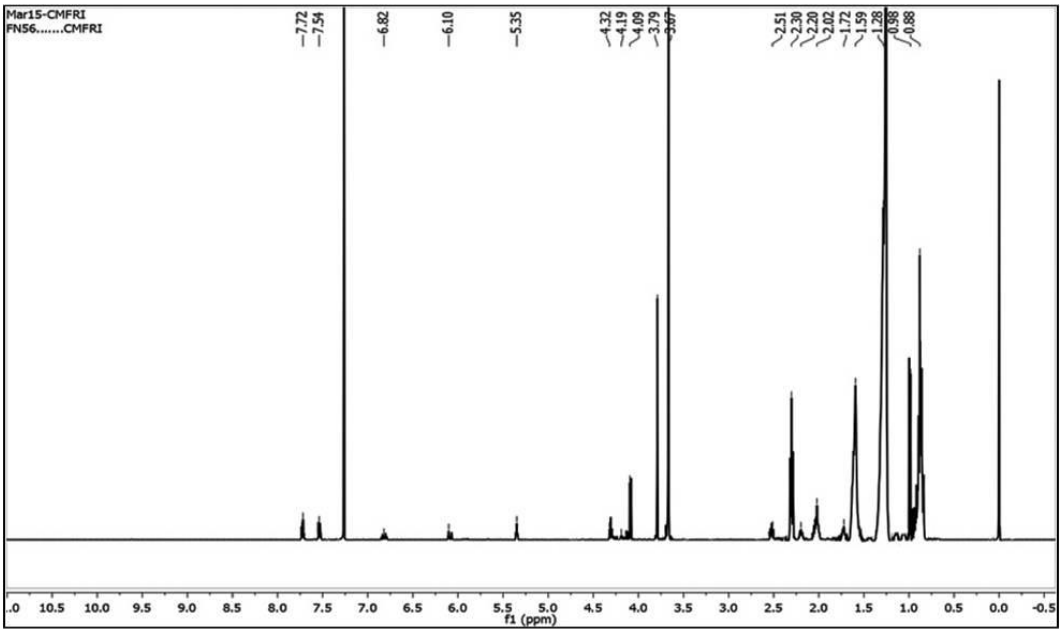

Figure 4.69. Figure showing the ^1H NMR spectrum of compound **G1**

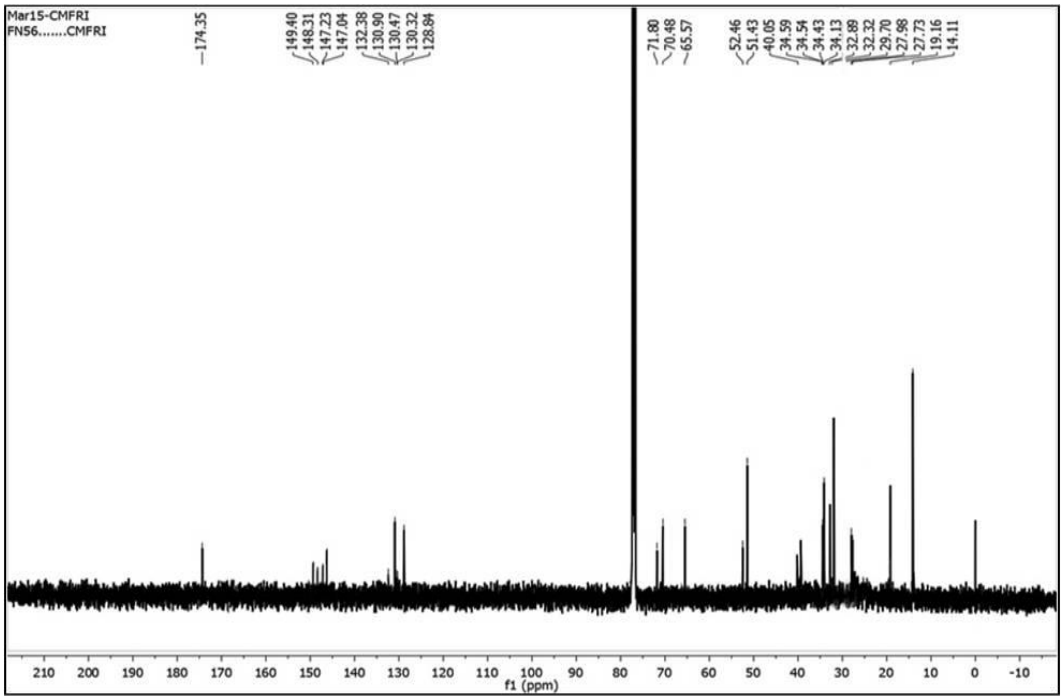

Figure 4.70. Figure showing the ^{13}C NMR spectrum of compound **G1**

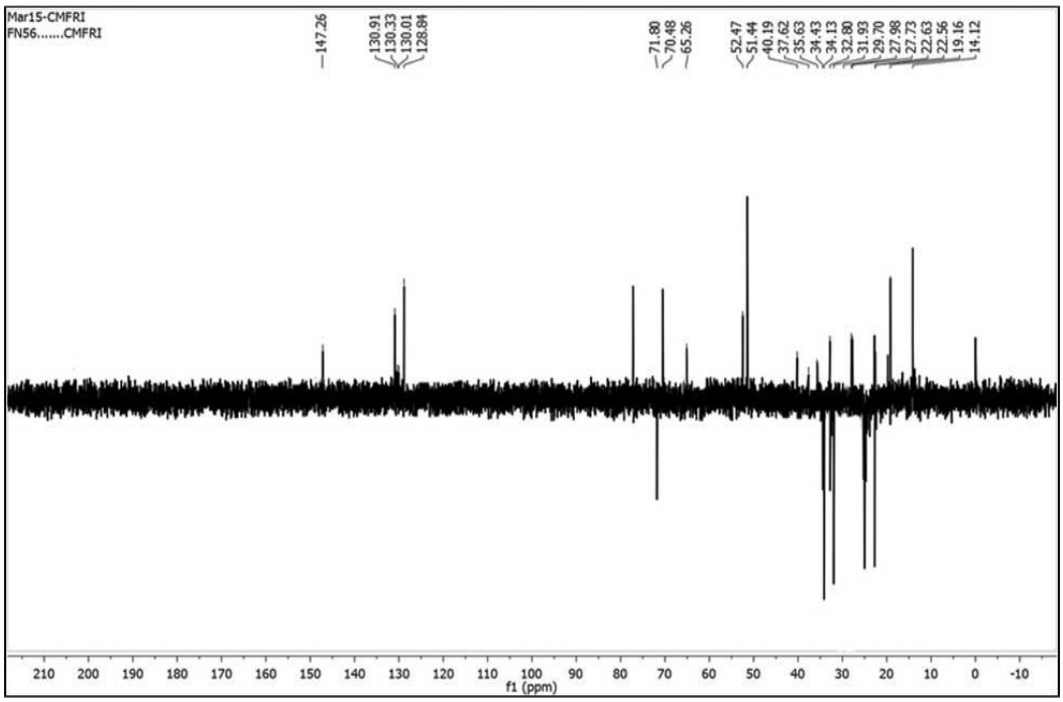

Figure 4.71. Figure showing the DEPT spectrum of compound **G1**

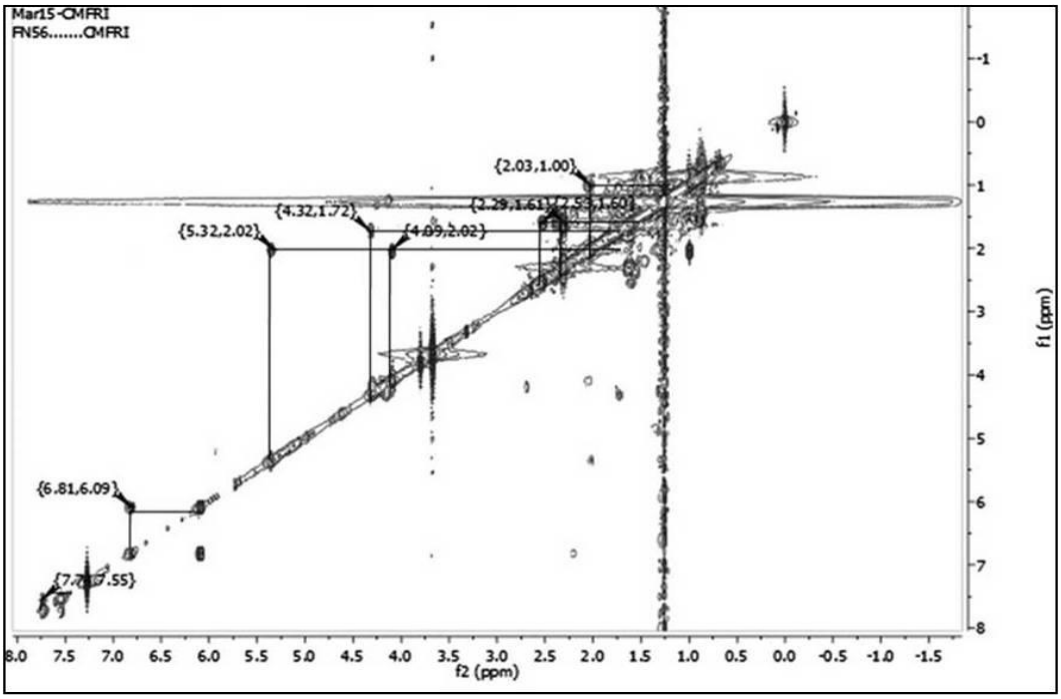

Figure 4.72. Figure showing the ^{1}H-^{1}H COSY spectrum of compound **G1**

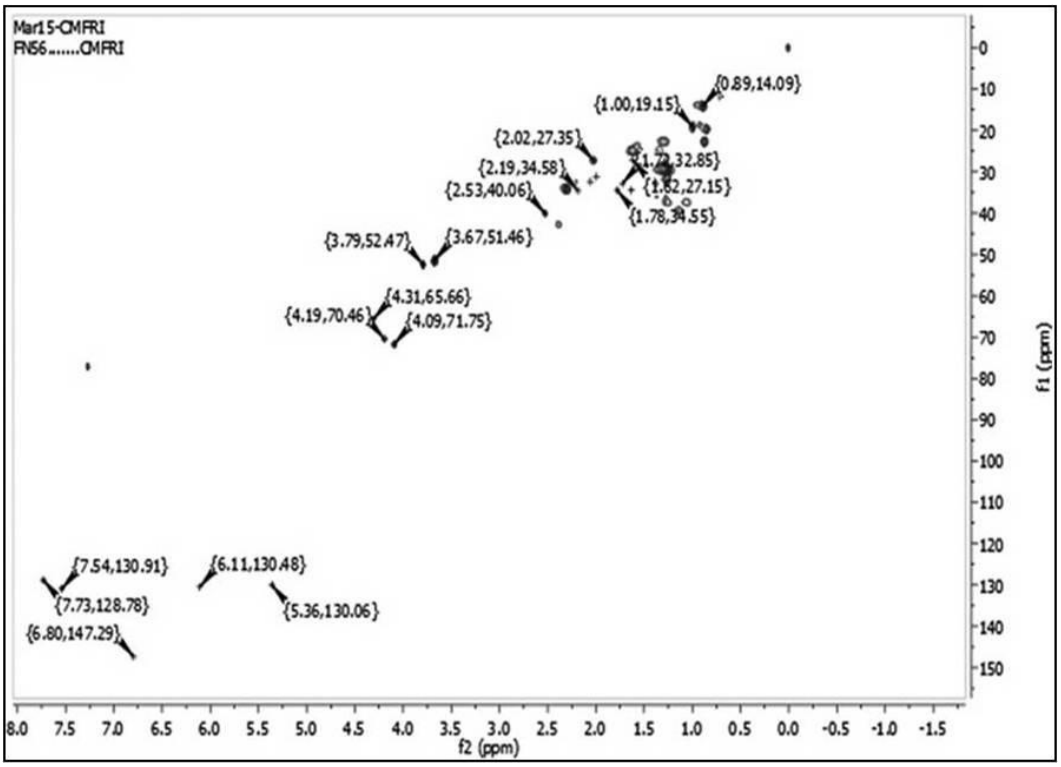

Figure 4.73. Figure showing the HSQC spectrum of compound **G1**

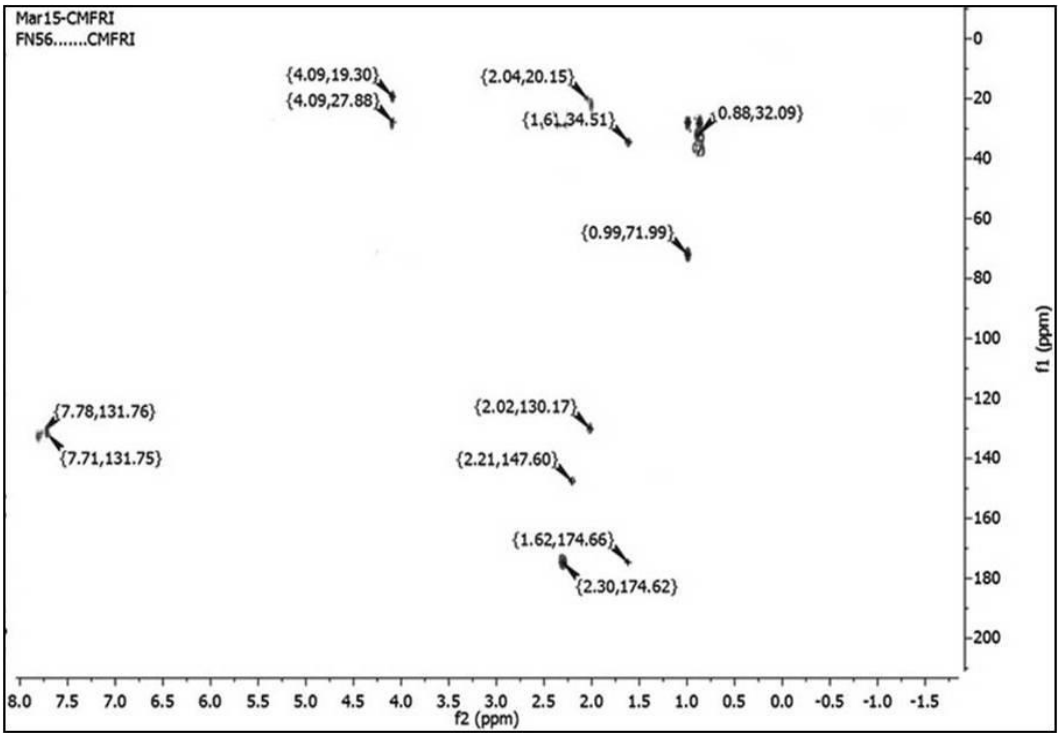

Figure 4.74. Figure showing the HMBC spectrum of compound **G1**

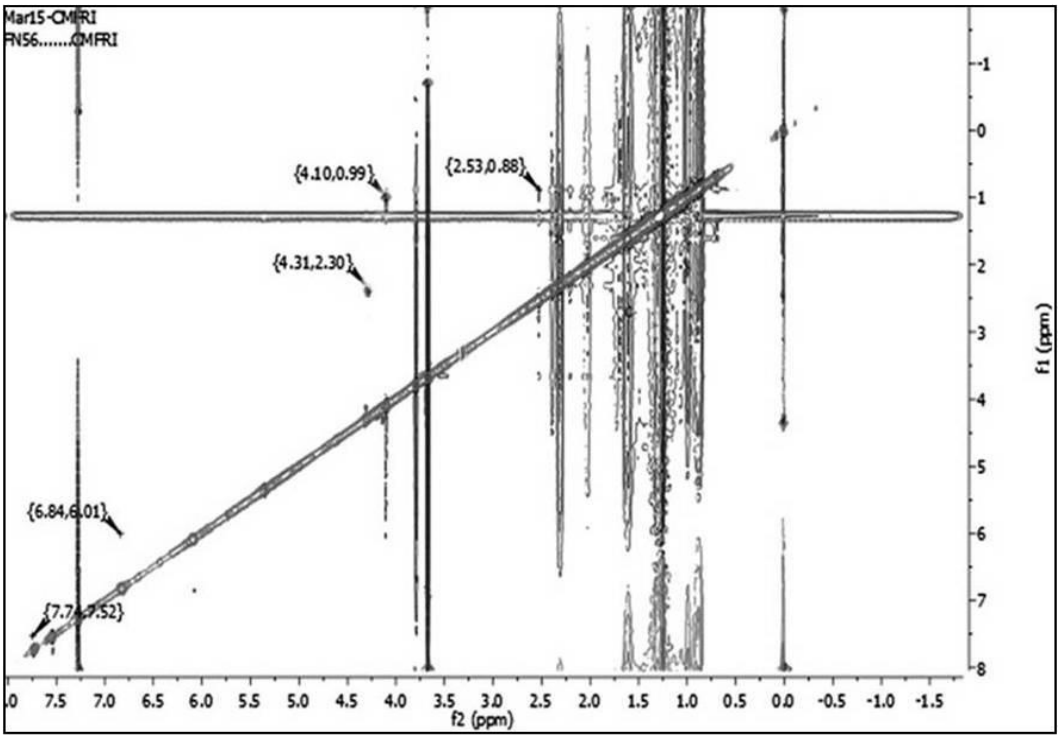

Figure 4.75. Figure showing the NOESY spectrum of compound **G1**

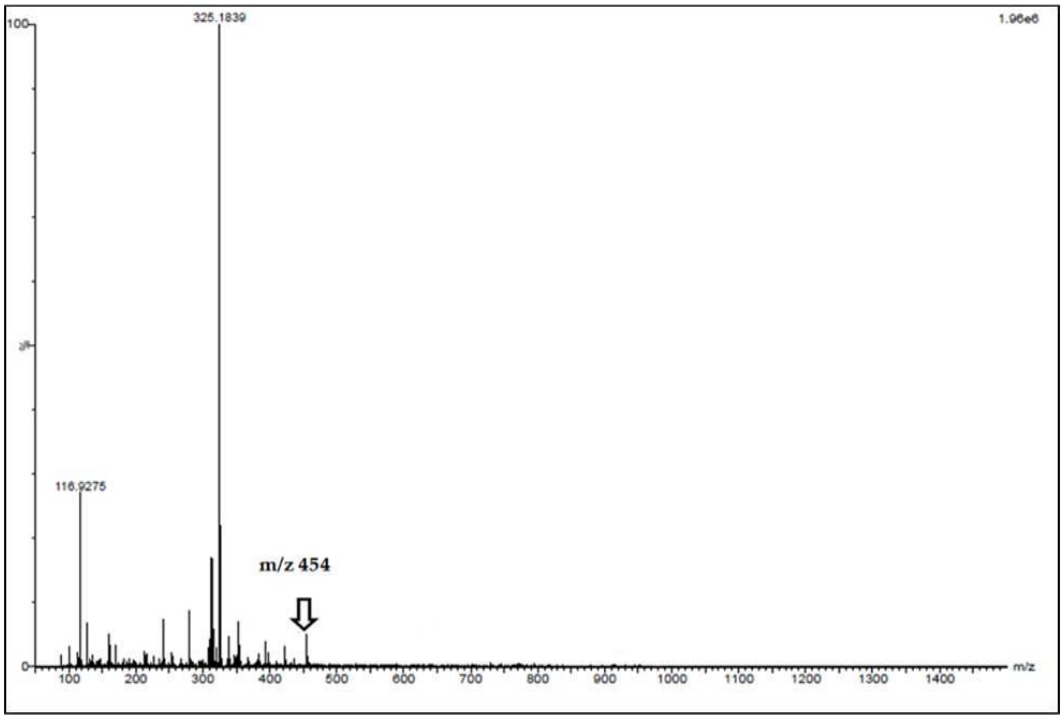

Figure 4.76. Mass spectrum of compound **G1**

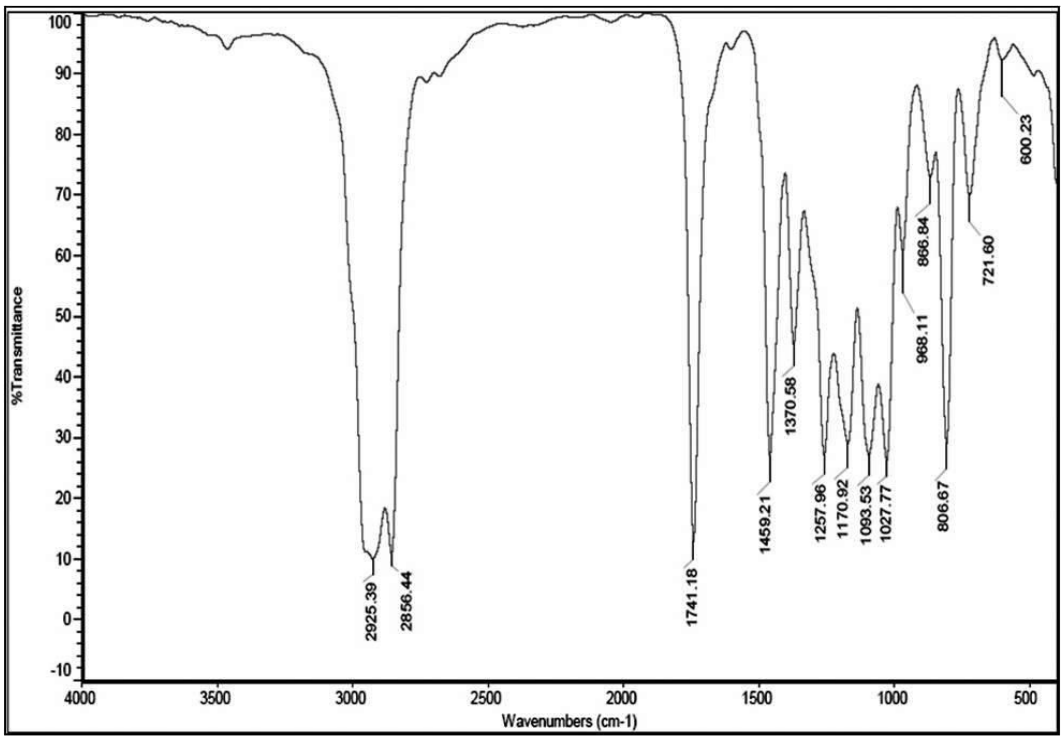

Figure 4.77. Figure showing the FTIR spectrum of compound **G1**

4.3.2.2. Structural Characterization of compound G2

2-(3-Ethyl-9-(2-methoxyethoxy)-1-oxo-2, 3, 4, 9-tetrahydro-1*H*-xanthen-2-yl) ethyl 5- hydroxy-9-methoxy-7, 8-dimethyl-8-(5-methylfuran- 2-yl) nona-3, 6-dienoate **(G2)**

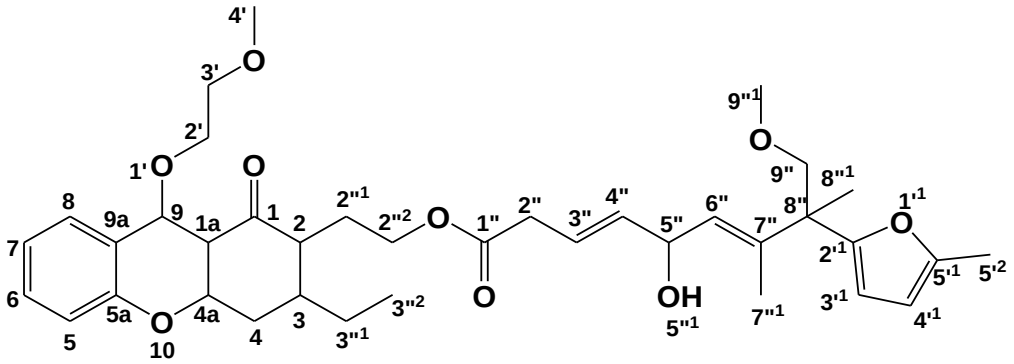

Sample yield	150 mg (0.625 %)
Physical description	Yellow oil
Molecular formula	$C_{37}H_{48}O_9$
Molecular weight	636.3308

2-**(3-Ethyl-9-(2-methoxyethoxy)-1-oxo-2, 3, 4, 9-tetrahydro-1*H*-xanthen-2-yl) ethyl 5-hydroxy-9-methoxy-7, 8-dimethyl-8-(5-methylfuran- 2-yl) nona-3, 6-dienoate :**Yellow oil; UV (MeOH: EtOAc) (log ε): 235 nm (3.237); TLC (Si gel GF_{254} 15 mm; MeOH: EtOAc 7:3, v/v) Rf: 0.76.; Rt (HPLC, CH_3CN: MeOH, 2:3 v/v): 14.147 min; IR (KBr, cm^{-1}) νmax (ν = stretching, δ = bending, ρ = rocking vibrations): 3425.10 (O-H ν), 2923.34, 2854.61 (C-H ν), 1708.08 (C=O ν), 1461.79 (C-H δ), 1297.86 (C-H ρ), 942.30 (=C-H δ), 724.28 (C-H ρ) ; ^{1}H NMR (500 MHz $CDCl_3$): δ_H 1.93 (2H, m), δ_H 1.93 (1H, m), δ_H 1.45 (2H, m), δ_H 0.80 (3H, t, *J*=6.88 Hz, H), δ_H 2.24 (1H, m), δ_H 1.54 (2H, m), δ_H 3.98 (2H, t, *J*=6.49 Hz), δ_H 2.75 (2H, d, *J*=4.62 Hz), δ_H 5.29 (1H, m), δ_H 5.26 (1H, t, *J*=8.19 Hz), δ_H 4.52 (1H, d, *J*=7.32 Hz), δ_H 3.24 (1H, s), δ_H 5.35 (1H, s), δ_H 1.62 (3H, s), δ_H 4.16 (1H, s), δ_H 4.06 (2H, t, *J*=7.18 Hz), δ_H 4.15 (2H, t, *J*=2.62 Hz), δ_H 3.59 (3H, s), δ_H 7.64 (1H, d, *J*=3.20 Hz), δ_H 7.29 (1H, t, *J*=2.05 Hz), δ_H 7.46 (1H, t,

J=3.07 Hz), δ_H 7.06 (1H, d, *J*=2.56 Hz), δ_H 2.06 (3H, s), δ_H 7.05 (1H, d, *J*=2.56 Hz), δ_H 7.06 (1H, d, *J*=2.56 Hz), δ_H 1.18 (3H, s), δ_H 3.92 (2H, s), δ_H 3.59 (3H, s); ^{13}C NMR (125 MHz, $CDCl_3$): δ_C 39.87 (C-4), δ_C 32.67 (C-3), δ_C 29.53 (C-3"^{1}), δ_C 14.1 (C-3"^{2}), δ_C 31.92 (C-2), δ_C 30.37 (C-2"^{1}), δ_C 64.39 (C-2"^{2}), δ_C 174.3 (C-1"), δ_C 25.63 (C-2"), δ_C 128.55 (C-3"), δ_C 128.99 (C-4"), δ_C 73.98 (C-5"), δ_C 128.18 (C-6"), δ_C 132.46 (C-7"), δ_C 38.76 (C-7"^{1}), δ_C 209.27 (C-1), δ_C 138.4 (C-1a), δ_C 74.75 (C-9), δ_C 60.8 (C-1'), δ_C 68.13 (C-2'), δ_C 51.39 (C-3'), δ_C 142.54 (C-9a), δ_C 128.85 (C-8), δ_C 124.44 (C-7), δ_C 130.83 (C-6), δ_C 125.09 (C-5), δ_C 147.67 (C-5a), δ_C 138.51 (C-4a), δ_C 147.07 (C-5'^{1}); δ_C 30.19 (C-5'^{2}), δ_C 123.42 (C-4'^{1}), δ_C 128.15 (C-3'^{1}), δ_C 142.6 (C-2'^{1}), δ_C 42.31 (C-8"), δ_C 31.79 (C-8"^{1}), δ_C 66.64 (C- 9"), δ_C 50.04 (C-9"^{1}); ^{1}H-^{1}H COSY and HMBC (Fig. 4.78 to Fig. 4.88, Table 4.14); HR (EI) MS *m/z* found 636.3308 $[M]^+$, calcd for $C_{37}H_{48}O_9$ 636.3305.

Compound **G2**, a previously undescribed furanyl derivative, was purified as yellow oil by extensive column chromatography on adsorbent silica gel. The mass spectral data of compound **G2** accounted for the molecular ion peak at *m/z* 636 (*m/z* 636.3308 $[M]^+$) enclosing fourteen degrees of unsaturation, and the molecular formula as $C_{37}H_{48}O_9$ was deduced from combined ^{1}H and ^{13}C NMR spectroscopic experiments. The IR spectrum showed bending vibration near 1708 cm^{-1}, which was attributed to the carbonyl group.

The absorption bands at 1461 and 2854 cm^{-1} in the FTIR spectrum showed the presence of olefinic (>C=C<) as well as alkyl groups, respectively. The characteristic hydroxyl stretching vibration appeared at 3425.10 cm^{-1}. The isolated compounds displayed ten quaternary carbons, in which, four carbons (δ_C 9a 142.54, δ_C 5a 147.67, δ_C 1a 138.4, δ_C 4a 138.51) were associated with substituted aromatic moiety, and two carbons {δ_C (C-1) 209.27, δ_C (C-1") 174.3} were attributed to the carbonyl groups in the side chain substitution of the aromatic framework, three carbons (δ_C 138.4, C-1a; δ_C 138.51, C-4a; and δ_C 132.46, C-7") were due to the olefinic groups, one quaternary carbon associated side chain substitution from furanyl moiety (δ_C 42.31, C-8") and remaining two carbons associated with furanyl skelton (δ_C 147.07, C-5'^{1} and δ_C 142.6, C-2'^{1}). These assignments supported the presence of 1*H*-xanthenyl methylfuranyl carbon skeleton. The ^{1}H-^{1}H COSY displayed the existence of three spin arrangements, H-6 to H-5{(δ_H 7.46 (H-6)/δ_H 7.06 (H-5)} which were due to the aromatic ring system, whereas the correlations between H-3"^{1} to H-3"^{2} {(δ_H 1.45 (H-3"^{1})/δ_H 0.80 (H-3"^{2})} designated ethyl substitution from xanthenyl moiety. ^{1}H-^{1}H COSY correlation between

H-2 to H-2"^{1}/H-2"^{2}{(δ_H 2.24 (H-2)/δ_H 1.54 (H-2"^{1})/δ_H 3.98 (H-2"^{2})}, H-2" to H-3" {(δ_H 2.75 (H-2")/δ_H 5.29 (H-3")} and H-4" to H-5" {(δ_H 5.26 (H-4")/δ_H 4.52 (H-5")} were assigned to the substitution from the furanyl framework, which were further confirmed from the detailed HMBC correlations.

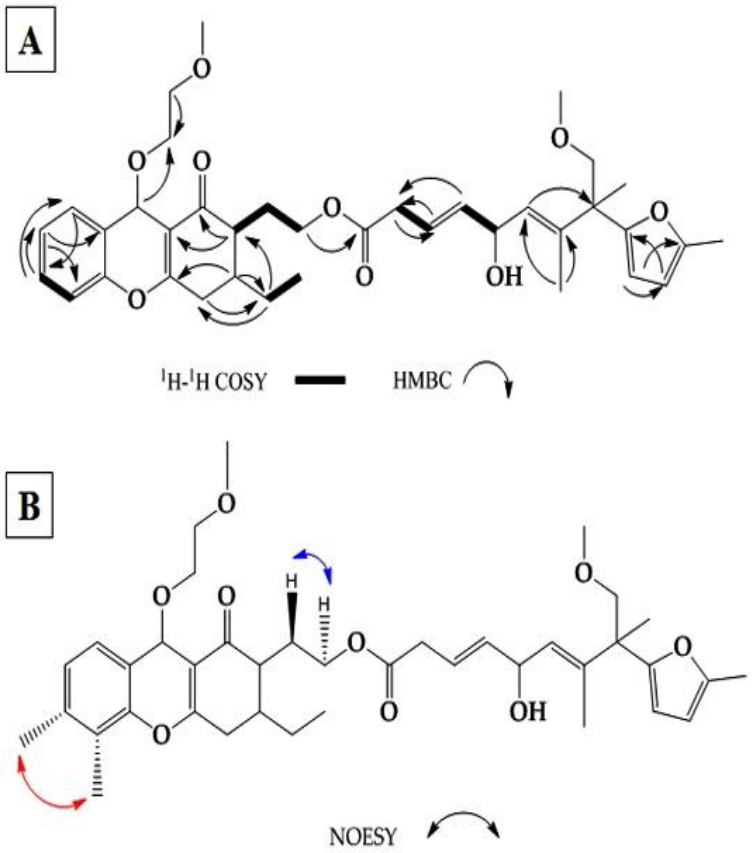

Figure 4.78. Figure showing key (**A**) ^{1}H-^{1}H COSY, HMBC, and (**B**) NOESY correlations of compound **G2**

Ultraviolet absorbance at λmax (log ε) 235 nm (3.237) was assigned to the xanthen chromophore, which was further supported by the IR bending vibrations at about 1461 cm^{-1} (Ochieng et al. 2012; Jiang et al. 2002). The ^{1}H NMR spectrum showed two doublets, and each integrated for one proton of furan with the same coupling constant (*J*=2.56 Hz) at δ_H 7.05 (H-4'^{1}) and (*J*=2.56 Hz) at δ_H 7.06 (H-3'^{1}) (Christoph et al. 2007). The ^{1}H NMR spectrum included eight methylene proton signals that appeared at H-1' {(δ_H 4.06 (H-1') corresponding to δ_C 60.18 (C-1') as deduced by HSQC experiments}, H-2' {(δ_H 4.15 (H-2'), δ_C 68.13 (C-2')}, H-4 {(δ_H 1.93 (H-4), δ_C

39.87 (C-4)}, H-3"^{1} {(δ_H 1.45 (H-3"^{1}), δ_C 29.53 (C-3"^{1})}, H-2"^{1} {(δ_H 1.54 (H-2"^{1}), δ_C 30.37 (C-2"^{1})}, H-2"^{2} {(δ_H 3.98 (H-2"^{2}), δ_C 64.39 (C-2"^{2})}, H-2" {(δ_H 2.75 (H-2"), δ_C 25.63 (C-2")} and H-9" {(δ_H 3.92 (H-9"), δ_C 66.64 (C-9")}, and terminal methyl group appeared as a triplet at H-3"^{2} {(δ_H 0.80 (H-3"^{2}, *J*=7 Hz), δ_C 14.1 (C-3"^{2})} attached to the xanthenyl ring framework (Table 4.14). The HMBC couplings between H-8 (δ_H 7.64)/C-6 (δ_C 130.83); H-7 (δ_H 7.29)/C-5 (δ_C 124.44); H-3 (δ_H 1.93)/C-3"^{1} (δ_C 29.53); H-3"^{1} (δ_H 1.45)/C-2 (δ_C 31.92), H-2" (δ_H 2.75)/C-3" (δ_C 128.55), H-3" (δ_H 5.29)/C-2" (δ_C 25.63), H- 4" (δ_H 5.26)/C-2" (δ_C 25.63) supported the above attributions. The ^{1}H NMR in combination with ^{13}C NMR exhibited highly deshielded oxymethylene protons at δ_H 4.06, H-1' (*J*=7.18 Hz) corresponding to C-1' (δ_C 60.18); δ_H 4.15, H-2' (*J*=2.62 Hz) C-2' (δ_C 68.13); δ_H 3.98, H-2"^{2} (*J*=6.49 Hz) C-2"^{2} (δ_C 64.39), and δ_H 3.92, H-9" (*J*=7.56 Hz) exhibiting HSQC correlation with C-9" (δ_C 66.64). Similarly highly deshielded oxymethine protons appeared at δ_H 4.16 H-9 (*J*=2.19 Hz) corresponding to C-9 (δ_C 74.75) due to the presence of electronegative oxygen and at δ_H 4.52 H-5" (*J*=7.32 Hz) C-5" (δ_C 73.83) due to the presence of neighboring –OH group, and therefore, were attributed to comprise the 1*H*-xanthenyl methylfuranyl ring system in compound **G2**. The additional olefinic signals were deduced at δ_H 5.29 (H-3", C-3"), δ_H 5.26 (H-4", *J*=8.19 Hz, C-4"), and δ_H 5.35 (H-6", *J*=5.35 Hz, C-6") whereas the methoxy group was found to appear as a singlet at δ_H 3.59 (H-3', 51.39 C-3'), δ_H 3.59 (H-9"^{1}, 50.04 C-9"^{1}), which were attributed to build the 2-(3-ethyl-9-(2-methoxyethoxy)-1-oxo-2, 3, 4, 9-tetrahydro-1*H*-xanthen-2-yl) ethyl-5-hydroxy-9-methoxy-7, 8-dimethyl-8-(5-methylfuran-2-yl) nona-3, 6-dienoate framework. The methyl protons at δ_H 7"^{1} (δ_H 1.62), 8"^{1} (δ_H 1.18) and 5'^{2} (δ_H 2.06) appeared as singlets. In addition hydroxyl group (-OH) appeared at H-5"^{1} (δ_H 3.24) as a singlet. The –CH proton at δ_H 2.24 {(H-2, C-2 (δ_C 31.92)}, δ_H 1.93 {(H-3, C- 3 (δ_C 32.67)}, and δ_H 4.16 {(H-9, C-9 (δ_C 74.75)} were distinct to the junction point of the substituted xanthenyl moiety with the side chain furanyl substitution. The intense HMBC interactions between H-3 (δ_H 1.93)/C-3"^{1} (δ_C 29.53)/C-4a (δ_C 138.51); H-3"^{1} (δ_H 1.45)/C-4 (δ_C 39.87); H-2 (δ_H 2.24)/C-1 (δ_C 209.27)/C-1a (δ_C 138.4); H-2"^{2} (δ_H 3.98)/C-1" (δ_C 174.3); H-7"^{1} (δ_H 1.62)/C-7" (δ_C 132.46)/C-6" (δc 128.18); H-6" (δ_H 5.35)/C-8" (δ_C 42.31); H-9 (δ_H 4.16)/C-1' (δ_C 60.18); H-2' (δ_H 4.15)/C-1' (δ_C 60.1); H-7 (δ_H 7.29)/C-9a (δ_C 142.54); H-6 (δ_H 7.46)/C-7 (δ_C 124.44)/C-8 (δc 128.85); H-4'^{1} (δ_H 7.05)/C-2'^{1} (δ_C 142.6); H-3'^{1} (δ_H 7.06)/C-4'^{1} (δ_C 123.42)/C-5'^{1} (δ_C 147.07) supported the above characteristics. The relative stereochemistries at C-3, C-2, C-9, and C-5" bearing the xanthenyl furanyl ring carbon

skeleton were attributed by detailed NOESY correlations and corresponding ^{1}H coupling constants (*J*-values). Notably, the aromatic protons at δ_H 7.46 {(H-6, C-6 (δ_C 130.83)} displayed NOESY correlations with the aromatic methine protons at δ_H 7.06 {(H-5, C-5 (δ_C 125.09)} in the xanthenyl furanyl ring skeleton. The proton at δ_H 1.54 {(H-2"^{1}, C-2"^{1} (δ_C 30.37)} resonated as a multiplet, which was at the α-face of the molecule having coupling at δ_H 3.98 {(H-2"^{2}, C-2"^{2} (δ_C 64.39)} (*J*=6.49 Hz), and subsequently the larger substituent 2, 3-diethyl-9-(2-methoxyethoxy)- tetrahydro-1*H*-xanthen-1-one at C-3 and C-2 was attributed to α-disposed.

Table 4.14 NMR spectroscopic data of compound **G2** in $CDCl_3$[a]

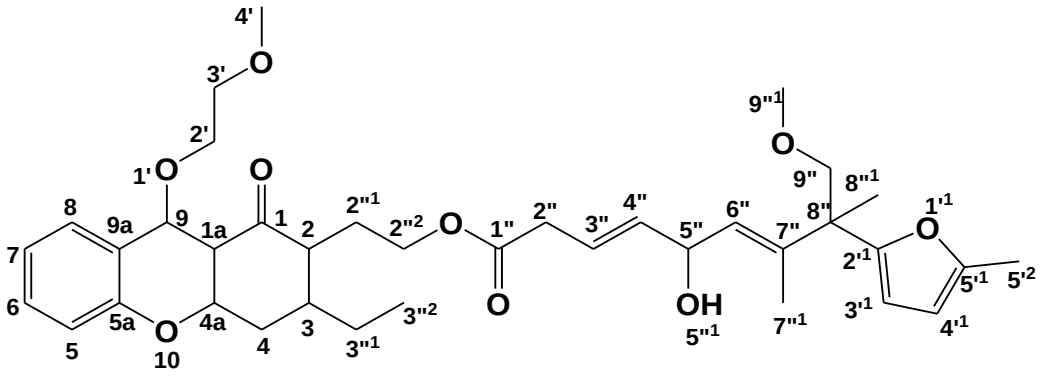

C. No	^{13}C (δ)	^{1}H NMR (mult., *J* in Hz, int.)[b]	^{1}H-^{1}H COSY	HMBC ($^{1}H^{13}C$)
1	209.27	-	-	-
1a	138.4	-	-	-
2	31.92	2.24 (m, 1H)	2"[1]-H	C-1, C-1a
2"[1]	30.37	1.54 (m, 2H)	2-H, 2"[2]-H	-
2"[2]	64. 39	3.98 (t, *J*=6.49 Hz, 2H)	2"[1]-H	C-1"
3	32.67	1.93 (m, 1H)	-	C-3"[1], C-4a
3"[1]	29.53	1.45 (m, 2H)	3"[2]-H	C-2, C-4
3"[2]	14.1	0.80 (t, *J*=6.88 Hz, 3H)	3"[1]-H	-
4	39.87	1.93 (m, 2H)	-	C-3"[1]
4a	138.51	-	-	-
5	125.09	7.06 (d, *J*=2.56 Hz, 1H)	6-H	-
5a	147.67	-	-	-
6	130.83	7.46 (t, *J*=3.07 Hz, 1H)	5-H	C-7, C-8
7	124. 44	7.29 (t, *J*=2.05 Hz, 1H)	-	C-9a, C-5
8	128.85	7.64 (d, *J*=3.20 Hz, 1H)	-	C-6
9	74.75	4.16 (s, 1H)	-	C-1'
9a	142.54	-	-	-
1'	60.18	4.06 (t, *J*=7.18 Hz, 2H)		
2'	68.13	4.15 (t, *J*=2.62 Hz, 2H)		C-1'
3'	51.39	3.59 (s, 3H)		
1"	174.3	-		
2"	25.63	2.75 (d, *J*=4.62 Hz, 2H)	3"-H	C-3"
3"	128.55	5.29 (m, 1H)	2"-H	C-2"
4"	128.99	5.26 (t, *J*=8.19 Hz, 1H)	5"-H	C-2"
5"	73.98	4.52 (d, *J*=7.32 Hz, 1H)	4"-H	-
5"[1]	-	3.24 (s, 1H)		
6"	128.18	5.35 (d, *J*=8.12 Hz,1H)		C-8"
7"	132.46	-		-
7"[1]	38.76	1.62 (s, 3H)		C-6", C-7"
8"	42.31	-	-	
8"[1]	31. 79	1.18 (s, 3H)	-	
9"	66.64	3.92 (s, 2H)	-	
9"[1]	50.04	3.59 (s, 3H)	-	
2'[1]	142.6	-	-	

3'[1]	128.15	7.06 (d, *J*=2.56 Hz, 1H)	-	C-4'[1], C-5'[1]
4'[1]	123.42	7.05 (d, *J*=2.56 Hz, 1H)	-	C-2'[1]
5'[1]	147.07	-		
5'[2]	30.19	2.06 (s, 3H)		

[a] NMR spectra recorded using Bruker AVANCE III 500 MHz (AV 500) spectrometer in $CDCl_3$ as aprotic solvent at ambient temperature with TMS as the internal standard (δ 0 ppm).

[b] Values in ppm, multiplicity and coupling constants (*J*=Hz) are indicated in parentheses. The assignments were made with the aid of the ^1H-^1H COSY, HSQC, HMBC and NOESY experiment

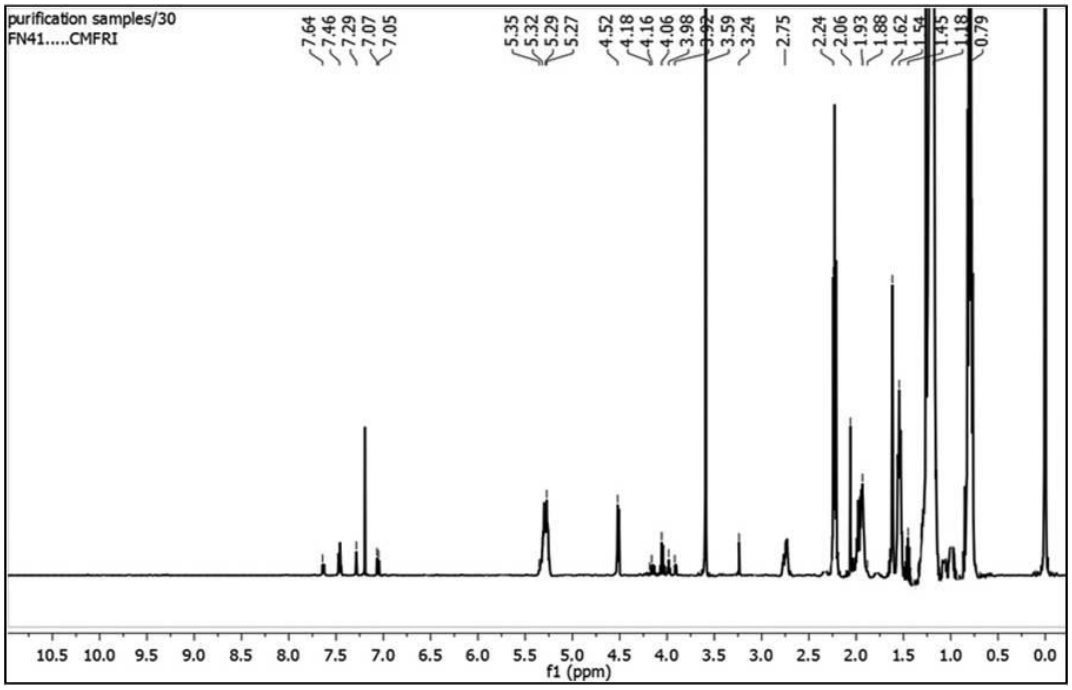

Figure 4.79. Figure showing the ^1H NMR spectrum of compound **G2**

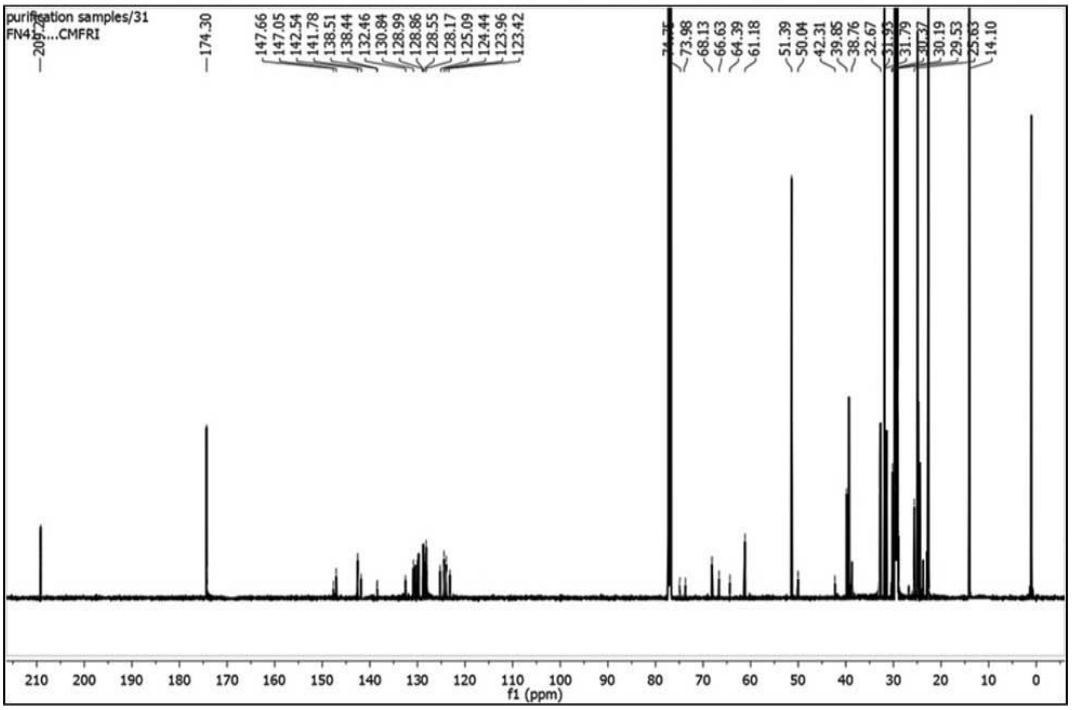

Figure 4.80. Figure showing the ^{13}C NMR spectrum of compound **G2**

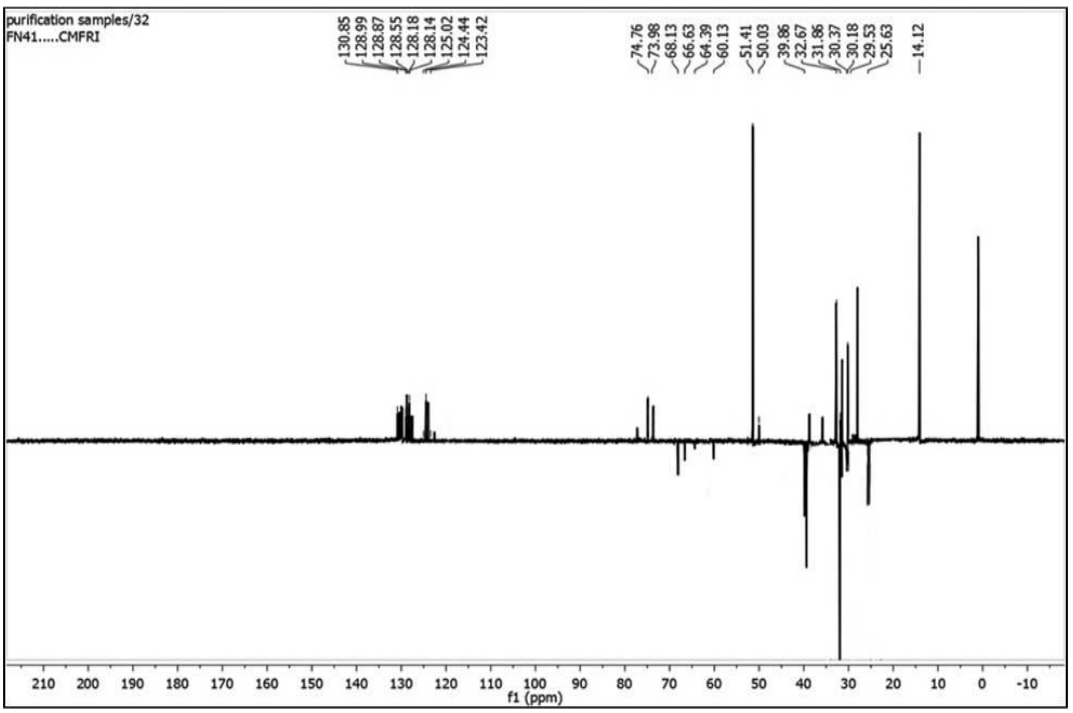

Figure 4.81. Figure showing the DEPT spectrum of compound **G2**

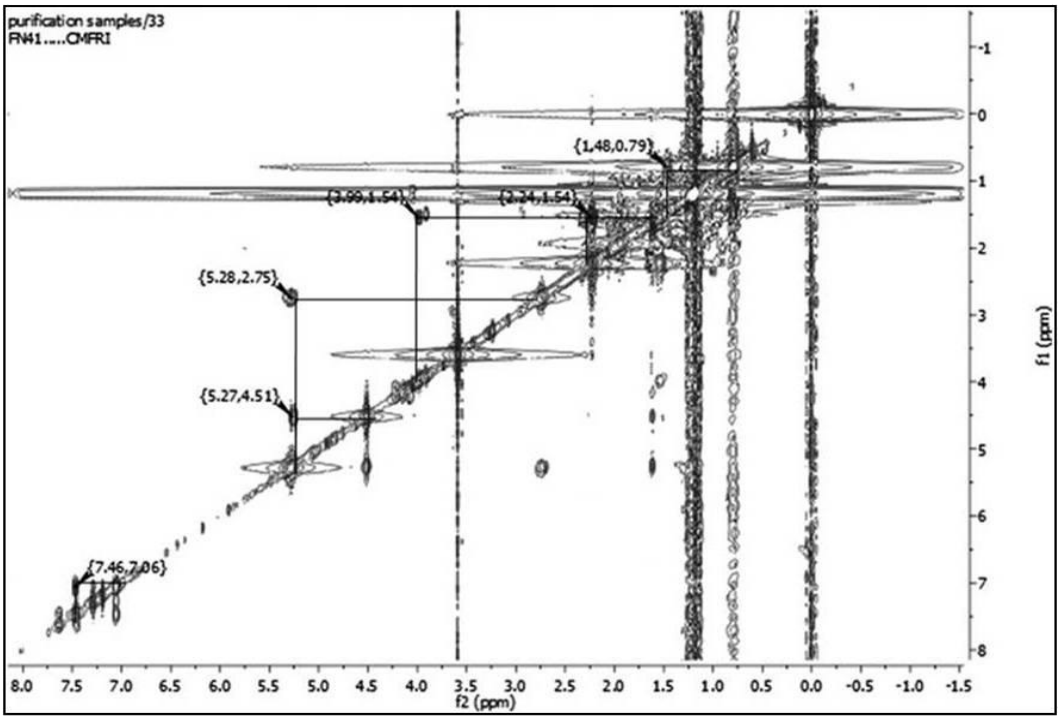

Figure 4.82. Figure showing the ^{1}H-^{1}H COSY spectrum of compound **G2**

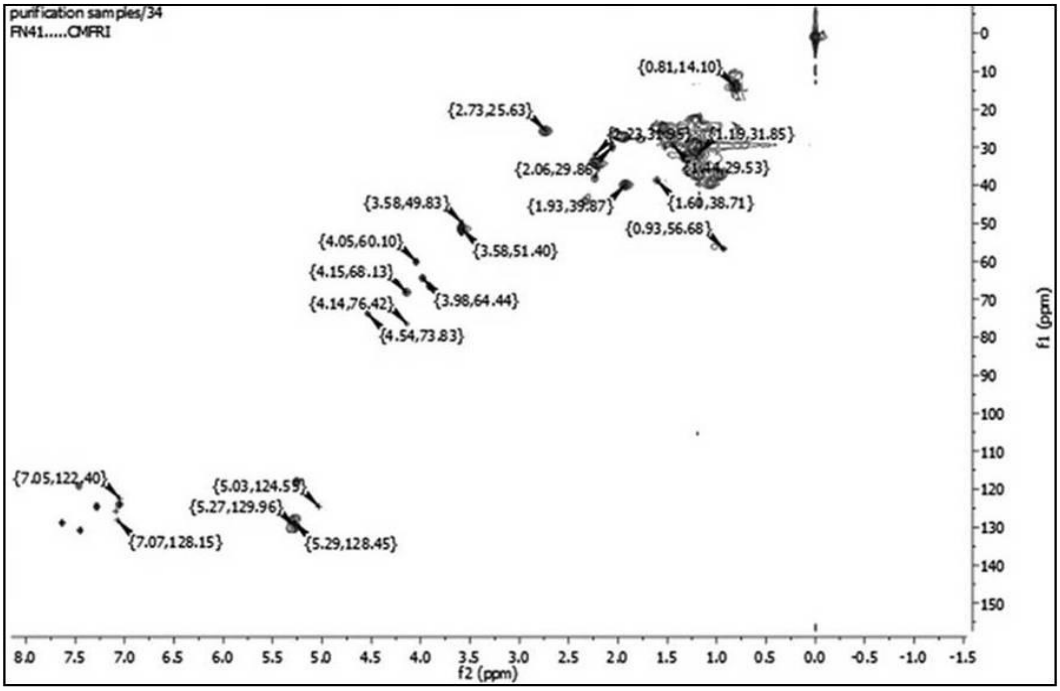

Figure 4.83. Figure showing the HSQC spectrum of compound **G2**

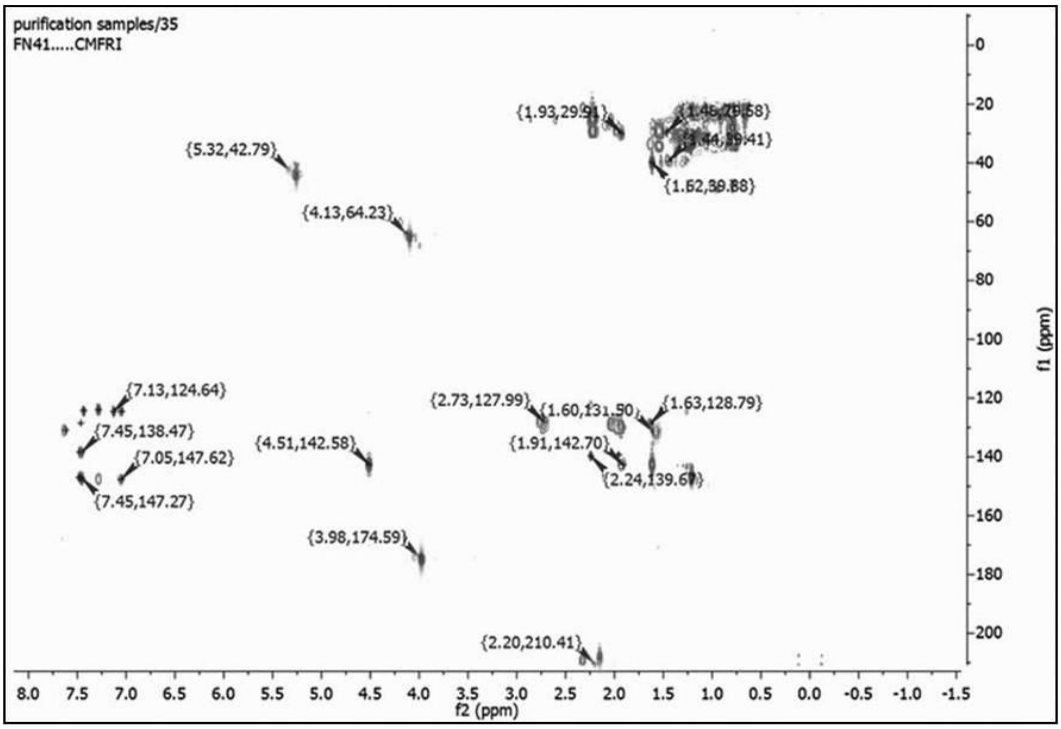

Figure 4.84. Figure showing the HMBC spectrum of compound **G2**

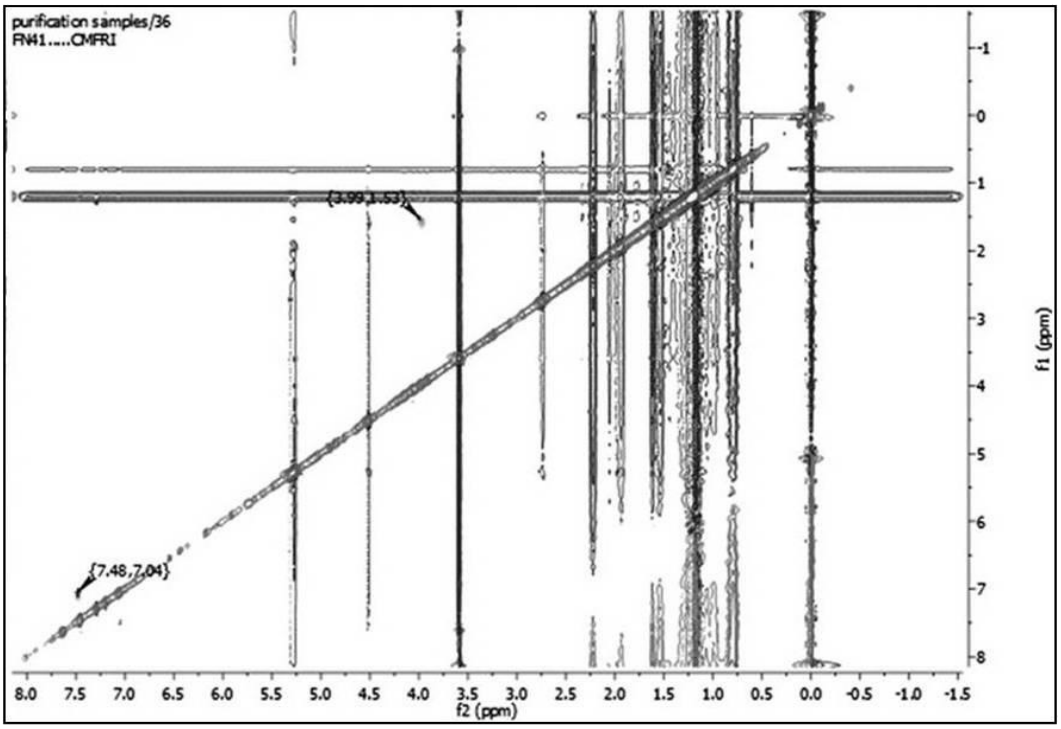

Figure 4.85. Figure showing the NOESY spectrum of compound **G2**

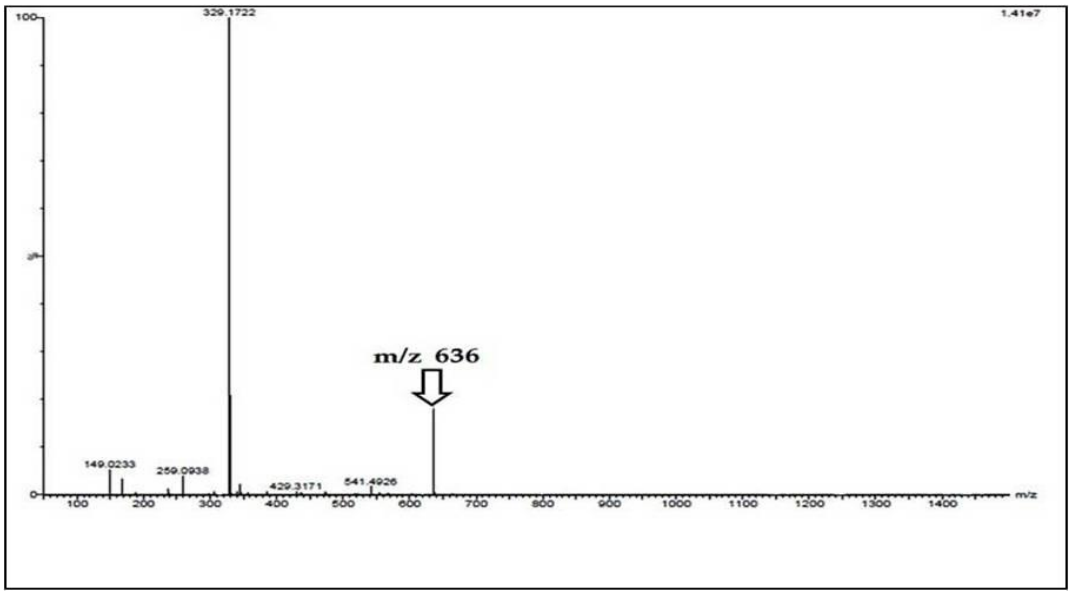

Figure 4.86. Mass spectrum of compound **G2**

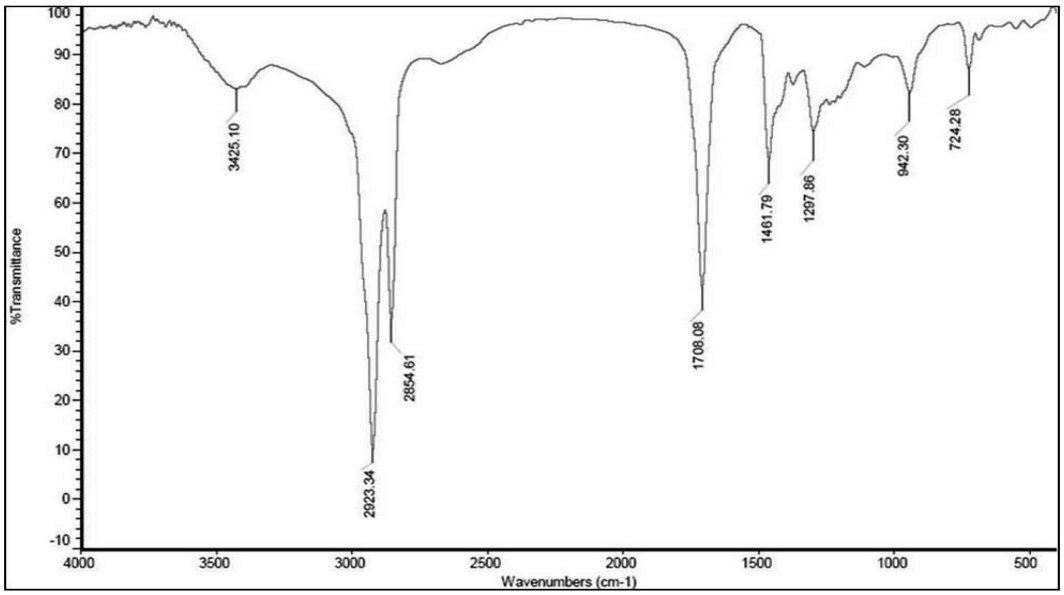

Figure 4.87. Figure showing the FTIR spectrum of compound **G2**

4.3.2.3. Bioactivities and Structure-Activity Relationship Analysis

The antioxidative properties of the furanyl derivatives as resolved by DPPH and ABTS free radical scavenging activities were found to be significantly greater (IC_{50}

~0.051–0.055 × 10^{-2} M) than those exhibited by α-tocopherol (IC_{50} > 0.146 × 10^{-2} M), and were similar to the synthetic antioxidants (BHT/BHA IC_{50} ~0.113–0.189 × 10^{-2} M, $P < 0.05$). It is of note that electron-delocalization through the electron-dense aromatic, carbonyl, methoxy, and olefinic bonds present in the molecular structure of the isolated compounds might apparently contribute towards their potential free radical scavenging properties (Pietta 2000; Cai et al. 2006).

The prostaglandins produced by proinflammatory constitutive enzyme COX-1 were reported to protect the stomach lining from gastric HCl secreted from the oxyntic and peptic glands, while blocking this enzyme isoform apparently increases the risk of stomach bleeding and ulcers. Notably, the commercially available NSAIDs, including salicylate analogs, aspirin and ibuprofen equally block two different cyclooxygenase isoforms, such as constitutive COX-1 and inducible COX-2. While this results in reduced pain and inflammation, it can potentially lead to serious gastrointestinal bleeding, heart attacks, and strokes. The furanyl derivatives isolated in this study displayed significantly greater inhibition towards COX-2 than its COX-1 isoform, and likewise, the selectivity indices (SI, anti-COX-1 IC_{50}/anti-COX-2 IC_{50}) of these compounds remained significantly lesser (1.08–1.09) than synthetic NSAIDs (aspirin and ibuprofen, SI: 0.02 and 0.44, respectively, $P < 0.05$), and consequently, appeared to be safer. The furanyl analogs exhibited no significant difference towards *in vitro* 5-LOX inhibitory activities (IC_{50} 0.209–0.173 × 10^{-2} M) with that displayed by ibuprofen (IC_{50} 0.451 × 10^{-2} M; $P < 0.05$). Sodium salicylate was found to be a weaker inhibitor of both COX isoforms (anti-COX-2 IC_{50} 1.655 × 10^{-2} M, anti-COX-1 IC_{50} 1.206 × 10^{-2} M), and demonstrated significantly lesser activity against 5-LOX (anti-LOX-5 IC_{50} 1.093 × 10^{-2} M) (Table 4.15-4.16). The hitherto undescribed furanyl derivatives from the red marine macroalga *G. opuntia*, might therefore, be used as potential anti-inflammatory and antioxidative pharmacophore leads in medicine and food. Structure–bioactivity correlation analyses of the furanyl derivatives isolated in this study were carried out by using different structural descriptor factors. The antioxidative properties of the isolated compounds were found to be directly proportional to their hydrophobic characters as resolved by octanol–water coefficient (log Pow). The larger the value of log Pow, the greater the molecular hydrophobicity of the compounds. Compound **G2** displayed lesser hydrophobic character (log Pow 3.37) than that recorded with **G1** (log Pow 4.59).

Table 4.15 Antioxidative and anti-inflammatory activities of the furanyl derivatives (**G1-G2**) from *G. opuntia vis-à-vis* the commercially available antioxidants and anti-inflammatory agents

Antioxidative activities†	**Bioactivities {**IC_{50} ($x10^{-2}$ M)}				
	Compound G1	**Compound G2**	**BHA**	**BHT**	**α-tocopherol**
$DPPH^{\cdot}$ scavenging	$0.051^{a} \pm 0.009$	$0.050^{a} \pm 0.009$	$0.144^{c} \pm 0.006$	$0.113^{b} \pm 0.009$	$0.146^{c} \pm 0.009$
$ABTS^{+\cdot}$ scavenging	$0.066^{a} \pm 0.004$	$0.055^{a} \pm 0.008$	$0.189^{c} \pm 0.011$	$0.118^{b} \pm 0.009$	$0.169^{c} \pm 0.116$
Anti-inflammatory activities†	**Compound G1**	**Compound G2**	**Aspirin**	**Na-salicylate**	**Ibuprofen**
COX -1 inhibition	$0.222^{b} \pm 0.009$	$0.185^{b} \pm 0.006$	$0.003^{a} \pm 0.00$	$1.206^{c} \pm 0.031$	$0.019^{a} \pm 0.00$
COX -2 inhibition	$0.202^{b} \pm 0.007$	$0.171^{b} \pm 0.014$	$0.117^{b} \pm 0.011$	$1.655^{c} \pm 0.031$	$0.044^{a} \pm 0.010$
Selectivity index††	$1.09^{c} \pm 0.06$	$1.08^{c} \pm 0.03$	$0.02^{a} \pm 0.02$	$0.72^{b} \pm 0.01$	$0.44^{b} \pm 0.02$
5-LOX inhibition	$0.209^{a} \pm 0.024$	$0.173^{a} \pm 0.006$	$0.216^{a} \pm 0.011$	$1.093^{c} \pm 0.075$	$0.451^{b} \pm 0.053$

† The samples were analyzed in triplicate (n=3) and expressed as mean ± standard deviation. Means followed by the different superscripts (a–c) within the same row indicate significant differences ($P < 0.05$).

†† Selectivity index has been calculated as the ratio of anti-COX-1(IC_{50}) to that of anti-COX-2 (IC_{50})

Table 4.16 Anti-diabetic and anti-hypertensive activities of the furanyl derivatives (**G1-G2**) from *G. opuntia vis-à-vis* the commercially available agents

	Bioactivities { $IC_{50}s$ ($x10^{-2}$ M)}		
Anti-diabetic activities†	**Compound G1**	**Compound G2**	**Standard**††
α-Amylase inhibitory	$0.062^{a} \pm 0.002$	$0.052^{a} \pm 0.002$	$0.062^{a} \pm 0.002$
α-Glucosidase inhibitory	$0.040^{a} \pm 0.007$	$0.031^{a} \pm 0.005$	$0.033^{a} \pm 0.002$
Inhibition of DPP-4	$0.002^{a} \pm 0.00$	$0.002^{a} \pm 0.009$	$0.003^{a} \pm 0.00$
Anti-hypertensive activities†	**Compound G1**	**Compound G2**	**Captopril**
ACE-1 inhibition	$0.024^{a} \pm 0.007$	$0.023^{a} \pm 0.005$	$0.037^{b} \pm 0.005$

† The samples were analyzed in triplicate (n=3) and expressed as mean ± standard deviation. Means followed by the different superscripts (a–b) within the same row indicate significant differences ($P < 0.05$).

†† Acarbose was used as the standard for α-amylase and α-glucosidase inhibitory activities; whereas diprotin A was the reference towards inhibition of DPP-4.

Figure 4.88. Graphical representation of bioactivities of compound **G1** and **G2**. The thalli of the studied marine macroalga were displayed as inset

The reduced activity of compound **G2** is justified based on the lesser hydrophobic properties and reduced membrane permeability and reactivity towards DPPH-free radical. It has been hypothesized that the free radical DPPH can easily interact with the compounds with greater hydrophobic coefficients (greater log Pow value), and therefore, exhibit higher radical scavenging ability towards lipophilic DPPH. Since antioxidants require diffusing into the liposomes to interact with the lipophilic free radicals in the biological systems, it is reasonable to expect that a greater hydrophobicity of antioxidants is related to their radical scavenging activity in liposomes and cells. On the basis of these results, it could be concluded that hydrophobicity has been the significant factor in determining the antioxidant and anti-inflammatory properties of the furanyl derivatives. Notably, acarbose and miglitol are competitive inhibitors of α-glucosidase, and were found to decrease the absorption of starch and disaccharides (Baylac and Racine 2003; Davis and Granner 2011). One of the remedial pathways for reducing the postprandial blood glucose levels in the patients with diabetes mellitus is to cut off carbohydrate consumption after food intake.

The α-amylase/α-glucosidase has been accepted as a family of endo-amylases catalyzing the initial hydrolysis of starch into smaller oligosaccharides by the cleavage of α-D-(1-4) glycosidic bonds. Inhibition of the enzymes, α-amylase and α-glucosidase appeared to minimize the increased postprandial blood glucose level in diabetes (Abu Soud et al. 2004; Conforty et al. 2005). The present study displayed that there were significant differences in α-glucosidase/α-amylase inhibitory activities of the purified compound **G1** than those recorded with compound **G2**. However, compound **G1** exhibited greater α-amylase inhibitory activity (IC_{50} 0.062 × 10^{-2} M) compared to compound **G2** (IC_{50} 0.052 × 10^{-2} M) and the activities were comparable with synthetic positive control (acarbose, IC_{50} 0.062 × 10^{-2} M) (Fig. 4.88, Table 4.15-4.16). Likewise, compound **G1** exhibited greater α-glucosidase inhibitory activity (IC_{50} 0.040 × 10^{-2} M) than that displayed by compound **G2** (IC_{50} 0.031 × 10^{-2} M) and the positive control (acarbose, IC_{50} 0.033 × 10^{-2} M). Marine macroalgae were reported to possess α-amylase and α-glucosidase inhibitory activities (Apostolidis et al. 2011), which appropriately substantiated the results obtained in the present study that the marine macroalgal species are potential source for anti-diabetic agents. DPP-4 inhibition was found to be a systematic approach to manage type 2 diabetes mellitus by potentiating insulin production (Mentlein 1999). The present study showed the biological effects of furanyl derivatives isolated from *G. opuntia*. The isolated compounds exhibited potential DPP-4 inhibitory activities (IC_{50} ~0.002 × 10^{-2} M) and were comparable with standard diprotin A (IC_{50} 0.003 × 10^{-2} M; $P < 0.05$). Vildagliptin, sitagliptin, saxagliptin, etc, are synthetic DPP-4 inhibitors available in market, and were reported to have several side effects, such as hypoglycemic disorders, headache, nausea, dizziness, weight gain, and swelling of the appendages due to excess fluid retention (Idris and Donnelly 2007). Likewise, other synthetic hypoglycemic agents, such as acarbose and voglibose that inhibit α-amylase and α-glycosidase were found to cause hepatic and gastrointestinal disorders (Murai et al. 2002). Bioactive potential of the isolated compounds was due to the interaction of functional groups in the furanyl derivative with DPP-4 by H-bonding and hydrophilic interactions. The isolated compounds showed significant number of electronegative functional groups, which could potentially form H-bond with DPP-4 resulting in greater anti-diabetic activity. The compounds in the present study can be effectively used for potential alternative therapy for treatment of diabetes. Notably, the isolated furanyl derivatives exhibited

potential ACE inhibitory activity (IC_{50} 0.023–0.024 × 10^{-2} M), and were comparable with the commercial ACE inhibitor, captopril (IC_{50} 0.037 × 10^{-2} M).

4.3.2.4. Structural Characterization of Compound G3

3-(2-Ethyl-6-((3, 7)-1, 2, 5, 6-tetrahydroazocin-5-yl) hexyl) morpholin-6-one (**G3**)

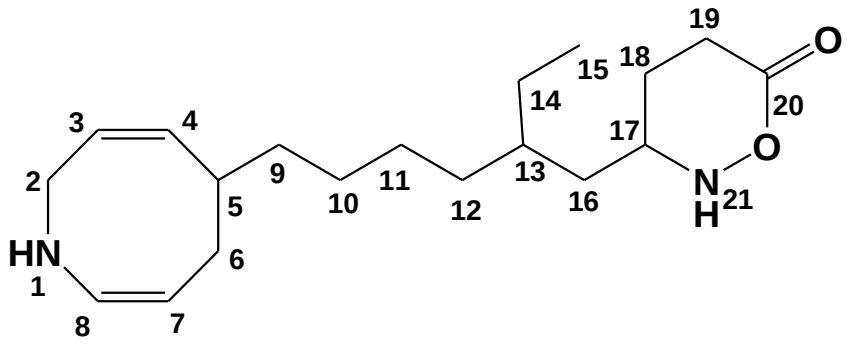

Sample yield	134 mg (1.34 %)
Physical description	Greenish oil
Molecular formula	$C_{19}H_{32}N_2O_2$
Molecular weight	320.2467

3-(2-Ethyl-6-((3, 7)-1, 2, 5, 6-tetrahydroazocin-5-yl) hexyl) morpholin-6-one: Greenish oil; UV (MeOH: EtOAc) λmax (log ε): 252 nm (3.76); TLC (Si gel GF_{254} 15 mm; EtOAc: *n*-hexane 3:7, v/v); Rf: 0.76.; Rt (HPLC, ACN: MeOH 2:3 v/v): 16.57 min; IR (KBr, cm^{-1}) ν_{max} (ν = stretching, δ = bending, ρ = rocking vibrations): 724.28 (C–H ρ), 942.30 (alkene C–H δ), 1297.86 (C–N ρ), 1461.79 (C–H δ), 1708.08 (C–CO–C ν), 2854.61 (C–H ν), 2923.34 (C–H ν), 3425.10 (N–H ν); ^{1}H-NMR ($CDCl_3$, 500 MHz), δ_H 2.64 (1H, s, NH), δ_H 4.16 (d, *J*=7.01 Hz, 2H), δ_H 5.4 (m, 1H), δ_H 5.43 (m, 1H), δ_H 2.81 (m, 1H), δ_H 2.01 (t, *J*=5.95 Hz, 2H), δ_H 5.34 (m, 1H), δ_H 5.36 (d, *J*=6.6 Hz, 1H), δ_H 1.5 (m, 2H), δ_H 1.11 (m, 2H), δ_H 1.26 (m, 2H), δ_H 1.26 (m, 2H), δ_H 1.32 (m, 1H), δ_H 1.28 (m, 2H), δ_H 0.88 (t, *J*=6.81 Hz, 3H), δ_H 1.25 (m, 2H), δ_H 4.16 (m, 1H), δ_H 1.62 (m, 2H), δ_H 2.36 (t, *J*=6.75 Hz, 2H), δ_H 3.79 (s, 1H); ^{13}C NMR (125 MHz, $CDCl_3$): δ_C 59.47 (C-2), δ_C 122.88 (C-3), δ_C 130.19 (C-4), δ_C 32.79 (C-5), δ_C 39.88 (C-6), δ_C 129.97 (C-7), δ_C 127.86 (C-8), δ_C 27.73 (C-9), δ_C 39.35 (C-10), δ_C 29.63 (C-11), δ_C 31.91 (C-12), δ_C 32.80 (C-13), δ_C 22.74 (C-14), δ_C 14.12 (C-15), δ_C 37.20 (C-16),

δ_C 61.62 (C-17), δ_C 24.72 (C-18), δ_C 33.83 (C-19), δ_C 178.6 (C-20); HMBC and ^{1}H-^{1}H-COSY data (Fig. 4.89 to Fig. 4.98, Table 4.17); HR (EI) MS *m/z* calcd for $C_{19}H_{32}N_2O_2$ 320.2464, found 320.2467 $[M]^+$.

In the present study, solvent methanol: ethyl acetate (1:1, v/v) soluble extract from the shade-dried thalli of red marine macroalga *G. opuntia* was submitted to repeated vacuum column chromatographic fractionation over silica gel, flash chromatography, and preparative thin layer chromatography (PTLC), using various combinations of mobile phase (*n*-hexane/EtOAc/MeOH) to afford hitherto unknown azocinyl morpholinone, named 3-(2-ethyl-6-((3, 7)-1, 2, 5, 6-tetrahydroazocin-5-yl) hexyl) morpholin-6-one. Furthermore, this novel bioactive lead from *G. opuntia* will be an abundant source for future research work. 3-(2-Ethyl-6-((3, 7)-1, 2, 5, 6-tetrahydroazocin-5-yl) hexyl) morpholin-6-one, a new derivative of the azocinyl morpholinone alkaloid, was purified as greenish oil by repeated chromatography (on adsorbent silica gel). The structure of the purified compound was attributed based on extensive 2D NMR experiments and mass spectra. The ^{1}H NMR along with ^{13}C NMR spectra recorded the presence of methylene protons at δ_H 1.62, δ_H 2.36, δ_H 1.25, δ_H 1.28, δ_H 1.26, δ_H 1.26, δ_H 1.11, δ_H 1.5, δ_H 2.01, δ_H 4.16 and the ^{1}H–^{1}H COSY cross peaks at H-18/H-19, H6/7, and H2/3 supported the occurrence of C-19 skeleton (Table 4.17). The downfield chemical shift of the >CH_2 signals at δ_H 2.36 and the C-19 carbon at δ_H 33.83 referred to a presence of ester carbonyl moiety. The olefinic protons were assigned at δ_H 5.32–5.45, and their proton integral values showed the existence of two olefinic bonds. The broad absorption band at 3425.10 cm^{-1} in the IR spectrum was attributed to the –NH groups, which has been supported by the ^{1}H NMR signal at δ_H 3.79 and δ_H 2.64. The presence of –NH protons was further validated by D_2O exchange. The occurrences of two nitrogen groups were also satisfied by nitrogen odd and even rule. The >CH_2 group of the protons at δ_H 4.16 and δ_H 2.36 were assigned to the C-2 and C-19 positions, respectively. Intense HMBC correlation was found between δ_H 2.01 (attributed to H-6) and δ_C 130.19 (assigned to C-4), which showed the existence of olefinic group near the >CH_2 group.

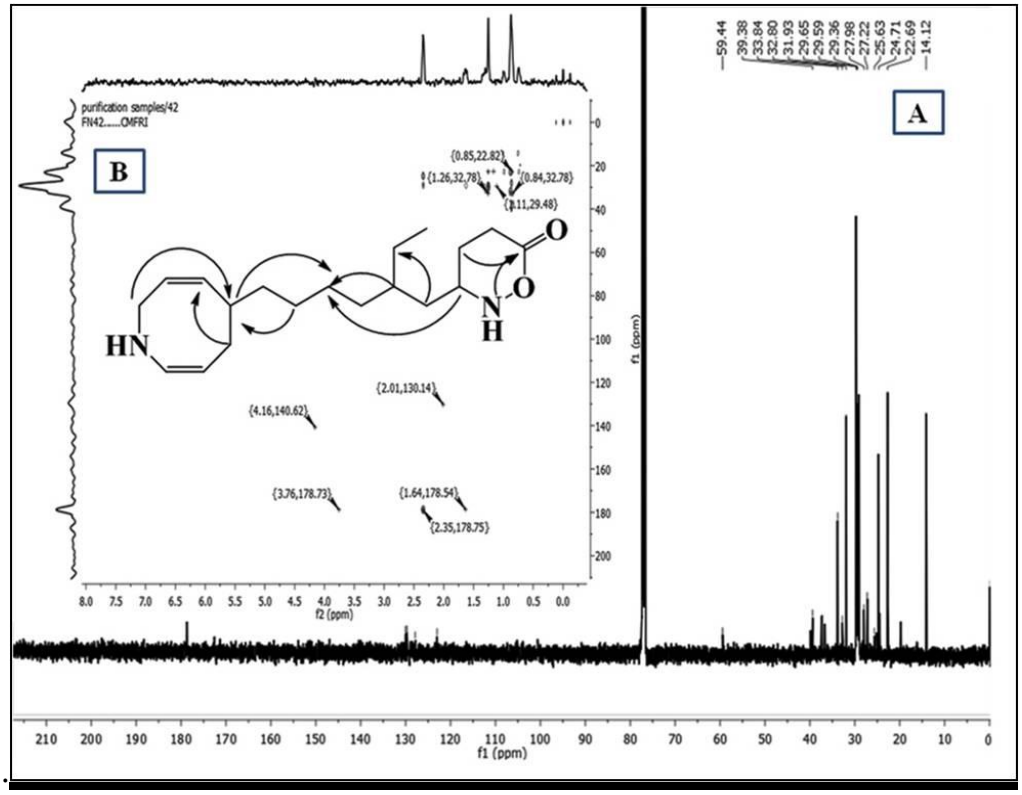

Figure 4.89. Figure showing the Key **(A)** ^{13}C-NMR, (**B**) HMBC spectra of compound **G3**

The proton due to methine group at δ_H 2.81 were deshielded due to the possible olefinic groups in their vicinity. Intense ^{1}H–^{1}H COSY cross peaks between H-6 (δ_H 2.01)/H-7 (δ_H 5.34), H-2 (δ_H 4.16)/H-3 (δ_H 5.4) along with the C/H connectivities (from the HMBC/HSQC experiments) attributed the tetrahydroazocine carbon skelton. The strong deshileding of the –NH protons at δ_H 3.79 was due to the presence of carboxyl ester group at C-20, and accordingly it was assigned to the junction point. The –CH– proton at δ_H 2.81 was attributed to the junction point of the tetrahydroazocinyl ring substituted with the side chain ethyl heptyl morpholine carbon skeleton. These assignments were further confirmed by ^{1}H–^{1}H COSY correlations and strong HMBC correlations. The location of the >NH proton at δ_H 3.79 was assisted by HMBC experiments. The cyclization point of the substituted morpholin ring was resolved by downfield shift of H-17 at δ_H 4.16, which was connected to the methylene protons at δ_H 1.62 (assigned to H-18) showing clear ^{1}H–^{1}H COSY correlation with H-19, thereby supporting the presence of the morpholin-6-one moiety. HSQC and HMBC experiments established the presence of tetrahydroazocinyl ring skelton connected to

the morpholin substitution at the C-9 carbon of the compound. Intense HMBC cross peaks were recorded between H-2 (δ_H 4.16)/C-5 (δ_C 32.79), H-5 (δ_H 2.81)/C-11 (δ_C 29.63), H-6 (δ_H 2.01)/C-4 (δ_C 130.19), H-10 (δ_H 1.11)/C-5 (δ_C 32.79), H-16 (δ_H 1.25)/C-14 (δ_C 22.74), H-13 (δ_H 1.32)/C-11 (δ_C 29.63), H-18 (δ_H 1.62)/C-20 (δ_C 178.6), H-21 (δ_H 3.79)/C-20 (δ_C 178.6), which supported the presence of 3-(2-ethyl-6-((3, 7)-1, 2, 5, 6-tetrahydro azocin-5-yl-hexyl) morpholin-6-one moiety. The –CH_2 signal at δ_H 1.62 (assigned to C-18) demonstrated HMBC connections with ester carbonyl carbon at δ_C 178.6 (attributed to C-20). The comparative stereochemical configuration of the chiral centers at C-5, C-13 belonging to 1, 2, 5, 6-tetrahydro azocin-5-yl-hexyl moiety, and C-17 of the morpholin- 6-one ring framework were summarized from the NOE spectral experiments and the coupling constant values. The equatorial proton Hb, of C-18b was found to resonate as a multiplet with the axial proton Ha-5, having an axial-axial coupling (*J*a,d=12 Hz) and axial equatorial coupling (*J*a,b=6 Hz) which attributed for the larger substituent 5-(5-methylheptyl)-1, 2, 5, 6-tetrahydroazocine group at C-16 as equatorially disposed. These assignments were established by a sequence of NOE cross peaks, which confirmed the C-17 proton as axial. Intense NOE correlation between the methine proton at Ha-5 and H-13, suggested that these protons were axial. The chair-like conformation might be due to intense 1,3-eclipsing interaction between the axial methylene proton at C-16 belonging to the bulky tetrahydro-5-(5-methylheptyl) azocine moiety and the He-19, which forced the latter into an equatorial disposition, and the morpholinone framework into a chair-like conformation. The existence of NOE between the axial –CH_2– proton Hd-19 and axial CH at Ha-5 indicated a chair-like configuration and these assignments were assisted by the absence of an NOE between the axial proton Hd-19, and the methylene proton Hc-18. The attributions for the chair-conformation might be explained by the lack of intense 1, 2-eclipsing interactions, since the equatorial position was occupied with bulky tetrahydro-5-(5-methylheptyl) azocine framework. The molecular ion peak at *m/z* 320 (HR-EI-MS *m/z* calcd. for $C_{19}H_{32}N_2O_2$ 320.2464, found 320.2467 $[M]^+$), which was combined with the detailed NMR experimental data to record the elemental composition of the compound **G3** with five degrees of unsaturation. Two degrees of unsaturation were due to the two olefinic double bonds (δ_H 5.32–5.42), whereas one degree of unsaturation was attributed to the carbonyl group (δ_C 178.6) and the remaining two were due to the two ring systems. The molecular ion peak at *m/z* 320 ($C_{19}H_{32}N_2O_2$, $[M]^+$) was found to undergo deamination yielding 6-ethyl-11-(prop-1-enyl) tetradec-13-enoic acid (*m/z*

294). Two $–CH_2$ groups eliminated from the fragment ion (*m/z* 294) to afford the fragments at *m/z* 280 (assigned to 6-ethyl-11-vinyltetradec-13-enoic acid) and *m/z* 266 (6-methyl-11-vinyltetradec-13-enoic acid). The fragment peak at *m/z* 148 (assigned to tetrahydro-6a*H*-cyclopenta azocine) was found to be the base peak. Intense IR stretching vibrations were apparent between 1461 and 2854 cm^{-1} that were attributed to the olefinic (C=C) and alkyl (C–H) groups. Intense ester carbonyl and N–H stretching vibrations were apparent near 1708 and 3425 cm^{-1}, respectively.

Table 4.17 NMR spectroscopic data of compound **G3** in $CDCl_3$[a]

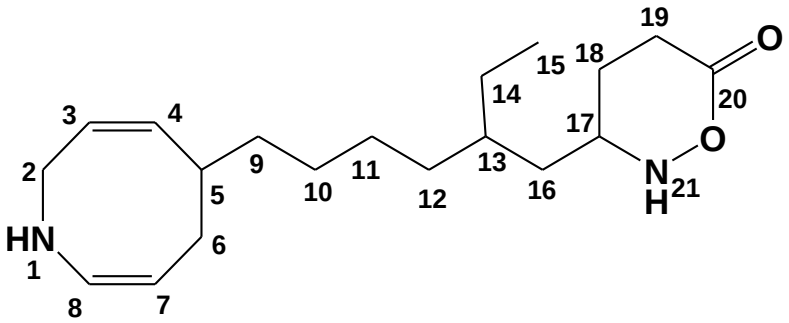

C. No	^{13}C (δ)	^{1}H-NMR[b] (int., mult., *J* in Hz)	^{1}H-^{1}H COSY	HMBC
1	-	2.64 (s, 1H)	-	-
2	59.47	4.16 (d, *J*=7.01 Hz, 2H)	3-H	C-5
3	122.88	5.4 (m, 1H)	2-H	-
4	130.19	5.43 (m, 1H)	-	-
5	32.79	2.81 (m, 1H)	-	C-11
6	39.88	2.01 (t, *J*=5.95 Hz, 2H)	7-H	C-4
7	129.97	5.34 (m, 1H)	6-H	-
8	127.86	5.36 (d, *J*=6.6 Hz, 1H)	-	-
9	27.73	1.5 (d, *J*=6.3 Hz, 2H)	-	-
10	39.35	1.11 (m, 2H)	-	C-5
11	29.63	1.26 (m, 2H)	-	-
12	31.91	1.26 (m, 2H)	-	-
13	32.80	1.32 (m, 1H)	-	C-11
14	22.74	1.28 (m, 2H)	-	-
15	14.12	0.88 (t, *J*=6.81 Hz, 3H)	-	-
16	37.20	1.25 (m, 2H)	-	C-14
17	61.62	4.16 (m, 1H)	-	-
18	24.72	1.62 (m, 2H)	19-H	C-20
19	33.83	2.36 (t, *J*=6.75 Hz, 2H)	18-H	-
20	178.6	-	-	-
21	-	3.79 (s, 1H)	-	C-20

[a] NMR spectra recorded using Bruker AVANCE III 500 MHz (AV 500) spectrometer in $CDCl_3$ as aprotic solvent at ambient temperature with TMS as the internal standard (δ 0 ppm).

[b] Values in ppm, multiplicity and coupling constants (*J*=Hz) are indicated in parentheses. The assignments were made with the aid of the ^1H-^1H COSY, HSQC, HMBC and NOESY experiment

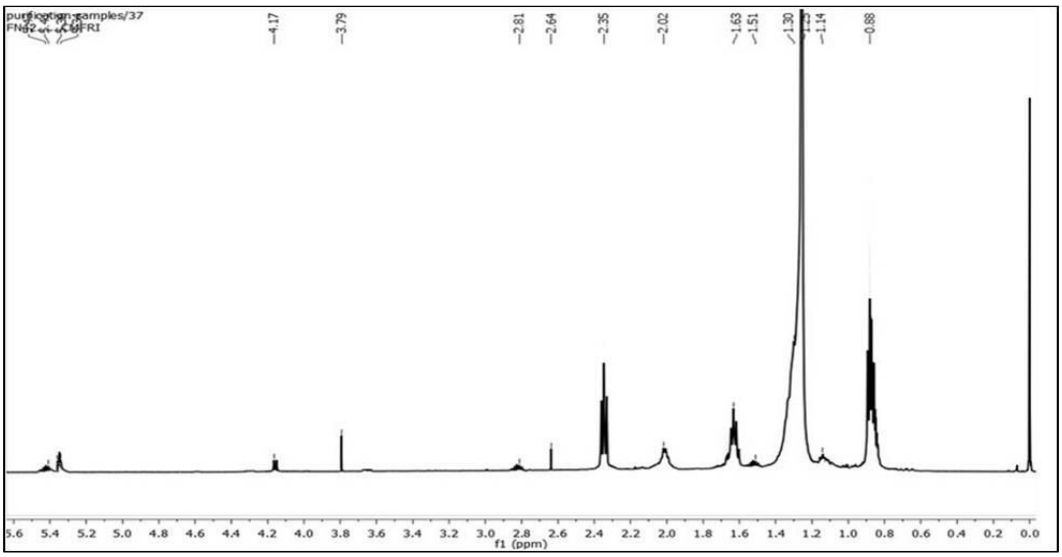

Figure 4.90. Figure showing the ^1H NMR spectrum of compound **G3**

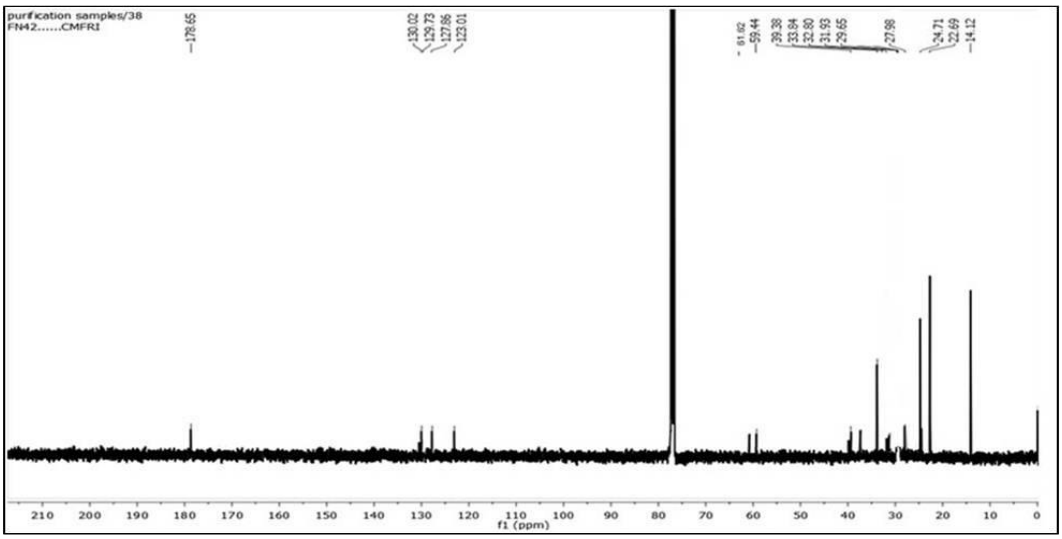

Figure 4.91. Figure showing the ^{13}C spectrum of compound **G3**

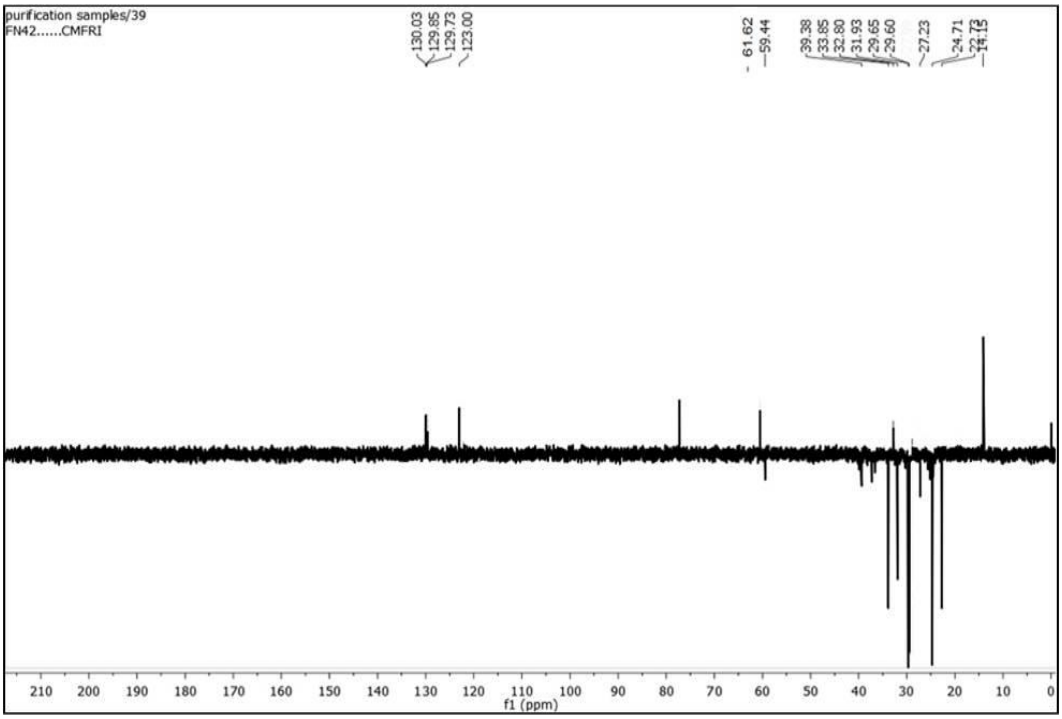

Figure 4.92. Figure showing the DEPT spectrum of compound **G3**

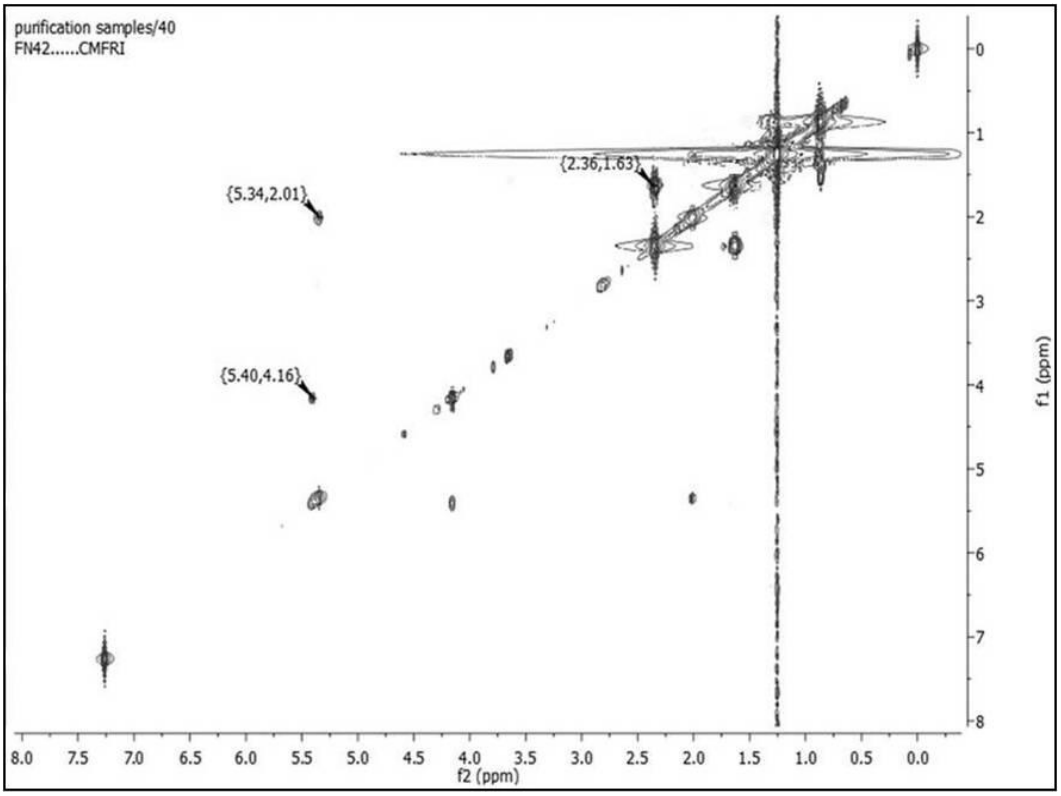

Figure 4.93. Figure showing the ^{1}H-^{1}H COSY spectrum of compound **G3**

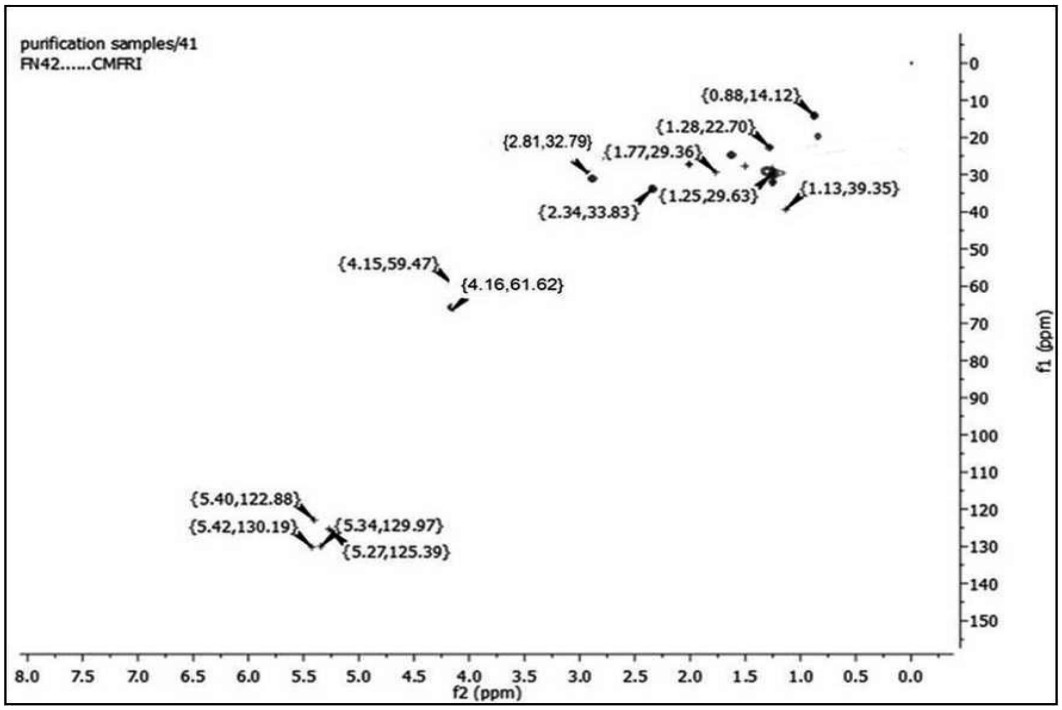

Figure 4.94. Figure showing the HSQC spectrum of compound **G3**

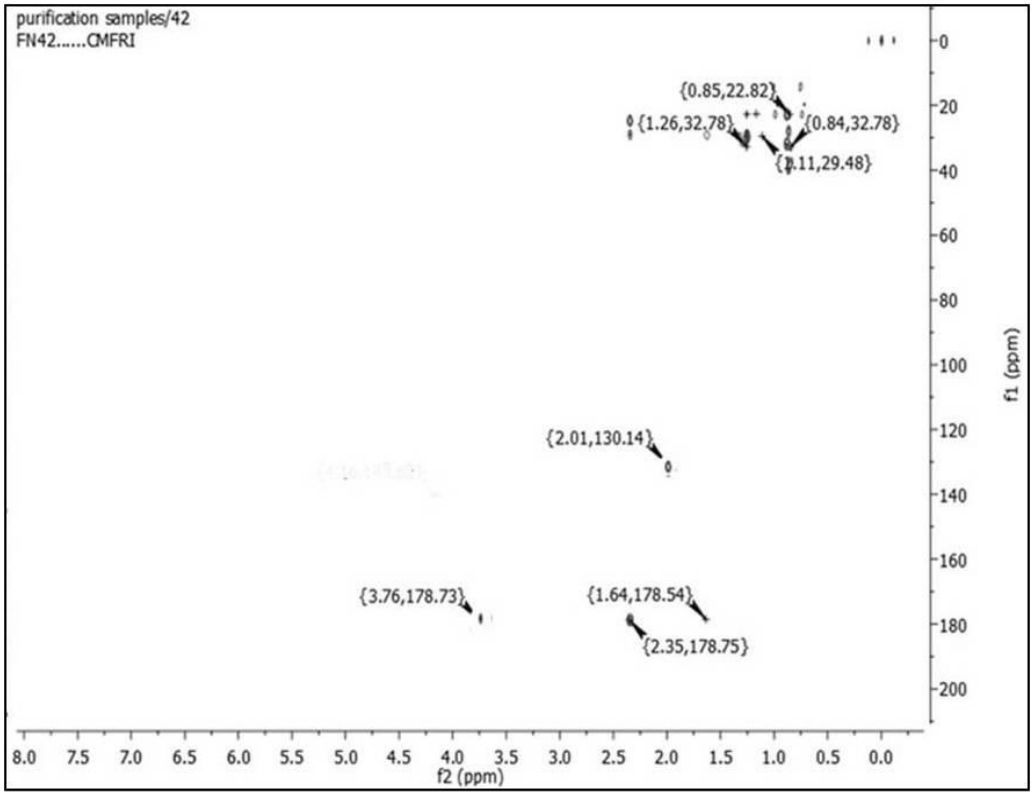

Figure 4.95. Figure showing the HMBC spectrum of compound **G3**

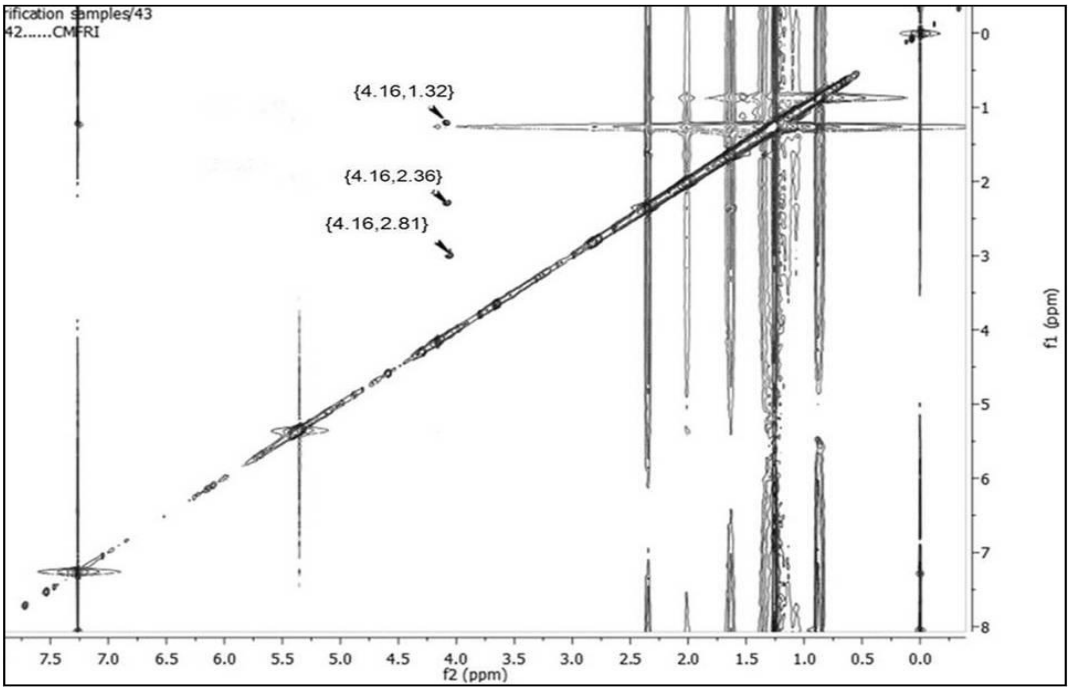

Figure 4.96. Figure showing the NOESY spectrum of compound **G3**

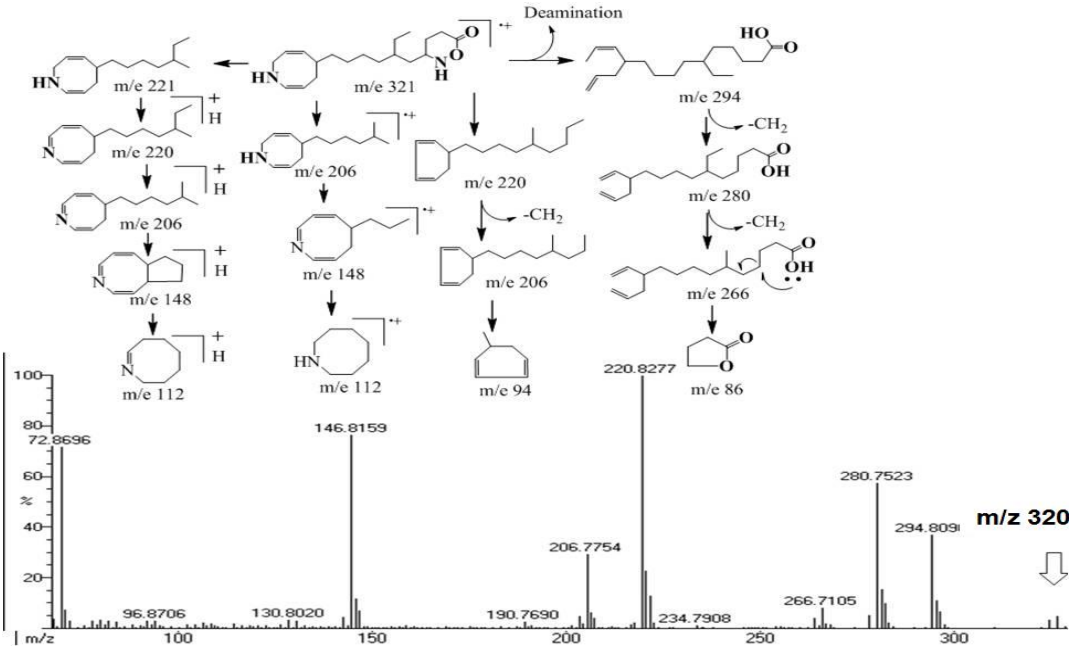

Figure 4.97. Mass spectrum of compound **G3**

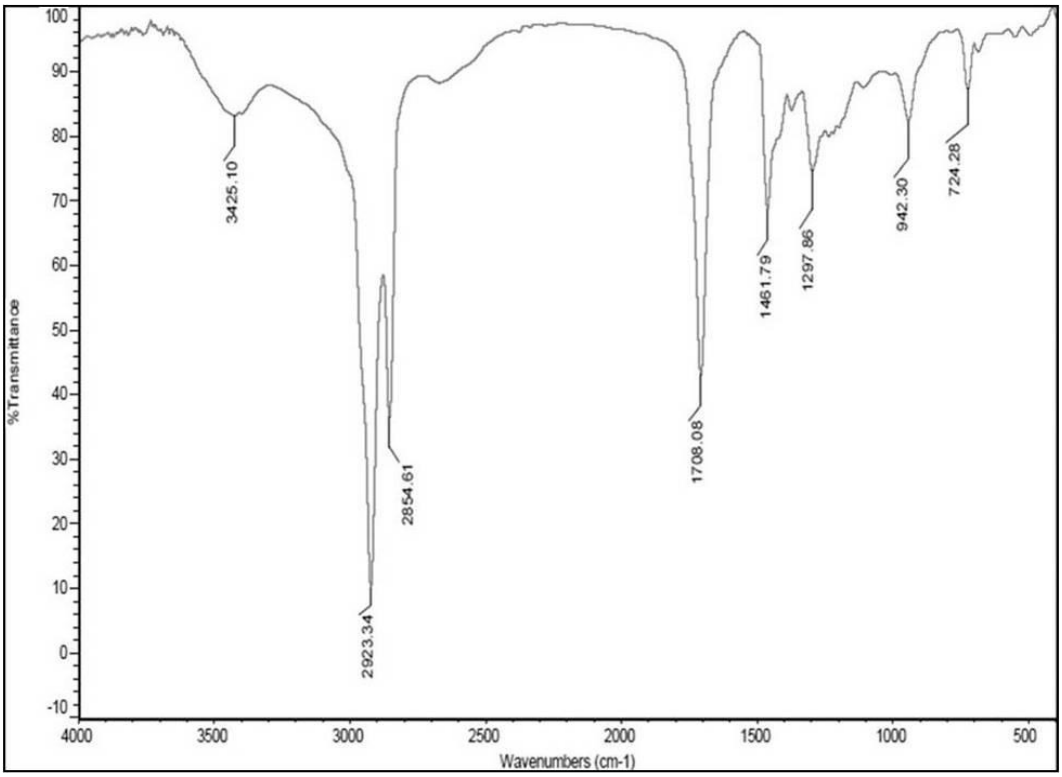

Figure 4.98. Figure showing the FTIR spectrum of compound **G3**

4.3.2.5. Bioactivities and Structure-Activity Relationship Analysis

The substituted azocinyl morpholinone recorded appreciably greater 1, 1-diphenyl-2-picryl-hydrazil (DPPH) free radical scavenging activities (IC_{50} ~ 0.086 mg/mL) compared to the commercially available synthetic antioxidants, butylated hydroxyanisole (BHA), butylated hydroxy toluene (BHT), and α-tocopherol (IC_{50} > 0.20 mg/mL). The lipophilic parameter Clog Pow (compound logarithmic scale of the octanol-water partition coefficient) was found to occupy a prominent part in determining the antioxidant property of the compounds. It is of note that while the Clog Pow of 3-(2-ethyl-6-((3, 7)-1, 2, 5, 6-tetrahydroazocin-5-yl) hexyl) morpholin-6-one was recorded as 0.55, the octanol-water partition coefficients of α-tocopherol (Clog Pow 120.4), BHA (Clog Pow 3.30), and BHT (Clog Pow 5.43) were found to be considerably greater, and this might considerably reflect towards the greater antioxidative potential of the compound **G3** than the commercially available synthetic and natural antioxidants. The antioxidant activity of α-tocopherol was found to be

considerably lesser apparently due to the greater steric bulk (Pr > 1000 cm^3) than the azocinyl morpholinone (Pr 783 cm^3) purified from *G. opuntia*. It is of note that the electronic parameter, topological polar surface area (tPSA) of the compound **G3** was significantly greater (tPSA 50.36) than the synthetic antioxidants, BHT (20.23), BHA (29.46) and α-tocopherol (29.46), and therefore, might contribute towards the higher DPPH radical scavenging activity (IC_{50} 0.086 mg/mL) than the synthetics (IC_{50} > 0.2 mg/mL). Likewise, no considerable variation in 2, 2′-azino-bis-3-ethylbenzothiozoline-6-sulfonic acid (ABTS) radical scavenging activity of the azocinyl morpholine (IC_{50} 0.42 mg/mL) was discernable with those of BHA and BHT (IC_{50} 0.34 and 0.26 mg/mL, respectively, $P > 0.05$), whilst, α-tocopherol recorded significantly lesser activity (IC_{50} 0.73 mg/mL) than the compound **G3** ($P > 0.05$). Apparently, the compound **G3** has two sp-hybridized –NH protons, which can be transferred to the free radicals (e.g. the hydrazinyl N – centered free radical of ABTS) by hydrogen atom transfer (HAT). It is evident that the HAT neutralize the free radicals (ABTS), as in phenolic antioxidants, is the mechanism of action of azocinyl morpholinone. In particular, the –NH proton that is a part of the morpholinone ring system, was deshielded, and appeared downfield at δ_H 3.79, which could be explained by the presence of the electronegative -O-C(=O) group at its vicinity. Earlier reports demonstrated that the radical scavenging activity of pharmacophore leads depends on electron donating groups, such as hydroxyl (-OH) and -NH group independent of their attachments, which can easily abstract free radicals and can potentially convert the highly reactive free radicals to their non-reactive forms (Cai et al. 2006). The radical scavenging activities of compounds were also reported to increase with the presence of double bonds due to effective electron-transfer through electron delocalization (Pietta 2000). It is interesting to note that the commercially available drugs, such as aspirin, sodium salicylate and ibuprofen along with COX-2 selective inhibitors {(Coxibs), celecoxib and rofecoxib} which were considered in the current study, displayed greater activities against cyclooxygenase-1 (COX-1) than cyclooxygenase-2 (COX-2), which might explain their undesirable side effects. Notably, greater inhibitory properties of the synthetic NSAIDs towards the constitutive enzyme COX-1 might lead to their shared therapeutic and side effects, which are undesirable, and lead to nephrotoxicity and gastrointestinal disorders (Rao and Knaus 2008). However, the compound **G3** exhibited greater activity against COX-2 (anti-COX-2 IC_{50} 0.84 mg/mL) than COX-1 isoform (COX-1 IC_{50} ~ 0.98 mg/mL). Sodium salicylate was found to be a weaker inhibitor of both COX isoforms (anti-COX-2 IC_{50}

2.65 mg/mL, anti- COX-1 IC_{50} 1.93 mg/mL) and demonstrated significantly lesser activity against 5-LOX (anti- LOX-5 IC_{50} 1.75 mg/mL). It was found that the synthetic NSAIDs, ibuprofen, sodium salicylate, and aspirin displayed significantly lesser activity against COX-2 than against COX-1 isoform, and the selectivity indices {ratio of anti-COX-1(IC_{50}) to that of anti-COX-2 (IC_{50})} remained considerably lesser (0.02–0.73 mg/mL) than the purified compounds (SI, 1.17). The azocinyl morpholinone exhibited potential COX-2 inhibitory activity/selectivity (IC_{50} 0.84 mg/mL) in conjunction with *in vitro* 5-LOX activity (IC_{50} 0.85 mg/mL) (Fig. 4.99, Table 4.18-4.19). The COX-2 selective inhibitors displayed potential selective COX-2 inhibitory activity (Celecoxib IC_{50} 29.60; Valdecoxib IC_{50} 61.50; Rofecoxib IC_{50} 272) (Tacconelli et al. 2002) than the purified compound. The selective COX-2 inhibitors were found to restrict the endothelial cell synthesis of prostacyclin (PGI2), an arachidonic acid product. PGI2 was reported to resist the effects of thromboxane leading to the disruption of physiological balance between thromboxane and prostacyclin resulting in the pathogenesis of atherosclerosis, thrombogenesis and other cardiovascular disorders (Fosslien 2005). These reports led to the restricted use of rofecoxib in 2004, followed by that of valdecoxib in 2005 (Fitz Gerald 2004). It was reported that rofecoxib induced nearly 28,000 heart attacks in the United States during the year 1999 and 2003 (Horton 2004). In addition COX-2 inhibitors, such as Celecoxib, with lesser selectivity, are also under restricted use (Fosslien 2005). The electronegative/hydrophilic groups in the compound **G3** appeared to inhibit the abstraction of hydrogen from arachidonic acid in the active site of cyclooxygenase (COX-1), thereby suppressing the synthesis of pro-inflammatory prostaglandins. Electronegative groups, such as NH in the compound **G3** can presumably be coordinated with the COX active site by ion pairing thereby preventing the prostaglandins synthesis. Notably, the animals challenged with the compound **G3** significantly mitigated the carrageenan-induced paw edema in a time-dependent manner till the end of the 6 h as compared to negative control animals. Structure-activity relationship analysis imparted that the bioactivities of azocinyl morpholinone were directed by the electronic and lipophilic parameters. Likewise, the greater anti-inflammatory potential of the compound **G3** was determined by the lesser Clog Pow value (0.55) as compared to the greater Clog Pow values of the synthetic NSAIDs, aspirin (1.02) and ibuprofen (3.68). The electronic parameter (polarizability, Pl and tPSA) also appeared to display significant role in determining the anti-inflammatory activity of the compound **G3**.

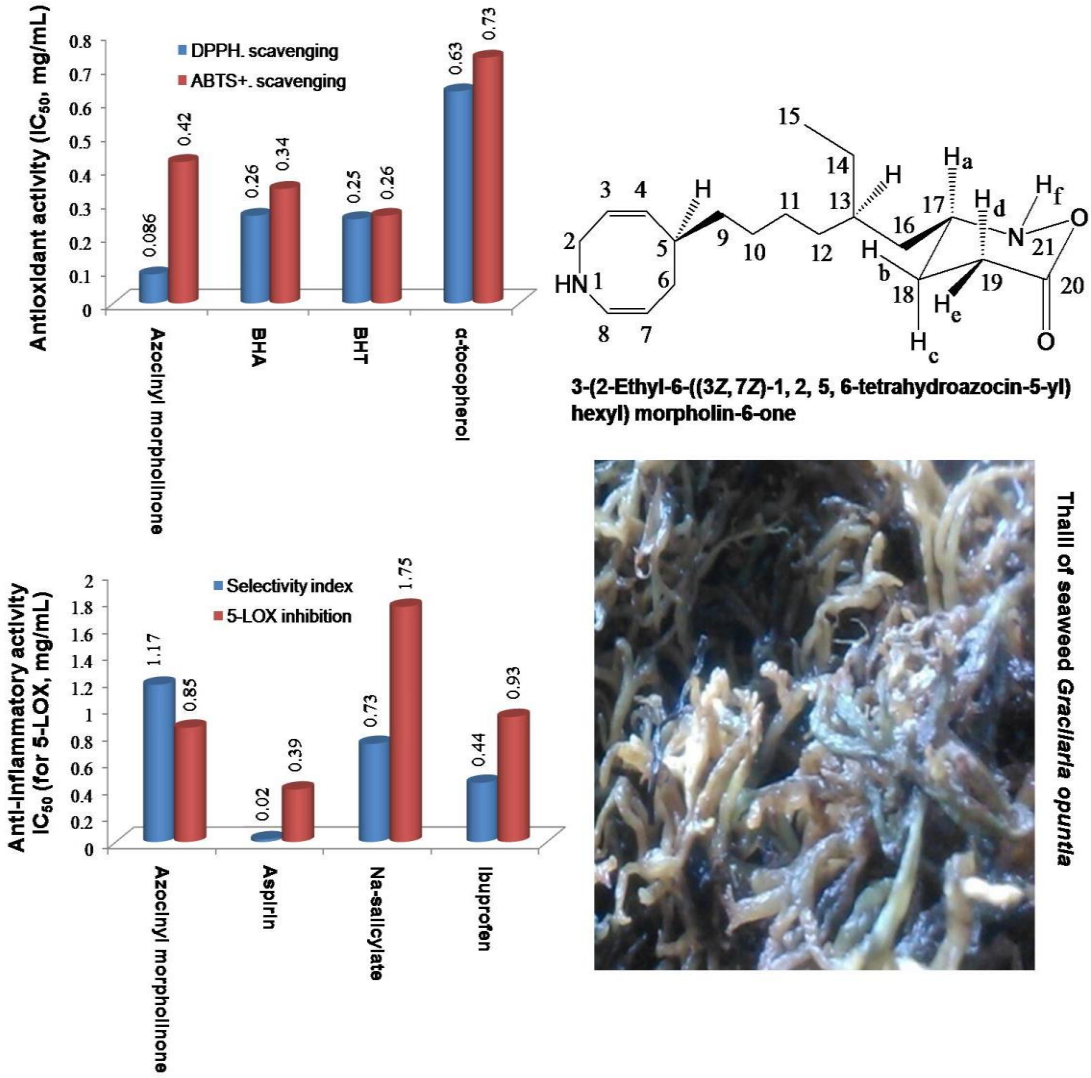

Figure 4.99. Graphical representation of bioactivities of compound **G3**. The thalli of the studied marine macroalga were displayed as inset

It is apparent that the electronic descriptor, Pl of the azocinyl morpholinone registered significantly greater value (~37 × 10^{-24} cm^3) than the NSAIDs (Pl aspirin 17.65 × 10^{-24} cm^3, Pl ibuprofen 24.09 × 10^{-24} cm^3), and therefore, the anti-inflammatory activity of the compound **G3** was found to be comparable to that of the synthetic NSAIDs. A greater selectivity index of the new azocinyl morpholinone isolated from *G. opuntia* signified the greater selectivity and significantly lesser side effect profiles than the current remedies by using nonsteroidal anti-inflammatory drugs used to combat the inflammatory diseases.

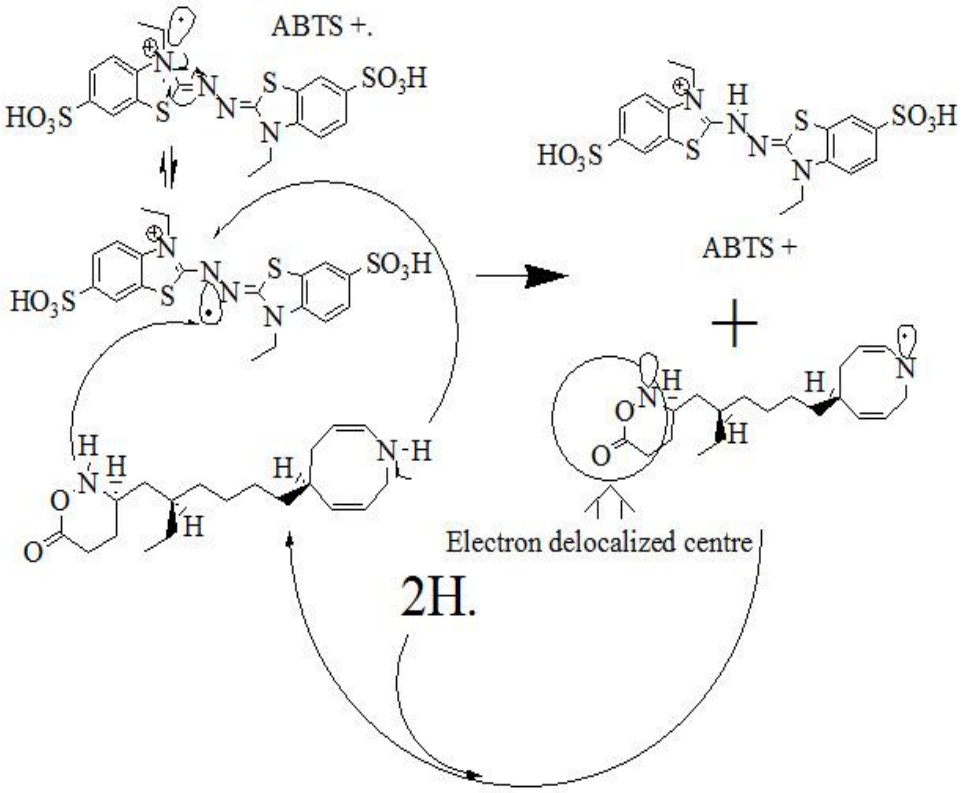

Figure 4.100. Antioxidative mechanism of the purified compound in the ABTS model system. The compound **G3** has two sp-hybridized –NH protons, which can be transferred to the free radicals (e.g., the hydrazinyl N –centered free radical of $ABTS^{+\cdot}$) by hydrogen atom transfer (HAT). HAT from the azocinyl morpholinone stabilized the free radicals ($ABTS^{+\cdot}$)

Table 4.18 Antioxidative and inflammatory activities of azocinyl morpholinone isolated from *G. opuntia vis-à-vis* the commercially available natural and synthetic antioxidants

Bioactivities*	**IC_{50} (mg/mL)**			
Antioxidative activities	**Azocinyl morpholinone**	**BHA**	**BHT**	**α-tocopherol**
DPPH scavenging	0.086^{a} ±0.07	0.26^{b} ± 0.01	0.25^{b} ± 0.02	0.63^{c} ± 0.04
ABTS scavenging	0.42^{b} ±0.23	0.34^{b} ± 0.02	0.26^{b} ± 0.02	0.73^{c} ± 0.05
Anti-inflammatory activities	**Azocinyl morpholinone**	**Aspirin**	**Na-salicylate**	**Ibuprofen**
COX -1 inhibition	0.98^{b} ±0.05	0.005^{a} ±0.00	1.93^{c} ±0.05	0.04^{a} ±0.00
COX -2 inhibition	0.84^{b} ±0.03	0.21^{b} ±0.02	2.65^{c} ±0.05	0.09^{a} ±0.02
Selectivity index**	1.17^{b} ±0.08	0.02^{b} ±0.01	0.73^{b} ±0.02	0.44^{b} ±0.03
5-LOX inhibition	0.85^{b} ±0.12	0.39^{a} ±0.02	1.75^{c} ±0.12	0.93^{b} ±0.11

* The bioactivities were expressed as IC_{50} values (mg/mL).

The samples were analyzed in triplicate (n=3) and expressed as mean ± standard deviation. Means followed by the different superscripts (a–c) within the same row indicate significant differences ($P < 0.05$).

**Selectivity index has been calculated as the ratio of anti-COX-1(IC_{50}) to that of anti-COX-2 (IC_{50}).

Table 4.19 Effect of the azocinyl morpholinone compared with the standard drug on carrageenan-induced hind paw edema in BALB/C mice at different time intervals.

	Paw edema (mm)*				
Samples Positive control (carrageenan induced)	**2h**	**3h**	**4h**	**5h**	**6h**
Normal saline	2.59^{bc} ±0.32	2.48^{b} ±0.27	2.53^{cd} ±0.24	2.62^{cd} ±0.26	2.65^{cd} ±0.21
Standard (ibuprofen)	1.98^{a} ±0.21	1.91^{a} ±0.16	1.84^{b} ±0.14	1.80^{a} ±0.13	1.79^{b} ±0.15
Azocinyl morpholinone	1.95^{a} ±0.18	1.87^{a} ±0.19	1.76^{a} ±0.20	1.72^{a} ±0.19	1.68^{a} ±0.11

*Initial paw diameter 1.38 mm (at 0^{th} h)

a-d: Column wise values with superscripts indicate significant differences ($P < 0.05$) within the samples.

4.3.2.6. Structural Characterization of Compound G4

2-Acetoxy-2-(5-acetoxy-4-methyl-2-oxotetrahydro-2*H*-pyran-4-yl) ethyl-4-(3-methoxy-2(methoxymethyl)-7-methyl-3, 4, 4a, 7, 8, 8a-hexahydro-2*H*-chromen-4-yloxy)-5 methylheptanoate (**G4**)

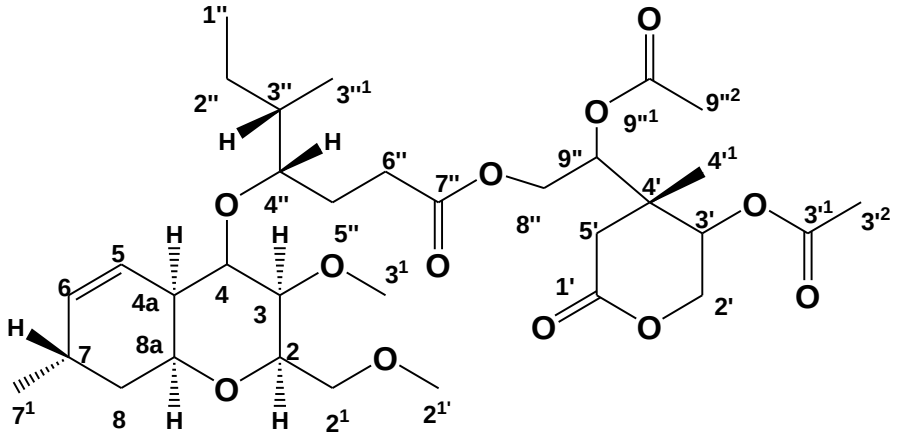

Sample yield	110 mg (1.0 %)
Physical description	Yellow oil
Molecular formula	$C_{33}H_{52}O_{12}$
Molecular weight	640.3182

2-Acetoxy-2-(5-acetoxy-4-methyl-2-oxotetrahydro-2*H*-pyran-4-yl) ethyl-4-(3-methoxy-2 (methoxymethyl)-7-methyl-3, 4, 4a, 7, 8, 8a-hexahydro-2*H*-chromen-4-yloxy)-5-methylheptanoate : Yellowish oil; UV (MeOH) λmax (log ε): 268 nm (3.01); TLC (Si gel GF_{254} 15 mm; EtOAc: *n*-hexane 3:7, v/v) Rf: 0.55; Rt (HPLC, MeOH: ACN, 3:2 *v*/*v*): 9.86 min; IR (KBr, cm^{-1}) *v*max (ν = stretching, δ = bending, ρ = rocking vibrations): 722.40 (C–H ρ), 794.82 (C–H ρ), 910.63 (alkene C–H δ), 1062.19 (C–O ν), 1252.45 (C–O ν), 1371.54 (CH_3 ν), 1458.63 (C–H δ), 1715.00 (C–CO–C ν), 2856.63 (C–H ν), 2923.39 (C–H ν); ^{1}H NMR (500 MHz, $CDCl_3$) δ_H 4.17 (m, 1H), δ_H 3.18 (*J*=4.40 Hz, d, 2H), δ_H 3.71 (s, 3H), δ_H 3.66 (*J*=3.10 Hz, t, 1H), δ_H 3.36 (s, 3H), δ_H 3.75 (*J*=5.55 Hz, t, 1H), δ_H 2.05 (m, 1H), δ_H 5.35 (*J*=7.36 Hz, t, 1H), δ_H 5.51 (*J*=7.87

Hz, t, 1H), δ_H 1.74 (m, 1H), δ_H 1.08 (*J*=4.16 Hz, d, 3H), δ_H 2.04 (*J*=3.13 Hz, t, 2H), δ_H 4.07 (m, 1H), δ_H 3.69 (*J*=3.10 Hz, d, 2H), δ_H 4.50 (*J*=8.11 Hz, t, 1H), δ_H 2.71 (s, 3H), δ_H 1.29 (s, 3H), δ_H 2.86 (s, 2H), δ_H 0.99 (*J*=6.07 Hz, t, 3H), δ_H 1.30 (m, 2H), δ_H 1.52 (m, 1H), δ_H 0.88 (*J*=6.64 Hz, d, 3H), δ_H 3.47 (m, 1H), δ_H 1.61 (m, 2H), δ_H 2.38 (*J*=7.87 Hz, t, 2H), δ_H 4.30 (*J*=8.97 Hz, d, 2H), δ_H 5.35 (*J*=7.36 Hz, t, 1H), δ_H 2.17 (s, 3H); ^{13}C NMR (125 MHz, methanol d4 δ in ppm): δ_C 75.21 (C-3), δ_C 73.45 (C-4), δ_C 73.32 (C-2^1), δ_C 65.13 (C-2), δ_C 53.96 (C-$2^{1'}$), δ_C 51.29 (C-3^1), δ_C 40.1 (C-4a), δ_C 129.55 (C-5), δ_C 132.53 (C-6), δ_C 40.07 (C-7), δ_C 26.56 (C-8), δ_C 71.62 (C-8a), δ_C 173.57 (C-1'), δ_C 70.31 (C-2'), δ_C 63.01 (C-3'), δ_C174.17 (C-$3'^1$), δ_C 39.07 (C-$3'^2$), δ_C 50.85 (C-4'), δ_C 14.03 (C-$4'^1$), δ_C 28.44 (C-5'), δ_C 21.63 (C-1''), δ_C 29.4 (C-2''), δ_C 27.77 (C-3''), δ_C 13.17 (C-$3''^1$), δ_C 72.01 (C-4''), δ_C 24.68 (C-5''), δ_C 33.62 (C-6''), δ_C 174.27 (C-7''), δ_C 65.77 (C-8''), δ_C 97.58 (C-9''), δ_C 184 (C-$9''^1$), δ_C 32.37 (C-$9''^2$), δ_C 18.16 (C-7^1). ^{1}H-^{1}H-COSY and HMBC data (Fig. 4.101 to Fig. 4.110, Table 4.20); HR (EI) MS *m/z* calcd for $C_{33}H_{52}O_{12}$ 640.3173, found 640.3182 $[M]^+$.

The EtOAc: MeOH extract of *G. opuntia* was subjected to repeated column chromatography over silica gel and preparative thin layer chromatography (PTLC) to yield the compound **G4** as yellowish oil. The compound showed absorption bands at 1715 cm^{-1} in the Fourier Transform Infrared (FTIR) spectrum due to the carbonyl functionalities. The olefinic (C=C) and alkyl (C–H) groups IR stretching vibrations were demonstrated by absorption bands at 1458 and 2856 cm^{-1}, respectively. The detailed ^{1}H, ^{13}C NMR and mass spectral analysis confirmed the structure. Its molecular formula, $C_{33}H_{52}O_{12}$, was deduced from the HR-EI-MS (*m/z* 640.3182) and ^{13}C NMR spectroscopic data, showing eight indices of hydrogen deficiency. The carbon signals at δ_C 174.27 (C-7''), δ_C 174.17 (C-$3'^1$), δ_C 173.57 (C-1') and δ_C 184 (C-$9''^1$) indicated the presence of four carbonyl carbons, and among them, one carbonyl groups formed the part of the 1-(5-acetoxy-4-methyl-2-oxotetrahydro-2*H*-pyran-4-yl) ethyl acetate moiety. The heteronuclear multiple- bond correlation spectroscopy (HMBC) relation between H-2^1 (δ_H 3.18; *J*=4.40 Hz)/C-$2^{1'}$ (δ_C 53.96)/C-2 (δ_C 65.13), H-3 (δ_H 3.66; *J*=3.10 Hz)/C-2^1 (δ_C 53.96), H-4a (δ_C 2.05)/C-5 (δ_C 129.55), H-6 (δ_H 5.51; *J*=7.87 Hz)/C-5 (δ_C 129.55), H-$3''^1$ (δ_H 0.88; *J*=6.64 Hz)/C-2'' (δ_C 29.4)/C-3'' (δ_C 27.77), H-5'' (δ_H 1.61)/C-7'' (δ_C 174.27)/C-6'' (δ_C 33.62), H-6'' (δ_H 2.38; *J*=7.87 Hz)/C-7'' (δ_C 129.55)/C-5'' (δ_C 24.68), H-9'' (δ_H 5.35; *J*=7.36 Hz)/C-8'' (δ_C 65.77), H-$9''^2$ (δ_H 2.17)/C-$9''^1$ (δ_C 184)/C-9'' (δ_C 97.58) established the side chain substitution of chromen (Table 4.20).

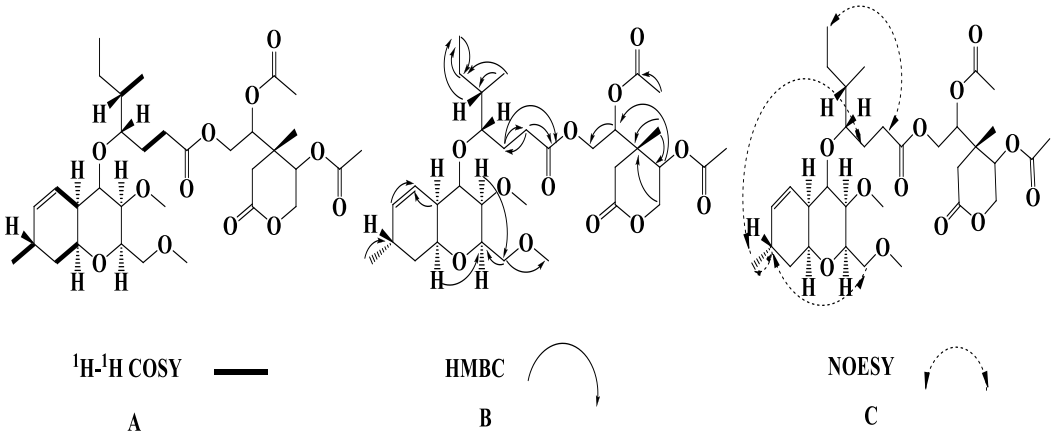

Figure 4.101. Figure showing the Key (**A**) ^{1}H-^{1}H COSY (**B**) HMBC and (**C**) NOESY correlations of compound **G4**

The ^{1}H NMR spectrum of the compound **G4** showed signals at δ_H 4.17 bearing carbon at δ_C 65.13 that unambiguously confirmed the presence of the characteristic signals of chromen carbons. The presence of the two acetyl groups has been confirmed by the singlet at δ_H 2.71 (H-3'^{2}) and δ_H 2.17 (H-9"^{2}). Intense HMBC correlation between H-9"^{2} (δ_H 2.17)/C-9"^{1} (δ_C 184)/C-9" (δ_C 97.58) established the side chain acetyl substitution of chromen. The ^{1}H-^{1}H COSY experiment displayed that the presence of three spin systems, H-4a to H-5 {(δ_H 2.05 (H-4a)/δ_C 5.35; *J*=7.36 Hz (H-5), H-7 to H-7^1{δ_H 1.74(H-7)/δ_H 1.08; *J*=4.16 Hz (H-7^1)}, H-8 to H-8a {(δ_H 2.04; *J*=3.13 Hz (H-8)/δ_H 4.07(H-8a)} in the methylcyclohexene ring, H-3" to H-3"^{1}{(δ_H1.52 (H-3")/δ_H 0.88; *J*=6.64 Hz (H-3"^{1}), H-5" to H-6" (δ_H 1.61(H-5")/δ_H 2.38; *J*=7.87 Hz (H-6")} in the propyl 4-hydroxy-5-methylheptanoate framework, which indicated the presence of substitution in the chromen groups that were further confirmed by the detailed HMBC correlations. The HMBC correlations from H-3 (δ_H 3.66; *J*=3.10 Hz)/C-2$^{1'}$ (δ_C 53.96), H-2^1 (δ_H 3.18; *J*=4.40 Hz)/C-2$^{1'}$ (δ_C 53.96) suggested the position of a methoxy group substituted at C-2 position. The presence of methoxy groups were also supported by two singlets at δ_H 3.36 and 3.71 recorded in the ^{1}H NMR spectrum. Strong HMBC correlations were exhibited by H-2^1 (δ_H 3.18; *J*=4.40 Hz)/C-2$^{1'}$ (δ_C 53.96)/C-2 (δ_C 65.13), H-3 (δ_H 3.66; *J*=3.10 Hz)/C-2^1 (δ_C 53.96), H-4a (δ_H 2.05)/C-5 (δ_C 129.55), H-6" (δ_H 2.38; *J*=7.87 Hz)/C-7" (δ_C 129.55)/C-5" (δ_C 24.68), H-9" (δ_H 5.35; *J*=7.36 Hz)/C-8" (δ_C 65.77), H-9"^{2} (δ_H 2.17)/C-9"^{1} (δ_C 184)/C-9" (δ_C 97.58), which supported the

structural attributions. The ^{13}C NMR in combination with DEPT spectra revealed the occurrence of one quaternary carbon along with intense HMBC correlations of H-2' (δ_H 3.69; *J*=3.10 Hz)/C-4' (δ_C 50.85) and H-4'^{1} (δ_H 1.29) C-4' (δ_C 50.85), which substantiated the presence of quaternary carbon at C-4' position. The NMR spectra displayed the presence of highly deshielded seven oxymethine signals (δ_H 4.17, δ_H 4.07, δ_H 3.66, δ_H 3.75, δ_H 3.47, δ_H 4.50, δ_H 5.35 corresponding to δ_C 65.13, δ_C 71.62, δ_C 75.21, δ_C 73.45, δ_C 72.01, δ_C 63.01, δ_C 97.58), one oxymethylene signals at (δ_H 3.18/δ_C 73.32, δ_H 4.30; *J*=8.97 Hz/δ_C 65.77, δ_H 3.69; *J*=3.10 Hz/δ_C 70.31) with eight degrees of unsaturation associated with three each of ring systems and carbonyl groups, with the remaining one attributed to the presence of olefinic group. The olefinic protons were recorded at δ_H 5.35 (*J*=7.36 Hz) and at δ_H 5.51 (*J*=7.87 Hz) of the ^1H NMR spectrum. In the proton correlation spectroscopy (^1H-^1H COSY) spectrum of the compound **G4**, couplings were apparent between the protons at δ_H H-4a to H-5 {(δ_H 2.05 (H-4a)/δ_H 5.35*; J*=7.36 Hz (H-5), H-7 to H-7^1 {δ_H 1.74 (H-7)/δ_H 1.08; *J*=4.16 Hz (H-7^1)}, H-8 to H-8a {(δ_H 2.04; *J*=3.13 Hz (H-8)/δ_H 4.07 (H-8a)}, H-3" to H-3"^{1} {(δ_H 1.52 (H-3")/δ_H 0.88 (H-3"^{1}), H-5" to H-6" (δ_H 1.61 (H-5")/δ_H 2.38; *J*=7.87 Hz (H-6")}, which formed three spin systems. The chromen framework of the compound **G4** was further evident from the characteristic proton and carbon signals in the literature data (Rateb and Ebel 2011). A combined 2D NMR analysis, in particular, ^1H-^1H COSY, heteronuclear single-quantum correlation spectroscopy (HSQC) and HMBC experiment unambiguously attributed the rest of the structure. The relative stereochemistries of the chiral centres of the compound **G4**, particularly that of C-7 (δ_H 1.74), C-8a (δ_H 4.07), C-4a (δ_H 2.05), C-4 (δ_H 3.75; *J*=5.55 Hz), C-3" (δ_H 1.52), C-4" (δ_H 3.47) and C-9" (δ_H 5.35 *J*=7.36 Hz) carrying the methine protons, were deduced from the NOESY spectrum and their *J*-values. The NOESY correlations between H-7^1 (δ_H 1.08)/H-5" (δ_H 1.62)/H-7 (δ_H 1.78), H-7 (δ_H 1.76)/H-2^1 (δ_H 3.18; *J*=4.40 Hz), H-1" (δ_H 0.99; *J*=6.07 Hz)/H-6" (δ_H 2.38; *J*=7.87 Hz) assigned the chair-like conformation of the 2*H*-chromen derivative. In addition, the coupling constant between the olefinic protons (*J*=7.36 Hz) at H-5 and H-6 attributed their *cis* configuration. The ^{13}C NMR spectrum in combination with DEPT indicated the presence of a total of 33 carbons, which enclosed four carbonyl groups, four CH_3, eight CH_2, nine CH, one olefinic, two methoxy, two acetyl and one quaternary carbon. The molecular ion peak at *m/z* 640 {HR (EI) MS *m/z* calcd for $C_{33}H_{52}O_{12}$ 640.3173, found 640.3182 $[M]^+$}, which in combination with its ^1H and ^{13}C NMR data designated the elemental composition of the compound **G4** as

$C_{33}H_{52}O_{12}$. Plastoquinones, chromanols and chromenes reside in a common class of natural compounds containing polyprenyl chain bound to a hydroquinone framework, and were reported to occur in marine macroalgae (Pereira et al. 2011). Mojabanchromanol is an example of an antioxidative chromen derivative isolated from marine macroalga *Sargassum siliquastrum*, and was reported to display free radical scavenging activity (Toth and Pavia 2000). Chromen derivatives from marine macroalga *Sargassum micracanthum* with potential antioxidative and anti-ulcer properties were reported in previous literature (Mori et al. 2003). Although there have been scanty reports of the occurrence of substituted chromenes from marine realm, several bioactive leads found their place in the literature with regard to the terrestrial plants. For example, new classes of quinones, chromenes and isoprenoid acetogenins were isolated from certain members of the family *Cyperaceae* of Australian origin (Allan et al. 1969). Naturally occurring anti-fungal 5, 7-dimethoxy-2-methyl-2*H*-chromene and 5, 7-dimethoxy-2, 8-dimethyl-2*H*-chromene were isolated from the leaf essential oil of *Calyptranthes tricona*. 7-Hydroxy-6-methoxy-4*H*-chromene was an example for naturally occurring 4*H*-chromene, which was obtained from the flower of *Wisteria sinensis*, and was reported to possess organoleptic property (Willem et al. 2005). The 4*H* chromene uvafzlelin was isolated from the stems of *Uvaria ufielii*, and showed anti-microbial activity against gram-positive and acid-fast bacteria (Charles et al. 1980). Chromen derivatives was also found to be an interesting template for the discovery of potential anti-cancer agents (Vosooghi et al. 2010), such as acronycine (lung, colon and ovary cancer).

Table 4.20 NMR spectroscopic data of compound **G4** in methanol d_4[a]

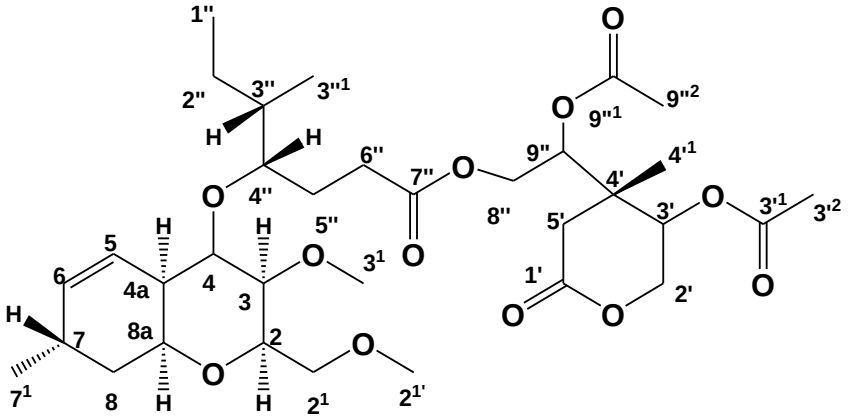

C. No	^{13}C (δ)	^{1}H-NMR[b] (int., mult., *J* in Hz)	^{1}H-^{1}H COSY	HMBC (^{1}H-^{13}C)
2	65.13	4.17 (1H, m)	-	-
2^{1}	73.32	3.18 (2H, *J*=4.40 Hz, d)	-	C-$2^{1'}$, C-2
$2^{1'}$	53.96	3.71 (3H, s)	-	-
3	75.21	3.66 (1H, *J*=3.10 Hz, t)	-	C-$2^{1'}$
3^{1}	51.29	3.36 (3H, s)	-	-
4	73.45	3.75 (1H, *J*=5.55 Hz, t)	-	-
4a	40.1	2.05 (1H, m)	5-H	C-5
5	129.55	5.35 (1H, *J*=7.36 Hz, t)	4a-H	-
6	132.53	5.51 (1H, *J*=7.87 Hz, t)	-	C-5
7	40.07	1.74 (1H, m)	7^{1}-H	-
7^{1}	18.16	1.08 (3H, *J*=4.16 Hz, d)	7-H	C-7
8	26.56	2.04 (2H, *J*=3.13 Hz, t)	8a-H	-
8a	71.62	4.07 (1H, m)	8-H	C-2
1'	173.57	-	-	-
2'	70.31	3.69 (2H, *J*=3.10 Hz, d)	-	C-4'
3'	63.01	4.50 (1H, *J*=8.11Hz, t)	-	C-9"
$3'^{1}$	174.17	-	-	-
$3'^{2}$	39.07	2.71 (3H, s)	-	-
4'	50.85	-	-	-
$4'^{1}$	14.03	1.29 (3H, s)	-	C-3', C-4'
5'	28.44	2.86 (2H, s)	-	-
1"	21.63	0.99 (3H, *J*=6.07 Hz, t)	-	C-2"
2"	29.4	1.30 (2H, m)	-	C-1"
3"	27.77	1.52 (1H, m)	$3"^{1}$-H	C-1"
$3"^{1}$	13.17	0.88 (3H, *J*=6.64 Hz, d)	3"-H	C-2", C-3"
4"	72.01	3.47 (1H, m)	-	-
5"	24.68	1.61 (2H, m)	6"-H	C-7", C-6"

6"	33.62	2.38 (2H, *J*=7.87 Hz, t)	5"-H	C-7", C-5"
7"	174.27	-	-	-
8"	65.77	4.30 (2H, *J*=8.97 Hz, d)	-	-
9"	97.58	5.35 (1H, *J*=7.36 Hz, t)	-	C-8"
9"[1]	184	-	-	-
9"[2]	32.37	2.17 (3H, s)		C-9"[1], C-9"

[a] NMR spectra recorded using Bruker AVANCE III 500 MHz (AV 500) spectrometer in methanol-d_4 as aprotic solvent at ambient temperature with TMS as the internal standard (δ 0 ppm).

[b]Values in ppm, multiplicity and coupling constants (*J*=Hz) are indicated in parentheses. The assignments were made with the aid of the ^{1}H-^{1}H COSY, HSQC, HMBC and NOESY experiments.

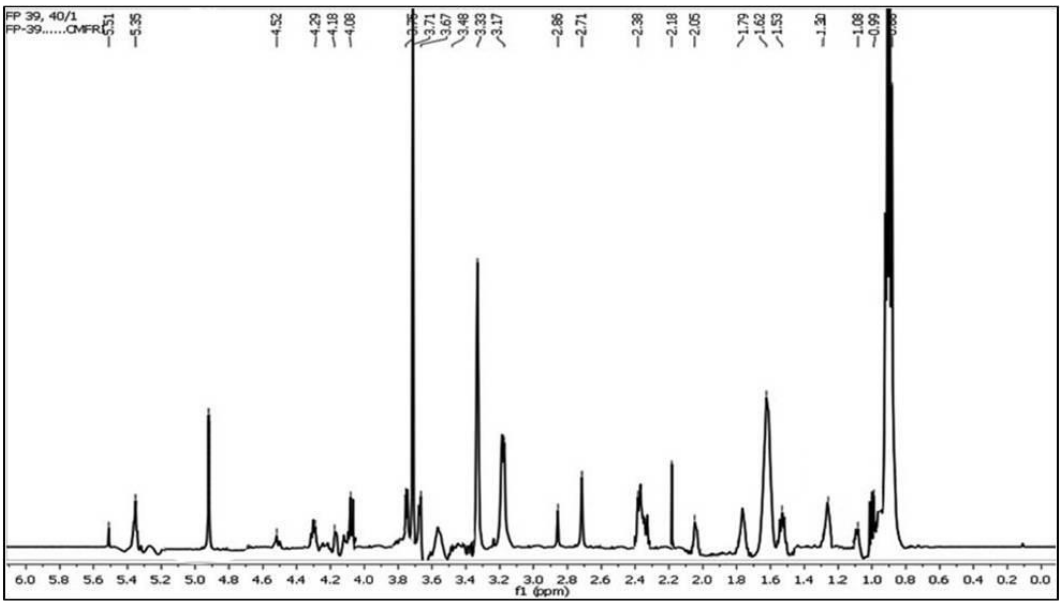

Figure 4.102. Figure showing the ^{1}H spectrum of compound **G4**

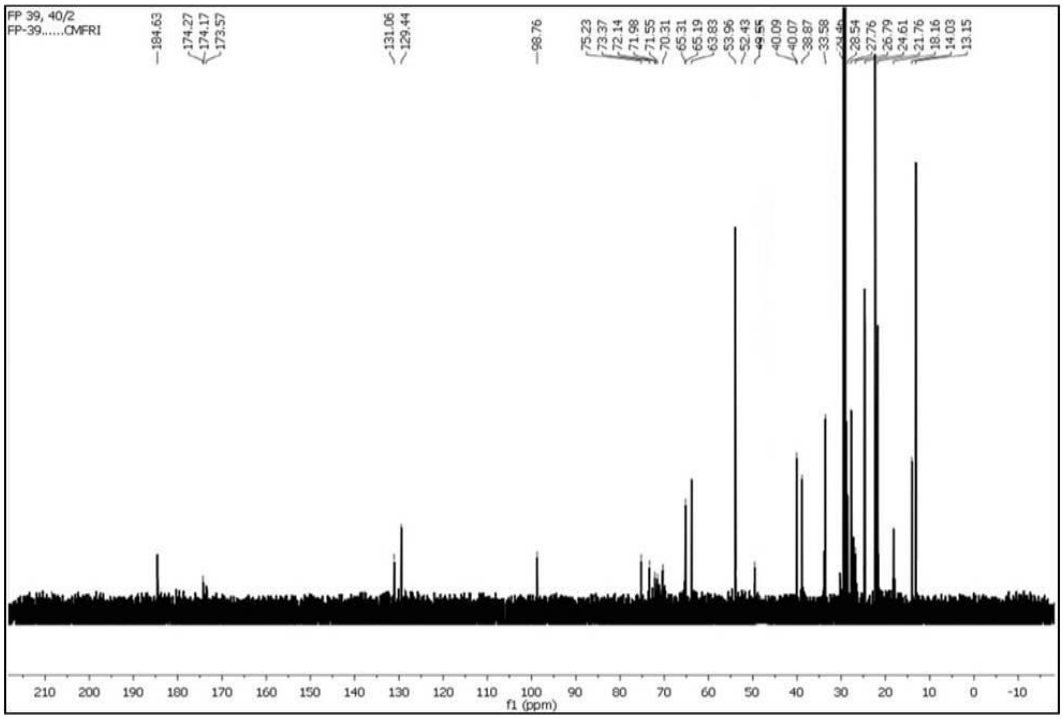

Figure 4.103. Figure showing the ^{13}C spectrum of compound **G4**

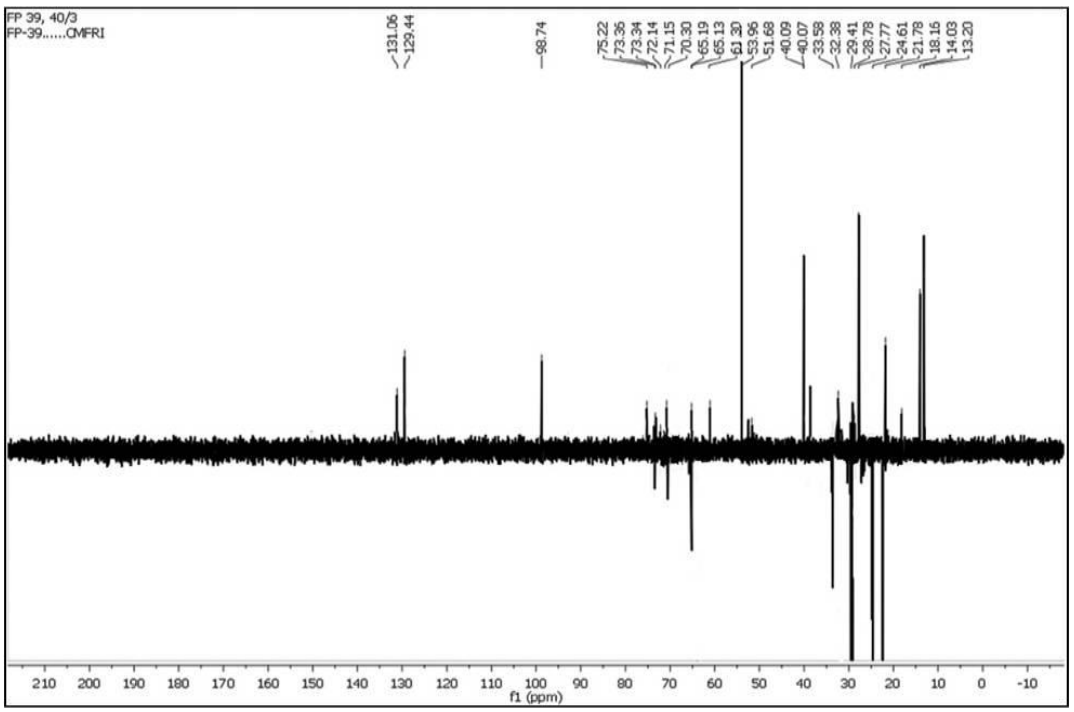

Figure 4.104. Figure showing the DEPT spectrum of compound **G4**

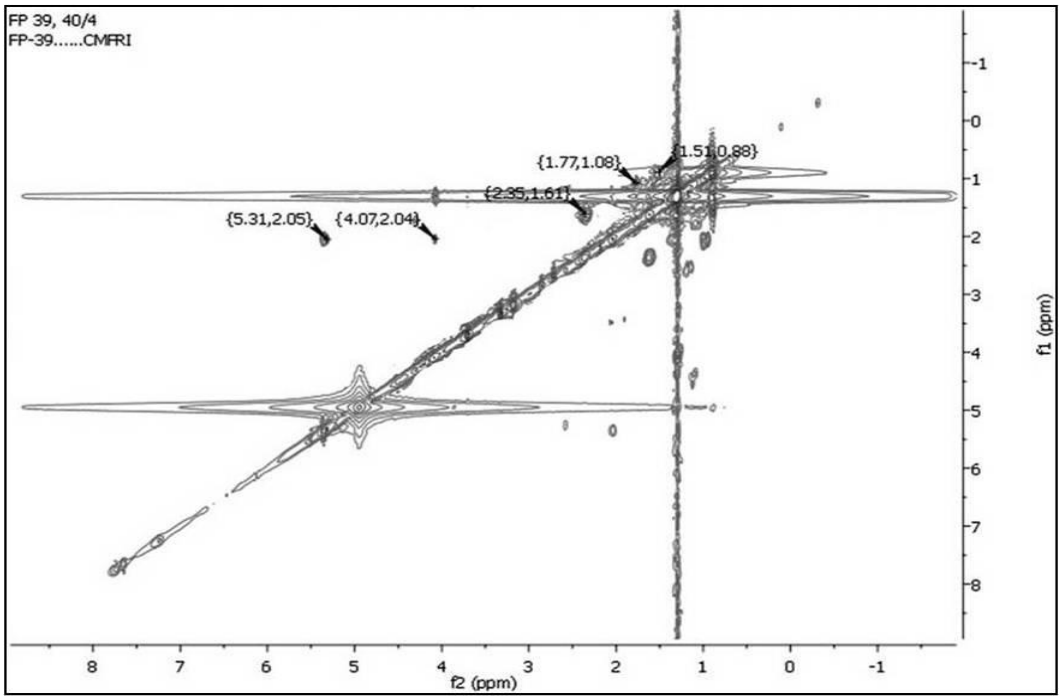

Figure 4.105. Figure showing the ^{1}H-^{1}H COSY spectrum of compound **G4**

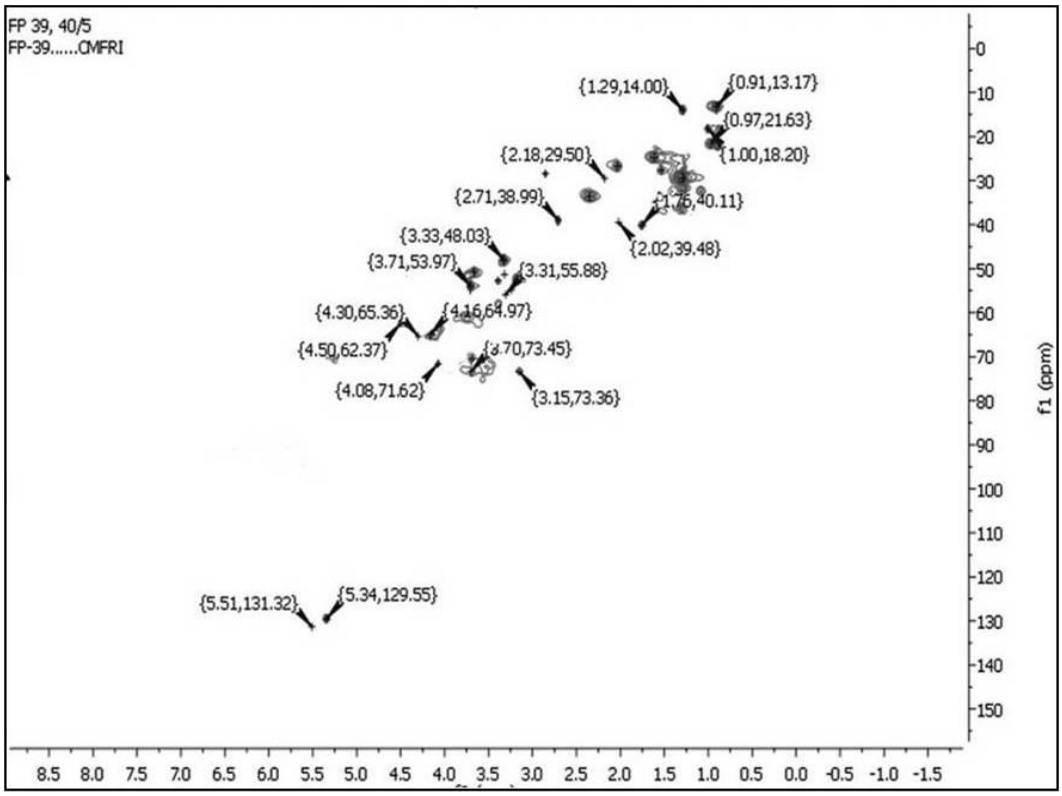

Figure 4.106. Figure showing the HSQC spectrum of compound **G4**

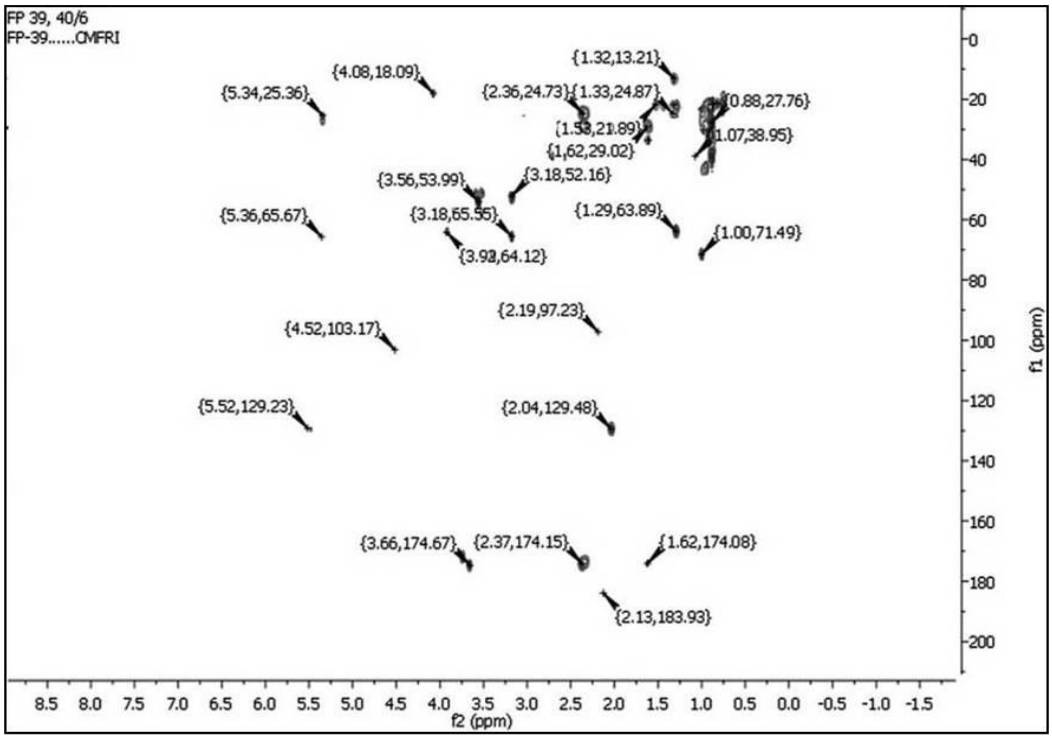

Figure 4.107. Figure showing the HMBC spectrum of compound **G4**

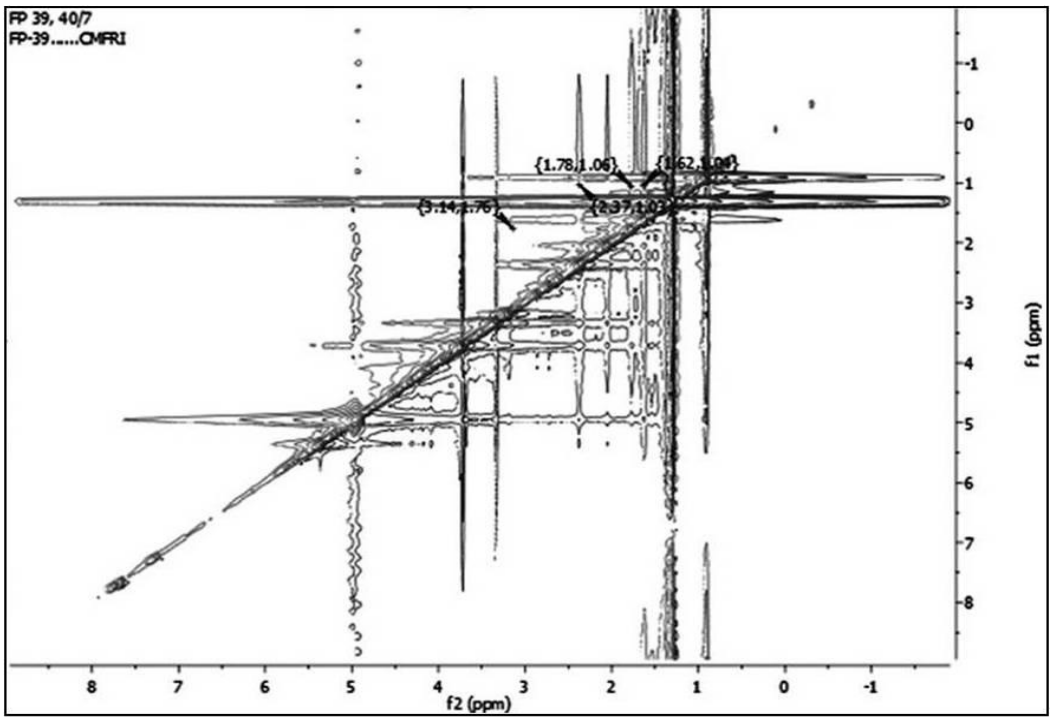

Figure 4.108. Figure showing the NOESY spectrum of compound **G4**

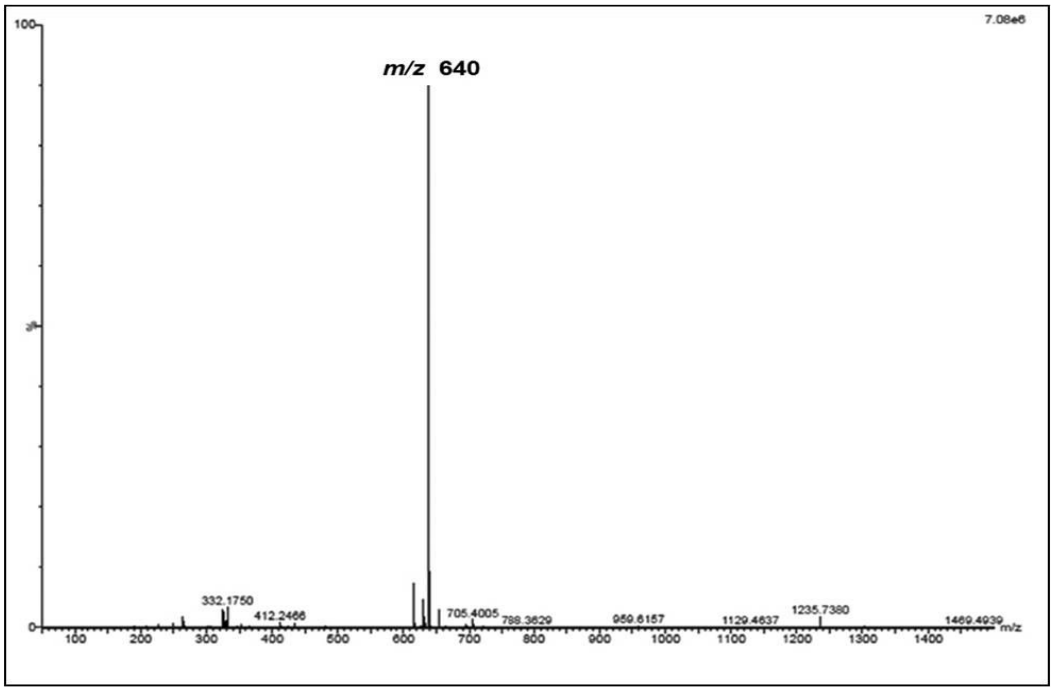

Figure 4.109. Mass spectrum of compound **G4**

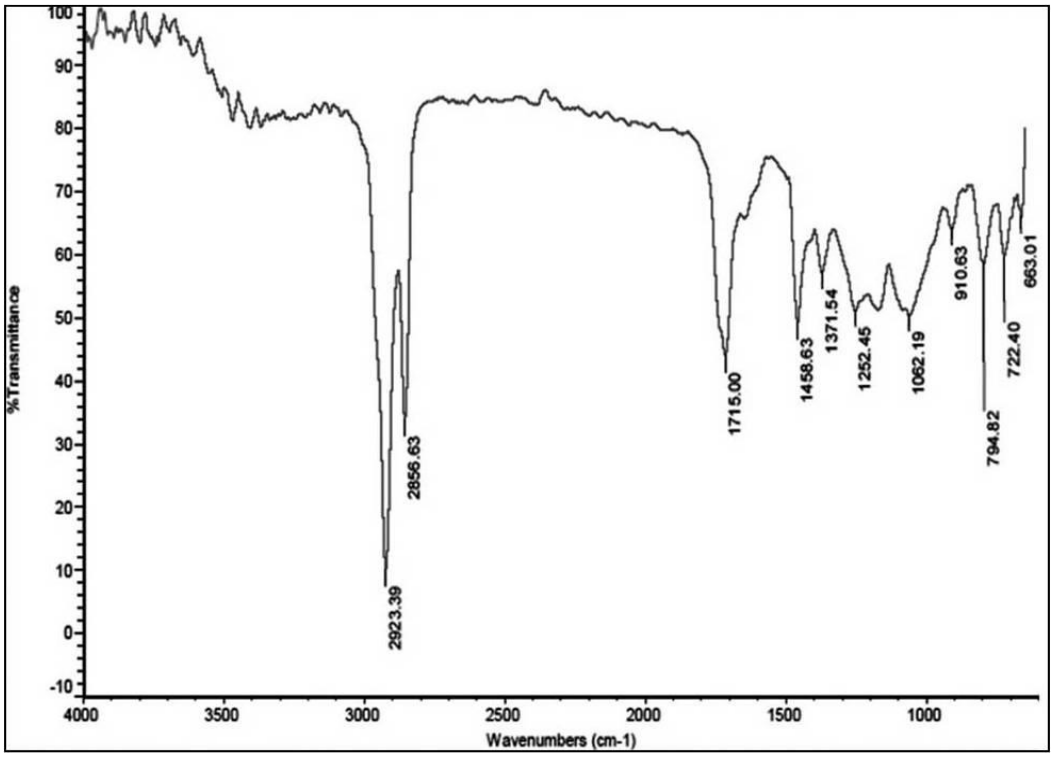

Figure 4.110. Figure showing the FTIR spectrum of compound **G4**

4.3.2.7. Bioactivities and Structure-Activity Relationship Analysis

Antioxidant activities have been displayed by various genera of marine macroalgae (Cornish and Garbary 2010; Kindleysides et al. 2012), although there were scanty reports of biogenic chromene derivatives with antioxidative and anti-inflammatory properties from this group of marine flora (Cornish and Garbary 2010). The antioxidative activity of the 2*H*-chromen derivative from the red marine macroalga *G. opuntia* was significantly greater as determined by DPPH and ABTS radical scavenging activities (IC_{50} 0.26–0.32 mg/mL) compared to α-tocopherol (IC_{50} > 0.6 mg/mL), and was comparable to the synthetic antioxidants BHT and BHA (IC_{50} ~ 0.25–0.34 mg/mL). The free radical scavenging property of the 2*H*-chromen derivative was found to be significantly influenced by the lipophilic descriptor (octanol-water coefficient, log Pow). It is of note that the octanol-water coefficient value of the compound **G4** was comparatively lesser (log Pow=2) as compared to those of the commercially available antioxidants (α-tocopherol log Pow 9.98, BHA log Pow 3.22, BHT log Pow 5.54), and this might be one of the factors leading to the significantly greater antioxidant activity of the 2*H*-chromen derivative. Although a greater lipophilic coefficient permits facile transportation of the molecule through the inter-membrane space, the lesser molecular hydrophobicity renders the molecule to harbor lesser radical scavenging properties. The log Pow of the chromene derivative is lesser apparently due to the presence of 1-(5-acetoxy-4-methyl-2-oxotetrahydro-2*H*-pyran-4-yl) ethyl acetate (log Pow 0.22) and dimethoxy-4-(methoxymethoxy)-2*H*-chromene (log Pow 1.23) frameworks. The majorities of the hydrophobicity and membrane permeability were imparted by the methylheptane moiety (log Pow 3.75) sandwiched between these two hydrophilic groups described earlier. It is of note that compounds with greater antioxidative properties in the *in vitro* systems might not prove themselves as potential radical scavengers in our metabolic systems, due to the fact that a balanced combination of hydrophilicity-lipophility is essential for antioxidative activities in the cellular framework. The 2*H*-chromen derivative isolated in the present study harbour 1-(5-acetoxy-4-methyl-2-oxotetrahydro-2*H*-pyran-4-yl) ethyl acetate and dimethoxy-4-(methoxymethoxy)-2*H*-chromene moieties, which might contribute towards the aggregate electronic property of the compound **G4** (aggregate topological surface area tPSA 142.12, polarisability Pl 53.26×10^{-24} cm^3).

Figure 4.111. Graphical representation of bioactivities of compound **G4**. The thalli of the studied marine macroalga were displayed as inset

The antioxidative activity of the compound **G4** might be contributed by the presence of electron donating groups, such as $–CH_2O$, –OMe, >C=O, etc., which could abstract and convert the free radicals to their non-reactive forms (Pietta 2000; Cai et al. 2006). It is interesting to note that the chromen from marine macroalga recorded significantly greater electronic properties than α-tocopherol (tPSA 29.46), BHT (20.23) and BHA (29.46) along with acceptable hydrophobicity (log Pow 2.88), which is comparable to that of BHT and BHA (log Pow 3–5). Interestingly, the hydrophobicity of α-tocopherol is significantly greater (log Pow 9.98) than other synthetics and the 2*H*-chromen, which can be attributed to the significantly lesser antioxidative activities of the former (IC_{50} 0.6–0.7 mg/mL, $P < 0.05$). Notably, the inhibition of the COX-1 isoform is subjected to many side effects of the conventional NSAIDs, and therefore, there were efforts to search anti-inflammatory leads with selective anti-COX-2 activities and lesser side effects. The purified compound showed greater anti-inflammatory activity against COX-2 isoform (IC_{50} 0.96 mg/mL) than COX-1 (IC_{50} 1.21 mg/mL), and this phenomenon is inverse with regard to the traditional NSAIDs, such as aspirin (anti-COX-1 IC_{50} 0.005, anti-COX-2 IC_{50} 0.21 mg/mL) and ibuprofen (anti-COX-1 IC_{50} 0.04, anti-COX-2 IC_{50} 0.09 mg/mL) (Fig. 4.111, Table 4.21).

Therefore, the anti-inflammatory selectivity index of the substituted 2*H*-chromen was found to be greater (SI: anti-cyclooxygense-1 IC_{50}/anti-cyclooxygense-2 IC_{50} ~ 1.26) than synthetic NSAIDs (aspirin and ibuprofen, SI: 0.02 and 0.44, respectively), and consequently, appeared to be safer. The *in vitro* 5-lipoxygenase (5-LOX) activity of the 2*H*-chromen (IC_{50} 1.22 mg/mL) was comparable to that of synthetic ibuprofen (IC_{50} 0.93 mg/mL). Sodium salicylate was found to be a weaker inhibitor of both COX isoforms (anti-COX-2 IC_{50} 2.65 mg/mL, anti-COX-1 IC_{50} 1.93 mg/mL) and demonstrated significantly lesser activity against 5-LOX (anti-COX-1 IC_{50} 1.75 mg/mL) ($P < 0.05$). In this context, it is important to note that the polarity (or electronic attributes) of the oxygenated 2*H*-chromen recorded greater values (tPSA 88.13) than NSAIDs (tPSA aspirin 63.60, tPSA ibuprofen 37.30), along side comparable hydrophobic-lipophobic (HLB) balance {log Pow (aspirin) 1.21, log Pow (ibuprofen) 3.75, log Pow (oxygenated 2*H*-chromen) 2.3)}. While the acceptable HLB would be of help for the compound **G4** to cross inter-membrane barrier, the greater polarity might enable the compound to effectively interact with the cyclooxygenase/lipoxygenase active site residues, which in turn, would result in greater anti-inflammatory activity.

Table 4.21 Antioxidative and anti-inflammatory activities of the 2*H*-chromen from *G. opuntia vis-à-vis* the commercially available antioxidants and anti-inflammatory agents

Bioactivities*	**IC_{50} (mg/mL)**			
Antioxidative activities	**Substituted 2*H*-chromen**	**BHA**	**BHT**	**α-tocopherol**
DPPH· scavenging	0.26^{a} ±0.02	0.26^{b}± 0.01	0.25^{b}± 0.02	0.63^{c}±0.04
$ABTS^{+\cdot}$ scavenging	0.32^{b} ±0.11	0.34^{b}± 0.02	0.26^{b}± 0.02	0.73^{c}±0.05
Anti-inflammatory activities	**Substituted *2H*-chromen**	**Aspirin**	**Na-salicylate**	**Ibuprofen**
COX -1 inhibition	1.21^{a} ±0.03	0.005^{a} ±0.00	1.93^{c} ±0.05	0.04^{a} ±0.00
COX -2 inhibition	0.96^{a} ±0.04	0.21^{b} ±0.02	2.65^{c} ±0.05	0.09^{a} ±0.02
Selectivity index**	1.26^{b} ±0.04	0.02^{b} ±0.02	0.72^{b} ±0.01	0.44^{b} ±0.02
5-LOX inhibition	1.22^{a} ±0.07	0.39^{a} ±0.02	1.75^{c} ±0.12	0.93^{b} ±0.11

* The bioactivities were expressed as IC_{50} values (mg/mL).

The samples were analyzed in triplicate (n=3) and expressed as mean ± standard deviation. Means followed by the different superscripts (a–c) within the same row indicate significant differences ($P < 0.05$).

**Selectivity index has been calculated as the ratio of anti-COX-1(IC_{50}) to that of anti-COX-2 (IC_{50})

4.4. Conclusions

Bioactivity-guided chromatographic fractionation of the organic extract obtained from the thalli of the red marine macroalga *K. alvarezii* yielded two halogenated compounds named as 2-butyl-7-4-(chloromethyl) cyclooct-1-enyl) hept-5-en-1-ol and 4-(2-chloroethyl)-5-7-(methoxymethyl) undec-3-enyl) cyclooct-4-enone. Three oxygenated meroterpenoids, characterized as 1-(3-methoxypropyl)-2-propylcyclohexane, 3-(methoxymethyl) heptyl 3-(cyclohex-3-enyl) propanoate, and 2-ethyl-6-(4-methoxy-2-((2-oxotetrahydro-*2H*-pyran-4-yl) methyl) butoxy)-6-oxohexyl-5-ethyloct-4-enoate along with an unprecedented non-isoprenoid oxocine carboxylate cyclic ether characterized as (3, 4, 5, 6)-3-(hexan-2'-yl)-3, 4, 5, 8-tetrahydro-4-methyl-2*H*-oxocin-5-yl acetate were also purified to homogeneity from the organic extract of the marine macroalga. Likewise chromatographic purification of the organic solvent extract of the thalli of the red marine macroalga *G. opuntia* yielded two unprecedented furanyl derivatives, named as 5-(7-(5-ethyl-3, 4-dimethoxycyclooctyl) benzofuran-6-yl)-7-methyl-tetrahydro-2*H*-oxocin-2-one and 2-(3-ethyl-9-(2- methoxyethoxy)-1-oxo-tetrahydro-1*H*-xanthen-2-yl) ethyl-5-hydroxy-9-methoxy-7, 8-dimethyl-8-(5-methylfuran-2-yl) nona-3, 6-dienoate. A rare antioxidative azocinyl morpholinone alkaloid characterized as of 3-(2-ethyl-6-((3, 7)-1, 2, 5, 6-tetrahydroazocin-5-yl) hexyl) morpholin-6-one along with a chromen derivative with highly oxygenated carbon skeleton, characterized as 2-acetoxy-2-(5-acetoxy-4-methyl-2-oxotetrahydro-2*H*-pyran-4-yl) ethyl-4-(3-methoxy-2-(methoxymethyl)-7-methyl-hexahydro-2*H*-chromen-4-yloxy)-5-methylheptanoate. The compounds were found to selectively inhibit pro-inflammatory inducible enzymes cyclooxygenase-2 and 5-lipoxygenase, and possessed significantly greater selectivity than the non-steroidal anti-inflammatory drugs. The target bioactivities of the isolated secondary metabolites were predominantly directed by the electronic and lipophilicity parameters. The newly reported compounds from the two studied marine macroalgae were found to be endowed with valuable bioactive potential as natural antioxidant and anti-inflammatory leads for use in the pharmaceutical and food applications.

Chapter 5

ISOLATION AND CHARACTERIZATION OF SULFATED POLYSACCHARIDES FROM *KAPPAPHYCUS ALVAREZII* AND *GRACILARIA OPUNTIA* AND THEIR PHARMACOLOGICAL APPLICATIONS

Contents

5.1. Background

The marine macroalgal polysaccharides were reported to possess valuable pharmacological properties, and have been found to constitute a fascinating chemical diversity (Pangestuti and Kim 2011; Souza et al. 2012; Maneesh and Chakraborty 2018). Previous reports of literature found that the macroalgae-derived polysaccharides could stimulate the immune system resulting in the decreasing onset of various life-threatening diseases (Leiro et al. 2007; Choi et al. 2005). The chemical structures of macroalgal hydrocolloids bearing oligosaccharide framework are heterogeneous, whereas these large families of macroalgal hydrocolloids were made up of homogenous or heterogenous group of linear repeating chains of monomeric saccharide units, with repeated sequence of 1, 3 and 1, 4-connectivity. The monosaccharide units were found to possess various combinations of ester-sulfate groups in their repeating framework. These structural complexities of macroalgal polysaccharide were attributed to the occurrence of a mixture of monomeric units, and their repeating sequence along with uronic acid and sulfate content in the polysaccharide backbone (Vandevelde et al. 2002). The brown marine macroalga '*wakame*' (*Undaria pinnatifida*), which is customarily consumed in Japan, was accounted for to have *in vitro* Angiotensin-I-converting enzyme (ACE) inhibitory and *in vivo* anti-hypertensive effects (Suetsuna and Nakano 2000). ACE-I inhibitory peptides were reported from the butanol portion of marine macroalga *U. pinnatifida* hydrolysate (Sato et al. 2002). Bioactive properties of the macroalgae were reported to be due to the presence of sulfated polysaccharides, phenolics, and terpenoids (Chakraborty and Paulraj 2010; Chakraborty et al. 2015).

The marine macroalgae were found to be potential inhibitors of α-glucosidase (Seung-Hong and You-Jin 2013). Bromophenols, 2-piperidione, benzene acetamide, *n*-hexadecanoic acid, and polysaccharide derivatives were found in red marine macroalgae like *Rhodomela confervoides*, *Symphyocladia latiuscula*, *Polysiphonia urceolata* and were found to exhibit hypoglycemic potentials by inhibiting α-glucosidase (Seung-Hong and You-Jin 2013).

Red marine macroalgae (Rhodophyta) were found to constitute a predominant natural resource in the coastal areas of Indian penninsular. Among different red marine macroalgae found in the Gulf of Mannar of the Indian subcontinent, *Kappaphycus alvarezii* (Doty) Doty ex Silva (family Solieriaceae, phylum Rhodophyta; voucher

specimen number MA/RS/KA-005/2016–2017) and *Gracilaria opuntia* (family Gracilariaceae, phylum Rhodophyta; voucher specimen number MA/RS/GO-003/2016–2017) are available all through the distinctive seasons. These genera of macroalgae were widely used in traditional medicine, and have been considered to be economically important since they are used in the pharmaceutical, nutraceutical, cosmetic and food industries (Blouin et al. 2011; Gressler et al. 2010; Holdt and Kraan 2011). Numerous studies have been carried out to determine the antioxidant activities in the red marine macroalga *K. alvarezii* extract (Chew et al. 2008; Matanjun et al. 2008; Ganesan et al. 2008; Kumar et al. 2008). The acetone extract of *K. alvarezii* was found to possess significant antioxidative activity (Farah Diyana et al. 2015). The organic extracts of *K. alvarezii* displayed significant protection against DNA damage induced by H_2O_2, and enhanced antioxidant potential and protection against tissue lipid peroxidation and cell damage (Nagarani and Kumaraguru 2013). The methanol extract derived from *K. alvarezii* was screened for the anti-diabetic (α-amylase) anti-inflammatory activity (hyaluronidase inhibition) and cytotoxicity against the stannous chloride in *E. coli* AB 1157 (Nagarani and Kumaraguru 2013). The red marine macroalga belonging to *Gracilaria* sp were found to be rich in sulfated polysaccharides, and were generally related with anti-inflammatory property (Mendonca and Freitas 2000).

In this background, the objectives of the present study were to screen these marine macroalgae belonging to *K. alvarezii* (family Solieriaceae, phylum Rhodophyta) and *G. opuntia* (family Gracilariaceae, phylum Rhodophyta) for lead polysaccharide fractions containing different sulfated galactan motifs by chemical derivatization and spectroscopic analyses. The pharmacological properties with regard to antioxidant, anti-hypertensive, anti-inflammatory and anti-diabetic activities of the purified polygalactans were evaluated by various selective assays as described in the following sections.

5.2. Materials and Methods

5.2.1. Algal Material

The red marine macroalgae used in this study were *Kappaphycus alvarezii* (Doty) Doty ex Silva (family Solieriaceae, phylum Rhodophyta; voucher specimen number MA/RS/KA-005/2016-2017) and *Gracilaria opuntia* Durairatnam (1962) (family Gracilariaceae, phylum Rhodophyta; voucher specimen number MA/RS/GO-003/2016-2017), which were freshly collected from the Gulf of Mannar in Mandapam region situated between 8º48′ N, 78º9′ E and 9º14′ N, 79º14′ E in the south east coast of India. The samples were washed in running water for 10 min to remove epiphytes, dirt, and salt particles, before being transported to the laboratory and shade-dried (35 ± 3 °C) for 72 h and utilized for further experiments.

5.2.2. Instrumentation

FTIR spectra of the compounds under KBr pellets were recorded in a Thermo Nicolet Avatar 370 in the IR range between 4000 and 400 cm^{-1}. UV spectra were obtained on a Varian Cary 50 ultraviolet visible (UV–VIS) spectrometer (Varian Cary, USA). The Gas chromatography–Mass spectrometry (GC-MS) analyses were performed in electronic impact (EI) ionization mode in a Perkin Elmer Clarus 680. GC-MS fitted with an Elite 5 MS non-polar, bonded phase capillary column (50 m × 0.22 mm i.d. × 0.25 μm film thicknesses). Helium (He) was used as the carrier gas, and the flow rate used was 1 mL min^{-1}. The temperature was programmed initially at 50 °C for 2 min, then increased at a rate of 10 °C min^{-1} to 180° C and kept for 2 min and raised at 4° C min^{-1} to 280 °C and held for 15 min. Thin layer chromatographic analysis was carried out using silica gel GF_{254} plates and visualized with a documentation system operating at 254 and 366 nm wavelength regions. A table-top high speed refrigerated centrifuge (Sorvall, Biofuge Stratos, Thermo Scientific, Germany) was used for centrifugation. Flash Chromatography (Biotage AB SP1-B1A, Biotage AB, Uppsala, Sweden). Chromatographic analysis was carried out using High performance liquid chromatography (Shimadzu SCL-10A vp, Shimadzu Co., Kyoto, Japan) equipped with a vacuum degasser, a binary pump (LC–20AD), a thermostatic column compartment (CTO–20A) and a diode array detector (SPD–M20A), connected to an LC solution software. Chromatographic separation was carried out at 30 ℃ on a reverse phase Luna C_{18} (250 mm x 4.6 mm, 5μm) phenomenex column. The ultra sonicator (Labline) was used for sonicating and a laboratory shaker (Shaker, Labline) was used for shaking. A

rotary vacuum evaporator (Heidolf, Germany) was used for evaporation of solvents. ^{1}H and ^{13}C NMR spectra were recorded on a Bruker AVANCE III 500 MHz (AV 500) spectrometer (Bruker, Germany) in $CDCl_3$ as aprotic solvent at ambient temperature with TMS as the internal standard (δ 0 ppm). Two-dimensional ^{1}H-^{1}H COSY, DEPT, HSQC, HMBC and NOESY experiments were carried out using standard pulse sequences. The NMR data were acquired by using the BrukerTopSpin™ 2 software, and processed by MestReNova-7.1.1-9649 (Mestrelab Research S.L.). All the reagents and solvents used in this study were of analytical grade and purchased from E-Merck.

5.2.3. Isolation and Purification of the Various Polysaccharide Fractions from the Marine Macroalgae *K. alvarezii* and *G. opuntia*

The dried and powdered material (200 g) derived from the marine macroalgae was refluxed for 4 h in *n*-hexane (40-60 °C, 1000 mL). The residual material acquired after filtration (Whatman number 1) was air-dried for 24 h before being treated with an alkaline solution (6 % KOH w/w) at 80–90 °C for 3–4 h. The treated samples were repeatedly washed with deionized water (3 × 1000 mL) to remove the excess KOH before being dried. The dried macroalgal powder (200 g) was thereafter extracted with hot deionized water (1200 mL) at 80–90 °C for 3–4 h to yield an aqueous extract, which was cooled and centrifuged (8,500 rpm for 15 min, 4 °C, Sorvell Biofuge Stratos, Thermo Scientific, USA) to remove the solid residues. The clarified supernatant (1000 mL) obtained after centrifugation was concentrated to 1/4th of the original volume (250 mL) by utilizing a rotational vacuum concentrator (Martin Christ RVC 2-33 IR, Martin Christ, Germany), cooled, and precipitated with three volumes of cold ethanol (750 mL, 3:1, v/v) overnight at 4 °C for the precipitation of mixture of sulfated polygalactan. Subsequently, ionic halide ($CaCl_2$ 1 % w/v, 15 g) was added to the supernatant, and the mixture was kept up overnight at 4 °C. The lyophilization of the precipitated material in a laboratory freeze-drier (Martin Christ alpha 1-4 LDplus, Germany) yielded sulfated polygalactan-enriched concentrate (**KA-1** from *K. alvarezii* and **GO-1** from *G. opuntia*) derived from the marine macroalgal species (yield based on powdered material, 72 %). The resultant polysaccharide concentrate was fractionated by anion-exchange chromatography (DEAE cellulose Cl^{-} previously equilibrated with 0.1 M NaCl, 3 × 10 cm, Bio-Rad, CA, USA), and the column was

continuously eluted with common salt (NaCl, 0-2 M). The polysaccharide fractions were vacuum-concentrated (Martin Christ RVC 2-33 IR, Germany) before being dialyzed for 48 h (against distilled water) and lyophilized (alpha 1-4 LD, Martin Christ, Germany). The purity of the fractionated polysaccharides were examined by reverse-phase high performance liquid chromatography (Shimadzu LC 20AD; Shimadzu Corp., Nakagyo-ku, Japan) accompanied by an reverse-phase amino column (SUPELCOSIL NH_2 column-5 µm, 25 cm × 4.6 mm; Supelco, Bellefonte, PA, USA) previously housed in an oven (maintained at 35 °C). Acetonitrile/water (3:1 v/v, flow rate of 0.5 mL/min) was used as the mobile phase to separate the polysaccharide fractions by using a refractive index detector. The purified polysaccharide fractions (**KA-1** from *K. alvarezii* and **GO-1** from *G. opuntia*) were further used for antioxidant and anti-hypertensive *in vitro* analysis.

In another process to fractionate the various polysaccharide fractions, the dried marine macroalgal powder (200 g) was extracted with hot water at 80–90 °C for 3–4 h to yield an aqueous extract (Praveen and Chakraborty 2013) which was cooled and centrifuged (8500 rpm for 15 min, 4 °C, Sorvell Biofuge Stratos, Thermo Scientific, USA) to remove the solid residues. The supernatant (1000 mL) obtained after centrifugation was concentrated to $1/10^{th}$ of the original volume (100 mL) by utilizing a rotational vacuum concentrator (Martin Christ RVC 2-33 IR, Germany), cooled, and precipitated with three volumes of ethanol (500 mL, 3:1, v/v) overnight at 4 °C for the precipitation of the sulfated polygalactans (**KA-2** from *K. alvarezii* and **GO-2** from *G. opuntia*). The lyophilization of the precipitated material in a laboratory freeze-drier (alpha 1-4 LD, Martin Christ, Germany) yielded sulfated polygalactan-enriched macroalgal concentrate (144 g; yield based on powdered macroalgae (72 %). The purified polysaccharide fractions (**KA-2** from *K. alvarezii* and **GO-2** from *G. opuntia*) were further used for anti-diabetic and anti-inflammatory *in vitro* analysis.

In a further different process to fractionate the various polysaccharides from the studied marine macroalga, the air-dried thalli of *K. alvarezii* (50 g) were extracted with alkali (1000 mL, 5 % KOH) at 80 °C (1 h), and were added with acid (1 M HCl) followed by extraction with mild alkaline solution of sodium bicarbonate ($NaHCO_3$, pH 8-9). The mild alkaline extract was treated with 1 % KCl solution to precipitate the polysaccharide fractions, which was freeze-dried (alpha 1-4 LD, Martin Christ, Germany) to yield a polysaccharide-concentrate (**KA-3** from *K. alvarezii*, 1000 g; 72 % yield on the basis of dry weight). Likewise, the air-dried thalli of *G. opuntia* (50 g)

were extracted with of mild alkaline solution of $NaHCO_3$ (1000 mL, pH 8-9). The extraction was carried out for 2 h, and the supernatant was collected. The clarified solution was evaporated to one-third of its original volume, and the polysaccharide fractions were precipitated by isopropyl alcohol. The centrifugation at 8000 rpm (4 °C for 20 min) was performed to recover precipitated polysaccharide fractions, which were freeze-dried to yield polysaccharide-enriched concentrate (**GO-3** from *G. opuntia*) (50 g; yield 75 %). The fractionation of polysaccharide concentrates using diethylaminoethyl cellulose (DEAE cellulose, Cl^-) anion-exchange chromatography (previously equilibrated with 0.1 M NaCl, 3 × 10 cm, Bio-Rad, CA, USA) with an increasing gradient of NaCl (0-2 M) was used to yield various fractions, which were vacuum-concentrated and dialyzed (against distilled water) before being freeze-dried. The reverse-phase high performance liquid chromatography (RP-HPLC; Shimadzu LC 20AD) with amino column (Supelcosil NH_2 column-5 μm) and mobile phase of acetonitrile/water (3:1 v/v) (flow rate of 0.6 mL/min) were used to analyze the homogeneity of the polysaccharides. The purified polysaccharide motifs were further used for anti-diabetic and anti-hypertensive *in vitro* analysis (**KA-3** from *K. alvarezii* and **GO-3** from *G. opuntia*). Monosaccharide composition was then measured by RP-HPLC with pulsed refractive index detector (RID detector), by external calibration with standard solutions of galactose (Sigma, St. Louis, MO, USA). In brief, trifluoro acetic acid (TFA, 1 M) was used to hydrolyze the sample (20 mg), and nitrogen gas was purged to remove the residues of TFA. The resulting hydrolysate was dissolved in 1 mL of HPLC-grade water, and was injected to the RP-HPLC mounted with an amino column and RI detector. Acetonitrile-water (80:20, v/v) mobile phase was used to separate the compounds, and methylation analyses of polysaccharides were performed by following previous reports of literature (Jun and Gray 1987; Kiwitt-Haschemie et al. 1993) with suitable modifications.

Methylated polysaccharide fractions (80 g) from *K. alvarezii* were recovered in EtOAc before being packed in glass column (90 cm X 4 cm) loaded with 60-120 meshed silica gel. Gradual increase of polarity of the mobile phase by addition of increasing gradient of EtOAc: *n*-hexane (1:99 to 7:3, v/v) yielded 10 fractions (8 mL each) that were combined to 4 fractions (FP_{10}- FP_{14}) on the basis of TLC experiments (EtOAc: *n*-hexane 1:4, v/v). The fraction FP_{11} (110 mg) recovered by using EtOAc: *n*-hexane (1:4, v/v) was a mixture that was flash chromatographed (Biotage AB SP1-B1A, Sweden) with a step-gradient of EtOAc/*n*-hexane (0-50 % EtOAc) to afford 160

sub-fractions (15 mL each). On the basis of analytical TLC experiments, the homogeneous fractions were combined to yield three fractions (FP_{15} – FP_{17}). The fraction $FP_{15\text{-}1}$ on further fractionation over preparatory RP-HPLC chromatography on a C_{18} RP column yielded 1, 3-*O*-diacetyl-2, 5, 6-tri hydroxyl-β-D-galactose-4-sulfate (**KA-3$_A$**; 85 mg, ~99 % purity).

The methylated polysaccharide fractions (80 g) from *G. opuntia* were recovered in EtOAc before being packed in glass column (90 cm X 4 cm) loaded with silica gel (60-120 mesh). Gradual increase of polarity of the mobile phase by addition of increasing gradient of EtOAc: *n*-hexane (1:99 to 7:3, v/v) yielded 15 fractions (15 mL each) that were combined to 5 fractions (FP_{30}- FP_{35}) on the basis of TLC experiments (EtOAc: *n*-hexane 1:4, v/v). The fraction FP_{33} (130 mg) recovered by using EtOAc: *n*-hexane (1:4, v/v) was a mixture that was flash chromatographed (Biotage AB SP1-B1A, Sweden) with a step-gradient of EtOAc/*n*-hexane (0-50 % EtOAc) to afford 150 sub-fractions (10 mL each). On the basis of analytical TLC experiments, the homogeneous fractions were combined to yield five fractions (FP_{36}–FP_{40}). The fraction $FP_{38\text{-}1}$ on further fractionation over preparatory RP-HPLC chromatography on a C_{18} RP column yielded 1, 3, 5-*O*-triacetyl-4-hydroxyl-6-*O*-methyl-D-galactose-2-sulfate (**GO-3$_A$**; 78 mg, ~ 99 % purity).

5.2.4. Analytical Methods

The polysaccharide fractions purified from the studied marine macroalgae were analyzed by the dinitrosalicyclic acid method, whereas uronic acid content was determined using the phenol-sulphuric acid reaction (Dubois et al. 1956). The sulfate content was evaluated by $BaCl_2$-gelatin method (Dodgson 1961). The yields were assessed from the dried weight of polysaccharide motifs. The pharmacological activities of the polysaccharide motifs were determined based on the *in vitro* assays performed as explained in the previous chapter (Chapter 3). The *in vitro* antioxidant activities were determined by ABTS, DPPH radical scavenging assays along with ferrous ion chelating assay (Sivasothy et al. 2012; Chakraborty et al. 2014). The anti-inflammatory properties were evaluated by COX-1 and COX-2 inhibition assays (Larsen et al. 1996) and 5-LOX inhibition assay (Baylac and Racine 2003). *In vitro* anti-diabetic studies were carried out by inhibition of dipeptidyl peptidase-4, α-amylase (Kojima et al. 1980; Hamdan and Afifi 2004) and α-glucosidase (Dong et al. 2012)

inhibition assays. The anti-hypertensive activities were determined by ACE-I inhibitory assay (Udenigwe et al. 2009). The IC_{50} value (mg/mL), named effective concentration, which is the concentration of the sulfated polygalactan enriched concentrate of *K. alvarezii* and *G. opuntia* inhibiting 50 % of the activity (COX-1 and COX-2), was calculated from the non linear regression curve. To calculate IC_{50}, a series of dose-response data have been used, whereas the simplest estimate of IC_{50} is to plot x-y and fit the data with a straight line. IC_{50} value was estimated using the fitted line, i.e., $y=mx+c$, and expressed as $IC_{50}= (0.5 - c)/m$.

5.2.5. Spectroscopic Methods

Fourier-transform infrared (FTIR) spectra of KBr pellets were recorded utilizing a Perkin–Elmer Series 400 FTIR spectrophotometer (Waltham, USA; scan range between 400-4000 cm^{-1}). The solid samples of dried sulfated polygalactan fraction (10 mg) were mixed with KBr (100 mg) and compressed to prepare as a salt disc. The frequencies of different components present in each sample were analyzed. Proton nuclear magnetic resonance (^{1}H-NMR) spectra were recorded on a Bruker AVANCE DRX 600 MHz (AV 600) spectrometer (Bruker, Karlsruhe, Germany) in deuterium oxide (D_2O) as aprotic solvent at ambient temperature (27 ^oC) with tetramethylsilane (TMS) as the internal standard (δ 0 ppm) equipped with 5 mm probes. The samples were deuterium exchanged by successive freeze-drying steps in D_2O (99.9 %) before being dissolved in D_2O (20-25 mg/mL).

5.2.6. Statistical Analysis

Data were expressed as mean values standard deviations. Statistical evaluation was carried out by Statistical Program for Social Sciences software (SPSS Inc, Chicago, USA, ver. 13.0). Analyses were carried out in triplicate and the means of all parameters were examined for significance ($P < 0.05$) by one-way analysis of variance (ANOVA). The Pearson correlation coefficient (r) was calculated ($P < 0.05$) to assess the strength of the linear relationship between two variables. The selected variables for principle component analysis (PCA) were the different bioactivities, as exhibited by different types of polysaccharides, which were extracted from the marine macroalgae.

5.3. Results and Discussion

5.3.1. Structural Characterization of Polysaccharide Fractions (KA-1 and GO-1) from Marine Macroalgae

The precipitation of polysaccharides from the crude extracts of *K. alvarezii* (**KA-1**) with ethanol brought about significantly greater yields (75 %) than that by utilizing $CaCl_2$ (56 %) ($P < 0.05$). Essentially, the aggregate recovery of polysaccharides from *G. opuntia* (**GO-1**) was recorded to be significantly lesser than those in *K. alvarezii* (**KA-1**) using ethanol (55 %) and $CaCl_2$ (50 %). The sulfated galactan was found to possess 34 % 3, 6-anhydro-D-galactose groups as a feature of its repeating structure and 25 % ester sulfate groups, which promptly diffused when warmed. Sulfated polygalactan was found to be the predominant polysaccharide acquired by $CaCl_2$ precipitation. It is evident that Ca^{2+} ions form bridges between the contiguous double helices through an electrostatic binding to two adjoining sulfate groups, consequently settling and reinforcing the polysaccharide system. The present examination demonstrated that a more significant yield of sulfated galactan could be obtained with alkaline (KOH) treatment.

The intense absorption bands in the 1210-1260 cm^{-1} region of the Fourier transform infrared (FT-IR) spectra showed the vicinity of S=O group of sulfate esters (ascribed to the glycosidic linkage) (Fig. 5.1). A particularly intense signal was recorded at 803-805 cm^{-1}, which was particular to 3, 6-anhydrogalactose-2-sulfate. The peaks were likewise identified at 925-935 cm^{-1} in the samples because of the vicinity of 3, 6-anhydro-D-galactose moieties (Villanueva et al. 2009). The S=O of the sulfate esters were obvious at 1258.92 and 1364.15 cm^{-1}, whilst the C-O-C of sugar and C-O-S sulfate ester were displayed at around 950-1100 cm^{-1}. The broad absorption band at 1240-1220 cm^{-1}, related to the ester sulfate group, is normal to every single sulfated polysaccharide. The ^{1}H-NMR spectra of polysaccharides derived from the marine macroalgae comprised of some well-resolved signals, tallying those of anomeric protons (δ_H 4.4-5.5), acetyl (δ_H 2) and methyl (δ_H 1.2) (Fig. 5.2 to Fig. 5.4). The ring protons connected to sulfate group showed up at δ_H 5.4-5.3, though the sulfated protons found at δ_H 6.1-6.8 was recorded in the ^{1}H-NMR spectra.

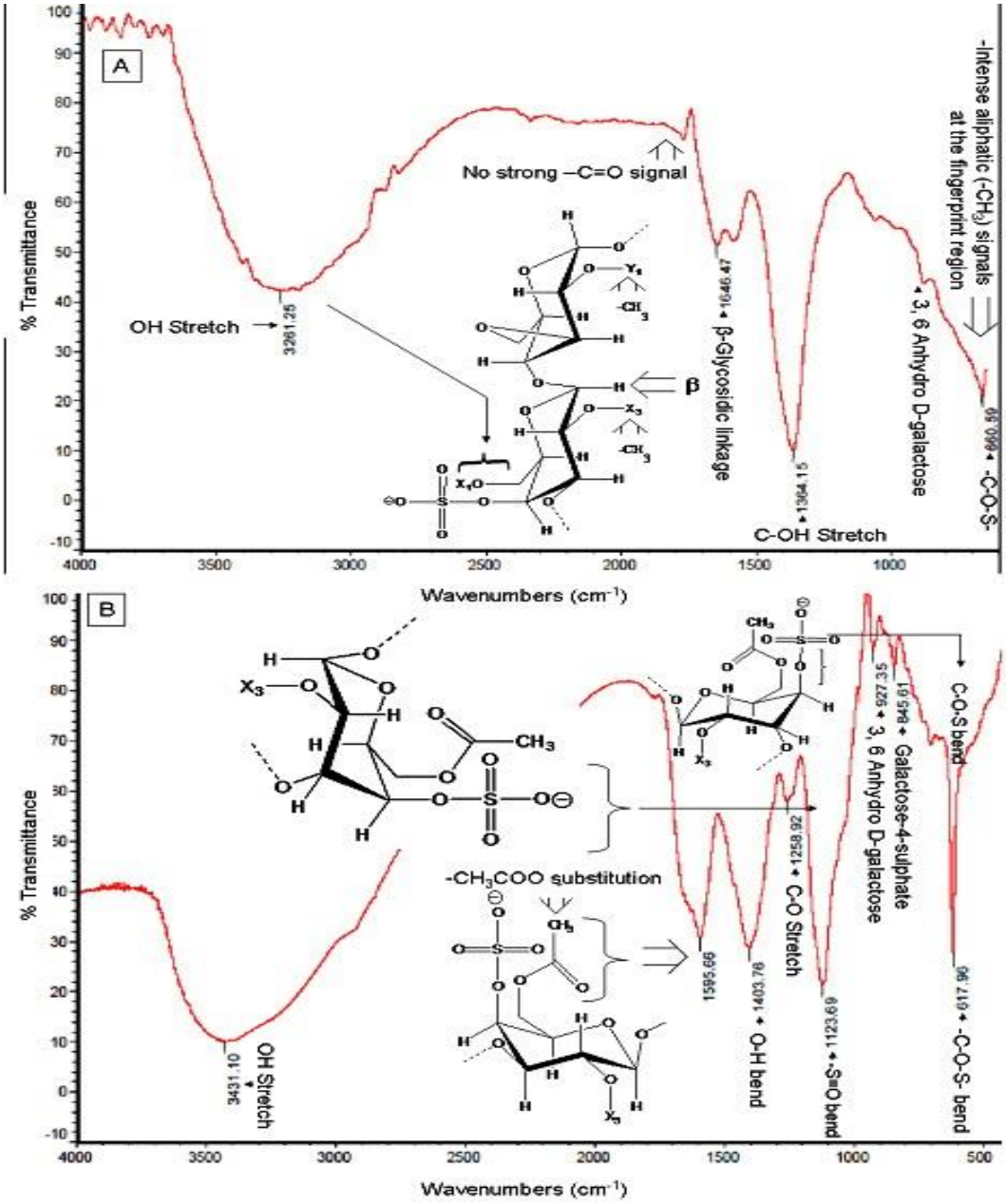

Figure 5.1. Infra red spectra of the sulfated polygalactans from (**A**) *K. alvarezii* (**KA-1**) and (**B**) *G. opuntia* (**GO-1**), the representative functional groups of the polysaccharides were indicated

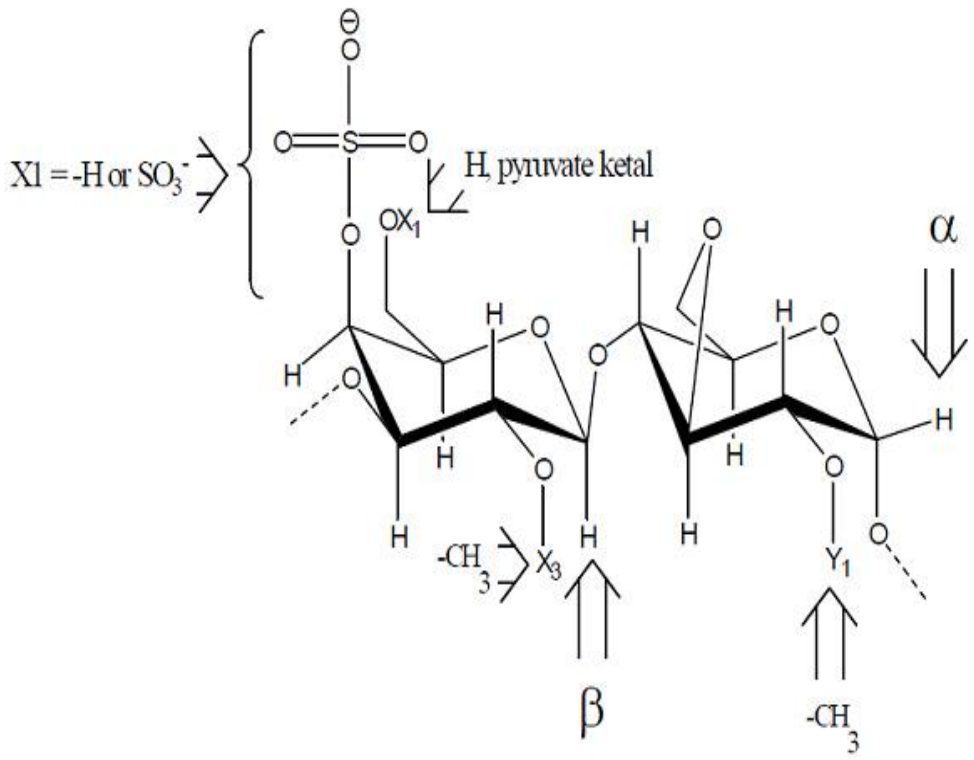

Figure 5.2. Schematic and global representation of sulfated polygalactans from *K. alvarezii* (**KA-1**)

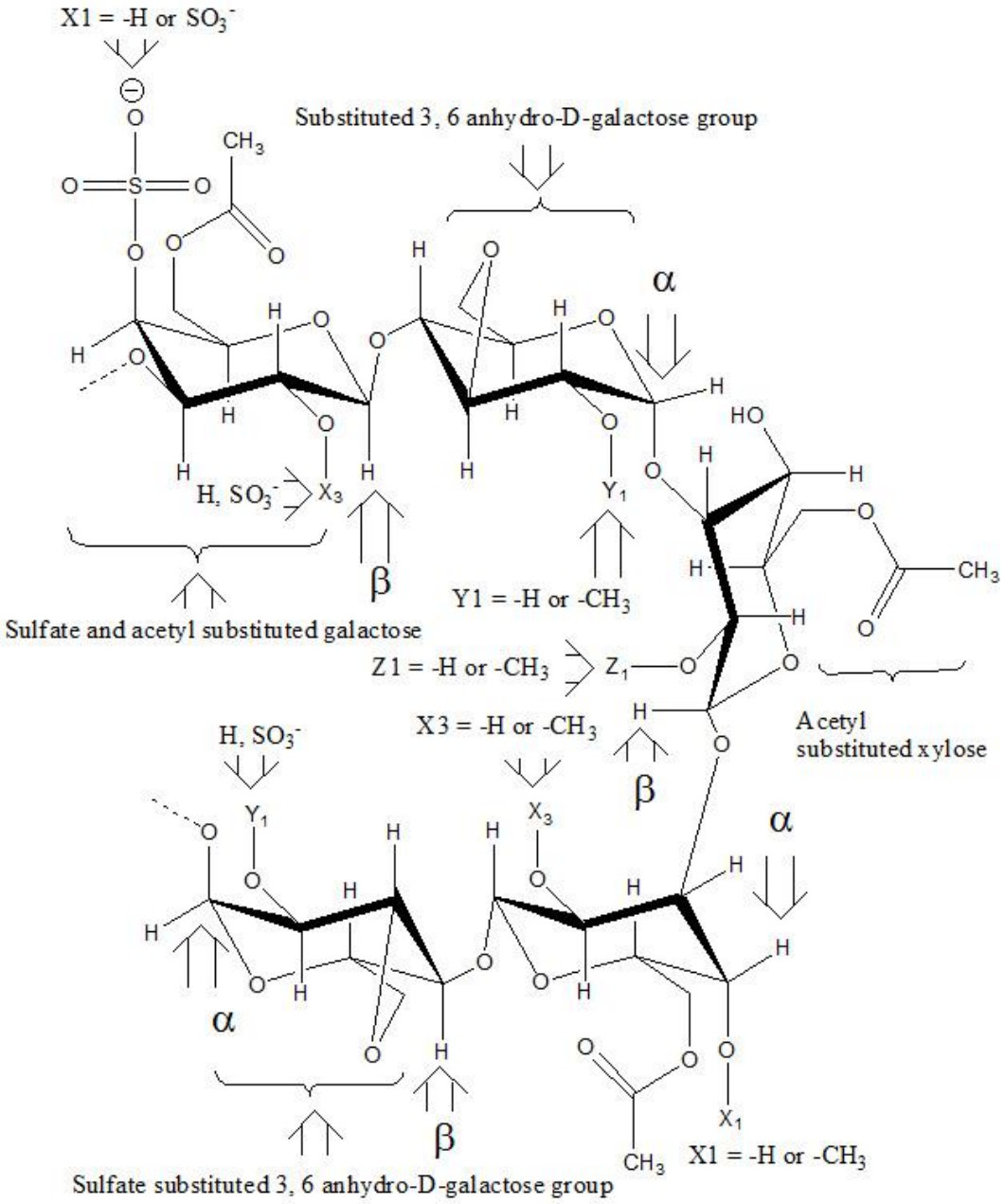

Figure 5.3. Schematic and global representation of sulfated polygalactans from *G. opuntia* (**GO-1**)

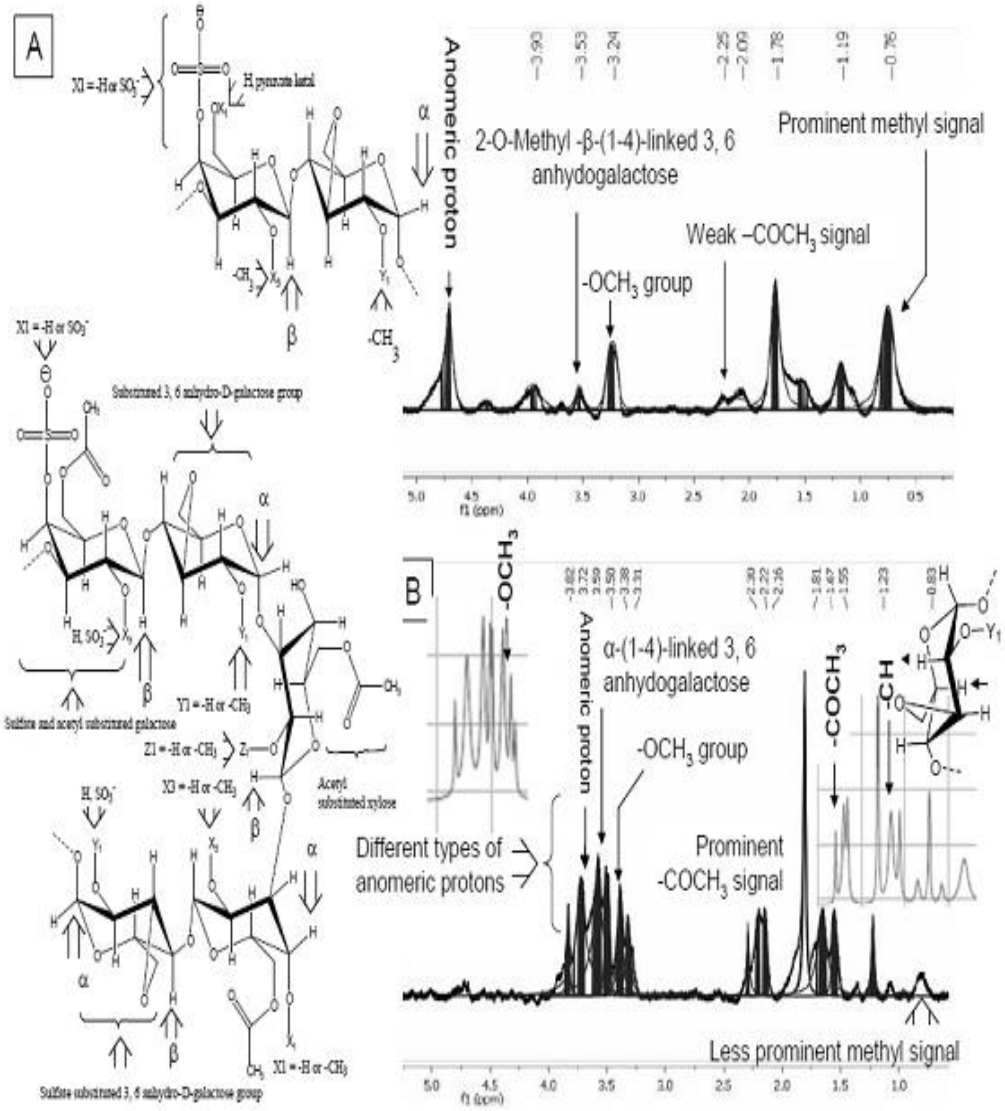

Figure 5.4. [1]H-NMR spectral representation of sulfated polygalactans motif from (**A**) *K. alvarezii* (**KA-1**) and (**B**) from *G. opuntia* (**GO-1**)

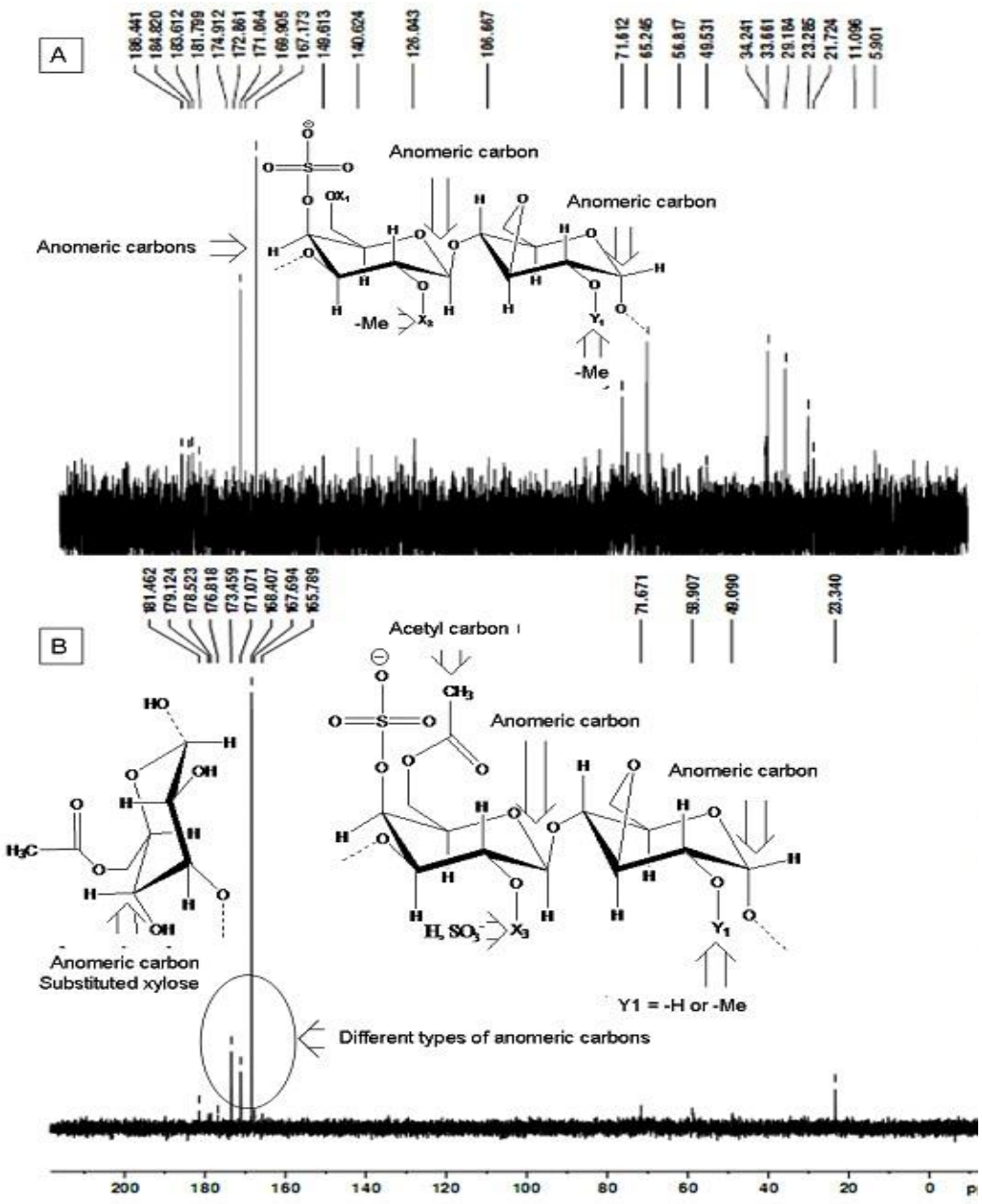

Figure 5.5. ^{13}C-NMR spectral representation of substituted galactan motifs from (**A**) *K. alvarezii* (**KA-1**) and (**B**) *G. opuntia* (**GO-1**)

The anomeric signals at δ_H 4.6 and δ_H 5.1 were characteristic of κ-sulfated polygalactan. The signal at δ_H 3.43 was assigned to the methyl proton of 6-*O*-methyl galactose. The sulfate group was situated at C-4 of (1→3)-linked galactopyranosyl residues of the native galactan, whereas the strong signals in the ^{1}H-NMR of *G. opuntia* (**GO-1**) at δ_H 2-2.5 attributed to the presence of strong -$COCH_3$ protons. Interestingly, very weak proton signals at δ_H 2-2.5 for *K. alvarezii* (**KA-1**) were assigned to be due to

the -$COCH_3$ protons. As diverged from *K. alvarezii* (**KA-1**), *G. opuntia* (**GO-1**) exhibited very sharp intense signals at δ_H 3.50 and δ_H 3.38, which ascribed to be due to the vicinity of 2-*O*-methyl α-(1-4)-linked 3, 6-anhydogalactose and 6-*O*-methyl-β-(1-3)-linked galactose residues, respectively. The anomeric carbon signals were found to be as C-1 of α-D-galactose-4-sulfate at δ_C 106.7, and this dyad was illustrative of a sulfated polygalactan. The ^{13}C-NMR chemical shifts of these characteristic signals were found at δ_C 27.6, δ_C 103.6 and δ_C 178, which showed the vicinity of methyl, acetyl and carboxyl carbon atoms, respectively (Fig. 5.5). The ^{13}C-NMR signals at δ_C 71.61, δ_C 71.67 and δ_C 65.25 were ascribed to the vicinity of C-5 and C-6 of 4-linked α-D-galactopyranoses (Fig. 5.5). The signals at δ_C 21.72 and δ_C 23.34 were because of the vicinity of methyl carbon atom of pyruvate moiety ($CH_3COCOOH$).

5.3.2. Structural Characterization of Polysaccharide Fractions (KA-2 and GO-2) from Marine Macroalgae

The precipitation of sulfated polygalactan from the crude extracts of *K. alvarezii* (**KA-2**) with ethanol brought about significantly greater recovery (75 %) than that in *G. opuntia* (55 %) (**GO-2**). The ethanol precipitated material was found to be rigid and crystalline. The elementary variables in extraction were the base used to generate the macroalgal material, and the temperature at which the reaction materialized, which affected the gelling properties and structure of sulfated galactan. The sulfated galactan was found to be a linear poly-galactose chain, where the galactose units integrate together and bear differing extent of sulfate entity (Fig. 5.6). A few of the D-galactoses involved a 6-sulfate ester group while some 3, 6-anhydro-D-galactoses consisting of a 2-sulfate ester group. In the presence of potassium ions, sulfated polygalactan gels dissolved by heating and subsequent cooling, resulting in the evolution of a three dimensional network by cationic interaction with sulfate group. The interesting aspects of mixture of sulfated polygalactan gel are its thermal reversibility, whereas it can gel and melt frequently, only defeating a little gel strength at each cycle. As potassium concentration increases, the gel stability was found to be increased until an optimum level is reached according to that potassium ions have a size and shape which comprise them fit into the mixture of sulfated polygalactan helix. This structure is sustained through the positively charged ions and the negatively charged sulfate groups in the sulfated galactan moiety.

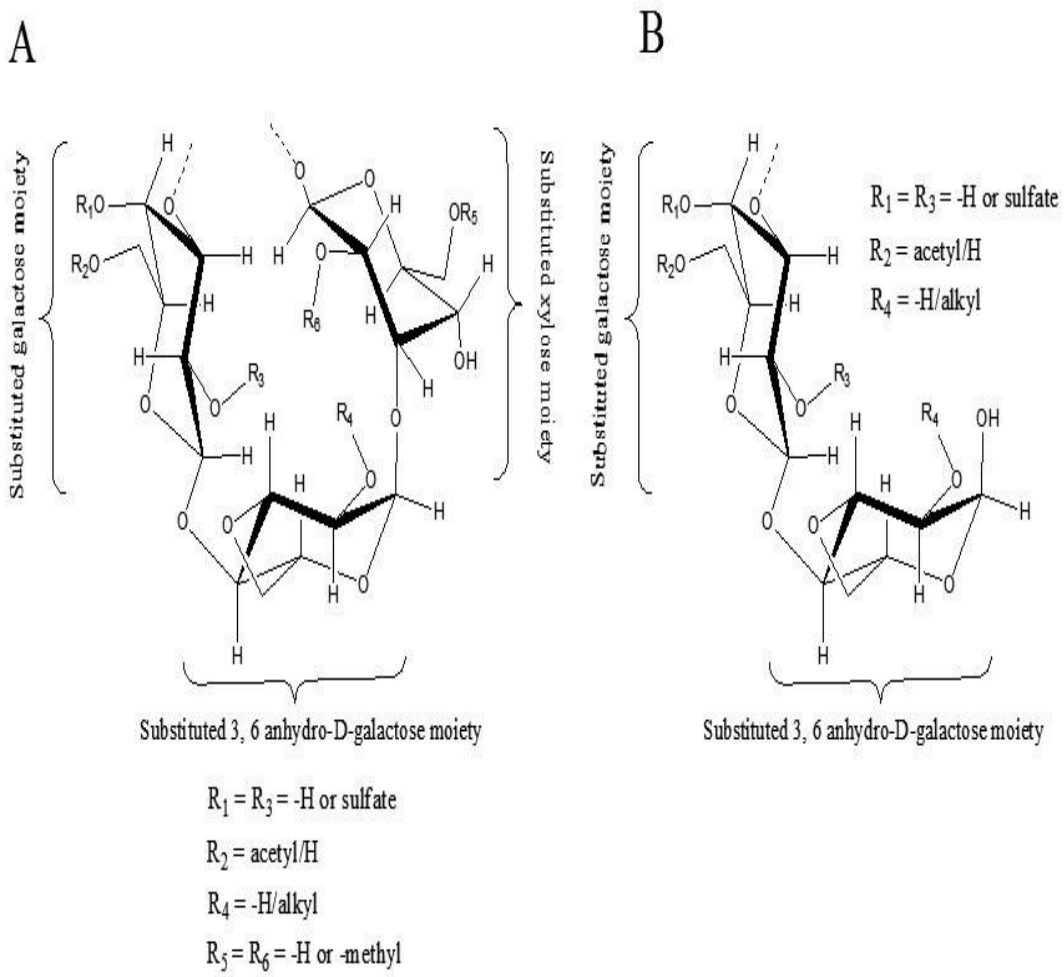

Figure 5.6. Structural representation of galactopyranan motifs of the sulfated polygalactans from (**A**) G. *opuntia* (**GO-2**) and (**B**) *K. alvarezii* (**KA-2**)

.

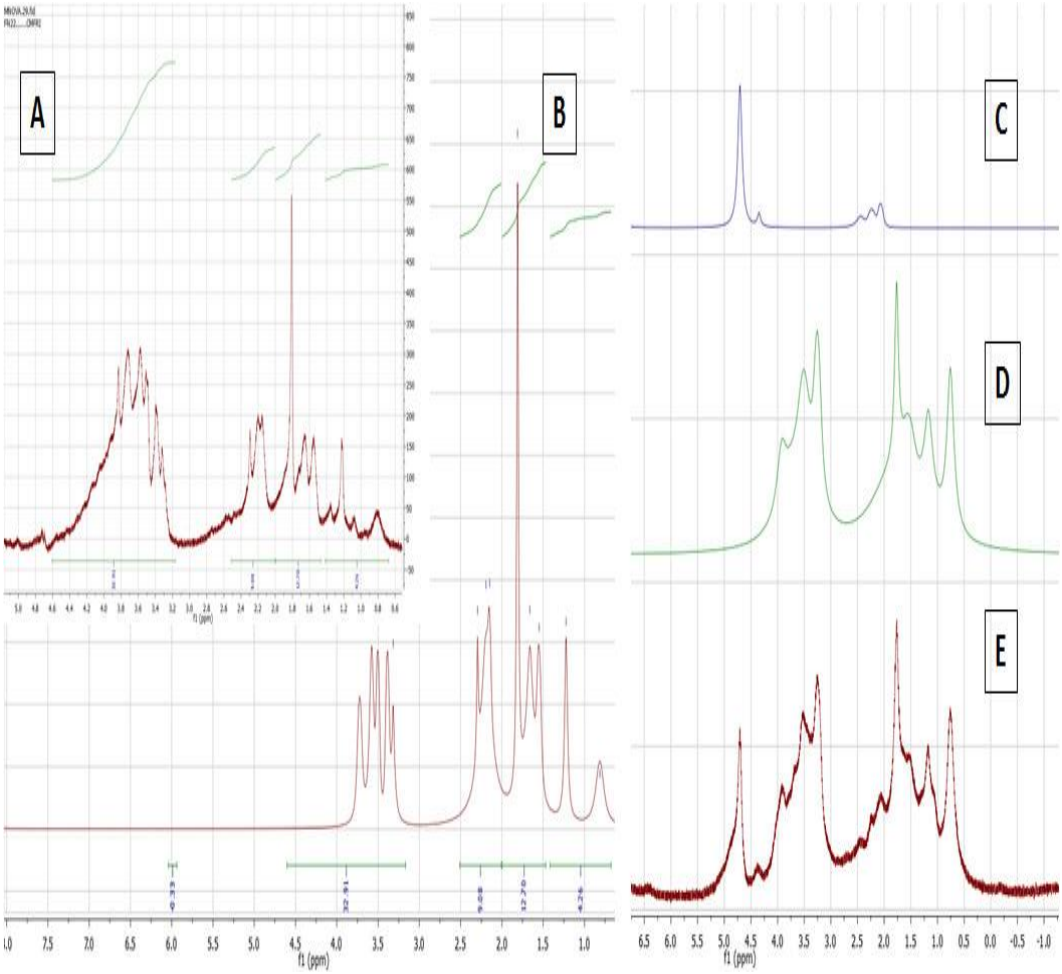

Figure 5.7. ^{1}H-NMR spectral representation of sulfated polygalactan from *G. opuntia* (**A-B**) (**GO-2**) and *K. alvarezii* (**C**-**E**) (**KA-2**)

The sulfated polygalactan has 34 % 3, 6 anhydro-D-galactose groups as segment of its repeating structure and 25 % ester sulfate groups, which promptly dispersed when heated. Thermo reversible gels engendered by polygalactan by the arrangement of the disjointed chains into double or triple helices. Hydrogen bonding, persuaded by aggregation of the ordered domains to form a firm, three dimensional stable gels. The gel strength of polysaccharides derived from the marine macroalgae *K. alvarezii* (**KA-2**) and *G. opuntia* (**GO-2**) was found to be greater, when heated in an alkaline solution of potassium hydroxide for about two hours. The hydroxide part of the reagent penetrates the macroalgae, diminished the amount of sulfate in the sulfated galactan and increasing the 3, 6-anhydro galactose unit, thereby developing the gel strength of the sulfated galactan. The contemporary inspection showed that greater yield of sulfated galactan could be achieved with KOH treatment. The conspicuous

attributes of the FT-IR spectra of sulfated polygalactan from the red marine macroalgae were because of the sulfate ester and carbohydrate groups in the infrared spectra. The strong absorption bands at 1210-1260 cm^{-1} of the FT-IR spectra demonstrated the region of S=O groups (attributed to the glycosidic linkage). The band at ~800 cm^{-1} was specific to 3, 6- anhydrogalactose-2-sulfate (Ganesan et al. 2008; Villanueva et al. 2009). The IR signals close to 3200-3400 cm^{-1} were credited to the region of -OH gatherings present in the sulfated polygalactans from the macroalgae. The S=O of the sulfate esters were showing up at 1250-1300 cm^{-1}, while the C-O-C of sugar and C-O-S sulfate ester were displayed at around 950-1100 cm^{-1}. The broad bands at 3200-3400 cm^{-1} were found to be a result of the sulfated polygalactan units. The C-H stretching vibrations were assigned to be present at around 2800-2900 cm^{-1}.

The absorbance peaks around 1050-1100 cm^{-1} displayed the pyranose ring structure. Intense absorbance at around 1700 cm^{-1} and bands of about 1420 cm^{-1} (C=O symmetric stretching vibrations), were due to carbonyl (acetyl) groups in the polysaccharide back bone chain. Three characteristic bands in the fingerprint anomeric region (950-700 cm^{-1}), connected to the ester sulfate bonds were attributed to a special feature of the sulfated polygalactan type of polysaccharides (Gomez-ordonez and Rupere 2011). The absorption bands at ~1400 cm^{-1} in FT-IR spectra deduced the normality of β-glycosidic linkages. Moreover, the IR absorption bands unique to the presence of anomeric locale (800-900 cm^{-1}), joined with the ester sulfate bonds are the special feature of the sulfated polygalactan type of polysaccharides (Kumar et al. 2008; Gomez-ordonez and Rupere 2011). NMR spectroscopy has been carried out for the structural prediction of any regular and complex polysaccharides. Intense signals acquired from the ^{1}H-NMR spectroscopy exhibited the region of hydrogen atoms at anomeric carbon (δ_H 5.4) (Fig. 5.7). The ^{1}H-NMR spectra of polysaccharides comprise of some well-resolved signals, counting those of anomeric protons (δ_H 4.4 - 5.5) (Fig. 5.7). By virtue of polysaccharides, the resonances due to the anomeric protons were grouped between δ_H 3-4. These results were in accordance to those reported in the literature (Cases et al. 1995). The Figure 5.7 exhibited the ^{1}H-NMR range of blend of sulfated polygalactans (κ-, ι-) separated from *K. alvarezii* (**KA-2**) and *G. opuntia* (**GO-2**). The peaks at δ_H 5 signified the vicinity of iota and κappa monomers of sulfated polygalactans (Nagarani and Kumaraguru 2013; Vandevelde et al. 2002). The ring protons associated with sulfate functionalities demonstrated ^{1}H-NMR signals at δ_H 5. The ^{1}H-NMR showed proton signal at δ_H 5.34, which was relegated to be a direct result

of the anomeric proton of the 3, 6- anhydrogalactose-2-sulfate (Cases et al. 1995). The anomeric proton signals at δ_H 4.5 and δ_H 5.0 were normal for κ-sulfated polygalactan. The ^{1}H-NMR signals in the scope of δ_H 3.6–4.9 were portrayed to whatever is left of the methylene and methine hydrogens of the sulfated polygalactan moiety. The ^{1}H-NMR spectrum of polysaccharides obtained from *K. alvarezii* (**KA-2**) got very much comprehended deshielded signals at δ_H 4.5-5, which demonstrated the region of κ and ι monomer of sulfated polygalactans. There absence of peaks at δ_H 5.26 indicated the absence of μ-monomers (precursor of κ-sulfated polygalactan) (Vandevelde et al. 2002). *Gracilaria opuntia* (**GO-2**) contains anomeric protons in the region between δ_H 3-4, which demonstrated that the sulfated polygalactan isolated from *G. opuntia* (**GO-2**) contains oligomeric building subunits, such as xylose and anhydro galactose besides κ and ι-type of monomeric units. Weak proton signals at δ_H 2-2.5 for *K. alvarezii* (**KA-2**) were relegated because of the acetyl protons. These outcomes have been supported by earlier studies (Chiovitti et al. 1998). Recognizable –*O*-alkyl signals (ideally -OCH_3) in the ^{1}H-NMR spectrum of galactan derivative from *G. opuntia* (**GO-2**) and *K. alvarezii* (**KA-2**) at δ_H 3.4 obviously revealed the region of more conspicuous number of alkoxy substitutions in the sulfated polygactans from the red macroalgae. The ^{13}C NMR spectrum of polygalactans sowed signals with specific multiplicities, which suggested the positional differences of 1→3 and 1→4 linked residues in the sulfation patterns. The anomeric region of ^{13}C-NMR exhibited the characteristic signals, and were relegated taking into account the data reported in the literature (Cases et al. 1995). Despite the normal sulfated polygalactan rehashing units, the samples were found to contain some minor constituents that were as often as possible experienced in carragenophytes. A small amount of 3-linked 6-*O*-methyl-D-galactose residues was found in the κ-sulfated polygalactan from *K. alvarezii* (**KA-2**) as additionally supported by past studies (Bellion et al. 1983). Pyruvic acid is a typical segment of numerous complex sulfated polygalactans. It outlines a cyclic acetal at positions C-4 and C-6 of the 3-linked galactose residues. The pyruvic acid ketals might likewise be experienced in the ^{1}H-NMR spectra of the polysaccharides in the present study as evident by the methyl proton resonances at δ_H 1.45. These outcomes have been supported by earlier studies (Chiovitti et al. 1998) .The anomeric region of ^{13}C-NMR exhibited the characteristic signals, and were assigned based on the literature data (Vandevelde et al. 2002). The ^{13}C-NMR signals at δ_C 58.91 and δ_C 65.25 were suggested as the –CH_2-groups on the C-6 of the 3-linked galactopyranosyl-4-sulfate moiety. In addition the

frail proton signals at δ_C 29.18 and δ_C 23.34 and carbon signals at δ_C 174-178 were related to the methyl and carboxyl carbons of the pyruvated galactopyranosyl residues. The ^{13}C-NMR chemical shift values in the present study were in accordance with the chemicals shifts reported for the basic sulfated polygalactan structure (Vandevelde et al. 2002). Based on the detailed NMR experiments the sulfated galactopyran motif of *G. opuntia* (**GO-2**) was designated as →3)-4-*O*-sulfonato-(6-*O*-acetyl)-β-D-galactopyranosyl-(1→4)-3, 6-anhydro-(2-*O*-sulfonato)-α-D-galactopyranosyl-(1→3)-4-*O*-sulfonato-(6-*O*-acetyl)-β-D-xylosyl-(1→3)-4-*O*-sulfonato-(6-*O*-acetyl)-β-D-galactopyranosyl-(1→4)-3, 6-anhydro-(2-*O*-sulfonato)-α-D- galactopyranan, whilst the one from *K. alvarezii* was demonstrated to be →4)-4-*O*-sulfonato-(2-*O*-methyl)-β-Dgalactopyranosyl-(1→4)-3, 6-anhydro-(2-*O*-methyl)-α-D-galactopyranan (Fig. 5.6).

5.3.3. Structural Characterization of Polysaccharide Fractions (KA-3$_A$ and GO-3$_A$) from Marine Macroalgae

NMR spectroscopy was used for the structural interpretation of polysaccharides (Bilan et al. 2004), whereas the pharmacological potential of this macropolymeric molecules were related with their structural parameters, such as series disposal of sugar units, branching arrangement, and orientation of functional groups (Rinaudo 2001). The HPLC profile of monosaccharide composition of polysaccharides revealed that they were mainly composed of galactose residues derived from the red marine macroalgae *K. alvarezii* (**KA-3**) and *G. opuntia* (**GO-3**) (Fig. 5.24).

5.3.3.1. Spectral Analysis of 1, 3-*O*-diacetyl-2, 5, 6-trihydroxyl-β-D-galactose-4-sulfate (KA-3$_A$)

White amorphous powder; HPLC R_t (H_2O: MeOH, 2:3 v/v): 7.21 min; TLC (15 mm Si gel GF_{254} *n*-hexane: EtOAc, 7:3 v/v); R_f: 0.82; UV (EtOAc) λ_{max} (log ε): 387 nm (1.722); IR (KBr, ν_{max} ν = stretching, δ= bending, ρ= rocking vibrations expressed in cm^{-1}): 720.35 (C-H ρ), 797.06 (C-H δ), 1023.26 (CH_3 ν), 1256.45 (C-CO-C ν, S=O ν), 1370.83 (CH_3 ν, S=O ν), 1458.44 (C-H δ), 1712.40 (-O-C=OCH_3 ν), 2855.51 (C-H ν), 2922.32 (C-H ν), 3339.03 (-OH ν); ^{1}H (500 MHz), ^{13}C-NMR (125 MHz) and 2D

NMR data (Table 5.1, Fig. 5.8 to 5.15); HR (EI) MS *m/z* calcd for $C_{10}H_{17}O_{11}S$ 345.0492; measured 345.0496 $[M]^+$ (Fig. 5.25).

1, 3-*O*-Diacetyl-2, 5, 6-trihydroxyl-β-D-galactose-4-sulfate was obtained as a white amorphous powder by methylation reaction of the polysaccharide fraction derived from *K. alvarezii* (**KA-3A**). The spectrum displayed characteristic resonance of signals from ring protons between δ_H 4.01 {H-1/C-1 (δ_C 65.33)} and δ_H 5.08 {H-5/C-5 (δ_C 72.40)}. The ^1H–^1H COSY correlation between δ_H 4.24 (H-4)/δ_H 5.07 (H-3); δ_H 4.01 (H-6)/δ_H 5.08 (H-5) and strong HMBCs between δ_H 4.24 (H-4)/δ_C 59.90 (C-2)/δ_C 66.03 (H-3)/δ_C 72.40 (C-5) supported the backbone framework of the ring system. The proton NMR accompanied with carbon NMR documented the existence of anomeric carbon appeared at δ_C 65.33 (C-1). The very high intensity two sharp singlet protons in the NMR spectrum {δ_H 2.20 (H-1"^{1}) and δ_H 2.13 (H-3"^{1})} were attributed to the acetyl group substitution in the 1, 3-*O*-diacetyl-2, 5, 6-tri hydroxyl-β-D-galactose-4-sulfate (**KA-3A**) residues. The strong HMBC correlations between δ_H 5.07 (H-1)/δ_C 167.7 (C-3"); δ_H 2.13 (H-3"^{1})/δ_C 167.7 (C-3"); δ_H 4.01 (H-1)/δ_C 167.02 (C-1"); δ_H 2.20 (H-1"^{1})/δ_C 167.02 (C-1") supported the above assignments.

It was inferred that the 3, 6-anhydro-galactose moiety were degraded during this particular reaction, and that supported the absence of IR signals at 845, 830 and 805 cm^{-1} (Mollet et al. 1998; Murano 1995; Murano et al. 1996). The characteristic absorption bands at 3339, 2922, 2855, 1712, 1458, 1370, 1256, 1177, 1023, 910, 797, 720 cm^{-1} in the FTIR spectrum of *K. alvarezii* (**KA-3A**) recorded the existence of galactose residue. The absorption band of S=O vibration appeared at 1370 cm^{-1} in the FTIR spectrum indicated the presence of sulfate groups (Melo et al. 2002; Fournet et al. 1997). The presence of –OH group in the IR spectroscopy (3339 cm^{-1}) considered that all the OH groups did not undergo the methylation, reduction and acetylation reactions. The ^{13}C resonances at δ_C 167.02, 167.7, 38.05 and 45.15 appropriately indicated the presence of acetyl carbons associated with carboxyl group of the galactose unit. Strong bending vibrations of the carbonyl group associated with acetyl group were found near 1712 cm^{-1}, which was further corroborated by the presence of ^{13}C NMR peak at δ_C 167.02 (C-1") and 167.7 (C-3"). The primary -CH_2- protons were assigned at δ_H 4.01 (H-6, d, *J*=6.65 Hz, 2H) showing HSQC correlation with δ_C 71.8 (C-6). Characteristic OSO_3^- group in the moiety of 1, 3-*O*-diacetyl-2, 5, 6-trihydroxyl-β-D-galactose-4-sulfate **(KA-3A)** were found to be situated at C-4 of the ring system, and these assignments was supported by the signals at δ_H 4.24 (H-4) showing HSQC cross-peak

with δ_C 65.56 (C-4). The 1, 3-*O*-diacetyl-2, 5, 6-trihydroxyl-β-D-galactose-4-sulfate were mainly unsubstituted with methoxy because the presence of -OH group were present in the primary alcoholic position (δ_H 3.70; H-6"). In addition, the unsubstituted -OH groups were recorded at δ_H 3.70 (H-6") and δ_H 3.88 (H-2"). The mass spectrum showed the peak at *m/z* 345 (molecular ion peak) (HR EI MS *m/z* calcd. for $C_{10}H_{17}O_{11}S^-$ 345.0492, measured at 345.0496 $[M]^+$). The presence of the strong NOEs between δ_H 5.08 (H-5) with δ_H 4.01 (H-1 *J*=6.65 Hz; H-6 *J*=6.65 Hz)/δ_H 2.20 (H-1"^{1}) showed axial-equatorial orientation of these proton pairs in the chair conformation of 1, 3-*O*-diacetyl-2, 5, 6-trihydroxyl-β-D-galactose-4-sulfate residue. Similarly, strong NOEs were observed between δ_H 5.08 (H-5) with δ_H 4.24 (H-4, *J*=6.31 Hz) that indicated the axial-axial orientation of these protons in the same polymeric backbone. In addition, the axial proton at δ_H 4.01 (H-1, H-6) displayed NOE correlation with the equatorial proton at δ_H 2.13 (H-3"^{1}) having axial-equatorial interaction between these protons.

5.3.3.2. Spectral Analysis of 1, 3, 5-*O*-triacetyl-4-hydroxyl-6-*O*-methyl-D-galactose-2-sulfate (GO- 3$_A$)

White amorphous powder; HPLC R_t (H_2O: MeOH, 2:3 v/v): 6.76 min; TLC (15 mm Si gel GF_{254} *n*-hexane: EtOAc, 7:3 v/v); R_f: 0.76; UV (EtOAc) λ_{max} (log ε): 387 nm (1.608); IR (KBr, ν_{max} in cm^{-1}): 1045.98 (CH_3 ν), 1201.04 (C-CO-C ν), 1416.30 (C-H *δ*), 1689.30 (-O-C=OCH_3 ν), 34445.36 (-OH ν); ^{1}H (500 MHz), ^{13}C-NMR (125 MHz) and 2D NMR data (Table 5.2; Fig. 5.16 to 5.25); HR (EI) MS *m/z* calcd for $C_{13}H_{21}O_{12}S$ 401.0754; measured 401.0758 $[M]^+$ (Fig. 5.25).

1, 3, 5-*O*-Triacetyl-4-hydroxyl-6-*O*-methyl-D-galactose-2-sulfate **(GO-3$_A$)** was isolated as white powder by repeated chromatography over adsorbent silica gel. The spectrum displayed characteristic resonance of signals from ring protons between δ_H 3.65 {(H-5/C-5 (δ_C 69.89)} and δ_H 3.81{H-1/C-1 (δ_C 81.83)}. The ^{1}H–^{1}H COSY correlation between δ_H 3.81 (H-1)/δ_H 3.73 (H-4)/δ_H 3.38 (H-3)/δ_H 3.65 (H-2) and intense HMBCs between δ_H 3.38 (H-3)/δ_C 81.83 (C-1); δ_H 3.65 (H-5)/δ_C 83.51 (C-6); δ_H 3.81 (H-1)/δ_C 62.28 (C-3)/δ_C 69.88 (C-2); δ_H 3.73 (H-4)/δ_C 62.28 (C-3) were recorded. The high intensity sharp singlet protons in the NMR spectrum at δ_H 2.17 (H-1"^{1}), δ_H 2.62 (H-3"^{1}), and δ_H 2.02 (H-5"^{1}) attributed to the acetyl group substitution in

the 1, 3, 5-*O*-triacetyl-4-hydroxyl-6-*O*-methyl-D-galactose-2-sulfate (**GO-3$_A$**) residues. The strong HMBC correlation between δ_H 3.81 (H-1)/δ_C 179.66 (C-1"); δ_H 3.65 (H-5)/δ_C 172.51 (C-5"); δ_H 2.02 (H-5"^{1})/δ_C 172.51 (C-5") supported the above assignments. NMR analysis of methylated polysaccharide from *G. opuntia* attributed the presence of acetylated and 1, 3, 5-*O*-triacetyl-4-hydroxyl-3-*O*-methyl-D-galactose-2-sulfate (**GO-3$_A$**) units. The IR spectrum inferred the presence of residual -OH group (3445 cm^{-1}) that indicated that all the hydroxyl groups did not undergo methylation reactions. The strong bending vibrations of carbonyl group associated with acetyl group were found near 1689 cm^{-1}, which further corroborated by the peak at δ_C 172.51 (C-5"), δ_C 176.07 (C-3") and δ_C 179.66 (C-1"). The primary-CH_2- protons were assigned at δ_H 3.81 {H-6 displaying HSQC with C-6 (δ_C 83.51)}. Characteristic OSO_3^- group in the moiety were present at the 2nd position of the ring system, and these attributions were inferred by the presence of δ_H 3.65 (H-2; δ_C 69.88 (C-2)) in the HSQC spectrum. The mass spectrum showed the molecular ion peak peak at *m/z* 401 (HR EI MS *m/z* calcd. for $C_{13}H_{21}O_{12}S$ 401.0754, measured at 401.0758 $[M]^+$). The strong NOE correlations between δ_H 2.17 (H-1"^{1}) with δ_H 3.38 (H-3 *J*=6.50 Hz) and δ_H 3.65 (H-5, H-2) showed axial-axial and axial-equatorial orientation of these proton pairs, respectively in the chair structure of 1, 3, 5-*O*-triacetyl-4-hydroxyl-3-*O*-methyl-D-galactose-2-sulfate (**GO-3$_A$**) residue. Similarly, intense NOEs between δ_H 2.62 (H-3"^{1}) with δ_H 3.67 (H-5, H-2) and δ_H 3.49 (H-6") indicated the axial–axial orientation between the protons. In addition, the axial proton at δ_H 3.65 (H-2, H-5) displayed NOE correlation with the equatorial proton at δ_H 2.85 (H-4") having axial-equatorial interaction between the protons. The presence of the strong NOEs correlation between δ_H 3.65 (H-5, H-2), δ_H 3.73 (H-4, *J*=8.52 Hz), and δ_H 3.38 (H-3 *J*=6.50 Hz) inferred their axial-axial orientation. The present study characterized the major polysaccharide fractions obtained from the red marine macroalgae *K. alvarezii* and *G. opuntia* as 1, 3-*O*-diacetyl-2, 5, 6-trihydroxyl-β-D-galactose-4-sulfate (**KA-3$_A$**) and 1, 3, 5-*O*-triacetyl-4-hydroxyl-6-*O*-methyl-D-galactose-2-sulfate (**GO-3$_A$**), respectively.

Table 5.1. NMR spectroscopic data of **KA-3$_A$** in $CDCl_3$[a]

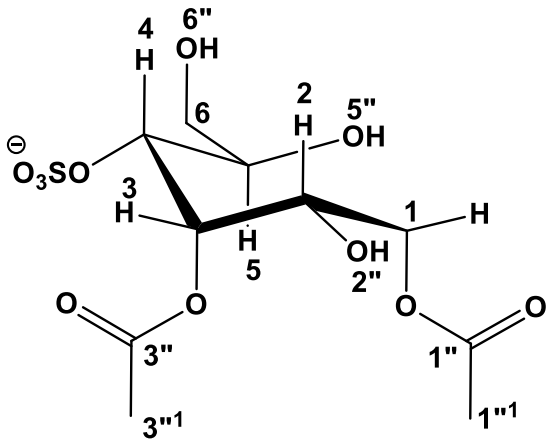

C. No	^{13}C (δ)	^{1}H-NMR[b] (int., mult., *J* in Hz)	^{1}H-^{1}H COSY	HMBC
1	65.33	4.01 (d, *J*=6.65 Hz, 2H)		C-1"
2	59.90	4.26 (m, 1H)		-
3	66.03	5.07 (t, *J*=6.89 Hz, 1H)	4-H	C-3"
4	65.56	4.24 (t, *J*=6.31 Hz, 1H)	3-H	C-5, C-3, C-2
5	72.40	5.08 (m, 1H)	6-H	-
6	71.8	4.01 (d, *J*=6.65 Hz, 2H)	5-H	-
1"	167.02	-	-	-
1"^{1}	38.05	2.20 (s, 3H)	-	C-1"
2"	-	3.88 (s, 1H)	-	
3"	167.7	-	-	-
3"^{1}	45.15	2.13 (s, 3H)	-	C-3"
5"	-	3.70 (s, 1H)		
6"	-	3.70 (s, 1H)	-	-

[a] NMR spectra recorded using Bruker AVANCE III 500 MHz (AV 500) spectrometers.

[b] Values in ppm, multiplicity and coupling constants (*J*=Hz) are indicated in parentheses. Assignments were made with the aid of the ^{1}H-^{1}H COSY, HSQC, HMBC and NOESY experiments.

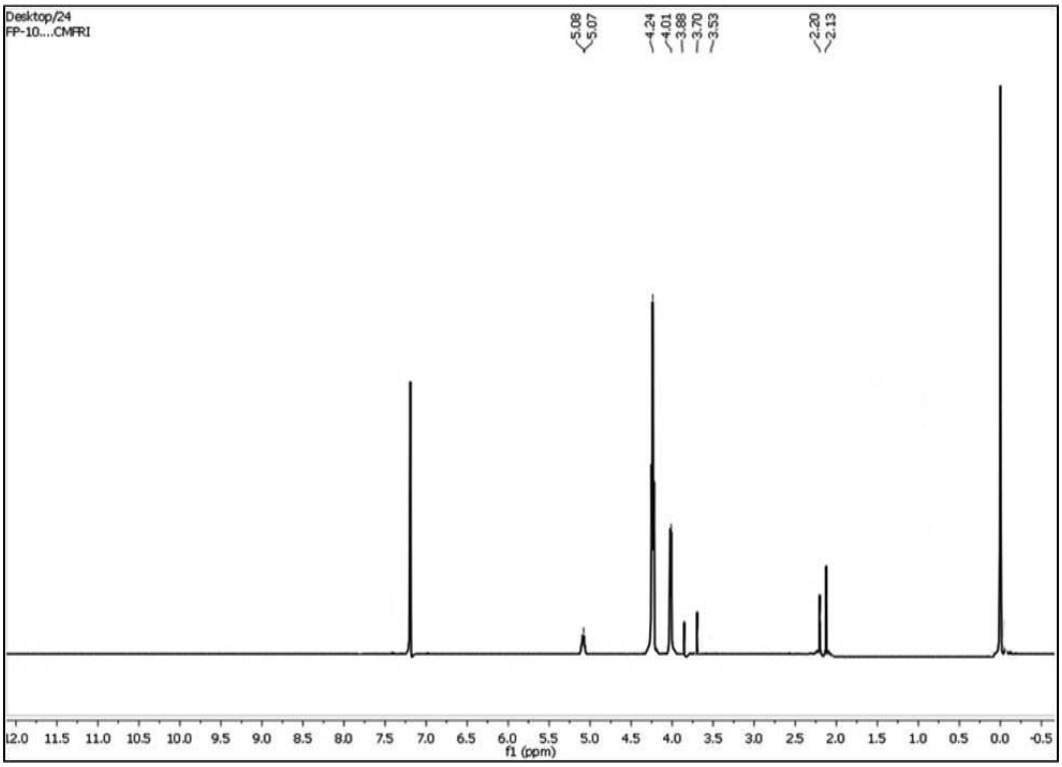

Figure 5.8. Figure showing the ^{1}H NMR spectrum of **KA-3$_A$**

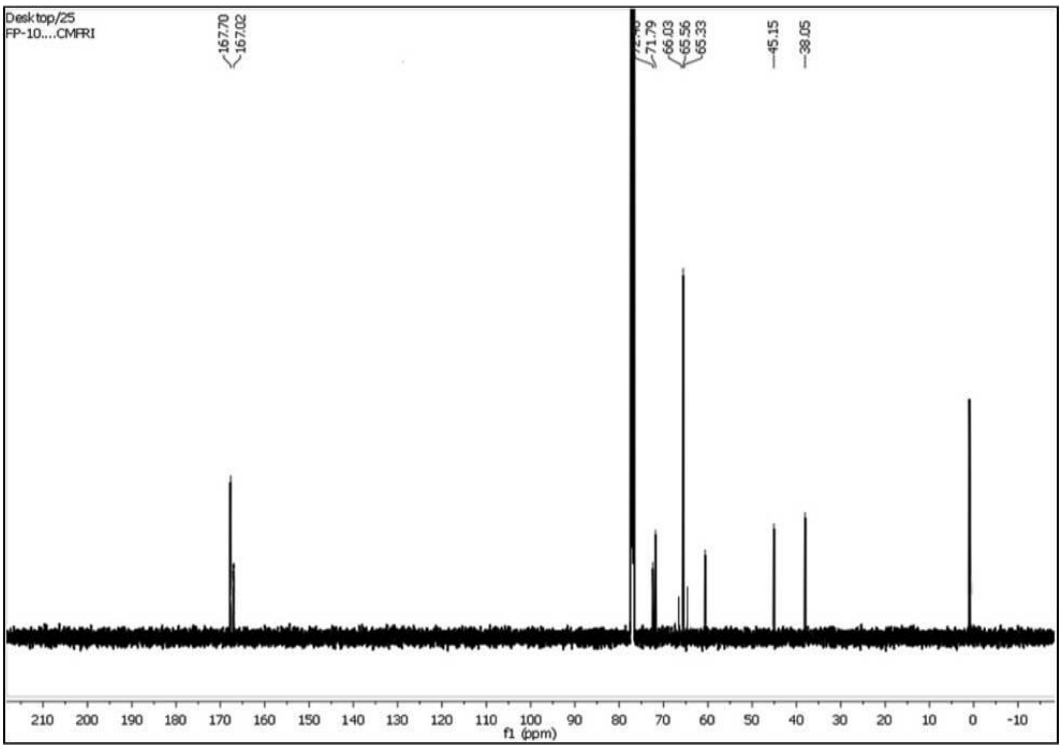

Figure 5.9. Figure showing the ^{13}C NMR spectrum of **KA-3$_A$**

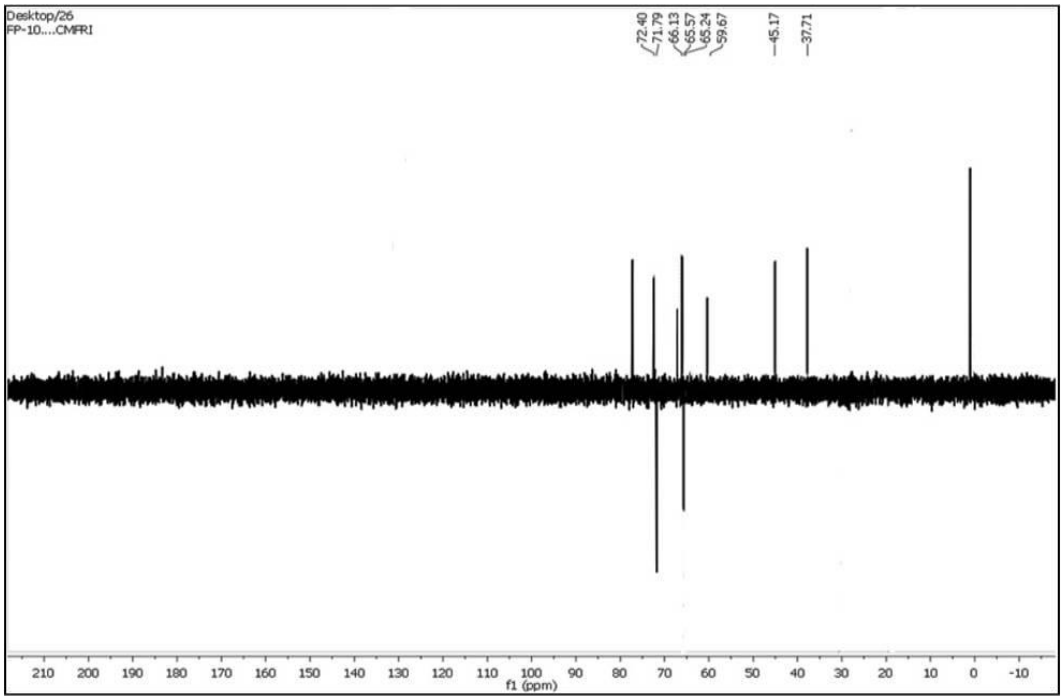

Figure 5.10. Figure showing the DEPT spectrum of **KA-3$_A$**

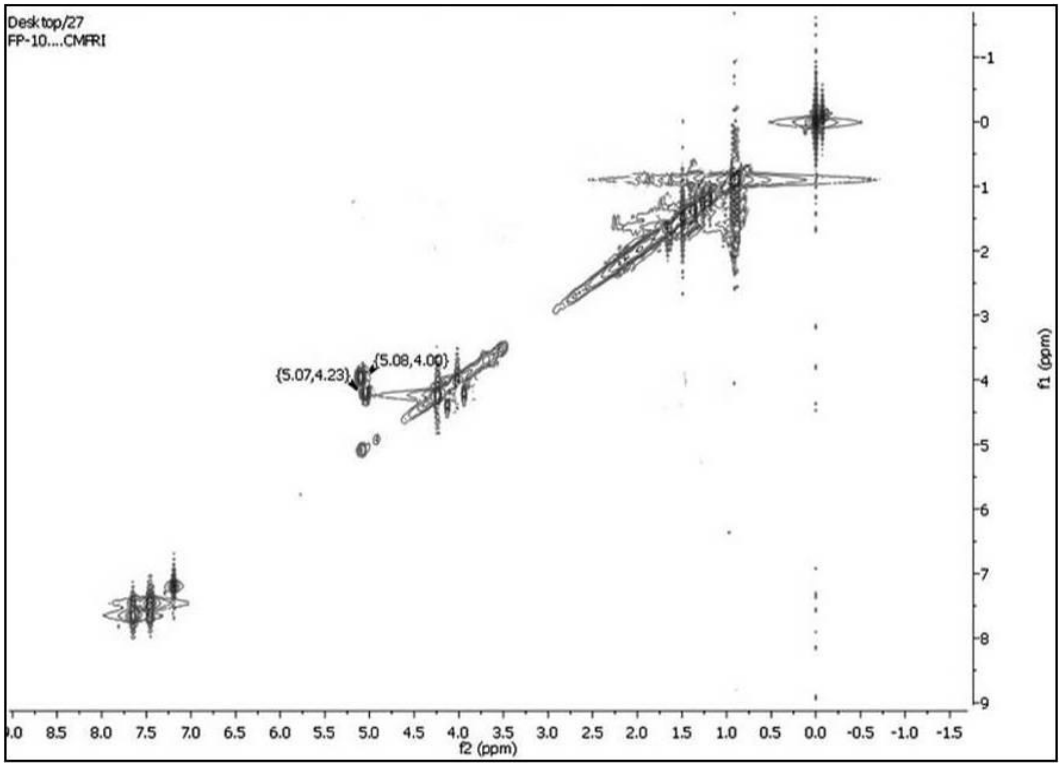

Figure 5.11. Figure showing the ^{1}H-^{1}H COSY spectrum of **KA-3$_A$**

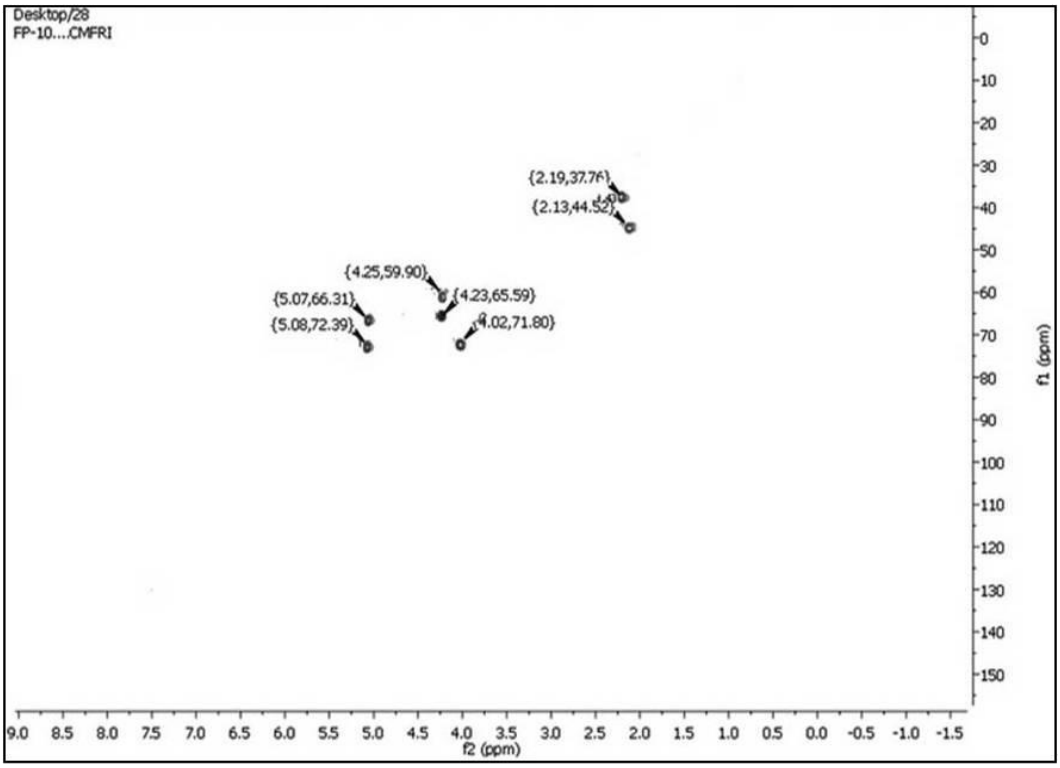

Figure 5.12. Figure showing the HSQC spectrum of **KA-3A**

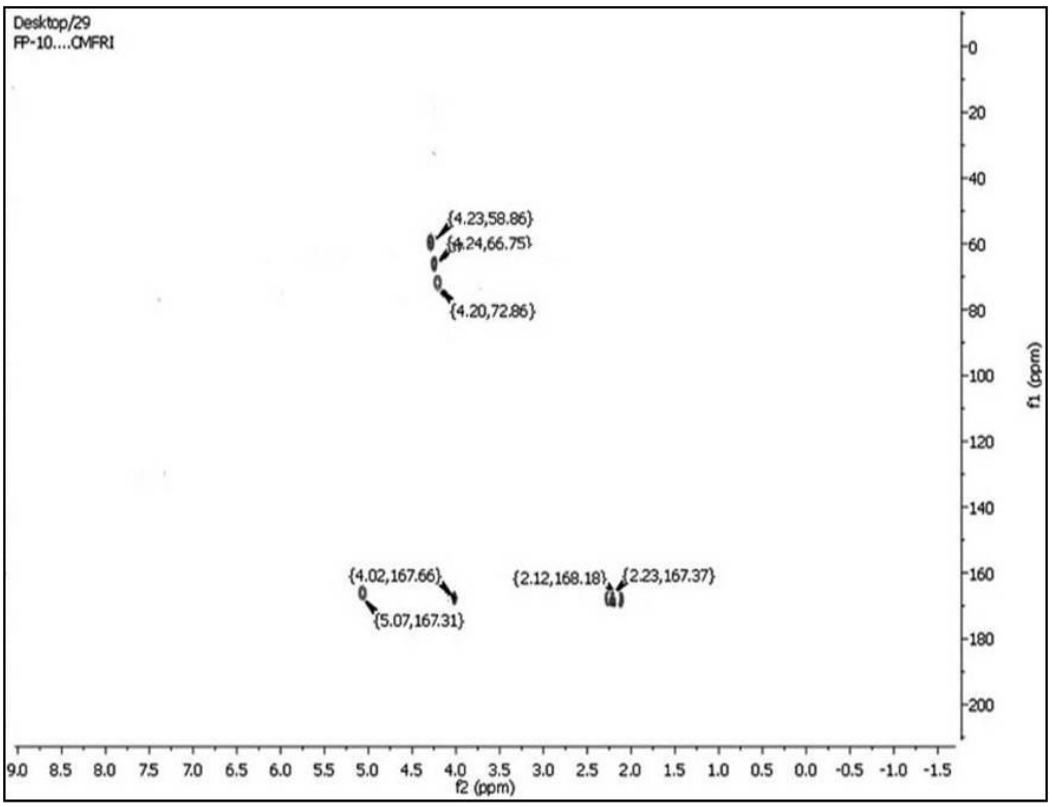

Figure 5.13. Figure showing the HMBC spectrum of **KA-3A**

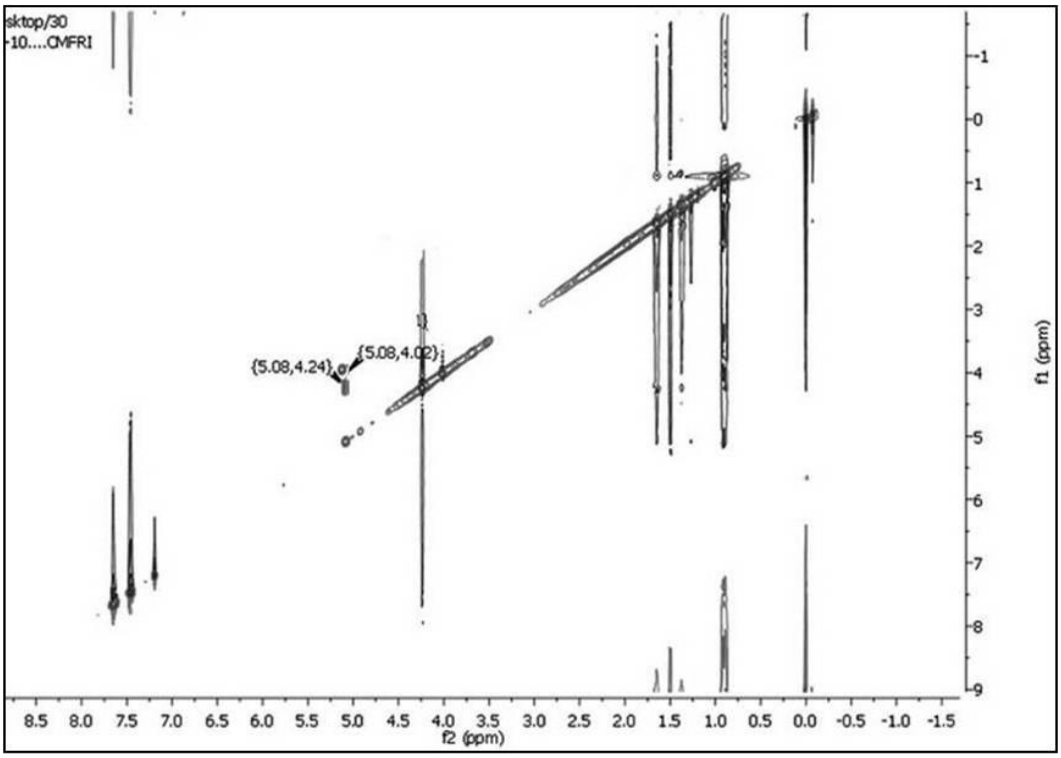

Figure 5.14. Figure showing the NOESY spectrum of **KA-3A**

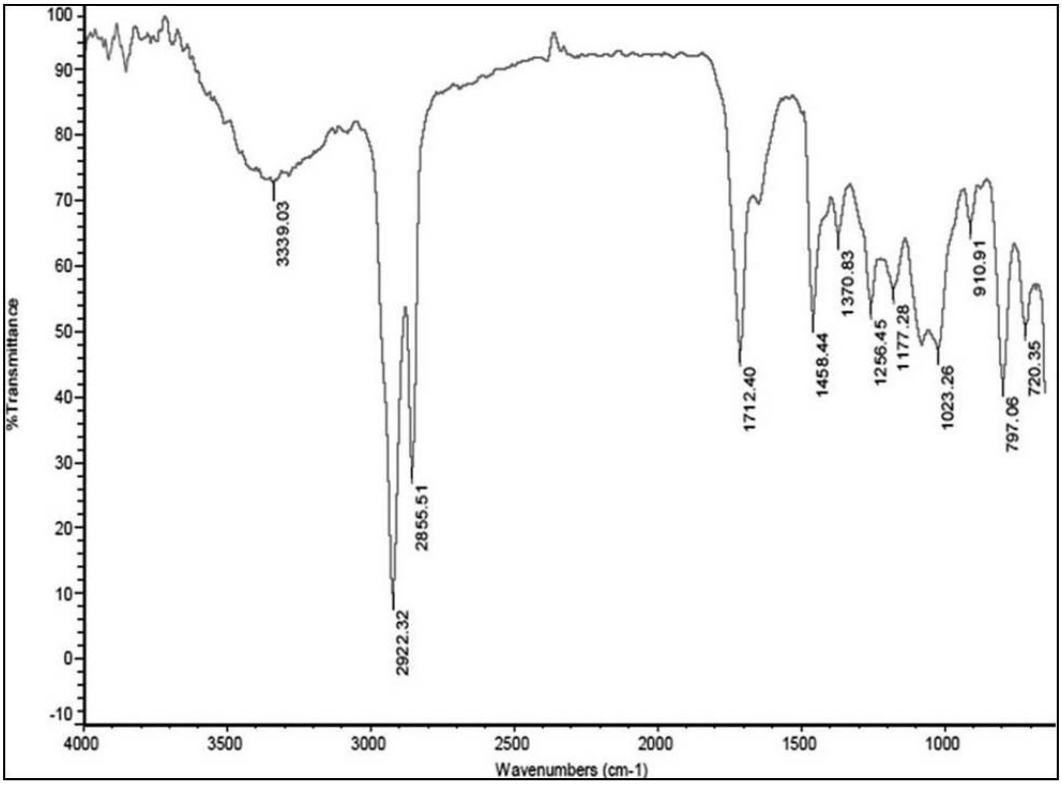

Figure 5.15. Figure showing the FTIR spectrum of **KA-3A**

Table 5.2. NMR spectroscopic data of **GO-3$_A$** in $CDCl_3$[a]

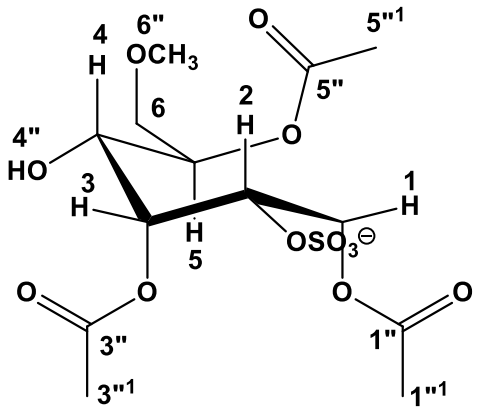

C. No	^{13}C (δ)	^{1}H-NMR[b] (int., mult., *J* in Hz)	^{1}H-^{1}H COSY	HMBC
1	81.83	3.81 (d, *J*=6.87 Hz, 2H)	2-H	C-3, C-2, C-1"
2	69.88	3.65 (m, 1H)	1-H, 3-H	
3	62.28	3.38 (t, *J*=6.50 Hz, 1H)	4-H, 2-H	C-1
4	74.7	3.73 (t, *J*=8.52 Hz, 1H)	3-H	C-3
5	69.89	3.65 (m, 1H)	-	C-6, C-5"
6	83.51	3.81 (d, *J*=6.87 Hz, 2H)	-	
1"	179.66	-	-	-
1"^{1}	30.93	2.17 (s, 3H)	-	-
3"	176.07	-	-	-
3"^{1}	40.98	2.62 (s, 3H)	-	-
4"	-	3.43 (s, 1H)	-	-
6"	59.84	3.49 (s, 3H)	-	-
5"	172.51			
5"^{1}	22.61	2.02 (s, 3H)		C-5"

[a]The NMR spectra were recorded using Bruker AVANCE III 500 MHz (AV 500) spectrometers.

[b] Values in ppm, multiplicity and coupling constants (*J*=Hz) are indicated in parentheses. Assignments were made with the aid of the ^{1}H-^{1}H COSY, HSQC, HMBC and NOESY experiments.

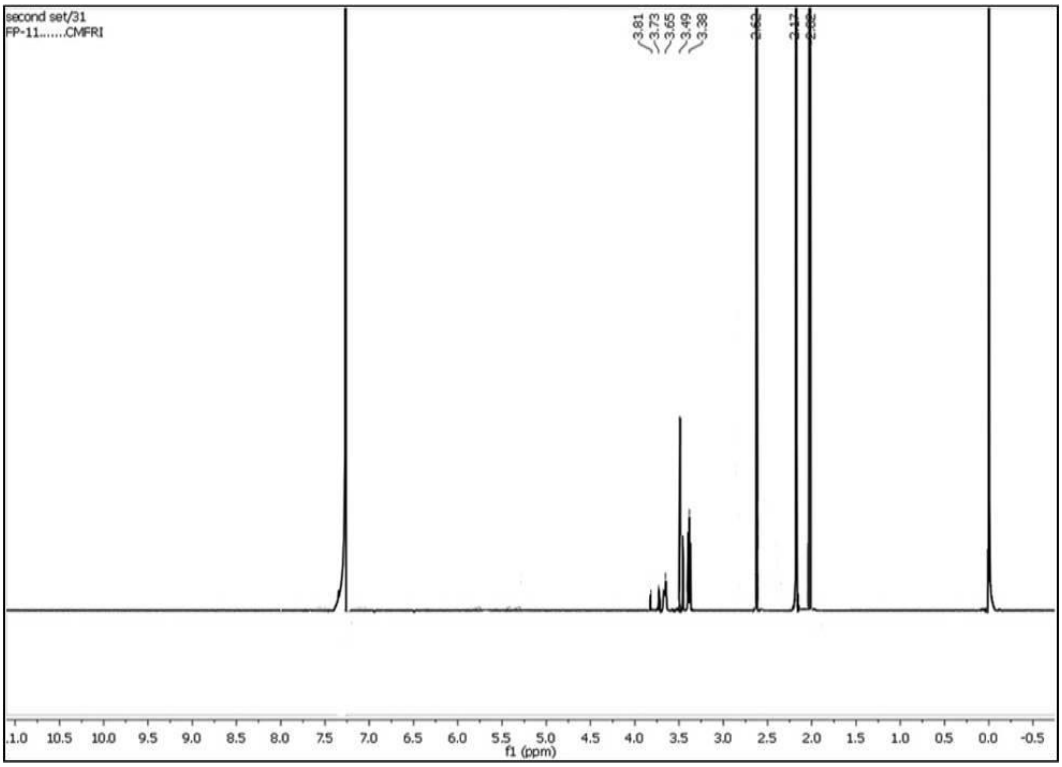

Figure 5.16. Figure showing the ^{1}H NMR spectrum of **GO-3A**

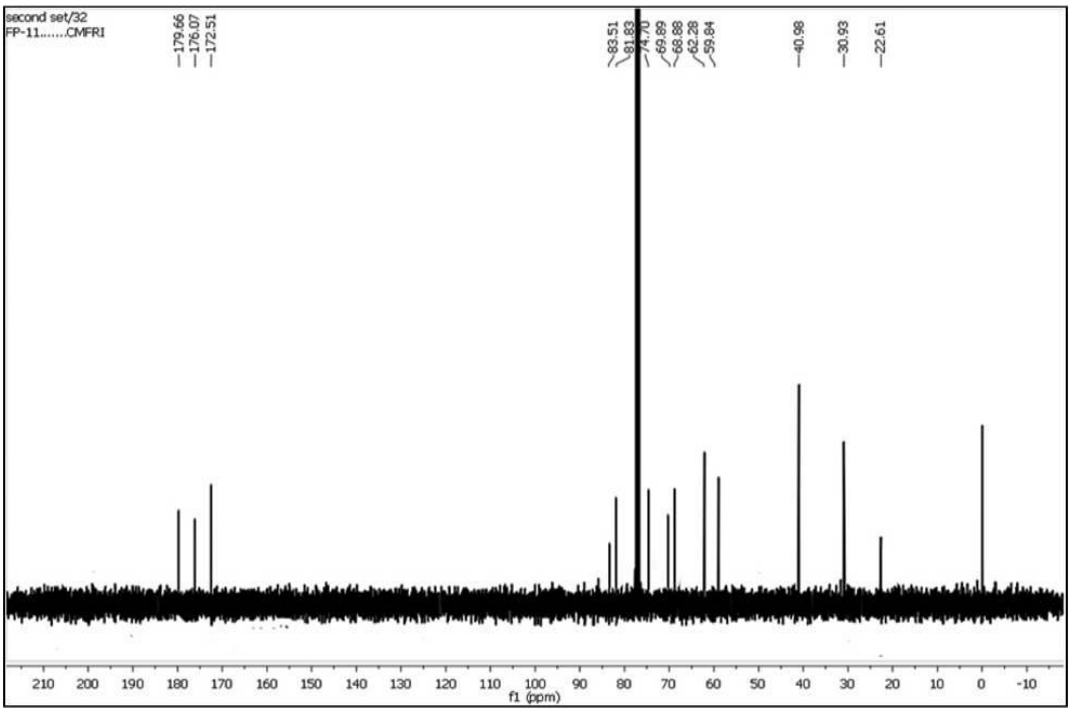

Figure 5.17. Figure showing the ^{13}C NMR spectrum of **GO-3A**

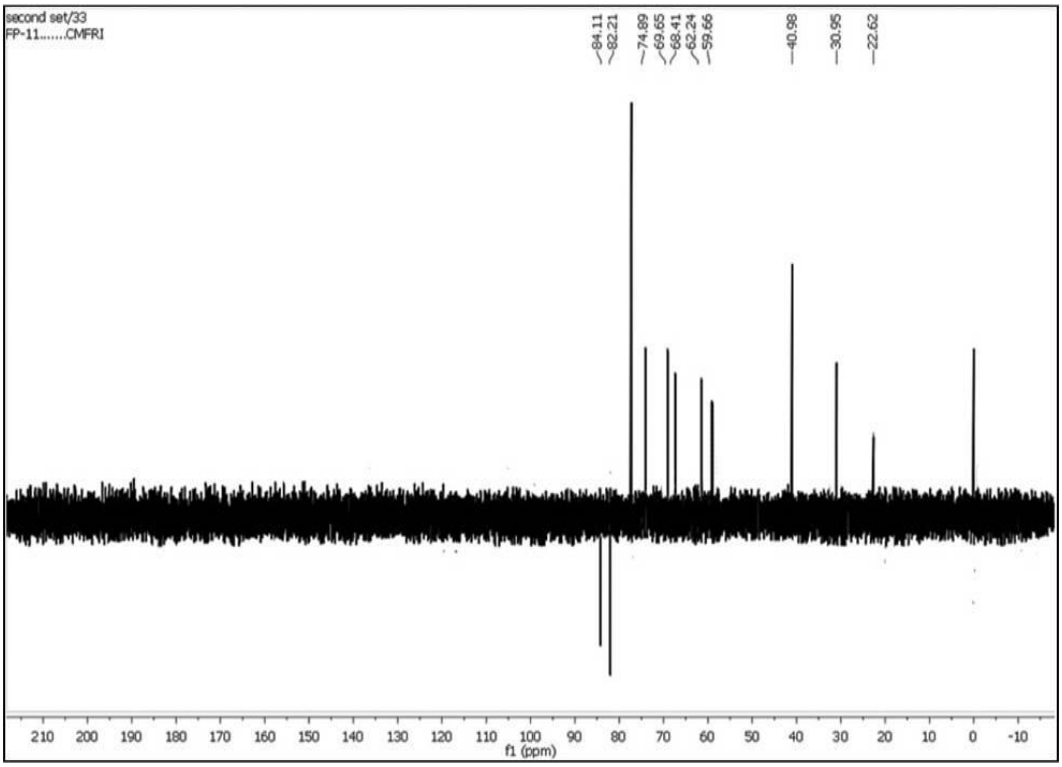

Figure 5.18. Figure showing the DEPT spectrum of **GO-3$_A$**

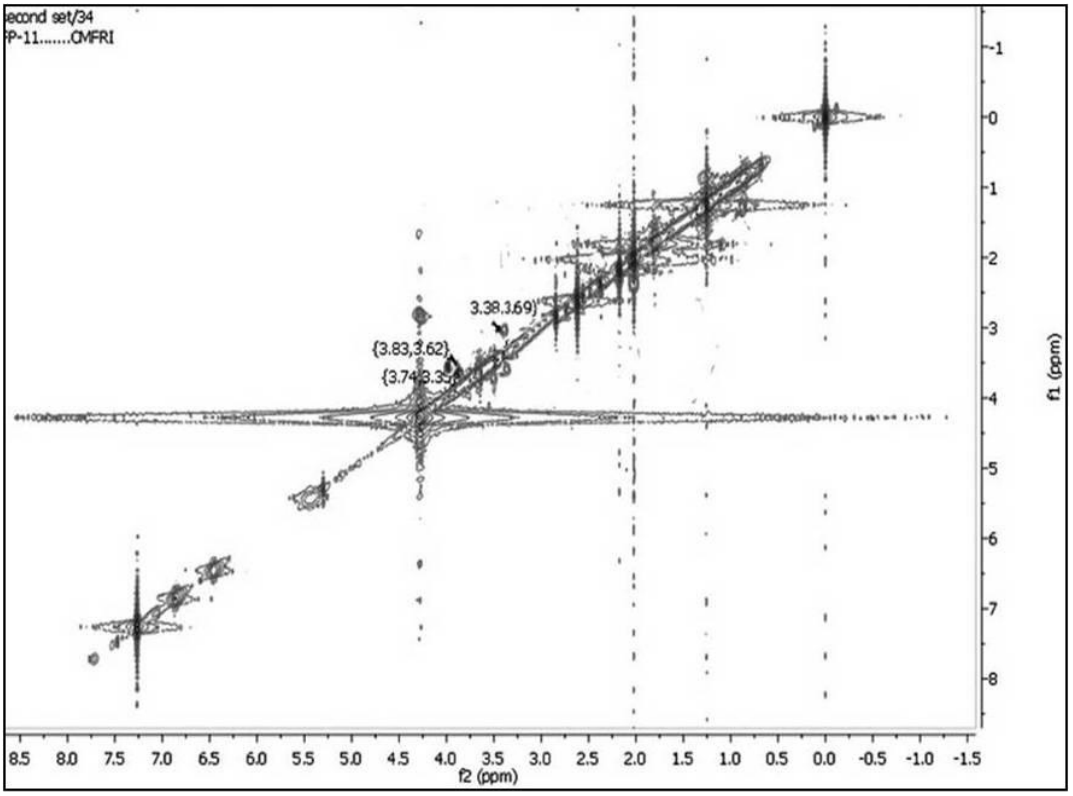

Figure 5.19. Figure showing the ^{1}H-^{1}H COSY spectrum of **GO-3$_A$**

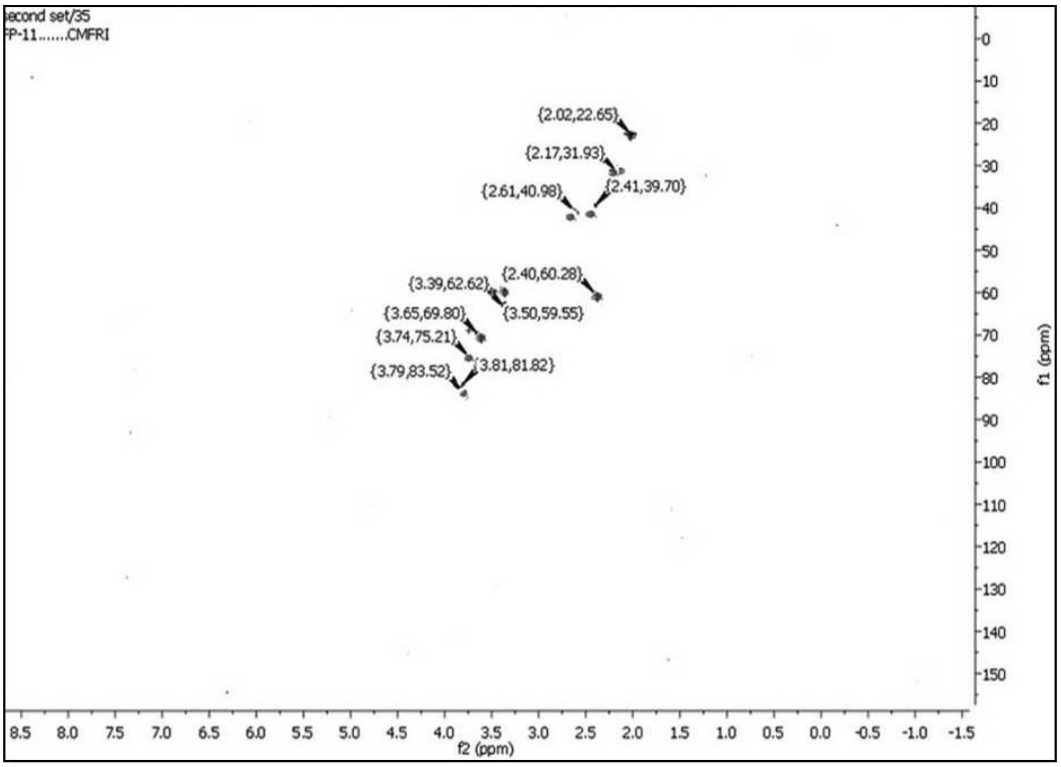

Figure 5.20. Figure showing the HSQC spectrum of **GO-3A**

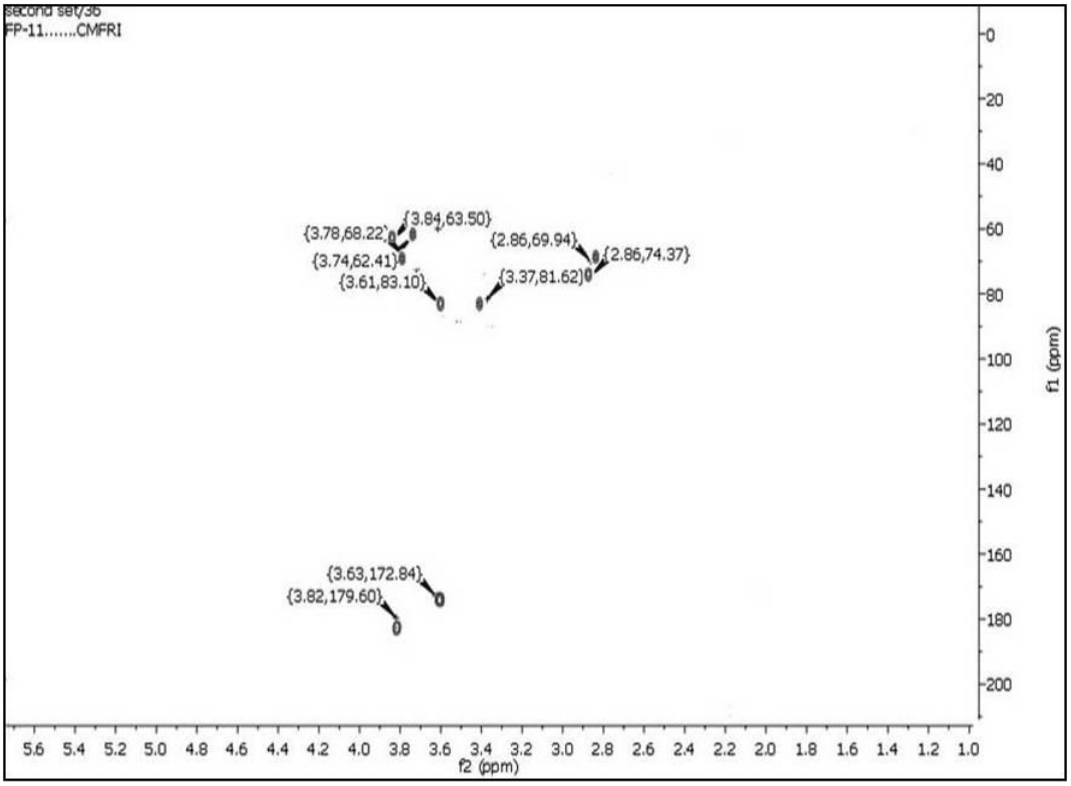

Figure 5.21. Figure showing the HMBC spectrum of **GO-3A**

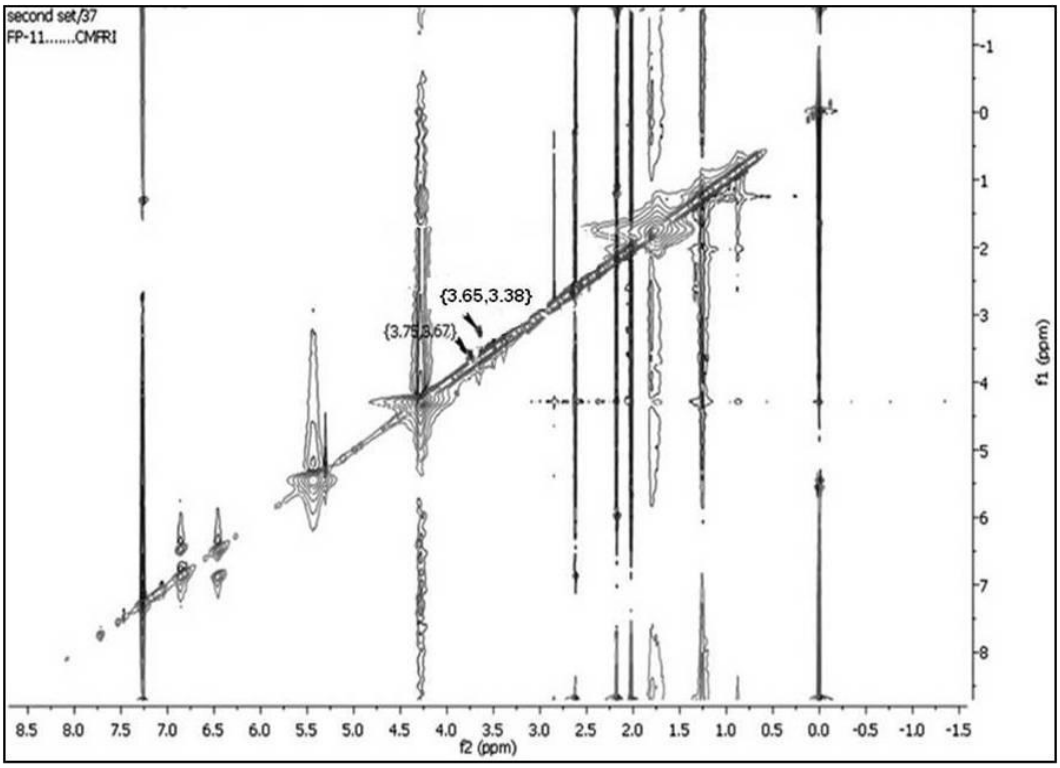

Figure 5.22. Figure showing the NOESY spectrum of **GO-3$_A$**

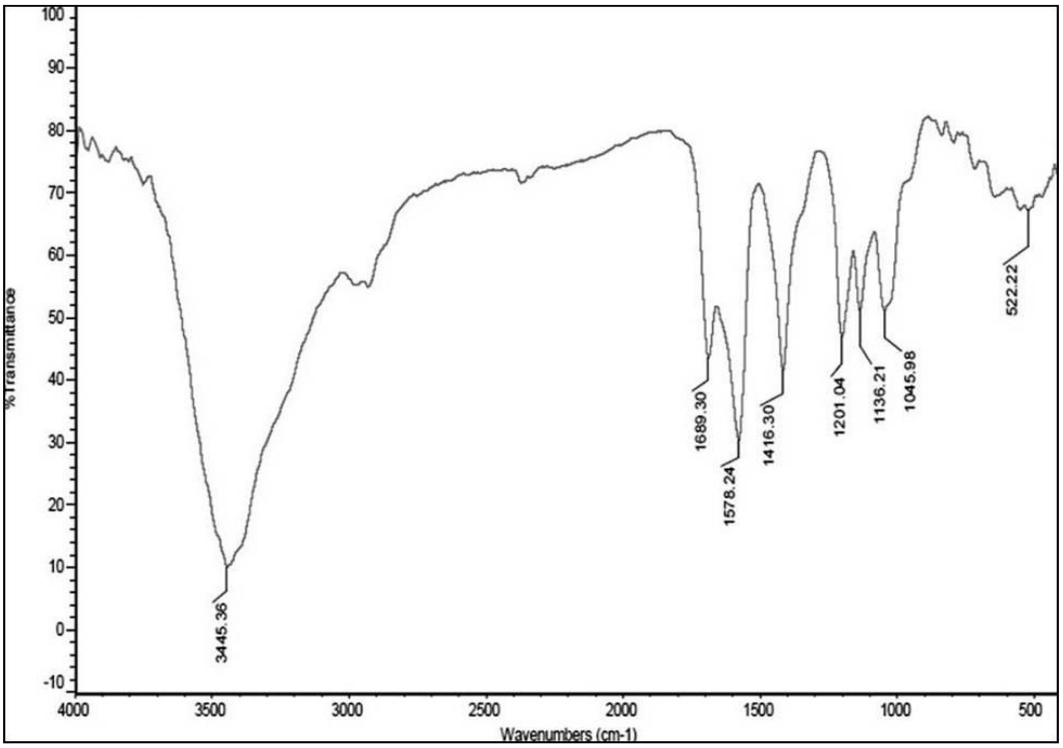

Figure 5.23. Figure showing the FTIR spectrum of **GO-3$_A$**

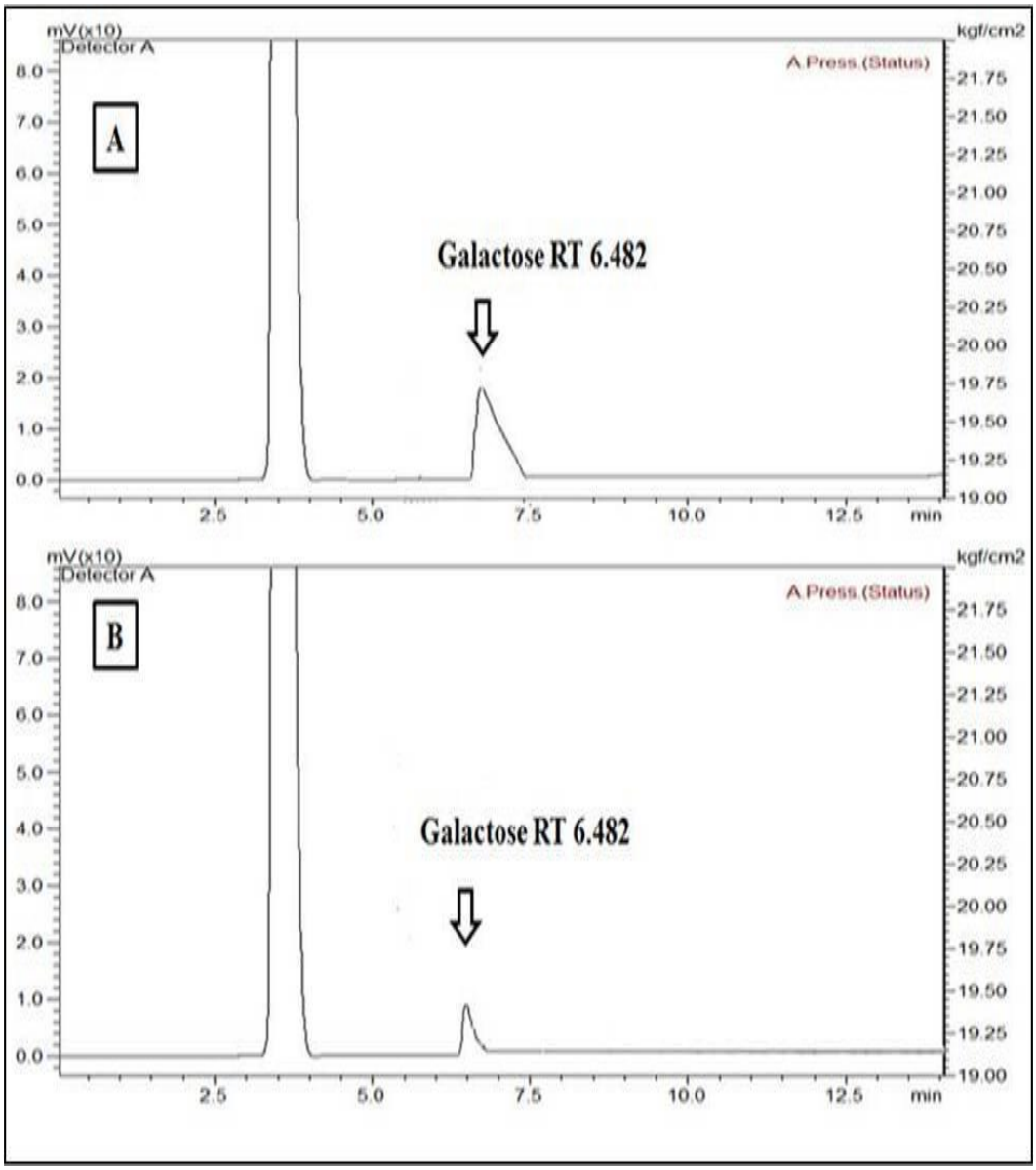

Figure 5.24. Figure showing Monosaccharide composition analysis of **KA-3$_A$** and **GO-3$_A$**

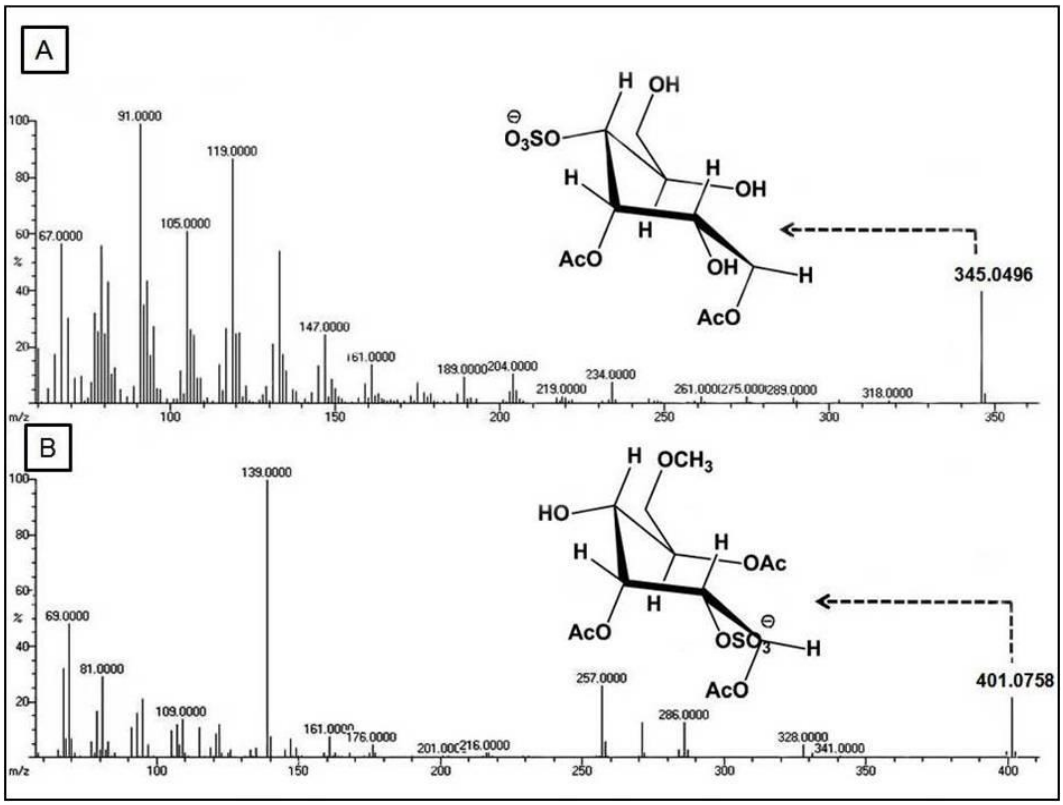

Figure 5.25. Mass spectrum of (**A**) from *K. alvarezii* (**KA-3A**) (**B**) and *G. opuntia* (**GO-3A**)

5.3.4. Pharmacological Potential of Various Polysaccharides from *K. alvarezii and G. opuntia*

The chemical analysis showed that the sulfated polygalactans derived from *K. alvarezii* (**KA-1**) was made essentially with carbohydrates (47 %) and showed higher sulfate content (> 70 %) than that recorded in *G. opuntia* (**GO-1**) (< 40 %). The aggregate content of carbohydrate in the latter was found to be 41.5 %, which was shown to be lesser than that in *K. alvarezii* (**KA-1**, Table 5.3). The uronic acid content in the sulfated polygalactan acquired from *K. alvarezii* (**KA-1**) by $CaCl_2$ precipitation was found to be significantly greater (7.2 %) than those in *G. opuntia* (**GO-1**) (6.6 %) ($P < 0.05$). There were other reports, which demonstrated that sulfated polysaccharides have been the major polysaccharides present in the marine algae (Ohno et al. 1994). The sulfated polygalactan from *G. opuntia* (**GO-1**) (> 400 mg of GAE/g) was found to possess greater content of total phenolics than that isolated from *K. alvarezii* (**KA-1**) (< 300 mg of GAE/g) (Table 5.3). ABTS scavenging activity of galactan separated from

K. alvarezii (**KA-1**) was greater (IC_{50} 0.72 mg/mL) than that from *G. opuntia* (**GO-1**) (IC_{50} 0.86 mg/mL) and commercially available antioxidant (gallic acid IC_{50} 0.92 mg/mL). The DPPH radical scavenging activity of sulfated polygalactan fraction derived from *K. alvarezii* (**KA-1**) was found to be greater (IC_{50} 0.97 mg/mL) than that in *G. opuntia* (**GO-1**, IC_{50} 1.20 mg/mL). The sulfated polygalactan from *K. alvarezii* displayed significantly greater Fe^{2+} chelating abilities (**KA-1**, IC_{50} 0.46 mg/mL) than that derived from *G. opuntia* (**GO-1**, IC_{50} 1.30 mg/mL). On account of lipid peroxidation inhibition assay, the sulfated polygalactan from the *G. opuntia* displayed greater lipid peroxidation inhibition activity (**GO-1**, 320.52 mM MDAEQ/kg) than that isolated from *K. alvarezii* (**KA-1**, 232.70 mM MDAEQ/kg). TBARS activity was denoted as mM of malondialdehyde equivalent compounds formed per kg sample (MDAEQ/kg sample) related to the control (lyophilised green mussel) leads to maximum lipid peroxidation on the same assay conditions. The capability of the polysaccharide fractions to capture lipid peroxidation was estimated by thiobarbituric acid reactive species (TBARS) assay. The guiding principles to determine the antioxidative activity of the sulfated polygalactans from the marine macroalgae could be attributed by utilizing different descriptor variables *viz.*, electronic, hydrophobic and steric parameters (Cinq-Mars et al. 2008). The electronic descriptors *viz.*, molecular polar surface area based on fragment contributions (aggregate topological polar surface area, tPSA), hydrophobic parameter Clog Pow to calculate *n*-octanol/water partition coefficient; steric (or bulk descriptor), molar refractivity (CMR) as computed by ChemDraw 12.0 were taken into consideration. We have considered 4-hydroxy-6-((3-hydroxy-4-methoxy-2, 6-dioxabicyclo [3.2.1] octan-8-yl) oxy)-2-(hydroxymethyl)-5-methoxytetrahydro-2*H*-pyran-3-yl sulfate moiety (designated as **KA-1**) of the galactan motif ((→4)-4-*O*-sulfonato-(2-*O*-methyl)-β-D-galactopyranosyl-(1→4)-3, 6-anhydro-(2-*O*-methyl)-α-D-galactopyranan) isolated from *K. alvarezii* for the accommodation to comprehend the atomic descriptors to adequately describe their anti-hypertensive properties. It is of note that, 2-(acetoxymethyl)-4, 5-dihydroxy-6-((3-hydroxy-4-methoxy-2, 6-dioxabicyclo [3.2.1] octan-8-yl) oxy) tetrahydro-2*H*-pyran-3-yl sulfate (designated as **GO-1**) was considered as a part of →3)-4-*O*-sulfonato-(6-*O*-acetyl)-β-D-galactopyranosyl-(1→4)-3, 6-anhydro-(2-*O*-sulfonato)-α-D-galactopyranosyl-(1→motif isolated from *G. opuntia*. The lipophilic (Clog Pow) and steric descriptors (CMR) were found to play a significant part to portray the greater antioxidative activities of sulfated galactan isolated from *K. alvarezii* **(KA-1)**. Although there were

no significant difference between the electronic descriptor (tPSA) variables (~188) in the macroalgal galactopyranan, the activity of the galactan extracted from *K. alvarezii (***KA-1)** displayed greater antioxidant activity than that obtained from *G. opuntia* **(GO-1)**, apparently due to greater steric bulk (estimated molar refractivity value, CMR = 9.10 cm^3) of **GO-1** than that exhibited by **KA-1** (CMR = 8.61 cm^3). Since MR is fundamentally a measure of the bulk of the substituent, the positive coefficient for this term indicates that molecules are contacting polar space in the enzyme (Hansch and Caldwell 1991) not the hydrophobic surface. A significant co-linearity was found to exist between CMR and Clog Pow. A positive correlation might propose an association with the polarisability of the substituents, albeit there is a little confirmation for the significance of such an effect. It is of note that unlike compound **KA-1** with 4, 6-dihydroxy-2-(hydroxymethyl)-5-methoxytetrahydro-2*H*-pyran-3-yl sulfate group, the compound **GO-1** with 2-(acetoxymethyl)-4, 5, 6-trihydroxytetrahydro-2*H*-pyran-3-yl sulfate moiety indicated more prominent lipophilic nature (Clog Pow -3.0628). The parameter Clog Pow of the compounds explained the hypothetically general computed lipophilicity of the molecule and governs the variations in activity. An increase in the lipophilicity apparently diminishes the antioxidative action of the galactans. The lipophilicity of the acetoxymethyl group was found to contribute towards reduced antioxidative property of the galactan isolated from *G. opuntia*. It was anticipated that the greater the acetyl substitution at the hydroxymethyl group of the galactan motif, lesser is the antioxidant activity. It can hence be induced that the stetric and lipophilic descriptors might essentially assume significant roles in determining the antioxidant activity. The electronic factor, such as tPSA was also found to significantly contribute towards the greater antioxidant activity of the macroalgal polygalactans.

The ACE inhibitory activities of the polygalactans from *G. opuntia* was lesser (**GO-1**, IC_{50} 0.70 μg/mL) than those separated from *K. alvarezii* (**KA-1**, IC_{50} 0.02 μg/mL) and the commercial ACE inhibitor, captopril (IC_{50} 0.05 μg/mL). The guiding principles to determine the anti-hypertensive activity of the sulfated polygalactans from the marine macroalgae was outlined by utilizing different descriptor variables *viz.*, electronic, hydrophobic and steric parameters. Despite the fact that the tPSA depicting the electronic descriptor were indistinguishable in the sulfated galactans isolated from *K. alvarezii* (**KA-1**) and *G. opuntia* (**GO-1**) the activity of the latter was lesser (IC_{50} 0.02 μg/mL) than of the previous (IC_{50} 0.70 μg/mL), evidently because of the greater steric values (CMR > 9 cm^3) of **GO-1** than that recorded in **KA-1** (CMR~ 8.6 cm^3). It

is intriguing to note that the lipophilicity of the 2-(acetoxymethyl)-4, 5, 6-trihydroxytetrahydro-2*H*-pyran-3-yl sulfate group has been double (Clog Pow 9.1058) than that of the corresponding 4, 6-dihydroxy-2-(hydroxymethyl)-5-methoxytetrahydro-*2H*-pyran-3-yl sulfate group of **KA-1** (Clog Pow 5.1021). Specifically, the tPSA of the polygalactans were recorded to be significantly greater (> 180) than the commercially available anti-hypertensive drug captopril with mercaptomethylpropanoyl pyrrolidine carboxylate moiety, which recorded a lesser tPSA value (tPSA 57.61). This might be due to the absence of the multiple electronegative sites (-OH, O-alkyl, $-SO_3^-$, etc.) in captopril.

The $–COCH_3$ group of the sulfated galactan might form a hydrogen bond with the imidazolyl proton of 2-amino-3-(1*H*-imidazol-4-yl) propanoic acid (His). The methoxy group on the anhydrogalactose ring fills the S3 pocket, and may conceivably shape a hydrogen bond with an auxiliary amine group of aromatic amino acid (such as Tyr). The terminal sulfate in position C-4 of the galactose ring grapples the tail in the dynamic site by framing a hydrogen bond with the aromatic amino acid (Tyr) and the enzyme metal cofactor Zn^{2+} in the S2' pocket of ACE (Fig. 5.26). The hydroxyl groups of the pyranose ring structure of sulfated polygalactan, at distinctive positions are different chemical attractions and hydroxyl group in the C-4 position was effectively supplanted by the sulfonato group, and a stronger interaction of $–SO_3^-$ with the Zn^{2+} (and tyrosyl –OH group) appeared to be responsible for anti-hypertensive activity. According to Ngo et al. (2008), the ACE inhibitory activity of aminoethyl-chitooligosaccharides (AE-COS) were greater than that of original chitooligosaccharides (COS). Essentially, Huang et al. (2005) have modified the structure of COS by carboxylation with $–COCH_2CH_2COO-$ groups to acquire particular structural features similar to captopril. Further, the greater ACE inhibitory activity of the 4-*O*-sulfonato-(2-*O*-methyl)-β-D-galactopyranosyl derivative (IC_{50} 0.02 μg/mL) than that of captopril (IC_{50} 0.51 μg/mL) might be due to the stronger electrostatic interactions between positively charged sites of enzymatic and negatively charged $–SO_3^-$ group of the latter. The sulfated polygalactan from *G. opuntia* (**GO-1**) was found to have additional $–COCH_3$ groups in the substituted galactose and anhydrogalactose units. It was, therefore, evident that the –OAc groups might have a negative effect on the target bioactivity.

Table 5.3. Yield, chemical compositions, antioxidative and ACE inhibitory activities of the sulfated polygalactans derived from *K. alvarezii* (**KA-1**) and *G. opuntia* (**GO-1**)

Activities	(**KA-1**)	(**GO-1**)
†**Yield (%)**	56.0	50.0
Biochemical contents		
†Uronic acid content	$7.20^{a} \pm 0.02$	$6.57^{b} \pm 0.12$
†Total sugar content	$46.99^{a} \pm 0.17$	$41.54^{a} \pm 0.10$
†Sulfate content	$75.0^{a} \pm 2.95$	$35.0^{b} \pm 1.37$
Total phenolic content (mg GAE/g)	$299.66^{b} \pm 0.04$	$480.45^{a} \pm 0.12$
Antioxidative activities		
x‡ABTS radical scavenging activity	$97.85^{a} \pm 0.68$ (0.72)	$90.67^{b} \pm 0.60$ (0.86)
x‡DPPH radical scavenging activity	$88.15^{a} \pm 0.63$ (0.97)	$83.04^{a} \pm 0.39$ (1.12)
x‡Fe^{2+} ion chelating ability	$73.15^{a} \pm 0.92$ (0.46)	$42.13^{b} \pm 0.56$ (1.30)
yLipid peroxidation inhibitory	$232.70^{b} \pm 0.36$	$320.52^{a} \pm 0.36$
Anti-hypertensive activities		
zACE inhibition	$82.69^{a} \pm 0.24$ (0.02)	$70.52^{b} \pm 1.11$ (0.70)

† The samples were analyzed in triplicate (n=3) and expressed as mean ± standard deviation. Means followed by the different superscripts within the same row indicate significant difference ($P < 0.05$).

†Percent mentioned in w/w

‡ Percentage inhibition of radicals/peroxides/metal ion (%) was calculated by, scavenging activity (%) = (Bc-Bs)/Bc X 100, where, Bc is the absorbance of the control and Bs is the absorbance of the sample.

x The IC_{50} values (the concentration at which it inhibits 50 % of its activity) were presented within the parentheses, and expressed as mg/mL. The IC_{50} was calculated from the graph plotted with concentrations of sample against percentage inhibition.

y Lipid peroxidation inhibitory (TBARS assay) was expressed as mM MDAEQ /kg.

z The ACE inhibition (%) was calculated as follows: $[1 - (\Delta A_{sample}/min \div \Delta A_{blank}/min)] \times 100$ % as detailed in the Materials section. The IC_{50} values were presented within the parentheses, and expressed as µg/mL.

Competitive inhibitor of α-glucosidase is acarbose and miglitol, which reduces consumption of starch and disaccharides (Baylac and Racine 2003; Davis and Granner 2011). Hence one of the therapeutic pathways for contracting postprandial blood glucose levels in patient with diabetes mellitus is to impede carbohydrate absorption after food intake. The α-amylase established a family of endo-amylases catalyzing the initial hydrolysis of starch into shorter oligosaccharides through the cleavage of α-D-(1-4) glycosidic bonds. Inhibition of these enzymes (α-amylase and α-glucosidase) reduced the high postprandial blood glucose peaks in diabetes (Hamdan and Afifi 2004; Conforty et al. 2005). Acarbose and miglitol are competitive inhibitor of α-glucosidase resulting in lower absorption of starch and disaccharides. Vicinity of ^{13}C-NMR signals at δ_H 170 of the extracts derived from the macroalgae are a decent sign about the acyl carbonyl carbon that were accounted for to repress α-glucosidase protein (Dong et al. 2012; Matsui et al. 2001). The results from the present study demonstrated that there were no difference in α-glucosidase inhibitory activity (IC_{50} 0.09 mg/mL) of the sulfated polygalactans purified from two marine macroalgae species considered in the present study (Table 5.4). However, the sulfated galactans of *G. opuntia* (**GO-2**) exhibited greater α-amylase inhibitory activity (IC_{50} 0.04 mg/mL) than that of *K. alvarezii* (**KA-2**, IC_{50} 0.15 mg/mL) and the positive control (acarbose, IC_{50} 0.2 mg/mL). The anti-diabetic effect of the sulfated polysaccharides from macroalgae might attribute to their inhibitory effects against α-amylase that retard the digestion of carbohydrate to delay the postprandial rise in blood glucose. Likewise, there was no significant difference in the α-glucosidase inhibitory activity of the sulfated galactans (**KA-2** and **GO-2**) derived from these two red macroalgal species (IC_{50} ~0.09 mg/mL). Marine macroalgae were reported to possess α-amylase and α-glucosidase inhibitory activities, (Villanueva et al. 2009; Apostolidis et al. 2011) which substantiate the results obtained in the present study that these macroalgal species are good source for anti-diabetic agents.

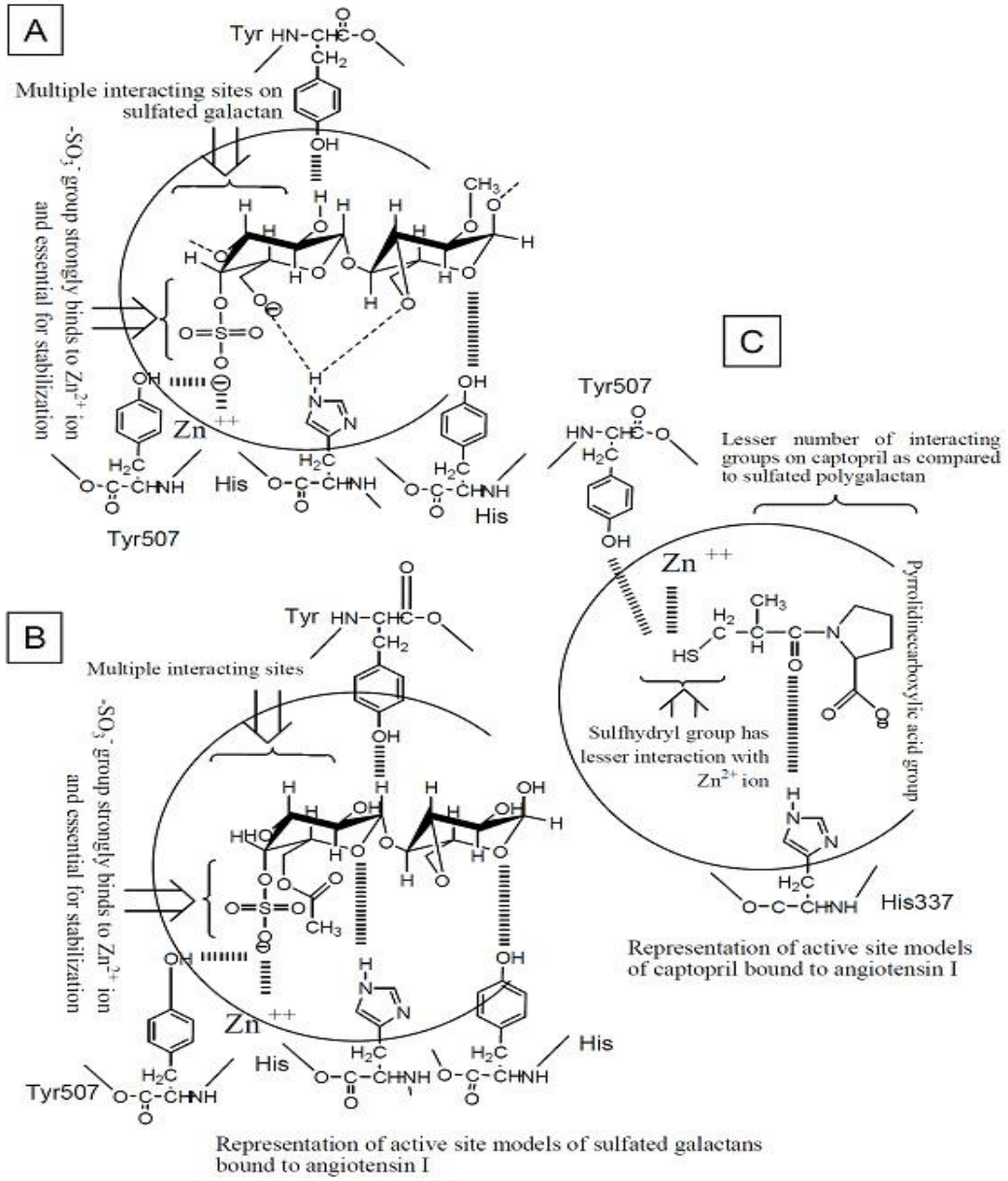

Figure 5.26. Representative active site models of substituted galactan motifs from (**A**) *K. alvarezii* (**KA-1**) (**B**) *G. opuntia* (**GO-1**) bound to the active centre of ACE (**C**) The ACE-ligand interaction of anti-hypertensive drug captopril has been shown

Dipeptidyl peptidase-4 (DPP-4) is involved in the inactivation of glucagon like peptide-1 (GLP-1), a potent insulinotropic peptide. Thus, DPP-4 inhibition can be an efficient approach to treat type-2 diabetes mellitus by potentiating insulin secretion (Mentlein 1999). The present study described the biological effects of sulfated polygalactan isolated from two different red marine macroalgae (**KA-2** and **GO-2**).

Significant differences were observed in the polysaccharide fractions, when compared with control.

Table 5.4. Anti-diabetic and anti-inflammatory inhibitory activities (IC_{50}) of the sulfated polygalactans derived from *K. alvarezii* (**KA-2)** and *G. opuntia* (**GO-2)**

Bioactivities	(**KA-2**)	(**GO-2**)
[x]**Anti-diabetic activities**		
α-Amylase	$0.15^{b} \pm 0.03$	$0.04^{a} \pm 0.02$
α-Glucosidase	$0.09^{a} \pm 0.02$	$0.09^{a} \pm 0.03$
DPP-4	$0.12^{b} \pm 0.01$	$0.09^{a} \pm 0.03$
[x]**Anti-inflammatory activities**		
COX-1	$0.01^{a} \pm 0.00$	$0.01^{a} \pm 0.00$
COX-2	$0.06^{b} \pm 0.01$	$0.03^{a} \pm 0.00$
5-LOX	$0.34^{b} \pm 0.02$	$0.24^{a} \pm 0.01$

The samples were analyzed in triplicate (n = 3) and expressed as mean ± standard deviation.

Means followed by the different superscripts within the same row indicate significant difference ($P < 0.05$).

[x] The IC_{50} values were expressed as mg/mL.

DPP-4 inhibitory activity of the sulfated galactans of *G. opuntia* (**GO-2)** was found to be significantly greater (IC_{50} 0.09 mg/mL) than that derived from *K. alvarezii* (**KA-2,** IC_{50} 0.12 mg/mL) and the standard diprotin A (IC_{50} 1.54 mg/mL) ($P < 0.05$). The synthetic DPP-4 inhibitors, such as, vildagliptin, sitagliptin, saxagliptin, etc, were reported to have several side effects like headache, dizziness, hypoglycemic disorders, nausea, weight gain and swelling of the legs and ankles due to excess fluid retention (Gomez-ordonez and Rupere 2011). Similarly, other synthetic hypoglycemic agents (acarbose and voglibose) that inhibit α-amylase and α-glucosidase were found to cause hepatic and gastrointestinal disorders (Cases et al. 1995; Murai et al. 2002). Polyphenols and sulfated polysaccharides present in macroalgae have been proven for anti-viral, anti-tumoral, anti-inflammatory and anti-coagulant activity (Vandevelde et

al. 2002; Cumashi et al. 2007). The bioactive compounds from macroalgae were reported to be effective for the treatment of major chronic diseases like diabetes through the inhibition of starch digesting enzymes and the regulation of glucose induced oxidative stress (Chiovitti et al. 1998; Lee et al. 2010). The bioactivity of the macroalgae extracts are due to the interaction of functional groups in the sulfated polygalactan with DPP-4 by H-bonding and hydrophilic interactions. The solvent fractions of *G. opuntia* were found to possess greater number of electronegative functional groups, which can form H-bond with DPP-4 resulting in greater anti-diabetic activity. The macroalgae considered in the present study can be used as potential alternative therapy for treatment of diabetes.

The sulfated polygalactan from *G. opuntia* **(GO-2)** exhibited significantly greater ($P < 0.05$) COX-1 and COX-2 inhibition activity (IC_{50} values of 0.01 and 0.03 mg/mL, respectively). *G. opuntia* **(GO-2),** polygalactan also exhibited greater 5-LOX inhibitory activity (**GO-2,** 0.24 mg/mL) than that of *K. alvarezii* (**KA-2,** IC_{50} 0.34 mg/mL) (Table 5.4). It is to be noted that sulfated polygalactan isolated in the present study showed greater anti-inflammatory activity in comparison with the positive control aspirin. Polysaccharides were reported to be one of the major bioactive components with selective activity against inflammation in the aqueous extract of macroalga *D. obtusata* (Frias et al. 2010; Silva et al. 1980). Red marine macroalgae were found to be the most important source of many biologically active metabolites in contrast to other algal classes (Frias et al. 2010). The sulfated galactans got from *G. opuntia* **(GO-2)** were found to have more prominent number of electronegative functional groups, which are characteristic of sulfated polygalactans, in the downfield space of the NMR spectra. These electronegative functional groups in the substituted polysaccharides derived from the macroalgae prevent abstraction of hydrogen from arachidonic acid in cyclooxygenases by ion pairing, and in this manner prevent synthesis of the pro-inflammatory prostaglandins.

The anti-diabetic potential of **KA-3** isolated from *K. alvarezii* measured in terms of the inhibitory activities against DPP-4 were deduced to be higher (IC_{50} 0.17 mg/mL) in comparison with that obtained from *G. opuntia* (**GO-3**, IC_{50} 0.21 mg/mL) and gold standard diprotein-A (IC_{50} 0.24 mg/mL). Similarly, the sulfated polygalactan derivatives showed significant increase in ($P > 0.05$) α-amylase inhibitory activities (**KA-3** and **GO-3**, $IC_{50} < 1$ mg/mL) when compared with the standard acarbose (IC_{50}

1.39 mg/mL). Notably, there has been a positive correlation between the sulfate content and anti-diabetic properties as reported previously (Cho et al. 2011).

Table 5.5. Pharmacological potential of sulfated polygalactan isolated from *K. alvarezii* (**KA-3**) and *G. opuntia* (**GO-3**)

Bioactivities	**Standard**	(**KA-3**)	(**GO-3**)
Anti-diabetic activity			
α-Amylase inhibitory activity	1.39 ± 0.06^{aC}	0.91 ± 0.04^{a}	0.93 ± 0.02^{b}
α-Glucosidase inhibitory activity	1.52 ± 0.03^{aC}	1.41 ± 0.02^{b}	1.43 ± 0.04^{b}
DPP-4 inhibitory activity	0.24 ± 0.01^{aD}	0.17 ± 0.02^{a}	0.21 ± 0.01^{b}
Anti-hypertensive activity			
ACE-I inhibitory activity	0.01 ± 0.01^{aE}	0.04 ± 0.01^{b}	0.07 ± 0.01^{b}

The samples were analyzed in triplicate (n=3) and expressed as mean ± standard deviation.

Means followed by the different superscripts (a-b) within the same row indicate significant difference ($P < 0.05$).

The IC_{50} values of anti-diabetic and anti-hypertensive activities were expressed as mg/mL.

Different superscripts (C-E) indicated the standards used for different activities; C-acarbose; D-diprotein-A; E-captopril

It was found that the α-amylase enzyme inhibitory activity of sulfated polysaccharide derived from *Ascophyllum nodosum* and *Saccharina longicruris* were lesser following complete removal of sulfate groups (Kim et al. 2014). Similarly, the polygalactan **KA-3** from *K. alvarezii* showed greater inhibitory properties against angiotensin-I (IC_{50} 0.04 mg/mL) when compared with **GO-3** (IC_{50} 0.07 mg/mL) (Table 5.5).

5.3.5. Correlation Analysis

A negative correlation was demonstrated between the total phenolic content (TPC) and different antioxidative activities of the sulfated polygalactans **(KA-1** and **GO-1)** isolated from the marine macroalgae, which apparently outlined that anti-hypertensive properties did not depend on aggregate phenol content, but rather additionally on other compounds, for instance, polysaccharides (Muzzarelli 1997).

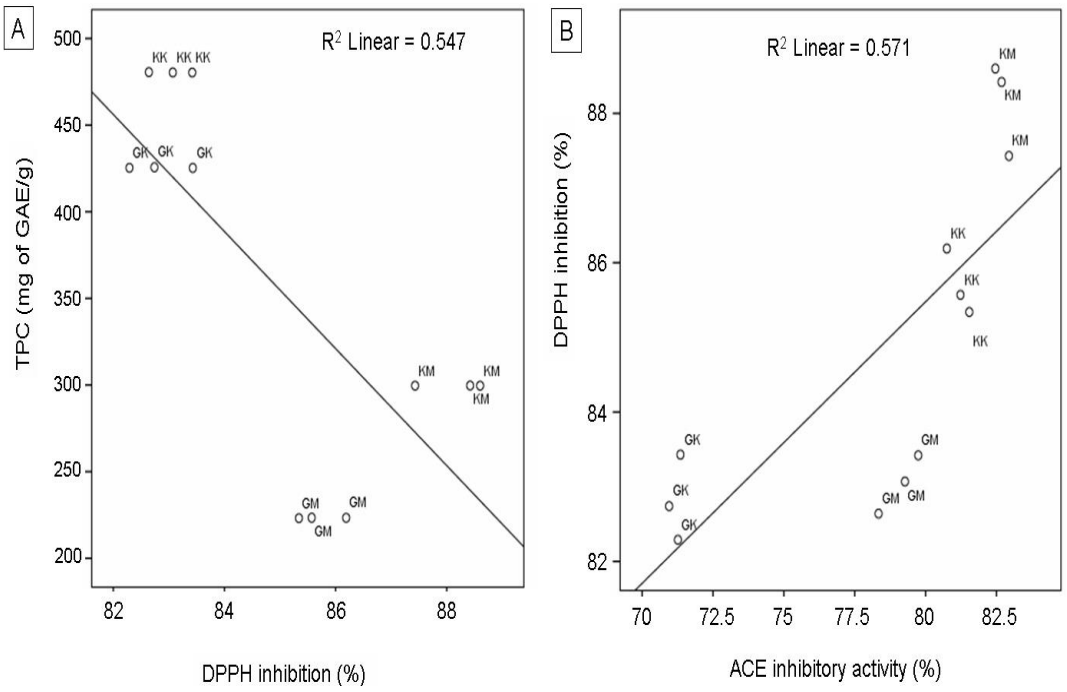

Figure 5.27. Correlation plot between (**A**) total phenolic contents (TPC) and antioxidative properties (DPPH inhibition) (**B**) antioxidative (DPPH inhibition) and anti-hypertensive properties (ACE inhibition)

The antioxidant activities as dictated by DPPH and ABTS activities were found to be significantly related to the anti-hypertension activity as displayed by ACE-I inhibitory properties (Fig. 5.27), which apparently demonstrated that the ACE-I inhibitory activities of the sulfated galactans **(KA-1** and **GO-1)** were due to their free radical scavenging properties. It is apparent that the multiple –OH and other electronegative groups bearing the hydrogen atoms contributed towards the hydrogen atom transfer (HAT), which resulted in the stabilization of the free radicals.

The relationships between anti-inflammatory and anti-diabetic activities of the sulfated polygalactan enriched concentrate of *K. alvarezii* **(KA-2)** and *G. opuntia* **(GO-2)** were statistically analyzed using PCA (Fig. 5.28). The loading of first and second principle components (PC1 and PC2) were accounted for 68.17 % and 31.8 % of the variance, respectively.

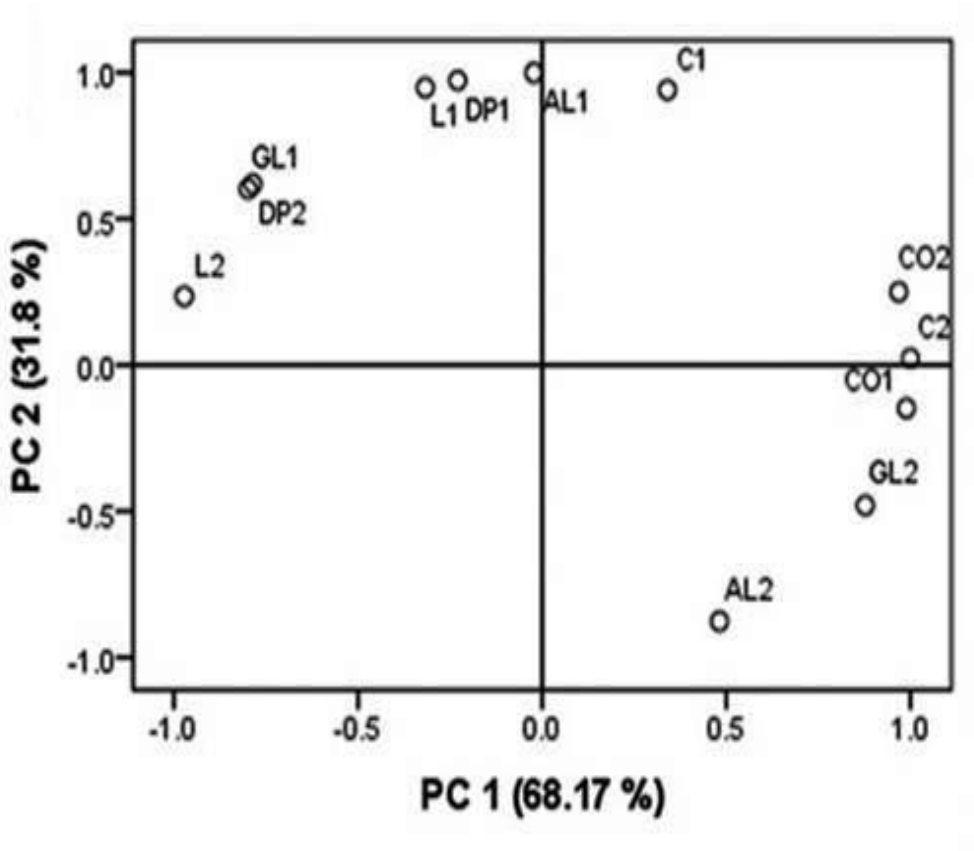

Figure 5.28. PCA loading plot diagrams showing the correlation between anti-diabetic and anti-inflammatory activities of the sulfated polygalactan fractions from *G. opuntia* **(GO-2)** and *K. alvarezii* **(KA-2)**.

The component, PC1 was mainly influenced by inhibitory activities of sulfated polygalactan derived from *G. opuntia* (**GO-2** and *K. alvarezii* (**KA-2**) towards the pro-inflammatory enzymes, COX-1 (denoted as C1; **GO-2** and C2; **KA-2**) and COX-2 (denoted as CO1; **GO-2** and CO2; **KA-2**), along with α-amylase (AL2; **KA-2**) and α-glucosidase (GL2; **KA-2**). On the other hand, 5-LOX (denoted as L1; **GO-2** and L2; **KA-2**), DPP-4 (DP1; **GO-2** and DP2; **KA-2**), α- amylase (AL1; **GO-2**), and α-

glucosidase (GL1; **GO-2**) inhibiotory properties of the sulfated polygalactans of the marine macroalgae were mainly contributed to PC2 (Fig. 5.28). The similarity in the greater loading of DPP-4, COX-2, 5-LOX·inhibitory activities, and a significant positive correlation between DPP-4 inhibition activity (DP1-DP2) with anti-COX and LOX properties of macroalgae derived sulfated polygalactans (**KA-2** and **GO-2)** apparently demonstrated that these bioactivities were in close relation. The significant correlation of anti-diabetic activities with anti-inflammatory properties of the sulfated polygalactans isolated from the macroalgae *G. opuntia* **(GO-2)** and *K. alvarezii* (**KA-2)** also indicated that these polysaccharides derived from macroalgae were responsible for potential anti-inflammatory and anti-diabetic properties.

5.4. Conclusions

The present study demonstrated that sulfated polygalactan characterized as→4)-4-*O*-sulfonato-(2-*O*-methyl)-β-D-galactopyranosyl-(1→4)-3, 6-anhydro-(2-*O*-methyl)-α-D-galactopyranan from *K. alvarezii* **(KA-1)** displayed significantly greater antioxidative and ACE inhibitory activities than →3)-4-*O*-sulfonato-(6-*O*-acetyl)-β-D-galactopyranosyl-(1→4)-3, 6-anhydro-(2-*O*-sulfonato)-α-D-galactopyranosyl-(1→3)-4-*O*-sulfonato-(6-*O*-acetyl)-β-D-xylosyl-(1→3)-4-*O*-sulfonato-(6-*O*-acetyl)-β-D-galactopyranosyl-(1→4)-3, 6-anhydro-(2-*O*-sulfonato)-α-D-galactopyranan from *G. opuntia* **(GO-1)**. The multiple hydroxyl groups of the pyranose ring structure of sulfated polygalactan from *K. alvarezii* **(KA-1)** and sulfonato group ($-SO_3^-$) at distinctive positions have stronger interactions with the Zn^{2+} (and tyrosyl –OH group), which were responsible for their anti-hypertensive activities. The sulfated polygalactan from *K. alvarezii* **(KA-1)** was found to be a potential therapeutic candidate to prevent the pathologies of hypertensive disorders.

The sulfated polygalactans isolated from the red marine macroalgae *K. alvarezii* **(KA-2)** and *G. opuntia* **(GO-2)** were found to possess a number of bioactivities against different disease targets, namely, inflammation and type-2 diabetes. The sulfated polygalactan enriched concentrate obtained from *G. opuntia* **(GO-2)** showed greater anti-inflammatory activities than that from *K. alvarezii* **(KA-2)** as determined by *in vitro* cyclooxygenase/lipoxygenase inhibitory activities. The activities showed significant positive correlation with the anti-diabetic activities as determined by *in vitro* α-amylase, α-glucosidase and dipeptidyl peptidase-4 inhibitory

properties. This study demonstrated the candidacy of red marine macroalgae particularly, *G. opuntia* **(GO-2)** as potential source of bioactive sulfated polygalactans for use as functional food supplements to deter inflammation and type-2 diabetes.

Further other polysaccharide fractions obtained from the red marine macroalgae *K. alvarezii* and *G. opuntia* were characterized as 1, 3-*O*-diacetyl-2, 5, 6-trihydroxyl-β-D-galactose-4-sulfate **(KA-3$_A$)** and 1, 3, 5-*O*-triacetyl-4-hydroxyl-6-*O*-methyl-D-galactose-2-sulfate **(GO-3$_A$)**, respectively, which were characterized by using extensive spectroscopic experiments. In particular, the polysaccharide fraction isolated from *K. alvarezii* **(KA-3)** exhibited potential DPP-4 and ACE-I enzyme inhibitory properties, and therefore, could function as candidate template for use in medicinal and food applications.

Chapter 6

SUMMARY

Marine macroalgae (otherwise named as seaweeds) were found to be the potential reservoir of bioactive secondary metabolites. Traditionally, marine macroalgae are considered as valuable marine flora, which are preferred delicacies in the South-east Asian countries due to their potential antioxidant and therapeutic properties. Species of the red marine macroalgae (class Rhodophyceae) were proven to be rich sources of structurally unique and biologically active secondary metabolites endowed with antioxidant, anti-bacterial, anti-inflammatory and anti-carcinogenic activities for applications in functional food and pharmaceuticals. The bioactive compounds extracted from the marine macroalgae are used as safer anti-inflammatory therapeutics. Marine macroalgae were found to be rich sources of bioactive compounds, such as terpenoids, phloroglucinol, phenolics, fucoidans, sterols, glycolipids and halogenated compounds, whereas the extracts or isolated components derived from these marine species exhibited a wide range of pharmaceutical properties. The potential applications offered by these valuable resources as ingredients in functional foods are significant because of their richness in bioactive principles, particularly antioxidants. Antioxidant effects have been reported from various macroalgae due to phenolic compounds, terpenoids and sulfated polysaccharides. Novel secondary bioactive metabolites from red marine macroalgae are attracting attention because of the growing demand for new compounds of marine natural origin, having potential applications in pharmaceutical fields and concerns about the toxic effects by synthetic drugs.

Among different red marine macroalgae, *Kappaphycus alvarezii* (Doty) (family Solieriaceae) and *Gracilaria opuntia* (Durairatnam) (family Gracilariaceae) are commercially important and cultivable species that are predominantly abundant in tropical coastal and marine habitats in the Southeast Asian countries. *K. alvarezii* is economically significant and predominantly farmed red marine macroalga in shallow tropical marine habitats. The genus *Gracilaria* is the largest in the order Gracilariales,

and was found to include more than 150 species, which were distributed in the tropical and temperate sea. Among different species of the genus *Gracilaria*, *G. opuntia* is one of the predominantly available red marine macroalga grown in the Gulf of Mannar region of the south-east coast of India. Despite the fact that red marine macroalgae, particularly *Laurencia* spp, have been studied extensively with respect to secondary metabolite chemistry, studies on members of the genus *K. alvarezii* and *G. opuntia* have been rare for the isolation of novel intriguing structures.

The organic ethyl acetate-methanol (EtOAc: MeOH) extracts of the studied marine macroalgae *K. alvarezii* and *G. opuntia* from the Gulf of Mannar region of Mandapam were screened for various pharmacological activities by different *in vitro* assays. The organic extracts obtained from the red macroalgae *K. alvarezii* and *G. opuntia* were found to possess a number of bioactivities against different disease targets, namely, hypertension, type-2 diabetes and inflammation. The organic extract of *K. alvarezii* possessed significantly greater antioxidative properties than those obtained from *G. opuntia*. The EtOAc: MeOH fraction of *K. alvarezii* registered greater Fe^{2+} ion chelating ability (IC_{50} 1.30 mg/mL), and were effective in stabilizing the ABTS (IC_{50} 1.26 mg/mL), and DPPH radicals (IC_{50} 1.24 mg/mL). The organic extract from *K. alvarezii* also showed greater angiotensin-I converting enzyme (ACE) inhibitory activity along with pro-inflammatory cyclooxygenase/lipoxygenase inhibitory activities than that exhibited by that acquired from *G. opuntia*. Likewise, EtOAc-MeOH crude extract obtained from *K. alvarezii* showed significant anti-diabetic activities as determined by *in vitro* α-amylase, α-glucosidase and dipeptidyl peptidase-4 inhibitory properties. The spectroscopic characterization of the solvent extracts provided the evidence regarding the occurrences of signature peaks and the prominent functional groups that were responsible for the target bioactivities.

The ethyl acetate-methanol extract of the thalli of *K. alvarezii* and *G. opuntia* was fractionated by repeated column chromatography to afford a number of previously undescribed compounds. The structures of these compounds were established by exhaustive spectroscopic experiments, including mass and two-dimensional nuclear magnetic resonance. The antioxidative and anti-inflammatory activities of the newly reported compounds were evaluated by different *in vitro* assays. Structure-bioactivity correlation analyses of the studied compounds were carried out using different electronic and hydrophobic molecular descriptor variables. Chromatographic fractionation of the organic extract obtained from the thalli of *K. alvarezii* yielded two

previously undescribed biogenic halogenated compounds named as 2-butyl-7-4-(chloromethyl) cyclooct-1-enyl) hept-5-en-1-ol (compound **K1**) and 4-(2-chloroethyl)-5-7-(methoxymethyl) undec-3-enyl) cyclooct-4-enone (compound **K2**), which demonstrated the rare skeletal framework featuring C_{20}-cyclooctene and C_{23}-cyclooctenyl ring system and three oxygenated meroterpenoids, characterized as 1-(3-methoxypropyl)-2-propylcyclohexane (C_{13}) (compound **K3**), 3-(methoxymethyl) heptyl 3-(cyclohex-3-enyl) propanoate (C_{18}) (compound **K4**) and 2-ethyl-6-(4-methoxy-2-((2-oxotetrahydro-*2H*-pyran-4-yl) methyl) butoxy)-6-oxohexyl-5-ethyloct-4-enoate (C_{29}) (compound **K5**) along with an unprecedented non-isoprenoid oxocine carboxylate cyclic ether characterized as (3, 4, 5, 6)-3-(hexan-2′ -yl)-3, 4, 5, 8-tetrahydro-4-methyl-2*H*-oxocin-5-yl acetate (compound **K6**)

The mass spectroscopic data of compound **K1** demonstrated a molecular ion peak at *m/z* 326, while the molecular formula $C_{20}H_{35}ClO$, implying three unsaturation degrees, and were associated with two olefinic bonds and one ring system. The infrared (IR) spectrum exhibited distinctive stretching vibration band for hydroxyl (3430 cm^{-1}) and olefinic group (3011 cm^{-1}). The existence of the hydroxyl proton at δ_H 3.67 was validated by ^1H NMR spectra and D_2O exchange reaction. The characteristic isotopic molecular ion peaks with typical isotopic pattern of 3:1 at *m/z* 326 and *m/z* 328 appropriately attributed the presence of one chlorine atom in compound **K1**. The NOE experiment of compound **K1** showed correlation peaks between the equatorial methine proton and methylene proton, which proposed that these protons were arranged on the same side of the reference plane (cyclooctene) with β-faced interaction. The mass spectroscopic experiments of compound **K2** showed a molecular isotopic ion peak at *m/z* 382, having four degrees of unsaturation (molecular formula $C_{23}H_{39}ClO_2$), and were associated with two olefinic bonds, along with one each of carbonyl group and ring system. The infrared (IR) spectrum exhibited distinctive stretching vibration band for carbonyl stretching (1727.88 cm^{-1} for C-CO-C ν) and olefinic group {3072.42 cm^{-1} (C-H)}. The NOE experiment showed correlation peaks between the oxygenated methine proton and axial proton, which proposed that these protons were on the opposite of the reference plane (cyclooctenyl) with β-faced interaction. The characteristic isotopic molecular ion peaks with typical isotopic pattern of 3:1 at *m/z* 382 and *m/z* 384 appropriately attributed the existence of one chlorine atom in compound **K2**. It is of note that the halogen derivatives isolated in the present study from *K. alvarezii* represented the first examples of naturally occurring halogen

derivative from the marine macroalga. The halogenated cyclooctenone (compound **K2**) displayed greater 5-LOX (IC_{50} 0.90 mg/mL) inhibitory activity when compared to the non steroidal anti-inflammatory drug ibuprofen (IC_{50} 0.93 mg/mL). Similarly, selectivity indices of the studied halogenated compounds (compounds **K1** and **K2**) were higher (anti-cyclooxygense-1 IC_{50}/anti-cyclooxygense-2 IC_{50} ~ 1.06-1.07) when compared to those exhibited by ibuprofen (0.44) and aspirin (0.02). The antioxidative activities of the halogen derivatives (compounds **K1** and **K2**) were found to be greater (IC_{50} < 0.30 mg/mL) in comparison with that displayed by α-tocopherol (IC_{50} > 0.50 mg/mL). This is the first report on structural characterization of unusual halogen analogues from *K. alvarezii* with duel cyclooxygenase-2 and 5-lipoxygenase inhibitory activities.

Compound **K3**, a methoxy-substituted C_{13} meroterpenoid, was purified as yellow oil by extensive column chromatography on adsorbent silica gel. The mass spectrum displayed the molecular ion peak at *m/z* 198 enclosing mono unsaturation, and the molecular formula as $C_{13}H_{26}O$ based upon combined ^{1}H and ^{13}C NMR spectral data. NOESY cross-peaks suggested their close proximity, and therefore, assigned to align on an identical plane of the cyclohexane ring system with di-equatorial β-faced interaction. Compound **K4**, an oxygenated C_{18} meroterpenoid displayed the molecular ion peak at *m/z* 296 enclosing three degrees of unsaturation the molecular formula as $C_{18}H_{32}O_3$ based upon combined ^{1}H and ^{13}C NMR spectral data. The IR-spectrum of compound **K4** displayed the presence of carbonyl group along with olefinic groups due to the bands recorded at 1458 and 2856 cm^{-1}. The chemistries of the stereogenic centres bearing protons were derived using coupling constant values and NOESY experiments. An intense NOE correlation was displayed between the protons suggested their equi-planer disposition, and was arbitrarily attributed as β-oriented. Compound **K5**, a highly oxygenated C_{29} meroterpenoid, was purified as yellow oil with *m/z* 510 bearing five degrees of unsaturation, and its structure was characterized by combined ^{1}H and ^{13}C NMR spectral experiments. The IR bending vibration near 1736 cm^{-1} was associated with the carbonyl group, whereas the olefinic groups were assigned to the absorption bands at 1455 cm^{-1} and 2857 cm^{-1}. NOE correlations between the di-equatorial protons apparently attributed to their close spatial arrangements, and therefore, were assigned to be at the β-face with reference to the molecular plane of symmetry. The highly oxygenated C_{29} meroterpenoid (compound **K5**) displayed potential antioxidative activities (IC_{50} < 0.35 mg/mL) as evaluated by 2, 2'-azino-bis (3-ethylbenzothiazoline)-6-

sulfonic acid and 1, 1-diphenyl-2-picryl-hydrazil free radical scavenging assays. The compound **K5** also displayed potential *in vitro* inhibitory activities towards pro-inflammatory 5-lipoxygenase (IC_{50} 1.04 mg/mL), which indicated its potential anti-inflammatory properties against inducible inflammatory mediators causing an inflammatory response. Structure-activity relationship analyses displayed the functional roles of lipophilic-hydrophobic characteristics and electronic parameter to determine its potential anti-inflammatory activity in terms of inhibiting inducible inflammatory cyclooxygenase and lipoxygenase. The mass spectrum supported the molecular formula of $C_{16}H_{28}O_3$ and the molecular ion peak at *m/z* 268 in the mass spectrum, which in combination with its ^{1}H and ^{13}C NMR data indicated the elemental composition of the compound **K6** as $C_{16}H_{28}O_3$ with three degrees of unsaturation. The olefinic (C=C) and alkyl (C–H) groups IR stretching vibrations were represented by the 1458 and 2855 cm^{-1} absorption bands, respectively. The strong bending vibration bands near 1712 cm^{-1} denoted the ester carbonyl absorption. The relative stereochemical configuration of the asymmetric centers bearing the 3, 4, 5, 8-tetrahydro-2*H*-oxocine ring framework, was proposed on the basis of NOE enhancements along with the coupling constants (*J*-values) of the NMR spectrum. The interpretation for the boat–chair conformation might be due to the bulky 3, 4, 5 ,8-tetrahydro-2*H*-oxocine group as equatorially disposed. The antioxidative activity of the non-isoprenoid oxocine carboxylate cyclic ether was found to be significantly greater as determined by DPPH and ABTS radical scavenging activities (IC_{50} ~ 0.3 mg/mL) compared to that displayed by α-tocopherol (IC_{50} > 0.6 mg/mL). The compound exhibited greater anti-inflammatory activity against COX-2 than COX-1 isoform, and therefore, the selectivity index remained significantly lesser (anti-COX-1 IC_{50}: anti-COX-2 IC_{50} 0.87) than synthetic anti-inflammatory drugs (0.02–0.44). No significant difference of *in vivo* 5-lipoxygenase activity (IC_{50} 0.95 mg/mL) than ibuprofen (IC_{50} 0.93 mg/mL) indicated the potential anti-inflammatory properties of the compound **K6**.

Chromatographic fractionation of the organic extract obtained from the thalli of *G. opuntia* yielded two furanyl derivatives, characterized as 5-(7-(5-ethyl-3, 4-dimethoxycyclooctyl) benzofuran-6-yl)-7-methyl-3, 4, 7, 8-tetrahydro-2*H*-oxocin-2-one (compound **G1)** and 2-(3-ethyl-9-(2-methoxyethoxy)-1-oxo-2, 3, 4, 9-tetrahydro-1*H*-xanthen-2-yl) ethyl-5-hydroxy-9-methoxy-7, 8-dimethyl-8-(5-methylfuran-2-yl) nona-3, 6-dienoate (compound **G2**) along with 3-(2-ethyl-6-((3, 7)-1, 2, 5, 6-tetrahydroazocin-5-yl) hexyl) morpholin-6-one (compound **G3**) and 2-acetoxy-2-(5-

acetoxy-4-methyl-2-oxotetrahydro-2*H*-pyran-4-yl) ethyl-4-(3-methoxy-2-(methoxymethyl)-7-methyl-3, 4, 4a, 7, 8, 8a-hexahydro-*2H*-chromen-4-yloxy)-5-methylheptanoate (compound **G4**). The isolated compounds were found to be the first furanyl natural products featuring methoxycyclooctyl benzofuran with tetrahydro-2*H*-oxocin framework and tetrahydro-1*H*-xanthenyl methoxy methylfuran skeletons. The compound **G1** was obtained as yellow oil, and its molecular ion peak at *m/z* 454 was deduced from the mass spectrum. The molecular formula of the isolated compounds was deduced as $C_{28}H_{38}O_5$ based on combined ^1H and ^{13}C NMR spectroscopic data. The IR spectrum displayed bending vibration appeared at 1741 cm^{-1}, which was attributed to the ester carbonyl group. The FTIR absorption bands at 1459 and 2856 cm^{-1} were attributed to the olefinic (>C=C<) as well as alkyl groups, respectively. The relative stereochemical configuration of the asymmetric centers, bearing the substituted furan ring framework was attributed by extensive NOESY experiments along with the coupling constants (*J*-values) in the ^1H NMR spectrum. The aromatic methine protons displayed NOESY correlations with the neighboring aromatic methane protons in the benzyl furan aromatic ring system. Compound **G2**, a previously undescribed furanyl derivative, was purified as yellow oil by extensive column chromatography on adsorbent silica gel. The mass spectral data of compound **G2** accounted for the molecular ion peak at *m/z* 636 enclosing fourteen degrees of unsaturation, and the molecular formula as $C_{37}H_{48}O_9$ was deduced from combined ^1H and ^{13}C NMR spectroscopic experiments. The IR spectrum showed bending vibration near 1708 cm^{-1}, which was attributed to the carbonyl group. The characteristic hydroxyl stretching vibration was recorded at 3425.10 cm^{-1}. The relative stereochemistries at chiral centers bearing the xanthenyl furanyl ring carbon skeleton were attributed by detailed NOESY correlations.

These studied compounds were assessed for anti-inflammatory activities against pro-inflammatory cyclooxygenase-2/5-lipoxygenase (COX-1, 2, and 5-LOX) and antioxidative effects in various *in vitro* models. The antioxidative properties of the furanyl derivatives as resolved by DPPH and ABTS free radical scavenging activities were found to be significantly greater (IC_{50} ~ 0.051–0.055 × 10^{-2} M) than those exhibited by α-tocopherol (IC_{50} > 0.146 × 10^{-2} M), and were similar to those displayed by the synthetic antioxidants BHT/ BHA (IC_{50} ~ 0.144–0.189 × 10^{-2} M, $P < 0.05$). The anti-inflammatory selectivity indices of the isolated compounds recorded significantly greater values (SI: anti-COX-1 IC_{50}/anti-COX-2 IC_{50} ~1.08–1.09) than NSAIDs

(aspirin, and ibuprofen, SI: 0.02 and 0.44, respectively, $P < 0.05$), and consequently, appeared to be safer. The isolated compounds showed significant anti-diabetic properties as determined by α-amylase/α-glucosidase ($IC_{50} < 0.052 \times 10^{-2}$ M) and dipeptidyl peptidase-4 (DPP-4, $IC_{50} < 0.002 \times 10^{-2}$ M) inhibitory activities. The angiotensin converting enzyme-I (ACE-I) inhibitory activity of the compounds (IC_{50} 0.023–0.024 $\times 10^{-2}$ M) was found to be comparable with that recorded by commercial ACE inhibitor, captopril (IC_{50} 0.037 $\times 10^{-2}$ M).

The molecular ion peak at *m/z* 320, which was combined with the detailed NMR experimental data to record the elemental composition of the compound **G3** with five degrees of unsaturation. The broad absorption band at 3425 cm^{-1} in the IR spectrum was attributed to the –NH groups, which has been supported by the ^{1}H NMR signal. The presence of –NH protons was further validated by D_2O exchange. The occurrences of two nitrogen groups were also satisfied by nitrogen odd and even rule. The comparative stereochemical configuration of the chiral centers belonging to 1, 2, 5, 6-tetrahydro azocin-5-yl-hexyl moiety, and morpholin-6-one ring framework were summarized from the NOE spectral experiments and the coupling constant values. The substituted azocinyl morpholinone recorded significant DPPH free radical scavenging activities (IC_{50} ~ 0.086 mg/mL) compared to the commercially available antioxidants, butylated hydroxyanisole, butylated hydroxytoluene, and α-tocopherol ($IC_{50} > 0.20$ mg/mL). The compound **G3** showed greater COX-2 inhibitory activity (IC_{50} 0.84 mg/mL) in conjunction with *in vitro* 5-lipoxygenase inhibitory activity (IC_{50} 0.85 mg/mL) than non-steroidal anti-inflammatory drugs (NSAIDs). The test compound had better selectivity index (COX-1/COX-2 ratio) (1.17 mg/mL) compared to those displayed by aspirin (0.02 mg/mL), sodium salicylate (0.73 mg/mL) and ibuprofen (0.44 mg/mL). The animals challenged with the substituted azocinyl morpholinone significantly mitigated the carrageenan-induced paw edema in time-dependent manner till the end of 6 h.

The compound **G4** showed absorption bands at 1715 cm^{-1} in the Fourier Transform Infrared (FTIR) spectrum due to the carbonyl functionalities. The IR stretching vibrations due to olefinic (C=C) and alkyl (C–H) groups were demonstrated by the absorption bands at 1458 and 2856 cm^{-1}, respectively. The molecular ion peak at *m/z* 640 in combination with its ^{1}H and ^{13}C NMR data designated the elemental composition of the compound **G4** as $C_{33}H_{52}O_{12}$. The detailed ^{1}H, ^{13}C NMR and mass spectral analysis confirmed the structure. The relative stereochemistries of the chiral

centres of the compound **G4**, assigned the chair-like conformation of the 2*H*-chromen derivative. The anti-inflammatory selectivity index of the compound **G4** was greater (SI: anti-cyclooxygense-1 IC_{50}/anti-cyclooxygense-2 IC_{50} ~ 1.26) than those exhibited by synthetic NSAIDs (aspirin and ibuprofen, SI: 0.02 and 0.44, respectively). The antioxidative activity of the compound **G4** was significantly greater as determined by DPPH and ABTS radical scavenging activities (IC_{50} 0.26–0.32 mg/mL) compared to α-tocopherol (IC_{50} > 0.6 mg/mL), and was comparable to the synthetic antioxidants BHT and BHA (IC_{50} ~ 0.25–0.34 mg/mL).

Antioxidant and anti-hypertensive potential of the sulfated polygalactans (**KA-1** and **GO-1**) isolated from the marine macroalgae *K. alvarezii* (**KA-1**) and *G. opuntia* (**GO-1**) was assessed by utilizing different *in vitro* systems. The intense absorption bands in the 1210-1260 cm^{-1} region of the fourier transform infrared spectra showed the vicinity of S=O group of sulfate esters. The sulfate group was situated at C-4 of (1→3)-linked galactopyranosyl residues of the native galactan, whereas the strong signals in the ^{1}H-NMR spectrum of *G. opuntia* (**GO-1**) attributed to the presence of strong -$COCH_3$ protons. Interestingly, very weak proton signals for *K. alvarezii* (**KA-1**) were assigned to be due to the -$COCH_3$ protons. As compared to the sulfated polygalactan isolated from *K. alvarezii* (**KA-1**), the one isolated from *G. opuntia* (**GO-1**) exhibited very sharp intense signals, which ascribed to be due to the vicinity of 2-*O*-methyl-α-(1-4)-linked 3, 6-anhydogalactose and 6-*O*-methyl-β-(1-3)-linked galactose residues. The anomeric carbon signals were found to be C-1 of α-D-galactose-4-sulfate, and this dyad was illustrative of a sulfated polygalactan. The galactans isolated from *K. alvarezii* (**KA-1**) possessed significantly greater antioxidative properties as determined by DPPH (**KA-1:** IC_{50} 0.97 mg/mL) and ABTS (**KA-1:** IC_{50} 0.72 mg/mL) scavenging activities than those isolated from *G. opuntia* (**GO-1**: DPPH IC_{50} 1.2 mg/mL and ABTS 0.86 mg/mL). The sulfated polygalactan →4)-4-*O*-sulfonato-(2-*O*-methyl)-β-D-galactopyranosyl-(1→4)-3, 6-anhydro-(2-*O*-methyl)-α-D-galactopyranan from *K. alvarezii* (**KA-1**) showed greater angiotensin-I-converting enzyme (ACE) inhibitory activity (**KA-1:** IC_{50} 0.02 μg/mL) than that displayed by →3)-4-*O*-sulfonato-(6-*O*-acetyl)- β-D-galactopyranosyl-(1→4)-3, 6-anhydro-(2-*O*-sulfonato)-α-D-galactopyranosyl-(1→3)-4-*O*-sulfonato-(6-*O*-acetyl)-β-D-xylosyl-(1→3)-4-*O*-sulfonato-(6-*O*-acetyl)-β-D-galactopyranosyl (1→4)-3, 6-anhydro-(2-*O*-sulfonato)-α-D-galactopyranan motif extracted from *G. opuntia* (**GO-1**: IC_{50} 0.70 μg/mL). Structure-activity correlation studies displayed that the ACE inhibitory properties of isolated

polygalactans were directly proportional to their electronic properties and inversely with the steric and hydrophobic characteristics. Putative ACE inhibitory mechanism of action of sulfated galactans from marine macroalgae corroborated the structure bioactivity correlation analysis.

Anti-diabetic and anti-inflammatory potential of sulfated polygalactans isolated from the red marine macroalgae *K. alvarezii* (**KA-2**) and *G. opuntia* (**GO-2**) were acquired by employing different *in vitro* systems. The strong absorption bands at 1210-1260 cm^{-1} of the FT-IR spectra demonstrated the region of S=O groups (attributed to the glycosidic linkage). The IR signals close to 3200-3400 cm^{-1} were credited to the region of -OH groups present in the sulfated polygalactans from the macroalgae. The broad bands at 3200-3400 cm^{-1} were found to be a result of the sulfated polygalactan units. The ^{1}H-NMR spectra of polysaccharides comprise of some well-resolved signals, counting those of anomeric protons. The ^{1}H-NMR spectrum of polysaccharides obtained from *K. alvarezii* (**KA-2**) got deshielded signals demonstrating the region of κ and ι monomer of sulfated polygalactans. Recognizable -*O*-alkyl signals (ideally –OCH_3) in the ^{1}H-NMR spectrum of galactan derivative from *G. opuntia* (**GO-2**) and *K. alvarezii* (**KA-2**) appropriately recognized the region of more conspicuous number of alkoxy substitutions in the sulfated polygactans from the red macroalgae. The ^{13}C NMR spectrum of polygalactans showed signals with specific multiplicities, which suggested the positional differences of 1→3 and 1→4 linked residues in the sulfation patterns. Based on the detailed NMR experiments the sulfated galactopyran motif of *G. opuntia* (**GO-2**) was designated as →3)-4-*O*-sulfonato-(6-*O*-acetyl)-β-D-galactopyranosyl-(1→4)-3, 6-anhydro-(2-*O*-sulfonato)-α-D-galactopyranosyl-(1→3)-4-*O*-sulfonato-(6-*O*-acetyl)-β-D-xylosyl-(1→3)-4-*O*-sulfonato-(6-*O*-acetyl)-β-D-galactopyranosyl-(1→4)-3, 6-anhydro-(2-*O*-sulfonato)-α-D- galactopyranan, whilst the one from *K. alvarezii* was demonstrated to be →4)-4-*O*-sulfonato-(2-*O*-methyl)-β-Dgalactopyranosyl-(1→4)-3, 6-anhydro-(2-*O*-methyl)-α-D-galactopyranan.

The sulfated galactopyran motif derived from *G. opuntia* possessed significant anti-diabetic properties as identified by α-amylase (**GO-2:** IC_{50} 0.04 mg/mL), α-glucosidase (**GO-2:** IC_{50} 0.09 mg/mL) and dipeptidyl peptidase-4 (**GO-2:** IC_{50} 0.09 mg/mL) inhibitory activities. The sulfated galactans from *G. opuntia* showed greater anti-inflammatory inhibitory activities as determined by cyclooxygenase-1 (**GO-2:** COX-1, IC_{50} 0.01 mg/mL), cyclooxygenase-2 (**GO-2:** COX-2, IC_{50} 0.03 mg/mL) and 5-lipoxygenase inhibitory activities (**GO-2:** IC_{50} 0.24 mg/mL). This study revealed that

the sulfated polygalactan enriched concentrate from *G. opuntia* could be used as potential therapeutic candidate to suppress the hyperglycemic response in diabetic conditions and inflammatory activity.

Two sulfated polygalactan derivatives characterized as 1, 3-*O*-diacetyl-2, 5, 6-tri hydroxyl-β-D-galactose-4-sulfate (**KA-3$_A$**) and 1, 3, 5-*O*-triacetyl-4-hydroxyl-6-*O*-methyl-D-galactose-2-sulfate (**GO-3$_A$**), were furthermore purified from *K. alvarezii* and *G. opuntia*, respectively, and were spectroscopically characterized. The compound **KA-3$_A$** showed absorption bands at 1712 cm^{-1} in the Fourier Transform Infrared (FTIR) spectrum due to the carbonyl functionalities. The molecular ion peak at *m/z* 345 in combination with its ^{1}H and ^{13}C NMR data designated the elemental composition of the compound **KA-3$_A$** as $C_{10}H_{17}O_{11}S$. The compound **GO-3$_A$** showed molecular ion peak at *m/z* 401, which in combination with its ^{1}H and ^{13}C NMR data designated the elemental composition of the compound **GO-3$_A$** as $C_{13}H_{21}O_{12}S$. The polygalactan from *K. alvarezii* (**KA-3**) showed greater inhibitory properties against angiotensin-I (IC_{50} 0.04 mg/mL) in comparison with polygalactan from *G. opuntia* (**GO-3**: IC_{50} 0.07 mg/mL). The anti-diabetic potential of polygalactan (**KA-3**), measured in terms of the inhibitory activities against dipeptidyl peptidase-4 was found to be greater (**KA-3:** IC_{50} 0.17 mg/mL) when compared with standard diprotein-A (IC_{50} 0.24 mg/mL). Likewise, the polygalactan derivatives showed higher α-amylase inhibitory activities (**KA-3:** $IC_{50} < 1$ mg/mL) when compared with the standard acarbose (IC_{50} 1.39 mg/mL).

Marine macroalgae-derived bioactive leads with potential therapeutic properties demonstrated to possess advantageous as functional food with added health benefits. Novel secondary bioactive metabolites from the marine macroalgae are attracting attention because of the growing demand for new compounds of 'marine natural' origin, having potential applications in pharmaceutical fields, and concerns about the toxic effects by synthetic drugs and their derivatives. Considering the promising perspective for the utilization of these groups of organisms, and limited research reports on their utilization as potential health food, their pharmaceutical potential began to receive considerable attention. The present study envisaged a systematic approach involving chemical profiling of two major species of red marine macroalgae *K. alvarezii* and *G. opuntia*, for bioactive pharmacophore leads for activity against various oxidative stress-induced diseases with a focus on hypertension, diabetes, inflammation, and a library of small molecular weight compounds with bioactive potential. The lead molecules were isolated to homogeneity and characterized using combined

chromatographic and spectroscopic experiments, whereas the novel leads were validated through bioassay and structure-activity relationship analyses to enrich the pool of bioactive leads. This research work also developed protocols to isolate and characterize polysaccharide compounds with bioactive properties against various drug targets for use against hypertension, diabetes, antioxidants and inflammatory pathologies. Furthermore, the discovery of new bioactive compounds from marine metabolites will form the basis for new drug leads. Thus, the new compounds will absolutely compose an abundant resource for future bioactivity research and drug development.

REFERENCES

Abad MJ, Bedoya LM, Bermejo P (2008). Natural marine anti-inflammatory products. Mini Review in Medicinal Chemistry, 8:740-754.

Abdel-Mageed WM, Ebel R, Valeriote FA, Jaspars M (2010). Laurefurenynes A-F, new cyclic ether acetogenins from a marine red alga, *Laurencia* sp. Tetrahedron, 66:2855-2862.

Abu Soud RS, Hamdan II, Afifi FU (2004). Alpha amylase inhibitory activity of some plant extracts with hypoglycemic activity. Scientia Pharmaceutica, 72:25-53.

Aguillar F, Crebelli R, Dusemund B, Galtier P, Gilbert J, Gott DM, Gundert-Remi U, Koenig J, Lambre C, Leblanc JC, Mortensen A, Mossesso P, Parent-Massin D, Rietjens IMCM, Stankovic I, Tobbcak P, Waalkens-Berendsen I, Woutersen RA, Wright M (2012). Scientific opinion on the re-evaluation of butylated hydroxytoluene BHT (E321) as a food additive. European Food Safety Authority Journal, 10:2392-2588.

Aknin M, Samb A, Mirailles J, Costantino V, Fattorusso E, Mangoni A (1992). Polysiphenol, a new brominated 9, 10-dihydrophenanthrene from the Senegalese red alga *Polysyphonia ferulacea*. Tetrahedron Letters, 33:555-558.

Alarif WM, Al-Lihaibi SS, Abdel-Lateff A, Ayyad SE (2011). New antifungal cholestane and aldehyde derivatives from the red alga *Laurencia papillosa*. Natural Product Communication, 6:1821-1824.

Allan RD, Correl RL, Wells RJ (1969). A new class of quinones from certain members of the family *Cyperaceae*. Tetrahedron Letters, 53:4669-4672.

Aller MA, Arias JL (2006). The inflammatory response: An efficient way of life. Medical Science Monitor, 12:225-234.

Ames BN, Shinenaga MK, Hagen TM (1993). Oxidants antioxidants and the degenerative diseases of aging. Proceeding of the National Academy of Sciences, USA, 90:7915-7922.

Amico V, Caccamese S, Neri P, Russo G, Foti M (1991). Brasilane type sesquiterpenoids from the Mediterranean red alga *Laurencia obtusa*. Phytochemistry, 30:1921-1927.

Ananthi S, Rao H, Raghavendran B, Sunil AG, Gayathri V, Ramakrishnan G (2010). *In vitro* antioxidant and *in vivo* anti-inflammatory potential of crude polysaccharide from *Turbinaria ornata* (Marine Brown Alga). Food and Chemical Toxicology, 48:187-192.

Anton R, Barlow S, Boskou D, Castle L, Crebelli R, Dekant W, Engel KH, Forsythe S, Grunow W, Larsen JC, Leclercq C, Mennes W, Milana MR, Rietjens I, Svensson K, Tobback P, Toldra F (2004). Opinion of the scientific palen on food additives, flavourings, processing aids and materials in contact with food on a request from the commission related to tertiary-butylhidroquinone (TBHQ). European Food Safety Authority Journal, 84:1-50.

Antunes AM, Afolayan AF, Chiwakata MT, Fakee J, Knott MG, Whibley CE, Hendricks DT, Bolton JJ, Beukes DR (2011). Identification and *in vitro* anti-esophageal cancer activity of a series of halogenated monoterpenes isolated from the South African seaweeds *Plocamium suhrii* and *Plocamium cornutum*. Phytochemistry, 72:769-772.

Apostolidis E, Karayannakidis PD, Kwon YI, Lee CM, Seeram NP (2011). Seasonal variation of phenolic antioxidant-mediated α-glucosidase inhibition of *Ascophyllum nodosum*. Plant Foods for Human Nutrition, 66:313-319.

Ashokkumar R, Ramaswamy M (2014). Phytochemical screening by FTIR spectroscopic analysis of leaf extracts of selected Indian medicinal plants. International Journal of Current Microbiology and Applied Sciences, 3:395-406.

Ask EI, Azanza RV (2002). Advances in cultivation technology of commercial eucheumatoid species: A review with suggestions for future research. Aquaculture, 206:257-277.

Astill BD, Fassett DW, Roudabush RL (1959). The metabolism of 2:4:5 trihydroxybutyrophenone in the rat and dog. Biochemical Journal, 72:451-459.

Ayyad SE, Al-Footy KO, Alarif WM, Sobahi TR, Bassaif SA, Makki MS, Asiri AM, Al Halwani AY, Badria AF, Badria FA (2011). Bioactive C_{15} acetogenins from the red alga *Laurencia obtusa*. Chemical and Pharmaceutical Bulletin, 59:1294-1298.

Bandoniene D, Murkovic M (2002). On-line HPLC-DPPH screening method for evaluation of radical scavenging phenols extracted from apples (*Malus domestica L*). Journal of Agricultural Food Chemistry, 50:2482-2487.

Bansemir A, Blume M, Schroder S, Lindequist U (2006). Screening of cultivated seaweeds for antibacterial activity against fish pathogenic bacteria. Aquaculture, 252:79-84.

Baruchel S, Wainberg MA (1992). The role of oxidative stress in disease. American Journal of Gastroenterology, 81:907-919.

Baylac S, Racine P (2003). Inhibition of 5-lipoxygenase by essential oils and other natural fragment extracts. International Journal of Aromatherapy, 13:138-142.

Bellion C, Brigand G, Prome JC, Welti D, Bociek S (1983). Identification characterization des precurseurs biologiques des carraghenanes par spectroscopie. Carbohydrate Research, 119:31-48.

Berge JP, Debiton E, Dumay J, Durand P, Barthomeuf C (2002). *In vitro* anti-inflammatory and anti-proliferative activity of sulfolipids from the red alga *Porphyridium cruentum*. Journal of Agricultural and Food Chemistry, 50:6227-6232.

Bilan MI, Grachev AA, Ustuzhanina NE, Shashkov AS, Nifantiev NE, Usov AI (2004). A highly regular fraction of a fucoidan from the brown seaweed *Fucus distichus L*. Carbohydrate Research, 339:511-517.

Bitencourt Fda S, Figueiredo JG, Mota MR, Bezerra CC, Silvestre PP, Vale MR, Nascimento KS, Sampaio AH, Nagano CS, Saker-Sampaio S (2008). Antinociceptive and anti-inflammatory effects of a mucin-binding agglutinin isolated from the red marine alga *Hypnea cervicornis*. Naunyn Schmiedebergs Archives of Pharmacology, 377:139-148.

Blackman J, Matthews DJ (1982). Halogenated phloroglucinols from *Rhabdonia verticillata*. Phytochemistry, 21:2141-2142.

Blondin C, Fischer E, Boisson-Vidal C, Kazatchkine MD, Jozefonvicz J (1994). Inhibition of complement activation by natural sulfated polysaccharides (fucans) from brown seaweed. Molecular Immunology, 31:247-253.

Blouin NA, Brodie JA, Grossman AC, Xu P, Brawley SH (2011). Porphyra: A marine crop shaped by stress. Trends in Plant Science, 16:29-37.

Blunt JW, Copp BR, Hu W, Munro MHG, Northcote PT, Prinsep M (2008). Marine natural products. Natural Product Report, 25:35-94.

Blunt JW, Copp BR, Keyzers RA, Munro MHG, Prinsep MR (2014). Marine natural products. Natural Product Report, 31:160-258.

Blunt JW, Copp BR, Munro MHG, Northcote PT, Prinsep M (2005). Marine natural products. Natural Product Report, 22:15-61.

Blunt JW, Copp BR, Munro MHG, Northcote PT, Prinsep MR (2006). Marine natural products. Natural Product Report, 23:26-78.

Blunt JW, Hartshorn MP, McLennan TJ, Munro MHG, Robinson WT, Yorke SC (1978). Thyrsiferol: A squalene-derived metabolite of *Laurencia thyrsifera*. Tetrahedron Letters, 1:69-72.

Blunt JW, Lake RJ, Munroe MHG, Yorke SC (1981). A new vinyl acetylene from the red alga *Laurencia thyrsifera.* Australian Journal of Chemistry, 34:2393-2400.

Blunt JW, Copp BR, Keyzers RA, Munro MH, Prinsep MR (2016). Marine natural products. Natural Product Report, 33:382-431.

Brennan MR, Erickson KL (1982). Austradiol acetate and austradiol diacetate, 4,6-dihydroxy-(+)-selinane derivatives from an Australian *Laurencia* sp. Journal of Organic Chemistry, 47:3917-3921.

Burreson BJ, Woolard FX, Moore RE (1975). Chondrocole A and B, two halogenated dimethylhexahydrobenzofurans from the red alga *Chondrococcus hornemanni* (mertens) Schmitz. Tetrahedron Letters, 26:2155-2158.

Burritt RL, Hahn T, Schaltegger St (2002). Towards a comprehensive framework for environmental management accounting-links between business actors and environmental management accounting tools. Australian Accounting Review, 12:39-50.

Buschmann AH, Correa JA, Westermeier R, Hernandez-Gonzalez MC, Norambuena R (2001). Red algal farming in chile: A review. Aquaculture, 194:203-220.

Caccamese S, Azzolina R, Duesler EN, Paul IC, Rinehart KL (1980). Laurencienyne, a new acetylenic cyclic ether from the marine red alga *Laurencia obtuse*. Tetrahedron Letters, 21:2299-2302.

Cafieri F, Ciminiello P, Santacroce C, Fattorusso E (1982). (1S)-1, 2-Dihydro-1-hydroxybromosphaerol, a minor bromoditerpene from the red alga *Sphaerococcus coronopifolius.* Phytochemistry, 21:2412-2413.

Cafieri F, Ciminiello P, Santacroce C, Fattorusso E (1983). Three diterpenes from the red alga *Sphaerococcus coronopifolius*. Phytochemistry, 22:1824-1825.

Cafieri F, De Napoli L, Fattorusso E, Impellizzeri G, Piattelli M, Sciuto S (1977). Bromosphaerodiol, a minor bromo compound from the red alga *Sphaerococcus coronopifolius.* Experientia, 33:1549-1550.

Cahyana AH, Shuto Y, Kinoshita Y (1992). Pyropheophytin as an antioxidative substance from the marine algae, *Arame* (*Eisenia bicyclis*). Bioscience Biotechnology and Biochemistry, 56:1533-1535.

Cai YZ, Mei S, Jie X, Luo Q, Corke H (2006). Structure-radical scavenging activity relationships of phenolic compounds from traditional Chinese medicinal plants. Life Sciences, 78:2872-2888.

Capon R, Ghisalberti EL, Jefferies PR, Skelton BW, White AH (1981). Sesquiterpene metabolites from *Laurencia filiformis*. Tetrahedron, 37:1613-1621.

Cardellina JH, Horsley SB, Clardy J, Leftow SR, Meinwald J (1982). Secondary metabolites from the red alga *Laurencia intricata*: Halogenated enynes. Canadian Journal of Chemistry, 60:2675-2677.

Carocho M, Ferreira ICFR (2013). A review on antioxidants, prooxidants and related controversy: Natural and synthetic compounds, screening and analysis methodologies and future perspectives. Food and Chemical Toxicology, 51:15-25.

Carter GT, Rinehart KL, Jr, Li LH, Kuentzel SL (1978). Brominated indoles from *Laurencia brongniartii*. Tetrahedron Letters, 46:4479-4482.

Cases MR, Cerezo AS, Stortz CA (1995). Separation and quantitation of enantiomeric galactoses and their mono-*O*-methylethers as their diastereomeric acetylated 1-deoxy-1-(2- hydroxypropylamino) alditols. Carbohydrate Research, 269:333-341.

Castro P, Huber ME (2013). Marine biology. McGraw-Hill, New York, pp 102-113.

Cavalcante-Silva LH, da Matta CB, de Araujo MV, Barbosa-Filho JM, de Lira DP, de Oliveira Santos BV, de Miranda GE, Alexandre-Moreira MS (2012). Ceptive and anti-inflammatory activities of crude methanolic extract of red alga *Bryothamnion triquetrum*. Marine Drugs, 10:1977-1992.

Cen Pacheco F, Villa–Pulgarin JA, Mollinedo F, Norte Martın M, Fernandez JJ, Daranas AH (2011). New polyether triterpenoids from *Laurencia viridis* and their biological evaluation. Marine Drugs, 9:2220-2235.

Chakraborty K, Joseph D (2013). Antioxidant activities and phenolic contents of three red seaweeds (Division: Rhodophyta) harvested from the Gulf of Mannar of Peninsular India. Journal of Food Science and Technology, 52:1924-1935.

Chakraborty K, Joseph D, Chakkalakal SJ (2014). Toxicity profile of a nutraceutical formulation derived from green mussel *Perna viridis*. BioMed Research International, 2016:1-14.

Chakraborty K, Joseph D, Joy M, Raola VK (2016). Characterization of substituted aryl meroterpenoids from red seaweed *Hypnea musciformis* as potential antioxidants. Food Chemistry, 212:778-788.

Chakraborty K, Joseph D, Praveen NK (2015). Antioxidant activities and phenolic contents of three red seaweeds (Division: Rhodophyta) harvested from the Gulf of Mannar of Peninsular India. Journal of Food Science and Technology, 52:1924-1935.

Chakraborty K, Lipton AP, Paulraj R, Chakraborty RD (2010). Guaiane sesquiterpenes from seaweed *Ulva fasciata Delile* and their antibacterial properties. European Journal of Medicinal Chemistry, 45:2237-2244.

Chakraborty K, Paulraj R (2010). Sesquiterpenoids with free-radical scavenging properties from marine macroalga *Ulva fasciata Delile*. Food Chemistry, 122:31-41.

Chandrasekaran S, Nagendran AN, Pandiaraja D, Krishnankutty N, Kamalakannan B (2008). Bioinvasion of *Kappaphycus alvarezii* on corals in the Gulf of Mannar, India. Current Science, 94:1167-1172.

Chapman V, Chapman DJ (1980). Sea vegetables (algae as food for man). In Seaweeds and their Uses, pp 62-97.

Charles DH, Babajide OO, Donna VE, David M, Jon C (1980). Vafzelin, uvafzelin novel constituents of *Uvaria afzelii*. Journal of the American Chemical Society, 102:7365-7367.

Chatter R, Ben Othman R, Rabhi S, Kladi M, Tarhouni S, Vagias C, Roussis V, Guizani-Tabbane L, Kharrat R (2011). *In vivo* and *in vitro* anti-inflammatory activity of neorogioltriol, a new diterpene extracted from the red algae *Laurencia glandulifera*. Marine Drugs, 9:1293-1306.

Chaves Lde S, Nicolau LA, Silva RO, Barros FC, Freitas AL, Aragao KS, Ribeiro Rde A, Souza MH, Barbosa AL, Medeiros JV (2013). Antiinflammatory and antinociceptive effects in mice of a sulfated polysaccharide fraction extracted from the marine red algae *Gracilaria caudata*. Immunopharmacology Immunotoxicology, 35:93-100.

Chen D, Wu XZ, Wen ZY (2008). Sulfated polysaccharides and immune response: Promoter or inhibitor. Panminerva Medica, 50:177-183.

Chen Q, Ke L, Song K, Huang H, Liu X (2004). Inhibitory effects of hexylresorcinol and dodecylresorcinol on mushroom (*Agaricus bisporus*) tyrosinase. The Protein Journal, 23:135-141.

Cheng JF, Ishikawa A, Ono Y, Thomas A, Alex N (2003). Novel chromen derivatives as TNF-α inhibitors. Bioorganic and Medicinal Chemistry Letters, 13:3647-3650.

Chevolot-Magueur M, Cave A, Potier P, Teste J, Chiaroni A, Riche C (1976). Composes bromes de *Rytiphlea tinctoria* (Rhodophyceae). Phytochemistry, 15:767-771.

Chew YL, Lim YY, Omar M, Khoo KS (2008). Antioxidant activity of three edible seaweeds from two areas in South East Asia. LWT Food Sciences and Technology, 41:1067-1072.

Chiovitti A, Bacic A, Craik DJ, Kraft GT, Liao ML, Falshaw R (1998). A pyruvated carrageenann from Australian specimens of the red alga *Sarconema filiforme*. Carbohydrate Research, 310:77-83.

Cho M, Han JH, You S (2011). Inhibitory effects of fucan sulfates on enzymatic hydrolysis of starch. Food Science and Technology, 44:1164-1171.

Choi EM, Kim AJ, Kim YO, Hwang JK (2005). Immunomodulating activity of arabinogalactan and focoidan *in vitro*. Journal of Medicinal Food, 8:446-453.

Christoph QS, Messmer Ruth, Bracher Franz, Krauss Jurgen (2007). A new approach to furan-containing macrolactones. Turkish Journal of Chemistry, 31:251-256.

Cinq-Mars CD, Hu C, Kitts DD, Li-Chan EC (2008). Investigations into inhibitor type and mode, simulated gastrointestinal digestion, and cell transport of angiotensin-I converting enzyme-inhibitory peptides in pacific hake (*Meriuccius productus*) fillet hydrolysate. Journal of Agricultural Food Chemistry, 56:410-419.

Clausen DJ, Wan S, Floreancig PE (2011). Total synthesis of the protein phosphatase 2A inhibitor lactodehydrothyrsiferol. Angewandte Chemie International Edition, 50:5178-5181.

Combaut G, Chantraine JM, Teste J, Soulier J, Glombitza KW (1978). Structure et conformation du dihydro-10, 15 tribromo-1, 6, 11 hexamethoxy-2, 3, 7, 8, 12, 13-5h-tribenzo [a,d,g] cyclononene. Tetrahedron Letters, 19:1699-1701.

Conforty F, Loizzo MR, Statty GA, Menichini F (2005). Comparative radical scavenging and antidiabetic activities of methanolic extract and fractions from *Achillea ligustica*. Biological and Pharmaceutical Bulletin, 28:1791-1794.

Cordero PA (2003). Encyclopedia of Food Sciences and Nutrition (Second Edition) 2003, pp 3726-3728.

Cornish ML, Garbary DJ (2010). Antioxidants from macroalgae: Potential applications in human health and nutrition. Algae, 25:155-171.

Cox PJ, Imre S, Islimyeli S, Thomson RH (1982). Obtusallene I, a new halogenated allene from *Laurencia Obtusa*. Tetrahedron Letters, 23:579-580.

Crews P (1977). Monoterpene halogenation by the red alga *Plocamium oregonum*. Journal of Organic Chemistry, 42:2634-2639.

Crews P, Kho-Wiseman E (1977). Acyclic polyhalogenated monoterpenes from the red algae *Plocamium violaceum*. Journal of Organic Chemistry, 42:2812-2815.

Crews P, Kho-Wiseman E, Montana P (1978). Halogenated alicyclic monoterpenes from the red algae (*Plocamium cartilagineum, Plocamium violaceum*). Journal of Organic Chemistry, 43:116-120.

Critchley AT, Ohno M (1998). Seaweed resources of the world. Yokosuka, Japan, Japan International Cooperation Agency, pp 429.

Crook M (2004). Type 2 diabetes mellitus: A disease of the innate immune system an update. Diabetic Medicine, 21:203-207.

Cumashi A, Ushakova NA, Preobrazhenskaya MEA (2007). Comparative study of the anti-inflammatory, anticoagulant, antiangiogenic, and antiadhesive activities of nine different fucoidans from brown seaweeds. Glycobiology, 17:541-552.

Daigo K (1959). Constituents of *Chondria arnata I*. Detection of anthelmintic constituents. Yakuga Zasshi, 79:350-353.

Davis SN, Granner DK (2001). Insulin, oral agents and the pharmacology of the endocrine pancreas. In: Hardman JG, Limbird LE, Gilman AG, editors. Goodman and Gilman's the pharmacological basis of therapeutics. 10th ed. New York: McGraw-Hill Co. Incorp, pp 1679-1714.

Davyt D, Fernandez R, Suescun L, Mombru AW, Saldana J, Dominguez L, Coll J, Fujii MT, Do Manta E (2001). New sesquiterpene derivatives from the red alga *Laurencia scoparia*. Isolation, structure determination and anthelmintic activity. Journal of Natural Product, 64:1552-1555.

De Sousa AA, Benevides NM, de Freitas Pires A, Fiuza FP, Queiroz MG, Morais TM, Pereira MG, Assreuy AM (2013). Galactan from marine alga *Gelidium crinale* with *in vivo* anti-inflammatory and antinociceptive effects. Fundamental and Clinical Pharmacology, 27:173-180.

De Souza MCR, Marques CT, Dore CMG, Da Silva FRF, Rocha HAO, Leite E (2007). Antioxidant activities of sulphated polysaccharides from brown and red seaweeds. Journal of Applied Phycology, 19:153-160.

De-Nys R, Wright AD, Konig GM, Sticher (1993). New halogenated furanones from the marine alga *Delisea pulchra* (cf. fmbriata). Tetrahedron, 49:11213-11220.

Dodgson KS (1961). Determination of inorganic sulphate in studies on the enzymic and non-enzymic hydrolysis of carbohydrate and other sulphate esters. Biochemical Journal, 78:312-319.

Dong HQ, Li M, Zhu F, Liu FL, Huang JB (2012). Inhibitory potential of trilobatin from *Lithocarpus polystachyus* Rehd against α-glucosidase and α-amylase linked to type 2 diabetes. Food Chemistry, 130:261-266.

Dubois M, Gilles KA, Hamilton JK, Rebers PA, Smith F (1956). Colorimetric method for determination of sugar and related substances. Analytical Chemistry, 28:350-356.

Dunlop RW, Murphy PT, Wells RJ (1979). A new polyhalogenated monoterpene from the red alga *Plocamium angustum*. Australian Journal of Chemistry, 32:2735-2739.

Ebada SS, Lin WH, Proksch P (2010). Bioactive sesterterpenes and triterpenes from marine sponges: Occurrence and pharmacological significance. Marine Drugs, 8:313-346.

Elliot RH, Strunin L (1993). Hepatotoxicity of volatile anaesthetics. British Journal of Anaesthaesia, 70:339-349.

Erickson KL (1983). Constituents of *Laurencia*. In: Scheuer PJ (ed) Marine Natural Products: Chemical and Biological Perspectives. Academic Press, New York, NY, pp 131-257.

Escrig AJ, Jimenez IJ, Pulido R, Calixto FS (2001). Antioxidant activity of fresh and processed edible seaweeds. Journal of the Science of Food and Agriculture, 81:530-534.

Evan AP, Gardner KD (1979). Nephron obstruction in nordihydroguaiaretic acid induced renalcystic disease. Kidney International, 15:7-19.

Farah Diyana A, Abdullah A, Shahrul Hisham ZA, Chan KM (2015). Antioxidant activity of red algae *Kappaphycus alvarezii* and *Kappaphycus striatum*. International Food Research Journal, 22:1977-1984.

Faulkner DJ (1984). Marine natural products: Metabolites of marine algae and herbivorous marine mollusks. Natural Product Reports, 1:251-280.

Fenical W, Schulte GR, Finer J, Clardy J (1978). Poitediol, a new nonisoprenoid sesquiterpene diol from the marine alga *Laurencia poitei*. Journal of Organic Chemistry, 43:3628-3630.

Ferreira ALG, Loureiro S, Soares AMVM (2012). Toxicity prediction of binary combinations of cadmium, carbendazim and low dissolved oxygen on *Daphniamagna*. Aquatic Toxicology, 89:28-39.

Festa AD, Agostino R, Howard G, Mykkanen L, Tracy, RP, Haffner SM (2000). Chronic subclinical inflammation as part of the insulin resistance syndrome: The Insulin Resistance Atherosclerosis Study (IRAS). Circulation, 102:42-47.

Fitz Gerald GA (2004). Coxibs and cardiovascular disease. The New England Journal of Medicine, 351:1709-1711.

Fleurence J (1999). Seaweed proteins: Biochemical, nutritional aspects and potential uses. Trends in Food science and Technology, 102:5-28.

Florence TM (1995). The role of free radicals in disease. Australian and New Zealand Journal of Ophthalmology, 23:3-7.

Fosslien E (2005). Cardiovascular complications of non-steroidal anti-inflammatory drugs. Annals of Clinical and Laboratory from red seaweed *Hypnea musciformis* as potential antioxidants. Food Chemistry, 212:778-788.

Fournet I, Gall EA, Deslandes E, Huvenne JP, Sombret B, Floch JY (1997). *In situ* measurements of cell wall components in the red alga *Solieria chordalis* (Solieriaceae, Rhodophyta) by FTIR micro spectrometry. Botanica Marina, 40:45-48.

Frias JP, Sobral P, Ferreira AM (2010). Organic pollutants in microplastics from two beaches of the Portuguese coast. Marine Pollution Bulletin, 60:1988-1992.

Fry DE (1992). Multiple system organ failure. In: Fry DE (ed). Mosby year book, St Louis, Missouri, pp 3-14.

Fukuzawa A, Kumagai Y, Masamune T, Furusaki A, Katayama C, Matsumoto T (1981). Acetylpinnasterol and pinnasterol, ecdysone-like metabolites, from the

marine red alga *Laurencia pinnata* Yamada. Tetrahedron Letters, 22:4085-4086.

Fukuzawa A, Kumagai Y, Masamune T, Furusaki A, Matsumoto T, Katayama C (1982). Pinnaterpenes A, B and C: New dibromoditerpenes from the red algal *Laurencia pinnata* Yamada. Chemistry Letters, 11:1389-1392.

Fukuzawa, Masamune T (1981). Laurepinnacin and isolaurepinnacin, new acetylenic cyclic ethers from the marine red alga *Laurencia pinnata* Yamada. Tetrahedron Letters, 22:4081-4084.

Ganesan P, Chandini SK, Bhaskar N (2008). Antioxidant properties of methanol extract and its solvent fractions obtained from selected Indian red seaweeds. Bioresource Technology, 99:2717-2723.

Ganesan S, Thiruppathi K, Eswaran CRK, Reddy B, Jha (2009). Cultivation of *Gelidiella acerosa* in the open sea on the southeastern coast of India. Marine Ecology Progress Series, 382:49-57.

Gershenzon J, Dudareva N (2007). The function of terpene natural products in the natural world. Nature Chemical Biology, 3:408-414.

Gharavi N, El-Kadi AOS (2005). Tert-Butylhydroquinone is a novel aryl hydrocarbon receptor ligand. Drug Metabolism and Disposition, 33:365-372.

Gomez-ordonez E, Rupere P (2011). FT-IR-ATR spectroscopy as a tool for polysaccharide identification in edible brown and red seaweeds. Food Hydrocolloids, 25:1514-1520.

Gonzalez AG, Aguiar JM, Darias J, Gonzalez E, Martin JD, Martin VS, Perez C, Fayos J, Martinez-Ripoll M (1978). Perforenol, a new polyhalogenated sesquiterpene from *Laurencia perforate*. Tetrahedron Letters, 19:3931-3934.

Gonzalez AG, Martin JD, Martin VS, Martinez-Ripoll M, Fayos J (1979a). X ray study of sesquiterpene constituents of the alga *Laurencia obtusa* leads to structure revision. Tetrahedron Letters, 20:2717-2718.

Gonzalez AG, Martin JD, Martin VS, Norte M (1979b). Carbon-13 NMR application to *Laurencia* polyhalogenated sesquiterpenes. Tetrahedron Letters, 20:2719-2722.

Gonzalez AG, Martin JD, Ptrez C, Ramirez MA, Ravelo P (1980). Total synthesis of 8-desoxy-isocaespitol, a new polyhalogenated sesquiterpene from *Laurencia caespitosa*. Tetrahedron Letters, 21:187-188.

Gonzalez G, Martin JD, Martin VS, Norte M, Perez R, Ruano JZ, Drexler SA, Clardy J (1982). Non-terpenoid C-15 metabolites from the red seaweed *Laurencia pinnatifida*. Tetrahedron, 38:1009-1014.

Gonzalez R, Rodriguez S, Romay C, Ancheta O, Gonzalez A, Armesta J, Remirez D, Merino N (1999). Anti-inflammatory activity of phycocyanin extract in acetic acid-induced colitis in rats. Pharmacological Research, 39:55-59.

Gregson RP, Marwood JF, Quinn RJ (1979). The occurrence of prostaglandins PGE_2 and $PGF_{2\alpha}$ in a plant-the red alga *Gracilaria lichenoides*. Tetrahedron Letters, 20:4505-4506.

Gressler V, Yokoya NS, Fujii MT, Colepicolo P, Mancini J, Torres RP, Pinto E (2010). Lipid, fatty acid, protein, amino acid and ash contents in four Brazilian red algae species. Food Chemistry, 120:585-590.

Guiry MD, Guiry GM (2016). Algae Base World-wide electronic publication. Galway: National University of Ireland.

Gutierrez-Cepeda A, Fernandez JJ, Gil LV, Opez- Rodrıguez ML, Norte M, Souto LM (2011a). Nonterpenoid C_{15} acetogenins from *Laurencia marilzae*. Journal of Natural Product, 74:441-448.

Gutierrez-Cepeda A, Fernandez JJ, Norte M, Souto ML (2011b). New Bicyclotridecane C_{15} Nonterpenoid Bromoallenes from *Laurencia marilzae*. Organic Letters, 13:2690-2693.

Guven KC, Bora A, Sunam G (1969). Alkaloid content of Marine algae. I. Hordenine from *Phyllophera nervosa*. Eczacihk Bulletin, 11:177-184.

Guven KC, Percot A, Sezik E (2010). Alkaloids in marine algae. Marine Drugs, 8:269-284.

Hamdan II, Afifi FU (2004). Studies on the *in vitro* and *in vivo* hypoglycemic activities of some medicinal plants used in treatment of diabetes in Jordanian traditional medicine. Journal of Ethnopharmacology, 93:117-121.

Hansch C, Caldwell J (1991). The structure-activity relationship of inhibitors of serotonin uptake and receptor binding. Journal of Computer Aided Molecular Design, 5:441-453.

Heo SJ, Cha SH, Lee KW, Jeon YJ (2006). Antioxidant activities of red algae from Jeju Island. Korean Society of Phycology, 21:149-156.

Higgs MD, Mulheirn LJ (1981). Hybridalactone, An unusual fatty acid metabolite from the red alga *Laurencia hybrida* (Rhodophyta, Rhodomelaceae). Tetrahedron, 37:4259-4262.

Higgs MD, Vanderah DJ, Faulkner DJ (1977). Polyhalogenated monoterpenes from *Plocamium cartilagineum* from the British coast. Tetrahedron, 33:2775-2780.

Holdt SL, Kraan S (2011). Bioactive compounds in seaweed: Functional food applications and legislation. Journal of Applied Phycology, 23:543-597.

Horsley SB, Cardellina JH, Meinwald J (1981). Secondary metabolites from a red alga (*Laurencia intricate*): Sesquiterpene alcohols. Journal of Organic Chemistry, 46:5033-5035.

Horton R (2004). Vioxx, the implosion of Merck, and aftershocks at the FDA. The Lancet, 364:1995-1996.

Howard BM, Fenical W (1978a). Obtusadiol, a unique bromoditerpenoid from the marine red alga *Laurencia obtusa*. Tetrahedron Letters, 19:2453-2456.

Howard BM, Fenical W (1978b). Structures of the irieols, new dibromoditerpenoids of a unique skeletal class from the marine red alga *Laurencia irieii*. Journal of Organic Chemistry, 43:4401-4408.

Howard BM, Fenical W (1979). Guadalupol and epiguadalupol, rearranged sesquiterpene alcohols from *Laurencia snyderiae var. guadalupensis.* Phytochemistry, 18:1224-1225.

Howard BM, Fenical W (1980). Isoconcinndiol, a brominated diterpenoid from *Laurencia snyderae var. guadalupensis*. Phytochemistry, 19:2774-2776.

Howard M, Schulte GR, Fenical W, Solheim B, Clardy J (1980). Three new vinyl acetylenes from the marine red alga *Laurencia*. Terrahedron, 36:1747-1751.

Huang R, Mendis E, Kim SK (2005). Improvement of ACE inhibitory activity of chitooligosaccharides (COS) by carboxyl modifications. Bioorganic Medicinal Chemistry, 13:3649-3655.

Hulsmans M, Van Dooren E, Holvoet P (2012). Mitochondrial reactive oxygen species and risk of atherosclerosis. Current Atherosclerosis Reports, 14:264-276.

Idris I, Donnelly R (2007). Dipeptidyl peptidase-4 inhibitors: A major new class of oral antidiabetic drug. Diabetes, Obesity and Metabolism, 9:153-165.

Iliopoulou D, Vagias C, Harvala C, Roussis V (2002). C_{15} acetogenins from the red alga *Laurencia obtusa*. Phytochemistry, 59:111-116.

Islam MN, Ishita IJ, Jin SE, Choi RJ, Lee CM, Kim YS, Jung HA, Choi JS (2013). Anti-inflammatory activity of edible brown alga *Saccharina japonica* and its constituents pheophorbide A and pheophytin A in LPS-stimulated RAW 264.7 macrophage cells. Food Chemical Toxicology, 55:541-548.

Izac RR, Sims JJ (1979). Marine natural products. 18. Iodinated sesquiterpenes from the red algal genus *Laurencia*. Journal of American Chemical Society, 101:6136-6137.

Ji NY, Wen W, Li XM, Xue QZ, Xiao HL, Wang BG (2009). Brominated selinane sesquiterpenes from the marine brown alga *Dictyopteris divaricata*. Marine Drugs, 7:355-360.

Jiang RW, Ma SC, He ZD, Huang XS, But PPH, Wang H, Chan SP, Ooi VEC, Xu HX, Mak TCW (2002). Molecular structures and antiviral activities of naturally occurring and modified cassane furanoditerpenoids and friedelane triterpenoids from *Caesalpinia minax*. Bioorganic and Medicinal Chemistry, 10:2161-2170.

Jiao N, Herndl GJ, Hansell DA, Benner R, Kattner G, Wilhelm SW, Kirchman DL, Weinbauer MG, Luo T, Chen F, Azam F (2011). The microbial carbon pump and the oceanic recalcitrant dissolved organic matter pool. Nature Reviews Microbiology, 9:555.

Joy M, Chakraborty K (2017a). Biogenic antioxidative and anti-inflammatory aryl polyketides from the venerid bivalve clam *Paphia malabarica*. Food Chemistry, 237:169-180.

Joy M, Chakraborty K (2017b). Previously undescribed antioxidative and anti-inflammatory chromenyls bearing 3*H*-isochromenone and furanyl-2*H*-chromenyl skeletons from the venerid clam, *Paphia malabarica*. Medicinal Chemistry Research, 26:1708-1722.

Juagdan EG, Kalidindi R, Scheuer P (1997). Two new chamigranes from Hawaiian red alga, *Laurencia cartilaginea*. Tetrahedron, 53:521-528.

Jun JG, Gray GR (1987). A new catalyst for reductive cleavage of methylated glycans. Carbohydrate Research, 163:247-261.

Kain JM (1991). Cultivation of attached seaweeds, In: Guiry, M.D. et al. (Ed.) Seaweed resources in Europe: Uses and potential, pp 309-377.

Kamada T, Vairappan CS (2013). New bioactive secondary metabolites from Bornean red alga, *Laurencia similis* (Ceramiales). Natural Product Communication, 8:287-288.

Kanai Y, Hiroki S, Koshino H, Konoki K, Cho Y, Cayme M, Fukuyo Y, Yotsu-Yamashita M (2011). Identification of novel oxidized levuglandin D_2 in marine red alga and mouse tissue. Journal of Lipid Research, 52:2245-2254.

Kang HS, Chung HY, Jung HA, Son BW, Choi JS (2003). A new phlorotannins from the brown alga *Ecklonia stolonifera*. Chemical and Pharmaceutical Bulletin, 51:1012-1014.

Kang HS, Chung HY, Kim JY, Son BW, Jung HA, Choi JS (2004). Inhibitory phlorotannins from the edible brown alga *Ecklonia stolonifera* on total reactive oxygen species (ROS) generation. Archives of Pharmacal Research, 27:194-198.

Kang KA, Bu HD, Park DS, Go GM, Jee Y, Shin T, Hyun JW (2005). Antioxidant activity of ethanol extract of *Callophyllis japonica*. Phytotherapy Research, 19:506-510.

Kato T, Kumanireng AS, Ichinose I, Kitahara Y, Kakinuma Y, Kato Y (1975). Structure and synthesis of active component from a marine alga, *Sargassum*. Chemistry Letters, 4:335-338.

Kazlauskas R, Lidgard RO, Wells RJ (1978). New polybrominated metabolites from the red alga *Ptilonia australasica*. Tetrahedron Letters, 34:3165-3168.

Kazlauskas R, Murphy PT, Qulnn RJ, U1ells RJ (1977a). A new class of halogenated lactones from the red alga *Delisea fimhriata* (Bonnemaisoneaceae). Tetrahedron Letters, 1:37-40.

Kazlauskas R, Murphy PT, Wells RJ (1982a). A brominated metabolite from the red alga *Vidalia spiralis*. Australian Journal of Chemistry, 35:219-220.

Kazlauskas R, Murphy PT, Wells RJ, Baird-Lambert JA, Jamieson DD (1983). Halogenated pyrrolo [2,3-d] pyrimidine nucleosides from marine organisms. Australian Journal of Chemistry, 36:165-170.

Kazlauskas R, Murphy PT, Wells RJ, Blackman A (1982b). Macrocyclic enol-ethers containing an acetylenic group from the red alga *Phacelocarpus labillardieri*. Australian Journal of Chemistry, 35:113-120.

Kazlauskas R, Murphy PT, Wells RJ, Daly JJ, Oberhansli WE (1977b). Heterocladol, a halogenated selinane sesquiterpene of biosynthetic significance from the red alga *Laurencia filiformis*: Its isolation, crystal structure andabsolute configuration. Australian Journal of Chemistry, 30:2679-2687.

Kigoshi H, Ojika M, Shizuri Y, Niwa H, Yamada K (1982).(10R, 11R)-(+)-squalene-10, 11-epoxide: Isolation from *Laurencia okamurai* and the asymmetric synthesis. Tetrahedron Letters, 23:5413-5414.

Kigoshi H, Shizuri Y, Niwa H, Yamada K (1981). Laurencenyne, a plausible precursor of various nonterpenoid C_{15}-compounds, and neolaurencenyne from the red alga *Laurencia okamurai*. Tetrahedron Letters, 22:4729-4732.

Kim KT, Rioux LE, Turgeon SL (2014). Alpha-amylase and alpha-glucosidase inhibition is differentially modulated by fucoidan obtained from *Fucus vesiculosus* and *Ascophyllum nodosum*. Phytochemistry, 98:27-33.

Kim SK, Pangestuti R (2011). Biological activities and potential health benefits of fucoxanthin derived from marine brown algae. Advances in Food and Nutrition Research, 64:111-128.

Kim YJ, Kim EH, Hahm KB (2012). Oxidative stress in inflammation-based gastrointestinal tract diseases: Challenges and opportunities. Journal of Gastroenterolgy Hepatology, 27:1004-1010.

Kindleysides S, Quek SY, Miller MR (2012). Inhibition of fish oil oxidation and the radical scavenging activity of New Zealand seaweed extracts. Food Chemistry, 133:1624-1631.

King H, Aubert RE, Herman WH (1998). Global burden of diabetes, 1995-2025: Prevalence, numerical estimates and projections. Diabetes Care, 2:1414-1431.

King TJ, Imre S, Oztuns A, Thomson RH (1979). Obtusenyne, a new acetylenic nine-membrered cyclic ether from *Laurenica obtuse*. Tetrahedron Letters, 20:1453-1454.

Kirkup MP, Moore RE (1983). Indole alkaloids from the marine red alga *Martensia fragilis*. Tetrahedron Letters, 24:2087-2090.

Kiwitt-Haschemie K, Heims H, Steinhart H, Mischnick P (1993). The analysis of agarose by the reductive cleavage method. Carbohydrate Research, 248:267-275.

Kladi M, Vagias C, Furnari G, Moreau D, Roussakis C, Roussis V (2005). Cytotoxic cuparene sesquiterpenes from *Laurencia microcladia*. Tetrahedron Letters, 46:5723-5726.

Kladi M, Vagias C, Papazafiri P, Brogi S, Tafi A, Roussis V (2009). Tetrahydrofuran acetogenins from *Laurencia glandulifera*. Journal of Natural Product, 72:190-193.

Kladi M, Vagias C, Roussis V (2004). Volatile halogenated metabolites from marine red algae. Phytochemistry Review, 3:337-366.

Kladi M, Vagias C, Stavri M, Rahman MM, Gibbons S, Roussis V (2008). C_{15} acetogenins with antistaphylococcal activity from the red alga *Laurencia glandulifera*. Phytochemistry Letters, 1:31-36.

Kladi M, Xenaki H, Vagias C, Papazafiri P, Roussis V (2006). New cytotoxic sesquiterpenes from the red algae *Laurencia obtusa* and *Laurencia microcladia*. Tetrahedron, 62:182-189.

Kojima K, Ham T, Kato T (1980). Rapid chromatographic purification of dipeptidyl peptidase-IV in human submaxiallry gland. Journal of Chromatography, 189:233-240.

Konig GM, Wright AD (1997a). *Laurencia rigida*: Chemical investigations of its antifouling dichloromethane extract. Journal of Natural Product, 60:967-970.

Konig GM, Wright AD (1997b). Sesquiterpene content of the antibacterial dichloromethane extract of the marine red alga *Laurencia obtusa*. Planta Medica, 63:186-187.

Kornprobst JM (2005). Substances naturelles d origine marine. Chimiodiversite-Pharmacodiversite-Biotechnologie. 1. Generalites-Micro-organismes-Algues. Lavoisier, Paris.

Kubo I, Xiao P, Fujita K (2001). Antifungal activity of octyl gallate: Structural criteria and mode of action. Bioorganic and Medicinal Chemistry Letters, 11:347-350.

Kulisic T, Radonic A, Katalinic V, Milos M (2004). Use of different methods for testing antioxidative activity of oregano essential oil. Food Chemistry, 85:633-640.

Kumar KS, Ganesan K, Subba Rao PV (2008). Antioxidant potential of solvent extracts of *Kappaphycus alvarezii* (Doty) Doty edible seaweed. Food Chemistry, 107:289-295.

Kurata K, Amiya T (1977). Two new bromophenols from the red alga, *Rhodomela larix*. Chemistry Letters, 6:1435-1438.

Kurata K, Amiya T (1980). Bis (2, 3, 6-tribromo-4, 5-dihydroxybenzyl) ether from the red alga, *Symphyocladia latiuscula.* Phytochemistry, 19:141-142.

Kurata K, Furusaki A, Katayama C, Kikuchi H, Suzuki T (1981). A new labile sesqiterpene diol having bromine from the marine red alga *Laurencia nipponica* Yamada. Chemistry Letters, 10:773-776.

Kurata K, Furusaki A, Suehiro K, Katayama C, Suzuki T (1982). Isolaurallene, a new nonterpenoid C_{15}-bromoallene, from the red alga *Laurencia nipponica* Yamada. Chemistry Letters, 11:1031-1034.

Kurata K, Suzuki T, Suzuki M, Kurosawa E, Furusaki A, Matsumoto T (1983). Constituents of marine plants. Laurenical, a novel sesquiterpene α, β-unsaturated aldehyde from the red alga *Laurencia Nipponica* Yamada. Chemistry Letters, 3:299-300.

Kurata K, Taniguchi K, Agatsuma Y, Suzuki M (1998). Diterpenoid feeding-deterrents from *Laurencia saitoi*. Phytochemistry, 47:363-369.

Kurosawa E, Fukuzawa A, Irie T (1973). Isoprelaurefucin, new bromo compound from *Laurencia nipponica Yamada*. Tetrahedron Letters, 14:4135-4138.

Kwangwoo C, Song-Kyu P, Hwan Mook K, Yongseok C, Myung-Hwa K, Chun-Ho P, Bo-Young J, Tae Gyu C, Hyun-Moo C, Hee-Yoon L (2008). Chromen-based TNF-α converting enzyme (TACE) inhibitors: Design, synthesis, and biological evaluation. Bioorganic and Medicinal Chemistry, 16:530-535.

Larsen LN, Dahl E, Bremer J (1996a). Peroxidative oxidation of leucodichloroluorescein by prostaglandin H synthase in prostaglandin biosynthesis from polyunsaturated fatty acids. Biochimica et Biophysica Acta, 1299:47-53.

Laurienzo (2010). Marine polysaccharides in pharmaceutical applications: An overview. Marine Drugs, 8:2435-2465.

Leal MC, Munro MHG, Blunt JW, Puga J, Jesus B, Calado R (2013). Biogeography and biodiscovery hotspots of macroalgal marine natural products. Natural Product Report, 30:1380-1390.

Lee DS, Park WS, Heo SJ, Cha SH, Kim D, Jeon YJ, Park SG, Seo SK, Choi JS, Park SJ (2011). Polyopes affinis alleviates airway inflammation in a murine model of allergic asthma. Journal of Bioscience, 36:869-877.

Lee HJ, Dang HT, Kang GJ, Yang EJ, Park SS, Yoon WJ, Jung JH, Kang HK, Yoo ES (2009). Two enone fatty acids isolated from *Gracilaria verrucosa* suppress the production of inflammatory mediators by down-regulating NF kappa B and STAT1 activity in lipopolysaccharide-stimulated RAW 264.7 cells. Archives of Pharmacal Research, 32:453-462.

Lee SH, Han JS, Heo SJ, Hwang JY, Jeon YJ (2010). Protective effects of dieckol isolated from *Ecklonia cava* against high glucose-induced oxidative stress in human umbilical vein endothelial cells. Toxicology in Vitro, 24:375-381.

Leiro JM, Castro R, Arranz JA, Lamas J (2007). Immunomodulating activities of acidic sulphated polysaccharides obtained from the seaweed *Ulva rigid*a C. Agardh. International Journal of Immunopharmacology, 7:879-888.

Leonard F, Collnot EM, Lehr CM (2010). A three-dimensional coculture of enterocytes, monocytes and dendritic cells to model inflamed intestinal mucosa *in vitro*. Molecular Pharmaceutics, 7:2103-2119.

Li K, Li XM, Gloer JB, Wang BG (2011). Isolation, characterization and antioxidant activity of bromophenols of the marine red alga *Rhodomela confervoides*. Journal of Agricultural Food Chemistry, 59:9916-9921.

Li F, Harmer P, Glasgow R, Mack KA, Sleet D, Fisher KJ (2008). Translation of an effective Tai Chi intervention into a community-based falls prevention program. American Journal of Public Health, 98:1195-1198.

Liebgott T, Miollan M, Berchadsky Y, Drieu K, Culcasi M, Pietri S (2000). Complementary cardioprotective effects of flavonoid metabolites and terpenoid constituents of Ginkgo biloba extract (EGb 761) during ischemia and reperfusion. Basic Research in Cardiology, 95:368-377.

Lindsay RC (1996). Food additives. In: Fennema OR, editor. Food chemistry. New York: Marcel Dekker, pp 778-780.

Lipinski C, Hopkins A (2004). Navigating chemical space for biology and medicine. Nature, 432:855-861.

Liu L, Heinrich M, Myers S, Dworjanyn SA (2012). Towards a better understanding of medicinal uses of the brown seaweed *Sargassum* in traditional Chinese medicine: A phytochemical and pharmacological review. Journal of Ethnopharmacology, 142:591-619.

Lobo V, Phatak A, Chandra N (2010). Free radicals and functional foods: Impact on human health. Pharmacognosy Reviews, 4:118-126.

Lordan S, Ross RP, Stanton C (2011). Marine bioactives as functional food ingredients: Potential to reduce the incidence of chronic diseases**.** Marine Drugs, 9:1056-1100.

Luning K (1990). Seaweeds: Their Environment, biogeography and ecophysiology. New York, John Wiely and sons.

Maneesh A, Chakraborty K (2018). Pharmacological potential of sulfated polygalactopyranosyl-fucopyranan from the brown seaweed *Sargassum wightii*. Journal of Applied Phycology, 30:1971-1988.

Manefield M, de Nys R, Kumar N, Read R, Givskov M, Steinberg P, Kjelleberg S (1999). Evidence that halogenated furanones from *Delisea pulchra* inhibit acylated homoserine lactone (AHL) - mediated gene expression by displacing the AHL signal from its receptor protein. Microbiology, 145:283-291.

Manta E (2001). New sesquiterpene derivatives from the red alga *Laurencia scoparia*. Isolation, structure determination and anthelmintic activity. Journal Natural Product, 64:1552-1555.

Mariana Barbosa, Patricia Valentao, Paula B, Andrade (2014). Bioactive Compounds from Macroalgae in the New Millennium: Implications for Neurodegenerative Diseases. Marine Drugs, 12:4934-4972.

Masuda M, Abe T, Sato S, Suzuki T, Suzuki M (1997). Diversity of halogenated secondary metabolites in the red alga *Laurencia nipponica* (Rhodomelaceae, Ceramiales). Journal of Phycology, 33:196-208.

Mata L, Wright E, Owens L, Paul N de Nys R (2013). Water soluble natural products from seaweed have limited potential in controlling bacterial pathogens in fish aquaculture. Journal of Applied Phycology, 25:1963-1973.

Matanjun P, Suhaila M, Noordin MM, Kharidah M, Ming CH (2008). Antioxidant activities and phenolic content of eight species of seaweeds from North Borneo. Journal of Applied Phycology, 20:367-373.

Matsui T, Ueda T, Sugita K, Terahara N, Matsumoto K (2001). α-Glucosidase inhibitory action of natural acylated anthocyanins. Journal of Agricultural Food Chemistry, 49:1952-1956.

Mayer AMS, Lehmann VKB (1998). Marine pharmacology in 1998: Marine compounds with antibacterial, anticoagulant, anti-inflammatory, anthelmintic, antiplatelet, antiprotozoal, and antiviral activities; with actions on the cardiovascular, endocrine, immune, and nervous systems; and other miscellaneous mechanisms of action. The Pharmacologist, 42:62-69.

McConnell OJ, Fenical W (1978). Ochtodene ochtodiol: Novel polyhalogenated cyclic monoterpenes from the red seaweed *Ochtodes secundiramea*. Journal of Organic Chemistry, 43:4238-4241.

McHugh DJ (2003). A guide to seaweed industry, FAO Fisheries Technical paper, No. 441. Rome, FAO, pp 105.

McLean JS, Byrick RJ (1993). ARDS and sepsis-definitions and new therapy. Canadian Journal of Anaesthaesia, 40:585-590.

Melo MRS, Feitosa JPA, Freitas ALP, de Paula RCM (2002). Isolation and characterization of soluble sulfated polysaccharide from the red seaweed *Gracilaria cornea*. Carbohydrate Polymers, 49:491-498.

Mendonca P, Freitas JC (2000). Topical antiedematous activity of the organic extract of *Liagora farinosa* algae (Rhodophyta, Nemaliales). Ciencia e Cultura, 52:175-178.

Mentlein R (1999). Dipeptidyl-peptidase IV (CD26): Role in the inactivation of regulatory peptides. Regulatory Peptides, 24:85-89.

Mikami D, Kurihara H, Kim SM, Takahashi K (2013). Red algal bromophenols as glucose 6-phosphate dehydrogenase inhibitors. Marine Drugs, 11:4050-4057.

Milan M, Mirjana M, Desanka B, Sanja M, Neda N, Vladimir M (2011). *In vitro* antioxidant of selected 4-hydroxy-chromen-2-one derivatives-SAR, QSAR and DFT studies. International Journal of Molecular Sciences, 12:2822-2841.

Minelli A, Chagas-junior A, Edgecombe GD (2009). Saltational evolution of trunk segment number in centipedes. Evolution and Development, 11:318-322.

Mollet JC, Rahaoui A, Lemoine Y (1998). Yield, chemical composition and gel strength of agarocolloids of *Gracilaria gracilis*, *Gracilariopsis longissima* and the newly reported *Gracilaria cf. vermiculophylla* from Roscoff (Brittany, France). Journal of Applied Phycology, 10:59-66.

Mori J, Hayashi T, Iwashima M, Matsunaga T, Saito H (2003). Effects of plastoquinones from the brown alga *Sargassum micracanthum* and a new chromen derivative converted from the plastoquinones on acute gastric lesions in rats. Biological and Pharmaceutical Bulletin, 29:1197-1201.

Murai A, Iwamura K, Takada M, Ogawa K, Usui T, Okumura JI (2002). Control of postprandial hyperglycaemia by galactosyl maltobionolactone and its novel anti-amylase effect in mice. Life Science, 71:1405-1415.

Murai, Murase H, Matsue H, Masamune T (1977). The synthesis of (±)-Laurencin. Tetrahedron Letters, 18:2507-2510.

Murano E (1995). Chemical structure and quality of agars from *Gracilaria*. Journal of Applied Phycology, 7:245-254.

Murano E, Toffanin R, Pedersini C, Carabot Cuervo A, Blunden G, Rizzo R (1996). Structure and properties of agar from two unexploited agarophytes from Venezuela. Hydrobiologia, 327:497-500.

Muzzarelli RAA (1997). Human enzymatic activities related to the therapeutical administration of chitin derivatives. Cellular and Molecular Life Science, 53:131-140.

Mynderse JS, Faulkner DJ (1974). Polyhalogenated acyclic and monocyclic monoterpenes have been found previously in red algae belonging to the genus *Plocamium*. Journal of American Chemical Society, 96:6771-6772.

Mynderse JS, Faulkner DJ (1978). Variations in the halogenated monoterpene metabolites of *Plocamium cartilagineum* and *Plocamium violaceum.* Phytochemistry, 17:237-240.

Nagarani N, Kumaraguru AK (2013). Evaluation of anti-inflammatory, antidiabetic, cytotoxic activity of *K. alvarezii*. International Journal of Pharma and Biosciences, 4:921-929.

Newman DJ, Cragg GM (2012). Natural products as sources of new drugs over the 30 years from 1981 to 2010. Journal of Natural Product, 75:311-335.

Ngo DH, Kim SK (2013). Sulfated polysaccharides as bioactive agents from marine algae. International Journal of Biological Macromolecules, 62:70-75.

Nicolaou KC, Pfefferkorn JA, Roecker AJ, Cao GQ, Barluenga S, Mitchell HJ (2000). Natural product-like combinatorial libraries based on privileged structures. 1. General principles and solid-phase synthesis of benzopyrans. Journal of American Chemical Society, 122:9939-9953.

Nisizawa K, Noda H, Kikuchi R, Watamaba T (1987). The main seaweeds food in Japan. Hydrobiologia, 151/152:5-29.

Numata A, Takahashi C, Ito Y, Takeda T, Kawai K, Osami Y, Matsumura E, Imachi M, Ito T, Hasegawa T (1993). Communesins, cytotoxic metabolites of a fungus isolated from a marine alga. Tetrahedron Letter, 34:2355-2358.

Nunnery JK, Mevers E, Gerwick WH (2010). Biologically active secondary metabolites from marine cyanobacteria. Current Opinion Biotechnology, 21:787-793.

Ochieng CO, Owuor PO, Manguro LAO, Akala H, Ishola IO (2012). Antinociceptive and antiplasmodial activities of cassane furanoditerpenes from *Caesalpinia volkensii H*. root bark. Fitoterapia, 83:74-80.

Ohno M (1993). Cultivation of the green alga, *Monostroma* and *Enteromorpha* "aonori", pp 51-56.

Ohno M, Largo DB, Ikumoto T (1994). Growth rate, sulphated galactan yield and gel properties of cultured kappa-carrageenan producing red alga *Kappaphycus alvarezii* (Doty) Doty in the subtropical waters of Shikoku, Japan. Journal of Applied Phycology, 6:1-5.

Olsen EK, Hansen E, Isaksson J, Andersen JH (2013). Cellular antioxidant effect of four bromophenols from the red algae, *Vertebrata lanosa*. Marine Drugs, 11:2769-2784.

Ovenden SPB , Nielson JL, Liptrot CH, Willis RH, Tapiolas DM, Wright AD, Motti CA, (2011). Callophycin A, a cytotoxic tetrahydro-beta-carboline from the red alga *Callophycus oppositifolius*. Phytochemistry Letters, 4:69-71.

Paiva L, Lima E, Neto AI, Baptista J (2016). Angiotensin I-converting enzyme (ACE) inhibitory activity of Fucus spiralis macroalgae and influence of the extracts storage temperature—A short report. Journal of Pharmaceutical and Biomedical Analysis, 131:503-507.

Pangestuti R, Kim SK (2011). Neuroprotective effects of marine algae. Marine Drugs, 9:803-818.

Parke A, Parke DV (1995). The pathogenisis of inflammatory disease: Surgical shock and multiple system organ failure. Inflammopharmacology, 3:149-168.

Parke DV (1994). The cyctochromes P450 and mechanisms of chemical carcinogenesis. Environmental Health Perspectives, 102:852-853.

Parshikov IA, Netrusov AI, Sutherland JB (2012). Microbial transformation of antimalarial terpenoids. Biotechnology Advances, 30:1516-1523.

Paul VJ, Fenical W (1980a). Palisadins A, B and related monocyclofarnesol-derived sesquiterpenoids from the red marine alga *Laurencia cf. palisade*. Tetrahedron Letters, 21:2787-2790.

Paul VJ, Fenical W (1980b). Toxic acetylene-containing lipids from the red marine alga *Liagorafarinosa lamouroux*. Tetrahedron Letters, 21:3327-3330.

Pereira DM, Cheel J, Areche C, San-Martin A, Rovirosa J, Silva LR, Valentao P, Andrade PB (2011). Antiproliferative activity of meroditerpenoids isolated from the brown alga *Stypopodium flabelliforme* against several cancer cell lines. Marine Drugs, 9:852-862.

Piccolella S, Fiorentino A, Pacifico S, D'Abrosca B, Uzzo P, Monaco P (2008). Antioxidant properties of sour cherries (Prunus cerasus L.): Role of colorless phytochemicals from the methanolic extract of ripe fruits. Journal of Agricultural Food Chemistry, 56:1928-1935.

Pietta PG (2000). Flavonoids as antioxidants. Journal of Natural Product, 63:1035-1042.

Pomin VH, Maurao PA (2008). Structure, biology, evolution, and medical importance of sulfated fucans and galactans. Glycobiology, 18:1016-1027.

Praveen NK, Chakraborty K (2013). Antioxidant and anti-inflammatory potential of the aqueous extract and polysaccharide fraction from brown marine macroalgae *Padina* sp from Gulf of Mannar of Peninsular India. Journal of Coastal Life Medicine, 1:38-48.

Quan (2008). Evolutionary and transcriptional analysis of karyopherin beta superfamily proteins. Molecular Cell Proteomics, 7:1254-69.

Ragan MA, Glombitza KW (1986). Phlorotannins, brown algal polyphenols. In: Round FE, Chapman DJ (eds) Progress in phycological research. Biopress, Bristol, pp 129-241.

Rao PNP, Knaus EE (2008). Evolution of nonsteroidal antiinflammatory drugs (NSAIDs): Cyclooxygenase (COX) inhibition and beyond. Journal of Pharmacy and Pharmaceutical Sciences, 11:81-110.

Rateb ME, Ebel R (2011). Secondary metabolites of fungi from marine habitats. Natural Product Report, 28:290-344.

Rinaudo M (2001). Relation between the molecular structure of some polysaccharides and original properties in sol and gel states. Food Hydrocolloids, 15:433-440.

Rochfort SJ, Capon RJ (1996). Parguerenes revisited: New brominated diterpenes from the southern Australian marine red alga *Laurencia filiformis*. Australian Journal of Chemistry, 49:19-26.

Rosanna DP, Salvatore C (2012). Reactive oxygen species, inflammation, and lung diseases. Current Pharmaceutical Design, 18:3889-3900.

Rose AF, Sims JJ (1977). Marine natural products XIV. 1-S-bromo-4-R-hydroxyselin-7-ene, a metabolite of the marine alga *Laurencia* sp. Tetrahedron Letters, 18:2935-2938.

Rose AF, Sims JJ, Wing RM, Wiger GM (1978). Marine natural products XVII. The structure of (1S, 4R, 7R)-1-bromo-4-hydroxy-7-chloroselinane, a metabolite of the marine alga *Laurencia* Sp. Tetrahedron Letters, 19:2533-2536.

San Martin A, Rovirosa J, Munoz O, Chen MHM, Guneratne RD, Clardy J (1983). The isolation and structure determination of chilenone A, a putative dimer of 2-methyl-3(2H)-furanone from the marine alga *Laurencia chilensis.* Tetrahedron Letters, 24:4063-4066.

Sasidharan S, Darah I, Jainc Witz K (1991). Antimicrobial activity and wound healing potential on infected rat of *Gracilaria Changii* methanolic extract. Pharmacologyonline, 2:661-670.

Sasidharan S, Darah I, Noordin MK (2008). Preliminary isolation and *in vitro* antiyeast activity of active fraction from crude extract of *Gracilaria changii*. Indian Journal of Pharmacology, 40:227-229.

Sato M, Hosokawa T, Yamaguchi T, Nakano K, Muramoto T, Kahara K, Funayama A, Kobayashi A (2002). Antihypertensive effects of hydrolysates of *wakame* (*Undaria pinnatifida*) and their angiotensin-I converting enzyme inhibitory activity. Annals of Nutrition and Metabolism, 46:259-267.

Savoia C, Schiffrin EL (2007). Vascular inflammation in hypertension and diabetes: Molecular mechanisms and therapeutic interventions. Clinical Sciences, 112:375-384.

Schramm A, Matusik P, Osmenda G, Guzik TJ (2012). Targeting NADPH oxidases in vascular pharmacology. Vascular Pharmacology, 56:216-231.

Selover SJ, Crews P (1980). Kylinone, a new sesqiterpene skeleton from the marine alga *Laurencia pacifica*. Journal of Organic Chemistry, 45:69-72.

Senni K, Gueniche F, Foucault-Bertaud A, Igondjo-Tchen S, Fioretti F, Colliec-Jouault S, Durand P, Guezennec J, Godeau G, Letourneur D (2006). Fucoidan a sulfated polysaccharide from brown algae is a potent modulator of connective tissue proteolysis. Archives of Biochemistry and Biophysics, 445:56-64.

Seung-Hong L, You-Jin J (2013). Anti-diabetic effects of brown algae derived phlorotannins, marine polyphenols through diverse mechanisms. Fitoterapia, 86:129-136.

Shen L, Park EJ, Kondratyuk TP, Guendisch D, Marler L, Pezzuto JM, Wright AD, Sun D (2011). Design, synthesis, and biological evaluation of callophycin A and

analogues as potential chemopreventive and anticancer agents. Bioorganic and Medicinal Chemistry, 19:6182-6195.

Sievanen L, Crawford B, Pollnac R, Lowe C (2005). Weeding through assumptions of livelihood approaches in ICM: Seaweed farming in the Philippines and Indonesia. Ocean and Coastal Management, 48:297-313.

Silva ED, Scheuer PJ (1980). Manoalide, an antibiotic sesterterpenoid from the marine sponge *Luffariella variabilis*. Tetrahedron Letters, 21:1611-1614.

Silva LM, Lima V, Holanda ML, Pinheiro PG, Rodrigues JA, Lima ME, Benevides NM (2010). Antinociceptive and anti-inflammatory activities of lectin from marine red alga *Pterocladiella* capillacea. Biological and Pharmaceutical Bulletin, 33:830-835.

Silva PC, Basson PW, Moe RL (1996). Catalogue of the benthic marine algae of the Indian Ocean. University of California Publications in Botany, 79:1-1259.

Sivasothy Y, Hadi AHA, Mohamad K, Leong KH, Ibrahim H, Sulaiman SF (2012). Spectaflavoside A, new potent iron chelating dimeric flavonol glycoside from the rhizomes of *Zingiber spectabile* Griff. Bioorganic and Medicinal Chemistry Letters, 22:3831-3836.

Slater TF (1979). Mechanisms of protection against the damage produced in biological systems by oxygen-derived radicals. Ciba Foundation Symposium, 65:143-162.

Souza BWS, Cerqueira MA, Bourbon AI, Pinheiro AC, Martins JT, Teixeira JA (2012). Chemical characterization and antioxidant activity of sulfated polysaccharide from the red seaweed *Gracilaria birdiae*. Food Hydrocolloid, 27:287-292.

Stierle DB, Wing RM, Sims JJ (1979). Marine natural products XV: Polyhalogenated cyclic monoterpenes from the red alga *Plocamium cartilegineum* of Antartica. Tetrahedron, 35:2855-2859.

Suetsuna K, Nakano T (2000). Identification of an antihypertensive peptide from peptic digest of *wakame* (*Undaria pinnatifida*). Journal of Nutritional Biochemistry, 11:450-454.

Sun HH, Erickson KL (1978). Sesquiterpenoids from the Hawaiian marine alga *Laurencia nidifica*. 7. (+)-selin-4, 7(11)-diene. Journal of Organic Chemistry, 43:1613-1614.

Sun WS, Su S, Zhu RX, Tu GZ, Cheng W, Liang H, Guo XY, Zhao YY, Zhang QY (2013). A pair of unprecedented spiro-trisindole enantiomers fused through a five-member ring from *Laurencia similis*. Tetrahedron Letters, 54:3617-3620.

Suzuki M, Furusaki A, Kurosawa E (1979). The absolute configurations of halogenated chamigrene derivatives from the marine alga, *Laurencia glandulifera*. Tetrahedron, 35:823-831.

Suzuki M, Kowata N, Kurosawa E (1980a). The structure of spirolaurenone, a halogenated sesquiterpenoid from the red alga *Laurencia glandulifera kutzing*. Tetrahedron, 36:1551-1556.

Suzuki M, Kurosawa E (1978). Two new halogenated sesquiterpenes from the red alga *Laurencia majuscule*. Tetrahedron Letters, 19:4805-4808.

Suzuki M, Kurosawa E (1979). Halogenated sesquiterpene phenols and ethers from the red alga *Laurencia glandulifera* Kutzing. Bulletin of the Chemical Society Japan, 52:3349-3351.

Suzuki M, Kurosawa E (1980). Venustin A and B, new halogenated C_{15} metabolites from the red alga *Laurencia venusta* Yamada. Chemistry Letters, 9:1177-1180.

Suzuki M, Kurosawa E (1981). Okamurallene, a novel halogenated C_{15} metabolite from the red alga *Laurencia okamuhai* Yamada. Tetrahedron Letters, 22:3853-3856.

Suzuki M, Kurosawa E, Furusaki A, Matsumoto T (1983a). The structures of (3Z)-epoxyvenustin, (3Z)-venustin and (3Z)-venustinene, new halogenated C_{15}-nonterpenoids from the red alga *Laurencia venusta* Yamada. Chemistry Letters, 12:779-782.

Suzuki T, Kikuchi H, Kurosawa E (1980b). (E)-γ-bisabolen-8, 9-epoxide and isocycloeudesmol, two new sesquiterpenoids from the marine red alga *Laurencia nipponica* Yamada. Chemistry Letters, 9:1267-1270.

Suzuki T, Koizumi K, Suzuki M, Kurosawa E (1983b). Kumausynes and deacetylkumausynes, four new halogenated C-15 acetylenes from the red alga *Laurencia nipponica* Yamada. Chemistry Letters, 12:1643-1644.

Swanson AK, Druehl LD (2002). Induction, exudation and the UV protective role of kelp phlorotannins. Aquatic Botany, 73:241-253.

Tacconelli S, Capone ML, Sciulli MG, Ricciotti E, Patrignani P (2002). The biochemical selectivity of novel COX-2 inhibitors in whole blood assays of COX-isozyme activity. Current Medicinal Research and Opinion, 18:503-511.

Takahashi C, Takai Y, Kimura Y, Numata A, Shigematsu N, Tanaka H (1995). Cytotoxic metabolites from a fungi adherent of a marine alga. Phytochemistry, 38:155-158.

Takaichi S (2011). Carotenoids in algae: Distributions, biosyntheses and functions. Marine Drugs, 9:1101-1118.

Topcu G, Aydogmus Z, Imre S, Goren AC, Pezzuto JM, Clement JA, Kingston DG (2003). Brominated sesquiterpenes from the red alga *Laurencia obtuse*. Journal of Natural Product, 66:1505-1508.

Toth G, Pavia H (2000). Lack of phlorotannin induction in the brown seaweed *Ascophyllum nodosum* in response to increased copper concentrations. Marine Ecology Progress Series, 192:119-126.

Troell M, Ronnback P, Halling C, Katusky, N, Buschmann A (1999). Ecological engineering in aquaculture: Use of seaweeds for removing nutrients from intensive mariculture. Journal of Applied Phycology, 11:89-97.

Tsujino I, Yabe K, Sekikawa I, Hamanaka N (1978). Isolation and structure of a mycosporine from the red alga *Chondrusyendoi*. Tetrahedron Letters, 16:1401-1402.

Turkez H, Gurbuz H, Aydin E, Aslan A, Dirican E (2012). The evaluation of the genotoxic and oxidative damage potentials of *Ulothrix tenuissima in vitro*. Toxicology and Industrial Health, 28:147-151.

Udenigwe CC, Lin Y, Hou W, Aluko RE (2009). Kinetic of the inhibition of renin angiotensin I-converting enzyme by flaxseed protein hydrolysate functions. Journal of Functional Food, 1:199-207.

Vairappan CS, Kamada T, Lee WW, Jeon YJ (2013). Anti-inflammatory activity of halogenated secondary metabolites of *Laurencia snackeyi* (Weber-van Bosse Masuda in LPS-stimulated RAW 264.7 macrophages). Journal of Applied Phycology, 25:1805-1813.

Vairappan CS, Kawamoto T, Miwa H, Suzuki M (2004). Potent antibacterial activity of halogenated compounds against antibiotic resistant bacteria. Planta Medica, 70:1087-1090.

Vairappan CS, Suzuki M, Abe T, Masuda M (2001). Halogenated metabolites with antibacterial activity from the *Okinawan Laurencia* species. Phytochemistry, 58:517-523.

Vallinayagam K, Arumugam R, Ragupathy raja kannan G (2009). Antibacterial activity of some selected seaweeds from Pudumadam coastal regions. Global Journal of Pharmacology, 3:50-52.

Van Wyk AWW, Zuck KM, McKee TC (2011). Lithothamnin A, the first bastadin-like metabolite from the red alga *Lithothamnion fragilissimum*. Journal of Natural Product, 74:1275-1280.

Vandevelde F, Knutsen SH, Usov AI, Rollema HS, Cerezo AS (2002). ^{1}H and ^{13}C high resolution NMR spectroscopy of carrageenans: Application in research and industry. Trends in Food Science and Technology International, 13:73-92.

Veena CK, Josephine A, Preetha SP, Varalakshmi P (2007). Beneficial role of sulfated polysaccharides from edible seaweed *Fucus vesiculosus* in experimental hyperoxaluria. Food Chemistry, 100:1552-1559.

Villanueva RD, Montano MNE, Romero JB (2009). Iota-carrageenan from a newly formed, rare variety of eucheumoid seaweed. Journal of Applied Phycology, 21:27-30.

Vosooghi M, Rajabalian S, Sorkhi M, Badinloo M, Nakhjiri M, Negahbani AS (2010). Synthesis and cytotoxic activity of some 2-amino-4-aryl-3-cyano-7-(dimethylamino)-4*H*-chromenes. Research in Pharmaceutical Sciences, 5:9-14.

Wael M, Abdel-Mageed AB, Rainer Ebel B, Fred A, Valeriote C, Jaspars M (2010). Laurefurenynes A-F, new cyclic ether acetogenins from a marine red alga, *Laurencia* sp. Tetrahedron, 66:2855-2862.

Wakibia JG, Bolton JJ, Keats DM, Rait LM (2006). Factors influencing the growth rate of three commercial eucheumoids grown in southern Kenya. Journal of Applied Phycology, 18:565-573.

Wang BG, Zhang WW, Duan XJ, Li XM (2009). *In vitro* antioxidative activities of extract and semi-purified fractions of the marine red alga, *Rhodomela confervoides* (Rhodomelaceae). Food Chemistry, 113:1101-1105.

Wang HMD, Chen, CC, Huynh, P, Chang JS (2015). Exploring the potential of using algae in cosmetics. Bioresource Technology, 184:355-362.

Waraszkiewicz SM, Erickson KL, Finer J, Clardy J (1977). Nidifocene: A reassignment of structure. Tetrahedron Letters, 18:2311-2314.

Waraszkiewicz SM, Sun HH, Erickson KL, Finer J, Clardy J (1978). C_{15}-Halogenated compounds from the Hawaiian marine alga *Laurencia nidifica*. Maneonenes and isomaneonenes. Journal of Organic Chemistry, 43:3194-3204.

Watanabe K, Umeda K, Miyakado M (1989). Isolation and identification of three insecticidal principles from the red algae *Laurencia nipponica* Yamada. Agricultural and Biological Chemistry, 53:2513-2515.

White RH, Hager LP (1978). Intricenyne and related halogenated compounds from *Laurencia intricate*. Phytochemistry, 17:939-941.

Willem AL, Lindani NE, Samuel K, Garreth LM, Simon SM, Charles BK (2005). Ring-closing metathesis for the synthesis of 2*H* and 4*H* chromenes. Tetrahedron, 61:9996-10006.

Williard PG, Grab LA, De Laszlo SE (1983). Synthesis of costatolide, a halogenated monoterpenoid from the red alga *Plocamium costatum*. Journal of Organic Chemistry, 48:1123-1125.

Wojdyło A, Oszmianski J, Czemerys R (2007). Antioxidant activity and phenolic compounds in 32 selected herbs. Food Chemistry, 105:940-949.

Woolard FX, Moore RE, Van Engen D, Clardy J (1978). The structure and absolute configuration of chondrocolactone, A halogenated monoterpene from the red alga *Chondrococcus hornemanni*, and a revised structure for chondrocole A. Tetrahedron Letters, 19:2367-2370.

Wright AE, Wing RM, Sims JJ (1983). Poitediene a new metabolite from the marine red alga *Laurencia Poitei*. Tetrahedron Letters, 24:4649-4652.

Xu X, Yin L, Gao L, Gao J, Chen J, Li J, Song F (2013a). Two new bromophenols with radical scavenging activity from marine red alga *Symphyocladia latiuscula*. Marine Drugs, 11:842-847.

Xu X, Yin L, Wang Y, Wang S, Song F (2013b). A new bromobenzyl methyl sulphoxide from marine red alga *Symphyocladia latiuscula*. Natural Product Research, 27:723-726.

Yan X, Chuda Y, Suzuki M, Nagata T (1999a). Fucoxanthin as the major antoxidant in *Hijikia fusiformis*, common edible seaweed. Bioscience, Biotechnology and Biochemistry, 63:605-607.

Yan XJ, Fang GM, Lou QX (1999b). Studies on free radical scavenging activity in Chinese seaweeds part I. screening results. Chinese Journal of Oceanology and Limnology, 17:240-246.

Yan XJ, Li XC, Zhou CX, Fan X (1996). Prevention of fish oil rancidity by phlorotannins from *Sargassum kjellmanianum*. Journal of Applied Phycology, 8:201-203.

Yang JI, Yeh CC, Lee JC, Yi SC, Huang HW, Tseng CN, Chang HW (2012). Aqueous extracts of the edible *Gracilaria tenuistipitata* are protective against H_2O_2-

induced DNA damage, growth inhibition, and cell cycle arrest. Molecules, 17:7241-7254.

Yangthong M, Nongporn HT, Phromkunthong W (2009). Antioxidant activities of four edible seaweeds from the southern coast of Thailand. Plant Foods Human Nutrition, 64:218-223.

Yoon WJ, Heo SJ, Han SC, Lee HJ, Kang GJ, Kang HK, Hyun JW, Koh YS, Yoo ES (2012). Anti-inflammatory effect of sargachromanol G isolated from *Sargassum siliquastrum* in RAW 264.7 cells. Archives of Pharmacal Research, 35:1421-1430.

Yotsu-Yamashita M, Yasumoto T, Yamada S, Bajarias FFA, Formeloza MA, Romero ML, Fukuyo Y (2004). Identification of polycavernoside A as the causative agent of the fatal food poisoning resulting from the ingestion of the red alga *Gracilaria edulis* in the Philippines. Chemical Research in Toxicology, 17:1265-1271.

Yvin JC, Chevolot-Magueur AM, Chevolot L, Lallemand JY, Potier P, Guilhem J (1982). Delesserine, a new metabolite of mixed biogenesis from the red marine Alga *Delesseria sanguinea* (Lamouroux). Journal of American Chemical Society, 104:4497-4498.

Zhang GN, Zhong LY, Bligh SWA, Guo YL, Zhang CF, Zhang M, Wang ZT, Xu LS (2005). Bi-bicyclic and bi-tricyclic compounds from *Dendrobium thyrsiûorum*. Phytochemistry, 66:1113-1120.

Zhao X, Xue C, Cai Y, Wang D, Fang Y (2005). Study of antioxidant activities of fucoidan from *Laminaria japonica*. High Technology Letters, 11:91-94.

Zhu JK (2001). Plant salt tolerance. Trends in Plant Science, 6:66-71.

LIST OF PUBLICATIONS

The list of published and accepted publications from the thesis work is detailed in this section.

1) Fasina Makkar, Kajal Chakraborty (2017). Antidiabetic and anti-inflammatory potential of sulphated polygalactans from red seaweeds *Kappaphycus alvarezii* and *Gracilaria opuntia*. International Journal of Food Properties, 20(6):1326-1337.
2) Fasina Makkar, Kajal Chakraborty (2017). Unprecedented antioxidative cyclic ether from the red seaweed *Kappaphycus alvarezii* with anti-cyclooxygenase and lipoxidase activities. Natural Product Research, 31:1131-1141.
3) Fasina Makkar, Kajal Chakraborty (2017). Antioxidative sulfated polygalactans from marine macroalgae as angiotensin-I converting enzyme inhibitors. Natural Product Research, 32(17): 2100-2106.
4) Fasina Makkar, Kajal Chakraborty (2017). Previously undescribed antioxidative azonicyl morpholinone alkaloid from red seaweed *Gracilaria opuntia* with anti-cyclooxygenase and lipoxidase properties. Natural Product Research, 32(10):1150-1160.
5) Fasina Makkar, Kajal Chakraborty (2018). Highly oxygenated antioxidative 2*H*-chromen derivative from the red seaweed *Gracilaria opuntia* with pro-inflammatory cyclooxygenase and lipoxygenase inhibitory properties. Natural Product Research, 32(23): 2756-2765.
6) Fasina Makkar, Kajal Chakraborty (2018). Novel furanyl derivatives from the red seaweed *Gracilaria opuntia* with pharmacological activities using different *in vitro* models. Medicinal Chemistry Research, 31:1131-1141.
7) Fasina Makkar, Kajal Chakraborty (2018). Antioxidant and anti-inflammatory oxygenated meroterpenoids from the thalli of red seaweed *Kappaphycus alvarezii*. Medicinal Chemistry Research, 27(8):2016-2026.
8) Fasina Makkar, Kajal Chakraborty (2018). First report of duel cyclooxygenase-2 and 5-lipoxygenase inhibitory halogen derivatives from the thallus of intertidal seaweed *Kappaphycus alvarezii*. Medicinal Chemistry Research, 27: 2331-2340.

PRESENTATION IN SEMINAR/SYMPOSIA

1) Fasina Makkar, Kajal Chakraborty (2017). Seminar presentation entitled "Previously undescribed and anti-inflammatory pharmacophores from red marine macroalga *Kappaphycus alvarezii*" in the National Seminar on Current Trends in Chemistry CTriC 2017 held at Cochin University of Science and Technology on 03rd and 4 th February 2017.
2) Fasina Makkar, Kajal Chakraborty (2017). Seminar presentation entitled "Antioxidative, anti-diabetic, anti-inflammatory and anti-hypertensive potential of sulfated polygalactans isolated from red macro algae *Kappaphycus alvarezii* and *Gracilaria opuntia*" in the National Seminar on Green Chemistry for Environmental Sustainability on 7 and 8 February 2017 held at Bharata Mata College, Thrikkakara , Kochi, Kerala.